

TEQIP II SPONSORED
1st National Power & Energy
System Conference
(NPESC-2014)
(APRIL 25th & 26th-2014)



PROCEEDINGS



**ELECTRICAL ENGINEERING DEPARTMENT
KAMLA NEHRU INSTITUTE OF TECHNOLOGY
SULTANPUR-228118 (INDIA)**

Lists of Key Note Address Speakers for NPESC-14



Prof. S P Singh, IIT (BHU), Varanasi



Prof. R K Mishra, IIT (BHU), Varanasi



Prof. R Mahanty, IIT (BHU), Varanasi



Prof. D Singh, IIT (BHU), Varanasi



Dr. UKD Dwivedi, RGIPT, Raebareli



Dr. Prabhakr Tiwari, GCET, Greater Noida

CONTENTS

About NPESC-2014

The Kamla Nehru Institute of Technology, Sultanpur

Conference Committee

Advisory Committee

Students Committee

Vice-Chancellor's Message

Patron's Message

Coordinator's Message

Convenor's Message

Co-convenor's Message

Organizing Secretary Message

Paper Presented Schedule



About NPESC-2014

The objective of the “1st National Power & Energy System Conference (NPESC-2014)” is to bring together academicians, researchers, professionals, executives, and practicing engineers from various industries, research institutes and educational bodies to share and exchange ideas and information on the theme of the conference. This conference will provide a forum to discuss various issues and problems pertaining to energy systems.



Kamla Nehru Institute of Technology, Sultanpur (U. P.)

Initially established as the Faculty of Technology in Kamla Nehru Institute of Science and Technology, Sultanpur in the year 1976 by Kamla Nehru Memorial Trust, this institute was taken over by the Government of Uttar Pradesh in 1979 with a view to develop a full-fledged engineering institute in the Eastern U.P. region better known as Avadh. Later, in the year 1983 it was registered as a separate society and renamed as Kamla Nehru Institute of Technology, Sultanpur.

The Institute is one of the leading technical institutions of the region and is responsible for producing top-grade engineers with skill sets comparable with the best in the world. It also renders the testing and consultancy services to the neighbouring industries and various other agencies. The institute is presently affiliated to G. B. Technical University (Formerly U. P. T. U.), Lucknow, India.

The institute offers B. Tech. and M. Tech. courses in Civil, Electrical, Mechanical, Electronics, Computer Science & Engineering and Information Technology disciplines in addition to M.C.A. course as well. Moreover, it offers Ph. D. in the aforesaid disciplines and also in Applied Science and Humanities. Department of Electrical Engineering also offers Ph. D. Program through QIP admission.

CONFERENCE COMMITTEE

CHIEF PATRON

Dr. R. K. Khandal

Hon'ble Vice Chancellor, U.P.T.U., Lucknow

PATRON

Prof. K. S. Verma

Director

CO-ORDINATORS

Prof. R. P. Payasi

Associate Professor & Head

Prof. Rakesh Kumar Singh

Assistant Professor

Prof. B. Singh

Assistant Professor

CO-COORDINATORS

Prof. Neelendra Badal

Assistant Professor

Prof. A. K. Chauhan

Assistant Professor

Prof. S. P. Gangwar

Assistant Professor

ORGANIZING SECRETARY

Prof. Harsh Vikram Singh

Assistant Professor

CONVENOR

Prof. S. P. Singh

Assistant Professor

Co-CONVENORS

Prof. Abhay Agrwal

Assistant Professor

Prof. S. M. Tripathi

Assistant Professor

Prof. Pradeep Kumar

Assistant Professor

ORGANIZING COMMITTEE

Prof. Varun Kumar

Assistant Professor

Prof. Amit Medhavi

Assistant Professor

Prof. Anupam Verma

Assistant Professor

Prof. Bipin Prajapati

Assistant Professor

ADVISORY COMMITTEE

Prof. D. S. Chauhan, Vice Chancellor, GLA University, Mathura
Prof. S. K. Kak, Vice Chancellor, MTU, Noida
Prof. Bhim Singh, IIT, Delhi
Prof. P. K. Kalra, Director, IIT, Rajasthan
Prof. S. C. Srivastava, IIT, Kanpur
Prof. S. N. Singh, IIT, Kanpur
Prof. K. B. Naik, Director, ABESIT, Ghaziabad
Prof. J. P. Saini, Principal, MMMEC, Gorakhpur
Prof. Kumar Vaibhav Srivastava, IIT, Kanpur
Prof. S. P. Singh, IIT (BHU), Varanasi
Prof. Anand Mohan, Director, NIT, Kurukshetra
Prof. Vivekananda Mukherjee, ISM Dhanbad
Prof. R. Mahanty, IIT (BHU), Varanasi
Prof. Devender Singh, IIT (BHU), Varanasi
Prof. Sudarsan Tiwari, Director, NIT Raipur
Prof. Satya Sheel, MNNIT, Allahabad
Prof. R. K. Singh, MNNIT, Allahabad
Prof. R. K. Tripathi, MNNIT, Allahabad
Prof. Asheesh K. Singh, MNNIT, Allahabad
Prof. Rajesh Gupta, MNNIT, Allahabad
Prof. Prabhakar Tiwari, GCET, Greater Noida
Prof. R. K. Saket, IIT (BHU), Varanasi
Prof. K. N. Pandey, MNNIT, Allahabad
Prof. R.P. S. Ganagwar, CTGBUAT, Pantnagar
Prof. K. G. Upadhyay, MMMEC, Gorakhpur
Prof. Vikram Singh, GBTU, Lucknow
Prof. Rajat Kumar Singh, IIIT, Allahabad
Prof. T. N. Shukla, KNIT, Sultanpur
Prof. S. K. Sinha, KNIT, Sultanpur
Prof. J. P. Pandey, MTU, Noida
Prof. A. S. Pandey, KNIT, Sultanpur
Prof . Deependra Singh, KNIT, Sultanpur
Prof. A. K. Singh, KNIT, Sultanpur
Prof. A. K. Singh, KNIT, Sultanpur
Prof. M. K. Gupta, KNIT, Sultanpur
Prof. R. K. Singh, KNIT, Sultanpur
Prof. D. N. Srivastava, KNIT, Sultanpur
Prof. Rakesh K. Singh, KNIT, Sultanpur

STUDENTS COMMITTEE

Anchoring

Mr. Ved Prakash (M. Tech.)

Ms. Aakriti Pandey (B. Tech.)

Ms. Apoorva Mishra (B. Tech.)

Ms. Poorva Mishra (B. Tech.)

Mr. Ishaan Pandey (B. Tech.)

Internet & Maintenance/ News & Editing

Mr. Hitendra Kr. Singh (M. Tech.)

Mr. Abhinav Kr. Gautam (M. Tech.)

Mr. Anuj Verma (M. Tech.)

Mr. Rajiv Kumar (M. Tech.)

Registration and Help Desk

Mr. Pavan P. Gupta (M. Tech.)

Ms. Anuradha Singh (M. Tech.)

Ms. Nishtha Anand (M. Tech.)

Mr. Ajay Kumar (B. Tech.)

Decoration

Ms. Roopal Gupta (B. Tech.)

Ms. VenuVerma (B. Tech.)

Ms. Kirti Singh (B. Tech.)

Ms. Deepika Vishnoi (B. Tech.)

Fooding & Accomodation

Mr. Ishrar Ahmad (M. Tech.)

Mr. Rizwan Haider (M. Tech.)

Mr. Jitendra Singh (M. Tech.)

Mr. Dinesh Singh (M. Tech.)

Mr. Ravi Yadav (M. Tech.)

Mr. Vinod Chaudhary (M. Tech.)

Transportation

Mr. Saurabh Singh (M. Tech.)

Mr. Vivek Soni (M. Tech.)

Mr. Anit Yadav (M. Tech.)

Mr. Mohit Jain (M. Tech.)

Mr. Sunil Singh (M. Tech.)

Mr. Dinesh Kandu (M. Tech.)

Volunteer

Mr. Prakash Azad (M. Tech.)

Ms. Abhiruchi Srivastava (M. Tech.)

Ms. Manisha (M. Tech.)

Mr. Ashok Kumar (M. Tech.)

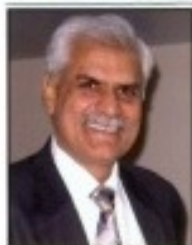
Mr. Prakrati Azad (M. Tech.)

Mr. Abhinav (M. Tech.)

Mr. Mohtasib Hasan (M. Tech.)

Ms. Amrapali Gupta (B. Tech.)

Dr. R.K. Khandal
Vice Chancellor



UTTAR PRADESH TECHNICAL UNIVERSITY
I.E.T. Campus, Sitapur Road, Lucknow-226 021 (U.P.)

Dated: April 16, 2014

MESSAGE

I am pleased to learn that **KNIT** would be organizing 1st **National Power & Energy System Conference (NPESC-2014)**; a topic of national importance. Considering the fact that the demand for energy is expected to rise with time due to the requirements of industry, agriculture and society, it has become imminent to assess all possible options of energy to ensure sustainable development and a conference on this subject is quite timely. In the case of India, newer and non-conventional ways of harnessing the potential resources of energy would have to be explored because the non-renewable reserves of fuel like hydrocarbons are not sufficient enough to even meet a notable fraction of the demand. The dependence on imports of fuel for producing energy has been growing even for coal due to the inferior quality of indigenous reserves of coal. In such a scenario adoption of states-of-the-art of technologies to produce energy, efficiently as also in environment-friendly manner, would be the subject of focus for policy makers. Further, all the essential devices used for efficient distribution of electricity would have to be put in place for ensuring that losses are minimized. It is timely and appropriate that this conference is being organized to deliberate on options available and the challenges involved in achieving the desired objectives related to meeting the demand of energy in future.

I am honoured to write this message to be included in the souvenir being brought out on the occasion of this conference. While felicitating the **Director of KNIT** and the **coordinator of the conference** for their endeavours in bringing experts of the field of power and energy systems to share their knowledge with the faculty and students, I wish them success.

With regards,

R.K.Khandal
(Prof. R.K. Khandal)
Vice Chancellor

Dr. K. S. Verma
Director,
KNIT, Sultanpur
Patron, NPESC-2014



Message from Director

I am very happy to note that Department of Electrical Engineering of the institute is organizing a “*1st National Power & Energy System Conference (NPESC-2014)*”. The recent researches made by Professors/ Scholars of IIT’s, NIT’s and other state technical universities would be a virtual feast for new thought in the respective domains. It will hopefully provide fresh and incisive vision and add a new fillip to the process of production in the country and abroad. New chapter of knowledge would set promising trend to the ongoing researches in the field of academia on such broad canvas and vast scales.

I want to thank the Organizing team for publishing Souvenir on this grand occasion.

I wish it all success.

Dr. K.S. Verma
Director,
KNIT, Sultanpur
Patron, NPESC-2014

Prof. R. P. Payasi
Head & Associate Prof.
Electrical Engg. Department
Co-ordinator, NPESC-2014



Message from Co-ordinator

Our country is continuously striving with electrical energy crisis because of increase in industrial, commercial and residential demand more than increase in electrical power production from different types of power plants. This conference (NPESC-2014) would be one of the steps to motivate the researchers to think and work to escape the country from power crisis and blackout problems. I believe that in this conference, the delegates from different parts of the country would exchange their views and explore regarding efficient, secure and reliable energy systems to overcome the electrical power crisis of country and would start dreaming for 24 hours electric power supply in every part of the country. I express my gratitude to everyone who involved in making this conference a great successful.

Prof. R. P. Payasi
Head & Associate Prof.
Electrical Engg. Department
Co-ordinator, NPESC-2014

Bindeshwar Singh
Assistant Professor
Electrical Engg. Department
Co-ordinator, NPESC-2014



Message from Co-ordinator

I am delighted to know that KNIT, Sultanpur is organizing a “*1st National Power & Energy System Conference (NPESC-2014)*” during 25-26 April, 2014, and on this occasion is bringing out a Souvenir.

The “*1st National Power & Energy System Conference (NPESC-2014)*” is the premier for the presentation of recent advances and research works in the field of emerging trends in Energy Systems. The Conference will bring together leading researchers, engineers and Scientist in the domain of interest from around the nation.

The theme of conference and contribute wider conclusions on Energy Systems and related topics which are indispensable for human progress in general and country in particular.

I would like to thanks the organizing committee, technical committee and referees who has put so much effort to make this a successful conference. My sincere thanks to participants of this conference whose kin interest in the field of Energy Systems, which I am sure help to build a powerful future through technology innovation.

Bindeshwar Singh
Assistant Professor
Electrical Engg. Department
Coordinator, NPESC-2014

S. P. Singh
Assistant Professor
Electrical Engg. Department
Convenor, NPESC-2014



Message from Convenor

It is a great pleasure that Department of Electrical Engineering of KNIT, Sultanpur is organizing a “*1st National Power & Energy System Conference (NPESC-2014)*”. It is landmark event for the Institute. The conference aims to be a key national forum for the exchange and dissemination of technical Information on “*1st National Power & Energy System Conference (NPESC-2014)*” among academicians and practicing engineers, scientists in the domain of interest around the nation.

Electrical energy is an essential ingredient for the industrial and all-round development of any country. The per capita consumption of electrical energy is a reliable indicator of a country’s state of development. Some important energy and environmental problems facing the third world countries and presents the current electric generation scenario in most of the developing countries with facts and figures in respect of India.

I would like to special thanks to Prof. K.S. Verma, Director, KNIT and Prof. R. P. Payasi, Head, Electrical Engineering Department for giving me this responsibility. My thanks are also due to the reviewers, editorial team-members, Organizing committe and student volunteers who have helped me in making the NPESC-2014 a reality.

S. P. Singh
Assistant Professor
Electrical Engg. Department
Convenor, NPESC-2014

A. K. Chauhan
Assistant Professor
Mechanical Engg. Department
Co-coordinator, NPESC-2014



Message from Co-coordinator

It is indeed a memorable day that a two day “*1st National Power & Energy System Conference (NPESC-2014)*” on April 25-26, 2014 is being organized at K N I T Sultanpur to achieve the well defined purpose of setting up an important landmark successfully by way of utilizing the activities consisting of expert lectures from exceptional achievers and presentations of researchers in relevant areas in an atmosphere of healthy interaction and sharing.

The enlisted topics shall set up a platform of spreading light of the recent technologies and enable us to grow by way of learning from knowledge reserves and absorbing expertise from treasury of learned academicians.

I am highly grateful to the members of the team for exercising painstaking effort in making this conference successful.

A. K. Chauhan
Assistant Professor
Mechanical Engg. Department
Co-coordinator, NPESC-2014

Mr. S P Gangwar
Assistant Professor,
Electronics Engg. Department
Co-convenor, NPESC-2014



Message from Co-coordinator

It has been a great honor and privilege to serve as the Co-coordinator of “*1st National Power & Energy System Conference (NPESC-2014)*”. Since in this conference, the technical experts from utilities and academia will opportunities to share their knowledge and experience in the Power & Energy System. The deliberations in the conference would be very fruitful to the nation.

I would like to extend my best wishes for the success of the conference in achieving its objectives.

Mr. S. P. Gangwar
Assistant Professor,
Electronics Engg. Department
Co-coordinator, NPESC-2014

Dr. Harsh Vikram Singh
Assistant Professor,
Electronics Engg. Department
Organizing Secretary, NPESC-2014



Message from Organizing Secretary

It is a matter of contentment and pride for all of us to organize “*1st National Power & Energy System Conference (NPESC-2014)*”. We have been thinking about organizing a conference for quite some time and the first aspect which we had to discuss was that would we be able to make it meaningful and fulfill the expectations of the participants and the aspirants. This took us around a year to think over the issues to be floated, the format, the key participants, their orientation, and so on. I am sure that you will gain from this event and please forgive us of any shortcomings.

I believe NPESC – 2014 is a strong platform for discussions on the recent advancements in this field, and it plays a crucial role to provide sophisticated analytical instrument support to the researchers from universities, national laboratories and also industries all over India. I am sure the technical and scientific program of the conference would certainly give the delegates an opportunity for fruitful discussions and stimulating interactions.

I would like to thank Prof. K. S. Verma and Prof. R. P. Payasi, for giving me this responsibility. My thanks are also due to the editorial team-members, reviewers, core team and student volunteers who have helped me in making the NPESC-2014 a reality.

Dr. Harsh Vikram Singh
Assistant Professor,
Electronics Engg. Department
Organizing secretary, NPESC-2014

| PAPER ID | PAPER PRESENTED TITLE | Proc. Page No. |
|--------------|---|----------------|
| NPESC_14_011 | Performance Analysis of Controllers for Linear Single Track Model of Sedan Car | 1-5 |
| NPESC_14_026 | Review Paper on Electricity Price Forecasting Using Hybrid Techniques | 6-11 |
| NPESC_14_030 | Power Quality Enhancement by using Synchronous Reference Theory for STATCOMS | 12-16 |
| NPESC_14_036 | Development of Dielectric Material for Application in Electronic Packaging Technique | 17-20 |
| NPESC_14_044 | State Feedback Controllers for Inverted Pendulum System using Lab view | 21-24 |
| NPESC_14_051 | Multi-Stage Optimal Placement of PMU using Reliability and Probabilistic Approach | 25-31 |
| NPESC_14_052 | Online Voltage Stability Monitoring using ANN-PSO based Technique | 32-36 |
| NPESC_14_054 | Network Reconfiguration of Radial Distribution System having DGs and Capacitors for Power loss Reduction Using Voltage Sensitivity Analysis | 37-42 |
| NPESC_14_057 | An Overview of Transmission Pricing Methods in a Pool based Power Market | 43-46 |
| NPESC_14_058 | Single Phase Matrix Converter Topology Based Implementation of Single Phase Boost –Buck Rectifier with Reduced Input Current THD | 47-52 |
| NPESC_14_059 | Thyristor Controlled Improvement of a Solid State Fault Current Limiter Using Simulink | 53-56 |
| NPESC_14_061 | Haptic System its Constituents and Application in Advanced Technology | 57-62 |

| | | |
|--------------|--|---------|
| NPESC_14_067 | Transient Stability Assessment of Multi Machine Power System and Enhancement Using Facts | 63-67 |
| NPESC_14_068 | Performance Investigation of PID and Hybrid Controllers for Speed Control of Induction Motor using Direct Field Oriented (DFO) Control Technique | 68-75 |
| NPESC_14_069 | Performance Investigation of SVPWM Controlled Diode Clamped and Flying Capacitor Multilevel Converters | 76-88 |
| NPESC_14_070 | Power Quality Enhancement by Single Switch AC-DC Converter | 89-96 |
| NPESC_14_073 | Review of Energy-Efficient Biometric Authentication Systems | 97-100 |
| NPESC_14_074 | Energy Efficient Image Watermarking in Spatial and Transform Domain | 101-107 |
| NPESC_14_075 | Survey for Wavelet Bayesian Network Image De noising | 108-113 |
| NPESC_14_076 | Survey for Image representation using block compressive sensing for compression Applications | 114-119 |
| NPESC_14_077 | Survey on Mining Order-Preserving Sub matrices | 120-125 |
| NPESC_14_078 | Impact of Voltage step Constraint and Mixed Load Models on Optimal Distributed Generation Placement | 126-135 |
| NPESC_14_079 | Direct Torque Controlled Permanent Magnet Synchronous Motor Drive: A Review | 135-139 |
| NPESC_14_080 | A Survey on Impact of DGs and FACTS Controllers on Power Systems | 140-162 |
| NPESC_14_083 | A Electrical Power Quality Problem & Its Solutions | 163-173 |
| NPESC_14_084 | Applications of FACTS Controllers in Emerging Power System Networks | 174-195 |
| NPESC_14_087 | Embedded Systems and their Reliability Testing | 196-200 |
| NPESC_14_088 | SL-Z- Source Inverter with Maximum Constant Boost Control | 201-205 |

| | | |
|--------------|--|---------|
| NPESC_14_089 | Performance Comparison of Hybrid Filter by Using Different Compensation Techniques | 206-210 |
| NPESC_14_090 | LIGHT-FIDELITY (Li-Fi) (VISIBLE LIGHT COMMUNICATION) | 211-217 |
| NPESC_14_091 | Transient Performance Investigation on CSI Fed Induction Motor Drive Employing A Variable Gain Proportional Integral (VGPI) Speed Controller | 218-222 |
| NPESC_14_094 | Iris Recognition | 223-226 |
| NPESC_14_095 | Application of Artificial Intelligence Computational Techniques in DC and AC Drives | 227-236 |
| NPESC_14_098 | Impact Assessment of Wind Farms and FACTS Controllers in Emerging Power System | 237-241 |
| NPESC_14_099 | Comparative Study on Signal Processing Techniques Applied to Human Sleep EEG Signals | 242-247 |
| NPESC_14_100 | Analysis and Evaluation of Impact of Domestic Load Unbalancing | 248-252 |
| NPESC_14_101 | Comparative Study of Different Fusion Techniques in Multimodal Biometric Recognition | 253-256 |
| NPESC_14_102 | Empirical Study of a Solar Still Coupled with an Evacuated Tube Collector | 257-261 |
| NPESC_14_103 | Grid Connected Photovoltaic System: A Review | 262-267 |
| NPESC_14_104 | Renewable Grid Integration : Analytical Approach | 268-272 |
| NPESC_14_105 | A Review on Micro Hydro Power Plant: Solution for Off-grid Renewable Energy Source in India | 273-277 |
| NPESC_14_106 | Assessment of Nuclear Power And It's Future In India | 278-284 |
| NPESC_14_107 | POWER QUALITY IMPROVEMENT BY UPQC USING ANN CONTROLLER | 285-292 |
| NPESC_14_108 | Role of Quality Models in Software Development | 293-297 |
| NPESC_14_109 | An Overview of Intrusion Detection System for Wireless | 298-302 |

| | Ad-hoc Networks | |
|--------------|---|---------|
| NPESC_14_110 | Grid connected Photovoltaic system An Assessment of Performance | 303-310 |
| NPESC_14_113 | Security Aspects In Vehicular ad hoc Network System (VANET'S) | 311-317 |
| NPESC_14_115 | POWER QUALITY IMPROVEMENT USING SHUNT ACTIVE POWER FILTER | 318-322 |
| NPESC_14_116 | Improvement of PQ in Electrical Distribution System Using Custom Power Devices: A Survey | 323-346 |
| NPESC_14_118 | Smart Grid Wide area Power System Load Protection Schemes | 347-353 |
| NPESC_14_120 | Non-Isolated Multiphase Bidirectional DC-DC Converter Design for Electric Vehicle Applications | 354-357 |
| NPESC_14_121 | Dynamic Voltage Restorer (DVR) for mitigation of Voltage SAG/SWELL in Distribution System | 358-364 |
| NPESC_14_123 | A Comparative Analysis of Various LNA Topologies Used in CMOS - LNA Design | 365-370 |
| NPESC_14_124 | Identification of Inrush Current of Transformer using Discrete Wavelet Transforms | 371-374 |
| NPESC_14_125 | Torque Ripples Minimization of Switched Reluctance Motor for Hybrid Electric Vehicle Applications | 375-377 |
| NPESC_14_126 | Suboptimal control of a higher order system by Balance Truncation method | 378-381 |

Performance Analysis of Controllers for Linear Single Track Model of Sedan Car

A. Alok Kumar Pandey, B. DevendraRawat, C. Naveen Kumar, D. Kritika Bansal and E. KhaingYadanaSw

Abstract—The objective of this paper is to present the timedomain performance of a linear single track model of a sedan car with state feedback controller. The linear dynamics of the car model has been considered along with actuator dynamics. The development of controller has also been presented. The simulated results are obtained using MATLAB.

Index Terms - Automatic steering, Pole Placement technique,State feedback controller.

I. INTRODUCTION

THE increasing number of crashes on highway has forced the researchers to start thinking about the control of vehicle dynamics as well as driving safety. Automatic steering of vehicle is of practical interest for factories and ship docks, for buses in narrow lanes. The main task of automatic steering is to track a reference path where the displacement from the guideline is measured by a front displacement sensor and a GPS, both of which are mounted on the front bumper of the vehicle [1]. This approach provides the advantage of both look down and look ahead reference system [2-3]. The aim of this paper is to design a controller for steering angle, road curvature & lateral displacement control and to stabilize the steering system so that the steering angle is maintained and hence collision can be avoided. In this paper, ideal design is based on look down reference control systems which is favorable due to its reliability, invariance to weather conditions and absence of occlusion by preceding vehicle. It is verified by different experiments [1-7]. Design is restricted to low speed of less than 20 m/s under practical constraints such as bandwidth limitations of actuator, comfort of passenger and stringent accuracy requirements. The extension of look down reference systems to practical conditions with speed 30m/s was not successful [6-7]. Therefore, one more sensor has been added to measure the lateral displacement from the lane reference at tail bumper. This provides a number of other possible control design directions [8] e.g., feedback of angular displacement and feedback of lateral displacement at the front

A. Alok Kumar Pandey is an M.Tech Student with Department of Electrical Engineering, National Institute of Technology, Kurukshetra, Haryana-136119, India (email: pandeyalok507@gmail.com).

B. DevendraRawat, C. Naveen Kumar, D. KritikaBansal and E. KhaingYadanaSwe are M.Tech Students with Department of Electrical Engineering, National Institute of Technology, Kurukshetra, Haryana-136119, India (email: devendrarawat85@gmail.com, naveenvermaindia@gmail.com, kbansal.711@gmail.com, khaingyadanaswe18@gmail.com).

bumper [5]. In this paper, Pole Placement technique has been applied for linear single track model of car and the same has been compared for change in mass of the vehicle.

Section II presents a single track vehicle dynamics model and actuator dynamics. Section III gives the control design methods to control the steering angle, road curvature and lateral displacement. Section IV carries the performance analysis using pole placement with state feedback control. Section V presents the time domain performance comparison of controller for change in mass of the vehicle. Finally conclusion is drawn in section VI.

II. MODEL DYNAMICS

A. Vehicle Dynamics:

This section describes the methodology used to get the position information of a controlled vehicle with the help of front sensor and GPS.

Model of vehicle used in this paper is a linear version of single track model [1] of a sedan car as shown in Fig. 1. In this model, two wheels are lumped of each axel into one wheel located at the middle of vehicle with displacement l_{tf} and l_{tr} from the centre of gravity. Lateral displacements d_{sf} & d_{sr} of the vehicle from the reference track are measured with the help of sensor placed at distances l_{sf} & l_{sr} from centre of gravity. β represents the side slip angle between vehicle speed v and longitudinal axis. Ψ represents the heading orientation, δ is the steering angle, r is yaw rate, ρ_{ref} denotes the curvature of the reference track and v is the vehicle velocity. Few assumptions have been taken during the derivation of this model which are listed below:

- i) Road coefficient ($= 1$ for dry road and $= 0.5$ for wet road).
- ii) Passengers distribute uniformly over the vehicle, centre of gravity (CG) is fixed and the moment of inertia I with respect to a vertical axis through the CG increases linearly with the mass m of vehicle.
- iii) In modeling the vehicle dynamics [8], it turns out the parameters m and I appears as only normalized mass.
- iv) All angles are small and are assumed to enter linearly.
- v) All states of the vehicle are controllable by front wheel steering with two exceptions,
 - a) At velocity zero the vehicle is uncontrollable, a minimum velocity must be assumed for automatic steering system.
 - b) Passterback [4] showed that there is a velocity at which controllability gets lost. A further analysis in [10] led to the conclusion that this occurs.

Vi All vehicle states are observable from the displacement. The state space representation of the vehicle dynamics for single track model of car is given [11]:

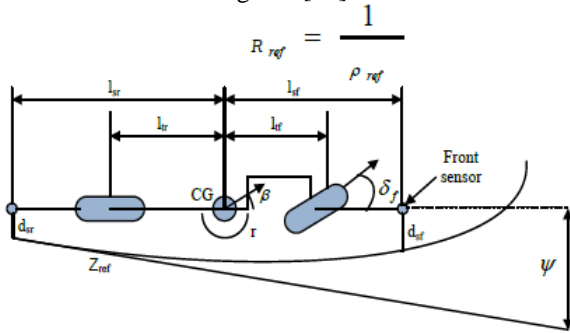


Fig.1 Single track Model.

$$\dot{\mathbf{X}} = \mathbf{AX} - \mathbf{BU}$$

$$\mathbf{X} = \begin{bmatrix} d_{sf} \\ d_{sf} \\ d_{sr} \\ d_{sr} \end{bmatrix}, \mathbf{U} = \begin{bmatrix} \delta_f \\ \rho_{ref} \end{bmatrix}$$

$$A = \begin{bmatrix} 0 & 1 & 0 & 0 \\ a_{12} & a_{22} & -a_{21} & -a_{24} \\ 0 & 0 & 0 & 1 \\ a_{41} & a_{42} & -a_{41} & a_{44} \end{bmatrix}, B = \begin{bmatrix} 0 & 0 \\ b_{21} & -v^2 \\ 0 & g_4 v \\ b_{41} & -v^2 \end{bmatrix}$$

$$\begin{aligned} a_{21} &= \frac{g_2}{mg_4} - \frac{l_g g_1}{Ig_4}, a_{22} = \frac{g_1 - l_x g_2}{mv g_4} + \frac{l_g (l_x g_1 - g_3)}{Iv g_4} \\ a_{24} &= -\frac{g_1 + l_g g_2}{mv g_4} + \frac{l_g (l_g g_1 + g_3)}{Iv g_4} \\ a_{41} &= \frac{g_2}{mg_4} + \frac{l_x g_1}{Ig_4}, a_{42} = \frac{g_1 - l_x g_2}{mv g_4} - \frac{l_x (l_x g_1 - g_2)}{Iv g_4} \\ a_{44} &= -\frac{g_1 + l_g g_2}{mv g_4} - \frac{l_x (l_g g_1 + g_3)}{Iv g_4} \\ b_{21} &= \mu c_f \left(\frac{1}{m} + \frac{l_g l_g}{I} \right), b_{41} = \mu c_f \left(\frac{1}{m} - \frac{l_x l_g}{I} \right) \end{aligned}$$

With

$$g_1 = \mu (c_f l_g - c_r l_g), g_2 = \mu (c_f + c_r)$$

$$g_3 = \mu (c_r l_x^2 + c_f l_g^2), g_4 = l_g + l_x$$

The plant's parameters value used in the simulation are summarized in Table I [2]

A. Actuator Dynamics:

A steering actuator A(s) is used to generate the front steering angle δ_f . A linear actuator model is used [1] with following transfer function:

$$T: A(s) = \frac{80000}{(s+62.8)(s+12.56+28.77j)(s+12.56-28.77j)}$$

| Symbol | Definition | Values |
|--------|--------------|--------|
| m | Vehicle Mass | 1573kg |
| | | |

TABLE I
VALUES OF THE PARAMETERS

| Symbol | Definition | Values |
|----------|-----------------------------------|--------------------------------|
| m | Vehicle Mass | 1573kg |
| I | Yaw moment of inertia | 2873kgm ² |
| l_x | Distance from rear axles to CG | 1.58m |
| l_g | Distance from front axles to CG | 1.1m |
| l_{sf} | Distance from front sensor to CG | 1.96m |
| l_{sr} | Distance from rear sensor to CG | 2.49m |
| c_f | Cornering stiffness of front tire | 80000N/rad |
| c_r | Cornering stiffness of rear tire | 80000N/rad |
| μ | Road adhesion factor | 1 (dry road) 0.5 (wet road) |
| l_g | Distance from front axles to CG | 1.1m |

III. CONTROLLER DESIGN METHOD

In this section, controller is designed using Pole placement method with state feedback.

A. Pole placement method

The pole placement design allows all closed loop poles to be placed in desired locations. The necessary and sufficient condition for the arbitrary placement of closed loop poles in the complex plane is that the system

$$\begin{aligned} \dot{x}(t) &= Ax(t) + Bu(t) \\ y(t) &= Cx(t) \end{aligned} \quad (3)$$

is controllable. If all n state variables x_1, x_2, \dots, x_n can be accurately measured at all times, according to linear control law of the form

$$u(t) = -k_1 x_1(t) - k_2 x_2(t) - \dots - k_n x_n(t) = -Kx(t) \quad (4)$$

$$K = [k_1, k_2, \dots, k_n] \quad (5)$$

Where, K is a constant state feedback gain matrix [4]. K matrix for this model is

$$K = \begin{bmatrix} 5.4589 & 6.3505 & 3.3450 & -0.3716 \\ .9202 & 1.5032 & 1.3379 & -0.1686 \end{bmatrix} \quad (6)$$

The closed loop system is described by the state differential equation

$$X(t) = (A - BK) x(t) \quad (7)$$

The feedback gain matrix K should be such that the closed loop system is robust, in the sense that its poles are as insensitive to any changes in system as possible.IV.

SIMULATION RESULTS

Results of Pole placement based state feedback controller without considering actuator dynamics are shown in Fig2 to Fig5 and later the results with actuator dynamics are given in Fig6 to Fig9. There are two inputs (δ_f & ρ_{ref}) and two outputs (Ψ & d_{sf}) in this model so there would be four combinations of transfer functions named G_1, G_2, G_3, G_4

i) With Actuator Dynamics:

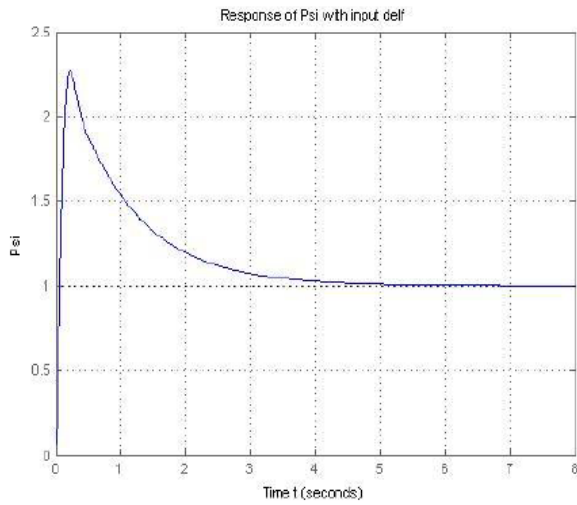


Fig.2. Pole Placement Based state feedback controller for G_1

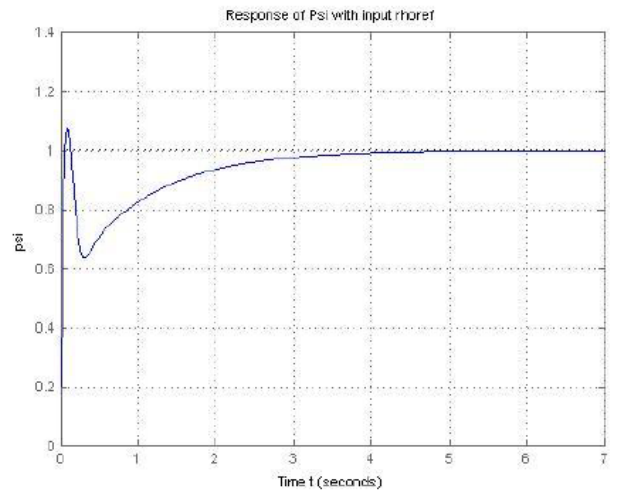


Fig.4. Pole Placement Based state feedback controller for G_2

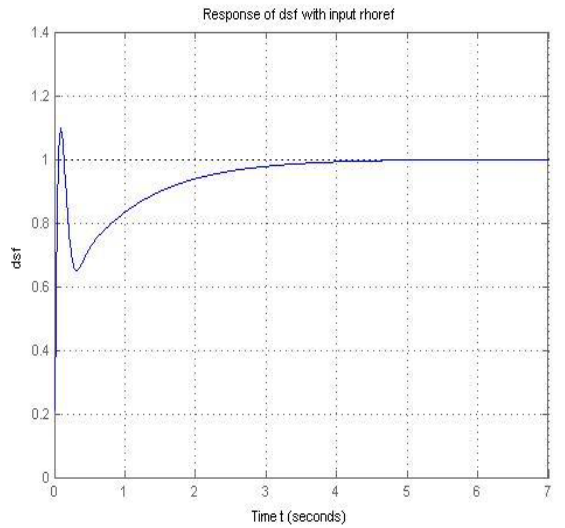


Fig.2. Pole Placement Based state feedback controller for G_1

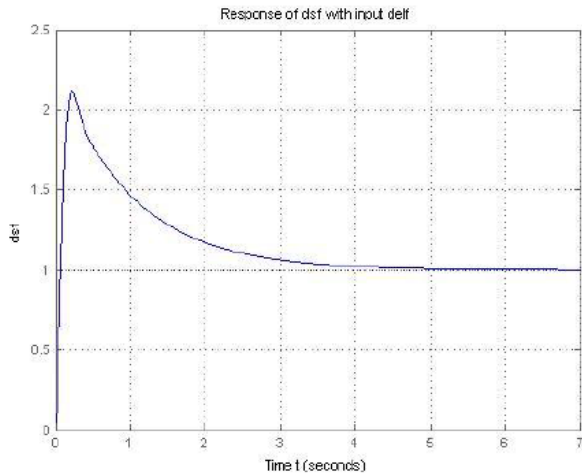


Fig.3. Pole Placement Based state feedback controller for G_2

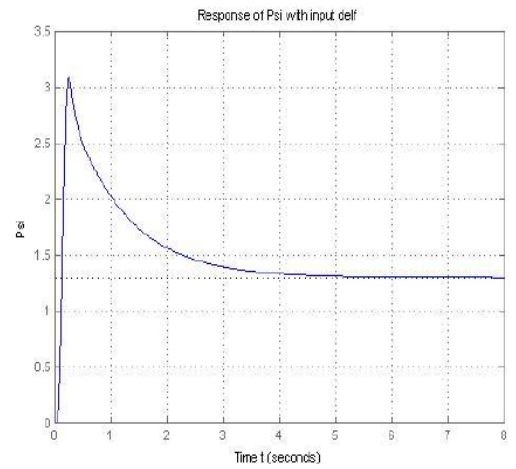


Fig.6. Pole Placement Based state feedback controller for G_1

Fig.9. Pole Placement Based state feedback controller for G_4

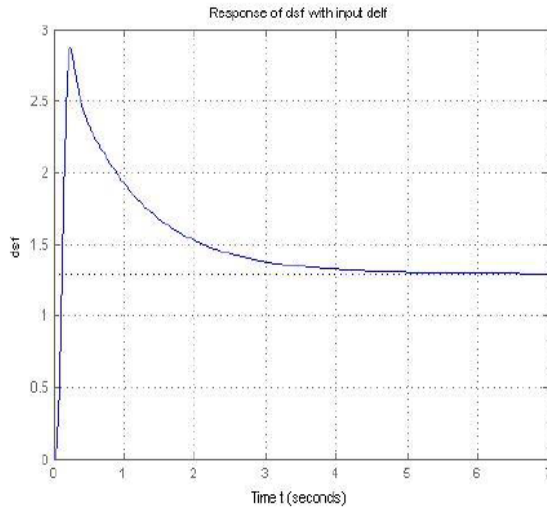


Fig.7. Pole Placement Based state feedback controller for G_2

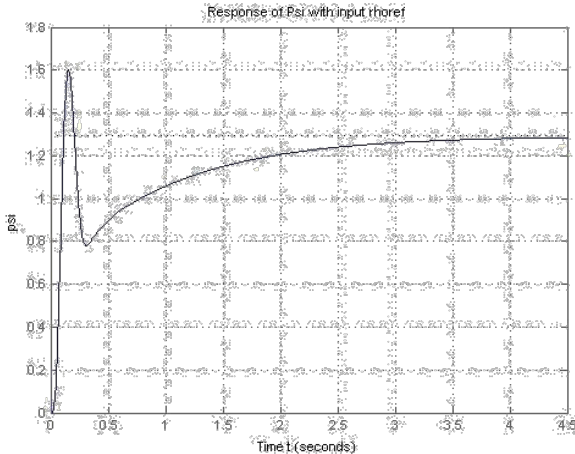
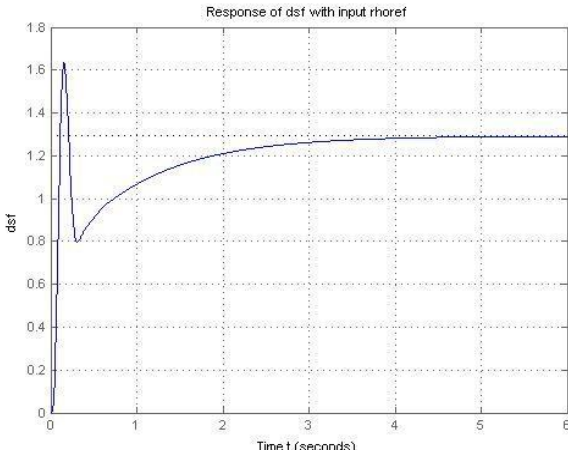


Fig.8. Pole Placement Based state feedback controller for G_3



V. PERFORMANCE COMPARISON& DISCUSSION

Performance of pole placement with state feedback controller for the steering model of a car on the basis of time domain specification is done. This analysis is categorized in two parts, without actuator and with actuator. With the change in total mass of vehicle controller is showing the robustness which is shown in Table II.

A. Change of Total Mass of Vehicle

When total mass of the body is increased by adding the 3 passengers of weight average 70 kg one by one, it is observed that rise time was almost same for all controllers except for G_1 in case of PID controller and G_3 in case of Pole placement technique is increased. Settling time is increased in case of G_1 & G_3 in pole placement technique. Percent overshoot in case of pole placement for G_1 is increased. Percent undershoot are zero in all case except for G_2 & G_3 in case of pole placement technique. Peak time is increased in case of pole placement for G_3 . The detail analysis of time domain parameters with change of mass of body is shown in table II. Values to construct the table are $m_1=1573$ kg, $m_2=1643$ kg and $m_3=1713$ kg.

TABLE II
RESULTS OF PID & POLE-PLACEMENT FOR CHANGE IN TOTAL MASS OF VEHICLE

| m | D. P | PID | | | | Pole Placement | | | |
|-------|---------|-------|-------|-------|-------|----------------|-------|-------|-------|
| | | G_1 | G_2 | G_3 | G_4 | G_1 | G_2 | G_3 | G_4 |
| m_1 | T_r | .154 | 1.26 | .136 | 1.25 | .197 | 2.32 | .759 | 2.28 |
| | T_s | 1.87 | 9.43 | 1.03 | 9.69 | 1.53 | 4.13 | 1.76 | 4.1 |
| | M_o | 10.2 | 24.4 | 20.9 | 24.9 | 35.6 | 0 | .202 | 0 |
| | M_u | 0 | 0 | 0 | 0 | 0 | 108.3 | 19.5 | 0 |
| | T_p | .874 | 3.27 | 0.326 | 3.31 | .536 | .21 | 3.09 | 7.81 |
| m_2 | T_r | .158 | 1.26 | .137 | 1.25 | .183 | 2.32 | .93 | 2.28 |
| | T_s | 1.84 | 9.43 | 1.04 | 9.69 | 1.81 | 4.14 | 2.26 | 4.1 |
| | M_o | 11.2 | 24.4 | 20.77 | 25 | 43.6 | 0 | 0 | 0 |
| | M_u | 0 | 0 | 0 | 0 | 0 | 120.7 | 18.6 | 0 |
| | T_p | .88 | 3.27 | .326 | 3.31 | .535 | .202 | 4.81 | 7.82 |
| m_3 | T_r | .163 | 1.26 | .138 | 1.25 | .169 | 2.31 | 1.13 | 2.27 |
| | T_s | 1.85 | 9.43 | 1.04 | 9.69 | 2.11 | 4.15 | 2.76 | 4.09 |
| | M_o | 11.9 | 24.36 | 20.6 | 24.9 | 53.4 | 0 | 0 | 0 |
| | M_u | 0 | 0 | 0 | 0 | 0 | 136.3 | 17.46 | 0 |
| | T_p | .895 | 3.27 | .34 | 3.31 | .525 | .219 | 8.37 | 7.81 |

VI. CONCLUSION

Steering control of a single track car model using pole placement with state feedback controller has been designed. Time domain performance of the controller is analyzed and it is found that the controller shows robustness with the change in total mass of the vehicle. The use of state observers can provide the robustness to changing operating conditions. Lateral position estimation can also give the real time lateral position of next obstacle. Further, the performance can be improved by using advanced control methods.

REFERENCES

- [1] J. Hernandez and C. Kuo, "Steering control of automated vehicles using absolute positioning GPS and magnetic markers," *IEEE Trans. Veh. Technol.*, vol. 52, no. 1, pp. 150–161, Jan. 2003.
- [2] J. Guldner, W. Sienel, H. S. Tan, J. Ackermann, S. Patwardhan, and T. Bunte, "Robust automatic steering control for look-down reference systems with front and rear sensors," *IEEE Trans. Control Syst. Technol.*, vol. 7, no. 1, pp. 2–11, Jan. 1999.
- [3] B. Litkouhi, A. Lee, and D. Craig, "Estimator and controller design for Lane Track, a vision-based automatic vehicle steering system," in Proc. IEEE Conf. Decision Control, San Antonio, TX, 1993, pp. 1868–1873.
- [4] S. Pasternack, Modern control aspects of automatically steered vehicles. Transportation Systems Centre , Cambridge Mass., Technical note , Dec. 1971.
- [5] Jing Yang, Edwin Hou, Meng Chu Zhou, "Front Sensor and GPS-Based Control of Automated Vehicles" *IEEE Trans. Intell. Transport. Syst.* vol 14.No.1, pp146-154, March 2013.
- [6] J. Guldner, H.-S. Tan, and S. Patwardhan, "Analysis of automatic steering control for highway vehicles with look-down lateral reference systems," *Veh. Syst. Dynamics*, vol. 26, no. 4, pp. 243±269, 1996.
- [7] S. Patwardhan, H.-S. Tan, and J. Guldner, "A general frame-work for automatic steering control: System analysis," in *Proc. Amer. Contr. Conf.*, Albuquerque, NM, 1997, pp. 1598±1602.
- [8] On fundamental issues of vehicle steering control for highway automation *Automatica* submitted in 1966.
- [9] M Gopal, Digital Control and State Variable Methods, 2nd Ed., Tata McGraw-Hill, Inc. 2003.
- [10] J. Ackermann, J. Guldner, and W. Sienel, et. al, "Linear and nonlinear controller design for robust automatic steering", *IEEE Transactions on Control Systems Technology*, 1995, vol. 3, no. 1, pp:132-143.
- [11] J. Ackermann and W. Sienel, "Robust Control for Automatic Steering.", *Proc. of the ACC, San Diego*. 1992.
- [12] R. E. Fenton, G. C. Melocik, and K. W. Olson, "On the steering of automated vehicles: Theory and experiment," *IEEE Trans. Autom. Control*, vol. 21, no. 3, pp. 306–315, Jun. 1976.

Review Paper on Electricity Price Forecasting Using Hybrid Techniques

Yashwant Kumar Singh¹, Nitin Singh²

Abstract—: Price forecasting has become an important issue in power markets, since it forms the basis for increasing profits of both consumer and supplier. This paper covers the approaches which are used in price forecasting and also includes comparison of different methods such as Wavelet, Auto Regressive Integrated Moving Average (ARIMA), Fuzzy Logic, Particle Swarm Optimization (PSO), and hybrid methods that overcome the problems arises due to individual methods.

Key words: Electricity price forecasting, wavelet, ARIMA, fuzzy and PSO.

Introduction

Electricity Price Forecasting has become a crucial area of research due to deregulation in electricity markets.

Price forecasting is of equal importance for both supplier and consumer [20]. Accurate electricity price forecasting is required for both supplier and consumer to increase their profit. Price forecasting has become an important factor for planning in generation, transmission and distribution systems and help in operation of competitive markets by accurate forecasting of electricity prices. Producers and consumers depend on price information for their bidding strategy [15]. Suppliers can maximize its benefit and similarly consumer can also maximize his utility. The remainder of the paper is organized as follows: Section II explains about different forecasting methods, section III explains about factors influencing the method of price forecasting. Section IV explains about wavelet transform and section V explains about different methodology of price forecasting such as Wavelet [2], [4], Autoregressive Integrated Moving Average (ARIMA) [1], Generalized Autoregressive Heterodasticity (GARCH) [24], Fuzzy Logic [16], Particle Swarm Optimization (PSO) [22] and hybrid methods along with accuracy criterion has been discussed. Section IV concludes the paper and different techniques are compared. This paper focuses on different methods for accurate and potential methodologies for forecasting.

A. ¹Electrical Engineering Department Motilal Nehru National Institute of Technology Allahabad, India.
(yashwant.y.p@gmail.com)²

B. Assistant Professor, Electrical Engineering Department Motilal Nehru National Institute of Technology Allahabad, India,
(nitins@mnnit.ac.in)

I. TYPES OF FORECASTING

Mainly there are three types of forecasting: Short-term, Medium and Long-term price forecasting. In which in India Long-term Forecasting is used. Short term forecasting requires data of 3 to 4 weeks, medium forecasting is used for months whereas long term forecasting requires data of 1 year or more.

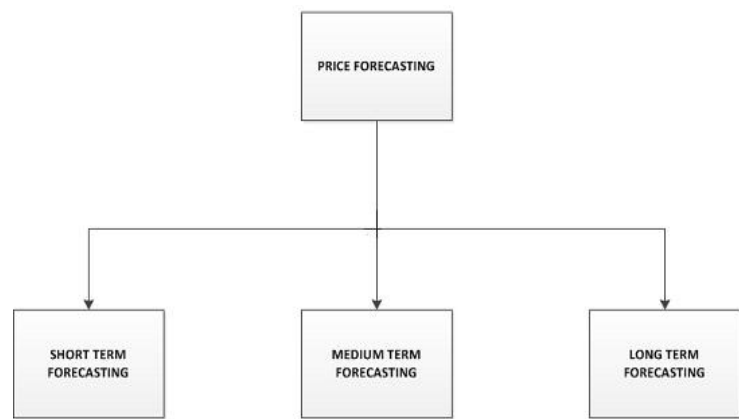


Fig 1. Types of Forecasting

II. PRICES FORECASTING METHODS

Different methods developed for Electricity Price Forecasting are shown below in fig 2; these methods can also be used for load forecasting. Different subclasses under each models used for forecasting are mentioned.

III. FACTORS AFFECTING ELECTRICITY PRICES

While developing an accurate forecasting technique it is better to consider these factors affecting the forecasted values. Weather condition, transmission congestion and other factors

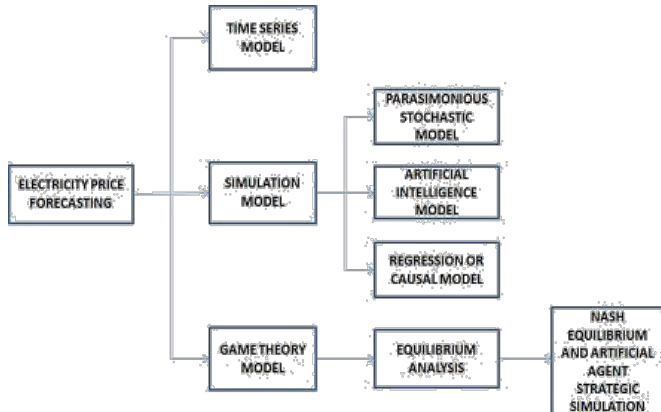


Fig 2. Classification of Forecasting Models

causes problem to price changes [19]. It is also affected much on weekend when demand is more thus calendar also plays a vital role in affecting price changes. The main factors influencing electricity prices are presented in figure 3 [6].

Different forecasting methods with different input affect these factors. Non stationary involve in the price series is handled by different forecast methods [7]. In ARIMA, integrated model is used to handle the non-stationary and further it is given to ARMA to forecast the values. Fuzzy is more flexible and consider these constraints. Thus selecting proper forecasting method with suitable inputs factors plays an important role in accurate forecasting.

IV. WAVELET TRANSFORM

It is a wave-like oscillation with amplitude that begins at zero, increases, and then decreases back to zero. Generally, wavelets are purposefully related to have specific properties that make them useful for signal processing. Wavelets can be combined, using a "reverse, shift, multiply and integrate" technique called convolution, with portions of a known signal to extract information from the unknown signal.

Wavelet removes all the non-stationary introduced in the price series due to seasonality included and makes it smoother [6]. Wavelet firstly decomposes the price series into two series i.e., approximate series and detail series and then remove the non-stationary and give back the final stationary price series by the help of inverse wavelet.

For practical applications, and for efficiency reasons, one prefers continuously differentiable functions with compact support as mother wavelet [2]. There are many functions chosen to be the mother wavelet, and here we list some important case. There are different types of wavelet but which

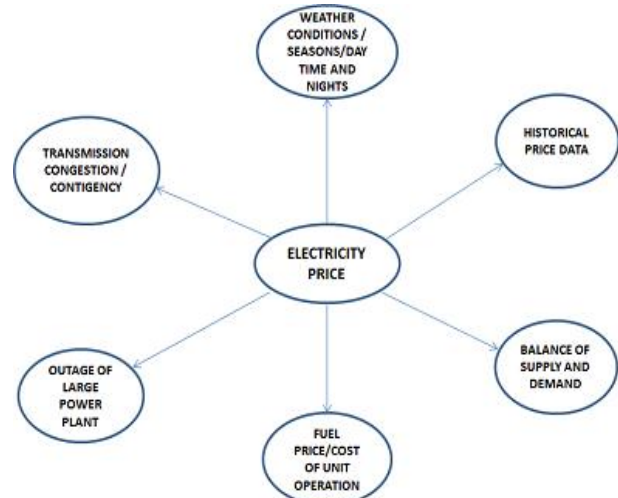


Fig 3. Factors affecting electricity prices

is used in most of the forecasting methods is Daubenchies decomposition level 3.

Wavelet transform is basically divided into categories: continuous wavelet transform and discrete wavelet transform. The continuous wavelet transform (CWT) $R_{(a,b)}$ of a signal $f(x)$ with respect to wavelet $\varphi(x)$ is given by [3]:

$$R_{(a,b)} = \frac{1}{\sqrt{a}} \int_{-\infty}^{+\infty} f(x)\varphi\left(\frac{x-b}{a}\right)dx \quad (1)$$

where scale parameter „a“ control the spread of wavelet, translation parameter „b“ determines its central position and $\varphi(x)$ is mother wavelet. Coefficients of function $R_{(a,b)}$ tells how nicely the function $f(x)$ and mother wavelet signal is matched.

Since mother wavelet can also be translated and scaled using another technique i.e., DWT (discrete wavelet transform). This technique is also as efficient and accurate as CWT [3]

$$R_{(a,b)} = 2^{-m/2} \sum_{n=0}^{T-1} f(t)\varphi\left(\frac{t-n2^m}{2^m}\right) \quad (2)$$

T is length of the signal $f(t)$, parameter „a“ is given by 2^m and

parameter „b“ is given by $n2^m$ and t is discrete time index. The multilevel decomposition series consisting of approximate series (A) and detail series (D) is shown in fig 2.

Wavelet transform has two steps decomposition and reconstruction. During decomposition two series are formed:

approximate series and detailed series. Decomposition of series involve down sampling and filtering where reconstruction involves up sampling and filtering [10].

V. TIME SERIES MODELS

A. ARIMA Model

It stands for auto regressive integrated moving average. ARIMA is used along with wavelet to provide robust price forecasting and wavelet provides a good local representation of the signal in frequency and time domain.

ARMA was also used in forecasting but it can't tackle the problems related to non-stationary of the series so ARIMA is used since it has integrated (differencing operator) model is used which remove the problem of non-stationary of the series.

General ARIMA model is given as ARIMA (p, d, q) where parameters p is order of autoregressive, d is order of integrated and q is order of moving average and p, d, q are non-negative integers [2]. When any of the parameter i.e. p, d, q is zero then we have to drop either "AR", "I", or "MA" from general model ARIMA(p,d,q). If any series is non-stationary then we look for difference operator of first order, second order or any other reliable order. This difference operator makes the series stationary. For example, if X_t is a non-stationary process, we look for first order difference as:

$$x_t' = x_t - x_{t-1} \quad (3)$$

We can use B to express differencing:

$$x_t' = x_t - x_{t-1} = x_t - Lx_t = (1-L)x_t \quad (4)$$

Thus ARIMA(p,d,q) is defined as:

$$\begin{aligned} & \underbrace{(1-\phi_1 L - \phi_2 L^2 - \dots - \phi_p L^p)}_{AR(p)} \underbrace{(1-L)^d}_{I(d)} x_t \\ & - c + \underbrace{(\psi_1 L + \psi_2 L^2 + \dots + \psi_q L^q)}_{MA(q)} \varepsilon_t \\ & \phi(L)(1-L)^d x_t = c + \psi(L)\varepsilon_t \end{aligned} \quad (5)$$

If there is no differencing (i.e. d=0), then ARIMA model can be called an ARMA model.

ARIMA model of a non-stationary time series forecasting is given by

$$\phi(B)(1-B)^d Y_t = \theta(B) \varepsilon_t \quad (6)$$

where Y_t is a non-stationary series, d is order of differencing, ε_t is a white noise, B is a backward shift operator, $\phi(B)$ is a autoregressive operator, and $\theta(B)$ is a moving average operator. A backshift operator is given by $BX_t = X_{t-1}$, autoregressive operator $\phi(B)=1-\phi_1 B-\phi_2 B^2-\dots-\phi_p B^p$, and moving average operator $\theta(B)=1-\theta_1 B-\theta_2 B^2-\dots-\theta_q B^q$. General ARIMA model is used to give price data and it has 4 steps, firstly if price data contains seasonality the operator $(1-B)^s$ is used in model where s represents a seasonality parameter. Secondly it estimate mean and variance and if both parameters are constant the series is stationary. Thirdly it estimates the parameters and finally it perform diagnostic checking.

The results shown below in table 1 describe the comparison of different methods individually and also along with wavelet [3]; the results shows that wavelet improves the accuracy of the model and helps in accurate prediction of forecasted price.

B. GARCH Model

GARCH stands for Generalized Autoregressive Conditional Heteroskedasticity which are used to model observed time series. The model GARCH (p,q) is defined as:

Consider a time series x_t with a constant mean offset, then

TABLE 1
MAPE (%) for 12 weeks of the Spanish market in 2002

| | ARIMA | ARIMA-GARCH | WT-ARIMA | ARIMA-GARCH-WAVELET |
|-----------|-------|-------------|----------|---------------------|
| January | 11.15 | 10.00 | 5.71 | 2.14 |
| February | 4.72 | 4.44 | 4.39 | 1.09 |
| March | 5.15 | 5.84 | 3.74 | 0.64 |
| April | 14.26 | 12.30 | 4.07 | 0.92 |
| May | 7.92 | 5.30 | 5.64 | 0.82 |
| June | 6.41 | 5.31 | 4.22 | 1.02 |
| July | 10.37 | 8.70 | 9.43 | 2.09 |
| August | 12.14 | 7.51 | 8.74 | 1.55 |
| September | 13.89 | 7.53 | 10.45 | 2.01 |
| October | 9.97 | 9.54 | 6.58 | 1.63 |
| November | 13.93 | 9.98 | 5.28 | 2.42 |
| December | 17.43 | 17.39 | 8.22 | 2.99 |
| Average | 10.61 | 8.65 | 6.37 | 1.61 |

TABLE 1MAPE (%) for 12 weeks of the Spanish market in 2002

Where μ is offset and $s_i = \sigma_i z_i$.

$$\sigma_i^2 = c + \sum_{i=1}^q \phi_i \varepsilon_{t-i}^2 + \sum_{i=1}^p \psi_i \sigma_{t-i}^2 \quad (8)$$

Where p is the order of GARCH terms σ^2 and q is the order of ARCH terms ε^2 .

As we can easily see in eq(9), in GARCH (p,q) model is $p=0$, i.e. a GARCH (0,q) model becomes an ARCH (q) model.

GARCH model can only specified for stationary time series so below equation must be satisfied for stationary time series.

$$\sum_{i=1}^q \phi_i + \sum_{i=1}^p \psi_i < 1 \quad (9)$$

Steps for GARCH model:

- (i) Identify the class of models.
- (ii) Identify the subsets of GARCH models.
- (iii) Parameters Estimation.
- (iv) Model Validation.
- (v) Apply Forecast.

C. Fuzzy Logic

Fuzzy logic is used to model a human reasoning. It is an approach to evaluate many valued logic which differs from binary set [8]. Binary set has two values 0 and 1 where 0 represents false and 1 represents true. Fuzzy logic has degree of truth whose values lies between 0 to 1. Fuzzy logic is also used to determine the partial truth since truth varies between completely true to completely false. It is a reasoning which approximate rather than exact and fixed. It is used in many sectors of control applications and artificial intelligence methods [10]. Fuzzy logic operates on model where degree of uncertainty is high (imprecise model) and it deals with approximate model rather than precise one. It provides an additional advantage that it is independent of the size of data used in model. Thus it improves the accuracy of forecasting methods and provides accurate forecasted values. It evaluates the typical calculation of system transition probabilities since identification become easier by using it if numbers of parameters are large.

D. Particle Swarm Optimization (PSO)

PSO is a population based robust stochastic optimization that is based on the movement of swarms. This algorithm is simple and performs optimization on a work space to find best position and velocity [22]. PSO operates on a population of particles or data and they are moved around in work space with certain formulae and they are guided by their own best known position and velocity in the work space along with the entire swarm best position and velocity. Each of the particle have the record of its coordinates in the solution space which are associated with best position which is so far achieved by that particle known as pbest and one more value is tracked which gives the best value attained by a particle in the neighborhood of that particle [23]. As improved position and velocity is discovered then these will guide the position and velocity of swarm. This process is repeated each time for accelerating particles towards its best position and velocity. The PSO technique is similar to GA (genetic algorithm) except that PSO is provided with memory.

Each particle tries to improve its position using following details: current position, current velocity, distance current space and pbest, distance between current position and gbest. Thus the changes done in the position of the particle to get accurate modification is mathematically modeled by using following equation [23]:

$$V_i^{k+1} = w V_i^k + c_1 \text{rand}_1(...)*(\text{pbest}_i - s_i^k) + c_2 \text{rand}_2(...)*(\text{gbest}_i - s_i^k) + \quad (10)$$

where V_i^k is the velocity of the particle at iteration k, w is a weighting function, c_j is a weighting factor, rand is an uniformly distributed random variable from 0 to 1, s_i^k is the current position of the particle at iteration k, pbest_i is pbest of the particle i and gbest is gbest of the group.

The result shown below in table 2 gives the variation of MAPE records of five forecasting structures such as Neural Network with Back Propagation tuning algorithm, Fuzzy Neural Network structure with Back Propagation tuning algorithm, Fuzzy Neural Network structure with Back Propagation tuning algorithm and varied learning rates, Fuzzy Neural Network structure with PSO (Particle Swarm Optimization), Particle Swarm optimization (PSO) are applied to obtain the following results.

TABLE 2
MAPE RECORDS FOR LONG-TERM LOAD FORECASTING

| | PSO | FNN-PSO | FNN-BP-V | FNN-BP | NN-BP |
|----------|-------|---------|----------|---------|---------|
| 2009 | 5.90% | 6.17% | 10.64 % | 11.04 % | 13.95 % |
| 2010 | 6.99% | 7.30% | 10.66 % | 11.48 % | 17.49 % |
| AVERA GE | 6.45% | 6.74% | 10.65 % | 11.26 % | 15.72 % |

TABLE 2: MAPE RECORDS FOR LONG-TERM LOAD FORECASTING

E. Hybrid Techniques

Recent survey has presented many hybrid techniques of forecasting and hybrid techniques to improve the forecasting accuracy parameter and to explain additional accuracy parameter. In it different algorithms are combined with different computing techniques to forecast the accurate value and thus percentage of error is reduced.

Hybrid techniques

help in accurate forecasting under the conditions when model complexity increases due to introduction of weather, transmission congestion, calendar etc. Recently many numbers of tuned algorithms are used with different artificial intelligence method to reduce the value of accuracy parameter for different model are described in many papers [22, 23]. In recent papers wavelet transform is also used with different techniques in order to improve accuracy of the forecasting model. PSO provides better result than GA in combination with other time series model [25].

V. FORECASTING MODEL ACCURACY

This section covers the parameters which help to find accurate value of forecasted error. Forecast error is the difference between the actual value and forecast value for the corresponding period [19].

$$\varepsilon_t = Y_t - F_t \quad (11)$$

Where, ε_t is the error for the period t, Y_t is the actual value for the period t, F_t is the forecasted value for the period t.

The measures of aggregate errors are:

The measures of aggregate errors are:

(i) Mean Absolute error:

$$MAE = \frac{\sum_{t=1}^N |\varepsilon_t|}{N} \quad (12)$$

(ii) Mean Absolute Percentage error:

$$MAPE = \frac{\sum_{t=1}^N \left| \frac{\varepsilon_t}{A_t} \right|}{N} \quad (13)$$

(iii) Mean Absolute Deviation:

$$MAD = \frac{\sum_{t=1}^N |\varepsilon_t - \bar{\varepsilon}_t|}{N} \quad (14)$$

(iv) Percentage Mean Absolute Deviation:

$$PMAD = \frac{\sum_{t=1}^N \left| \frac{\varepsilon_t - \bar{\varepsilon}_t}{A_t} \right|}{\sum_{t=1}^N |A_t|} \quad (15)$$

(v) Mean Square error:

$$MSE = \frac{\sum_{t=1}^N \varepsilon_t^2}{N} \quad (16)$$

(vi) Root Mean Square error:

$$RMSE = \sqrt{\frac{\sum_{t=1}^N \varepsilon_t^2}{N}} \quad (17)$$

(vii) Forecast Skill (SS)

$$SS = 1 - \frac{MSE_{forecast}}{MSE_{reference}} \quad (18)$$

Where N represents the number of observations used for analysis.

MAPE and MSE is frequently used to analyze the error of the price forecast results; it is more robust and easy to understand.

VI. CONCLUSION

The combination of different time series technique and their choices play an important role in accurate prediction of forecasted values. Hybrid techniques overcome the short comings of other individual model used for forecasting and also handle different influencing factor tactfully and predict the forecasted values accurately.

Wavelet transform is used to convert an ill-behaved series into a better one by removing the non-stationary. Wavelet along with other time series techniques forecast an accurate result as shown in table 1 i.e. wavelet along with ARIMA, GARCH or ARIMA-GARCH combination. Thus wavelet plays an important role in reducing forecasting error and improve the accuracy of the forecasted values.

Similarly, PSO model is used to adjust the interval length for accurate forecasting and reduces the RMSE value and provide good validity and feasibility in forecasting.

PSO also provides reduced MAPE and accurate result as shown in table 2. Due to inclusion of PSO in forecasting model computational time is also reduced [22].

So based on the above conclusion it can be decided that which method of price forecasting is applicable for the respective problem.

REFERENCES

- [1] Contreras J, Espinola R, Nogales F, Conejo A. "ARIMA models to predict next-day electricity prices", IEEE Trans Power Syst 2003;18(3):1014–20.
- [2] Conejo A, Plazas M, Espinola R, Molina A. "Day-ahead electricity price forecasting using the wavelet transform and ARIMA models", IEEE Trans Power Syst 2005;20(2):1035–42.
- [3] Zhongfu Tan, Jinliang Zhang, Jianhui Wang, Jun Xu "Day-ahead electricity price forecasting using wavelet transform combined with ARIMA and GARCH models", IEEE Trans Power Syst 2010.
- [4] Ying-Yi Hong, Chuan-Fang Lee Department of Electrical Engineering, Chung Yuan Christian University, Chung Li 320, Taiwan, "A neuro-fuzzy price forecasting approach in deregulated electricity markets" Electric Power Systems Research 73 (2005)151–157 .
- [5] Yao-Lin Huang, Shi-Jinn Horng , Tzong-Wang Kao, Terano Takao, "A hybrid forecasting model based on adaptive fuzzy time Series and particle swarm optimization" Oct. 2012 International Symposium on Biometrics and Security Technologies.
- [6] Linlin Hu, Brunel University UK, Gareth Taylor Brunel University UK, Hai-Bin Wan Brunel University UK, Malcolm Irving,
- [7] Brunel University UK, "A Review of Short-term Electricity Price Forecasting Techniques in Deregulated Electricity Markets", IEEE Conference Publications Publication Year 2009.
- [8] Michael Egnevitsky, Senior Member, IEEE, Paras Mandal, Member, IEEE, and Anurag K. Srivastava, Member, IEEE, "An Overview of Forecasting Problems and Techniques in Power Systems", IEEE Conference Publications Publication Year: 2009.
- [9] Linlin Hu Brunel Institute of Power Systems, Brunel University, UK Gareth Taylor Brunel Institute of Power Systems, Brunel University, UK Malcolm Irving Brunel Institute of Power Systems, Brunel University, UK, "Fuzzy-logic Based Bidding Strategy for Participants in the UK Electricity Market", IEEE Conference Publications Publication Year: 2008
- [10] Ajay Shekhar Pandey, Devender Singh, and Sunil Kumar Sinha, "Intelligent Hybrid Wavelet Models for Short-Term Load Forecasting" IEEE TRANSACTIONS ON POWER SYSTEMS, VOL. 25, NO. 3, AUGUST 2010.
- [11] Amjad N, Keynia F. "Day-ahead price forecasting of electricity markets by a mixed data model and hybrid forecast method". Electr Power Energy Syst 2008;30(9):533–46.
- [12] P.T.T.Binh, N.T.Hung, P.Q.Dung, Lee-Hong Hee, "Load Forecasting Based on Wavelet Transform and Fuzzy Logic", IEEE Conference Publications Publication Year 2012.
- [13] Z. Obradovic and K. Tomsovic, "Time series methods for forecasting electricity market pricing," in Proc. IEEE Power Eng. Soc. Summer Meeting, vol. 2, Edmonton, AB, Canada, 1999, pp. 1264–1265.
- [14] Garcia R, Contreras J, Van Akkeren M, Garcia J. A, "GARCH forecasting model to predict day-ahead electricity prices", IEEE Trans Power Syst 2005;20(2):867–74.
- [15] Amjad N. "Day-ahead price forecasting of electricity markets by a new fuzzy neural network", IEEE Trans Power Syst 2006;21(2):887–96.
- [16] Conejo AJ, Contreras J, Plazas MA, Espinola R. "Forecasting electricity prices for a day-ahead pool based energy market", Int J Forecast 2005;21:435–62.
- [17] J. R. Hwang, S. M. Chen, and C. H. Lee, "Handling forecasting problems using fuzzy time series," Fuzzy Sets and Systems, vol. 100, pp. 217–228, 1998.
- [18] G. Bakirtzis, J. B. Theocharis, S. J. Kiartzis, and K. J. Satsios, "Short-term load forecasting using fuzzy neural networks," IEEE Trans. Power Syst., vol. 10, pp. 1518–1524, Aug. 1995.
- [19] S. Al Wadi, Mohd Tahir Ismail "Selecting Wavelet Transforms Model in Forecasting Financial Time Series Data Based on ARIMA Model" Applied Mathematical Sciences, Vol. 5, 2011 no. 7, 315–326.
- [20] Sanjeev Kumar Aggarwal, Lalit Mohan Saini, Ashwani Kumar "Electricity Price Forecasting in Deregulated Markets: A Review and Evaluation." ELSEVIER Science Direct Electrical Power and Energy Systems 31(2009) 13-22.
- [21] Reinaldo C. Garcia, Javier Contreras, Macro Van Akkeren, João Batista C. Garcia "A GARCH Model to Predict Day-Ahead Electricity Prices" IEEE Transactions on Power Systems, VOL 20, No. 2, May 2005. Proceedings of the 2012 International Conference on Machine
- [22] Learning and Cybernetics, Xian, 15-17 July, 2012 "Design of intelligent long-term load forecasting with fuzzy neural network and particle swarm optimization" Rong-jongwai*, Yu-Chih Huang, Yi-Chang Chen, Department of Electrical Engineering, Yuan Ze University, Chung Li 32003, Taiwan.

Power Quality Enhancement by using Synchronous Reference Theory for STATCOMS

A. G. Ganjewar, B. Dr. M.M.Waware, C. J. M. Shaikh

Abstract - In modern days power electronic devices are playing a crucial role leading to power quality problems. Power quality is an occurrence manifested as a nonstandard voltage, current or frequency that results in a failure of end user equipment. D-STATCOM is one of the most promising facts devices that can be effectively used for mitigation of power quality problems especially voltage sag and swell in power distribution network. This paper deals with modelling and simulation of a Distribution STATCOM (DSTATCOM) based on instantaneous SRF theory for power quality improvement. D-STATCOM based current control VSI injects current into system to compensate voltage sag and swell. The control scheme based on Hysteresis current control (HCC) technique is used to control VSC. The proposed D-STATCOM model is simulated in MATLAB/ SIMULINK environment and the results are presented.

Keywords: Hysteresis current control (HCC), FACTS devices, power quality (PQ), static compensator (STATCOM), point of common coupling (PCC), voltage source convertor (VSC).

I. INTRODUCTION

Electric problems always occur at any rate of time and place. This affects the electric supply, may affect the manufacturing industry also and finally it affects the economic development in a country. Three-phase four-wire distribution systems are going through various severe power quality problems such as poor voltage regulation, Voltage sag, harmonic, transient, overvoltage and under voltage are major impacts to a distribution system and have been discussed by the electrical engineers around the world. Since power quality problems have become a major issue due to the rapid development of sophisticated and sensitive equipment in the manufacturing and production industries. In three phase four wire distribution systems, the power quality problems can reduce the supplied power to the utility from its nominal value[2]. The customers and the end users are responsible in polluting the supply network due to use of large load. In order to mitigate the power quality problems, many standards are proposed such as IEEE 519 standard mainly have their origin in the higher voltage levels. Different types of faults are one of the most common causes of voltage sags on overhead lines.

If the economic losses due to voltage sags are noticeable then and then mitigation actions can be profitable for the customer and each mitigation action must be carefully planned and evaluated. There are different ways to mitigate voltage sags, swell and interruptions in transmission and distribution systems [1]. At present, FACTS controllers, which contribute on newly available power electronic components, are becoming prominent for custom power applications. The problem of voltage mitigation by reactive current injection and absorption is investigated. The capability of the FACTS devices to compensate voltage sag and swell is also demonstrated. And to reduce the harmonics present in output of FACTS controller passive filters are employed [3].

For mitigation purpose shunt and series connecting facts devices are available. Some FACTS devices normally used are SVC, DVR, UPFC and STATCOM. But STATCOM have so many advantages over other facts devices are as [5]

Voltage sags are one of the most occurring power quality problems. It happens frequently which leads to severe problems and economical losses. Utilities usually points towards disturbances occurred in end-user equipment as the main power quality problems and are correct for many disturbances like flicker, harmonics, etc., but voltage sSTATCOM has almost the same impact on the system behavior as long as they operate within their control ranges.

The STATCOM is more robust and effective than an SVC in providing voltage support and stability improvements.

The STATCOM provides better damping characteristics than the SVC and DVR as it is able to exchange active power with the system.

The reactive power provided by STATCOM is independent of the actual voltage on the connection point of STATCOM.

A modular design of the STATCOM allows for high availability i.e. without the loss of the entire, compensation system we can change faulty module of the STATCOM [3].

II. STATCOM

In 1999 the first SVC with Voltage Source Converter called STATCOM (STATicCOMpensator) went into operation [1]. STATCOMs are based on different topologies of Voltage Sourced Converter (VSC) and uses either GTO or IGBT devices. STATCOM is one of the most

-
- A. P.G student Department of electrical engg,Walchand college of engineering sanglia(M.S) india
 - B. Assistant professor Department of electrical engg, Walchand college of engineering sangli(M.S) india.
 - C. Assistant professor Department of electrical engg. KITS RamtekNagpu (M.S)india

advantageous custom power devices, used for supplying reactive power for correction of voltage sag and swell. It is a device connected in derivation, basically composed of a coupling transformer, that serves of link between the electrical power systems and the voltage source converter (VSC), that generates the voltage wave comparing it to the one of the electric system to realize the exchange of reactive power to correct the power quality. The STATCOM is like an electronic synchronous condenser. For three phase STATCOM the reactive power in each phase is supplied by circulating the real power between the other phases [3].

A STATCOM consists of a three phase inverter (generally a PWM inverter) using SCRs, MOSFETs or IGBTs, a D.C capacitor which provides the D.C voltage for the inverter, a link reactor which links the inverter output to the a.c supply side, filter components to filter out the high frequency components due to the PWM inverter. From the d.c. side capacitor, a three phase voltage is generated by the inverter. This is synchronized with the a.c supply. The link inductor links this voltage to the a.c supply side. This is the basic principle of operation of STATCOM [6]. Such configuration allows the device to absorb or generate controllable active and reactive power .

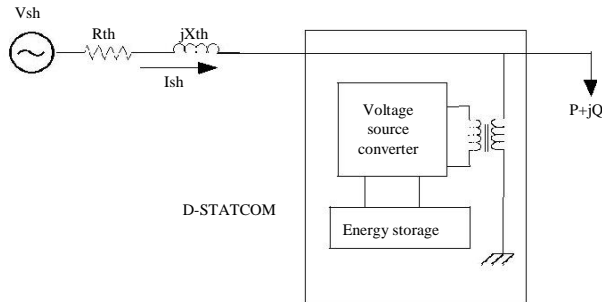


Fig. 1. Block Diagram of STATCOM

The DSTATCOM (distribution static compensator) is a shunt connected FACTS controller best and economical for compensation of power quality problems in the current and voltage. Some of the topologies for DSTATCOM three-phase four-wire system for the mitigation of power quality problems are three phase three-leg VSC (voltage source converter), three single phase VSC, three -leg VSC with split capacitors, three-leg VSC with neutral terminal at the positive or negative of dc bus [6] . A three- leg VSC is advantageous because an easily available 3-leg VSC is used, which reduces the complexity and cost of the system.

A STATCOM can improve power-system performance in such areas as the following [1]:

- The dynamic voltage control in Transmission and distribution systems;
- The power-oscillation damping in power transmission

systems;

- The transient stability;
- The voltage flicker control; and
- It also controls real power in line when it is needed

III. PROPOSED CONTROL SCHEME

Reference current generation is very important [7]. The current generation methods are compared and simulated under MATLAB environment using SIMULINK. Simulations shall be performed and compared based on-

Steady state and dynamic load conditions.

Under balanced/unbalanced nonlinear reactive loads.

Reference currents obtained from load current without considering source voltage. Reference signal is unaffected due to voltage unbalance and distortion. It increases compensation robustness and performance. The DSTATCOM shall be realized by means of a hysteresis current-controlled voltage-source inverter (VSI) [8].

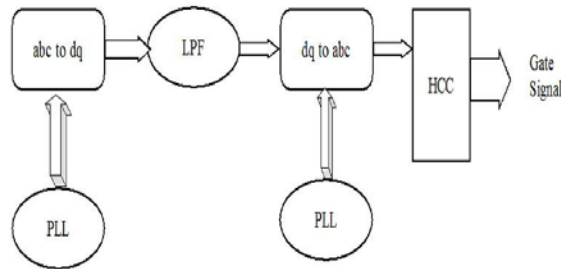


Fig. 2. Block diagram for control scheme of STATCOM

A. SRF- Synchronous Reference Frame Method (D-Q)

Reference Frame transformation is the transformation of coordinates from a three-phase *a-b-c* stationary co-ordinate system to the two phase *0-d-q* rotating coordinate system as shown [9].

This transformation is important because it is in *0-d-q* reference frame the signal can effectively be controlled to get the desired reference signal. Transformation is made in two steps: First a transformation from the three-phase stationary co-ordinate system to the two-phase so-called *α-β-0* stationary coordinate system. And two phase stationary to two phase rotating *dq0*. Load currents and voltages at Point of Common Coupling (PCC) are transformed to *0αβ* co-ordinates [10].

The transformation from *a-b-c* frame to *α-β-0* frame is given by

$$\begin{bmatrix} i_{\alpha} \\ i_{\beta} \end{bmatrix} = \sqrt{\frac{2}{3}} \begin{bmatrix} 1 & -\frac{1}{2} & \frac{1}{2} \\ 0 & \frac{\sqrt{3}}{2} & -\frac{\sqrt{3}}{2} \end{bmatrix} \begin{bmatrix} i_{La} \\ i_{Lb} \\ i_{Lc} \end{bmatrix} \quad (1)$$

The axes *a*, *b*, and *c* are fixed on the same plane and are separated
13

from each other by 120 degree. Axis being synchronized with the α - axis of a-b-c plane and β the axis being orthogonal to the α -axis. $0\alpha\beta$ is still rotating with the frequency of ω radians/second. To eliminate this frequency, further step is taken, a transformation from the $0-\alpha-\beta$ stationery coordinate system to the $0-d-q$ rotating coordinate transformation is performed [11].

The transformation from $\alpha-\beta-0$ frame to $d-q-0$ frame is given by,

$$\begin{bmatrix} i_d \\ i_q \end{bmatrix} = \begin{bmatrix} \sin \theta & -\cos \theta \\ \cos \theta & \sin \theta \end{bmatrix} \begin{bmatrix} i_\alpha \\ i_\beta \end{bmatrix} \quad (2)$$

The DC quantities and all other harmonics are transformed to non-DC quantities using a low pass filter as shown in fig.2. The algorithm is further carried a step forward, where the current reference signal in $0-d-q$ rotating frame is converted back into a $-b-c$ stationery frame. The inverse transformation from $0-d-q$ rotating frame to $a-b-c$ stationery frame is achieved with two steps $0-d-q$ to $0-\alpha-\beta$ and again $0-\alpha-\beta$ to $a-b-c$ by using inverse transformation [7].

These reference currents are used for the generation of the pulses by using the HCC i.e. hysteresis current controller. In the HCC we compare reference current with the load current and filter current to get the pulses for the inverter. These pulses will be used for triggering of the IGBT's used in the inverter circuit. The o/p of the inverter is fed to the system to compensate the harmonics and other power quality problems in the system. These current is nothing but Filter current for the system [10].

IV. SIMULATION MODEL

Simulink model for STATCOM by using synchronous reference frame theory to Sag and Swell as:

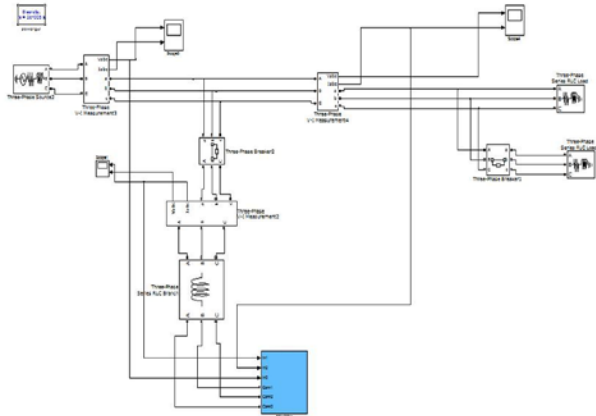


Fig. 3. Simulink model of STATCOM for sag and swell.

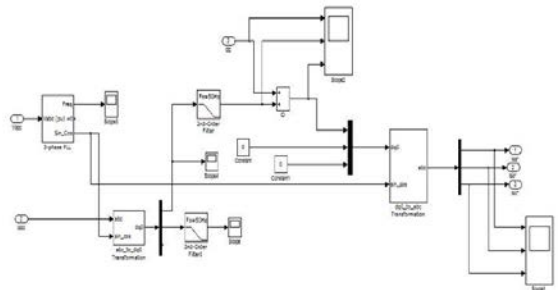


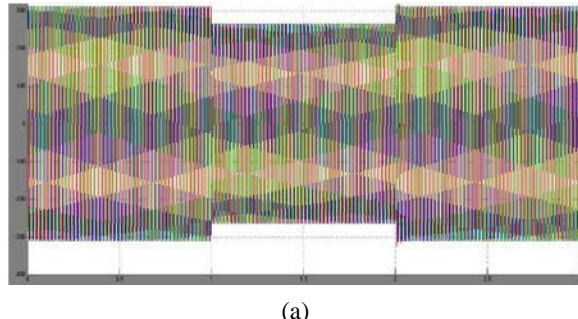
Fig. 4.SRF theory for STATCOM.

V. SIMULATION RESULTS

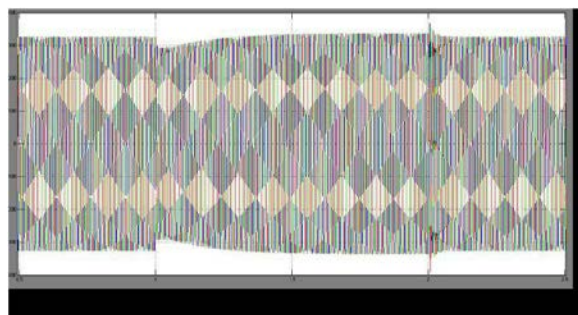
Fig .3 and Fig.4 are the test system implemented in MATLAB/SIMULINK to carryout simulations for the D-STATCOM. The test system is a distribution system having a voltage of 415 V.

1) Fig .a shows the simulation results without D-STATCOM. During the time interval of 1 to 2 sec, load on system is suddenly increased, this leads to voltage sag on three phase system. The voltage sag at the load point is 20% with respect to the reference voltage.

2) Fig .b simulation is carried out using the same scenario as above but now D-STATCOM is connected to the system. It takes few milliseconds to overcome the sag and maintain the voltage profile upto 99% thus leading to mitigation of voltage sag.



(a)



(b)

Fig. 5.voltage sag (a) without D-STATCOM and (b) with STATCOM

1) Following Fig .a shows the simulation results without D-STATCOM. During the time interval of 1 to 2 sec, load on system is suddenly removed, this leads to voltage swell on three phase system. The voltage swell at the load point is 18% with respect to the reference voltage.

2) Fig .b simulation is carried out using the same scenario as above but now D-STATCOM is connected to the system. It takes few milliseconds to overcome the swell and maintain the voltage profile upto 99% thus leading to mitigation of voltage swell.

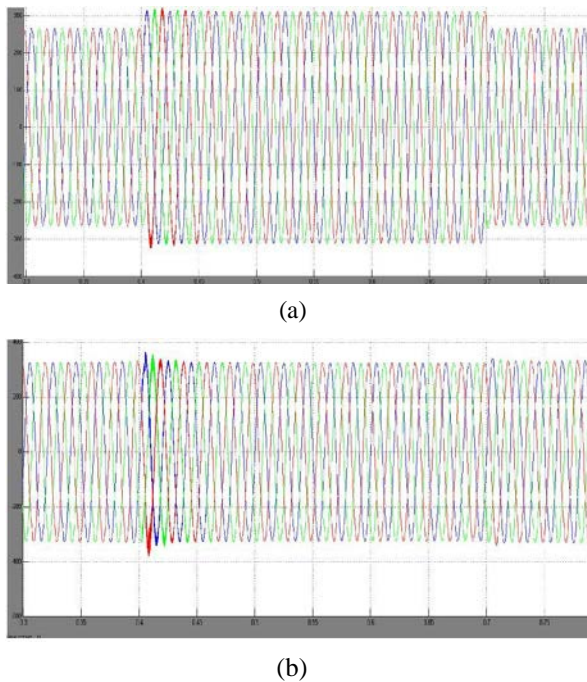


Fig. 6.voltage swell (a) without D-STATCOM and (b) with STATCOM

VI. CONCLUSION

This paper recommends STATCOM- based control scheme using instantaneous SRF theory for improving the power quality of distribution system .The performance of DSTATCOM has been validated at the radial distribution system by examining the voltage waveform before and after the STATCOM operation .When there is voltage sag and swell on system, STATCOM injects current into the three phase system to compensate the sag and absorbs the current from the system when there is swell thus enhancing the quality of power at distribution level .The design and applications of D-STATCOM for voltage sags, swells are simulated in MATLAB/SIMULINK software and the comprehensive results are presented that shows DSTATCOM provides relatively better voltage regulation capabilities.

VII. FUTURE SCOPE

The power demand is always increasing day by day. The power quality problems are also following the same trend and increasing day by day. So there is need to reduce such power quality problems like voltage sag and swell and make the supply system efficient. STATCOM is one of the promising technologies to enhance the power quality of system. The power quality can be still improved by using soft computing techniques like Unified power flow controller, Dynamic Voltage Restorer etc. FACT devices can be controlled through different control techniques to get better coordination between real and reactive power.

VIII. REFERENCES

- [1] Ravilla Madhusudan, Student Member, IEEE, G. RamamohanRao, "Modeling and Simulation of a Distribution STATCOM (D-STATCOM) for Power Quality Problems-Voltage Sag and Swell Based on Sinusoidal Pulse Width Modulation (SPWM)", IEEE-International Conference On Advances In Engineering, Science And Management (ICAESM -2012) March 30, 31,2012 436.
- [2] Gurijbal Singh, "Electric Power Quality-Issues, Effects and its Mitigation" International Journal of Engineering Research & Technology (IJERT) ISSN: 2278-0181, Vol. 2 Issue 6, June - 2013.
- [3] M. A. Abido "Power System Stability Enhancement Using Facts Controllers" A REVIEW
- [4] Jyothishila NayakBharothu, K Lalitha , "Compensation of voltage flicker by using facts devices" American Journal of Electrical Power and Energy Systems 2013; 2 (3) : 66-80Published online May 30,2013.
- [5] Dae-Wook Kang, Woo-Chol Lee, Dong-Seok Hyun "The Distribution STATCOM for Reducing the Effect of Voltage Sag and Swell", Department of Electrical Engineering,HanYangUniversity,HaengDang Dong, SungDong GU ,SEOUL 133-791
- [6] B.Singh, R.Saha, A.Chandra, K.Al Haddad "Static synchronous compensators (STATCOM)" a review Department of Electrical Engineering, Indian Institute of Technology, New Delhi 110 016, India.
- [7] E.Latha Mercy, R.Karthick, and S.Arumugam, "A comparative performance analysis of four control algorithms for a three phase shunt active power filter," IJCSNS International Journal of Computer Science and Network Security, vol.10 no.6, June 2010.
- [8] Consalva J. Msigwa, Beda J. Kundu and Bakari M.M. Mwinyiwiwa, "Control algorithm for shunt active power filter using synchronous reference frame theory," World Academy of Science, Engineering and Technology 34 2009.
- [9] Avik Bhattacharya, ChandanChakraborty, And Subhashish Bhattacharya, "Reviewing traditional methods of reference current generation," IEEE Industrial Electronics Magazine N September 2009 1932-4529/09/2009 IEEE.
- [10] Chennai Salim and Benchouia Mohamed Toufik, "Intelligent controllers for shunt active filter to compensate current harmonics based on srf and scr control strategies," International Journal on Electrical Engineering and Informatics - Volume 3, Number 3, 2011.
- [11] María Isabel Milánés Montero, Enrique Romero Cadaval, and Fermín Barrero González, "Comparison of control strategies for shunt active power filters in three-phase four-wire systems," IEEE Trans. on Power Electronics, vol. 22, no. 1, January 2007.



Sunayana .G. Ganjewar has obtained B.E. (Electrical) from PES College of Engg Aurangabad, India, in 2011. Currently she is pursuing M.Tech in Electrical Power System, from Walchand College of Engg. Sangli, India under the guidance of Prof. Dr. M. M. Waware.



Joya M. Shaikh has obtained B.E. (Electrical) from ADCET, College of EnggAshta, India, in 2012. Currently she is pursuing M.Tech in Electrical Power System, from Walchand College of Engg. Sangli, India under the guidance of Prof. R. P. Hasabe.



Prof. Dr. M. M. Waware obtained B.E and M.E. in Electrical Engineering from Walchand College of Engineering (WCE) Sangli, Maharashtra, India. He obtained Ph.D from Indian Institute of Technology Roorkee (IITR) in 2012. Currently he is Assistance Professor in Electrical

Department in WCE, Sangli. His fields of interest include Power Electronics, Power Quality, ActivePowerFilters, Multilevel inverter



Rahul Chakole has obtained his BE in Electrical , Electronics and Power from P.E.S. college of engg. Aurangabad. He has worked as Jr. Testing Engineer at BNC Power Project pvt ltd pune for 14 months. He is now working as assistant professor in KITS Ramtek, Nggpur from last 17 months. His area of interests are Power System and Power Quality and transformer.

Development of Dielectric Material for Application in Electronic Packaging Technique

A. Preeti Kumari, B. S. P. Gangwar, C. Harsh Vikram Singh, D. Rabinder K. Singh

Abstract— Dielectric materials developed using compositions consisting basically Magnesium borosilicate (MBS). The developed MBS Glass-Ceramic materials were characterized to find its suitability as a substrate for electronic packaging. The experimental study was made on the MBS glass-ceramic itself, MBS glass-ceramic containing MAS (Magnesium Alumino-Silicate) based glass-ceramic as an additive and the MBS glass-ceramic containing TiO_2 as additives. The results of doped MBS glass-ceramics were compared with the pure MBS glass-ceramic. Axial and radial shrinkage data were deliberated. The effects of additives on the densification and shrinkage anisotropy after sintering of MBS glass-ceramic samples were investigated. Also the dilatometry behaviour of these materials was studied. The thermal expansion was observed in decreasing order with addition of additives. A microwave dielectric characterization was also performed. It was observed that the material possess low permittivity. These materials are found suitable for usage as Low Temperature Co-fired Ceramics (LTCC) substrate material.

Keyword— Electronic packaging, Glass-ceramics, Dilatometry, Permittivity, LTCC.

I. INTRODUCTION

Electronic packaging is a major discipline within the field of electronic engineering and includes a wide variety of technology. It refers to the enclosures and protective features built into the product itself, and not to shipping containers. It applies both to end products and to components. It includes mounting and interconnection of integrated circuits and other components onto printed circuit boards.

The various types of packaging techniques are sheet metal, cast metal, machined metal, moulded plastic, hermetic metal/glass cases, hermetic ceramic packages and printed circuit assemblies etc. Packages consisting of a lead frame embedded in a vitreous paste layer between flat ceramic top and bottom covers are more convenient than metal/glass¹ packages for some products, but give equivalent performance. Examples are integrated circuit chips in ceramic Dual In-line Package form, or complex hybrid assemblies of chip components on a ceramic base plate.

This type of packaging can also be divided into two main types: multilayer ceramic packages (like LTCC and HTCC) and pressed ceramic packages.

Low temperature co-fired ceramic (LTCC) devices are monolithic, ceramic microelectronic devices. In this context "co-fired ceramic" means that the ceramic support structure and any conductive, resistive, and dielectric materials are fired in a kiln at the same time, and "Low temperature" means that the sintering temperature is less than 1000°C. LTCC devices include capacitors, inductors, resistors, transformers, and hybrid circuits. LTCC processes can also be used to make packages for ICs. LTCC devices are made by processing a number of layers independently and assembling them into a device as a final step. This differs from semiconductor device fabrication where layers are processed serially; each new layer being fabricated on top of previous layers. Co-fired ceramics were first developed in the late 50's and early 60's to make more robust capacitors [1]. The technology was later expanded in the 60's to include multilayer printed circuit board like structures[2]. LTCC technology is especially beneficial for RF and high-frequency applications. In RF and wireless applications, LTCC technology is also used to produce multilayer hybrid integrated circuits, which can include resistors, inductors, capacitors, and active components in the same package.

Glass-ceramics are polycrystalline materials of fine microstructure that are produced by the controlled crystallisation (devitrification) of a glass. These glass-ceramics are attractive as microwave dielectric materials for usage as Low temperature co-fired ceramics (LTCC) substrate. In the new era of communication technology we have revolutionary developments in satellite communication, global positioning systems and mobile communication systems, which have helped the developments in multilayer technologies like low temperature co-fired ceramics (LTCC). There is a requirement for the development of materials and process technologies that can offer the rapid production of low-cost, light weight, small, multifunctional and highly reliable devices. The firing of the electrodes and the ceramic substrate material simultaneously requires a low sintering temperature with electrodes that are compatible with ceramics. In addition to these basic requirements, the LTCC substrate materials should exhibit a low permittivity to reduce the signal propagation delay and low dielectric losses ($\tan\delta$), i.e. high quality factor ($Q=1/\tan\delta$) [3]. In contrast to the conventional ceramic technology, LTCC technology is growing continuously especially for industrial and telecommunication area due to the low investment and short process [4-5].

-
- A. PG Scholar, ECD, KNIT Sultanpur
preetikumari5501@gmail.com
 - B. Assistant Professor, ECD, KNIT Sultanpur
gangwar_sp@rediffmail.com
 - C. Assistant Professor, ECD, KNIT Sultanpur
harshvikram@gmail.com
 - D. HOD, ECD, KNIT Sultanpur
singhrabinder57@gmail.com

Glass-ceramic materials share many properties with both glasses and ceramics. Glass-ceramics have an amorphous phase and one or more crystalline phases and are produced by a so-called "controlled crystallization" in contrast to a spontaneous crystallization, which is usually not wanted in glass manufacturing. Glass-ceramics have the fabrication advantage of glass as well as special properties of ceramics. Glass-ceramics are mostly produced in two steps: First, a glass is formed by a glass manufacturing process. The glass is cooled down and is then reheated in a second step. In this heat treatment the glass partly crystallizes. In most cases nucleation agents are added to the base composition of the glass-ceramic. These nucleation agents aid and control the crystallization process. Glass-ceramics based on CaO-B₂O₃-SiO₂ system have been widely investigated by several researchers. These glass ceramics are promising LTCC substrate materials because of their low dielectric losses, low firing temperature and compatibility with several metal electrodes [6-8].

In this study, we selected different compositions of MgO-B₂O₃-SiO₂ (MBS) based glass-ceramics. The main purpose is to develop and characterize its sintering behaviour and microwave dielectric properties for its suitability as LTCC substrate material.

II. EXPERIMENTAL PROCEDURES

Two glass compositions, namely GC-1 and GC-2 were prepared with the compositions furnished in Table-1. Powder of Quartz, Magnesium Oxide, Boric Acid, Anatase, Rajmahal China Clay, Talc Powder and Calcined alumina with much purity. The raw materials and chemicals were mixed thoroughly by using agate mortar & pestle. Each mixed batch was taken in alumina crucible and heated in an electric furnace (Nabertherm, Germany) for melting at 1350°C. The soaking time at peak temperature was maintained for 2 hours to get melted glass and then quenched into the cold water separately. The quenched Glass so obtained is called frit. These quenched glasses of each batch were ground separately for 6 hrs using Pot mill. The finely ground glasses were then passed through a 200 mesh sieve and then stored separately. The chemical composition of the ground glasses (GF-1 and GF-2) are given in Table-1.

Three batches of MBS glass-ceramics (i.e. MBS₀, MBS_{10GC} and MBS_{12Ti}) were prepared as per Table-2 and mixed thoroughly. Test specimens were prepared by uniaxial pressing at 100 MPa pressure using Hydraulic Press (HIECO, New Delhi, India). A steel die was used for making the test specimens having diameter 15 mm with ~3mm thickness.

All the green test specimens were dried in an electric oven at 110°C for 3 hrs. Then these specimens were fired for sintering at 920°C with 3 hours soaking time at the peak temperature. Again the same cooled samples were reheated up to 900°C with 5 hrs soaking time at peak temperature for proper crystallisation of glass-ceramics. After crystallization at 900°C, the samples were cooled naturally up to room temperature. Cooled test specimens were polished using the Polishing Machine (Metatech, Mumbai, India) as per desired

size. The sintering and densification behaviours of the test samples were evaluated. For the measurement of thermal expansion, rectangular specimens were prepared using same pressure and firing temperature as applied for cylindrical samples. Linear thermal expansion was analysed by Dilatometer (V. B. Ceramics and Consultant, Chennai, India). The microwave dielectric measurements of the polished test specimens were performed by Alpha-A High Performance Frequency Analyzer (Novo Control Technologies).

TABLE 1: CHEMICAL COMPOSITION OF CRYSTALLISING GLASSES

| Constituents | Glass-Ceramics | |
|--------------------------------|----------------|-------|
| | GF-1 | GF-2 |
| SiO ₂ | 19.94 | 43.42 |
| Al ₂ O ₃ | 0.64 | 27.8 |
| TiO ₂ | 0.11 | 10.56 |
| Fe ₂ O ₃ | 0.14 | 0.82 |
| CaO | 0.08 | 1.62 |
| MgO | 34.48 | 14.86 |
| Na ₂ O | 0.02 | 0.22 |
| K ₂ O | 0.06 | 0.26 |
| B ₂ O ₃ | 44.31 | — |
| L.O.I | 0.18 | 0.35 |

TABLE -2: BATCH COMPOSITION (Parts by weight)

| Constituents | Batches | | |
|------------------|------------------|---------------------|---------------------|
| | MBS ₀ | MBS _{10GC} | MBS _{12Ti} |
| GF-1 | 100 | 100 | 100 |
| GF-2 | | 10 | |
| TiO ₂ | | | 12 |

III. RESULTS AND DISCUSSION

The **green density** was measured and furnished in Table-3. The results indicated in increasing order from 1.81 to 2.04 g/cc. The **water absorption, apparent porosity and bulk density** were evaluated after reheating the samples at 900°C and the results were furnished in Table-3.

The **theoretical density (D_{th})** of the glass-ceramics is calculated using the following equation:

$$D_{th} = \frac{W_1 + (W_2 + W_3)}{\frac{D_1}{W_1} + \frac{D_2}{W_2} + \frac{D_3}{W_3}}$$

where, W₁, W₂ and W₃ are the weight percentage of the glass ceramic matrix with densities D₁, D₂ and D₃ in the mixture, respectively [9]. It was observed that bulk density of the samples sintered at 900°C lie in the range 2.45 to 2.58. The bulk density was found close to the theoretical density. This was because the glass-ceramic samples were sintered up to temperature 900°C. From a macroscopic viewpoint, during sintering not merely the dimensions of the products change but also the shape of the products may vary as a consequence of anisotropic sintering shrinkage, phase transformations, swelling or bloating effects, etc. Moreover, anisotropic

shrinkage behaviour of composite powders can cause formation of cavities and other micro-structural changes in sintered compacts [10]. The observed value of the **radial and axial shrinkage** with the sintering anisotropy factor (k) had been illustrated in Table-3.

If the sintering of the samples is isotropic, then the axial and radial shrinkage are equal. On the other hand, for anisotropic behaviour, the axial shrinkage is not equal to the radial shrinkage. A more convenient way to compute the shrinkage anisotropy of sintering materials is the calculation of the shrinkage anisotropy factor k. This parameter can be calculated by taking the ratio of radial shrinkage to the axial shrinkage. If k = 1, the sintering is isotropic otherwise the sintering is anisotropic [11].

TABLE-3: PROPERTIES OF TEST SPECIMENS SINTERED AT 900°C

| Properties | MBS ₀ | MBS _{10GC} | MBS _{12Ti} |
|--------------------------------|------------------|---------------------|---------------------|
| Green Density(gm/cc) | 1.81 | 2.01 | 2.04 |
| Fired Axial Shrinkage | 0.1731 | 0.1805 | 0.1746 |
| Fired Radial Shrinkage | 0.1733 | 0.1667 | 0.1600 |
| Sintering anisotropy factor, k | 1.001 | 0.923 | 0.916 |
| Water Absorption(%) | 1.011 | 2.071 | 1.878 |
| Apparent Porosity(%) | 2.525 | 5.07 | 4.837 |
| Bulk Density(gm/cc) | 2.496 | 2.448 | 2.576 |
| Theoretical Density (gm/cc) | 2.807 | 2.84 | 2.91 |

In liquid phase sintering, the densification occurs through the enhanced rearrangement of particles through low viscous liquid and in due course removes pores in the solid body. The primary glass B₂O₃ is regarded as a typical glass network former that has a lower glass transition temperature [12]. It is generally agreed that a non-wetting glassy network leads to porosity and hence the densification will be lower if the solubility of the ceramic in the liquid phase is poor.

A comparative study of the variation of the green density with respect to additives revealed that green density (above 65% of their respective theoretical densities) was observed for both the cases, which on sintering resulted in a final densification of about 86 – 89 % of their theoretical densities (Table-4). The true porosity of the specimens fired at the maturing temperatures is also shown. It was observed that porosity of samples sintered at 900°C was between 11 – 13%.

Table-4: Relative Densities Of Different Body Mix After Firing At 900°C.

| Mix No./900°C | Bulk Density (gm/cc) | True Density (gm/cc) | Relative Density | %True Porosity |
|---------------------|----------------------|----------------------|------------------|----------------|
| MBS ₀ | 2.496 | 2.807 | 0.8892 | 11.08 |
| MBS _{10GC} | 2.448 | 2.84 | 0.8619 | 13.81 |
| MBS _{12Ti} | 2.576 | 2.910 | 0.8852 | 11.48 |

The length of an object changes when it is heated or cooled, by an amount proportional to the original length and the change in temperature. Rectangular test specimens having dimension 50mm×5mm×5mm were obtained by uniaxial pressing. A **dilatometer** was used to measure the percent thermal expansion of the sintered test specimens up to 700°C with heating rate of 10°C per minute. The variation of the percent linear thermal expansion as a function of temperature is shown in Figure-1. All the Test Specimens reheated at 900°C with 5 hours soaking at the peak temperature were taken for the tests. The rectangular bar was used in dilatometer and the readings of percent thermal expansion were recorded from room temperature to 700°C at the heating rate of 10°C/min. At 500°C, the coefficient of thermal expansion was 9.29×10^{-6} , 7.25×10^{-6} & 8.22×10^{-6} and at 700°C, it was 1.16×10^{-6} , 9.54×10^{-6} & 9.42×10^{-6} for the MBS₀, MBS_{10GC} and MBS_{12Ti} respectively. The thermal expansion was minimum in case of MBS_{10GC}, this might be due to the maximum crystallising phase.

A variety of techniques like dielectric resonator techniques at C-band and X-band, mode filtered cavity techniques at K-band, parallel plate capacitor method from dc to 1 MHz and open resonator techniques at frequencies from 15 to 100 GHz etc have been used to evaluate the dielectric properties of materials [13]. The glass-ceramic substrate is characterized from 0.01 Hz to 1 MHz using the Alpha-A High Performance Frequency Analyzer (Novo Control Technologies).

Permittivity describes the interaction of a material with an electric field E and is a complex quantity.

$$\mathbf{k} = \boldsymbol{\epsilon}/\epsilon_0 = \boldsymbol{\epsilon}_r = \boldsymbol{\epsilon}' - j\boldsymbol{\epsilon}''$$

Dielectric constant (k) is equivalent to relative permittivity (ϵ_r) or the absolute permittivity ϵ relative to the permittivity of free space (ϵ_0). The real part of permittivity (ϵ') is a measure of how much energy from an external electric field is stored in a material. The imaginary part of permittivity ϵ'' is called the loss factor and is a measure of how dissipative or lossy a material is to an external electric field. The imaginary part is usually much smaller than real part. The loss factor includes the effects of both dielectric loss and conductivity. The simplest way to define dissipation factor (loss tangent) is the ratio of the energy dissipated to the energy stored in the dielectric material. The more energy that is dissipated into the material the less is going to make it to the final destination. This dissipated energy typically turns into heat or is radiated as RF (Radio Frequencies) into the air. With “high power” signals, a material with a large dissipation factor could result in the development of a tremendous amount of heat, possibly culminating in a fire (advanced dielectric heating). When the signals are very weak a high loss material means that little or no signal is left at the end of the transmission path. In order to retain maximum signal power, a low loss material should be used [14].

The values of permittivity, loss tangent ($\tan\delta$), capacitances and impedances have been recorded from dc to 1 MHz at

various temperatures. The recorded values of above parameters at 1MHz of three samples at different temperatures was shown in Tables-5-7. The variation of permittivity of all the sintered glass-ceramic samples as a function of temperature at 1MHz frequency can be seen from the table. It was observed that in case of MBS_{10GC}, the addition of glass-ceramic GF-2 (10% by parts) cause decrement in the permittivity. The permittivity of the MBS_{10GC} was found in the range 5-7, which is best suitable for the LTCC technology. It was also observed that the addition of noticeable amount of TiO₂ cause an increment in the value of permittivity of the MBS glass-ceramics as seen in case of MBS_{12Ti}. The titanium possess the higher dielectric polarizability as compared to that of other constituting elements in the glass. The permittivity value of TiO₂ is very high i.e. 105 [15]. At 300°C, the permittivity observed for the MBS_{12Ti} and MBS₀ are 10.28 and 8.87, respectively. The quality factor (i.e. inverse of loss tangent, 1/tanδ) has also been increased on addition of GF-2 and TiO₂ content, correspondingly in MBS glass ceramic. Consequently, the dielectric losses were also reduced to a great extent. Thus it meets the requirement for LTCC technology.

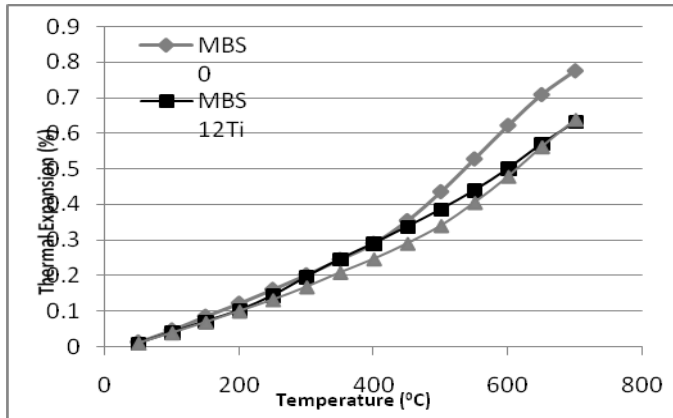


Fig. 1 : Percentage of linear thermal expansion of matured test specimens as a function of temperature

TABLE 5: DIELECTRIC PROPERTIES OF MBS₀ AT 1 MHz AT DIFFERENT TEMPERATURES

| Te mp. (°C) | ε' | ε'' | Cp' [F] | Cp'' [F] | Tan(δ) | Zs' [Ohms] | ε _r |
|-------------------|----------|----------|----------|-----------|----------|---------------|----------------|
| 30 | 1.20E+01 | 1.98E+00 | 6.24E-12 | -1.03E-12 | 1.64E-01 | 4.08E+03 | 12.20 |
| 70 | 9.01E+00 | 2.19E-01 | 4.67E-12 | -1.14E-13 | 2.43E-02 | 8.28E+02 | 9.01 |
| 100 | 8.96E+00 | 1.51E-01 | 4.65E-12 | -7.85E-14 | 1.69E-02 | 5.78E+02 | 8.96 |
| 150 | 8.84E+00 | 5.49E-02 | 4.59E-12 | -2.85E-14 | 6.21E-03 | 2.15E+02 | 8.84 |
| 200 | 8.90E+00 | 3.50E-02 | 4.62E-12 | -1.81E-14 | 3.93E-03 | 1.35E+02 | 8.90 |
| 300 | 8.87E+00 | 8.76E-02 | 4.60E-12 | -4.54E-14 | 9.87E-03 | 3.42E+02 | 8.87 |

IV. CONCLUSION

Results revealed that sintering behaviours of MgO-B₂O₃-SiO₂ based (MBS) glass-ceramics samples were anisotropic. Thermal expansion coefficients were recorded from room temperature to 700°C at heating rate of 10°C/min and were

found to be 9.29×10^{-6} , 7.25×10^{-6} & 8.22×10^{-6} for the MBS₀, MBS_{10GC} and MBS_{12Ti} respectively at 500°C. From the data it was observed that with addition of additives in the MBS glass ceramics, the percent thermal expansion decreases at all the test temperatures (Fig.1). The MBS_{12Ti} glass-ceramics exhibit permittivity of 9-10, bulk density of 2.576gm/cc and loss tangent is less than 3.59×10^{-2} . While in the case of MBS_{10GC}, which exhibit low permittivity of 5-7, bulk density of 2.45gm/cc and loss tangent is less than 3.17×10^{-2} . The bulk density obtained is close to theoretical density and thus the relative density is around 86-89% at such a low sintering temperature of 920°C. The quality factor values increased with the addition of additives. These improved values of quality factor and lesser dielectric losses due to selective addition of GF-2, also enhanced the crystallisation process. Developed MBS glass-ceramics can be used with deliberated improved performance in Low Temperature Co-fired Ceramics (LTCC) substrate preparation.

V. REFERENCES

- [1] Rodriguez, Antonio R. & Arthur B. Wallace, "Ceramic capacitor and method of making it", US Patent 3004197, October 10, 1961.
- [2] Stetson, Harold W., "Method of making multilayer circuits", US Patent 3189978 , June 22, 1965.
- [3] Urban Dosler, M.M.Krzmanc, D.Suvorov, "Phase evolution & microwave dielectric properties of MgO-B₂O₃-SiO₂ based glass-ceramics", *Ceram. Int.* 38 , pp. 1019-1025, 2012.
- [4] H.Schubert, and G. Petzow, "Preparation and characterization of ceramic powders", *Advance Ceramics III, Elsevier Science Publisher Ltd*, pp. 45-56, 1990.
- [5] W. M. Sigmund, N. S. Bell and L. Bergstrom,"Novel Powder-Processing Methods for Advanced Ceramics", *J. Am. Ceram. Soc.*, 83(7), pp. 1557-1574, 2004.
- [6] S.H.Wang and H.P.Zhou, "Densification and dielectric properties of CaO-B₂O₃-SiO₂ system glass ceramics", *Mater. Sci. Eng. B* 99 , pp. 597-600, 2003.
- [7] H.K.Zhu, H.Q.Zhou, M. Liu,P.F.Wei and G. Ning, "Low temperature sintering and properties of CaO-B₂O₃-SiO₂ system glass-ceramics for LTCC application", *J. Alloys Compd.* 482 pp. 272-275, 2009.
- [8] J.H.Jean, C.R.Chang and C.D.Lei, "Sintering of a crystallizable CaO-B₂O₃-SiO₂ glass with silver", *J. Am. Ceram. Soc.* 87(7), pp.1244-1249, 2004.
- [9] K.P.Surendran, P.Mohanam and M.T.Sebastian, "The effect of glass additives on the microwave dielectric properties of Ba(Mg_{1/3}Ta_{2/3})O₃ ceramics", *Journal of solid state chemistry* 177 pp. 4031-4046, 2004.
- [10] M.J. Hoffmann, A. Nagel, P. Greil and G. Petzow, "Slip casting of SiC whisker-reinforced Si₃N₄", *J. Am. Ceram. Soc.* 72, 765-769, 1989.
- [11] J.H. Jean and T.K.Gupta, "Crystallization kinetics of binary borosilicate glass composite", *J. Mater. Res.* 7, No.11, pp. 3103-3111, 1992.
- [12] Liang Chai, Aziz Shaikh, Vern Stygar et al., "Characterization of LTCC Material Systems at Microwave Frequencies", Ferro Electronic Materials, IMAPS Advanced Technology Workshop on Ceramic Technologies for Microwave, March 26-27, 2001, Denver.
- [13] D. Sen, T. Mahata, A.K. Patra, S. Mazumder and B.P. Sharma, 'Small angle neutron scattering investigation and the low frequency dielectric response of sintered ZrO₂-8 mol % Y₂O₃ ceramic compacts: the effect of pore characteristics', *Jr. Phy: Condensed Matter*, 16, pp. 6229-6242, 2004.
- [14] S. H. Yoon, D. W. Kim, S. Y. Cho, K. S. Hong, "Phase analysis and microwave dielectric properties of LTCC TiO₂ with glass system", *J. Eur. Ceram. Soc.*, 23, pp. 2549-2552, 2003.

State Feedback Controllers for Inverted Pendulum System using Lab view

A. Devendra Rawat, B. Jyoti Ohri

Abstract—Lab VIEW is an application software used in virtual instrumentation. Lab VIEW is an essential part of a VI because it offers data acquisition and better interfacing with hardware. Inverted Pendulum is the benchmark control problem because it is a nonlinear and highly unstable system. In this paper the modeling of inverted pendulum system is given and a virtual instrument for pole placement based state feedback controller and Linear Quadratic Regulator is simulated. The performance of controllers is observed with the help of virtual instrument.

Index Terms --Inverted Pendulum, LQR, Lab view, Lagrangian, Pole placement, State Feedback, Virtual Instrumentation.

I. INTRODUCTION

The inverted pendulum is one of the most important problems of classical control engineering. Inverted Pendulum on a cart is a nonlinear and unstable control problem. The complexity of the problem depends also on the flexibility of pendulum rod. The problem is to balance a pole on a mobile platform that can move in only two directions, to the left or to the right. The basic principle in rocket or missile propulsion uses the concept of this inverted pendulum system. Virtual instrumentation is the measurement technique with which we can perform real time measurements by creating user defined applications in LabVIEW software. Software component of a virtual instrument is the main difference between natural and virtual instrumentation. With the help of software complex and expensive equipment are being replaced by simpler and less expansive hardware [11]. In this paper, the inverted pendulum system modeling i.e. the mathematical model of the pendulum system is described in the section II. The mathematical modeling is based on the Lagrangian which is the conservation of energy. In III and IV section the pole placement based state feedback controller and LQR controllers are described. The simulation results of the both pole placement and LQR controllers are given in the section V and conclusion is given in section VI. Finally the references are given in section VII.

II. INVERTED PENDULUM SYSTEM

An inverted pendulum is a basic important control problem shown in Fig.1. This is a non linear and highly unstable process. It is one input and two output signals. Here our objective is to balance a pendulum vertically on a motor driven wagon. When the wagon moves along the x direction the pendulum should not fall. A DC motor is used to drive the wagon, a controller is controlling the motor.

The objective here is to balance the pendulum at a vertical position on a motor driven cart. We want settling time for ¹

angular position of pendulum and displacement of cart to be less than 5 seconds. The angular displacement of the inverted pendulum from vertical should be zero. The linearized model is derived using the Lagrangian equations of motion. The Lagrangian can be defined as $L=K-U$ where K is kinetic energy of system and U is the potential energy.

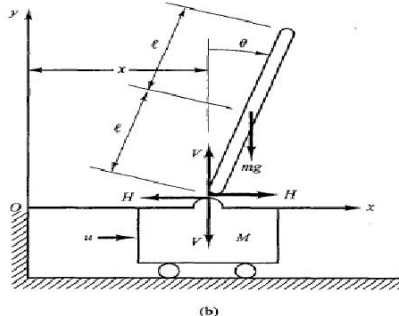
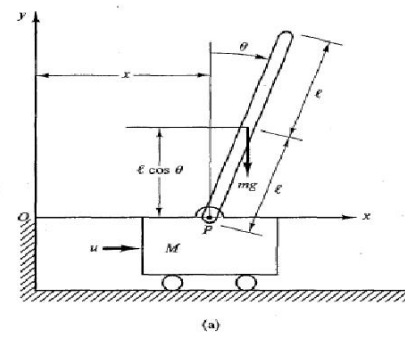


Fig. 1. (a) Inverted Pendulum System (b) FBD
The Lagrangian equations can be written as

$$\frac{\partial}{\partial t} \left(\frac{\partial L}{\partial \dot{\theta}} \right) - \frac{\partial L}{\partial \theta} = 0 \quad \frac{\partial}{\partial t} \left(\frac{\partial L}{\partial \dot{x}} \right) - \frac{\partial L}{\partial x} = u \quad (1)$$

These lagrangian equations are just an equivalent representation of Newton's equations of motion.
The system parameters for inverted pendulum on a moving cart are given following.

x position of the cart or displacement of the cart

θ Pendulum angle from vertical

F force applied on the cart

M mass of the cart

m mass of the pendulum

l length to pendulum centre of mass

So we get the system equations in state space form as

A. PG Scholar, EED, NIT Kurukshetra, Haryana
devendra.rawat85@gmail.com
B. Professor, EED, NIT Kurukshetra, Haryana
ohrijyoti@rediffmail.com

$$\begin{bmatrix} \cdot \\ x \\ \cdot \\ \cdot \\ \theta \\ \cdot \\ \ddot{\theta} \end{bmatrix} = \begin{bmatrix} 0 & 1 & 0 & 0 \\ \left(\frac{mg}{Ml} + \frac{g}{l}\right) & 0 & 0 & 0 \\ 0 & 0 & 0 & 1 \\ -\left(\frac{mg}{M}\right) & 0 & 0 & 0 \end{bmatrix} \begin{bmatrix} x \\ \cdot \\ x \\ \theta \\ \cdot \\ \dot{\theta} \end{bmatrix} + \begin{bmatrix} 0 \\ -\frac{1}{Ml} \\ 0 \\ \frac{1}{M} \end{bmatrix} u \quad (2)$$

$$\begin{bmatrix} y_1 \\ y_2 \end{bmatrix} = \begin{bmatrix} 1 & 0 & 0 & 0 \\ 0 & 0 & 1 & 0 \end{bmatrix} \begin{bmatrix} x \\ \cdot \\ x \\ \theta \\ \cdot \\ \dot{\theta} \end{bmatrix} + [0]u$$

III. POLE PLACEMENT CONTROLLER INVERTED PENDULUM SYSTEM

The pole placement design is a method to place all the closed Loop poles at the desired locations. The necessary and sufficient condition for the arbitrary placement of closed loop poles in the complex plane is that the system

$$\begin{aligned} x(t) &= Ax(t) + Bu(t) \\ y(t) &= Cx(t) \end{aligned} \quad (3)$$

is controllable, If all n state variables x_1, x_2, \dots, x_n can be accurately measured at all times, according to linear control

$$\begin{aligned} u(t) &= -k_1 x_1(t) - k_2 x_2(t) - \dots - k_n x_n(t) = -kx(t) \\ K &= [k_1, k_2, \dots, k_n] \end{aligned} \quad (4) \quad (5)$$

where K is a constant state feedback gain matrix. The closed loop system is described by the state differential equation

$$x(t) = (A - BK)x(t) \quad (6)$$

The feedback gain matrix K should be insensitive to any changes in system. It should be robust in nature. The closed loop should not be affected by any disturbance.

IV. LQR CONTROLLER FOR INVERTED PENDULUM

LQR is a state feedback controller which minimizes the performance index J of a controllable and linear system. Consider the linear system

$$\begin{aligned} x(t) &= Ax(t) + Bu(t) \\ y(t) &= Cx(t) \end{aligned} \quad (7)$$

and the quadratic objective function J (or cost function) as

$$J = \frac{1}{2} \int_0^T (x^T Q x + u^T R u) dt \quad (8)$$

LQR minimize J with respect to the control input $u(t)$. Now

we see that J represents the weighted sum of energy of the state and control. In general case, Q and R represent respective weights on different states and control channels. The main design parameters are Q and R , such that Q be symmetric positive semi definite and R symmetric positive definite for a meaningful optimization problem. The controller of the feedback form is given as

$$U(t) = -k(t)x(t) \quad \text{where } k(t) = R^{-1}B^T P(t) \quad (9)$$

Here also k state feedback gain matrix is of the form

$$K = [k_1, k_2, \dots, k_n]$$

LQR approach gives us optimal value of k for which system is stable under constraints.

V. SIMULATION RESULTS FOR POLE PLACEMENT AND LQR CONTROLLER

System parameter s for inverted pendulum system are taken as given in Table I.

TABLE I

| Symb ol | Parameter | Value |
|---------|------------------------|----------------------|
| M | Mass of cart | 10 kg |
| m | Mass of pendulum rod | 1 kg |
| l | Length of pendulum | 0.5 m |
| g | Gravitational constant | 9.8 m/s ² |

VALUES OF THE SYSTEM PARAMETERS

On putting these system parameters values in state space equations we get following results.

$$A = \begin{bmatrix} 0 & 1 & 0 & 0 \\ 21.56 & 0 & 0 & 0 \\ 0 & 0 & 0 & 1 \\ -0.98 & 0 & 0 & 0 \end{bmatrix} B = \begin{bmatrix} 0 \\ -0.20 \\ 0 \\ .10 \end{bmatrix} \quad (11)$$

$$C = \begin{bmatrix} 1 & 0 & 0 & 0 \\ 0 & 0 & 0 & 0 \end{bmatrix} D = [0] \quad (12)$$

A. Pole Placement controller

The pole placement method successfully gives the stable responses for pendulum angle and cart displacement. we obtained the state feedback gain matrix by placing the closed loop poles at a desired location [5].

$$K = [-1604.9 - 357.73 - 914.29 - 473.47]$$

And settling time for both the output parameters are 2 seconds. With the state feedback gain matrix K obtained above the closed loop is formed and the response for pendulum angle and cart position is obtained as shown in fig. 2. Thus pole placement state feedback controller is able to

maintain the pendulum at its vertical position.

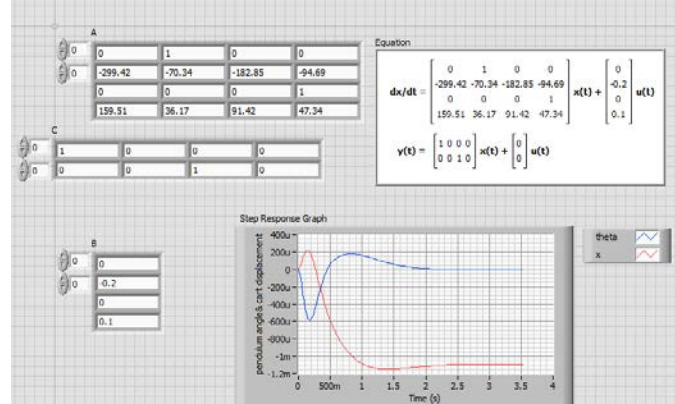


Fig. 2 Screen shot of Lab View Front panel for pole placement response of inverted pendulum system.

B. LQR controller

$$Q = C^T * C = \begin{bmatrix} 1 & 0 & 0 & 0 \\ 0 & 0 & 0 & 0 \\ 0 & 0 & 1 & 0 \\ 0 & 0 & 0 & 0 \end{bmatrix}$$

And we have taken R=1.

we obtained the state feedback gain matrix as

$$K = [-236.36 - 51.13 - 1.0 - 5.12]$$

Then the closed loop equation (A-BK) will be formed. The step response of closed loop equation for both the system's output pendulum angle and cart position is shown in Fig.3

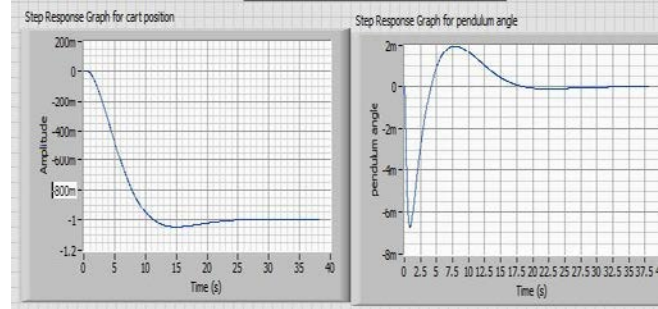


Fig. 3 Screen Shot of Lab view front panel for LQR response of inverted pendulum system with Q_1 .

The settling time for both the pendulum angle and position of cart is about 20 seconds but we want it to be less than 5 seconds. So the Q matrix will be tuned for improving the settling time and other specification. Q the state weighted matrix must be symmetric and positive semi definite as to keep the error squared positive.

q_{11} - weights to the position of cart

q_{33} -weights to the pendulum angle

Since there is a constraint on position of cart it has to be in a range so this factor is very important in tuning of Q so we will weight to it more $q_{11} >> q_{33}$.

We can do this by increasing the non zero diagonal values in the matrix Q [6]

Now we select Q such that

$$Q_2 = \begin{bmatrix} 1000 & 0 & 0 & 0 \\ 0 & 0 & 0 & 0 \\ 0 & 0 & 200 & 0 \\ 0 & 0 & 0 & 0 \end{bmatrix} \quad (16)$$

we obtained the state feedback gain matrix for newly selected weighted error matrix as

$$K = [-307.39 - 66.80 - 14.14 - 24] \quad (17)$$

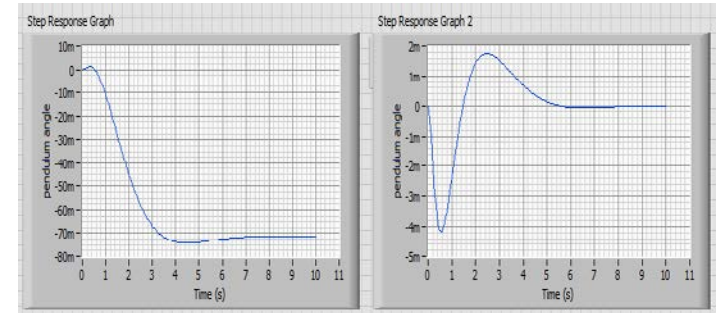


Fig. 4 screen shot of Labview front panel for LQR response of Inverted pendulum system with Q_2

VI. CONCLUSION

Inverted Pendulum is very difficult system to control due its intrinsic non linearity and instability. Two state feedback based control techniques namely pole placement and linear quadratic regulator is simulated with the help of LabVIEW.

The state feedback gain matrices are obtained and then closed loop responses for both pendulum angle and cart position are found to be satisfactory.

Further the work can be extended to verify the results on inverted pendulum system model by interfacing and acquiring the data with the help of LabVIEW.

VII. REFERENCES

- [1] National Instruments, "LabVIEW Course LV1 & LV2", 2011.
- [2] www.ni.com/white-paper/4752/en
- [3] Hongliang Wang, Haobin Dong, Lianghua He, Yongle Shi, Yuan Zhang, "Design and Simulation of LQR Controller with the Linear Inverted Pendulum," International Conference on Electrical and Control Engineering (ICECE), pp. 699-702, June 2010.
- [4] Stanislaw H. Zak, "Systems and Control" Oxford University Press, New York, 2003.
- [5] K. Ogata, Modern Control Engineering, 4th ed, Pearson Education (Singapore) Pvt. Ltd., New Delhi, 2005, ch. 12.
- [6] F. L. Lewis, "Linear Quadratic Regulator (LQR) State Feedback Design", Lecture notes in Dept. Elect. Engineering, University of Texas, Arlington, Oct 2008.
- [7] M.G. Henders, A.C. Soudack, "Dynamics and stability state-space of a controlled inverted pendulum", *International Journal of Non-Linear Mechanics*, vol.31, no.2, pp. 215-227, March 1996.
- [8] Chandan Kumar, Santosh Lal, Nilanjan Patra, Kaushik Halder,

- Motahar Reza "Optimal Controller Design for Inverted Pendulum System based on LQR Method", International Conference on Advanced Communication Control and Computing Technologies(ICACCCT),DOI:10.1109/ICACCCT.2012.6320782,R amm athapuram,Tamilnadu, August 2012.
- [9] Changkai Xu; Ming Li ; Fangyu Pan " The System Design and LQR control of a Two- wheels Self-balancing Mobile Robot", Electrical and Control Engineering (ICECE),2011 International Conference on, page(s): 2786 - 2789
- [10] Ekici, M. ; Kahveci, H. ; Akpinar, A.S. "A LabVIEW Based Submarine Depth Control Simulator with PID and Fuzzy Controller", Innovations in Intelligent Systems and Applications (INISTA), 2013 IEEE International Symposium on , page(s): 1-6
- [11] Chaturi Singh and K. Poddar "Implementation of a LabVIEW-Based Automated Wind Tunnel Instrumentation System", India Conference, 2008. INDICON 2008. Annual IEEE 2008,page(s) 103-108
- [12] Daniel Kaminsky, Jan Zidek, Petr Bilik, 2011, "Virtual Instrumentation Based Power Quality Analyzer", Intelligent Data Acquisition and Advanced Computing Systems (IDAAACS), 2011 IEEE 6th International Conference on, year 2011, page(s): 184-187
- [13] Zhang Lin, Song Yin, "Design of PID Temperature Controlling System Based on Virtual Instrument Technique", The Eighth International.

Multi-Stage Optimal Placement of PMU using Reliability and Probabilistic Approach

Sanjay Kumar, Ajay Rana, KS Sajan, Vishal Kumar

Abstract—In this paper, a technique has been devised to identify the optimal locations of Phase Measurement Units (PMU) with complete observability in the power system. The paper has also performed staging for the obtained PMU locations. The approach of Probability and Reliability has been utilized and its impact on staging and optimal PMU placements has been explained. Two indices known as Probability of Observability (PO) and Reliability Observability Criteria (ROC) has been introduced and evaluated for each bus. PO has been averaged and aggregated for each solution (APO). The option with maximum APO has been selected. ROC has been considered as the main index for Multistage Optimal Placement of PMUs. The proposed technique has been demonstrated on IEEE 14 and 24 bus systems.

Keywords—Phase Measurement Unit (PMU); Multi-stage; Optimal PMU Placement (OPP); Probability of Observability (PO); Reliability; Reliability Observability Criteria (ROC); Analytical Hierarchical Process (AHP); Integer Linear Programming; Genetic Algorithm.

I. INTRODUCTION

In a power system, PMU gives time synchronized phasor measurements by time stamping of voltage & current wave form utilizing a common synchronizing signal obtained from Global Positioning System (GPS) [1]. The ability to obtain synchronizing phasors makes PMU one of the most important measuring devices in power system monitoring and control. The functional diagram has been explained in [2]. PMU measures voltage phasor of the bus where PMU is installed and current phasor of the all buses incident to it.

A PMU can estimate the state of system directly or indirectly. PMU installation at every bus becomes a major problem due to cost factor or due to unavailability of communication facilities in some sub-station. However, Ohm's law allows us to measure the state of the buses which are directly connected to the PMU installed bus [3]. Hence required numbers of PMUs are less than the number of buses. Most important issue that needs attention is the site selection of PMU. The PMU placement problem is NP-Complete [4]. Two types of algorithm named Mathematical algorithm and Heuristic algorithm have been

discussed in [5]. Work on PMU placement using an ILP approach has been proposed by Abur [6], [7]. This paper deals with optimal PMU placement algorithm for complete observability. The main problem arises when there comes multiple optimal PMU placement solutions. Probabilistic Approach is considered for adopting the final PMU placement. Reliability of various components is considered for calculating PO. Earlier, the electric power systems were limited to relatively small geographical regions but today the connection of regional power network forms a highly interconnected large system. The number of PMUs required for the complete observability for such power system comes out to be large. Every OOP techniques only give optimal number of PMU and their location in a power system network. The cost of PMU and its installation is very high. There is a need to install PMU in stages. Hence it is required to study some decision making criteria on which multi staging of PMU will depend. Certain criteria like tie-line oscillation observability and voltage control area observability have been considered for multi staging of PMU in earlier work [7], [8], [9]. The main contribution of this work is the development of a new criterion called as Reliability Observability Criteria (ROC) and, subsequently, using it to install PMUs in stages according to their relative ranking. Analytical Hierarchical Process (AHP) has been used to define the priority to different criteria. In this work, multi-staging is done by selecting the OPP solution with the help of Probabilistic Approach. The criteria considered for decision making is Generator Observability Criteria (GOC), Bus Observability Criteria (BOC) and ROC. In [9], authors have used indices like bus observability index (BOI), voltage control area observability index (VOI) and tie-line oscillation observability index (TOI). They have taken TOI as the most important index in performing staging of PMU Locations. Numerical studies are applied to a IEEE 14 and 24 bus system.

Section II discussed about formulation of PMU placement problem taking effect of non-zero and zero injection buses. It also discussed the computation frame work for probabilistic observability [13]. Multi-phasing framework [9] using AHP is illustrated in Section III. Section IV examined the performance of proposed technique on IEEE 14 and 24 bus systems. Concluding remarks are discussed in Section V.

A. Department of electrical engineering Indian institute of TechnologyRoorkee uttarakhand india
(sanjay4kumar@gmail.com)

II. PMU PLACEMENT PROBLEM

A. Problem Formulation

PMU placement problem aims to find out minimum number of PUMs and their location for complete observability of system. In mathematical form, Integer Linear Problem for finding optimal solutions for a N bus system can be formulated as [10]

$$\text{Minimize } \sum_{k=1}^N k \quad (1)$$

Subject to:

$$A_{PMU}^T x \geq b_{PMU} \quad (2)$$

where

$$X = [x_1 \ x_2 \ x_3 \ x_4 \ x_5 \ x_6 \ x_7 \dots \ x_N]^T$$

$$x_i \in \{0,1\}$$

$$b_{PMU} = [1 \ 11]^T$$

$$A_{PMU} \in \mathbb{R}^{1 \times N}$$

The matrix A_{PMU} can be called as Bus Connectivity

Matrix that can be obtained directly from bus admittance matrix by transforming its entries into binary form. The matrix b_{PMU} indicates that there should be at least one PMU

placed at one bus involved in respective equation. If we assume zero injection bus to be present in the system then Objective Function will remain same and only constraint will be modified. The equation can be modified as in [7]. Zero injection bus is a bus which does not inject any current into the system. It allows the zero injection bus to be observable with the help of other indirectly observed buses using Ohm's Law.

B. Need for Probabilistic Approach

As above are ILP problems, so we get different combinations of optimal solutions. Now, there is the problem to select the best possible solution among the different combination. There are various contingencies [11] present in the Power System which can make Power System unobservable for some time until that contingency is removed. We need to select such a combination which will keep the system observable for maximum time. So, the Reliability of all the components on which these contingencies depend is considered [12]. Reliability of these components can be correlated with the availability of characteristics of the system. Reliability parameter with each contingency is linked which has been used to calculate the probability of observability (PO) for each bus in the system. The placement option which gives the maximum PO is selected. The Probabilistic Approach is discussed in the next Section.

C. Characteristics of Component Used For Computing PO

Table I shows all the various characteristics of components which is used for calculating PO value for each bus. As discussed in [13] PO for Electrical Power System without Zero Injection bus can be evaluated using equations

(3) and (4). These values have been aggregated and averaged to provide a quantitative sight on the observability performance of the WAMS network.

$$PO = A_{ss} = A_{ss}^{Vm} * A_{ss}^{PMU} * A_{ss}^{Link} \quad (3)$$

TABLE I
PHYSICAL PARAMETER ON WHICH RELIABILITY DEPEND

| Parameter | Characteristics |
|-----------------|---|
| A_{i}^{Vm} | Availability of voltage measurement at bus i |
| A_{i}^{PMU} | Availability of PMU at bus i |
| A_{i}^{Link} | Availability of communication link for PMU at bus i |
| A_{ij}^{Cm} | Availability of current measurement at line ij |
| A_{ij}^{Line} | Availability of line ij |

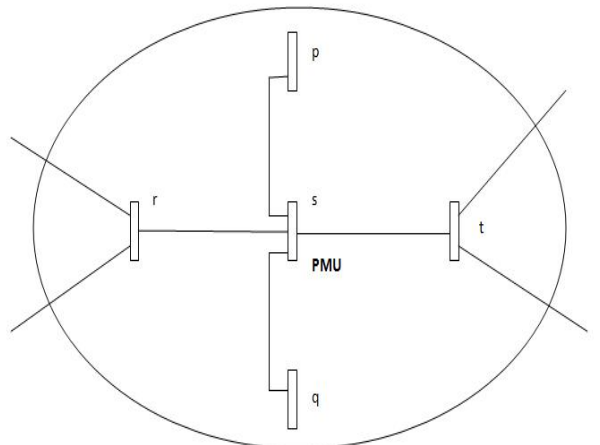


Fig. 1 A Portion of Large Power Network

A_{ss} is the probability of observability of bus s with the installed PMU at that bus. In Fig 1, bus r is made observable through the observability of bus s . So, the observability of bus r required the availability of PMU at bus s , its corresponding communication link, corresponding voltage measurement, current measurement of line rs , and the line rs itself. Hence,

$$PO = A_{ss} = A_{ss}^{Vm} * A_{ss}^{PMU} * A_{ss}^{Link} * A_{ss}^{Cm} * A_{ss}^{Line} \quad (4)$$

Zero Injection buses have been discussed in Section II. For understanding Probabilistic Approach on system involving Zero Injection buses, assume that bus s is Zero Injection bus

and PMU is installed on bus t in Figure 1. PMU installed at bus t made buses t, s and q observable directly but buses r and p are made observable using Zero Injection effect of bus s. Here PO for buses t, s and q is calculated in the same way. But PO for the buses r and p is calculated using cut set method [14]. According to this method, the Probability of failure is calculated and it is subtracted from one to obtain PO at given buses. Therefore

$$PO_r = 1 - (1 - A_s^{IM}) + (1 - A_{rs}^{Line}) + \sum_{t,q} A_{si}^{Line} (1 - PO_i) \quad (5)$$

III. MULTI STAGING OF PMU INSTALLATION

A. PMU Selection Criteria

In this work, three criteria are used to identify the importance of PMU location. These are Generator Observability Criteria (GOC), Bus Observability Criteria (BOC) and Reliability Observability Criteria (ROC)

1. Generator Observability Criteria

Power systems are highly inductive in nature due to the abundance of motors and industrial loads in the system. Generators and synchronous condensers assist in supplying the required reactive power to such loads in the system. The reactive power generation should be commensurate with the reactive power consumed by the loads. In order to have more close and real time control and to contain damage to the power system in case of eventuality the Generator buses should be observable. In this case Generator bus will have a higher weight than those connected to neighbor or neighbor-to-neighbor Generator buses. A weighting process related to GOC for PMU bus is given by,

$$GOC_K = \sum_{\forall G}^G KG + 0.8 * \sum_{\forall NG}^G KNG + 0.6 * \sum_{\forall NN}^G KNN \quad (6)$$

G_{OCK} is GOC weight of PMU Bus k. G_{KG} is the number of Generator buses connected to k^{th} PMU Bus. G_{NG} is the number of neighboring Generator buses connected to k^{th} PMU Bus. G_{KNN} is the number of neighbor-to-neighbor

Generator buses connected to k^{th} PMU Bus. G, NG, and NN are generator buses, neighbor to generator bus and neighbor-to-neighbor to Generator buses respectively.

2. Reliability Observability Criteria

ROC of a bus is associated with the PO of every bus in the system. A PMU installed bus made every bus connected to that bus observable. Reliability will increase or decrease depending on the PO of neighbouring buses. For calculating the ROC of a PMU installed bus, it is required to multiply PO of all the connected buses. It can be considered one of the important criteria for multi-staging of

PMU placement as if system is not reliable then PMU should be installed only at the later stage rather than installing PMU in first stage.

$$ROC_k = \prod_{\forall \text{ connected buses to } k} PO_i \quad (7)$$

3. Bus Observability Criteria

Bus Observability Criteria (BOC) for any Optimal PMU bus location is equal to the total number of buses connected to it. This is a quantitative criterion and is included in the phasing problem to maximize the observability of the power system by giving more preference to the buses have maximum connectivity with other buses. Bus Observability Criteria (BOC) for PMU bus k, is given by (8). Here N is totalnumber of buses and B_{kj} is 1 if bus k and j is directly connected otherwise zero.

$$BOC_k = \sum_{j=1}^N B_{kj} \quad (8)$$

B. Weight Selection Process using Analytical Hierarchical Process

Analytical Hierarchical Process (AHP) is a decision making technique and was introduced by Belton and Gear in the year 1983 [15]. The decision making process involves many intangibles that need to be traded off in a decision process. The basic idea of the approach is to convert subjective assessments of relative importance to a set of overall scores or weights. These criteria's have to be measured alongside these tangibles and need to be evaluated how well they serve the objectives of decision maker. AHP is a theory of measurements through pair wise comparisons and relies on judgments of experts to derive priority scales. In this process, the decision maker has to convert the opinion in terms of value of pair wise comparison, one at a time [15].

The AHP of decision making starts with defining the main goal and then identifying some main criteria's organized in a decision hierarchy which contributes in final decision making [8]. Set these criteria's in a hierarchy, make the comparisons based on the importance or dominance of one criterion over another. The methodology of AHP is based on pair wise comparisons of the following type 'How important is criterion C_i relative to criterion C_j ?' These comparisons are made on 9 point linguistic scale as given in Table IX. After doing pair wise comparisons the first step is to form an Overall Weight Matrix (W). The three criteria: 1. BOC (weight W1); 2. GOC (weight W2); 3. ROC (weight W3) discussed in section IV.A is used to form the Overall Weight Matrix (W)

$$W = \begin{bmatrix} w_1/w_1 & w_1/w_2 & w_1/w_3 \\ w_2/w_1 & w_2/w_2 & w_2/w_3 \\ w_3/w_1 & w_3/w_2 & w_3/w_3 \end{bmatrix}$$

The fractional value of criteria w_i / w_j is a relative comparison of criteria i against criteria j .

C. PMU installation index (PMI)

PMI is the final assessment for multi staging the PMU installation. Its value determines the ranking of PMU to be phased in different stage. PMI is calculated using values of the proposed indices V_{kj} (calculated as described in Section III.A) and the weights of the three criteria W_j (Section III.B), the PMI value of each alternative can be calculated as[9]:

$$PMI_k = \sum_{j=1}^3 j^V_{kj} \quad (9)$$

IV. CASE STUDIES

A case study on IEEE 14 and IEEE 24 bus system has been conducted to calculate Probabilistic system index (PO) and Reliability Observability Criteria (ROC). It is used to find out the best optimal solution of PMU Placement among the various combinations. The various combinations of optimal solution are calculated using Genetic Algorithm (GA). The optimal solution obtained is then used for the multi-staging of PMU installation location using different criteria. In following section we will first discuss how to calculate PMU Placement problem considering 14 bus system and 24 bus system and then apply computational frame work for computing PO values for different optimal solutions.

A. 14 Bus System

The 14 bus system is depicted in the Figure 2. It has 20 transmission lines. The system has no existing conventional measurements and only PMUs are making it observable. The placement problem is solved using the Genetic Algorithm Approach to find all optimal solution. The Genetic Algorithm gives 4 different combinations of optimal solutions for 14 bus system as shown in the Table II. Each solution is identified by an option number. Table II also shows optimal solutions for 14 bus system including zero injection bus. There is only one zero injection buses present in the system i.e. bus number 7. We get only one optimal solution for PMU Placement using three PMU.

Now the PMU placement problem is analyzed using the Probabilistic Approach proposed in Section II.C. Reliability data is given in the Appendix. The equations in Section II are used to calculate values of Probability of Observability (PO). Table III shows the proposed bus indices and average probability of observability for all the placement options. It can be noticed that PO values come out to be maximum for those buses where PMU is installed and it comes out to be minimum for those buses which are made observable by the zero injection effect of zero injection buses. The PO values

are coming out to be same for the buses where the PMUs are installed.

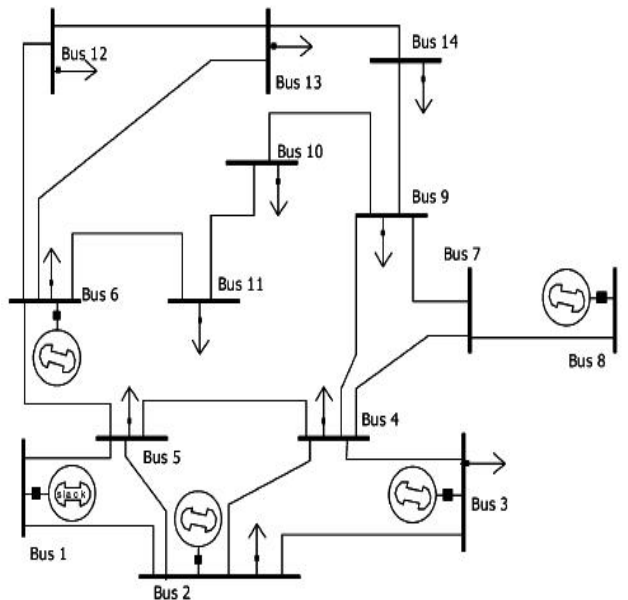


Figure 2: A IEEE 14 Bus System

TABLE II
OPTION OF PMU PLACEMENT PROBLEM FOR 14 BUS SYSTEM

| Solutions | PMU installation buses (without zero injection buses) | PMU installation buses (with zero injection buses) |
|-----------|--|---|
| Option 1 | 2,6,7,9 | 2,6,9 |
| Option 2 | 2,7,10,13 | |
| Option 3 | 2,8,10,13 | |
| Option 4 | 2,7,11,13 | |

TABLE III
PROBABILITY OF OBSERVABILITY FOR 14 BUS SYSTEM

| | Option 1 | Option 2 | Option 3 | Option 4 | Option 1 (with zero injection bus) |
|----|----------|----------|----------|----------|--|
| 1 | 0.9850 | 0.9850 | 0.9850 | 0.9850 | 0.9850 |
| 2 | 0.9902 | 0.9902 | 0.9902 | 0.9902 | 0.9902 |
| 3 | 0.9866 | 0.9866 | 0.9866 | 0.9866 | 0.9866 |
| 4 | 0.9839 | 0.9823 | 0.9813 | 0.9823 | 0.9842 |
| 5 | 0.9830 | 0.9815 | 0.9815 | 0.9815 | 0.9830 |
| 6 | 0.9902 | 0.9861 | 0.9861 | 0.98561 | 0.9902 |
| 7 | 0.9902 | 0.9902 | 0.9845 | 0.9902 | 0.98667 |
| 8 | 0.9845 | 0.9845 | 0.9902 | 0.9845 | 0.9567 |
| 9 | 0.9902 | 0.9850 | 0.9839 | 0.9867 | 0.9902 |
| 10 | 0.9832 | 0.9902 | 0.9902 | 0.9827 | 0.9833 |
| 11 | 0.9852 | 0.9827 | 0.9827 | 0.9902 | 0.9852 |

| | | | | | |
|-----|---------------|--------|--------|--------|---------------|
| 12 | 0.9862 | 0.9876 | 0.9876 | 0.9876 | 0.9863 |
| 13 | 0.9861 | 0.9902 | 0.9902 | 0.9902 | 0.9861 |
| 14 | 0.9842 | 0.9831 | 0.9831 | 0.9831 | 0.9842 |
| APO | 0.9863 | 0.9861 | 0.9859 | 0.9862 | 0.9841 |

| | | | |
|-----|--------|--------|---------------|
| 16 | 0.9902 | 0.9902 | 0.9902 |
| 17 | 0.9489 | 0.9489 | 0.9489 |
| 18 | 0.9279 | 0.9279 | 0.9279 |
| 19 | 0.9659 | 0.9659 | 0.9659 |
| 20 | 0.9568 | 0.9568 | 0.9568 |
| 21 | 0.9902 | 0.9902 | 0.9902 |
| 22 | 0.8986 | 0.8986 | 0.8986 |
| 23 | 0.9902 | 0.9902 | 0.9902 |
| 24 | 0.8800 | 0.8800 | 0.9902 |
| APO | 0.9490 | 0.9485 | 0.9495 |

A. 24 Bus System

IEEE 24 Bus system has 38 transmission lines buses number 11, 12, 17 and 24 are buses with zero injection effect.³ optimal solutions for PMU Placement are obtained for the system which has no zero injection bus as shown in Table IV. Seven PMUs are required for each option. Probability of Observability (PO) for all optimal solutions is shown in Table V which indicates that PO is maximum for option number 3. This means by using this option for PMU Placement, the system can be kept observable for most of the year. number 11, 12, 17 and 24 are buses with zero injection effect.³ optimal solutions for PMU Placement are obtained for the system which has no zero injection bus as shown in Table IV. Seven PMUs are required for each option. Probability of Observability (PO) for all optimal solutions is shown in Table V which indicates that PO is maximum for option number 3. This means by using this option for PMU Placement, the system can be kept observable for most of the year.

TABLE IV
**PMU PLACEMENT PROBLEM FOR THE 24 BUS SYSTEM
WITHOUT ZERO INJECTION BUSES**

| Optimal Solutions | PMU installation buses |
|-------------------|------------------------|
| Option 1 | 2,3,8,10,16,21,23 |
| Option 2 | 2,8,10,16,21,23,24 |
| Option 3 | 2,3,7,10,16,21,23 |

If zero injection buses are considered, then we get 10 OPP for the system in which every option required 6 PMUs. Optimal solutions are listed in Table VI. It can be noticed that the number of PMUs required become less than that required in system which has no zero injection bus

PO values of three options are shown in the Table VII. Here PO value is maximum for option number 8.

TABLE VI
**PMU PLACEMENT PROBLEM FOR THE 24 BUS SYSTEM WITH
ZERO INJECTION BUSES**

| Optimal Solutions | PMU installation buses |
|-------------------|------------------------|
| Option 1 | 3 4 7 10 19 22 |
| Option 2 | 1 4 8 10 19 21 |
| Option 3 | 1 7 9 10 18 19 |
| Option 4 | 1 7 9 10 19 21 |
| Option 5 | 1 7 9 10 19 22 |
| Option 6 | 1 8 9 10 19 21 |
| Option 7 | 1 8 9 10 19 22 |
| Option 8 | 2 7 9 10 19 21 |
| Option 9 | 2 8 9 10 19 21 |
| Option 10 | 1 1 8 10 19 21 |

TABLE VII
**PROBABILITY OF OBSERVABILITY FOR THE 24 BUS SYSTEM
WITH ZERO INJECTION BUSES**

| Bus No. | Option 3 | Option 8 | Option 10 |
|---------|----------|----------|-----------|
| 1 | 0.9902 | 0.9767 | 0.9902 |
| 2 | 0.9323 | 0.9902 | 0.9902 |
| 3 | 0.9086 | 0.9605 | 0.9086 |
| 4 | 0.9902 | 0.8999 | 0.8879 |
| 5 | 0.9774 | 0.9888 | 0.9774 |
| 6 | 0.9010 | 0.8956 | 0.8956 |
| 7 | 0.9902 | 0.9902 | 0.9449 |
| 8 | 0.9574 | 0.9574 | 0.9902 |
| 9 | 0.9902 | 0.9902 | 0.9592 |
| 10 | 0.9902 | 0.9902 | 0.9902 |
| 11 | 0.9554 | 0.9554 | 0.9877 |
| 12 | 0.9249 | 0.9249 | 0.8790 |
| 13 | 0.8721 | 0.8721 | 0.7957 |
| 14 | 0.7953 | 0.7953 | 0.7279 |
| 15 | 0.8609 | 0.9110 | 0.9110 |
| 16 | 0.9659 | 0.9659 | 0.9659 |

B. MULTI-STAGING ON IEEE 24 BUS SYSTEM

In this work multi-staging is considered for the OOP solution which is obtained with the help of Probabilistic Approach. The optimal solution having highest value of APO will be multi-staged. The AHP of decision making starts with defining the main goal and then identifying some main criteria's organized in a decision hierarchy which contributes in final decision making. Set these criteria's in a hierarchy, make the comparisons based on the importance or dominance of one criterion over another. These comparisons are made on 9 point linguistic scale as given in Table VIII. After comparing all the criteria with each other, next step is to form weight matrix (W) using criteria discussed in Section III. The weight matrix is shown in Table X is taken from [9]. The elements of weight matrix is calculated using Table X

TABLE VIII
LINGUISTIC COMPARISON

| Priority | Linguistic Comparison |
|----------|----------------------------------|
| 1 | Equally preferred |
| 3 | Moderately preferred |
| 5 | Strongly (essentially) preferred |
| 7 | Very strongly preferred |
| 9 | Extremely strongly preferred |
| 2,4,6,8 | Intermediate values |

TABLE IX
LINGUISTIC STATEMENT FORMING PAIRWISE MATRIX

| Serial No. | Weight Ratio | Statement |
|------------|--------------|--|
| 1 | W3/W2=9 | ROC is considered an extremely important factor as compared to BOC |
| 2 | W3/W2=5 | GOC is considered Strongly (essentially) preferred factor as compared to BOC |
| 3 | W3/W2=3 | ROC is considered moderately important to GOC |

The weight corresponding to the respective criteria will be obtained by calculating the Eigen Vector (V) corresponding to highest Eigen Value.

TABLE X
PAIRWISE MATRIX FOR WEIGHT CALCULATION WITH PREFERENCE GIVEN TO RELIABILITY OBSERVABILITY CRITERIA [17]

| Criteria | BOC | GOC | ROC |
|----------|-----|-----|-----|
| BOC | 1 | 1/5 | 1/9 |
| GOC | 5 | 1 | 1/3 |
| ROC | 9 | 3 | 1 |

$$W = \begin{bmatrix} 1 & 1/5 & 1/9 \\ 5 & 1 & 1/3 \\ 9 & 3 & 1 \end{bmatrix}$$

The weight matrix has maximum Eigen value of 3.0291 and the corresponding right eigenvector is [0.0868, 0.3662, and 0.9265]. After normalizing, weights come of each criterion come out to be [0.0629, 0.2654, 0.6716]. These values are taken from [9]. After this, the value of all the criteria i.e. GOC, BOC and ROC is calculated using equations (6), (7) and (8). PMU installation index will be calculated using (9). The normalized values of three criteria and PMI are shown in the Table XII. Table XII shows the Ranking of Bus location for PMU installation considering ROC as the main criteria. This result can be compared with the result obtained in [9] for 14 bus system

TABLE XI
NORMALIZED SELECTION CRITERIA AND PMI VALUES FOR IEEE 14-BUS SYSTEM

| Opp Bus | BOC | GOC | ROC | PMI | Ranking |
|---------|-----|--------|--------|--------|---------|
| 2 | 1 | 1 | 0.9799 | 0.9864 | 1 |
| 6 | 1 | 0.9130 | 0.9819 | 0.9645 | 2 |
| 7 | 0.8 | 0.6957 | 1 | 0.9066 | 4 |
| 9 | 1 | 0.7391 | 0.9829 | 0.9192 | 3 |

TABLE XII
NORMALIZED SELECTION CRITERIA AND PMI VALUES FOR IEEE 24-BUS SYSTEM

| Opp Bus | BOC | GOC | ROC | PMI | Ranking |
|---------|--------|--------|--------|--------|---------|
| 2 | 0.6667 | 0.7826 | 0.8220 | 0.8017 | 6 |
| 3 | 0.6667 | 0.6957 | 0.8725 | 0.8125 | 5 |
| 7 | 0.3333 | 0.3913 | 1 | 0.7964 | 7 |
| 10 | 1 | 1 | 0.8555 | 0.9029 | 1 |
| 16 | 0.8333 | 1 | 0.7814 | 0.8426 | 3 |
| 21 | 0.6667 | 1 | 0.8206 | 0.8583 | 2 |
| 23 | 0.6667 | 0.7826 | 0.8597 | 0.8270 | 4 |

V. CONCLUSION

In this paper, first optimal solution for location of PMU is obtained by using probabilistic Approach. After this, staging is performed on the optimal location obtained. ROC is considered the most important criteria for multi-staging of PMU Locations. Since, ROC of a bus is related to the Reliability of various parameters like availability of voltage, current measurement from CT and PT, availability of Lines connected to that bus. ROC will take care of outage of any line or component. It also includes availability of PMU and its communication link which is required to be installed at the bus. PMU installation will be more advantageous and beneficial at those buses which are most reliable. Hence considering ROC as the criteria for highest priority is justified. This can be proved more useful for the utility

VI. APPENDIX

The reliability data used for PMU, CT, PT, Link [11], [12] for twenty four bus system is presented in Table XIII,

TABLE XIII
RELIABILITY VALUES FOR COMPONENTS

| Parameter | PMU A_i | PT A_i | CT A_{ij} | Link A_i |
|-----------|--------------|-------------|----------------|---------------|
| Values | 0.99549768 | 0.99854238 | 0.99958447 | 0.999 9 |

Reliability values for Transmission line are generated by random numbers in reasonable range between 0 and 1. These values for twenty four bus system are shown in Table XIV

TABLE XIV
RELIABILITY VALUES FOR TRANSMISSION LINE FOR TWENTY FOURS BUS SYSTEM

| | | | |
|--------------------|---------|--------------------|---------|
| A_{12}^{Line} | 0.9876 | $A_{12,13}^{Line}$ | 0.9656 |
| A_{13}^{Line} | 0.9188 | $A_{12,23}^{Line}$ | 0.9988 |
| A_{15}^{Line} | 0.9868 | $A_{13,23}^{Line}$ | 0.9198 |
| A_{24}^{Line} | 0.8978 | $A_{14,16}^{Line}$ | 0.8760 |
| A_{26}^{Line} | 0.9001 | $A_{15,16}^{Line}$ | 0.9999 |
| $A_{3,24}^{Line}$ | 0.8899 | $A_{15,21}^{Line}$ | 0.9387 |
| A_{49}^{Line} | 0.9222 | $A_{15,22}^{Line}$ | 0.9212 |
| $A_{5,10}^{Line}$ | 0.9999 | $A_{15,24}^{Line}$ | 0.9191 |
| A_{39}^{Line} | 0.9713 | $A_{16,17}^{Line}$ | 0.9595 |
| $A_{6,10}^{Line}$ | 0.9111 | $A_{16,19}^{Line}$ | 0.9767 |
| A_{78}^{Line} | 0.9555 | $A_{17,18}^{Line}$ | 0.9845 |
| A_{89}^{Line} | 0.9699 | $A_{17,22}^{Line}$ | 0.9090 |
| $A_{8,10}^{Line}$ | 0.9789 | $A_{18,21}^{Line}$ | 0.9898 |
| $A_{9,11}^{Line}$ | 0.9333 | $A_{19,20}^{Line}$ | 0.9887 |
| $A_{9,12}^{Line}$ | 0.9817 | $A_{20,23}^{Line}$ | 0.9675 |
| $A_{10,12}^{Line}$ | 0.9988 | $A_{11,13}^{Line}$ | ----- |
| $A_{11,14}^{Line}$ | 0.8888 | | 0.92825 |
| | 0.97778 | | |

REFERENCES

- [1] A. G. Phadke, "Synchronised phasor measurements in power systems," IEEE Comput. Applicat. Power, vol. 6, no. 2, pp. 10–15, Apr. 1993.
- [2] Phadke, A.G., Thorp, J.S, "History and applications of phasor measurements," In: Power Syst. Conf. Expo., pp. 331–335 (2006)
- [3] X. Dongjie, H. Renmu, W. Peng, and X. Tao, "Comparision of several PMU placement algorithms for state estimation," In Proc. Inst.Elect. Eng.E Int. Conf. Develop. Power Syst. Protection, Apr. 2004,pp. 32–35.
- [4] D. J. Brueni and L. S. Heath, "The PMU placement problem," SIAM J. Discrete Math., vol. 19, no. 3, pp. 744–761, Dec. 2005.
- [5] Nikolaos M. Manousakis, George N. Korres, "Taxonomy of PMU placement methodologies," IEEE Transactions on Power Systems, Vol. 27, NO. 2, 1070-1077(2012)
- [6] Rajpal Saini, Manj, "Optimal placement of phasor measurement units for power systemobservability without considering zero injection buses," International Journal of Smart Sensor, ISSN No. 2248-9738, Vol. 1, Issue 4(2011)
- [7] Dua, D., Dambhare, S., Gajbhiye, R.K., Soman, "Optimal multistage scheduling of PMU placement: an ILP approach," IEEE Trans. Power Deliv. 23(4), 1812–1820 (2008)
- [8] Josias Ziestsman, "Transport corridor decision making with multi-attribute utility theory," International Journal Manage Decision Making, 7(2) (2006). 254-256.
- [9] R. Sodhi, S.C. Srivastava, S.N. Singh, "Multi-criteria decision-making approach for multistage optimal placement of phasor measurement units," Generation, Transmission & Distribution, IET, 5(2), (2011) 181 – 190.
- [10] Nuqui, R.F., Phadke, A.G.: "Phasor measurement unit placement techniques for complete and incomplete observability," IEEE Trans. Power Deliv., 2005, 20, (4), pp. 2381–2388
- [11] Aminifar, F., Khodaei, A., Fotuhi-Firuzabad, M., Shahidehpour, M
"Contingency-constrained PMU placement in power networks," IEEE Trans. Power Syst. 25(1), 516–523 (2010)
- [12] F Aminifa, Bagheri-Shouraki, S., Fotuhi-Firuzabad, M., Shahidehpour, M.: "Reliability modeling of PMUs using fuzzy sets," IEEE Trans. Power Deliv. 25(4), 2384–2391 (2010)
- [13] F. Aminifar, M. Fotuhi-Firuzabad, M. Shahidehpour, A. Khodaei,
"Observability enhancement by optimal PMU placement considering random power system outages," Energy System Vol 2,45-65(2011)
- [14] Billinton, R., Allan, R.: Reliability Evaluation of Engineering Systems: Concepts and Technique, 2nd edn. Plenum, New York (1994)
- [15] Belton V., Gear A E, On a shortcoming of Saaty's Method of Analytic Hierarchies, Omega, 11(3) (1983) 228-230

Online Voltage Stability Monitoring using ANN-PSO based Technique

A.Ajay Rana, B.Sanjay Kumar, and C.KS Sajan, Vishal Kumar

Abstract-- This paper has proposed hybrid Artificial Neural Network approach for online monitoring of long-term voltage stability. Evolutionary technique like ANN gives better results than the conventional load flow techniques, it has been shown that the Particle Swarm Optimization (ANN-PSO) can be further used to improve the accuracy of ANN by optimizing their meta-parameters such as number of nodes in hidden layer, input and output activation function and learning rate. The proposed approach has used the voltage magnitude and phase angle obtained from Phasor measurement units (PMUs) as the input vectors and the output is the Voltage Stability Margin Index (VSMI) vector. The efficacy of the proposed approach has been justified on New England 39-bus test system. The results of the proposed ANN-PSO approach for voltage stability monitoring have been compared with ANN model on same data set.

Keywords— Artificial Neural Network (ANN), Particle Swarm Optimization (PSO), Phasor Measurement Units (PMUs), Voltage Stability Margin Index (VSMI).

I. INTRODUCTION

Hitherto, the reach of power systems were limited to relatively small geographical regions but today the connectivity of regional power network forms a highly interconnected large system. Such large power system aggravates the voltage monitoring and operation, as disturbance in one part of the system may adversely impact the entire system. The power system observability has been a necessary condition for real-time power system monitoring, protection and control for effective implementation of Wide Area Monitoring Protection and Control Systems (WAMPC). The Phasor Measurement Unit (PMU) is the main technology enabler of WAMPC. PMU measures voltage phasors at the installed buses and current phasors to all connected buses [1]. PMU provides synchronized voltage phasors, current phasors, frequency and rate of change of frequency. Synchronization in PMU is achieved through a common referenced clock of Global Positioning System (GPS) [2]. In recent years, voltage collapse has been a major cause for many power system blackouts [3] around the globe. The traditional method for voltage stability analysis depended on static analysis using the conventional power flow methods such as Gauss-Seidel or Newton-Raphson method. In references [4]-[8], voltage stability indices galore based upon conventional power flow have been proposed. The main drawback of these techniques is the singularity of the Jacobian matrix at maximum loading

Point. To overcome this problem, Ajjarapu, and Christy has proposed Continuation Power Flow (CPF) method to compute voltage stability margin [9]. Gao et al. [10] has proposed the modal analysis technique to compute the voltage stability level of the system. The aforementioned techniques require comparatively large computations and are not efficient for online applications.

Recently, the machine learning techniques such as ANN, fuzzy logic, pattern recognition, support vector machine etc. have been used for power system analysis. Reference [11] has introduced a method of using the ANN model for predicting the voltage stability margin of a power system. The author has proposed artificial feed forward neural network (FFNN) approach for the assessment of power system voltage stability [12]. Zhou et.al. [13], proposed a new online monitoring technique for voltage stability margin using synchrophasor measurement. Usually, ANN is considered to be more powerful, flexible method known for performing nonlinear regressions. However, ANNs suffer from the amount of training time and the scores of the learning parameters, if the ANN meta-parameters are not selected optimally.

In this paper, ANN-PSO approach, which not only relieves the user from selecting these meta-parameters but also gives the optimum values of these parameters to minimize the generalization error. The approach has used ANN as the nonlinear process modelling paradigm, and further employed PSO for optimizing the meta-parameters of the ANN model such that an improved prediction performance is realized. ANN-PSO has been used to emulate the continuation power flow for estimation of voltage stability margin index (VSMI) for steady state voltage stability analysis. The input features of ANN-PSO are formed by voltage magnitudes and voltage phase angles obtained from PMUs. The effectiveness of the proposed method has been justified on the New England 39-bus test system and the performance indices of ANN-PSO are also compared with ANN model.

II. PROBLEM FORMULATION

A. Voltage Stability Assessment (VSA)

The main objective of voltage stability analysis is to determine whether the current operating point of power system is stable, meeting various operational criteria. The voltage vs real power curve (P-V curve) [6] as shown in Fig. 1 can be used directly to obtain voltage stability margin. Considering, the current operating point the total active power delivered to the load is P_{current} and the maximum active power transfer is P_{\max} , then the Voltage Stability Margin (VSM) for each load bus can be calculated as

$$VSM_i = P_{\max,i} - P_{\text{current},i}, \text{ where } i=1,2,\dots (1)$$

A. Department of Electrical Engineering, Indian Institute of Technology, Roorkee, India (e-mail: ajay.rana043@gmail.com).

B. Department of Mechanical Engineering, Indian Institute of Technology, Roorkee, India.

C. Department of Electrical Engineering, Department of Mechanical Engineering, Indian Institute of Technology, Roorkee, India.

D. Department of Mechanical Engineering, Department of Mechanical Engineering, Indian Institute of Technology, Roorkee, India.

Where, l is the total number of load buses in the power system. The Voltage stability margin index (VSMI) for the network is given by:

$$VSMI = \min (VSM_i / P_{max,i}) \quad (2)$$

VSMI is an indicator of voltage collapse in the power system. The VSMI varies in a range between 1 (no load) and 0 (maximum loadability).

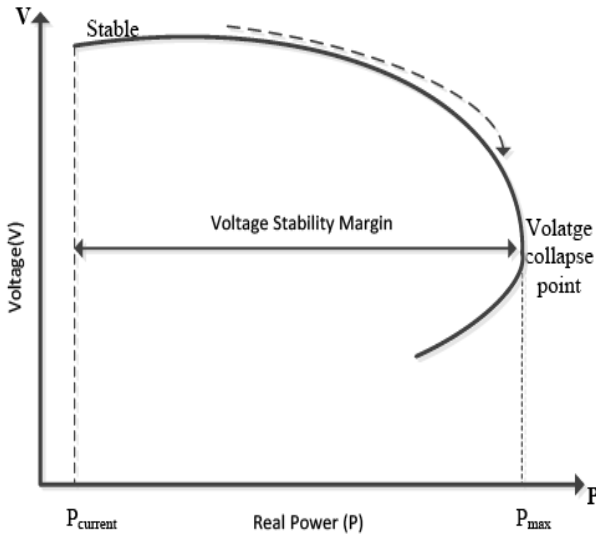


Fig. 1. P-V Curve

To determine the collapse point, PV curve has been drawn using the CPF because conventional power flow (Gauss Seidel or Newton-Raphson) method fails to converge as the operating point reaches the nose point of PV curve [7, 14]. The CPF program calculates the voltage stability limit starting from a specified initial operating point. The flow of the procedure involved in the determination of VSMI has been shown in Fig. 2. Every power network has different types of nodes. For PV-node, real power and voltage magnitude are known and for PQ-nodes, real and reactive power is specified. Therefore, this known parameter is fed to conventional power flow to calculate the current values of voltage magnitude ($V_{current}$), voltage phase angle ($\theta_{current}$), real power (P) and reactive power (Q) at the current operating condition. With these calculated values, the CPF is used to trace the PV curve and to determine the parameters corresponding to voltage collapse point V_{max} , P_{max} , Q_{max} , θ_{max} . Then these parameters are used to calculate VSM and VSMI using (1) and (2). To predict the voltage stability margin index, the computations shown inside dotted area in Fig 2 is replaced by ANN model. The major advantage of using ANN is that it avoids the traditional iterative procedure to find VSMI and can be used for real time application. Voltage magnitudes and phase angles have been taken as inputs to the ANN which are to be obtained from PMUs.

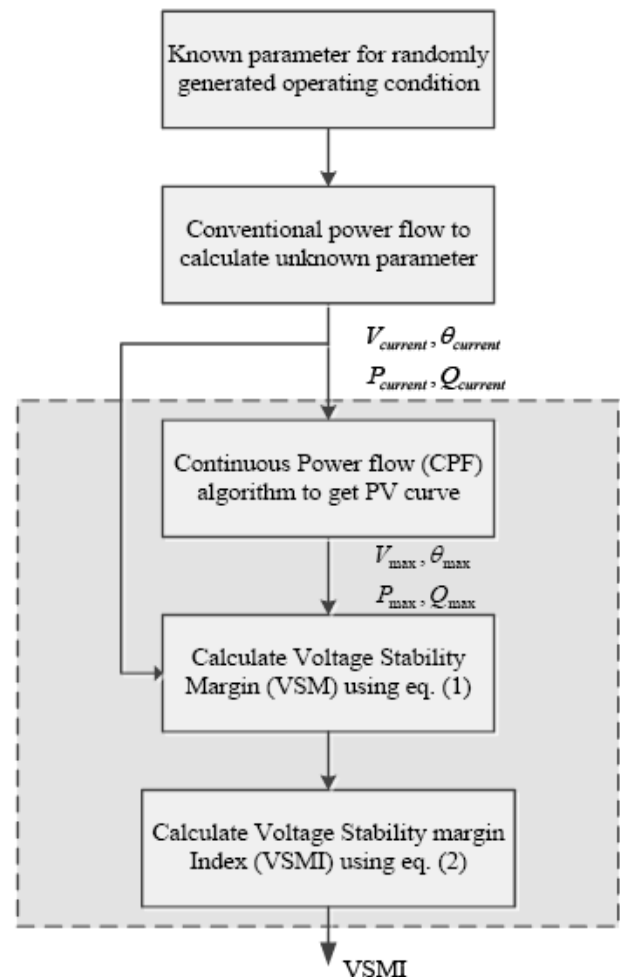


Fig. 2. Procedure to calculate VSMI

III. ARTIFICIAL NEURAL NETWORK

Artificial Neural Network (ANN) can be defined as union of simple processing units based on neurons that are connected to each other to obtain a performance similar to a human's performance when solving problem. These connections contain the "knowledge" of the network and the patterns of connectivity express the objects represented in the network. And the knowledge about the network is obtained through a learning process. ANN is a viable alternative to solve the problem where mathematical description of the process is abstruse but where it is possible to obtain the data that describe the problem.

Among the several artificial neural networks that have been proposed, the most widely used type of neural network is the Multilayer Perceptron (MLP) networks, also known as the multilayer feed-forward network [15]. The ANN structure and learning process has been shown in Fig. 3. The ANN consists of an input layer, hidden layers and an output layer of neurons. The parameters obtained by the ANN model have been obtained and now we are interested in optimizing the ANN parameters using some other techniques like GA, PSO etc.

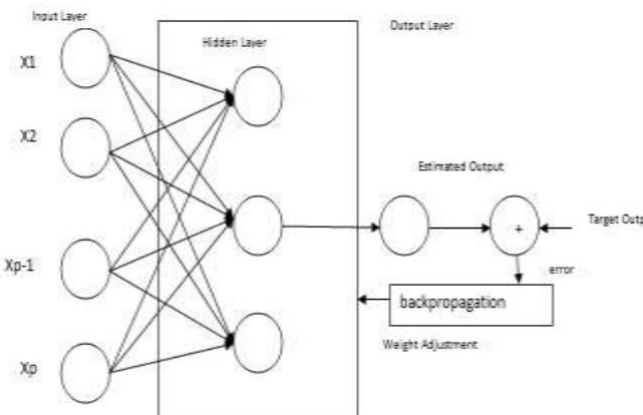


Fig.3. ANN structure and learning process

A. ANN-PSO approach for Regression

The selections of meta-parameters are very important in ANN modelling to get better estimation accuracy. The tuning meta-parameters of ANN have been delineated below:

1. Number of nodes in hidden layer: The number of nodes in hidden layer has a profound effect on ANN performance. Few nodes cannot learn the relationship of data properly and too large number of nodes increases the network complexity and execution time.
2. The activation functions in input layer: Each hidden node and output node applies the activation function to its input. Five type of activation function are available and are shown in table I. Y_i is the output from node i and inp_i is the input to node i.

TABLE I
DIFFERENT ACTIVATION FUNCTIONS

| Case | Activation function | Equation |
|------|---------------------------|---|
| 1 | Log sigmoid (logsig) | $Y_i = 1 / (1 + \exp(-inp_i))$ |
| 2 | Tan hyperbolic (tansig) | $Y_i = \tanh(inp_i)$ |
| 3 | Linear function (purelin) | $Y_i = (inp_i)$ |
| 4 | Radial basis (radbas) | $Y_i = \exp(-inp_i \wedge 2)$ |
| 5 | Triangular basis (tribas) | $Y_i = \begin{cases} 1 - \text{abs}(inp_i) & \text{if } -1 \leq inp_i \leq 1 \\ 0 & \text{Otherwise} \end{cases}$ |

3. The activation function in output layer: Same activation functions have been used as shown in table I.

4. The learning rate: The performance of the back propagation algorithm can be improved by estimating optimal learning rate. The learning rate is multiplied with the negative of the gradient to determine the changes to the weights and biases. The larger the learning rate, the bigger the step. If the learning rate is made too large, the algorithm becomes unstable. If the learning rate is set too small, the algorithm takes a long time to converge.

In this paper, ANN-PSO has been used to optimize the meta-parameters to ameliorate the accuracy of ANN model and the results have been compared with the simple ANN model.

B. PSO based optimization of ANN model

In hybrid ANN model obtained, ANN-PSO has further been used for optimizing its meta-parameters. The objective of the problem is to minimize mean square error (MSE). And the optimal problem of ANN model is represented as follows:

$$\min f = \text{MSE}(X)$$

$$MSE = \frac{1}{n} \sum_{i=1}^n (A_i - P_i)^2$$

$$X \in \{x1, x2, x3, x4\}$$

Where, X_1 is Number of nodes in hidden layer and varies from $10 \leq x_1 \leq 50$, x_2 and x_3 are input layer and output activation function and can have values between 1 to 5 corresponding to five activation function as shown in table I and x_4 is learning rate which is varied between 0 – 5. A_i and P_i are the actual and predicted values and n is the number of training data samples. The above-formulated problem has been solved for optimal solution using PSO[16]. Table II enunciates PSO parameters setting used for the tuning of ANN meta-parameters.

TABLE II
PARTICLE SWARM OPTIMIZATION PARAMETER SETTING

| | |
|--------------------------------|------|
| Testing data | 500 |
| Swarm size | 20 |
| Velocity function(vmax1,vmax2) | 10,2 |
| Weighting function | 0.5 |
| Acceleration constants(c1,c2) | 2 |

C. ANN-PSO performance measures

To evaluate the performance of the ANN-PSO model, following indices have been evaluated:

1. Mean Absolute percentage Error (MAPE)
2. Maximum Percentage Error (MPE)
3. Willmott's Index of Agreement (WIA) [17]

Table III shows the Performance indices and their expressions to find the deviation between actual output and predicted output. The smaller the value of MAPE and MPE, the closer is the predicted value to the actual value. The WIA measures the regression degree and varies from 0 (complete

disagreement) to 1 (perfect agreement). WIA close to 1 represents more accurate predicted value.

TABLE III
PERFORMANCE INDICES AND THEIR EXPRESSIONS

| Indices | Expressions |
|--|---|
| MAPE (mean absolute percentage error) | $MAPE = \frac{1}{n} \sum_{i=1}^n \left \frac{A_i - P_i}{A_i} \right * 100$ |
| MPE (maximum percentage error) | $MPE = \max \left(\left \frac{A_i - P_i}{A_i} \right \right) * 100$ |
| WIA (Willmott's Index of Agreement) | $WIA = 1 - \frac{\sum_{i=1}^n (A_i - P_i)^2}{\sum_{i=1}^n (\ A_i - \bar{A}\ + \ P_i - \bar{A}\)^2}$ $\bar{A} = \frac{1}{n} \sum_{i=1}^n A_i$ |

IV. RESULTS

The proposed hybrid ANN-PSO based method for online voltage stability monitoring has been applied to the New England 39-bus test system [18]. It consists of 20 load buses, 10 generator buses and 35 transmission lines. Input feature for voltage stability margin could be expressed as a function of the four variables i.e. voltage magnitude, voltage phase angle, real power and reactive power that defines the system operating point. In the proposed work, voltage magnitudes and phase angles have been taken as the input that have been assumed to be obtained from PMUs. These PMUs have been installed in the system for complete observability such that all the data is available for all the load buses.

In ANN-PSO model, PSO is used to determine the optimal values of ANN meta-parameters i.e. number of nodes in hidden layer, input layer and output layer activation functions and learning rate. Within the overall searching process, the optimal fitness value is 0.202% and table IV shows the optimal values of ANN meta-parameter for New England 39- bus system.

TABLE IV
ANN META-PARAMETER OPTIMIZED BY PSO

| ANN meta-parameters | Optimum values |
|----------------------------|--------------------------|
| Number of nodes | 18 |
| Input activation function | Tansig |
| Output activation function | Linear function(purelin) |
| Learning rate | 1.28 |

For generating sample data for the ANN-PSO, active and reactive powers at the load buses are varied randomly within random operating points are generated for training and another 500 operating points were used to verify the performance of proposed ANN-PSO method.

The plot shown in Fig. 4 is the regression plot of Target VSMI against output VSMI by the ANN-PSO, for the 500 unseen test cases.

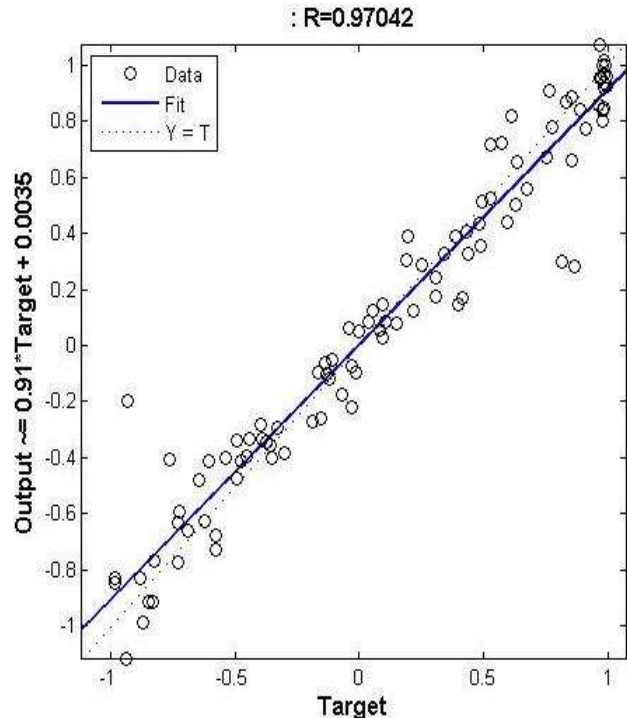


Fig. 4 VSMI estimation by ANN-PSO for New England 39-bus system

Table V lists the performance indices of both training data used as input and 500 unseen test cases for New England 39-bus system.

TABLE V
PERFORMANCE INDEX FOR TRAINING AND TESTING DATA FOR NEW ENGLAND-39 BUS SYSTEM

| Performance indices | Training data | Testing data |
|---------------------|---------------|--------------|
| MAPE | 0.1804 | 0.1426 |
| MPE | 8.76 | 0.649 |
| WIA | 0.9968 | 0.9989 |

To find the effectiveness of the ANN-PSO model presented in this paper, comparison of ANN-PSO model with ANN model is carried out. In both the model the same data set has been taken for analysis.

The meta-parameters considered and the performance indices calculated for ANN-PSO and ANN have been shown in table VI. Table VI delineates that ANN-PSO model has optimized the ANN model meta-parameters. The performance indices MAPE and MPE with smaller values indicate small deviation between the predicted and the actual values. The higher value of WIA

rating indicates that VSMI predicted by ANN-PSO has more precision as compared to ANN model.

TABLE VI
COMPARISON OF PERFORMANCE OF ANN MODEL VS ANN-PSO MODEL

| Indices | ANN model | ANN-PSO model |
|---------------------------------------|----------------------------------|----------------------------------|
| Mean Absolute percentage Error (MAPE) | 0.1821 | 0.1426 |
| Maximum Percentage Error (MPE) | 5.0343 | 0.649 |
| Willmott's Index of Agreement (WIA) | 0.98624 | 0.9989 |
| Number of nodes | 20 | 18 |
| Input activation function | Tan hyperbolic function (tansig) | Tan hyperbolic function (tansig) |
| Output activation function | Linear function (purelin) | Linear function (purelin) |
| Learning rate | 1.12 | 1.28 |

V.CONCLUSION

An online voltage stability monitoring scheme has been proposed in this paper. The proposed technique is based on hybrid ANN and its meta-parameters optimization by particle swarm optimization (PSO) model. The ANN-PSO has been used to estimate voltage stability margin index (VSMI) under normal operating conditions. The ANN-PSO has considered voltage magnitudes and phase angles as the inputs. The efficacy of the proposed approach has been justified on New England 39-bus system. A comparative study of the results of ANN and PSO has been carried out and the results delineates that PSO yields better results than the conventional ANN method by optimizing its meta-parameters. The performance indices calculated shows that the proposed technique for estimating the VSMI can be used for online voltage stability monitoring in practical system.

REFERENCE

- [1] V. Terzija, G. Valverde, C. Deyu, P. Regulski, V. Madani, J. Fitch, S. Skok, M. M. Begovic, and A. Phadke, "Wide-area monitoring, protection and control of future electric power networks", Proc. IEEE, vol. 99, no. 1, pp. 80–93, Jan. 2011.
- [2] A.G. Phadke, J.S. Thorp, "Synchronized phasor measurements and their applications", Springer January pp 3-27, 2008.
- [3] J. De La Ree, V. Centeno, J. S. Thorp, A. G. Phadke, "Synchronized phasor measurement applications in power systems", IEEE Trans. Smart Grid, vol. 1 pp. 20-27, June 2010.
- [4] K. P. Kessel and H. Glavitsch, "Estimating the voltage stability of a power system", IEEE Transactions on Power Delivery, Vol. PWRD-1, No. 3, pp.346-354, July 1986.
- [5] Y. Tamura, K. Sakamoto, Y. Tayama, "Voltage instability proximity index (VIPI) based on multiple load flow solutions in 111conditioned power systems", Proceedings of the 27th EEE Conference on Decision and Control, Austin, Texas, December 1988.
- [6] A Tiranuchit and R. J. Thomas, "A posturing strategy against voltage instabilities in electric power systems", IEEE Trans. on Power Systems, Vol.3, No. 1, pp. 87-93 , February 1988.
- [7] V. Ajjarapu and B. Lee, "Bibliography on voltage stability," IEEE Trans. Power System, vol. 13, pp. 115–125 1998.
- [8] Taylor C.W, "Power system voltage stability", EPRI Power System Engineering Series, McGraw-Hill, 1993.
- [9] V. Ajjarapu, C. Christy, "The continuation power flow: a tool for steady state voltage stability analysis", IEEE Trans. Power Syst. Vol. 7 pp. 416– 423, 1992.
- [10] B. Gao, G.K. Morisan, P. Kundur, "Voltage stability evaluation using modal analysis", IEEE Trans. Power Syst. Vol. 7 pp. 1529–1542, 1992.
- [11] V. R. Dinavahi and S. C. Srivastava, "ANN based voltage stability margin prediction", in Proc. IEEE Power Eng. Soc. Summer Meeting, vol. 2, pp. 1275–1280, July 2001.
- [12] S. Kamalasadan, A. K. Srivastava, and D. Thukaram, "Novel algorithm for online voltage stability assessment based on feed forward neural network", in Proc. IEEE Power Eng. Soc. General Meeting, pp. 18–22, June 2006.
- [13] Zhou D. Q., Annakkage U. D., Rajapakse A. D., "Online monitoring of voltage stability margin using an artificial neural network", IEEE Transaction on Power System, vol. 25(3) pp. 1566-1574, 2010.
- [14] H.-D. Chiang, A. J. Flueck, K. S. Shah, and N. Balu, "CPFLOW: A practical tool for tracing power system steady-state stationary behaviour due to load and generation variations", IEEE Trans. Power Syst., vol. 10, no. 2, pp.623–634, May 1995.
- [15] P. Devijver and J. Kittler, "Pattern Recognition: A statistical approach", Englewood Cliffs, NJ: Prentice-Hall, 1982.
- [16] J. Kennedy and R. Eberhart, "Particle swarm optimization", Proceedings of IEEE International Conference on Neural Networks, pp.1942-1948, 1995.
- [17] Willmott, C. J., "On the evaluation of model performance in physical geography", Spatial Statistics and Models Springer, pp. 443–460, 1984.
- [18] P. W. Sauer and M. A. Pai, "Power System Dynamics and Control", Upper Saddle River, NJ: Prentice-Hall, 1998.

Network Reconfiguration of Radial Distribution System having DGs and Capacitors for Power loss Reduction Using Voltage Sensitivity Analysis

Somvir, Assoc. Prof. Sunita Chauhan,

Abstract-- This paper presents an efficient Heuristic optimization algorithm for technical power loss reduction and voltage profile improvement. In order to obtain the optimal radial network, switching is done by opening the candidate switch which results in reduction of total power loss of the radial system. In this algorithm, switching decision is based on the Voltage magnitude information obtained from radial distribution power flow. The whole network reconfiguration process is completed in two parts. The first section of algorithm starts with distribution power flow of radial network to calculate voltage magnitude at each bus. The basic idea of switches to be open is based on the magnitude of the voltage deviation (VD). The second section of the algorithm is, based on the branch exchange operation. The effectiveness of the proposed algorithm has been evaluated on IEEE 33-bus radial distribution system with distribution generators (DGs) and capacitors. The computer simulation results have been compared to the initial distribution network and with other methods [6], [4], [8]. It shows that the performance of proposed method is better than that of the other [6], [4], [8].

Index terms-- Distribution Generators (DGs), Distribution Network reconfiguration, distribution power flow, Heuristic optimization algorithm, radial distribution system, Technical power loss.

I. INTRODUCTION

Distribution network reconfiguration (DNR) is a very important process for operating the distribution system at minimum cost and to improve the system efficiency. Network reconfiguration is defined as altering the topological structure of distribution feeders by changing the open/closed states of the sectionalizing and ties switches. In primary distribution systems, sectionalizing switches (normally close switches) are used for protection, to isolate a fault and for configuration management. Tie switches are normally open switches and they are used to reconfigure the network and improve the reliability of the network. DNR may significantly improve the operating conditions of the overall system by transferring loads from heavily loaded feeder to relatively less heavily loaded feeders.

Such transfers are effective not only in terms of altering the level of loads on the feeders being switched, but also in improving the voltage profile along the feeders and effecting reductions in the overall system power losses.

Continuous increasing of load growth in distribution system make necessary to construct new power plants. Several advantages like Tendency towards applying clean energies, economic benefits and independence from fossil fuel, have drawn a great attention to use different kinds of renewable energy sources like wind energy, PV cells, bio-gas energy, fuel cells etc. in the distribution voltage level. Distribution generator is a small-scale power generation, at distribution voltage, that is installed in the network at near the site where they are to be used. The impact of DG on system may be positive or negative, depending on the system's operating conditions, characteristics and location of installation. This paper paid attention towards economic benefits presented in terms of active power loss reduction. The active power loss varies with the square of branch current flow. In this paper, distributed generators are considered as a negative active power load units. Normally, DG units can help in reduction of current flow in the feeder, depending on the optimal size and site of installation.

Allocation of capacitors locally at optimum location with optimum size reduces the Reactive power requirement of the system and also helps in minimization of the active power loss to some extent. In this paper, capacitors are considered as a negative reactive power load units.

Since last three decades, Studies and experiments on feeder reconfiguration are ongoing in many utilities. To solve the network reconfiguration problem, many algorithms has been developed based on heuristic algorithms Merlin and Back [1] first proposed a heuristic method to determine minimum loss configuration for the network represented by a spanning tree structure. An improved method represented by Shirmohamadi [4] to get convergence to the optimal or near optimal solution. Goswami and Basu [5] presented a heuristic algorithm based on the concept of optimal flow pattern. Civenlar *et al* [3] has suggested branch exchange based algorithm. Kashem et al. [9] have suggested a new method based on distance measurement (DMT) that first locate the loops in the system and then switching operation was done for load balancing. A fast heuristic method, based on sensitivity analysis has been presented by Cheragi [8] and also refined the solution using branch exchange operation. This method also reduces the computational efforts by reducing the no. of load flow requirement. [5], [11], [8] has obtained minimum loss configuration using some heuristic methods and a near minimum configuration has obtained by [4]

A. Somvir, Electrical engineering Department, NIT, Kurukshetra, Haryana, India(e-mail: Sameer08feb@yahoo.com)

B. Prof. sunita Chauhan, Electrical engineering Department, NIT, Kurukshetra, Haryana, India(e-mail: Sameer08feb@yahoo.com)

II. PROPOSED METHODOLOGY

Distribution network reconfiguration need proper planning to find the most reliable system that fulfils a group of objectives and constraints. The objective function of Distribution network reconfiguration problem is as follow:

- 1) Minimize the total power loss
- 2) Improve the voltage profile

This objective function is subjected to the following constraints:

- 1) The voltage magnitude at each node must be keep within its specified limits:

$$V_{\min} \leq [V_i] \leq V_{\max} \quad i=1, 2, 3 \dots n$$

n= no. of nodes

- 2) Feeder current capability limits:

$$[I_j] \leq I_{j,\max}$$

$j \in \{1, 2, 3, \dots, b\}$ (no. of branches)

- 3) Radiality of the network must be retained.

- 4) No feeder section can be left out of service.

The most of the switching approaches for finding optimal network reconfiguration need to check out the effectiveness of every candidate switch for power loss minimization. These approaches require considerable numerical computation and time. Figure 1 shows the flow chart of the proposed method, which is based some simple heuristic rules. The proposed algorithm may help to minimize the computational complexity and time for solving network reconfiguration problem.

The reconfiguration procedure of the proposed method is completed in two sections.

A. First Procedure

This section starts with distribution power flow of the radial system.

1. Read distribution network data(bus, load and branch data);
2. Run distribution power flow program for radial network and compute initial total power loss (TPL) and voltage at each bus;
3. Identify the minimum voltage bus in network and also its adjacent (connected) bus having lower voltage magnitude;
4. Open that branch and close the respective tie line of the that loop;
5. Check the radiality of configuration. If radiality violate then close that branch and identify next minimum voltage bus and go to step 3;

6. Run distribution load flow and compute total power loss. Compare the result with last configuration and open the branch which gives least total power loss. Save the new configuration ;
7. Identify the new minimum voltage bus in network and also its adjacent (Connected) bus having lower voltage magnitude;
8. Go to step 4 and proceed until get a feasible solution;
9. Print the new configuration, total active and reactive power loss and voltage profile;

B. Second Procedure

The first procedure cannot guarantee optimum solution. Therefore, second procedure (branch exchange operation [3]) attempt to improve the result of the first procedure. In some cases, better result may be obtained using branch exchange operation. In this process, for each open switch i, two exchange operation are performed with its adjacent switches (one from left side and one from right side). For each new configuration, the total power losses are calculated and compared with last configuration results. If there is reduction of loss then new configuration will be taken to replace the configuration obtained in the first procedure.

III. CASE STUDY

The 33-bus balanced system [2] is used to verify the validity of the proposed algorithm. The test system, as shown in figure 2, is a 12.66 kV radial distribution system having one transformer, 4 feeders, 33 buses and 37 branches (32 sectionalizing switches and 5 tie-switches). The sectionalizing switches (s1 to s32) are represented by solid line and tie-switches (s33 to s37) are represented by dotted lines. The load and line data of the test system is taken from [2]

Four cases are considered for testing:

Case 1: Initial radial distribution network. Shown in Figure 2. The initial active and reactive power losses of the system are 202.68 kW and 135.16 kVAR

Case 2: It represents the reconfigured network of case 1.

Case 3: It represents a radial distribution network, as taken in

Case 1, with 3 DG units and 5 Capacitors are connected. The DG units with firm active power Capacities of 250, 250 and 500 kW are located [6] at buses 16, 22 and 30 respectively while capacitor units with reactive power capacities of 300, 300, 300, 600 and 300 kVAR are placed at bus no. 15, 18, 29, 30, 31 respectively.

Case 4: It represented the reconfigured network of case 3. As shown in Figure 3

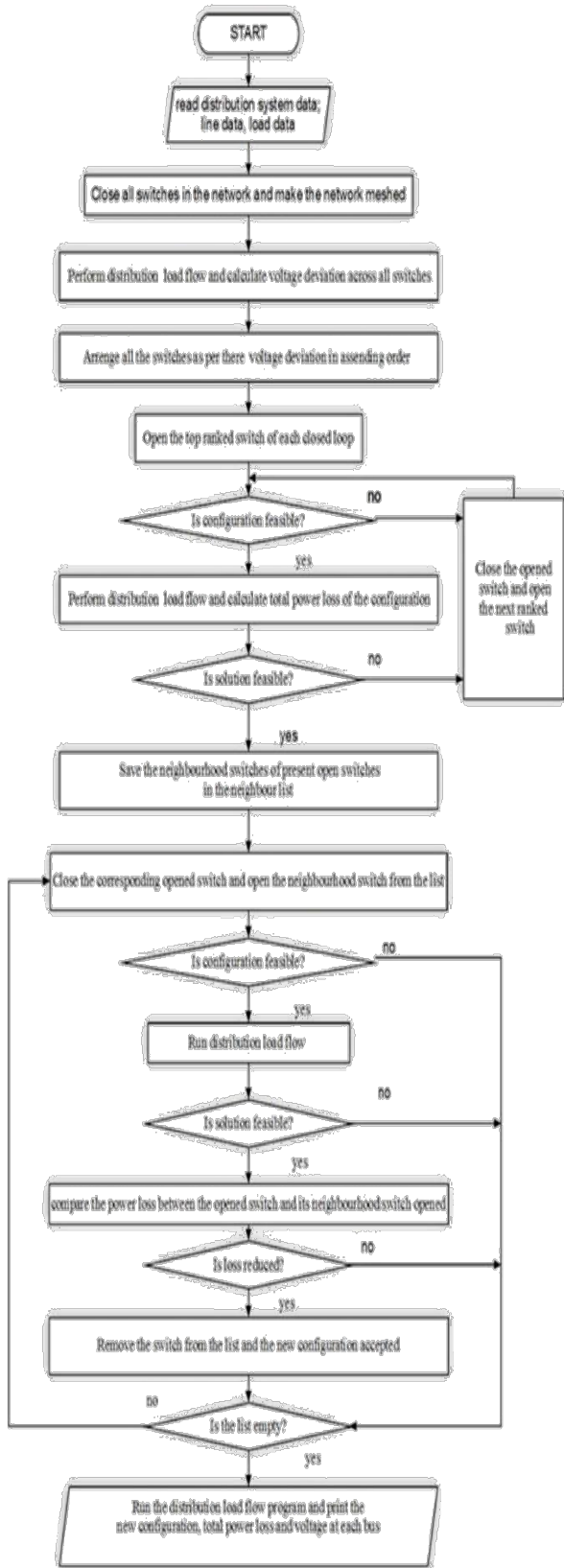


Fig. 1. Flow chart of the proposed algorithm

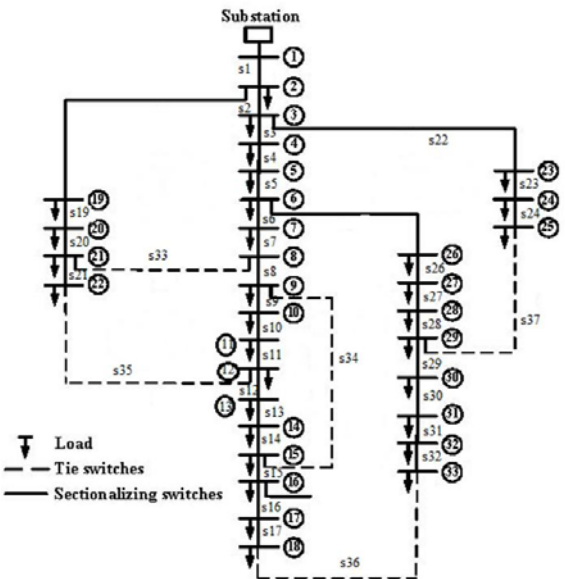


Fig. 2. Test system of 33-bus radial system

For the calculation of total distribution power loss, voltage and other parameters, a MATLAB program is implemented. First of all run distribution load flow program and calculate initial power loss and identify minimum voltage bus of the network and its adjacent buses voltage magnitudes, as shown in table I:

TABLE I

| Bus no. | Voltage (p.u.) |
|---------|----------------|
| 12 | 0.9714 |
| 11 | 0.9718 |
| 10 | 0.9720 |

As shown in Table I, bus no. 12 has least voltage magnitude and among its adjacent connected buses, bus no. 11 has lower voltage. Therefore open the branch s11 (11-12) and close the respective loop's tie-switch s35. Table V shows a comparison of TPL values, by opening the adjacent branch of bus no.12. It is observed that opening of switch s11 will give more loss reduction than tie-switch (s35) open. Therefore, the first optimal switching operation is obtained by closing the tie switch s35 and opening the switch s11. For the second switching operation, the voltage magnitude across each bus is arranged in ascending order, as shown in Table II:

TABLE II

| Bus no. | Voltage (p.u.) |
|---------|-----------------|
| 11 | 0.9724 (reject) |
| 10 | 0.9725 (reject) |
| 33 | 0.9742 |
| 32 | 0.9746 |
| 18 | 1.008 |

In Table II voltage magnitude across bus no. 11 is least among all buses but opening of its any adjacent branch will lead to violation the readability constraint and similar reason with selection of bus no. 10 for second switching. Therefore,

next least voltage bus is 33 is taking in to consideration for next switching and bus 32 is its adjacent least voltage bus. Table V shows TPL values, by opening the adjacent branch of bus no.33. It is observed, that opening of switch s32 will give more loss reduction. Therefore, the second optimal switching operation is obtained by closing the tie switch s36 and opening the switch s32.

TABLE III

| Bus no. | Voltage (p.u) |
|-----------|---------------|
| 11 | rejected |
| 10, 9 | rejected |
| 25 | 0.9767 |
| 24 | 0.9804 |
| 29 | 0.9802 |

TABLE III shows that Selection of bus no.11, 10 and 9 will lead to violation of radiality constraints. Therefore, next least voltage bus, 25 is taken in to consideration for next switching. Its adjacent minimum voltage bus is 29. Branch s37 (25-29) is tie-line of that loop (already opened). Therefore, no need of new switching for this loop.

TABLE IV

| Bus no. | Voltage (p.u.) |
|---------------|----------------|
| 11,10,9,32,31 | rejected |
| 8 | 0.9825 |
| 7 | 0.9854 |
| 21 | 0.9894 |

Selection of bus no.11, 10, 9, 32 and 31 will lead to violation of radiality constraints. Therefore, next least voltage bus is 8 is taking in to consideration for next switching and bus no 7 is its adjacent least voltage bus. Therefore, open branch s7 (7-8). Table VI shows a comparison of TPL values, by opening the adjacent branches of bus no.8. It is observed, that opening of switch s7 will give more loss reduction. Therefore, the fourth optimal switching operation is obtained by closing the tie switch s33 and opening the switch s7. Repeating the same procedure, the next least voltage magnitude buses arranged in ascending order is shown in Table V

TABLE V

| Bus no. | Voltage (p.u.) |
|---------------|----------------|
| 11,10,9,32,31 | rejected |
| 9 | 0.9811 |
| 8 | 0.9825 |
| 15 | 0.9924 |

Next considered, least voltage bus is 9. Bus no. 8 is its connected adjacent least voltage bus. It is observed, that opening of switch s8 will give more TPL than last switching (tie switch). Therefore, there is no need of 5th switching.

TABLE VI

| Switching | Least voltage bus | Tie-switch closed | Sectionalizing Switch opened | Power loss (kW) |
|-----------------|-------------------|--------------------|------------------------------|----------------------------|
| 1 st | 12 | S35(12-22) | S11 (11-12) | 59.34 |
| 2 nd | 33 | S36(18-33) | S32 (32-33) | 56.62 |
| 3 rd | 25 | | | 56.62 |
| 4 th | 8 | S33(8-21) | S7(7-8) | 50.45 |
| 5 th | 9 | | | 50.45 |
| Branch exchange | | S11 S37 (25-29) | S10 - S28 (28-29) | 49.94 - 48.63 |

Finally start branch exchange operation, the total power loss come out to be 48.63 kW with the exchange of branch s11 (close) with s10 (open) and s37 (close) with s28 (open).

TABLE VII
Comparison of proposed method with other [6] for case 2(reconfiguration of network without DGs and capacitors)

| Case 2 | Proposed method | [6] | shirmohamma di [4] | Keshem [9] |
|------------------------------|------------------|-------------------|--------------------|------------------|
| Initial loss (kW) | 202.68 | 202.70 | 202.68 | 202.68 |
| Final opened switches | 7,10,14 28,32 | 11,27,32 33,34 | 7,10,14 32,37 | 7,11,14 28,32 |
| Final Total Power Loss (kW) | 140.70 | 146.5 | 140.28 | 141.63 |
| Minimum voltage (p.u.) | 0.9412 | 0.938 | 0.9378 | 0.9401 |
| Percentage of loss reduction | 30.58 | 27.72 | 30.78 | 30.12 |

Figure VI shows the final numerical result comparison, for the case 2, of the proposed method with [6], [4], [9]. Proposed method find the configuration having minimum total power loss (TPL) with better voltage profile then [6], [4], [9].

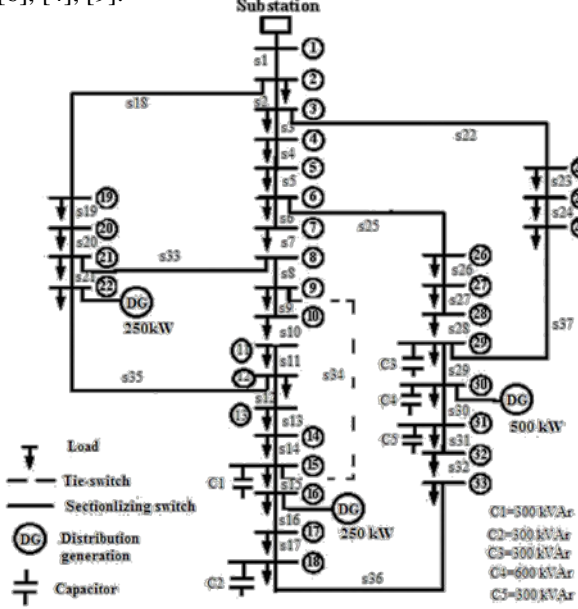


Fig. 3. Test system of 33-bus radial system having DGs and capacitors reconfigured network

TABLE VII

| | Proposed method | [6] |
|------------------------------|-----------------|--------------|
| Initial loss (kW) | 202.68 | 202.70 |
| Final opened switches | 7,10,14,28,36 | 7,9,15,27,34 |
| Final Total Power Loss (kW) | 48.63 | 48.06 |
| Minimum voltage (p.u.) | 0.938 | 0.938 |
| Percentage of loss reduction | 76.01 | 76.32 |

TABLE VII shows the final numerical result comparison of proposed method with other [6], for case 4 (reconfiguration of network with DGs and capacitors).

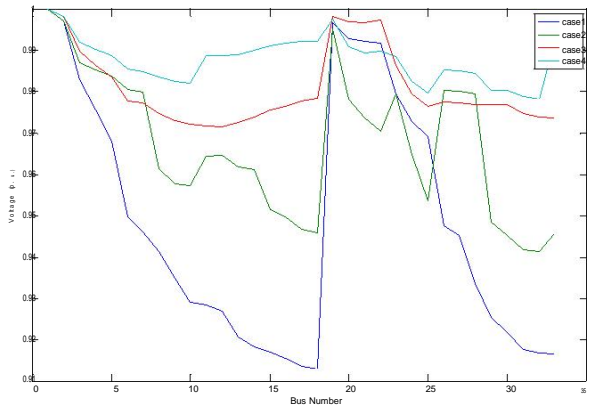


Fig. 4. Comparison of voltage (p.u.) for all four cases

Figure 4 shows that the voltage profile improves with reconfiguration (case 2), with DGs and capacitor placement (case 3) and with final reconfigured distribution system having DGs and capacitors (case 4). Case 4 presents best voltage profile among all four cases.

IV CONCLUTIONS

This paper has presented a new simple and effective heuristic methodology to solve a network reconfiguration problem having a mutual impact of Distribution Generators and reactive power source. The network reconfiguration result on IEEE-33 bus test system shows that the present algorithm give nearly optimum configuration, minimum total power loss (TPL) with better voltage profile then [6], [4], [9] , with simple network and nearly equal results [6] with connection of distribution generators and capacitors. This algorithm also reduces the computational efforts by reducing the no. of load flow required and also reduce the switching complexity.

REFERENCES

- [1] A. Merlin, H. Back, "Search for a minimal-loss operating spanning tree configuration in an urban power distribution system" Proceedings of 5th Power System Computation Conference (PSCC), Cambridge, UK, 1975, pp. 1-18.
- [2] M. E2. Baran and F.Wu, "Network reconfiguration in distribution system for loss reduction and load balancing," IEEE Trans. Power Del., vol. 4, no. 2, pp. 1401–1407, April 1989.
- [3] S. Civanlar, J. Grainger, H. Yin, and S. Lee, "Distribution feeder reconfiguration for loss reduction," IEEE Trans. Power Del., vol. 3, no. 3, pp. 1217–1223, July 1988.
- [4] D. Shirmohammadi and H. Wayne Hong, "Reconfiguration of electric distribution networks for resistive line losses reduction," IEEE Transaction on Power Delivery, vol. 4, no. 2, pp. 1492-1498, April 1989.
- [5] S. Goswami and S. Basu, "A new for the reconfiguration of distribution feeders for loss minimization," IEEE Trans. Power Del., vol. 7, no. 3, pp. 1484–1491, July 1992.
- [6] N. Rugthaicharoencheep, S. Nedphograw, and W. Wanaratwijit, "Distribution System Operation for Power Loss Minimization and Improved Voltage Profile with Distributed Generation and Capacitor Placements" IEEE International Conference on DRPT, pp. 1185 – 1189, July 2011.
- [7] Israfil Hussain and Anjan Kumar Roy," A New Heuristic approach for Optimal Reconfiguration of distribution systems for improvement of power delivery efficiency through", IEEE-International Conference On Advances In Engineering, Science And Management (ICAESM-2012) March 30, 31, 2012.
- [8] M. Cheraghi, and P. Ramezanpour, "An Efficient-Fast Method for

1st National Power & Energy System Conference (NPESC), April 25-26, 2014, KNIT Sultanpur

- [9] Determining Minimum Loss Configuration in Radial Distribution Networks Based on Sensitivity Analysis," IEEE International Conference PEDCO, pp. 46 – 51, June 2012.
- [10] M. A. Kashem, V. Ganapathy, G.B. Jasmon, and M. I. Buhari, "A Novel model for loss minimization in distribution networks", IEEE International Power Technologies 2000 Conference on Electric Utility deregulation, restructuring at City University London, 4-7 April 2000, pp. 251-256.
- [11] R. Srinivasa Rao, S.V.L. Narasimham, A new heuristic approach for optimal network reconfiguration in distribution systems, Int. J. Appl. Sci. Eng. Technol. 5(1)(2009)15-21.
- [12] T. E. McDermott, J. Drezga, and R. P. Broadwater, "A heuristic nonlinear constructive method for distribution system reconfiguration," IEEE Trans. Power Syst., vol. 14, no. 2, pp.478-483, May 1999.
- [13] Z. Dong, et al., Capacitor switching and network reconfiguration for loss reduction in distribution system, in Proc Power Engineering Society General Meeting Conf., pp. 1-6, 2006.
- [14] H. A. Gil and G. Joos, Models for quantifying the economic benefits of distributed generation, IEEE Transaction on Power Systems, vol. 23, no. 2, pp. 327-335, May. 2008.
- [14] C. F. Chang, "Reconfiguration and capacitor placement for loss reduction of distribution systems by ant colony search algorithm," IEEE Transaction on Power Systems, vol. 23, no. 4, pp. 1747-1755, November. 2008.
- [15] J. S. Savier and D. Das, "Impact of network reconfiguration on loss allocation of radial distribution systems," IEEE Transactions on Power Delivery, vol. 2, no. 4, pp. 2473-2480, Oct. 2007.
- [16] Rakesh Ranjan and D. Das, "Simple and Efficient Computer Algorithm to Solve Radial Distribution Networks," Electric Power Components and Systems, Taylor and Francis, 31:95–107, 2003.
- [17] G.K.V. Raju and P.R. Bijwe, "Efficient reconfiguration of balanced and unbalanced distribution systems for loss minimisation," IET Gener. Transm. Distrib. , 2008, 2, (1), pp. 7–12.
- [13] F. V. Gomes, S. Carneiro, J. L. R. Pereira, M. P. Vinagre, and P. A. N. Garcia, "A new distribution system reconfiguration approach using optimum power flow and sensitivity analysis for loss reduction," IEEE Trans. Power Syst., vol. 21, no. 4, pp. 1616–1623, Nov. 2006

An Overview of Transmission Pricing Methods in a Pool based Power Market

M.Murali, *Student Member, IEEE*, M.Sailaja Kumari, *Member, IEEE*, and M. Sydulu, *Member, IEEE*
Electrical Engineering Department, N.I.T Warangal, A.P, India

Abstract—In a restructured power market, it is necessary to develop an appropriate pricing scheme that can provide the useful economic information to market participants, such as generation, transmission companies and customers. Proper pricing method is needed for transmission network to ensure reliability and secure operation of power system. Accurately estimating and allocating the transmission cost in the transmission pricing scheme still remains challenging task. This paper gives an overview of different costs incurred in transmission transaction, types of transmission transactions and the transmission pricing methodologies. Transmission pricing methods such as Embedded and Incremental cost methods are explained. It mainly focused on determining the embedded transmission cost by various methods and tested all the methods on IEEE14 bus system, New England39 bus system and Indian75 bus power system and then illustrated the results.

Keywords—Bialek Tracing, Embedded Cost, GGDF, Kirschen tracing, MVA-Mile, MW-Mile, Postage Stamp

I. INTRODUCTION

The rapidly changing business environment for electric power utilities all around the world has resulted in unbundling of services provided by these utilities. With the introduction of restructuring into the electric power industry, the price of electricity has become the focus of all activities in the power market. The objective of transmission pricing is to recover all or part of the existing and new cost of transmission system. Pricing of transmission services plays a crucial role in determining whether providing transmission crucial role in determining whether providing transmission services is economically beneficial to both the wheeling utility and the wheeling customers. Engineering analysis which deals mainly with determining the feasibility and the cost of providing transmission services is only one of many considerations in the overall process of pricing transmission services. So, it is important to distinguish between transmission costs and prices.

A. Categories of Transmission Transactions

The following are the categories [2, 3] of transmission transactions:

1) Firm Transmission Transactions

These transactions are not subject to discretionary interruptions and are specified in terms of MW of transmission capacity that must be reserved for the transaction. The transco makes arrangements for enough capacity on the network to meet these transaction needs. These

could either be on a long-term basis, in the order of years or on short-term contracts (up to one year).

2) Non-firm Transmission Transactions

These transactions may be curtailable or as-available. Curtailable transactions are ongoing transactions that may be curtailed at the utility's discretion. As-available transactions are short-term, mainly economy, transactions that take place when transmission capacity becomes available at specific areas of the system at specific times.

3) Long-term Transmission Transactions

A long-term transaction takes place over a period spanning several years. Long-term transmission transaction is long enough to allow building new transmission facilities. Transmission service provided as part of long -term firm power sales is an example of long-term transaction [3].

4) Short-term Transmission Transactions

A short-term transmission transaction may be as short as a few hours to as long as a year or two and as such are not generally associated with transmission reinforcements. Short term transaction may be a bilateral contract or pool trading [3].

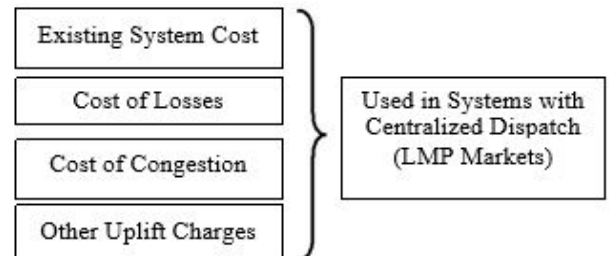
B. Components of the Transmission Cost

The major components of the transmission cost of transmission transactions are: [17]

- i) Operating Cost
- ii) Opportunity Cost
- iii) Reinforcement Cost
- iv) Embedded Cost or Existing System Cost

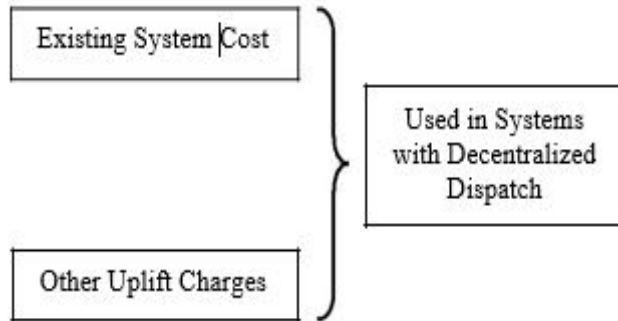
C. Transmission Pricing Approaches

Approach 1:



This is a popular approach which was under practice mostly in US and European markets. Later it was found that, this approach is mostly suitable for recovering congestion cost and losses cost but major drawback of this approach is, it can recover only 20-30% of existing system cost and other uplift charges. So another approach is proposed to overcome this drawback.

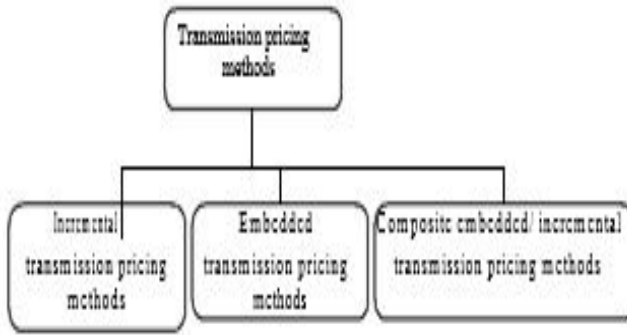
Approach 2:



The remaining 80% of existing system cost and other uplift charges of approach1 can be recovered with approach2 but it cannot account for congestion cost and losses cost. So a combination of approach1 and approach2 is required for a perfect transmission pricing mechanism and this type of mechanism is practised by PJM market in USA.

II. TRANSMISSION PRICING METHODS

The main objective of any transmission pricing method is to recover the transmission system cost plus some profit. Transmission pricing methods are the overall processes of translating transmission costs into overall transmission charges. These methods are shown in Figure 1:



A. Incremental Transmission Pricing

These pricing methods allocate the incremental cost (i.e., variable cost) of the transmission transaction. Figure 2 shows different types of incremental pricing methods.

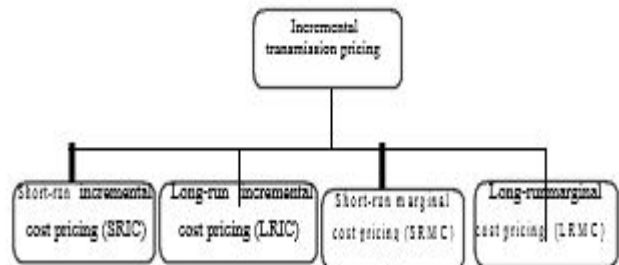


Fig. 2. Types of incremental transmission pricing methods

B. Embedded Transmission Pricing

These pricing methods allocate the embedded system costs i.e., fixed cost among transmission system users. Embedded pricing methods can be categorized as in Figure 3:

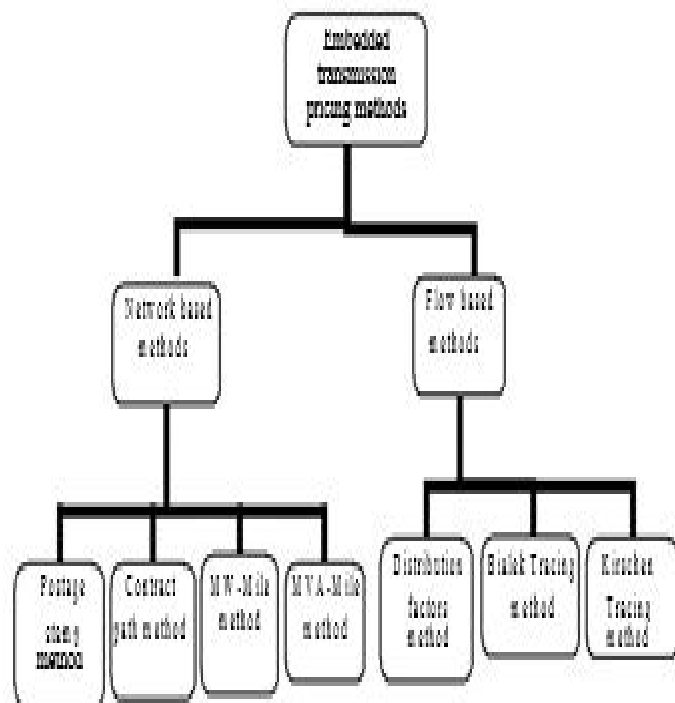


Fig. 1. Different transmission pricing methods

Operating cost, opportunity cost and reinforcement cost of section 1.3 constitute the incremental cost of the transmission transaction. Incremental costs are two types. They are short run and long run incremental costs. "Short-Run Incremental Cost" refer to operating cost and opportunity cost, "Long-Run Incremental Cost" refers to operating cost, opportunity cost and reinforcement cost. The pricing method adopted for these costs is Incremental Transmission Pricing method which comes under Approach1 of section 1.4. Embedded Transmission Pricing method accounts for Embedded Cost or Existing System Cost and this method comes under Approach2 of section 1.4. These two pricing methods are discussed below in detail. A combination of these two methods leads to proper pricing structure for any market. This paper mainly focuses on brief discussion of Embedded Transmission Pricing methods and their case studies.

1) Network Based Methods

These methods depend on the structure of the transmission system but do not recognize the physical laws governing its operation [8].

a) Postage Stamp Method

Postage-stamp rate method is traditionally used by electric utilities to allocate the fixed transmission cost among the users of firm transmission service. This method is an embedded cost method, which is also called the rolled-in embedded method. This method does not require power flow calculations and is independent of the transmission distance and network configuration. The magnitude of the transacted power for a particular transmission transaction is usually measured at the time of system peak load condition:

$$R_T = TC * (P_t / P_{peak}) \quad (2)$$

Where R_t is the transmission price for transaction t , TC is the total transmission charges and P_t and P_{peak} are transaction t load and the entire system load at the time of system peak load condition [13]. The main purpose of using this methodology is the entire system is considered as a centrally operated integrated system. This method is simpler. Since this method ignores the actual system operation, it is likely to send incorrect economic signal to transmission customers.

b) Distance Based MW-Mile Method

This method allocates the transmission charges based on the magnitude of transacted power and the geographical distance between the delivery point and the receipt point i.e., it is the product of power due to a transaction times the distance this power travels in the network [8]. This method is DC power flow based method.

$$TC_t = TC \cdot \frac{\sum_{k \in K} C_k L_k MW_{t,k}}{\sum_{t \in T} \sum_{k \in K} C_k L_k MW_{t,k}} \quad (3)$$

In (3)
 TC_t = cost allocated to transaction t
 TC = total cost of all lines in \$
 L_k = length of line k in mile
 C_k = cost per MW per unit length of line k
 $MW_{t,k}$ = flow in line k , due to transaction t
 T = set of transactions
 K = set of lines

1) Flow Based Methods

This approach allocates the charges of each transmission facility to a wheeling transaction based on the extent of use of that facility by the transaction. This is determined as a function of magnitude, the path, and the distance travelled by the transacted power. The flow based methods are Bialek tracing method and Distribution factors method.

a) Distribution Factors Method

Distribution factors are calculated based on DC load flows. These factors are used to determine the impact of generation and load on transmission flows. The various distribution factors are Generation shift distribution factors (GSDF's) and Generalized Generation/ load distribution factors (GGDF's/GLDF's) have been used extensively in power system security analysis to approximate the transmission line flows and generation /load values. GSDF's or A factors provide line flow changes due to a change in generation. These factors can be used in determining maximum transaction flows for bounded generation and load injections. GGDF's are applied to estimate the contribution by each generator [15,16] to the line flow on the transmission grid and GLDF's determine the contribution of each load to line flows.

b) Bialek Tracing Method

This algorithm works only on lossless flows when the flows at the beginning and end of each line are the same. The simplest way of obtaining lossless flows from the lossy ones is by assuming that a line flow is an average over the sending and receiving end flows and by adding half of the line loss to the power injections at each terminal node of the line [14].

The total flow P_i through node i (i.e., the sum of inflows or outflows) may be expressed, when looking at the inflows as [15]

$$P_{ij}^g = \frac{\sum_{j \in \alpha_i^d} P_{jk}}{\sum_{k=1}^n P_{jk}} \sum [A_u^{-1}]_{ik} P_{Gk}; j \in \alpha_i^d \quad (4)$$

In (4)

$$P_i^g = \sum_{j \in \alpha_i^d} |P_{ij}^g| + P_{Gk}$$

$$[A_u]_{ij} = \begin{cases} 1 & i=j \\ \frac{|P_j|}{P_j} & j \in \alpha_i^u \\ 0 & \text{otherwise} \end{cases}$$

and

r_{ij}^g = an unknown gross line flow in line $i-j$

P_i^g = an unknown gross nodal power flow through node i

A_u = upstream distribution matrix

P_{Gk} = generation in node k

α_i^d = set of nodes supplied directly from node i

α_i^u = set of buses supplying directly to bus i

c) Kirschen Tracing Method

This method is based on a set of definitions for domains, commons and links.

A domain is a set of buses that obtain power from a particular generator. A common is a set of contiguous buses supplied by the same set of generators. Links are branches that interconnect commons. The rank of a common is defined as the number of generators supplying power to the buses comprising this common. It can never be lower than one or higher than the number of generators in the system. Based on these definitions, the state of a system (an acyclic state graph) is represented by a directed graph that consists of commons and links, with directed flows between commons and the corresponding data for generation/loads in commons and flows on links. The method assumes that the proportion of inflow traced to a particular generator is equal to the proportion of outflow traced to the same generator. As, in Bialek's tracing method, Kirschen's tracing method can determine contributions from individual generators to line flows, and determine contributions of individual loads to line flows. The method is applicable to both ac and dc load flow solutions. This traceable allocation method does not rely on a linearized model of the network and is therefore not limited to incremental changes in injections. The method starts by calculating line flows through an optimal power flow.

To calculate the contribution of each generation to commons and line flows, the method calculates the inflow to each common. The inflow to common k is the sum of generation at common k and the flow to common k from other commons with a lower rank j . mathematically:

$$I_k = g_k + \sum_j F_{jk} \quad (5)$$

I_k = inflow of common k

g_k = net generation in common k

F_{jk} = flow (from j to k) in a link connecting commons j and k

The next step is to recursively calculate relative contributions by each generator to the load and outflow of each common, starting from the root common (that has rank 1). Relative contributions are calculated based on absolute contributions to a common. Let

R_{ij} = relative contribution of common i to the load and the outflow of common j

A_{ij} = absolute inflow contribution of common j to common i

N_c = number of commons

F_{ki} = flow between commons k and i

III. RESULTS

In this section different case studies and their results are discussed. IEEE14 bus system, New England39 bus system and Indian75 bus Power system (Uttar Pradesh State Electricity Board data i.e., 400kV and 220kV grid data) are used as the case studies to demonstrate some of the above discussed methods. IEEE14 bus system [18] has 2 generators. New England39 bus system [20] has 10 generators. Indian75 bus Power system [30] has 15 generators. In this paper line lengths are assumed to be proportional to the line reactance for 14 and 75 bus systems whereas for 39 bus system lengths are given in the data file. For transformers line lengths are taken as 1 km for all the three systems. DC optimal power flow is used to get line flows in all the methods. Postage stamp method doesn't consider system line lengths, and hence gives a very inferior result compared to other methods. MW-Mile method, GGDF method, Bialek Tracing method and Kirschen Tracing method accounts for line lengths. GGDF method uses Power transfer Distribution factors for pricing and are used to approximately determine the impact of generation and load on transmission flows. Bialek tracing method uses proportional sharing principle based algorithm and it traces the actual power flow of each line by each participant. Kirschen Tracing method uses domains and commons for tracing the line flow in each line by each generator. The results shows that, power flow tracing based methods present more accurate pricing compared to Postage stamp method, MW-Mile method and GGDF method. Bialek tracing method is a topological approach to determine the contribution of individual generators to every line flow based on the calculation of topological distribution factors. But one drawback of this method is the results obtained by this method are not 100% accurate. Finally it is observed that among the tracing methods; results obtained by Kirschen tracing method are 100% accurate and so this method considered to be the best way of transmission pricing.

Tables I to III illustrate cost per MW generation for each generator using various methods for 14, 39 and 75 bus systems. In all the methods for all bus systems transmission charges are allocated to generators only.

TABLE I.
COMPARISON OF VARIOUS METHODS FOR IEEE14 BUS
SYSTEM

| | G1 | G2 |
|---|----------|----------|
| Postage stamp method Total cost = 5746.08 \$ | | |
| Trans. cost (\$) | 100 | 100 |
| Cost (\$/MW) | 0.69 | 0.85 |
| MW-Mile method Total cost = 70077.11 \$ | | |
| Trans. cost (\$) | 1386.67 | 1386.67 |
| Cost (\$/MW) | 9.03 | 13.13 |
| GGDF method Total cost = 71796.6 \$ | | |
| Trans. cost (\$) | 1722.062 | 1051.287 |
| Cost (\$/MW) | 11.22 | 9.96 |
| Bialek tracing method Total cost = 70082 \$ | | |
| Trans. cost (\$) | 1871.6 | 901.7 |
| Cost (\$/MW) | 12.19 | 8.54 |
| Kirschen tracing method Total cost = 69302.82 \$ | | |
| Trans. cost (\$) | 1846.08 | 927.26 |
| Cost (\$/MW) | 13.00 | 7.92 |

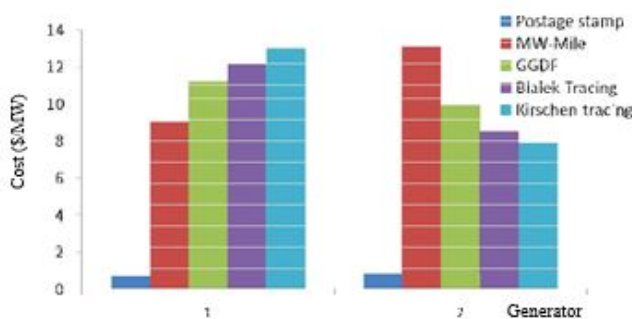


Fig. 4. Comparison of 14 bus system results for different methods

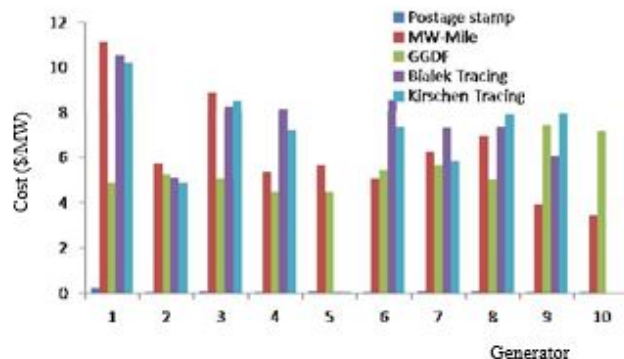


Fig. 5. Comparison of 39 bus system results for different methods

TABLE II.
COMPARISON OF VARIOUS METHODS FOR NEW ENGLAND39 BUS SYSTEM

| | G30 | G31 | G32 | G33 | G34 | G35 | G36 | G37 | G38 | G39 |
|---|---------|---------|---------|---------|--------|---------|---------|--------|---------|---------|
| Postage stamp method Total cost = 128595.18 \$ | | | | | | | | | | |
| Each transaction cost (\$) | 46 | 46 | 46 | 46 | 46 | 46 | 46 | 46 | 46 | 46 |
| Cost (\$/MW) | 0.24 | 0.074 | 0.03 | 0.071 | 0.099 | 0.0652 | 0.079 | 0.081 | 0.06 | 0.042 |
| MW-MILE method Total cost = 709360.3 \$ | | | | | | | | | | |
| Each transaction cost (\$) | 3443 | 3443 | 3443 | 3443 | 3443 | 3443 | 3443 | 3443 | 3443 | 3443 |
| Cost (\$/MW) | 11.12 | 5.72 | 8.83 | 5.35 | 5.66 | 5.04 | 6.25 | 6.94 | 3.94 | 3.44 |
| GGDF method Total cost = 5.15519e+7 \$ | | | | | | | | | | |
| Each transaction cost (\$) | 1516.45 | 3204.07 | 3733.75 | 2899.00 | 2720.6 | 3366.31 | 3289.92 | 2934.6 | 5229.36 | 5735.32 |
| Cost (\$/MW) | 4.39 | 5.27 | 5.07 | 4.46 | 4.47 | 5.45 | 5.66 | 5.03 | 7.43 | 7.19 |
| Bialek Tracing method Total cost = 6.942306519917834e+006 \$ | | | | | | | | | | |
| Each transaction cost (\$) | 1407.87 | 3109.02 | 6044.35 | 5297.95 | 30.14 | 6029.68 | 4267.31 | 4128.4 | 4115.18 | 0 |
| Cost (\$/MW) | 10.55 | 5.10 | 8.23 | 8.15 | 0.049 | 8.55 | 7.31 | 7.33 | 6.06 | 0 |
| Kirschen Tracing method Total cost = 6763923.0 \$ | | | | | | | | | | |
| Each transaction cost (\$) | 2247.50 | 2987.06 | 6382.59 | 4681.94 | 30.94 | 4458.03 | 2380.45 | 5068.8 | 6190.69 | 0 |
| Cost (\$/MW) | 10.21 | 4.90 | 8.51 | 7.20 | 0.05 | 7.36 | 5.86 | 7.92 | 7.96 | 0 |

TABLE III.
COMPARISON OF VARIOUS METHODS FOR INDIAN75 BUS POWER SYSTEM

| | G1 | G1 | G3 | G4 | G5 | G6 | G7 | G8 | G9 | G10 | G11 | G12 | G13 | G14 | G15 |
|--|--------|-------|-------|-------|------|-------|------|-------|-------|-------|-------|------|-------|------|-------|
| Postage stamp method Total cost = 159228.088 \$ | | | | | | | | | | | | | | | |
| Cost (\$/MW) | 0.079 | 0.33 | 0.22 | 0.4 | 0.23 | 0.29 | 0.4 | 0.35 | 0.62 | 0.35 | 0.30 | 0.9 | 0.065 | 0.25 | 0.11 |
| MW-MILE method Total cost = 496661.8 \$ | | | | | | | | | | | | | | | |
| Cost (\$/MW) | 0.36 | 0.69 | 0.83 | 2.08 | 9.37 | 1.06 | 1.46 | 1.30 | 0.56 | 1.30 | 1.12 | 0.16 | 0.35 | 0.93 | 0.51 |
| GGDF method Total cost = 1.06717e+6 | | | | | | | | | | | | | | | |
| Cost (\$/MW) | 0.51 | 0.62 | 0.77 | 0.77 | 1.04 | 1.04 | 1.07 | 0.99 | 0.49 | 0.58 | 0.75 | 0.47 | 0.48 | 0.8 | 0.75 |
| Bialek Tracing method Total cost = 4.7064e+5 | | | | | | | | | | | | | | | |
| Cost (\$/MW) | 1.085 | 0.685 | 0.67 | 0.201 | 2 | 0.383 | 6 | 0.538 | 1.003 | 0.418 | 0.529 | 5 | 0.275 | 4 | 0.339 |
| Kirschen Tracing method Total cost = 473190.824 | | | | | | | | | | | | | | | |
| Cost (\$/MW) | 1.0065 | 0.684 | 0.671 | 0.182 | 6 | 0.38 | 6 | 0.538 | 0.935 | 0.4 | 0.526 | 7.5 | 0.275 | 0.33 | 0.36 |

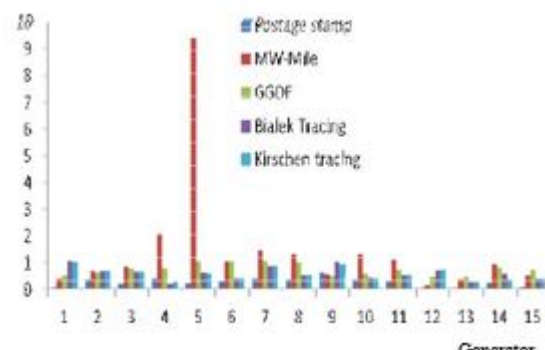


Fig. 6. Comparison of 75 bus system results for different methods

IV. DISCUSSIONS

Figures 4, 5, 6 of 14, 39 and 75 bus systems show the cost per MW flow to be paid by generators to Transco for utilizing transmission network. Since postage stamp method values are near to zero, they are not clearly visible in the graphs. From figure 6 it can be observed that transmission cost (cost per MW flow paid by generator to Transco for utilizing the transmission network) allocated to generator5 through MW-Mile method is very high. Because in MW-Mile method the transaction cost allocated to the transactions is not proportional to the generation of the generator belongs to that transaction. All the transactions owed equal transaction cost in this method. Since power generation for generator5 is 25MW only which is a minimum value and transaction cost is 234.35\$ which is uniform to all transactions; the generator5 has to pay 9.37\$ as cost per MW flow to Transco which is the highest value among all other transactions. This is a major drawback of MW-Mile method. This drawback can be overcome with flow based methods. Another observation is, in table4 (39bus system results) for Bialek and Kirschen tracingmethods the value of cost per MW allocated to generator39 is equal to zero. Because the power generated from generator39 is totally supplied to the load connected to bus39. So the power of this generator39 is not flown into any of the lines connected to bus39. Thus transaction cost and cost per MW allocated for this generator39 should be zero which is obtained in Bialek and Kirschen tracing methods only. With this example the authors claim that tracing methods produce most accurate results for tracing and pricing than all other methods

V. CONCLUSION

In this paper embedded cost based methods of transmission pricing with DCOPF have been discussed. Different cost components incurred by the transmission transaction were explained. Case studies of Postage stamp method, MW-Mile method, Distribution factors method, Bialek tracing method and Kirschen tracing method for IEEE14 bus system, NewEngland39 bus system and Indian75 bus Power system are presented. Postage stamp method for calculating embedded cost provides very poor results. Among all the embedded transmission pricing methods, flow based methods are proven to be better than network based methods for pricing. Next among all these flow based methods, Kirschen tracing method is the best method because it gives most accurate and reliable results of tracing and also for transmission pricing. It can be concluded that embedded pricing methods only cannot recover total transmission cost; a combination of incremental and embedded pricing methods could result in the recovery of true transmission system cost

REFERENCE

- [1] P.S. Kulkarni, O.P. Yadav, "SRMC based Transmission Pricing for Wheeling Transactions under Deregulated Environment of Power Sector", IE (I) Journal-EL, May 2008.
- [2] R.A.Wakefield, J.S.Graves and .F.Vojdani, "A transmission services costing framework", IEEE Transactions on Power systems, vol 12, No.2, May.1997.

- [3] D.Shirmohammadi, C.Rajagoapalan, E.R.Alward and C.L.Thomas, "Cost of transmission transactions: An introduction", IEEE Transactions on Power systems, Nov.'91, pp.1546-1556.
- [4] D.Shirmohammadi, P.R.Gribik, E.T.K.Law, J.H.Malinowski and R.E.O Donnel, "Evaluation of transmission network capacity use for wheeling transactions", IEEE transactions on Power Systems, Oct.'89, pp.1405-1413.
- [5] Y.Z.Li and A.K.David, "Wheeling rates of reactive power flow under marginal cost pricing", IEEE Transactions on Power Systems, Aug.'94, pp.1263-1269
- [6] C.W.Yu and A.K.David, "Pricing transmission services in the context of industry deregulation", IEEE Transactions on Power systems, Feb.'97, pp.503-510.
- [7] M.C.Caramanis, R.E.Bohn and F.C.schwepppe, "The cost of wheeling and optimal wheeling rates", IEEE Transactions on Power Systems, Feb.'86, pp.63-73.
- [8] Mohamed A.M.Shaaban, "Cost-based pricing of transmission system services: An overview", IEEE Conference
- [10] M.B. Rosenzweig, J. Bar-Lev, "Transmission Access and Pricing: Some Other Approaches", Public Utilities Fort-nightly, August 21, 1986, pp. 20-26. A.S. Holmes, "A Review and Evaluation of Selected Wheeling Arrangements and a Proposed General wheeling Tariff", FERC Paper, September 1983.
- [11] D. Shirmohammdi, "An Engineering Perspective of Transmission Access and Wheeling", Proceedings of the 3rd International Symposium of Specialists in Electric Operational and Expansion Planning (SEPOPE III), Belo- Horizonte, Brazil, 1992.
- [12] P.R. Gribik, D. Shirmohammadi, S. Hao, C.L. Thomas, "Optimal Power Flow Sensitivity Analysis", IEEE Transaction on Power Systems, Vol. 5, No. 3, August 1990, pp. 969-976.
- [13] D. Shirmohammadi, Xisto Vieira, Boris Gorenstein, Mario V.P.Pereira, "Some fundamental technical concepts about cost based transmission pricing", IEEE Transactions on Power Systems, Vol. 11, No. 2,May 1996.
- [14] J. Bialek, "Tracing the flow of electricity", IEE Proc-Gener. Transm. Distrib., Vol 143, No.4 July1996.
- [15] Mohammad Shahidehpour, Hatim Yamin, Zuyi Li, "Market operations in Electric Power Systems", New York:Wiley, 2002.
- [16] O.P.Rahi, Y.R.Sood, R.C.Chauhan, "Transmission pricing methodologies under restructured environment: An overview", NPSC 2004 paper.
- [17] Kankar Bhattacharya, Math H.J.Bollen, Jaap E.Daalder, "Operation of Restructured Power Systems", Springer, 2001.
- [18] P.K.Iyambo, R.Tzomeva, "Transient Stability Analysis of the IEEE 14-Bus Electric Power System", IEEE conference, Africon 2007. (14 bus data)
- [19] Ching-Tzong Su,Ji-Horng Liaw, "Power wheeling pricing using power tracing and MVA-KM method", IEEE Proto Power Tech Conference, Proto, Portugal,2001.
- [20] New England 39 bus system data "<http://sys.elec.kitami-it.ac.jp/ueda/demo/WebPF/39-New-England.pdf>". (39 bus data)
- [21] Orfaros G.A, Tziassiou G.T, Georgilakis P.S, Hatziargyriou N.D, "Evaluation of transmission pricing methodologies for pool based electricity markets", IEEE conference, Power Tech, 2011.
- [22] Manescu L.G, Rusinaru D, Dadulescu P, Anghelina V, "Usage based cost allocation for transmission cost under open access", IEEE conference, Power Tech, 2009.
- [23] M.Yi, B.Jeyasurya, "Investigation of transmission cost allocation using a power flow tracing method", Proceedings of IEEE Power Engineering Society General Meeting, June 2007, pp.1-7.
- [24] N.Kumar, Y.R.V. Reddy, D.Das, N.P.Padhy, "Allocation of transmission charge by using MVA-Mile approaches for restructured Indian power utility", IEEE conference, Power and Energy Society General Meeting, 2011.
- [25] Ghayeni M, Ghazi R, "Transmission network cost allocation with nodal pricing approach based on Ramsey pricing concept", IET Journal on Generation, Transmission & Distribution, 2011

Single Phase Matrix Converter Topology Based Implementation of Single Phase Boost –Buck Rectifier with Reduced Input Current THD

Ajay Giri, M.Tech. Student, Prof. L. M. Saini

Abstract-- Simulation of single phase buck boost rectifier with reduced input current THD using single phase matrix converter topology is describe in this paper. Due to the bidirectional feather the operation for buck- boost rectifier can be made through matrix converter topology. And this is possible by the proper switching algorithm to control the switches for their boost and buck operation. The input current nature is almost sinusoidal with low current total current harmonics and the level of THD is below than limit that was defined in the standards of IEEE. With the proper variation in modulation index corresponding changes in the output voltage is observed of buck- boost rectifier. For the synthesis of the output voltage Pulse width modulation (PWM) technique is used. The simulation results using MATLAB/Simulink are providing to validate the feasibility of this proposed method.

Keywords-- single phase matrix converter, pulse width modulation, boost and buck rectifier.

I. INTRODUCTION

The AC-DC converters which are also called rectifiers conventionally. These are developed by using thyristors and diodes. These provide controlled and uncontrolled dc power flow .due to the injected current harmonics they have poor power quality causing current distortion and poor power factor at input. in the light of their increased application a new type of rectifier has been developed by using insulated gate bipolar transistor (IGBT) The rectifier which gives output voltage more than input voltage called boost rectifier and rectifier which gives the less output voltage than input voltage called buck rectifier.

First of all matrix converter topology was introduce by Gyugyi in 1976 and the single phase matrix converter (SPMC) topology was realize first of all by Zuckerburger in 1997[1]. Which was based on direct AC-AC converter.

A. Ajay Giri, Department of Electrical Engineering, National Institute of Technology, Kurukshetra, Haryana ,India (e-mail: ajaygiri56@gmail.com).

B. Prof. L. M. Saini, Department of Electrical Engineering, National Institute of Technology, Kurukshetra, Haryana ,India

Matrix converter topology has a distinct advantage of affording bi-directional power flow with any desired number of input and output phase .in the absence of DC link capacitor increased power density with reduction in size and weight. It may be possible to generate various output irrespective of the type of load from various type of input.

In this paper use of single phase matrix converter is used in the single phase boost and buck rectifier and the operation and behaviour of the circuit are examined through MATLAB/SIMULINK by varying the modulation index.

II. CONVENTIONAL CONTRPLLED RECTIFIERS

Conventionally we use two different circuits for boost and buck operation as shown in fig.1 and fig.2 respectively. For the boost and buck operation of the rectifier here the circuit is divided into two stages[2] in first stage combination of diodes are there for rectification of AC input voltage to DC voltage and in second stage a step-up or step-down chopper is there for boost and buck operation respectively.

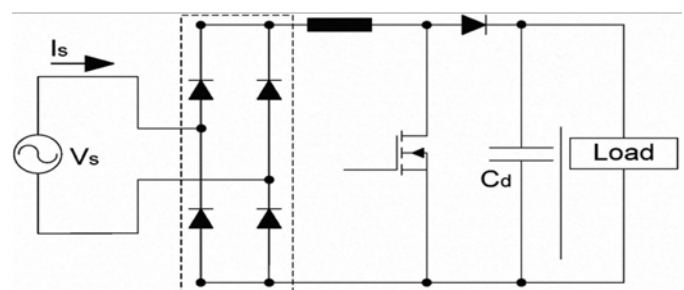


Fig. 1. Boost Rectifier

PWM pulse train

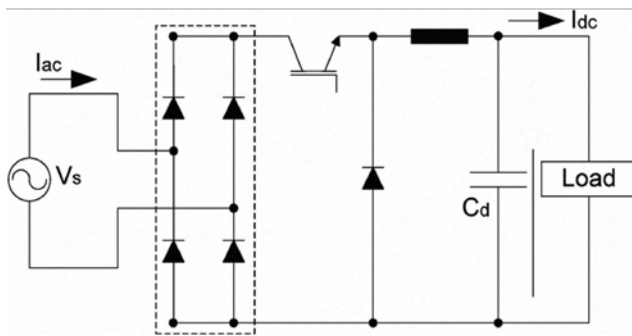
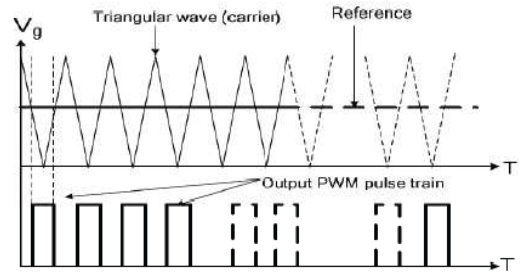


Fig.2. Buck Rectifier

III. SPMC TOPOLOGY

Single phase matrix converter is the combination of four bi-directional switches which have the capacity of blocking the voltage and conducting current in the both direction. Due to the high switching frequency and high current capacity for high power application a common emitter anti-parallel insulated gate bipolar transistors (IGBT) with diode pair can be used for bi-directional switches. In this module diode have the reverse blocking capacity. The major advantage of this topology is that we can get DC output from AC input or AC output from DC input. The circuit arrangement is shown below in figure.3

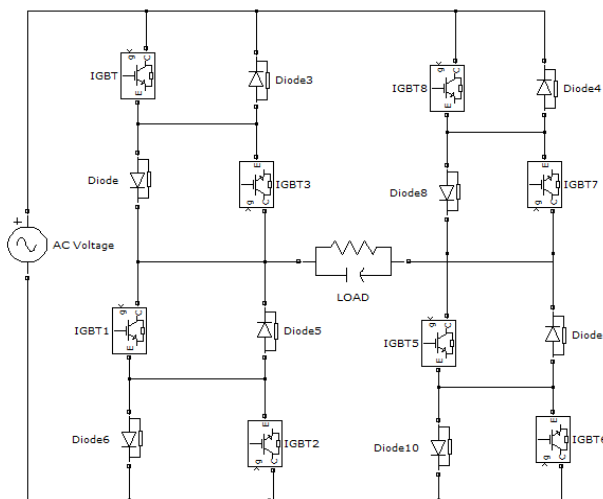


Fig. 3. SPMC

IV. PULSE WIDTH MODULATION

To control the output of the boost-buck rectifier pulse width modulation technique is used. To generating PWM signal the carrier signal is compared with the reference signal. As we see in the figure.4 a triangular wave is compared with the reference dc signal and a generate a

Fig. 4. (PWM)

Due to the inductive load in the circuit voltage spikes are there which affect the current. If the change in the current across the inductor instantaneous [7] then it will produce large voltage spikes and due to these spikes the switches will destroy. In the SPMC topology there is a possibility of reversal of current from the inductive load when the IGBT's are in turn-off mode. To avoid this type of problem we have to use a proper switching sequence for the energy flowing through the insulated gate bi-polar transistors (IGBT).

V. COMMUTATION STRATEGIES FOR THE BOOST AND BUCK OPERATION.

The average output of the single phase boost rectifier should be greater than the input voltage and the average output of the single phase buck rectifier should be less than the input voltage. Conventionally we use the different switching pattern for both boost and buck rectifier. But in this paper the switching pattern is same for both boost and buck rectifier [6-7] and we get the output by varying the modulation index. The switching pattern is tabulated in the table I

Table. I
(Switching strategies for the boost and buck rectifier

| Switches | | | |
|----------|-------|------------|-----------------|
| Cycle | Modes | On/control | Off |
| Positive | 1 | S2b | S3b,S4b,S1a,S4a |
| | 2 | S3b, | S1a,S2b,S4b,S4a |
| Negative | 3 | S1a,S4a | S2b,S3b,S4b, |
| | 4 | S1a,S3a | S4b,S3b,S4a |

rectifier

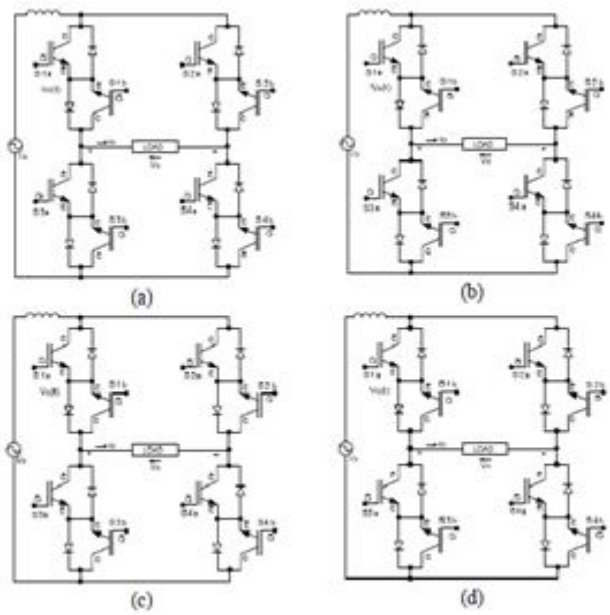


Fig. 5. circuit arrangements for the boost and buck rectifier. For positive half cycle (a) & (b) for negative cycle (c) & (d)

Switching strategies for the boost and buck rectifier can be divided into two cycle and each cycle have two modes of operation .in the first mode of operation switch S2b is in on state and switches S1a, S3b, S4a, and S4b are in off state. The input current flows through the inductor L. In mode two switch S3b is in on state and switches S1a, S2b, S4a and S4b are in off state now input current flows through the load and inductor current falls and the energy stored in inductor 1 transfer to load. In the negative half cycle first switches S1a and S4a are in on state and switches S2b, S3b and S4b are in off state and in mode four switches S1a and S3a are in on state and switches S3b, S4a and S4b are in off state.

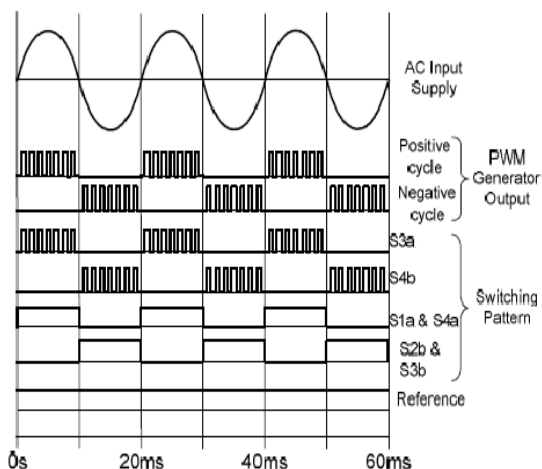


Fig. 6. Switching pattern for the boost –buck

VI. SIMULATION MODELS

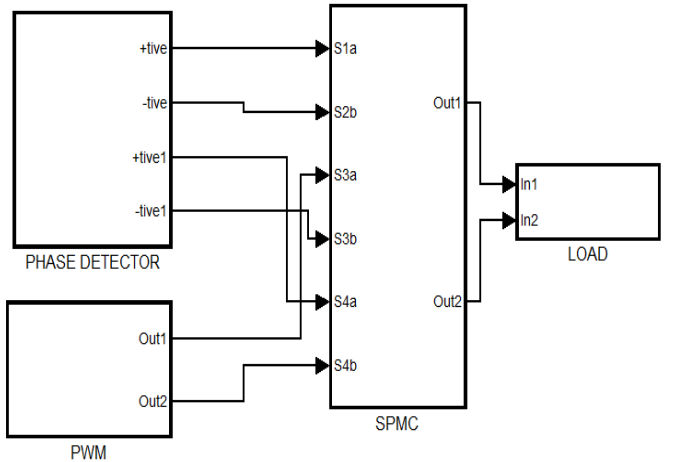


Fig. 7. Main model of boost buck rectifier with SPMC

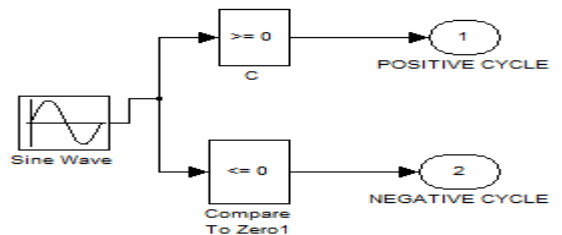


Fig. 8. Phase detector

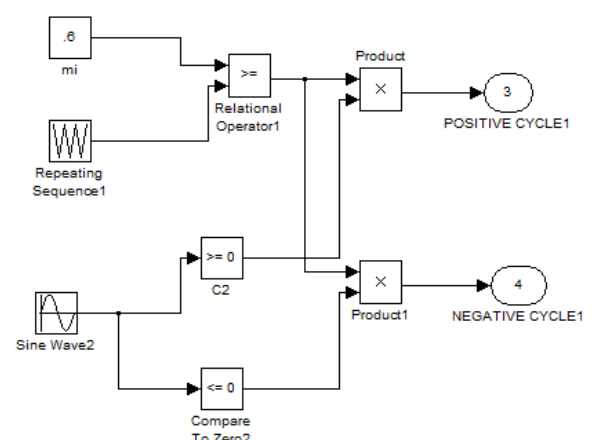


Fig. 9. PWM generator

VII. RESULTS

Simulation model of Single phase boost-buck rectifier using single phase matrix converter topology has been developed in MATLAB/Simulink. This connected with the supply voltage of 100 V, 50Hz. A parallel connected resistive and capacitive load with the values of 40ohm and 5microferred respectively are used .modulation index of 0.2, 0.3, 0.4, 0.5, 0.6 are used with the switching frequency of 5khz. We observe from the results coming from the simulation that if we increase the modulation index then the output voltage also increases its values. when we take modulation index 0.2 to .04 then rectifier works as a buck rectifier. the results for output voltage and input current THD are shown in figure 10,figure 11, figure 12, figure 13, figure 14 and figure 15 respectively. When we take modulation index 0.5 and 0.6 then the rectifier works as a boost rectifier. the results for output voltage and input current THD are shown in figure 16 figure 17 figure 18 and figure 19 respectively. The results for the input current THD are also indicating that the input current THD is below the limit that was defined in the standards of IEEE in every case either it is buck rectifier or boost rectifier. Figure 20 and figure 21 are shows the input voltage and input current respectively.

VIII. RESULT FOR INPUT POWER FACTOR AND EFFICIENCY

Input power factor of the boost- buck rectifier is changing its value with the modulation index. The values of power factor are 0.88 and 0.90 with 0.2 and 0.3 modulation index respectively and efficiency is also increasing with the increment in modulation index. The values of efficiency are 81% and 83% with 0.2 and 0.3 modulation index respectively

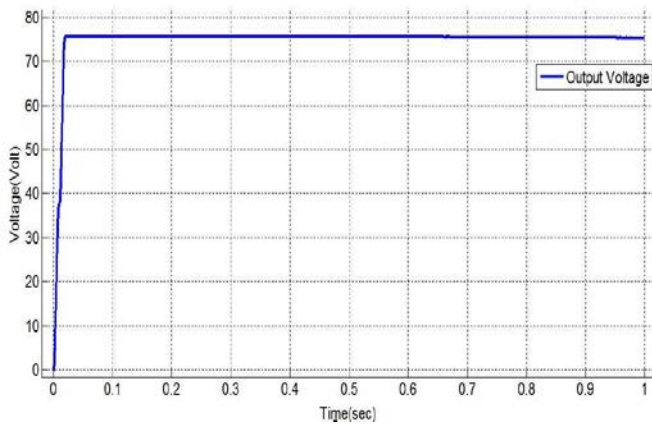


Fig. 10. Output voltage for buck rectifier with MI=0.2

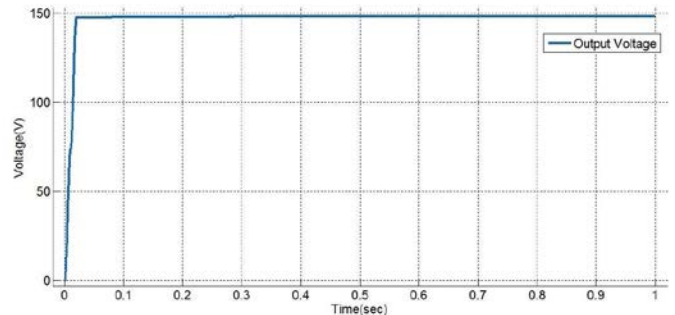


Fig. 11. Output voltage for buck rectifier with MI=0.3

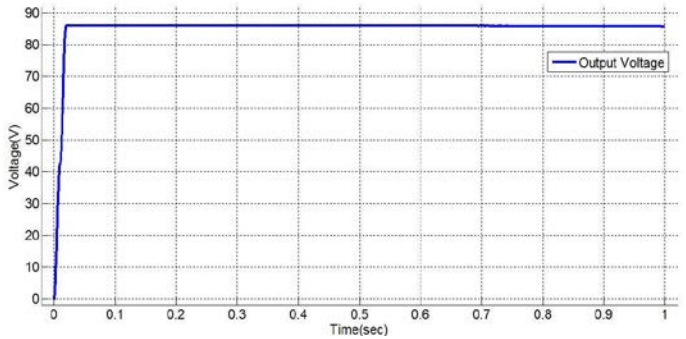


Fig. 12. Output voltage for buck rectifier with MI=0.4

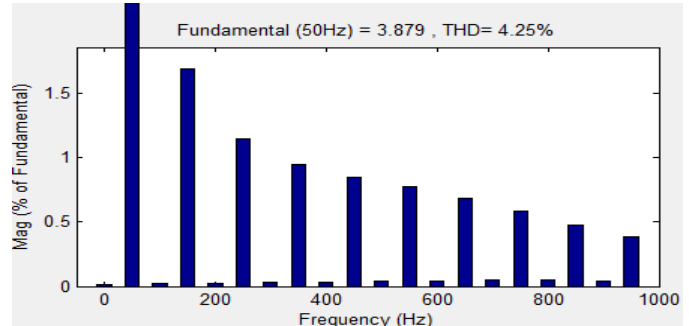


Fig. 13. Input current THD with MI=0.2

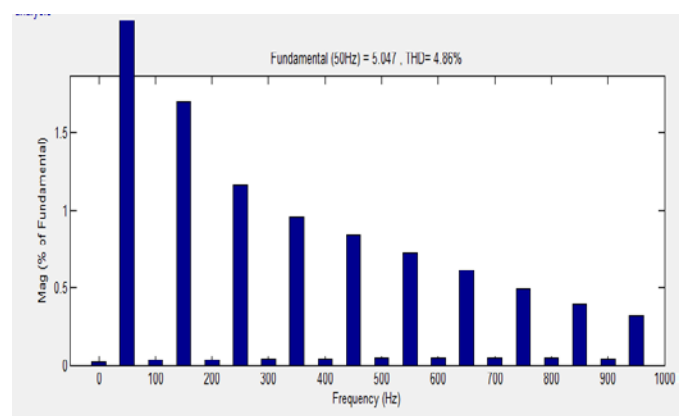


Fig. 14. Input current THD with MI=0.3

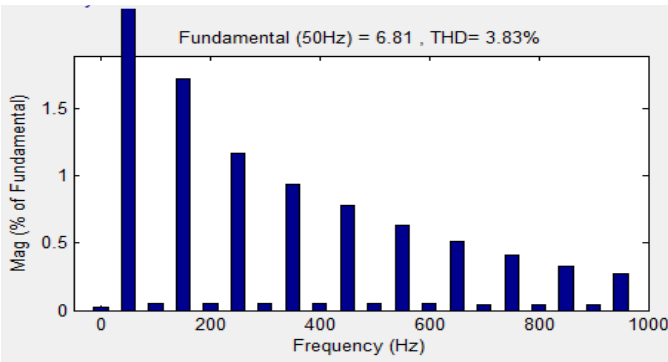


Fig. 15. Input current THD with MI=0.4

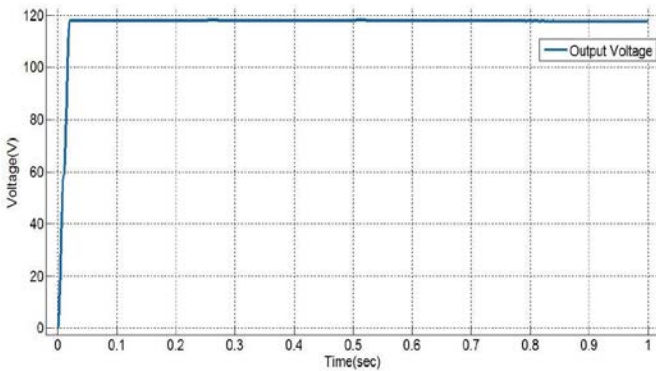


Fig. 16. Output voltage for boost rectifier with MI=0.5

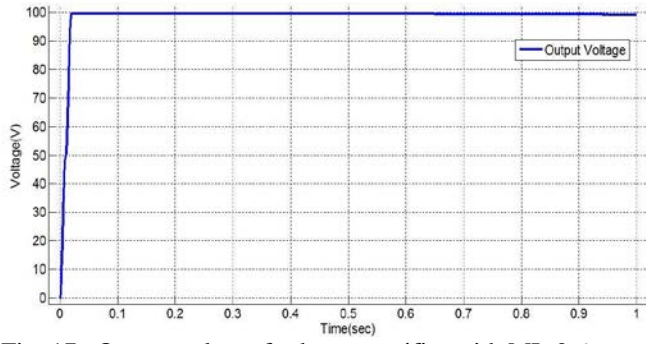


Fig. 17. Output voltage for boost rectifier with MI=0.6

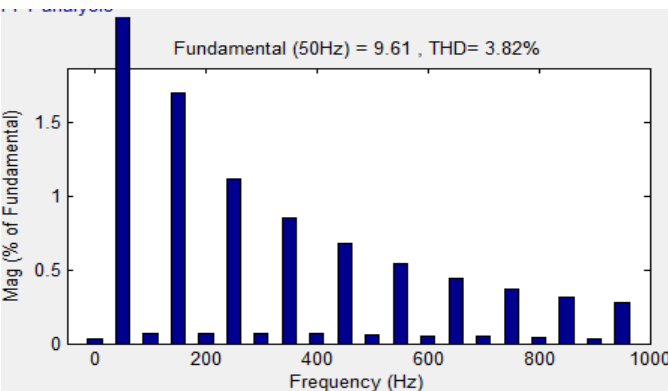


Fig. 18. Input current THD for boost rectifier with MI=0.5

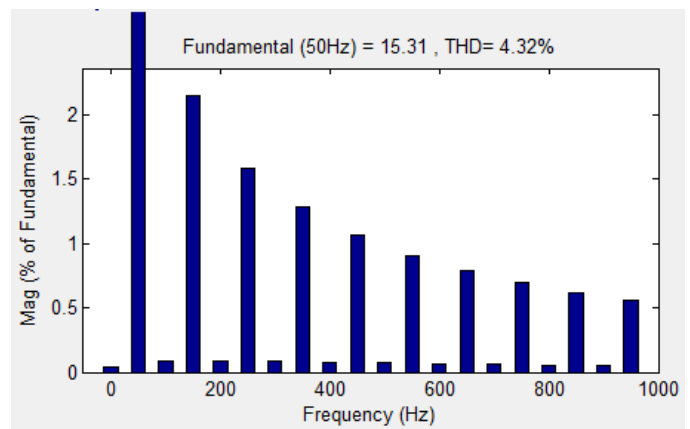


Fig. 19. Input current THD for boost rectifier with MI=0.6

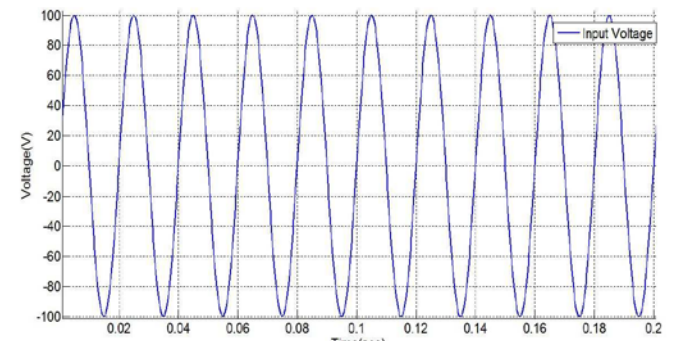


Fig. 20. Supply input voltage waveform

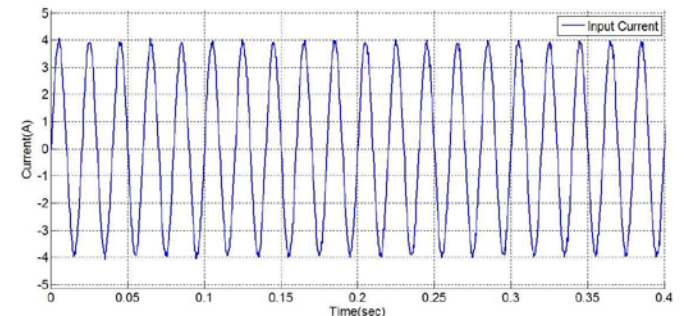


Fig. 21. Supply input current waveform

IX. CONCLUSION

This paper briefly describe the successful implementation of single phase boost- buck rectifier using Single phase matrix converter topology. We observe from the results that if we vary the modulation index then output voltage is also vary mutinously with THD of input current less than the limit. The rectifier works as a buck rectifier when modulation index in between 0.2 to 0.4 and when its range in between of 0.5 to .06 then rectifier works as a boost. Efficiency and input power factor are also discuss. All the results verified in MATLAB/SIMULINK

REFERENCES

- [1] Zuckerberger, A.; "Single phase Matrix Converter", *IEEE Proceeding Electric Power App.*, 1997, PP.235-240
- [2] Z.Idris.,S.Zaliha.,M.K.humzah. "Safe Commutation Strategy SinglePhase Matrix Converter", *IEEE PEDS 2005*
- [3] M.H.Rashid."Power electronic circuit Devices and application", Third edition 2004 prentice hall
- [4] Patrick W.Wheeler, Jose Rodriguez,Jon C.Clare,Lee Empringham, and Alejandro Weinstein; "Matrix Converters: A Technology Review", *IEEE Transactions on Industrial Electronics*, 2002.
- [5] Nishanthi, S.; Kumar, N.S., "Design and simulation of single phase z- source buck boost matrix converter", *International Conference on ICCEET, 2012*, Publication Year: 2012, Page(s): 186 – 192
- [6] H. M. Hanafi, et al., "Improved switching strategy of single phase matrix converter as a direct AC-AC converter," *IEEE Conference on Industrial Electronics and Applications in 2008. ICIEA 2008*. pp. 1157-1162
- [7] M.Noor,S.Z,Kamal Hamzah.,M.Farid Abidin."A modelling and simulation of a DC chopper using SPMC topology", International conference on power electronic and drive systems.2005
- [8] Badeli, A.A.; Baharom, R.; Hidayat, N. ; Hamzah, M.K. "Single-phase matrix converter with reduced switch count operating as buck or boost rectifier," *IEEE Symposium on Computer Applications and Industrial Electronics (ISCAIE)*, 2012 Publication Year: 2012 , Page(s): 20–25.
- [9] M. K. Hamzah, et al., "A New Single-Phase Inverter using Single-Phase Matrix Converter Topology," *IEEE International on Power and Energy Conference (PECon '06)*, 2006, pp. 459-464.
- [10] Hosseini,S.H.;Babaei, E."A New Generalized Direct Matrix Converter" industrial Electronics. 2001. Proc.ISLE 2001.Vol (2), pp.1071-1076

Thyristor Controlled Improvement of a Solid State Fault Current Limiter Using Simulink

A. Maloth Naresh, B. Gajendra Kumar, and C. Navneet Kumar Singh

Abstract--The paper focus on application of thyristor-controlled solid state fault current limiter for the medium voltage distribution systems (6.35 KV-10KV), switchgear and other equipments of the power system. So here the proposed Fault Current Limiter and Interrupting Device (FCLID) with Solid State Fault Current Limiting (SSFCL) reduces the short circuit currents due to voltage sag. Short circuit currents contain high energy and can damage electrical equipments so when a fault occurs the circuit breakers automatically opens in three to six cycles of the fault. Model of the power system with the limiter has been developed and simulation has been carried out in MATLAB/SIMULINK, and performance evaluation of the proposed system is done against voltage and current of the limiter

Index Terms--Fault Current Limiter and Interrupting Device, Solid State Fault Current Limiter, Switchgear, Thyristor controlled, Voltage Sag.

I. INTRODUCTION

THE extension of power system has resulted in an increase in the use of solid state fault current limiter for the limitation of fault current [1].these paper will be focusing on the thyristor – controlled fault current limiters (power system based) resonant Fault Current Limiters (FCLs) for voltage sag mitigation. For solid state resonant FCLs power electronic switches are used to instant limiting impedance to the system. Immediately after the sensing of a fault the thyristor – controlled resonant FCL is found in [2] to be able to limit the fault current efficiency .The operations of the resonant FCLs excite series and parallel L-C circuit formed by the customer step down transformer and the low voltage capacitor. Advantages of using a fault current limiter include reduced fault level of the supply and smaller voltage sag during a short-circuit fault. These will avoid upgrading

A. Maloth Naresh, Department of Electrical Engineering, Motilal Nehru National Institute of Technology, Allahabad-211004, India (e-mail: naresh219.m@gmail.com).

B. Gajendra Kumar, Department of Mechanical Engineering, Motilal Nehru National Institute of Technology, Allahabad-211004, India (e-mail: kumar.gajendra76@gmail.com).

C. Navneet Kumar Singh, Department of Electrical Engineering, Motilal Nehru National Institute of Technology, Allahabad-211004, India (e-mail: nvnt.kmr.sng@gmail.com).

switchgears during system expansion and improve the power quality delivered to the customers. This paper first outlines the construction and operation of the new solid-state fault current limiter. The design with impedance insertion switched using semiconductor device [3], for a high level current application for its inherent backward [4]. Solid state Fault current limiter has been in important component of Flexible AC Transmission System (FACTS), bridge type of solid state fault current limiter [3] in the SSFCL to high or extra-high voltage of the power systems. When the SSFCL is used in high-voltage power system, a number of high-voltage thyristor must be connected in series, series and parallel controlled resonant.

II. PRINCIPLE OF OPERATION AND TYPES OF FAULTS

A fault current limiter is a series device its must present low impedance to current flow under normal condition, this impedance should be quickly increase the current. The fault current limiters there are mainly four types,

1. Inductive
2. Power Electronics
3. Electromagnetic
4. Super Conductor (Resistive)

A. The Resistance Fault Current Limiter and Interrupting Device (FCLID)

The solid state fault current connected in these study actually a fault current is limiting and interrupting device [3] shown in figure (1)

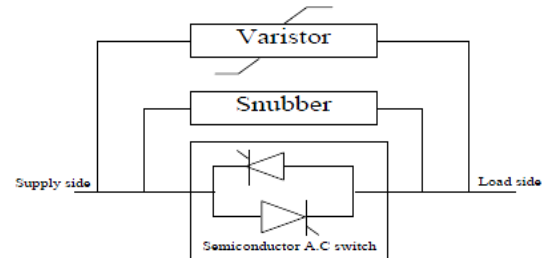


Fig.1 Construction of FCLID

The configuration of single phase FCLID is shown in Fig. 1. It

consists of a high speed bi-directional switch realized using power semiconductor device. Such as IGBT, a snubber and varistor circuits all connected in parallel. When the SSFCL is used in high-voltage power system, a number of high-voltage thyristor must be connected in series to constitute bridge arms. Complicated voltage sharing and drive circuit will lead to increased cost and reduced reliability. To these points, we can use a series three-phase buck transformer to reduce requirement of thyristors voltage rating, which can greatly reduce the cost of SSFCL and greatly increase its reliability.

In these operations without fault the semiconductor device are constantly gated on. The FCLID can be passed using circuit breaker to avoid the losses. The bypass circuit is opened when the FCLID is required to operate. Consider that short circuit fault occur on the load side , a semiconductor device will initially conduct the fault current .the switch is turned off when the fault current reaches a preset value I_{max} which should to be within the interrupting capability of the Semiconductor device. The fault current is thus diverted to the varistor. The clamping voltage of the varistor is set to be higher than the peak supply voltage. The semiconductor device is turned on the gain to reestablish the current as it reduces to a preset low value I_{min} . Switching logic is the same for both positive and negative half cycle of the fault current.

B. Resonant Circuit Current Limiters

The resonant LC circuit consists of an inductance and capacitance connected either in parallel or in series, turned to the supply frequency 60 Hz. The impedance of this resonant circuit increases rapidly when inserted in the system and reduces the fault current, in the steady state condition. Which is now possible with the development of power electronics switches [1].

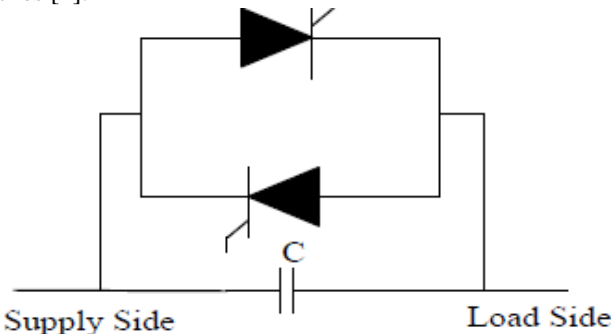


Fig. 2 Thyristor controlled resonant

C. Series Resonant FCL

Series resonant current limiters use series tuned LC circuits connected in series in the system. The tuning frequency of the series LC circuit is chosen to be the fundamental supply

frequency. The Thyristor-Controlled Series Resonant FCL limits fault current by the insertion of an inductor in series with the line during normal steady state operations. The resonant circuit offers very low impedance when the frequency is closer to fundamental frequency and offers very high impedance during fault conditions. This type of configuration is shown in Fig-4[5]. The bus voltages are not affected from high frequency oscillations. However there are small voltage sags large L (small C) can reduce these sags significant drop in fault currents occurs due to large L value. For the Series Reactor FCL the voltage across the FCL capacitor is approximately zero

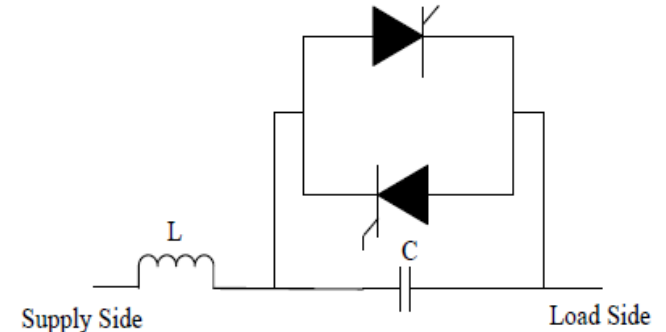


Fig. 3 Thyristor controlled series resonant FCL

D. Thyristor Controlled Series and Parallel FCL

The schematic principle for the Thyristor-Controlled Series-Parallel Resonant FCL is given in Fig(4) .Two resonant circuits, tuned at the supply frequency, are used in the formation of the Series- Parallel Resonant FCL. Thyristors are not fired during normal system state. The series connected inductors and capacitors are tuned to resonate at supply frequency and voltage drop across the FCL will be negligible. When a fault is detected thyristor will be turned on and hence the parallel resonant circuit thus formed will limit the fault current. Due to incorporation of the combination of series parallel resonant circuits, the proposed FCL performance is quite better as compared to those of the original Resonant FCL. The fault current, through a Series-Parallel Resonant FCL shown in Fig. 4, consists of a steady state, two transient and two DC components. Since the FCL is tuned to the supply frequency, the steady-state impedance will be infinite and hence the steady-state component will be zero. The transient frequency β is higher than the supply frequency, and is expresses as follows [5].

$$\beta = \frac{I}{LC} \sqrt{\frac{L + L_S}{L_S}} = \omega \sqrt{\frac{L + L_S}{L_S}}$$

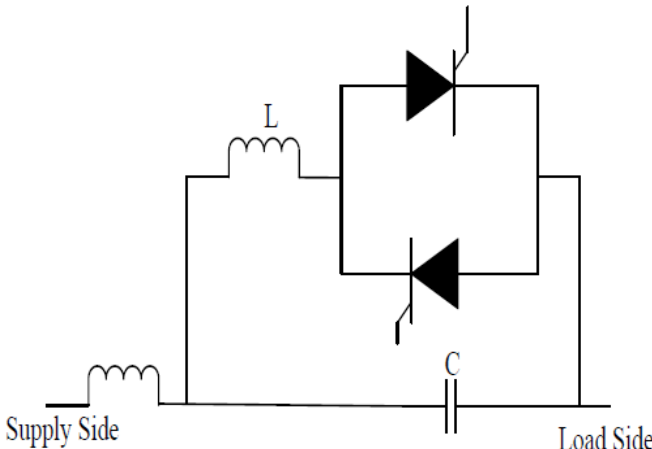


Fig. 4 Thyristor controlled series -parallel resonant FCL

III. DESIGN ANALYSIS AND SIMULATION RESULTS

To illustrate the above operating principle, a simulation model is using MATLAB/SIMULINK for the single-phase 230 V system shown in Fig. (6) [6]. It is assumed that the pre-fault load current is less than 40 A. Without the fault current limiter, the prospective peak short-circuit current at the bus bar of Load 4 is 1 kA. Change the value of 2kA, 3kA and 4 kA, if the fault location is at Load 3, Load 2, and Load 1, respectively. Bus bar A is the Point of Common Coupling (PCC) with other cable feeders.

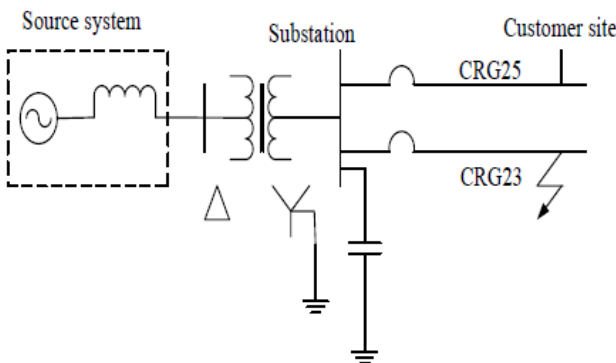


Fig. 5 Single line diagram for distribution system

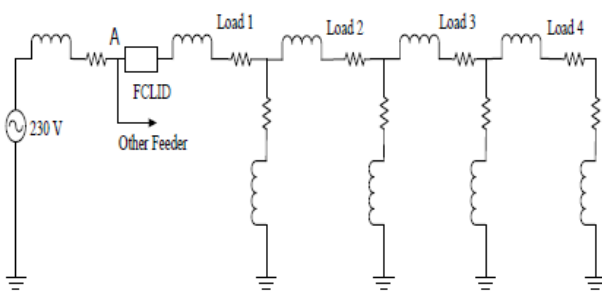


Fig. 6 FCL Incorporated in a distribution system

Extensive dynamic simulation has been carried out in order to justify the proposed control methodology in MATLAB/SIMULINK environment. The simulation parameters are as follows

Source Side

1. Supply system 230V/60 Hz
2. Transformer 6.35kV / 240 Volts, 150 kVA
3. Limiting Resistance = 0.35Ω .

Distribution feeders

1. Resistance = $0.00825 \Omega/\text{km}$.
2. Inductance = $0.3137e-03 \text{ H/km}$.
3. Capacitance = $1.237e-09 \text{ F/km}$.
4. Length of feeder = 1 km.
5. Load = $1+j0.75 \Omega$

Single line diagram for distribution system is shown in figure (5) the parameter of the circuit has been mentioned above.

In case of a fault at Load 4, the maximum through current, which is potentially 1 kA without the FCLID, is limited by the fault current limiter to $I_{\max}=120\text{A}$.

The simulation is performed for three half cycles only. The thyristor-Controlled Series Resonant FCL limits fault current by the insertion of an inductor in series with the line. The small leakage current of the varistor, I_{\min} , is set the zero ampere and then simulation is performed. The current through the fault current limiter is shown in figure 7.

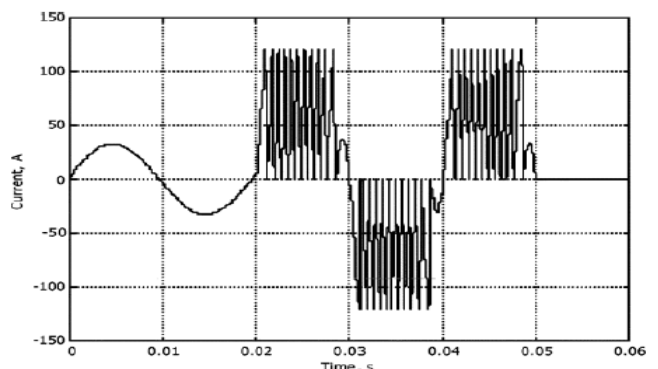


Fig.7 Current through FCLID

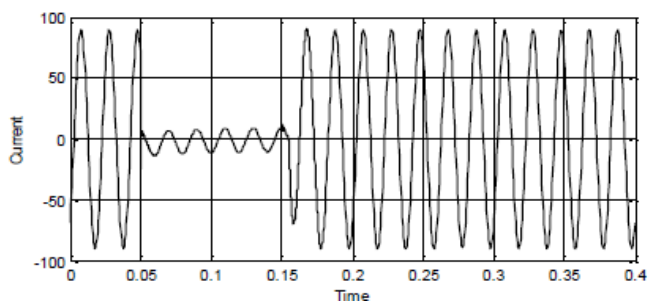


Fig. 8(a) Current Feeder-1

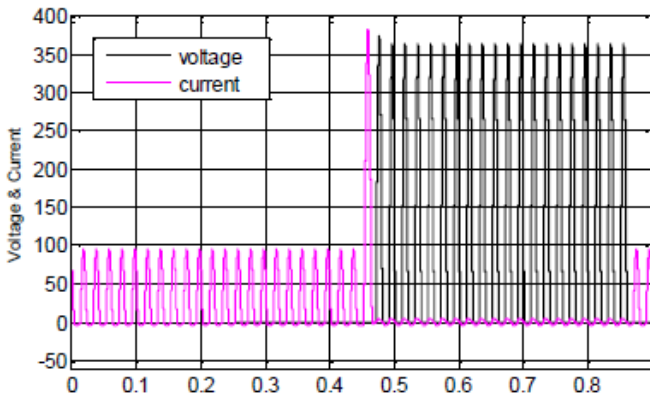


Fig. 8(b) SSFCL voltage and current

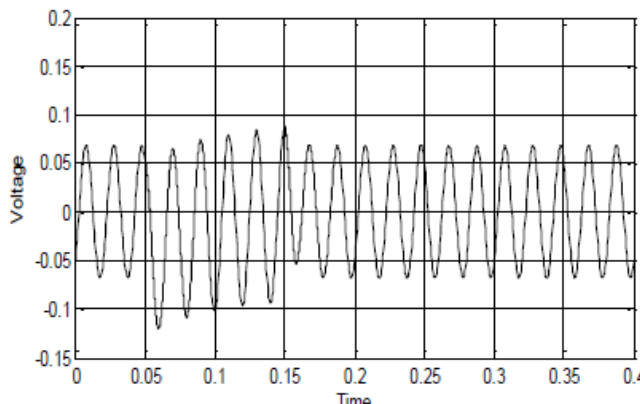


Fig. 8(c) Voltage at PCC

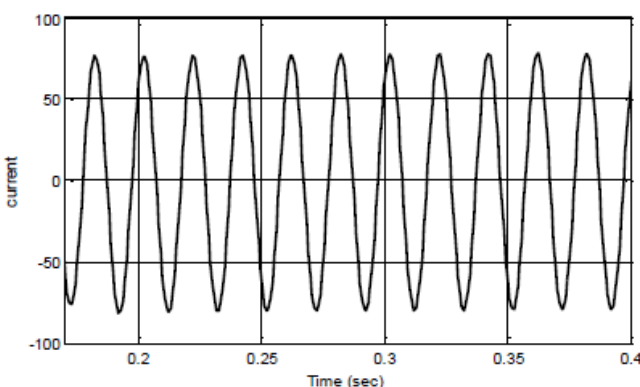


Fig. 8(d) Current Feeder-2

Fault is created at the moment of 0.05 s, rated current is 242A. The value of the peak value of fault current is 2160A. The simulation results are shown in Fig 8(a) to Fig-8(d) in order to evaluate the performance of the proposed control techniques against the different sets of voltage and currents. From Fig-8(c) and 8(d) it is clear that the line current rises at the high value and bus voltage drops to a low level during the faults.

IV. CONCLUSION

This paper thus shows that the fault current limiter used in distribution systems has to be thyristor controlled resonant FCL. Simulation in MATLAB/SIMULINK environment is carried out for resistive type SSFCL When the SSFCL is used in high-voltage power system, a number of high-voltage thyristor must be connected in series/series and parallel controlled resonant FCL. To these points, we can use a series single-phase 230V, transformer to reduce the thyristors voltage rating, which can greatly reduce the cost of SSFCL and reliability of the system is enhanced. The FCLID's such as thyristor, snubber and varistor circuits all connected in parallel.

V. REFERENCES

- [1]. R.K. Smith, P.G. Slade, and H. Mehta, "Solid-state distribution current limiter and circuit breaker application requirements and control strategies", IEEE Trans. on Power Delivery, vol.8, No.3 July 1993, pp.1155-1164.
- [2]. P. G. Slade, J. L. Wu, E. J. Stacey, W.F. Stubla, R E Voshall, J. J.Bonk, J. Porter and LHong, "IEEE Utility Requirements for a Fault Current Limiter," IEEE Trans.Pwr Delivery, vol. 7, no. 2, April 1992, pp. 507- 515.
- [3]. M. M. R. Ahmed, Ghanim A. Putrus, Li Ran, and Lejun Xiao "Harmonic Analysis and Improvement of a New Solid-State Fault Current Limiter" IEEE TRANSACTIONS ON INDUSTRIAL APPLICATIONS, VOL. 40, NO. 4, JULY/AUGUST 2004.
- [4]. Gang Chen, Daozhuo Jiang, Zhengyu Lu, and Zhaolin Wu "Simulation Study on A New Solid State Fault Current Limiter for High-Voltage Power Systems" IEEE International Conference April 2004.
- [5]. Wu Zhaolin, Chen Pingping, Tan Lingyun, and Jiang Daozhuo, "Short Circuit Current Limiter in AC Network," Journal of Zhejiang University (SCIENCE), Vol. 2, No. 1, pp. 41-45, Jan.-Mar. 2001.
- [6]. T. Ueda, M. Morita, and H. Arita, "Solid-state current limiter for power distribution system", IEEE Trans. On Power Delivery, Vol.8, No.4, October, 1993, pp. 1796-1801.
- [7]. G.G. Karady, "Principles of a Fault Current Limiter by a Resonant LC Circuit," IEE Proceedings-C, vol. 139, no. 1, January 1992, pp. 1-6.
- [8]. Hector G. Sarmiento, C. Tovar and E. Molero, "A Feasibility Study for a Fault Current Limiter to reduce Voltage Sags at Sensible Loads," Power Systems Technical Conference, 1995, pp. 99-103.
- [9]. Gang Chen, Daozhuo Jiang, Zhengyu Lu, and Zhaolin Wu, "Simulation Study on A New Solid State Fault Current Limiter for High-Voltage Power Systems" 2004 IEEE International Conference on Electric Utility deregulation, restructuring and Power Technologies (drpt2004) April 2004 Hong kong.
- [10]. C. S. Chang, Member, IEEE, P. C. Loh, Student Member, IEEE, "Design Synthesis of Resonant fault current Limiter for Voltage Sag mitigation and Current Limitation".
- [11]. 3-Phase Fault Current Limiter for distribution systems Vijay K. Sood, Fellow, IEEE, and Shahabur Alam. 0-7803-9772-X/06/\$20.00 2006 IEEE.

Haptic System its Constituents and Application in Advanced Technology

A. Naveen Kumar, and B. Jyoti Ohri,

Abstract--Haptic is an emerging technology having vast scopes in the different areas such as medical, military training enhancement & performing evaluation task. It is a multidisciplinary field involving computer engineers, control engineers, biomechanics & neurologist. Although a lots of research work has been done in this field but still it has various transparency & stability issues in different disciplines, on which more work is needs to be done for better system's performance. A review of haptic system from its basic definition via subcomponents (haptic interface, haptic information and various rendering algorithm), the constituent parts of subcomponents (sensors and other measuring elements) and working of its along with the various issues in different discipline, is presented here.

Index Terms--Fault Haptic, interface, sensor, information & rendering algorithms

I. INTRODUCTION

HAPTIC is a Greek word “Haptethai” which means sense of touch i.e. contacts. Haptic system refers to the science of manual sensing (via sensor tactile or kinesthetic) and manipulation of surrounding objects and environment in the virtual world and vice-versa [1]. Objects and environments rendered in the virtual world may be reality based or some imaginary. Haptic makes virtual object seems real, much interactive and tangible. It makes touch a unique sense similar to human sense system and enable the bidirectional flow of energy which connects the virtual world with real. In haptic system, input is taken from user in terms of force, velocity or acceleration. This input is sensed by haptic sensors and these sensors convert it to electrical form with the help of transducers inside the haptic interface. This input signal is then executed in the virtual world using rendering algorithm. Interaction between the objects & environment in

the virtual world is transferred to user in terms of force or velocity called haptic feedback. Hence when user interacts with the virtual world through haptic interface, it feels realistic.

It is multidisciplinary [1] field of technology which includes neurophysiology, psychology, biomechanics and different disciplines of engineering such as mechanical, computer & control etc. Here neurologist have the role of

understanding the working & behavior for perception of information through nerves, psychologist for understanding the working of human actuation system under brain signals. Biomechanics & mechanical together have role for designing the mechanical user interface with best perception and actuation useful for biomedical & other applications. The computer engineers have the key role for implementing, interacting and evaluation the behavior of objects & environment in virtual world. Control engineers have role to make an analysis of coupling between virtual & real world and maintain the transparency & stability of the system so that the information reached to user would be same as generated into virtual world and vice-versa.

In the haptic system, as like human sensing system, there are sensors to measure the force, temperature, surface, vibration and position of the user. There are actuators, controller which works like human muscle and brain respectively. By these actuators, it provides the feedback whereas, with controller it handle all activities in the system. It further have a haptic device in which all virtual tasks are to be performed and haptic interface system which combine the haptic device's virtual environment with real world. There are different haptic rendering algorithms such as tool based rendering algorithm, contact-model algorithm and direct-hand rendering algorithm for implementing, interacting and evaluating the behavior of objects & environment in the virtual world [2, 3].

Haptic system has wide range of application in the cutting edge instruments. It has been accomplished in medical domain for evaluating the training skill and improves the performance of medical interventions [4], in military for training the combatant before placing in the adversary environment [5].

II. HAPTIC SYSTEM

Haptic is science of manual sensing and implementing the objects & environment into virtual world. In the haptic system, as like human sensing system, there are sensors to measure the force, temperature, surface, vibration and position of the user, there are actuators, controller which works like human muscle and brain respectively. By these actuators, it provides the feedback whereas, with controller it handle all activities in the system.

A working of haptic system is similar to human sensory and

actuation system. Taking an example to grasp the glass of water, if a person want to grasp it, first, person have to make an image of location, shape, texture of surface, analyze the mass, force required for it. Then a command signal will be generated by brain, transferred to hand via nerve system, muscles acting as actuator. During the process, relative information of hand such as direction, location, force required are continuously transferred to brain for better controlling the movement. This information is called haptic information. When hand is near by the glass speed decrease, fingers moves according the shape of glass. Then similarly, in machine system sensing (skin) task is perform by sensor, muscle task are performed by actuators and brain task performed by controller as shown in fig. 1.

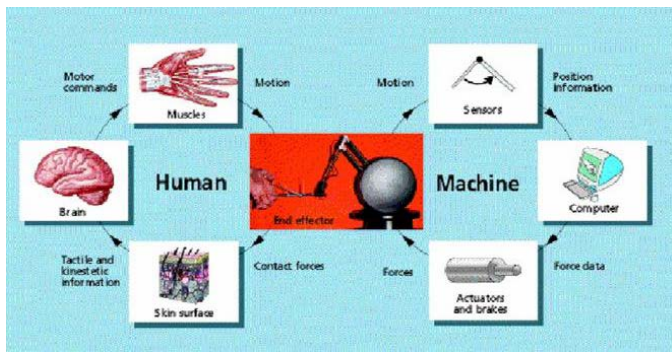


Fig. 1. Haptic sensory system similar to human [6]

A haptic system is a combination of basically three segments: haptic interface, haptic information and rendering algorithms.

A. Haptic Interface

An interface is mechanical part of haptic system which connects virtual world to the real world and enables the signal flow in terms of force, velocity & acceleration. It is considered as two port network as in [7]. It covers everything between user and virtual environment such as haptic device, virtual coupling and other components as shown in fig. 2. It gives feedback to user in form of force or velocity. An input to interface is in terms of either velocity or force results in either force or velocity as shown in fig. 2. v_c & f_h are the human/user velocity and force respectively. This input is then converted to the electrical equivalent with the help of sensors & transducer. Information inside the system is in discrete form. So v_c^* & f_h^* shows velocity & force information in discrete one [8].

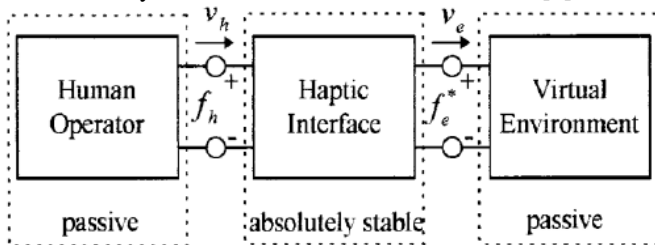


Fig. 2. Haptic interface combining human operator & virtual environment.

In the haptic interface, there are two key issues which are required to consider while designing: Transparency & Stability of system. Transparency here means the amount of input signal in terms of force or velocity, which is applied at input terminal of device should reached to the virtual world and in feedback cycle, amount of signal developed by the mutual interaction of objects and environment in the virtual world should reached to user. In the haptic system, due to disturbance signal which is consist of un-modeled dynamics of system, noises, uncertain parameter's, signal gets disturbed and results reduction in transparency. Maximize the transparency will results more realistic feel by haptic system and vice-versa. Stability here means response of system gets settle over certain period of time. In the absence of stability, system may vibrate or reduce the performance of the system. Since haptic system actively generate physical energy in the form of haptic feedback, which may lead system to unstable or can give a physical threat to user. Control engineers are here required to analyze various cause and effects of instability related issues. They also require to maintain the system's transparency so that the signal generate due to interaction between the objects in the virtual world can be transferred to user in the same extent and interaction feels more realistic. A work has been proposed by Eom et al in [9] to maintain the transparency and stability of one degree of freedom haptic system.

Haptic interface is combination of haptic display and virtual coupling as shown in fig. 3. Both of these are also two port network. On the one end there is human/user force, and on the other end, there is virtual environment.

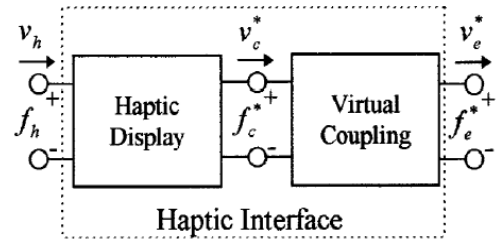


Fig. 3. Haptic

1. Haptic Display

A Haptic Display as shown in fig. 4, includes the physical structure of manipulator as well as actuators, sensors (tactile & kinesthetic) to capture the input information, analog filters for rejection of noise signal in analogues form, amplifiers to boost the weak recognized signal, DAC & ADC for conversion of signal to other required form, digital filters and virtual environment as control software. It has two haptic ports, first one is physical port, a handle to which a user transmits and receives the energy. Other one is information port, having discrete variable, velocity and force.

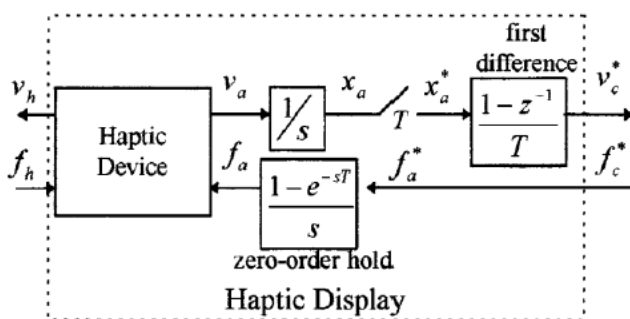


Fig. 4. Haptic display

Here first signal is amplified and then it is discretize using sample & hold circuit and in feedback, a discrete signal is convert back to analogues one using zero order hold (ZOH) circuit as shown in fig. 4.

Two type of haptic display are there which either “measure motion & display force” or “measure force & display motion”. First one is called impedance display having V_c a velocity at coupling end, as output. And later one is admittance type having V_c as an input and force f_c a coupling force, as output [8]. An impedance type display is commonly used, is consist of optical encoder or potentiometer to measure device position. It measure the device position, then discretize it at sampling rate “T” then device velocity is measure using different method, here first difference approximation. The digital force signal is converted to analogue and then given as input to actuator for feedback force to user. An admittance display is used in industries where high inertia requires. Both impedance type and admittance display are shown in fig. 5.

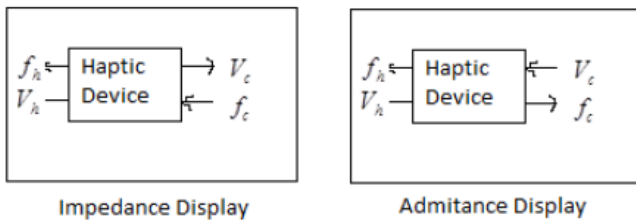


Fig. 5. Types of haptic display

2. Virtual Coupling

Virtual coupling implementation is a part of haptic interface. It have various control elements and impedance matching circuitry to couple the device with the virtual world such that interface is stable [8]. It is also a two port network designed to specific topologies, explicit design criteria. These are classified in two ways: impedance type and admittance type. Impedance display uses impedance virtual coupling, which induces a limit on the maximum impedance that can be rendered. In effect, it acts a spring-damper placed between the virtual environment and the haptic display. It never allows the virtual environment to drive the system unstable by generating an excessively rigid constraint. For admittance display,

admittance virtual coupling are used which acts as a frequency-dependent damper, providing the required level of impedance to stabilize the system. For performance, we would like impedance to be as small as possible, permitting unconstrained free motion, while still meeting the requirements for absolute stability.

B. Haptic Information

It is the immersive element of the haptic system called as signal information. A haptic perception system is similar to human sensing system. It perceives information in two ways: Tactile information & kinesthetic information. This information's are tracked by tactile and kinesthetic sensors. Tactile information emulates the force, texture & temperature of the surface whereas kinesthetic information emulates the angle at different joints of end effectors.

Tactile sensors are being sensitive device with a limited range of displacement (in millimeter range). These sensors are mounted on end effector to makes highly continuous measurement of force and pressure. These provide the geometric profile of the touched object. A most popular tactile sensors uses are conductive elastomer, piezoelectric effects or piezoresistive properties to measure the contact force profile. Generally used tactile sensors are piezoresistive sensors because of their sensing and stiffness ability for small force measurement. These sensors are consists of force sensing resister (FSR) elements as shown in fig. 6(a).

They have elastic pad over the sensor called elastic overlay to contact with non-uniform surface as shown in fig. 6(b). An array of FSR consists of 16 X 16 matrix of pressure sensing points respectively [10]. These FSR elements have decreasing electrical resistance. FSR elements sense the compression force so that these are placed on rigid back. The elastic overlay limits the force applied on FSR through a damping effect and hence ensure the physical protection of FSR.

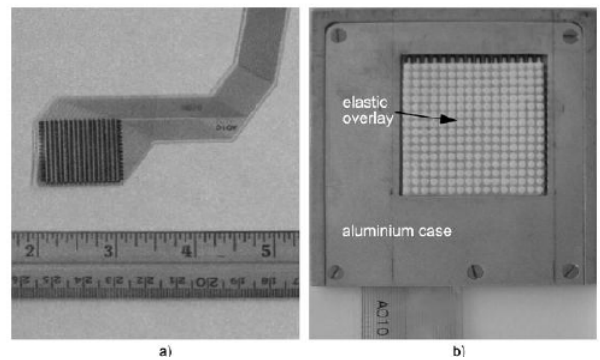


Fig. 6 a). Force sensing resister array, and b) Elastic overlay mounted on it

When an object force is applied on the sensor device, it is transmitted through an elastic overlay to force sensitive array of transducers as shown in fig. 6(b). The elastic pad here, acts

as low pass filter as well as displacement to force convertor while force sensor array accomplishes a two dimensional sampling and a one direction sensing. This principle of operation is shown in fig. 7.

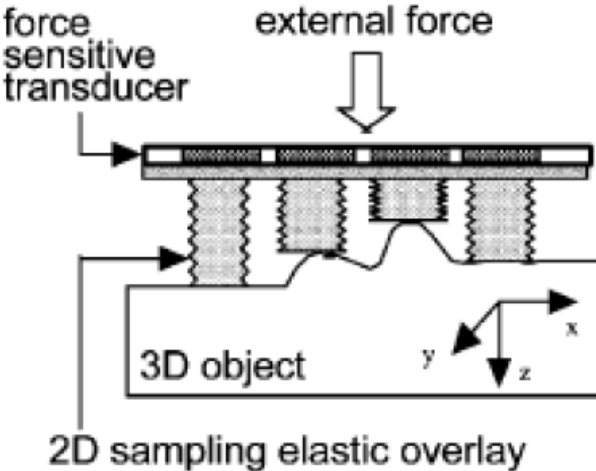


Fig. 7. Principle of operation of FSR.

Kinesthetic information is measured through the sensors situated in the joints as shown in fig. 8. These sensors measure the joint angle continuously and then calculate the position of end effector with the help of kinematic matrix.



Fig. 8. Kinesthetic sensor at joints.

C. Haptic Rendering Algorithms

Rendering algorithms are also major element of haptic system. These algorithms have the computational technology that allows us to interact with the virtual world. It depends on the various algorithms that simulate a virtual world similar to real and compute the interaction in terms of force, velocity & acceleration. Various algorithms are present today for simulating this. The main objective of these algorithms is to simulate a virtual system that feels real, control the movement of the objects and compute the real time interaction in terms of force & velocity between them. Then this information transferred to the real world considering the various coupling effect which gives slow update simulation. Various approached have been used by authors and found the

fundamental approached for modeling a complex contact is to maximize the efficiency of collision detection, dynamics simulation and collision response algorithm in [11, 12, 13]. Performance of these algorithms may be limited by scene complexity [3]. To overcome the above drawbacks Carloss et al. have presented some algorithm which are: tool based algorithm, robust contact modeling algorithm and direct algorithm. A tool based algorithm simulate the virtual design of tool, objects and environments while a robust contact modeling algorithm execute contact velocity & force between tool and other objects in the virtual environment whereas a direct hand rendering algorithm track & computes the force & velocity to be transfer for the user [3].

So the reader's objective should be to find such an approach which has generalized behavior over complexity of different scene so that system transparency would maximize.

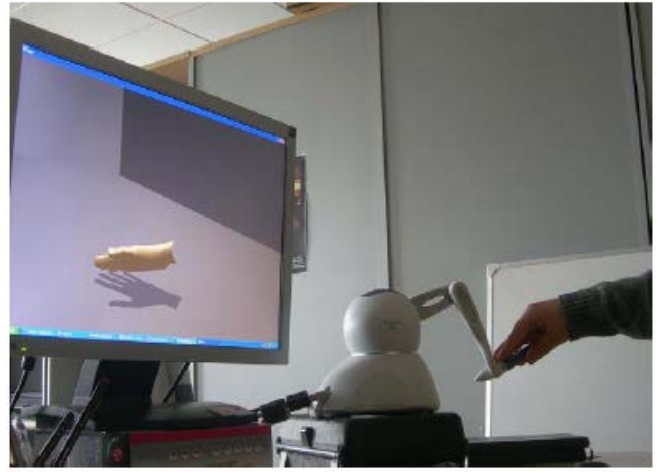


Fig. 9. Haptic manipulation of hand in virtual environment

III. APPLICATIONS

Haptic system has numerous applications in the training and performance enhancement for medical officers, combat in military and pilots.

A. Medical Application

In medical profession, clinical skills strongly rely on sense of touch along with the anatomical and diagnostic knowledge. Haptic feedback has key role in medical technology. For example, a surgeon makes an incision, a dental surgeon drills into a carious lesion or veterinarian sutures a wound. The use of haptic technology is yet to maximize in training. Earlier simulator was based on force feedback glove which was created for abdominal palpation to detect subsurface of liver tumor [14]. It featured with multiple finger support and used into deformation depth for lookup in force detection curves [14]. Later PHANTOM devices were also used in the medical technology. Haptic system have vital role of training, task improvement & performing from far end.

1. Medical Examination Evaluation & Training

Haptic system have vital role in medical training to the researchers and young medical officers with the help of haptic simulator. These simulators provides various realistic objects in medical professions and discipline including surgery, interventional radiology, veterinary medicine and allied health professions, to work upon along with haptic feedback. Human haptic perception and execution system are used for medical examination and procedures enhancement in institutes shown in figure 10-12. A fig. 10 shows close-up view of palpation interaction on a virtual patient for the medical trainee. By applying the action as shown in fig. 11 by robotic manipulator, effect of same can be seen on the virtual patient shown in fig. 10. The overall process and interaction between the medical trainee and virtual patient can be seen in fig. 12. These also provide a vital role in evaluation of clinical skill [4].

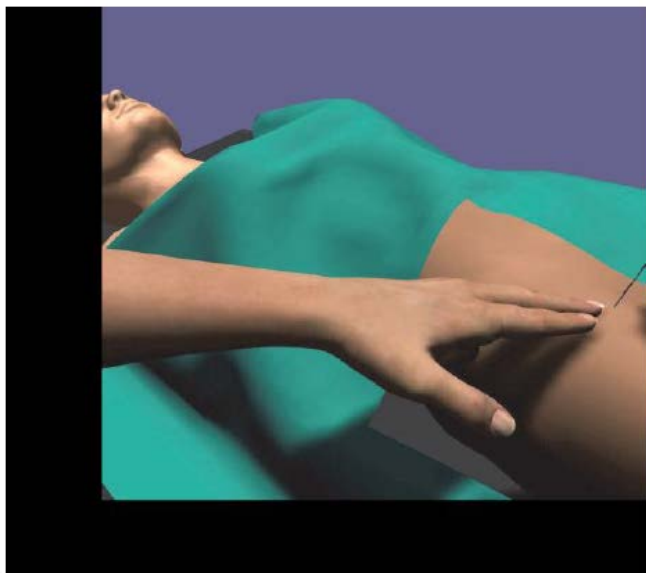


Fig. 10. A close-up view of palpation interaction on a virtual patient.

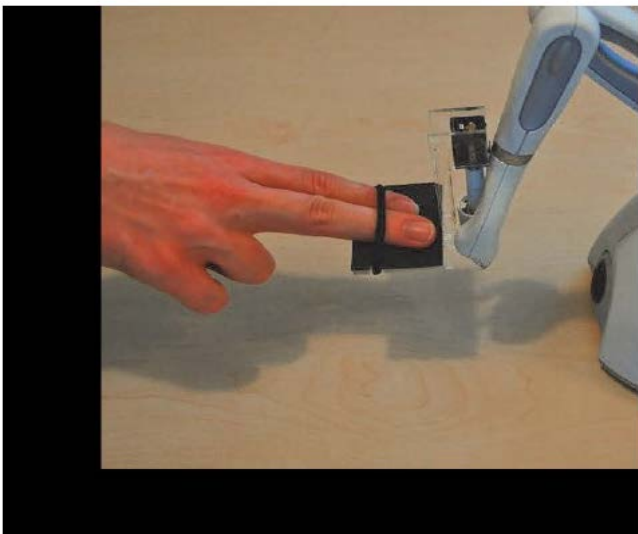


Fig. 11. A light weight palpation pad as a hardware for a haptic device.

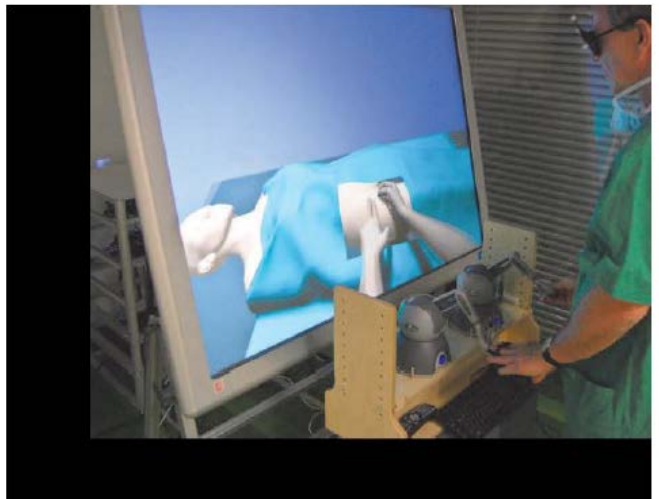


Fig. 12. Medical training simulator prototype used in medical expert.

2. Medical Intervention

With the help of haptic feedback system, medical officer can perform various remote surgeries from a central location with less intervention as shown in figure 10-12. Hence this technology saves time as well as a skilled professional can serve to a number of patient sitting on a single place [4, 15].

B. Military: For training of combat

Haptic systems are very useful in the training of military person by providing them realistic environment with haptic feedback to trainer through tactile and other kinesthetic sensors. In this particular system, a simulator develop virtual environment and enemy seems real.

The combat attacks them and simulator changes the condition as per realistic environment. These types of technical aid reduce the risk of lives and money for the organization and prepare the combat according to various critical situations.



Fig. 13. Haptic system for training the combat.

Haptic system simulators are also useful in air force and pilot training. It provides the realistic adversary environmental condition through big display. The user here moves there on and condition inside the simulator changes as per direction given by user. This system provides the feedback to user in terms of force, velocity & sound so that a pilot here feels realistic and can experience & improve his skills to worst condition [5].

IV. CONCLUSION

Haptic system have huge potential to work in different areas such as training and performance enhancement for medical officers, combat in military and pilots. Although a lots of research work has been done in the field of haptic but still various issues related to transparency & stability including sensing system, perception of information and simulation of complex scene are there for researchers of different discipline to work upon. Before starting the work, a researcher should have knowledge of various components & working of all domain for better understanding of system and hence performance.

V. REFERENCES

- [1]. Abdulmotaleb El Saddik —Potential of Haptic Technologyl IEEE Instrumentation & Measurement Magazine, pp. 10-17, Feb. 2007
- [2]. http://www.springer.com/cda/content/document/cda_downloaddocument/9783642226571-c1.pdf?SGWID=0-0-45-1205038p174133657
- [3]. Carlos Garre, Miguel A. Otaduy —Haptic rendering of objects with rigid and deformable partsl Computers & Graphic (Elsevier), 34, pp. 689-697, 2010.
- [4]. Allison M. Okamura, Sarah Baillie and William S. Harwin, —Haptics in Medicine and Clinical Skill Acquisitionl, IEEE Trans. on Haptic, Vol. 4, No. 3, pp. 153-154 July-September 2011.
- [5]. <http://www.sis.uta.fi/~hui/mobile/papers/Immonen-paper.pdf>
- [6]. <http://citeseerx.ist.psu.edu/viewdoc/download?doi=10.1.1.19.3058&rep=rep1&type=pdf>
- [7]. Zhang J, Li J, —Stability Control of Haptic Interfacel, Proceeding of IMECE 2007/ ASME Int. Mechanical Engineering Congress and Exposition, pp. 1-6, Nov. 2007.
- [8]. Richard J. Adams and Blake Hannaford, —Control Law Design for Haptic Interface to Virtual realityl, IEEE Trans. on Control Systems Technology, Vol. 10, No. 1, pp. 3-13, January 2002.
- [9]. K.S.Eom, I.H.Suh, and B.-J.Yi, —A Design Method of Haptic Interface Controllerl Proceedings of 2000 IEEE/RSJ Int. Conf. on Intelligent Robotics and Systems, pp. 961-966, 2000.
- [10]. 8Pierre Payeur, Codrin Pasca, Ana-Maria Cretu and Emil M.Petriu, —Intelligent Haptic Sensor System for robotic manipulationl, IEEE Transaction on Instrumentation and Measurement, Vol. 54, No. 4, August 2005.
- [11]. McNeely W, Puterbaugh K, Troy J, —Six Degree-of-Freedom Haptic Rendering Using Voxel Samplingl, Proceedings of ACM SIGGRAPH, pp. 401–408, 1999.
- [12]. http://www.google.co.in/url?sa=t&rct=j&q=&esrc=s&source=web&cd=2&cad=rja&ved=0CDkQFjAB&url=http%3A%2Fwww.cs.utah.edu%2Fgdc%2Fpublications%2Fpapers%2FTVCGSIHapticsDJohnson.pdf&ei=8hrQUo22NsO_rgfLyoBg&usg=AFQjCNFPIuTqSpSfdI7amTa8JVveirAs6VQ&sig2=0CXAdEYyxrl8lyNSBnT1zvQ&bvm=bv.59026428,d.bmk
- [13]. <http://citeseerx.ist.psu.edu/viewdoc/download?doi=10.1.1.19.3058&rep=rep1&type=pdf>
- [14]. M. Dinsmore, N. Langrana, G. Burdea, and J. Ladeji, —Virtual reality training simulation for palpation of subsurface tumorsl, in Proceedings of the 1997 Virtual Reality Annual International Symposium (VRAIS '97), pp. 54–60, Mar. 1997.
- [15]. Sebastian Ullrich, Torsten Kuhlen, —Haptic Palpation for Medical Simulation in Virtual Environmentsl, IEEE Trans. On Visualization and Computer Graphics, Vol. 18, No. 4, pp. 617-625, April 2012

Transient Stability Assessment of Multi Machine Power System and Enhancement Using Facts

A. Alok Pratap Singh, B. Kartik Kumar, and C. Malvika Upadhyay

Abstract--This paper discusses Extended Equal Area Criteria (EEAC) and conversion of multi machine power system into Single Machine Infinite Bus (SMIB) to apply Equal Area Criteria (EAC) for transient stability of multi machine power system using the parameter Critical Clearing Time (CCT).This paper also discusses about the facts controller in enhancing the transient stability and effect of them over CCT.

Index Terms--Equal area criteria, Extended equal area criteria (EEAC), Critical clearing time, Clearing time (CT), Single machine infinite bus.

I. INTRODUCTION

POWER systems transient stability phenomena are associated with the operation of synchronous machines in parallel, and become important with long power transmission lines. Physically, transient stability is defined as the ability of power system to maintain machine's synchronous operation when subjected to heavy disturbance. As it is a strongly nonlinear and high-dimensional problem, to access it accurately, the numerical integration method can be used, which is commonly referred as the time-domain (T-D) methods. Historically, the time-domain methods came in the picture before the advent of computer. At that time the high dimensional nonlinear transient stability problem was reduced to simplified version and calculated manually. In this way the machine's swing curves were obtained [1] i.e. machine's rotor angle plot were evaluated.

Transient stability of a system refers to its capability of being stable when subjected to large disturbances such as instant faults, loss of generation or tripping of lines. This type of stability depends on the initial operation condition of the system and the severity of the disturbance as well. For any specified disturbance, there is always an associated power

A. Alok Pratap Singh, Department of Electrical Engineering , Indian Institute of Technology (BHU), Varanasi, India (e-mail: alok.eee12@iitbhu.ac.in).

B. Kartik Kumar, Department of Electrical Engineering , Indian Institute of Technology (BHU), Varanasi, India (e-mail: kartik.eee12@iitbhu.ac.in).

C. Malvika Upadhyay, Department of Electrical Engineering , Indian Institute of Technology (BHU), Varanasi, India (e-mail: malvika.eee12@iitbhu.ac.in).

transference limit, called the transient stability limit, above which the system will become dynamically unstable. Also, the transient stability limit is always below the steady-state stability limit [2]. It may have many different values, depending upon the nature and magnitude of the disturbance. The stability can be generally classified as rotor angle stability and voltage stability. I emphasize mainly on rotor-angle stability which depends upon t_{CCR} . Where t_{CCR} is defined as the maximum time interval between the instant of fault initiation and that of its clearing, up to which the power system remains transiently stable. There are two stability limits power limits and CCTs. As the computation of CCTs is easier than that of the power limits so computation of CCTs is more popular and useful. CCTs may be used to tell about a system directly that whether the system is stable or unstable.

Popular method based on graphical interpretation of kinetic and potential energy, known as Equal-Area Criterion (EAC) has been used since thirties for power system stability analysis. This method can be implemented on a one machine infinite bus (OMIB) system. The treatment of a large real system as a single machine equivalent (SMIB) is very popular and effective tool the EAC has been used to determine the transient stability limits and reduced the complete system into OMIB system this work is popularly known as Extended Equal-Area Criterion (EEAC) It is a direct method for computing critical clearing time (CCT)[3].

A much generalized application of EEAC on the basis of first-swing stability classifies the machines in any power network into two types Critical Machines (CM's) and Non-Critical Machine (NM's) mathematically. In revised EEAC for an assigned contingency (or fault, or disturbance) decompose the multi-machine system into two subsets: the “cluster of critical machine(s)” called for short the “critical cluster”, and the group of the remaining machines and two equivalent machines are replaced by an OMIB [4]. By doing the analysis of IEEE14 bus system when a fault occurred near a bus the machine affected most is considered as critical machine and the rest of others are called non critical machines and thus a number of machines is divided into two groups critical machines and non critical machines now they can be

simplified as one machine infinite bus(OMIB) and now the equal area criteria can be applied and assessment of transient stability can be done using the parameter critical clearing time(CCT).

The factors influencing the transient stability of power system are the transmission line reactance reactive power absorptions & injection.[5]. Since, transient stability of power system is directly related to the power flow in the transmission corridor and it is considered as a matter of energy balance. The mismatches in power can be well regulated by insertion of series and shunt capacitances by enhancing the power flow in the line [6].In this paper we have also simulated a model and shown the effect of facts device such as svc and series capacitors on the transient stability of power system and how the CCT can be increased so that system will remain stable.

II. EXTENDED EQUAL AREA CRITERIA (EEAC) & SINGLE MACHINE EQUIVALENT (SMIB)

The incapability of EAC for multi-machine power system paid attention towards other techniques for transient stability analysis. Extended equal-area criterion is basically the modification of EAC, in which a multi-machine power system is realized by two equivalent machines, namely critical machine (CM) & non-critical machine (NM), with equivalent inertia constant and centre of inertia (COI).

For a multi-machine system containing ‘n’ number of generator buses and loads are considered as constant impedances, n rotor angle second order differential equations, popularly known as swing equations and algebraic power flow equations are given by

$$M_i \frac{d^2 \delta_i}{dt^2} = p_{mi} - p_{ei} = p_{ai}$$

and

$$\left[p_{ei} = E_i \sum_{j=1}^n [G_{ij} \cdot \cos(\delta_i - \delta_j) + B_{ij} \cdot \sin(\delta_i - \delta_j)] \right] z$$

where

Pm= mechanical power input of ith generator, in p.u.

Pe = electrical power output of ith generator, in p.u.

Mi = inertia constant of ith generator

δ_m = rotor angle of the ith generator

Ei= emf behind transient reactance of the ith generator

G_i, B_i= real & imaginary parts of admittance

Neglecting the real part of all the admittances (resistances of the line) the power flow equations becomes very simple that has already been stated above in case of two machine model.

$$p_{ei} = \frac{E_i * E_j}{X_t} \sin(\delta_i - \delta_j) \quad \dots \dots \dots \quad (1)$$

$$M_c = \frac{d^2 \delta_c}{dt^2} = p_{mc} - p_{ec}$$

Where

$$M_c = \sum_{i \in CM's} M_i \text{ and } \delta_c = \frac{1}{M_c} \sum_{i \in CM's} M_i \delta_i$$

And

$$M_n \frac{d^2 \delta_n}{dt^2} = P_{mn} - P_{en}$$

Where

$$M_n = \sum_{i \in NM's} M_i \delta_n = \frac{1}{M_n} \sum_{i \in NM's} M_i \delta_i$$

Now converting these two machines equivalent to single machine equivalent (SIME) by considering the equivalent rotor angle deviation

$$\delta = \delta_c - \delta_n$$

The equivalent swing equation is given as

$$M \frac{d^2 \delta}{dt^2} = P_m - [P_o + P_{e,max} \sin(\delta - \theta)]$$

Where

$$M = M_c M_n M^{-1}_r$$

$$M_r = \sum_{i=1}^n M_i$$

$$P_m = [M_n P_{mc} - M_c \sum_{i \in NM's} P_{mi}] M^{-1}_r$$

$$P_o = \left(M_n E_c^2 G_{cc} - M_c \sum_{i,j \in NM's} E_i E_j G_{ij} \right) M^{-1}_r$$

$$P_{e,max} = \sqrt{C^2 + D^2}$$

$$\theta = -\tan^{-1}(C/D)$$

$$C = (M_n - M_c) M^{-1}_r \sum_{i \in NM's} E_c E_i G_{ci}$$

$$D = \sum_{i \in NM's} E_c E_i B_{ci}$$

If we neglect the resistance of the lines, the above equations become very simple after substituting values of θ , C, P_o to zero.

$$M \frac{d^2 \delta}{dt^2} = P_m - P_{e,max} \sin \delta$$

$$P_{e,max} = \sum_{i \in NM's} E_c E_i B_{ci}$$

These are very interesting expressions and similar to the equations derived for OMIB system. This method will be graphically supported for a 14-bus test system in the case study.

III. TRANSIENT STABILITY ENHANCEMENT USING FACTS

From the power flow equations stated above, the power flows in the line depend upon the voltage magnitude of the bus, phase angle difference of the bus voltages and the impedance of the line. The concept behind FACTS controllers are to enable control of these parameter in real-time and, thus, vary the transmitted power according to system conditions. The ability to control power rapidly, within appropriately defined boundaries, can increase transient and dynamic stability, as well as the damping of the system. For example, a change in line reactance X changes the power flow in the line. For a given power flow, a change of X also change the phase angle between the buses. Regulating the magnitude of bus voltages also changes the power flow. The real power flow is more sensitive to the change in line reactance and phase angle difference and reactive power flow is more coupled with voltage magnitude of the buses. For the entire FACTS controller, the STATCOM/SVC/VRT has the ability to increase or decrease the terminal voltage magnitude in turn, enables reactive power exchange. STATCOM injects the current always in quadrature (either capacitive or inductive) with bus voltage. SVC is basically a variable susceptance connected in shunt with the power network. VRT changes the voltage magnitude at either side of the line by changing tapping. The SSSC controls the active power flow by injecting a series voltage in quadrature with the line control. Same can be done by direct controlling of line reactance in case of TCSC. TCPAR changes the angle difference between the buses for the same. UPFC can control all these parameters independently for controlling active and reactive power flows simultaneously [7].

IV. CASE STUDY AND RESULTS

(A) Transient Stability Assesment (IEEE 14 Bus Test System)

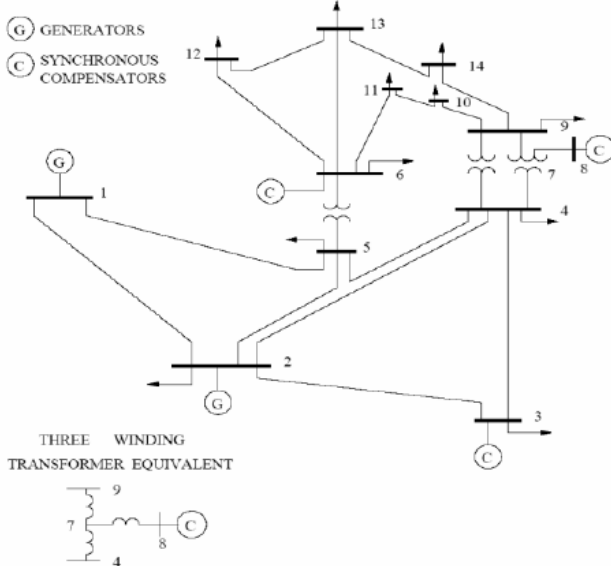


Fig.1: IEEE 14-Bus, 5-Machine System

The rotor angle differences of all the generators connected at generator buses of 14-bus, 5 machine test system (Fig: 1) followed by a three phase to ground fault near several buses have plotted and new steady state rotor angle is evaluated after tripping faulty line. Bus-2 is the swing bus and bus-1 is generator bus. Two synchronous compensators are connected at bus bus-6 and 8. Rest are load buses. After fault, some of the generators are separated from the system called as critical machine group and the remaining are termed as non-critical machine group. If the fault is occurred on line 3-4 near bus-4, the machine at bus-8 forms critical machine group. The CCT measured is 305 ms. In Fig: 2, it is clearly seen that the rotor angle of machine at bus-8 decelerates and getting unbounded from the remaining system. If fault is cleared within the CCT (Fig: 3), then also deviation in δ_8 is more compared to remaining system. Similarly, fault on line 1-5, near bus-5 is simulated at 330 ms (Fig: 4) and 310 ms (Fig:5) after and within CCT (315 ms) respectively.

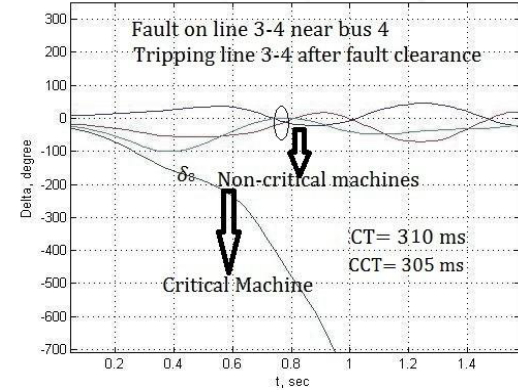


Fig. 2: Fault on line 3-4 near bus-4, cleared after CCT

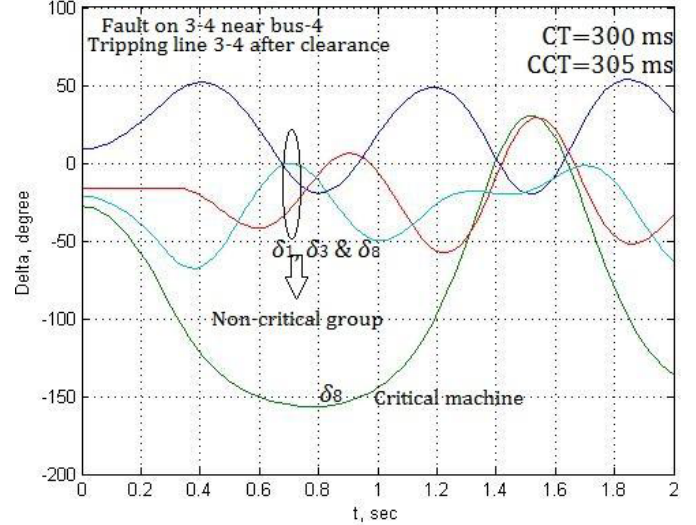


Fig. 3: Fault on line 3-4 near bus-4, cleared within CCT

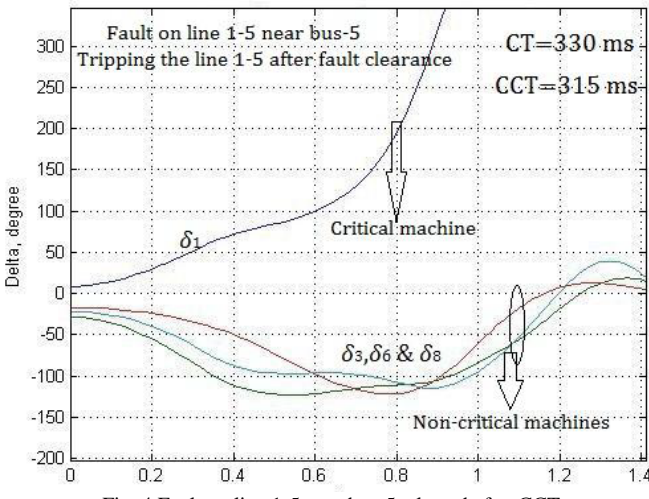


Fig. 4 Fault on line 1-5 near bus-5, cleared after CCT

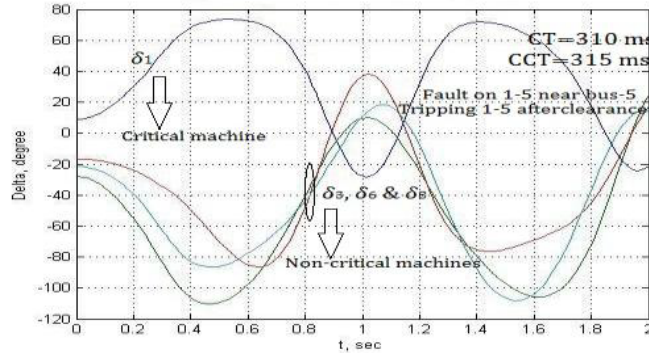


Fig. 5 Fault on line 1-5 near bus-5, cleared within CCT

(B) Transient Stability Enhancement Using Facts

(1) A Two Machine System

Two generating unit of power rating 5000 MW and 1000MW is connected through a two single circuit transmission lines (connected at a bus B₂) and feeding a load of 5000 MW connected at the large generating unit. The line flow is 950 MW. Although the PSS's are installed at each generator for multi-swing damping, we are concentrating on first swing stability and computing CCT. A three phase ground fault is taken at the bus B₁,

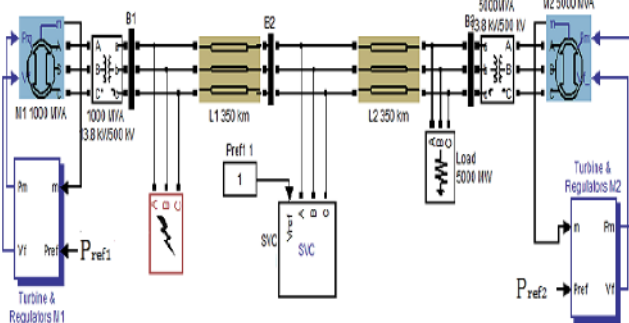


Fig. 6. Two machine model with SVC

The CCT obtained without SVC is 87 ms and fault clears at 88ms. If SVC of reactive power rating 500 MW, then CCT will increases to 141 ms. The Plot of voltage magnitude at different bus, power flow in the line, the phase difference between buses B1& B3, the angular speed of machines and the generator terminal voltages is shown in Fig: 7. In Fig: 8 these parameters have plotted when the CCT=141ms with SVC.

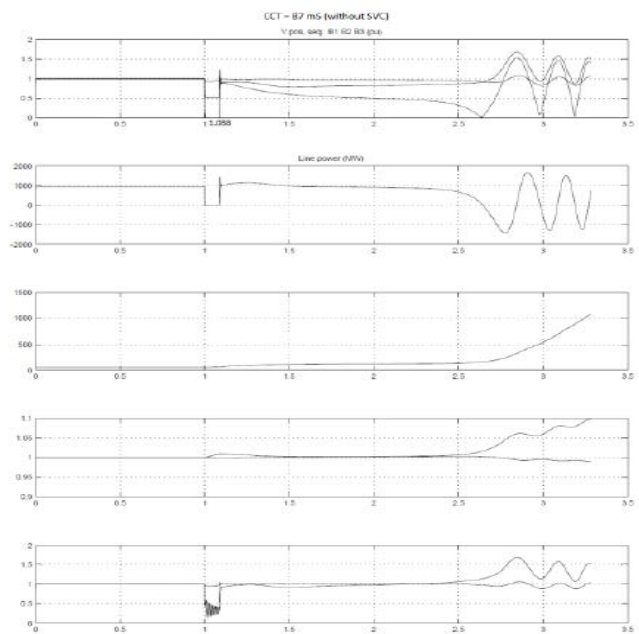


Fig. 7: Two machine system plot without SVC

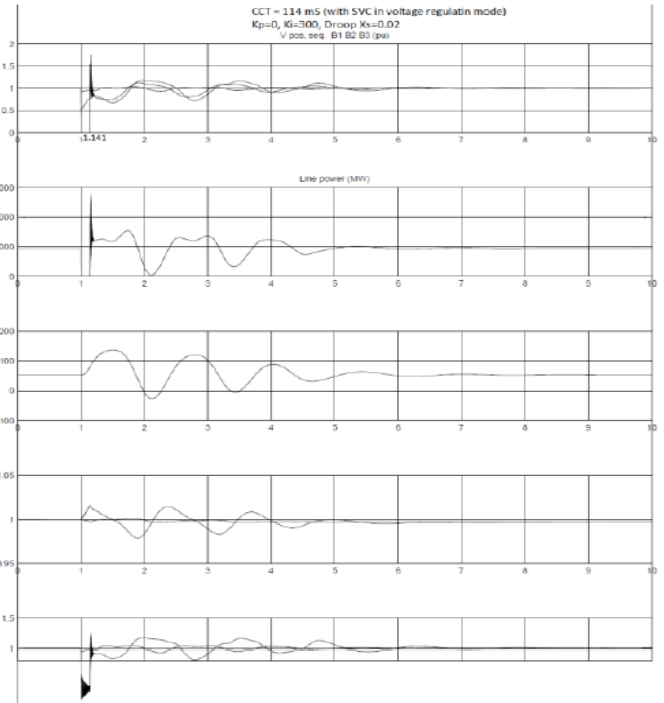


Fig. 8: Two machine system plots, Clearing time is 141 sec with SVC.

Thus we concluded that the unstable system without svc for a clearing time more than 87ms is transformed into a stable system with svc as CCT is increased from 87ms to 141ms.

(2) A Single Machine Infinite Bus System

Consider a test system, a generator having inertia constant $H = 5 \text{ MJ/MVA}$ and a direct axis transient reactance $X_d' = 0.3 \text{ p.u.}$ is connected with an infinite bus through a transformer of leakage reactance 0.2 p.u. and a purely reactive double circuit line of reactance 0.3 p.u. per phase. Simulating a bolted fault at the middle of any of the line and tripping by operating circuit breakers. The power angle plot is shown in Fig: 5. the critical clearing angle and CCT are found to be 98.83° and 289.6 ms . The initial power flow is $S = 0.8 + j0.074 \text{ p.u.}$

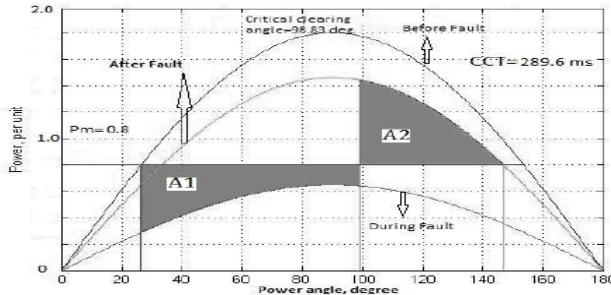


Fig. 9: Power angle curve without series capacitor

If a capacitor of reactance $-j0.15 \text{ pu}$ is connected in series with the un-affected line, the CCT is increased to 314 ms . The power angle curve in Fig: 10 shows the increase in critical clearing angle clearly. If a series capacitor of reactance $-j0.15 \text{ p.u.}$ is more added for some time, the CCT is increased to 334 ms..

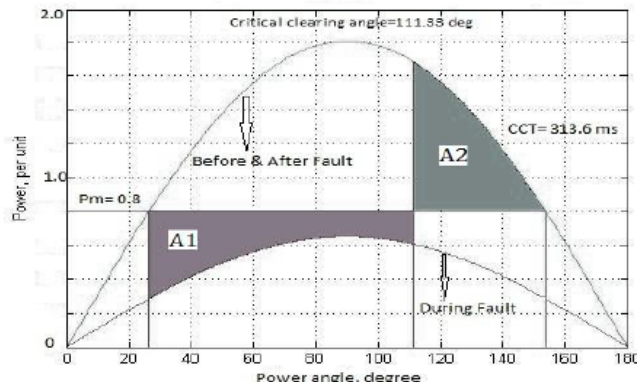


Fig. 10: Equal-area criterion depicting critical clearing with series capacitor

V. CONCLUSION

Transient stability analysis is studied by different methods for SMIB system, two machine model and for multi-machine system also. Different approaches for analysis are observed out of which EEAC and new simplified version of single machine equivalent is more suitable and takes less computation time. We have seen that the transformation of multi-machine system into single machine equivalent for transient stability analysis and CCT computation needs less effort. The effect of SVC and series capacitor on transient stability is studied. Use of these FACTS controllers enables increase in stability margin (increase CCT) of a power system.

VI. REFERENCES

- [1]. R.H. Park and E.H. Bancker. "System Stability as a Design Problem" AIEE Trans., 48:170–194, 1929.
- [2]. Edward Wilson Kimbark" Power system stability, volume 1," IEEE Press, 445 Hoes Lane Piscataway, NJ 08855, 1995, A John Wiley & sons, inc., publication, Hoboken, New Jersey.
- [3]. Dhal, H.H. Skilling and M.H. Yamakawa. "A Graphical Solution of Transient Stability". Electrical Engineering, Vol 59: 462–465, 1940
- [4]. Y. Xue, Th. Van Cutsem, and M. RibbensPavella. "A Simple Direct Method for Fast Transient Stability Assessment of Large Power Systems".IEEE Trans. on PWRS, PWRS3: 400–412, 1988.
- [5]. P. Kundur: "Power system stability and control" (McGraw- Hill, 1994), pp. 1103-127.
- [6]. P.M. Anderson and A.A. Fouad, "Power system control and stability" IEEE Press, A John Wiley & Sons Publication, 1977.
- [7]. N.G.Hingorani and L.Gyagyi" Understanding FACTS concepts and technology of flexible AC transmission systems," IEEE Press, New York, 2000.

Performance Investigation of PID and Hybrid Controllers for Speed Control of Induction Motor using Direct Field Oriented (DFO) Control Technique

Shobha Rani, S. P. Singh, *Member, IEEE*, A. K. Gautam, *Student Member, IEEE*

Abstract—In this work, we have done speed control of a direct field-oriented induction motor (DFOIM) using a PID plus fuzzy logic control (FLC) Technique. The reason behind the selection of PID because its parameter values can be chosen using a simple and useful rule of thumb. The FLC is developed based on the output of the PID controller, and the output of the FLC is the torque command of the DFCIM. The simulation has been carried out on a 0.14 hp induction motor and resulting waveforms are obtained under different stiff conditions to exhibit the effectiveness of the proposed controller and investigate the starting and transient performance of drive using a PID plus fuzzy logic control (FLC) scheme in MATLAB/SIMULINK environment. Moreover the performance comparison between the PID controller and the hybrid (PID + Fuzzy) controller is also carried out.

Index Terms—Direct Field oriented Induction motor(DFOIM), Induction motor, Fuzzy Logic Control (FLC), Performance Investigation etc.

I. INTRODUCTION

IN recent years, field-oriented induction machine (FOIM) drives have been increasingly utilized in motion control applications due to easy implementation and low cost. Besides, they have the advantage of decoupling the torque and flux control, which is the desirable feature. However, the decoupling control feature can be adversely affected by load disturbances and parameter variations in the motor so that the variable-speed tracking performance of an IM is degraded. In general, both conventional PI and PID controllers have the difficulty in making the motor closely follow a reference speed trajectory under torque disturbances. To overcome this difficulty, an effective and robust speed controller design is needed.

Shobha Rani, S. P. Singh, and A. K. Gautam are with Department of Electrical Engineering, Kamla Nehru Institute of Technology, Sultanpur-228118, India (e-mail:saxenashobha7@gmail.com, singhsurya12@gmail.com, and abhinavgautam97@gmail.com).

Hence fuzzy-logic-based intelligent controllers have been proposed for speed control of FOIM drives. These intelligent controllers are associated with adaptive gains due to fuzzy inference and knowledge base. As a result, they can improve torque disturbance rejections in comparison with best trial-and-error PI or PID controllers. Nonetheless, no performance advantages of intelligent controllers in combination with a PI or PID controller are investigated.

Fuzzy control is a non-linear control and it permits the design of optimized non-linear controllers to improve the dynamic performance of conventional regulators. Due to the various advantages and applications, a hybrid PID plus fuzzy controller consisting of a PID controller and a fuzzy logic controller (FLC) in a serial arrangement for speed control of FOIM drives, more specifically, direct field-oriented IM (DFOIM) drives is proposed. Moreover a fuzzy logic controller is designed to carry out fuzzy tuning of the output of the PID controller to issue adequate torque commands.

II. MATHEMATICAL MODELING OF INDUCTION MOTOR

A. Equivalent circuit model

To analyze the operating and performance characteristics of an induction motor, an Equivalent Circuit can be drawn.

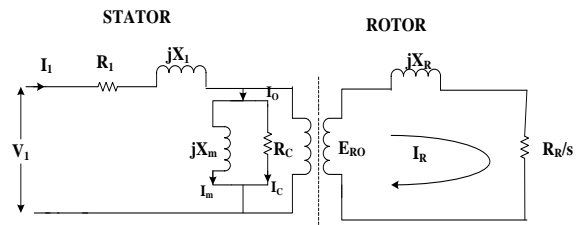


Fig.1 Equivalent circuit of one-phase out of three-phase of an induction motor
Let I_1 =Stator current per phase

R_1 =Stator winding resistance per phase

X_1 =Stator winding reactance per phase

R_R and X_R are the rotor winding resistance and reactance per phase, respectively

I_R =Rotor current

V_1 =Applied voltage to the stator per phase

$I_0 = I_c + I_m$

I_m =Magnetizing current

I_c =Core-loss component of current

Induced voltages

Let E_{R0} be the induced voltage in the rotor at stand-still

$$\therefore E_{R0} = 4.44N_R \Phi_m f_r \quad (1)$$

Since $f_r = f_e$, at standstill,

$$\therefore E_{R0} = 4.44N_R \Phi_m f_e \quad (2)$$

If E_R is the induced voltage in the rotor winding with, $f_r = sf_e$, ($s \neq 1$) then

$$E_R = 4.44N_R \Phi_m f_r \quad (3)$$

$$E_R = 4.44N_R \Phi_m s f_e \quad (4)$$

. From eq. (2.3) & (2.5)

$$E_R = sE_{R0} \quad (5)$$

Rotor current

$$I_R = \frac{E_R}{R_R + jX_R} = \frac{s.E_{R0}}{R_R + s.jX_{R0}} \quad (6)$$

$$I_R = \frac{E_{R0}}{\frac{R_R}{s} + jX_{R0}} \quad (7)$$

Transformation is done using the effective turns ratio, a_{eff} for currents

$$I_2 = \frac{I_R}{a_{eff}} \quad (8)$$

Impedance transfer is made using the a_{eff}^2 ; where R_2 and X_2 are transferred values

$$R_2 = a_{eff}^2 R_R$$

$$X_2 = a_{eff}^2 X_R$$

Phase impedance is given by

$$Z_{in} = R_1 + jX_1 + \frac{jX_m \left(\frac{R_2}{s} + jX_2 \right)}{\frac{R_2}{s} + j(X_2 + X_m)} \quad (9)$$

Now, phase current is given by

$$I_1 = \frac{V_1}{Z_{in}} \quad (10)$$

. From eq. (2.9) & (2.10)

$$I_1 = \frac{V_1}{R_1 + jX_1 + \frac{jX_m \left(\frac{R_2}{s} + jX_2 \right)}{\frac{R_2}{s} + j(X_2 + X_m)}} \quad (10)$$

B. Control structure of induction motor

The DFOIM drive is shown in Fig. 2.3. The dynamics of an induction motor can be described by synchronously rotating reference frame direct-quadrature (d-q) equations as;

$$\begin{bmatrix} v_{qs}^e \\ v_{ds}^e \\ 0 \\ 0 \end{bmatrix} = \begin{bmatrix} R_s + pL_s & \omega_e L_s & pL_m & \omega_e L_m \\ -\omega_e L_s & R_s + pL_s & -\omega_e L_m & pL_m \\ pL_m & (\omega_e - \omega_r)L_m & R_r + pL_r & (\omega_e - \omega_r)L_r \\ -(\omega_e - \omega_r)L_m & pL_m & (\omega_e - \omega_r)L_r & R_r + pL_r \end{bmatrix} \begin{bmatrix} i_{qs}^e \\ i_{ds}^e \\ i_{qr}^e \\ i_{dr}^e \end{bmatrix} \quad (11)$$

$$J_m p\omega_{rm} + B_m \omega_{rm} + T_L = T_e \quad (12)$$

$$T_e = \frac{3N}{4} L_m (i_{qs}^e i_{dr}^e - i_{ds}^e i_{qr}^e) \quad (13)$$

$$\omega_{rm} = \frac{2}{N} \omega_r \quad (14)$$

where the notational superscript “e” stands for the synchronous reference frame.

$v_{ds}^e, v_{qs}^e, i_{qs}^e$ & i_{qr}^e are the d-axis and the q-axis stator voltages, stator currents and rotor currents respectively.

R_s, R_r, L_s & L_r denote the resistances and self-inductances of the stator and the rotor respectively.

L_m denotes the mutual inductance.

T_e & T_L represent the electromagnetic and external force load torques, respectively.

J_m & B_m are the rotor inertia and the coefficient of viscous damping, respectively.

ω_r & ω_{rm} denote the rotor and motor mechanical speeds.

ω_e stands for electrical angular velocity;

N is the number of poles of the motor mechanical speed.

p stands for the differential operator (d/dt) .

The notational superscript “s” stands for stationary reference frame.

For a DFOIM drive, the flux has to fall entirely on d-axis. Therefore, the q- axis rotor flux ϕ_{qr}^e is set to zero. The controllers PI-1, PI-2, and PI-3 are chosen to ensure that $i_{qs}^* \cong i_{qs}^e, i_{ds}^* \cong i_{ds}^e$, and the flux command ϕ_r and the

estimated d-axis rotor flux ϕ_{dr}^e satisfies $\phi_r = \phi_{dr}^e$, respectively. The parameters τ and σ are given by

$$\tau = \frac{L_r}{R_r} \quad (15)$$

$$\sigma = 1 - \frac{L_m^2}{L_s L_r} \quad (16)$$

To control the speed of the IM, the speed controller of the DFOIM drive transforms the speed error signal e into an appropriate electromagnetic torque command T_e^* .

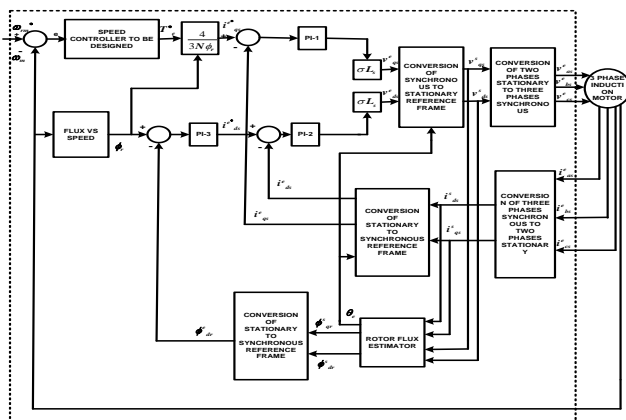


Fig. 2 Block diagram for speed control of Induction motor using DFO technique

III. CONTROL TECHNIQUES

The speed of an induction machine can be controlled by adjusting the magnitude and frequency of the applied stator voltages. The specific control strategy implemented is dependent on the requirements of the specific application. The two control techniques can be categorized as below:

- 1) Scalar control
- 2) Vector control

Vector control techniques can be further divided into

- a) Direct torque control
- b) Field oriented control

❖ Field Oriented Control:

FOC involves controlling the components of the motor stator currents, represented by a vector, in a rotating reference frame. In the case of induction machines, the control is normally performed in a reference frame aligned to the rotor flux space vector. To perform the alignment on a reference frame revolving with the rotor flux requires information about the modulus and the space angle of the rotor flux space vector.

In order to estimate the rotor flux vector either of the below mentioned strategies can be adopted:

❖ DFOC (Direct Field Oriented Control)

In this strategy rotor flux vector is either measured by means of a flux sensor mounted in the air-gap or by using the voltage equations starting from the electrical machine parameters.

❖ IFOC (Indirect Field Oriented Control)

In this strategy rotor flux vector is estimated using the field oriented control equations (current model) requiring a rotor speed measurement.

Considering the d-q model of the induction machine in the reference frame rotating at synchronous speed ω_e . The field-oriented control implies that the i_{ds} component of the stator current would be aligned with the rotor field and the i_{qs} component would be perpendicular to i_{ds} . This can be accomplished by choosing ω_e as speed of the rotor flux and locking the phase of the reference frame system such that the rotor flux is aligned with the d axis, as shown in Fig. 3.2 below:

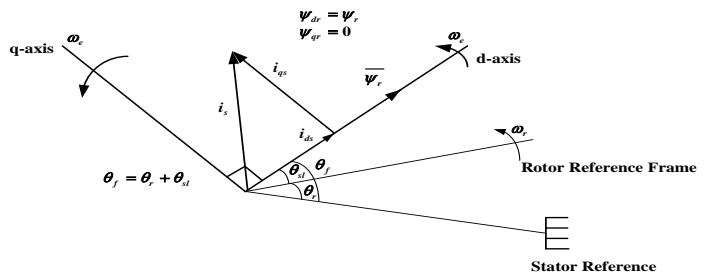


Fig. 3 Phasor diagram describing the FOC scheme

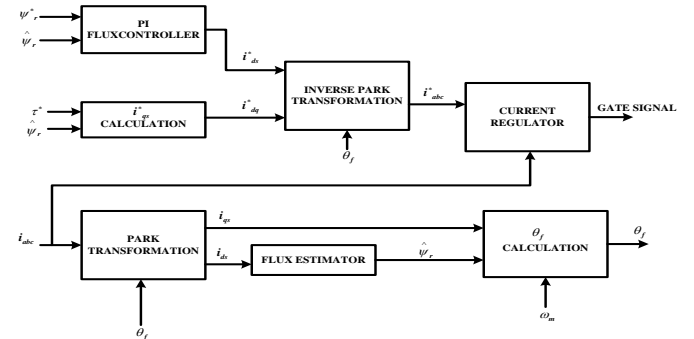


Fig. 4 Block diagram of FOC

The block diagram of FOC as shown in Fig.3.3 has the following blocks:

i. Flux Estimator

This block is used to estimate the motor's rotor flux. This calculation is based on motor equation synthesis.

$$\psi_r = \frac{L_m}{1+T_r s} (i_{ds}) \quad (17)$$

ii. θ_f Calculation

This block is used to find the phase angle of the rotor flux rotating field using the following equations

$$\theta_f = \theta_r + \theta_m \quad (18)$$

$$\frac{d\theta_f}{dt} = \frac{d\theta_r}{dt} + \frac{d\theta_m}{dt} \quad (19)$$

$$\theta_f = \int (\omega_r + \omega_m) dt \text{ & } \omega_r = \frac{L_m i_{ds}}{T_r \psi_r} \quad (20)$$

iii. Park Transformation

This block performs the translation of a, b & c phase variables into d-q components of the rotor flux rotating field reference frame.

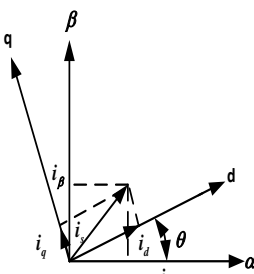
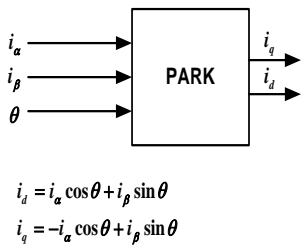


Fig. 5 Park Transformation

iv. Inverse Park Transformation

This block performs the conversion of the d-q component of the rotor flux rotating field reference frame into a, b and c phase variables.

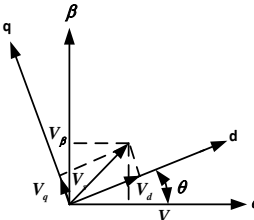
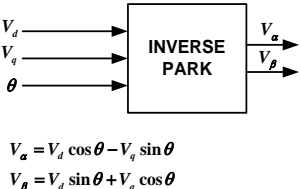


Fig.6 Inverse Park Transformation

v. i_{qs}^* Calculation

This block uses the calculated rotor flux and the torque reference to compute the stator current quadrature component required to produce the electromagnetic torque on the motor's shaft.

vi. Flux PI

This block compares the estimated rotor flux and the reference rotor flux as the input to a Proportional Integrator which calculates the flux to be applied to the motor which in turn is used to compute the stator current direct component required to produce the required rotor flux in the machine.

IV. THE HYBRID (PID + FUZZY) CONTROLLER

The hybrid (PID + Fuzzy) logic controller of the direct field oriented induction motor drive transforms the speed error

signal into the electromagnetic torque command. The fuzzy system is built by graphical user interface tool provided by the fuzzy logic tool box in MATLAB environment system.

Fuzzy Inference System Editor for FLC

All the information for a given fuzzy inference system is contained in the FIS editor structure, including variable names, membership function etc. The fuzzy inference system editor firstly consists of the name of FIS file that can be imported from the workspace. In this system the FIS editor file for the FLC is named as "Fuzzy". The following important parameters related to fuzzy inference system of the FLC are shown:

Name="Fuzzy"

Type="mamdani"

NumInputs=2

NumOutputs=1

NumRules=9

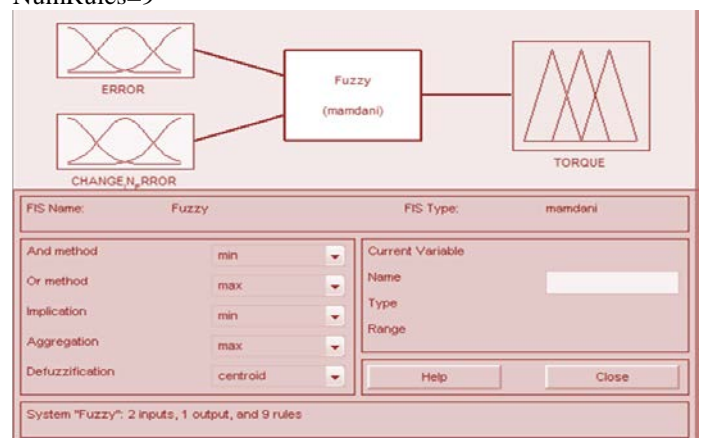


Fig.7. Fuzzy Inference system editor of the FLC

AndMethod="min"

OrMethod="max"

ImpMethod="min"

AggMethod="max"

DefuzzMethod="centroid"

Membership Function Editor for FLC

The input membership functions used in the fuzzification process are μ_{N_x} , μ_{Z_x} and μ_{P_x} to map a crisp input to a fuzzy set with a degree of certainty where $X = g(t)$ or $\square g(t)$ with $g(t) = K_1 f(t)$ & $\square g(t) = K_2 \square f(t)$. These three membership functions are chosen because of their simplicity for computation since a large number of membership functions and rules can cause high computational burden for a fuzzy controller. For any $x \in N$, where N denotes the interval $(-\infty, 0]$, its corresponding linguistic value is 'N'. Moreover, for any $x \in P$, where P denotes the interval $(0, \infty)$, its corresponding linguistic value is 'P'. For any $x \in Z$, where Z denotes the interval $[-b, b]$, its corresponding linguistic value is 'Z'. The membership functions μ_{N_x} , μ_{Z_x} and μ_{P_x} are given by

$$\mu_N(x) = \begin{cases} 1 & x \leq -b \\ \frac{-x}{b} & -b < x \leq 0 \\ 0 & \text{otherwise} \end{cases} \quad (21)$$

$$\mu_Z(x) = \begin{cases} \frac{x+b}{b} & -b < x \leq 0 \\ \frac{b-x}{b} & 0 < x \leq b \\ 0 & \text{otherwise} \end{cases} \quad (22)$$

$$\mu_P(x) = \begin{cases} 1 & b \leq x \\ \frac{x}{b} & 0 < x \leq b \\ 0 & \text{otherwise} \end{cases} \quad (23)$$

The fuzzy inference engine, based on the input fuzzy sets in combination with the expert's experience, uses adequate IF-THEN rules in the knowledge base to make decisions and produces an implied output fuzzy set u .

- i. If $\Delta g(t) \in N$, then $u(g(t), \Delta g(t)) = b$.
- ii. If $\Delta g(t) \in P$, then $u(g(t), \Delta g(t)) = -b$.
- iii. If $\Delta g(t) \in Z$ and $\Delta g(t) \in N$, then $u(g(t), \Delta g(t)) = -b$.
- iv. If $\Delta g(t) \in Z$ and $\Delta g(t) \in P$, then $u(g(t), \Delta g(t)) = b$.
- v. If $\Delta g(t) \in Z$ and $g(t) \in Z$, then $u(g(t), \Delta g(t)) = 0$.

Fig. 8 shows the structure of the hybrid (PID + Fuzzy) controller consisting of a PID controller and a fuzzy logic controller (FLC) in a serial arrangement for speed control of direct field oriented induction motor drive.

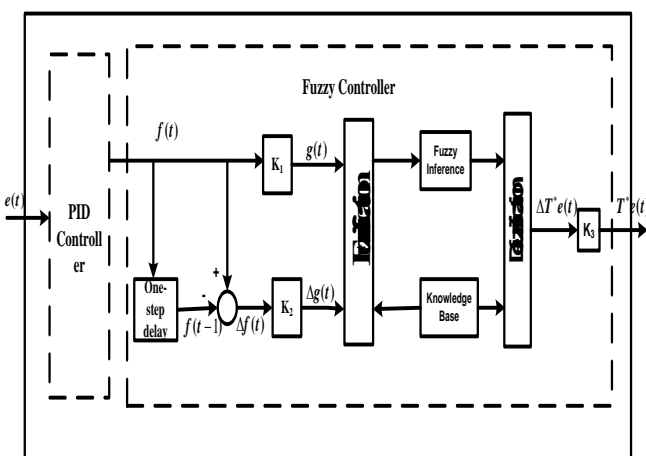


Fig. 8 The block diagram of the hybrid (PID + Fuzzy) controller

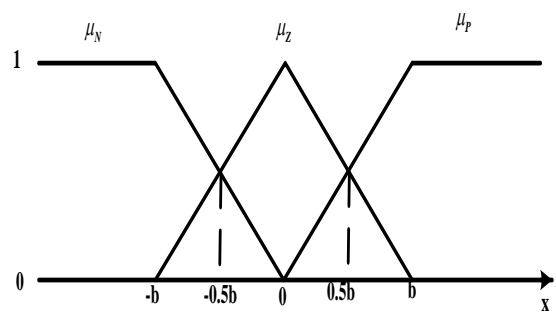


Fig. 9 Membership functions with $X = g(t)$ or $\Delta g(t)$

Table I shows the fuzzy rule base which are based on if-then rule.

TABLE I
FUZZY RULE BASE

| u | N | Z | P |
|---------------|----|----|----|
| $g(t)$ | | | |
| $\Delta g(t)$ | | | |
| N | b | b | b |
| Z | -b | 0 | b |
| P | -b | -b | -b |

Rule Editor of FLC

As there are two inputs each having three membership functions hence both inputs are combined using "AND" operator to form nine combinations of rule and these combinations are given to the output of rule editor named as "Fuzzy" which are shown in Fig. 10.

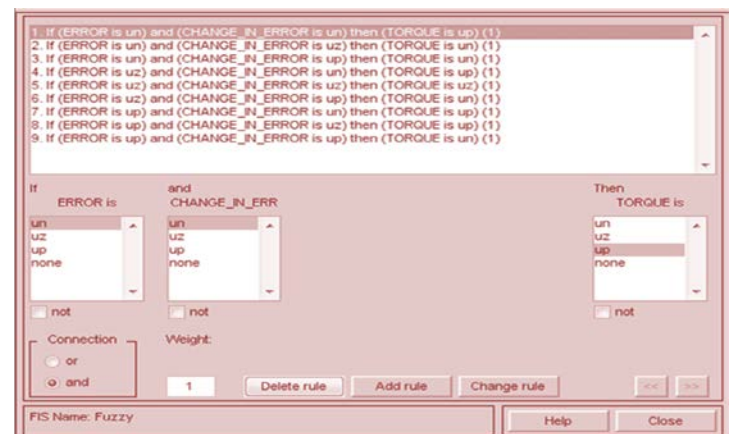


Fig. 10 Rule editor of the FLC

In the defuzzification process, ‘center of mass’ defuzzification method is used for transforming the implied output fuzzy set into a crisp output, and obtain

$$\Delta T_e^*(t) = \frac{\sum_{i \in FL(g(t))} \sum_{j \in FL(\Delta g(t))} \min\{\mu_i(g(t)), \mu_j(\Delta g(t))\} \times u(i, j)}{\sum_{i \in FL(g(t))} \sum_{j \in FL(\Delta g(t))} \min\{\mu_i(g(t)), \mu_j(\Delta g(t))\}}$$

Where

$$FL(a) = \begin{cases} \{N, Z\} & \text{if } a \in N \text{ and } a \in Z \\ \{P, Z\} & \text{if } a \in P \text{ and } a \in Z \\ \{N\} & \text{if } a \in N \text{ and } a \notin Z \\ \{P\} & \text{if } a \in P \text{ and } a \notin Z \end{cases}$$

The output of the fuzzy controller is given by

$$T_e^* = K_3 \cdot \Delta T_e^*(t)$$

V. RESULTS AND DISCUSSIONS

The performance for the speed control of direct field oriented control induction motor using PID and hybrid (PID + Fuzzy) controllers are investigated through MATLAB simulation. The performance is analyzed for different cases. The results obtained are discussed along with the performance evaluation. In the first case the performance of PID controller is evaluated while for the second case the performance of a hybrid (PID plus Fuzzy) controller for speed control of Induction motor is evaluated. The command speed is increased from 0 to 900 rpm and a load disturbance of 1.1 N-m is suddenly applied to the shaft at 4.2 sec.

A. System parameters

The system parameters of the 0.14 hp squirrel-cage induction motor used in this thesis are as following:

TABLE I
SYSTEM PARAMETERS

| System Parameters | Values of parameters |
|------------------------|--|
| Stator resistance | 17Ω |
| Rotor resistance | 11Ω |
| Stator self inductance | 0.196H |
| Rotor self inductance | 0.196H |
| Mutual inductance | 1.88×10^{-3} H |
| No. of poles | 4 |
| Moment of inertia | 2.4×10^{-4} kg - m ² |

B. Simulation under study

The two simulation models under study are:

- Speed control of a direct field oriented induction motor drive using PID controller.
- Speed control of a direct field oriented induction motor drive using a hybrid (PID + Fuzzy) controller

C. Performance comparison of induction motor using PID and a hybrid (PID plus Fuzzy) controller through waveforms

Case I: At a load of 1.1 N-m (Rated Torque)

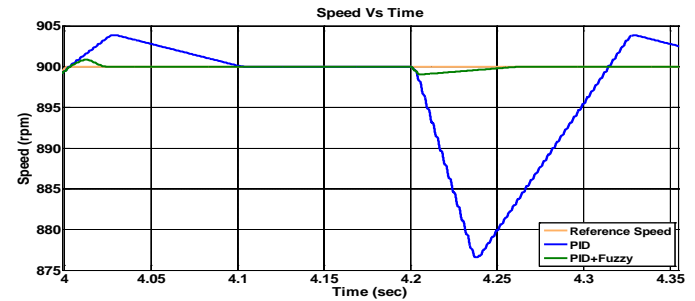


Fig. 11 Simulation results of the DFOIM using the hybrid controller and the PID under a load disturbance of 1.1 N-m

From the Fig. 11 it is clear that when a load disturbance of 1.1 N-m is applied to an induction motor of 0.14 hp at 4.2 sec, the speed of PID controller drops to 876 rpm from 900 rpm which is reference speed. The performance parameters such as steady state error, overshoot and setting time are 0.002%, 0.4% and 0.2 sec respectively while in case of a hybrid (PID + Fuzzy) controller speed drops to 899 rpm from 900 rpm which is reference speed. The performance parameters such as steady state error, overshoot and setting time are 0%, 0.11% and 0.06 sec respectively.

Case II: At 0 N-m (No load)

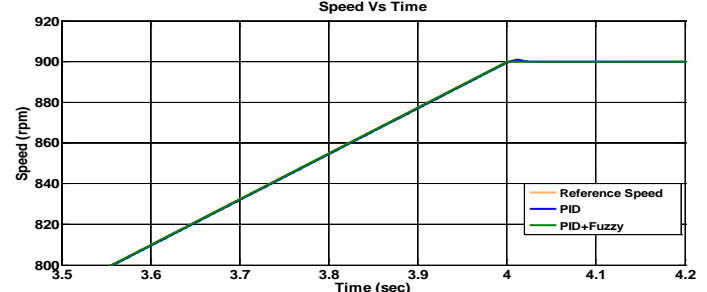


Fig. 12 Simulation results using the hybrid controller and the PID under no load

From the Fig. 12 it is clear that when no load disturbance is applied, the PID controller shows negligible steady state error and overshoot of 0.11% while in case of hybrid (PID + Fuzzy) controller no steady state error and no overshoot is obtained.

Case III: At a load of 0.5 N-m (Under load)

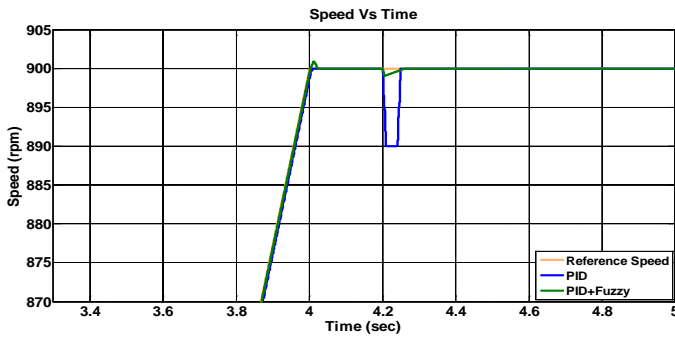


Fig. 13 Simulation results of the DFOIM using the hybrid controller and the PID under a load disturbance of 0.5 N-m

From the Fig. 13 it is clear that when a load disturbance of 0.5 N-m is applied to an induction motor of 0.14 hp at 4.2 sec, the speed of PID controller drops to 890 rpm from 900 rpm which is reference speed. The performance parameters such as steady state error, overshoot and setting time are 0.003%, 1.1% and 0.05 sec respectively while in case of a hybrid (PID + Fuzzy) controller speed drops to 899.1 rpm from 900 rpm which is the reference speed. The performance parameters such as steady state error, overshoot and setting time are 0%, 0.1% and 0.04 sec respectively.

Case IV: At a load of 2 N-m (Overload)



Fig. 14 Simulation results of the DFOIM using the hybrid controller and the PID under a load disturbance of 2 N-m

From the Fig. 13 it is clear that when a load disturbance of 2 N-m is applied to an induction motor of 0.14 hp at 4.2 sec, the speed of PID controller drops to 860 rpm from 900 rpm which is reference speed. The performance parameters such as steady state error, overshoot and setting time are 0.002%, 4.5% and 0.05 sec respectively while in case of a hybrid (PID + Fuzzy) controller speed drops to 899.03 rpm from 900 rpm which is reference speed. The performance parameters such as steady state error, overshoot and setting time are 0%, 0.12% and 0.03 sec respectively.

D. Performance comparison of PID and hybrid (PID+ fuzzy) controllers

Performance comparison of PID and Hybrid (PID + Fuzzy) controllers for speed control of Induction motors using DFO technique at a reference speed of 900 rpm and different loading conditions are given in the following table.

TABLE II
PERFORMANCE COMPARISON OF PID AND HYBRID (PID + FUZZY)
CONTROLLERS

| Controllers | PID Controller | | | | PID + Fuzzy Controller | | | |
|-------------------------------------|----------------|-------------|------------------------|---------------|------------------------|-------------|------------------------|---------------|
| | Par. | Speed (rpm) | Steady State Error (%) | Overshoot (%) | Settling Time (sec) | Speed (rpm) | Steady State Error (%) | Overshoot (%) |
| Load | | | | | | | | |
| At a load of 1.1 N-m (Rated Torque) | 876 | 0.002 | 0.4 | 0.2 | 899 | 0.00 | 0.11 | 0.06 |
| At 0 N-m (no load) | 899.9 | 0.001 | 0.11 | 0.02 | 900 | 0.00 | 0.00 | 0.01 |
| At a load of 0.5 N-m (Under load) | 890 | 0.003 | 1.1 | 0.05 | 899.1 | 0.00 | 0.1 | 0.04 |
| At a load of 2 N-m (Over load) | 860 | 0.002 | 4.5 | 0.05 | 899.03 | 0.00 | 0.12 | 0.03 |

VI. CONCLUSIONS

In this paper, PID and a hybrid (PID + Fuzzy) Controller based speed control of a direct field oriented induction motor (DFOIM) drive is discussed for the analysis of various load conditions. The hybrid (PID + Fuzzy) controller has exhibited the combined advantages of a PID controller and a Fuzzy Logic Controller. It also has the capability of improving the stability, the transient response and load disturbance rejection of speed control of a DFOIM.

Moreover a performance comparison between PID & a hybrid (PID + Fuzzy) controller for the speed control of Induction motor is studied through simulation in MATLAB/Simulink environment. With results obtained from simulation and its comparison on the basis of steady state error, settling time and overshoot, it is clear that for the same operating conditions the hybrid (PID + Fuzzy) controller performs better than the PID controller. The steady state error is remarkably less in the case of the hybrid (PID plus fuzzy) controller. The fuzzy logic only with three membership functions are used for each input and output for low computational burden, which can achieve satisfactory results.

VII. REFERENCES

- [1] T. J. Ho and L.Y. Yeh, "Design of a Hybrid PID plus Fuzzy Controller for Speed Control of Induction Motors," *IEEE Conference on Industrial Electronics and Applications; 2010*, pp.1352-1357.
- [2] R. Arulmozhiyal, K. Baskaran, and R. Manikandan, "A Fuzzy Based PI Speed Controller for Indirect Vector Controlled Induction Motor drives," *IEEE 2011*.
- [3] N. B. Muthuselvan, Subharansu Sekhar Dash & P. Somasundaram, "A High Performance Induction Motor Drive System Using Fuzzy Logic Controller," *IEEE 2006*.
- [4] Li Zhen and Longya Xu, "A Comparison Study of Three Fuzzy Schemes for Indirect Vector Control of Induction Machine Drives," *IEEE 1996*.
- [5] Minh Ta-Cao, J.L. Silva Neto and Homg Le-Huy, "Fuzzy Logic Based Controller for Induction Motor Drives," *IEEE 1996*, pp.631-634.
- [6] Pedro Ponce and Juan C. Ramirez, "Fuzzy Logic Controller Based on Space Vector Modulation for Induction Motor Control", *IEEE 2004*, pp.1285-1290.
- [7] Md. Nurul Islam, Mashud Haider, and M. Bashir Uddin, "Fuzzy Logic Enhanced Speed Control System of a VSI-Fed Three Phase Induction Motor," *IEEE 2005*, pp.296-301.
- [8] M. Nasir Uddin, Tawfik S. Radwan, and M. Azizur Rahman, "Performances of Fuzzy-Logic-Based Indirect Vector Control for Induction Motor Drive," *IEEE Transactions on Industry Applications*, vol. 38, no. 5, September/October 2002, pp.1219-1225.
- [9] R. Arulmozhiyal and K. Baskaran, "Space Vector Pulse Width Modulation Based Speed Control of Induction Motor using Fuzzy PI Controller," *International Journal of Computer and Electrical Engineering*, vol. 1, no. 1, April 2009, pp. 1793-8198.
- [10] Bahram Kimiaghalam, Meisam Rahmani and Hassan Halleh, "Speed & Torque Vector Control of Induction Motors with Fuzzy Logic Controller," *International Conference on Control, Automation and Systems*, Oct. 14-17, 2008.
- [11] Eleftheria S. Sergaki, "Motor Flux Minimization Controller based on Fuzzy Logic Control for DTC AC Drives," *IEEE 2010*.

Performance Investigation of SVPWM Controlled Diode Clamped and Flying Capacitor Multilevel Converters

Vikas Shukla, S. P. Singh, *Member, IEEE*, and A. K. Gautam, *Student Member, IEEE*

Abstract- In this paper, we have done dynamic performance of SVPWM controlled diode clamped and flying capacitor multilevel converters. These converters shows the better dynamic performances.. The different cases of load disturbances are analyzed like fixed load, increase in load and decrease in load. The analysis is also performed for source perturbation like Increase & decrease in source voltage. The proposed multilevel converters work here as ac-dc converter at constant frequency of supply and boost up in output voltage without use of transformer. Due to power electronic switches used in conversion process vulnerability of power system is increased and results in different power quality issues power factor, Harmonics injection in supply and reactive power compensation. But both of the converters are showing more resiliencies to such impacts. The simulation results of converters are attentive about power factor very near to unity and harmonics in specified limits. Thus converters used in this paper perform transformer less boosting, conversion and less vulnerability to power quality.

Index Terms—Multilevel Converter, Diode clamped, Flying Capacitor, Performance Investigation, SVPWM, Power Quality etc.

I. INTRODUCTION

THE era of high power converters and Medium voltage (MV) drives evolved in mid 1980s when 4500 volt Gate Turn off Thyristor (GTO) became commercially available.

They have the drawback of poor power quality in terms of injection of current harmonics, resultant voltage waveform distortion and poor power factor at input ac supply. Also slowly varying rippled dc output at load side, low efficiency, and bulky size of ac and dc filters. Because of the conflicts with power quality problems some other methods such as passive filters, active filters (AFs), and hybrid filters are also employed.

A. Vikas Shukla,EED Sultanpur 228118, India (e-mail:life.vikas@gmail.com)

B. S. P. Singh,EED Sultanpur 228118, India (e-mail:singhsurya12@gmail.com)

C. A. K. Gautam, EED Sultanpur 228118, India, (e-mail:abhinavgautam97@gmail.com).

Power quality improvement using MLC: Multilevel converters present great advantages compared with conventional and very well-known two-level converters. These advantages are fundamentally focused on improvements in the output signal quality and a nominal power increase in the converter. The power converter output voltage improves its quality as the number of levels increases reducing the total harmonic distortion (THD) of the output waveforms. These properties make multilevel converters very attractive and researchers are spending great efforts trying to improve multilevel converter performances such as the control simplification and the performance of different optimization algorithms in order to enhance the THD of the output signals, and the ripple of the currents. For instance, nowadays researchers are focused on the harmonic elimination using pre-calculated switching functions , harmonic mitigation to fulfills specific grid codes, the development of new multilevel converter topologies (hybrid or new ones), and new control strategies. Also conversion of 3 phase ac to dc, line side voltage and current waveforms are getting polluted with conventional pulses schemes like 12, 24, 48..... Pulse convertors as shown in Fig. 1. So multilevel converters are showing much effectiveness in this area with new control technique.

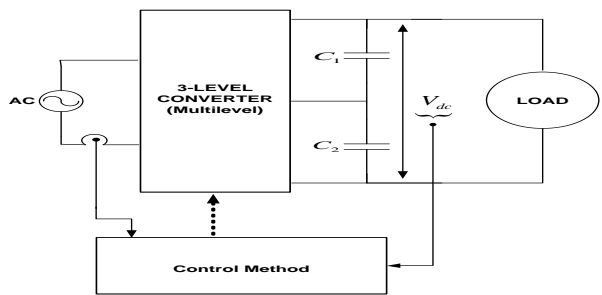


Fig. 1.Block diagram representation of a multilevel converter

II. DIODE CLAMPED AND FLYING CAPACITOR MULTILEVEL CONVERTERS

a) *Three-phase three-level diode clamped converter:* The drawbacks of the two-level converters are the high voltage stress across the devices, large passive components and hence due to the inherent advantages of the three-level Diode

Clamped converters were proposed to draw the sinusoidal line currents in phase with mains voltage. And improving the waveform quality and reducing voltage stress on the power devices. The voltage stress on the open power devices is constrained by clamping capacitors.

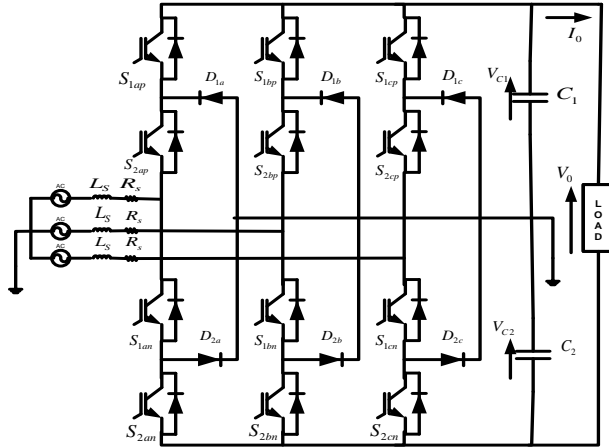


Fig.2. A 4-level Diode Clamped Multilevel Converter

b) Three-phase three-level flying capacitor multilevel converter: Three-phase flying capacitor converter is illustrated in Fig. 3. In this topology capacitor are not shared among different legs of the converter; each phase has its own set of capacitors. Regulation of capacitor voltages is possible without using an external circuit regardless of the number of levels of the converter. This is one of the advantages of this topology. Because the voltage of the outer capacitors is higher than the inner ones, several capacitors need to be connected in a series to reach to the required voltage (the tolerable voltage for each capacitor bank). Therefore, the number of capacitors drastically increases when the number of voltage levels increases. Furthermore, the number of capacitors is proportional to the number of phases of the converter. This is one of the primary drawbacks of this topology.

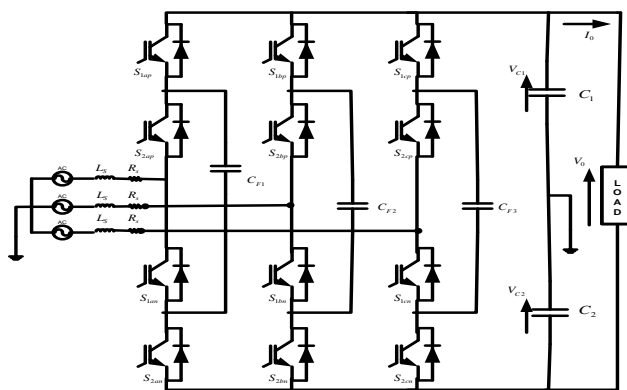


Fig.3. A 4-Level Flying Capacitor Multilevel Converter

III. SVPWM CONTROL TECHNIQUE FOR DIODE CLAMPED AND FLYING CAPACITOR

A standard Space vector PWM has been used for three-phase Diode clamped and Flying capacitor multilevel

converters. The basic principle of operation of a Converter employing SVPWM technique block diagram is shown below.

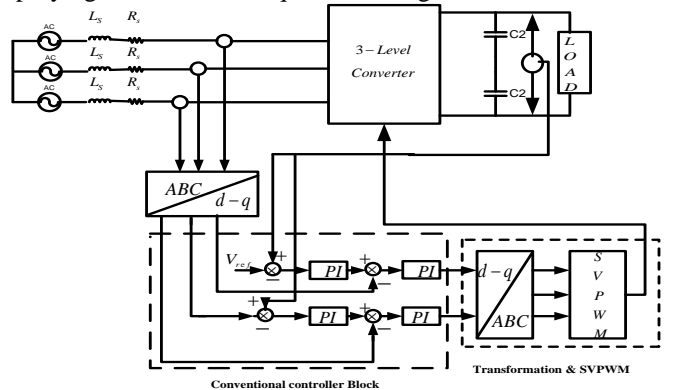


Fig. 4. Control Scheme of Multilevel converter in two-frame of references

This scheme involves 3-basic actions performed by system as for switching operation and ride through from any abnormal operation.

1) Transformation Stage

The input terminals of rectifier a, b and c are connected to terminals of three phase ac supply through source inductance. The input three phase supply voltage can be written as,

$$\begin{aligned} v_a &= V_m \cos(\omega t + 0^\circ) \\ v_b &= V_m \cos\left(\omega t - \frac{2\pi}{3}\right) \\ v_c &= V_m \cos\left(\omega t + \frac{2\pi}{3}\right) \end{aligned} \quad (1)$$

Where V_m is peak phase voltage of supply and ω is angular frequency of source.

For the diode clamped three level converters, line to ground voltages can be derived from switching states S_a, S_b, S_c . If the converter is connected to a balanced three phase source, corresponding phase voltages can be derived from line to ground voltages using (2). Then these phase voltages are transformed into the $d-q$ reference frame by (3) and the resultant coordinates for the vectors in sector can be computed. This can implemented using Clarke's function and easily applied using MATLAB embedded Function or .m file approach

$$\begin{bmatrix} v_{as} \\ v_{bs} \\ v_{cs} \end{bmatrix} = \frac{1}{3} \begin{bmatrix} 2 & -1 & -1 \\ -1 & 2 & -1 \\ -1 & -1 & 2 \end{bmatrix} \begin{bmatrix} v_{ag} \\ v_{bg} \\ v_{cg} \end{bmatrix} \quad (2)$$

$$\begin{bmatrix} v_{ds} \\ v_{qs} \\ v_0 \end{bmatrix} = \frac{1}{3} \begin{bmatrix} 1 & -1 & -1 \\ -1 & -\frac{\sqrt{3}}{2} & -\frac{\sqrt{3}}{2} \\ 1 & 1 & 1 \end{bmatrix} \begin{bmatrix} v_{as} \\ v_{bs} \\ v_{cs} \end{bmatrix} \quad (3)$$

2) Concept of Space vector calculation

The space vector diagram with equivalent circuit representation of Diode clamped rectifier can be used for following analysis of the space vectors are defined as follows:

$$\left. \begin{aligned} v &= \frac{2}{3}(v_a + a.v_b + a^2.v_c) \\ v' &= \frac{2}{3}(v'_a + a.v'_b + a^2.v'_c) \\ i &= \frac{2}{3}(i_a + a.i_b + a^2.i_c) \end{aligned} \right\} \quad (4)$$

This equation can be expressed in a rotating reference frame (d-q), with the d-axis oriented in the direction of source voltage vector v as shown in Fig. 5.

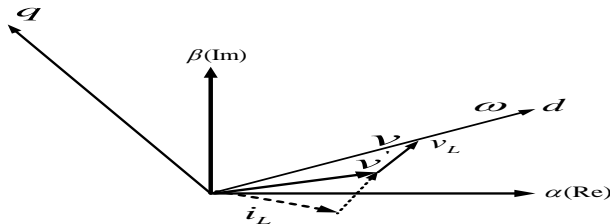


Fig. 5 Vector diagram of multilevel converter in two frame of references

The equation can be written as below

$$\left. \begin{aligned} v_d &= L \cdot \frac{di_d}{dt} - \omega \cdot L \cdot i_q + v_d' \\ v_q &= L \cdot \frac{di_q}{dt} - \omega \cdot L \cdot i_d + v_q' \end{aligned} \right\} \quad (5)$$

Where ω is angular frequency of three - phase voltage and v_d , v_d' , i_d and v_q , v_q' , i_q are components of v , v' and i . v_d is in d and q axis respectively. Here both equations depict behavior of i_d and i_q can be controlled using voltages v_d and v_q generated by rectifier.

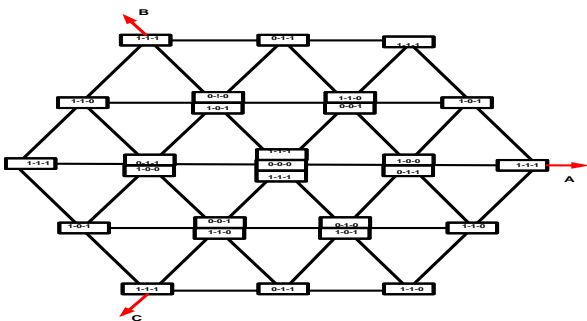


Fig.6. Space vector diagram for all switching states in three phase converters

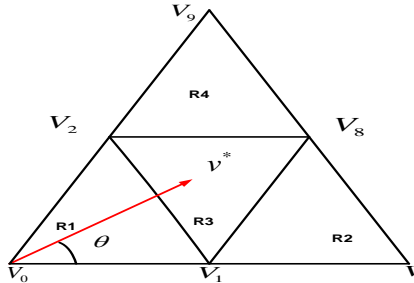


Fig.7. One sector of space vectors representation with time of switching

It is to be emphasized that this method only controls the total DC bus voltage. The current controllers deliver the reference values for voltages in d and q frame of reference. By using coordinates frame transformation, we obtain V_α^* and V_β^* in stationary frame of reference. The voltages V_α^* and V_β^* are used to derive the reference command input v and its angle θ . These are now fed to space vector modulator and used for generation of control pulses for 12 semiconductor switches.

All 27 possible conduction states of NPC or Flying capacitor multilevel converter produce 19 different space vectors. The complex plane can be subdivision of 6 sectors and 24 triangles with four triangles in each sector as shown in fig.6. The sector triangle can be formed using voltage components V_0 , V_7 and V_9 . Also it is assumed command voltage vector v^* will reside in region R_1 when following equations of (4.6) and (4.7).

$$V_1 T_a + V_8 T_b + V_2 T_c = V^* T_{samp} / 2 \quad (6)$$

$$T_a + T_b + T_c = T_{samp} / 2 \quad (7)$$

Where V_1 , V_2 and V_8 are corner voltage triangles of selected region. Respective time intervals are represented as T_a , T_b and T_c whether T_{samp} is sampling time of these vectors.

In order to find out all the sector representation we should keep region one as a reference then we can obtain analytical time expression for time intervals T_a , T_b and T_c .

$$\text{Region 1: } \begin{cases} T_a = 2m \cdot T_{samp} \cdot \sin\left(\frac{\pi}{3} - \theta\right) \\ T_b = T_{samp} \cdot \left[1 - 2m \sin\left(\frac{\pi}{3} - \theta\right)\right] \\ T_c = 2m \cdot T_{samp} \cdot \sin \theta \end{cases} \quad (8)$$

| System Parameters | |
|--|-----------------------------------|
| Load side Parameters | Input Side Parameters |
| Load R=15Ω, L=5 mH | Supply voltage= 1000 volts, 50 Hz |
| DC Bus capacitors C1=C2= 4700μF | Source R= 0.5 ohm, L = 5 mH |
| Chopping Frequency of Switches=5000 Hz | |
| DC Bus voltage (Reference)=3000 volts | |

$$\text{Region 2: } \begin{cases} T_a = 2T_{\text{samp}} \cdot \left[1 - m \sin\left(\frac{\pi}{3} + \theta\right) \right] \\ T_b = 2m \cdot T_{\text{samp}} \cdot \sin \theta \\ T_c = T_{\text{samp}} \cdot \left[2m \sin\left(\frac{\pi}{3} - \theta\right) - 1 \right] \end{cases} \quad (9)$$

$$\text{Region 3: } \begin{cases} T_a = T_{\text{samp}} \cdot [1 - 2m \sin \theta] \\ T_b = T_{\text{samp}} \cdot \left[2m \sin\left(\frac{\pi}{3} + \theta\right) - 1 \right] \\ T_c = T_{\text{samp}} \cdot \left[1 + 2m \sin\left(\theta - \frac{\pi}{3}\right) \right] \end{cases} \quad (10)$$

$$\text{Region 4: } \begin{cases} T_a = T_{\text{samp}} \cdot [2m \sin \theta - 1] \\ T_b = T_{\text{samp}} \cdot 2m \sin\left(\frac{\pi}{3} - \theta\right) \\ T_c = 2T_{\text{samp}} \cdot \left[1 - m \sin\left(\frac{\pi}{3} + \theta\right) \right] \end{cases} \quad (11)$$

Where θ is command vector angle, modulation index $m = 2/\sqrt{3}(V^*/V_0)$, V^* command voltage vector and V_0 is dc bus voltage of converter. In similar fashion two other region time vectors can be calculated.

IV. SIMULATION RESULTS AND DISCUSSIONS

A MATLAB/SIMULINK model is developed to investigate the performance comparison of PI based SVPWM controlled Flying capacitor and Diode clamped converters. The performance is analyzed for different cases in which changes in load done.

System parameters for simulation: For comparison of two different systems it is important to fix few parameters and different parameter which helps at time of different cases as preset indicators and responses in a manner of ease in comparison. So for this objective few parameters named as Source side and Load side are fixed and referring to these system parameters are examined in disturbed and without any disturbance.

TABLE I
SYSTEM PARAMETERS

A. SIMULATION RESULTS OF DIODE CLAMPED MULTILEVEL CONVERTER

Case1. Operation with fixed source voltage and variable load

a) *Operation with fixed load:*

In this case operation is performed with fixed load of 15 ohm, 5mH and 1000 volt ac (rms). Also no variation is applied in source voltage. Then the performance evaluation of Diode clamped converter is performed.

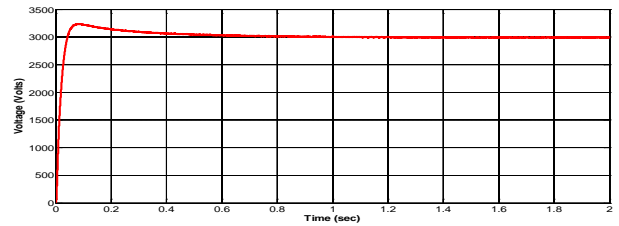


Fig.8. Output voltage waveform

As shown in Fig.8. The peak overshoot is 320 volts and start to settle after peak value. At time $t=0.6$ sec it completely settled down to reference.

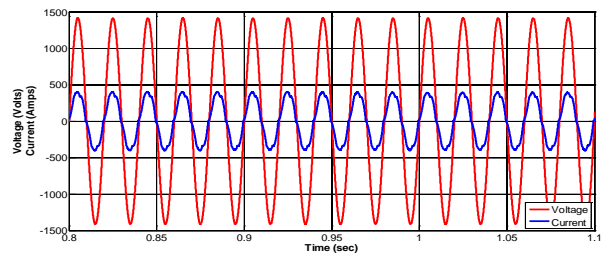


Fig. 9. Waveform of source voltage and current

As shown in Fig. 9. Waveforms are depicted from source side current and phase angle no lagging operation is visualized. And waveform is having little distortion.

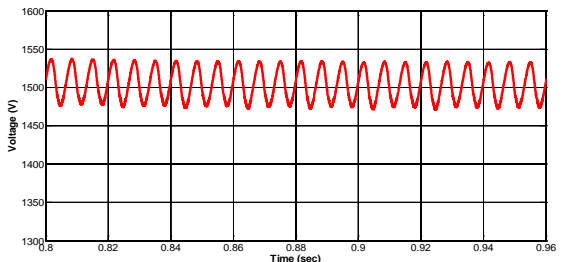


Fig.10. Voltage across upper capacitor

As shown in the Fig.10. V_{C1} Is crossing and swinging over 1500 volts. The same property is showing by Fig.11.

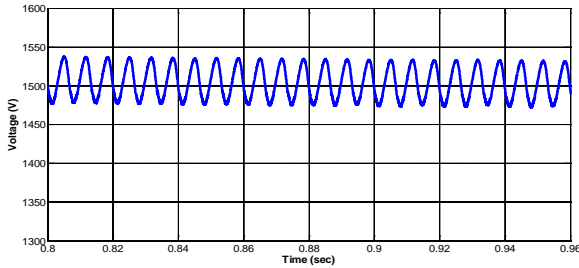


Fig.11. Voltage across lower capacitor

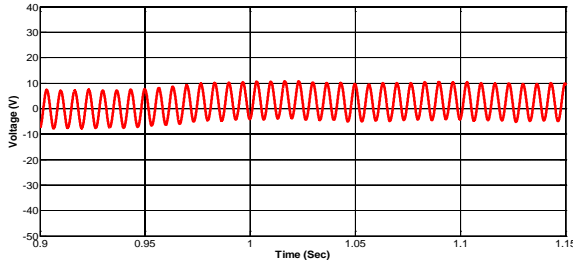


Fig.12. Voltage difference across capacitors,

$$\Delta V_C = V_{C1} - V_{C2}$$

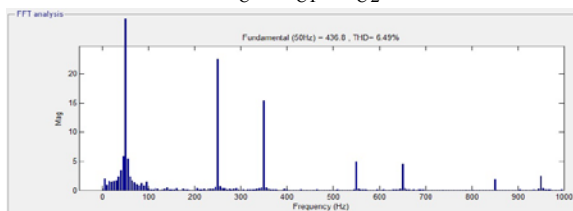


Fig.13. Harmonic spectrum of source current

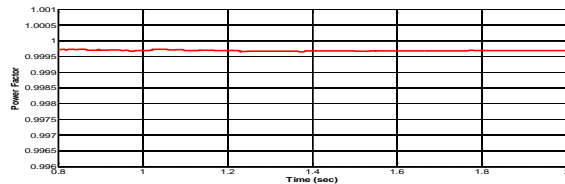


Fig.14. Power Factor of Source

Fig.14. shows the power factor of supply which is approximate to unity.

b) Operation with sudden Increase in load:

Here in this case operation is started with fixed load. During entire operation the supply voltage is fixed. But load is suddenly increased at $t=1$ sec. In this condition the performance and behavior of Diode Clamped Converter is analyzed with such change in load.

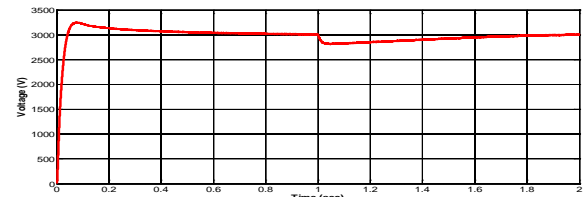


Fig.15. Output Voltage waveform for Sudden Increase in Load
As shown in Fig.15 load is suddenly increased at $t=1$ sec. The dip in output supply voltage of 240 volt and settled down at time $t = 1.8$ sec

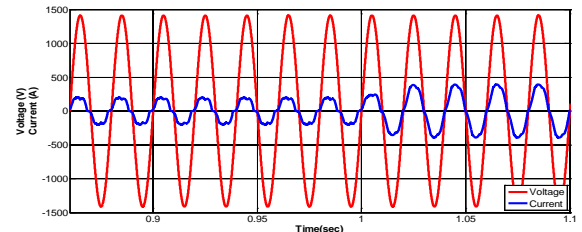


Fig.16 Waveforms of source voltage and current for sudden Increase in Load

As shown in Fig.16 source voltage and current Waveforms are depicted from source side current and phase angle no lagging operation is visualized.

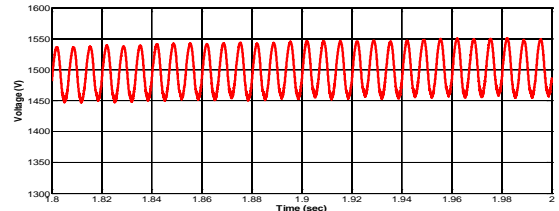


Fig.17. Voltage across upper capacitor

As shown in the fig.17 voltage across upper capacitor is shown which crossing and swinging over 1500 volts are. The same property is showing by Fig.18.

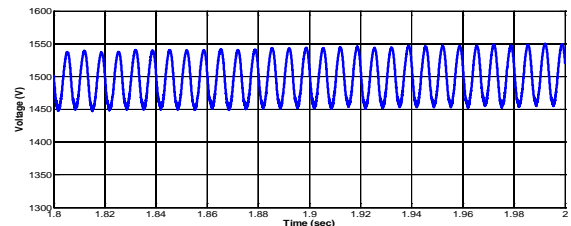


Fig.18. Voltage across lower capacitor

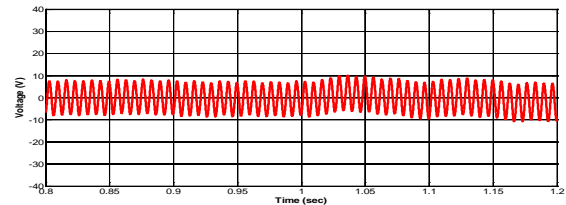


Fig.19. Voltage difference across capacitors,

$$\Delta V_C = V_{C1} - V_{C2}$$

Fig.19 shows Voltage difference across capacitors, which is range of 8 volts.

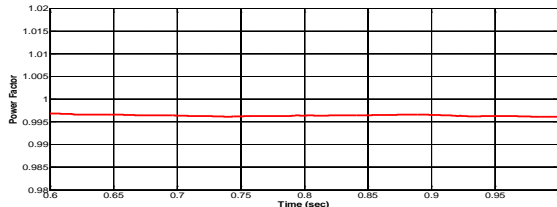


Fig.20 Power Factor of source

Fig. 20 shows the power factor of supply which is approximate to unity.

c) Operation with sudden Decrease in load

Here in this case operation is started with fixed load. During entire operation the supply voltage is fixed. But load is suddenly decreased at $t=1$ sec. In this condition the performance and behaviour of Diode Clamped Converter is analyzed with such change in load.

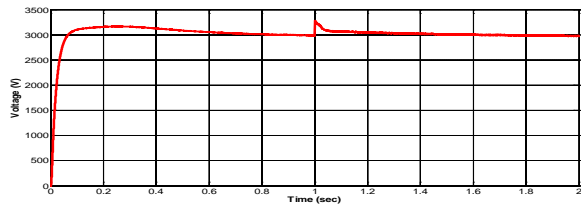


Fig.21. Output Voltage Waveform during Sudden Decrease in Load

As shown in Fig.21. Load is suddenly decreased at ($t=1$) sec. The rise in output supply voltage of 220 volt and settled down at time ($t = 1.5$) sec.

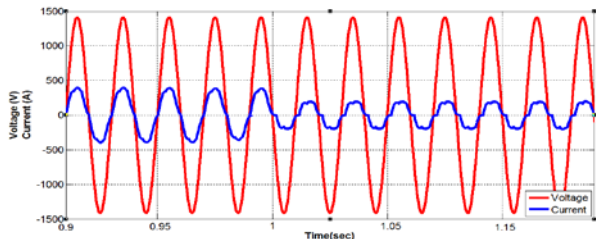


Fig. 22 Waveform of source voltage and current for sudden Load Decrease

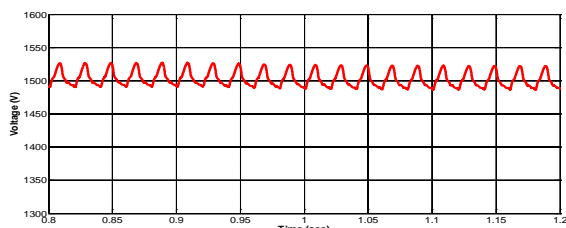


Fig.23. Voltage across upper

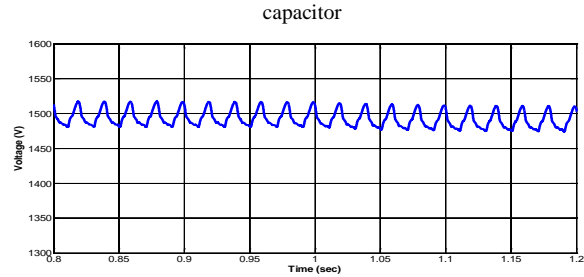


Fig.24. Voltage across lower capacitor

As shown in the fig. 23 voltage across upper capacitor is shown which is crossing and swinging over 1500 volts. The same property is showing by Fig.24.

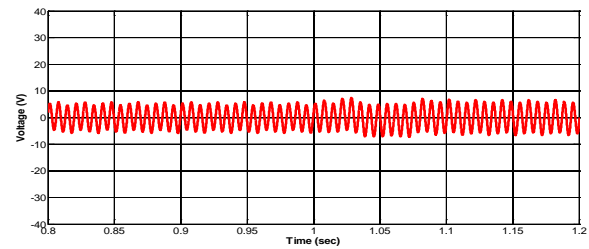


Fig.25 Voltage difference across capacitors,

$$\Delta V_C = V_{C1} - V_{C2}$$

Fig. 25 shows Voltage difference across capacitor which are of range 7 volts.

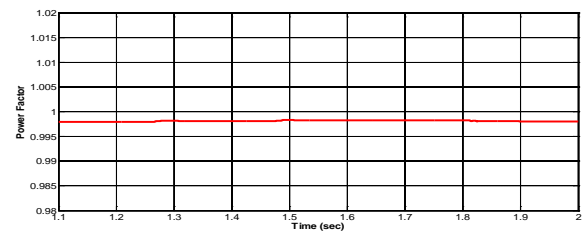


Fig.26. Power Factor of system

Fig.26 shows the power factor of supply which is approximate to unity.

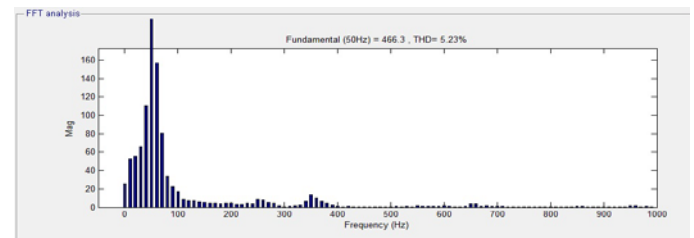


Fig. 27. Harmonic analysis of source current

Case II. Operation with fixed load and variable source voltage

a) Operation with increase in source voltage

The analysis is performed with three phase ac source on line side of rating 1100 volt (rms) value on frequency of 50 Hz. In this case the source voltage is increased. But the load is fixed and no transient condition is examined. The increase in voltage is of 10 % and for this case the analysis is carried out.

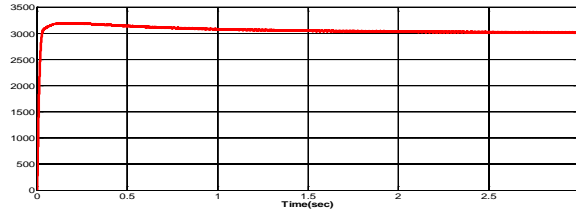


Fig. 28. Output voltage waveform for increase in Source Voltage

As shown in Fig.28 the output waveform of DC supply is with fixed load of 15 ohm, 5mH and 1000 volt ac (r.m.s.). During entire operation the load is fixed, But increase of 10% source voltage is done. The peak overshoot is 250 volts and start to settle after peak value. At time t = 2.4 sec it completely settled down to reference.

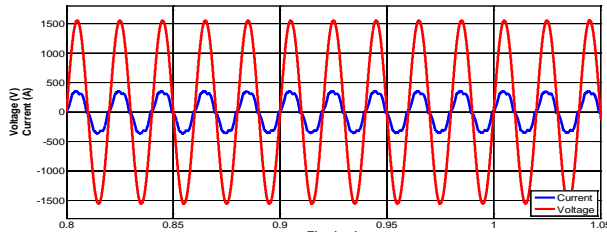


Fig. 29 Waveform of source voltage and current for increase in source voltage

As shown in Fig. 29 Waveform are depicted from source side current and phase angle no lagging operation is visualized. Also waveform is having little distortion.

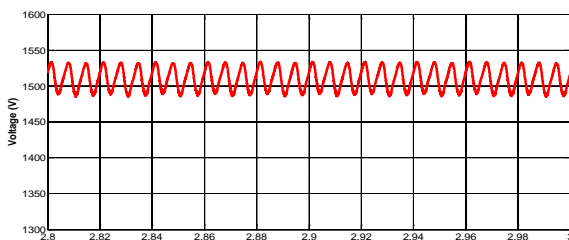


Fig. 30. Voltage across upper capacitor

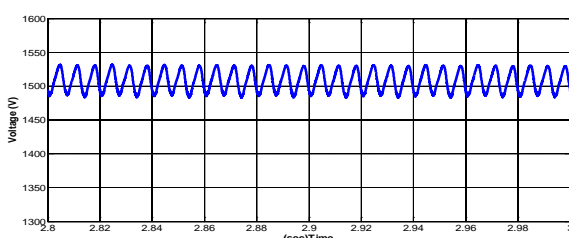


Fig. 31. Voltage across lower capacitor

As shown in the Fig. 30 voltage across upper capacitor is shown which is crossing and swinging over 1500 volts. The same property is showing by Fig. 31.

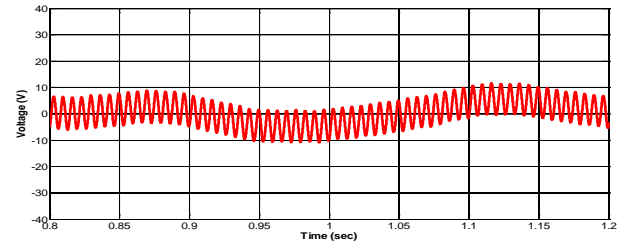


Fig. 32. Voltage difference across capacitors,

Fig. 32 shows Voltage difference across capacitors, which are of range 10 volts.

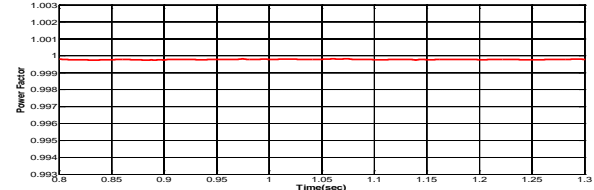


Fig. 33 Power Factor of source

Fig. 33 shows the power factor of supply which is approximate to unity.

b) Operation with Decrease in source voltage

Here in this case operation is started with fixed load. But at Supply voltage is decreased to 900 volt and in this condition the performance and behaviour of controller is analyzed with such reduction in source voltage.

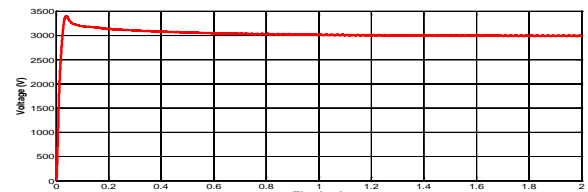


Fig. 34. Output voltage waveform for decrease in Source Voltage

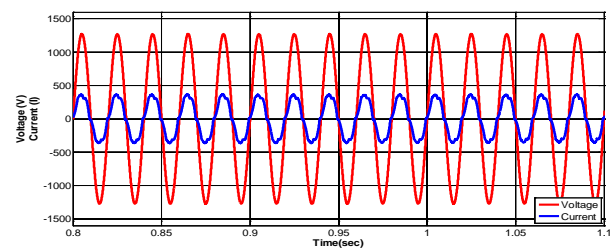


Fig. 35 Waveform of source voltage and current for Decrease in source voltage

As shown in Fig. 34 the output waveform of DC supply is with fixed load, but decrease of 10% source voltage is done. The peak overshoot is 400 volts and start to settle after peak value. At time t = 0.9 sec it completely settled down to

reference.

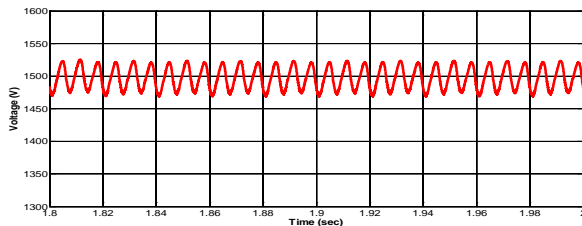


Fig. 36 Voltage across upper capacitor

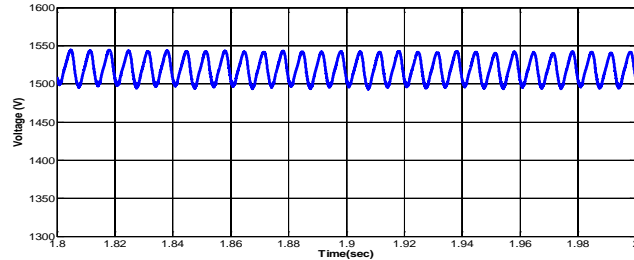


Fig. 37 Voltage across lower capacitor

As shown in the Fig. 36 voltage across upper capacitor is shown which is crossing and swinging over 1500 volts. The same property is showing by Fig. 37.

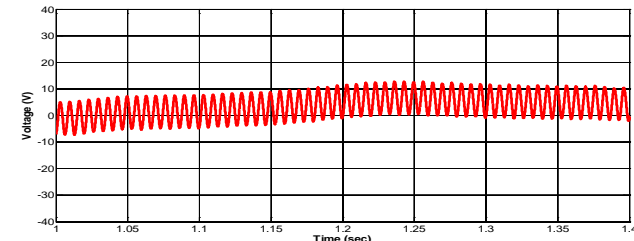


Fig. 38 Voltage difference across capacitors,

Fig. 38 shows Voltage difference across capacitors, which are of range 7 volts.

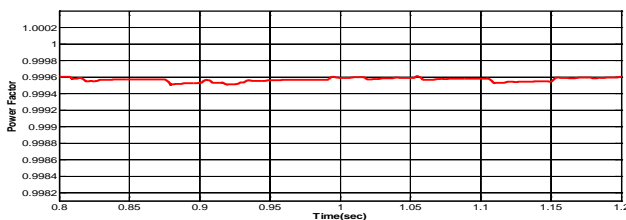


Fig. 39 Power Factor of source

Fig. 39 shows the power factor of supply which is approximate to unity.

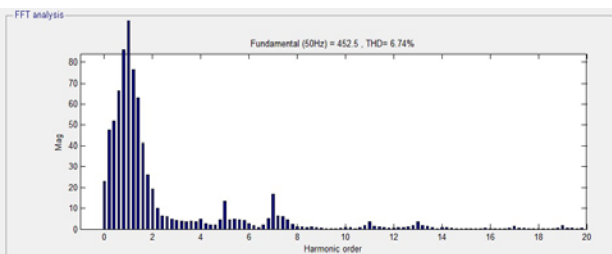


Fig. 40 Harmonic analysis of source current during load disturbance

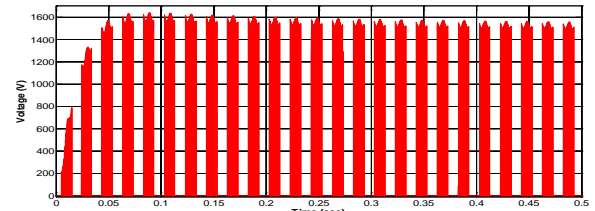


Fig. 41 Switching stress across a switch

Fig. 41 shows the switching stress across a switch during its operation and showing peak value of voltage across it as 1600 volts. This voltage is of intermittent nature because of switch getting regularly turning On and Off.

B. SIMULATION RESULT OF FLYING CAPACITOR MULTILEVEL CONVERTER

Case I. Operation with fixed source voltage and variable load

a) Operation with fixed load:

In this case operation is performed with fixed load. Also no variation is applied in source voltage. Then the performance evaluation of flying capacitor converter is performed.

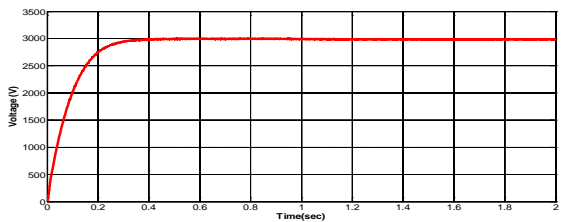


Fig.42. Output voltage waveform

As shown in Fig.42. The peak overshoot is not found and start to settle after peak value. At time $t = 0.4$ sec it completely settled down to reference.

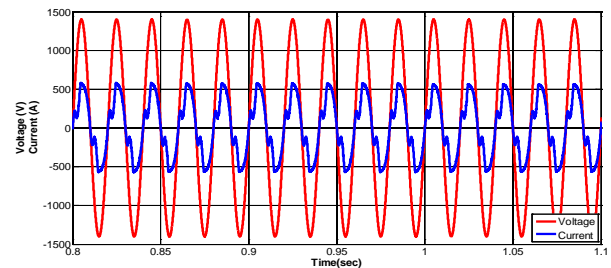


Fig. 43 Waveform of source voltage and current

As shown in Fig. 43, Waveform are depicted from source side current and phase angle no lagging operation is visualized. Also waveform is having little distortion.

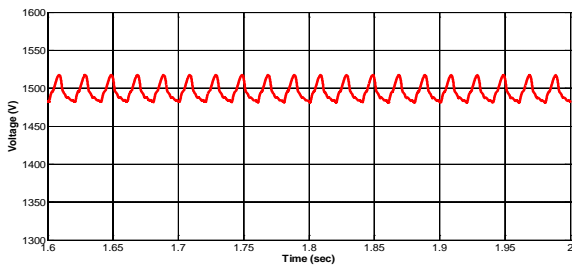


Fig. 44 Voltage across upper capacitor

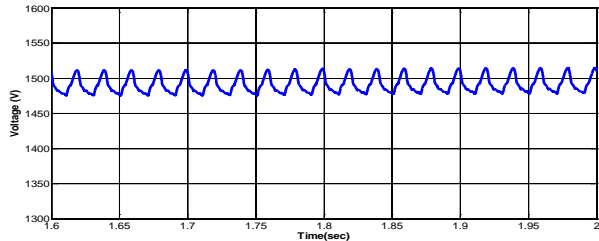


Fig. 45 Voltage across lower capacitor

As shown in the Fig. 44 voltage across capacitor one V_{C1} is shown which is crossing and swinging over 1500 volts. The same property is showing by Fig.45

Fig. 46 shows Voltage difference across capacitors which are of range 7 volts

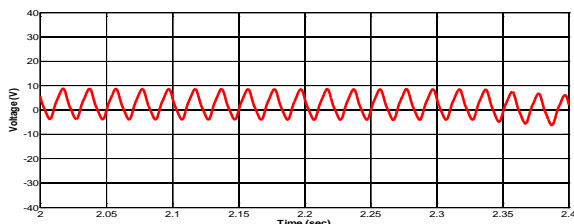


Fig. 46 Voltage difference across capacitors

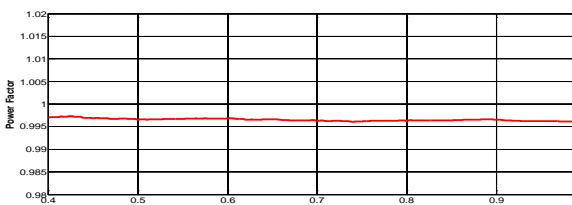


Fig. 47. Power Factor of Source.

Fig. 47 shows the power factor of supply which is approximate to unity.

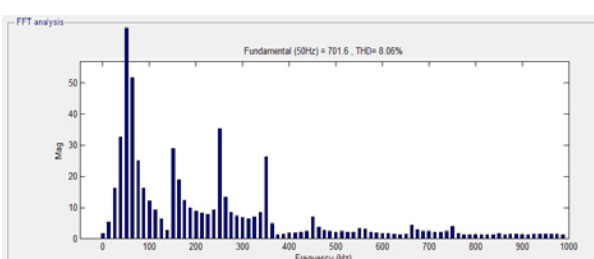


Fig.48 Harmonic analysis of source current

b) Operation with sudden Increase in load:

Here in this case operation is started with fixed load. But load is suddenly increased at $t=1$ sec. In this condition the performance and behaviour of Flying Capacitor Converter is analyzed with such change in load.

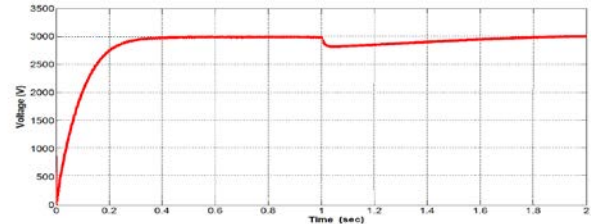


Fig. 48 Output Voltage waveform for Sudden increase in Load

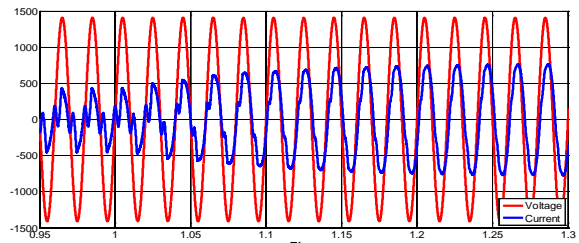


Fig. 49 Waveform of source voltage and current for sudden increase in Load

As shown in Fig.48. The dip in output supply voltage of 200 volt and settled down at time ($t = 1.8$) sec. As shown in Fig.48 , Waveforms are depicted from source side current and phase angle no lagging operation is visualized.

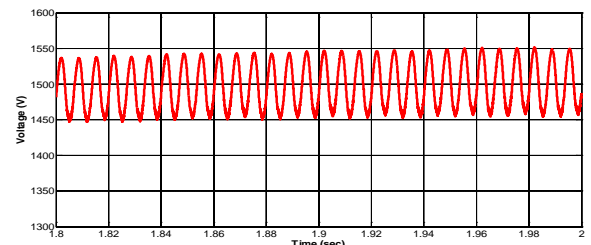


Fig .50.Voltage across upper capacitor

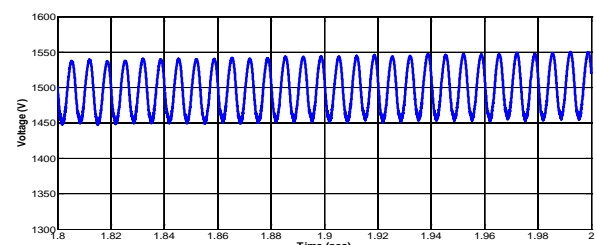


Fig. 51 Voltage across lower capacitor

Fig. 50 and Fig. 51 shows the balancing of capacitor voltage which is of variable in nature. Whenever a capacitor voltage is increasing other voltage is getting decreased.

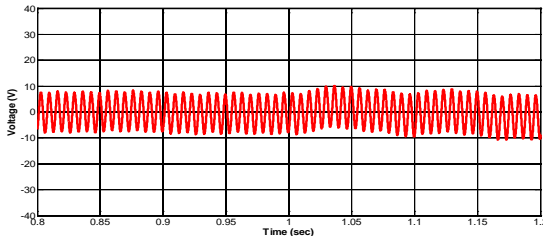


Fig. 52 Voltage difference across capacitors,

Fig. 52 shows Voltage difference across capacitors which are of range 8 volts.

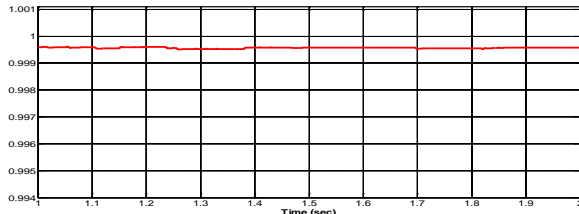


Fig.53 Power factor of source

Fig. 53 shows the power factor of supply which is approximate to unity.

C. Operation with sudden Decrease in load :

Here in this case operation is started with fixed load. But load is suddenly decreased at $t=1$ sec. In this condition performance and behaviour of Flying Capacitor Converter is analyzed with such change in load.

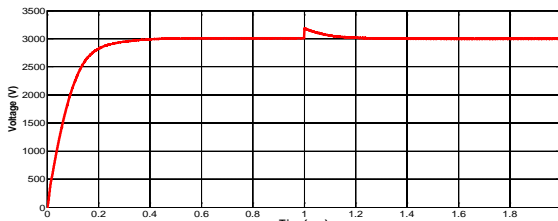


Fig. 54 Output Voltage Waveform during Sudden decrease in Load

As shown in Fig. 54. Load is suddenly decreased at $t = 1$ sec. The rise in output supply voltage of 210 volt and settled down at time $t=1.3$ sec.

Due to sudden drop of load the output voltage is getting increased at time $t=1$ sec. This supply current is suddenly sensed by controller and controller starts to response the final settling is performed at time $t=1.3$ seconds and output supply is maintained at 3000 volts reference.

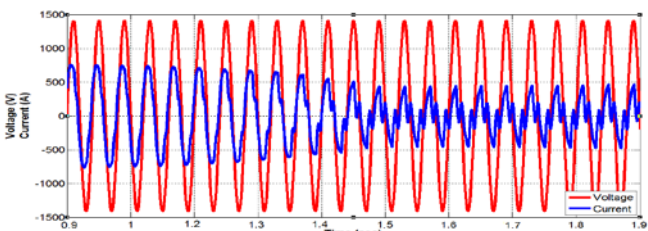


Fig. 55 Waveform of source voltage and current for sudden Decrease in Load

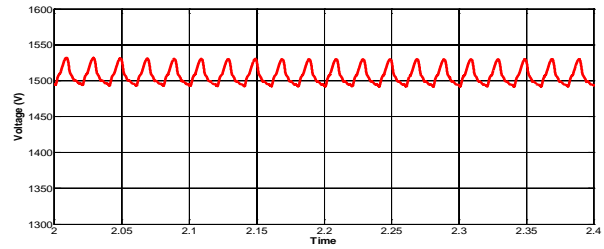


Fig. 56 Voltage across upper capacitor

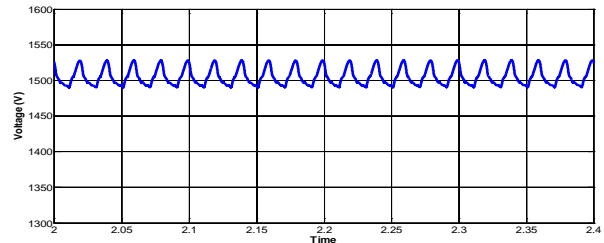


Fig. 57 Voltage across lower capacitor

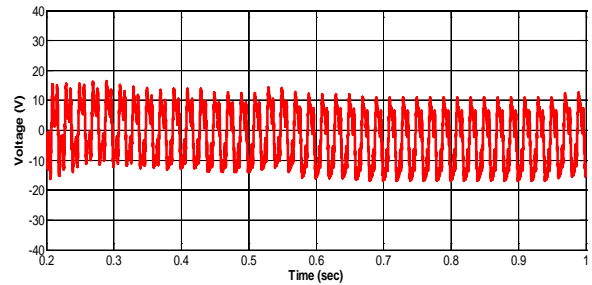


Fig. 58 Voltage difference across capacitors,

Fig. 58 shows Voltage difference across capacitors which are of range 15 volts.

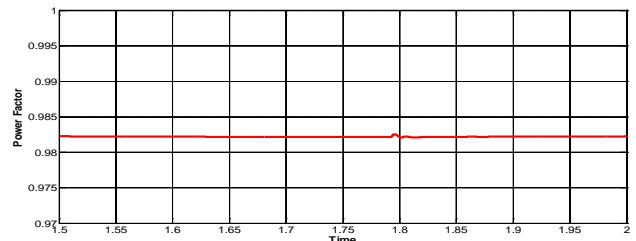


Fig. 59 Power Factor of system

Fig. 59 shows the power factor of supply which is approximate to unity.

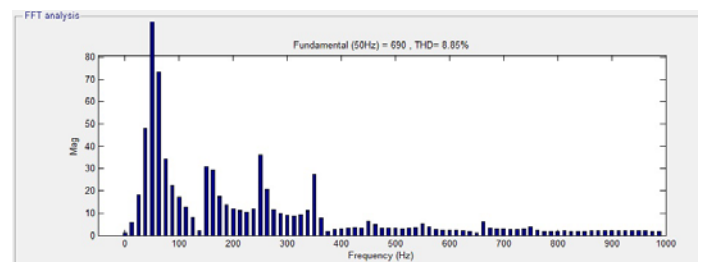


Fig. 60 Harmonic analysis of source current during load disturbance

Case II. Operation with fixed load and variable source voltage

a) Operation with increase in source voltage:

In this case the source voltage is increased. But the load is fixed and no transient condition is examined.

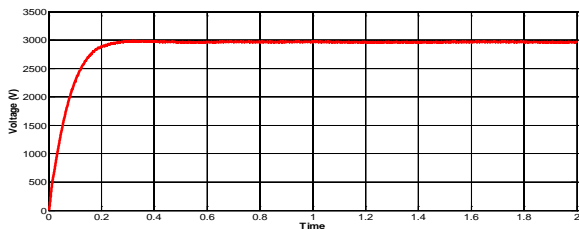


Fig. 61 Output voltage waveform for Increase in Source Voltage

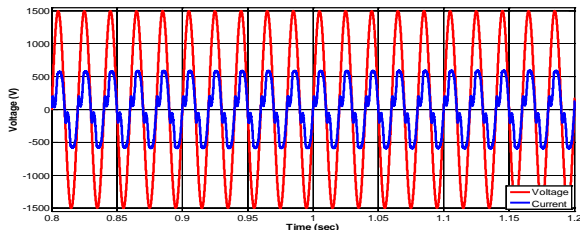


Fig.62 Waveform of source voltage and current for increase in source voltage

As shown in Fig. 61, DC supply is with fixed load. During entire operation the load is fixed, but increase of 10% source voltage is done. At time ($t=0.3$) sec it completely settled down to reference.

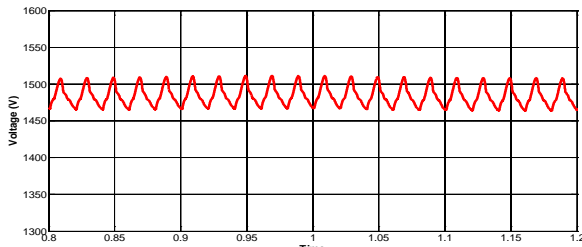


Fig.63 Voltage across upper capacitor

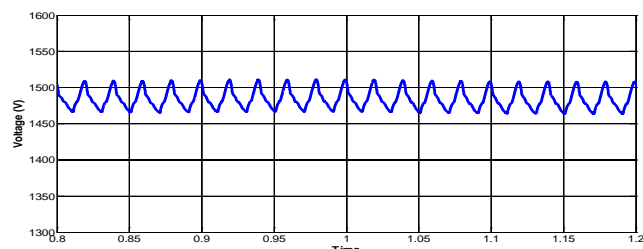


Fig.64 Voltage across lower capacitor

As shown in the Fig.63 voltage across capacitor one V_{C1} is shown which is crossing and swinging over 1500 volts. The same property is showing by Fig. 64.

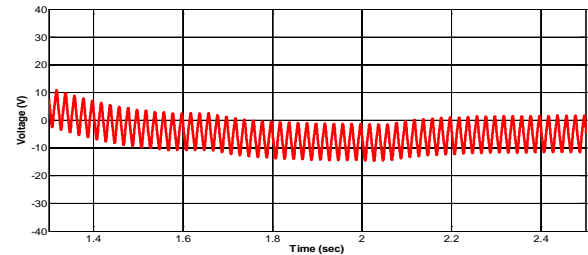


Fig.65 Voltage difference across capacitors,

Fig. 65 shows Voltage difference across capacitors which are of range 10 volts.

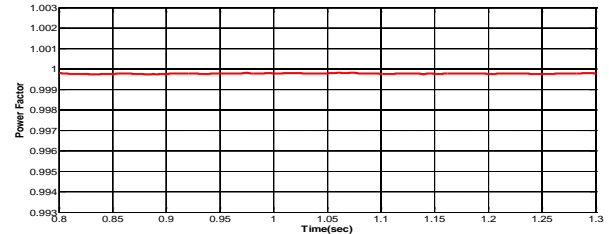


Fig. 66 Power Factor of source

Fig.66 shows the power factor of supply which is approximate to unity.

b) Operation with Decrease in source voltage:

Here in this case operation is started with fixed load. But at Supply voltage is decreased to 900 volt and in this condition the performance and behaviour of controller is analyzed with such reduction in source voltage.

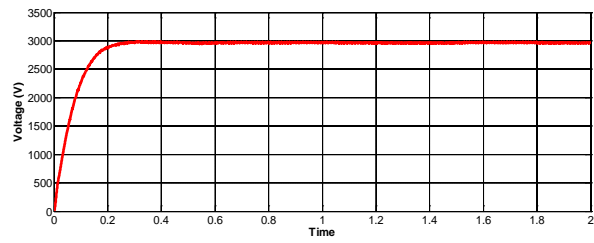


Fig. 67 Output voltage waveform for decrease in Source Voltage

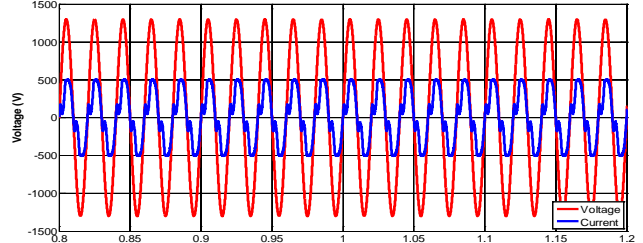


Fig. 68 Waveform of source voltage and current for decrease in source voltage

As shown in Fig.67 the output waveform of DC supply is with fixed load. But increase of 10% source voltage is done. At time $t = 0.3$ sec it completely settled down to reference.

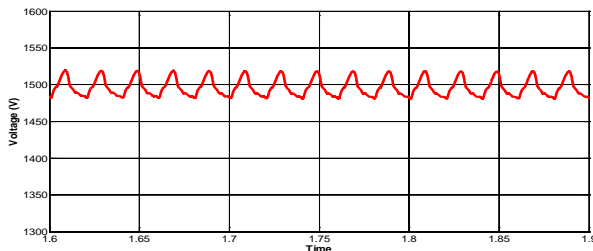


Fig.69 Voltage across upper capacitor

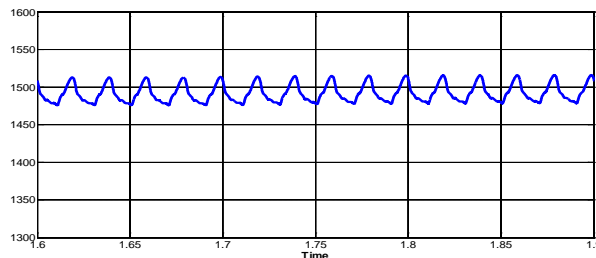


Fig.70 Voltage across lower capacitor

As shown in the Fig. 69 voltage across capacitor one V_{C1} is shown which is crossing and swinging over 1500 volts. The same property is showing by Fig. 70.

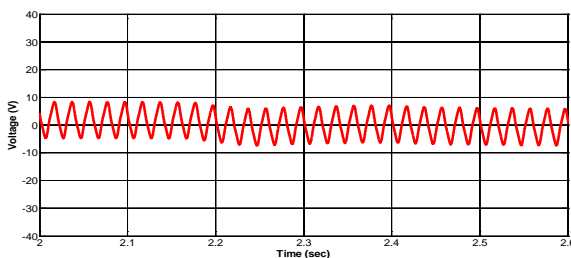


Fig. 71 Voltage difference across capacitors,

Fig.71 shows Voltage difference across capacitors which are of range 10 volts.

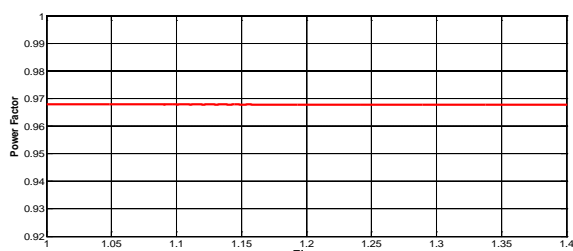


Fig. 72 Power Factor of source

Fig. 72 shows the power factor of supply which is approximate to unity.

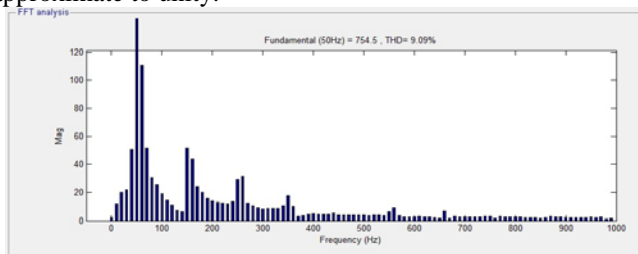


Fig. 73 Harmonic analysis of source current during load disturbance

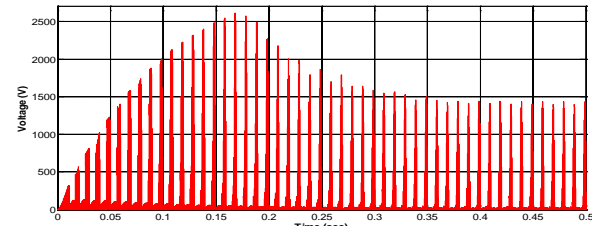


Fig.74 Switching stress across a switch

Fig. 74 show the switching stress across a switch during its operation and showing peak value of voltage across it as 2600 volts. This voltage is of intermittent nature because of switch getting regularly turning ON and Off of switch.

V. PERFORMANCE COMPARISON OF DIODE CLAMPED AND FLYING CAPACITOR MULTILEVEL CONVERTERS

Performance comparison of SVPWM controlled Diode clamped and flying capacitor multilevel converters can be summarized from simulation results.

TABLE II
DYNAMIC PERFORMANCE COMPARISON OF BOTH CONVERTERS USING SVPWM

| S. No. | Performance Parameters | Diode Clamped Multilevel Converter | Flying Capacitor Multilevel Converter |
|--------|-------------------------------|------------------------------------|---------------------------------------|
| 1. | Delay time (sec) | 0.01 | 0.1 |
| 2. | Rise Time (sec) | 0.1 | 0.26 |
| 3. | Peak Time (sec) | 0.15 | 0.4 |
| 4. | Settling time (sec) | 0.7 | 0.4 |
| 5. | DC bus voltage Overshoot (%) | 11.33 | 0 |
| 6. | DC bus voltage Undershoot (%) | 10 | 10.1 |
| 7. | Nature of Response | Under damped | Over damped |

VI. CONCLUSIONS

The main conclusions drawn from work which is carried out in this paper are summarizes for saliency of work:

- The harmonic content increase in source side results in different kind of problems as reduction of life of equipment; heat up of windings, distorted waveform of source current etc. THD of line side current should also be within prescribed limit IEC standard and is about 5%-10% for both of converters. But Diode clamped converter is working in limit of 6% THD.

- The proposed SVPWM Diode clamped and Flying Capacitor converters are able to operate without transformer at source side for step up of voltage and then conversion to DC.
- These converters show their ability to ride through from variation of loads. Also usefulness of converters is reflects in case of supply voltage variation.

VII. REFERENCES

- [1] F. Z. Peng, J. S. Lai, J. McKeever, and J. VanCoevering, "A multilevel voltage-source converter system with balanced DC voltage," in *Proc. IEEE PESC'95*, 1995, pp. 1144-1150
- [2] P. G. Kamp, B. Endres, and M. Wolf, "Modular high power DC-link converter units for power system application," in *Proc. EPE'97*, 1997, pp. 4305-4310.
- [3] L. H. Walker, "10 MW GTO converter for battery peaking services," *IEEE Trans. Ind. Applicat.*, vol. 26, pp. 63-72, Jan./Feb. 1990.
- [4] E. M. Berkouk and G. Manesse, "Multilevel PWM rectifier-multilevel inverter cascade application to the speed control of the PMSM," in *Proc. IEEE ICCA'98*, pp. 1031-1035, 1998.
- [5] Y. Chen and B. T. Ooi, "Multimodular multilevel rectifier/inverter link with independent reactive power control," *IEEE Trans. Power Delivery*, vol. 13, pp. 902-908, July 1998.
- [6] E. C. Nho, I. D. Kim, and T. A. Lipo, "A new boost type rectifier for a DC power supply with frequent output short circuit," in *Conf. Rec. IEEE-IAS Annu. Meeting*, vol. 2, pp. 1165-1172, 1999.
- [7] L. M. Tolbert, F. Z. Peng, and T. G. Habetler, "Multilevel converters for large electric drives," *IEEE Trans. Ind. Applicat.*, vol. 35, pp. 36-44, Jan./Feb. 1999.
- [8] K. T. Wong, "Harmonic analysis of PWM multilevel converters," *Proc. IEE-Elect. Power Applicat.*, vol. 148, pp. 35-43, Jan. 2001.
- [9] N. Celanovic and D. Boroyevich, "A fast space-vector modulation algorithm for multilevel three-phase converters," *IEEE Trans. Ind. Applicat.*, vol. 37, pp. 637-641, Mar./Apr. 2001.

Power Quality Enhancement by Single Switch AC-DC Converter

K. P. Yadav, S. P. Singh, *Member, IEEE*, and A. K. Gautam, *Student Member, IEEE*

Abstract-- In this paper, power factor and efficiency enhancement can be done using single switch AC-DC converter. A detailed analysis and design is presented for single-switch topologies, namely Forward, Buck, Fly back, Cuk, Sepic and Zeta Buck-Boost Converters, with high frequency isolation for Discontinuous Conduction Modes (DCM) of operation. With an awareness of modern design trends towards improved performance, these switching converters are designed for low power rating and low output voltage, typically 20.25 W with 13.5 V in DCM operation. MATLAB/Simulink Environment of the proposed single-switch converters in DCM operation.

Index Terms—AC-DC converter, discontinuous conduction mode (DCM), power quality, performance parameters etc.

I. INTRODUCTION

Single ended Converters, such as the Forward, Fly back, Cuk, Sepic, Zeta and others, are often chosen for enhancement simple low cost and low power converters. The use of only one switch and the relatively simple control circuit required are strong reasons for their choice. The discontinuous mode operation (DCM) of all single-switch topologies is most suitable for low power applications where these converters present excellent characteristics of Power Factor correction using a very simple control scheme with only one voltage feedback loop.

The conventional single-phase diode rectifier draws pulsating current due to the direct connection of the diode to an electrolytic capacitor. The amount of line current distortion produced by the single low power converter is minimal. A large number of electronic devices generate a large amount

of current distortion, and these results in environmental pollution such as electromagnetic interference.

For consumer electronics and other similar equipment with relatively low power, a solution to suppress its input current distortion, i.e. to improve its Power Factor, is required. Therefore, a simple-structure PFC converter is desirable. On the other hand, sufficient suppression of the output-voltage ripple and high power efficiency are also required. Power quality has become an important consideration when designing any converter. As a result, more attention has been given to the design of converters with good Power Factor correction, reduced input harmonics and better Efficiency. The aim is to produce a converter that draws sinusoidal input current while providing well regulated output voltage at the required power rating.

In this paper, Converters in DCM are carried out for Power Factor and Efficiency improvement. For wave shaping in single-phase single-switch AC-DC Converters different techniques are used with various combinations of inductors and capacitors [1, 2].

II. AC-DC CONVERTER

Converters can be defined as electrical circuits which convert electrical energy from one stage of voltage/current/frequency to another using semiconductor based electronic switch.

The purpose of this paper is to explore the converter modulation issue in detail as it relates to high power AC/DC (Rectifying) Converters, with particular emphasis on the process of open-loop pulse width modulation (PWM) applied to these types of Converters.

The AC-DC Converters (Rectifiers) are convert input AC to variable magnitude DC supply. The input is single phase or three phase AC supply normally available from the mains. The output is the controlled DC voltage and current.

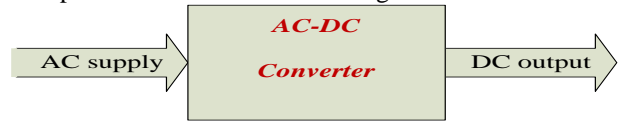


Fig. 1 AC-DC Converter

The AC to DC Converters includes diode rectifiers as well as control rectifiers. The control rectifier mainly uses SCRs.

Since the input is AC supply, the SCRs are turn off by natural commutation circuit is not required. Hence the AC-DC Converters is also called as a line (supply) commutated converter.

Switch mode AC-DC Converters are the first building block to supply power from AC mains to downstream converters for the electronics circuits normally known as loads. Therefore, they should provide performance characteristics that are acceptable by both the ac mains and the output load. From the AC mains point of view, a power supply should provide good power quality, such that, input current and input voltage are purely sinusoidal at the line frequency (50 or 60 Hz) and are in phase.

In order to conserve energy, high overall power conversion efficiency is required. However, conventional AC-DC Switch mode power supplies introduce some adverse effects on the AC side. Examples of such effects are distortion of input current/voltage, input voltage dip due to the presence of bulk capacitors and electromagnetic interference (EMI) due to high frequency switching [11].

III. CONVERTER CIRCUIT AND OPERATION

A single phase AC-DC converter with power factor correction in DCM operation as shown in Fig. 2

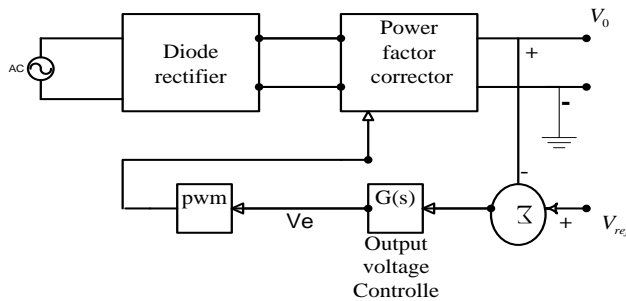


Fig. 2 Block diagram of single phase AC-DC Converter with Power Factor Correction and feedback control in DCM operation

In AC-DC Converter for discontinuous conduction mode (DCM) uses a very simple control feedback, which only requires output voltage sensing. The bridge rectifier is used at the input AC side with a Power Factor corrector. Now, a small value of output voltage, compared to the reference value and resulting value, passes through the output voltage controller $G(s)$, which generates the PWM output and is used for switching the converter[3]. The output voltage regulation is provided by the feedback loop as shown in Fig 3

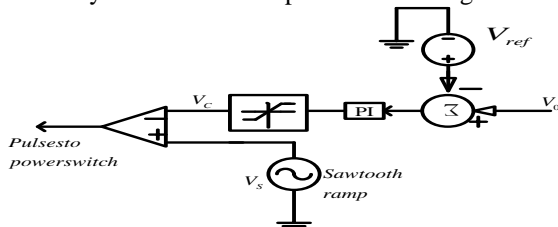


Fig. 3 Voltage follower approach for PWM control

Where the output sensed voltage V_o is compared with a reference V_{oref} value and the error is amplified in a proportional integral (PI) controller which is compared with a saw-tooth ramp V_s , thus providing the pulse to power switch. Therefore, this circuit is controlled by the difference in the on time interval and the constant switching frequency f_s .

IV. CONVERTER TOPOLOGIES FOR AC-DC CONVERTER

In single-phase single-switch AC-DC Converters different techniques are used with various combinations of inductors and capacitors for Power Factor and Efficiency enhancement.

- a) Cuk converter
- b) Flyback converter
- c) Sepic converter
- d) Zeta converter
- e) Forward converter

The above converters are work as Buck, Boost and Buck-Boost Converter topology.

V. POWER FACTOR CORRECTION AND EFFICIENCY ENHANCEMENT

The rise in the industrial, commercial and residential applications of electronic equipment's has resulted in a huge variety of electronic devices requiring mains supply. These devices have rectification circuits, which is the prominent reason of harmonic distortion. These devices convert AC-DC power supply which causes current pulses to be drawn from the ac network during each half cycle of the supply waveform [11].

a) Power factor correction:

The objective of Power Factor Correction circuits is to make the input to a power supply behaves like purely resistive or a resistor.

When the ratio between the voltage and current is a constant, then the input will be resistive hence the power factor will be 1.0. When the ratio between voltage and current is other than one due to the presence of non-linear loads, the input will contain phase displacement, harmonic distortion and thus, the Power Factor gets degraded Reduction of line current harmonics is needed in order to comply with the standard The Power Factor is defined as

$$\text{Power factor} = \frac{\text{Active power}}{\text{Apparent power}}$$

For purely sinusoidal voltage and current, the classical definition is obtained

$$p.f. = \cos\phi$$

The line current is non-sinusoidal when the load is nonlinear. For sinusoidal voltage a non-sinusoidal current the p. f. can be expressed as

$$p.f. = \frac{V_{rms} I_{1rms}}{V_{rms} I_{rms}} \cos\phi = \frac{I_{1rms}}{I_{rms}} \cos\phi = K_p \cos\phi$$

$$K_p = \frac{I_{1,rms}}{I_{rms}}, K_p \sum(0,1)$$

Where K_p describes the harmonic content of the current

The total harmonic distortion factor THD is defined as:

$$THD_i = \sqrt{\sum_{n=2}^{\infty} I_{n,rms}^2} / I_{1,rms}$$

$$K_p = \frac{1}{\sqrt{1+THD_i^2}}$$

Output voltage peak to peak ripple of converter define as:

$$\% \text{ Output Ripple} = \frac{(\text{max.value} - \text{mean value})}{\text{max.value}} \times 100$$

b) Techniques for power factor correction

Many methods have been used to remove current harmonics and thus improve the overall system Power Factor. There are two main methods to eliminate or at least reduce the input line current harmonics.

- 1) Passive Power Factor Correction
- 2) Active Power Factor Correction

c) Power efficiency

Power Efficiency of a Buck Converter changes with a change in the load. Efficiency of a Buck Converter is affected by resistive impedances and the switching losses due to the capacitive parasitic impedances of the circuit components.

$$\text{Efficiency} = \frac{\text{Output power}}{\text{Input power}} = \frac{\text{Output voltage} \times \text{Output current}}{\text{Input voltage} \times \text{Input current}}$$

VI. RESULTS AND DISCUSSIONS

Single Ended Converters, such as the Cuk, Sepic, Zeta, Forward, Flyback, are often chosen for improvement simple low cost and low power converters. These converters present excellent characteristics of Power Factor Correction using a control scheme with only one voltage feedback Loop [1].

I have taken following converters for simulation studies under two cases:

Case 1: For 100% load

Case 2: For 50% load

To verify and investigate the design and performance of the preliminary stage, a simulation study of all converters is performed in DCM operation for input AC voltage 220 V at 50 Hz and output DC voltage of 13.5 V and 20.25 W output power rating using the MATLAB 7.8 platform.

In order to demonstrate all converters, the simulation parameters are summarized in Table I.

TABLE I
SIMULATION PARAMETERS OF SINGLE-PHASE, SINGLE SWITCH AC-DC CONVERTERS IN DCM OPERATION

| Parameters | Cuk Convertor | Sepic Convertor | Zeta Convertor | Forward Convertor | Flyback Convertor |
|-----------------------------|---------------|-----------------|----------------|-------------------|-------------------|
| Transformer Turn ratio (n) | 20 | 20 | 20 | 15 | 20 |
| Magnetizing Inductance (mH) | 2.5 | 2.5 | 2.5 | 3.5 | 2.5 |
| Input Inductor (mH) | 4.7 | 4.5 | 7.1 | 5.5 | 5.1 |
| Output Inductor (μH) | 19.2 | - | 67 | 17.6 | - |
| Output Capacitor (mF) | 17.5 | 22.5 | 19.5 | 20.5 | 22.5 |

The source voltage and current waveform for all the Converter is shown in Fig.4 for DCM operation.

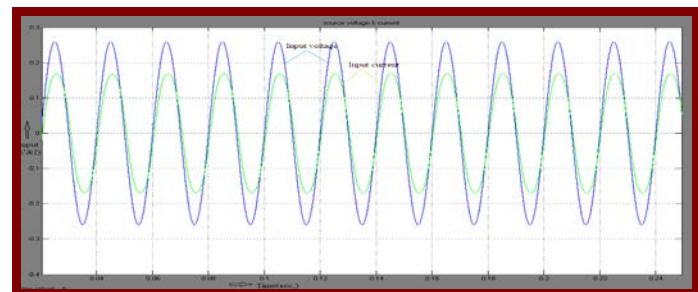


Fig. 4 Source Voltage and Current waveform for all convertor in DCM Operation

a) Simulation result of cuk converter

Case 1: For 100% load

The maximum ripple 1.2% and maximum THD 4.48% measured in output voltage and current for DCM operation. The output power of Cuk Converter is 20.25W.

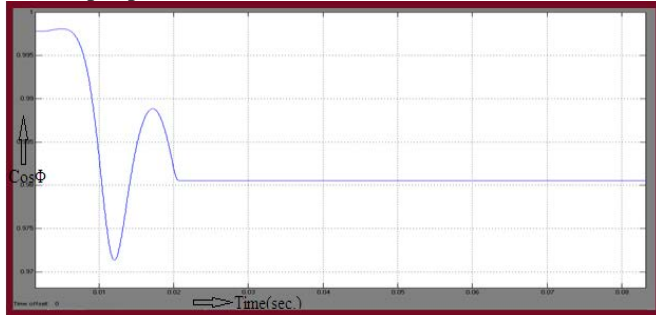


Fig. 5 Steady state input Power Factor of Cuk Converter in DCM at 100% load

The output Efficiency of Cuk Converter more than 79.8%, less than 1.3% output voltage peak to peak ripple.

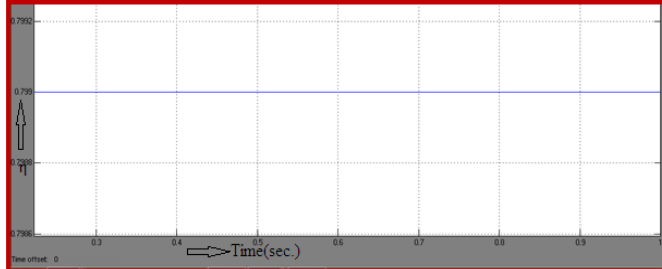


Fig. 6 Steady state output Efficiency of Cuk Converter in DCM at 100% load

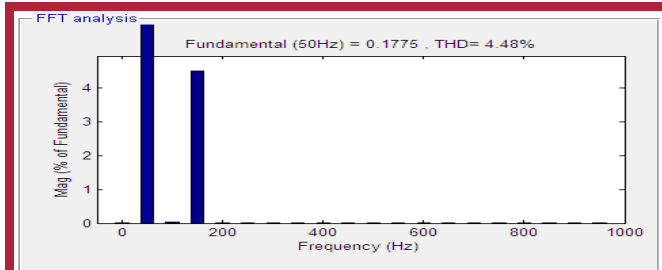


Fig. 7 Input THD of Cuk Converter at 100% load

Case 2: For 50% load

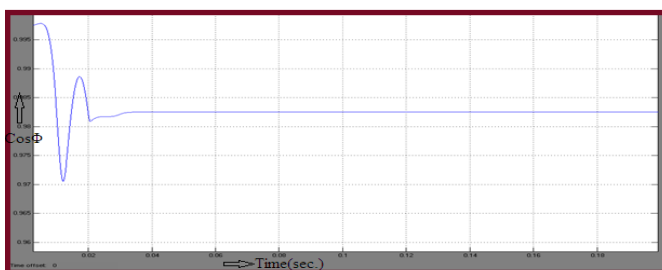


Fig. 8 Steady state input Power Factor of Cuk Converter in DCM at 50% load

The output Efficiency of Cuk Converter more than 78.8%, less than 1% output voltage peak to peak ripple.

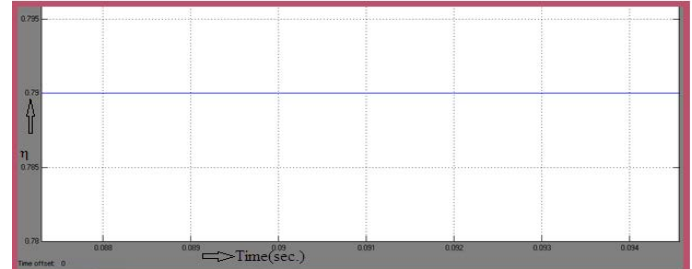


Fig. 9 Steady state output Efficiency of Cuk Converter in DCM at 50% load

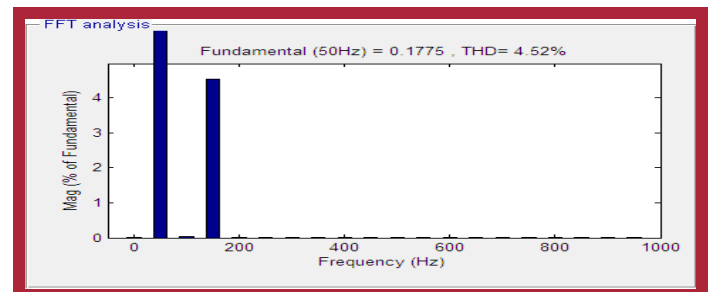


Fig. 10 Input THD of Cuk Converter at 50% load

b) Simulation result of sepic converter

Case 1: For 100% load

The maximum ripple 0.94% and maximum THD 4.63% measured in output voltage and current for DCM operation. The output power of Sepic Converter is 20.25W

The Power Factor is around 0.903, which is high in DCM operation is shown in Fig.10

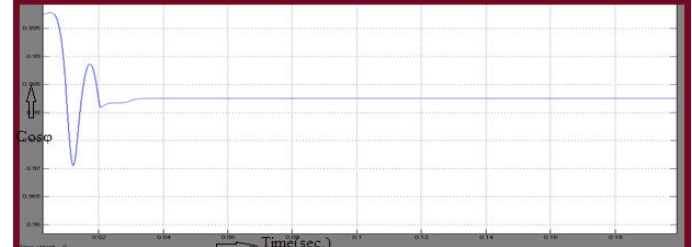


Fig. 11 Steady state input Power Factor of Sepic Converter in DCM at 100% load

The output Efficiency of Sepic Converter more than 80%, less than 1% output voltage peak to peak ripple.

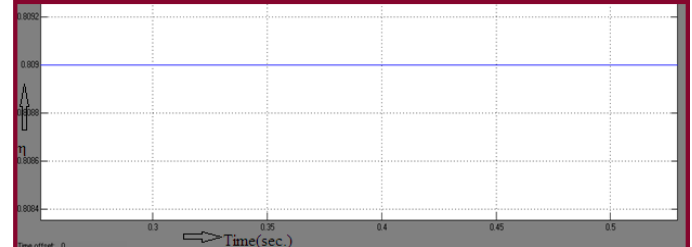


Fig. 12 Steady state output Efficiency of Sepic Converter in DCM at 100% load

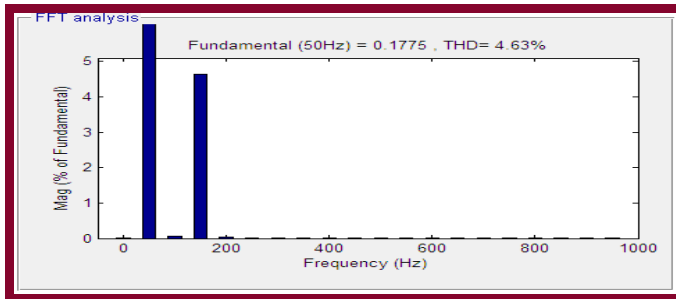


Fig. 13 Input current THD of Sepic Converter at 100 % load

Case 2: For 50% load

The steady state input Power Factor of Sepic Converter is 0.902 at 50% load is show in Fig.14.

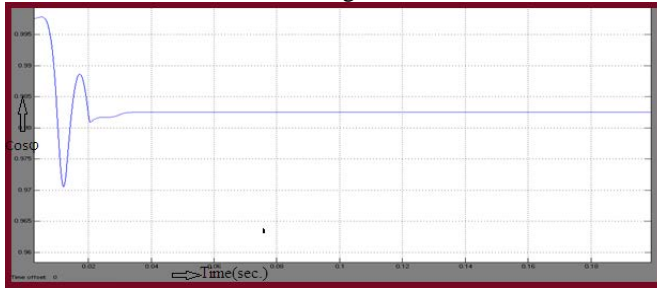


Fig. 14 Steady state input Power Factor of Sepic Converter in DCM at 50% load

The output Efficiency of Sepic Converter more than 79%, less than 1% output voltage peak to peak ripple.

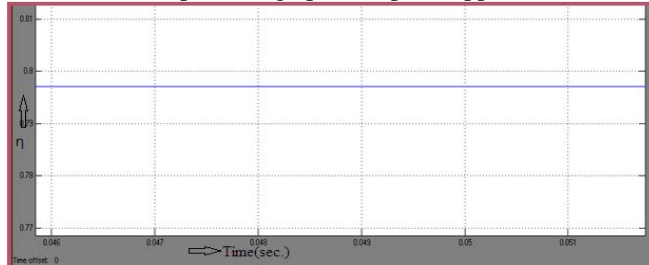


Fig. 15 Steady state output Efficiency of Sepic Converter in DCM at 50% load

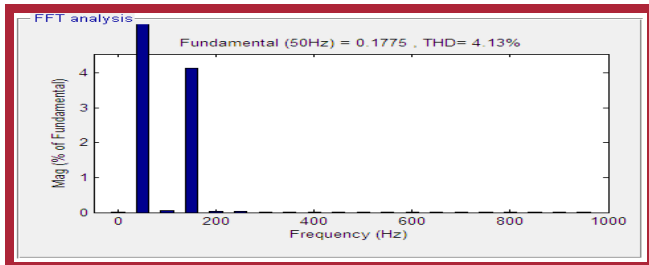


Fig.16 Input current THD of Sepic Converter at 50% load

c) Simulation result of zeta converter

Case 1: For 100% load

The maximum ripple 1.05% and maximum THD 4.0% measured in output voltage and current for DCM operation. The output power of Zeta Converter is 20.25W.

The Power Factor is around 0.984 in DCM operation is show in Fig. 17.

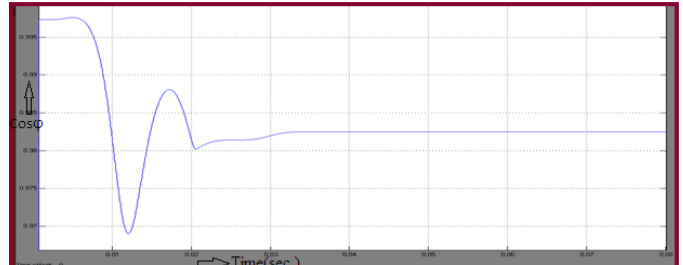


Fig. 17 Steady state input Power Factor of Zeta Converter in DCM at 100% load

The output Efficiency of Zeta Converter more than 81 %, less than 1.1% output voltage peak to peak ripple is show below

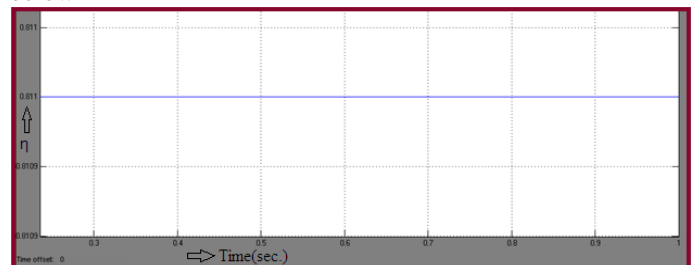


Fig.18 Steady state output Efficiency of Zeta Converter in DCM at 100% load

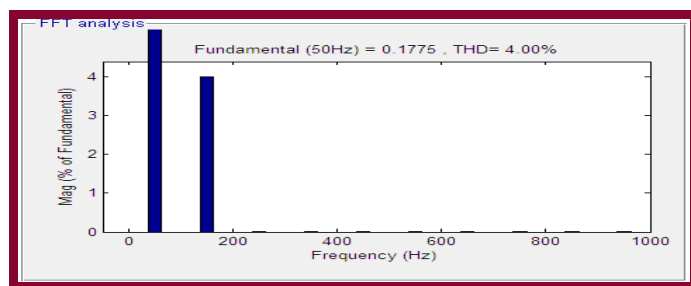


Fig. 19 Input current THD of Zeta Converter at 100% load

Case 2: For 50% load

Steady state input Power Factor of Zeta Converter is 0.980 in DCM operation at 50% load is show below

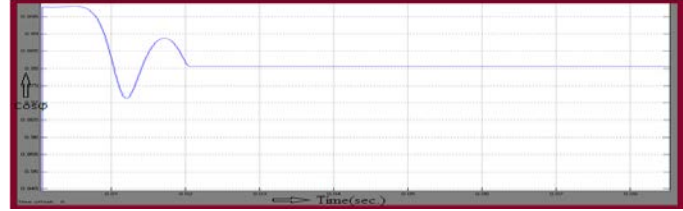


Fig. 20 Steady state input Power Factor of Zeta Converter in DCM at 50% load

The output Efficiency of Zeta Converter more than 78.5 %, less than 1% output voltage peak to peak ripple is show below

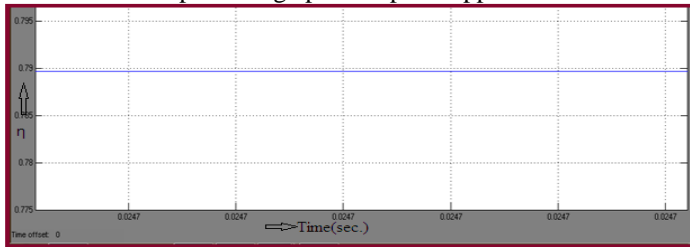


Fig. 21 Steady state output Efficiency of Zeta Converter in DCM at 50% load

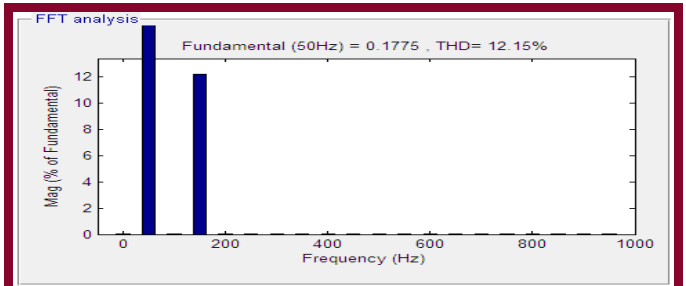


Fig. 25 Input current THD of Forward Converter at 100% load

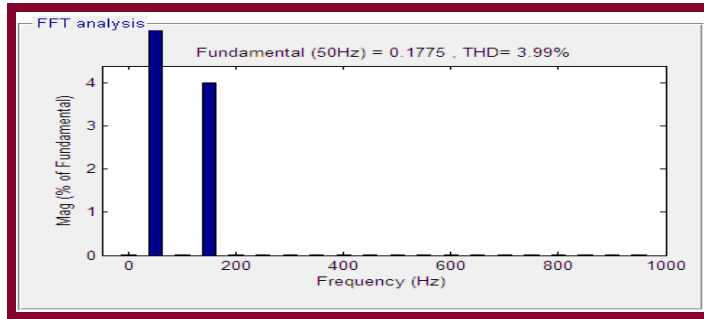


Fig. 22 Input current THD of Zeta Converter at 50% load

d) Simulation result of forward converter

Case 1: For 100% load

The maximum ripple 1.3% and maximum THD 12.15% measured in output voltage and current for DCM operation. The output power of Forward Converter is 20.25W.

The Power Factor is around 0.982, which is very high in DCM is shown in Fig.23.

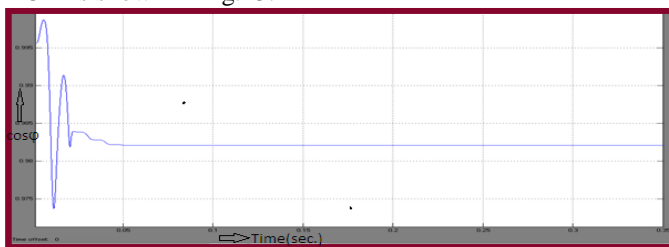


Fig. 23 Steady state input Power Factor of Forward Converter in DCM at 100% load

The output Efficiency of Forward Converter more than 82%, less than 1.4% output voltage peak to peak ripple

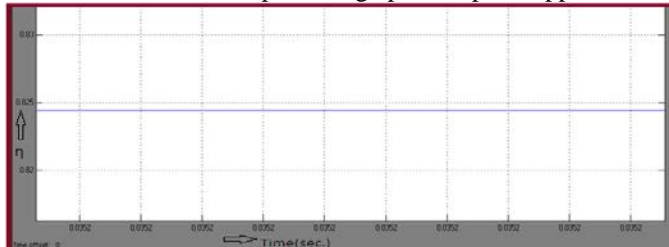


Fig. 24 Steady state output Efficiency of Forward Converter in DCM at 100% load

Case 2: For 50% load

The Steady state input Power Factor is 0.98 of Forward Converter in DCM at 50% load shown in Fig.26

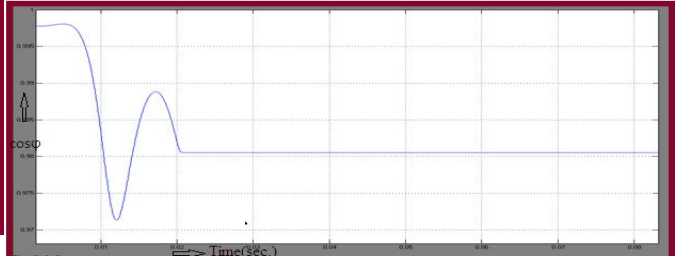


Fig. 26 Steady state input Power Factor of Forward Converter in DCM at 50% load

Steady state output Efficiency of Forward Convert79%.

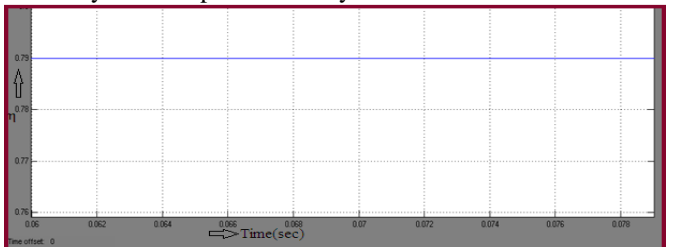


Fig. 27 Steady state output Efficiency of Forward Converter in DCM at 50% load

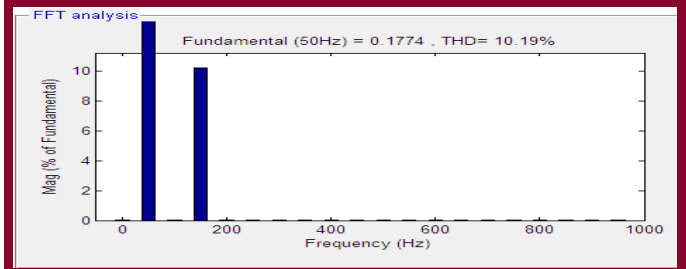


Fig. 28 Input current THD of Forward Converter at 50% load

e) Simulation result of flyback converter

Case 1: For 100% load

The maximum THD 4.80% measured in output current for DCM operation. The output power of Forward Converter is 20.25W.

The Power Factor is around 0.981, which is high .

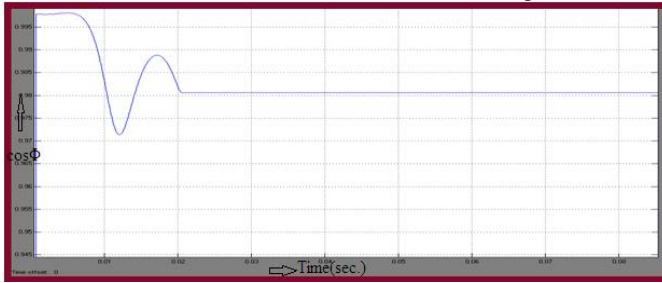


Fig.29 Steady state input Power Factor of Flyback Converter in DCM at 100% load

The output Efficiency of Flyback Converter more than 80%, less than 1.5% output voltage peak to peak ripple shown in Fig.30

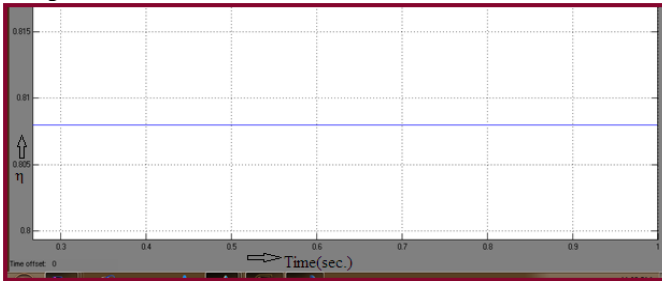


Fig. 30 Steady state output Efficiency of Flyback Converter in DCM at 100% load

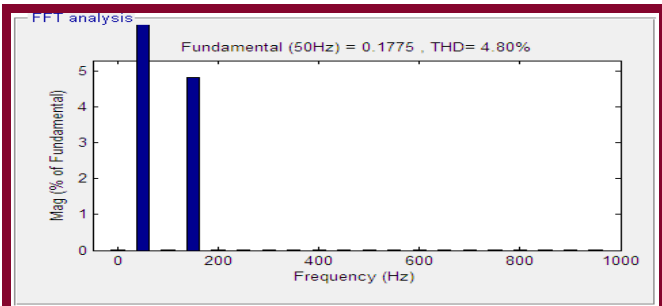


Fig.31 Input current THD of Flyback Converter at 100% load

Case 2: For 50% load

The Power Factor of Flyback Converter is 0.961 shown in Fig.32



Fig. 32 Steady state input Power Factor of Flyback Converter in DCM at 50% load

The output Efficiency of Flyback Converter more than 78%, less than 1.2% output voltage peak to peak ripple shown in Fig. 33.

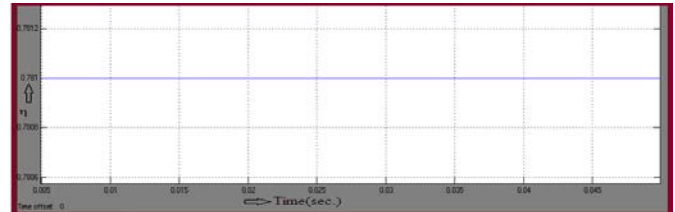


Fig. 33 Steady state output Efficiency of Flyback Converter in DCM at 50% load

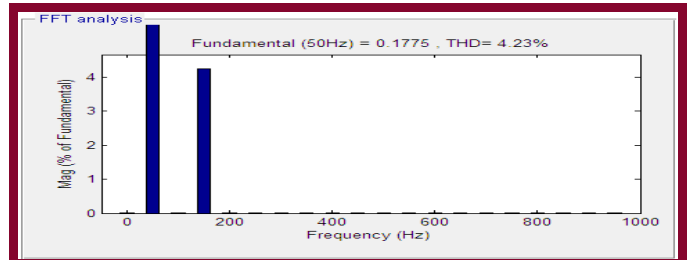


Fig.34 Input current THD of Flyback Converter at 50% load

The prototypes for single-switch converters are developed for power rating 20.25 watt with 13.5 volt output voltage at 50 kHz switching frequency in DCM operation using PWM controller technique, a Power Factor of 0.99, Efficiency more than 80%, less than 1% output voltage peak to peak Ripple and less source current harmonic distortion at full load. The power quality observations for all single-switch converters are summarized in Table II, which shows the comparison between simulations results at 100% load.

TABLE II SIMULATION RESULTS OF SINGLE SWITCH AC-DC CONVERTERS IN DCM OPERATION

| Paramete r | Cuk Converte r | | Sepic Converte r | | Zeta Converte r | | Forwar d Convert er | | Flyback Convert er | |
|---------------------|----------------|--------------|------------------|-------------|-----------------|--------------|---------------------|-------------|--------------------|--------------|
| | 50 % | 100 % | 50 % | 100 % | 50 % | 100 % | 5 0 % | 10 0 % | 50 % | 100 % |
| THD (%) | 4.52 | 4.48 | 4.13 | 4.63 | 3.99 | 4.0 | 1.0 | 12.14 | 4.23 | 4.8 |
| Powe r Facto r | 0.92 | 0.981 | 0.902 | 0.903 | 0.98 | 0.984 | 0.98 | 0.982 | 0.961 | 0.981 |
| Effici ency (%) | 79.0 | 79.9 | 79.8 | 80.9 | 78.9 | 81.1 | 7.9 | 82.4 | 78.1 | 80.7 |
| Outp ut Rippl e (%) | 0.92 | 1.206 | 0.79 | 0.94 | 0.90 | 1.05 | 1.12 | 1.30 | 1.1 | 1.429 |

VII. CONCLUSIONS

The analysis of **Single Switch AC to DC Converter for Power Quality Enhancement** is carried out in DCM operation for 13.5V, 20.25W output. High power quality is obtained with design parameters with Power Factor on the order of 0.98

and Efficiency more than 80%. The Zeta, Forward, Flyback, Sepic and Cuk Converters show close to unity Power Factor at full load with more than 80% Efficiency, on the other hand, the Forward Converter shows very good Efficiency, which comes out to 82.4% So, depending on the requirements we can choose a converter for low power applications, but little compromise between Efficiency, THD, Power Factor (PF) and Output Ripple are required and full load.

VIII. REFERENCES

- [1] Javier Sebastian, Marta Maria Hernando, Arturo Fernandez, "Input Current Shaper Based On the Series Connection of a Voltage Source and a Loss-Free Resistor," *IEEE Transactions on industry applications*, vol. 37, no. 2, march/April2001.
- [2] Laszlo Huber, Brian T. Irving, and Milan M. Jovanovich "Review and Stability Analysis Of PLL-Based Interleaving Control of DCM/CCM Boundary Boost PFC Converters" *IEEE transactions on power electronics*, vol. 24, no. 8, August 2009.
- [3] D. S. L Simonetti, J. Sebastiin, F. S. dos Reis and J. Uceda. "Design Criteria for Sepic and Cuk Converters as Power Factor Preregulators in Discontinuous Conduction Mode" *IEEE Xplore*.on April 12, 2009.
- [4] J. M. Kwon, W.-Y. Choi, J.-J. Lee, E.-H. Kim and B.-H. Kwon "Continuous conduction Mode SEPIC converter with low reverse-recovery loss for power factor correction," *IEEE Proc. Electr. Power Appl.*, Vol. 153, No. 5, September 2006.
- [5] Esam H. Ismail, Abbas A. Fardoun, "SEPIC Converter with Continuous Output Current and Intrinsic Voltage Doublers Characteristic" *Czech technical university* on June 5, 2009 from *IEEE xplore*
- [6] G. Ranganathan L. Umanand "Power factor improvement using DCM Cuk converter with coupled inductor" *IEEE Trans. Power Electron.* 1995, 10, (5).
- [7] Laszlo Huber, Milan M. Jovanović, "Single-Stage Single-Switch Input Current Shaping Technique with Fast Output Voltage Regulation" *IEEE transactions on power electronics*. vol. 13, no. 3, May 1998.
- [8] Per Karlsson "DC Distributed Power Systems Analysis, Design and Control for Renewable Energy System" *IEEE Power Electronics Specialists Conference*, PESC 2001 Conf. Rec.,Vancouver, BC, Canada, Jun. 17-21, 2001, vol. 1, pp. 33-37.
- [9] Vesa Tuomainen "low-power pfc and forward converters methods to improve performance" *Helsinki University of Technology Institute of Intelligent Power Electronics Publications Espoo* 2004.
- [10] M. Savithri and Jebasalma "ac-dc converter with quasi-active power factor correction" *International Conference on Computing and Control Engineering (ICCCE 2012)*, 12 &13 April, 2012

Review of Energy-Efficient Biometric Authentication Systems

Anil Bharti^A, Harsh Vikram Singh^B

Abstract- Over the last few years a new area of engineering science has been established whose products are likely to create a large market in the near future. It has been called "biometrics". The pioneers of this new domain intend to construct devices which would allow identification of a person on the basis of his/her "biological" characteristics: voice, dynamics of movements, features of face and other parts of the body, retina or iris pattern. Nature has made human beings with different characteristics which may vary from one person to another. This property is made use of by *Biometric technology* to distinctly identify each person. Due to the crucial developments of low power in the sensors, security mechanisms and key distribution schemes are now available.

I. INTRODUCTION

The first modern biometric device was introduced on a commercial basis over 25 years ago when a machine that measured finger length was installed for a time keeping application at Shearson Hamil on Wall Street. In the ensuing years, hundreds of these hand geometry devices were installed at high security facilities operated by Western Electric, Naval Intelligence, the Department of Energy, and the like. There are now over 20,000 computer rooms, vaults, research labs, day care centers, blood banks, ATMs and military installations to which access is controlled using devices that scan an individual's unique physiological or behavioral characteristics. Reduced prices have lead to increased awareness of biometric technologies; this coupled with lower overall prices will certainly bode well for this industry as we move through the new millennium.

II. BIOMETRICS

The term biometrics refers to the emerging field of technology devoted to the identification of individuals using biological traits or behaviors. In practice, this means capturing an image of a unique feature of an individual such as a fingerprint, hand, eye or face, and comparing it with a template captured previously. For ease of explanation this has been oversimplified, but in essence this is how biometric technology works. This paper gives an overview of key biometric technologies and basic technique involved. The various opportunities for biometrics are mentioned, followed by the uses, benefits, drawbacks, and applications.

1

-
- A. PG Scholar, ECD, KNIT Sultanpur
B. Assistant Professor, ECD, KNIT Sultanpur

III. DEFINITION

The statistical use of the characteristic variations in unique elements of living organisms is known as biometrics.

a) Why we need biometrics?

In order to avoid the problems of forgetting passwords and ID codes, Biometrics based authentication helps us in verifying your finger prints, iris pattern and voice for your identity at A.T.M's, Airports etc., you can unlock your houses, withdrawing money from a bank with just a blink of an eye, a tap of your finger or by just showing your face.

b) Biometrics-what is it?

Biometrics refers to the automatic identification of a person based on his/her physiological or behavioral characteristics. This method of identification is preferred over traditional methods involving password's and PIN numbers for various reasons:

1. The person to be identified is required to be physically present at the point of identification.
2. Identification based on biometric techniques obviates the need to remember a password or carry a token. By replacing PIN's, biometric techniques can potentially prevent unauthorized access to or fraudulent use of A.T.M's, Smart cards, computer networks.
3. PIN's passwords may be forgotten, and token based methods of identification like passwords and driver's licenses may be forged, stolen or lost. A biometric system is essentially a pattern recognition system which makes a personal identification by determining the authenticity of a specific physiological or behavioral characteristic possessed by the user.

Design issues of biometric systems :

An important issue in designing a practical system is to determine how an individual is identified and are designed by keeping two characteristics in mind, they are:

Physical characteristics

-Fingerprint, Handprint

- Face
- Scent,
- Thermal image
- Iris Pattern

Personal traits

- Voice pattern
- Handwriting
- Acoustic Signature

Depending on the context a biometric system can be either a verification(authentication) system or an identification system

Verification Vs Identification:

There are two different ways to resolve a person's identity: verification and identification. Verification (Am I whom I claim I am?) involves confirming or denying a person's claimed identity. In identification, one has to establish a person's identity (Who am I?). Each one of these approaches has its own complexities and could probably be solved best by a certain biometric system.

Types of biometric devices and their services:

Now let's see some of the biometric devices being widely used in many areas like computer/network security, government organizations, prisons.... They are:

Fingerprint identification, Face recognition, Iris recognition, Hand geometry, Signature recognition, Retinal scanning, Voice verification....

Fingerprint recognition:

Finger prints are unique to each individual and no two fingerprints are alike. Fingerprint recognition is most widely accepted biometric among the technology being used today. Fingerprints contain patterns of ridges and valleys as well as minutiae points. Minutiae points are local ridge characteristics that occur at either the ridge bifurcation or a ridge ending.

There are three methods for scanning finger prints:

- (1) Optical scanners,
- (2) Thermal scanners and
- (3) Capacitance (solid state) scanners

Currently, there are two accepted methods for extracting the fingerprint data

- (I) Minutia-based and
- (II) Correlation-based

"Minutia-based is the more microscopic of the two. This method locates the ridge characteristics (branches and endings) and assigns them a XY-coordinate that is then stored in a file.

The correlation-based method looks at the entire pattern of ridges and valleys in the fingerprint. The location of the whorls, loops and arches and the direction that they flow in are extracted and stored. Neither method actually keeps the captured image; only the data is kept, therefore making it impossible to recreate the fingerprints."

Once the scanning is complete, the analysis is done by a comparison of several features of the fingerprint known as minutia. Investigators are systems look at where the ridge lines end or where one ridge splits into two (bifurcation). The scanning system uses complicated algorithms to recognize and analyze the minutia. If two prints have three ridge endings, two bifurcations, and form the same shape with the same dimensions, then it is likely the same person's fingerprints.

Advantages:

High accuracy rate, it can perform 1-to-many comparisons, Inexpensive equipment, Easy to use (samples are easy to capture and maintain), Most established and oldest of the biometric technology.

Disadvantages:

Actual finger scan images cannot be recreated from a template image

Users relate fingerprint recognition to criminal activity.

Face (or Facial) recognition:

Face recognition is one of the newer biometrics technologies. The technology analyzes facial characteristics and attempts to match it to database of digitized pictures. This technology is relatively new and has only been commercially available since the 1990's. Face recognition has received a surge of attention since of disaster of 11/9 for its ability to identify known terrorists and criminals.

Face recognition uses distinctive features of the face – including the upper outlines of the eye socket, the areas surrounding the cheekbones, the sides of the mouth, and the location of the nose and ears – to perform verification and identification. The first step in the face recognition is to obtain an image of an individual and store it in a database for later use. Usually, several pictures (or video images) at different angles are taken. Individuals may also be asked to make different facial expressions for the data base. Next, the images are analyzed and extracted to create a template. The last step is to verify the individual's identity by matching images to those images that been stored in database.

There are four main methods being used for facial recognition:

Eigen faces: a tool developed by MIT that extracts characteristics through the use of two-dimensional grayscale imagery.

Feature Analysis (also known as Local Feature Analysis (LFA)): is the most widely used technique because of its ability to accommodate for facial changes and aspect. LFA uses an algorithm to create a face print (84 bytes in size) for comparison.

Neural network: a method that extracts features from the face and creates a template of contrasting elements that is then matched to a template in database.

Automated Face Processing (AFP): a technique that looks for distances and ratios between certain facial features, and is more ideal for poorly lit areas.

Advantages:

High accuracy rate, Can be performed from a distance, Accepted by most users, Non-intrusive, Hands-free.

Disadvantages:

Cannot not always account for the effects of aging.

Sensitive to lighting conditions.

Can perform limited 1-to-many comparisons.

Iris recognition:

No two irises are alike, not even in one individual or in identical twins. The iris consists of over 400 distinguished characteristics. Compared to the 40 or 50 points of distinct fingerprint characteristics, the iris has more than 250 distinct features. Therefore, iris scanning is much more accurate than

fingerprints or even DNA analysis of the distinguishing features.

Iris scanning is executed by scanning the measures of the colored circle that surrounds the pupil. With video technology, a camera scans the iris pattern, which consists of corona, pits, filaments, crypts, striations, and radial furrows (page). The system software then digitizes the unique information of the iris and stores it for authentication at a later time. Iris scanning is easy, accurate, and convenient. One significant downfall of Iris recognition is the initial startup costs as they are extremely high.

In identifying one's Iris, there are two types of methods that are used by Iris identification systems, passive and active. The active Iris system method requires that a user be anywhere from six to 14 inches away from the camera. It also requires the user to move back and forth so that the camera can adjust and focus in on the user's iris. The passive system allows the user to be anywhere from one to three feet away from the camera(s) that locate and focus in on the iris.

This technology's main uses are for authentication, identification, and verification of an individual.

Advantages:

- High accuracy rate
- Imitation is almost impossible

Disadvantages:

- perceived to be intrusive and invasive
- Can be done from a short distance
- optical readers are difficult to operate requiring advanced training for employees

Hand geometry:

Hand geometry is concerned with measuring the physical characteristics of the user's hand and fingers and it is believed to be sufficiently unique for use as a means of biometric authentication. The technology records various dimensions of the human hand, it is relatively easy to use, and offers a good balance of performance characteristics. Reader configurations vary among a softball-shaped device which the subject grabs in his hand and a flat plate which the subject places his/her hand, a bar which the subject grabs as if opening a door, and a flat plate which the subject places his/her hand on.

Hand geometry readers are developed in a wide range of scenarios, including time and attendance recording where they have proved extremely popular. The methodology may be suitable where there is a large user base or there are users who access the system infrequently. Accuracy can be very high if desired.

Hand geometry readers are relatively large and expensive but the ease of integration into other systems and processes, small template size (only 9 bytes for pure hand geometry template) and ease of use makes it a good choice for many projects.

Hand geometry Vs Fingerprints:

Unlike fingerprints the human hand isn't unique. One can use finger length, thickness and curvature for the purposes of verification but not for identification. For some kinds of access control like immigration and border control, invasive biometrics (e.g., fingerprints) may not be desirable as they infringe on privacy. In such situations it is desirable to have a biometric system that is sufficient for verification. As hand geometry is not distinctive, it is idle choice. Furthermore, hand geometry data is easier to collect. With fingerprint collection good frictional skin is required by imaging systems, and with retina-based recognition systems, special lighting is necessary. Additionally, hand geometry can be easily combined with other biometrics, namely fingerprint. One can envision a system where fingerprints are used for (in frequent) identification and hand geometry is used for (frequent) verification.

Application Areas:

The uses for biometric security are varied and growing. It was developed in response to a need to associate human action with identity – whether conducting a transaction, accessing a computer or a critical information system, or entering secure physical area. Some of the existing and proposed applications in general we use are described below:

Computer/Network security:

Many stand-alone and network computer systems carry valuable and sensitive information. Controlling access to these systems is another major use of biometric authentication systems.

Internet transactions:

Due to growing security requirements that results from the boom in e-commerce, many think of on-line transactions as being an obvious area for biometrics. The biometric authentication generates a greater degree of vendor confidence because he knows that person that the person at the terminal is he who he claims to be.

Physical area security:

Conclusion:

It is important to recognize that although biometric authentication has served extensively in high security applications in defense industry, it is still fledgling technology in commercial world, both in terms of its technical sophistication and current extent of deployment. There are no established standards for biometric system architecture, for template formation, or even for biometric reader testing. In the absence of standards and direction, the rapid and wide spread deployment of biometric authentication system could easily facilitate the problematic proliferation of authentication and tracking of the people.

REFERENCES

- [1] Jain, A., Hong, L., & Pankanti, S. (2000). "Biometric Identification".
- [2] Jain, Anil K.; Ross, Arun (2008). "Introduction to Biometrics" ..
- [3] Weaver, A.C. (2006). "Biometric Authentication".

- [4] Jain, A.K.; Bolle, R.; Pankanti, S., eds. (1999). *Biometrics: Personal Identification in Networked Society*.
- [5] Sahoo, SoyujKumar; Mahadeva Prasanna, SR, Choubisa, Tarun (1 January 2012). "Multimodal Biometric Person Authentication : A Review".
- [6] "Questions Raised about Iris Recognition Systems". *Science Daily*. 12 July 2012.
- [7] Saylor, Michael (2012). *The Mobile Wave*:
- [8] Bill Flook (3 October 2013). "This is the 'biometric war' Michael Saylor was talking about".
- [9] A. Rattani, "Adaptive Biometric System based on Template Update Procedures," PhD thesis, University of Cagliari, Italy, 2010
- [10] R. Palaniappan, and S. M. Krishnan, "Identifying individuals using ECG signals,"
- [11] McConnell, Mike (January 2009). Biometric Consortium Conference.
- [12] Schneider, Bruce. "The Internet: Anonymous Forever". Retrieved 1 October 2011.

Energy Efficient Image Watermarking in Spatial and Transform Domain

A. Raj Vikram Singh, B. Dr. Rakesh Kumar Singh, C. Dr. Harsh Vikram Singh

ABSTRACT: Digital watermarking embeds an imperceptible signature or watermark in a digital file containing audio, image, text, or video data. The watermark can be used to authenticate the data file and for tamper detection. It is particularly valuable in the use and exchange of digital media, such as audio and video, on emerging handheld devices. However, watermarking is computationally expensive and adds to the drain of the available energy in handheld devices. Amongst these, image watermarking is known to have an edge over other steganography mediums or techniques. In this paper we discussed performance analysis of mainly two kinds of image watermarking; the one in spatial or image domain and the other in transform domain.

KEYWORDS: Image Steganography, Spatial Domain, Frequency or Transform Domain.

I. INTRODUCTION

Since ages secure communications has a vital role to play in information transfer. Information security has a major role to play both for legal purposes (such as police) and also illegitimate purposes (such as for criminals and militants). There have been various methods of secure communication as recorded in history and present.

Cryptography, Steganography and Watermarking are methods for secure data transmission. In cryptography we allow encryption of the secure information to be transferred. The secret information is encrypted and decoded by the authenticated decoder. Thus, on one hand, any third person can judge that a secret message is being transferred from encoder to decoder. It also ensures authentication of the decoder. There are mainly three main techniques of encryption. First, secret key cryptography, in which there is only a single key for encryption and decryption. Second, public key cryptography, in which there are two separate keys. One key is used for encryption while the other is used for decryption. Third, hash functions, which is also known as one way cryptography. Hash functions encrypt a message in such a manner that encrypted message, that is, the cipher text cannot be recovered from plain text.
1

Many different steganography methods have been proposed during the last years; most of them can be seen as

A. PG Scholar, ECD, KNIT Sultanpur
B. Assistant Professor, ECD, KNIT Sultanpur
C. Assistant Professor, ECD, KNIT Sultanpur
harshvikram@ieee.org

substitution systems. Such methods try to substitute a redundant part of a signal with secret message; their main disadvantage is the relative weakness against cover modification. Although steganography provides a method for secure data transmission but limitations of method like LSB (Least Significant Bit) substitution can lead to security threats. In LSB insertion method, if the LSBs of the stego-image are changed either accidentally or intentionally by the attackers the data will be totally lost. The variety of challenges that arise in the LSB substitution is due to the action of Human Visual System (HVS) and typical modification that image undergoes.

II. IMAGE OR SPATIAL DOMAIN STEGANOGRAPHY

In spatial domain methods a steganographer modifies the secret data and the cover medium in the spatial domain, which involves encoding at the level of the LSBs. This method although simpler, has a larger impact compared to the other two types of methods. Spatial domain techniques perform data embedding by directly manipulating the pixels, code value or bit stream of the host image signal and they are computationally simple and straight forward. The data hiding involves direct replacement of host media data by message data. *Least significant bit (LSB) substitution, patchwork, and quantization index modulation* are some of the important spatial domain techniques. Out of these LSB substitution is a popular method of spatial domain steganography where a pixel of the digital image cover is randomly selected and the *LSB* of this pixel is replaced with a data bit and this process is iterated until all data bits have been embedded.

A. LSB INSERTION TECHNIQUE

LSB is the lowest bit in a series of numbers in binary. e.g. in the binary number: 10110001, the least significant bit is far right 1. The LSB based Steganography is one of the steganographic methods, used to embed the secret data in to the least significant bits of the pixel values in a cover image. e.g. 240 can be hidden in the first eight bytes of three pixels in a 24 bit image.

PIXELS: (00100111 11101001 11001000)
(00100111 11001000 11101001)
(11001000 00100111 11101001)

240 : 011110000

RESULT: (00100110 11101001 11001001)
(00100111 11001001 11101000)
(11001000 00100110 11101000)

Here number 240 is embedded into first eight bytes of the grid and only 6 bits are changed. Least significant bits (LSB) insertion is a simple approach to embedding information in image file. The simplest steganographic techniques embed the bits of the message directly into least significant bit plane of the *cover-image* in a deterministic sequence. Modulating the least significant bit does not result in human-perceptible difference because the amplitude of the change is small. In the above example, consecutive bytes of the image data – from the first byte to the end of the message – are used to embed the information. This approach is very easy to detect. A slightly more secure system is for the sender and receiver to share a secret key that specifies only certain pixels to be changed. Should an adversary suspect that LSB steganography has been used, he has no way of knowing which pixels to target without the secret key.

While using a 24 bit image gives a relatively large amount of space to hide messages, it is also possible to use a 8 bit image as a cover source. Because of the smaller space and different properties, 8 bit images require a more careful approach. Where 24 bit images use three bytes to represent a pixel, an 8 bit image uses only one. Changing the LSB of that byte will result in a visible change of color, as another color in the available palette will be displayed. Therefore, the cover image needs to be selected more carefully and preferably be in grey scale, as the human eye will not detect the difference between different gray values as easy as with different colors. These techniques are based on modifying the least significant bits (LSBs), of the pixel values in the space domain. In a basic implementation, these pixels replace the entire LSB-plane with the stego-data; on average, 50% of the LSBs are flipped (see Figure 1). It can be shown that fidelity of the stego-image measured in peak-signal-to-noise ratio with respect to the cover is 51.1dB, representing a very high degree of imperceptibility compared to the lower bound of 39dB generally accepted by researchers of watermarking. With more sophisticated schemes in which embedding locations are adaptively selected, depending on human vision characteristics, even less distortion is achievable. Popular tools include EzStego, S-Tools, and Hide and Seek. In general, simple LSB embedding is susceptible to image processing, especially lossy compression.

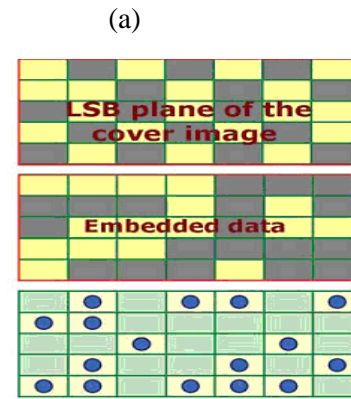
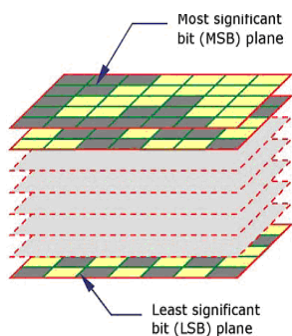


Fig. 2: An LSB Approach (Circles represent flipped bits; the stego image is visually identical to the cover)

B. 5th BIT INSERTION TECHNIQUE

In the proposed method, we have used 5th bit of pixel value. In 5th Significant bit Insertion Method, the 5th significant bit of each 8-bit pixel of a cover image is used to hide the binary data. To hide 240 (11110000) can be hidden in the first eight bytes of 8-bit grayscale image.

| | | | |
|---------------|----------|----------|----------|
| 00100111 | 11101001 | 11001000 | 00100111 |
| 11001000 | 11101001 | 11001000 | 00100111 |
| 240: 11110000 | | | |

RESULT:

| | | | |
|-------------------|-------------------|-------------------|-------------------|
| 0010 <u>1</u> 111 | 1110 <u>1</u> 001 | 1100 <u>1</u> 000 | 0010 <u>1</u> 111 |
| 1100 <u>0</u> 000 | 1110 <u>0</u> 001 | 1100 <u>0</u> 000 | 0010 <u>0</u> 111 |

Here number 240 is embedded into first eight bytes of the grid and only 5 bits are changed. But the value of the pixel is changed by 8 values up or 8 values down.

PROPOSED ALGORITHM FOR 5th BIT INSERTION TECHNIQUE

There are two parts to the algorithm: Part 1 deals with embedding the data at the transmitting end while part 2 considers decoding the information

Part 1: Embedding Algorithm

- i. Read the cover image $I(M,N)$ in BMP format of size $M \times N$.
- ii. Read the Secret text message
- iii. Read the Secret key
- iv. find the length of the secret text (T)
- v. Find the maximum text length which can be embedded in the Image(T_{max})
- vi. If $T_{max} > T$
- vii. Convert the secret text into binary form

- viii. Encoding: Hide stream of bits of secret message into the image at 5th bit positions sequentially.
- ix. Save the stego image (Encoded image), I'(M,N) in BMP format of size MxN.

Cover and stego images are shown in Figure and respectively from which it can be seen that there is no significant perceptual difference between these two images.

Part 2: Extracting Algorithm

The working of the extracting is described as follows:

- (i) Read the stego image I'(M,N) of size MxN.
- (ii) Read the Secret Key
- (iii) Convert the secret key into binary form
- (iv) Extract stream of bits of Secret key
- (v) Compare both the secret keys
- (vi) Extract stream of bits of secret message from stego image by extracting the LSBs sequentially.

Rearrange the extracted bits and regenerate the ASCII message

III. TRANSFORM DOMAIN TECHNIQUES

Digital steganography is the art of secretly hiding information inside a multimedia signal in such a way that its very existence is concealed. In this paper, we present a new steganographic technique for covert communications. The technique embeds the hidden information in the transform domain after decorrelating the image samples in the spatial domain using a key. This results in a significant increase in the number of transform coefficients that can be used to transmit the hidden information, and therefore, increases the data embedding capacity. The hidden information is embedded in the transform domain after taking a block DCT of the decorrelated image. A quantization technique is used to embed the hidden data. The decoding process requires the availability of the same key that was used to decorrelate the image samples. By using quantization techniques, the hidden information can be recovered reliably. If the key is not available at the decoder it is impossible to recover the hidden information. Hence, this system is secure against removal attacks. The statistical properties of the cover and the stego image remain identical for small quantization steps. Therefore, the hidden data cannot be detected. The data embedding system is modeled as transmitting information through a Gaussian channel.

A. DCT BASED IMAGE STEGANOGRAPHY TECHNIQUE

DCT is a general orthogonal transform for digital image processing and signal processing with advantages such as high compression ratio, small bit error rate, good information integration ability and good synthetic effect of

calculation complexity. One dimensional DCT can be described with the help of equation 1 and 2.

$$F(0) = \frac{1}{\sqrt{N}} \sum_{x=0}^{N-1} f(x) \quad (1)$$

$$F(u) = \sqrt{\frac{2}{N}} \sum_{x=0}^{N-1} f(x) \cos\left(\frac{2(x+1)u\pi}{2N}\right) \quad (2)$$

Where F (u) is cosine transform coefficient, u is general frequency variable, u=1, 2, 3...., N-1; if f(x) is M sequence of time domain, x= 1, 2, 3... N-1, one dimensional inverse discrete cosine transform is defined as given in equation 3:

$$f(x) = \sqrt{\frac{1}{N}} F(0) + \sqrt{\frac{2}{N}} \sum_{u=1}^{N-1} F(u) \cos\left(\frac{2(x+1)\pi}{2N}\right) \quad (3)$$

Two dimensional DCT is defined below (equation4):

$$f(x,y) = C(u)C(v) \sum_{u=0}^{N-1} \sum_{v=0}^{N-1} F(u,v) \cos\left(\frac{(2x+1)u\pi}{2N}\right) \cos\left(\frac{(2y+1)v\pi}{2N}\right) \quad (4)$$

The inverse of two dimensional DCT can be defined as given in equation 4:

For x, y =0, 1, 2... N -1. N is horizontal and vertical pixel number of pixel block, generally N=8. If N is more than 8, efficiency is increased a little but complexity is increased many times.

DCT allows an image to be broken up into different frequency bands namely the high, middle and low frequency bands thus making it easier to choose the band in which the message is to be inserted. The literature survey reveals that mostly the middle frequency bands are chosen because embedding the message in a middle frequency band does not scatter the message to most visual important parts of the image i.e. the low frequencies and also it do not overexpose them to removal through compression and noise attacks where high frequency components are targeted. Numerous steganography techniques based on DCT are proposed. Although some of the steganography techniques embed the message in the DC component, most techniques utilize the comparison of middle band DCT coefficients to embed a single bit of information into a DCT block. The middle-band frequencies (FM) of an 8*8 DCT block can be shown below in figure 2.1. DCT block consists of three frequency bands- Low frequency band (FL), High frequency band (FH), mid frequency band (FM). We have chosen FM for embedding the message.

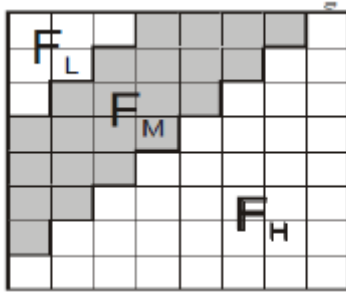


FIG 3: DCT Regions

B. DWT BASED IMAGE STEGANOGRAPHY TECHNIQUE

The frequency domain transform we applied in this research is Haar-DWT, the simplest DWT. A 2-dimensional Haar-DWT consists of two operations: One is the horizontal operation and the other is the vertical one. Detailed procedures of a 2-D Haar-DWT are described as follows: At first, scan the pixels from left to right in horizontal direction. Then, perform the addition and subtraction operations on neighboring pixels. Store the sum on the left and the difference on the right as illustrated in. Repeat this operation until all the rows are processed. The pixel sums represent the low frequency part (denoted as symbol L) while the pixel differences represent the high frequency part of the original image (denoted as symbol H). Secondly, scan the pixels from top to bottom in vertical direction. Perform the addition and subtraction operations on neighboring pixels and then store the sum on the top and the difference on the bottom as illustrated in. Repeat this operation until all the columns are processed. Finally we will obtain 4 sub-bands denoted as LL, HL, LH, and HH respectively. The LL sub-band is the low frequency portion and hence looks very similar to the original image.



Fig. 4: (a) Original image (b) Image after DWT based Embedding

IV. PERFORMANCE PARAMETERS AND COMPARATIVE ANALYSIS

Comparative analysis of LSB based and DCT based steganography has been done on basis of parameters

like PSNR, MSE and BER. Both gray scale and colored images have been used for experiments. Peak signal to noise ratio is used to compute how well the methods perform. PSNR computes the peak signal to noise ratio, in decibels, between two images. This ratio is used as a quality measurement between two images. If PSNR ratio is high then images are best of quality. Imperceptibility takes advantage of human psycho visual redundancy, which is very difficult to quantify. The (weighted) mean squared error between the cover image and the stego-image (embedding distortion) is used as the measure to assess the relative perceptibility due to the embedded text. Mean square error (MSE) and Peak Signal to Noise Ratio (PSNR) can be used as metrics to measure the degree of imperceptibility. After the computations of various computer-based calculations on the basis of three performance metrics of the image steganographic techniques presented in this thesis our next step is to analyze the performance of the three performance metrics w.r.t the discussed methods of image steganography techniques for various lengths of the secret text.

A. Peak Signal to Noise Ratio (PSNR)

Figure below show the Peak Signal to Noise Ratio verses different length of the secret text using LSB Method, 5th Significant Bit Method and DCT Method.

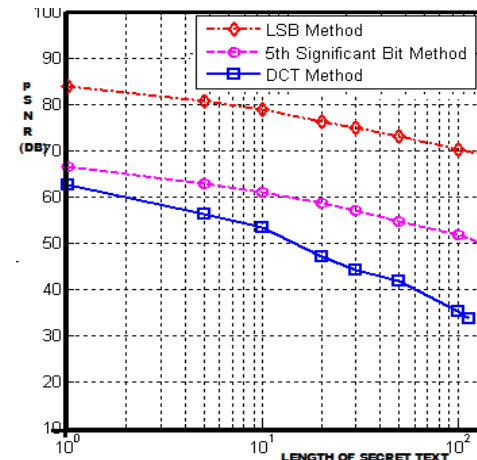


Fig. 5 : Comparative chart of PSNR verses characterlength of the secret text using LSB Method, 5th Significant Bit Method & DCT Method for lena.bmp image(shown in fig 4(a))

Frome above, it can be obsevered that, for the same length of the secret text, the PSNR values are not same. In LSB Method, the PSNR values are comparatively high. It shows that the imperceptibility of the stego image is comparatively high. In 5th significant bit insertion method, the PSNR values are

less than the LSB Method but more than the DCT Method. It shows that the imperceptibility of the watermarked image is better than the DCT Method but less than LSB Method. In case of the DCT Method, the PSNR values are comparatively low.

B. Bit Error Rate (BER)

Figure below show the Bit Error Rate (in %) verses different length of the secret text using LSB Method, 5th Significant Bit Method and DCT Method.

In digital transmission, the number of **bit errors** is the number of received bits of a data stream over a communication channel that has been altered due to noise, interference, distortion or bit synchronization errors. The **bit error rate** or **bit error ratio (BER)** is the number of bit errors divided by the total number of transferred bits during a studied time interval. BER is a unit less performance measure, often expressed as a percentage. The **bit error probability** p_e is the expectation value of the BER. The BER can be considered as an approximate estimate of the bit error probability. This estimate is accurate for a long time interval and a high number of bit errors. Mathematically, BER is given as:

$$BER (\%) = \frac{\text{No. of dissimilar bits between two images}}{\text{Total no. of bits of the image}} \times 100$$

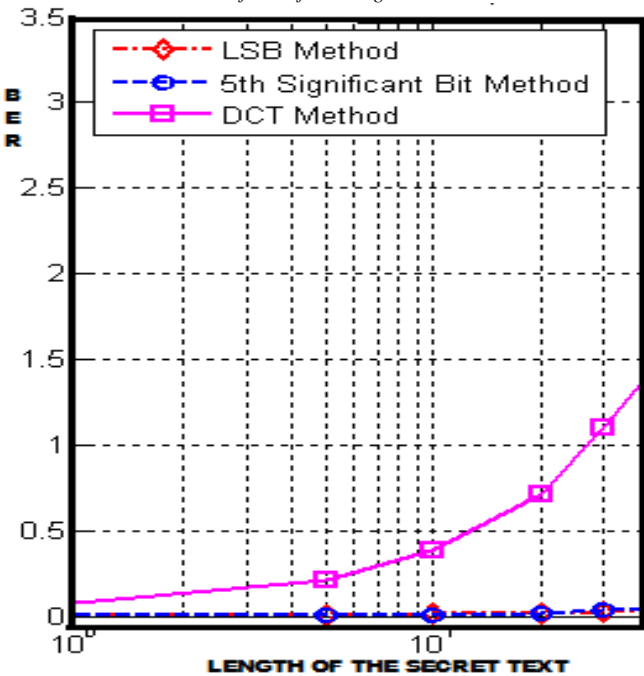


Fig. 6: Comparative chart of BER (in %) versus character length of the secret text using LSB Method, 5th Significant Bit Method & DCT Method for lena.bmp

From above, it can be observed that, using the LSB Method or using the 5th significant bit insertion method, the bit error rates are almost same. In case of the DCT Method, the BERs are comparatively high. It shows that, for the same length of the secret text, DCT Method changes more number of bits of the image.

C.MEAN SQUARE ERROR (MSE)

Figure below show the Mean Square Error verses different length of the secret text using LSB Method, 5th Significant Bit Method and DCT Method. The MSE is the second moment (about the origin) of the error, and thus incorporates both the variance of the estimator and its bias. For an unbiased estimator, the MSE is the variance. Like the variance, MSE has the same units of measurement as the square of the quantity being estimated. In an analogy to standard deviation, taking the square root of MSE yields the **root mean square error** or **root mean square deviation(RMSE or RMSD)**, which has the same units as the quantity being estimated; for an unbiased estimator, the RMSE is the square root of the variance, known as the standard deviation.

$$MSE = \frac{1}{MN} \left[\sum_{i=1}^M \sum_{j=1}^N (f_{i,j} - g_{i,j})^2 \right] \quad (5)$$

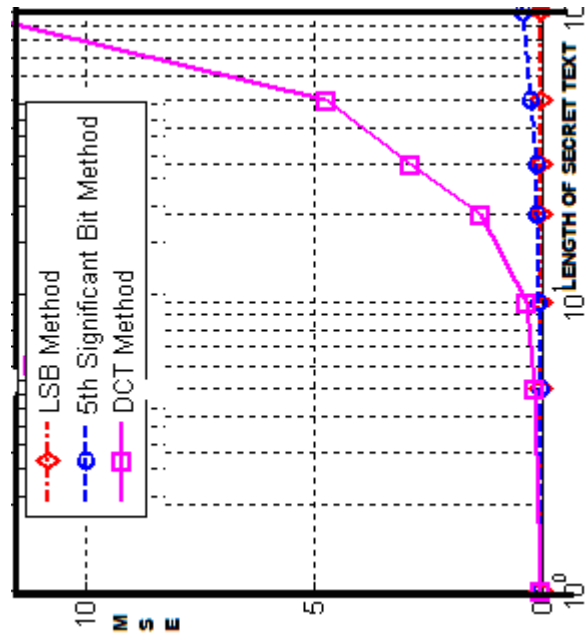


Fig. 7 : Comparative chart of MSE versus characterlength of the secret text using LSB Method, 5th Significant Bit Method & DCT Method for lena.bmp image

From figure below, it can be observed that in LSB Method, the MSE values are zero whereas, it is very less using 5th significant bit method. But in case of the DCT Method, the MSE values grow rapidly. It concludes that using DCT Method, the length of the secret text should be low.

D.CONCLUSION TABLE

The conclusion of the analysis, that have been conducted in this section, is tabulated in table1. It is shown next which shows a comparative analysis between spatial domain techniques.

| ITEMS | LSB insertion method | 5 th significant bit insertion method |
|------------------------|----------------------|--|
| DOMAIN | Spatial | Spatial |
| SECURITY | Weak | Moderate |
| DETECTION | Suspicious | Difficult to be suspected |
| REQUIRED SIZE OF IMAGE | Small | Small |
| ROBUSTNESS | Low | Moderate |
| IMPERCEPTIBILITY | High | Moderate |

V. CONCLUSION AND FUTURE SCOPE

The report presents three techniques for image steganography, namely; LSB insertion, 5th bit insertion, DCT method. 5th bit insertion is a new idea which requires detailed performance evaluation this report is an initial step in this direction. We have focused mainly on grey scale images and their variations when a secret message gets embedded into them. These variations are measured in terms of performance metrics like PSNR, MSE and BER. From the results obtained a broad and simple conclusion can be inferred; the higher value of PSNR makes more difficult for a stego image to detect, thus improving imperceptibility. All the three performance metrics characterizes image steganography techniques on perceptibility, capacity, robustness, tamper resistance and other characteristics. Since ancient times, man has found a desire in the ability to communicate covertly. The recent explosion of research in watermarking to protect intellectual property is evidence that steganography is not just limited to military or espionage applications. Steganography, like cryptography, will play an increasing role in the future of secure communication in the "digital world."

While this thesis has presented a complete working algorithm using the LSB insertion technique, 5th bit insertion technique and DCT technique for steganography, there is further research that can be done. First of all, the images used for this thesis were BMP files so adapting this method for different image file formats would make it more practical given that jpeg and other compressed file formats are much more readily than BMP files. Also, all of the files used in this thesis were grayscale images and since few people trade grayscale images modifying the algorithm to work with color images would help to better conceal hidden messages. Another way to improve the usefulness of this technique is to improve the data capacity. With a greater data capacity different error correcting codes can be used to further reduce the error rate. Also a greater capacity allows for audio or video messages to be hidden. One way to increase capacity is to hide a large message across multiple images. Also, once the algorithm can work with compressed color images, it could be extended to be used in video file, which could allow for a much greater data capacity than images alone. Finally, a steganographic algorithm is good only so long as the hidden messages cannot be detected. A detected message can be read (if it is not encrypted), tampered with or destroyed so thorough steganalysis should be performed. In the near future, the most important use of steganographic techniques will probably be lying in the field of digital watermarking. Content providers are eager to protect their copyrighted works against illegal distribution and digital watermarks provide a way of tracking the owners of these materials. Although it will not prevent the distribution itself, it will enable the content provider to start legal actions against the violators of the copyrights, as they can now be tracked down.

VI. REFERENCES

- [1] J. J. K. O Ruanaidh, W. J. Dowling, and F. M. Boland, "Watermarking digital images for copyright protection." *I.E.E. Proceedings on Vision, Signal and Image Processing*, vol. 143, Aug. 1996.
- [2] M. G. Kuhn and R. J. Anderson, "Soft tempest: Hidden data transmission using electromagnetic emanations." In Aucsmith, ISBN 3-540-65386-4.
- [3] Aucsmith, ed., *Information Hiding: Second International Workshop*, vol. 1525 of *Lecture Notes in Computer Science*, Portland, Oregon, U.S.A., 1998, Springer-Verlag, Berlin, Germany, ISBN 3-540-65386-4.
- [4] G. J. Simmons, "Subliminal channels: Past and present." *European Transaction on Telecommunications*, vol. 5, no. 4, July/August 1994.
- [5] G. W. Braudaway, "Results of attacks on a claimed robust digital image watermark." In van Renesse, ISBN 0-8194-2556-7.
- [6] J. Cox, J. Kilian, T. Leighton, and T. Sha-moon, "A secure, robust watermark for multi-media." In Anderson , ISBN 3-540-61996-8.
- [7] Kundur and D. Hatzinakos, "Digital watermarking using multiresolution wavelet decomposition." In *International*

1st National Power & Energy System Conference (NPESC), April 25-26, 2014, KNIT Sultanpur

- [8] *Conference on Acoustic, Speech and Signal Processing (ICASP)*, British Standard, BSI, London, *Information technology Generic coding of moving pictures and associated audio information / Part 3: au-dio.*, Oct. 1995, implementation of ISO/IEC 13818-3:1995.
- [9] P. Leary, *The second cryptographic Shakespeare: a monograph wherein the poems and plays attributed to William Shakespeare are proven to contain the enciphered name of the concealed author, Francis Bacon*. Omaha, Nebraska, U.S.A.: Westchester House, 2nd edn., 1990, ISBN 0-9617917-1-3.
- [10] A.W. Naji, A.A.Zaidan, B.B.Zaidan, Ibrahim A.S.Muhamadi, "New Approach of Hidden Data in the portable Executable File without Change the Size of Carrier File Using Distortion Techniques", Proceeding of World Academy of Science Engineering and Technology (WASET), Vol.56, ISSN:2070-3724.
- [11] A.W. Naji, A.A.Zaidan, B.B.Zaidan, Ibrahim A.S.Muhamadi, "Novel Approach for Cover File of Hidden Data in the Unused Area Two within EXE File Using Distortion Techniques and Advance Encryption Standard.", Proceeding of World Academy of Science Engineering and Technology (WASET), Vol.56, ISSN:2070-3724.
- [12] M. Abomhara, Omar Zakaria, Othman O. Khalifa , A.A.Zaidan, B.B.Zaidan, "Enhancing Selective Encryption for H.264/AVC Using Advance Encryption Standard ", International Journal of Computer and Electrical Engineering (IJCEE), ISSN: 1793-8198, Vol.2 , NO.2, April 2010, Singapore..
- [13] Md. Rafiqul Islam, A.W. Naji, A.A.Zaidan, B.B.Zaidan " New System for Secure Cover File of Hidden Data in the Image Page within vol. 5, IEEE, Seattle, Washington, U.S.A., May1998.
- [14] Executable File Using Statistical Steganography Techniques", International Journal of Computer Science and Information Security (IJCSIS), ISSN: 1947-5500, P.P 273-279, Vol.7 , NO.1, January 2010,USA..
- [15] Hamid.A.Jalab, A.A Zaidan, B.B Zaidan, "New Design for Information Hiding with in Steganography Using Distortion Techniques", International Journal of Engineering and Technology (IJET)), Vol 2, No. 1, ISSN: 1793-8236, Feb (2010), Singapore.
- [16] R. Chandramouli, N. Memon, "Analysis of LSB Based Image Steganography Techniques", IEEE , 2001.
- [17] R.J. Anderson, F.A.P. Petitcolas, "On The Limits of Steganography", IEEE Journal of Selected Area in Communications,May 1998.
- [18] R.Popu,"An Analysis of Steganographic System", The "Politehnica" University of Timisoara, Faculty of Automatics and Computers, Department of Computer Science and Software Engineering, May 25, 1998.
- [19] S. Katzenbeisser and F.A.P. Peticolas, "Defining Security in Steganographic Systems", in Proceeding of Electronic Imaging, Photonics West, SPIE, vol. 4675, 2002.
- [20] S. Tanako, K. Tanaka and T. Sugimura, "Data Hiding via Steganographic Image Transformation", IEICE Trans. Fundamentals, vol. E83-A, February, 2000.
- [20] W. Bender, D. Gruhl, N. Morimoto and A. Lu, "Techniques for Data Hiding", Systems Journal, vol. 35, 1996.

Survey for Wavelet Bayesian Network Image Denoising

Pallavi Sharma, Department of Information Technology SATI Vidisha India, R.C. Jain, Department of Information Technology SATI Vidisha India, and Rashmi Nagwani, Department of Information Technology SATI Vidisha India,

Abstract— In now days, wavelet-based image denoising method, which extends a recently emerged “geometrical” Bayesian framework. The new scheme combines three criteria for distinctive theoretically useful coefficients from noise: coefficient magnitudes, their advancement across scales and spatial clustering of bulky coefficients close to image edges. These three criteria are united in a Bayesian construction. The spatial clustering properties are expressed in a earlier model. The statistical properties regarding coefficient magnitudes and their development crossways scales are expressed in a joint conditional model. We address the image denoising difficulty, where zero-mean white and homogeneous Gaussian additive noise is to be uninvolved from a given image. We employ the belief propagation (BP) algorithm, which estimates a coefficient based on every one the coefficients of an picture, as the maximum-a-posterior (MAP) estimator to derive the denoised wavelet coefficients. We illustrate that if the network is a spanning tree, the customary BP algorithm can achieve MAP estimation resourcefully. Our research consequences show that, in conditions of the peak-signal-to-noise-ratio and perceptual superiority, the planned approach outperforms state-of-the-art algorithms on a number of images, mostly in the textured regions, with a range of amounts of white Gaussian noise.

Keywords— Image denoising, Bayesian network, Wavelet transform, image restoration, Bayesian estimation.

I. INTRODUCTION

The class of natural images that we encounter in daily Life is only a small subset of the set of all possible images. This subset is called an image manifold. Digital image processing applications are becoming increasingly important and they all start with a mathematical representation of the image. In Bayesian restoration methods, the image manifold is encoded in the form of prior knowledge that express the probabilities that specified combinations of pixel intensities can be experiential in an image. Because image spaces are high-dimensional, one often isolates the manifolds by decomposing images into their

components and by fitting probabilistic models on it [1]-[2]. The construction of a Bayesian network involves prior knowledge of the probability relationships between the variables of interest. Learning approaches are widely used to construct Bayesian networks that best represent the joint probabilities of training data. In practice, an optimization process based on a heuristic search technique is used to find the best structure over the space of all possible networks. However, the approach is computationally intractable because it must explore several combinations of dependent variables to derive an optimal Bayesian network. The difficulty is resolved in this paper by representing the data in wavelet domains and restricting the space of possible networks by using certain techniques, such as the “maximal weighted spanning tree”. Three wavelet properties - sparsely, cluster, and motion - can be oppressed to reduce the computational complexity of learning a Bayesian network [3]-[7]. During the last decades, multi resolution image representations, like wavelets, have received much attention for this purpose, due to their sparseness which manifests in highly non-Gaussian statistics for wavelet coefficients. Marginal histograms of wavelet coefficients are typically leptokurtosis and have heavy tails [8]-[9]. In literature, many wavelet-based image denoising methods have arisen exploiting this property, and are often based on simple and elegant shrinkage rules. In addition, joint histograms of wavelet coefficients have been studied in. Taking advantage of correlations between wavelet coefficients either across space, scale or orientation, additional improvement in denoising performance is obtained. The Gaussian Scale Mixture (GSM) model, in which clusters of coefficients are modeled as the artifact of a Gaussian random vector and a positive scaling variable, has been shown to produce outcome that are appreciably better than marginal models [10]. Image restoration aims to construct an estimate sharing the significant features still present in the degraded image, but with the artifacts censored.

II. PROBLEM FORMULATION

In our construction, we use image patches to take into account complex spatial interactions in images. In contrast to exemplar-based approaches for image modeling. An unsupervised method that uses no collection of image patches and no computational intensive training algorithms. Our adaptive smoothing works in the joint spatial-range domain as the nonlocal means filter but have a more powerful adaptation to the local structure of the data since the size of windows and control parameters are estimated from local image statistics [11]. We create the presentation of the proposed denoising algorithm by first introducing how sparsely and redundancy are brought to exploit. We do that via the beginning of the Sparse land reproduction Once this is set, we will talk about how local management on image patches turns into a global prior in a Bayesian rebuilding framework. The second part of the paper attempts to further validate recent claims that loss compression can be used for denoising. The Bayes Shrink threshold can aid in the parameter selection of a coder designed with the intention of denoising, and thus achieving concurrent denoising and looseness. Specifically, the zero-zone in the quantization step of compression is analogous to the threshold value in the threshold function. The left behind coder design parameters are selected based on a criterion derived from Rissanen's minimum description length (MDL) theory [12]. Experiments show that this compression method does indeed remove noise extensively, especially for great noise power. Although it introduces quantization noise and should be used only if bit rate were an additional concern to denoising. In meticulous, the transform-domain denoising methods normally assume that the true signal can be well approximated by a linear combination of few basis elements. That is, the signal is sparsely represent in the transform domain. Thus, by preserving the few high-magnitude transform coefficients that convey typically the accurate-signal energy and discarding the rest which are mainly due to noise, the correct signal can be successfully estimated. The sparsely of the representation depends on both the transform and the true-signal's properties. The multi resolution transforms can achieve first-class sparsely for spatially localized fine points, for instance edges and singularities. When this prior-learning plan is combined with sparsely and redundancy, it is the glossary to be used that we target as the learned set of parameters [13].

III. IMAGE DENOISING

Image denoising is an important image processing assignment, both as a process itself, and as a module in other processes. Very several ways to denoise an image or a set of records exists. The main properties of an excellent image denoising model are that it will eliminate noise while preserving edges. Generally linear models have been used. One common technique is to use a Gaussian filter, or homogeneously solving the heat-equation with the noisy image as input-data, i.e. a linear, 2nd order PDE-reproduction. For some purposes this kind of denoising is sufficient. One large advantage of linear noise removal models is the speed. But a reverse draw of the linear models is that they are not able to preserve edges in a excellent way: edges, which are recognized as discontinuities in the image, are dirty out. Nonlinear models on the other hand can handle edges in a much better way than linear models can. This filter is very good at preserving edges, but smoothly unstable regions in the input image are transformed into piecewise constant regions in the output image. Using the TV-filter as a denoiser leads to solve a 2nd order nonlinear PDE because smooth regions are transformed into piecewise constant regions when using the TV-filter, it is desirable to generate a model for which smoothly changeable regions are transformed into smoothly unreliable regions, and yet the edges are preserved. This can be done for example by solving a 4th order PDE instead of the 2nd order PDE from the TV-filter. Result show that the 4th order filter produces greatly better results in smooth regions, and unmoveing preserves edges in a very excellent way.

IV. IMAGE DENOISING TECHNIQUES

Image denoising algorithms may be the oldest in image processing. Various methods, in spite of implementation, share the similar basic plan noise reduction through image blurring. Blurring can be done nearby, as in the Gaussian smoothing model or in anisotropic filtering; by calculus of variations; or in the frequency domain, such as Weiner filters. But a universal "best" approach has yet to be found.

A) Patch-Based Image Denoising

A novel adaptive and patch-based approach is proposed for image denoising and representation. The method is based on a point wise selection of small image patches of fixed size in the variable neighborhood of each pixel. Our involvement is to associate with each pixel the weighted sum of data

points within an adaptive neighborhood, in a manner that it balances the exactness of approximation and the stochastic error, at each spatial location. This method is general and can be applied under the assumption that there exist repetitive patterns in a local neighborhood of a point. By introducing spatial adaptively, we expand the work earlier described by Buades *et al.* which can be measured as an addition of bilateral filtering to image patches. Finally, we recommend a nearly parameter-free algorithm for image denoising. The scheme is applied to both artificially despoiled (white Gaussian noise) and real images and the performance is extremely close to, and in some cases yet surpasses, that of the already published denoising schemes. A novel adaptive and exemplar-based approach is proposed for image restoration and representation. The method is based on a point wise selection of small image patches of fixed size in the variable neighbourhood of each pixel. The core idea is to associate with each pixel the weighted sum of data points within an adaptive neighbourhood. This method is general and can be applied under the assumption that the image is a locally and fairly stationary process. In this paper, we spotlight on the problem of the adaptive neighbourhood selection in a manner that it balances the accuracy of approximation and the stochastic error, at each spatial location. Thus, the new proposed point wise estimator mechanically adapts to the degree of underlying smoothness which is unidentified with minimal a priori assumptions on the function to be recovered [14].

B) Wavelet Based Image Denoising

Wavelet-based image denoising method, which extends a newly emerged “geometrical” Bayesian framework. The new method merges three criteria for distinguishing supposedly valuable coefficients from noise: coefficient magnitudes, their development across scales and spatial clustering of large coefficients close to image edges. These three criteria are pooled in a Bayesian construction. The spatial clustering properties are expressed in a prior model. The statistical properties regarding coefficient magnitudes and their progression across scales are expressed in a joint conditional model. The three middle novelties with respect to related approaches are

- 1) The inter scale-ratios of wavelet coefficients are statistically characterized and different local criteria for distinguishing valuable coefficients from noise are evaluated.
- 2) A joint provisional model is introduced.

3) A novel anisotropic Markov random field prior model is designed. The results demonstrate an enhanced denoising performance over related earlier techniques [15].



Fig. 1. Left: reference images: 1: “Lena,” 2: “Goldhill,” 3: “Fruits,” and 4: “Barbara.” Right: reference edge positions for vertical orientation of details at resolution scale.

Several issues were addressed to improve Bayesian image denoising using prior models for spatial clustering. A new MRF prior model was introduced to preserve image details better. A joint significance measure, which combines coefficients magnitudes and their evolution through scales, was introduced. For the resulting, joint conditional model a simple practical realization was proposed and motivated via Simulations. The advantage of the joint conditional model in terms of noise suppression performance was demonstrated on different images and for different amounts of noise. Some aspects that were analyzed in this paper may be useful for other denoising schemes as well: the realistic conditional densities of interscale ratios obtained via simulations and objective criteria for evaluating noise suppression performance of different significance measures [15].

C) Sparse and Redundant Representations based Image Denoising

We address the image denoising difficulty, where zero-mean white and homogeneous Gaussian additive noise is to be detached from a given image. The move toward taken is based on sparse and redundant representations over trained dictionaries. Using the K-SVD algorithm, we achieve a dictionary that describes the image content effectively. Two training options are measured: using the corrupted image itself, or training on a amount of high-quality image database. Since the K-SVD is limited in management

small image patches, we expand its deployment to arbitrary image sizes by defining a global image prior that forces sparsity over patches in every location in the image. We illustrate how such Bayesian treatment leads to a simple and effective denoising algorithm. This lead to a state-of-the-art denoising presentation, equivalent and sometimes surpassing recently published leading alternative denoising methods. Image denoising, leading to state-of-the-art presentation, equivalent to and sometimes surpassing recently published leading alternatives denoising methods. The planned method is based on local operations and involves sparse decompositions of each image block under one fixed over-complete dictionary, and a simple average calculation. The content of the dictionary is of main importance for the denoising method we have shown that a dictionary trained for natural real images, as well as an adaptive glossary trained on patches of the noisy image itself, both present very well [16].

D) Adaptive Wavelet Thresholding for Image Restoration (denoising)

An adaptive, data-driven threshold for image denoising via wavelet soft-thresholding. The threshold is derivative in a Bayesian framework, and the previous used on the wavelet coefficients is the generalized Gaussian distribution (GGD) widely used in image processing applications. The anticipated threshold is simple and closed-form, and it is adaptive to each sub band because it depends on data-driven estimates of the parameters. Investigational results show that the proposed method, called *BayesShrink*, is usually within 5% of the MSE of the best soft-thresholding benchmark with the image assumed known. It also outperforms Donohue and Johnston's *Sure Shrink* most of the time. The subsequent part of the paper attempt to further validate recent claims that lossy compression can be used for denoising. The *Bayes Shrink* threshold can serve in the parameter selection of a coder designed with the intention of denoising, and thus achieving instantaneous denoising and compression. Particularly, the zero-zone in the quantization step of compression is analogous to the threshold value in the thresholding function. The residual coder design parameters are chosen based on a criterion derived from Rissanen's minimum description length (MDL) principle. Experiments show that this compression scheme does indeed remove noise considerably, especially for huge noise power. However, it introduces quantization noise and should be used only if bitrates were an additional concern to denoising is often corrupted by noise in its acquisition or transmission. The goal of denoising is

to eliminate the noise while retaining as much as possible the important signal features. Conventionally, this is achieved by linear processing such as Wiener filtering. A vast literature has emerged freshly on signal denoising using nonlinear techniques, in the location of additive white Gaussian noise [17].



Fig. 2. Shows the wavelet based Adaptive Wavelet Thresholding for Image Denoising .

E) Image Denoising by Sparse 3D Transform-Domain Collaborative Filtering

Image denoising strategy based on an enhanced sparse representation in transform domain. The improvement of the sparsity is achieved by grouping similar 2D image fragments (e.g. blocks) into 3D data arrays which we call "groups". Collaborative filtering is a special procedure developed to deal with these 3D groups. We appreciate it using the three successive steps: 3D transformation of a group, reduction of the transform band, and inverse 3D transformation. The result is a 3D approximate that consists of the together filtered grouped image blocks. By attenuating the noise, the simultaneous filtering reveals even the finest details shared by grouped blocks and at the same time it preserves the essential unique features of each character block. The filtered blocks are returned to their original locations. Since these blocks are overlapping, for each pixel we obtain several different estimates which need to be combined. Aggregation is a particular averaging process which is exploited to take advantage of this redundancy. An important improvement is obtained by a specially developed collaborative Wiener filtering. An algorithm based on this description denoising approach and its efficient implementation

is presented in full detail; an extension to color-image denoising is also developed. The experimental results display that this computationally scalable algorithm achieves state-of-the-art denoising performance in terms of both peak signal-to-noise ratio and subjective visual quality [18].

F) Image Denoising Using Mixtures of Projected Gaussian Scale Mixtures

A new statistical model for image restoration in which neighborhoods of wavelet sub bands are modeled by a discrete mixture of linear projected Gaussian Scale Mixtures . In each projection, a lower dimensional approximation of the local neighborhood is obtained, thus modeling the strongest correlations in that neighborhood. The model is a generalization of the just developed Mixture of GSM (MGSM) model that offers a significant improvement both in PSNR and visually compared to the current state-of-the-art wavelet techniques though the computation cost is very high which hampers its use for practical purposes. We present a quick EM algorithm that takes advantage of the projection bases to speed up the algorithm. The results explain that, when foretelling on a fixed data-independent basis, even computational advantages with a imperfect loss of PSNR can be obtained with respect to the BLS-GSM denoising method, although data-dependent bases of Principle Components offer a higher denoising presentation, both visually and in PSNR compared to the current wavelet-based state-of-the-art denoising methods. The Mixtures of Projected Gaussian Scale Mixtures (MPGSM) as a means to further improve upon the recently proposed MGSM model. The new model is a generalization of the existing SVGSM, OAGSM and MGSM techniques and allows for a lot of flexibility with regard to the neighborhood size, spatial adaptation and even when modeling dependencies between different wavelet sub bands. We developed a fast EM algorithm for the model training, based on the “winner-take all” approach, taking benefit of the Principal Component bases. We discussed how this technique can also be used to speed up the denoising itself. We discussed how data independent projection bases can be constructed to allow flexible neighborhood structures, offering computational savings compared to the GSM-BLS method which can be useful for real-time denoising applications. Finally we showed the PSNR improvement of the complete MPGSMBLS method compared to recent wavelet-domain state-of the- art methods [19].

G) Bayesian Network Image Denosing

From the perspective of the Bayesian approach, the denoising problem is basically a prior probability modeling and estimation task. In this paper, we suggest an approach that exploits a hidden Bayesian system, constructed from wavelet coefficients, to model the previous probability of the original image. Then, we use the belief propagation (BP) method, which estimates a coefficient based on all the coefficients of an image, as the maximum-a-posterior (MAP) estimator to develop the denoised wavelet coefficients. We explain that if the network is a spanning tree, the standard BP algorithm can execute MAP estimation competently. Our experiment results demonstrate that, in conditions of the peak-signal-to-noise-ratio and perceptual quality, the projected approach outperforms state-of-the-art algorithms on various images, particularly in the textured regions, with various amounts of white Gaussian noise [20].

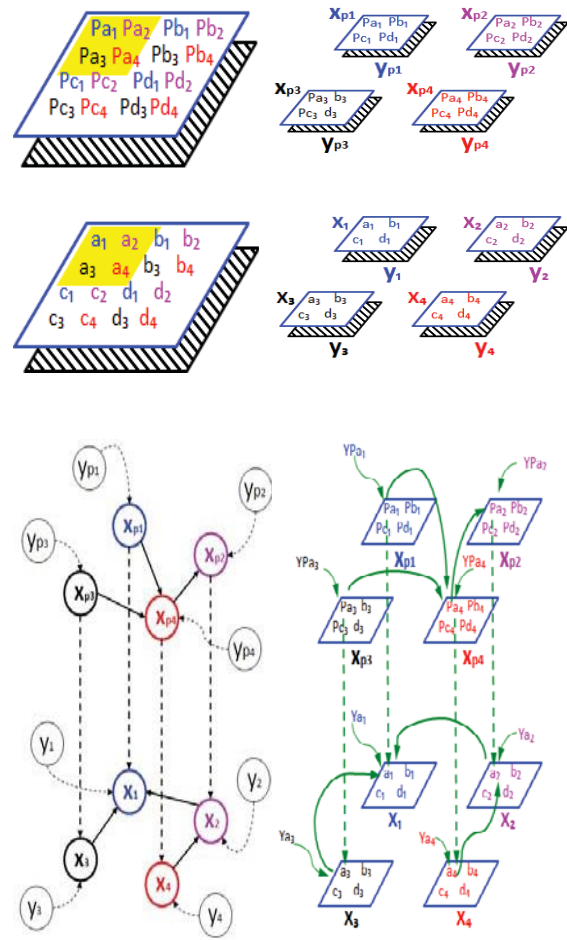


Fig. 3. Bayesian Network Image Denoising

V. CONCLUSION

Bayesian image denoising using prior models for spatial clustering. A new MRF prior model was introduced to preserve image details better. A joint significance measure, which combines coefficients magnitudes and their evolution through scales, was introduced. For the resulting, joint conditional model a simple practical realization was proposed and motivated via simulations. We have described a novel adaptive denoising algorithm where patch-based weights and variable window sizes are jointly used. An advantage of the method is that internal parameters can be easily chosen and are relatively stable. The algorithm is able to denoise both piecewise-smooth and textured natural images since they contain enough redundancy. Actually, the performance of our algorithm is very close, and in some cases still surpasses, to that of the previously published denoising methods. Also we just mention that the algorithm can be easily parallelized since at iteration, each pixel is processed independently. However, some problems may occur when the texture sample contains too many texels making hard to find close matches for the locality context window.

REFERENCES

- [1] B. Goossens, A. Pizurica, and W. Philips, "Image denoising using mixtures of projected Gaussian scale mixtures," *IEEE Trans. Image Process.*, vol. 18, no. 8, pp. 1689–1702, Aug. 2009.
- [2] A. Srivastava, A. B. Lee, E.P. Simoncelli, and S-C. Zhu, "On Advances in Statistical Modeling of Natural Images," *Journal of Mathematical Imaging and Vision*, vol. 18, pp. 17–33, 2003.
- [3] J. Ho and W.-L. Hwang, "Wavelet Bayesian Network Image Denoising," *IEEE Trans. Image Process.* vol. 22, no. 4, Apr. 2013.
- [4] G. F. Cooper and E. Herskovits, "A Bayesian method for the induction of probabilistic networks from data," *Mach. Learn.*, vol. 9, no. 4, pp.309–347, Oct. 1992.
- [5] D. Heckerman, D. Geiger, and D. M. Chickering, "Learning Bayesian networks: The combination of knowledge and statistical data," *Mach. Learn.*, vol. 20, no. 3, pp. 197–243, 1995.
- [6] D. Heckerman, "A tutorial on learning Bayesian networks," Microsoft Research, Mountain View, CA, Tech. Rep. MSR-TR-95-06, 1995.
- [7] D. M. Chickering, D. Heckerman, and C. Meek, "A Bayesian approach to learning Bayesian networks with local structure," in *Proc. 13th Conf. Uncertainty Artif. Intell.*, 1997, pp. 80–89.
- [8] D. J. Field, "Relations between the statistics of natural images and the response properties of cortical cells," *J. Opt. Soc. Am. A*, vol. 4, no. 12, pp. 2379–2394, 1987.
- [9] S. Mallat, "Multi frequency channel decomposition of images and wavelet models," *IEEE Trans. Acoust., Speech, Signal Proc.*, vol. 37, no. 12, pp. 2091–2110, Dec. 1989.
- [10] J. Portilla, V. Strela, M. Wainwright, and E. Simoncelli, "Image denoising using Gaussian Scale Mixtures in the Wavelet Domain," *IEEE Trans. Image Processing*, vol. 12, no. 11, pp. 1338–1351, Nov. 2003.
- [11] J. Mairal, F. Bach, J. Ponce, and G. Sapiro, "Non-local sparse models for image restoration," in *Proc. IEEE Int. Conf. Comput. Vis.*, Kyoto, Japan, 2009, pp. 2272–2279.
- [12] G. Chang, B. Yu, and M. Baraniuk, "Spatially adaptive wavelet thresholding with context modeling for image denoising," *IEEE Trans. Image Process.*, vol. 9, no. 9, pp. 1522–1531, Sep. 2000.
- [13] M. Elad and M. Aharon, "Image denoising via sparse and redundant representations over learned dictionaries," *IEEE Trans. Image Process.*, vol. 15, no. 12, pp. 3736–3745, Dec. 2006.
- [14] C. Kervrann and J. Boulanger, "Optimal spatial adaptation for patchbased image denoising," *IEEE Trans. Image Process.*, vol. 15, no. 10, pp. 2866–2878, Oct. 2006.
- [15] A. Pizurica, W. Philips, I. Lemahieu, and M. Achery, "A joint inter- and intra-scale statistical model for Bayesian wavelet based image denoising," *IEEE Trans. Image Process.*, vol. 11, no. 5, pp. 545–557, May 2002.
- [16] M. Elad and M. Aharon, "Image denoising via sparse and redundant representations over learned dictionaries," *IEEE Trans. Image Process.*, vol. 15, no. 12, pp. 3736–3745, Dec. 2006.
- [17] G. Chang, B. Yu, and M. Baraniuk, "Spatially adaptive wavelet thresholding with context modeling for image denoising," *IEEE Trans. Image Process.*, vol. 9, no. 9, pp. 1522–1531, Sep. 2000.
- [18] K. Dabov, A. Foi, V. Katkovnik, and K. Egiazarian, "Image denoising by sparse 3-D transform-domain collaborative filtering," *IEEE Trans. Image Process.*, vol. 16, no. 8, pp. 2080–2095, Aug. 2007.
- [19] B. Goossens, A. Pizurica, and W. Philips, "Image denoising using mixtures of projected Gaussian scale mixtures," *IEEE Trans. Image Process.*, vol. 18, no. 8, pp. 1689–1702, Aug. 2009.
- [20] J. Ho and W.-L. Hwang, "Wavelet Bayesian Network Image Denoising," *IEEE Trans. Image Process.* vol. 22, no. 4, Apr. 2013.

Survey for Image representation using block compressive sensing for compression Applications

Ankita Hundet, Department of Information Technology SATI Vidisha, India,R.C. Jain ,Department of Information Technology SATI Vidisha, India, and Vivek Sharma, Department of Information Technology SATI Vidisha, India,

Abstract— Compressing sensing theory have been favourable in evolving data compression techniques, though it was put forward with objective to achieve dimension reduced sampling for saving data sampling cost. In this paper two sampling methods are explored for block CS (BCS) with discrete cosine transform (DCT) based image representation for compression applications - (a) coefficient random permutation (b) adaptive sampling. CRP method has the potency to balance the sparsity of sampled vectors in DCT field of image, and then in improving the CS sampling efficiency. To attain AS we design an adaptive measurement matrix used in CS based on the energy distribution characteristics of image in DCT domain, which has a good impact in magnifying the CS performance. It has been revealed in our experimental results that our proposed methods are efficacious in reducing the dimension of the BCS-based image representation and/or improving the recovered image quality. The planned BCS based image representation scheme could be an efficient alternative for applications of encrypted image compression and/or robust image compression.

Keywords—Image representation, compressive sensing, random sampling, Block compressive sensing, Coefficient random permutation.

I. INTRODUCTION

Recent years have seen important interest in the paradigm of compressed sensing (CS) which permit, in certain conditions, signals to be sampled at sub-Nyquist rates via linear projection onto a random basis while still enabling exact reconstruction of the original signal. As applied to 2D images, though, CS faces some challenges including a computationally expensive reconstruction process and huge memory required to store the random sampling operator in recent times, numerous fast algorithms have been developed for CS rebuilding, while the latter challenge was addressed in [1] using a block-based sampling operation. Additionally in projection-based Land weber iterations were planned to achieve fast

CS reconstruction while simultaneously imposing smoothing with the goal of improving the reconstructed-image quality by eliminating blocking artifacts. Sparse representation and compressive sensing establishes a more rigorous mathematical framework for studying high-dimensional data and ways to discover the structures of the data, giving rise to a large range of efficient algorithms. When transmitting data over insecure bandwidth-limited channels, data compression and encryption is for all time needed. An encryption algorithm converts the data from comprehensible to incomprehensible structure, thus making the encrypted data difficult to compress using any of the classical compression algorithms, which relies on intelligence embedded in the data. Hence, traditionally the encryption always follows compression. While such a scheme is suitable for most of the applications, there are some applications which need encryption to be carried out before compression [2]. Consider for example, an information owner and a network operator who does not trust each other. In such a case, to protect his content, the information owner encrypts his data before giving it to network operator. Due to the bandwidth limitation the network operator is forced to compress this encrypted data stream [3-5].

II. PROBLEM FORMULATION

The idea of CS is to represent the signal by non adaptive random projections to reduce the sampling rate, which is considered as an advantage of CS. However, the main challenges existed in CS for practical applications include how to reduce efficiently measurement rate with preserving good recovered image quality and decreasing the implementation complexity. To address these problems, many researches [6] have reported to use the prior knowledge of the sampled signal to enhance the performance of CS. Although most of them focused on decoder-based reconstruction optimization, encoder-based sampling optimization may have important sense for addressing these

problems. Block-based sampling for fast CS of natural images, where the original image is divided into small blocks and each block is sampled independently using the same measurement operator. The possibility of exploiting block CS is motivated by the great success of block DCT coding systems which are widely used in the JPEG and the MPEG standards [7]. The main advantages of our proposed system include: (a) Measurement operator can be easily stored and implemented through a random under sampled filter bank. Block-based measurement is more advantageous for real-time applications as the encoder does not need to send the sampled data until the whole image is measured; (b) Since each block is processed independently, the initial solution can be easily obtained and the reconstruction process can be substantially speeded up; For natural images, our preliminary results show that block CS systems offer comparable performances to existing CS schemes with much lower implementation cost.

III. IMAGE REPRESENTATION

The objective is to signify and express the resulting aggregate of segmented pixels in a form suitable for further computer processing after segmenting an image into regions.

- Two choice for representing a region:
External characteristics: its boundary.

Internal characteristics: the pixels comprise the region. For example, a region may be represented by (a) its boundary with the boundary describe by features such as its length, (b) the orientation of the straight line joining the extreme points, and (c) the number of concavities in the boundary.

- An external representation is chosen while the primary focus is on shape characteristics.
- An internal representation is chosen when the primary focus is on reflectivity properties, such as colour and texture. The segmentation techniques yield raw data in the form of pixels along a boundary or pixels contained in a region. Although these data are sometimes used directly to obtain descriptors (as in determining the texture of a region), standard practice is to use schemes that compact the data into representations that are considerably more useful in the computation of descriptors. This section introduces some basic representation schemes for this purpose. To represent a boundary by a connected sequence of straight line segments of specified length and direction.

IV. IMAGE REPRESENTATION TECHNIQUES

Over the last two decades, great improvements have been made in image and video compression techniques driven by a growing demand for storage and transmission of visual information. By far, many image and video compression standards, such as JPEG, JPEG2000 and MPEG-4 AVC/H.264 etc., have been proposed. However, these mainstream compression coding techniques still may be not very efficient in some special compression applications, for examples of robust image coding and encrypted image compression. Robust coding is very important in digital multimedia transmission over internet and wireless networks, where the image codec needs to have not only excellent compression performance to reduce data rate, but also high robustness performance to resist transmission error due to channel noise and/or packet loss.

A) CRP Based Block Compressive Sensing

As mentioned above, the theory foundation of CS is that the signal sampled is sparse or compressible, and the required minimal number of measurement dimension for perfect recovery is determined by the sparsity of the sampled signal. When an image is represented by a BCS scheme, it will be inefficient to assign the same number of measurement dimension to each sampled vector corresponding to the different image block, because the image block with different spatial characteristic has significantly different sparsity from each other. In general, the image blocks located at smooth region should have stronger sparsity than those located at rich edge or texture region. The method of bits random permutations has been used in channel coding in communication system for design of interleaved, which can maximally scatter the burst error generated in the process of data channel transmission, thus plays a very important role in increasing the reliability of data transmission. Motivated by the above fact, the CRP in DCT domain of image is exploited to equalize the sparsity of the sampled vectors in CS encoding stage for enhancing measurement efficiency of BCS of image in this Section, which is followed by a CRP based BCS scheme. The proposed CRP can be at the same time used to achieve encrypting image in transform domain at information owner side. In traditional BCS, the CS sampling does not exploit the inter coefficient correlation within a sampled signal vector, so coefficient permutations across signal vectors will not adversely affect encoding performance. On the other hand, because the random Permutations make the distribution of coefficients become randomization and homogenization, such random permutations will make sparsity of all the

sampled vectors nearly identical, which improves reconstruction performance since it is likely that before CRP some less sparse vectors will not be reconstructed well[8].

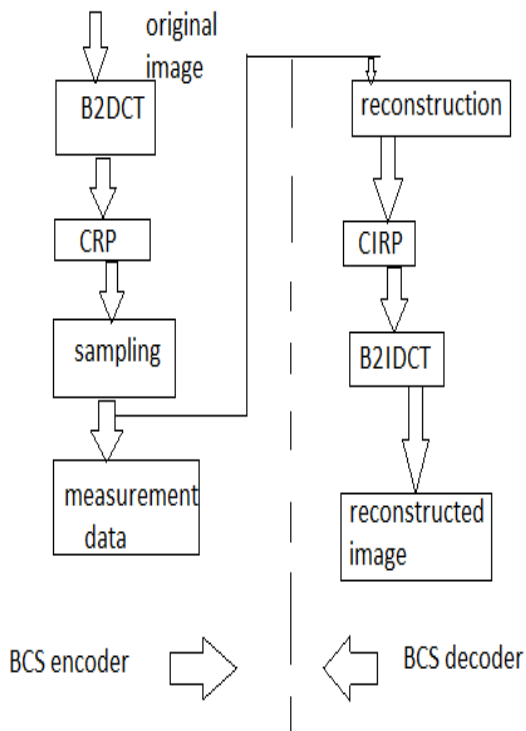


Fig. 1. The architecture of BCS scheme with CRP

B) AS Based block Compressive Sensing

In conventional CS scheme, a fixed measurement matrix is used to achieve non-adaptively sampling signal. This scheme is simple but not high efficiency, because it identically samples all signals with different feature, and non-distinctively extracts all information components of a signal that maybe have different importance to recovery signal quality [9]. In this Section, a novel method of developing adaptive measurement matrix is proposed to achieve adaptive Sampling (AS) in our BCS in DCT domain. As what we have known, image signals are bandwidth limited, and their energy are mostly distributed in the low-frequency components. In addition, the human eyes have certain masking effect on some parts of the frequency spectrum of image signals, which like low-pass filters that makes them more sensitive to low frequency components than high frequency ones. So, the low frequency components occupying large part of energy of image signals are more important to image quality than the high frequency components occupying less part of energy. Considering these

facts, we propose to develop an adaptive measurement matrix in BCS framework based on the energy distribution characteristic of the sampled image signal in DCT domain to enhance the performance of BCS. The key idea is to adaptively extract more information of the important frequency components than that of the relatively non-important frequency components in sampling stage to reduce recovery error. It is implemented by adaptively scaling the coefficients of measurement matrix according to the sampled image's characteristic, i.e. unequally measuring the different frequency components based on their importance to image quality.

C) Compressed Sensing

Compressed sensing is a signal processing technique for ably acquire and reconstructing a signal, by finding solution to underdetermined linear systems. This takes profit of signals sparseness or compressibility in particular domain, we design compressed data acquisition protocols which perform as if it were possible to directly acquire just allowing the entire signal to be determined from relatively few measurements. The important information about the signals/images in effect, not acquiring that part of the data that would eventually just be “thrown away” by lossy compression [10]. Moreover, the protocols are non adaptive and parallelizable; they do not require knowledge of the signal/image to be acquired in advance other than knowledge that the data will be compressible and do not attempt any “understanding” of the underlying object to guide an active or adaptive sensing strategy. The measurements ended in the compressed sensing protocol are holographic thus, not easy pixel samples and must be process nonlinearly. In specific applications, this principle might enable dramatically reduced measurement time, dramatically reduced sampling rates, or reduced utilize of analog-to digital converter resources [10]. Shuffling the class attribute values belonging to heterogeneous leaves of a decision tree. If a leaf corresponds to a group of records having different class attribute values, then the leaf is identified to be a heterogeneous leaf.

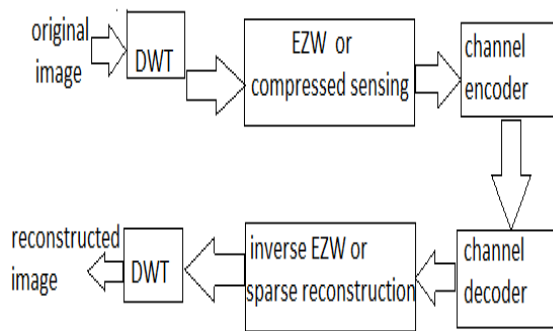


Fig. 2. Overall joint source-channel coding system block diagram [11]

Recently, we developed an interactive and adaptive joint source-channel coding algorithm by which the centre and size of the image are specified by the user after receiving the low-resolution background image.

D) Random Permutations Based Block Compressive Sensing

Compressive sensing (CS) is a novel theory framework for signal acquisition, which has been widely concerned in many application fields. A new block CS scheme for image compression applications, in which a method of coefficients random permutations (CRP) in transform domain is exploited for optimal sampling of CS, considering the fact that the image blocks with different spatial characteristics have different sparsity or compressibility [12]. The proposed random permutations technique makes the sparsity of all the sampled coefficients vectors more evenly, which results in requiring approximate equal number of measurement for well restoration. New results show that our proposed scheme can efficiently enhance the CS performance in increasing reconstructed image quality or reduce the measurement ratio.

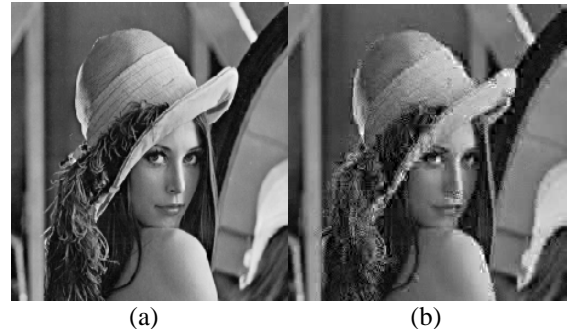


Fig. 3. Visual quality comparisons with measurement rate equaling to 0.4 and block size of 8×8. (a) Original image, (b) reconstruction image by CRP-based CS method.

A novel scheme of image compressive sensing for compression applications is proposed in this paper. By employing the coefficients random permutations technique in sampling process, the sparsity of all sampled vectors could be balanced efficiently, which can considerably increase the utilization of sensing resources. The simulation results illustrate that our proposed sampling scheme can enhance the performance of compressive sensing efficiently in both objective and subjective assessment manners with little increasing the complexity.

E) Reweighted Compressive Sampling for Image Compression

Shannon sampling theory tells us that if we want to reconstruct a band limited signal without distortion, then sampling the original signal at a rate which is at least twice of its highest frequency is necessary. However, a newly emerged theory called Compressive Sampling (CS), also known as Compressive Sensing proves that this is not always true. It tells that as long as the signal is sparse or compressible, then we can exactly recover the original signals through only a few measurements, namely, we can achieve data sampling and compression at the same time for designing highly efficient data compression techniques while the performance of existing ones seem to reach the bottleneck. Some initial exploration about applying CS theory in data compression has been made; however, the performance is limited. The main problem that prevents CS framework from being applied in real data compression system is the efficiency decrease for complex signals which are usually hard to be perfectly sparsely represented. One major reason causing this efficiency dropping is that conventional CS framework samples data randomly without showing discrimination to different components, in other words, it does not consider about the characteristics of the signals. However, this may not be the best way to sample when it comes to

the complex signals, resembling images. A lot of efforts have been made trying to improve the performance of the CS signal recovery algorithms by adjusting the behavior of the decoder adaptively to the signal characteristics. However, usually their methods are based on the blind estimation of the signal magnitudes and iterative refining process in the decoding side. For instance, in, the authors propose an iterative reweighting scheme to enhance the sparsity of the reconstruction results. In their work, the solution of an unweighted minimization reconstruction is used as the initial guess, and then the weighting coefficients are refined iteratively, until the convergence is reached. However, the complexity for these iterative processing schemes is too high for the methods to be practical, and they are often guaranteed only to converge to a local (not necessarily) optimum. In this paper, we propose a reweighted Compressive Sampling for CS based image compression by introducing a weighting scheme into the encoding procedure. This method works on the block-based processing mechanism. First the images will be divided into small blocks, and then the weighting coefficients are determined by taking advantage of the statistical characteristics of natural images and subsequently sent together with the CS measurements to help the decoder to achieve better reconstruction results. The main advantage of our proposed method is that it can sufficiently utilize image characteristics to achieve considerable performance gain without notably increasing the complexity of the system structure or the computation procedures [13].

G) Robust Image Compression Based on Compressing Sensing

The existing image compression methods (e.g., JPEG2000, etc.) are vulnerable to bit-loss, and this is generally tackle by channel coding that follow. Though, source coding and channel coding have contradictory requirement. In this paper, we deal with the problem with an alternative paradigm, and a novel compressive sensing (CS) based compression scheme is therefore pro- posed [14]. Discrete wavelet transform (DWT) is applied for sparse representation, and base on the property of 2-D DWT, a fast CS measurements captivating technique is presented. Unlike the un- equally important discrete wavelet coefficients, the resultant CS measurements hold nearly the same amount of information and have minimal effects for bit-loss. At the decoder side, one can merely recreate the image via minimization. New-results show that the proposed CS-based image codec with- out resorting to error protection is more

robust compared with existing CS technique and relevant joint source channel coding (JSCC) schemes.

V. CONCLUSION

With the help of compressive sensing using the recently developed HALS algorithm based on nonlinear thresholding a progressive transmission system has been introduced in this paper. The main contributions of this effort are on *a.* selection and coding of a small number of samples (sampled below Nyquist rate) and *b.* introducing an adaptive thresholding technique for selection and reconstruction of those samples. Keep the inferences that disclose private information about organizations or individuals at a minimum.Compression of encrypted image is not possible by using any of the classical compression techniques. We proposed a system and showed that lossy compression of encrypted image data is indeed possible by using compressive sensing techniques. The basis pursuit algorithm was appropriately modified to enable joint decompression and decryption. Simulation results were provided to demonstrate the compression results of the proposed method.

VI. REFERENCES

- [1] S. Mun, J.E. Fowler, "Block compressed sensing of images using directional Transforms", in: Proc. Int. Conf. Image Processing (ICIP), 2009, pp. 3021–3024.
- [2] M. Johnson, P. Ishwar, V. Prabhakaran, D. Schonberg and K. Ramachandran, "On compressing encrypted data", IEEE Trans. Signal Processing vol. 52, pp. 2992-3006, Oct. 2004.
- [3] D. Schonberg, S. Draper and K. Ramachandran, "On compression of encrypted images", Proc. International conference on Image processing, Atlanta, GA, pp. 269-272, Oct. 2006.
- [4] A. A. Kumar and A. Makur,"Distributed source coding based encryption and lossless compression of gray scale and color images", Proc. IEEE 10th workshop on multimedia and signal processing, Cairns, Australia, pp. 760-764, Oct. 2008.
- [5] A. Mitra, Y. V. S. Rao and S. R. M. Prasanna, " A new image encryption approach using combinational permutation techniques", International J. of comp. Sc., Vol. 1, PP. 127-131, May 2006.
- [6] L. Gan, Block compressed sensing of natural images, in: Proc. Of Int. Conf. Digital Signal Processing, 2007, pp. 403–406.
- [7] R. Baranuik, "Compressive Sensing", IEEE signal processing magazine, Vol. 24, PP. 118-120, July 2007.
- [8] L. Gan, Block compressed sensing of natural images, in: Proc. of Int. Conf. Digital Signal Processing, 2007, pp. 403–406.
- [9] E. J. Candes and M. B. Wakin, "An introduction to compressive sampling", IEEE signal processing magazine, Vol. 25, pp. 21-30, Mar. 2008.
- [10] D.L. Donoho, Compressed sensing, IEEE Trans. Inform. Theory 52 (4) (2006) 1289–1306.
- [11] S. Sanei, A. H. Phan, J.-L. Lo V. Abolghasemi and A. Cichocki, "A compressive sensing approach for progressive

- transmission of images”, in Proc. Int. Conf. DSP’2009, pp. 1–5, 2009.
- [12] Z. Gao, C. Xiong, C. Zhou, H. Wang, “Compressive Sampling with Coefficients Random Permutations for Image Compression”, in: Proc. Int. Conf. on Multimedia and Signal Processing, 2011, pp. 321–324.
- [13] Y. Yang, O.C. Au, L. Fang, X. Wen, W. Tang, “Reweighted compressive sampling for image compression”, in: Proc. Int. Conf. Picture Coding Symposium (PCS), 2009, pp. 89–92.
- [14] C. Deng, W. Lin, B.-S. Lee, C.T. Lau, “Robust image compression based on compressive sensing”, in: Proc. Int. Conf. Multimedia & Expo (ICME), 2010, pp. 462–467
- [15] R.G. Baraniuk, V. Cevher, M. Duarte, C. Hegde, “Model-based compressive sensing”, IEEE Trans. Inf. Theory 56 (4) (2010) 1982–2001.

Survey on Mining Order-Preserving Sub matrices

Pallavi Sharma, Department Of Information Technology SATI Vidisha, India, Dr. R.C. Jain Department of Information Technology SATI Vidisha ,India, and Prof. Rashmi Singh, Department of Information Technology SATI, Vidisha India

Abstract: Order-preserving sub matrices (OPSM's) have been shown useful in capturing concurrent patterns in data when the relative magnitudes of data items are more important than their exact values. For example, in analyzing gene expression profiles obtained from micro-array experiments, the relative magnitudes are important both since they represent the change of gene activities across the experiments, and since there is typically a high level of noise in data that makes the exact values untrustable. To manage with data noise, repeated experiments are often conducted to collect multiple measurements.

Keywords: -Order-preserving sub matrices, Simultaneous Clustering.

I. INTRODUCTION

In bioinformatics community, a large number of genes are studied by using DNA micro-array technology to obtain gene expression data. Gene expression data are usually organized as matrices, in which each row represents one gene and each column represents a sample for the experiment, and each item records the expression value of one gene under an experiment sample. Through the analysis of expression data, we can discover information about the genes.

Clustering is helpful to find different functional categories of genes. Among various kinds of clustering approaches, Order-Preserving Sub Matrix has been a useful method to discover groups of genes that share some common functions.

Simultaneous clustering, usually designated by bi-clustering, co-clustering, 2-way clustering or block clustering, is an important method in two-way data analysis. A number of algorithms that perform simultaneous clustering on rows and columns of a matrix have been proposed to date. The goal of simultaneous clustering is to find sub-matrices, which are subgroups of rows and subgroups of columns that

exhibit a high correlation. This type of algorithms has been proposed and used in many fields, such as bio-informatics [1], web mining [2], text mining [3] and social network analysis [4].

II. OVERVIEW OF SIMULTANEOUS CLUSTERING PROBLEM

Clustering is the grouping together of similar subjects. Standard clustering methods consider the value of each point in all dimensions, in order to form group of similar points. This kind of one-way clustering techniques is based on similarity between subjects across all variables. Simultaneous clustering algorithms seeks “blocks” of rows and columns that are interrelated. They aim to identify a set of biclusters $B_k(I_k, J_k)$, where I_k is a subset of the rows X and J_k is a subset of the columns Y. I_k rows exhibit similar behavior across J_k columns, or vice versa and every bicluster B_k satisfies some criteria of homogeneity. A biclustering method may assume a specific structure and data type. Madeira and Oliveira launch in their survey [5] some biclustering structures defined by: single bicluster, exclusive rows biclusters, exclusive columns biclusters, non-overlapping biclusters with tree arrangement, and arbitrarily positioned overlapping biclusters. Biclusters can be with constant values, with constant values on rows or columns, with coherent values or with non-coherent evolution. There are many advantages in a simultaneous rather than one way clustering (table 1). In fact, simultaneous clustering may highlight the association between the row and column clustering that appears from the data analysis as a linked clustering. In addition, it allows the researcher to deal with sparse and high dimensional data matrices [6]. Simultaneous clustering is also an interesting paradigm for unsupervised data analysis as it is more useful, has less parameters, is

scalable and is able to effectively interlink row and column information.

Table 1. Comparison between Clustering and Simultaneous Clustering

| Clustering | Simultaneous Clustering |
|---|--|
| Applied to each the rows or the columns of the data matrix separately =>Global model. | performs clustering in the two dimensions simultaneously =>Local model. |
| Produce clusters of rows or clusters of columns. | Seeks blocks of rows and columns that are interrelated. |
| Each subject in a given subject cluster is defined using all the variables. Each variable in a variable cluster characterizes all subjects. | Each subject in a bicluster is selected using only a subset of the variables and each variable in a bicluster is selected using only a subset of the subjects. |
| Clusters are exhaustive | The clusters on rows and columns should not be exclusive and/or exhaustive |

Simultaneous Clustering Approaches

A survey of simultaneous clustering algorithms applied on biological data has been given by Madeira and Oliveira. These algorithms are based on five approaches: Iterative Row and Column Clustering Combination (IRCCC), Divide and Conquer (DC), Greedy Iterative Search (GIS), Exhaustive Bicluster Enumeration (EBE) and Distribution Parameter Identification (DPI). The IRCCC approach consists to apply clustering algorithms to the rows and columns of the data matrix, independently, and then to combine results using some sort of iterative process the algorithms based on DC approach begin with the entire data in one block (bicluster) and identifies biclusters at each iteration by splicing a given block into two pieces. GIS approach creates biclusters by adding or removing rows/columns from them, using a criterion that maximizes the local increase EBE approach identifies biclusters using an exhaustive enumeration of all possible biclusters in the data matrix. DPI approach assumes that the biclusters are generated using a given statistical model and tries to identify the distribution parameters that fit the available data, by minimizing a

certain criterion through an iterative move toward All the algorithms presented in this survey analyze biological data from gene expression matrices. Given that there are a number of algorithms based on bipartite graph model [7], mixture model [8] and information theory [9], which are applied in other fields such as text mining, web mining and information recovery, we propose to categorize simultaneous clustering methods into five categories: bipartite Graph methods, variance minimization techniques, two-way clustering methods, motif and pattern recognition methods and probabilistic and generative methods.

The bipartite graph methods consists in modeling rows and columns as a weighted bipartite graph and assigning weights to graph edges using similarity measure methods. The created bipartite graph is then partitioned in a way that minimizes the cut of the divider i.e. the sum of the weights of the crossing edges between parts of the partition. In [10], the authors created a word-document bipartite graph. The graph was partitioned using a partial singular value decomposition of the associated edge weight matrix of the bipartite graph. Dhillon [11] used the spectral method for partitioning the bipartite graph constructed in the same way as in [12]. Authors proposed an isoperimetric co-clustering algorithm (ICA) for partitioning the word file matrix. ICA used the same model than spectral partitioning but instead of searching the solutions of the singular word-document system of linear equations, it converts the scheme to a nonsingular system of equations which is easier to solve. The bipartite graph techniques are also used for gene expression analysis. One case is Statistical-Algorithmic Method for Bicluster Analysis (SAMBA).

The variance minimization methods define clusters as blocks in the matrix with minimal deviation of their elements. This definition has been already measured by Hartigan and extended by Tibshirani et al. Some examples are the δ -cluster methods, such as δ -ks clusters, δ -p Clusters and δ -biclusters, which search for blocks of elements having a deviation below δ . flexible Overlapped bi-Clustering (FLOC) introduced by extend Cheng and Church δ -biclusters by dealing with missing values. – Two-way clustering methods use one-way clustering such as k-means Self-Organizing Maps, Expectation-Minimization algorithm or hierarchical clustering algorithm to produce clusters on both dimensions of the data matrix separately. One-

dimension results are then combined to produce subgroups of rows and columns called biclusters. These methods identify clusters on rows and columns but not directly biclusters. Motif and pattern recognition methods define a bicluster as samples sharing a common prototype or motif. To simplify this task, some methods discretize the data such as xMOTIF [13] or binarize the data such as Bimax [14]. Order-Preserving Sub Matrices (OPSM) [15] searches for blocks having the same order of values in their columns. Spectral clustering (SPEC) [16] performs a singular value decomposition of the data matrix after normalization. Contiguous column coherent (CCC bi-clustering) [17] is a method for gene expression time series, which finds patterns in nearby columns.

Probabilistic and generative methods use model-based techniques to define biclusters [18]. Probabilistic Relational Models (PRMs) [19] and their extension ProBic [20] are fully generative models that combine probabilistic modeling and relational logic. C Monkey [21] is a generative approach which models biclusters by Markov chain processes. GU and Liu [22] generalized the plaid models proposed in [23] to fully generative models called Bayesian BiClustering model (BBC). The latter models introduced in [24] is generative models which have the advantage that they select models using well-understood model selection techniques such as maximum likelihood. Costa et al. [25] introduced a hierarchical model-based co-clustering algorithm. In their method the co-occurrence matrix is characterized in probabilistic terms, by estimating the joint distribution between rows and columns.

III. STUDY ON MINING ORDER-PRESERVING SUB MATRICES

Order-Preserving Sub matrix (OPSM) is a data pattern particularly useful for discovering trends in noisy data. The OPSM problem applies to a matrix of numerical data values. The objective is to discover a subset of attributes (columns) over which a subset of tuples (rows) exhibit similar rises and falls in the tuples' values. For instance, when analyzing gene expression data from microarray experiments, genes (rows) with concurrent changes of mRNA expression levels across different time points (columns) may share the same cell-cycle related properties [26]. Due to the high level of noise in typical microarray data, it is typically more

meaningful to compare the relative expression levels of different genes at different time points rather than their total values. Genes that exhibit simultaneous rises and falls of their expression values across different time points or experiments reveal interesting patterns and knowledge.

The original OPSM problem was first proposed by Ben-Dor and company. [27]:

Definition 1: Given an $n \times m$ matrix (dataset) D , an order-preserving sub matrix (OPSM) is a pair $(R; P)$, where R is a subset of the n rows (represented by a set of row ids) and P is a permutation of a subset of the m columns (represented by a sequence of column ids) such that for each row in R , the data values are monotonically increasing with respect to P , i.e., $D_{iP_j} < D_{iP_{j_0}} ; \forall i \in R; 1 \leq j < j_0 = jP_j$, where D_{rc} denotes the value at row r and column c of D .

TABLE 1

A Dataset without Repeated Measurements

| | <i>a</i> | <i>b</i> | <i>c</i> | <i>d</i> |
|--------------|----------|----------|----------|----------|
| row 1 | 49 | 38 | 115 | 82 |
| row 2 | 67 | 96 | 124 | 48 |
| row 3 | 65 | 67 | 132 | 95 |
| row 4 | 81 | 115 | 133 | 62 |

For example, Table 1 shows a dataset with 4 rows and 4 columns. The values of rows 2, 3 and 4 rise from a to b, so $\{(2, 3, 4), \langle a, b \rangle\}$ is an OPSM. For simplicity, in this study we assume that all values in a row are unique.

We say that a row supports a permutation if its values increase monotonically with respect to the permutation. In the above example, rows 2, 3 and 4 support the permutation $\langle a, b \rangle$, but row 1 does not. For a fixed dataset, the rows that support a permutation can be unambiguously identified. In the following discussion, we will refer to an OPSM simply by its variation which will also be called a *pattern*.

An OPSM is said to be frequent if the number of supporting rows is not less than a support threshold, ρ . Given a dataset, the basic OPSM mining problem is to identify all frequent OPSM's. In the gene expression context, these OPSM's correspond to groups of genes

that have similar activity patterns, which may suggest shared regulatory mechanisms and/or protein functions. In microarray experiments, each value in the dataset is a physical measurement subject to different kinds of errors. A drawback of the basic OPSM mining problem is that it is sensitive to noisy data. In our previous example, if the value of column a is slightly increased in row 3, say from 65 to 69, then row 3 will no longer support the pattern $\langle a, b \rangle$, but will support $\langle b, a \rangle$ instead.

To combat errors, experiments are often repeated and multiple measured values (called replicates) are recorded. The replicates allow a better estimate of the actual physical quantity. Certainly as the cost of microarray experiments has been dropping, research groups have been obtaining replicates to strike for higher data quality. For example, in some of the microarray datasets we use in our study, each experiment is repeated 3 times to produce 3 measurements of every data point. Studies have clearly shown the importance of having multiple replicates in improving data quality.

TABLE 2

A dataset with repeated measurements

| | a_1 | a_2 | a_3 | b_1 | b_2 | b_3 | c_1 | c_2 | c_3 | d_1 | d_2 | d_3 |
|---|-------|-------|-------|-------|-------|-------|-------|-------|-------|-------|-------|-------|
| r | 4 | 5 | 80 | 38 | 51 | 8 | 11 | 10 | 79 | 8 | 1 | 5 |
| o | 9 | 5 | | | | 1 | 5 | 1 | | 2 | 1 | 0 |
| w | | | | | | | | | | | 0 | |
| 1 | | | | | | | | | | | | |
| r | 6 | 5 | 13 | 96 | 85 | 8 | 12 | 92 | 94 | 4 | 3 | 3 |
| o | 7 | 4 | 0 | | | 2 | 4 | | | 8 | 7 | 2 |
| w | | | | | | | | | | | | |
| 2 | | | | | | | | | | | | |
| r | 6 | 4 | 62 | 67 | 39 | 2 | 13 | 11 | 83 | 9 | 8 | 6 |
| o | 5 | 9 | | | | 8 | 2 | 9 | | 5 | 9 | 4 |
| w | | | | | | | | | | | | |
| 3 | | | | | | | | | | | | |
| r | 8 | 8 | 10 | 11 | 11 | 8 | 13 | 10 | 10 | 6 | 5 | 5 |
| o | 1 | 3 | 5 | 5 | 0 | 7 | 3 | 8 | 5 | 2 | 2 | 1 |
| w | | | | | | | | | | | | |
| 4 | | | | | | | | | | | | |

Different replicates, however, may support different OPSM's. For example, Table 2 shows a dataset with two more replicates added per experiment. From this dataset, we see that it is no longer clear whether row 3 supports the $\langle a, b \rangle$ pattern. For instance, while the replicates a_1, b_1 support the pattern, the replicates a_1, b_2 do not.

Our example illustrates that the original OPSM definition is not robust against noisy data. It also fails to take advantage of the additional information provided by replicates. There is thus a need to modify the definition of OPSM to handle repeated measurements. Such a definition should satisfy the following requirements:

- 1) If a pattern is supported by all combinations of the replicates of a row, the row should contribute a high support to the pattern. For example, for row 3, the values of column b are clearly smaller than those of column c . All $3 \times 3 = 9$ replicate combinations of b and c values $(b_1, c_1), (b_1, c_2) \dots (b_3, c_3)$ support the $\langle b, c \rangle$ pattern. Row 3 should thus strongly support $\langle b, c \rangle$.
- 2) If the value of a replicate largely deviates from other replicates, it is most likely due to error. The replicate should not severely affect the support of a given pattern. For example, we see that row 2 generally supports the pattern $\langle a, c \rangle$ if we ignore a_3 , which is abnormally large (130) when compared to a_1 (67) and a_2 (54), and is thus likely an error. The support of $\langle a, c \rangle$ contributed by row 2 should only be mildly reduced due to the presence of a_3 .
- 3) If the replicates largely disagree on their support of a pattern, the overall support should reflect the uncertainty. For example, in row 4, the values of b and c are mingled. Thus, row 4 should neither strongly support $\langle b, c \rangle$ nor $\langle c, b \rangle$.

The first two requirements can be satisfied by summarizing the replicates by robust statistics such as medians, and mining the resulting dataset using the original definition of OPSM. However, the third requirement cannot be satisfied by any single summarizing statistic. This is because under the original definition, a row can only either fully support or fully not support a pattern, and thus the information of uncertainty is lost. To tackle this problem, we propose a new definition of OPSM and the corresponding mining problem based on the concept of fractional support:

Definition 2: The partial support $s_i(P)$ of a pattern P contributed by a row I is the number of replicate combinations of row I that support the pattern, divided by the total number of replicate combinations of the columns in P .

For example, for row 1, the pattern $\langle a,b,d \rangle$ is supported by 8 replicate combinations: ha_1,b_2,d_1i , ha_1,b_2,d_2i , ha_1,b_3,d_1i , ha_1,b_3,d_2i , ha_2,b_3,d_1i , ha_2,b_3,d_2i , ha_3,b_3,d_1i , and ha_3,b_3,d_2i out of $3^3 = 27$ possible combinations. The fractional support $s_1(\langle a,b,d \rangle)$ is therefore 8/27. We use $sn_i(P)$ and $sd_i(P)$ to denote the numerator and the denominator of $s_i(P)$, respectively. In our example, $sn_1(\langle a,b,d \rangle) = 8$ and $sd_1(\langle a,b,d \rangle) = 27$.

If we use fractional support to indicate how much a row supports an OPSM, all the three requirements we stated above are satisfied. Firstly, if all replicate combinations of a row support a certain pattern, the fractional support contributed will be one, the maximum fractional support. Secondly, if one replicate of a column j deviates from the others, the replicate can at most change the fractional support by $\frac{1}{r(j)}$, where $r(j)$ is the number of replicates of column j . This has small effects when the number of replicates $r(j)$ is large. Finally, if only a fraction of the replicate combinations supports a pattern, the resulting fractional support will be fuzzy (away from 0 and 1), which reflects the doubt

Based on the definition of fractional support, the support of a pattern P is defined as the sum of the fractional supports of P contributed by all the rows: $s(P) = \sum_i s_i(P)$. A pattern P is frequent if its support is not less than a given support threshold ρ . Our new OPSM mining problem OPSM-RM (OPSM with repeated measurements) is to identify all frequent patterns in a data matrix with replicates:

Definition 3: Given a dataset, the OPSM-RM difficulty asks for the set of all OPSMs each of which having a total fractional support from all rows not less than a given support threshold.

From the definition of fractional support, we can observe the combinatorial nature of the OPSM-RM problem — the number of replicate combinations grows exponentially with respect to the pattern length. The objective of this work is to derive efficient algorithms for mining OPSM-RM. By proving a number of interesting properties and theorems, we propose pruning techniques that can significantly reduce mining time [28].

IV. OVERVIEW OF DATASET

The readout of a DNA chip containing n genes consists of n real numbers that represent the expression level of each gene, either as an absolute or as a relative quantity (with respect to some reference). When the readouts for m experiments (tissues) are joint, each gene yields a vector of m real numbers.

Table 1. The Ranks of the Three Genes g1:g2:g3 Induce a Common Permutation When Restricted to Columns t1;t2;t3;t4;t5

| Gene n tissue | t1 | t2 | t3 | t4 | t5 |
|------------------------|----|----|----|----|----|
| g1 | 7 | 13 | 19 | 2 | 50 |
| | | | | | |
| g2 | 19 | 23 | 39 | 6 | 42 |
| g3 | 4 | 6 | 8 | 2 | 10 |
| Induced permutation | 2 | 3 | 4 | 1 | 5 |

To make our results independent of the scaling of the data, we think only the relative ordering of the expression levels for each gene, as different to the correct values. This motivates us to consider the permutation induced on the m numbers by sorting them. so, we view the expressed data matrix, D , as an n -by- m matrix, where each row corresponds to a gene and each column to an experiment. The m entries in each row are a permutation of the numbers $\{1 \dots m\}$. The (I, j) entry is the rank of the readout of gene in tissue j , out of the m readouts of this gene. Characteristic values for n and m are in the ranges $500 \leq n \leq 15,000$ and $10 \leq m \leq 150$.

The computational task we address is the identification of large order-preserving sub matrices (OPSMs) in an $n \times m$ matrix D . A sub matrix is order preserving if there is a permutation of its columns under which the sequence of values in every row is strictly increasing. In the case of expression data, such a sub matrix is determined by a set of genes G and a set of tissues T such that, within the set of tissues T , the term levels of all the genes in G have the same linear ordering.

V. CONCLUSION

In this paper we review Order-preserving sub matrices (OPSM's) which is useful in capturing concurrent patterns in data when the relative magnitudes of data items are more important than their exact values. To cope with data noise, repeated experiments are often conducted to collect multiple measurements. We also review some basic methods of Simultaneous Clustering Problem.

REFERENCES

- [1]. Madeira, S.C., Oliveira, A.L." Biclustering Algorithms for Biological Data Analysis: A Survey." IEEE/ACM Trans. on Comp. Biol. and Bioin for., 24–45 (2004).
- [2]. Charrad, M., Lechevallier, Y., Ahmed, M.b., Saporta, G."Block Clustering for Web Pages Categorization." In: Corchado, E., Yin, H. (eds.) IDEAL 2009. LNCS, vol. 5788, pp. 260–267. Springer, Heidelberg (2009).
- [3]. Bichot, C.E."Co-clustering documents and words by minimizing the normalized cut objective function." JMMA 9, 131–147 (2010).
- [4]. Grimal, C., Bisson, G."Classification a partird'une collection de matrices."CAp2010 (2010).
- [5]. Prelic, A., Bleuler, S., Zimmermann, P.: A systematic comparison and evaluation of bi clustering methods for gene expression data. Bioinformatics, 122–129 (2006).
- [6]. Balbi, S., Miele, R., Scepi, G."Clustering of documents from a two-way viewpoint." In: 10th Int. Conf. on Statistical Analysis of Textual Data (2010).
- [7]. Dhillon, I.S."Co-clustering documents and words using bipartite spectral graph partitioning." In: 7th ACM SIGKDD 2001, California, pp. 269–274 (2001).
- [8]. Nadif, M., Govaert, G."Block clustering of contingency table and mixture model." In: Famili, A.F., Kok, J.N., Pen˜a, J.M., Siebes, A., Feelders, A. (eds.) IDA 2005.
- [9]. Dhillon, I.S., Mallela, S., Modha, D.S., "Information theoretic co-clustering. "In: ACM SIGKDD, pp. 89–98. ACM, Washington DC (2003).
- [10]. Zha, H., He, X., Ding, C., Simon, H., Gu, M." Bipartite Graph Partitioning and Data Clustering." In: ACM Conf. on Inf. and Knowledge Management, pp. 25–32 (2001).
- [11]. Tanay, A., Sharan, R., Shamir, R."Biclustering Algorithms: A Survey." In: Aluru,S. (ed.) Handbook of Comp. Molecular Biology, Chapman, Boca Raton (2004).
- [12]. Malika Charrad and Mohamed Ben Ahmed, "Simultaneous Clustering: A Survey", LNCS 6744, pp. 370–375, 2011. Springer-Verlag Berlin Heidelberg 2011.
- [13]. Murali, T.M., Kasif, S."Extracting conserved gene expression motifs from gene expression data." In: Pacific Sym. on Biocomputing, Hawaii, USA, pp. 77–88 (2003).
- [14]. Prelic, A., Bleuler, S., Zimmermann, P."A systematic comparison and evaluation of bi clustering methods for gene expression data." Bioinformatics, 122–129 (2006).
- [15]. Ben-Dor, A., Chor, B., Karp, R."Discovering local structure in gene expression data: The order-preserving submatrix problem." J. of Comput. Biol. 10, 373–384 (2003).
- [16]. Klugar, Y., Basri, R., Chang, J.T., Gerstein, M."Spectral bi clustering of microarray data: co clustering genes and conditions. "Genome Research 13, 703–716 (2003).
- [17]. Madeira, S.C., Teixeira, M.C." Identification of regulatory modules in time series gene expression data using a linear time bi clustering algorithm." IEEE ACM (2010).
- [18]. Hochreiter, S., Bodenhofer, U., Heusel, M., Mayr," A. FABIA: factor analysis for bicluster acquisition." Bioinformatics journal 26(12), 1520–1527 (2010).
- [19]. Getoor, L., Friedman, N., Koller, D., Taskar, B." Learning probabilistic models of link structure." J. Mach. Learn. Res. 3, 679–707 (2002).
- [20]. Van den, B.T., "Robust Algorithms for Inferring Regulatory Networks Based on Gene Expression Measurements." PhD Thesis (2009).
- [21]. Reiss, D.J., "Integrated bi clustering of heterogeneous genome-wide datasets for the inference of global regulatory networks." BMC Bioinfor. 280–302 (2006).
- [22]. Lazzeroni, L., Owen, A., "Plaid models for gene expression data. Technical report, Stanford University (2002).
- [23]. Caldas, J., Kaski, S."Bayesian bi clustering with the plaid model."In: IEEE Intern. Workshop on Machine Learning for Signal Processing, pp. 291–296 (2008).
- [24]. Gu, J.: Bayesian, "Biclustering of gene expression data." BMC Genomics (2008).
- [25]. Costa, G., Manco, G., Ortale, R."A hierarchical model-based approach to co clustering high-dimensional data." In: ACM sym. on App. comput. pp. 886–890 (2008).
- [26]. P.T. Spellman, G. Sherlock, M.Q. Zhang, V.R. Iyer, K. Anders, M.B. Eisen, P.O. Brown, D. Botstein, and B. Futcher, "Comprehensive Identification of Cell Cycle-regulated Genes of the Yeast *Saccharomyces cerevisiae* by Microarray Hybridization." MolecularBiology of the Cell, vol. 9, no. 12, pp. 3273–3297, 1998.
- [27]. A. Ben-Dor, B. Chor, R.M. Karp, and Z. Yakhini, "Discovering Local Structure in Gene Expression Data: The Order-Preserving Sub matrix Problem," J. Computational Biology, vol. 10, nos. 3/4, pp. 373–384, 2003.
- [28]. Kevin Y. Yip, Ben Kao, Xinjie Zhu, Chun Kit Chui, Sau Dan Lee, and David W. Cheung, "Mining Order-Preserving Sub matrices from Data with Repeated Measurements" IEEE Transactions on knowledge and data Engineering , vol. 25, no. 7, july 2013.

Impact of Voltage Step Constraint and Mixed Load Models on Optimal Distributed Generation Placement

Rajendra Prasad Payasi, *Member, IEEE*, Asheesh K. Singh, *Member, IEEE*, Devender Singh

Abstract— The optimal distributed generation placement (ODGP) is aimed to provide best location and size of distributed generation (DG) within system constraints for optimized electrical distribution network operation. In this paper, the important factors considered are voltage step constraint and mixed load models to explore the influence of these in ODGP. The optimal location, size, and operating power factor of DG are obtained by minimizing real power loss using Simple Genetic Algorithm (SGA). The analyses presented in the paper, reveal that the mixed load models and voltage step limit significantly affect the optimal location and size of DG.

Index Terms— *Distributed generation, Distribution system, Optimal distributed generation placement, Simple Genetic Algorithm*

| | |
|--------------------------|---|
| $NVSLVB$ | Number of voltage step limit violated buses. |
| P_{0i}, Q_{0i} | Real and reactive load at bus i at nominal Voltage (p.u.). |
| P_D, Q_D | Total system real and reactive power Demand (p.u.). |
| P_{DG}, Q_{DG}, S_{DG} | Real, reactive, and MVA power DG (p.u.). |
| P_i, Q_i | Real and reactive power injection at bus i (p.u.). |
| P_L, Q_L | System real and reactive power loss (p.u.). |
| PF_{DG} | Operating power factor of DG |
| V_{0i}, V_i | Nominal voltage at i^{th} bus (p.u.), Voltage of i^{th} bus (p.u.). |
| V_{stepi}, VSL | Voltage step at i^{th} bus (p.u.), Voltage step limit (%). |

| Nomenclature | |
|-----------------|---|
| α, β | Voltage exponent of real and reactive loads. |
| CP | Constant power load model. |
| SDM, SNM | Summer day and summer night mixed load models |
| WDM, WNM | Winter day and winter night mixed load models |
| $CS_{i,j}$ | MVA capacity of line $i - j$ (p.u.). |
| S_{intake} | Apparent power (MVA) intake at bus 1 (p.u.). |
| $NLCLVL$ | Number of line capacity limit violated Lines. |
| $NVLVB$ | Number of voltage limit violated buses. |
| $WDG, WODG$ | With and without DG. |
| $WVSL, WOVSL$ | With and without VSL. |
| N_B, N_L | Number of buses and number of lines. |

I. INTRODUCTION

In electric power system most of the electric energy loss occurs in the distribution lines because of higher R/X ratio. The distributed generation is one of the options to reduce the energy loss by generation of electricity near to the load centers. Distributed generation, unlike traditional generation, aims to generate part of required electrical energy on small scale closer to the places of consumption. Distributed generation, termed as embedded generation or dispersed generation or decentralized generation, is defined as “electric power source that can be connected to a distribution network at any node or by customer at the customer side of the meter” [1].

Nowadays, DG penetration has renewed interest of possible solutions [25-26]. In [27-29], authors have because of liberalization of electricity market, constraint implemented Genetic Algorithm (GA) for real power in expansion of transmission and distribution lines, loss minimization but they have not considered voltage technological developments in DG, and benefits accrued step constraint and seasonal mixed loads at each bus. to DG [2]-[4]. The real power loss reduction is one of the benefits of DG for economical operation of electrical distribution network. The loss reduction is also important because distribution network operators (DNOs) are economically rewarded for that. The DG owners assist DNOs for reduction in network loss and DNOs may give the part of reward to DG owners [5]. The optimal location, size, and operating power factor of DG could be obtained by minimizing real power loss. The load model and voltage step constraint may affect the optimal location and size of DG. So, the consideration of load model and voltage step constraints is inevitable in optimal DG placement (ODGP).

The load throughout the year is not constant instead it varies with seasonal day and night. Further, the load at every bus may be the composition of different type of voltage dependent loads such as industrial, residential, and commercial. The composition of voltage dependent loads can be represented by mixed load models [6], [7], [8]. In [9], authors considered the DG capable of supplying both real and reactive power, and determined the optimal power factor of DG along with its optimal size and location corresponding to minimum loss. In [10], the distributed generation capacity analysis is performed with voltage step constraint within narrow range of DG power factor variation (between 0.95 leading and lagging) for fixed location with constant power load. Thus, seasonal mixed load models, wide range of DG power factor variation (between 0.8 leading and 0.8lagging), and voltage step constraint are the important components to be considered together for ODGP.

In [8, 11-13], different kinds of load models have been considered but the mixed load model at every bus has not been considered except in [8]. The variable load, but not voltage dependent, has been adopted in [14-16]. In [17-23], the type of DG has been considered which is capable of supplying both real and reactive power but without considering load models. In literature review [24], very few literature have been found which considered seasonal mixed load models, voltage step constraint and wide range of DG operating power factor.

The optimal siting, sizing, and operating power factor of DG involves large computation time when exhaustive power flow with exhaustive search or traditional optimization techniques are used. Because of this reason, simple Genetic Algorithms (SGA) has been implemented in order to overcome some limits of conventional methods. GA has the capability to obtain optimum solution with high probability of best one by a finite number of evolution steps performed on a finite number

In this paper, real power loss minimization is considered as an objective function to determine optimal location, size, and operating power factor of DG for seasonal mixed loads as well as constant power load with and without consideration of voltage step constraint.

A 38 bus system, as described in [12,13,32], is adopted for ODGP based on real power loss minimization using SGA, and Newton Raphson load flow method for different load scenario represented by mixed load model. The voltage step limit of 3%, which is recommended for planned outages of DG [10], is considered along with usual constraints i.e. bus voltage limits and line power capacity limit. To keep the problem focused on impact of voltage step constraint and mixed load models, this works presents the case of ODGP for single location. However, the methodology is generalized and can be implemented for multiple DG locations by making the number of variables larger in number. It is also considered that the DG system is capable of operating with wide variation of operating power factor.

This paper is structured as follows: Section 2 introduces the voltage step change by way of simple two-bus network. Section 3 describes the load models and test cases. Section 4 describes the indices to compare the results. Section 5 describes the problem formulation. Section 6 describes the implementation of SGA. Section 7 presents the simulation results and analysis, and Section 8 presents the conclusions of the analysis.

II. VOLTAGE RISE AND VOLTAGE STEP

The voltage rise and voltage step are illustrated using two bus network (Fig. 1) consists of a grid supply point (GSP) at Bus A, load ($P_{DB} + jQ_{DB}$) and DG (capable of supplying both real power and reactive power

($P_{DGB} + Q_{DGB}$) at bus B. The some of the load power met by DG, and hence the power drawn from the grid through impedance ($R+jX$) is reduced. Thus DG results steady state voltage rise at B (V_{riseB}) is expressed approximately (assuming that the voltage at A remains constant i.e. 1 p.u.) as follows [10].

$$V_{riseB} = (P_{DGB} - P_{DB})R + (Q_{DGB} - Q_{DB})X \quad (1)$$

On subtracting the voltage at B without DG (V_{WDGB}) from the voltage at B with DG (V_{WDGB}), gives the voltage step at bus B (V_{stepB}) on loss of the DG which is expressed as follows.

$$V_{stepB} = V_{WDGB} - V_{WODGB} = -(P_{DGB}R - Q_{DGB}X) \quad (2)$$

For a given percentage limit of voltage step limit (VSL), the DG capacity is restricted more than commonly considered for bus voltage limit for fixed location of DG. As per the UK standards, the voltage step limit is specified as 3% for planned switching or outages of DG and 6% for unplanned outages (under fault condition) of DG [10].

In this paper, the voltage step limit corresponding to planned switching outages of DG is adopted and bus 1 (GSP) of 38 test bus system (Fig. 6 in Appendix) is taken as slack bus for power flow study. The voltage step at i^{th} bus (V_{stepi}) in p.u. is calculated as follows:

$$V_{stepi} = \frac{(V_{WDGi} - V_{WODGi})}{V_{WDGi}}, \text{ for } i = 2 \text{ to } N_B \quad (3)$$

$PDG\ B + jQDG\ B$

Above equations (4) and (5) neglect frequency dependency of load, assuming that the range of frequency variation is relatively narrow. In practice, the load on each bus are the composition of industrial, residential, and commercial loads in certain proportion which may vary with seasonal day and night. Therefore, in this paper the mixed load model is considered to represent the load at i^{th} bus in the following form.

$$P_i = I_{Pi} \cdot P_{Qi} \left(\frac{|V_i|}{|V_{oi}|} \right)^{\alpha} + R_{Pi} \cdot P_{Qi} \left(\frac{|V_i|}{|V_{oi}|} \right)^{\beta} + C_{Pi} \cdot P_{Qi} \left(\frac{|V_i|}{|V_{oi}|} \right)^{\gamma}$$

$$Q_i = I_{Qi} \cdot Q_{Qi} \left(\frac{|V_i|}{|V_{oi}|} \right)^{\delta} + R_{Qi} \cdot Q_{Qi} \left(\frac{|V_i|}{|V_{oi}|} \right)^{\theta} + C_{Qi} \cdot Q_{Qi} \left(\frac{|V_i|}{|V_{oi}|} \right)^{\beta}$$

Where, exponents i and i are corresponding to industrial load; r and r are corresponding to residential load; c and c are corresponding to commercial load. The values and are zeros corresponding to constant power load model.

I_{Pi} & I_{Qi} , R_{Pi} & R_{Qi} and C_{Pi} & C_{Qi} are the composition factors for real & reactive powers for industrial, residential and commercial loads respectively at i^{th} bus except for unloaded buses (UB). The composition factors are assumed such that

$$I_{Pi} + R_{Pi} + C_{Pi} = 1 \quad \text{for } i = 2 \text{ to } N_B, \quad i \neq UB \quad (8)$$

$$I_{Qi} + R_{Qi} + C_{Qi} = 1 \quad \text{for } i = 2 \text{ to } N_B, \quad i \neq UB. \quad (9)$$

Fig. 1. Two-bus system for voltage step analysis

III. LOAD MODELS AND TEST CASES

In conventional load flow analysis, normally constant power loads are assumed i.e. loads are not dependent on voltage or frequency. While in fact, the loads in distribution system are voltage dependent. So, the voltage dependent load model is adopted to represent the loads in practice. The load models for active and reactive power are represented as follows [6, 7].

$$P_I = P_{Qi} \left(\frac{V_i}{V_{oi}} \right)^{\alpha} \quad (4)$$

$$Q_i = Q_{Qi} \left(\frac{V_i}{V_{oi}} \right)^{\beta} \quad (5)$$

The values for exponents of voltage for real and reactive component of SDM , SNM , WDM , and WNM load models are given in Table I [7, 8]. The composition factors of basic load models assumed at each bus are given in Table 2. In this study it is also assumed that $I_{Pi} = I_{Qi}$, $R_{Pi} = R_{Qi}$ and $C_{Pi} = C_{Qi}$

The studies are performed considering the following conditions: 1) each bus has a composition of industrial, residential, and commercial load in a certain proportion; 2) voltage dependency of load varies with seasonal day and night.

The analysis of DG is performed for the following test cases.

- 1) DG operates under wide range of power factor without VSL constraint.
- 2) DG operates under wide range of power factor with V

TABLE I

| EXONENT VALUES FOR DIFFERENT LOAD MODELS [6] | | | | | | | | | |
|--|-----------------|-------------|------------|------------|-----------|------------|-----------|------------|-----------|
| Duration | Exponent values | | | | | | | | |
| | Industrial | Residential | Commercial | α_i | β_i | α_r | β_r | α_c | β_c |
| Summer | Day | 0.18 | 6.00 | 0.72 | 2.96 | 1.25 | 3.50 | | |
| | Night | 0.18 | 6.00 | 0.92 | 4.04 | 0.99 | 3.95 | | |
| Winter | Day | 0.18 | 6.00 | 1.04 | 4.19 | 1.50 | 3.15 | | |
| | Night | 0.18 | 6.00 | 1.30 | 4.38 | 1.51 | 3.40 | | |

TABLE II

Reactive Power Loss Index (QLI): The reactive power loss index is defined

$$QLI = \frac{Q_{LWDG}}{Q_{LOWDG}} \times 100$$

The lower value of this index indicates better benefits in terms of reduction in Q_L .

Voltage Profile Index (VPI): It is associated with the maximum voltage drop between each bus and root bus. The lower value of this index indicates better voltage profile. It is defined as:

$$VPI = \max \left(\frac{V_1 - V_i}{V_1} \right) \times 100 \quad \text{for } i=2 \text{ to } N_B \quad (12)$$

Where, V_i is the voltage at bus one (main substation) considered as slack bus.

Line Capacity Index (LCI): Lower value of this index indicates that more line capacity is available and further load can be increased

$$LCI = \max \left(\frac{S_{ij}}{CS_{ij}} \right) \times 100 \quad \text{for } i,j=1 \text{ to } N_L \quad (13)$$

V. PROBLEM FORMULATION

A. Objective Function and Constraints

The objective is to minimize the total real power loss in the distribution system with ODGP. The P_L in the system is expressed as.

$$P_L = \sum_{i,j \in N_L} \left(\frac{P_{ij}^2 - Q_{ij}^2}{V_{ij}^2} r_{ij} \right) \quad (14)$$

Loss is the function of all system bus voltage (V_i) and line resistances (r_{ij}). The total loss mainly depends on voltage profile. In case of load models, P_L is dependent on α and β .

With the inclusion of DG at optimum location in the network, the P_L and hence S_{intake} and S_{sys} are affected. So, these quantities are evaluated to show the effect of Load models and voltage step constraint.

IV. INDICES

The following Indices are considered to quantify the impact of DG. These indices are defined as follows:

Real Power Loss Index (PLI): The real power loss index is defined as:

$$PLI = \frac{P_{LWDG}}{P_{LOWDG}} \times 100 \quad (10)$$

The lower value of this index indicates better benefits in terms of reduction in P_L .

The above objective function is minimized subject to various operational constraints of the system. The constraints considered are as follows.

$$V_{\min} \leq V_i \leq V_{\max} \quad \text{For } i=2 \text{ to } N_B \quad (15)$$

$$S_{ij} \leq CS_{ij}^{\max}, \text{ for } i,j \in N_L \quad (16)$$

$$V_{stepi} \leq V_{step}^{\max}, \text{ for } i=2 \text{ to } N_B$$

(17)

$$S_{DG} \leq S_{intakeWODG} \quad (18)$$

Where,

$$V_{min} = 0.95 \text{ p.u. } V_{max} = 1.03 \text{ p.u. and } V_{step}^{\max} = 3\%$$

B. Optimum Location

The optimum location in a network corresponding to minimum real power loss could be different for different loading conditions. To obtain one optimum location, the minimum energy loss criterion is adopted. The placement of DG depends on many other factors such as availability of space and practical suitability. Therefore, if the optimum location corresponding to seasonal loading conditions (summer day, summer night, winter day, and winter night) is practically suitable, then one optimum location suitable for all seasonal loading condition could be obtained on the basis of lowest aggregate energy loss. The aggregate energy loss

Corresponding to each candidate location is determined by formula expressed as follows.

Energy Loss =

$$w_{SD} \cdot P_{LSD} + w_{SN} \cdot P_{LSN} + w_{WD} \cdot P_{LWD} + w_{WN} \cdot P_{LWN} \quad (19)$$

Where, $w_{SD} + w_{SN} + w_{WD} + w_{WN} = 1$

$w_{SD}, w_{SN}, w_{WD}, w_{WN}$ are the normalized weights for durations corresponding to *SDM*, *SNM*, *WDM*, *WNM* load models respectively. $P_{LSD}, P_{LSN}, P_{LWD}, P_{LWN}$ are real power loss corresponding to *SDM*, *SNM*, *WDM*, and *WNM* loading conditions.

In this paper, the normalized weights are assumed as follows.

$$w_{SD}=0.33; w_{SN}=0.33; w_{WD}=0.17; w_{WN}=0.17$$

C. Distributed Generation

There are different types of traditional and non-traditional distributed generation classified from the constructional, technological, size, and power-time duration points of view [3]. However, on the basis of terminal characteristics in terms of real and reactive power delivering capability, DGs have also been grouped into four major types [9]. According to [2], DGs are connected to grid at distribution level to serve the customer on site by providing the support to the distribution network. The DG technologies include engines, small (and micro) turbines, fuel cells, and photovoltaic systems. It generally excludes wind power, because it mostly produced on wind farms instead of on-site power requirements. In this paper, the study is performed for optimum location, size and power factor of DG which may have wide variation of power factor (0.8 ld to 0.8 lg) such as converters/inverters-connected photovoltaic, micro-turbines, and fuel cells.

VI. COMPUTATION

A. Test system

The simulation studies are carried out to obtain the optimum size, power factor, and location of a DG in 38 bus system [12, 13, 32] (Fig. 6 in appendix). In this paper, the line impedances, load data and the line power limits are expressed in p.u. at the base voltage of 12.66 kV and base MVA of 1.0 MVA [12,13,32] (Table VI in Appendix). GA based real power loss minimization approach is implemented in above system with seasonal mixed load models and voltage step constraint.

B. GA implementation

GA is an efficient tool based on evolutionary strategy to solve the optimization problems. A simple GA (SGA) starts with an initial population of individuals and population is modified by means of operators for the formation of next generation. The process continues until convergence criterion is satisfied.

The criterion of proper implementation of SGA, the network configuration is kept unchanged and the objective function depends only on location, size (P_{DG}), and power factor (PF_{DG}) of DG. The solution is checked for proper location (ranging from 2 to N_B), size (limited to P_{intake}) and power factor (limited between 0.8 ld to 0.8lg) of DG unit.

The SGA starts with random generation of initial population corresponding to individuals. For each solution a size, power

Factor, and a location (bus) of DG are generated within system constraints. The numbers of size-power_factor-location pairs are randomly selected, objective function is evaluated, and system constraints are verified. The solution is accepted if any constraint is not violated else solution is rejected.

The genetic operators are applied, after formation of initial population, for a certain number of times to produce new solutions and those new solutions are accepted which are not violating the constraints. The new population is formed by selecting best among old and new solution. The algorithms terminated when difference between value of objective function of the best and worst individuals becomes smaller than the specified value. The steps for SGA based solution are given in Appendix.

VII. SIMULATION RESULTS AND ANALYSIS

The results are tabulated in Tables III, IV, and V. The indices are depicted in Fig. 2 to 5 to show the effect of *VSL*, and load models. The optimal size, location, and operating power factor of DG are determined corresponding to minimum P_L , with and without inclusion of *VSL* constraint. The analyses of results are as follows.

A. Impact of Load Models on *VSL* Violation

Without inclusion of *VSL* constraint in GA based loss minimization, it is found that the *VSL* is violated at number of buses for *CP*, *SDM*, *SNM* load models as given in Table III. It is observed that for *CP*, *VSL* violated at more number of buses compared to seasonal mixed load models. It is also

observed that there is no violation of VSL for WDM and WNM load models.

Thus, it is revealed that voltage step constraint is more effective in case of constant power load whereas less severe for mixed load models.

TABLE III
Number of VSL Violated Buses

| Load model | <i>N_{VSLVB}</i> |
|------------|--------------------------|
| CP | 25 |
| SDM | 11 |
| SNM | 3 |
| WDM | 0 |
| WNM | 0 |

B. Impact of load models and VSL on ODGP

The optimum size, operating power factor, and location of DG corresponding to minimum real power loss are given in Table IV. It is observed that in case of CP, SDM, and SNM the DG size and P_L are different with inclusion of VSL constraint because for these loading conditions the VSLs violates as given in Table III. The optimum operating power factor in case of seasonal mixed load models is 0.8 with and without VSL constraint whereas in case of CP, it is 0.8 and 0.82 with and without inclusion of VSL respectively. The optimum locations for seasonal mixed load models are 29, 31, and 32 with inclusion of VSL whereas those of without inclusion of VSL are 30, 31, and 32. The location of DG for CP is near to the main substation i.e. bus 6 and DG size is also more for both cases (with and without inclusion of VSL). Thus assumption of CP may not give the appropriate size and location of DG because in practice the loads are composition of voltage dependent loads.

It is also observed from Table IV that S_{sys} is reduced when DG is connected because of reduction in loss. The S_{intake} for CP is less compared to seasonal mixed load models in both cases (with and without VSL) because in case of CP the optimal location is near to the root bus and penetration of DG is high.

TABLE IV
PL Minimization With and Without Inclusion of VSL Constraint

| Load model | W/WO DG | W/WO VSL | P_{sys} (MW) | P_{Fsys} | DG bus | S_{sys} (MVA) | S_{intake} | P_L (MVA) (p.u.) |
|------------|---------|----------|---------------------------|------------|--------|----------------------------|--------------|-------------------------------|
| CP | WODG | - | - | - | - | 4.5963 | 4.3963 | 0.1889 |
| | WDG | WOVSL | 2.4574 | 0.8214 | 6 | 1.4584 | 4.4422 | 0.0577 |
| SDM | WODG | - | 1.3680 | 0.8014 | 6 | 2.7712 | 4.4706 | 0.0822 |
| | WDG | WOVSL | 0.7426 | 0.8014 | 30 | 4.4372 | 4.4372 | 0.1667 |
| SNM | WODG | - | 0.7183 | 0.8014 | 29 | 3.5604 | 4.4533 | 0.0940 |
| | WDG | WOVSL | 0.5335 | 0.8014 | 31 | 4.4304 | 4.4304 | 0.1855 |
| WDM | WODG | - | 0.5280 | 0.8014 | 31 | 3.7845 | 4.4475 | 0.1049 |
| | WDG | WOVSL | 0.4358 | 0.8014 | 31 | 4.4224 | 4.4224 | 0.1645 |
| WNM | WODG | - | 0.4358 | 0.8014 | 31 | 3.8959 | 4.4374 | 0.1129 |
| | WDG | WOVSL | 0.3280 | 0.8014 | 32 | 4.0206 | 4.4281 | 0.1229 |
| | | WVSL | 0.3280 | 0.8014 | 32 | 4.0206 | 4.4281 | 0.1229 |

the voltage drop.

Voltage Profile Index (VPI): It is observed from Fig. 4 that the increase in VPI is more for CP compared to seasonal mixed load models with inclusion of VSL. This shows that VSL is more effective if load is assumed as constant power load. In case of with and without DG, it is found that constant power load shows more improvement in voltage profile than mixed load models which signifies that assumption of constant power load for analysis will give misleading result.

Line Capacity Index (LCI): The capacity release is more for CP compared to seasonal mixed load models in both cases (with and without VSL). This signifies that VSL is more effective for CP compared to seasonal mixed load models.

Thus, indices reveal that assumption of CP may not give the appropriate results regarding ODGP because in practice most of the loads are voltage dependent and of mixed type.

C. Impact of VSL on Indices

The indices PLI, QLI, VPI, and LCI, obtained corresponding to minimum loss are depicted in Fig. 2 to 5. The analysis of indices as follows.

Real Power Loss Index (PLI): It is observed from Fig. 2 that PLI is more for CP, SDM, and SNM with inclusion of VSL constraint because with this constraint DG size is less compared to without VSL constraint. Hence, the real power drawn from grid is increased which increases the voltage drop.

Fig. 3. QLI corresponding to minimum P_L

Reactive Power Loss Index (QLI): It is observed from the Fig. 3 that QLI is more for CP, SDM, and SNM with inclusion of VSL because this constraint reduces the DG size and reactive power drawn from grid is more which increases

Indices show that the effect of voltage step constraint on real and reactive power losses, voltage profile and line capacity release is significant for constant power load compared to mixed load models.

The size of DG for constant power load is larger compared to mixed load models for both with and without VSL cases. The optimal location of DG in case of constant load model is near to the root bus, whereas in case of load models it is far away from the root bus. The optimum location corresponding to minimum energy loss is bus-29

APPENDIX

D. DG Placement

All the possible locations obtained corresponding to minimum P_L for all load models (excluding CP) with VSL (Table IV) are considered as candidate buses for final implementation. Thus, the candidate buses are 29, 31, and 32 for minimum P_L . At each candidate location the optimal size and power factor of DG corresponding to minimum P_L for all loading conditions are determined. The energy loss corresponding to each candidate location is calculated using (19) and depicted in Table V. It is observed from the Table V that energy loss (0.10791 p.u.) is minimum corresponding to bus-29. The maximum DG_size is 0.7183 p.u. and operating power factor is 0.80 to meet the demand at all loading conditions. Thus, optimal size, operating power factor, and location are 0.7183 p.u. 0.80, and bus-29 respectively.

A. System

Fig. 6. The 38 bus test system [12, 13, 32]

TABLE V
Energy loss Minimization with Inclusion of VSL Constraint

| Candidate DG bus | Load Models | P_L (P. U.) | P_{DG} (p.u.) | PF_D | Energy loss (p.u.) |
|------------------|-------------|---------------|-----------------|--------|----------------------------------|
| 29 | SDM | 0.09388 | 0.7183 | 0.80 | 0.10791 (Minimum energy loss) |
| | SNM | 0.10800 | 0.5220 | 0.80 | |
| | WDM | 0.11641 | 0.4320 | 0.80 | |
| | WNM | 0.12627 | 0.3240 | 0.80 | |
| 31 | SDM | 0.10586 | 0.5544 | 0.84 | 0.10973 |
| | SNM | 0.10514 | 0.5520 | 0.83 | |
| | WDM | 0.11289 | 0.4360 | 0.80 | |
| | WNM | 0.12298 | 0.3280 | 0.80 | |
| 32 | SDM | 0.10870 | 0.5208 | 0.84 | 0.11161 |
| | SNM | 0.10802 | 0.5250 | 0.84 | |
| | WDM | 0.11290 | 0.4360 | 0.80 | |
| | WNM | 0.12291 | 0.3280 | 0.80 | |

VIII. CONCLUSION

The impact of mixed load models and voltage step constraint in optimal placement of distributed generation in 38-bus system is analyzed.

The voltage step limit violation for constant power load model is more severe compared to voltage dependent load model

B. Steps for SGA Based Solution

Step 1: Read the load data, line data, number of buses, and

For all load models, voltage limits, voltage step change limit ($VSL=3\%$), power factor (pf) limits (0.8 ld to 0.8 ld), Maximum number of iterations ($mi=50$), Maximum number of runs ($mr=10$).

Step 2: Select one of the load models by selecting exponent values, α, β .

Step 3: Run power flow program without DG and save the required quantities corresponding to WODG.

Step 4: Randomly generate size-pf-location of DG in a predefined range of DG sizes, buses (2 to N_B), and power factor. Set $k=1$.

Step 5: if $kr>mr$ go to 16

Step 6: If $k>mi$, go to 14

Step 7: Run power flow and calculate real power loss of system for each of the size-pf-location pairs for selected load model and record the power loss and its corresponding size-pf

TABLE VI
LINES PARAMETER AND LOAD DATA FOR 38 BUS SYSTEM [12,13]

| F | T | Line impedance (p. u.) | | L | S_L | Load on to bus (p. u.) | |
|----|----|---------------------------|----------|----|-------|---------------------------|-------|
| | | R | X | | | P | Q |
| 1 | 2 | 0.000574 | 0.000293 | 1 | 4.60 | 0.10 | 0.06 |
| 2 | 3 | 0.003070 | 0.001564 | 6 | 4.10 | 0.09 | 0.04 |
| 3 | 4 | 0.002279 | 0.001161 | 11 | 2.90 | 0.12 | 0.08 |
| 4 | 5 | 0.002373 | 0.001209 | 12 | 2.90 | 0.06 | 0.03 |
| 5 | 6 | 0.005100 | 0.004402 | 13 | 2.90 | 0.06 | 0.02 |
| 6 | 7 | 0.001166 | 0.003853 | 22 | 1.50 | 0.20 | 0.10 |
| 7 | 8 | 0.004430 | 0.001464 | 23 | 1.05 | 0.20 | 0.10 |
| 8 | 9 | 0.006413 | 0.004608 | 25 | 1.05 | 0.06 | 0.02 |
| 9 | 10 | 0.006501 | 0.004608 | 27 | 1.05 | 0.06 | 0.02 |
| 10 | 11 | 0.001224 | 0.000405 | 28 | 1.05 | 0.045 | 0.03 |
| 11 | 12 | 0.002331 | 0.000771 | 29 | 1.05 | 0.06 | 0.035 |
| 12 | 13 | 0.009141 | 0.007192 | 31 | 0.50 | 0.06 | 0.035 |
| 13 | 14 | 0.003372 | 0.004439 | 32 | 0.45 | 0.12 | 0.08 |
| 14 | 15 | 0.003680 | 0.003275 | 33 | 0.30 | 0.06 | 0.01 |
| 15 | 16 | 0.004647 | 0.003394 | 34 | 0.25 | 0.06 | 0.02 |
| 16 | 17 | 0.008026 | 0.010716 | 35 | 0.25 | 0.06 | 0.02 |
| 17 | 18 | 0.004538 | 0.003574 | 36 | 0.10 | 0.09 | 0.04 |
| 2 | 19 | 0.001021 | 0.000974 | 2 | 0.50 | 0.09 | 0.04 |
| 19 | 20 | 0.009366 | 0.008440 | 3 | 0.50 | 0.09 | 0.04 |
| 20 | 21 | 0.002550 | 0.002979 | 4 | 0.21 | 0.09 | 0.04 |
| 21 | 22 | 0.004414 | 0.005836 | 5 | 0.11 | 0.09 | 0.04 |
| 3 | 23 | 0.002809 | 0.001920 | 7 | 1.05 | 0.09 | 0.05 |
| 23 | 24 | 0.005592 | 0.004415 | 8 | 1.05 | 0.42 | 0.20 |
| 24 | 25 | 0.005579 | 0.004366 | 9 | 0.50 | 0.42 | 0.20 |
| 6 | 26 | 0.001264 | 0.000644 | 14 | 1.50 | 0.06 | 0.025 |
| 26 | 27 | 0.001770 | 0.000901 | 15 | 1.50 | 0.06 | 0.025 |
| 27 | 28 | 0.006594 | 0.005814 | 16 | 1.50 | 0.06 | 0.02 |
| 28 | 29 | 0.005007 | 0.004362 | 17 | 1.50 | 0.12 | 0.07 |
| 29 | 30 | 0.003160 | 0.001610 | 18 | 1.50 | 0.20 | 0.60 |

| | | | | | | | |
|----|----|----------|----------|----|------|------|------|
| 30 | 31 | 0.006067 | 0.005996 | 19 | 0.50 | 0.15 | 0.07 |
| 31 | 32 | 0.001933 | 0.002253 | 20 | 0.50 | 0.21 | 0.10 |
| 32 | 33 | 0.002123 | 0.003301 | 21 | 0.10 | 0.06 | 0.04 |
| 8 | 34 | 0.012453 | 0.012453 | 24 | 0.50 | 0.00 | 0.00 |
| 9 | 35 | 0.012453 | 0.012453 | 26 | 0.50 | 0.00 | 0.00 |
| 12 | 36 | 0.012453 | 0.012453 | 30 | 0.50 | 0.00 | 0.00 |
| 18 | 37 | 0.003113 | 0.003113 | 37 | 0.50 | 0.00 | 0.00 |
| 25 | 38 | 0.003113 | 0.002513 | 10 | 0.10 | 0.00 | 0.00 |

F = From bus, T = To bus, L = line number, S_L = Line apparent power limit in p.u., P = Real power load in p.u., Q = Reactive power load in p.u.

location

Step 8: Check the voltage limits and VSL at all the buses, and line capacity limit for all the lines for each of the size-pf-location pairs.

Step 9: Accept the pairs for next generation of population for which NVLVB=NLCVLV =0 (and NVSLVB =0 when VSL constraint is considered). If population is zero go to step 4

Step 10: Obtain the size-pf-location (k) pair for minimum power loss ($P_L(k)$).

Step 11: Use the available population of size-pf-location pair (parent population) for cross over and mutation for obtaining new generation (offspring) of population.

Step 12: Use the newly generated population size i.e. offspring and parents as new generation.

Step 13: $k = k+1$ and go to step 6

Step 14: size-pf-location (kr) = size-pf-location (k) and $P_L(kr) = P_L(k)$.

Step 15 : $kr = kr+1$ go to 5

Step 16: The size, pf, and location corresponding to minimum loss out of number of runs is the optimum size-pf-location pair. For optimum size, pf, and location run the power flow and obtain all the relevant quantities such as P_{DG} , Q_{DG} , P_L , Q_L ,

S_{intake} , P_{intake} , Q_{intake} , S_{sys} , PLI, QLI, VPI, LCI,

Step 17: go to step 2 till all load models are selected.

Step 18: stop

IX. REFERENCES

- [1] Ackermann T., Andersson G., Soder L., "Distributed generation: a definition," *Electric Power Systems Research*, vol. 57, no. 3 pp. 195– 204, April 2001.
- [2] IEA, Distributed Generation in Liberalized Electricity Markets. Paris, France: OECD, 2002.
- [3] El-Khattam W., and Salma M. M. A., "Distributed Generation Technologies, Definitions and Benefits," *Electric Power System Research* vol. 71, no. 2, pp. 119-128, Oct. 2004.
- [4] Pepermans G., Driesen J., Haeseldonckx D., Belmans R., D'haeseleer W., "Distributed generation: definition, benefits and issues," *Energy Policy*, vol. 33 pp. 787–798., 2005.
- [5] Payyala SL, Green TC. An estimation of economic benefit values of DG, IEEE power engineering society general meeting, Tampa, USA; June, 2007. pp. 1–8.
- [6] IEEE Task Force on Load Representation for Dynamic Performance, "Load representation for dynamic performance analysis," *IEEE Trans. Power Syst.*, vol. 8, no. 2, pp. 472–482, May 1993.
- [7] IEEE Task Force on Load Representation for Dynamic Performance, "Bibliography on load models for power flow and dynamic performance simulation," *IEEE Trans. Power Syst.*, vol. 10, no. 1, pp. 523–538, Feb. 1995.
- [8] Qian Kejun, Zhou Chengke, Allan Malcolm, and Yuan Yue, "Effect of load models on assessment of energy losses in distributed generation planning," *Int J. Electrical power and Energy Systems*, 33, pp 1243-1250, 2011.
- [9] Hung D. Q., Mithulanthan N., and Bansal R. C., "Analytical expression for DG allocation in primary distribution network," *IEEE Trans. Energy Convers.*, vol. 25, no. 3, pp. 814-820, Sept. 2010.
- [10] Dent C. J., Ochoa L. F., and Harrison G. P., "Network distributed generation capacity analysis using OPF with voltage step constraints," *IEEE Trans. Power Syst.*, vol. 25, no. 1 pp. 296-304, Feb. 2010.
- [11] Gozel T., Hocaoglu M. H., Eminoglu U., and Balikci A., "Optimal placement and sizing of distributed generation on radial feeder with different static load models," in *Proc. Int. Conf. Future Power Systems*, pp. 1–6, Nov. 2005.
- [12] Singh Devender, Mishra R. K., and Singh Deependra, "Effect of

1st National Power & Energy System Conference (NPESC), April 25-26, 2014, KNIT Sultanpur

- Load Model in Distributed Generation Planning," *IEEE Trans. Power Syst.*, vol. 22, no. 4, pp. 2204–2212, Nov.. 2007.
- [13] Singh Deependra, Singh Devender, and Verma K. S., "Multiobjective Optimization for DG Planning with Load Models," *IEEE Trans. Power System*, vol. 24, no. 1, pp. 427-436, Feb. 2009 .
- [14] Zhu D., Broadwater R. P., Tam K. S., Seguin R, and Asgeirsson H., "Impact of DG placement on reliability and efficiency with time-varying loads," *IEEE Trans. Power Syst.*, vol. 21, no. 1 pp. 419-427, Feb. 2006.
- [15] Ochoa L. F., Feltrin A. Padilha, and Harrison G. P., "Time-series based maximization of distributed wind power generation integration," *IEEE Trans. Energy Conv.*, vol. 23, no. 3, pp. 968–974, Sep. 2008.
- [16] Atwa Y.M., El-Saadany E.F., Salama M.M.A., and Seethapathi R, "Optimal renewable resources mix for distribution system energy loss minimization," *IEEE Trans. Power Syst.*, vol. 25, no. 1 pp. 360-370, Feb. 2010.
- [17] El-Khattam W., Hegazy Y.G., and Salama M.M.A..., "An integrated distributed generation optimization model for distribution system planning," *IEEE Trans., Power System*, vol 20, no. 2, pp.1158-1165, May 2005.
- [18] Vovos P.N., Harrison G.P., Wallace A.R., Bialek J.W., "Optimal power flow as a tool for fault level-constrained network capacity analysis," *IEEE Trans. Power Syst.*, vol. 20, no.2, pp. 734–74 1, May, 2005.
- [19] Vovos P. N. and Bialek J. W., "Direct incorporation of fault level constraints in optimal power flow as a tool for network capacity analysis," *IEEE Trans. Power Syst.*, vol. 20, no. 4, pp. 2125–2134, Nov. 2005.
- [20] Harrison G. P., Piccolo A., Siano P., and Wallace A. R., "Hybrid GA and OPF evaluation of network capacity for distributed generation Connections," *Elect. Power Syst. Res.*, vol. 78, no. 3, pp. 392–398, Mar. 2008.
- [21] Algarni Ayed A. S. and Bhattacharya Kankar, "Disco operation considering DG units and their goodness factors", *IEEE Trans. Power System*, vol. 24, no. 4, pp.1831-1840, Nov. 2009.
- [22] Kumar Vishal, Kumar H. C. Rohith, Gupta Indra, and Gupta Hari Om, "DG Integrated approach for service restoration under cold load pickup," *IEEE Trans. Power Del.*, vol. 25, no. 1, pp. 398-406, Jan. 2010
- [23] Kumar A., and Gao W., "Optimal distributed generation location using mixed integer non-linear programming in electricity markets," *IET Gen. Trans. & Distrib.* Vol 4, no. 2, PP. 28 1-298, 2010.
- [24] Payasi R. P., Singh Asheesh K., and Singh Devender, "Review of Distributed Generation Planning: Objectives, Constraints and Algorithms," *Int. Journ. of Sc., Engg, and Technology*, Vol. 3, No. 3, pp. 133-153, July 2011.
- [25] Goldberg D. E., *Genetic Algorithms in Search, Optimization & Machine Learning*. Reading, MA: Addison Wesley, 1989.
- [26] Beasley, Bull D.R., and Martin R.R., "An overview of genetic algorithms: Part 1, fundamentals," *University Computing*, 15(2):58{69, 1993.
- [27] Silvestri A., Berizzi A., and Buonanno S., "Distributed generation planning using genetic algorithms," in Proc. IEEE Power Tech, 1999, p.257.
- [28] Kim K. H., Lee Y. J., and Rhee S. B., "Dispersed generator placement using fuzzy-GA in distribution systems", Proc. IEEE Power Engineering Society Summer Meeting, Chicago, USA,21–25 July 2002, pp. 1148– 1153
- [29] Singh Deependra., Singh Devender, and Verma K. S., "GA based energy loss minimization approach for optimal sizing and placement of distributed generation," *Int. J. Knowledge-Based and Eng. Intell. Syst.*, vol. 12, no. 2, pp.147–159, 2008.
- [30] Singh R.K., and Goswami S.K., "Optimum siting and sizing of distributed generations in radial and networked systems," *Electric Power Components and Systems*, vol 37, 127–145, 2009.

Direct Torque Controlled Permanent Magnet Synchronous Motor Drive: A Review

A. H.K.Singh, *Student Member, IEEE* B. S.M.Tripathi, *Member IEEE*, and C. R.P.Payasi, *Member IEEE*

Abstract--In this paper, an attempt has been made to a review on Direct Torque Controlled Permanent magnet Synchronous Motor (DTC-PMSM) Drive. In this paper an overview is given. It also reviews various controlled methodologies of AC drives. The basic principles of DTC for PMSMs are explained. Topologies and algorithms are described in the literature for surface mounted PMSMs. As a result of this review, it is observed that the increase of the electromagnetic torque is directly proportional to the increase of the angle between the stator and rotor magnetic flux linkages. The main focus of this paper is to give an outline of what is already done for DTC-PMSM Drive and to determine the points for further work.

Index Terms--Direct torque control, Permanent magnet synchronous motor, Speed control

I. INTRODUCTION

DIRECT Torque Control was introduced in the 1980's for Induction Motors as a new approach for torque and flux control. Direct Torque Control (DTC) directly controls the inverter states based on the errors between the reference and estimated values of torque and flux. It selects one of six voltage vectors generated by a Voltage Source Inverter to keep torque and flux within the limits of two hysteresis bands. [8]The torque of the Permanent Magnet Synchronous Motor (PMSM) is controlled by inspecting the armature current since electromagnetic torque is proportional to the armature current. For high dynamic performance, the current control is applied on rotor flux (*dq*) reference system that is rotated at synchronous speed. In this system, if the change of the back electromotor force (emf) and the inductance are

A. H.K.Singh, Department of Electrical Engineering, Kamla Nehru Institute of Technology, Sultanpur-228118, India (e-mail: hitu244001@yahoo.com).

B. S.M.Tripathi, Department of Electrical Engineering, Kamla Nehru Institute of Technology, Sultanpur-228118, India (e-mail: mani_excel@yahoo.co.in)

C. R.P.Payasi, Department of Electrical Engineering, Kamla Nehru Institute of Technology, Sultanpur-228118, India (e-mail: payasirp@rediffmail.com)

D. Babita Raj,Department of Electrical Engineering, RK. University, Rajkot-360001 (Gujrat) India (e-mail: babita.raj@rku.ac.in).

sinusoidal, armature circuit inductance and magnet magnetic flux are constant. [12-14] The main principle of DTC is to select the appropriate voltage vectors according to the stator magnetic flux, difference between the reference and real torque. The current control circuit that is constituted with the pulse width modulation (PWM) comparator circuit is not used in DTC. Therefore, if the DTC method is compared to PWM current control, it yields advantages such as; less parameter dependence and fast torque response. If the initial position of the rotor is known, it is possible to work with DTC without sensors. [19-21].

II. MATHEMATICAL MODEL OF PERMANENT MAGNET SYNCHRONOUS MOTOR^[9, 23]

Permanent magnet (PM) synchronous motors are widely used in high-performance drives such as industrial robots and machine tools because of their well-known advantages as: high power density, high-torque/inertia ratio, and free maintenance. In recent years, the magnetic and thermal capabilities of the PM have been considerably increased by employing the high-coercive PM materials. Permanent Magnet Synchronous Motor is an AC motor that has windings in the stator slots. The flux generated by stator currents is almost sinusoidal. Therefore, the same control methods used for the induction motors can also be used for the permanent magnet synchronous motors. These controls are; V/f control, field oriented control, and direct torque control. The stator of the PMSM and the Wound Rotor Synchronous Motor (SM) are similar. In addition there is no difference between the back emf produced by a permanent magnet and that produced by an excited coil.

Hence the mathematical model of a PMSM is similar to that of the wound rotor SM. The equivalent circuit model of PMSM in the rotor reference frame is shown in Fig.1. The voltage and flux equations for a PMSM in the rotor oriented coordinates d-q can be expressed as:

$$v_{sd} = R_s j_{sd} + \frac{d\psi_{sd}}{dt} - P\omega_m \psi_{sq} \quad (1)$$

$$v_{sq} = R_s i_{sq} + \frac{d\psi_{sq}}{dt} + P\omega_m \psi_{sd}$$
(2)

Where

$$\psi_{sd} = L_d i_{sd} + \psi_{pm}$$

$$\psi_{sq} = L_q i_{sq}$$

and the electromagnetic torque equation is

$$T_e = \frac{3}{2} P(\psi_{sd} i_{sq} - \psi_{sq} i_{sd})$$
(5)

$$T_e = \frac{3}{2} P(\psi_{PM} i_{sq} - (L_d - L_q) i_{sd} i_{sq})$$
(6)

Where,

P is the number of pole pairs,

R_s is the stator winding resistance,

ω_m is the angular frequency,

v_{sd} , v_{sq} and i_{sd} , i_{sq} are d , q components of the stator winding voltage and current,

ψ_{sd} , ψ_{sq} are d , q components of the stator flux linkage,

L_d , L_q are d and q axis inductances,

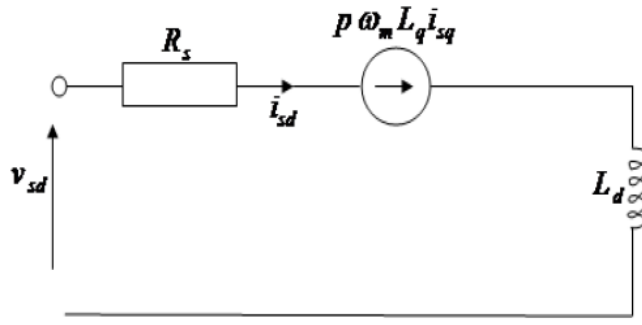
and ψ_{PM} is the PM rotor flux linkage.

Finally, the motion equation is expressed as:

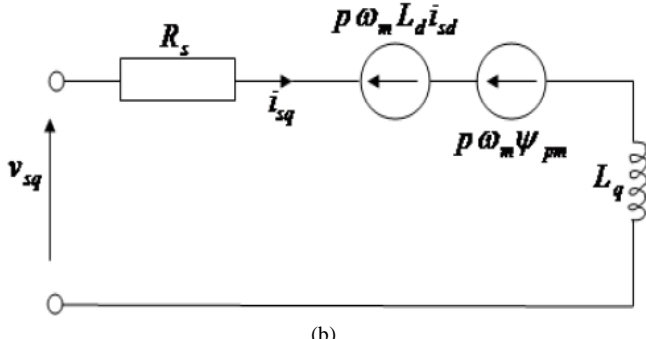
$$\frac{d\omega_m}{dt} = \frac{1}{J}(m_e - m_L - d\omega_m)$$
(7)

where

J is moment of inertia, m_L is motor load and d is damping constant.



(a)



(b)

Fig. 1: Equivalent circuit model of PMSM in the rotor reference frame. (a) Rotor d-axis equivalent circuit (b) Rotor q-axis equivalent circuit

From the vector diagram of Fig.1 and (3) & (4), the following relation is obtaining as

$$m_e = \frac{3}{2} p \frac{\psi_{s_ref}}{L_d L_q} [\psi_{PM} L_q \sin \delta +$$
(8)

$$+ \frac{1}{2} \psi_{s_ref} (L_d - L_q) \sin 2\delta]$$

From (8) it can be see that for constant stator flux amplitude and flux produced by permanent magnet, the electromagnetic torque can be changed by control of the torque angle. This is the angle between the stator and rotor flux linkage, when the stator resistance is neglected. The torque angel δ , in turn, can be changed by changing position of the stator flux vector in respect to PM vector using the actual voltage vector supplied by PWM inverter. In the steady state, δ is constant and corresponds to a load torque, whereas stator and rotor flux rotate at synchronous speed. In transient operation, δ varies and the stator and rotor flux rotate at different speeds (Fig.2).

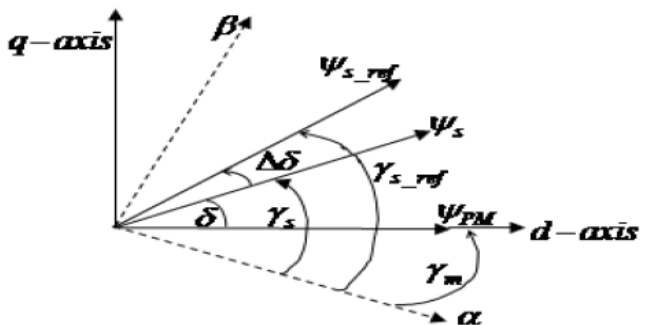


Fig. 2: Vector diagram of illustrating torque control conditions

Based on above equations the block scheme of the PMSM machine can be creates. Where the input signals are the voltage components in d , q reference frame v_{sd} , v_{sq} and the output signal is the mechanical speed of the rotor ω_m . As the external load torque m_L is disturbance.

III. DIRECT TORQUE CONTROL SYSTEM [21]

In most control systems as in Field Oriented Control, the control algorithm calculates a control signal whose amplitude depends on the difference between desired and actual value. This control signal can assume any value in a given interval. In Direct Torque Control the control algorithm chose a control signal that increases the quantity in question if actual value is lower than desired and vice versa. Whether the difference is big or small the same control signal is chosen. There are three signals which affect the control action in a DTC system; torque, flux linkage and the angle of the resultant flux linkage vector. One revolution is divided into six sectors. In each sector the DTC chose between 4 voltage vectors. Both flux and torque errors are compared in 2-level hysteresis comparators. Two of the vectors increase and the other two decrease torque. Another pair of vectors increase and decrease

flux. For each combination of the torque and flux hysteresis comparator states there is only one of the four voltage vectors which at the same time compensate torque and flux as desired. Fig.3 shows the block diagram of the DTC.

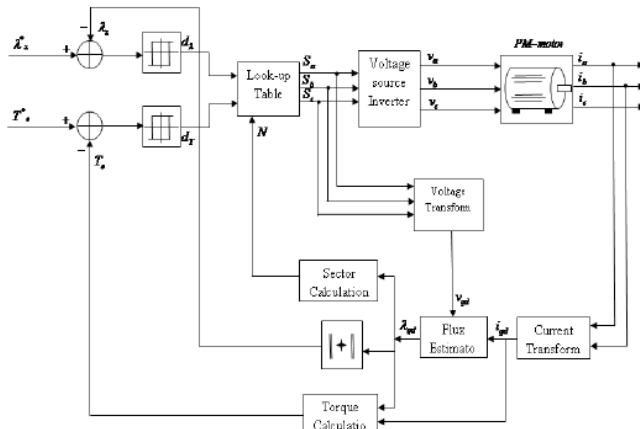


Fig. 3: The different blocks in a DTC system

IV. CONTROL TECHNIQUE

Permanent Magnet Synchronous Motor is an AC motor, which has windings in the stator slots. The flux generated by stator current is almost sinusoidal. Therefore the same control methods used for the induction motor can also be used for the PMSM [13, 20]. The main principle of DTC is to select the appropriate voltage vectors according to the stator magnetic flux, difference between the reference and real torque [19]. The control techniques are-V/F control, Field oriented control and direct torque control.

The choice of Direct Torque Control gives the advantages such as faster torque control, high torque at low level speed and high speed sensitivity [8, 12, 13, 20, 21]. The DTC technique is different from the conventional vector control method, where torque is controlled in the rotor references via current control loops. Over the advantages of DTC, some disadvantages are variable switching frequency, current and torque distortion caused by sector changes [9]. The Direct Torque control technique is also used for multiphase motor drive. This scheme is used in some application with multi-level inverters such as three-level or five-level inverter [11, 12, 18]. In case of PMSM DTC both the stator voltage and rotor magnetic flux determine together the stator magnetic flux linkage [12]. In the DTC scheme, the electromechanical torque is delivered at the shaft of the motor and should kept close to its reference torque by maintaining it between the lower and upper limits of torque i.e. minimum and maximum limits. To avoid the motor saturation, the magnitude of the stator flux should be kept between the minimum and maximum band of limits [12, 19].

V. SELECTION OF INVERTER TOPOLOGY [9, 11-14, 17-19]

Among the different types of the inverter topologies, a voltage source inverter is generally used in Direct Torque Control scheme for AC motor drives such as induction motors drives, permanent magnet synchronous motors drives [1-3]. A voltage source inverter is used for the selection of voltage vector switching from a six space vectors of voltage matrix.

The main control objective related to the inverter operation consists in minimizing the average switching frequency (or switching losses) on the inverter legs [19]. For constant flux operation region, the reference value of stator flux amplitude is equal to the flux amplitude produced by the permanent magnet [9].

VI. STATOR FLUX CONTROL

Direct stator flux linkage control is used for Permanent Magnet Synchronous Motors drives in Direct Torque Control scheme [8, 12-14, 17-21]. A pulse width modulator is used to generate an increment of stator flux linkage. This scheme controls the load angle and amplitude of the stator flux linkage. The reference value for the load angle can be calculated from the torque reference [14].

VII. VOLTAGE SPACE VECTOR GENERATION AND SELECTION

Main working of Direct Torque Control is to determine the correct voltage vectors using the appropriate switching table. The determination process is based on the torque and stator magnetic flux hysteresis control [8, 20]. Voltage space vector table has six and eight voltage vectors switching strategies. In each region flux is increasing or decreasing functions of time. In most of the previous work a six voltage vector scheme is used. The use of six voltage vectors switching table implies that the stator flux linkage is always kept in motion [17]. The circular stator flux vector trajectory can be divided into six symmetrical sectors (according to the nonzero voltage vectors), which are defined as:

| | |
|----------|---------------------------------------|
| Sector 1 | $-30^\circ \leq \gamma_s < 30^\circ$ |
| Sector 2 | $30^\circ < \gamma_s \leq 90^\circ$ |
| Sector 3 | $90^\circ < \gamma_s \leq 150^\circ$ |
| Sector 4 | $150^\circ < \gamma_s \leq 210^\circ$ |
| Sector 5 | $210^\circ < \gamma_s \leq 270^\circ$ |
| Sector 6 | $270^\circ < \gamma_s < -30^\circ$ |

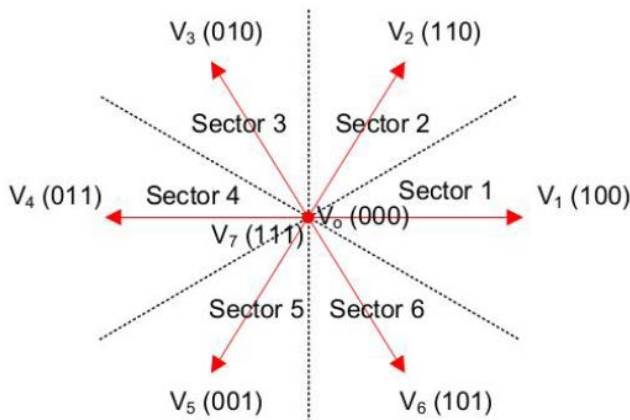


Fig. 4: Sector definitions for DTC

In each region, two adjacent voltage vectors, which give the minimum switching frequency, may be selected to increase or decrease the amplitude of stator flux and electromagnetic torque.

When stator flux vector is located in first sector Ψ_s and rotates clockwise in order to increase the torque ($d_{Me}=1$) the vectors V_2 , V_3 can be used. In order to reduce torque the opposite two vectors are used.

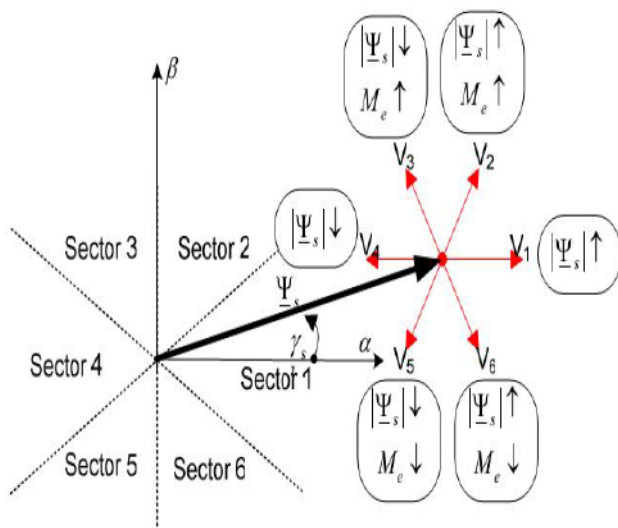


Fig. 5: Voltage vector effects in sector 1 on stator flux and torque.

The presented rule for first sector can be extended for other sectors.

VIII. POWER QUALITY ASPECTS^[15]

In Direct Torque Control scheme, electrical power conversion is performed by converting the AC mains voltage to a DC voltage using an AC-DC power converter. The resulting DC voltage is converted in to a variable frequency; variable voltage AC by voltage source inverter to feeds the PMSM. For low power range of less than 2kW, a very little effort is made on AC-DC converters for the VSI fed PMSM drive system. In this conversion the input AC supply current is drawn in narrow

pulses. This narrow pulses current causes power quality problems to nearby customers. The main power quality problems during DTC are as following-

- High value of total harmonic distortion of supply current.
- High total harmonic distortion (THD) of input supply voltage.
- Low value of power factor and displacement factor and poor distortion factor.

The problem becomes more serious when several drive units are connected to a single-phase power supply. To get out from these problems an AC-DC Zeta converter topology is used for providing regulated DC voltage to feed the voltage source inverter employed in the DTCPMSM drive.

IX. SOME COMMON CONTROL SCHEMES FOR PMSM DRIVE^[4-5, 7]

PMSM control techniques can be divided in to scalar and vector control. Scalar control is based on relationships valid in steady-state. Amplitude and frequency of the controlled variables are considered. In vector control amplitude and position of a controlled space vector is considered. These relationships are valid even during transients which is essential for precise torque and speed control.

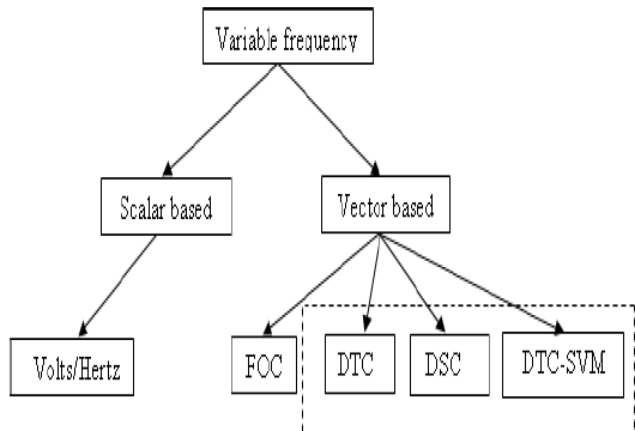


Fig. 6: Some common control techniques used for PMSM. Control methods in the dashed box belong to the DTC family.

X. CONCLUSION

This paper has dealt with the Direct Torque Control and one of its improved variants proposed in the research literature. Vector control was introduced in 1972 by F. Blaschke which was the technique since known as Field Oriented Control. In vector control both amplitude and position of the field flux is known, so the controller can control the armature flux amplitude and angle relative the field flux. In a DC motor the field flux, which in this case is the stator flux, and the armature flux (rotor) are held orthogonal mechanically by the

commutator. When the fields are orthogonal, armature flux does not affect the field flux and the motor torque responds immediately to a change in armature flux or equivalently, armature current. In an AC motor the field flux (which now is in the rotor) rotates, but in a FOC the controller rotates the armature (stator) flux so that armature and field flux are kept orthogonal, and hence, the motor-controller system behaves as a DC motor system. The decreased performance of DTC drives in terms of torque, flux and current ripple, with respect to FOC, is partly compensated for by its simplicity since this allows for higher sample frequencies. The problem is that the inverter sets an upper limit for its switching frequency. Since the introduction of DTC a lot of research has been done to improve performance of DTC drives while maintaining the good properties, such as

- Low complexity
- Good dynamic response
- High robustness.

The main drawback of the DTC is its relatively high torque and flux ripple. In this paper one of the many improved DTC systems proposed is presented.

XI. FUTURE WORK

The influence of saturation and parameter-estimation errors on the performance of DTC for PMSMs, especially on model based estimators and controllers have to be investigated. A focus on sensor less controllers and estimators is intended. Sensor less position estimation also has applications other than DTC PMSM. Digital implementation of DTC PMSM and associated discrete modeling of PMSM, together with new DTC schemes offers many opportunities for more research. In conjunction with the research on DTC schemes, research into the most appropriate switching strategies has to be undertaken.

XII. REFERENCES

- [1]. Rashid, Mohammad H., "Power Electronics", Prentice Hall of India Pvt. Ltd, New Delhi, 2005.
- [2]. Bose, B. K., "Modern power electronics and ac drives", Prentice Hall PTR, 2002.
- [3]. Bimbhra, Dr. P. S, "Power Electronics", Khanna publishers, New Delhi, 2006.
- [4]. Bimbhra, Dr. P. S, "Electrical Machinery", Khanna publishers, New Delhi, 2008.
- [5]. P. C. Sen, "Principle of electric machines and power electronics", John Wiley and sons, 1989.
- [6]. Dubey, G. K., "Fundamental of electric drives", Narosa publishing house, New-Delhi, 2009.
- [7]. R. Krishnan, "Electric motor drives, modelling, analysis, and control", PHI Inc, 2003.

- [8]. Selin Ozcira, Nur Bekiroglu, Engin Aycicek, "Simulation of Direct Torque Controlled Permanent Magnet Synchronous Motor drive" Technical University Dept. of Electrical Engineering, 34349 Besiktas, Istanbul, Turkey, 2000.
- [9]. Dariusz Swierczynski, Marian P.Kazmierkowski, "Direct Torque Controlled Permanent Magnet Synchronous Motor (PMSM) Using Space Vector Modulation (DTC-SVM) Simulation and Experimental Results" IEEE, 2002.
- [10]. Haque, Lixin Tang, Limin Zhong, "Problems Associated With The Direct Torque Control of an Interior Permanent-Magnet Synchronous Motor Drive and Their Remedies" Industrial Electronics, IEEE vol:51,Issue:4, 02 August 2004.
- [11]. Xavier Kestelyn, Eric Semail and Dominique Loriot, " Direct Torque Control of a Multi-Phase Permanent Magnet Synchronous Motor Drive: Application to a Five-Phase One" IEEE, 2005.
- [12]. K. E. B. Quindere, E. Ruppert, Milton E. De Oliveira, "Direct Torque Control of Permanent Magnet Synchronous Motor Drive With a Three- Level Inverter" Dept of system and energy control, CP 6101, CEP 13083-970, Brazil, 2005.
- [13]. Zhuqiang Lu, Honggang Sheng, Herbert L. Hess, Kevin M. Buck, "The Modeling and Simulation of a Permanent Magnet Synchronous Motor with Direct Torque Control Based on Matlab/Simulink" IEEE, 2005.
- [14]. Thomas J. Vyncke, Ren K. Boel and Jan A. A. Melkebeek, "Direct Torque Control of Permanent Magnet Synchronous Motors – An Overview" IEEE, GHENT, Belgium, April 2006.
- [15]. Bhim Singh, B. P. Singh and Sanjeet Dwivedi "ACDC Zeta converter for Power Quality Improvement in Direct Torque Controlled PMSM Drive", Journal of Power Electronics, vol.6,No.2, April 2006.
- [16]. Marek Stulrajter, Valeria Hrabovcova, Marek Franko, "Permanent magnet synchronous motor control theory" Journal of electrical engineering, vol.58, no.2,79–84, 2007.
- [17]. Mohamed Kadjoudj, Soufiane Taibi, Noureddine Golea, Hachemi Benbouzid, "Modified Direct Torque Control of Permanent Magnet Synchronous Motor Drives" IJ-STA, vol.1,no.2, pp.167–180, December 2007.
- [18]. M. N. Abdul Kadir, Saad Mekhilef, HewWooi Ping, "Direct Torque Control of Permanent Magnet Synchronous Motor Drive with Asymmetrical Multilevel Inverter Supply" The 7th International Conference on Power Electronics, October 22- 26,2007/ EXCO, IEEE, Daegu, Korea, 2008.
- [19]. Tobias Geyer, Giovanni A. Beccuti, Georgios Papafotiou, and Manfred Morari, "Model Predictive Direct Torque Control of Permanent Magnet Synchronous Motor", IEEE, 2010.
- [20]. D. Siva Krishna, C. Srinivasa Rao, "Speed Control of Permanent Magnet Synchronous Motor Based on Direct torque Control Method" International Journal of Advances in Science and Technology, vol.2, no.3, 2011.
- [21]. Nitin Kelkar, V. A. Joshi, "Direct Torque Control of Permanent Magnet Synchronous Motor" International Journal of Scientific & Engineering Research , vol.3, Issue 8, August-2012.
- [22]. M. S. Merzoug, and F. Naceri, "Comparison of Field- Oriented Control and Direct Torque Control for Permanent Magnet Synchronous Motor (PMSM)", World Academy of Science, Engineering and Technology, vol.21. Sep.22, 2008.
- [23]. Dariusz Swierczynski, "Direct Torque Control with Space Vector Modulation (DTC-SVM) of Inverter- Fed Permanent Magnet Synchronous Motor Drive", Ph.D. Thesis, Warsaw, Poland – 2005

A Survey on Impact of DGs and FACTS Controllers on Power Systems

Bindeshwar Singh,*Member, IEEE*, Vivekanand Mukherjee, *IEEE*, and Praphakar Tiwari,*Member, IEEE*

Abstract: This paper presents a critical survey on impact assessment of optimally placed and coordinated control of Distributed Generations (DGs) and Flexible Alternating Current Transmission Systems (FACTS) controllers in power systems for the different performance parameters of power systems viewpoint such as minimize the active power losses and cost of system, improve the voltage profile, increase the load ability of systems, increase available power transfer capacity of system, enhance power system stability, reduce power system oscillations, improve environmental conditions, and provide the reactive power support in emergency case such fault occur or suddenly change in field excitation of alternators, or suddenly load increased in power systems. In this paper also presents a survey on the computational artificial intelligent techniques for optimally placement and coordinated control of DGs and FACTS controllers in power systems for enhancement of power system performance parameters. Authors strongly believe that this survey article will be very much useful to the researchers, scientific engineers, industrial persons for finding out the relevant references in the field of impact assessment of optimally placed and coordinated control of DGs and FACTS controllers in power systems for the different performance parameters of power systems viewpoint enhancement.

Index Terms:-DGs, FACTS Controllers, Optimal Load Flow (OPF), Artificial Computational Intelligent Techniques, Optimal placement, Coordinated control, Power System Performance Parameters, Power Systems.

NOMENCLATURE

| | |
|-----------|--|
| DGs | Distributed Generations |
| FACTS | Flexible Alternating Current Transmission System |
| TCSC | Thyristor Controlled Series Capacitor |
| SVC | Static Var Capacitor |
| SSSC | Sub Synchronous Series Compensator |
| STATCOM | Static Compensator |
| D-STATCOM | Distributed Static Compensator |
| IPFC | Inter-link Power Flow Controller |
| UPFC | Unified Power Flow Controller |
| HPFC | Hybrid Power Flow Controller |
| PQ | Power Quality |
| VP | Voltage Profile |
| APTC | Available Power Transfer Capacity |
| WT | Wind Turbine |
| MT | Micro-Turbine |
| SSS | Steady State Stability |
| TS | Transient Stability |
| PSS | Power System Stability |

I. INTRODUCTION

DISTRIBUTED generation aims to generate part of required electrical energy on small scale closer to the places of consumptions. According to [1] two major driving forces that created renewed interest in DGs are electrically market liberalization, and environmental concerns. The other driving forces are: standby capacity or peak use capacity, reliability and PQ, alternative to expansion, grid support, combined generation of heat, electricity, ancillary of services of DGs, and efficient use of cheap fuel opportunities.

In the current context of high fluctuation in energy prices, concerns over fossil fuel depletion and increased awareness of greenhouse gas emission, the European Union sees energy efficiency as a major challenge for the years to come. In its communication, the Commission of the European communities (2006) estimates that the European Union can save up to 20% of its energy consumption over the period 2007- 2020. In several countries such as the United Kingdom, a wide range of possibilities are currently explored including DG.

DGs are one of the new trends in power systems used to support the increased energy-demand. There is not a common accepted definition of DG as the concept involves many technologies and applications. Different countries use different notations like “embedded generation”, “dispersed generation” or “decentralized generation” or “distributed energy resources”.

“DG is an electric power source connected directly to the distribution network or on the customer site of the meter”. (Ackermann et al., 2001) [2].

“Dondi et al. (2002) [3], define DG as a generator with small capacity close to its load that is not part of a centralized generation system”.

“Pepermans et al. (2005) [4], the definition varies significantly in terms of characteristics of the generators mentioned”.

“The Government’s Energy Review Report of July 2006 highlighted the challenges we face in addressing climate change and ensuring security of energy supplies. A key part of responding to this challenge is to investigate to what extent DG could complement, or in the longer term potentially offer an alternative to, a centralized system.” (Ofgem, 2007)[5].

Although it is now over a decade since DGs became a significant and topical phenomenon in power systems, there is

as yet no universal agreement on the definition of DGs, which is also known as embedded generation or distributed generation. Current definitions of DGs are very diverse and range from 1 kWpV installations, 1MWengine generators to 1000MW offshore wind farms. The various examples of DGs technologies include the following as follows [6]:

- Photovoltaic or Solar Systems
- Wind Turbines Systems
- Fuel Cells System
- Small Micro-Sized Turbines
- Wave Energy Systems
- Tidal Energy Systems
- Sea or Ocean Energy Systems
- Bio-Gas Systems
- Diesel Engine Systems
- Geo-Thermal Energy Systems
- Gas Engine Systems
- Sterling Engine Based Generators
- Internal Combustion Engine Generators

The open literature review has strongly pronounced the need of integration to technical as well as economical benefits of the system with FACTS controllers and DG integration to the power system. The impact of DGs and FACTS controllers on power systems are enhancement of various power system parameters such as flexibility of operation of system, minimize the real and reactive power losses, improve voltage profile of system, increase the available power transfer capability of system, improve the power system oscillations, increase the loadability of system, increase the reactive power support in the system, elimination of power quality problems, enhance the power system stability, provide the greenhouse environments, increase the system reliability, and increase the efficiency of system.

(a) Concepts of Optimal Placement of DGs and FACTS Controllers

The optimally placed of DGs and FACTS controllers in power system networks are very important issues. Since all the power system performance parameters such as real power losses, reactive power support, voltage profile, power system oscillations, available power transfer capacity, loadability, and environmental friendless, etc. are achieved better when DGs and FACTS controllers are optimally placed in power system networks. So that all DGs and FACTS controllers are optimally placed in power system network are very important issues.

(b) Concepts of Coordinated Control of DGs and FACTS Controllers

The drive towards distributed systems may result in simultaneous installation of DGs and FACTS controllers in power systems. These DGs and FACTS controllers have the potential to interact with each other. This interaction may either deteriorate or enhance system stability depending upon the chosen controls and placement of DGs and FACTS controllers. Hence there is a need to study the interaction between the DGs and FACTS controllers.

The various interactions can potentially occur between the DGs and FACTS controllers, as well as, between multiple FACTS controllers in power system environments. These likely interactions have been classified into different frequency ranges and various interaction problems between DGs and FACTS controllers or between multiple FACTS controllers from voltage stability/ small signal stability viewpoint are presented in [7].

The implementation of more than one FACTS controller or multi-function FACTS controller in DGs may lead to adverse interactions. These interactions can occur in the following combinations [7]:

- Multiple FACTS controllers of a similar kind with DGs
- Multiple FACTS controllers of diverse kind with DGs
- Multiple FACTS controllers and HVDC controllers with DGs

These different control interactions have been classified into five frequency ranges [8]:

| S.No. | Frequency range | Type of Interactions between DGs and FACTS controllers |
|-------|-----------------|--|
| 1 | 0 Hz | Steady-State Interactions |
| 2 | 0-3 or 5 Hz | Electro-Mechanical Oscillations |
| 3 | 2-15 Hz | Small-Signal or Control Oscillations |
| 4 | 10-50/60 Hz | Sub-Synchronous Resonance Interactions |
| 5 | >15 Hz | Electro-Magnetic Transients, High Frequency Resonance or Harmonic Resonance Interactions, and Network Resonance Interactions |

In practical installation and integration of DGs in power systems with consideration of FACTS controllers, these are five common requirements as follows [7]:

- What kinds of DGs and FACTS controllers should be installed in power systems?
- Where in the system it should be placed?
- How to estimate economically the number, optimal size of DGs and FACTS controllers to be installed in a practical power system networks?
- How to coordinate dynamically the interaction between multiple DGs , FACTS controllers and the network to better exploit the DGs and FACTS controllers to improve the index power quality?
- How to review and adjust the system protection devices to assure service continuity and keep the index power quality at the margin security limits?

A study by the *Electric Power Research Institute* (EPRI) indicates that by 2010, 25% of the new generation will be distributed; a study by the *Natural Gas Foundation* concluded that this figure could be as high as 30% [9]. The *European Renewable Energy Study* (TERES), commissioned by the *European Union* (EU) to examine the feasibility of EU CO₂-reduction goals and the EU renewable energy targets, found that around 60% of the renewable energy potential that can be utilized until 2010 can be categorized as decentralized power sources [10]. It is predicted that distributed generation may account for up to 25% of all new generation by year 2010 [11]-[12].

(c) Type & Size of DGs

The technical issues related to distributed generation, however, can vary significantly with the rating. Therefore, it is appropriate to introduce categories of distributed generation. We suggest the following distinction for these categories are discussed in table 1 as follows:

Table 1: Type and Size of Distributed Generations

| S.No. | Type | Rating |
|-------|-------------------------------|------------|
| 1 | Micro distributed generation | 1 W-5kW |
| 2 | Small distributed generation | 5kW-5MW |
| 3 | Medium distributed generation | 5 MW-50MW |
| 4 | Large distributed generation | 50MW-300MW |

These are the next generation of power system devices taking advantages of new materials technologies, nanotechnologies, advanced digital designs etc., to produce higher power densities, better reliability, and improved real time diagnostics to greatly improve grid performance. Such technologies include superconducting transmission cable, fault current limiters, composite conductors, FACTS controllers-(SVC, TCSC, TSSC, TCSR, TSSR, TCPAR, SSSC, STATCOM, TCVR, TVR, UPFC, GUPFC, IPFC, GIPFC, HPFC), custom power devices (D-STATCOM, DVR, SSTS), advanced energy storage (SMES, BESS), HVDC devices, distribution generations (wind, solar, micro-turbine etc.), advanced transformers and circuit breakers, and smart loads.

This paper is organized as follows: Section II discusses the definitions of distributed generations. Section III presents the types of distributed generations. Section VI presents the conclusions of the paper.

II. DEFINITIONS OF DGs [13]-[46]

DGs are not a new concept but it is an emerging approach for providing electric power in the heart of the power system. It mainly depends upon the installation and operation of a portfolio of small size, compact, and clean electric power generating units at or near an electrical load (customer). Till

now, not all DGs technologies and types are economic, clean or reliable. Some literature studies delineating the future growth of DGs are:

- The Public Services Electric and Gas Company (PSE&G), New Jersey, started to participate in fuel cells (FCs) and photo-voltaic (PVs) from 1970 and micro-turbines (MTs) from 1995 till now. PSE&G becomes the distributor of Honeywell's 75kW MTs in USA and Canada. Fuel cells are now available in units range 3–250kW size [13].
- The Electric Power Research Institutes (EPRI) study shows that by 2010, DGs will take nearly 25% of the new future electric generation, while a National Gas Foundation study indicated that it would be around 30% [14].
- PV industries and companies expect about one million rooftops equipped by PV modules within the coming decade [15].
- The largest commercial 1MW FC (five 200kW units) installed by the US Postal Service at the Anchorage Mail Processing Center, Alaska and is connected to the utility grid [14].
- In the year 2000, new wind farms of 3000MW capacities were installed [13].

Surveying DG concepts may include DG definitions, technologies, applications, sizes, locations, DG practical and operational limitations, and their impact on system operation and the existing protective devices. This paper focuses on surveying different DG types, technologies, definitions, their operational constraints and operational and economical benefits. Furthermore, we aim to present a critical survey by proposing new DG classifications. In the open literature, a large number of terms and definitions are used in relation to distributed generation in power system networks.

For example, Anglo-American countries often use the term '*embedded generation*', North American countries the term '*dispersed generation*', and in Europe and parts of Asia, the term '*de-centralized generation*' is applied for the same type of generation.

In addition, in regards to the rating of distributed generation power units, the following different definitions are currently used:

- Preston and Rastler define the size as 'ranging from a few kilowatts to over 100 MW' [5];
- The *Electric Power Research Institute* defines distributed generation as generation from 'a few kilo watts up to 50 MW' [6];
- According to the *Gas Research Institute*, distributed generation is 'typically [between] 25 and 25 MW'[7];
- Cardell defines distributed generation as generation 'between 500 kW and 1 MW' [8];

- The *International Conference on Large High Voltage Electric Systems (CIGRE)* defines DG as ‘smaller than 50 –100 MW’ [9];

And because of different government regulations, the definition of the rating of each distributed power station also varies between countries, for example [10]:

- In the English and Welsh market, DG plants with a capacity of less than 100 MW are not centrally dispatched and if the capacity is less than 50 MW, the power output does not have to be traded via the wholesale market [11]. The term distributed generation is, therefore, predominantly used for power units with less than 100 MW capacity;
- Swedish legislation gives special treatment to small generation with a maximum generation capacity of up to 1500 kW, [12]-[14]. Hence, DG in Sweden is often defined as generation with up to 1500 kW. But under Swedish law, a wind farm with one hundred 1500 kW wind turbines is still considered DG, as the rating of each wind energy unit, and not the total wind farm rating, is relevant for the Swedish law. For hydro units, in comparison, it is the total rating of the power station that is relevant. Some of the proposed offshore wind farms for Sweden have a maximum capacity of up to 1000 MW. This would still be considered DG as they plan to use 1500 kW wind turbines [45]-[46].

Due to the large variations in the definitions used in the literature, the following different issues have to be discussed to define distributed generation more precisely as follows:

- The purpose.
- The location.
- The rating of distributed generation.
- The power delivery area.
- The technology.
- The environmental impact.
- The mode of operation.
- The ownership.
- The penetration of distributed generation.

A. Purpose

There is an agreement among different authors and organizations regarding the definition of the purpose of DG.

Definition A1. *The purpose of distributed generation is to provide a source of active electric power.*

According to this definition, distributed generation does not need to be able to provide reactive power.

B. Location

The definition of the location of the distributed generation plants varies among different authors. Most authors define the location of DG at the distribution side of the network, some authors also include the customers’ side, and some even include the transmission side of the network [5]. We think that the following definition is appropriate:

Definition B1. *The location of distributed generation is defined as the installation and operation of electric power generation units connected directly to the distribution network or connected to the network on the customer site of the meter.*

The motivation for using this definition is that the connection of generation units to the transmission network is done traditionally by the industry. The central idea of distributed generation, however, is to locate generation close to the load, hence on the distribution network or on the customer side of the meter.

Having defined distributed generation now as electric power generation at distribution level or below, the definition requires a more detailed distinction between a transmission and a distribution system. A distinction based on voltage levels, e.g. 220 kV and higher is considered as transmission and below as distribution, is not very useful as distribution companies sometimes own and operate 220 kV lines and transmission companies operate 110 kV lines. As the voltage level does not provide any internationally useful distinction between distribution and transmission, another approach is needed. The approach suggested in this paper is based on the legal definition.

Definition B2. *In the context of competitive electricity market regulations, only the legal definition for transmission and distribution systems provides a clear distinction between the two systems [17].*

In a competitive electricity system, the legal regulations define the transmission system, which is usually operated by an independent company that is not involved in power generation, distribution or retail service. In countries without a clear legal definition, however, further discussions will be required. In some countries, e.g. Sweden, also regional networks are included in the legal definitions. These regional networks are located between the nation-wide transmission network and the local distribution networks.

However, usually they are considered to be part of the distribution network system. Based on the above definition, another question arises: What is a small generation unit, e.g. a wind farm or a CHP system, connected to the transmission network? Theoretically, the two following situations can occur:

- A CHP system is located on a large industrial site and the industrial customer is directly connected to the

transmission network. In this case, the CHP system can be described as distributed generation as it is connected on the customer side of the meter;

- a medium-sized wind farm is directly connected to the transmission system, due to the capacity limit of the local distribution network. In this case, the wind farm cannot be described as distributed generation.

C. Rating of distributed generation

The maximum possible rating of the distributed generation source is often used within the definition of distributed generation in the literature (see beginning of Section 2). Our definition, however, does not include any information regarding the rating of the distributed generation source.

Definition C1. *The rating of the DG power source is not relevant for our proposed definition.*

The motivation for this approach is that:

- The rating is ‘not critical to the definition of what constitutes distributed generation’ [5];
- The maximum rating that can be connected to a distribution system depends on the capacity of the distribution system, which is correlated to the voltage level within the distribution system. The technical design of each distribution system is unique, therefore, no general definition of the maximum generation capacity that can be connected to a distribution system can be given.

Taking into account these initial remarks, general data can be provided, of course. According to Klopfer et al. power units with more than 100–150 MW cannot be connected to 110 kV voltage levels, due to technical constraints [17]. As this is in most cases the maximum voltage level owned and operated by distribution companies, the maximum capacity for distributed power stations seems to be in the 100–150 MW range.

In Berlin, however, the local utility BEWAG built a CCGT power station in the centre of the city. The power plant produces both electricity (capacity 300MW) as well as district heat (capacity 300 MW). The power station actually feeds into various 110 and 33 kV distribution lines, owned and operated by BEWAG.

The power as well as the heat is predominantly used locally. Hence, this power station can be considered distributed generation, according to definition DefinitionB1 this case, however, is certainly very special. The above discussion shows that DG can vary between couples of kilowatts to up to ~300 MW.

The technical issues related to distributed generation, however, can vary significantly with the rating. Therefore, it is appropriate to introduce categories of distributed generation.

We suggest the following distinction for these categories in table 2.

Table 2: Type and Size of the DGs

| S.No. | Type | Rating |
|-------|-------------------------------|--------------|
| 1 | Micro distributed generation | ~1 W <5kW |
| 2 | Small distributed generation | 5kW <5MW |
| 3 | Medium distributed generation | 5 MW <50MW |
| 4 | Large distributed generation | 50MW <~300MW |

Some authors define generation between 1 kW and 1 MW as dispersed generation. However, this definition is not used consistently in the literature and should therefore not be applied in this way.

D. Power delivery area

Some authors also define the power delivery area, e.g. all power generated by DG is used within the distribution network. In certain circumstances, defining the power delivery area is not very helpful, as the following example illustrates:

The New Zealand utility *Wairarapa Electricity* operated a 3.5 MW wind farm within its 11/33 kV southern distribution network (the wind farm is now owned by the *Electricity Cooperation of New Zealand*). The produced energy is almost totally used within its own network, however, during nights with very low demand and high wind speeds the wind farm actually exports energy back into the transmission system [18].

A definition of the area of power delivery restricted to the distribution network would disqualify this project as distributed generation, despite the fact that it is a very typical DG project. Furthermore, any restriction of the power delivery areas in the definition of DG would result in complex analyses of the power flow in the distribution network. Therefore:

Definition D1. *The area of the power delivery is not relevant for our proposed definition of DG.*

The term *embedded distributed generations* seems to be more appropriate to describe that the power output of the distributed generation source is only used locally. Unfortunately, the term *embedded* is not used consistently in the literature.

E. Technology

Often the term distributed generation is used in combination with a certain generation technology category, e.g. renewable energy technology. According to our definition, however, the technology that can be used is not limited.

Definition E1. *The technology used for DG is not relevant for the here proposed definition.*

Current praxis also shows that available technology for distributed generation varies widely (seen in Table1). A detailed technical description and analysis of the current status for each of the technologies presented in Table 1 is beyond the scope of this paper. The paper will limit itself to discussing typical features of some of these technologies, which can be used to further categories them.

First, many of the technologies utilize renewable energy resources. According to the *International Energy Agency* (IEA), renewable energy resources are defined as resources that are generally not subject to depletion, such as the heat and light from the sun, the force of wind, organic matter (biomass), falling water, ocean energy and geothermal heat [19]. As about 1000 times more energy reaches the earth as fossil fuel is currently consumed, renewable energy resources can be described as abundant. However, availability of the different resources varies significantly between areas and countries, as well as technology efficiency to harvest the renewable energy resources. The following technologies for distribution generations are presently used in all over worlds as follows in table 3;

Table 3: Technologies for Distributed Generations*

| S.No. | Technology | Typical available size per module |
|-------|------------------------------------|-----------------------------------|
| 1 | Combined cycle gas T. | 35–400 MW |
| 2 | Internal combustion engines | 5 kW–10 MW |
| 3 | Combustion turbine | 1–250 MW |
| 4 | Micro-Turbines <i>Renewable</i> | 35 kW–1 MW |
| 5 | Small hydro | 1–100 MW |
| 6 | Micro hydro | 25 kW–1 MW |
| 7 | Wind turbine | 200 Watt–3 MW |
| 8 | Photovoltaic arrays | 20 Watt–100 kW |
| 9 | Solar thermal, central receiver | 1–10 MW |
| 10 | Solar thermal, Lutz system | 10–80 MW |
| 11 | Biomass, e.g. based ongasification | 100 kW–20 MW |
| 12 | Fuel cells, phosphoric acid | 200 kW–2 MW |
| 13 | Fuel cells, molten carbonate | 250 kW–2 MW |
| 14 | Fuel cells, proton exchange | 1 kW–250 kW |
| 15 | Fuel cells, solid oxide | 250 kW–5 MW |
| 16 | Geothermal | 5–100 MW |
| 17 | Ocean energy | 100 kW–1 MW |
| 18 | Stirling engine | 2–10 kW |
| 19 | Battery storage | 500 kW–5 MW |
| 20 | Wave energy | 5MW-50MW |

*Source: Linden et al. [20], IEA [21], p. 64, Duffie et al. [22], pp. 638 and author.

Secondly, technologies such as micro-hydro units, PV arrays, wind turbines, diesel engines, solar thermal systems, fuel cells and battery storage consist of a number of small modules, which are assembled in factories. These modules can be installed in a very short time at the final power station location. Manufacturing and construction on site requires significantly less time than for large centralized power stations.

Furthermore, each modular unit can start to operate as soon as it is installed on site, independent of the status of the other modules. In case a module fails, the other modules are not affected by it. As each module is small compared to the unit size of large centralized power stations, the effect of module failures on the total available power output is considerably smaller. And finally, these technologies allow for adding on modules later or move modules to another site, if required [23]–[25].

Another important aspect is the combined production of heat and power (CHP). Combined cycle gas turbines, internal combustion engines, combustion turbines, biomass gasification, geothermal, sterling engines as well as fuel cells are suitable for a combined production of heat and power. The combined local production of heat and power has the advantage of a high efficiency, if the heat is used locally. In most cases, heat and power output have an almost (positive) fixed correlation, as the heat production utilizes the heat losses of the power production. The heat demand usually defines the operation process, unless there is a back-up system for the heat production. The technology of combined heat and power production is already widely used with combined cycle gas turbines, internal combustion engines, combustion turbines and biomass gasification. A commercial version of a 1 kW fuel cell for the combined production of heat and power for houses is expected to be available by 2001 [26]–[27].

For the discussion of the technical and economic issues related to distributed generation technologies, technology categories seem useful. We suggest the following categories; others are also possible, though:

- Renewable distributed generation;
- Modular distributed generation;
- CHP distributed generation.

F. Environmental impact

Often DG technologies are described as more environmentally friendly than centralized generation. According to our definition, however, the environmental impact of the DG technology is not relevant.

Definition F1. *The environmental impact of DG is not relevant for the here proposed definition.*

The motivation for this approach is that the analysis of the environment impact is too complex, to be included in the here proposed definition. Table 2, for example, provides an overview of the most important emissions related to electricity production based on different technologies. The data comprises direct emissions and indirect emissions. Indirect emissions are emissions that occur during the manufacturing of the power unit and the exploration and transport of the energy resources.

The calculation is based on the average German energy mix and on typical German technology efficiency, [30]-[31]. Table 2 shows that the emissions from typical DG technologies are significantly lower than that from coal power stations. *Combined cycle gas turbines* (CCGT) and large hydro units, too, have significantly lower SO₂ and CO₂ emissions than coal power stations. Biomass is not included in the figure, as it is considered CO₂ neutral, as the amount of CO₂ emitted into the atmosphere when biomass is burned is equal to the amount of CO₂ absorbed during its growth. NO_x emissions of combustion of bio-fuels are reported to be 20–40% lower than that of fossil fuel plants, and SO₂ emissions are reported to be insignificant [32].

Battery storage as well as fuel cells has no direct emissions. Beside the emissions occurring during the manufacturing process, however, the fuel mix used for the production of the electricity stored in the batteries must be considered in the calculations of the indirect emissions of battery storage. In the case of fuel cells, the indirect emissions also depend on the energy mix that is required to produce hydrogen, as hydrogen cannot be exploited.

Additional environmental benefits, resulting from e.g. the reduction of transmission line losses, achieved by proper siting in terms of location and unit size, could further improve the environmental balance of DG. Apart from that, some argued that a large amount of DG might force the large units to operate below their optimum efficiency, which will lead to an increase in emissions per produced kWh [33]. Other aspects, which make an environmental comparison very difficult, are different perceptions regarding the risk of nuclear power stations or regarding the visual impact, noise impact and land requirements of wind turbines, for example. The details of comparison of energy amortization time and emission of various energy technologies are discussed in table 4.

Table 4: Comparison of Energy Amortization Time and Emissions of Various Energy Technologies^{a&b}

| Technology | Energy pay back time in months ^a | SO ₂ in kg/GWh ^a | NO _x in kg/GWh ^a | CO ₂ in t/GWh ^a | CO ₂ and CO ₂ equivalent for methane in t/GWh ^b |
|---|---|--|--|---------------------------------------|--|
| Coal fired (pit) | 1.0–1.1 | 630–1370 | 630–1560 | 830–920 | 1240 |
| Nuclear | N.A. | N.A. | N.A. | N.A. | 28–54 |
| Gas (CCGT) | 0.4 | 45–140 | 650–810 | 370–420 | 450 |
| Large hydro | 5–6 | 18–21 | 34–40 | 7–8 | 5 |
| Renewable distributed generation technologies | | | | | |
| Mico-hydro | 9–11 | 38–46 | 71–86 | 16–20 | N.A. |
| Small-hydro | 8–9 | 24–29 | 46–56 | 10–12 | 2 |
| Wind turbine | | | | | |
| 4.5 m/s | 6–20 | 18–32 | 26–43 | 19–34 | N.A. |
| 5.5 m/s | 4–13 | 13–20 | 18–27 | 13–22 | N.A. |
| 6.5 m/s | 2–8 | 10–16 | 14–22 | 10–17 | 11 |
| Photo-voltaic | | | | | |

| | | | | | |
|-------------------|-------|---------|---------|---------|-------|
| Mono-crystalline | 72–93 | 230–295 | 270–340 | 200–260 | N.A. |
| Multi-crystalline | 58–74 | 260–330 | 250–310 | 190–250 | 228 |
| Amorphous | 51–66 | 135–175 | 160–200 | 170–220 | N.A. |
| Geothermal | N.A. | N.A. | N.A. | N.A. | 50–70 |
| Tidal | N.A. | N.A. | N.A. | N.A. | 2 |

^aSource: Kalsch+mitt et al. [28]. ^bSource: Lewin [29], Fritsch et al. [30], also Ackermann [31]; All figures include direct and indirect emissions based on average German energy mix, technology efficiency, solar radiation and typical lifetime.

Therefore, the technologies that can be used for distributed generation cannot be described in general as environmentally friendly. But regarding the main current environmental issue, the increased greenhouse effect, all DG technologies lead to significantly lower emissions than coal-based technologies.

G. Mode of operation

The issue of the mode of operation is based on the wide-spread view that DG is ‘relatively unencumbered by the rules of operation of central systems (scheduling, pool pricing, dispatch, etc.)’ [5]. According to our definition, however, the mode of operation is not relevant.

Definition G1. *The mode of operation of distributed power generation is not relevant for the here proposed definition.*

The motivation for this approach is based on large variations in the international regulations regarding the operation of electricity network. Taking the English and Welsh regulations as an example, a power unit connected to the distribution system with a capacity of more than 100 MW would be treated by the market regulations as a centralized power unit, but a unit with less than 100 MW would be less encumbered in the rules of operation [11].

Therefore, it cannot be assumed in general that distributed generation is relatively unencumbered by the rules of operation. In situations, however, where distributed generation receives a special treatment by the regulations, this can be specially mentioned, for example: *not centrally dispatched distributed generation*.

H. Ownership

It is frequently argued that DG has to be owned by independent power producers or by the customers themselves, to qualify as DG. According to our definition, however, the ownership is not relevant.

Definition H1. *The ownership of DG is not relevant for the here proposed definition.*

The motivation for this approach is based on different international experiences regarding the ownership of distributed

generation. In Sweden, for example independent generators as well as traditional generators are involved in DG. However, the current experience in many countries shows that large power generation companies are often too inflexible to develop small DG systems. Furthermore, there is strong evidence that projects developed by local companies and partly financed with regional involvement have more public support than projects of other organizations [34]. Large power generation companies, however, become more and more interested in the topic and there is no obvious reason why distributed generation should be limited to independent ownership.

Nevertheless, it is important to emphasize that ownership issues of DG can be of importance for the development of distributed generation. Therefore, the ownership of DG could be mentioned, for example, *independently-owned distributed generation*

I. Penetration of distributed generation

Regarding the total amount of DG within a distribution network, some authors assume that DG stands for completely decentralized power generation that does not require any transmission lines or large centralized power plants [27]. Other authors assume that distributed generation will be able to provide only a fraction of the local energy demand. According to our definition, however, the penetration level of DG is not relevant.

Definition I1. *The penetration level of DG is not relevant for the here proposed definition.*

The motivation for this approach is based on the fact that the definition of the penetration level itself is problematic. This amount of DG must be put into relation to an area, e.g. local distribution system or nation-wide power network. The definition of this area, however, could significantly influence the penetration level.

It is, however, important to emphasize that if the predictions of the *Electric Power Research Institute* (EPRI) and the *Natural Gas Foundation*, which predict that by the year 2010, 25–30% of new generation will be distributed, will become reality, it will be likely that DG satisfies the majority of the energy needs within certain distribution networks. Therefore, the analysis of DG should always take into consideration that the penetration of DG could reach a significant level.

The proposed definition for distribution generation as follows [2].

Different definitions regarding *Distributed Generation* (DG) are used in the literature and in practice. These variations in the definition can cause confusion. Therefore, this paper suggests an approach towards a general definition of distributed generation.

The general definition for distributed generation suggested here is:

Definition 1. *Distributed generation is an electric power source connected directly to the distribution network or on the customer site of the meter.*

The distinction between distribution and transmission networks is based on the legal definition. In most competitive markets, the legal definition for transmission networks is usually part of the electricity market regulation. Anything that is not defined as transmission network in the legislation can be regarded as distribution network.

The definition of distributed generation does not define the rating of the generation source, as the maximum rating depends on the local distribution network conditions, e.g. voltage level. It is, however, useful to introduce categories of different ratings of distributed generation. The following categories are suggested in table 5:

Table 5: Type and Size of the DGs

| S.No. | Type | Rating |
|-------|-------------------------------|-------------|
| 1 | Micro distributed generation | ~1 W <5kW |
| 2 | Small distributed generation | 5kW <5MW |
| 3 | Medium distributed generation | 5 MW <50MW |
| 4 | Large distributed generation | 50MW <300MW |

Furthermore, the definition of distributed generation does neither define the area of the power delivery, the penetration, the ownership nor the treatment within the network operation. It cannot be assumed, as it is often done, that distributed generation stands for local power delivery, low system penetration, independent ownership and special treatment within the network operation in general. If these aspects are of interest, they should be mentioned additionally. For example, if the power output of distributed generation is used only within the local distribution network, we suggest the term *embedded distributed generation*. And if the distributed generation source is not centrally dispatched, it should be called: *not centrally dispatched distributed generation*.

Also, the definition of distributed generation does not define the technologies, as the technologies that can be used vary widely. However, a categorization of different technology groups of distributed generation seems possible. We suggest the following categories, but others are also possible.

| | |
|-----------|-------------------------|
| Renewable | distributed generation; |
| Modular | distributed generation; |
| CHP | distributed generation. |

III. DGs [47]-[66]

A. A Brief Historical Background of DGs

1. Backgrounds

Section 1817 of the Energy Policy Act (EPACT) of 2005, calls for the Secretary of Energy to conduct a study of the potential benefits of cogeneration and small power production, otherwise known as distributed generation, or DG. The benefits to be studied include those received “either directly or indirectly by an electricity distribution or transmission service provider, other customers served by an electricity distribution or transmission service provider and/or the general public in the area served by the public utility in which the co-generator or small power producer is located.” Congress did not require the study to include the potential benefits to owners/operators of DG units.

DG is not a new phenomenon. Prior to the advent of alternating current and large-scale steam turbines - during the initial phase of the electric power industry in the early 20th century - all energy requirements, including heating, cooling, lighting, and motive power, were supplied at or near their point of use. Technical advances, economies of scale in power production and delivery, the expanding role of electricity in American life, and its concomitant regulation as a public utility, all gradually converged to enable the network of giga-watt-scale thermal power plants located far from urban centers that we know today, with high-voltage transmission and lower voltage distribution lines carrying electricity to virtually every business, facility, and home in the country.

At the same time this system of central generation was evolving, some customers found it economically advantageous to install and operate their own electric power and thermal energy systems, particularly in the industrial sector. Moreover, facilities with needs for highly reliable power, such as hospitals and telecommunications centers, frequently installed their own electric generation units to use for emergency power during outages. These “traditional” forms of DG, while not assets under the control of electric utilities, produced benefits to the overall electric system by providing services to consumers that the utility did not need to provide, thus freeing up assets to extend the reach of utility services and promote more extensive electrification.

Over the years, the technologies for both central generation and DG improved by becoming more efficient and less costly. Implementation of Section 210 of the Public Utilities Regulatory Policy Act of 1978 (PURPA) sparked a new era of highly energy efficient and renewable DG for electric system applications. Section 210 established a new class of non-utility generators called “Qualifying Facilities” (QFs) and provided financial incentives to encourage development of cogeneration and small power production. Many QFs have since provided energy to consumers on-site, but some have sold power at rates and under terms and conditions that have been either negotiated or set by state regulatory authorities or non-regulated utilities.

Today, advances in new materials and designs for photovoltaic panels, micro-turbines, reciprocating engines, thermally-activated devices, fuel cells, digital controls, and remote monitoring equipment, among other components and technologies, have expanded the range of opportunities and applications for “modern” DG, and have made it possible to tailor energy systems that meet the specific needs of consumers. These technical advances, combined with changing consumer needs, and the restructuring of wholesale and retail markets for electric power, have opened even more opportunities for consumers to use DG to meet their own energy needs, as well as for electric utilities to explore possibilities to meet electric system needs with distributed generation.

2. Major Findings

- Distributed generation is currently part of the U.S. energy system. There are about 12 million DG units installed across the country, with a total capacity of about 200 GW. Most of these are back-up power units and are used primarily by customers to provide emergency power during times when grid-connected power is unavailable. This DG capacity also includes about 84 GW² of consumer-owned combined heat and power systems, which provide electricity and thermal energy for certain manufacturing plants, commercial buildings, and independently-owned district energy systems that provide electricity and/or thermal energy for university campuses and urban areas. While many electric utilities have evaluated the costs and benefits of DG, only a small fraction of the DG units in service are used for the purpose of providing benefits to electric system planning and operations.
- There are several economic and institutional reasons why electric utilities have not installed much DG. For example, the economics of DG are such that financial attractiveness is largely determined on a case-by-case basis, and is very site-specific. As a result, many of the potential benefits are most easily captured by customers so that the incentives for customer-owned DG are often far greater than those for utility-owned DG. This has led to the current situation where standard business model(s) for electric utilities to invest profitably in DG have not emerged. In addition, in instances where financially attractive DG opportunities for electric utilities have been identified, there is often a lack of familiarity with DG technologies, which has contributed to the perception of added risks and uncertainties, particularly when DG is compared to conventional energy solutions. This lack of familiarity has also contributed to a lack of standard data, models, or analysis tools for evaluating DG, or standard practices for incorporating DG into electric system planning and operations.

- Under certain circumstances, and depending on the assumptions, DG can also have beneficial effects on land use and needs for rights-of-way for electric transmission and distribution.
- Regulation by the states of electric rates, environmental siting and permitting, and grid interconnection for DG play an important role in determining the financial attractiveness of DG projects. These rules and regulations vary by state and utility service territory, which in itself can be an impediment for DG developers who cannot use the same approach across the country, thus raising DG project costs beyond what they might otherwise be. In addition, utilities, often with the concurrence of regulators, have rules and charges that result in rate-related impediments that discourage DG. Recently, there have been actions to address some of these impediments, such as the work of the Institute of Electrical and Electronic Engineers (IEEE) to implement uniform DG interconnection standards. In addition, *Subtitle E – Amendments to PURPA of the Energy Policy Act of 2005*, contains provisions for state public utility commissions to consider adopting time-based electricity rates, net metering, smart metering, uniform interconnection standards, and demand response programs, all of which help address some of the rate-related impediments to DG.
- A key for using DG as a resource option for electric utilities is the successful integration of DG with system planning and operations. Often this depends on whether or not grid operators can affect or control the operation of the DG units during times of system need. In certain circumstances, DG can pose potentially negative consequences to electric system operations, particularly when units are not dis-patchable, or when local utilities are not aware of DG operating schedules, or when the lack of proper interconnection equipment causes potential safety hazards. These instances depend on local system conditions and needs and must be properly assessed by a full review of all operational data.
- Nevertheless, DG offers potential benefits to electric system planning and operations. On a local basis there are opportunities for electric utilities to use DG to reduce peak loads, to provide ancillary services such as reactive power and voltage support, and to improve power quality. Using DG to meet these local system needs can add up to improvements in overall electric system reliability. For example, several utilities have programs that provide financial incentives to customer owners of emergency DG units to make them available to electric system operators during peak demand periods, and at other times of system need. In addition, several regions have employed demand response (DR) programs, where financial incentives and/or price signals are provided to customers to reduce their electricity consumption during peak periods. Some customers who participate in these programs use DG to maintain near-normal operations while they reduce their use of grid-connected power.
- In addition to the potential benefits for electric system planning and operations, DG can also be used to decrease the vulnerability of the electric system to threats from terrorist attacks, and other forms of potentially catastrophic disruptions, and to increase the resiliency of other critical infrastructure sectors as defined in the National Infrastructure Protection Plan (NIPP) issued by the Department of Homeland Security, such as telecommunications, chemicals, agriculture and food, and government facilities. There are many examples of customers who own and operate facilities in these sectors who are using DG to maintain operations when the grid is down during weather-related outages and regional blackouts.

B. Concept of Distribution Generations

1. Traditional Concept of Power Systems

Currently, most of the power systems generate and supplies electricity having into account the following considerations is shown in fig 1 [47]-[66]:

- Electricity generation is produced in large power plants, usually located close to the primary energy source (for instance: coal mines) and far away from the consumer centres.
- Electricity is delivered to the customers using a large passive distribution infrastructure, which involves high voltage (HV), medium voltage (MV) and low voltage (LV) networks.
- These distribution networks are designed to operate radially. The power flows only in one direction: from upper voltage levels down-to customers situated along the radial feeders.
- In this process, there are three stages to be passed through before the power reaching the final user, i.e. generation, transmission and distribution.

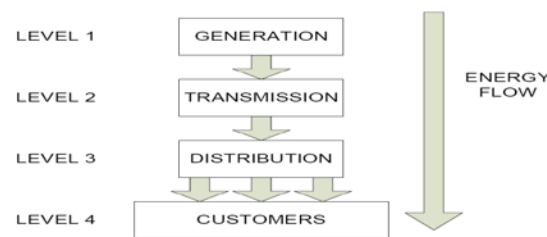


Fig 1.Traditional industrial conception of the electrical energy supply [1]-[3]

In the first stage the electricity is generated in large generation plants, located in non-populated areas away from loads to get round with the economics of size and environmental issues. Second stage is accomplished with the support of various equipment such transformers, overhead transmission lines and underground cables. The last stage is the distribution, the link between the utility system and the end customers. This stage is

the most important part of the power system, as the final power quality depends on its reliability [2].

The electricity demand is increasing continuously. Consequently, electricity generation must increase in order to meet the demand requirements. Traditional power systems face this growth, installing new support systems in level 1 (see figure). Whilst, addition in the transmission and distribution levels are less frequent.

2. New Concept of Power Systems

Nowadays, the technological evolution, environmental policies, and also the expansion of the finance and electrical markets, are promoting new conditions in the sector of the electricity generation [2].

New technologies allow the electricity to be generated in small sized plants. Moreover, the increasing use of renewable sources in order to reduce the environmental impact of power generation leads to the development and application of new electrical energy supply schemes.

In this new conception, the generation is not exclusive to level 1. Hence some of the energy-demand is supplied by the centralized generation and another part is produced by *distributed generation*. The electricity is going to be produced closer to the customers. The new concept of power system shown in fig. 2.



Fig 2. New industrial conception of the electrical energy supply [1]-[3]

C. Technologies of DGs

1. Internal Combustion Engines (ICEs)

The predominant DG technology is currently given by the internal combustion engines (ICEs) driving electric generators. ICEs have gained widespread acceptance in many sectors of the economy, serving in most cases as backup generators for sensitive loads for which long-duration energy supply failures would have serious consequences. ICEs are currently available from many manufacturers in all DG sizes ranging from few kW to 50 MW (and over). Smaller engines are primarily designed for transportation and can be converted to power generation with little modification. Larger engines are, in general, designed for power generation, mechanical drive, or marine propulsion. A subset of ICE technologies (which also include rotary engines) is given by the reciprocating engines. These engines were developed more than 100 years ago, are still

widely used and can be considered the first of the fossil fuel-driven DG technologies.

Reciprocating engines are mostly four stroke engines in which pistons move back and forth in cylinders and are based on either the Otto (spark ignition) or the Diesel cycle (compression ignition). For the former type the possible fuels are gasoline, natural gas and also biogas from sewage works while for the latter type diesel and also bio-diesel are the feasible fuels. There are also dual fuel engines with a diesel pilot fuel (instead of a spark) to start the combustion of the primary natural gas fuel. Figure 3 shows a diesel-fuelled ICE with the coupled generator. The pressure of the hot, combusted gases drives the piston down the cylinder. Energy in the moving piston is translated to rotational energy by a crankshaft. As the piston reaches the bottom of its stroke the exhaust valve opens and the exhaust is expelled from the cylinder by the rising piston.

The efficiency of earlier ICE was relatively low at around 30%, but more recent designs have average efficiencies of 35-38% reaching even 48% for diesel engines. Most internal combustion engines are designed to run at 1500 or 3000 rpm driving either a four pole or two-pole electric generator and have good control features enabling these machines to run in parallel to the grid. Particularly, diesel engines are designed to drive a synchronous generator at 750, 1500 or 3000 rpm: they can be put on line very quickly. ICEs have low startup times (less than a minute) and are responsive enough to change load rapidly. The power factor can be adjusted. The engines are fairly bulky and normally require a small building to house engine, generator, control equipment and water cooling system. It is possible to incorporate these engines into cogeneration systems as lower grade heat is available from the cooling jacket and lubricating oil, and high grade heat from the exhaust.

The utilization of such engine generators creates location specific environmental issues associated with the equipment's operational characteristics as well as potential DG system interconnection issues. In fact, the combustion process of ICEs produces NO_x and, as a result of improper fuel/air mixtures and excessive cylinder cooling, CO, CO₂, and particulate emissions. Furthermore, engine generators represent a potential noise nuisance to their immediate surroundings. While noise abatement materials and enclosures may be applied at fairly low costs to address the latter issue, the remedies for the emissions, such as selective catalytic reduction (SCR), are quite costly. Among ICEs, diesel engines are more polluting. They are primarily being used for emergency or standby applications where their low installed equipment cost, performance track record, and availability of trained mechanics make them the technology of choice. Dual fuel ICEs offer an alternative that combines the efficiency and reliability of a diesel engine with the emission benefits of a natural gas engine. These engines tend to be both more efficient and produce fewer emissions than diesel engines. Diesels can be used, however, for power supply to local communities on isolated islands or localities far

from a main grid system. Here, the high efficiency of diesel engines and the transportability and storability of the fuel are of considerable advantage.

Other issues are related to the maintenance demands which are high with spark plugs and lubricating oil having to be regularly changed. For diesel engines maintenance demands are lower than those ones for natural gas engines.

From an electric DG utility perspective, distributed engine generators, with their low installed costs and fairly high operational costs, represent peaking capacity that could be more economically dispatched in peaking demand conditions. Under such operational scenarios, the total contribution of emissions by engine generators, as a percentage of the total from all generation, would be fairly low. With regards to the interactions of these DG technologies with the rest of the power system, most existing engine generators are sized to provide power to critical and emergency loads only.

Diesel-based ICEs, although of currently limited interest due to their pollution features, have a good potential in the future in helping the EU to meet its CO₂ emission requirements as they Utilizes bio-diesel fuel very efficiently.

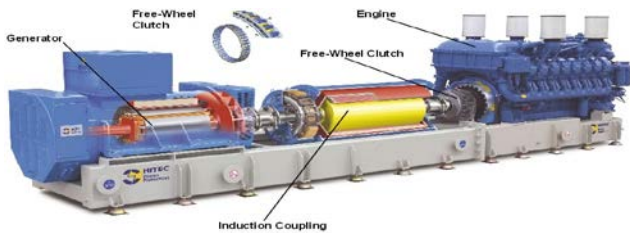


Fig. 3- A diesel-fuelled ICE with the coupled generator [4].

2. Industrial Combustion Turbines

A combustion turbine is a device in which air is compressed and a gaseous or liquid fuel ignited and the combustion products expanded directly through the blades in a turbine to drive an electric generator. The compressor and turbine usually have multiple stages and axial balading. This differentiates them from smaller micro-turbines that have radial blades and are single staged. Figure 4.2 shows a combustion turbine scheme.

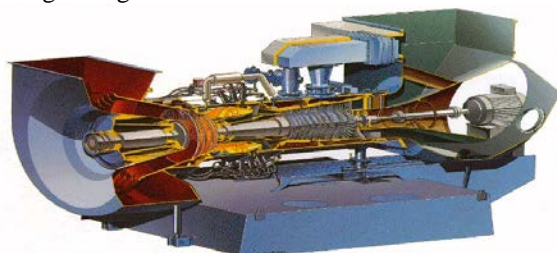


Fig. 4- A combustion turbine scheme [4].

Combustion turbines have been used for power generation for decades and range in size from simple cycle units starting at about 1 MW to over a hundred MW. Unlike in reciprocating engines, in combustion turbines combustion occurs outside the area of the prime mover (the turbine) rather than inside. This allows for greater flexibility in reducing NO emissions. Typically, emissions control of combustion turbines is performed in the combustion process.

Combustion turbines have relatively low installation costs, low emissions, heat recovery through steam and low maintenance requirements, but also reduced electric efficiency (30% on average). With these traits, combustion turbines are typically used for cogeneration DG when a continuous supply of steam or hot water and power is desired, a speakers, and in combined Cycle configurations.

3. Sterling Engines

Sterling engines are being promoted for production of electricity in domestic CHP (micro-CHP) systems. The Sterling engines are external combustion engines: in these engines the potential energy difference between the hot end and cold end is used to establish a cycle (the Stirling cycle) of a fixed amount of gas expanding and contracting within the engine. Thus, a temperature difference is converted across the machine into mechanical power. The heat is external and the burning of a fuel-air mixture can be more accurately controlled. For these reasons, the creation of pollutants such as NOx can be mostly avoided or limited and the Stirling engine can be considered a cleaner technology than ICEs. The external combustion aspect enables a Sterling engine to operate equally well on multiple types of fuel producing this external heat, such as natural gas, propane, gasoline, diesel, ethanol, bio-diesel, hydrogen or even solar energy. The best working gas in this engine is hydrogen. There are different configurations and types of Stirling engines, also depending on the respective heat source. The currently available Stirling modules are in size ranging from few kW up to a hundred kW. Figure 4.5 shows a 55 kW Stirling engine. The Stirling engine as a whole is much less complex than other reciprocating engine types. The thermodynamic efficiency is higher than in steam engines and even in some ICEs: the electrical efficiency is in the range 25-30 % for modern engines of this type, while the overall efficiency in cogeneration applications can reach 80-90 %. The very quiet operation of some types of Stirling engine is also one of the engine's best features. This prime mover can be coupled to power generator (synchronous or induction type) to be connected to the grid. A converter may be also needed for grid connection.

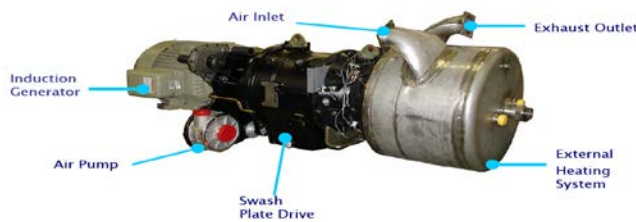


Fig. 5 - A 55 kW Stirling engine [5].

4. Photovoltaic System

The photovoltaic (PV) module or array is an unregulated dc power source, which has to be treated and conditioned before being connected to the power system. A dc/dc converter (chopper) is used at the PV array output for maximum power tracking (MPPT) as shown in Figure 2. It can extract maximum available power at a given insulation level, which means maintaining the voltage as close as possible to the maximum power point [6].

Numerous benefits are expected for both the utility company and the consumer by integration of photovoltaic (PV) energy resource into the utility's conventional resources. This form of energy, besides being renewable, also possesses other advantages, such as its ability to improve service reliability by reducing the number of system outages and by avoiding line extensions to remote areas. Such systems can also relieve thermal overloads in selected utility distribution systems. Other important benefits also exist, such as loss reduction on both distribution and transmission lines and voltage support. There are many such applications that have proven to be cost effective [7].

Photovoltaic (PV) systems are composed of arrays of modules of discrete cells connected together that convert light radiation into electricity. The PV cells produce DC electricity, which needs to be converted from DC to AC using a converter (inverter). Figure 4.6 shows a basic PV system.

Photovoltaic systems are currently widely available, produce no emissions during their operation, are reliable, and require minimal maintenance to operate. Photovoltaic systems have not been largely used so far mainly because they are one of the most costly DG technologies. However, the continual decline of manufacturing costs is expanding the range of cost-effective uses including road-signs, home power generation and even grid connected electricity generation.

Insolation is a term used to describe available solar energy that can be converted to electricity: it is a measure of solar radiation power incident on a surface. The factors that affect insolation are the intensity of the light and the operating temperature of the PV cells. Light intensity depends on the local latitude and climate and generally increases as the site gets closer to the equator.

Another major factor is the position of the solar module. In order to maximize light intensity, the panel should be positioned to maximize the duration of perpendicular incident light rays. Even with these adjustments, the maximum efficiency that can be currently obtained by a commercial PV module is about 25%. Fig. 8 shows the basic photovoltaic system.

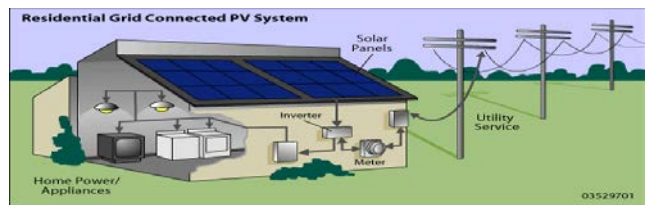


Fig. 6- A basic photovoltaic system [8].

The Schematic diagram of a photovoltaic system and physical interpretation diagram of a photovoltaic system are shown in Fig. 7 & 8.

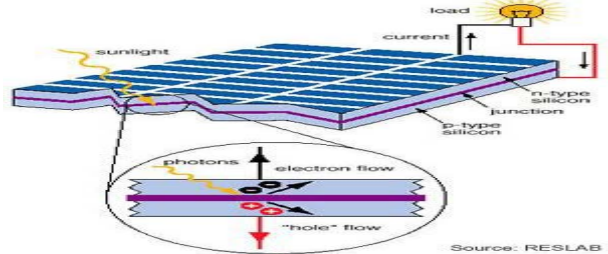


Fig. 7 Schematic diagram of a photovoltaic system [9]



Fig. 8.Physical interpretation diagram of a photovoltaic system [9]

The grid connection of PV system is shown in Fig.9.

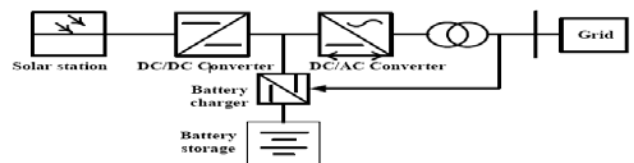


Fig. 9. Grid connection of PV system [6]-[7]

5. Wind Turbine System

Wind turbines are nowadays widespread in the European power system: Germany, Denmark and also Spain are among the

countries with the highest penetration of wind technology worldwide. Wind turbines are commonly employed in remote locations. Most wind turbines currently being used are small units designed for the residential sector, or larger units installed in on-shore or off-shore wind parks. The biggest wind turbine size has reached 6 MW of installed capacity. Figure 4.7 shows a wind turbine scheme. However, the wind farms (especially the off-shore systems) cannot be considered as DG being necessary to connect them to high capacity or high voltage systems. The wind turbine scheme shown in Fig. 10.



Fig. 10-A wind turbine scheme [8]

The schematic operation diagram of a wind turbine and variable speed induction generator diagram are shown in Fig.11 &12.

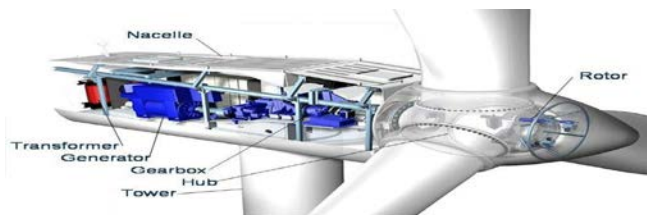


Fig. 11-Schematic operation diagram of a wind turbine [10]

Grid connected wind turbines (WT) as an effective DG source has developed noticeably in the recent past. WT can be operated at nearly constant or variable speed and coupled to induction generators to produce power. Induction generators are widely used in WT, and variable speed technology is preferred in almost all newer installations. A squirrel cage induction generator could be connected to the power system through a power electronic interface as shown in Fig.12 [6].

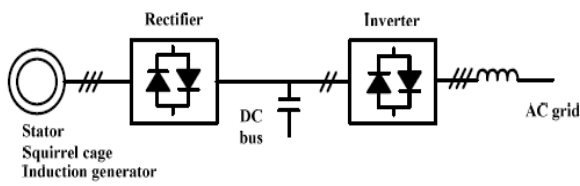


Fig. 12- Variable speed induction generator [6]

6. Micro-Turbine System

Micro-turbines are essentially very small combustion turbines: in most configurations, the micro-turbine is a single-shaft machine with the compressor and turbine mounted on the same Shaft as the electric generator. With a single rotating shaft, gearboxes and associated parts are eliminated, helping to reduce manufacturing costs and improve operational reliability.

Power outputs for this class of machine range from 1000 kW down to 1 kW. It becomes more difficult to maintain good efficiency as machine rating is reduced: gas turbines of the micro type are limited to efficiencies of 25-30% and this is only achieved with the use of a high temperature heat exchanger Called re-cooperator.

The advantage of micro-turbines is that their power output is very high in proportion to their volume. Extremely high speed, typically 100000 rpm (however in the range from 50000 to 200000 rpm), enables the generator size to be reduced by a factor of 100 compared to those of spark ignition or diesel engines. This high-frequency electricity output is first rectified and then converted to 50 Hz. Fig.13 shows a micro-turbine scheme. Micro-turbines are capable of burning a number of fuels at high- and low pressure levels, including natural gas, waste (sour) gas, landfill gas, or propane. Hydrogen, since it is much more reactive than natural gas, would be even more suited to catalytic combustion. If the gas turbine was burning bio fuels, a small high pressure pump would be needed to get the fuel into the combustion chamber. Although micro gas turbines are promoted as being suited to cogeneration, the electrical efficiency is not very high. There are also problems with the temperature of the heat emanating from the exhaust: this only permits about two thirds of the heat to be recovered. The development of condensing heat exchangers should improve the heat recovery performance, but such exchangers will have to be carefully designed as the electrical efficiency is very sensitive to pressure drops.

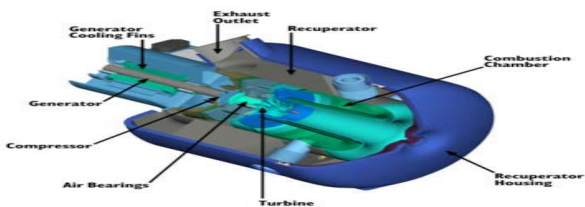


Fig.13- A micro-turbine scheme [11].

Gas fired micro-turbines in the range of 25kW to 1MW can be used to generate electricity. These micro turbines run at high speeds (50,000-90,000 rpm) with air foil bearings. The ac generator is a high frequency generator that cannot be directly connected to the power system, and hence a power electronic interface is used [14]. Generated voltage is first rectified by a diode rectifier. Dc/ac voltage source type inverter is employed to obtain utility-grade ac for injection into the grid as shown in Fig.14 [7].

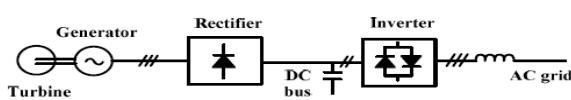


Fig. 14-Micro-turbine electrical system [7]

Micro-turbines are essentially very small combustion turbines: in most configurations, the micro-turbine is a single-shaft machine with the compressor and turbine mounted on the same shaft as the electric generator. With a single rotating shaft, gearboxes and associated parts are eliminated, helping to reduce manufacturing costs and improve operational reliability.

A micro-turbine is a mechanism that uses the flow of a gas, to convert thermal energy into mechanical energy. The combustible (usually gas) is mixed in the combustor chamber with air, which is pumped by the compressor. This product makes the turbine to rotate, which at the same time, impels the generator and the compressor. In the most commonly used design the compressor and turbine are mounted above the same shaft as the electric generator. This is shown in Fig. 15. The output voltage from micro-turbines cannot be connected directly to the power grid or utility, it has to be transferred to DC and then converted back to AC in order to have the nominal voltage and frequency of the utility.

The main advantage of micro-turbines is the clean operation with low emissions produced and good efficiency. On the other hand, its disadvantages are the high maintenance cost and the lack of experience in this field. Very little micro-turbines have been operated for enough time periods to establish a reliable field database. Furthermore, methods of control and dispatch for a large number of micro turbines and selling the remaining energy have not been developed yet [12].

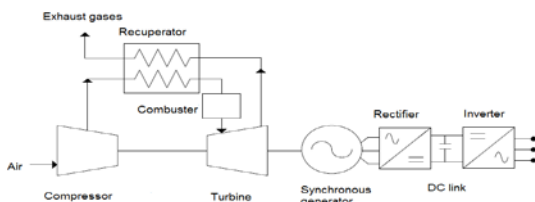


Fig 15- Schematic diagram of a micro-turbine [12]

7. Micro/small hydroelectric units

Micro/small hydroelectric power units consist of small turbines connected to electric generators and the structures necessary to regulate the flow of water to the turbines. Hydroelectric power currently represents the largest share of power production from renewable energy, both world-wide and in the EU. Hydropower units convert the kinetic energy of water into electricity. The vertical difference between the upper reservoir (where water is stored) and the level of the turbine(s) is known as the head. The

water falling through the head gains kinetic energy which it then imparts to the turbine blades. The fast-moving water pushes the turbine blades, thus turning the rotor and generating electricity. Thanks to the modern forecasting tools for hydrology resources, long-term planning for hydro energy is now also possible. This has made hydro power suitable for load control, also due to the fast start-up time of hydraulic turbines. Hydropower plants can be classified by their capacity as it follows:

- Micro and mini hydropower plants: up to 100 kW;
- Small hydropower plants: 100 kW to 10 MW;
- Large hydropower plants: > 10MW.

However, there is no consensus in EU Member States on the definition of small hydropower and the threshold of 10 MW is widely discussed.

The large majority of small hydro plants are 'run-of-river' schemes, meaning simply that the turbine generates when the water is available and provided by the river. When the river dries up and the flow falls below some predetermined amount, the generation ceases. This means that small independent schemes may not always be able to supply energy, unless they are sized in a way that there is always enough water. On the contrary, energy storage in a reservoir can more easily guarantee the energy supply. It permits to store energy during off-peak hours and to release it during peak hours.

8. Fuel Cell System

A fuel cell is a device that generates electricity by a chemical reaction. Every fuel cell has two electrodes, one positive and one negative, called, respectively, the anode and cathode. The reactions that produce electricity take place at the electrodes. Every fuel cell also has an electrolyte, which carries electrically charged particles from one electrode to the other, and a catalyst, which speeds the reactions at the electrodes [16].

Hydrogen is the basic fuel, but fuel cells also require oxygen. One great appeal of fuel cells is that they generate electricity with very little pollution—much of the hydrogen and oxygen used in generating electricity ultimately combines to form a harmless byproduct, namely water. A fuel cell is an electrochemical energy conversion device, where chemical energy in the fuel is directly and isothermally converted to electrical energy. The dc power produced by the fuel cell is converted into ac using a dc/ac inverter. The output DC power of fuel cell is converted via an inverter to grid compatible AC power as shown in Figure 3 [17].

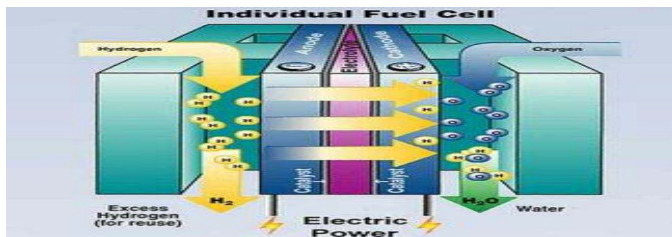


Fig. 16 Schematic diagram of a fuel cell [6]

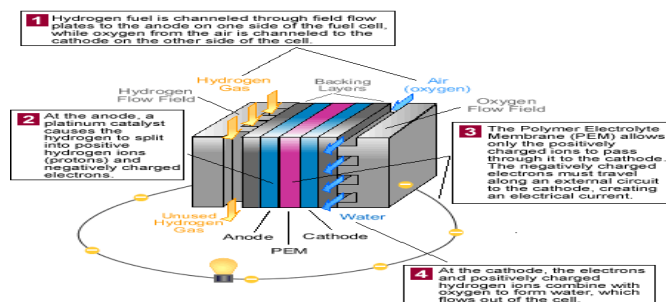


Fig. 17 – A PEM fuel cell scheme [41].

Fuel cells probably represent the power production technology receiving the most development attention. Because of their high efficiency levels (up to 55-60%), fuel cells offer several good opportunities in terms of CHP and environmental impact. There are many types of fuel cells, but each uses the same basic principle to generate power. A fuel cell consists of two electrodes (an anode and a cathode) separated by an electrolyte. Hydrogen fuel is fed into the anode; while oxygen (or air) enters the fuel cell through the cathode. With the aid of a catalyst, the hydrogen atom splits into a proton (H^+) and an electron. The proton passes through the electrolyte to the cathode, and the electrons travel through an external circuit connected as a load, creating a DC current. The electrons continue on to the cathode, where they combine with hydrogen and oxygen, producing water and heat. Fuel cells have very low levels of NO_x and CO emissions because the power conversion process is an electrochemical rather than a combustion one. For this reason, as emission standards become increasingly stringent, fuel cells will offer a clear advantage.

The main differences between fuel cell types are in their electrolytic material. Each different electrolyte has both benefits and disadvantages, based on materials and manufacturing costs, operating temperature, achievable efficiency, power to volume (or weight) ratio, and other operational considerations. The main types of fuel cells are:

- Alkaline fuel cell (AFC): This is one of the earliest fuel cell technologies successfully deployed in space missions. AFCs use a liquid solution of potassium hydroxide as the electrolyte with an operating temperature of 100-250 °C. The lower operating temperature facilitates rapid start-up of the unit. One of the major disadvantages of this

technology is its intolerance of CO_2 and the requirement to install expensive CO_2 scrubbers.

- Proton exchange membrane fuel cell (PEMFC): This fuel cell technology (see Figure 4.4) utilizes a solid polymer as the electrolyte. The polymer is an excellent conductor of protons and an insulator of electrons; it does not require liquid management. This unit features a low operating temperature of 70- 90 °C, which facilitates rapid start-up. The PEM fuel cell has a high power density and is a leading candidate for portable power, mobile and residential sector applications. PEMFC has been in the demonstration and testing stage and is starting to be commercially available.
- Solid oxide fuel cell (SOFC): A solid ceramic material is used for the electrolyte at operating temperatures of 600-1000 °C. This high operating temperature, while hampering rapid start-up as required for most mobile applications, helps to increase the efficiency and frees up the SOFC to use a variety of fuels without a separate reformer. This technology is primarily targeted at medium and large-scale stationary power generation applications.
- Molten carbonate fuel cell (MCFC): A molten carbonate salt mixture is used for the electrolyte and requires operating temperatures of 600-700 °C. This technology is targeted at medium- and large-scale stationary power generation applications.
- Phosphoric acid fuel cell (PAFC): A liquid phosphoric acid contained in a Teflon matrix is used as the electrolyte for these fuel cells. The operating temperature is 175-200 °C to facilitate the removal of water from the electrolyte. This technology is very tolerant to impurities in the fuel stream and is the most mature in terms of system development. It is currently commercially available.

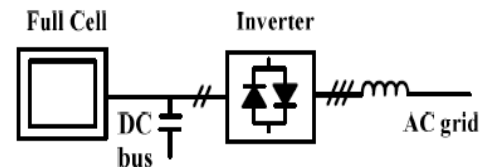


Fig. 18 Fuel cell electrical conversion system

9. Biomass Power Units

Biomass can be seen as an alternative to conventional fuel. According to the EU Directive 2001/77/EC [6], biomass is intended to be the biodegradable fraction of products, waste and residues from agriculture (including vegetal and animal substances), forestry and related industries, as well as the biodegradable fraction of industrial and municipal waste.

Biomass cannot be considered as a real DG technology, but as a fuel. In fact, it can remain unaltered and can be used directly to be burnt (e.g. in the Rankine cycle for traditional steam turbines) both separately and together with coal in the co-firing process, or it can be converted into liquid or gas and used as a

fuel for DG technologies like micro turbines, gas turbines, fuel cells, ICEs, Stirling engines. Biomass-fuelled schemes are suitable for CHP and therefore include installations designed to Run on solid, liquid and gaseous fuels. Biomass-fuelled CHP is widespread in countries such as Sweden, Finland and Austria, e.g. for using forestry residues. Typical fields of application are Wood-processing industries, district heating systems, industries with a high process heat demand, and co-combustion of biomass in existing fossil fuel-fired CHP plants.

For biogas plants a number of waste products from households, industry and agriculture can be used as fuels: municipality waste is the dominant fuel in incineration plants. Distributed biomass-fuelled CHP can provide important environmental benefits in terms of reduced greenhouse gas emissions and preservation of the limited global stock of fossil fuel resources. Biomass combustion is *CO₂*-neutral under the condition that the amount of biomass burnt is replaced, thereby keeping the overall stock of biomass constant. In addition, biomass combustion produces less toxic gases like *NO_x*.

Concerning the technology development, combustion of biomass and waste is a mature and proven technology. At present, the sizes of the combustion plants are relatively small compared to fossil-fired plants. However, for commercial exploration larger plants with capacity higher than 20 MW are preferred. According to the definition of distributed power generation as introduced in this work, future biomass combustion plants will have to be considered as centralized power plants.

As a pre-treatment technology at mainly coal fired power plants, gasification is also a mature technology. In the gasification process, wood and other biomass materials are gasified to produce so-called 'producer gas' for electricity generation. With gasification becoming also a competitive technology, as for the combustion, gasification plants will have to be considered as centralized power plants as well.

10. Solar Thermal Units

Solar thermal energy aims at exploiting solar power for practical applications spanning from solar heating to electrical power generation. For electrical power generation a solar thermal power plant generates electricity via the heat resulting from concentrating the sun's energy and driving a thermal power plant. For this reason this type of electricity production is also known as concentrated solar power generation. Different types of concentrating solar panels exist: among these technologies, the solar dish coupled to a Stirling engine has the highest solar energy conversion efficiency, equal to ca. 40%.

These coupled systems are still in the development stage and may be applied for DG purposes. In the United States there are the largest solar thermal power plants, reaching several hundreds of MW of capacity. In Europe the biggest plant is in

Spain and reaches the capacity of 50 MW. Other projects are under development. However, for bigger plant capacities it is inappropriate to consider them for DG applications; high capacity or high voltage transmission networks are the most suitable systems to accommodate this power.

10. Ocean Energy Power Units





Fig.19. (a) - (g) Technical Readiness of Ocean Thermal Energy Conversion (OTEC)

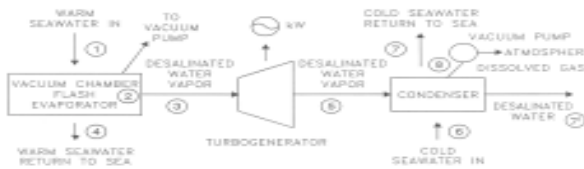


Fig.20 Schematic diagram of an open-cycle OTEC system (*Diagram: courtesy of Luis Vega, Hawaii*)

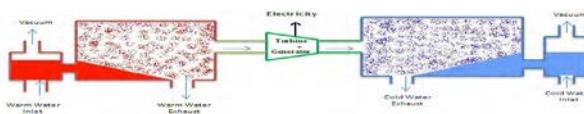


Fig. 21. Principles of operation of an open-cycle OTEC Facility

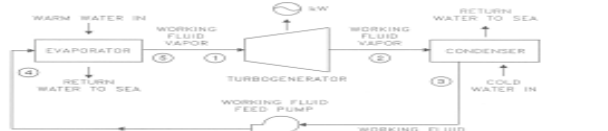


Fig. 22 Schematic diagram of a closed-cycle OTEC system (*Diagram: courtesy of Luis Vega, Hawaii*)

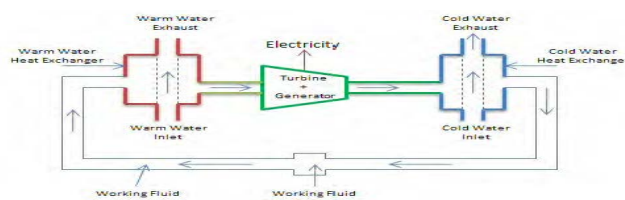


Fig. 23 Principles of operation of a closed-cycle OTEC facility

D. Electric Power System with DGs

The distributed generation Backgrounds are shown in Fig. The details of electric power system network [1] without distributed generations as shown in Fig.

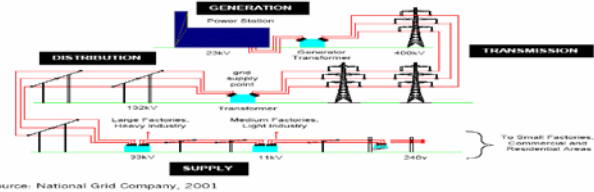


Fig.24 Electric Power System Networks without DGs

The details of distributed generation in electric power system networks [1] as shown in Fig.

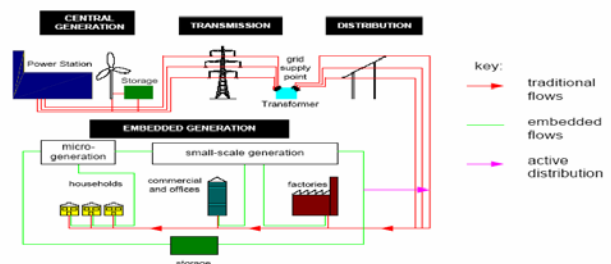


Fig. 25 Distributed Generation in Electric Power System Networks

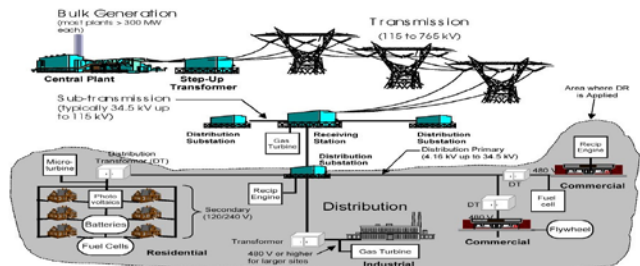


Fig. 26 Distributed Generation in Electric Power System Networks

E. Types of Distribution Generations

The different types of traditional and nontraditional DGs are classified and described in (El-Khattam and Salama, 2004) from the constructional, technological, size, and power time duration point of view. The DGs may also be grouped into four major types based on terminal characteristics in terms of real and reactive power delivering capability as described in (Hung et al, 2010). In [], the four major types are considered for comparative studies which are described as follows:

Type 1: This type DG is capable of delivering only active power such as photovoltaic, micro turbines, fuel cells, which are integrated to the main grid with the help of converters/inverters. However, according to current situation and grid codes the photovoltaic can and in sometimes are required to provide reactive power as well.

Type2: DG capable of delivering both active and reactive power. DG units based on synchronous machines (cogeneration, gas turbine, etc.) come under this type

Type3: DG capable of delivering only reactive power. Synchronous compensators such as gas turbines are the example of this type and operate at zero power factors.

Type4: DG capable of delivering active power but consuming reactive power. Mainly induction generators, which are used in wind farms, come under this category. However, doubly fed induction generator (DFIG) systems may consume or produce reactive power i.e. operates similar to synchronous generator.

In [-IEST-PAYASI---], the analysis of T1, T2, T3, and T4 for optimal size and location is done on the basis of terminal characteristic of basic DGs in terms of their power delivering capability.

F. Penetration of DG

As the yearly electric energy demand grows, there is a significant increase in the penetration of distributed generation (DG) to fulfill this increase in demand. Interconnecting DG to an existing distribution system provides various benefits to several entities as for example the owner, utility and the final user. DG provides an enhanced power quality, higher reliability of the distribution system and can peak shaves and fill valleys. However, the integration of DG into existing networks has associated several technical, economical and regulatory questions.

The penetration level (*PL*) can be defined in two ways as follows [3].

$$\% PL = \frac{P_{DG}}{P_{Load}} \times 100$$

$$\% PL = \frac{P_{DG}}{P_{Load} + P_{DG}} \times 100$$

Where *P_{DG}* stands for the total active power of all distributed generators installed in a given area and *P_{Load}* is the total active power of the load in the same area.

G. Issues of DGs

The various issues of DGs are explaining in details as follows:

1. DGs Electrical Interconnection

The interconnection with the network is a complicated procedure that involves the realization of a DG application. The DG operation is usually referred to as synchronized or parallel operation. In this configuration the DG is connected to the network the same time that it's producing power and in the case that the load is met any excess energy is also transmitted to that.

The parallel DG operation is the most complicated in contrast with a stand-alone DG application. The complexity of DG operation generally depends on the level of interaction with the existing network.

- *Isolated, stand-alone source (fig.):*

In this case the load is met by DG only with no network connection as follows:

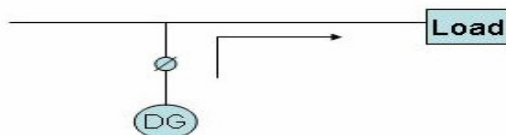


Fig.27 Isolated, stand-alone source

- *Isolated system with automatic transfer (fig.):*

DG provides power in Load 2. The network covers Load 1 and Load 2 when needed. DG does not work in parallel except for a few sec.

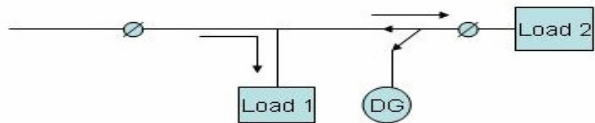


Fig. 28 Isolated system with automatic transfer

- *DG connected to the network with no power export (fig.):*

DG operates in parallel to the grid by transmitting power to one or more loads without sending any excess energy to the grid.

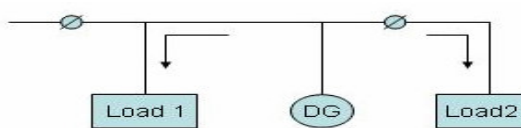


Fig. 29 DG connected to the network with no power export

- *DG grid interconnected with power export (fig.):*

DG operates in parallel to the grid and there exists the option to supply any excess power to the grid.

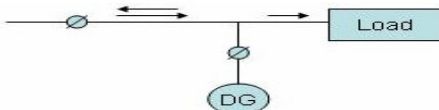


Fig.30 DG grid interconnected with power export

- *Grid interconnected with power export- utility side (fig.):*

The system supplies the base load, standby power, and peak load. DG operates in parallel.

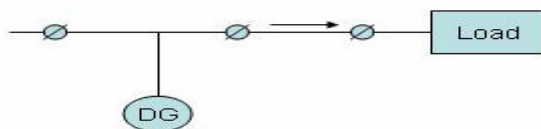


Fig.31 Grid interconnected with power export- utility side



2. Technical Issues

The main technical issues for DG connection relate to reliability and quality of supply, protection, metering, and operating protocols for connection and disconnection, islanding and reactive power management. Voltage regulation, voltage flicker, harmonic voltages and DC injection are key quality of supply issues. Protection issues arise both for DG equipment and network equipment. The DG protection issues depend on the type of generator and the characteristics of the network. Network protection issues depend on the type and location of the DG installation and network characteristics. Thus protection design requires good communication between DG project developer and network service provider during the design process. It may be difficult to develop economically sound policies on how to pay for any required upgrades in the utility infrastructure to protect against those risks. Experts generally agree that the current risks to the distribution system from the parallel operation of small generators, representing only a small fraction of a local distribution network's capacity, are usually manageable. But the cumulative effects of many generators would be another matter. The utility network might require significant upgrades and additional protective devices to manage distributed generators that could use a large fraction of the local distribution network's capacity.

- Power Quality Issues
- Protection Issues
- Commercial and Planning Issues

H. Possible Benefits or challenges and Drawbacks of DGs and FACTS Controllers in Power Systems[4]

The possible benefits of DGs incorporated with FACTS controllers in power systems as follows:

- Minimized Real Power Losses
- Improve Voltage Profile
- Improve steady state stability
- Improve transient stability
- Elimination of Power Quality Problems
- Increase the Reactive Power Support
- Increase the Loadability of Systems
- Increase the Available Power Transfer Capacity of Systems
- Enhance the Power System Stability
- Reduce the Power System Oscillations
- Provide the Green House environments
- Increase the System Reliability
- Increase the Efficiency of System
- Improve the power factor of system
- Connection of DG is intended to increase the reliability of power supply provided to the customers, using local sources, and if possible, reduce the losses of the transmission and distribution systems.
- The connection of DG to the power system could improve the voltage profile, power quality and support voltage stability. Therefore, the system can withstand higher loading situations.
- The installation of DG takes less time and payback period. Many countries are subsidizing the development of renewable energy projects through a portfolio obligation and green power certificates. This incentives investment in small generation plants.
- Some DG technologies have low pollution and good overall efficiencies like combined heat and power (CHP) and micro-turbines. Besides, renewable energy based DG like photovoltaic and wind turbines contribute to the reduction of greenhouse gases.
- The provision of ancillary services.
- An emergency supply of power.
- Reducing the vulnerability of a system to terrorism.
- Diminished land use effects and right-of-way acquisition costs.
- Offsets to investments in generation, transmission, or distribution facilities that would otherwise be recovered through rates.

The possible drawbacks of DGs incorporated with FACTS controllers in power systems as follows:

- Voltage and Current Interaction Problems are Occurs
- Proper placement and coordination problems
- Active and Passive Filters are Required
- Installation or Capital Cost will be Increase.
- Many DG are connected to the grid via power converters, which injects harmonics into the system.

- The connection of DG might cause over-voltage, fluctuation and unbalance of the system voltage if coordination with the utility supply is not properly achieved.
- Depending on the network configuration, the penetration level and the nature of the DG technology, the power injection of DG may increase the power losses in the distribution system.
- Short circuit levels are changed when a DG is connected to the network. Therefore, relay settings should be changed and if there is a disconnection of DG, relay should be changed back to its previous state.
- Power Generation by DGs and FACTS Controllers are Limited (around 25- 30% of total new generations)

I. Applications and Technologies of DGs

The details of distributed generation applications and Technologies [2]-[7].

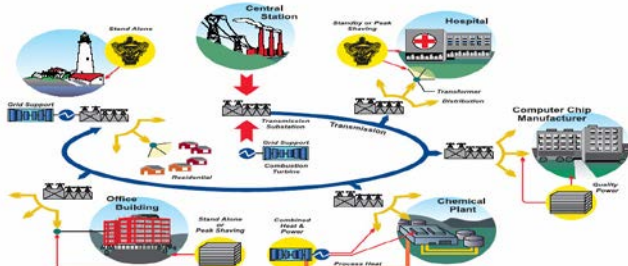


Fig.32. Summary of DG applications [2]

IV. CONCLUSIONS

In this paper presents the optimal placement techniques for distributed generations form different performance parameter of systems viewpoints such as improve the voltage profile, reduce active power losses, reduce the voltage deviation and cost of systems, increase the loadability of systems.

V. ACKNOWLEDGMENT

The authors would like to thanks Dr. S. C. Srivastava, and Dr. S. N. Singh, Indian Institute of Technology, Kanpur, U.P., India, Dr. K.S. Verma, Dr. R.P. Payasi, and Dr. D. Singh, Kamla Nehru Institute of Technology, Sultanpur, U.P., 228118, India, for their valubales suggestions regarding optimal placement and coordination techniques for distributed generations with FACTS controllers form different performance parameter of systems viewpoints such as improve the voltage profile, reduce active power losses, reduce the voltage deviation and cost of systems, increase the loadability of systems.

VI. REFERENCES

- [1] G. Pepermans, J. Deereisen, D. Heeseldonckx, R. Belmans, WE. D'haeseleer, "Distribution generation: Definitions, Benefits, and issues," Energy Policy, Vol. 33, 2005, pp. 787-798.
- [2] Ackermann, T., Andersson, G., Soder, L., (2001). "Distributed generation: a definition". Electric Power Systems Research 57, pp. 195–204, 2001.
- [3] Dondi, P., Bayoumi, D., Haederli, C., Julian, D., Suter, M., (2002). "Networkintegration of distributed power generation". Journal of Power Sources 106, pp. 1–9, 2002.
- [4] Pepermans, G., Driesen, J., Haeseldonckx, D., Belmans, R., D'haeseleer, W., (2005). "Distributed Generation: definition, benefits and issues". Energy Policy, 33, pp. 787-798, 2005.
- [5] OFGEM, 2007. "Review of Distributed Generation". Office of Gas and Electricity Markets (www.dti.gov.uk/energy/whitepaper).
- [6] Vovos, P.N., Kiprakis, A. E., Wallace, A. R. & Harison, G.P., "Centralized and Distribution Voltage Control: Impact on Distribution Generation Penetration, IEEE Trans. on Power systems, Vol.22, No.1, pp. 476-683.
- [7] Belkacem Mahdad, Tarek Bouktir, and Kamel Srairi, "Optimal Coordination and Penetration of Distributed Generation with Multi-Shunt FACTS Compensators Using GA/Fuzzy Rules," Distributed Generation, D. N. Gaonkar (Ed.), ISBN: 978-953-307-046-9, in tech, Available from: www.intechopen.com, February' 2010, pp. 327-350.
- [8] M.Mokhtari, J. Khazaie, D. Nazarpour, M. Farsadi, "Interaction analysis of multi-function FACTS and D-FACTS controllers by MRGA," Turkish Journal of Electrical Engineering & Computer Sciences, Vol. 21, pp.1685-1702, October 2013.
- [9] R.H. Lasseter, Control of distributed resources, in: L H. Fink, C.D. Vournas (Eds.), Proceedings: Bulk Power Systems Dynamics and Control IV, Restructuring, organized by IREP and National Technical University of Athens, Santorini, Greece, August 23–28, 1998, pp. 323–329.
- [10] M. Grubb, Renewable Energy Strategies for Europe-Volume I, Foundations and Context, The Royal Institute of International Affairs, London, UK, 1995.
- [11] J. Zhang, H. Cheng, and C. Wang, "Technical and economic impacts of active management on distribution network," International Journal of Electrical Power and Energy Systems, Vol. 31, No.2-3, pp. 130-138, Feb./March. 2009.
- [12] A Zangeneh, S. Jadid, and A. Rahimi-Kian, "A fuzzy environmental technical economic model for distributed generation planning," Energy, Vol. 36, No. 5, pp. 3437-3445, May 2011.
- [13] J.L. Del Monaco, The role of distributed generation in the critical electric power infrastructure, in: Proceedings of the Power Engineering Society Winter Meeting IEEE, vol. 1, 2001, 144–145.
- [14] A. Thomas, A. Göran, S. Lennart, Distributed generation: a definition, Electric Power Syst. Res. 57 (3) (2001) 195–204.
- [15] P.P. Barker, R.W. De Mello, Determining the impact of distributed generation on power systems. I. Radial distribution systems, in: Proceedings of the Power Engineering Society Summer Meeting IEEE, vol. 3, 2000, pp. 1645–1656.
- [16] S. Gilbert, The nation's largest fuel cell project, a 1MW fuel cell power plant deployed as a distributed generation resource, Anchorage, Alaska project dedication 9 August 2000, in: Proceedings of the Rural Electric Power Conference, 2001, pp. A4/1-A4/8.
- [17] D. Sharma, R. Bartels, Distributed electricity generation in competitive energy markets: a case study in Australia, in: The Energy Journal Special issue: Distributed Resources: Toward a new Paradigm of the Electricity Business, The International Association for Energy Economics, Cleveland, Ohio, USA, 1998,pp. 17–40.
- [18] See Electric Power Research Institute web-page (January 1998):<http://www.epri.com/gg/newgen/disgen/index.html>.
- [19] Gas Research Institute, Distributed Power Generation: A Strategy for a Competitive Energy Industry, Gas Research Institute, Chicago, USA 1998.
- [20] J. Cardell, R. Tabors, Operation and control in a competitive market: distributed generation in a restructured industry, in: The Energy Journal Special Issue: Distributed Resources: Toward aNew Paradigm of the Electricity Business, The International Association for Energy Economics, Cleveland, Ohio, USA, 1998,pp. 111–135.
- [21] CIGRE, Impact of increasing contribution of dispersed generation on the power system; CIGRE Study Committee no 37, Final Report, September 1998.
- [22] CIRED, Dispersed Generation; Preliminary Report of CIRED (International Conference on Electricity Distribution), Working Group WG04, Brussels, Belgium, June 1999.
- [23] J. Watson, Perspective of Decentralized Energy Systems in aliberalised Market: The UK Perspective, in: Rolf Wu'stenhagen,Thomas Dyllick, St. Gallen, Institute for Wirtschaft und Okologie (IWO)-

- [24] Diskussionsbeiträge Nr. 72: Nachhaltige Marktchancen Dank dezentraler Energie? Ein Blick in die Zukunft der Energiedienstleistung, Switzerland, January 1999, pp. 38–47.
- [25] R. Menges, K. Barsantny, Die Liberalisierung der Strommarkte in Norwegen und Schweden; in: Zeitschrift für Energiewirtschaft, Vol. 21; Heft 1/1997; Energiewirtschaftliches Institute an der University Ko In, Germany, 1997, pp. 39–56.
- [26] VDEW, Die Nordische Elektrizitätswirtschaft im Wettbewerb; Bericht über die VDEW Studienreise nach Norwegen, Schweden und Finnland, Frankfurt/Germany, April 1998.
- [27] Swedish Electricity Act, SFS 1997: 857.
- [28] T. Wizelius, Series of Offshore Projects Planned; in: Wind PowerMonthly, Vol. 14, No.10, October 1998, pp. 23–24.
- [29] R.P. Payasi, A.K. Singh, and D. Singh, "Review of distributed generation planning: objectives, constraints, and algorithms," International Journal of Engineering, Science and Technology, Vol.3, No.3, pp.133-153, 2011.
- [30] T. Klopfer, P. Kreuzberg, W. Schulz, F. Starrmann, O. Werner, Das Pool-System in der Elektrizitätswirtschaft — Möglichkeiten einer umweltorientierten Gestaltung von Poolregeln; Herausgegeben vom Umweltbundesamt, Bericht 4/96, Forschungsbericht 101 06 062 UBA-FB 96-047, Berlin, Germany, 1996.
- [31] D. Hammond, J. Kendrew, The Real Value of Avoided Transmission Costs; Conference Proceedings EECA/NZWEA (Energy Efficiency and Conservation Authority/New Zealand Wind Energy Association), New Zealand, 1997.
- [32] International Energy Agency, Energy Technologies for the 21st Century; Paris, 1997.
- [33] H.R. Linden, Distributed Power Generation-The logical Response to Restructuring and Convergence, available at: <http://www.dpc.org/publications/index.html>.
- [34] International Energy Agency, Enhancing the Market Deployment of Energy Technology: a Survey of Eight Technologies, Paris, 1997.
- [35] J. A. Duffie, W. A. Beckman, Solar Engineering of Thermal Processes, Second, John Wiley & Sons, New York, USA, 1991.
- [36] T. E. Hoff, National Renewable Energy Laboratory, Integrating Renewable Energy Technologies in the Electric Supply Industry: A Risk Management Approach; December 1996, http://wwwleland.stanford.edu/_tomhoff/cv.htmcreports.
- [37] T. E. Hoff, Merig, Managing risk using renewable energy technologies; in: Shimon Awerbuch, AliStair Preston, The VirtualUtility: Accounting, Technology and Competitive Aspects of the Emerging Industry, Kluwer, Boston, 1997.
- [38] M. Grubb, R. Vigotti, Renewable Energy Strategies for Europe—Volume II, Electricity Systems and Primary Electricity Sources, The Royal Institute of International Affairs, London, UK, 1997.
- [39] R. Diethelm, How fuel cells could change the market place: perspectives of a decentralized Swiss Energy System in 200x; in: Rolf Wu'stenhagen, Thomas Dyllick, St. Gallen, (Eds.), Institut für Wirtschaft und Ökologie (IWO)-Diskussionsbeiträge Nr.72: Nachhaltige Marktchancen Dank dezentraler Energie? EinBlick in die Zukunft der Energiedienstleistung, Swiss, January 1999, pp. 27–37.
- [40] D. Milborrow, Renewables and the real world; in: Wind PowerMonthly, Vol. 14, No. 4, Knebel, Denmark, April 1998, pp.38–45.
- [41] M. Kaltschmitt, T. Stelzer, A. Wiese, Ganzheitliche Bilanzierung am Beispiel einer Bereitstellung elektrischer Energie aus regenerativen Energien; in: Zeitschrift für Energiewirtschaft, Vol. 20;Heft 2 / 1996; Energiewirtschaftliches Institute an der Universität Ko In, Germany, 1996, pp. 177–178.
- [42] B. Lewin, CO₂-Emission von Energiesystemen zur Stromerzeugung unter Berücksichtigung der Energiewandlungsketten; Ph.D.Thesis, Fachbereich 16, Bergbau und Geowissenschaften, Technical University Berlin, Germany, 1993.
- [43] Fritsch et al. (1989): Umweltwirkungsanalyse von Energiesystemen,Gesamt-Emissions-Modell integrierter Systeme; Hessisches Ministerium für Wirtschaft und Technologie (Ed.), Wiesbaden,Germany, 1989.
- [44] Berücksichtigung der Windenergie-Eine system analytische Untersuchung; Diplomarbeit (Master Thesis), Lehrstuhlführer Loft und Ranmfahrt, Prof. Gaseb, Technical University Berlin, Germany, February 1995.
- [45] Research Council of Norway, New Renewable Energy — Norwegian Development; published by The Research Council of Norway in cooperation with The Norwegian Water Resources and Energy Directorate (NVE), Second ed., Oslo, Norway, December 1998.
- [46] Fischedick Kaltschmitt, Wind- und Solarstrom im Kraftwerksverbund-Möglichkeiten und Grenzen; Hrsg. vom Institut für Energiewirtschaft und Rationelle Energieanwendung(IER) an der Universität Stuttgart, C.F. Muller Verlag, Heidelberg, Germany, 1995.
- [47] M. Grubb, Renewable Energy Strategies for Europe—Volume I, Foundations and Context, The Royal Institute of International Affairs, London, UK, 1995.
- [48] K Kauhaniemi, L. K. (2004). Impact of Distributed Generation on the Protection of Distribution Networks, „University of Vaasa, Finland, VTT Technical Research Centre of Finland, Finland
- [49] Mario Vignolo, R. Z. (2002). Transmission Networks or Distributed Generation?. Montevideo, Uruguay.
- [50] Angel Fernández Sarabia, "Impact of distributed generation on distribution system," Department of Energy Technology, A Dissertation Submitted to the Faculty of Engineering, Science and Medicine, Aalborg University in Partial Fulfilment for the Degree of Master Graduate , June 2011, Aalborg, Denmark.
- [51] Hitec Electric. Website: www.hitecelectric.com.
- [52] STM Power Inc. Website: <http://www.stmpower.com>.
- [53] V. P. Mahadanaarachchi, R. Ramakuma, "Impact of distributed generation on distance protection performance - A review," in Proc.IEEE Conf. Power and Energy Society General Meeting-Conversion and Delivery of Electrical Energy, USA, 2008, pp. 1-7.
- [54] B. H. Chowdhury, and A. W. Sawab, "Evaluating the value of distributed photovoltaic generations in radial distribution systems," IEEE Trans. Energy Conversion, vol. 11, no. 3, pp. 595-600, Sep. 1996.
- [55] U.S. Department of Energy (DOE), Energy Efficiency and Renewable Energy. Website:www.eere.energy.gov.
- [56] Ingenieros, A. M. (2011). grupoglobalgreen. Retrieved May 20, 2011, from grupoglobalgreen: www.grupoglobalgreen.es.
- [57] tutorvista. (n.d.). Retrieved February 18, 2011, from tutorvista: <http://www.tutorvista.com/physics/wind-electric-power>.
- [58] Energieprojecten.com.Website: www.energieprojecten.nl.
- [59] Gonzalez-Longatt, F. M. (2008, Junio). Impacto de la Generación Distribuida en el Comportamiento de los Sistemas de Potencia. Universidad Central de Venezuela., 2008.
- [60] Energy OR Technologies Inc. (n.d.). Retrieved February 15, 2011, from EnergyORTechnologiesInc: http://www.energyor.com/energyor/fuel_cell.cfm
- [61] Konstantinos Angelopoulos, "Integration of Distributed Generation in Low Voltage Networks: Power Quality and Economics," PHD Thesis, submitted in 2004, Department of Mechanical Engineering, University of Strathclyde in Glasgow, 2004.
- [62] "Distributed Generation: It's Role in Emerging Economies", Rajat K.Sen, Chris Namovicz, Jennifer Kish- SENTECH, Inc.
- [63] "Distributed Generation", U.S. Department of Energy, Federal Energy Technology Center.
- [64] "Distributed Generation: Policy Framework and Regulators", Arthur D. Little White Paper, 1999.
- [65] "Distributed Generation: Understanding the Economics", Arthur D. Little White Paper, 1999.
- [66] "Networks for Embedded Generation" EEA/EA Technology Travel Award 2001, Summary report.
- [67] "Distributed Generation: System Interfaces" An Arthur D. Little White Paper, 1999.

BIBLIOGRAPHIES



Bindeshwar Singh received the M.Tech. in electrical engineering from the Indian Institute of Technology, Roorkee, in 2001. He is now a Ph. D. student at ISM, Dhanbad, Jharkhand, India. His research interests are in Optimal placement and Coordination of DGs and FACTS controllers in power systems and Power system Engg.. Currently, he is an Assistant Professor with Department of Electrical Engineering, Kamla Nehru Institute of Technology, Sultanpur, U.P., India, where he has been since August'2009.

Mobile: 09473795769

Email:bindeshwar.singh2025@gmail.com



Dr. Prabhakar Tiwari received the B.Tech. from MMM Engineering College, Gorakhpur in 1998, M. Tech from IITD in 1999 and Ph.D in electrical engineering from the JMI Central University New Delhi in 2012. Currently, he is a Professor & Head EEE Department, Galgotias College of Engineering & Technology, Gr. Noida. His interests are in the areas of Power System Restructuring, Deregulation, Stability and Pricing of Power systems. Mobile: 08130460622,

Email: profptiwari@gmail.com



Dr. Vivekananda Mukherjee received the Ph.D. in electrical engineering from the NIT, Durgapur in 2008. Currently, he is a Assistant Professor in Electrical Engineering Department, ISM Dhanbad. His interests include Small signal stability, restructured power systems, distributed generation, and evolutionary computing techniques. Mobile: 09474512640, Email: vivek_agamani@yahoo.com

A Electrical Power Quality Problem & Its Solutions

Bindeshwar Singh¹, Rajiv Kumar², Pavan Prakash Gupta³, and Ashok Kumar⁴

¹ Asst. Professor, Department of Electrical Engineering, Kamla Nehru Institute of Technology (KNIT), Sultanpur-228118, U.P., India
^{2,3&4} Student Member IEEE, M. Tech. (PE&D) Regular Student, Department of Electrical Engineering, Kamla Nehru Institute of Technology (KNIT), Sultanpur-228118, U.P., India

Abstract- This paper presents a electrical power quality problems (PQ) such as transients, instantaneous (interruption, swell & sag), long duration variations (interruption, under voltage, over voltage), harmonics, voltage unbalance, voltage fluctuation, power frequency variations, power factor of system, and waveform distortion such as current and voltage in the system and its solution by FACTS controllers such as DVR, STATCOM, DSTATCOM, DDSTATCOM, FDSTATCOM, and third generation of FACTS controllers and also discuss power quality standerds.

Keywords: Power Quality, Flexible AC Transmission System (FACTS), FACTS Controllers, Voltage sag, Voltage swell, DVR, STATCOM, DSTATCOM.

NOMENCLATURES

| | |
|----------|--|
| FACTS | Flexible Alternating Current Transmission System |
| FC-TCR | Fixed capacitor Thyristor Controlled Reactor |
| TCSC | Thyristor Controlled Series Capacitor |
| TCPAR | Thyristor Controlled Phase Angle Regulator |
| SSSC | Static Synchronous Series Compensator |
| TCPST | Thyristor Controlled Phase Shifting Transformer |
| TSSC | Thyristor Switched Series Capacitor |
| TCSR | Thyristor Controlled Series Reactor |
| TCR | Thyristor Controlled Reactor |
| TSR | Thyristor Switched Reactor |
| SVC | Static Var Compensator |
| STATCOM | Static Synchronous Compensator |
| DSTATCOM | Distribution Static Compensator |
| IPFC | Interline Power Flow Controller |
| UPFC | Unified Power Flow Controller |
| GUPFC | Generalized Unified Power Flow Controller |
| HPFC | Hybrid Power Flow Controller |
| SMES | Superconducting Magnetic Energy Storage Systems |
| BESS | Battery Energy Storage Systems |
| UIPC | Unified Interphase Power Controller |
| PFC | Power System Stabilizers |
| AP | Active Power |
| RP | Reactive Power |
| VSC | Voltage Source Converter |
| VSI | Voltage Source Inverter |
| VS | Voltage Stability |
| VI | Voltage Instability |
| VC | Voltage Collapse |
| VP | Voltage Profile |
| VR | Voltage Regulation |
| SSVS | Steady State Voltage Stability |
| TS | Transient Stability |
| APTC | Available Power Transfer Capacity |
| PQ | Power Quality |
| SSR | Sub-synchronous Resonance |
| SS | Steady State |
| α | Firing Angle |
| HFC | Hybrid Flow Controller |
| PST | Phase Shifting Transformer |
| PSS | Power system stability |

DVR

Dynamic Voltage Restorer

I. INTRODUCTION

Modern power systems are continuously being expanded and upgraded to cater the need of ever growing power demand. This paper explains the problems that are due to poor Power Quality in electrical systems. Flexible AC transmission systems or FACTS are devices which allow the flexible and dynamic control of power systems[1]. Latest innovative ideas to make the life easier using the technology depends upon the application of power electronics in turn about power quality. With increasing quantities of non-linear loads being added to electrical systems, it has become necessary to establish criteria for limiting problems from system voltage degradation. This paper presents the power quality problems, issues, related international standard, effect of power quality problem in different apparatuses and methods for its correction. This is important for design engineers and researchers in power quality to know the international standards used for power quality.[2]

II. A LITRATURE SURVAY

A. Capability(2000-2013)

G. Vishwakarma, and N. Saxena [6], has been presented a novel methodology for enhancement of VP by using FC-TCR. M. S. H. Lipu, and T. Fahrin Karim [7], has been proposod a novel technology for effectiveness of FACTS controllers and HVDC transmissions for improving PSS and increasing power transmission capability. M. Bhanu Siva *et al.* [8], has been presented a novel approach for PQ improvement of three-phase for-wire D-STATCOM with fuzzy logic controller. I. Kumaraswamy *et al.* [9], has been presented a novel suggested for amelioration of PQ in isolated power system. V. G. Mathad *et al.* [10], has been presented a novel reported for review on comparison of FACTS controllers for (PSS) enhancement. M. A. Gargeya [11], has been presented a novel methodology for a new proposal for mitigation of PQ problems using D-STATCOM. J. Namratha Manohor and J. Amarnath [12], statistical analysis of PS on enhancement of (ATCP) applying FACTS. T. A. R. Kumar, and I. A. Chidambaram [13], has been presented for PS security enhancement using FACTS devices in a PS network with voltage dependent loads and ZIP loads. T. S. Sudheer *et al.*

[14], has been presented a novel approach for optimal location of the FACTS devices using the sensitivity approach for the enhancement of ATC and VP in deregulated PS. G. Beck, *et al.* [15], has been represented the novel survey for use of FACTS for system performance improvement. C. Vasavi *et al.* [16], has been presented a novel methodology for FACTS placement for maximum power transfer capability and stability in a transmission line.

B. Custom Power Devices (2000-2013)

In[17], Satyaveer Gupt *et al.*, has been presented suggestion on custom power devices for PQ improvement: a review. D. K. Tanti *et al.* [18], has been presented a novel approach on optimal placement of custom power devices in power system network to mitigate voltage sag under faults. K. Hussain and J. Praveen, has been advised on PQ enhancement using VSC based D-STATCOM [19]. Dr. S. S. Kumar *et al.* [20], suggested on Enhancement for PQ in distribution side using CPD.

C. Loadability (2000-2013)

Harjeet Johal [21], has been advised to a novel approach on design considerations for series-connected distributed FACTS converters. Navid Ghaffarzadeh, Haniyeh Marefatjou *et al.* [22], has been proposed to a novel approach on investigation and comparison of the effect of facts devices, capacitors and lines reactance variations on VS improvement and loadability enhancement in two area PS. S. Asha Kiranmai, M. Manjula *et al.* [23], has been suggested on a novel approach on mitigation of various power PQ using unified series shunt compensator on PSCAD/EMTDC. K. Venkateswararao and P. K. Agarwal [24], has been presented to a novel approach on distribution system VP improvement with series FACTS devices using line flow-based equation. J. Sandeep soni, H. P. Agrawal *et al.* [25], has been suggested to a novel approach on potentials and capabilities of FACTS controllers for quality and performance enhancement of PS. M. A. Kamarposhiti and M. Alinezhad [26], has been advised to a novel approach on comparison of SVC and STATCOM in static voltage margin enhancement. B. V. Manikandan, Sathiasamuel Charles Raja *et al.* [27], has been presented to a novel approach on enhancement of available transfer capability with facts device in the competitive power market. Qazi Waqar Ali and Prof. Dr. Azzam ul Asar [28], has been suggested on a novel approach on smart power transmission system using FACTS device. S. N. Singh[29], has been proposed on a novel approach on location UPFC for enhancing PS loadability.

D. Long Duration Variation (2000-2013)

A. Handy, *et al.* [30], has been advised to novel approach on recognition of PQ events using artificial neural networks.

E. Power Factor (2000-2013)

I. K. Kiran and Jaya Laxmi. A [31], has been suggested to a novel approach on shunt versus series compensation in the improvement of PS performance. Jan A. Wiik, Takanori Isobe *et al.* [32], has been technology to a novel approach on feasible series compensation application using magnetic energy recovery switch (MERS). K. K. Pinapatruni and Krishna Mohan L [33], has been advised to novel approach on DQ based control of D-STATCOM for PQ improvement.

F. Power Frequency Variation (2000-2013)

B. K. Prusty and M. Ali [34], has been suggested to a novel approach on PQ issues and its parameters measurement technique with improvement features in a distribution system.

G. Real and Reactive Power (2000-2013)

P. Bapaiah [35], has been suggested to a novel approach on PQ improvement by using DSTATCOM. K. K. Pinapatruni, and K. Mohan L, [36] has been present a novel technology on DQ based control of D-STATCOM for PQ improvement. Saleem Swarupa and V. S. Ramchandra Murthy [37], has been advised to a novel approach on control strategy for UPFC. DIB Djalel, A. Rezaiguia *et al.* [38], has been proposed to a novel approach on improving the electric power by UPFC system in electrical networks. Ashish Jain and Anand Singh [38], has been presented to a novel approach on performance and analysis of FACTS controller SVC and SSSC using MATLAB/Simulink. D. Murali and Dr.M.Rajaram [40], has been suggested to a novel approach on ARPFC using FACTS. Abhishek Kumar, Vinay Kumar Dwivedi *et al.* [41], has been suggested to a novel approach on performance comparisons of control algorithms for load compensation using D-STATCOM under abnormal source voltage. Vinita Vasundhara, Rintu Khanna *et. al.* [42], has been proposed to a novel approach on improvement of PQ by UPQC using different intelligent controls: a literature review. T. Srikanth [43], has been advised to a novel approach on compensating linear and non linear loads using distribution static compensator (D-STATCOM). Snehasish Pal, Suvarun Dalapati *et al.* [44], has been technology to a novel approach on application of multilevel VSC in FACTS devices for PS voltge control and reactive power compensation. K. R. Uyyury and M. K. Mishra [45], has been present a novel methodology on comparison of control strategies for DSTATCOM in power distribution system. RDV Rama Rao and Dr. Subhransu. Sekhar. Dash [46], has been advised to a novel approach on PQ enhancement by unified PQ conditioner using ANN with hysteresis control. K. Kiran, and J. Laxmi. A. [47], has been presented a novel technology on shunt versus series compensation in the improvement of power system performance. B. M. Naveen Kumar Reddy, Mr. G. V. Rajashekhar *et al.* [48], has been suggested to a novel approach on PSS enhancement using SSSC. Gerardo Escobar and Aleksander M. Stankovic [49], has been proposed to a novel approach on an adaptive controller in stationary reference frame for D-STATCOM in unbalance operation. Raju Pandey

and A. K. Kori [50], has been suggested to a novel approach on real and reactive PFC using FACTS connected to a transmission line: a power injection concept. Arvind Kumar Singh, Upendra Prasad *et al.* [51], has been proposed to a novel approach on modeling of single phase UPFC with DC capacitor. M.Prashanthi [52], has been suggested to a novel approach on reduction of reactive power in a disturbance system using D-STATCOM. R. Pandey, and A. K. Kori [53], has been present a novel approach on enhancement of PQ in transmission line using flexible ac transmission system. Miss Sobha rani Injeti and K.Ratna Raju [54], has been proposed to a novel approach on PQ improvement by UPQC device in doubly fed induction generator wind farm to weak-grid connection.

H. Short Duration Variation (2000-2013)

Sudharshan Rao Gandineni and Vijay Kumar K [55], has been proposed to a novel approach on UPQC during voltage sag and swell. Mr. V. Pratapa Rao, Mr. O.Hemakeshavulu [56], has been advised to a novel approach on performance of flexible D-STATCOM as flexible generation in mitigation faults. Dhanorkar Sujata and Himabindu [57], has been suggested a novel approach on voltage sag mitigation analysis using D-STATCOM under different faults in distribution system. Swarupa Pinninti and V. Naga Raju Nayak [58], has been advised to a novel approach on important of PQ using STATCOM applied for grid at various load conditions. C. H. Ram Jethmalani , V. Karthikeyan *et al.* [59], has been suggested to a novel approach on implementation of UPFC for voltage sag mitigation. S. Sundeep and Dr. G. Madhusudhana Rao [60], has been advised to a novel approach on modeling and analysis of custom power devices for improve PQ. Shazly A.Mohammad, Aurelio G. Cerrada [61], has been proposed to a novel approach on conventional DVR for mitigation of voltage sag in power distribution systems. M. Ramadan Sayed, M. A. Moustafa Hassan *et al.* [62], has been advised to a novel approach on PSQ improvement using flexible AC transmission system based on adaptive neuron-fuzzy interface system. D. K.Tanti, M. K.Verma *et al.* [63], has been suggested to a novel approach on optimal placement of custom power devices in PS network to mitigation voltage sag under faults. Ahmad Jamshidi, S. Masoud Barakati *et al.* [64], has been proposed to a novel approach on impact of distribution PFC to improve PQ based on synchronous reference frame method. Ahmad N. Al-Husban [65], has been advised to novel approach on An optimal location of a capacitive reactance compensator in electrical in electric PS.Mohmoud S.Awad [66], has been suggested to a novel approach on review PQ Issues.

I. Transient (2000-2013)

Dr. Tralochan Kaur and Sandeep Kakran [67], has been proposed a novel approach on transient stability improvement of long transmission line system by using SVC. Sidhartha Panda and Ramnarayan N. Patel [68], has been advised a

novel approach on improvement PS transient stability with an off-centre location of shunt FACTS devices. M. Kavitha and N. Ratnakar *et al.* [69], has been suggested a novel approach on integration of FACTS into energy storage system for future PS applications. Salim. Haddad and A. Haddouche *et al.* [70], has been proposed a novel approach on the use of facts devices in DPS -modeling, interface, and case study. Srinivasa Rao and Sivanagaragu *et al.* [71], has been advised a novel approach on comparison of performance of TCPS and SMES in automatic generation control of reheat thermal system. Z. Eleschova *et al.* [72], has been proposed a novel approach on evaluation of PS transient stability and definitition of the basic criterion. S. Muthukrishnan and Dr. A. Nirmal Kumar [73], has been advised to a novel approach on comparison of simulation and experimental results of UPFC used for PQ improvement. Math H.J.Bollen and Yu-Hua Gu[74], has been proposed to a novel approach on categorization and analysis of PS transients. Jignesh S. Patel and Manish N. Sinha [75], has been advised to a novel approach on PS transient stability analysis using ETAP software. K. S. Deshmukh and D. B. Meshram [76], has been proposed to a novel approach on how to improve stability by using FACTS controller. B. Singh, N.K.Sharma, *et al.* [77], has been suggested to a novel approach on a status review of incorporation of FACTS controllers in multi-machine PS for enhancement of damping of PS and voltage stability. A. N. Hussain, F. Malek *et al.* [78], has been proposed to a novel approach on performance improvement of PSS by using multiple damping controllers based on PSS and the UPFC. A. K. Kori and Ratnesh Singh [79], has been advised to a novel approach transient stability and power flow models of STATCOM coordination controllers with ULTC transformer for VS improvement. L. Jin *et al.* [80], has been presented the novel technology on PS transient stability design using reach ability based stability-region computation. K. M. Amirthalingam and R. P. Ramachandran [81], has been suggested to a novel approach on improvement of transient stability of PS using solid state circuit breaker. P. Sunilkumar [82], has been proposed to a novel approach on transient stability enhancement of PS using TCSC.

J. Voltage Fluctuation (2000-2013)

Abdelazeem A and Abdelsalam *et al.* [83], has been proposed to a novel approach on PQ Improvement using FACTS power filter compensation scheme. Jyothil Nayak Bharothu and K Lalitha [84], has been advised to a novel approach on compensation of voltage flicker by using facts devices. R. Vijayakumar and R.Subramanian [85], has been suggested to novel approach on compensation of voltage variation in distribution system by using DVR based separate energy storage devices. Vasudeo B. Virulkar and Mohan V. Aware [86], has been advised to a novel approaches on modeling and control of D-STATCOM with BESS for mitigation of flicker. Xiao-Yuan Chen and Jian-Xun *et al.* [87], has been proposed to a novel approaches on high temperature superconducting magnetic energy storage and its power control technology.

Sugain P.R and Dr. T. Ruban Deva Prakash *et al.* [88], has been proposed a novel approach on ANN based voltage flicker mitigation with UPFC using SRF algorithm. Sai Kiran Kumar, Sivakoti and Y. Naveen Kumar *et al.* [89], has been advised a novel approach on PQ improvement in distribution system using D-STATCOM in transmission lines.

K. Voltage Stability (2001-2013)

M. Noroozian and C. W. Taylor [90], has been presented a novel approach on benefits of SVC and STATCOM for electric utility application. B. Singh [91], has been presented a application of FACTS controller in PS for enhance the PS stability: a state-of-the-art. M. S. H. Lipu and T. Karim [92], has been presented a novel approach on effectiveness of FACTS controllers and HVDC transmissions for improving PSS and increasing power transmission capability. B. Singh, *et al.* [93], has been presented a comprehensive survey of optimal placement and coordination control techniques of FACTS controllers in multi-machine PS environments. DJJ Djalel, A. Rezaiguia *et al.* [94], has been advised a novel approach on improving the electric PQ by UPFC systems in electrical networks. S. Jalilzadeh, M. Darabian *et al.* [95], has been suggested a novel approach on PSS improvement via TCSC controller employing a multi-objective strength praeator evolutionary algorithm approach. P. Suman Pramod Kumar, N. Vijaysimha *et al.* [96], has been presented a novel approach on static synchronous series compensator for series compensation of EHV transmission line. Amim Safari [97], has been advised a novel approach on optimal design of POD controller for FACTS devices in interconnected PS. G.Naveen Kumar, M. Surya Kalavathi *et al.* [98], has been suggested a novel approach on optimal placement of SVC STATCOM for voltage stability enhancement under contingency using cat swarm optimization. A. Elkholly, F.H.Fahmy *et al.* [99], has been presented a novel approach on PSS enhancement using the UPFC. M. A. Abido [100], has been advised a novel approach on PSS enhancement using FACTS controller: a review. Prof. P. Venkat Kishore and Dr. S. Rama Reddy [101], has been suggested a novel approach on modeling and simulation of fourteen bus system employing D-STATCOM for PQ improvement. Ashish Choubey and Deepa Choudhary [102], has been suggested a novel approach on voltage stability with the help of STATCOM. S. Sowjanya and Prof. J. Srinivasarao [103], has been suggested a novel approach on design of FACTS device for the improvement of PSS using mathematical matching controller. Alok Kumar Mohanty and Amar Kumar Barik [104], has been advised to a novel approach on PSS improvement using FACTS devices. P. R. Sharma and Ashok Kumar *et al.* [105], has been suggested a novel approach on optimal location for shunt connected FACTS devices in a series compensated long transmission line. Aarti Rai [106], has been advised a novel approach on enhancement of voltage stability and reactive power control of distribution system using facts devices. J. Sandeep and H. P.

Agarwal *et al.* [107], has been suggested a novel approached on potential and capabilities of FACTS controllers for quality and performance enhancement of PS. Sangram Keshori Mohapatra and Sidharth Panda [108], has been advised a novel approached on stability improvement by SSSC and STATCOM based damping controller employing differential evolution algorithm. E. S. Ali and S. M. Abd-Elazim [109], has been proposed a novel approached on bacteria foraging: a new technique for optimal design of FACTS controller to enhance PS stability. Alok Kumar and Surya Bhushan Dubey [110], has been suggested a novel approached on enhancement of transient stability in transmission line using SVC FACTS controller. Satvinder Singh and Atma Ram *et al.* [111], has been proposed a novel approached on transient stability enhancement of multi-machine system using FACTS controllers. H. B. Nagesh and P. S. Puttaswamy [112], has been advised to a novel approached on enhancement of voltage stability margin using FACTS controllers.

L. Voltage Unbalance (2000-2013)

I.Parveena and M.Mahendran [113], has been presented a novel approach on the compensation unbalanced 3 phase currents in transmission system on UPFC. Navid Khorrami [114], has been advised a novel approach on analyzing of dynamic voltage restorer in series compensation voltage. Kein Huat Chua, *et al.* [115], has been proposed a novel approach on voltage unbalance mitigation in low voltage distribution network with photovoltaic systems.

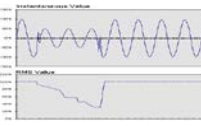
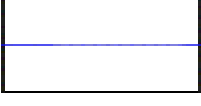
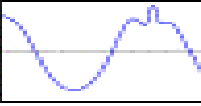
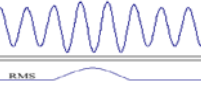
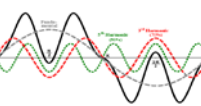
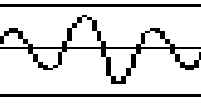
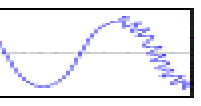
M. Waveform Distortion (2000-2013)

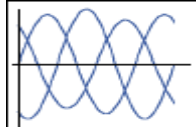
E.Rambabu, *et al.* [116], has been reported a novel approach on mitigation of harmonics in distribution system using D-STATCOM.

H.Dag *et al.* [117], has been present the novel approach for the application of series and shunt compensation to turkish national power transmission system to improve system loadability. L. Gyugyi *et al.* [118], has been present the novel methodology for static synchronous series compensator: a solid-state approach to the series compensation of transmission line. M.H.H.A. Shayanfar, and M. F. Firuzabad [119], has been present the novel technology for modeling of series and shunt distribution FACTS devices in distribution system load flow.

III. POWER QUALITY PROBLEMS

The details of the following PQ problems and relevant waveforms are discussed in this table as follows:

| | | |
|--------------------------|---|--|
| Voltage sag(or dip) |  | Description: A decrease of the normal voltage level between 10 and 90% of the nominal rms voltage at the power frequency, for durations of 0,5 cycle to 1 minute. Causes: Since the electric motors draw more current when they are starting than when they are running at their rated speed, starting an electric motor can be a reason of a voltage sag. When a line-to-ground fault occurs, there will be a voltage sag until the protective switch gear operates. Sudden load changes or excessive loads can cause a voltage sag. Consequences: Malfunction of information technology equipment, namely microprocessor-based control systems (PCs, PLCs, ASDs, etc) that may lead to a process stoppage. Tripping of contactors and electromechanical relays. Disconnection and loss of efficiency in electric rotating machines. |
| Very short interruptions |  | Description: Total interruption of electrical supply for duration from few milliseconds to one or two seconds. Causes: Mainly due to the opening and automatic reclosure of protection devices to decommission a faulty section of the network. The main fault causes are insulation failure, lightning and insulator flashover. Consequences: Tripping of protection devices, loss of information and malfunction of data processing equipment. Stoppage of sensitive equipment, such as ASDs, PCs, PLCs, if they're not prepared to deal with this situation. |
| Long interruptions |  | Description: Total interruption of electrical supply for duration greater than 1 to 2 seconds. Causes: Equipment failure in the power system network, storms and objects (trees, cars, etc) striking lines or poles, fire, human error, bad coordination or failure of protection devices. Consequences: Stoppage of all equipment. |
| Voltage spike |  | Description: Very fast variation of the voltage value for durations from a several microseconds to few milliseconds. These variations may reach thousands of volts, even in low voltage. Causes: Lightning, switching of lines or power factor correction capacitors, disconnection of heavy loads. Consequences: Destruction of components (particularly electronic components) and of insulation materials, data processing errors or data loss, electromagnetic interference. |
| Voltage swell |  | Description: Momentary increase of the voltage, at the power frequency, outside the normal tolerances, with duration of more than one cycle and typically less than a few seconds. Causes: Start/stop of heavy loads, badly dimensioned power sources, badly regulated transformers (mainly during off-peak hours). Consequences: Data loss, flickering of lighting and screens, stoppage or damage of sensitive equipment, if the voltage values are too high. |
| Harmonic distortion |  | Description: Voltage or current waveforms assume non-sinusoidal shape. The waveform corresponds to the sum of different sine-waves with different magnitude and phase, having frequencies that are multiples of power-system frequency. Causes: <i>Classic sources:</i> electric machines working above the knee of the magnetization curve (magnetic saturation), arc furnaces, welding machines, rectifiers, and DC brush motors. <i>Modern sources:</i> all non-linear loads, such as power electronics equipment including ASDs, switched mode power supplies, data processing equipment, high efficiency lighting. Consequences: Increased probability in occurrence of resonance, neutral overload in 3-phase systems, overheating of all cables and equipment, loss of efficiency in electric machines, electromagnetic interference with communication systems, errors in measures when using average reading meters, nuisance tripping of thermal protections. |
| Voltage fluctuation |  | Description: Oscillation of voltage value, amplitude modulated by a signal with frequency of 0 to 30 Hz. Causes: Arc furnaces, frequent start/stop of electric motors (for instance elevators), oscillating loads. Consequences: Most consequences are common to undervoltages. The most perceptible consequence is the flickering of lighting and screens, giving the impression of unsteadiness of visual perception. |
| Noise |  | Description: Superimposing of high frequency signals on the waveform of the power-system frequency. Causes: Electromagnetic interferences provoked by Hertzian waves such as microwaves, television diffusion, and radiation due to welding machines, arc furnaces, and electronic equipment. Improper grounding may also be a cause. |

| | | |
|-------------------|---|---|
| | | Consequences: Disturbances on sensitive electronic equipment, usually not destructive. May cause data loss and data processing errors. |
| Voltage Unbalance |  | Description: A voltage variation in a three-phase system in which the three voltage magnitudes or the phase angle differences between them are not equal. Causes: Large single-phase loads (induction furnaces, traction loads), incorrect distribution of all single-phase loads by the three phases of the system (this may be also due to a fault). Consequences: Unbalanced systems imply the existence of a negative sequence that is harmful to all three-phase loads. The most affected loads are three-phase induction machines. |

IV. SUMMARY OF THE PAPER

Table.1 Summary of Literature Reviewed from Electrical Power Quality View points

The summary of literature reviewed regarding with PQ problems and its solutions. So that the FACTS controllers are best solution for this problems. The FACTS controller such as series, series-series, series-shunt, FACTS controllers in power system network are discussed with respect to PQ problems in table 1.

| AUTHORS | PARAMETERS (YEARS) | PERFORMANCE PARAMETER |
|--|--------------------------------------|--|
| G. Vishwakarma <i>et al.</i> ; Molla Shahadat Hossain Lipu <i>et al.</i> ; M.Bhanu Siva <i>et al.</i> ; I.Kumaraswamy <i>et al.</i> ; V.G.Mathad <i>et al.</i> ; M. A. Gargeya; J.Namratha Manohar <i>et al.</i> ; T.A.R. Kumaar <i>et al.</i> ; T. S. Sudheer <i>et al.</i> ; G.Beck <i>et al.</i> ; C. Vasavi <i>et al.</i> | Capability(2000-2013) | Voltage Profile[6], Power transmission Stability and Capability[7], Power Quality Improvement[8], Amelioration of Power Quality[9], Power system stability enhancement[10], Power quality problems[11], Static analysis of Power system[12], Power system security enhancement[13], Voltage profile in deregulated Power system[14], Power system performance improvement[15], Power transfer capability and stability[16] |
| Satyaveer Gupt <i>et al.</i> ; D. K. Tanti <i>et al.</i> ; K. Hussain <i>et al.</i> ; Dr. S. S. Kumar <i>et al.</i> | Custom Power Device(2000-2013) | Custom power devices for power quality improvement[17], optimal placement of custom power devices[18], power quality enhancement[19], distribution using custom power device[20] |
| H. Johal <i>et al.</i> ; N. Ghaffarzadeh <i>et al.</i> ; S. A. Kiranmai <i>et al.</i> ; K. Venkateswararao <i>et al.</i> ; J. S. Soni <i>et al.</i> ; M. A. Kamarpushti <i>et al.</i> ; B. V. Manikandan <i>et al.</i> ; E. Q. W. Ali <i>et al.</i> ; S. N. Singh <i>et al.</i> | Loadability(2000-2013) | Design consideration for series FACTS[21], voltage stability improvement and loadability enhancement[22], Mitigation of various power quality problems[23], Distribution system voltage profile improvement[24], Potentials and capabilities of FACTS controller[25], Comparison of SVC and STATCOM[26], Enhancement of available transfer capability[27], Smart Power Transmission System using FACTS device[28], enhancing power system loadability[29]. |
| Amany Handy <i>et al.</i> | Long duration variation(2000-2013) | Recognition of Power Quality Events[30] |
| Irinjila Kranti Kiran <i>et al.</i> ; JanA.Wiik <i>et al.</i> ; Kiran Kumar Pinapatruni <i>et al.</i> | Power Factor(2000-2013) | improvement of Power System Performance[31], Feasible Series Compensation Applications[32], DSTATCOM for Power Quality Improvement[33] |
| B.K.Prusty <i>et al.</i> | Power Frequency Variation(2000-2013) | Power Quality Issue and its Parameters Measurment[34]. |
| P.Bapaiah; K. K. Pinapatruni <i>et al.</i> ; Seelam Swarupa <i>et al.</i> ; DIB Djalel <i>et al.</i> ; Mr.Ashish <i>et al.</i> ; D.Murali <i>et al.</i> ; Abhishek Kumar <i>et al.</i> ; Vinita Vasundhara <i>et al.</i> ; T.Srikanth <i>et al.</i> ; Snehasish Pal <i>et al.</i> ; K. R. Uyyuru <i>et al.</i> ; RVD Rama Rao <i>et al.</i> ; I. K. Kiran <i>et al.</i> ; B.M.N.K.Reddy <i>et al.</i> ; G.Escobar <i>et al.</i> ; R.Pandey <i>et al.</i> ; Dr.A.K.Singh <i>et al.</i> ; M. Prashanthi <i>et al.</i> ; R. Pandey <i>et al.</i> ; Miss.S. R.Injeti <i>et al.</i> | Real and Reactive power(2000-2013) | Power Quality Improvement by using DSTATCOM[35], DQ based control of DSTATCOM[36], Control Strategy for Unified Power Flow Controller[37], Improving the Electric Power Quality[38], Performance and analysis of FACTS[39], Active and Reactive Power Flow Control[40], Performance Comparision of Control Algorithms for Load Compensation[41], Improvement of power Quality by UPQC[42], Compensation linear and non linear loads[43], multilevel source converter for power system voltage control and reactive power[44], Comparison of Control strategies for DSTATCOM[45], power quality enhancement by UPQC[46], Shunt versus series compensation[47], power system stability enhancement by SSSC[48], DSTATCOM in unbalance operation[49], real and reactive power flow control[50], modeling of single phase UPFC[51], Reduction of Reactive Power in a Disturbance System[52], Enhancement of power quality in transmission line[53], Power Quality improvement by UPQC in doubly fed induction generator[54]. |
| Sudarshan Rao Gandineni <i>et al.</i> ; Mr.V.Ratappa Rao <i>et al.</i> ; Dhanorkar Sujata <i>et al.</i> ; Swarupa Pinninti <i>et al.</i> ; C.H.Ram Jethmalani <i>et al.</i> ; S.Sundeep <i>et al.</i> ; Shazly A.Mohammed <i>et al.</i> ; M.Ramadan Sayed <i>et al.</i> ; D.K.Tanti <i>et al.</i> ; Ahmad Jamshidi <i>et al.</i> ; Ahmad N.Al-Husban <i>et al.</i> ; Mahmoud S.Awad <i>et al.</i> | Short duration variation(2000-2013) | UPQC during voltage sag and swell[55], flexible distributed generation in mitigation fault[56], voltage sag mitigation[57], STATCOM applied for grid[58], implementation of UPQC[59], modeling and analysis [60], DVR for mitigation voltage sag[61], FACTS based on neuro-fuzzy[62], optimum placement of custom power device[63], impact of distribution[64], optimum location of capacitive reactance[65], power quality issues[66]. |
| Dr. Tarlochan Kaur <i>et al.</i> ; Siddharth Panda <i>et al.</i> ; M. Kavitha <i>et al.</i> ; Salim. Haddad <i>et al.</i> ; Srinivasa Rao <i>et al.</i> ; Z.Eleschova <i>et al.</i> ; S.Muthukrishnan <i>et al.</i> ; Math. H.J.Bollen <i>et al.</i> ; Jigneh S.Patel <i>et al.</i> ; Kirti S.Deshmukh <i>et al.</i> ; Bindeshwar Singh <i>et al.</i> ; A.N.Hussain <i>et al.</i> ; A.K.Kori <i>et al.</i> ; Licheng Jin <i>et al.</i> ; Kalai Murugan Amirthalingam <i>et al.</i> ; P.Sunilkumar. | Transient(2000-1013) | Transient stability improvement[67], improving power system transient stability[68], integration of FACTS[69], power system modeling interface[70], comparison of performance of TCPS and SMES[71], evaluation of power system transient stability[72], comparison of simulation and experimental[73], categorization and analysis of power system transient[74], transient stability analysis using ETAP[75], how to improve stability[76], damping of power system and voltage stability[77], performance improvement of power system stability[78], transient stability and power flow models[79], power system transient stability design[80], improvement of transient stability using solid state circuit breaker[81], transient stability using TCSC[82]. |
| Abdelazeem A <i>et al.</i> ; Jyothil Nayak Bharothu <i>et al.</i> ; R.Vijayakumar <i>et al.</i> ; Vasudeva B.Virulkar <i>et al.</i> ; Xiao-Yuan Chen <i>et al.</i> ; Sugun P.R <i>et al.</i> ; Sai Kiran Kumar.Sivakoti <i>et al.</i> | Voltage Fluctuation(2000-2013) | Power quality improvement using FACTS[83], compensation of voltage flicker[84], compensation of voltage variation[85], modeling and control of DSTATCOM[86], high temperature superconducting magnetoe energy[87], voltage flicker mitigation[88], power quality improvement using DSTATCOM[89]. |

| | | |
|---|--------------------------------|--|
| M.Noroozian <i>et al.</i> ; Bindeshwar singh; Molla Shahadat Hossain Lipu <i>et al.</i> ; Bindeshwar Singh <i>et al.</i> ; DIB Djalel <i>et al.</i> ; S.Jalilzadeh <i>et al.</i> ; P.Suman Pramod Kumar <i>et al.</i> ; Amin Safari; G.Naveen Kumar <i>et al.</i> ; A.Elkholy <i>et al.</i> ; M A. Abido <i>et al.</i> ; Prof. P.Venkat Kishore <i>et al.</i> ; Ashish Choubey <i>et al.</i> ; S.Sowjanya <i>et al.</i> ; Alok Kumar Mohanty <i>et al.</i> ; P.R.Sharma <i>et al.</i> ; Aarti Rai; J.Sandeep Soni <i>et al.</i> ; Sangram Keshori Mohapatra <i>et al.</i> ; E.S.Ali <i>et al.</i> ; Alok Kumar <i>et al.</i> ; Satvinder Singh <i>et al.</i> ; H.B.Nagesh <i>et al.</i> | Voltage Stability(2000-2013) | Benefits of SVC and STATCOM[90], Application of FACTS[91], effectiveness of FACTS controller[92]. A comprehensive survey[93], Improving the electric power quality[94], power system stability improvement via TCSC[95], SSSC for EHV transmission line[96], optimum design for FACTS device interconnected[97], voltage stability enhancement under contingency[98], power system stability enhancement using UPFC[99], power system stability using FACTS[100], modeling and simulation of fourteen bus[101], voltage stability using STATCOM[102], power system stability improvement using mathematical matching controller[103], power system stability improvement using FACTS[104], optimum location for shunt connected FACTS[105], enhancement of voltage and reactive power[106], potentials and capability of FACTS[107], stability improvement by SSSC and STATCOM[108], a new technique for optimal design of FACTS[109], enhancement of transient stability[110], transient stability enhancement of multi-machine[111], enhancement of voltage stability margin[112]. |
| I.Parveena <i>et al.</i> ; Navid Khorrami <i>et al.</i> ; Kein Huat Chua <i>et al.</i> ; | Voltage Unbalance(2000-2013) | Compensation of unbalance three phase transmission system[113], analysis of dynamic voltage restorer[114], voltage unbalance mitigation[115] |
| E.Rambabu <i>et al.</i> | Waveform distortion(2000-2013) | Mitigation of harmonics in distribution system[116]. |

V. SOLUTION OF BOTH SIDE OF THE METER

| Disturbance | Possible causes | Utility-Side Solution | Customer- Side Solution |
|---------------------|---|---|---|
| Voltage Sag | • Lightning strike • Tree or animal contact with lines | • Dynamic voltage restorer • Static condenser | • Line conditioner • Uninterruptible power supply |
| Overvoltage | • Fault on another phase • Load rejection | • Dynamic voltage restorer • Fault current limiter • High-energy surge arrester | • Line conditioner • Voltage regulator • Uninterruptible power supply |
| Interruption | • Blown fuse • Breaker operation in response to fault | • Solid-state circuit breaker • Static condenser | • Uninterruptible power supply • Motor-generator set |
| Transient | • Lightning strike • Utility switching | • High-energy surge arrester | • Line conditioner • Surge suppressor |
| Harmonic distortion | • Nonlinear loads • Ferroresonance | • Filter • Static condenser • Dynamic voltage restorer | • Line conditioner • Filter |
| Electric noise | • Improper customer wiring or grounding | | • Grounding and shielding • Line conditioner • Filter |

1. Energy Storage System

(A) Flywheels: A flywheel is an electromechanical device that couples a rotating electric machine (motor/generator) with a rotating mass to store energy for short durations. The motor/generator draws power provided by the grid to keep the rotor of the flywheel spinning. During a power disturbance, the kinetic energy stored in the rotor is transformed to DC electric energy by the generator, and the energy is delivered at a constant frequency and voltage through an inverter and a control system.

(B) Supercapacitors: Supercapacitors (also known as ultracapacitors) are DC energy sources and must be interfaced to the electric grid with a static power conditioner, providing energy output at the grid frequency. A supercapacitor provides power during short duration interruptions or voltage sags.

(C) Superconducting Magnetic Energy Storage(SMES):

A magnetic field is created by circulating a DC current in a closed coil of superconducting wire. The path of the coil circulating current can be opened with a solid-state switch, which is modulated on and off. Due to the high inductance of the coil, when the switch is off (open), the magnetic coil behaves as a current source and will force current into the power converter which will charge to some voltage level. Proper modulation of the solid-state switch can hold the voltage within the proper operating range of the inverter, which converts the DC voltage into AC power.

2. Distributed Generations

Distributed Generation (DG) units can be used to provide clean power to critical loads, isolating them from disturbances with origin in the grid. DG units can also be used as backup generators to assure energy supply to critical

loads during sustained outages. Additionally DG units can be used for load management purposed to decrease the peak demand. Distributed generation is defined as a generation with a limited size (roughly 10MW or less), which is interconnected at the substation, distribution feeder or customer load levels. DG technologies include wind turbines (WT), photovoltaics (PV), gas turbines (GT), micro turbines (MT) and internal combustion (IC) engine, and so on.

3. Enhanced Interface Devices

(A) Dynamic Voltage Restorer:

A dynamic voltage restorer (DVR) acts like a voltage source connected in series with the load. The output voltage of the DVR is kept approximately constant voltage at the load terminals by using a step-up transformer and/or stored energy to inject active and reactive power in the output supply trough a voltage converter.

(B) Transient Voltage Surge suppressors (TVSS):

Transient voltage surge suppressors are used as interface between the power source and sensitive loads, so that the transient voltage is clamped by the TVSS before it reaches the load. TVSSs usually contain a component with a nonlinear resistance (a metal oxide varistor or a zener diode) that limits excessive line voltage and conduct any excess impulse energy to ground.

(C) Constant Voltage Transformer:

Constant voltage transformers (CVT) were one of the first PQ solutions used to mitigate the effects of voltage sags and transients. To maintain the voltage constant, they use two principles that are normally avoided: resonance and core saturation.

(D) Noise filters:

Noise filters are used to avoid unwanted frequency current or voltage signals (noise) from reaching sensitive equipment. This can be accomplished by using a combination of capacitors and inductances that creates a low impedance path to the fundamental frequency and high impedance to higher frequencies, that is, a low-pass filter. They should be used when noise with frequency in the kHz range is considerable.

(E) Isolation Transformers:

Isolation transformers are used to isolate sensitive loads from transients and noise deriving from the mains. In some cases (Delta-Wye connection) isolation transformers keep harmonic currents generated by loads from getting upstream the transformer.

(F) Static VAR compensators:

Static VAR compensators (SVC) use a combination of capacitors and reactors to regulate the voltage quickly. Solid-state switches control the insertion of the capacitors and reactors at the right magnitude to prevent the voltage from fluctuating. The main application of SVC is the voltage regulation in high voltage and the elimination of flicker caused by large loads (such as induction furnaces).

(G) Harmonic Filters:

Harmonic filters are used to reduce undesirable harmonics. They can be divided in two groups: passive filters and active filters.

VI. POWER QUALITY CODES AND STANDARDS

Below is a list of the most commonly used standards and recommendations used in the field of power quality within the European community and USA.

- i. **EN 50 160 (2000)** 'Voltage characteristics of electricity supplied by public distribution systems'.
- ii. **EN 61000-2-2 (1993)** EMC Environment section. 'Compatibility levels for low-frequency conducted disturbances and signalling in public LV power supply systems'.
- iii. **EN 61000-3-2 (1999)** EMC Limits. 'Limits for harmonic current emissions (Equipment input current less than or equal to 16 A per phase)'.
- iv. **EN 61000-3-3 (1998)** EMC Limits. 'Limitation of voltage fluctuations and flicker in low voltage supply systems for equipment with rated current less than or equal to 16A'.
- v. **EN 61000-3-4 (1998)** EMC Limits. 'Limits for harmonic current emissions (Equipment input current greater than 16 A per phase)'.
- vi. **EN 61000-3-5 (1994)** EMC Limits. 'Limitation of voltage fluctuations and flicker in low voltage supply systems for equipment with rated current greater than 16A'.
- vii. **EN 61000-3-6 (1996)** EMC Limits. 'Assessment of emission limits for distorting loads in MV and HV power systems'.
- viii. **EN 61000-4-7 (1995)** 'EMC testing and measurement techniques-General guide on harmonics and inter harmonics measurements and instrumentation, for power supply systems and equipment connected thereto'.
- ix. **EN 61000-4-11 (1994)** 'EMC testing and measurement techniques-Voltage dips, short interruptions and voltage variation immunity tests'.
- x. **IEEE 446 (1995)** 'Recommended practice for emergency and standby power systems for industrial and commercial applications-IEEE orange book'.
- xi. **IEEE 519 (1992)** 'Recommended practice and requirements for harmonic control in electrical power system'.
- xii. **IEEE 1100 (1993)** 'Recommended practice for powering and grounding electronic equipment- IEEE Emerald Book'.
- xiii. **IEEE 1159 (1995)** 'Recommended practice for monitoring electric power quality'.
- xiv. **IEEE 1250 (1990)** 'Guide for service to equipment sensitive to momentary voltage disturbances'.
- xv. **IEEE 1346 (1998)** 'Recommended practice for evaluating electric power system compatibility with electronic process equipment'.

VII. CONCLUSIONS

This paper presents a survey on PQ problems & its solution follows: The PQ problem such as voltage fluctuation, frequency, harmonics etc. can be solved by using FACTS controller such as SVC, TCSC, SSSC, STATCOM, DSTATCOM, UPFC, IPFC, GUPFC, HPFC, GIPFC, TCPAR. Finally it is concluded that the most powerful and versatile FACTS controller from enhancement of power quality parameters are STATCOM & DSTATCOM, are utilized in the system. Also discuss some power quality standards in this paper.

VIII. ACKNOWLEDGMENT

The authors would like to thank Dr. K.S. Verma, Dr. R. P. Payasi, and Dr. D. Singh, Kamala Nehru Institute of Technology, Sultanpur, U.P., 228118, India, for their valuable suggestions regarding A power quality problems in power system environments.

IX. REFERENCES

- [1] A.rada krishna, CH. K. Rama Krishna Reddy, International Journal of Engineering Trends and Technology, vol. 4 issue 5, May 2013.
- [2] S. Khalid, Bharti Dwivedi, International Journal of Advances in Engineering & Technology, vol. 1, Issue 2, pp. 1-11 May 2011.
- [3] S. Nilsson, "Special application considerations for Custom Power systems," in Proc. IEEE Power Eng. Soc., Winter Meeting 1999, vol. 2, 1999, pp. 1127-1130.
- [4] G. Venkataraman and B. Johnson, "A pulse width modulated power line conditioner for sensitive load centers," *IEEE Trans. Power Delivery*, vol. 12, pp. 844-849, Apr. 1997.
- [5] J. O. Q. Tande 'Applying Power Quality Characteristics of wind turbine for Assessing impact on Voltage Quality', Wind Energy, pp 52, 2002.
- [6] G. Vishwakarma, and N. Saxena, "Enhancement of Voltage Profile by using FC-TCR," *International Journal of Electrical, Electronics and Computer Engineering*, vol. 2, Issue 2, pp. 18-22, 2013.
- [7] Molla Shahadat Hossain Lipu, and Tahia Fahrin Karim, "Effectiveness of FACTS controllers and HVDC transmissions for improving power system stability and increasing power transmission capability," *International Journal of Energy and Power Engineering*, vol.2, Issue 4, pp. 154-163, 2013.
- [8] M.Bhanu Siva, M.R.P Reddy, and Ch.Rambabu, "power quality improvement of three-phase for – wire DSTATCOM with fuzzy logic controller," *International Journal of Computer Science and Information Technologies*, vol.2, Issue 5, pp.2273-2276, 2011.
- [9] I.Kumaraswamy, W.V.Jahnavi, and P.Ramesh, "Amelioration of Power Quality in Isolated Power System," *International Journal of Scientific and Research Publications*, vol. 2, Issue 4, April 2012.
- [10] V.G.Mathad, B.F.Ronad, and S.H. Jangamshetti, "review on comparison of FACTS controllers for power system stability enhancement," *International Journal of Scientific and Research Publications*, vol. 3, Issue 3, March 2013.
- [11] M. A. Gargeya, "A New Proposal for Mitigation of Power Quality Problems Using D-STATCOM," *International Journal of Scientific Engineering and Technology*, vol. 2, Issue 5, pp. 317-321, May 2013.
- [12] J.Namratha Manohar, and J. Amarnath, "Statistical Analysis of Power System on enhancement of Available Transfer Capability Applying FACTS," *International Journal of Multidisciplinary Science and Engineering*, vol. 3, no. 7, July 2012.
- [13] T.A.R. Kumaar, and I.A. Chidambaram, "Power System Security Enhancement using FACTS devices in a Power system network with voltage dependent loads and ZIP loads," *International Journal of Computer Applications*, vol. 45, no. 4, May 2012.
- [14] T. S. Sudheer, J. S. Rao, and J. Amarnath, "Optimal Location of the Facts Devices using the Sensitivity Approach for the Enhancement of ATC and Voltage Profile in Deregulated Power System," *International Journal of Computer Applications*, vol. 76, no.10, August 2013.
- [15] G.Beck, W. Breuer, D. Povh, and D.Retzmann, "Use of FACTS for System Performance Improvement," *CEPSI Conference*, 6-10 November 2006.
- [16] C. Vasavi, and Dr. T. G. Manohar, "Facts Placement for Maximum Power Transfer Capability and Stability in a Transmission Line," *International Journal of Computational Engineering Research*, vol. 2, issue. 7, Nov. 2012.
- [17] Satyadeep Gupta, Ankit Dixit, Nikhil Mishra and S. P. Singh, "Custom power devices for power quality improvement: A review," *International journal of research in engineering & applied science*, vol. 2, issue-2, pp. 1646-1659, Feb. 2012.
- [18] D. K. Tanti, M.K. Verma, Brijesh Singh and O.N. Mehrotra, "optimal placement of custom power devices in power system network to mitigate voltage sag under faults," *International journal of power electronics and drive system*, vol. 2, no. 3, pp. 267-276, sept. 2012.
- [19] K. Hussain and J. Praveen, "Power quality enhancement using VSC based DSTATCOM," *International journal of engineering and technology*, vol. 2, no. 1, pp. 93-98, Jan. 2012.
- [20] Dr. S. S. Kumar, M. Kalyansundaram and Ammu Wilson, "Enhancement for power quality in distribution side using custom power devices," *IOSR journal of electrical and electronics engineering*, vol. 5, issue 6, pp. 81-87, May-Jun 2013.
- [21] H. Johal, and D. Divan, "Design consideration for series-connected FACTS converters," *IEEE transaction on industry application*, vol. 43, no. 6, Nov./Dec. 2007.
- [22] N. Ghaffarzadeh, H. Marefatjou, and I. Soltau, "Investigation and comparison of the effect of FACT devices, capacitors and line reactance variation on voltage stability improvement and loadability enhancement in two area power system," *International Journal of Applied Power Engineering*, vol. 1, no. 3, pp. 145-158, December 2012.
- [23] S. A. Kiranmai, M. Manjula, and A. V. R. S. Sarma, "Mitigation of various power quality problems using unified series shunt compensator in PSCAD/EMTDC," *16th National power system conference*, pp. 192-197, 15-17 December 2010.
- [24] K. Venkateswararao, and P. K. Agrawal, "Distribution system voltage profile improvement with series FACTS devices using line flow based equations," *16th National power system conference*, pp. 386-392, 15-17 December 2010.
- [25] J. S. Soni, H. P. Agrawal, R. Gupta, and H.O. Bansal, "Potentials and capabilities of FACTS controller for quality and performance enhancement of power system," *International Journal of Innovative Technology and exploring Engineering*, vol. 2, issue. 4, March 2013.
- [26] M. A. Kamarposhiti, and M. Alinezhad, "Comparison of SVC and STATCOM in static voltage stability margin enhancement," *World academy of science, Engineering and Technology*, pp. 860-865, 2009.
- [27] B. V. Manikandan, S. C. Raja, and P. Venkatesh, "Enhancement of available transfer capability with FACTS device in the competitive power market," *Science Research*, vol. 2, pp. 337-343, 2010.
- [28] E. Q. W. Ali, and Prof. A. ul Asar, "Smart Power Transmission System using FACTS device," *International Journal of Engineering & Computer Science*, vol. 12, no. 6, pp. 14-20, 2012.
- [29] S. N. Singh, and I. Erlich, "Locating Unified power flow controller for enhancing power system loadability," *IEEE*.
- [30] Amany Handly, Almotar Y.Abdelaziz and Mohamed Abd El-Latif Badi, "Recognition of Power Quality Events Using Artificial Neural Networks," *International Journal on Power Engineering and Energy*, vol. 4, issue. 1, Jan 2013.
- [31] Irinjila Kranti Kiran and Jaya Laxmi,A, "Shunt versus Series Compensation in the improvement of Power System Performance," *International Journal of Applied Engineering Research*, vol. 2, issue. 1, 2011.
- [32] Jan.Wiik, Takanori Isobe, Taku Takaku, F.Danang Wijaya and Kazuhiro Usuki, "Feasible Series Compensation Applications using Magnetic Energy Recovery Switch (MERS)," *IEEE*, 2010.
- [33] Kiran Kumar Pinapaturi and Krishna Mohan L, "DQ based Control of DSTATCOM for Power Quality Improvement," *VSRD International Journal of Electrical,Electronics and Communication Engineering*, vol. 2, issue. 5, 2012.
- [34] B.K.Prusty and S.M.Ali, "Power Quality Issues and its Parameters Measurment Technique with Improvement Features in a Distribution System," *special Issue of International Journal on Advanced Computer Theory and Engineering*, vol. 2, issue. 1, 2013.
- [35] P.Bapaiah, "Power Quality Improvement by using DSTATCOM," *International Journal of Emerging Trends in Electrical and Electronics*, vol. 2, issue. 4, April 2013.
- [36] K. K. Pinapaturi, and K. Mohan L, "DQ based control of DSTATCOM for power quality improvement," *VSRD International Journal of Electrical, Electronics & Communication Engineering*, vol. 2, Issue. 5, pp. 207-227, 2012.
- [37] Seelam Swarupa and K.S.Ramachandra Murthy, "Control Strategy for Unified Power Flow Controller," *IJETEE*, vol. 2, issue. 1, April 2013.
- [38] DIB Djalel, A.Rezaiguia and Z.Abada, "Improving the Electric Power Quality by UPFC System Electrical Network," *IJ of Energy*, vol. 6, issue. 4, 2012.
- [39] Mr.Ashish Jain and Asst.Prof.Anand Singh, "Performance and analysis of FACTS Controller Using MATLAB/Simulink," *IJARCSEE*, vol. 2, issue. 1, Jan 2013.
- [40] D.Murali and Dr.M.Rajaram, "Active and Reactive Power Flow Control using FACTS Device," *IJ of Computer Applications*, vol. 9, issue. 8, Nov 2010.
- [41] Abhishek Kumar, Vijay Kumar Dwivedi, Santanu Maity and Mohit Bajaj, "Performance Comparison of Control Algorithms for Load Compensation Using Abnormal Source Voltage," *Journal of Automation and Control Engineering*, vol. 2, issue. 1, March 2013.
- [42] Vinita Vasundhara , Ritika khanna and Manoj Kumar, "Improvementof power Quality by UPQC Using Different Intelligent Controls:A Literature," *IJRTE*, vol. 2, issue. 1, March 2013.
- [43] T.Srikanth, "Compensation linear and non linear loads using distribution static compensator (DSTATCOM)," *J.Electrical.Eng.Res.*, vol. 5, issue. 2, Aug 2013.
- [44] Snehasish Pal, Suvarun Dalpati and N.C.Ganguly, "Application of Multilevel-Source-Converter in FACTS Devices for Power System Voltage Control and Reactive Power Compensation," *IJMER*, vol. 2, issue. 6, Dec 2012.
- [45] K. R. Uyyuru, and M. K. Mishra, "Comparison of Control strategies for DSTATCOM in power distribution system," *International Journal of emerging electric power system*, vol. 12, Issue. 3, Jun 2011.
- [46] RVD Rama Rao and Dr.Subhransu.Sekhar.Dash, "Power Quality Enhancement by Unified Power Quality Conditioner Using ANN with Hysteresis Control," *IJCA*, vol. 6, issue. 1, Sept 2010.
- [47] I. K. Kiran, and J. Laxmi. A, "Shunt versus series compensation in the improvement of power system performance," *International Journal of applied engineering research Dingidigul*, vol. 2, no. 1, 2011.
- [48] B.M.N.K.Reddy, Mr.G.V.Rajashekhar and Dr.H.Goyal, "Power System Stability Enhancement Using Static Synchronous Series Compensator (SSSC)," *IJMER*, vol. 3, issue. 4, Aug 2013.
- [49] G.Escobar and A.M.Stankovic, "An Adaptive Controller in Stationary Reference Frame for D-Statcom in Unbalanced Operation," *IEEE Transactions on Industrial Electronics*, vol. 51, issue. 2, April 2004.
- [50] R.Pandey and A.K.Kori, "Real and Reactive Power flow Control Using Flexible Ac Transmission System connected to a Transmission line: A Power Injection Concept," *IJARCET*, vol.1, issue. 6, Aug 2012.
- [51] Dr.A.K.Singh, Dr.U.Prasad, R.Pudur and Satyendra kumar, "Modelling of Single Phase UPFC without DC Capacitor," *IEST*, vol. 3, issue. 5, May 2011.
- [52] M. Prashanthi, Dr. Himani, "Reduction of reactive power in a distribution system using D-STATCOM," *Journal of Research in electronics engineering*, vol. 2, Issue. 4, July 2013.

1st National Power & Energy System Conference (NPESC), April 25-26, 2014, KNIT Sultanpur

- [53] R. Pandey, and A. K. Kori, "Enhancement of power quality in transmission line using Flexible Ac transmission System," *International Journal of Science, Engineering and Technology Research*, vol. 2, Issue 8, August 2013.
- [54] Miss.S. R.Injeti and K.R.Raju, "Power Quality Improvement by UPQC device in Doubly Fed Induction Generator Wind Fram to Weak-Grid Connection," IJSER, vol. 2, issue. 12, Dec 2011.
- [55] Sudarshan Rao Gandimeni and Vijay Kumar K, "Unified Power Quqlity Conditioner (UPQC) During Voltage Sag and Swell," *VSRD International Journal of Electrical, Electronics and Communication Engineering*, vol. 2, Issue 8, 2012.
- [56] Mr.V.Ratapa Rao, Mr.O.Hemakeshavulu, Mrs.M.Rama Subbamma and Dr.M.Padma Lalitha, "Performance of Flexible D-STATCOM as a Flexible Distributed Generation in Mitigation Faults," *American Journal of Sustainable cities and Society*, vol. 1, Issuu 1, July, 2012.
- [57] Dhanorkar Sujata and E.Himabindu, "Voltage Sag Mitigation Analysis Using DSTATCOM Under Different Faults in Distribution System," *International Journal of Emerging Trends in Electrical and Electronics*, vol. 9, Issue 1, Nov, 2013.
- [58] Swarupa Pinninti and V.Naga Raju Nayak, "Improvement of Power Quality Using Statcom Applied for Grid at Various Load Conditions," *International Journal of over Quality and Energy Management*, vol. 4, Issuu 1, 2013.
- [59] C.H.Ram Jethmalani, V.Karthikyan and Narayananappa, "Implementation of UPQC for Voltage Sag Mitigation," *International Journal of Computer Communication and Information System*, vol. 2, Issue 1, Dec, 2010.
- [60] S.Sundeep and Dr. G.Madhusudhana Rao, "Modeling and Analysis of Cuctom Power Devices for Improve Power Quality," *International Journal of Electrical and Computer Engineering*, vol. 1, Issue 1, Sept, 2011.
- [61] Shazly A.Mohammed, Aurelio G.Cerrada, Abdel-Moamen M.A and B.Hasanin, "Conventional Dynamic Voltage Restorer (DVR) for Mitigation of Voltage Sag in Power Distribution Systems," *International Journal of Advances in Enginnering and Technology*, vol. 6, Issuu 1, Mar, 2013
- [62] M.Ramadan Sayed, M.A.Moustafa Hssan and A.A.Hassan, "Power System Quality Improvement Using Flexible AC Transmission System Based on Adaptive Neuro-Fuzzy Inference System," *WSEAS Transitions on Power Systems*, vol. 8, Issue 2, April, 2013.
- [63] D.K.Tanti, M.K.Verma, Brijesh Singh and O.N.Mehrotra, "Optimal Placement of Custom Power Devices in Power System Network to Mitigation Voltage Sag under Faults," *International Journal of Power Electronic and Drives System*, vol. 2, Issue 3, Sept, 2012.
- [64] Ahmad Jamshidi, S.Masoud Barakati and M.Moradi Ghaderjani, "Impact of Distribution Power Flow Controller to Improve Power Quality Based on Synchronous Reference Frame Method," *IACSIT International Journal of Engineering and Technology*, vol. 4, Issue 5, Oct, 2012.
- [65] Ahmad N.Al-Husban, "An Optimal Location of Capacitive Reactance Compensator in Electric Power System," *Innovative Systems Design and Engineering*, vol. 3, Issue 10, 2012.
- [66] Mahmoud S.Awad, "Review Power Quality Issues," *Canadian Center of Science and Education*, vol. 6, no. 2, Feb. 2012.
- [67] Dr. Tarlochan Kaur and Sandeep Kakran, "Transient Stability Improvement of Long Transmission Line System by Using SVC," *International Journal of Advanced Rearch in Electrical*, vol. 1, Issue 4, Oct, 2012.
- [68] Sidharth Panda and Ramanarayanan N. Patel, "Improving Power System Transient Stability with An Off-Centre Location of Shunt FACTS Devices," *Journal of Electrical Engineering*, vol. 57, Issue 6, 2006.
- [69] M. Kavitha, N.Rthakar and Mohan Reddy, "Integration of FACTS into Energy Storage System for Future Power Systems Applications," *International Jornal of Avanced Research in Electrical*, vol. 2, Issue 2, Feb, 2013.
- [70] Salim. Haddad, A. Haddouche and H. Bouyeda, "The use of Facts Devices in Distributed power Systems-Modeling, Interface, and Case Study," *International Journal of Computer and Electrical Engineering*, vol. 1, Issuu 1, April, 2009.
- [71] Srinivasa Rao, Sivanagaraj and Sangameswara Raju, "Comparison of Performance of TCPS and SMES in Automatic Generation Control of Reheat Thermal System," *Acta Electrotechnica et Informatica*, vol. 10, Issue 4, 2010.
- [72] Z.Eleschova, M.Smitkova and A.Belan, "Evaluation of Power System Transient Stability and Definition of the Basic Criterion, *International Journal of Energy*, vol. 4, Issue 1, 2010.
- [73] S.Muthukrishnan and Dr. A.Nirmal Kumar, "Coparison of Simulation and Experimental Results of UPFC used for Power Quality Improvement," *International Journal of Computer and Electrical*, vol. 2, Issuu 3, June, 2010.
- [74] Math H.J.Bollen and Yu-Hua, "Categorization and Analysis of Power System Transients," *IEEE Transactions on Power Delivery*, vol. 20, Issue 3, July, 2005.
- [75] Jigneh S.Patel and Manish N.Sinha, "Power System Transient Stability Analysis Using ETAP Software," *National Conference on Recent Trends in Engineering and Technology*, May, 2011.
- [76] Kirti S.Deshmukh and D.B.Meshram, "How to Improve Stability by Using Facts Controller," *International Journal of Engineering and Innovative Tectnology*, vol. 3, Issue 2, Aug, 2013.
- [77] Bindeshwar Singh, N.K.Sharma, A.N.Tiwari, K.S.Verma and Deepender Singh, "A Status review of Incorporation of FACTS Controllers in multi-Machine Power System for Enhancement of Damping of Power System and Voltage Stability," *International Journal of Engineering Science and Technology*, vol. 2, Issue 6, 2010.
- [78] A.N.Hussain, F.Malek, M.A.Rashid and M.F.Haji Abd Malek, "Performance Improvement of Power System Stability by Using Multiple Damping Controllers Based onPSS and the UPFC," *International Journal of Engineering and Technology*, vol. 4, Issue 4, Sep, 2013.
- [79] A.K.Kori and Ratnesh Singh, "Transient Stability and Power Flow Models of STATCOM coordination Controllers with ULTC transformer for Voltage Stability improvement," *International Journal of Science, Engineering and Technology Research*, vol. 1, Issue 5, Nov, 2012.
- [80] Licheng Jin, Haifeng Liu, Ratnesh Kumar, James D. McCalley, Nicola Elia, Venkataramana Ajjarupu, "Power System Transient Stability Design using Reachability based Stability-Region Computation," *Electric Power networks efficiency and security*.
- [81] Kalai Murugan Amirthalingam and Raja Prabu Ramachandran, "Improvement of Transient Stability of Poer System Using Solid State Circuit Breaker," *American Journal of Applied Science*, vol. 10, Issue 6, 2013.
- [82] P.Sunilkumar, "Transient Stability Enhancement of Power System Using TCSC," *International Journal of Electrical and Computer Engineering*, vol. 2, Issue 3, June, 2012.
- [83] Abdelazeem A, Abdelsalam, Mohammed E, Desouki, Adel M.Sharaf, "Power Quality Improvement Using FACTS Power Filter Compensation Scheme," *Journal of Electrical System*, vol. 9, Issue 1, 2013.
- [84] Jyothilal Nayak Bharothu and K Lalitha, "Compensation of Voltage Flicker by using Facts Devices," *American Journal of Electrical Power and Energy Systems*, vol. 2, Issue 3, May, 2013.
- [85] R.Vijayakumar and R.Subramanian, "Compensation of Voltage Variation in Distribution System by using DVR Based Separate Energy Storage Devices," *International Electrical Engineering Journal*, vol. 4, Issue 1, 2013.
- [86] Vasudeo B.Virulkar and Mohan V.Aware, "Modeling and Control of DSTATCOM with BESS for Mitigation of Flicker, *Asian Power Elecronics Journal*, vol. 4, Issue 1, April, 2010.
- [87] Xiao-Yuan Chen, Jian-Xun Jin, Kai-Meng Ma, JU Wen, Ying Xin, Wei-Zhi Gong, An-Lin and Jing-Yin Zhang, "High Temperature Superconducting Magnetic Energy Storage and Its Power Control Techology," *Journal of Electronic Science and Technology on China*, vol. 6, Issue 2, June, 2008.
- [88] Sugun P.R, Dr. T.Ruban Deva Prakash and Dr.L.Padam Suresh, "ANN Based Voltage Flicker Mitigation With UPFC Using SRF Algorithm," *Trend in Advanced Science and Engineering*, vol. 4, Issue 1, 2012.
- [89] Sai Kiran Kumar.Sivakoti, Y.Naveen Kumar and D.Archana, "Power Quality Improvement In Distribution System Using D-Statcom In Transmission Lines," *International Journal of Engineering Research and Applications*, vol. 1, Issue 3, 2013.
- [90] M.Noroozian and C.W.Taylor, "Benefits of SVC and STATCOM for Electric Utility Application,"
- [91] Bindeshwar singh, "Application of Facts Controllers in Power System for Enhance the Power System Stability : A State-of-the-Art," *International Journal of Reviews in Computing*, vol. 6, Issue 1, July, 2011.
- [92] Molla Shahadat Hossain Lipu and Tahia Fahrin Karim, "Effectiveness of FACTS controllers and HVDC transmissions for improving power system stability and increasing power transmission capability," *International Journal of Energy and Power Engineering*, vol. 2, Issue 4, 2013.
- [93] Bindeshwar Singh, N.K.Sharma and A.N.Tiwari, "A Comprehensive Survey of Optimal Placement and Coordinated Control Techniques of FACTS Controllers in Multi-Machine Power System Environments," *Journal of Electrical and Technolodgy*, vol. 5, Issue 1, 2010.
- [94] DIB Djalel, A.Rezaiguiia and Z.Abada, "Improving the Electric Poer Quality by UPFC Systems in Electrical Networks," *International Journal of Energy*, vol. 6, Issue 4, 2012.
- [95] S.Jalilzadeh, M.Darabian and M.Azari, "Power System Stability Improvement via TCSC Controller Employing a Multi-objective Strength Pareto Evolutionary Algorithm Approach," *Journal of Operation and Automation in Power Engineering*, vol. 1, Issue 1, March, 2013.
- [96] P.Suman Pramod Kumar, N.Vijaysimha and C.B.Saravanan, "Static Synchronous Series Compensator for Series Compensation of EHV Transmission Line," *International Journal of Advanced in Electrical, Electronics and Instrumentation Engineering*, vol. 2, Issuu 7, July, 2013.
- [97] Amin Safari, "Optimum Design of POD Controller for FA0CTS Device in Interconnected Power System," *International Journal of Control and Automation*, vol. 6, Issue 3, June,2013.
- [98] G.Naveen Kumar, M.Surya Kalavathi and R.Harini Krishna, "Optimal Placement of SVC and STATCOM for Voltage Stability Enhancement Under Contingency Using Cat Swarm Optimization," *International Journal of Advanced in Engineering and Technology*, Nov,2012.
- [99] A.Elkholy, F.H.Fahmy and A.A.Abou El-Ela, "Power System Stability Enhancement using The Unified Power Flow Controller," *International Middle East System Conference*, Dec, 2010.
- [100] M A. Abido, "Power System Stability Enhancement Using FACTS Controllers: A Review," *The Arabian Journal for Science and Engineering*, vol. 34, Issue 1B, Nov, 2008.
- [101] Prof. P.Venkatal Kishore and Dr. S.Rama Reddy, "Modeling and Simulation of fourteen Bus System Employing D-STATCOM fpr Power Quality Improving," *ACEEE International Journal on Control and Instrumentation*, vol. 2, Issue 3, Oct, 2011.
- [102] Ashish Choubey and Deepa Choudhary, "Voltage Stability with the help of STATCOM," *International Journal of Research Engineering and Technology*, vol. 2, Issue 3, June, 2013.
- [103] S.Sowjanya and Prof. J.Srinivasarao, "Design of FACTS Device For The Improvement of Power System Stability using Mathematical Matching Controller," *IOSR Journal of Electrical and Electronics Engineering*, vol. 1, Issue 3, Aug, 2012.
- [104] Alok Kumar Mohanty and Amar Kumar Barik, "Power System Stability Improvement Using FACTS Devices," *International Journal of Modern Engineering Research*, vol. 1, Issue 2, 2013.
- [105] P.R.Sharma, Ashok kumar and Narendra Kumar, "Optimal Location for Shunt Connected FACTS Devices in a Series Compensated Long Transmission Line," *Truk Journal Electrical Engineering*, vol. 15, Issue 3, 2007.
- [106] Aarti Rai, "Enhancement of Voltage and Reactive Power Control of Dtribution System Using Facts Devices," *International Kournal of Scientific Research Engineering and Technology*, vol. 1, Issue 9, Dec, 2012.
- [107] J.Sandeep Soni, H.P.Agarwal, R.Gupta and H.O.Bansal, "Potentials and Capabilities of FACTS Controllers for Quality and Performance Enhancement of Power System," *International Journal of Technology and Exploring Engineering*, vol. 2, Issue 4, March, 2013.
- [108] Sangram Keshori Mohapatra and Sidharth Panda, "Stability Improvement by SSSC and STATCOM based Damping Controller Employing Differential Evolution Algorithm," *International Journal of Technology and Engineering*, vol. 24, Issue 1, 2013.
- [109] E.S.Ali and S.M.Abd-Elzazim, "Bacteria Foraging: A New Technique for Optimal Design of FACTS Controller to Enhance Power System Stability," *Wseas Transactions on Systems*, vol. 12, Issue 1, Jan, 2013.

1st National Power & Energy System Conference (NPESC), April 25-26, 2014, KNIT Sultanpur

- [110] Alok Kumar and Surya Bhushan Dubey, "Enhancement of Transient Stability in Transmission Line Using SVC Facts Controller," *International Journal of Recent Technology and Engineering*, vol. 2, Issue 2, May, 2013.
- [111] Satvinder Singh, Atma Ram, Nitin Goel and Pawan Kumar, "Transient Stability Enhancement of Multi-Machine System Using FACTS Controllers," *International Journal of Engineering Science and Innovative Technology*, vol. 2, Issue 2, March, 2013.
- [112] H.B.Nagesh and P.S.Puttaswamy, "Enhancement of Voltage Stability Margin Using FACTS Controllers," *International Journal of Computer and Electrical Engineering*, vol. 5, Issue 2, April, 2013.
- [113] I.Parveena and M.Mahendran, "The Compensation of Unbalanced 3 Phase Transmission Systems of Utilized Power flow Controller," *International Journal of Scientific and Research Publication*, vol. 2, Issue 4, April 2013.
- [114] Navid Khorrami, "Analyzing of Dynamic Voltage Restorer in Series Compensation Voltage," *Research Journal of Applied Sciences*, vol. 4, Issue 3, 2012.
- [115] Kein Huat Chua, Yun Seng Lim, Jianhui Wong, Philip Taylor, Ezra Morris and Stella Morris, "Voltage Unbalance Mitigation in Low Voltage Distribution Network with Photovoltaic Systems," *Journal of Electronic science and Technolodgy*, vol. 10, Issue 1, march 2012.
- [116] E.Rambabu, E.Parveen and Prof.P.K.Kishore, "Mitigation of Harmonics in Distribution System Using D-STATCOM" *International Journal of Scientific and Engineering Research publications*, vol. 2, Issue 11, Nov 2011.
- [117] H. Dag, B. Ozturk, and A. Ozyurek, "Application of Series and Shunt Compensation to Turkish National Power Transmission System to Improve System Loadability," *ELECO'99 International conf. on Electrical and Electronics Engineering*, 1999.
- [118] A. de Almeida, L.M.J. Delgado, "Power quality problems and New solution," ISR-Departement of Electrical and Computer Engineering University of Coimbra.

BIBLIOGRAPHIES



Bindeshwar Singh received the M.Tech. In electrical engineering from the Indian Institute of Technology, Roorkee, in 2008. He is now a Ph. D. student at ISM Dhanbad, Jharkhand, India. His research interests are in Coordination of DGs & FACTS controllers in power systems and Power system Engg.. Currently, he is an Assistant Professor with Department of Electrical Engineering, Kamla Nehru Institute of Technology, Sultanpur, U.P., and India, where he has been since August'2010.

Mobile: 09473795769.

Email id: bindeshwar.singh2025@gmail.com



Rajiv Kumar is a M.Tech student (Regular).In specialization of Power Electronics and Drives in electrical engineering department, KNIT Sultanpur-228118 (U.P.), India. His interests are in the areas of Power Electronics and Drives.

E-mail ID: rajiv.kumar177@gmail.com



Pavan Prakash Gupta is a M.Tech student (Regular) . In specialization of Power Electronics and Drives in electrical engineering department, KNIT Sultanpur- 228118 (U.P.), India. His interests are in the areas of Power Electronics and Drives.

E-mail ID: pavan.kashyp@gmail.com



Ashok Kumar is a M.Tech student (Regular) . In specialization of Power Electronics and Drives in electrical engineering department, KNIT Sultanpur-228118 (U.P.), India. His interests are in the areas of Power Electronics and Drives.

E-mail ID: kashyapashok44@gmail.com

Applications of FACTS Controllers in Emerging Power System Networks

Bindeshwar Singh¹, Manisha² and Abhiruchi Srivastava³, and Aanchal Baranwal⁴

¹Asst. Professor, Department of Electrical Engineering, Kamla Nehru Institute of Technology (KNIT), Sultanpur-228118, U.P., India
^{2&3}M. Tech. (PE&ED) Regular Student, Department of Electrical Engineering, Kamla Nehru Institute of Technology (KNIT), Sultanpur-228118, U.P., India
⁴Asst. Prof., Department of Electrical ,Electronics & Instrumentation Engineering, MIT Moradabad, U.P., India

Abstract- This paper presents a comprehensive survey on historical background of FACTS controllers such as series, shunt, series-series, and series-shunt FACTS controllers. Authors strongly believe that this survey article will be very much useful to the researchers, scientific, engineers and industrial persons for finding out the relevant references in the field of historical back ground on FACTS controllers.

Keywords: Control Coordination, Flexible AC Transmission System (FACTS), FACTS Controllers ,GUPFC,HPFC,IPFC,SVC,SSSC,STATCOM, TCSC,TCPAR,TCR,TSR,TSSC,TCSR,TSSR,UPFC,Interactions, Placements, Coordination Voltage Stability, frequency stability and rotor angle stability.

NOMENCLATURES

| | |
|----------|---|
| FACTS | Flexible Alternating Current Transmisssion System |
| TCSC | Thyristor Controlled Series Capacitor |
| TCPAR | Thyristor Controlled Phase Angle Regulator |
| SSSC | Static Synchronous Series Compensator |
| TCPST | Thyristor Controlled Phase Shifting Transformer |
| TSSC | Thyristor Switched Series Capacitor |
| TCSR | Thyristor Controlled Series Reactor |
| TCR | Thyristor Controlled Reactor |
| TSR | Thyristor Switched Reactor |
| SVC | Static Var Compensator |
| STATCOM | Static Synchronous Compensator |
| DSTATCOM | Distribution Static Compensator |
| IPFC | Interline Power Flow Controller |
| UPFC | Unified Power Flow Controller |
| GUPFC | Generalized Unified Power Flow Controller |
| HPFC | Hybrid Power Flow Controller |
| SMES | Superconducting Magnetic Energy Storage Systems |
| BESS | Battery Energy Storage Systems |
| UIPC | Unified Interphase Power Controller |
| PFC | Power System Stabilizers |
| AP | Active Power |
| RP | Reactive Power |
| VSC | Voltage Source Converter |
| VSI | Voltage Source Inverter |
| VS | Voltage Stability |
| VI | Voltage Instability |
| VC | Voltage Collapse |
| VP | Voltage Profile |
| VR | Voltage Regulation |
| SSVS | Steady State Voltage Stability |
| TS | Transient Stability |
| APTC | Available Power Transfer Capacity |
| PQ | Power Quality |
| SSR | Sub-synchronous Resonance |
| SS | Steady State |
| α | Firing Angle |
| HFC | Hybrid Flow Controller |
| PST | Phase Shifting Transformer |

I. INTRODUCTION

THE drive towards deregulated environment may result in simultaneous installation of different FACTS controllers in power system networks.

These multiple FACTS controllers have the potential to interact with each other. This interaction may either deteriorate or enhance system stability depending upon the chosen controls and placement of FACTS controllers. Hence there is a need to study the interaction between the FACTS controllers.

The various interactions can potentially occur between the different FACTS controllers, as well as, between FACTS controllers and Power System Stabilizers (PSS) in a multi-machine power system environment. These likely interactions have been classified into different frequency ranges and various interaction problems between FACTS controllers or FACTS to PSS's from voltage stability/ small signal stability view point The various frequency ranges are:

| | |
|---------|---------------------------------------|
| 0 Hz | Steady State Interaction |
| 0-3/5Hz | Electro-mechanical Oscillation |
| 2-10Hz | Small-Signal Or Control Oscillation |
| 10-15 | Sub synchronous resonance Interaction |
| >15 | Electromagnetic transient . |

A. Definition of FACTS [1]

According to IEEE, FACTS, which is the abbreviation of *Flexible AC Transmission Systems*, is defined as follows : “Alternating current transmission systems incorporating power electronics based and other static controllers to enhance controllability and PTC”.

B. Generation of FACTS Controllers [2]

The following generation of FACTS controllers for the development of FACTS controllers from last century :

1. First Generation of FACTS Controllers(1950-1970)

The following FACTS controllers such as SVC, TCSC ,TCPAR and TCPST are developed in the first generation of FACTS controllers:

2. Second Generation of FACTS Controllers(1971-2010)

The following FACTS controllers such as STATCOM, SSSC, UPFC, and IPFC are developed in the second generation of FACTS controllers.

3. Third Generation of FACTS Controllers(2011-2014)

-
- A. Assistant Professor, Department of electrical engineering, KNIT Sultanpur. Email : bindeshwar.singh2025@gmail.com
 - B. And C ARE M. Tech(PE&ED) Student Department of electrical engineering, KNIT Sultanpur. Email : yadavmyy@gmail.com.

The following FACTS controller such GUPFC, HPFC are developed in third generation of FACTS controllers.

C. Connection of FACTS Controllers [3]

- a) *Series controllers* such as TCSC, TCPAR , TCPST and SSSC
- b) *Shunt controllers* such as SVC,STATCOM and DSTATCOM
- c) *Combined series-series controllers* such as IPFC &GIPFC
- d) *Combined series-shunt controllers* such as UPFC,GUPFC & HPFC

D. Possible Benefit & Drawback of FACTS Technology [4]

Within the basic system security guidelines, the FACTS devices enable the transmission system to obtain one or more of the following benefits:

- Control of power flow as ordered.
- Increase utilization of lowest cost generation.
- Dynamic stability enhancement.
- Increase the loading capability of lines to their thermal capabilities.
- Provide secure tie-line connections.
- Upgrade of transmission lines.
- Reduce RP flows, thus allowing the lines to carry more active power.
- Loop flow control.
- Improve the power system oscillations.
- Provide flexible operation & control.
- Improve steady state stability.
- Enhance APTC of system.
- Enhance power system security.
- Enhance Green House Gas environments.
- Less mechanical maintenance required.

E. Drawbacks of FACTS[4]

- It produces large no. of harmonics in the system.
- It requires filters.
- More expensive than other conventional devices.

F. Application of FACTS Controller [5]

In interconnected as well as in long-distance transmission systems technical problems occur which can limit the loadability and reliability of the system. Some problems result from normal changes and developments in power systems. A number of FACTS controllers are suitable for improving these technical problems. The application of these devices depends on the problem which has to be solved. The technical benefits of the principal for dynamic applications of FACTS in addressing problems in TS, dampening, post contingency VC and VS are summarized. FACTS devices are required when there is a need to respond to dynamic (fast-changing) network conditions. The conventional solutions are normally less expensive than FACTS devices, but limited in their dynamic behavior. It is the task of the planners to identify the most economic solution.

There are several literatures survey regarding FACTS controllers such as definition of FACTS controller [1], generation of FACTS controllers [2], connection of FACTS controllers [3], possible benefits and drawbacks of FACTS controllers [4] and application of FACTS controllers [5].

There are several literatures survey regarding connections of FACTS controllers like series FACTS controllers which includes TCSC [6]-[44], TCPAR[45]-[46],SSSC[47]-[59],TCPST[60]-[66],TSSC [67]-[69],TCSR[70]-[71], shunt FACTS controllers which include TCR , TSR [72]-[75], SVC[76]-[101],STATCOM[102]-[113],DSTATCOM[114]-[118], series-series FACTS controllers which include IPFC[119]-[132], series-shunt FACTS controllers which includes UPFC [133]-[195].

There are several literatures survey regarding third generation of FACTS controller i.e. GUPFC [196]-[201], energy storage FACTS controllers i.e. SMES [204]-[212], BESS [213]-[218] and additional FACTS controllers

UIPC [219]-[224].There is a comparative chart which compares all the FACTS on the basis of various subjects, related problems and their corrective actions.

This paper is organized as follows: Section II discusses the connection of FACTS controllers in power systems. Section III presents the 3rd generation FACTS controllers, energy storage FACTS controllers and an additional FACTS controller UIPC. Section IV presents comparative charts on various FACTS controllers & its features. . Section V presents the summary of the paper. Section VI presents the conclusion of the paper.

II. CONNECTION OF FACTS CONTROLLERS

A. Series FACTS Controllers

Series FACTS devices could be a variable impedance, such as capacitor, reactor, etc., or a power electronics based variable source of main frequency, subsynchronous and harmonic frequencies (or a combination) to serve the desired need. In principle, all series FACTS devices inject voltage in series with the transmission line.The series FACTS controllers connection diagram shown in fig.1

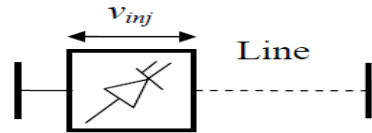


Fig .1 Series FACTS Controller Connection Diagram

i) TCSC [6]-[44]

i. Origination

It is the member of the first generation of FACTS devices, that uses silicon controlled rectifiers to manage a capacitor bank connected in series with a line. TCSC allows utility to transfer more power further on a particular line. The worlds first three phase TCSC was developed by ABB and installed at Kayenta substation, Arizona in 1992, that raises the capacity of a transmission line by almost 30%. By the end of year 2004, seven TCSCs have been installed worldwide. In Asia, three TCSC came into operation; two in China and one in India, bringing Asia into the forefront of the advanced FACTS technology. shows the complete list of TCSC installed worldwide as of December 2004.

ii. Its Features, Related Mathematical Modeling, and Control Block Diagram and all Stages of TCSC

A TCSC is a capacitive reactance compensator, which consists of a series capacitor bank shunted by a thyristor TCR in order to provide a smoothly variable series capacitive reactance.

Even through a TCSC in the normal operating range in mainly capacitive, but it can also be used in an inductive mode. The power flow over a transmission line can be increased by controlled series compensation with minimum risk of SSR. TCSC is a second generation FACTS controller, which controls the impedance of the line in which it is connected by varying the firing angle of the thyristors. A TCSC module comprises a series fixed capacitor that is connected in parallel to a TCR i. e. Shown in Fig.2. A TCR includes a pair of anti-parallel thyristors that are connected in series with an inductor. In a TCSC, a metal oxide varistor (MOV) along with a bypass breaker is connected in parallel to the fixed capacitor for overvoltage protection. A complete compensation system may be made up of several of these modules.

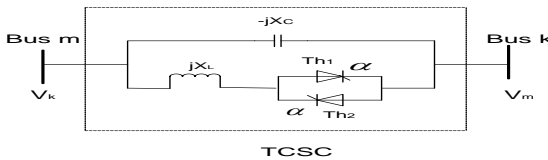


Fig .2. TCSC module

The SS impedance of the TCSC is that of a parallel LC circuit, consisting of fixed capacitive impedance, X_c , and a variable inductive impedance, $X_L(\alpha)$, that is,

$$X_{TCSC}(\alpha) = \frac{X_c X_L(\alpha)}{X_L(\alpha) - X_c}$$

Where

$$X_L(\alpha) = X_L \frac{\pi}{\pi - 2\alpha - \sin 2\alpha}, X_L \leq X_L(\alpha) \leq \infty$$

$X_L = \omega L$, and α is the delay angle measured from the crest of the capacitor voltage (or, equivalently, the zero crossing of the line current). The impedance of the TCSC by delay is shown in Fig.2. The TCSC has three basic modes of operation are as follows:

- Thyristor valve bypass mode (inductive region operation $0 \leq \alpha \leq \alpha_{L\lim}$):
 - Thyristor valve blocked mode (resonance region for inhibited operation $\alpha_{L\lim} \leq \alpha \leq \alpha_{c\lim}$):
 - Vernier control mode (capacitive region operation: $\alpha_{c\lim} \leq \alpha \leq \pi/2$):
- a) Thyristor Valve Bypass Mode (Inductive Region Operation $0 \leq \alpha \leq \alpha_{L\lim}$): In the bypass mode thyristors are gated for full conduction and the current flow in the reactor is continuous and sinusoidal. In this case the net reactance is slightly inductive because the susceptance of reactor is larger than that of the capacitor. This mode is mainly used for protecting the capacitor against overvoltage (during transient overcurrents in the line). In this mode of operation the behavior of reactance of TCSC module as follows.
- b) Thyristor Valve Blocked Mode (Resonance Region For Inhibited Operation $\alpha_{L\lim} \leq \alpha \leq \alpha_{c\lim}$): In the inserted mode with thyristor blocked, no current flows through the valve as the gate pulses are suppressed. In this mode, the TCSC reactance is the same as that the fixed capacitor. This mode is also termed as waiting mode. This mode is used to provide control and protective measures. The breaker is generally provided to remove TCSC from service when there are internal TCSC failures. In this mode of operation the behavior of reactance of TCSC module as follows.
- c) Vernier Control Mode (Capacitive Region Operation $\alpha_{c\lim} \leq \alpha \leq \pi/2$): In vernier control mode, thyristors are gated in such a manner that a controlled amount of inductive current can be circulate through the capacitor thereby increasing effective capacitive/reactive reactance of the module. In this mode of operation the behavior of reactance of TCSC module as follows. All the modes of operation (regions of operation) of TCSC are shown in Fig.3.

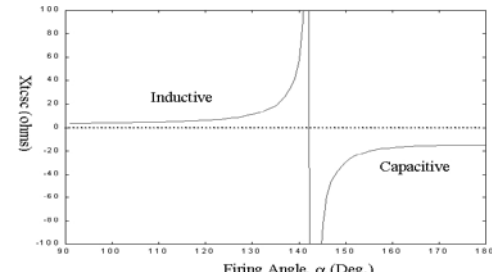


Fig.3. TCSC equivalent Reactance as a function of firing angle

- d) Explanations of above TCSC characteristics: The TCSC thus presents a tunable parallel LC circuit to the line current that is substantially a constant alternating current source. As the impedance of the controlled reactor, $X_L(\alpha)$ is varied from its maximum (infinity) towards its minimum (ωL), the TCSC increases its minimum capacitive impedance, $X_{TCSC\min} = X_c = 1/\omega C$, (and thereby the degree of series capacitive compensation) until parallel resonance at $X_c = X_L(\alpha)$ is established and $X_{TCSC\max}$ theoretically becomes infinite. Decreasing $X_L(\alpha)$ further, the impedance of the TCSC, $X_{TCSC}(\alpha)$ becomes inductive, reaching its minimum value of $X_c X_L(\alpha)/X_L(\alpha) - X_c$ at $\alpha = 0$, where the capacitor is in effect bypassed by the TCR. Therefore, with the usual TCSC arrangement in which the impedance of the TCR reactor, X_L , is smaller than that of the capacitor, X_c , the TCSC has two operating ranges around its internal circuit resonance; one is the $\alpha_{c\lim} \leq \alpha \leq \pi/2$ range, where $X_{TCSC}(\alpha)$ is becomes capacitive, and the other is the $0 \leq \alpha \leq \alpha_{L\lim}$ range, where $X_{TCSC}(\alpha)$ is inductive, as illustrated in fig.3. From above characteristics it is observed that TCSC can't work in a particular band of firing angle i.e. shown in above figure due to resonance phenomena occurs in TCSC in this zone. This is the drawback of TCSC operations in power systems. The variable reactance and current injection model of TCSC are shown in fig.4 respectively.

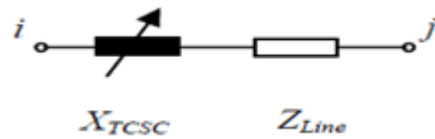


Fig. 4(a) Variable Reactance Model

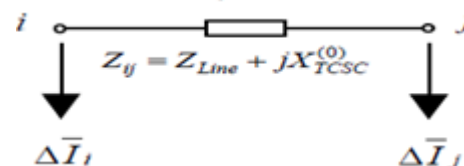


Fig. 4(b) Current Injection Model

iii. Its Application In Research

- a) Initial experience with TCSC installation has been favorable. A TCSC has been installed on the American Electric Power (AEP) 345 kV system in 1991 and another on the Western Area Power Administration (WAPA) 230 kV system in northeastern Arizona at the Kayenta substation in 1992. A third TCSC has been connected to the BPA 500 kV system at Slatt in 1993 for power flow control and improvement of system performance.

- b) The total ASC system, dedicated in 1992, which includes a TCSC and a conventional series capacitor, was installed at the Kayenta 230 kV substation in Western Area Power Administration (WAPA) in Northeast Arizona. This ASC was employed to increase the reliable transmission capacity of a 230 kV line between Glen Canyon and Shiprock. The ASC consists of two 55 Ω series capacitor banks each rated for 165 Mvar and 1000 A.

The results of the project have proved that the ASC is a reliable means of using existing transmission capacity while maintaining system security.

2) TC-PAR [45]-[46]

The TC-PAR is equipment that can control power flow in transmission lines of power system by regulating the phase angle of the bus voltage. Environment restrictions usually restrict opportunities of reinforcement through the consideration of new routes. In such a situation, FACTS controllers such as TCPAR play an important role in increasing loadability of the existing system and controlling the congestion in the network.

FACTS device like TC-PAR can be used to regulate the power flow in the tie-lines of interconnected power system. When TC-PAR is equipped with power regulator and frequency based stabilizer it can also significantly influence the power flow in the transient states occurring after power disturbances. In the case of simple interconnected power system, consisting of two power systems the control of TC-PAR can force a good damping of both power swings and oscillations of local frequency. In the case of larger interconnected power system consisting of more than two power systems the influence of the control of TC-PAR on damping can be more complicated. Strong damping of local frequency oscillations and power swings in one tie-line may cause larger oscillations in remote tie-lines and other systems. Hence using devices like TC-PAR as a tool for damping of power swings and frequency oscillations in a large interconnected power system must be justified by detailed analysis of power system dynamics.

The power injection model of TC-PAR is shown in Fig.5.

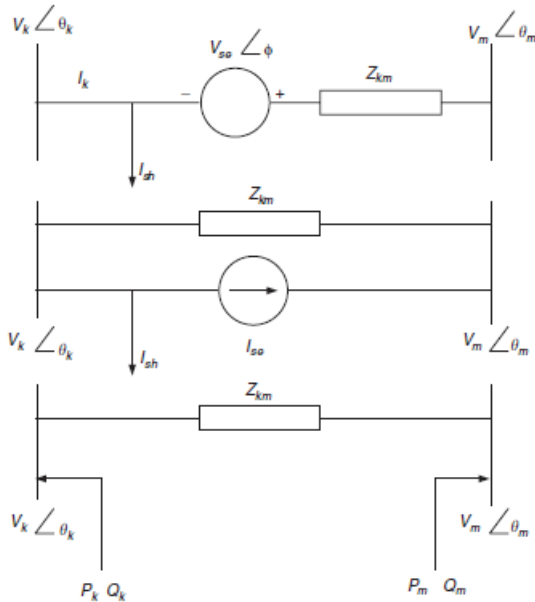


Fig.5. Power injection model of TC-PAR

3) SSSC [47]-[59]

"A SSSC is a static synchronous generator operated without an external electric energy source as a series compensator whose output voltage is in quadrature with, and controllable independently of the line current for the purpose of increasing or decreasing the overall reactive voltage drop across the line and thereby controlling the transmitted electric power. The SSSC may

include transiently rated energy source or energy absorbing device to enhance the dynamic behavior of the power system by additional temporary real power compensation, to increase or decrease momentarily, the overall real voltage drop across the line".

An SSSC incorporates a solid state voltage source inverter that injects an almost sinusoidal voltage of variable magnitude in series with a transmission line. The SSSC has the same structure as that of a STATCOM except that the coupling transformer of an SSSC is connected in series with the transmission line. The injected voltage is mainly in quadrature with the line current. A small part of injected voltage, which is in phase with the line current, provides the losses in the inverter. Most of injected voltage, which is in quadrature with the line current, emulates a series inductance or a series capacitance thereby altering the transmission line series reactance. This emulated reactance, which can be altered by varying the magnitude of injected voltage, favorably influences the electric power flow in the transmission line. The structure of SSSC shown in Fig.6.

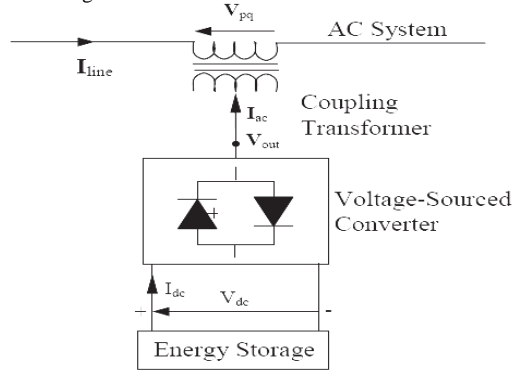


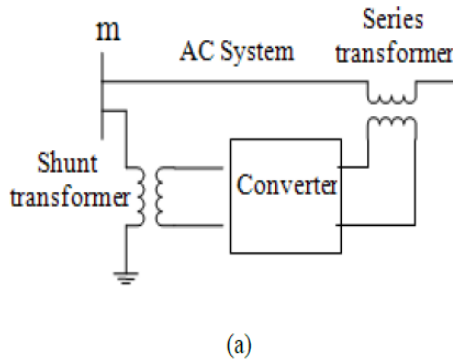
Fig. 6.The basic structure of SSSC

SSSC is a solid-state synchronous voltage source employing an appropriate DC to AC inverter with gate turn-off thyristor. It is similar to the STATCOM, as it is based on a DC capacitor fed VSI that generates a three-phase voltage, which is then injected in a transmission line through a transformer connected in series with the system. In SSSC, the resonance phenomena has been removed. So SSSC is having more superior performance as compare to TCSC. The main control objective of the SSSC is to directly control the current, and indirectly the power, flowing through the line by controlling the RP exchange between the SSSC and the AC system. The main advantage of this controller over a TCSC is that it does not significantly affect the impedance of the transmission system and, therefore, there is no danger of having resonance problem.

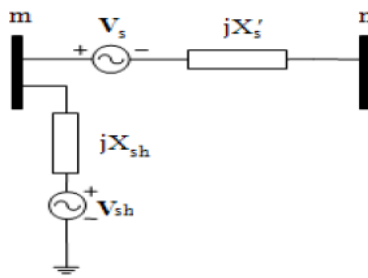
4) TC-PST [60]-[66]

The TC-PST consists of two transformers; a shunt transformer or magnetizing transformer connected in parallel and a series transformer or booster transformer in series to the line. The current through the magnetizing transformer induces a voltage on the primary side of the booster transformer. The turn ratio of the shunt transformer is 1: n, and the turn ratio of the series transformer is 1:1. Compared to conventional PST, the mechanical tap changer is replaced by a thyristor controlled equivalent. The purpose of the TC-PST is to control the power flow by shifting the transmission angle. In general, phase shifting is obtained by adding a perpendicular voltage vector in series with a phase. This vector is derived from the other two phases via shunt connected transformers. The perpendicular series voltage is made variable with a variety of power electronics topologies. A circuit concept that can handle voltage reversal can provide phase shift in either direction. This Controller is also referred to as TC-PAR. A phase shifter model can be represented by an equivalent circuit. It consists of admittance in series with an ideal transformer having a complex turns ratio. The schematic diagram of the TC-PST. The series transformer injects the voltage in series in the system. The AP and RP injected by the series transformer is taken from the shunt transformer. For sake simplicity of analysis, the insignificant losses from transformer and converter is neglected. Thus the net complex power (real and reactive power) exchange between the TCPS and the system is zero. The injection of this complex power depends on the injection of a series voltage controlled by a converter. Vs and Vsh are represented by the synchronous

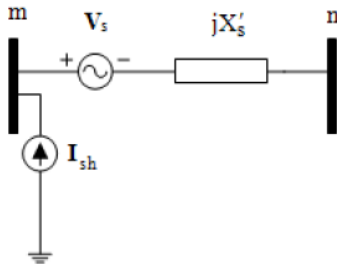
voltage sources in series and shunt, respectively. X_{sh} is the leakage reactance of the shunt transformer. X_s' is the leakage reactance seen from primary side of series transformer is given by $X_s' = X_s + n^2 X_{sh}$ where n is the turn ratio number of the shunt transformer and X_s is the leakage reactance of the series transformer. The schematic connection diagram of TC-PST shown in fig.7 (a)&(b)



(a)



(b)



(c)

Fig.7: TCPST; (a) Schematic diagram of a TCPST; (b) a series and shunt synchronous voltage source equivalent; (c) a series injected voltage source and a shunt injected current source.

The series transformer injects a voltage in series with the system. The AP and RP injected by the series transformer is taken from the shunt transformer. For the sake of simplicity, the losses in the transformers and the converter are neglected. Thus the net complex power (AP and RP) exchange between the TCPS and the system is zero. The injected complex power of the series transformer depends on the complex injected voltage and the line current, where V_s and V_{sh} represent by the voltage of the series and shunt transformer, respectively. X_s and X_{sh} represent the leakage reactance of the series and shunt transformers, respectively. X_s' represents the leakage reactance seen from the primary side of the series transformer and is given by $X_s' = X_s + n^2 X_{sh}$ where n is the turns ratio of the shunt transformer. The shunt voltage source and the associated leakage reactance X_{sh} can be represented by a shunt injected current source (I_{sh}) as shown in Figure.. The

shunt injected current has two components: in phase component (I_p) and quadrature component (I_q) with respect to the bus voltage V_m . Thus I_{sh} can be expressed as

$$I_{sh} = (I_p - I_q)e^{j\delta}$$

Consider a TCPS is placed at bus m of the single machine infinite bus (SMIB) system. Here X_1 is the sum of generator transient reactance, main transformer leakage reactance and the equivalent reactance of lines 1 and 2; X_2 is the sum of X_s and the equivalent reactance of lines 3 and 4. Figure shows the phasor diagram of the system showing various voltages and currents.

The complex power (S_{st}) injected by the series transformer can be written as

$$S_{st} = V_s (-I)^* = \left[\frac{-V_m + V_s + E_2}{jX_2} \right]^*$$

The active (P_{st}) and reactive (Q_{st}) powers injected by the series transformer are given by

$$\begin{aligned} P_{st} &= \Re[S_{st}] \\ &= bV_s V_m \sin(\theta_s - \delta_m) = bV_s E_2 \sin(\theta_s) \\ Q_{st} &= \Im[S_{st}] \\ &= -bV_s V_m \cos(\theta_s - \delta_m) + bV_s^2 + bV_s E_2 \cos(\theta_s) \end{aligned}$$

Here $b=1/X_2$ and θ_s is the angle of V_s . Similarly, the active (P_{sht}) and reactive (Q_{sht}) powers drawn by the shunt transformer are given by

$$\begin{aligned} P_{sht} &= \Re[S_{sht}] = -V_m I_p \\ Q_{sht} &= \Im[S_{sht}] = -V_m I_q \end{aligned}$$

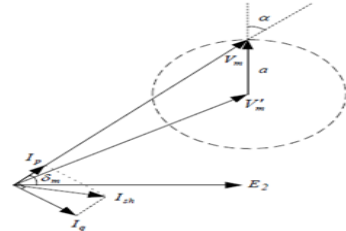


Fig. 8 Phasor Diagram of TC-PST

e) TSSC [67]-[69]

TSSR is an inductive reactance compensator, which consists of a series reactor shunted by a TCR to provide a stepwise control of series inductive reactance. The basic element of a TSSC is a capacitor shunted by bypass valve. The capacitor is inserted into the line if the corresponding thyristor valve is turned off, otherwise it is bypassed.

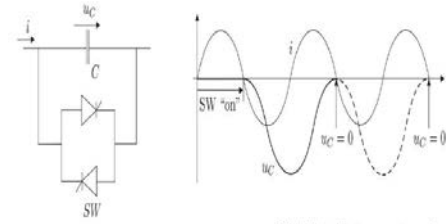


Fig.9 Course of capacitor voltage for a basic element in a TSSC

A thyristor valve is turned off in an instance when the current crosses zero. Thus, the capacitor can be inserted into the line by the thyristor valve only at the zero crossings of the line current. On the other hand, the thyristor valve should be turned on for bypass only when the capacitor voltage is zero in

order to minimize the initial surge current in the valve, and the corresponding circuit transient. This results in a possible delay up to one full cycle to turn the valve on. Therefore, if the capacitor is once inserted into the line, it will be charged by the line current from zero to maximum during the first half-cycle and discharged from maximum to zero during the successive half-cycle until it can be bypassed again.

f) TCSR [70]-[71]

The compensator TCSR consists of variable inductance (L_1) connected in series with the transmission line controlled by thyristors mounted in antiparallel and controlled by an firing angle (α) which varies between 90° and 180° , and a fixed value inductance (L_2) connected in shunt.

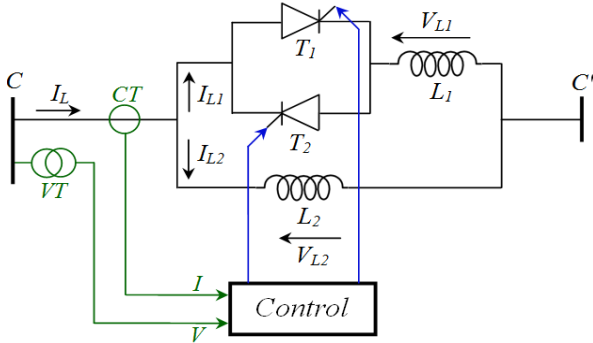


Fig.10 Principal operation of TCSR

This compensator can be modeled as a variable reactance (X_{TCSR}) as shown in Fig.11

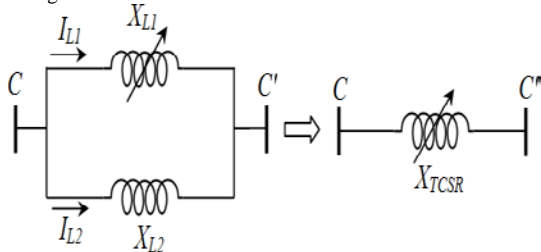


Fig.11 Apparent reactance injected by TCSR

From Fig. 2, the apparent reactance of the TCSR injected on transmission line is defined by the following equation.

$$X_{TCSR} = X_{L1(\alpha)} \parallel X_{L2} = \frac{X_{L1(\alpha)} \cdot X_{L2}}{X_{L1(\alpha)} + X_{L2}}$$

The reactance of the first inductance X_{L1} (α) controlled by thyristors is defined by equation

$$X_{L1}(\alpha) = X_{L1-\max} \left[\frac{\pi}{\pi - 2\alpha - \sin \alpha} \right]$$

Where

$$X_{L1-\max} = L_1 \cdot \omega$$

And the second reactance of inductance (X_{L2}) is defined by formula

$$X_{L2} = L_2 \cdot \omega$$

From above equations and the final equation becomes

$$X_{TCSR} = \frac{L_2 L_1 \omega^2 \left[\frac{\pi}{\pi - 2\alpha - \sin 2\alpha} \right]}{\omega \left[L_2 + L_1 \left[\frac{\pi}{\pi - 2\alpha - \sin 2\alpha} \right] \right]}$$

The AP and RP on transmission line with TCSR are defined by following equations:

$$P(\delta) = \frac{V_A \cdot V_B}{Z_{AB} + X_{TCSR}(\alpha)} \sin(\delta)$$

$$Q(\delta) = \frac{V_B^2}{Z_{AB} + X_{TCSR}} - \frac{V_A \cdot V_B}{Z_{AB} + X_{TCSR}(\alpha)} \cos(\delta)$$

where, Z_{AB} is impedance of transmission line, δ is line angle, V_A and V_B voltage on extremity of transmission line.

B. Shunt FACTS Controllers

Shunt FACTS devices may be variable impedance, variable source, or a combination of these. They inject current into the system at the point of connection.

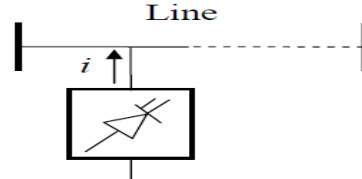


Fig. 11 Shunt FACTS Controllers Connection Diagram

A. TCR & TSR [72]-[75]

TCR is a shunt-connected thyristor-controlled inductor whose effective reactance is varied in a continuous manner by partial-conduction control of the thyristor valve. TCR has been used as one of the economical alternatives of FACTS controllers. An elementary single-phase TCR is shown in Figure . The current in the reactor can be controlled from maximum to zero by the method of firing delay angle control. That is the duration of the current conduction intervals is controlled by delaying the closure of the thyristor valve with respect to the peak of the applied voltage in each half-cycle. For $\alpha = 0^\circ$ the amplitude is at its maximum and for $\alpha = 90^\circ$ the amplitude is zero and no current is flowing during the corresponding half cycle. Like this the same effect is provided as with an inductance of changing value.

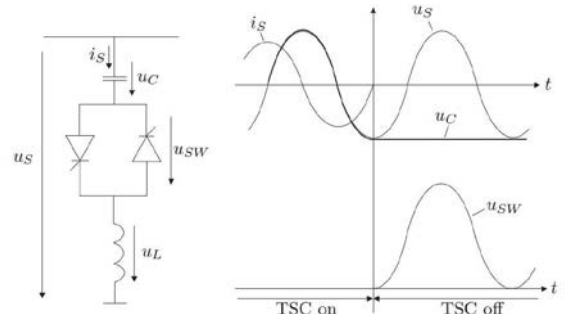


Fig.12 Thyristor-Switched Capacitor

A TSR has similar equipment to a TCR, but is used only at fixed angles of 90° and 180° , i.e. full conduction or no conduction. The reactive current $i_S(t)$ will be proportional to the applied voltage. Several TSRs can provide a reactive admittance controllable in a step-like manner. A Non-conducting thyristor varies in phase with the applied AC voltage. single-phase thyristor-switched capacitor (TSC) is shown in Figure 8. The TSC branch can be switched out at a zero crossing of the current. At this time instance the capacitor value has reached its peak value.

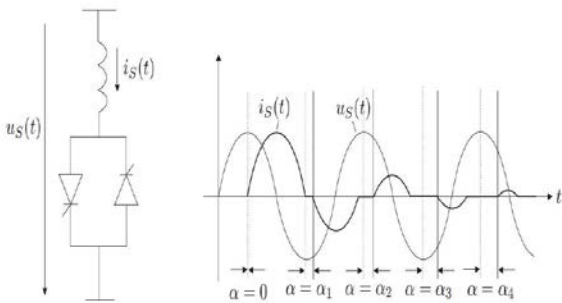


Fig.13 Thyristor Switched Reactor

Normally, the voltage across the capacitor does not remain constant during the time when the thyristor is switched out, but it is discharged after disconnection. To minimize transient disturbances when switching the TSC on, the reconnection has to take place at an instance where the AC voltage and the voltage across the conductor are equal, that is when the voltage across the thyristor valve is zero. However, there will still be transients caused by the non-zero du_S/dt at the instant of switching, which, without the reactor, would result an instant current in the capacitor ($i_S = C.du_S/dt$). The interaction between the capacitor and the current (and di_S/dt) limiting reactor produces oscillatory transients on current and voltage.

B. SVC [76]-[101]

i. Origination

The world's first demonstration of SVC for utility application was installed in 1974, which was commercialized by General Electric (GE). As a consequence of deregulation in UK in 1990, voltage control became difficult. To accommodate the risk associated with the uncertain future and changing power system condition, UK installed relocatable SVC (RSV). At present 12 RSVC (60 MVar each) are operational in the NGC (National Grid Company) system.

ii. Its Features, Related Mathematical Modeling and Control Block Diagram and all Stages of SVC

According to IEEE-CIGRE co-definition, a SVC is a static var generator whose output is varied so as to maintain or control specific parameters (e.g. voltage or RP of bus) of the electric power system.

SVC is a first generation FACTS controller that is already in operation at various places in the world. In its simplest form it uses a TCR in conjunction with fixed capacitor (FC) or (TSC). A pair of opposite poled thyristors is connected in series with a fixed inductor to form a TCR module while the thyristors are connected in series with a capacitor to form a TSC module. An SVC can control the voltage magnitude at the required bus thereby improving the voltage profile of the system. The primary task of an SVC is to maintain the voltage of a particular bus by means of RP compensation (obtained by varying the firing angle of the thyristors). It can also provide increased damping to power oscillations and enhance power flow over a line by using auxiliary signals such as line AP, line RP, line current, and computed internal frequency. SVC is a shunt connected FACTS controller whose main functionality is to regulate the voltage at a given bus by controlling its equivalent reactance. Basically it consists of a fixed capacitor (FC) and a TCR. Generally they are two configurations of the SVC.

- a) **SVC total susceptance model:** A changing susceptance B_{SVC} represents the fundamental frequency equivalent susceptance of all shunt modules making up the SVC as shown in Figure.14(b)
- b) **SVC firing angle model:** The equivalent reactance X_{SVC} , which is function of a changing firing angle α , is made up of the parallel combination of a TCR equivalent admittance and a fixed capacitive reactance. This model provides information on the SVC firing angle required to achieve a given level of compensation as shown in fig.14(a).

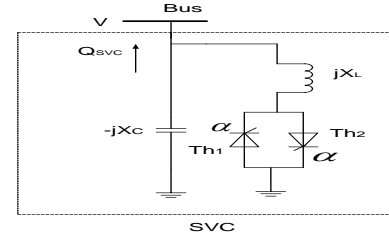


Fig.14. (a) SVC Firing Angle Model

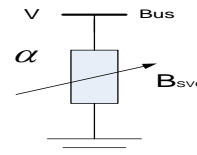


Fig.14 (b) SVC Total Susceptance Model

Fig 15 shows the steady-state and dynamic voltage-current characteristics of the SVC. In the active control range, current/susceptance and reactive power is varied to regulate voltage according to a slope (droop) characteristic. The slope value depends on the desired voltage regulation, the desired sharing of reactive power production between various sources, and other needs of the system. The slope is typically 1-5%. At the capacitive limit, the SVC becomes a shunt capacitor. At the inductive limit, the SVC becomes a shunt reactor (the current or RP may also be limited).

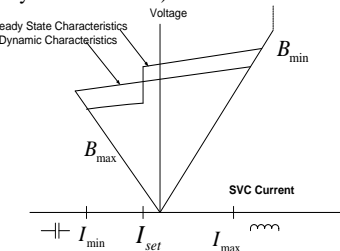


Fig.15. Steady-State and Dynamic Voltage/Current Characteristics of the SVC

SVC firing angle model is implemented in this paper. Thus, the model can be developed with respect to a sinusoidal voltage, differential and algebraic equations can be written as

$$I_{SVC} = -jB_{SVC}V_k$$

The fundamental frequency TCR equivalent reactance X_{TCR}

$$X_{TCR} = \frac{\pi X_L}{\sigma - \sin \sigma}$$

Where $\sigma = 2(\pi - \alpha)$, $X_L = \omega L$

And in terms of firing angle

$$X_{TCR} = \frac{\pi X_L}{2(\pi - \alpha) + \sin 2\alpha}$$

σ and α are conduction and firing angles respectively

At $\alpha = 90^\circ$, TCR conducts fully and the equivalent reactance X_{TCR} becomes X_L , while at $\alpha = 180^\circ$, TCR is blocked and its equivalent reactance becomes infinite.

The SVC effective reactance X_{SVC} is determined by the parallel combination of X_C and X_{TCR}

$$X_{SVC}(\alpha) = \frac{\pi X_C X_L}{X_C [2(\pi - \alpha) + \sin 2\alpha] - \pi X_L}$$

Where $X_C = 1/\omega C$

$$Q_k = -V_k^2 \left\{ \frac{X_C [2(\pi - \alpha) + \sin 2\alpha]}{\pi X_C X_L} \right\}$$

The SVC equivalent reactance is given above equation. It is shown in Fig. that the SVC equivalent susceptance ($B_{SVC} = -1/X_{SVC}$) profile, as function of firing angle, does not present discontinuities, i.e., B_{SVC} varies in a continuous, smooth fashion in both operative regions. Hence, linearization of the SVC power flow equations, based on B_{SVC} with respect to firing angle, will exhibit a better numerical behavior than the liberalized model based on X_{SVC} . In SVC, the resonance phenomenon is present as similar to TCSC. So, this device can't operate in a particular zone due to these phenomena.

This is the drawback of SVC operations in power systems. Figure 18 Shows the SVC equivalent susceptance profile.

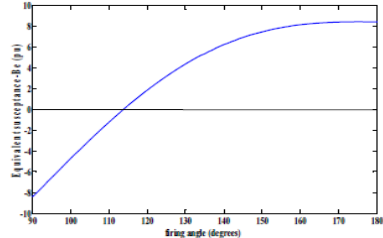


Fig.16 SVC Equivalent Susceptance Profile

C. STATCOM [102]-[113]

i. Origination

STATCOM is the second generation of FACTS controllers that has a very promising future application. STATCOM has several advantages of being small/compact, high response speed and no harmonic pollution. The world's first commercial STATCOM (± 80 MVA, 154 kV) was developed by Mitsubishi Electric Power Products, Inc and was installed at Inuyama substation in Japan in 1991. There are around 20 STATCOM operating successfully around the world.

ii. Its Features, Related Mathematical Modeling and Control Block Diagram and all Stages of STATCOM

A STATCOM is a static synchronous generator operated as a shunt connected SVC whose capacitive or inductive output current can be controlled independent of the ac system voltage.

A STATCOM is a solid state switching converter capable of generating or absorbing independently controllable AP and RP at its output terminals, when it is fed from an energy source or an energy storage device of appropriate rating. A STATCOM incorporate a VSI that produces a set of three phase ac output voltages, each of which is in phase with, and coupled to the corresponding ac system voltage via a relatively small reactance. This small reactance is usually provided by the per phase leakage reactance of the coupling transformer. The VSI is driven by a dc storage capacitor. By regulating the magnitude of the output voltage produced, the reactive power exchange between STATCOM and the ac system can be controlled. The STATCOM is a power electronic-based Synchronous Voltage Generator (SVG) that generates a three-phase voltage from a dc capacitor in synchronism with the transmission line voltage and is connected to it by a coupling transformer. By controlling the magnitude of the STATCOM

voltage, V_s , the reactive power exchange between the STATCOM and the transmission line and hence the amount of shunt compensation can be controlled.

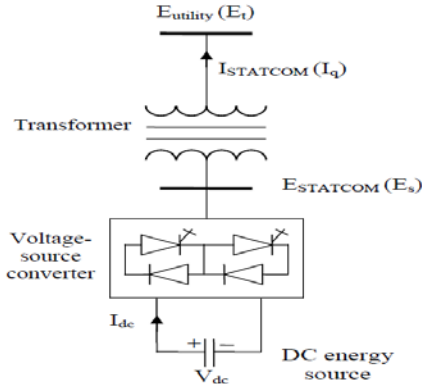


Fig.17 The Structure Of STATCOM

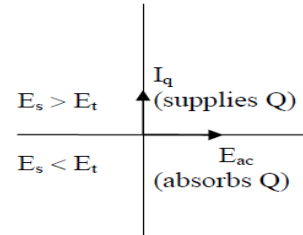


Fig.18 Characteristics of STATCOM

Fig.18 shows the schematic diagram and terminal characteristic of STATCOM, respectively. From Figure, STATCOM is a shunt-connected device, which controls the voltage at the connected bus to the reference value by adjusting voltage and angle of internal voltage source. From Figure, STATCOM exhibits constant current characteristics when the voltage is low/high under/over the limit. This allows STATCOM to deliver constant reactive power at the limits compared to SVC.

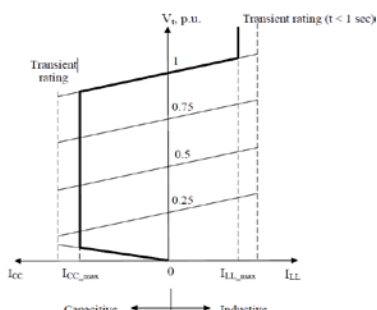


Fig.19. Terminal Characteristic of STATCOM.

The following mode of operation of STATCOM given as:

- Over Excited Mode of Operation ($V_o \geq V_{bus}$):* That is, if the amplitude of the output voltage is increased above that of the ac system voltage, then the current flows through the reactance from the STATCOM to the ac system and the STATCOM generates reactive (capacitive) power for the ac system.
- Under Excited Mode of Operation ($V_o \leq V_{bus}$):* On the other hand, if the amplitude of the output voltage is decreased below that of the ac system, then the reactive current flows from the ac system to STATCOM, and the STATCOM absorbs the reactive (inductive) power.

- c) *Normal (Floating) Excited Mode of Operation ($V_o = V_{bus}$):* If the output voltage is equal to the ac system voltage, the RP exchange is zero. In STATCOM, the resonance phenomenon has been removed. So STATCOM is having more superior performance as compare to SVC.

iii. Its Application In Research

This first high-power STATCOM in the United States was commissioned in late 1995 at the Sullivan substation of the Tennessee Valley Authority (TVA) for transmission line compensation. The STATCOM is employed to regulate the 161 kV bus voltages during the daily load buildup so that the tap changer on the transformer bank will be used less often. The nominal capacity of the STATCOM is ± 100 MVar. This application shows that STATCOM is versatile equipment with outstanding dynamic capability, that will find increasing application in power transmission systems.

e) DSTATCOM [114]-[118]

i. Its Features, Related Mathematical Modeling and Control Block Diagram and all Stages of DSTATCOM

A D-STATCOM is a shunt voltage controller, which is schematically depicted in Fig.20, consists of a two-level VSC, a dc energy storage device, a coupling transformer connected in shunt to the distribution network through a coupling transformer. The VSC converts the dc voltage across the storage device into a set of three-phase ac output voltages. These voltages are in phase and coupled with the ac system through the reactance of the coupling transformer. Suitable adjustment of the phase and magnitude of the D-STATCOM output voltages allows effective control of AP and RP exchanges between the D-STATCOM and the ac system. Such configuration allows the device to absorb or generate controllable AP and RP. The VSC connected in shunt with the ac system provides a multifunctional topology which can be used for up to three quite distinct purposes:

- Voltage regulation and compensation of RP
- Correction of power factor; and
- Elimination of current harmonics.

Here, such device is employed to provide continuous voltage regulation using an indirectly controlled converter.

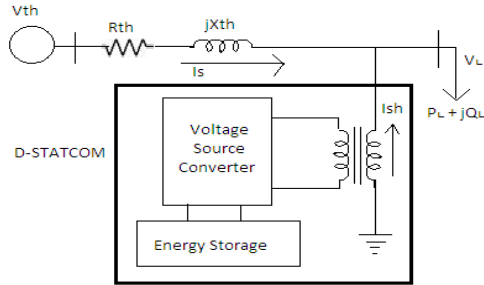


Fig.20 Schematic Dig. of D-STATCOM

The shunt injected current I_{sh} corrects the voltage sag by adjusting the voltage drop across the system impedance Z_{th} . The value of I_{sh} can be controlled by adjusting the output voltage of the converter. The shunt injected current I_{sh} can be written as:

$$I_{sh} = I_L - I_s = I_L - \left(\frac{V_L - V_{Th}}{Z_{Th}} \right)$$

$$I_{sh} \angle \eta = I_L \angle -\theta - \frac{V_{Th}}{Z_{Th}} \angle (\delta - \beta) + \frac{V_L}{Z_{Th}} \angle -\beta$$

The complex power injection of the D-STATCOM can be expressed as,

$$S_{sh} = V_L I_{sh}^*$$

It may be mentioned that the effectiveness of the D-STATCOM in correcting voltage sag depends on the value of Z_{th} or fault level of the load bus. When

the shunt injected current I_{sh} is kept in quadrature with V_L , the desired voltage correction can be achieved without injecting any active power into the system. On the other hand, when the value of I_{sh} is minimized, the same voltage correction can be achieved with minimum apparent power injection into the system .

ii. Its Application In Research

Initial application of DSTATCOM (using GTO devices) was primarily for the control of (fundamental frequency) reactive power control and voltage regulation. SVCs have been applied for this purpose earlier. A DSTATCOM has obvious advantages over a SVC. A major advantage relates to the improved speed of response, capacity for transient overload (up to one second) in addition to the improved performance at reduced voltages. A case study on a § 12 MVAR STATCOM connected at a 12.5 kV, 150 MW substation of Commonwealth Edison of Chicago, U.S.A.

C. Series-Series FACTS Controllers

Combined series-series FACTS device is a combination of separate series FACTS devices, which are controlled in a coordinated manner.

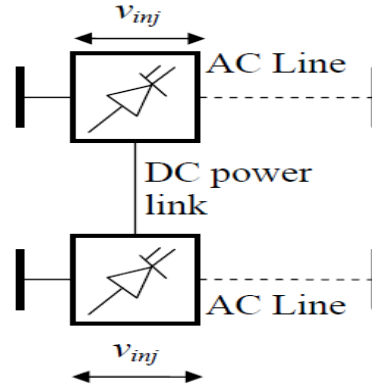


Fig. 21 Series-Shunt FACTS Controller Connection Diagram

1) IPFC [119]-[132]

Generally, IPFC is a combination of two or more independently controllable SSSC which are solid-state VSC which inject an almost sinusoidal voltage at variable magnitude and couples via a common DC link as shown in Fig.22. Conventionally, series capacitive compensation fixed, thyristor controlled or SSSC based, is employed to increase the transmittable real power over a given line and to balance the loading of a normally encountered multi-line transmission system. They are controlled to provide a capability to directly transfer independent real power between the compensated lines while maintaining the desired distribution of reactive flow among the line. The fig.23 shows the Simplified schematic of two-converter IPFC model and basic Two-Inverter IPFC respectively.

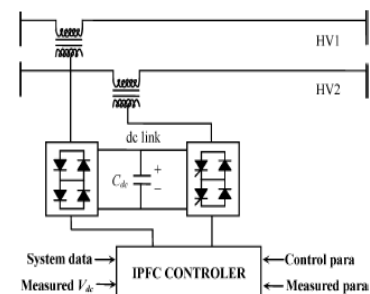


Fig 22 Simplified Schematic of Two-Converter IPFC Model

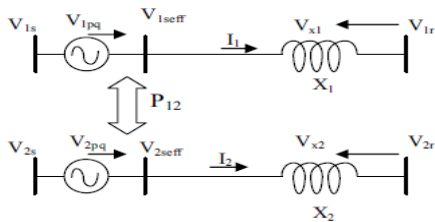


Fig. 23 Basic Two-Inverter Interline Power Flow Controller.

The fig.24 &25 shows the equivalent circuit diagram of the IPFC and power injection model of two converters IPFC respectively.

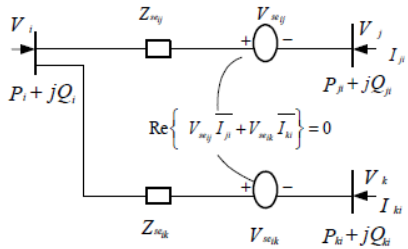


Fig. 24. Equivalent Circuit Diagram of the IPFC

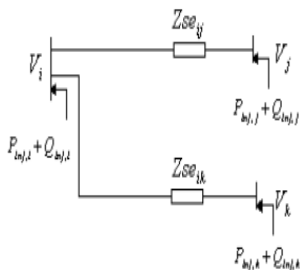


Fig. 25 Power Injection Model of Two Converters IPFC

D. Series-shunt FACTS controllers

Combined series-shunt FACTS device is a combination of separate shunt and series devices, which are controlled in a coordinated manner or one device with series and shunt elements.

1) UPFC [133]-[195]

i. Origination

Combining the STATCOM and the SSSC into a single device with a common control system represents the third generation of FACTS known as UPFC. It has the unique ability to control AP and RP flow independently. The first utility demonstration of a UPFC is being constructed at the Inez substation of American Electric Power in 1998. Recently, 80 MVA UPFC is being constructed at Gangjin substation in South Korea.

ii. Its Feature, Related Mathematical Modeling and Control Block Diagram and all Stages of UPFC

A combination of STATCOM and a SSSC which are coupled via a common dc link, to allow bidirectional flow of real power between the series output terminals of the SSSC and the shunt output terminals of the STATCOM, and are controlled to provide concurrent real and reactive series line compensation without an external electric energy source. The UPFC, by means of angularly unconstrained series voltage injection, is able to control,

concurrently or selectively, the transmission line voltage, impedance, and angle or, alternatively, the real and reactive power flow in the line. The UPFC may also provide independently controllable shunt reactive compensation.

The UPFC is the most versatile and powerful FACTS device. UPFC is also known as the most comprehensive multivariable FACTS controller. Simultaneous control of multiple power system variables with UPFC posses enormous difficulties. In addition, the complexity of the UPFC control increases due to the fact that the controlled and the variables interact with each other. UPFC is used to control the power flow in the transmission systems by controlling the impedance, voltage magnitude and phase angle. This controller offers advantages in terms of static and dynamic operation of the power system. It also brings in new challenges in power electronics and power system design. The basic structure of the UPFC consists of two VSI; where one converter is connected in parallel to the transmission line while the other is in series with the transmission line.

The UPFC consists of two VSC; series and shunt converter, which are connected to each other with a common dc link. Series converter or SSSC is used to add controlled voltage magnitude and phase angle in series with the line, while shunt converter or STATCOM is used to provide reactive power to the ac system, beside that, it will provide the dc power required for both inverter. Each of the branches consists of a transformer and power electronic converter. These two VSC shared a common dc capacitor. The energy storing capacity of this dc capacitor is generally small. Therefore, AP drawn by the shunt converter should be equal to the AP generated by the series converter. The RP in the shunt or series converter can be chosen independently, giving greater flexibility to the power flow control. The coupling transformer is used to connect the device to the system. Shows the schematic diagram of the three phases UPFC connected to the transmission line.

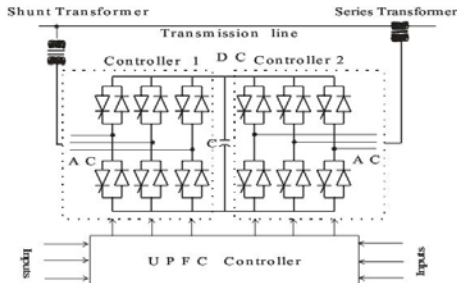


Fig. 26 Schematic Diagram of Three Phases UPFC Connected To a Transmission Line

With the presence of the two converters, UPFC not only can supply reactive power but also active power. Fig. 27 shows the equivalent single line circuit diagram representation of UPFC in power system and UPFC model schematic. The figure shows the UPFC model equivalent.

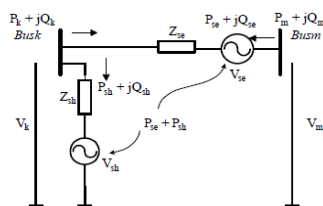


Fig. 27 Equivalent Single Line Circuit Diagram Representation of UPFC in Power Systems

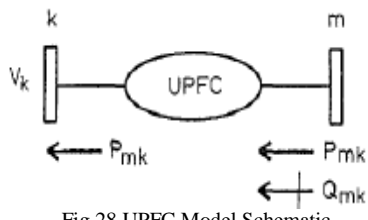


Fig.28 UPFC Model Schematic

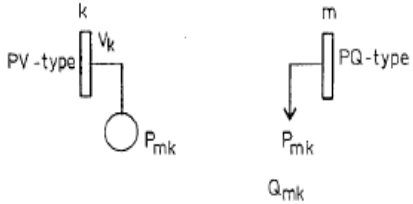


Fig.29 UPFC Model Equivalent

The sending end of the UPFC is transformed into a PQ bus, whilst the receiving end is transformed into a PV bus. The active and reactive power loads in the PQ bus are set to the values being controlled by the UPFC. The voltage magnitude at the PV bus is set at the value to be controlled by the UPFC. A standard load flow solution is carried out with the equivalent model given in Fig. 5. After load flow convergence, an additional set of nonlinear equations is solved by iteration to compute the UPFC parameters. This method is simple but will only work if the UPFC is used to control voltage magnitude, active power and reactive power, simultaneously. If one only wishes to control one or two variables, the method is no longer applicable. Moreover, since the UPFC parameters are computed after the load flow has converged, there is no way of knowing during the iterative process whether or not the UPFC parameters are within limits.

iii. Its Application In Research

This first UPFC in the world was commissioned in mid-1998 at the Inez station of the American Electric Power (AEP) in Kentucky for voltage support and power flow control. This UPFC was designed to provide fast reactive shunt compensation with a total control range 320 MVar, and control power flow in the 138 kV high-capacity transmission line. Furthermore, it can be applied to force the transmitted power, under contingency conditions, up to 950 MVA.

III. OTHER GENERATIONS OF FACTS CONTROLLERS

A. Third Generation FACTS controllers

1) GUPFC [196]-[201]

An innovative approach to utilization of FACTS controllers providing a multifunctional power flow management device. There are several possibilities of operating configurations by combining two or more converter blocks with flexibility. Among them, there are two novel operating configurations, namely the IPFC and the GUPFC, which are significantly extended to control power flows of multi-lines or a sub-network rather than control power flow of single line by a UPFC or SSSC.

In contrast to the practical applications of the GUPFC in power systems, very few publications have been focused on the mathematical modeling of this new FACTS controller in power system analysis. A fundamental frequency model of the GUPFC consisting of one shunt converter and two series converters for EMTP study was proposed quite recently in open literatures. While modeling the GUPFC in power flow, optimal power flow (OPF) analysis has not been reported yet. Therefore, in open literatures, a mathematical model of the GUPFC suitable for power flow and optimal power flow study is established. In the past three decades, techniques such as Newton method, sequential linear and quadratic programming method, PQ de-coupling method, etc. Have been used to solve optimal power flow problems. The GUPFC with

combing three or more converters working together extends the concepts of voltage and power flow control beyond what is achievable with the known two-converter UPFC FACTS controller. The simplest GUPFC consists of three converters, one connected in shunt and the other two in series with two transmission lines in a substation. It can control total five power system quantities such as a bus voltage and independent AP and RP flows of two lines. Such a GUPFC, which is shown in Fig.30, is used to show the basic operation principle for the sake of simplicity. However, the mathematical derivation is applicable to a GUPFC with an arbitrary number of series converters. In the SS operation, the main objective of the GUPFC is to control voltage and power flow. The equivalent circuit of the GUPFC consisting of one controllable shunt injected voltage source and two controllable series injected voltage sources is shown in Figure. Real power can be exchanged among these shunt and series converters via the common DC link. The sum of the real power exchange should be zero if we neglect the losses of the converter circuits. For the GUPFC shown in Figures, it has total 5 degrees of control freedom, which means it can control five power system quantities such as one bus voltage, and 4 AP and RP flows of two lines. It can be seen that with more series converters included within the GUPFC, more degrees of control freedom can be introduced and hence more control objectives can be achieved. The simplest GUPFC consists of three switching converters. These converters are operated from two common dc link provided by two dc storage capacitors as shown in Fig.30

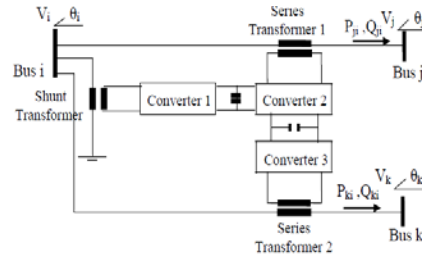


Fig.30 Basic Circuit Arrangement of GUPFC

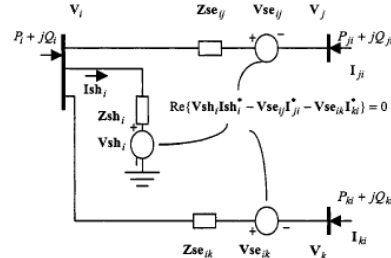


Fig.31 The Equivalent Circuit of The GUPFC

2) HPFC [202]-[203]

It introduced a HFC as a new member of FACTS controllers for steady-state and power-flow control of power transmission lines. HFC is a hybrid compensator (i.e., provides series and/or shunt compensation). Structurally, an HFC unit is composed of a mechanically switched PST, a mechanically switched shunt capacitor, and multi-module, series connected, thyristor-switched capacitors and inductors. The steady-state operation, single-phase equivalent circuit, power flow model, and $V-I$ and $P-Q$ characteristics of the HFC. It highlighted the steady-state technical features of the HFC for power-flow control of a study system and also provides a quantitative comparison of the HFC, UPFC, and PST.

It introduced a HFC as a new FACTS controller which:

- describes its SS principles of operations;
- develops its single-line equivalent circuit and power-flow model; and
- Investigates its SS power flow control characteristics.

Conceptually, HFC is not a new circuit configuration and rather an amalgamation of existing and well established power-flow controllers, that is,

- Conventional mechanically switched PST
- A conventional mechanically switched shunt capacitor (MSC);
- A multi-module TSSC;
- A multi-module TSSR.

TSSC and TSSR subsystems of an HFC are electronically switched, and thus are adequately fast to 1) respond to system dynamics and 2) provide dynamic power-flow control. However, this paper investigates only steady-state behavior and characteristics of an HFC. Due to the inherent discrete operational nature of the HFC, its dynamic control and behavior are best investigated based on a discrete-event supervisory control strategy and will be the subject of a separate article. HFC belongs to the family of hybrid compensators since it provides power-flow control through series and/or shunt compensation, analogous to the UPFC. Although HFC does not offer all versatility and technical features of the UPFC, its salient features make it an alternative to the UPFC. These features are:

- Cost effectiveness;
- Simplicity of concept, control, and operational strategies;
- Maturity and ruggedness of the technologies of its various subsystems;
- Lower losses and, thus, higher efficiency.

HFC provides economical incentive in a scenario that an existing PST is augmented with TSSC and/or TSSR modules to form an HFC. Furthermore, since TSSC and TSSR modules are not phase-controlled and only switched in and out by thyristor switches, HFC does not generate harmonics and has no adverse impact on power quality. Figure shows a schematic diagram of an HFC that is connected between buses i and j within a transmission line and is comprised of:

- A PST which can inject a lead/lag, quadrature-phase voltage.
- Multimodule TSSC system that can insert a variable series capacitive reactance, in discrete steps, to adjust the line series reactance.
- Multimodule TSSR system that can insert a variable series inductive reactance, in discrete steps, to prevent overflow.
- An MSC for reactive power compensation.

Due to their inherent large time-constants, PST and MSC can only impact steady-state power flow, while the TSSC and the TSSR modules can provide both dynamic and steady-state power-flow control. By replacing one TSSC module with a TCSC module, continuous control of series reactance also can be achieved. Based on the configuration of Fig. 32, a per-phase schematic representation of the HFC is given in Fig. 33. The details to reduce the single-phase PST of Fig. 33 from that of Fig. 32, under balanced conditions. The extraction of per phase representations of the TSSC, TSSR, and MSC of Fig. 33 from those of Fig. 32, under a balanced condition.

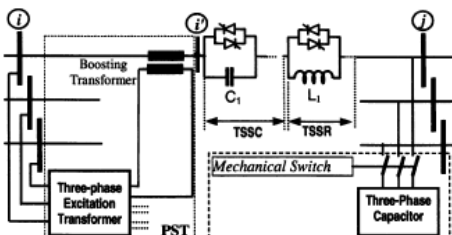


Figure 32 Schematic diagram of an HPFC

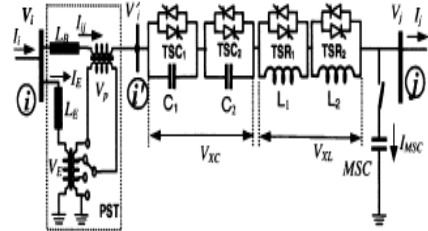


Figure 33 Per-phase schematic representation of HPFC

A steady-state $V - I$ characteristic of the HFC of Fig. 32 is shown in Fig. 34. I V and j V voltage phasors of buses i and j , respectively. The PST injects quadrature-phase voltage p V , and ' i ' V is the voltage of the HFC internal bus (i.e., ' i ' bus). A steady-state $V - I$ characteristic of the HFC of Fig. 34 is shown in Fig. 34. I V and j V are voltage phasors of buses i and j , respectively. The PST injects quadrature-phase voltage p V , and ' i ' V is the voltage of the HFC internal bus (i.e., bus ' i '). In Fig. 34(b), the phasor of line current ij I is lagging i V by angle ϕ . Fig. 34(a) also shows the TSSC voltage XC V for $\phi = 0^\circ$ and $m \phi = \phi_m$, and the corresponding voltage at bus j (i.e., j V), corresponding to a pre-specified reactance of MSC. Magnitude of XC V depends on 1) the magnitude of line current ij I and 2) the number of TSSC modules in service. It should be noted that the TSSC is less effective to control real power flow when the line current is small.

However the magnitude of the injected voltage by the PST is almost independent of the line current and can be controlled only by the PST voltage ratio, from 0 to p_{max} V . As a result, for those conditions where the HFC operates under a lightly loaded line, the PST subsystem of HFC can effectively control real power flow, and the TSSC modules can be used to adjust the power flow only in small steps. Under heavy power-flow conditions, TSSC can effectively control the power flow and also reduce adverse impact of high current switching on the PST mechanical taps. The Fig. 35(a) & 35(b) shows the steady-state V - I characteristics of HPFC.

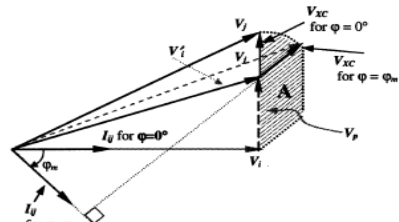


Fig.34(a)

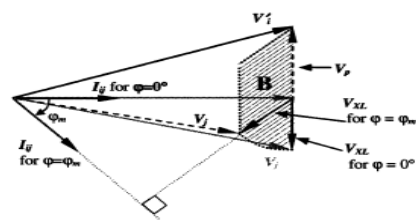


Fig.34(b)

Figure 34(A) &34(B) Steady-State V - I Characteristic of HPFC, TSSC in Service. (B) TSSR in Service

Fig. 34(b) shows a $V - I$ characteristic of the HFC when the TSSC modules are shorted and the TSSR is operational. Fig. 34(b) shows TSSR voltage phasor XL V for $\phi = 0^\circ$ and, $m \phi = \phi_m$, and the corresponding j V bus j . A combination of shaded areas A and D of Fig. 22 specifies the - area that the HFC can control the line power flow. If the PST is capable of injecting lagging quadrature voltage, the corresponding V - I characteristics regions are added to regions A and B of Fig. 35 to determine the overall V - I area.

Conceptually, there are three approaches to develop an HFC model for power-flow analysis. The first one is the classical approach which is based on augmenting the system matrix to include the HFC model. The drawback of this approach is that the augmented becomes asymmetrical, and thus can be used neither in a decoupled power-flow analysis, nor for efficient storage. The power flow model of HPFC shown in fig.35

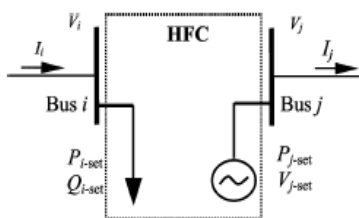


Fig.35. Power-flow model of HPFC

B. Energy Storage FACTS Controllers

1) SMES [204]-[212]

i. Its Features ,Related Mathematical Modeling and Control Block Diagram and all Stages of SMES

The SMES recharges within minutes and can repeat the charge/discharge sequence thousands of times without any degradation of the magnet. Recharge time can be accelerated to meet specific requirements, depending on system capacity. This is an energy storage device with a lot of promise in effectiveness in terms of capacity and efficiency. SMES units use liquid helium to keep the coil of niobium-titanium at 4.2K, the temperature required for its material to become superconducting. The block diagram is shown in fig.35

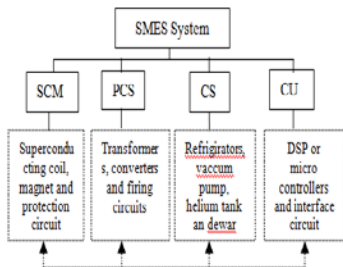


Fig.35 Block Diagram of SMES

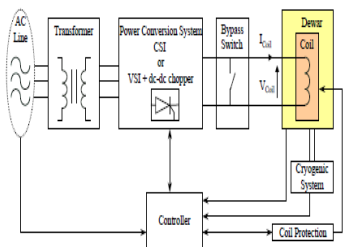


Fig.36 Super Conducting Magnetic Energy Storage System

An SMES unit consists of a large superconducting coil at the cryogenic temperature. This temperature is maintained by a cryostat or Dewar that contains helium or nitrogen liquid vessels. A power conversion/ conditioning system (PCS) connects the SMES unit to an ac power system, and it is used to charge/discharge the coil. Two types of power conversion systems are commonly used. One option uses a current source converter (CSC) to both interface to the ac system and charge/discharge the coil. The second option uses a VSC to interface to the ac system and a dc-dc chopper to

charge/discharge the coil. The VSC and dc-dc chopper share a common dc bus. The modes of charge/discharge/standby are obtained by controlling the voltage across the SMES coil. The SMES coil is charged or discharged by applying a positive or negative voltage across the superconducting coil. The inductively stored energy (in joules) which is shown below.

$$E = \frac{1}{2} L I^2$$

$$p = \frac{dE}{dT} = LI \frac{dI}{dT}$$

SMES' efficiency and fast response capability (MW/millisecond) have been, and can be further exploited in applications at all levels of electric power systems. Some of them are:

- Frequency support (spinning reserve) during loss of generation.
- Enhancing transient and dynamic stability.
- Dynamic voltage support (VAR compensation).
- Improving power quality.
- Increasing transmission line capacity, thus enhancing overall security and of reliability Power systems.
- It has efficiency greater than or equal to 90%.

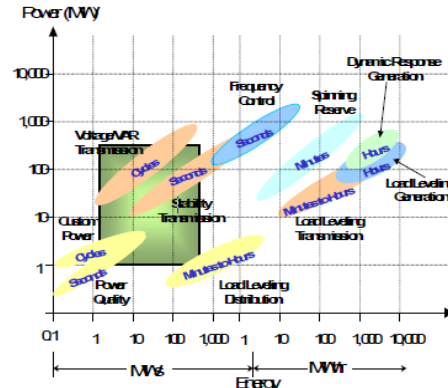


Fig.36 Energy-Power Characteristics For Potential SMES Applications For Generation, Transmission, And Distribution.

ii. Its Application In Research

- An advantage of SMES is that power is available almost instantaneously, and very high power output is provided for a brief period of time. There is no loss of power, and are no moving parts.
- Already dramatically used in such applications as high-speed, magnetic-levitated trains, superconductors are also being developed for use in microelectronics and communications

2) BESS [213]-[218]

In December 2011 the first pilot installation of a BESS in a Swedish distribution system commissioned by Falbygdens Energy was energized in the city of Falköping. A BESS is a packaged solution of power equipment such as coupling transformer and sensing transformer, medium and low voltage switchgear together with automation equipment such as inverters in a complete segregated enclosure. The energy is stored in batteries for use at a later time or to effectively optimize cost. This solution can store electrical energy and supply it to the loads as a primary or supplementary source. It provides a stable and continuous power supply regardless of the supply source status and voltage. Moreover, generation smoothing and transient support for renewable energies are feasible with this solution.

a) Low voltage distribution and control switchboard

The low voltage distribution and control switchboard (see LV in) includes the incoming AC circuit breaker, BESS station local control system's components and other protection and control equipment needed for the operation of the facility.

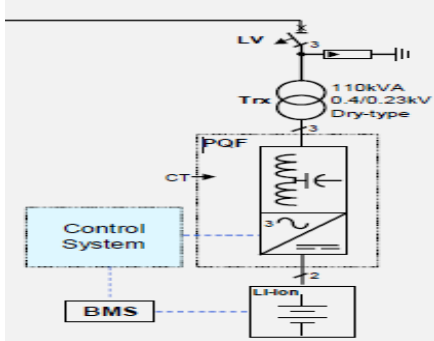


Fig.37

b) Coupling transformer

In order to connect the battery system to the 400 VAC grid, a 110kVA dry-type coupling transformer has been used, due to the low voltage present in the battery array.

c) Power electronic bi-directional converter

The bi-directional power electronic converter is one of the main components of the BESS. It acts as a rectifier during the charging of the batteries and as an inverter during the supplying of the energy from the batteries to the grid. For this application, the converter selected is the PQFI -V1- M25 - IP21 manufactured by ABB.

The internal control, with a closed loop strategy, is able to generate a compensation current for each harmonic frequency. This is in perfect phase opposition to the polluting current taking into account the high frequency rejection filter included in this solution. The current transformers (CTs) are installed on the incoming busbars of the LV Switchboard inside the existing CSS (CT) in order to monitor the power flow on the grid.

d) Battery Management System (BMS)

The BMS performs the measurement necessary to manage the batteries (voltage, temperature, current) in order to extend the battery life and increase the safety of the system.

e) Batteries

The batteries have been selected according to the power and energy requirements. The LiFePO4 battery array has a nominal voltage of 547Vdc (428 Vdc – 616 Vdc), 80.5Kw nominal power and 85kWh nominal energy. The deviation in the nominal power from 75kW is to compensate the losses inside the converter and the coupling transformer and the degradation in the batteries during their lifetime.

C. ADDITIONAL FACTS CONTROLLERS

1) UIPC [220]-[224]

FACTS came into existence in order to overcome the changing conditions in power systems. Among all of the FACTS devices IPC has many capabilities like power-flow control, voltage isolation and fault current limitation. By modeling IPC can be realized as decoupling interconnector, FCLT, PFC, and assisted phase-shifting transformer. A general model of IPC is shown in Fig.38. From the fig.38 it is clearly seen, each phase consists of two parallel branches. And each branch consists of a reactance (inductor or capacitor) connected in series with the phase-shifting device. Different IPC structures have been suggested the in depending upon IPC control variables like reactance, internal phase angles, or both. In the reactance control strategy, different reactance levels will result in different active power flows. For the

tuned IPC, having equal reactance for the inductor and capacitor, many unique structures have been reported based on the reactance or phase-angle control. The relative increase of the voltage drop across the reactance followed by an increasing growth of the reactance rating is the main problem of this strategy.

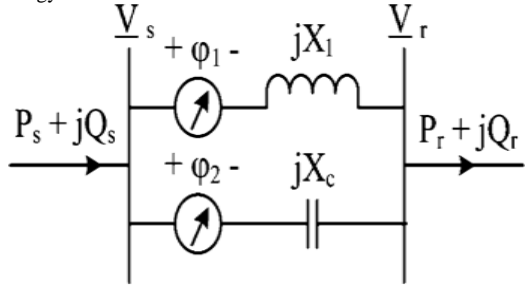


Fig.38 IPC Model

The range of power control of IPCs is limited due to the PSTs phase-shift limitations. PSTs are replaced by SSSCs in this paper in order to increase the power control range of IPCs. The ideal lossless converter can be modeled by a dc voltage-converter ac voltage source transmitting the active power between ac and dc sides at the fundamental frequency.

The fundamental frequency equations are completed by the active power conservation between the ac sides and dc sides, as follows:

$$P_{AC} = \text{Re}[V_{AC} \cdot I^*_{AC}] = P_{DC} = V_{DC} \cdot I_{DC}$$

where P_{AC} and P_{DC} are active powers in the ac and dc sides, respectively

IV. COMPARATIVE CHARTS OF FACTS CONTROLLERS

The various FACTS controllers such as TCSC, SSSC, TC-PSR, TC-PST, TCR, TCS, SVC, STATCOM, UPFC, HPFC, SMES, BESS, UIPC, IPFC, GUPFC & their special features are explained in table.1

Table .1 FACTS Controllers And Its Features

| Subject | Problem | Corrective action | FACTS |
|---------------------|--------------------------------------|---|-----------------|
| Voltage limits | Low voltage at heavy load | Supply reactive power | SVC,STATCOM |
| | | Reduce line reactance | TCSC |
| | High voltage at low load | Absorb reactive power | SVC,STATCOM |
| | High voltage following an outage | Absorb reactive power, prevent overload | SVC,STATCOM |
| | Low voltage following an outage | Supply reactive power, prevent overload | SVC,STATCOM |
| Thermal limits | Transmission circuit overload | Increase transmission capacity | TCSC,SSSC,UPFC |
| Load flow | Power distribution on parallel lines | Adjust line reactance | TCSC, SSSC |
| | | Adjust phase angle | UPFC, SSSC, PAR |
| | Load flow reversal | Adjust phase angle | UPFC, SSSC, PAR |
| Short circuit power | High short circuit current | Limitation of short circuit current | TCSC, UPFC |
| Stability | Limited transmission power | Decrease line impedance | TCSC, UPFC |

Table .2 FACTS Controllers And Its Control Variables

| Controller | Constraint Equations | Control Variable(s) |
|------------|----------------------|---------------------|
| | | |

| | | |
|---------|--|------------|
| SVC | $V_p = 0, V_r = 0, I_p = 0, I_r = -B_{SVC}V_1$ | B_{SVC} |
| TCSC | $I_p = 0, I_r = 0, V_p = 0, V_r = X_{TCSC}I_2$ | X_{TCSC} |
| TCPAR | $V_1I_p = V_pI_2 = I_2V_r$ | ϕ |
| STATCOM | $V_p = 0, V_r = 0, I_p = 0$ | I_r |
| SSSC | $I_p = 0, I_r = 0, V_p = 0$ | V_r |

V. SUMMARY OF PAPER

A) Series FACTS controller

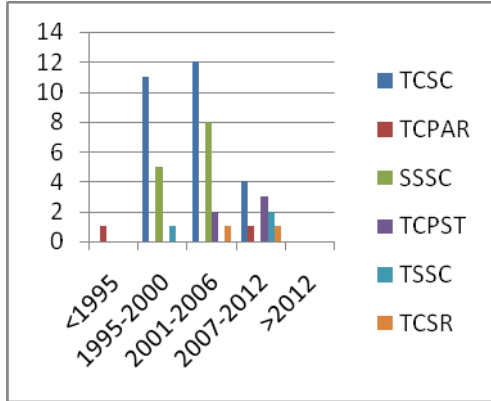


Fig.39 Comparative Graph of Series FACTS Controllers

Fig.40 Total No. of Literature Review

| YEAR | TCSC | TCPAR | SSSC | TCPST | TSSC | TCSR |
|-----------|------|-------|------|-------|------|------|
| <1995 | | 1 | | | | |
| 1995-2000 | 11 | | 5 | | 1 | |
| 2001-2006 | 12 | | 8 | 2 | | 1 |
| 2007-2012 | 4 | 1 | | 3 | 2 | 1 |
| >2012 | | | | | | |

From the above table & Fig.39 it is concluded that above 52 literatures are reviewed based on various series FACTS Controllers for the betterment power flow control in power system from 1995-2012.

B) Shunt FACTS Controller

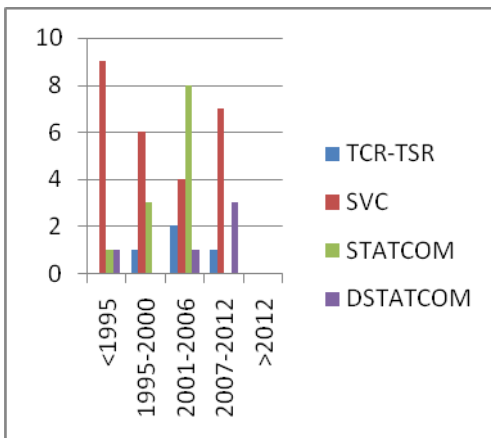


Fig.41 Comparative Graph of Shunt FACTS Controllers

Fig.42 Total No. of Literature Review

| YEAR | TCR - TSR | SVC | STATCOM | DSTATCOM |
|-----------|-----------|-----|---------|----------|
| <1995 | | 9 | 1 | 1 |
| 1995-2000 | 1 | 6 | 3 | |
| 2001-2006 | 2 | 4 | 8 | 1 |
| 2007-2012 | 1 | 7 | | 3 |
| >2012 | | | | |

From the above table & fig.41 it is concluded that above 47 literatures are reviewed based on various shunt FACTS Controllers for the reactive power control in power system from 1995-2012.

C) Series -Series FACTS Controller

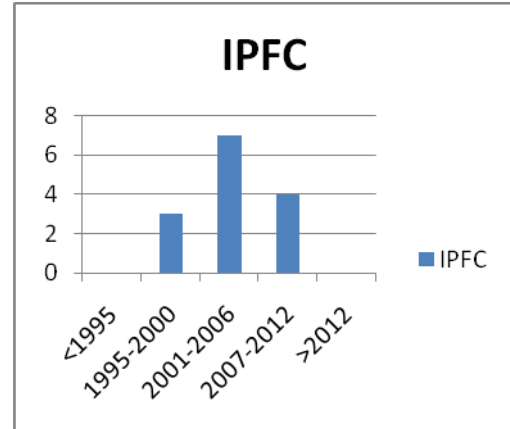


Fig.43 Bar Graph of Series-Series FACTS Controllers

Fig.44 Total No. of Literature Review

| YEAR | IPFC |
|-----------|------|
| <1995 | |
| 1995-2000 | 3 |
| 2001-2006 | 7 |
| 2007-2012 | 4 |
| >2012 | |

From the above table & fig .43 it is concluded that above 14 literatures are reviewed based on various series-series FACTS Controllers for the power flow control in power system from 1995-2012.

D) Series Shunt FACTS Controller

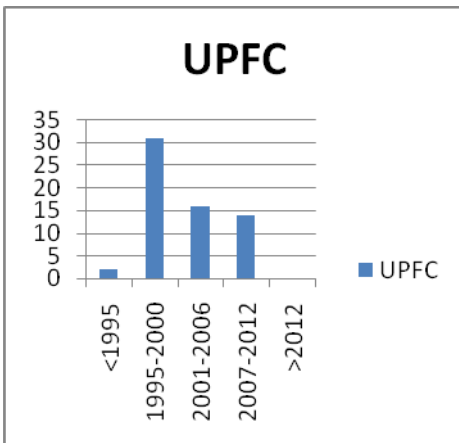


Fig.44 Bar Graph of Series-Shunt FACTS Controllers

Fig.46 Total No. of Literature Review

| YEAR | UPFC |
|-----------|------|
| <1995 | 2 |
| 1995-2000 | 31 |
| 2001-2006 | 16 |
| 2007-2012 | 14 |
| >2012 | 0 |

From the above table & fig. 44 it is concluded that above 63 literatures are reviewed based on various series-shunt FACTS Controllers for the power flow control as well as reactive power control in power system from 1995-2012.

E) *3rd Generation FACTS Controllers*

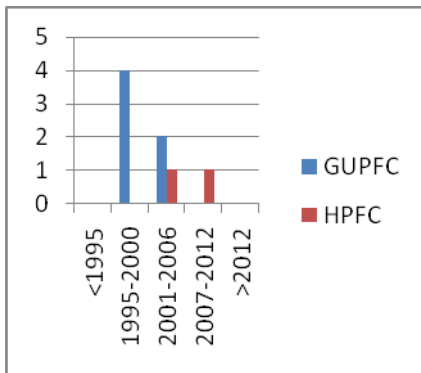


Fig.47 Comparative Graph of 3rd generation FACTS Controllers

Fig.48 Total No. Of Literature Review

| YEAR | GUPFC | HPFC |
|-----------|-------|------|
| <1995 | 4 | 0 |
| 1995-2000 | 2 | 1 |
| 2001-2006 | 0 | 1 |
| 2007-2012 | 0 | 0 |
| >2012 | 0 | 0 |

From the above table & fig.47 it is concluded that above 8 literatures are reviewed based on various 3rd generation FACTS Controllers for the power flow control as well as reactive power control along with reactance control in power system from 1995-2012.

F) *Energy Storage FACTS Controllers*

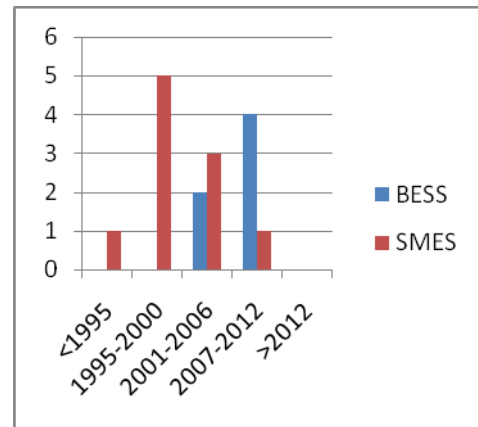


Fig.49 Comparative Graph of Energy Storage FACTS Controllers

Fig.50 Total No. of Literature Review

| YEAR | BESS | SMES |
|-----------|------|------|
| <1995 | 0 | 1 |
| 1995-2000 | 0 | 5 |
| 2001-2006 | 2 | 3 |
| 2007-2012 | 4 | 1 |
| >2012 | 0 | 0 |

From the above table & fig.49 it is concluded that above 16 literatures are reviewed based on various energy storage FACTS Controllers when coupled with other VSI based FACTS Controllers used for the power flow control as well as reactive power control along with reactance control in power system from 1995-2012.

G) *Additional FACTS Controller*

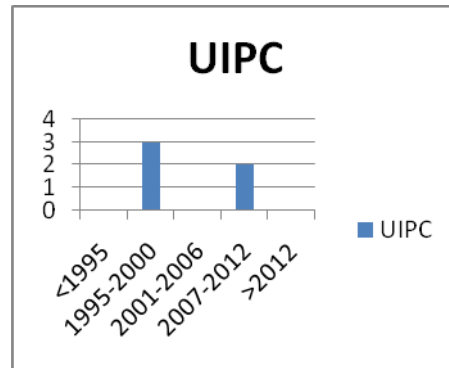


Fig.51 Bar Graph of Series-Shunt FACTS Controllers

Fig.52 Total No. of Literature Review

| YEAR | UIPC |
|-----------|------|
| <1995 | 0 |
| 1995-2000 | 3 |
| 2001-2006 | 0 |
| 2007-2012 | 2 |
| >2012 | 0 |

From the above table & fig.51 it is concluded that above 5 literatures are reviewed based on an additional FACTS Controllers to extend the range of power flow control in power system from 1995-2012.

VI. CONCLUSION

Finally it is concluded that the maximum research work is carried out regarding various FACTS controllers in power system environment for enhancement of different power system parameters such as APTC, voltage profile, minimum real power loss, minimum reactive power loss, improve steady state stability, improve transient stability, improve power system oscillations in last 2 decades.

VII. ACKNOWLEDGMENT

The authors would like to thanks Prof.(Dr) K.S Verma, Director, and Prof. (Dr) R.P. Payasi, HEED, KNIT Sultanpur, U.P.-228118, India, for discussions regarding with comprehensive survey regarding of a historical background of FACTS controllers in power system environments..

REFERENCES

- [1] Y. H. Song, A. T. Johns. *Flexible AC Transmission Systems (FACTS)*, IEE Press, London, 1999. ISBN 0-85296-771-3.
- [2] J.Y. Liu; Y.H. Song; P.A. Mehta, "Strategies for handling UPFC constraints in steady-state power flow and voltage control". *IEEE Transactions on Power Systems*. VOL. 15, May 2000, pp. 566–571 .
- [3] S. Gerbex, R. Cherkaoui, and A. J. Germond, "Optimal location of multi-type FACTS devices in a power system by means of genetic algorithms," *IEEE Trans. Power Systems*, vol. 16, August. 2001, pp. 537-544.
- [4] J.Y. Liu; Y.H. Song; P.A. Mehta, "Strategies for handling UPFC constraints in steady-state power flow and voltage control". *IEEE. Transactions on Power Systems*. VOL. 15, May 2000, pp. 566–571
- [5] R.J.Nelson, J-Bian, D.G.Ramey, T.A.Lemak, T-R-Reitman, J.E.Hil1 " Transient Stability enhancement with FACTS controllers" *Sixth International Conference on AC & DC Transmission*, No.423, 1997
- [6] N. Hingorani and L. Gyugyi, *Understanding FACTS—Concepts and Technology of Flexible AC Transmission Systems*. Piscataway, NJ: IEEE Press/Wiley, 2000.
- [7] Claudio A. Canizares, and Zeno T. Faur, " Analysis of SVC and TCSC Controllers in Voltage Collapse," *IEEE Trans on Power Systems*, Vol. 14, No. 1, February 1999.
- [8] Ashwani kumar Sharma,"Optimal Number and Location of TCSC and Loadability Enhancement in Deregulated Electricity Markets Using MINLP," *International Journal of Emerging Electric Power Systems*, Vol.5, Issue 1, 2006.
- [9] Guang Ya Yang, Geir Hovland, Rajat Majumder, and Zhao Yang Dong, "TCSC Allocation Based on Line Flow Based Equations Via Mixed-Integer Programming," *IEEE Trans on Power Systems*, Vol.22, No.4, November 2007.
- [10] Srinivasa Rao Pudi, and S.C.Srivastava, "Optimal Placement of TCSC Based on A Sensitivity Approach for Congestion Management," *Fifteenth National Power Systems Conference (NPSC)*, IIT Bombay, December 2008, pp.558-563.
- [11] S.Gerbex, R. Cherkaoui, and A.J.Germond, "Optimal Location of Multi-Type FACTS Devices in a Power System by Means of Genetic Algorithms," *IEEE Trans. on Power Systems*, vol.16, No.3, pp. 537-544, August 2001.
- [12] A. Kazemi, and B. Badrzadeh, "Modeling and Simulation of SVC and TCSC to Study Their Limits on Maximum Loadability Point," *Electrical Power & Energy Systems*, Vol. 26, pp. 619-626, 2004.
- [13] J.G. Singh, S. N. Singh, and S. C. Srivastava, "Placement of FACTS Controllers for Enhancing Power System Loadability", *IEEE Trans. on Power Delivery*, Vol. 12, No.3, July 2006.
- [14] B. Chaudhuri, and B. C. Pal, "Robust Damping of Multiple Swing Modes Employing Global Stabilizing Signals with a TCSC," *IEEE Trans on Power Systems*, Vol. 19, No.1, February 1999.
- [15] S. N. Singh and A. K. David, "A new approach for placement of FACTS Devices in Open Power Market," *IEEE Power Engg. Rev.*, 2001, 21(9), pp. 58-60.
- [16] N. K. Sharma, A. Ghosh, and R. K. Verma, "A Novel Placement Strategy for FACTS Controllers", *IEEE Trans. on Power Delivery*, Vol. 18, No.3, July 2003.
- [17] W. H. Litzenberger, R. K. Verma and J. D. Flanagan, "An Annotated Bibliography of HVDC transmission and FACTS Devices 1996-1997," *Electric Power Research Institute*, WO-3022 06 , June 1998.
- [18] E. J. Oliveira, J. W. M. Lima, and K de. Almeida, "Allocation of FACTS devices in Hydrothermal Systems," *IEEE Trans. on Power Systems*, Vol. 15, No.1, pp. 276-282, February 2000.
- [19] Tjing T. Lie and WanHong Deng, "Optimal Flexible AC Transmission Systems (FACTS) Devices Allocation," *Electrical Power & Energy Systems*, Vol. 19, No.2, pp. 125-134, 1997.
- [20] J.J. Sanchez-Gasca, "Coordinated Control of two FACTS devices for Damping Inter-area Oscillations," *IEEE Trans. on Power Systems*, Vol.13, No.2, pp. 428-434, May 1998.
- [21] Ping Lam So, Yun Chung Chu, and Tao Yu, "Coordinated Control of TCSC and SVC for system Damping Enhancement," *International Journal of Control Automation and Systems*, Vol. 3, No.2, (special edition), pp. 322-333, June 2005.
- [22] L. J. Cai, and I. Erlich, "Fuzzy Coordination of FACTS Controllers for Damping Power Oscillations," *IEEE Trans. on Power Systems*, Vol. 21, No.3, 2006.
- [23] Dheeman Chatterjee and Arindam Ghosh, "Application of Trajectory Sensitivity for the Evaluation of the Effect of TCSC Placement on Transient Stability," *International Journal of Emerging Electric Power Systems*, Vol. 8, Issue 1, 2007.
- [24] K. Clark, B. Fardanesh, and R. Adapa, "Thyristor Controller Series Compensation Application Study – Control Interaction Considerations," *IEEE Transactions on Power Delivery*, vol. 10, pp. 1031-1037, 1995.
- [25] S. Zelingher, B. Shperling, J. D. Mountford, and R. J. Kiessler, "Analytical Studies for Thyristor-Controlled Series Compensation in New York State, Part II - Dynamic Stability Analysis," *EPRI FACTS 2 Conference*, May1992, Boston.
- [26] X. Wei, *Network Sensitivities of TCSC and SVC for Power Dispatching and Damping Control Design*, MS Thesis, Rensselaer Polytechnic Institute, May 2002.
- [27] A. D. Del Rosso, C. A. Ca-nizares, and V. M. Do-na, \A Study of TCSC Controller Design for Power System Stability Improvement," *IEEE Trans. On Power Systems*, vol. 18, no. 4, November 2004, pp. 1487/1496.
- [28] N. Yang, Q. Liu, and J. D. McCalley, \TCSC Controller Design for Damping Interarea Oscillations," *IEEE Trans. on Power Systems*, vol. 13, no. 4,November 1998, pp. 1304/1309.
- [29] N. Martins, H. Pinto, and J. Paserba, \Using a TCSC for Power System Scheduling and System Oscillation Damping-Small Signal and Transient Stability Studies". In Proc. of IEEE/PES Winter Meeting, Singapore, January 2000.
- [30] J. Paserba, N. Miller, E. Larsen, and R. Piwko, \A Thyristor Series Controlled Compensation Model for Power System Stability Analysis," *IEEE Trans. On Power Systems*, vol. 10, no. 4, November 1995.
- [31] F. Wang, G. B. Shrestha, "Allocation of TCSC devices to optimize total transmission capacity in a competitive power market". *Power Engineering Society Winter Meeting*, IEEE , Vol. 2 , pp. 587–593, 28 January-1 February 2001.
- [32] T.S. Sidhu and M. Khederzadeh, "TCSC Impact on Communication – Aided Distance Protection Schemes and its Mitigation," *IEE Proceedings: Generation, Transmission and Distribution*, Vol. 152, Issue 5, September 2005.
- [33] T. Luor, Y. Hsu, T. Guo, J. Lin, and C. Huang, "Application of Thyristor- Controlled Series Compensators to Enhance Oscillatory Stability and Transmission Capability of Longitudinal Power System", *IEEE Transactions on Power System*, Vol. 14, No. 1, pp. 179-185, Feb. 1999.
- [34] X. Zhou and J. Liang, "Overview of Control Methods for TCSC in Enhance the Stability of Power Systems", *IEE Proc., Generation, Transmission and Distribution*, Vol. 146, No. 2, pp. 125-130, March 1999.
- [35] A. M. Simoes, D. C. Savelli, P. C. Pellanda, N. Martins, and P. Apkarian, "Robust Design of a TCSC Oscillation Damping

- Controller in a Weak 500-kV Interconnection Considering Multiple Power Flow Scenarios and External Disturbances ,” *IEEE Transactions on Power Systems*, vol. 24, pp. 226 – 236, February 2009
- [36] Q. Liu, V. Vittal, and N. Elia, “LPV supplementary damping controller design for a thyristor controlled series capacitor (TCSC) device,” *IEEE Transactions on Power Systems*, vol. 21, pp. 1242–1249, August 2006.
- [37] D. N. Kosterev, W. Kolodziej, R. Mohler, and W. Mittelstadt, “Robus Transient Stability Control Using Thyristor-Controlled Series Compensation,” in *Proceedings of IEEE 4th Conf. on Control Applications*, pp. 215 – 220, 1995.
- [38] J. G. Singh, S. N. Singh, and S. C. Srivastava, “Enhancement of Power System Security through Optimal Placement of TCSC and UPFC,” in *Proceedings of IEEE Power Engineering Society General Meeting*, pp. 1–6, 2007.
- [39] P. M. Anderson and R. G. Farmer, *Series Compensation of Power Systems*, p. 241. PBLSH/ Inc., 1996
- [40] R. Billinton, M. Fotuhi-Firuzabad and S.O. Faried, “Power System ReliabilityEnhancement using a Thyristor Controlled Series Capacitor,” *IEEE Transactions on Power Systems*, Vol. 14, No. 1, February 1999, pp. 369-374
- [41] C. Gama and L. Angquist, “Commissioning and Operative Experience of TCSC for Damping Power Oscillation in the Brazilian North-South Interconnection,” *CIGRE, Session 2000, Paris*.
- [42] H.A. Othman and L. Angquist, “Analytical Modeling of Thyristor-Controlled Series Capacitors for SSR Studies,” *IEEE Transactions on Power Systems*, Vol. 11, No. 1,February 1996.
- [43] B.K. Perkins and M.R. Iravani, “Dynamic Modeling of a TCSC with Application to SSR Analysis,” *IEEE Transactions on Power Systems*, Vol. 12, No. 4, pp. 1619-1625, 1997.
- [44] H. Shayeghi, H. A. Shayanfar, S. Jalilzadeh and A. Safari, “TCSC Robust Damping Controller Design Based on Particle Swarm Optimization for a Multi-Machine Power System”, *Energy Conver. Manage.*, vol. 51, (2010)
- [45] A. Kumar, S. C. Srivastava, and S. N. Singh, “Impact of TCPAR on Cluster-Based Congestion Management Using Improved Performance Index,” *Iranian Journal of Electrical and Computer Engineering*, Vol. 7, No. 2, Summer-Fall 2008, pp.89-97.
- [46] M.R.Iravani, D.Maratkulam, “Review of semiconductor-controlled (static) Phase shifiers for power system applications”, *IEEE Transactions on Power Systems*, Vo1.9, No.4, Nov 1994, pp. 1833-1839.
- [47] N.K.Sharma, “A Novel Placement Strategy for FACTS Controllers in Multi-machine Power Systems,” *Ph. D. Thesis, IIT Kanpur, India, 2003*.
- [48] Liu Jun, Tang Guangfu, and Li Xingyuan, “Interaction Analysis and Coordination Control between SSSC and SVC,” *Power System Technology*, 2006, POWERCON’2006, *International Conference*, 22-26 Oct., 2006, pp.7-10.
- [49] X. P. Zhang, “Advanced modeling of the multi-control functional static synchronous series compensator (SSSC) in Newton power flow,” *IEEE Trans. Power Syst.*, vol. 18, no. 4, pp. 1410–1416, Nov. 2003.
- [50] K. K. Sen, “SSSC-static synchronous series compensator theory, modeling, and application,” *IEEE Trans. Power Del.*, vol. 13, no. 1, pp. 241–246, Jan. 1998.
- [51] L Zhang, M.L. Crow, Z. Yang, and S. Chen, “The Steady State Characteristics of an SSSC Integrated with Energy Storage,” *IEEE, 2001*,
- [52] L. Dong, M.L. Crow, Z. Yang, C. Shen, L. Zhang, and S. Atcity, “A Reconfigurable FACTS System for University Laboratories,” *IEEE Trans Power Systems*, vol. 19, no. 1, Feb. 2004.
- [53] R. Mihalic and I Papie, “Mathematical Models and Simulation of a Static Synchronous Series Compensator,” *Electric Power Engineering 1999, PowerTech Budapest 1999*, Aug. 2002.
- [54] F. W. Huang, B. S. Rigby, and R. G. Harley, “A Static Synchronous Series Compensator Model for EMTDC,” *IEEE Africon 2002*
- [55] H. F. Wang, “Design of SSSC Damping Controller to Improve Power System Oscillation Stability,” *IEEE Africon*, vol. 01, Oct. 1999
- [56] K. H. Kupers, R.E. Morrison, and S.B. Tennakoon, “Power Quality Implications Associated with a Series FACTS Controller,” *Ninth International Conference Proceedings on Harmonics and Quality of Power*, vol. 1, Oct. 2000
- [57] B. M. Han, J. K. Park, S I. Moon, and G. G. Karady, “Switching-Level Simulation Model for SSSC with EMTP,” *IEEE Winter Meeting Power Engineering Society..*, vol.31, Jan. 1999.
- [58] B. Han, S. Moon, and G. Karady, “Dynamic Characteristic Analysis of Multi-Bridge PWM Inverter for SSSC,” *IEEE Power Engineering Society Winter Meeting.*, vol. 3, July 2000
- [59] Xiao-Ping Zhang, “Advanced Modeling of the Multicontrol Functional Static Synchronous Series Compensator (SSSC) in Newton Power Flow,” *IEEE Trans Power Systems.*, vol. 18, no. 4, Nov. 2003.
- [60] Prechanon Kumratug, “Improvement of Transient Stability of Power System by Thyristor Controlled Phase Shifting Transformer” *American Journal of Applied Sciences*7(11):1495-1499,2010 ISSN 1546-9239
- [61] Noroozian, M., and Anderson, G., “Power flow Control by use of controllable seriescomponent”, *IEEE Trans. PD*, Vol. 8, No. 3,1993, pp. 1420-1429
- [62] A. Marinakis, M. Glavic, and T. V. Cutsem, “Control of phase shifting transformers by multiple transmission system operators,” in *Proceedings of IEEE PowerTech*, pp. 119 – 124, 2007.
- [63] J. A. Momoh, J. Z. Zhu, G. D. Boswell, and S. Hoffman, “Power System Security Enhancement by OPF with Phase Shifter,” *IEEE Transactions on Power Systems*, vol. 16, pp. 287 – 293, May 2001.
- [64] B. Sweeney, “Application of phase-shifting transformers for the enhanced interconnection between Northern Ireland and the Republic of Ireland,” *Power Engineering Journal*, vol. 16, no. 3, pp. 161 – 167, 2002
- [65] M. Belivanis and K. R. W. Bell, “Use of phase-shifting transformers on the Transmission Network in Great Britain,” *Proceedings of the Universities Power Engineering Conference (UPEC)*, pp. 1–5, August 2010.
- [66] N. Johansson, *Control of dynamically assisted phase-shifting transformers, Licentiate Thesis, Royal Institute of Technology, Stockholm, Sweden*, pp. 13–15, 49–67, 79–89, 147–155. Available at www.kth.se, 2008
- [67] N.G. Hingorani and L. Gyugyi. Understanding FACTS concepts and technology of flexible AC transmission systems. *IEEE Press, New York, 2000*.
- [68] S.V. Ravi Kumar, S. Siva Nagaraju, 2007, “Transient Stability Improvement using UPFC and SVC,” *ARPN Journal of Engineering and Applied Sciences*, 2(3), pp. 38-45.
- [69] Pavlos S. Georgilakis and Peter G. Vernados, “Flexible AC Transmission System Controllers: An Evaluation” *Materials Science Forum, Trans Tech Publications, Switzerland*, Vol. 670, pp 399-406, 2011
- [70] R.M. Mathur, and R.K. Varma, “Thyristor based FACTS Controllers for Electrical Transmission Systems”, John Wiley & Sons, Inc. Publication ant *IEEE Press, New York, USA, 2002*.
- [71] K.K. Sen, and M.L. Sen, “Introduction to FACTS Controllers: Theory, Modeling and Applications”, Published by John Wiley & Sons, Inc., and *IEEE, New Jersey, USA, July 2009*
- [72] Alok Kumar Mohanty, Amar Kumar Barik, “Power System Stability Improvement Using FACTS Devices” *International Journal of Modern Engineering Research (IJMER)*, Vol.1, Issue.2, pp- 666-672 ISSN: 2249-6645.
- [73] S.V. Ravi Kumar, S. Siva Nagaraju, 2007, “Transient Stability Improvement using UPFC and SVC,” *ARPN Journal of Engineering and Applied Sciences*, 2(3), pp. 38-45.
- [74] S. Jalali, I. Dobson, R. H. Lasseter, G. Venkataraman, *IEEE Transactions on Circuits and Systems-I: Fundamental Theory and Applications* 43(3), 209 (1996).
- [75] R.M. Mathur and R.K. Varma. Thyristor-based facts controllers for electrical trans-mission systems. *IEEE Press, Piscataway*, 2002.
- [76] <http://www.nationalgrid.com>, 2005
- [77] R. K. Verma, “Control of Static VAR systems for Improvement of Dynamic Stability and Damping of Torsional Oscillations,” *Ph. D. Thesis, IIT Kanpur, April 1998*.

1st National Power & Energy System Conference (NPESC), April 25-26, 2014, KNIT Sultanpur

- [78] Yuan-Lin Chen, "Weak Bus-Oriented Optimal Multi-Objective VAR Planning," *IEEE Trans on Power Systems*, Vol. 11, No.4, November 1996.
- [79] R. M. Hamouda, M. R. Iravani, and R. Hacham, "Coordinated Static VAR Compensators for Damping Power System Oscillations," *IEEE Trans. on Power Systems*, Vol. PWRS-2, No.4, November 1987.
- [80] W. Zhang, F. L., and Leon M. Tolbert, "Optimal Allocation of Shunt Dynamic VAR Source SVC and STATCOM: A Survey", *IEEE Trans on Power systems*, Vol.22, No. 3, Oct 2007.
- [81] Y. Mansour, W. Xu, F. Alvarado, and C. Rinzin, "SVC Placement Using Critical Modes of Voltage Stability," *IEEE Trans. on Power Systems*, Vol. 9, pp. 757-762, May 1994.
- [82] Cigre Working Group, "Modeling of Static VAR Systems for Systems Analysis," *Electra*, Vol. 51, pp.45-74, 1977.
- [83] Malike M. Farsangi, Hossein Mezamabadi-pour, "Placement of SVCs and Selection of Stabilizing Signals in Power Systems, " *IEEE Trans. on Power Systems*, Vol. 22, No. 3, August 2007.
- [84] Roberto Mingues, Federico Milano, Rafael Zarate-Minano, and Antonio J. Conejo, "Optimal Network Placement of SVC Devices," *IEEE Trans. on Power Systems*, Vol.22, No.4, November 2007.
- [85] Y. Chang, "Design of HVDC and SVC Coordinate Damping Controller Based on Wide Area Signal," *International Journal of Emerging Electric Power Systems*, Vol. 7, Issue 4, 2006.
- [86] N. Martins and L. T. G. Lima, "Determination of Suitable Locations for Power System Stabilizers and Static Var Compensators for Damping Electro-mechanical Oscillation in large Scale Power Systems," *IEEE Trans. on Power Systems*, Vol. 5, No.4, pp. 1455-1469, November 1990.
- [87] M. K. Verma, and S. C. Srivastava, "Optimal Placement of SVC for Static and Dynamic Voltage Security Enhancement," *International Journal of Emerging Electric Power Systems*, Vol.2, issue-2, 2005.
- [88] C. S. Chang, and J. S. Huang, "Optimal SVC Placement for Voltage Stability Reinforcements," *Electric Power System Research*, Vol.42, pp.165-172, 1997.
- [89] Mohd WAzir Mustafa, and Wong Yan Chiew, "Optimal Placement of Static VAR Compensator Using Genetic Algorithms," *Elektrika*, Vol. 10, No.1, pp.26-31, 2008.
- [90] Z. Y. Dong, Y. Wang, D. J. Hill, and Y. V. Makarov, " A New Approach to Power Systems VAr Planning Aimed at Voltage Stability Enhancement with Feedback Control," In Proc. 1999, *Electric Power Engineering Power Tech.Budapest'99*, pp.33-39.
- [91] V.Ajjarapu, Ping Lin Lau, and S. Battula, "An Optimal Reactive Power Planning Strategy Against Voltage Collapse," *IEEE Trans on Power Systems*, Vol.9, No.2, May 1994.
- [92] L. Gyugi, N. G. Hingorani, P. R. Nannery, and N. Tai, "Advanced Static VAR Compensator Using Gate Turn-off Thyristor for Utility Applications," *CIGRE,23-203, 1990 Session, Paris*.
- [93] Jing Zhang, J. Y. Wen, S. J. Cheng, and Jia Ma, "A Novel SVC Allocation Method for Power System Voltage Stability Enhancement by Normal Forms of Diffeomorphism," *IEEE Trans. on Power Systems*, Vol. 22, No. 4, November 2007.
- [94] Youyi wang, Yoke Lin Tan, and Guoxiao Guo, "Robust Non-linear Coordinated Excitation and SVC Control for Power Systems," In Proc. of the 4th International Conf. on Advances in Power System Control, Operation and Management, *APSCOM'97, Hong Kong*, Nov. 1997.
- [95] J. V. Milanovic, and I. A. Hiskens, "Damping Enhancement by Robust Tuning of SVC Controllers in the Presence of load Parameters Uncertainty," *IEEE Trans on Power Systems*, Vol.13, No.4, November 1997.
- [96] L. J. Cai, and I. Erlich, "Simultaneous Coordinated Tuning of PSS and FACTS Damping Controllers in Large Power Systems," *IEEE Trans. on Power Systems*, Vol. 20, No. 1, February 2005.
- [97] M. W. Mustafa, Nuraddeen Magaji, and "Optimal Location of Static Var Compensator Device for Damping Oscillations," *American Journal of Engineering and Applied Sciences*, Vol. 2, No.2, 2009
- [98] E. V. Larsen and J. H. Chow, "SVC Control Design Concepts for System Dynamic Performance," in *IEEE Power Engineering Society Publication 87TH0187-5-PWR Application of Static Var Systems for System Dynamic Performance*, 1987.
- [99] A. Hammad and B. Roesle, "New Roles for Static VAR Compensators in Transmission Systems," *Brown Boveri Review*, vol. 73, pp. 314-320, June 1986
- [100] J. Zhang, J. Y. Wen, S. J. Cheng, and J. Ma, "A Novel SVC AllocationMethod for Power System Voltage Stability Enhancement by Normal Forms of Diffeomorphism", *IEEE Transactions on Power Systems*, Vol. 22, No. 4, pp. 1819-1822, November 2007.
- [101] Canadian Electrical Association, "Static Compensators for Reactive Power Control," *Context Publications*, 1984.
- [102] K.K. Sen , "STATCOM-static synchronous compensator theory, modeling, and applications," in *Proc. IEEE Power Eng. Soc. Winter Meeting*, 1999, vol. 2, pp. 1177-1183.
- [103] C. Schauder, M. Gernhardt, E. Stacey, T. Lemak, L. Gyugyi, T. W. Cease, and A. Edris, "TVA STATCOM project: design, installation, and commissioning," presented at the *CIGRE Meeting, Paris, France*, Aug. 1996, *Paper 14-106, unpublished*.
- [104] E. M. John, A. Oskouie, and A. Petersson, "Using a STATCOM to RetireUrban Generation," *IEEE PES Power Systems Conference and Exposition*, vol.2, pp. 693-698, 2004.
- [105] A. W. Scarfone, B. K. Oberlin, J. P. Di Luca Jr., D. J. Hanson, and C.Horwill, "A □/150 MVar STATCOM for Northeast Utilities' Glenbrooksubstation," *Proceedings of the 2003 IEEE PES General Meeting*, Vol. 3, July 2003.
- [106] G. Reed, J. Paserba, T. Croasdaile, R. Westover, S. Jochi, N. Morishima, M. Takeda, T. Sugiyama, Y. Hamazaki, T. Snow, and A. Abed, "SDG&E Talega STATCOM Project - System Analysis, Design, and Configuration," *Proceedings of the IEEE PES T&D-Asia Conference and Exposition, Yokahama, Japan, October 2002*.
- [107] D. J. Hanson, C. Horwill, B. D. Gemmell, and D. R. Monkhouse, "STATCOM-Based Relocatable SVC Project in the UK for National Grid," *Proceedings of the IEEE PES Winter Power Meeting, New York, January 2002*.
- [108] R. J. Piwko, Ed., Applications of Static Var Systems for System Dynamic Performance, *IEEE Publication 87TH01875-5-PWR*, 1987.
- [109] N. Mithulananthan, C. A. Ca~nizares, J. Reeve, and G. J. Rogers, \ Comparison of PSS, SVC and STATCOM Controllers for Damping Power System Oscillations," *IEEE Trans. on Power System*, vol. 18, no. 2, May 2003.
- [110] K. El-Arroudi, G. Joos and D.T. McGillis," Operation of Impedance Protection Relays with the STATCOM," *IEEE Transactions on Power Delivery*, Vol. 17, No. 2, April 2002.
- [111] T. S. Sidhu, R.K. Varma, P.K. Gangadharan, F.A. Albasri and G.R. Ortiz, "Performance of Distance Relays on Shunt-FACTS Compensated Transmission Lines," *IEEE Transactions on Power Delivery*, Vol. 20, No. 3, July 2005.
- [112] M. Molinas, S. Vazquez, T. Takaku, J.M. Carrasco, R. Shimada, T. Undeland, "Improvement of transient stability margin in power systems with integrated wind generation using a STATCOM: An experimental verification," *International Conference on Future Power Systems*, 16-18 Nov. 2005.
- [113] L. Chun, J. Qirong, X. Jianxin, "Investigation of Voltage Regulation Stability of Static Synchronous Compensator in Power System," *IEEE Power Engineering Society Winter Meeting*, vol. 4, 2642-47, 23-27 Jan. 2000.
- [114] Singh, R. Singh, D.K. Simulation of D-STATCOM for Voltage Fluctuation Page(s): 225 - 230 Advanced Computing & Communication Technologies (ACCT), 2012 Second International Conference.
- [115] M. K. Mishra, A. Ghosh and A. Joshi, "Operation of a DSTATCOM in voltage control mode," *IEEE Transactions on Power Delivery*, vol. 18, no. 1, 2003.
- [116] H. Fugita and H. Akagi, "Voltage-regulation performance of a shunt active filter intended for installation on a power distribution system," *IEEE Trans. on Power Electron.*, vol. 22, no.1, pp.1046-1053, May 2007.
- [117] H. Akagi, E H Watanabe and M Arede, Instantaneous power theory and applications to power conditioning, *John Wiley & Sons, New Jersey, USA*, 2007.
- [118] *IEEE Recommended Practices and Requirements for Harmonics Load current and the harmonic spectrum Control in Electric Power Systems*, *IEEE Std. 519, 1992*.

- [119] S. Ali Nabavi Niaki, Reza Iravani, and Mojtaba Noroozian, "Power-Flow Model and Steady-State Analysis of the Hybrid Flow Controller," *IEEE Transactions On Power Delivery*, Vol. 23, No. 4, October 2008, pp.2330-2338.
- [120] Suman Bhawmick, Biswarup Das, and Narendra Kumar, "An Advanced IPFC Model to Reuse Newton Power Flow Codes," *IEEE Transactions On Power Systems*, Vol. 24, No. 2, May 2009, pp. 525-532.
- [121] Y. Zhang, Y. Zhang, and C. Chen, "A novel power injection model of IPFC for power flow analysis inclusive of practical constraints," *IEEE Trans. Power Syst.*, vol. 21, no. 4, pp. 1550–1556, Nov. 2006.
- [122] L. Gyugyi, K. K. Sen, and C. D. Schauder, "The Interline Power Flow Controller concept: A new approach to power flow management in transmission systems," *IEEE Trans. Power Del.*, vol. 14, no. 3, pp. 1115–1123, Jul. 1999.
- [123] E. Uzunovic, B. Fardanesh, S. Zelinger, S. J. Macdonald and C. D. Schauder, "Interline Power Flow Controller(IPFC): A Part of Convertible Static Compensator(CSC)," in *North American Power Symposium*, Oct. 2000.
- [124] X-P. Zhang, "Modelling of the Interline Power Flow Controller and theGeneralized Unified Power Flow Controller in Newton Power Flow," *IEE Proceedings-Generation, Transmission and Distribution*, Vol. 150, No. 3, May 2003.
- [125] B. Lu, L. Hou, B. Li, Y. Liu, 2007, "A New Unified Power Flow Fuzzy Control Method", *In.novative Computing, Information and Control, Second International Conference*.
- [126] Lutfu Saribulut, Mehmet Tumay, and dlyas Eker, 2007, "Performance Analysis of Fuzzy Logic Based Unified Power Flow Controller" *Second International Conference*.
- [127] Timothy J. Ross, 1995, "Fuzzy Logic with engineering application", McGraw-Hill, Inc.
- [128] X.Wei, J. H. Chow, B. Fardanesh, and A.-A. Edris, 2004 "A dispatch strategy for an Interline power flow controller operating at rated capacity," in *Proc. Power Systems Conf. Expo., New York, Oct. 10–13*.
- [129] C. Jianhong, T. T. Lie, and D. M. Vilathgamuwa, 2002 "Basic control of Interline power flow controller," in *Proc. IEEE Power Eng. Soc. Winter Meeting*.
- [130] R. L. Vasquez-Arnez and L. C. Zanetta Jr., Jun 2005, "Multiline power flow control: An evaluation of the GIPFC (generalized Interline power flow controller)," *presented at the 6th Int. Conf. Power Systems Transients, Montreal, QC,Canada, 19–23*.
- [131] V. Diez-Valencia, U. D. Annakkage, A. M. Gole, P. Demchenko, and D. Jacobson, "Interline power Flow Controller concept steady-state operation," *IEEE Canadian Conference on Electrical and Computer Engineering, Vol. 1*, pp. 280-284, Winnipeg, May 2002.
- [132] J. Chen, T. T. Lie, and D. M. Vilathgamuwa, "Basic control of interline power flow controller," *IEEE Power Engineering Society, Vol. 1*, pp. 521– 525, Winter 2002.
- [133] B.A. Renz, A. Keri, A.S. Mehraban, C. Schauder, E. Stacey, L. Kovalsky L. Gyugyi, A. Edris, " AEP Unified Power Flow Controller Performance", *IEEE Trans. PD*, Vol. 14, No. 4, pp. 1374-1381, 1999.
- [134] S. A. N. Niaki, "Modeling and applications of unified power flow controller (UPFC) for power systems," *Ph.D. dissertation, Dept. Elect. Comput. Eng., Univ. Toronto, Toronto, ON, Canada, 1996*.
- [135] K. S. Verma and H. O. Gupta, "Impact on Real and Reactive Power Pricing in Open Power Market Using Unified Power Flow Controller," *IEEE Transactions On Power Systems*, Vol. 21, No. 1, February 2006, pp.365-371.
- [136] K. K. Sen, "UPFC-unified power flow controller theory-modeling and applications," *IEEE Trans. Power Del.*, vol. 13, no. 4, pp. 1453–1460, Oct. 1998.
- [137] A.Nabavi-Niaki, and M.R. Iravani, "Steady-State and Dynamic Models of UPFC for Power System Studies," *IEEE Trans. on PS*, Vol. 11, No. 4, pp. 1937-1943, Nov. 1996.
- [138] Seungwon An, John Condren, and Thomas W. Gedra, "An Ideal Transformer UPFC Model, OPF First-Order Sensitivities, and Application to Screening for Optimal UPFC Locations," *IEEE Transactions On Power Systems*, Vol. 22, No. 1, February 2007, pp.68-75.
- [139] J. Y. Liu, Y. H. Song, and P. A. Mehta, "Strategies for handling UPFC constraints in steady—State power flow and voltage control," *IEEE Trans. Power Syst.*, vol. 15, no. 2, pp. 566–571, May 2000.
- [140] S.M. Alamelu, and R. P. Kumudhini Devi, "Novel Optimal Placement UPFC Based on Sensitivity Analysis and Evolutionary Programming ,"*Journal of Engineering and Applied Sciences*, Vol.3, No.1, pp.59-63, 2008.
- [141] Srekanth Reddy Donapati, and M. K. Verma, "An Approach for Optimal Placement of UPFC to enhance Voltage Stability Margin under Contingencies," *Fifteenth National Power Systems Conference (NPSC), IIT Bombay, December 2008* pp.441-446.
- [142] S. N. Singh, and I. Erlich, "Locating Unified Power Flow Controllers for Enhancing Power System Loadability," *Future Power Systems, 2005, International Conference , 18 Nov 2005*, pp 5-5.
- [143] H.I. Shaheen, G. I. Rashed, and S.J. Cheng, "Optimal Location and Parameters Setting of UPFC based on GA and PSO for Enhancing Power System Security Under Single Contingencies," *Power and Energy Society General Meeting-Conversion and delivery of Electrical Energy in The 21st Century, 2008,IEEE*, 20-24 July, 2008, pp.1-8..
- [144] L. Ippolito, " A novel Strategy for Selection of the Optimal Number and Location of UPFC devices in Deregulated Electric Power Systems," *Power Tech, 2005, IEEE Russia, 27-30 June, 2005*, pp.1-9.
- [145] W.L.Fang, and H. W. Ngan, "Optimizing location of UPFC using the Methods of Augmented Lagrange Multipliers," *IEE Proc., Gener., Transm.,Distrib.,Vol 146, No.5, Sep. 1999*.
- [146] K. Visakha, D. Thukaram, L. Jenkins, and H.P. Khincha, "Selection of UPFC Suitable Locations for System Security Improvement Under Normal and Network Contingencies," *TENCON 2003, Conference on Convergent Technologies for Asia –Pacific Region, Vol-2, 15-17 Oct, 2003*, pp755-760.
- [147] D. Thukarana, L. Jenkins, and K. Visakha, "Improvement of System Security with UPFC at Suitable Locations Under Network Contingencies of Interconnected Systems," *IEE Proc., Gener., Transm., Distrib., Vol. 152, No.5, Sep 2005*.
- [148] R.P.Kalyani, M. L. Crow, and D. R. Tauritz, "Optimal Placement and Control of UPFC devices Using Evolutionary Computing and Sequential Quadratic Programming," *Power Systems Conference and Exposition 2006, PSCE'06, 2006 IEEE PES, 29 Oct.,2006- 1 Nov.,2006*, pp 959-964.
- [149] J. G. Singh, S. N. Singh, and S. C. Srivastava, "Optimal Placement of Unified Power Flow Controller Based on System Loading Distribution Factors," *Electric Power Components and Systems, Vol. 37, Issue 4, April 2009*, pp.441-463.
- [150] J. Bian, D. G. Ramey, R. J. Nelson, and A. Edris, "A study of equipment sizes and constraints for a unified power flow controller," *IEEE Trans. Power Del.*, vol. 12, no. 3, pp. 1385–1391, Jul. 1997.
- [151] R. L. Vasquez-Arnez and L. C. Zanetta, "A novel approach for modeling the steady-state VSC-based multiline facts controllers and their operational constraints," *IEEE Trans. Power Del.*, vol. 23, no. 1, pp. 457–464, Jan. 2008.
- [152] C. D. Schauder, M. R. Lund, D. M. Hamai, T. R. Rietman, D. R. Torgerson, and A. Edris, "Operation of the unified power flow controller (UPFC) under practical constraints," *IEEE Trans. Power Del.*, vol. 13, no. 2, pp. 630–637, Apr. 1998.
- [153] H. Ambriz-Perez, E. Acha, C. R. Fuerte-Esquivel, and A. De la Torre, "Incorporation of a UPFC model in an optimal power flow using Newton's method," *Proc. Inst. Elect. Eng., Gen., Transm., Distrib.*, vol. 145, no. 3, pp. 336–344, May 1998.
- [154] C. R. Fuerte-Esquivel, E. Acha, and H. Ambriz-Perez, "A comprehensive Newton-Raphson UPFC model for the quadratic power flow solution of practical power networks," *IEEE Trans. Power Syst.*, vol. 15, no. 1, pp. 102–109, Feb. 2000.
- [155] M. Noroozian, L. Ängquist, M. Ghadhari, and G. Andersson, "Use of UPFC for optimal power flow control," *IEEE Trans. Power Del.*, vol. 12, no. 4, pp. 1629–1634, Oct. 1997.
- [156] Christopher Collins, Neville Watson, and Alan Wood, *Member*, "UPFC Modeling in the Harmonic Domain," *IEEE Transactions On Power Delivery*, Vol. 21, No. 2, April 2006, pp. 933-938.
- [157] J. Monteiro, J. Fernando Silva, S. F. Pinto, and J. Palma, "Matrix Converter-Based Unified Power-Flow Controllers: Advanced Direct

1st National Power & Energy System Conference (NPESC), April 25-26, 2014, KNIT Sultanpur

- Power Control Method," *IEEE Transactions On Power Delivery*, Vol. 26, No. 1, January 2011, pp.420-430.
- [158] B. Geethalakshmi and P. Dananjayan, "Investigation of performance of UPFC without DC link capacitor," in *Elect. Power Energy Res.*. New York: Elsevier, 2008, pp. 284–294, 736-746..
- [159] X. Jiang, X. Fang, J. Chow, A. Edris, E. Uzunovic, M. Parisi, and L. Hopkins, "A novel approach for modeling voltage-sourced converter based FACTS controllers," *IEEE Trans. Power Del.*, vol. 23, no. 4, pp. 2591–2598, Oct. 2008.
- [160] I. Papic, P. Zunko, D. Povh, M. Weinhold, "Basic Control of Unified Power Flow Controller," *IEEE Transactions on Power Systems*, vol. 12, pp.1734-1739, Nov. 1997.
- [161] Y. Morioka, M. Kato, Y. Mishima, Y. Nakachi, M. Asada, and K. Tokuhara, "Implementation of Unified Power Flow Controller and Verification for Transmission Capability Improvement," *IEEE Transactions on Power Systems*, vol. 14, pp. 575-581, 2000
- [162] H. F. Wang, "A Unified Model for the Analysis of FACTS Devices in Damping Power System Oscillations. III. Unified Power Flow Controller," *IEEE Transactions on Power Delivery*, vol. 15, pp. 978-983, July 2000.
- [163] H. Cai, Z. Qu, and D. Gan, "Determination of the Power Transfer Capability of a UPFC with Consideration of the System and Equipment Constraints and of Installation Locations," *IEE Proceedings – Generation, Transmission and Distribution*, vol.149,
- [164] S. Bruno, E. De Tuglie, M. La Scala, and P. Scarpellini, "Dynamic Security Corrective Control by UPFCs," *IEEE Transactions on Power Systems*, vol. 16, pp. 490-497, 2001.
- [165] Z. Y. Huang, Y. Ni, C. M. Shen, F. F. Wu, S. Chen, and B. Zhang, "Application of Unified Power Flow Controller in Interconnected Power Systems-Modeling, Interface, Control Strategy, and Case Study," *IEEE Transactions on Power Systems*, vol. 15, pp. 817-824, May 2000.
- [166] K. R. Padiyar and K. U. Rao, "Modeling and Control of United Power Flow Controller for Transient Stability," *Int. J. Electr. Power Energy Stst.*, vol. 21, no. 1, pp. 1-11, Feb. 1999
- [167] K. S. Smith, L. Ran, J. Penman, "Dynamic Modelling of a Unified Power Flow Controller," *IEE Proceedings on Generation, Transmission and Distribution*, vol. 144, no.1, pp. 7-12, Jan. 1997
- [168] M-Toufan, U-D-Annakkage " Simulations of the Unified Power Flow Controller performance using PSCAD-EMTDC" *Electric Power Systems Research*, Vo1.46,1998,
- [169] A. J. F. Keri, A. S. Mehraban, X. Lombard, A. Elriachy, and A. A. Edris, "Unified Power Flow Controller (UPFC): Modeling and Analysis," *IEEE Transactions on Power Delivery*, vol. 14, pp. 648-654, 1999
- [170] A. L'Abbate, M. Trovato, C. Becker, and E. Handschin, "Advanced steady-state models of UPFC for power system studies," *Proc. of IEEE Power Engineering Society Summer Meeting*, vol. 1, pp. 449-454, July 2002
- [171] X. Zhou, H. Wang, R.K. Aggarwal, and P. Beaumont, "Performance Evaluation of a Distance Relay as Applied to a Transmission System with UPFC," *IEEE Transactions on Power Delivery*, Vol. 21, No. 3, July 2006
- [172] L. L. Li and J. T. Ma, "Power Flow Control with UPFC Using Genetic Algorithms", *International Conference on Intelligent Systems Applications to Power Systems*, Orlando, FL, Feb 1996
- [173] L. L. Li and J. T. Ma, "Power Flow Control with UPFC Using Genetic Algorithms", *International Conference on Intelligent Systems Applications to Power Systems*, Orlando, FL, Feb 1996
- [174] A. Kazemi, D. Arabkhabori, M. Yari, and J. Aghaei, "Optimal Location of UPFC In Power Systems for Increasing Loadability By Genetic Algorithm", *Universities Power Engineering Conference, UPEC '06*, UK, Vol. 2, pp. 774 – 779, 6-8 Sept. 2006
- [175] D. Arabkhabori, A. Kazemi, M. Yari, and J. Aghaei, "Optimal Placement of UPFC In Power Systems using Genetic Algorithm", *IEEE International Conference on Industrial Technology (ICIT)*, India, pp. 1694 - 1699, 18-21 Dec. 2006
- [176] H. C. Leung, and T. S. Chung, "A Hybrid GA Approach for Optimal Control Setting Determination of UPFC", *IEEE Power Engineering Review*,Vol. 21, pp. 62 - 65, Dec. 2001.
- [177] B. Mahdad, T. Bouktir, and K. Srairi, "Dynamic Methodology for Control of Multiplie-UPFC to Relieve Overloads and Voltage Violations", *The International Conference on (Computer as a Tool) EUROCON 2007*, Poland, Vol. 1, pp. 1579 – 1585, 9-12 Sept. 2007.
- [178] F. Taki, S. Abazari, and G. R. Markadeh, "Transient Stability Improvement using ANFIS Controlled UPFC based on Energy Function", *18th Iranian Conference Electrical Engineering (ICEE)*, Iran, pp. 994 – 948, 11-13 May 2010.
- [179] K. Schoder, A. Hasanovic, and A. Feliachi , "Load-Flow and Dynamic Model of the Unified Power Flow Controller (UPFC) within the PowerSystem Toolbox (PST) ", *Circuits and Systems Proc. of the 43rd IEEE Midwest Symposium*, USA, Vol. 2, pp. 634 – 637, 8-11 August 2000.
- [180] A. M. Othman, A. Gaun, M. Lehtonen, and M. M. Alarini, "Real World Optimal UPFC Placement and its Impact on Reliability", *5th IASME / WSEAS International Conference on (EE'10)*, Cambridge University, UK, pp. 90-95, February 2010.
- [181] Fugita and Watanaba. (2008) „Control and Analysis of UPFC”, *IEEE Transactions on Power Electronics* Vol.14, No.6 pp. 1021-1027.
- [182] E.Lerch, D-Povh, R-Witzmann, H.Hlebcar, R-Mihilac " Simulation and performance analysis of unified power flow controllers", *CZGRE 1994*
- [183] Z.Huang, Y.Ni, F-Wu, S.Chen, B-Zhang, " Application of Unified power flow controller in interconnectd power systems-Modeling, interface, control strategy and case study" *IEEE Transactions on Power Systems*, Vol. 15, No.2. May 2000
- [184] S.D.Round, Q&, L.E.Nomm, T.M.Undeland " Performance of a Unified Power flow controller using a D-Q Control system" *Sixth International Conference on AC & DC Transmission*, No.423. 1997.
- [185] X.Lombard7 P.G.Themod " Control of Unified power flow controller: Comparison of methods on the basis of a detailed numerical rnode", *IEEE Transactions on Power Systems*, Vo1.12, No.2. May 1997.
- [186] S.A.Al-mawasawi, A.Coonick "Analysis, Simulation and implementation of PWM based UPFC " *Sixth International Conference on AC & DC Transmission, N0.423. 1997.*
- [187] E.Uzunovic, C.Canizeres, J.Reeve " Fundamental frequency Model of Unified Power flow contrdler" *North American Power Symposium (NAPS)*, Cleveland, Ohio, October 1998
- [188] E-Uzunovic, C.Canizeres, J.Reeve " EMTP Studies of UPFC power oscillation damping" *North American Power Symposium (NAPS)*, San Luis Obispo, California, October 1999.
- [189] Dizdarevic,2001, Unified Power Flow Controller in Alleviation of Voltage Stability Problem. Ph. D. Thesis, University of Zagreb, Faculty of electrical engineering and computing.
- [190] Fouad A.A. and V. Vittal, 1992, Power System Analysis Using the Transient Energy Function Methods, Prentice Hall, Englewood Cliffs , New Jersey 07632
- [191] Prechanon Kumkratug, 2009, "Application of UPFC to Increase Transient Stability of Inter-Area Power System" *ACADEMY PUBLISHER JOURNAL OF COMPUTERS*, VOL. 4, NO. 4.
- [192] Zhengyu Huang, et al , 2000,' Application of Unified Power Flow Controller in Interconnected Power Systems—Modeling, Interface ,Control Strategy, and Case Study' *IEEE Transactions on power systems* vol.15,No2,p.817-823.
- [193] R.Mihalic *et al.*, "Improvement of transient stability using unified power flow controller' *IEEE Trans.Power Del.*, vol. 11, no. 1, pp. 485-492, Jan 1996.
- [194] E. Gholipour and S.Saadate, " A new method for improving transient stability of power systems by using UPFC," in Proc. European Power Electronics, Toulouse, France, Sep. 2003.
- [195] Wang B and Venkataraman.G, 'Evaluation of shunt and series power conditioning strategies for feeding sensitive loads', "IEEE applied electronics", pp. 1445-1451, 2004.
- [196] X. P. Zhang, "Modelling of the Interline Power FlowController and the generalized unified power flow controller in Newton power flow," *Proc. Inst. Elect. Eng., Gen., Transm., Distrib.*, vol. 150, no. 3, pp. 268–274, May 2003.
- [197] L. Gyugyi, C. D. Schauder, S. L. Williams, T. R. Rietman, D. R. Torgerson, and A. Edris, "The unified power flow controller: A new

1st National Power & Energy System Conference (NPESC), April 25-26, 2014, KNIT Sultanpur

- approach to power transmission control,” *IEEE Trans. Power Del.*, vol. 10, no. 2, pp. 1085–1097, Apr. 1995.
- [198] Xiao-Ping Zhang, Edmund Handschin, and Maojun “Mike” Yao, “Modeling of the Generalized Unified Power Flow Controller (GUPFC) in a Nonlinear Interior Point OPF,” *IEEE Transactions On Power Systems*, Vol. 16, No. 3, August 2001, pp.367-373.
- [199] S. Arabi, P. Kundur, and R. Adapa, “Innovative Techniques in Modeling UPFC for Power System Analysis,” *IEEE Transactions on Power Systems*, vol. 15, pp. 336-341, 2000.
- [200] J.-Y. Liu, Y.-H. Song, and P. A. Mehta, “Strategies for Handling UPFC Constraints in Steady-State Power Flow and Voltage Control,” *IEEE Transactions on Power Systems*, vol. 15, pp. 566-571, 2000.
- [201] B. Fardanesh, B. Shperling, E. Uzunovic, and S. Zelingher, “Multi-Converter FACTS Devices: the Generalized Unified Power Flow Controller(GUPFC),” *Proc. Winter Power Meeting*, vol. 4, pp. 2511-2517 2000.
- [202] S. Ali Nabavi Niaki, Reza Iravani, and Mojtaba Noroozian, ”Power-Flow Model and Steady-State Analysis of the Hybrid Flow Controller”, *IEEE Transactions On Power Delivery*, Vol. 23, No. 4, October 2008, pp.2330-2338
- [203] I. A. Hiskens and M. A. Pai, \Hybrid systems view of power system modelling,” in *Proceedings of the IEEE International Symposium on Circuits and Systems*, no. 2, Geneva, Switzerland, May 2000, pp. 228{231}.
- [204] D. Sutanto, “Energy Storage System to Improve Power Quality and System Reliability”, 2002 *Student Conference on Research and Development Proceedings*, pp. 8-11, Shah Alam, Malaysia.
- [205] John D. Boys, “Overview of Energy Storage Applications”, *IEEE Power Engineering Society Summer Meeting*, pp. 1514-1516, July 2000.
- [206] X.D. Xue, K.W.E. Cheng, D. Sutanto, “Power System Applications of Superconducting Magnetic Energy Storage Systems”, *Industry Applications Conference, 2005. Fourtieth IAS Annual Meeting*, pp. 1524-1529.
- [207] V. Karasik, K. Dixon, C. Weber, B. Batchelderr, etc, “SMES For Power Utility Applications: A Review of Technical and Cost Considerations”, *IEEE Transactions on Applied Superconductivity*, page 541-546, Vol. 9, No.2, June 1999.
- [208] Roger W. Boom and Harold A. Peterson, “Superconductive Energy Storage for Power Systems”, 1972 INTERMAG CONFERENCE, pp. 701-703.
- [209] P.F. Ribeiro, “SMES For Enhanced Flexibility and Performance of FACTS Devices”, Panel Session on FACTS Controllers Applications and Operational Experiences T&D and Substations Committee, Edmonton, Canada, July 1999.
- [210] S. Kolluri, “Application of Distributed Superconducting Magnetic Energy Storage System (D-SMES) in the Entergy System to Improve Voltage Stability”, *IEEE Conference*, pp. 838-841, 2002.
- [211] Paulo. F. Ribeiro, Aysen Arsoy and Yiliu Liu, “Transmission Power Quality Benefits Realized by a SMES-FACTS Controller,” *Harmonics and Quality of Power, 2000 Proceedings*, pp. 307-312, *Ninth International Conference*, October 2000.
- [212] Cesar A. Luongo, “Superconducting Storage Systems: An Overview”, *IEEE Trans. On Magnetics*, Vo.32, No.4, July 1996, pp. 2214-2223.
- [213] Sathans, Akhilesh S (2011). “Automatic generation control of two area power system with and without SMES: from conventional to modern and Intelligent control” *International Journal of Engineering Science and Technology (IJEST)*. Vol. 3 No. 5.pp 3693-3707, May 2011.
- [214] TANG, S., YANG, H., ZHAO, R., GENG, X. “Influence of battery storage system on steady state stability of power system”. *Proceedings of Int. Conference on Electrical Machines and Systems*, 2009, pp.1-4.
- [215] OUDALOV, A., CHERKAOUI, R., BEGUIN, A. “Sizing and Optimal Operation of Battery Energy storage system for Peak Shaving Application”. *Proceedings of the IEEE Power Tech*, 2007, pp. 621-625.
- [216] ZENG, J. et al. “Use of BESS to Improve the Power Quality and Stability of Wind Farms”. *Proceedings of Int. Conf. on Power System Technology*, 2006, pp.1-6.
- [217] ABB Energy Storage Modules. [on line].<[http://abblibrary.abb.com/global/scot/scot235.nsf/veritydisplay/f09413974e2f041cc12579e3004fa562/\\$file/energy_storage_modules_broc_hure_rev_e.pdf](http://abblibrary.abb.com/global/scot/scot235.nsf/veritydisplay/f09413974e2f041cc12579e3004fa562/$file/energy_storage_modules_broc_hure_rev_e.pdf)> [Consulted: December, 12, 2012].
- [218] Z. Yang, C. Shen, L. Zhang, M. L. Crow, S. Atcitty, “Integration of a StaCom and Battery Energy Storage”, *IEEE Transactions on Power Systems*, Vol. 16, No. 2, pp. 254-260, May 2001.
- [219] K.C. Divya and J.Ostergaard, “Battery Energy Storage Technology for Power Systems: An Overview”, *Electric Power Systems Research*, vol.79, pp.511-520, April 2009.
- [220] J.Brochu, F.Beauregard, J.Lemay, G.Morin,P.Pelletier, and R.S.Thallam, “Application of the interphase power controller technology for transmission line power flow control,” *IEEE Trans. Power Del.*, vol. 12,no. 2, pp. 888-894, Apr. 1997.
- [221] J. Lemay, J. Brochu, P. Pelletier, and F. Beauregard,“Inter-phase Power Controllers: Complementing the family of FACTS controllers,” *J. IEEE Can. Rev.*, vol. 34,pp. 9-12, Spring 2000.
- [222] M. S. Naderi, G. B. Gharehpetian, K. Rahmani, M. B. Abolhasani, and N.Mansoubi, “Application of interphase power controller to control and limit short circuit current,” presented at the *18th Iranian Conf.Elect. Eng., Isfahan, Iran*, May 11-13, 2010.
- [223] L.Zahedi, M.S.Naderi, M.S.Naderi, G.B.Gharehpetian, and E.Babaei, “Interphase power controller application to mitigate transmission network short circuit level,” presented at the *Int. Conf. Renew. Energies Power Qual., Las Palmas de Gran Canaria, Spain*, Apr. 13-15,2011.
- [224] J. Lemay, P. Berube, M.M. Brault,M. Gvozdanic, M.I.Henderson, M.R. Graham, G.E .Smith,R.F.Hinners, L.R.Kirby, F.Beauregard, and J. Brochu, “The Plattsburgh inter-phase power controller,” in *Proc. Transm. Distrib. Conf, New Orleans*, Apr. 11-16, 1999, pp. 648-653.

BIBLIOGRAPHIES



Bindeshwar Singh received the M.Tech. In electrical engineering from the Indian Institute of Technology, Roorkee, in 2008. He is now in ISM Dhanbad , India. His research interests are in Coordination of FACTS & DGs controllers in power systems and Power system Engg.. Currently, he is an Assistant Professor with Department of Electrical Engineering, Kamla Nehru Institute of Technology, Sultanpur, U.P., and India, where he has been since August'2010.
Mobile: 09473795769.

Email id: bindeshwar.singh2025@gmail.com



Manisha is a M.Tech student (Regular) in specialization of Power Electronics and Drives in Department of electrical engineering, KNIT Sultanpur- 228118(U.P.), India. Her interests are in the areas of Power Electronics and Drives & Modelling of Electrical Machines.
E.Mail id: yadavmyyy@gmail.com



Abhiruchi Srivastava is a M.Tech student (Regular) . In specialization of Power Electronics and Drives in Department of electrical engineering , KNIT Sultanpur- 228118 (U.P.), India. Her interests are in the areas of Power Electronics and Drives & Modelling of Electrical Machines.
E.Mail id: abhiruchisri@gmail.com



Aanchal Baranwal is presently working as an Assistant Professor in Department of electrical and Electronics Engineering of Moradabad Institute of TechnologyMoradabad, U.P., India since 1st July 12 to till date. Her interest in power systems, FACTS controllers, Power Electronics and drives, Distribution Generation
Email id: baranwal.aanchal@gmail.com

Embedded Systems and their Reliability Testing

Biswajit Choudhury Dr. RK Singh

Abstract— The number of operational embedded systems has already surpassed the human population on this planet. We can, therefore, understand the degree of its widespread use in human life. Since most of the embedded systems have actuators that influence the environment, the safety and reliability aspects are very important. High reliability in embedded systems reduces the frequency of failure and mishaps in the mission in which the system is intended to. Here the term reliability covers both hardware and software reliability as use of software in embedded systems is a common affair. Hence, to ensure high reliability in these systems, enormous tests are conducted by simulating the actual field environment during operation. This is known as Reliability testing which is necessary because the designer cannot usually be aware of or be able to analyse all the likely causes of their designs in service.

Key words—Electronic equipment, thermal management, environmental tests, reliability.

I. INTRODUCTION

These days embedded systems have been integral part of human life and routine work of home and office occupies such a volume that normal life gets disturbed greatly due to the malfunction of it. From automobiles to elevators, kitchen appliances to televisions, and water heaters to cell phones, we increasingly depend upon embedded systems to operate as expected. A few obviously critical embedded application domains, such as aviation, have traditionally benefited from extraordinary care during development to ensure that everything is done correctly. But increasingly, everyday embedded applications are becoming “mission critical,” with little fanfare and perhaps without the full attention to dependability properties that they truly deserve. Consider the following potentially significant failure modes for embedded systems: A cell phone that doesn’t work when the owner needs to call for emergency medical attention. A domestic hot water heater that overheats water, causing scalding burns on a child. A thermostat that doesn’t turn on heat when needed, causing household water pipes to freeze and burst. A microwave oven that turns on with the door open.

Although the number and the diversity of embedded systems is huge, they share a set of common and important characteristics are as follows: Most of the embedded systems perform a fixed and dedicated set of functions. For example, the microprocessor which controls the fuel injection system

in a car will perform the same functions for its entire life time. Embedded systems work as reactive systems which are connected to the physical world through sensors and react to the external stimuli. Embedded systems have to be dependable. For example, a car should have high reliability and maintainability features while ensuring that fail-safe measures are present for the safety of the passengers in case of emergency. Embedded systems have to satisfy varied, tight and at times conflicting constraints. For example, a mobile phone, apart acting as a phone, has to act as digital camera, an MP-3 player and as a game console. In addition, it has to be light-weight, cost-effective and with a very long battery life time.

II. COMPLEXITY IN EMBEDDED SYSTEMS

The relentless scaling of technology and increase in transistor densities are a primary reason for complex embedded systems and Multi-Processor System-on-Chips (MPSoCs) to have become possible. However, power requirements have not scaled accordingly, causing power densities to skyrocket and on-chip temperatures to increase at alarming rates. One of the main effects of the thermal increase is the premature aging of the CMOS devices, reducing the mean-time-to-failure (MTTF) metric. Therefore, the need for improved power and thermal management techniques still exist, however, now expanding those techniques to incorporate reliability metrics is crucial as we head into the future.

Power dissipation in electronic systems should be evaluated carefully, because the reliability and the mean time between failures (MTBF) can be sharply reduced by excessive component temperatures. It may be necessary to investigate many different sets of conditions to prove the thermal design of an electronic system. For example, a high altitude and high temperature environment may produce the highest temperatures in the logic section of the system rather than in the power supply section. Instead, a high altitude, low temperature environment may be the most severe for power supplies, because this condition draws maximum heater power for the warm-up period. High currents demands, even for short periods, may create hot spots in the electronic components that control the power. Power dissipation in electronic systems in general and microcomputers with high density hybrid chips in particular dictates the method of heat removal which in turn determines the hot spot component temperatures. Humidity is another aspect which can cause serious problems in the electronic equipment when the internal circulating air is cooler than outside ambient air. Moisture can condense on the electronic components,

M.Tech (pursuing) Dept. of Electronics Engineering, KNIT Sultanpur Uttar Pradesh, INDIA b_jeet003@rediffmail.com Head of Dept. Electronics Engineering, KNIT, Sultanpur Uttar Pradesh, INDIA singhrabinder57@gmail.com

connectors and circuit boards producing short circuits or radical changes in the resistance between components.

III. MOUNTING COMPONENTS ON PCBs

For effective cooling of components such as DIPs, VLSIs, hybrids and microprocessors used very frequently in embedded systems, it is necessary to plan in advance the heat flow mechanism and the heat flow path from the components to the sink. Metal heat sinks are often laminated to the PCBs because the thermal conductivity. The two most popular metals are aluminium and copper, which can be laminated in several different ways. The thermal resistance from IC case, through 0.008 in thick epoxy fiber glass lamina, to aluminium heat sink plate is given in Table -1 and the thermal resistance for resistors mounted on an Aluminium heat sink is given in table 1.

Table-1 Thermal Resistance from Integrated Circuit Case, through 0.008 in Thick Epoxy Fiberglass Lamina, to Aluminum Heat Sink Plate

| Component | Resistance with Cement under Component | Resistance with Air Gap under Component |
|---|---|--|
| $\frac{1}{4} \times \frac{1}{4}$ in flat pack | 20°C/watt with 0.001 in Humiseal conformal coat | — |
| $\frac{1}{4} \times \frac{1}{4}$ in flat pack | 29°C/watt with 0.003 in thick double-sided Mylar tape | 60°C/watt with 0.005 in air gap |
| $\frac{1}{4} \times \frac{1}{4}$ in flat pack | 30°C/watt with 0.002 in thick RTV adhesive over 0.004 in thick Styccast epoxy, which insulates copper runs on PCB | 35°C/watt with 0.001 in air gap over 0.004 in thick Styccast epoxy, which insulates copper runs on PCB |

Table-2
Aluminum Heat Sink

| Component | Interface Cemented with Humiseal Conformal Coating | Resistance with No Cement |
|-----------------------------------|--|---------------------------|
| $\frac{1}{4}$ watt Resistor RC 07 | 46.2°C/watt | 75°C/watt |
| $\frac{1}{2}$ watt Resistor RC 20 | 34.2°C/watt | 58°C/watt |
| 1 watt Resistor RC 32 | 19.1°C/watt | 26°C/watt |

IV. RELIABILITY PREDICTION METHODS

In today's competitive electronic products market, having higher reliability than competitors is one of the key factors for success. To obtain high product reliability, consideration of reliability issues should be integrated from the very beginning of the design phase. This leads to the concept of *reliability prediction*. Historically, this term has been used to denote the process of applying mathematical models and component data for the purpose of estimating the field reliability of a system before failure data are available for the system. However, the objective of reliability prediction is not limited to predicting whether reliability goals, such as MTBF, can be reached. It can also be used

- Identifying potential design weaknesses.
- Evaluating the feasibility of a design.
- Comparing different designs and life-cycle costs.
- Providing models for system reliability/availability analysis.
- Establishing goals for reliability tests.
- Aiding in business decisions such as budget allocation and scheduling.

A. Empirical (or Standards Based) Prediction Methods

Empirical prediction methods are based on models developed from statistical curve fitting of historical failure data, which may have been collected in the field, in-house or from manufacturers. These methods tend to present good estimates of reliability for similar or slightly modified parts. Some parameters in the curve function can be modified by integrating engineering knowledge. MIL-HDBK-217 is very well known in military and commercial industries. It is probably the most internationally recognized empirical prediction method, by far.

Figure 1 shows an example using the MIL-HDBK-217 method (in ReliaSoft's [Lambda Predict](#) software) to predict the failure rate of a ceramic capacitor. According to the handbook, the failure rate of a commercial ceramic capacitor of 0.00068 mF capacitance with 80% operation voltage, working under 30 degrees ambient temperature and "ground benign" environment is $0.0216/10^6$ hours. The corresponding MTBF (mean time before failure) or MTTF (mean time to failure) is estimated to be 46,140,368 hours.

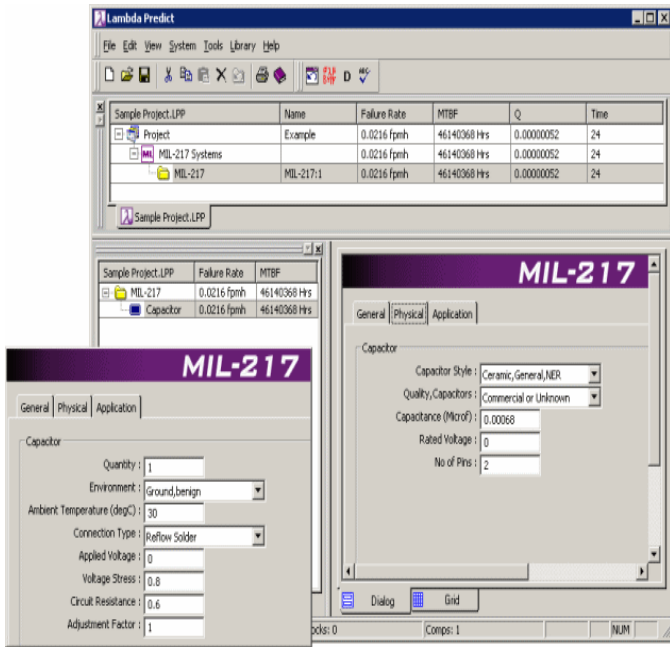


Fig. 1 Empirical (or Standards Based) Prediction Methods

B. Bellcore/Telcordia Predictive Method

The Bellcore/Telcordia standard assumes a serial model for electronic parts and it addresses failure rates at the infant mortality stage and at the steady-state stage with Methods I, II and III [2-3]. Method I is similar to the MIL-HDBK-217F parts count and part stress methods.

Figure 2 shows an example in Lambda Predict using SR-332 Issue 1 to predict the failure rate of the same capacitor in the previous MIL-HDBK-217 example (shown in Figure 1). The failure rate is 9.654 Fits, which is $9.654 / 10^9$ hours. In order to compare the predicted results from MIL-HBK-217 and Bellcore SR-332, we must convert the failure rate to the same units. 9.654 Fits is $0.000965 / 10^6$ hours. So the result of $0.0216 / 10^6$ hours in MIL-HDBK-217 is much higher than the result in Bellcore/Telcordia SR-332. There are reasons for this variation. First, MIL-HDBK-217 is a standard used in the military so it is more conservative than the commercial standard. Second, the underlying methods are different and more factors that may affect the failure rate are considered in MIL-HDBK-217.

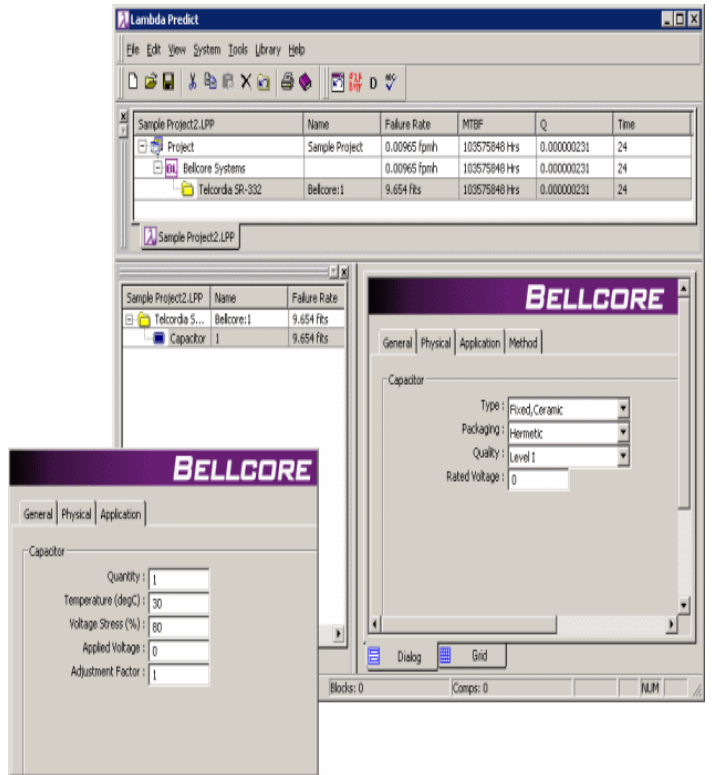


Fig. 2 Bellcore/Telcordia Predictive Method

C. RDF 2000 Predictive Method

RDF 2000 provides a unique approach to handle mission profiles in the failure rate prediction. Component failure is defined in terms of an empirical expression containing a base failure rate that is multiplied by factors influenced by mission profiles. These mission profiles contain information about how the component failure rate may be affected by operational cycling, ambient temperature variation and/or equipment switch on/off temperature variations.

RDF 2000 disregards the wearout period and the infant mortality stage of product life based on the assumption that, for most electronic components, the wearout period is never reached because new products will replace the old ones before the wearout occurs. For components whose wearout period is not very far in the future, the normal life period has to be determined. The infant mortality stage failure rate is caused by a wide range of factors, such as manufacturing processes and material weakness, but can be eliminated by improving the design and production processes. Figure 3 shows the implementation of the failure rate prediction using RDF 2000 in Lambda predict.

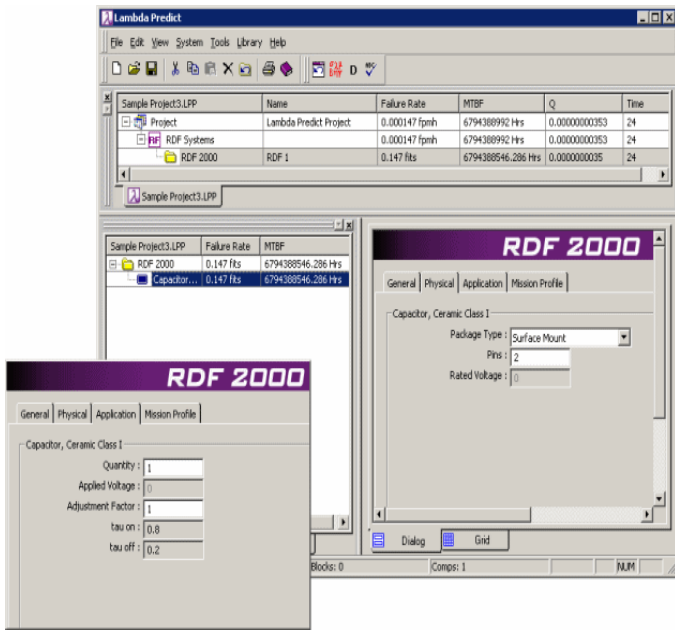


Fig. 3 RDF 2000 Predictive Method

V. RELIABILITY TESTING

It is therefore very clear that, to obtain high product reliability, consideration of reliability issues should be integrated from the very beginning of the design phase. This leads to the concept of *reliability prediction*. Historically, this term has been used to denote the process of applying mathematical models and component data for the purpose of estimating the field reliability of a system, failure data are available for the system.

Testing is an essential part of any engineering development programme and thus, the reliability test programme must cover the range of environmental conditions which the product is likely to have to endure. The main reliability-affecting environmental factors are temperature, vibration, shock, humidity, power input and output, dirt and people. In addition electronic equipment might be subjected to Electromagnetic effects (EMI) and voltage transients including electrostatic discharge (ESD).

The environmental aspects of the reliability test programme must take account of the environmental requirements stated in the design specification and of the planned environmental test. However, to be effective as a means of ensuring a reliable product, the environmental aspects of reliability testing must be assessed in much greater detail.

The environmental aspects of reliability testing must be determined by considering which environmental condition, singly and in combination with others, are likely to be the most critical from reliability point of view. A typical reliability test environment for an electronic system to be used

in vehicle or aircraft might be as shown in fig. 1. Such testing is known as combined environmental reliability testing (CERT).

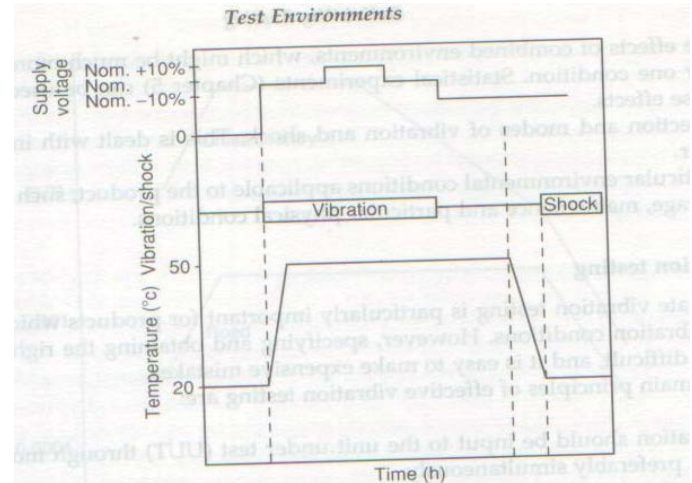


Fig. 4 Typical CERT environmental cycles: electronic equipment.

A. Vibration testing

Electronic equipment can be subjected to many different forms of vibration over wide frequency ranges and acceleration levels. It is probably safe to say that all electronic equipment will be subjected to some type of vibration at some time in its life. If the vibration is not due to an active association with some sort of machine or moving vehicle, the vibration may be due to the act of transporting the equipment from manufacturer to the customer. Embedded systems used in airplanes and missiles generally have a high packing density. The vibration frequency spectrum for airplanes will vary from about 3 Hz to 1000Hz with acceleration levels that can range from 1G to 5 G peak. The highest acceleration G levels appear to occur in vertical direction in the frequency range of 100-400 Hz and the lowest acceleration G levels appear to occur in the longitudinal direction, with maximum levels of about 1G in the same frequency.

The simplest vibration test is a fixed frequency shake with a sine wave input. Swept frequency sine testing is useful for resonance searches to enable the design to be modified if acceptable resonances are detected. Peak acceleration for a given frequency of sine wave vibration is calculated using the formula

$$A=0.002f^2 D$$

where A = peak acceleration (g)
 f =Frequency Hz
 D = peak to peak displacement

Alternatively, the spectrum could be a random input within a specified range and density function. Random vibration testing in which input contains many frequencies is more effective than swept frequency for reliability testing, to show up vibration-induced failure modes, since it

simultaneously excites all resonances. A typical random vibration spectrum is shown in Fig. 5

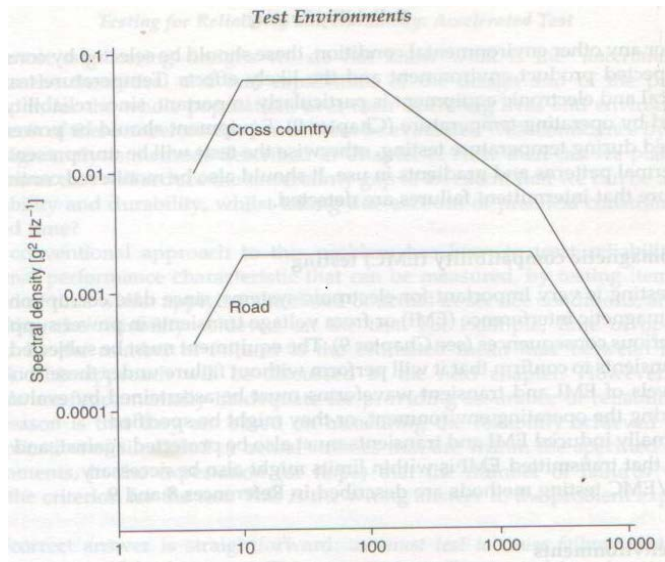


Fig. 5 Road transport vibration levels.

It is important to apply power to electronic equipment to monitor its performance while it is being vibrated, so that intermittent failures can be detected and investigated.

B. Temperature testing

High temperature can cause damage or incorrect operation in electrical and electronic components. Wire coils such as inductors, solenoids, transformers and motors can become short circuited if high temperature, caused by high currents or high ambient temperature, causes insulation charring. Similarly low temperatures can also cause components to fail due to parametric changes in electrical characteristics. However, such failures are usually reversible, and correct function is regained if the temperature rises.

Temperature testing for reliability is, however, less complex subject than vibration testing. The only aspects that need to be considered are extreme values of temperature (high and low) and rate of change. Equipment should be powered and operated during temperature testing, otherwise the test will be unrepresentative of the thermal patterns and gradients in use. It should be monitored continuously to ensure that intermittent failures are detected.

C. Software Reliability

Software is now part of the operating system of a very wide range of product and embedded systems and this trend continues to accelerate with the opportunities presented by low cost microcontroller devices. Hence, there is requirement of high reliability in both operating and application software so that the embedded system operates with very high reliability. There are various standards and tools available for software testing, debugging, software verification and validation.

VI. CONCLUSION

In conclusion, the reliability of embedded systems is improved right from the design and specification stages. But the reliability testing with consideration of environmental stresses and power cycling help in not only removal of weakness in production process including poor workmanship but also rendering long durability.

VII. REFERENCES

- [1] Patrick D. T. O'Connor, Practical Reliability Engineering. Fourth edition
- [2] Manish Verma & Peter Marwedel, Advanced memory optimization techniques for Low-Power Embedded Processor. Edition-2007
- [3] Dave S. Steinberg, vibration analysis for electronic equipment
- [4] Dave S. Steinberg, Cooling techniques for electronic equipment..
- [5] Charles A. Harper, Electronic materials and processes handbook..
- [6] M. Young, The Technical Writer's Handbook. Mill Valley, CA: University Science, 1989

SL-Z- Source Inverter with Maximum Constant Boost Control

A. Gaurav Sharma, B. Kavya Mittal, C. Bhupesh Kumar Pal, and D. Ankita Kosti

Abstract--This paper explores Switched Inductor (SL) Z-source inverter to enlarge voltage adjustability. The proposed inverter employs a unique SL impedance network to couple the main circuit and the power source . Compared with the classical Z-source inverter, the proposed inverter increases the voltage boost inversion ability significantly and power quality of the main circuit. In addition is presented A Maximum Constant Boost for controlling the SL-ZSI system which gives the benefit that the output voltage can be available to increase in vast scope also improving total harmonic distortion in current. The control methods, relationships of voltage gain versus modulation index are analyzed in detail and verified by simulation.

Index Terms--Boost inversion ability, converter, switched inductor (SL), topology, voltage conversion ratio, Z-source inverter.

I. INTRODUCTION

VOLTAGE and current-source inverters [1],[3] are widely used in industries for various purposes like for ac motor drives, distributed power systems, uninterruptible power supplies, hybrid electric vehicles etc. However, these inverters suffer from some major problems such as a voltage source inverter cannot have an ac output voltage higher than dc source voltage. Moreover it can only provide buck dc-ac power conversion. Similarly, a current-source inverter cannot have an ac output voltage lower than dc source voltage and hence can only provide only voltage boost dc-ac power conversion. So, for applications where both buck and boost voltage are demanded, there two-stage power conversion is performed by both voltage- and current-source inverter and this leads to high cost and low efficiency [2].

A. Gaurav Sharma, Department of Electrical Engineering, , India (e-mail: gaurav21987@gmail.com).

B. Kavya Mittal, Department of Mechanical Engineering, India (e-mail: kavyamittal89@gmail.com).

C. Bhupesh Kumar Pal, Department of Electrical Engineering, India (e-mail: bhupeshkumar09@gmail.com).

D. Ankita Kosti , Department of Electrical Engineering, India (e-mail: ankitakosti@gmail.com m).

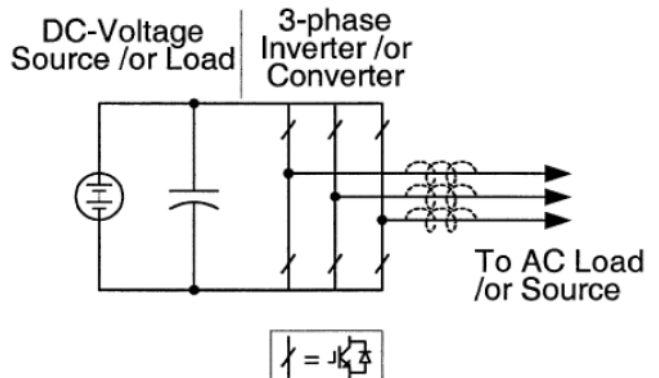


Fig.1. Traditional V- source converter

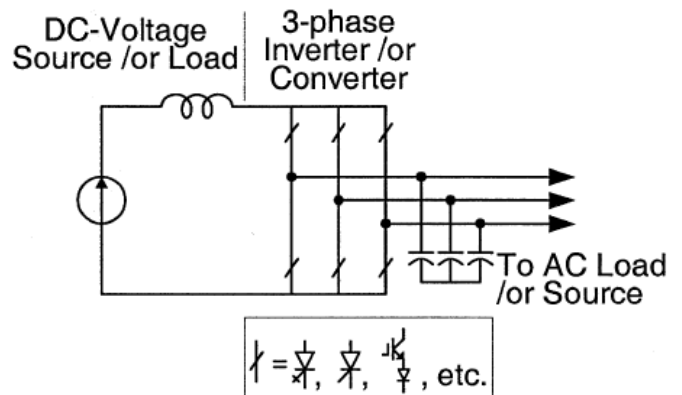


Fig.2. Traditional I-source converter

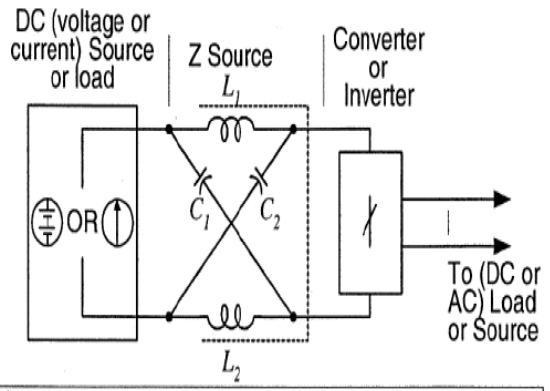


Fig.3. General Structure of the SL-Z-source inverter.

As there are certain limitations in case of VSI and CSI, so Z-source (impedance source) power converter come into existence which employs a unique impedance network or circuit to couple the converter main circuit to the power source, load or other features that cannot be observed in the traditional V- and I-source converters. Z-source converter overcomes the limitations of VSI and CSI.

In this paper, the techniques of SL are integrated into classical Z-source impedance network and hence new SL Z-source impedance network is proposed and its maximum constant boost control is done through simulation [4].

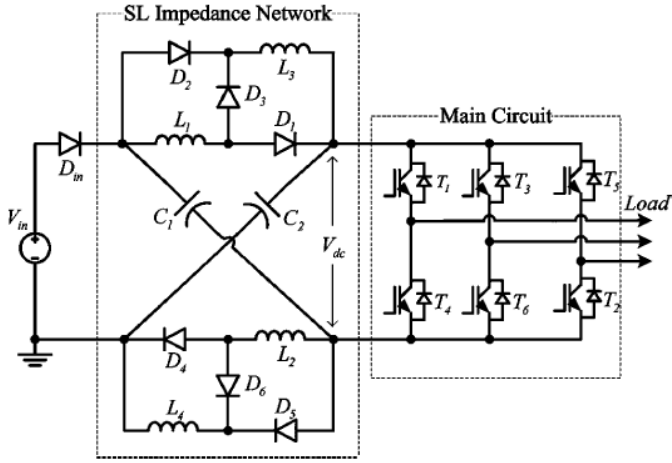


Fig.4. Topology of proposed SL Z source inverter.

In this paper, the concept of the SL techniques has been integrated into the classical Z-source impedance network, and consequently, a new SL Z-source impedance network is proposed.

II. ANALYSIS OF TOPOLOGY OF SL Z-SOURCE INVERTER

The proposed SL Z-source inverter shown in fig.4.consists of four inductors (L_1, L_2, L_3 and L_4), two capacitors (C_1 and C_2), and six diodes (D_1, D_2, D_3, D_4, D_5 and D_6). The combination of $L_1-L_3-D_1-D_3-D_5$ performs the function of top SL cell and the combination of $L_2-L_4-D_2-D_4-D_6$ performs the function of bottom SL cell. Both of these cells are meant for storing and transferring energy from the capacitors to the dc bus under the switching action of the main circuit.

A. Operating Principle:

On the basis of switching states of the main circuit connected with SL impedance network, the operating principles of SL-ZSI are similar to that of classical ZSI network as viewed from the dc bus as shown in Fig.5 in which an active switch S and a passive switch D_o are used for the simulation of the practical shoot-through actions of the top and bottom arms. Thus the proposed impedance network has the substates which are

classified into shoot-through state and non-shoot-through state, respectively.

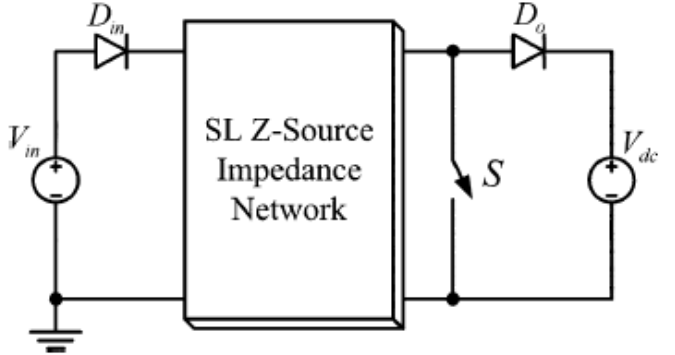


Fig.5. Equivalent circuit of the SL Z-source inverter viewed from the dc-linkbus.

1) *Shoot-Through State*: In this substate , S is ON, while both D_o and D_{in} are OFF. D_1 and D_2 are ON and D_3 is OFF for the top SL cell. L_2 and L_4 are charged by C_2 in parallel. This state leads to additional zero state produced by the shoot-through actions of the top and bottom arms. The equivalent circuit is shown in Fig.6 (a). Both top and bottom SL cells perform the same function of absorbing the energy stored in the capacitors.

2) *Non-Shoot-Through State*: This state has two zero states and six active states of the main circuit as shown in Fig.6(b). During this sub state, S is OFF, while both D_o and D_{in} are ON. D_1 and D_3 are OFF and D_5 is ON for the top SL cell. L_1 and L_2 are connected in series and the energy stored is transferred to the main circuit. D_4 and D_6 are OFF and D_6 is ON for the bottom SL cell, L_3 and L_4 are connected in series and the energy stored is transferred to the main circuit. During the shoot-through state, C_1 is charged by V_{in} via bottom SL cell, and C_2 is charged by V_{in} via top SL cell.

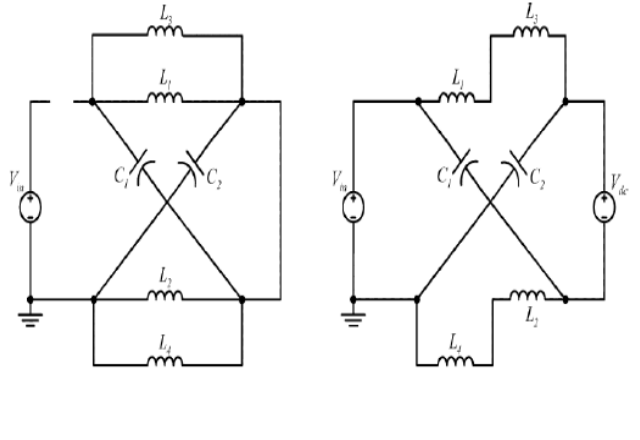


Fig.6. Equivalent circuits.
(a) Shoot-through zero state (i.e., switching ON).
(b) Non-shoot-through states (i.e., switching OFF).

B. Boost Ability Analysis of SL-Z Source Inverter:

We assume the same values of inductance (L) and capacitance (C). Since the values of C₁ and C₂ are very large so in a steady state we have

$$V_{C1}=V_{C2}=V_C$$

The inductor current value i_{L1} increases at the time of switching ON ,and decreases during switching OFF. During switching ON, the voltage across L₁,V_{L1-ON} is equal to V_C. Applying the volt-sec analysis across we can obtain the voltage during switching OFF,which is expressed by

$$V_{L1-OFF} = \frac{D}{1-D} V_C \quad (1)$$

$$= V_{L3-OFF} \quad (2)$$

Applying the volt-second balance principle to L₃, we have

$$V_C = \frac{1-D}{1-3D} V_{in} \quad (3)$$

$$= V_{C1}=V_{C2} \quad (4)$$

Therefore,

$$V_{dc} = \frac{1+D}{1-3D} V_{in} = B V_{in} \quad (5)$$

Boost factor of SL Z-source impedance, B is thus expressed by :

$$B = \frac{1+D}{1-3D} = \frac{1+T_o/T}{1-3T_o/T} \quad (6)$$

For the comparison of individual boost ability ,the curves of boost factor B versus duty ratio D for classical Z- source impedance network and the proposed network is compared in fig 7. As seen boost ability of the proposed impedance network has increased .

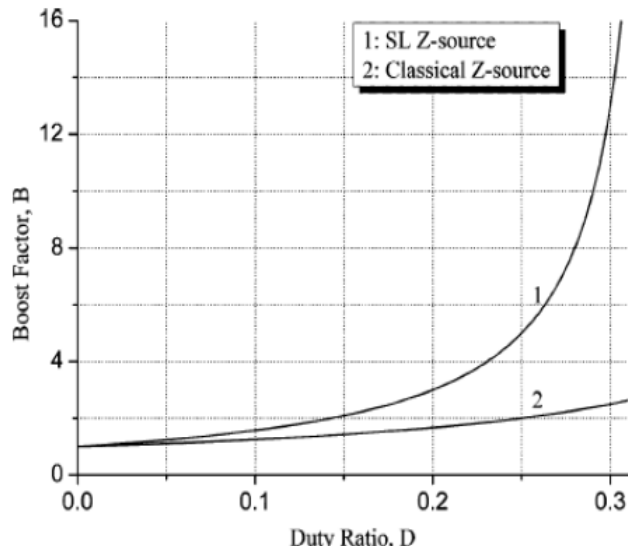


Fig .7.Boost ability comparison of the classical Z-source and the proposed SL Z- source

C. Stress Comparison of inverters:

By considering the same value of D and V in, we can compare stress for classical and proposed inverter through the table 1.

TABLE 1

| | SL-ZSI | ZSI |
|------------------|--------------------|------------------|
| V _{inv} | $\frac{1+D}{1-3D}$ | $\frac{1}{1-2D}$ |
| i _D | $2i_L - i_l$ | $2i_L - i_l$ |

III. COMPARISON OF VARIOUS CONTROL STRATEGIES

Fig 8(a),8(b) and 8 (c) shows voltage conversion ratios versus modulation index under various control strategies i.e simple boost control ,maximum boost control and maximum constant boost control .

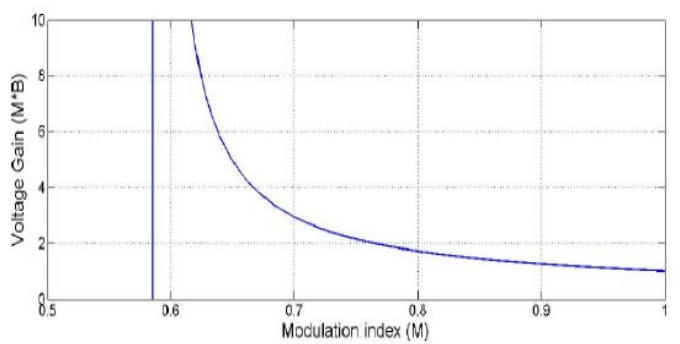


Fig 8(a) voltage conversion versus modulation index for simple boost control

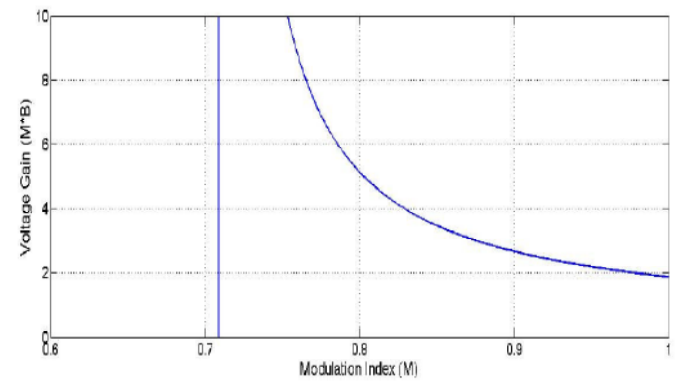


Fig 8(b) voltage conversion versus modulation index for simple boost control

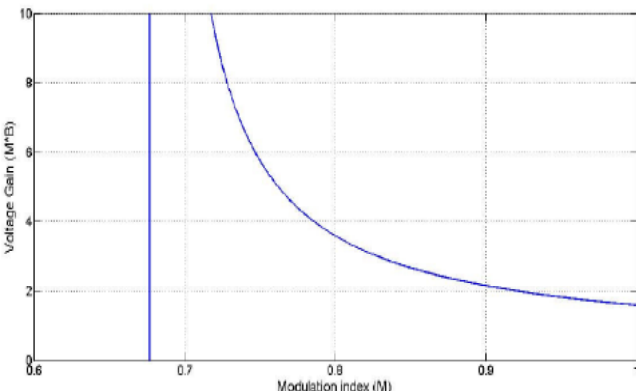


Fig 8(c) voltage conversion versus modulation index for simple boost control

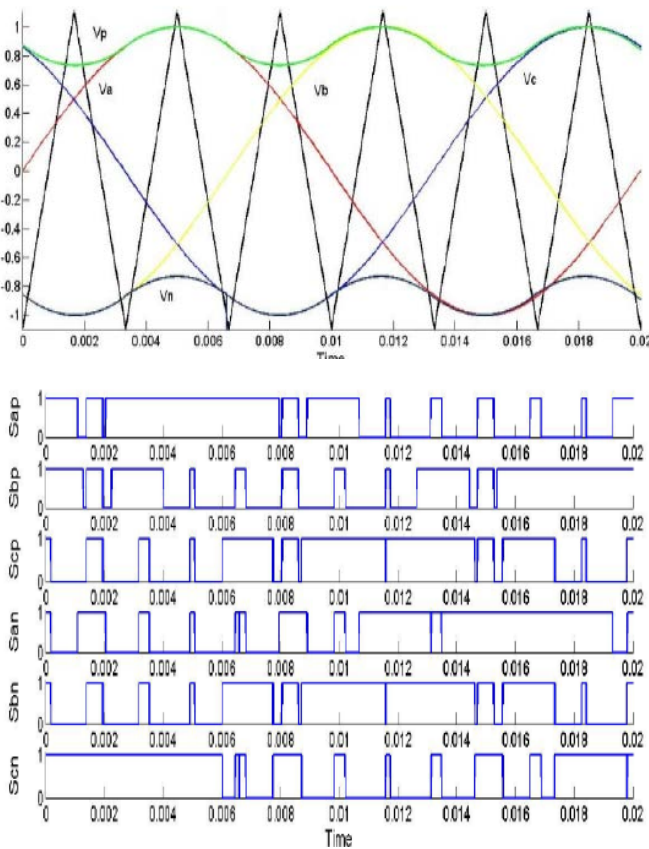


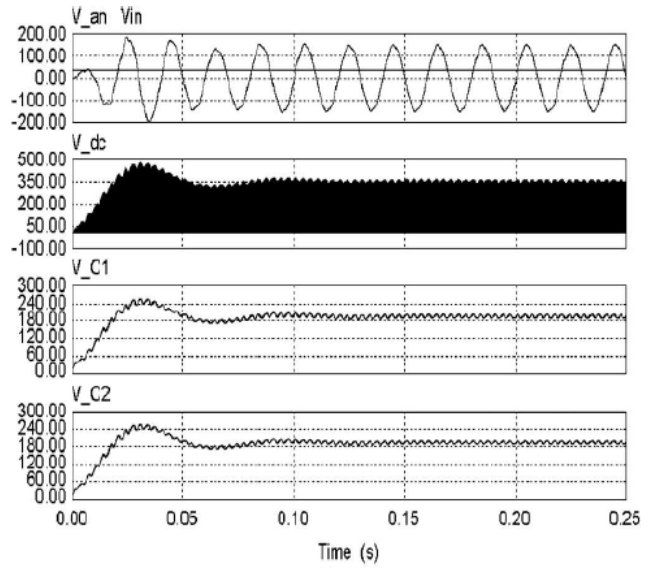
Fig .9. Waveform of Maximum Constant boost Control

IV. EXPERIMENTAL VERIFICATION:

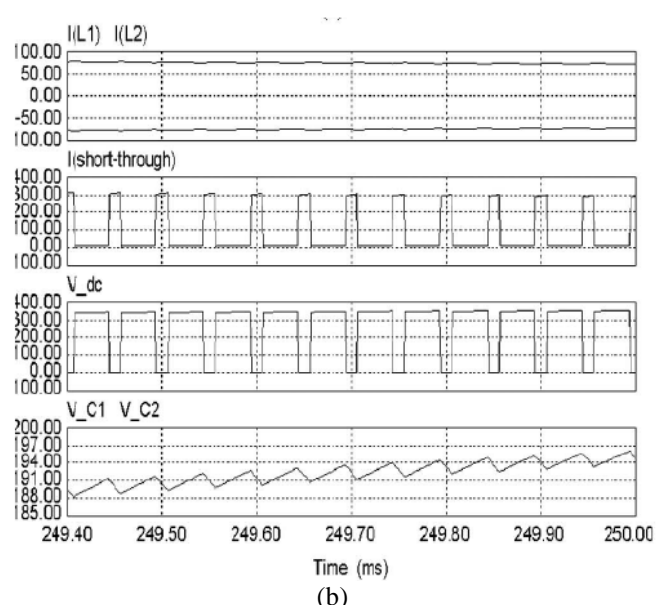
Parameters used in the simulation of maximum boost control of SL-qZSI are shown in **table 2**.

TABLE 2
SIMULATION PARAMETERS

| | |
|--|--------|
| Input DC voltage | 40V |
| Output line voltage | 90V |
| L ₁ =L ₂ =L ₃ | 10mH |
| C ₁ =C ₂ | 1000uF |
| Carrier frequency | 10KHz |
| L _f | 20mH |
| C _f | 30uF |
| Resistive load three phase | 900W |



(a)



(b)

Fig 10(a) and 10 (b) shows the simulation results under the Maximum Constant Boost control

V. CONCLUSION

In the paper the focus is on rapidly changing z- source network .SL-ZSI improves the input current ,reduces passive count . To control maximum constant boost is used which has been verified by simulation .It is clear from the simulation results the ripples in maximum constant boost control is used and peak value of shoot through current decreases.

VI. REFERENCES

- [1]. C. Yang and K.Smedley ,“Three -phase boost type grid connected inverter”, *IEEE Trans Power Electron* ,vol.23,no.5.pp 2301-2309,Sep 2008.
- [2]. F.Z Peng, “Z Source Inverter”, *IEEE Trans .Ind Application*, vol39, no.2.pp.504-510, April 2003.
- [3]. T. Kerekes, R. Teodorescu and M. Summer , “Evaluation of three phase transformer less Photovoltaic inverter”, *IEEE Trans*,vol24, no 9,pp.2202-2211,Sep .2009.
- [4]. F.Z. Peng ,M.Shen, “Maximum boost Control of Z- Source inverter”, *IEEE Trans*. Vol.20,no4, pp. 833-838 July 2005.

Performance Comparison of Hybrid Filter by Using Different Compensation Techniques

A. Gaurav Sharma, B. Kavya Mittal, C. Ankita Kosti, and D. Bhupesh Kumar Pal

Abstract-- This paper basically deals with the objective to improve the Power Quality (PQ) and enhance the reliability of power supply by using Hybrid Active Power Filter (HAPF) and calculating Total Harmonic Distortion (THD) as per IEEE-519 Standard limits. In this paper the harmonic compensation is obtained by two different compensation strategies (pq and dq) in hybrid active power filter. To assess the performance of each method, simulation results are compared. Both of these compensation techniques show an acceptable compensation performance.

Index Terms-- hybrid active power filter (HAPF), pq method, dq method, IEEE 519 harmonic standard, total harmonic distortion (THD).

I. INTRODUCTION

WITH the increasing use of non-linear devices either for residential or industrial applications, the power distribution system is polluted with harmonics. These harmonics not only lead to current and voltage stress but also responsible for other effects such as electromagnetic interference, more losses and capacitor failure. For a particular type of load, IEEE-519 Standard limits the maximum amount of harmonics that a supply system can tolerate. Thus filters are very much essential for the harmonic compensation and improving the power quality and hence increases the reliability of the distribution system.

The harmonic compensation can be obtained by Passive Filters (PF), Active Power Filters (APF) and hybrid filters (HPF) [1]. PF and APF have some advantage and disadvantages, but hybrid active power filters contain their advantages but not their disadvantages.

A. Gaurav Sharma, Department of Electrical Engineering, , India (e-mail: gaurav21987@gmail.com).

B. Kavya Mittal, Department of Mechanical Engineering, India (e-mail: kavyamittal89@gmail.com).

C. Bhupesh Kumar Pal, Department of Electrical Engineering, India (e-mail: bhupeshkumar09@gmail.com).

D. Ankita Kosti , Department of Electrical Engineering, India (e-mail: ankita.kosti@gmail.com m).

Passive filter have been traditionally used for the mitigation of distortion due to harmonic current in industrial power systems but due to some drawbacks such as resonance problem, dependency of their performance on the system impedance, absorption of harmonic current of nonlinear load, which could lead to further harmonic propagation through the power system.

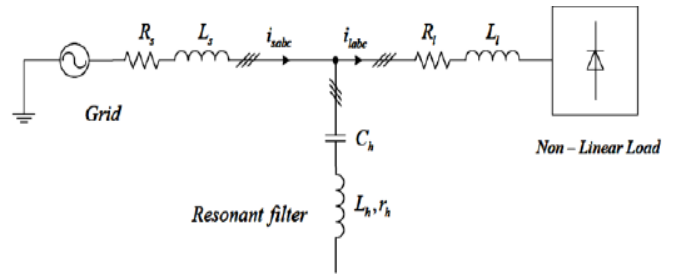


Fig.1 Passive Filter Topology

Active power filters (APF) generate either harmonic currents or voltages in a manner such that the grid current or voltage waves conserve the sinusoidal form. The APFs can be connected to the grid in series (Series APF), shunt (SAPF) to compensate voltage harmonics or current harmonics respectively. Or can be associated with passive filters to construct the hybrid filters (HAPF).

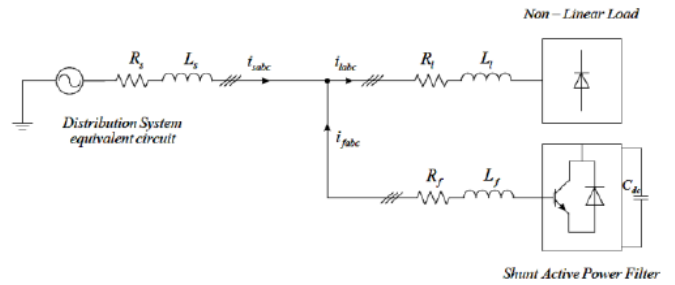


Fig.2. Shunt Active Filter Topology

There are different models of hybrid filters [2]. The common HAPF is obtained by connecting PF and APF as shown in fig.1.

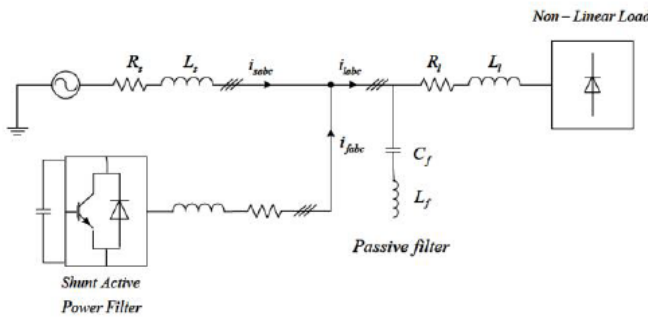


Fig.3. Hybrid Filter Topology

APF generally consists of two distinct main blocks: the Current-Controlled Voltage-Source Inverter (CCVSI) and active filter controller [3]. APF sense the load current i_L continuously with control algorithm, and calculate the instantaneous values of the compensating current reference for the VSI.

The passive filter consists of simple LC filters per phase tuned near the lowest harmonics (5th or 7th or...). It performs main functions: reactive compensation, absorption of harmonic currents produced by the loads. This paper presents the configuration of HAPF. Then different control strategies including pq method [4], dq method [5] are presented. Final section present simulation results that are conducted in MATLAB/Simulink environment and under various non ideal mains test scenarios. Then a comparison of the methods is made for various conditions.

II. HARMONIC CURRENT EXTRACTION METHODS

A. Instantaneous Reactive Power Theory (pq Method):

This method is also known as pq method. Most APFs have been designed on the basis of instantaneous reactive power theory or pq method to calculate the desired compensation current. This theory was first proposed by Akagi and co-workers in 1984 [4].

The p-q theory is based on a set of instantaneous powers defined in the time domain. The three-phase supply voltages (u_a, u_b, u_c) and currents (i_a, i_b, i_c) are transformed using the Clarke (or $\alpha\beta$) transformation into a different coordinate system yielding instantaneous active and reactive power components.

This transformation may be viewed as a projection of the three-phase quantities onto a stationary two-axis reference frame.

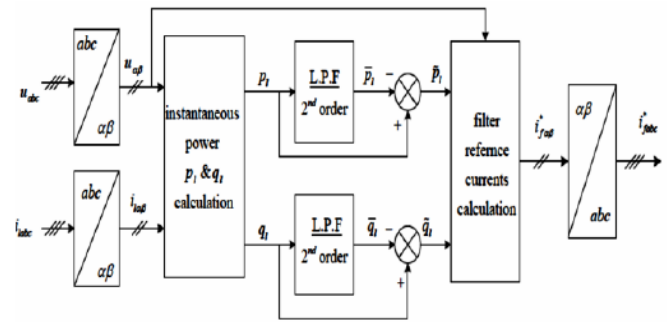


Fig.4. Principle of instantaneous active and reactive power theory.

B. Synchronous Reference Theory (d-q Method):

In this method, called also the method of instantaneous currents i_d, i_q , the load currents are transformed from three phase frame reference abc into synchronous reference in order to separate the harmonic contents from the fundamentals [6]. It gives better performance even in the case where the three phase voltage is not ideal.

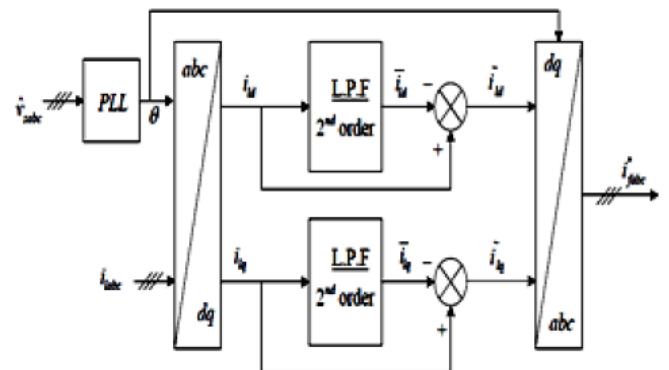


Fig.5. Principle of the synchronous reference method

III. MODELLING OF CURRENT EXTRACTION METHODS

A. Instantaneous Reactive Power Theory (pq Method)

The Clarke transformation for the voltage variables is given by [6]:

$$\begin{bmatrix} u_\alpha \\ u_\beta \\ u_0 \end{bmatrix} = \sqrt{\frac{2}{3}} \begin{bmatrix} 1 & -\frac{1}{2} & -\frac{1}{2} \\ 0 & \frac{\sqrt{3}}{2} & -\frac{\sqrt{3}}{2} \\ \frac{1}{\sqrt{2}} & \frac{1}{\sqrt{2}} & \frac{1}{\sqrt{2}} \end{bmatrix} \begin{bmatrix} u_a \\ u_b \\ u_c \end{bmatrix} \quad (1)$$

Similarly, this transform can be applied on the distorted load currents to give:

$$\begin{bmatrix} i_{l\alpha} \\ i_{l\beta} \\ i_{l0} \end{bmatrix} = \sqrt{\frac{2}{3}} \begin{bmatrix} 1 & -\frac{1}{2} & -\frac{1}{2} \\ 0 & \frac{\sqrt{3}}{2} & -\frac{\sqrt{3}}{2} \\ \frac{1}{\sqrt{2}} & \frac{1}{\sqrt{2}} & \frac{1}{\sqrt{2}} \end{bmatrix} \begin{bmatrix} i_{la} \\ i_{lb} \\ i_{lc} \end{bmatrix} \quad (2)$$

The instantaneous active power $p(t)$ is given by:

$$p(t) = u_a i_{la} + u_b i_{lb} + u_c i_{lc} \quad (3)$$

This expression can be given in the stationary frame by:

$$p(t) = u_\alpha i_{l\alpha} + u_\beta i_{l\beta} \quad (4)$$

$$p_o(t) = u_0 i_{l0} \quad (5)$$

Where, $p(t)$ is the instantaneous active power, $p_0(t)$ is the instantaneous homo-polar sequence power. Similarly the instantaneous reactive power can be given by:

$$q(t) = -\frac{1}{\sqrt{3}} [(u_a - u_b)i_{lc} + (u_b - u_c)i_{la} + (u_c - u_a)i_{lb}] \quad (6)$$

$$= u_\alpha i_{l\beta} - u_\beta i_{l\alpha} \quad (7)$$

In matrix form, the instantaneous active and reactive power can be given by:

$$\begin{bmatrix} p \\ q \end{bmatrix} = \begin{bmatrix} u_\alpha & u_\beta \\ -u_\beta & u_\alpha \end{bmatrix} \begin{bmatrix} i_{l\alpha} \\ i_{l\beta} \end{bmatrix} \quad (8)$$

After separating the direct and alternating terms of instantaneous power, the harmonic components of the load currents can be given by using the inverse of equation (8) which gives:

$$\begin{bmatrix} i_{l\alpha} \\ i_{l\beta} \end{bmatrix} = \frac{1}{v_{s\alpha}^2 + v_{s\beta}^2} \begin{bmatrix} v_{s\alpha} & v_{s\beta} \\ -v_{s\beta} & v_{s\alpha} \end{bmatrix} \begin{bmatrix} \tilde{i}_l \\ \tilde{q}_l \end{bmatrix} \quad (9)$$

The APF reference current can be then given by:

$$\begin{bmatrix} i_{fa}^* \\ i_{fb}^* \\ i_{fc}^* \end{bmatrix} = \sqrt{\frac{2}{3}} \begin{bmatrix} 1 & 0 \\ -\frac{1}{2} & \frac{\sqrt{3}}{2} \\ -\frac{1}{2} & -\frac{\sqrt{3}}{2} \end{bmatrix} \begin{bmatrix} \tilde{i}_{l\alpha} \\ \tilde{i}_{l\beta} \end{bmatrix} \quad (10)$$

B. Synchronous Reference Theory (d-q Method)

Transformation from three phase frame reference abc into synchronous reference is given by [7]:

$$\begin{bmatrix} i_{ld} \\ i_{lq} \\ i_{l0} \end{bmatrix} = \sqrt{\frac{2}{3}} \begin{bmatrix} \cos \theta & \cos(\theta - \frac{2\pi}{3}) & \cos(\theta + \frac{2\pi}{3}) \\ -\sin \theta & -\sin(\theta - \frac{2\pi}{3}) & \sin(\theta + \frac{2\pi}{3}) \\ \frac{1}{\sqrt{2}} & \frac{1}{\sqrt{2}} & \frac{1}{\sqrt{2}} \end{bmatrix} \begin{bmatrix} i_{la} \\ i_{lb} \\ i_{lc} \end{bmatrix} \quad (11)$$

The currents in the synchronous reference can be decomposed into two parts as:

$$\begin{cases} i_{ld} = \bar{i}_{ld} + \tilde{i}_{ld} \\ i_{lq} = \bar{i}_{lq} + \tilde{i}_{lq} \end{cases} \quad (12)$$

The APF reference currents are given by:

$$\begin{bmatrix} i_{fd}^* \\ i_{fq}^* \end{bmatrix} = \begin{bmatrix} \tilde{i}_{ld} \\ \tilde{i}_{lq} \end{bmatrix} \quad (13)$$

In three phase system, APF currents can be calculated by the inverse Park transform which is defined as:

$$\begin{bmatrix} i_{fa}^* \\ i_{fb}^* \\ i_{fc}^* \end{bmatrix} = \sqrt{\frac{2}{3}} \begin{bmatrix} \cos \theta & -\sin \theta \\ \cos(\theta - \frac{2\pi}{3}) & -\sin(\theta - \frac{2\pi}{3}) \\ \cos(\theta + \frac{2\pi}{3}) & \sin(\theta + \frac{2\pi}{3}) \end{bmatrix} \begin{bmatrix} i_{fd}^* \\ i_{fq}^* \end{bmatrix} \quad (14)$$

IV. SIMULATION RESULTS

On applying PQ harmonic current extraction technique, the following simulation results are obtained which clearly explains the power quality improvement from THD analysis by using Hybrid Filter.

Fig.6. shows the source current waveform before filter using PQ method. Figure shows the effect of load variation.

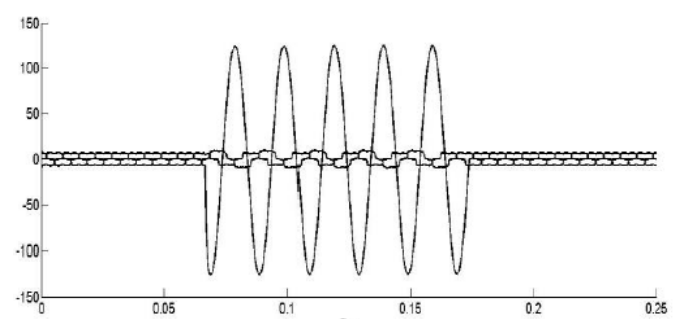


Fig.6. Source Current before Filter

Fig.7. shows the THD analysis before filter which is found to be many more times as per IEEE-519 standard limits.

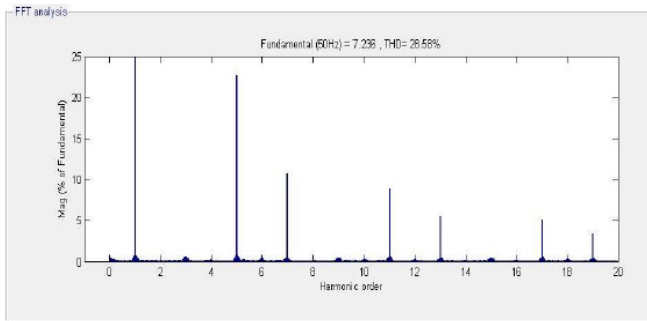


Fig.7. THD of Source Current before Filter

Fig.8. shows the source current waveform after using hybrid filter which clearly shows the transient period and steady state period of the current waveform.

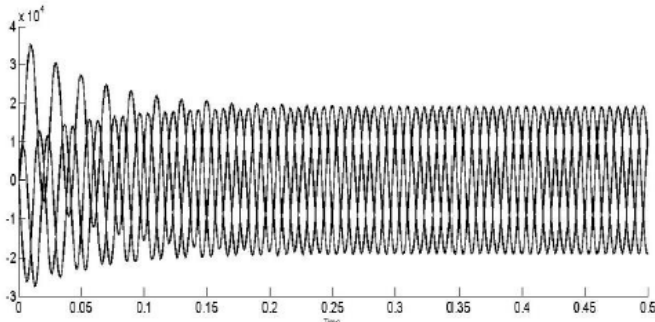


Fig.8. Source Current after Filter

Fig.9. shows the THD analysis after filter which is found to be approximate as per IEEE-519 standard limits. This clearly explains the power quality improvement by reducing the THD.

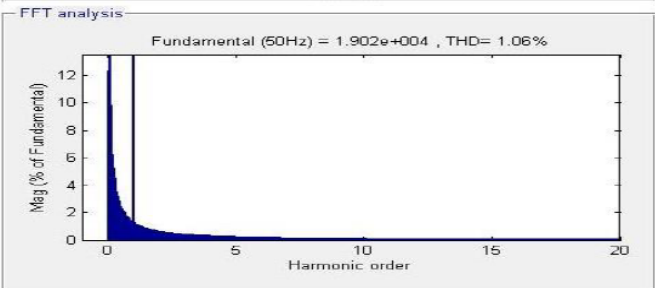


Fig.9. THD of Source Current after Filter

Fig.9 shows the waveform of load voltage.

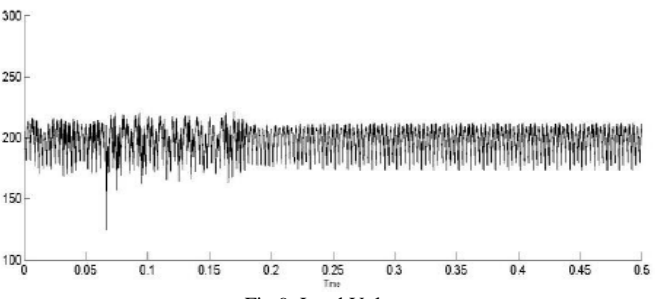


Fig.9. Load Voltage

By DQ harmonic current extraction technique:

Fig.10. shows the source current waveform after using hybrid filter which clearly shows the transient period and steady state period of the current waveform.

It can be seen that the transient period by using dq technique is less than using pq technique.

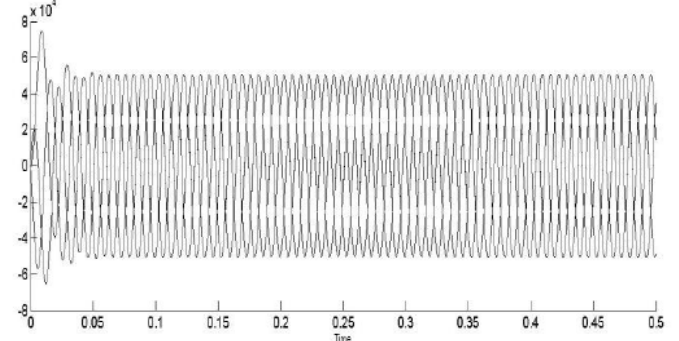


Fig.10. Source Current after Filter

Fig.11. shows the THD analysis after filter which is found to be approximate as per IEEE-519 standard limits. This clearly explains the power quality improvement by reducing the THD.

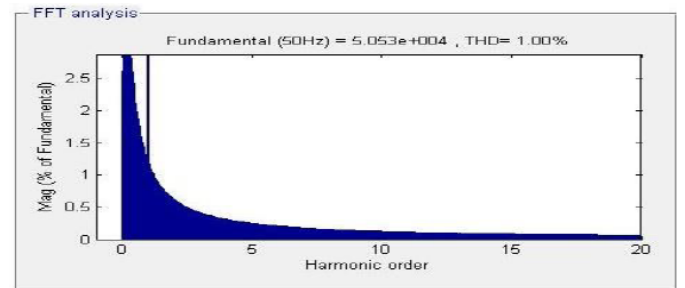


Fig.11. THD of Source Current after Filter

V. SIMULATION PARAMETERS

TABLE I

| | | |
|------------------|-----------------------------------|--------|
| Supply System | Line Voltage (r.m.s. value) | 220V |
| | Line Frequency | 50 Hz |
| | Source inductance, L _s | 0.1mH |
| Active Filter | AC inductor to the rectifier | .002mH |
| | V _{dc} (V) | 650 |
| | C _{dc} (μF) | 0.1 |
| Passive Filter | L _c (mH) | 0.2 |
| | C _f (μF) | 1 |
| Nonlinear load 1 | L _f (mH) | 1 |
| | R _L (Ω) | 30 |
| Nonlinear load 2 | L _L (mH) | 0.3 |
| | R _L (Ω) | 50 |
| | L _L (mH) | 0.1 |

VI. CONCLUSION

In this paper, different control methodologies are implemented and simulated to understand the performance of HAPF under different load conditions. On the basis of simulation results performed in MATLAB/Simulink environment, it is concluded that dq method is more stable than pq method and hence improved the power quality by reducing the THD.

VII. REFERENCES

- [1]. M. Ranjbar, M. A. Masoumand A. Jalilian, "Comparison of compensation strategies for shunt active power filter control in unbalanced three-phase four-wire systems," in *Proc. 22nd Canadian Conference on Electrical and Computer Engineering (CCECE'09)*, pp. 1061-1066, May 2009.
- [2]. S.Rahmani, K. Al-Haddad, H. Y. Kanaan, and B. Singh, "Implementation and simulation of modified PWM with Two current control techniques applied to single-phase shunt hybrid power filter," *IEEE Proc.-Electr. Power Appl.*, Vol. 153, No. 3, May 2006.
- [3]. V. F. Corasaniti, M. B. Barbieri, P. B. Arnera and M. I. Valla, "Hybrid active filter for reactive and harmonics compensation in a distribution network," *IEEE Trans. on Industrial Electronics*, Vol. 56, No. 3, pp. 670-677, March 2009.
- [4]. H. Akagi, E. H. Watanabe, M. Arede and J. H. Marks, "Instantaneous power theory and applications to power conditioning," *IEEE Press 445 Hoes Lane Piscataway, NJ 08854*.
- [5]. V. F. Corasaniti, M. B. Barbieri, P. B. Arnera and M. I. Valla, "Hybrid power filter to enhance power quality in a medium-voltage distribution network," *IEEE Trans. on Industrial Electronics*, Vol. 56, No. 8, pp. 2885-2893, Aug. 2009.
- [6]. N. Hanna Mandalek, "Qualité de L'ondeElectrique et Moyens de Mitigation", *Thèse de Doctorat, Ecole de Technologie Supérieure Univ.Quebec*, 2003.
- [7]. C. Sharneela, M. R. Mohan, G. Uma, J. Baskaranet A.C. College, "Fuzzy Logic Controller Based Three-Phase Shunt Active Filter for Line Harmonics Reduction", *Univ Anna*, Vol. 3, No. 2, 2007, pp. 76-80.

LIGHT-FIDELITY (Li-Fi) (VISIBLE LIGHT COMMUNICATION)

A.Vikram Singh, B.Rajneesh Lodhi,C. Suneel Kushwaha, and D.R. K. Singh

Abstract-- With the vast growing gadgets, their usage and their developments led to the advancement in the Wi-Fi which provides a technology so called Li-Fi. Li-Fi is a technology that makes use of LED light which helps in the transmission of data much faster and flexible than data that can be transmitted through Wi-Fi. Light reaches nearly everywhere so communication can also go along with light freely. Light Fidelity is a branch of optical wireless communication which is an emerging technology. By using visible light as transmission medium, Li-Fi provides wireless indoor communication. The bit rate achieved by Li-Fi cannot be achieved by Wi-Fi. Dr Herald Haas, the professor of mobile communications at the University of Edinburgh School of engineering, first time publically displayed the proof of Light Fidelity (Li-Fi), a method of Visible Light communication (VLC). Li-Fi is the transfer of data through light by taking fibre out of fibre optics and sending data through LED light.

I. INTRODUCTION

Li-Fi basically known as "light fidelity" is an outcome of twenty first century. The basic ideology behind this technology is that the data can be transmitted through LED light whose intensity varies even faster than the human eye. As the transmission of the data takes place through the light emitting diodes (LED's) the amount is comparatively small .In modern times, it is called as the optimized version of WI-FI .The advantageous thing is the wireless communication which decreases the cost enormously. HARALD HASS, who is considered to be the father of Li-Fi from university of Edinburgh, UK says that the heart of this technology lies in the intensity and the potential of the light emitting diodes. The major reason which lead the modern man through this invention is that the confinement of Wi-Fi to comparatively small distance. As there are more and more devices coming up day-by-day the signals are being clogged up due to heavy traffic, there arises a need for an error free transmission technology. And the solution to this problem was the Li-Fi technology. It has been designed in such a way that it overcomes the disadvantages that occurs during the usage of Wi-Fi. In general terms, Li-Fi works even under water thereby causing a great benefit to the military operations.

A.ECD KNIT, Sultanpur-228118 (U.P.) India
(e-mail: vik081189@gmail.com)

B. ECD KNIT,Sultanpur-228118 (U.P.) India
(e-mail: rajneesh.nra@gmail.com)

C. ECD KNIT,Sultanpur-228118 (U.P.) India

(e-mail: suneel.er@gmail.com)

D.ECD KNIT,Sultanpur-228118 (U.P.) India

(e-mail: singhrabinder57@gmail.com)

The physics envisions that this technology would make a great difference between the assumption and the proof in this case.The demonstration took place using two Casio smart phones. The data was made to exchange between the phones using light. Even though the distance was nominal, it is sure that there would be a rapid increase in the distance of transmission.As there is a limited amount of Radio basedwireless spectrum available, a number of companies formed a consortium called Li-Fi consortium in order to promote high speed optical wireless systems .The members of this consortium believes that a speed of 10 Gbps can be achieved in no time. In simple terms, Li-Fi can be thought of as a light-based Wi-Fi. That is, it uses light instead of radio waves to transmit information. And instead of Wi-Fi modems, Li-Fi would use transceiver-fitted LED lamps that can light a room as well as transmit and receive information. Since simple light bulbs are used, there can technically be any number of access points. This technology uses a part of the electromagnetic spectrum that is still not greatly utilized- The Visible Spectrum. Light is in fact very much part of our lives for millions and millions of years and does not have any major ill effect. Moreover there is 10,000 times more space available much more. The technology truly began during the 1990's in countries like in this spectrum and just counting on the bulbs in use, it also multiplies to 10,000 times more availability as an infrastructure, globally.

It is possible to encode data in the light by varying the rate at which the LEDs flicker on and off to give different strings of 1s and 0s. The LED intensity is modulated so rapidly that human eyes cannot notice, so the output appears constant. More sophisticated techniques could dramatically increase VLC data rates. Teams at the University of Oxford and the University of Edinburgh are focusing on parallel data transmission using arrays of LEDs, where each LED transmits a different data stream. Other groups are using mixtures of red, green and blue LEDs to alter the light's frequency, with each frequency encoding a different data channel.

Li-Fi, as it has been dubbed, has already achieved blisteringly high speeds in the lab. Researchers at the Heinrich Hertz Institute in Berlin, Germany, have reached data rates of over 500 megabytes per second using a standard white-light LED. Haas has set up a spinoff firm to sell a consumer VLC

transmitter that is due for launch next year. It is capable of transmitting data at 100 Mbps faster than most UK broadband connections.

II. HISTORY

has the possibility to change how we access the internet, stream videos, receive emails and much more. The technology truly began during the 1990's in countries like Germany, Korea, and Japan where they discovered LED's could be retrofitted to send information. This type of light would come in familiar forms such as infrared, ultraviolet and visible light. Research into VLC has been conducted in earnest since 2003, mainly in the UK, US, Germany, Korea and Japan. Experiments have shown that LEDs can be electronically adapted to transmit data wirelessly as well as to provide light. VLC is faster, safer and cheaper than other forms of wireless internet, advocates say -- and so could eliminate the need for costly mobile-phone radio masts.

Haas has a small lab stuffed with equipment, including the now-famous table lamp and its box of electronics. It was here in 2007 that his research assistant, MostafaAfgani, first sent

III. DEVELOPMENT

Two latest technologies in telecommunication have been revealed in last few months.

- It was demonstrated that the data can be transmitted through LED light. So the data will be transmitted through the LED light without any physical optical fibre. If there will be an LED, there will be data.
- Meanwhile Steve Perlman of Rearden lab has introduced another technology named DIDO which will break the Shannon's limit by 100 times.

IV. WORKING OF LI-FI

In order to know the working of Li-Fi we need to know the necessity for Li-Fi. With the vast development in living the use of gadgets and invention of new gadgets is increasing which lead to the technological developments

There are many situations in which people get frustrated with the dull performance signals of Wi-Fi at a place with many network connections in seminars conferences etc. Li-Fi fulfills these needs .This fantabulous idea first strike the mind of Harald Haas from University of Edinburgh, UK, in his TED Global talk on VLC. His idea was very simple that if the LED is “on” then the digital 1 can be transmitted and if the LED is “off” then the digital 0 can be transmitted. LED's

Harald Haas continues to hit the world that there is a possibility for communication through light.LI-FI technology

data using light signals. Haas's invention centres on how these signals are modulated: the information, embedded within. visible light emitted from the LEDs, is transmitted by means of many subtle changes made to the intensity of the light at the ultra-high rate of 100 million cycles per second (100MHz).

The photo-detector in Haas's box monitors these tiny variations and converts them back into a digital signal, from which the transmitted information is extracted. In October 2011 a number of companies and industries formed the Li-Fi Consortium, to promote high-speed optical wireless system sand to enhance the limited bandwidth provided by radio-based wireless spectrum available. The consortium believes it is possible to achieve more than 10Gbps speed using this optical wireless technology also known as Li-Fi. The communication is done by deploying transmitter and receiver in direct line of sight manner. It gets affected if line of sight is not used, the speed of data transmission will reduce or data transmission will stop. It is also more secure than other wireless networks as only photo receptors are used, which can receive data within transmitted cone of light signals.

can be switched on and off very quick. For transmitting data this way all that we require is LED's and controller that code data into LED's. Parallel data transmission can be done by using array of LED's or by using red, green, blue LED's to alter light frequency with the frequency of different data channel. Advancements and enhancements in this field generate a speed of 10 gbps! But amazingly fast data rates and lowering band widths are not the only reasons that enhance this technology. LI-FI usually is based on light and so it can be probably implemented in aircrafts and hospitals that are prone to inference from radio waves. Unlike Wi-Fi Li-Fi can work even underwater which makes it more advantageous for military operations. Radio waves are replaced by light waves in data transmission called Li- Fi.Light emitting diodes can be switched on and off very much faster than the human eye allowing the light source to appear continuously. The data transmission is done through binary codes which involve switching on LED can be done by logic 1 and switch off using logic 0.The encoding of information in light can therefore be identified by varying the rate at which the LED's flicker on and off to give strings of 0's and 1's.visible light communication is this method of using rapid pulses of light to transmit information wirelessly.

V. VISIBLE LIGHT COMMUNICATION

VLC is a data communication. The general term visible light communication (VLC), includes any use of the visible light

portion of the electromagnetic spectrum to transmit information. The term Li-Fi was coined by Harald Haas from the University of Edinburgh in the UK. The D-Light project at Edinburgh's Institute for Digital Communications was funded from January 2010 to January 2012. Harald Haas promoted this technology in his 2011 TED Global talk and helped start a company to market it. Pure VLC is an original equipment manufacturer (OEM) firm set up to commercialize LiFi products for integration with existing LED - lighting systems.

In October 2011, companies and industry groups formed the Li-Fi Consortium, to promote high-speed optical wireless systems and to overcome the limited amount of radio-based wireless spectrum available by exploiting a completely different part of the electromagnetic spectrum. A number of companies offer uni-directional VLC products. VLC technology was exhibited in 2012 using Li-Fi. By August 2013, data rates of over 1.6 Gbps were demonstrated over a single colour LED. In September 2013, a press release said that Li-Fi, or VLC systems in general, do not require line-of-sight conditions. In October 2013, it was reported Chinese manufacturers were working on Li-Fi development kits.

VLC communication is modelled after communication protocols established by the IEEE 802 workgroup. This standard defines the physical layer (PHY) and media access control (MAC) layer. The standard is able to deliver enough data rates to transmit audio, video and multimedia services. It takes count of the optical transmission mobility, its compatibility with artificial lighting present in infrastructures, the defiance which may be caused by interference generated by the ambient lighting. The MAC layer allows to use the link with the other layers like the TCP/ IP protocol.

The standard defines three PHY layers with different rates:

- The PHY I was established for outdoor application and works from 11.67 kbit/s to 267.6 kbit/s.
- The PHY II layer allows to reach data rates from 1.25 Mbit/s to 96 Mbit/s.
 - The PHY III is used for many emissions sources with a particular modulation method called colour shiftkeying (CSK). PHY III can deliver rates from 12 Mbit/s to 96 Mbit/s.

The modulations formats preconized for PHY I and PHY II are the coding on-off keying (OOK) and variable pulse position modulation (VPPM). The Manchester coding used for the PHY I and PHY II layers include the clock inside the transmitted data by representing a logic 0 with an OOK symbol "01" and a logic 1 with an OOK symbol "10", all with a DC component. The DC component avoids the light extinction in case of an extended line of logic 0. Optical

orthogonal frequency-division multiplexing (O-OFDM) modulation methods were modelled for data rates, multiple-access and energy efficiency.

Medium, which uses visible light between 400 THz (780 nm) and 800 THz (375 nm) as optical carrier for data transmission and illumination. Fast pulses are used for wireless transmission. Communication system components are:

1. A high brightness white LED which acts as communication source
2. Silicon photo diode which shows good response to visible wavelength region.

LED illumination can be used as a communication source by modulating the LED light with the data signal. The LED light appears constant to the human eye due to the fast flickering rate. The high data rate can be achieved by using high speed LED's and appropriate multiplexing techniques. Each LED transmits at a different data rate which can be increased by parallel data transmission using LED arrays. Many different reasons exist for the usage of LED light in spite of fluorescent lamp, incandescent bulb etc. which are available.

VI. DEVICES USED IN VLC

Devices which are used for transmission purpose in VLC are visible light LED and fluorescent lamp. LED light intensity is modulated by controlling its current. The technology uses fluorescent lamps to transmit signals at 10bit/s, or LED's for up to 500 Mbit/s. Devices which are used for reception purpose in visible light communication are pin photodiode (high speed reception up to 1Gbps), Avalanche photo diode (very sensitive reception) and Image sensor(simultaneous image acquisition and data reception) as shown in fig



Fig: LED and a photo detector



At the heart of LI-FI is the bulb sub-assembly where a sealed bulb is embedded in a dielectric material. This design is more reliable than conventional light sources that insert degradable electrodes into the bulb. The dielectric material serves two

The world will become gradually green mobile internet masts that will permit to respond to the impressive increasing demand of mobile connectivity. Also, this will allow reducing the electromagnetic pollution generated by the numerous radio wave solutions developed until now.

VII. LI-FI CONSTRUCTION

The LI-FI product consists of 4 primary sub-assemblies:

- Bulb
- RF power amplifier circuit (PA)
- Printed circuit board (PCB)
- Enclosure

The world of lighting companies experiences a true revolution with the development of Led lighting devices. With reduced energy consumption and a longer lifetime, LEDs appear as a solution that cannot be overlooked to face up to the challenge of the CO₂ emission reduction at the worldwide scale. The sale

purposes; first as a waveguide for the RF energy transmitted by the PA and second as an electric field concentrator that focuses energy in the bulb. The energy from the electric field rapidly heats the material in the bulb to a plasma state that emits light of high intensity and full spectrum. The design and construction of the LI-FI light source enable efficiency, long stable life, and full spectrum intensity that is digitally controlled and easy to use.

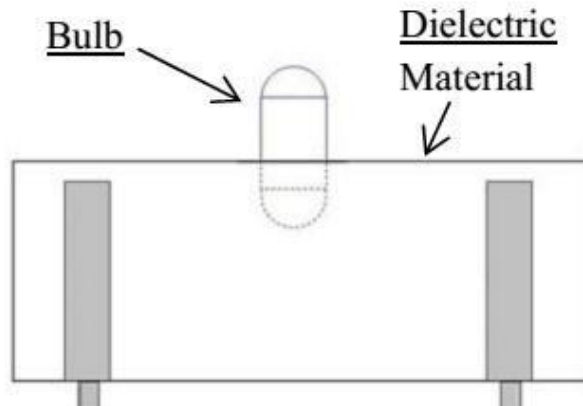
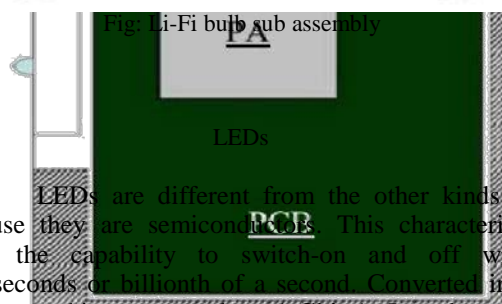


Fig: Li-Fi block diagram

The PCB controls the electrical inputs and outputs of the lamp and houses the microcontroller used to manage different lamp functions. An RF (radio-frequency) signal is generated by the solid-state PA and is guided into an electric field about the bulb. The high concentration of energy in the electric field vaporizes the contents of the bulb to a plasma state at the bulb's centre; this controlled plasma generates an intense source of light. All of these subassemblies are contained in an aluminium enclosure.

FUNCTION OF THE BULB SUB ASSEMBLY



LEDs are different from the other kinds of lamps because they are semiconductors. This characteristic gives them the capability to switch-on and off within few nanoseconds or billionth of a second. Converted in terms of data rates, this corresponds to 1 Gbit/s. In order to compare, at best Wi-Fi can reach 100 M bits/s data rates and so 10 times lower. Thanks to the Li-Fi technology, the 14 billion lamps

inof LEDs Lighting units knows an impressive increase these last years.

COMPARISION BETWEEN LI-FI AND WI-FI

Li-Fi is a terminology which is used to describe visible light communication technology applied to high speed wireless communication. Wi-Fi is great for general wireless coverage within buildings, and Li-Fi is ideal for high density wireless data coverage in confined area and for relieving radio interference issues, so the two technologies can be considered complimentary. Comparisons of two technologies are given below in table

| PARAMETERS | WIRELESS TECHNOLOGIES | |
|---|---|---|
| | Light Fidelity | Wireless Fidelity |
| Speed for data transfer | Greater than 1 Gbps | 150 Mbps |
| Medium through which data transfer occurs | Light as carrier | Radio spectrum |
| Spectrum range | Visible spectrum has 10,000 times broad spectrum in comparison to radio frequency | Radiofrequency spectrum range is less than visible light spectrum |
| Network topology | Point to point | Point to point |
| Cost | Cheaper than Wi-Fi Because free band doesn't need license and it uses light | Expensive in comparison to Li-Fi because it uses radio spectrum |
| Operating frequency | Hundreds of Tera Hz | 2.4 GHz |

Table1: Comparison of Li-Fi and Wi-Fi

HOW IT IS DIFFERENT??

Li-Fi technology is based on LEDs for the transfer of

data. The transfer of the data can be with the help of all kinds of light, no matter the part of the spectrum that they belong. That is, the light can belong to the invisible, ultraviolet or the visible part of the spectrum. Also, the speed of the internet is incredibly high and you can download movies, games, music etc. in just a few minutes with the help of this technology. Also, the technology removes limitations that have been put on the user by the Wi-Fi. You no more need to be in a region that is Wi-Fi enabled to have access to the internet. You can simply stand under any form of light and surf the internet as the connection is made in case of any light presence. There cannot be anything better than this technology.

TECHNOLOGY DEMONSTRATION

It was demonstrated that table lamp that successfully transmit data at speed exceeding 10 Mbps using light waves from LED light to a computer located below the lamp. To prove that the light bulb was the source of the data stream, he (Harald Hass) periodically blocked the light beam, causing the connection to drop.

BRIGHTNESS OF Li-Fi SOURCE

The LI-FI source has very high lumen intensity. In other words, a single source, only a few millimetres in size can produce 2300 lumens of brilliant white light. At this level of output, you will only need to use one light source per street light in most cases. This makes the mechanical and optical implementation of light much simpler and less expensive.

SPECIAL FACTS FOR Li-Fi TECHNOLOGY

Li-Fi is a new way to establish wireless communication links using the LED lighting networks. The Li-Fi protocols are defined by the international standard IEEE 802.15 established since 2011 by the IEEE committee. This is the same committee that has defined previously the Ethernet 802.3 and Wi-Fi 802.11 standards.

- For numerous specialists, Li-Fi is a major breakthrough technology for the mobile Internet community and for the connected objects domain.
- After more than 4 years of scientific research at the University of Versailles, OLEDCOMM is the first European company that start to commercialize Li-Fi communication solutions a worldwide level.
- 14 billion of new lamps are generated each years.
- 25 billion Euros of turnover in 2011.

VIII. APPLICATIONS

There is a wide necessity for data transfer and by the end of the day every field involves the use of technologies. one such technology is Li-Fi which can have its applications extended

in areas where the Wi-Fi technology lack its presence like medical technology, power plants and various other areas where Li-Fi proved its excellence of the undersea awesomeness.

FUTURE APPLICATIONS

EDUCATION SYSTEMS

As with the advancement of science the latest technology is the LI-FI which is the fastest speed internet access service. so this will lead to the replacement of WI-FI at institutions and at companies so that all the people can make use of LI-FI with same speed intended in a particular area.

MEDICAL FACILITIES

As operation theatres do not allow WI-FI due to radiation concerns. Usage of WI-FI at hospitals interfere with the mobile and pc which blocks the signals for monitoring equipment. Therefore the replacement for this Wi-Fi is Li-Fi as Hass has mentioned in his TED TALK that LI-FI has 10,000 times the spectrum of Wi-Fi. Because the lights are not only allowed in operation theatres but also the most dazzling fixtures in the room.

REDUCTION IN ACCIDENT NUMBERS

At traffic signals, we can use LI-FI in order to communicate with LED lights of the cars by the number of accidents can be reduced. Data can be easily transferred by making use of LI-FI lamps with the street lamps.

REPLACEMENT FOR OTHERS TECHNOLOGIES

- with the LED lights of cars and might alert drivers when other vehicles are too close so accident numbers can be decreased.
- Traffic lights could better regulate traffic flow using data.
- It can also be used in hospitals and aeroplanes where radio signals are prohibited.
- It will transform air travel by allowing overhead cabin light to connect mobiles and laptops in flight and it will improve conditions for those working underwater on oil rigs where radio waves can't go through.
- Thousands and millions of street lamps can be transferred to Li-Fi lamps to transfer data.
- It can be used in petroleum and chemical plants where other transmission or frequencies could be hazardous.

This technology doesn't deal with radio waves, so it can easily be used in the places where Bluetooth, infrared, WI-FI and Internet are banned. In this way, it will be most helpful transferring medium for us. It includes other benefits like:

- A very wide spectrum over visible wave length range.
- Extremely high colour fidelity.
- Instant start time.
- Easy terminal Management.
- Dynamic dark i.e. brightness Modulation of lamp output to enhance video contrast.
- Trouble-free integration into existing light engine platform.

Li-Fi is the upcoming and on growing technology acting as competent for various other developing and already invented technologies. Since light is the major source for transmission in this technology it is very advantageous and implementable in various fields that can't be done with the Wi-Fi and other technologies. Hence the future applications of the Li-Fi can be predicted and extended to different platforms like education fields, medical field, industrial areas and many other fields.

ADVANTAGES OF Li-Fi

Visible light communication advantages in hazardous or tough conditions.

Li-Fi used in sensitive areas such as aircraft for data transmission without causing interference.

- Light waves can't penetrate walls this phenomena makes it secure.
- It is used in places where it is difficult to lay optical fibres like operation theatres and at traffic signal.
- In traffic signals, Li-Fi can be used to communicate

CHALLENGES FOR Li-Fi

Apart from many advantages over Wi-Fi, Li-Fi technology is facing some challenges.

- Li-Fi requires line of sight.
- When set up outdoors, the apparatus would need to deal with ever changing conditions.
- Indoors, one would not be able to shift the receiving device.
- A major challenge facing Li-Fi is how the receiving device will transmit back to transmitter.
- One more disadvantage is that visible light can't penetrate through brick walls as radio waves
- and is easily blocked by somebody simply walking in front of LED source.
- A side effect of Li-Fi is that your power cord immediately becomes your data stream, so if you have power, you have internet.

IX. CONCLUSION

Li-Fi is the upcoming and on growing technology acting as competent for various other developing and already invented technologies. Since light is the major source for transmission in this technology it is very advantageous and implementable in various fields that can't be done with the Wi-Fi and other technologies. Hence the future applications of the Li-Fi can be predicted and extended to different platforms like education fields, medical field, industrial areas and many other fields. The possibilities are numerous and can be explored further. If this technology can be put into practical use, every bulb can be

REFERENCES

1. International Journal of Scientific & Engineering Research, Volume 4, Issue 5, May2013 ISSN 2229-5518 (<http://www.ijser.org>)
2. seminarprojects.com/s/seminar-report-on-Li-Fi
3. <http://en.wikipedia.org/wiki/Li-Fi>
4. <http://teleinfobd.blogspot.in/2012/01/what-is-Li-Fi.html>
5. technopits.blogspot.comtechnology.cgap.org/2012/01/
6. [/a-Li-Fi-world/](http://a-Li-Fi-world/)
7. www.Li-Ficonsortium.org/
8. the-gadgeteer.com/2011/08/29/Li-Fi-internet-at-the-speed-Of-light/
9. en.wikipedia.org/wiki/Li-Fi
10. www.macmillandictionary.com/buzzword/entries/Li-Fi.html
11. advice.com/archives/2012/08/Li-Fi-ten-ways-i.php
12. Will Li-Fi be the new Wi-Fi?, New Scientistt, by Jamie Condliffe, dated 28 July 2011
13. <http://www.digplanet.com/wiki/Li-Fi>

used something like a Li-Fi hotspot to transmit wireless data and we will proceed toward the cleaner, greener, safer and brighter future. The concept of Li-Fi is currently attracting a great deal of interest, not least because it may offer a genuine and very efficient alternative to radio-based wireless. As a growing number of people and their many devices access wireless internet, the airwaves are becoming increasingly clogged, making it more and more difficult to get a reliable, highspeed signal. This may solve issues such as the shortage of radio-frequency bandwidth and also allow internet where traditional radio based wireless isn't allowed such as aircraft or hospitals. One of the shortcomings however is that it only works in direct line of sight.

Transient Performance Investigation on CSI Fed Induction Motor Drive Employing A Variable Gain Proportional Integral (VGPI) Speeed Controller

A,S. M. Tripathi,B. Ashish Mishra,C. A. K. Pandey

Abstract- This paper presents a variable gain PI (VGPI) controller for speed control of a self commutating current source inverter-fed induction motor drive with volts/Hz control strategy. First, a VGPI speed controller is designed then its simulated performances for various transient conditions are then compared to those of a classical PI controller. The closed loop mathematical modeling of the complete drive system is presented in the synchronously rotating d^e-q^e reference frame

Keywords – Induction motor, Closed-loop control, current source inverter, variable gain PI controller, pulse width modulation (PWM), transient performance, V/f control.

I. INTRODUCTION

Induction motors in high performance variable speed drive applications have a series of advantages. The current source inverter (CSI) as variable speed drive is characterized by its simplicity, ruggedness, and lower cost. Proportional plus integral (PI) controllers, which are conventionally employed for CSI-fed induction motor drives suffer from some limitations of high overshoots. To overcome this problem, we propose the use of variable gains PI controllers. A variable gain PI (VGPI) controller is a generalization of a classical PI controller where the proportional and integrator gains vary along a tuning curve.

II. VARIABLE GAIN PI(VGPI) BASED SPEED CONTROLLER

In this paper a variable gain PI (VGPI) speed controller based current source inverter (CSI) fed induction motor (IM) drive comprising of PI current controller in inner current loop and VGPI speed controller in outer speed loop along with its mathematical modeling is described. A variable gain PI (VGPI) controller is a generalization of a classical PI controller where the proportional and integrator gains vary along a tuning curve.

Each gain of the proposed controller has four tuning parameters:

- Gain initial value or start up setting which permits overshoot elimination.

- Gain final value or steady state mode setting which permits rapid load disturbance rejection.
- Gain transient mode function which is a polynomial curve that joins the gain initial value to the gain final value.
- Saturation time which is the time at which the gain reaches its final value.

The degree n of the gain transient mode polynomial function is defined as the degree of the variable gain PI controller. The signal input to the VPGI controller then the output is given by:

$$y(t) = K_p e(t) + \int_0^t K_i e(\tau) d\tau \quad (1)$$

With

$$K_p = \begin{cases} (K_{pf} - K_{pi}) \left(\frac{t}{T_s} \right)^n + K_{pi} & \text{if } t < T_s \\ K_{pf} & \text{if } t \geq T_s \end{cases} \quad (2)$$

$$K_i = \begin{cases} (K_{if}) \left(\frac{t}{T_s} \right)^n & \text{if } t < T_s \\ K_{if} & \text{if } t \geq T_s \end{cases} \quad (3)$$

Here is a

proposed method of tuning a VGPI controller:

1. Choose a first degree VGPI controller with a high value of K_{if} (rapid load disturbance rejection).
2. Choose an initial value of the saturation time T_s .
3. Determine K_{pi} and K_{pf} for speed overshoot elimination by using the following steps:
 - (a) Consider K_p to be constant and simulate the controlled system for a small initial value of K_p .
 - (b) Increase K_p gradually and simulate the controlled system again until speed overshoot gets to its optimum. Simulation shows that as K_p increases, speed overshoot decreases until an optimal value is obtained, then it begins to increase again. Choose K_{pi} to be the value of K_p that gives optimal overshoot.

A Department of Electrical Engg., Kamla Nehru Institute of Technology, Sultanpur (U.P.), India, (E-mail: mani_excel@yahoo.co.in)

B Department of Electrical & Electronics Engineering, RRSIMT, Amethi (U.P.), India, (E-mail:ashish06cest@gmail.com)

C Department of Electrical Engineering, M. M. M. Engineering College, Gorakhpur (U.P.), India, E-mail: apk1234@gmail.com)

(c) Simulate the controlled system for an initial value of K_{pf} equal to the chosen value of K_{pi} .

(d) Increase gradually the value of K_{pf} and simulate the controlled system again until speed overshoot is totally eliminated or gets to its optimal value.

Simulation shows that as K_{pf} increases, speed overshoot decreases until a total elimination or gets to an optimal value. If overshoots are totally eliminated then K_{pf} is obtained and the controller is tuned.

4. If overshoots are not totally eliminated, then the value of the saturation time T_s is not sufficiently high, increase it gradually without exceeding a limiting value and repeat step 3 until overshoot is totally eliminated.

$$I_c = k_{11} \omega_e^2 \quad (4)$$

Where K_{11} can be written as:

$$k_{11} = \frac{I_c(\text{rated})}{(\omega_e(\text{rated}))^2} \quad (5)$$

If at the limiting value of T_s overshoot is still not eliminated, then the degree of the controller is not high enough. Increase it and repeat the controller tuning again.

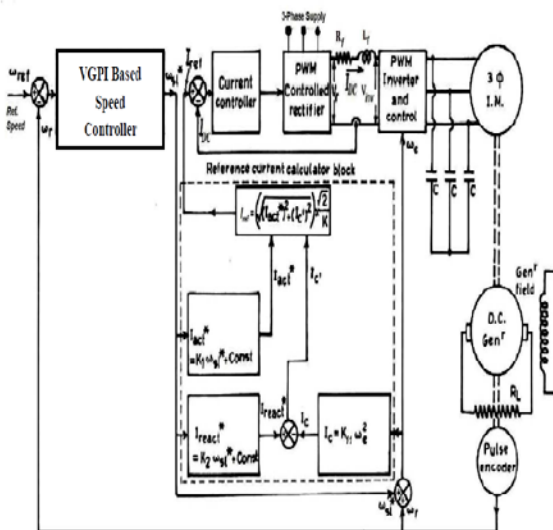


Fig. 1 Self commuting CSI fed IM drive with VGPI speed and PI current controller

The CSI-fed induction motor drive consists of a three phase AC source, a PWM rectifier, a DC link smoothening reactor, a current-controlled inverter, a three-phase squirrel cage induction motor, and a three-phase capacitor bank, as shown in Fig. 1.

The outer speed regulator compares the reference speed and the actual rotor speed and processes the speed error to obtain the reference slip speed (ω_{sl}^*) which is required to estimate the reference stator

active current (I_{act}^*) and reference stator reactive current (I_{react}^*) of the induction motor and hence, reference DC link current (I_{ref}).

The reference stator active current (I_{act}^*) and reference stator reactive current (I_{react}^*) of induction motor is estimated by reference slip speed and is given below:

$$I_{act}^* = k_1 \omega_{sl}^* + \text{constant} \quad (6)$$

$$I_{react}^* = k_2 \omega_{sl}^* + \text{constant} \quad (7)$$

Switching frequency (ω_e) of inverter is given by:

$$\omega_e = \omega_r + \omega_{sl}^* \quad (8)$$

The error between reference DC link current and the actual DC link current is regulated by PI controller in inner current feedback loop. The widths of pulse of PWM rectifier are decided by output of PI current controller and hence output voltage of PWM rectifier is controlled which in turn controls the DC link current.

The output voltage of rectifier in terms of current controlled parameters is given by:

$$V_r = \left(k_{pi} + \frac{k_{i_i}}{p} \right) (I_{ref} - I_{DC}) \quad (9)$$

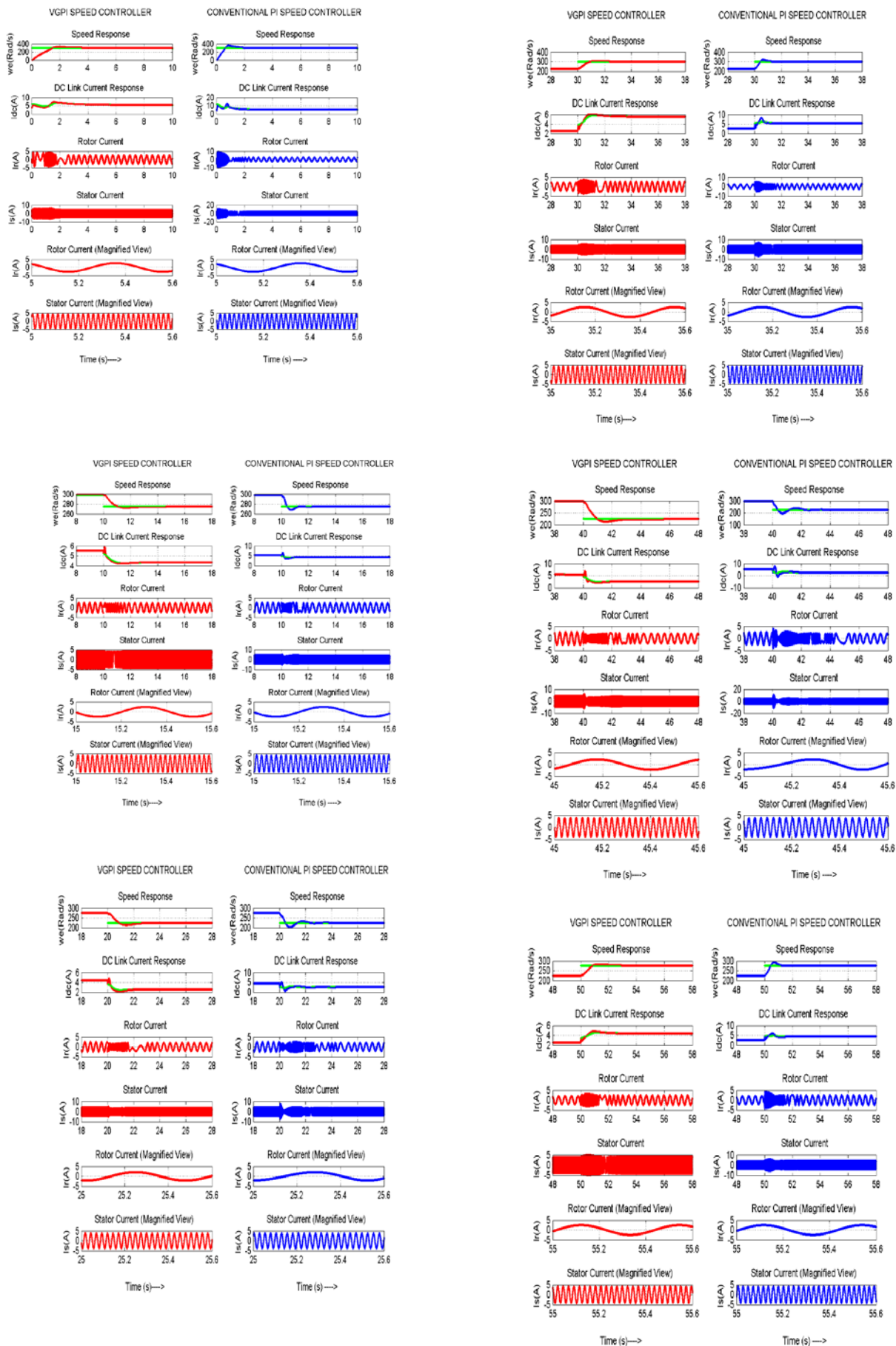
The reference DC link current is determined by:

$$I_{ref} = \left(\sqrt{(I_{act}^*)^2 + (I_{react}^* - I_c)^2} \right) \cdot \left(\frac{\sqrt{2}}{k} \right) \quad (10)$$

III. SIMULATION RESULTS AND DISCUSSIONS

Here performance of CSI fed induction motor drive is investigated through MATLAB for various transient conditions. For different variations in reference speed, performance of the drive is investigated, compared and analyzed in case of both PI speed controller as well as VGPI speed controller and results are shown here accordingly.

The main motive of analysis is to confirm whether VGPI speed controller is better than PI controller or not by comparing their effectiveness during various transient conditions.



- Following different cases for step change in reference speed are taken:
 - (1). Start up by step change in reference speed from 0 rad/s to 298.29 rad/s.
 - (2). Deceleration by step change in reference speed from 298.29 rad/s to 275 rad/s.
 - (3). Deceleration again by step change in reference speed from 275 rad/s to 225 rad/s.
 - (4). Acceleration by step change in reference speed from 225 rad/s to 298.29 rad/s.
 - (5). Deceleration again by step change in reference speed from 298.29 rad/s to 225 rad/s.
 - (6). Acceleration again by step change in reference speed from 225 rad/s to 275 rad/s.

Here for different variations in reference speed, performance of CSI fed induction motor drive is investigated, compared and analyzed with both PI speed controller as well as VGPI speed controller and results are shown accordingly.

By comparing their effectiveness during various transient conditions, it has been concluded that VGPI speed controller based drive system has better overall response as compare to that of PI speed controller based drive system.

The percentage overshoot in speed of the drive during starting for the reference speed command of rated value (298.29 rad/s) from initial speed has been observed 20.98 % and 7.78 % seconds for PI and VGPI based speed controllers respectively. The percentage overshoot for reference speed commands of 275 rad/sec from 298.29 becomes 4.36 % in case of PI speed controller and 0.80 % in case of VGPI speed controller. Further for reference command of 225 rad/sec from 275 rad/sec, 298.29 rad/sec from 225 rad/sec, 225 rad/sec from 298.29 rad/sec, 275 rad/sec from 225 rad/sec, percentage overshoots became 2.57 %, 5.50 %, 2.57 %, 4.3 % for PI speed controller and 4.04 %, 2.38 %, 5.20 %, 2.54 % for VGPI speed controller respectively which shows effectiveness of VGPI speed controller over PI speed controller. The steady state DC link current is

almost same in both cases. However settling time taken by drive is more for VGPI speed controller as compared to PI speed controller. The results for both controllers under each variation in reference speed are compared and analyzed. Moreover, the CSI fed induction motor drive system using a VGPI speed controller has highly reduced peak overshoot and better steady state DC link currents as compared to the system with a PI speed controller. This way, the results in MATLAB environment have proved the feasibility and better performance of the proposed VGPI speed controller based for closed-loop control of a self-commutating current source inverter-fed induction motor drive

Table 1: Performance of drive for each alteration in reference speed

| Sr . | Step change in ref. Speed(rad/s) | | Steady state DC link current(A) | | Speed Overshoot(%) | | Drive settling time(s) | |
|------|----------------------------------|--------|----------------------------------|-------|---------------------|-------|------------------------|-------|
| | From | To | VG PI | VG PI | VG PI | VG PI | VG PI | VG PI |
| 1 | 0 | 298.29 | 5.51 | 5.50 | 7.78 | 20.98 | 4.35 | 3.24 |
| 2 | 298.29 | 275 | 4.33 | 4.36 | 0.80 | 2.36 | 2.61 | 2.75 |
| 3 | 275 | 225 | 2.54 | 2.57 | 4.04 | 9.82 | 2.85 | 3.92 |
| 4 | 225 | 298.29 | 5.51 | 5.50 | 2.38 | 7.27 | 3.00 | 2.75 |
| 5 | 298.29 | 225 | 2.54 | 2.57 | 5.2 | 12.4 | 2.90 | 3.96 |
| 6 | 225 | 275 | 4.33 | 4.36 | 2.54 | 6.76 | 3.30 | 2.49 |

IV. CONCLUSIONS

In this paper, a proposed variable gain PI (VGPI) speed controller based current source inverter (CSI) fed induction motor (IM) drive comprising of PI current controller in inner current loop and VGPI speed controller in outer speed loop has been described. The mathematical model of the drive has

been developed by considering different sections of the drive scheme.

The objectives of this paper were to survey CSI fed IM drives, to develop mathematical model of a proposed variable gain PI controller based CSI fed induction motor drive system in synchronously rotating reference frame, to tune proposed variable gain PI (VGPI) controller as speed controller, development of control law, to analyze transient performance of drive for various conditions and to compare performance of VGPI speed controller based CSI fed induction motor drive system with conventional PI speed controller based CSI fed induction motor drive system in MATLAB environment.

For different variations in reference speed, performance of the drive is investigated, compared and analyzed in case of both PI speed controller as well as VGPI speed controller and results are shown here accordingly. The transient performance curves have been obtained and compared with both PI and VGPI based speed controllers in MATLAB environment.

However settling time taken by drive is more for VGPI speed controller as compared to PI speed controller but the CSI fed induction motor drive system using a VGPI speed controller has highly reduced peak overshoot and better steady state DC link currents as compared to the system with a PI speed controller.

By comparing their effectiveness during various transient conditions, it has been concluded that VGPI speed controller based drive system has better overall response as compare to that of PI speed controller based drive system.

APPENDIX

MOTOR SPECIFICATIONS

Name Plate Ratings of Induction Motor

1 HP, 3-phase, 400V, 50 Hz, 4-pole, 1425 r.p.m, Star connected

Induction Motor Parameters

$$R_s = 3.520 \Omega, R_r = 2.780 \Omega, L_s = 0.165 \text{ H}$$

$$L_r = 0.165 \text{ H}, L_m = 0.150 \text{ H}, J = 0.01289 \text{ kg-m}^2$$

DC Link Parameters

$$R_f = 0.250 \Omega, L_f = 0.040 \text{ H}$$

V. REFERENCES

- [1] Kamalesh Hatua, V.T.Ranganathan, "A Novel VSI and CSI fed Dual Stator Induction Motor Drive Topology for Medium Voltage Drive Applications," IEEE accepted, March, pp. 1-10, 2010.
- [2] Kamal Jamshidi and Vedam Subrahmanyam, "Modified Controller for Closed Loop Control Of CSI-Fed Induction Motor," IEEE, 1995.
- [3] A. R. Beig and V. T. Ranganathan, "A Novel CSI fed Induction Motor Drive," IEEE Trans. Power Electron., vol. 21, no. 4, pp. 1073-1082, Jul. 2006.
- [4] P. Agarwal and V. K. Verma, "Performance Evaluation of Current Source Inverter-fed Induction Motor Drive", Journals of Institution of Engineers, Vol.72, pp. 209-217, February 1992.
- [5] J. R. Espinoza and G. Joos, "A Current Source Inverter fed Induction Motor Drive System with Reduced Losses," IEEE Trans. Ind. Appl., vol. 34, no. 4, pp. 796-805, Jul./Aug. 1998.
- [6] A.K. Pandey and S.M. Tripathi, "Determination of Regulator Parameters and Transient Analysis of Modified Self-commutating CSI-fed IM Drive", Journal of Electrical Engineering and Technology, Vol. 6, No. 1, pp. 48-58, January 2011.
- [7] A. K. Pandey, Pramod Agarwal and V. K. Verma, "Optimal Capacitor Selection for Modified Self- Commutated CSI-fed Induction Motor Drive" IEEE ISIE 2006, July 9-12Montreal, Quebec, Canada, pp. 1166-1171, 2006.
- [8] S.M. Tripathi and A.K. pandey, "Dynamic Performance Analysis of Self-commutating PWM CSI-fed Induction Motor Drive under MATLAB Environment", Asian Power Electronics Journal, Vol.5 No.1, Aug 2011.
- [9] S. M. Tripathi , A. K. Srivastava and A. K. Pandey , " A Novel Speed Controller Based on Lagrange's Interpolation for Closed-loop Control of a CSI-fed Induction Motor Drive".
- [10] Eid Al-radadi , " Direct Torque Neuro Fuzzy Speed Control Of An Induction Machine Drive Based On A New Variable Gain Pi Controller", Journal Of Electrical Engineering, Vol. 59, No. 4, 2008.
- [11] Milaudi and Draou," Speed control based on variable gain PI controller and rotor resistance estimation of an indirect vector controlled induction machine drive.
- [12] A. Miloudi, Al-Radadi , Y. Miloud , Draou," A New Variable Gain PI Controller Used For Direct Torque Neuro Fuzzy Speed Control Of Induction Machine Drive".

Iris Recognition

Suneelkumar kushwaha¹,Vikram singh²,kavish kumar³,Dr. R.K.singh⁴

Abstract -Iris recognition is the process of recognizing a person by analysing the random pattern of the iris, which is unique for each person. The iris is called the living password because of its unique, random features. It is always with you and cannot be stolen or faked. Iris recognition systems are being used today to control physical access, to facilitate identity verification and for computer authentication. Real-world iris recognition applications have been implemented for airport and prison security, automatic teller machines, authentication using single sign-on, to replace ID cards, and to secure schools and hospitals.

Keywords – Iris recognition, Iris localization, biometrics

I. INTRODUCTION

In today's information technology world, security for systems is becoming more and more important. The number of systems that have been compromised is ever increasing and authentication plays a major role as a first line of defence against intruders. The three main types of authentication are something you know (such as a password), something you have (such as a card or token), and something you are (biometric). Passwords are notorious for being weak and easily crackable due to human nature and our tendency to make passwords easy to remember or writing them down somewhere easily accessible. Cards and tokens can be presented by anyone and although the token or card is recognisable, there is no way of knowing if the person presenting the card is the actual owner. Biometrics, on the other hand, provides a secure method of authentication and identification, as they are difficult to replicate and steal. If biometrics is used in conjunction with something you know, then this achieves what is known as two-factor authentication. Two-factor authentication is much stronger as it requires both components before a user is able to access anything.

Iris recognition, a biometric, provides one of the most secure methods of authentication and identification thanks to the unique characteristics of the iris. Once the image of the iris has been captured using a standard camera, the authentication process, involving comparing the current subject's iris with the stored version, is one of the most accurate with very low false acceptance and rejection rates.

Suneel.er@gmail.com,vik081189@gmail.com,kavishkumar@gmail.com
Department of Electronics Knit sultanpur

This makes the technology very useful in areas such as information security, physical access security, ATMs and airport security.

The technology is accurate, easy to use, non-intrusive, difficult to forge, and despite what people may think, is actually quite a fast system once initial enrolment has taken place. However, it does require the co-operation of the subject, needs specific hardware and software to operate and administrators need to ensure they have a fallback plan should the resources required to operate the system fail, for example power. Iris recognition technology does provide a good method of authentication to replace the current methods of passwords, token cards or PINs and if used in conjunction with something the user knows in a two-factor authentication system then the authentication becomes even stronger.

HISTORY

- In 1936, ophthalmologist Frank Burch proposed the concept of using iris patterns as a method to recognize an individual.
- In 1985, Dr. Leonard Flom and Dr. AranSafir, [1] ophthalmologists, proposed the concept that no two irises are alike, and were awarded a patent for the iris identification concept
- In 1987, Dr. Flom approached Harvard Professor Dr. John Daugman to develop an algorithm to automate identification of the human iris.
- In 1993, the Defence Nuclear Agency began work to test and deliver a prototype unit, which was successfully completed by 1995 due to the combined efforts of Dr. Flom Dr. Safir, and Dr. Daugman.
- In 1994, Dr. Daugman [5] was awarded a patent for his automated iris recognition algorithms.

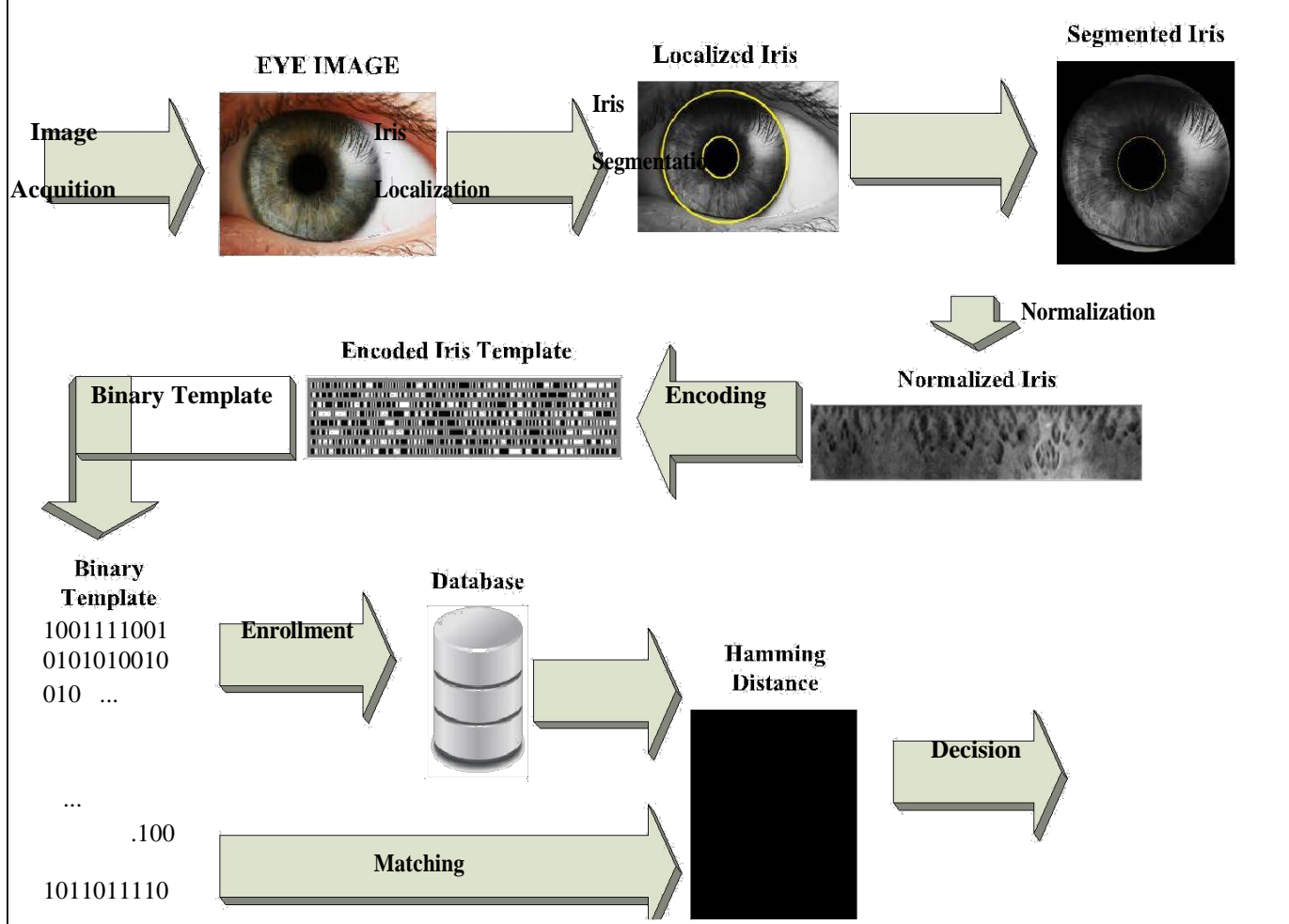
In 1995, the first commercial products became available.

- In 2005, the broad patent covering the basic concept of iris recognition expired, providing marketing opportunities for other companies that have developed their own algorithms for iris recognition.
- The patent on the Iris Codes implementation of iris recognition developed by Dr. Daugman expired in 2011.

III. STEPS IN IRIS RECOGNITION

The process Iris recognition consists of five steps:

- 1.Image Acquisition.
- 2.Iris localization and segmentation
- 3.Normalization
- 4.Feature extraction
- 5.Storing and Matching



Iris acquisition module can use visible light or near infrared light for acquisition

IV. IRIS IMAGE ACQUITION

The first step of iris recognition system is the acquisition of iris images using a special iris camera. The small size of the iris combined with the possibility of varying iris colours arises need of a special camera, especially for people with darker colour irises.

At the time of acquisition, the user has to stand in a range of 4-24 inches from the acquisition device and stare at the acquiring window with eyes widely open so that a clear iris image can be acquired.

V. IRIS LOCALIZATION

Localization and segmentation of iris from iris image should be automatic and reliable. Different methods are used to determine the inner boundary (pupil) and outer boundary (sclera) of iris



First J. Daugman [2] proposed to use an integro-differential operator for locating inner and outer boundaries of iris by using fallowing operator

$$\max_{(r, x_0, y_0)} |G_\sigma(r) * \frac{\partial}{\partial r} \oint_{r, x_0, y_0} \frac{I(x, y)}{2\pi r} ds|$$

Where $I(x, y)$ is an image containing an eye. The IDO searches over the image domain (x, y) for the maximum in the blurred partial derivative with respect to increasing radius r , of the normalized contour integral of $I(x, y)$ along a circular arc ds of radius r and centre coordinates (x_0, y_0) . The symbol $*$ denotes convolution and (\cdot) is a smoothing function such as a Gaussian of scale σ .

R.P Wildes [3] proposed to use edge detection to detect edges followed by circular Hough transform to localize iris boundaries. The Hough transform searches the optimum parameters of the following,

$$\max_{(r, x_0, y_0)} \sum_{j=1}^n h(x_j, y_j, x_0, y_0, r)$$

$$\text{Where } h(x_j, y_j, x_0, y_0, r) = \begin{cases} 1 & \text{if } g(x_j, y_j, x_0, y_0, r) \\ 0 & \text{otherwise} \end{cases}$$

$$\text{With } g(x_j, y_j, x_0, y_0, r) = (x_j - x_0)^2 + (y_j - y_0)^2 - r^2$$

For edge point (x_j, y_j) , $j=1, \dots, n$

VI. NORMALIZATION

After segmentation of iris region from eye image the next step is normalization. Normalization is the process of transforming segmented iris region into a fixed dimension to enable comparison.

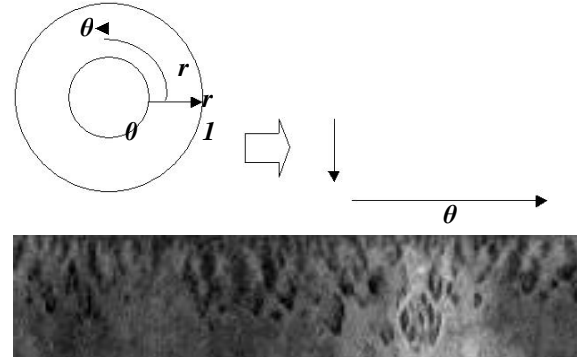
J. Daugman proposed daugman's rubber sheet model which projects the segmented iris disk into a rectangle region with fixed size using fallowing formula

$$\theta \in [0, 2\pi], r \in [0, 1], I(x(r, \theta), y(r, \theta)) \rightarrow I(r, \theta)$$

$$x(r, \theta) = (1 - r)x_p(\theta) + rx_i(\theta)$$

$$y(r, \theta) = (1 - r)y_p(\theta) + ry_i(\theta)$$

Where $I(x, y)$ is the iris region image, (x, y) and (r, θ) are the Cartesian and normalized polar coordinates respectively, and (x_p, y_p) and (x_i, y_i) are the coordinates of pupil and iris boundaries along θ direction



VII. FEATURE EXTRACTION

To enable accurate and efficient iris recognition the most discriminating information present in iris pattern must be extracted. Only significant feature of normalized iris pattern should be extracted so that comparison between templates can be made. Band pass decomposition of iris image is used in most iris recognition systems to create a biometric template.

Dr. J. Daugman used 2D Gabor filter for iris feature extraction.

A 2D Gabor filter is represented as

$$G(x, y) = e^{-\pi[x^2/\sigma_x^2 + y^2/\sigma_y^2]} e^{-\pi i[\mu x + \nu y]}$$

It is Gaussian modulated by oriented complex sinusoidal functions. Where σ_x and σ_y are the scale parameters of the Gaussian function, μ and ν are the frequency parameters of Gabor. The convolution of the normalized iris image with 2D Gabor filter results in complex valued coefficients.

Using Daugman's phase quantization method, the phase information of these coefficients are quantized into four levels, one for each possible quadrant in the complex plane. Thus to create the iris code that corresponds to iris features, each pixel in the normalized iris image produces two bits of data in the iris code.

The disadvantage of Gabor filter is that even symmetric filter will have a DC component. Log Gabor filter [9] has less limited bandwidth and zero dc component due to the algorithm operation. The 1D Log Gabor filter log-polar coordinate is

$$G(f) = \exp\left(\frac{-(\log(f/f_0))^2}{2(\log(\sigma/f_0))^2}\right)$$

Where f_0 represents the central frequency, σ is the bandwidth of the filter.

VIII. MATCHING

Matching is the last step in iris recognition system. Hamming distance (HD) between two iris codes is used to calculate the percentage of mismatched bits between a pair of iris codes. (0-100%)

$$HD = \frac{\text{No. of bits different}}{\text{Total no. of bits}} = \frac{1}{N} \sum_{j=1}^{j=N} A_j \oplus B_j$$

Where N is the number of bits in iris code

If HD < Separation Point Then the two irises are alike

The Hamming distance as matching metric is employed by J. Daugman.

IX. CONCLUSION

Based on the applications, reliability, ease of use, and software and hardware devices that currently support it, iris recognition technology has potential for widespread use. Iris recognition costs compare favourably with many other biometric products on the market today. Iris recognition is the most secure biometric technology available.

Iris recognition removes the need for physical contact with the biometric recording device and is recommended for both verification and identification. The algorithms developed for iris recognition have been well tested and perform well when implemented on today's computer hardware.

For ATMs at banks, iris recognition seems to be the perfect biometric. However, it will take longer to enrol customers using a biometric device than it does to simply assign and change a PIN. Since cards with PIN are already in use, it may be a while before any type of biometric device becomes prevalent in the banking industry. The beauty of iris recognition, however, is that it is non-intrusive and very secure, and it could eliminate the need for a card for ATM transactions. This could drastically reduce the effects of credit card theft because the cards would be useless at the ATM. Secure banking that relies on who you are rather than what you have would certainly be convenient. The increase in requirements for securing airports could drive up the use of biometric devices for transportation security. Since there were not many identification/verification systems in airports prior to September 11, 2001, the opportunity is ripe to install state-of-the-art identification systems for travellers. Iris recognition systems seem to fill that need well, and there is already evidence that the transportation industry recognizes

the usefulness of iris recognition. Terrorist activity increases the need for secure access to restricted areas, so there may also be increases in installation of biometric devices for building entry. In addition to its reliability, the lack of physical contact required for verification may make iris recognition more attractive to the general public than fingerprint or hand geometry biometric devices.

Iris recognition has made great strides in the last 5 years. It scores well compared to the other biometric technologies, both in ease of use and in reliability. Perhaps someday, iris recognition will be prevalent for many more applications.

X. REFERENCES

- [1] L. Flom and A. Safir, "Iris Recognition system", U.S. Patent No. 4641394, 1987.
- [2] J. Daugman, "High Confidence Visual Recognition of Persons by a Test of Statistical Independence," IEEE Trans. on Pattern Analysis and Machine Intelligence, vol. 15, no. 11, pp. 1148 – 1161, 1993.
- [3] R. P. Wildes, "Iris Recognition: An Emerging Biometric Technology," Proc. of the IEEE, vol. 85, no. 9, 1997, pp. 1348-1363.
- [4] J. Daugman, "How iris recognition works", Proceedings of International Conference on Image Processing, Vol. 1, 2002.
- [5] J. Daugman, United States Patent No. 5,291,560 (issued on March 1994). Biometric Personal Identification System Based on Iris Analysis, Washington DC: U.S. Government Printing Office, 1994.
- [6] Li Ma, Tieniu Tan, Yunhong Wang, Dexin Zhang, "Efficient Iris Recognition by Characterizing Key Local Variations", IEEE Transactions on Image processing, Vol. 13, June 2004, pp. 739-750.
- [7] Z. He, T. Tan, Z. Sun, and X. Qiu, "Towards accurate and fast iris segmentation for iris biometrics", IEEE Transactions on Pattern Analysis and Machine Intelligence, Vol. 31, No. 9, pp. 1670–1684, September 2009.
- [8] J. Daugman, "The Importance of Being Random: Statistical Principles of Iris Recognition," Pattern Recognition, vol. 36, no. 2, pp 279-291, 2011.
- [9] D. J. Field, "Relations between the statistics of natural images and the response properties of cortical cells," J. Opt. Soc. Am. A, vol. 4, no. 12, pp. 2379-2394, 1987.

Application of Artificial Intelligence Computational Techniques in DC and AC Drives

Bindeshwar Singh¹, Varun Kumar, ²Prakrati Azad³, Shubhendu Anand⁴ and Vijay Shankar⁵

¹

Abstract- This paper presents the application of artificial intelligence computational techniques in DC and AC drives such as DC series motors, DC shunt motors, DC compound motors, permanent magnet DC motors, single phase induction motors, three phase induction motors, three phase synchronous motors and other special purpose motors. This paper also presents the current status of AI techniques used in DC and AC drives. This article is very useful for researchers, scientific persons, and industrial persons for finding out relevant articles of application of artificial intelligence computational techniques in DC and AC drives.

Keywords: Artificial Intelligence computational techniques, AC Drives, DC Drives

NOMENCLATURES

| | |
|--------|---|
| AI | Artificial intelligence |
| FL | Fuzzy Logic |
| ANN | Artificial Neural Network |
| ABC | Artificial Bee Colony |
| GA-FNC | Genetic Algorithm-Fuzzy Neural Controller |
| AN-FIS | Adaptive Neuro-Fuzzy Inference System |
| HPSO | Hybrid Particle Swarm Optimization |
| PWM | Pulse Width Modulation |
| PM | Permanent Magnet |

I. INTRODUCTION

From last two decades the artificial intelligence techniques such as fuzzy logic, neural network and hybrid techniques are used for better enhancement of ac and dc drives performance parameter as compared to conventional controllers such as proportional, proportional-derivative, proportional-integral, and proportional-integral-derivative controllers.

The AC and DC drives performance parameters such as stator current, rotor current, torque, speed etc. These parameters are controlled by main controllers (hardware) and auxiliary controller (software). The basic role of auxiliary controllers is the fine adjustment of parameters whereas the main controllers used to control 90-95% of rated value of parameters.

^{&2}Asst. Professor, Department of Electrical Engineering, Kamla Nehru Institute of Technology (KNIT), Sultanpur-228118, U.P., India

^{2,3&4}M. Tech. (PE&D) Regular Student, Department of Electrical Engineering, Kamla Nehru Institute of Technology (KNIT), Sultanpur-228118, U.P., India

In this paper, various open literatures regarding with AI techniques and its applications in AC and DC drives are surveyed. The organization of this paper is as follows:
Section II discusses the fundamentals of AI techniques.
Section III discusses the survey of open literatures.

II. FUNDAMENTALS OF AI TECHNIQUES

Basically electric drives can be classified into two major types, on the basis of supply it is using for its operation, i.e. DC drives and AC drives. Explanation the application of artificial intelligence computational techniques such as Fuzzy Logic and Artificial Neural Network (ANN) to control the operation of DC and AC drives. As we can use AI Techniques in Control of Drives along with conventional Controllers like Proportional(P), Integral(I), Differential(D) and combination of all these controllers like PI, PD and PID. The modeling of various AI techniques in Drives as follow:

1. Fuzzy Logic Control[1]:

Fuzzy logic is a complex computational technique that allows getting solution of difficult simulated problems with multiple inputs and multiple output variables. Fuzzy logic gives results in the form of suggestion for a specific interval of output state, so this computational technique is different from more familiar logics like Boolean algebra.

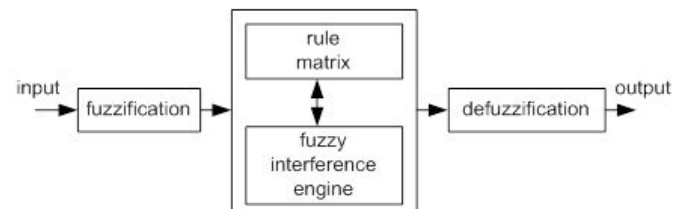


Fig. 1: Block Diagram of Fuzzy Logic Control

Fuzzy logic control has basically three stages i.e.

a. *Fuzzification:*

Fuzzy Set: A fuzzy set μ is a function from the reference set X to the unit interval, i.e.

$$\mu: X \rightarrow [0,1]$$

$\mu(X)$ represents the set of all fuzzy sets of X .

Membership Function: It is a graphical representation of fuzzy sets, $\mu_F(X)$

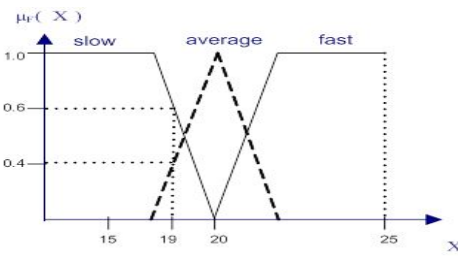


Fig. 2: Membership Function

Fuzzification Method:

First step of fuzzy logic control is to provide input parameters for given fuzzy system which act as a base for calculation of output. These parameters are fuzzified with use of pre-defined input membership functions, which can have different shapes. The mostly used shapes are: triangular shape, however bell, trapezoidal, sinusoidal and exponential. A simple membership function does not require complex computing and will not overload the implementation. The degree of membership function is determined by placing a chosen input variable on the horizontal axis, while vertical axis shows quantification of grade of membership of the input variable. The only condition a membership function must meet is that it must vary between zero and one. The value zero means that input variable is not a member of the fuzzy set, while the value one means that input variable is fully a member of the fuzzy set.

With each input parameter there is a unique membership function associated. The membership functions associate a weighting factor with values of each input and the effective rules. These weighting factors determine the degree of influence or degree of membership (DOM) each active rule has. By computing the logical product of the membership weights for each active rule, a set of fuzzy output response magnitudes are produced. All that remains is to combine and defuzzify these output responses.

b. Rule Matrix and Fuzzy Inference Engine:

Rule Matrix

The rule matrix is used to describe fuzzy sets and fuzzy operators in form of conditional statements. A single fuzzy if-then rule can be as follows

If x is A then y is Z,

Where A is a set of conditions that have to be satisfied and Z is a set of consequences that can be inferred.

In rule with multiple parts, fuzzy operators are used to combine more than one input: AND = min, OR = max and NOT = additive complement. Geometrical demonstration of fuzzy operators is shown in Figure 4.

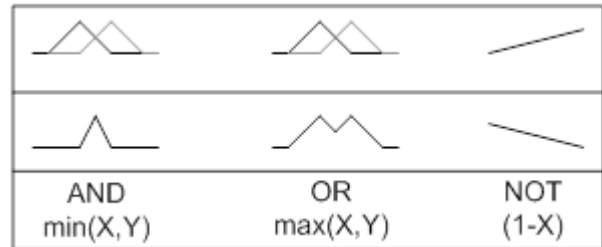


Fig. 3 Graphical interpretation of fuzzy operators

The rule matrix is a simple graphical tool for mapping the fuzzy logic control system rules. It accommodates two or more input variables and expresses their logical product (AND or OR) as one output response variable. The degree of membership for rule matrix output can take value of maximum, minimum of the degree of previous of the rule [1]. It is often probable, that after evaluation of all the rules applicable to the input, we get more than one value for the degree of membership. In this case, the simulation has to take into consideration, all three possibilities, the minimum, the maximum or an average of the membership-degrees.

Inference Mechanisms

Inference mechanism allows mapping given input to an output using fuzzy logic. It uses all pieces described in previous sections: membership functions, logical operations and if-then rules. The most common types of inference systems are Mamdani and Sugeno. They vary in ways of determining outputs.

c. Defuzzification Mechanisms:

Defuzzification task is to find one single crisp value that summarizes the fuzzy set. There are several mathematical techniques available: centroid, bisector, mean, maximum, maximum and weighted average. Figure demonstrates illustration of how values for each method are chosen.

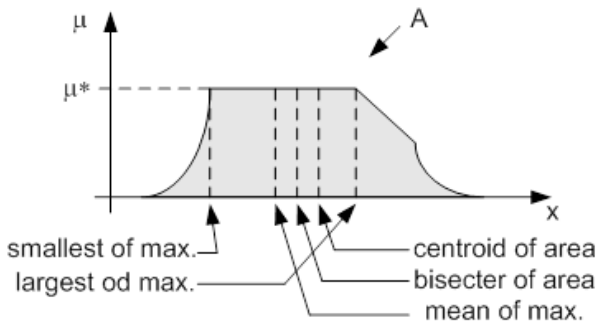


Fig. 4: Graphical demonstration of defuzzification methods

Centroid defuzzification is the most commonly used method, as it is very accurate. It provides centre of the area under the curve of membership function. For complex membership functions it puts high demands on computation. It can be expressed by the following formula

$$z_0 = \frac{\int \mu_i(x) \cdot x dx}{\int \mu_i(x) dx}$$

where z_0 is defuzzified output, μ_i is a membership function and x is output variable.

Bisector defuzzification uses vertical line that divides area under the curve into two equal areas.

$$\int_{\alpha}^z \mu_A(x) dx = \int_z^{\beta} \mu_A(x) dx$$

Mean of maximum defuzzification method uses the average value of the aggregated membership function outputs.

$$z_0 = \frac{\int x dx}{\int dx'}$$

Where $x' = \{x; \mu_A(x) = \mu^*\}$.

Smallest of maximum defuzzification method uses the minimum value of the aggregated membership function outputs.

$$z_0 \in \{x | \mu(x) = \min \mu(\omega)\}$$

Largest of maximum defuzzification method uses the maximum value of the aggregated membership function outputs.

$$z_0 \in \{x | \mu(x) = \max \mu(\omega)\}$$

Weighted average defuzzification method, based on peak value of each fuzzy set, calculates weighted sum of these peak values [4]. According to these weight values and the degree of membership for fuzzy output, the crisp value of output is determined by the following formula

$$z_0 = \frac{\sum \mu(x)_i \times W_i}{\sum \mu(x)_i}$$

Where μ_i is the degree of membership in output singleton i , W_i and is the fuzzy output weight value for the output singleton i .

The block diagram of DC drives using fuzzy logic controller [2] is as shown below:

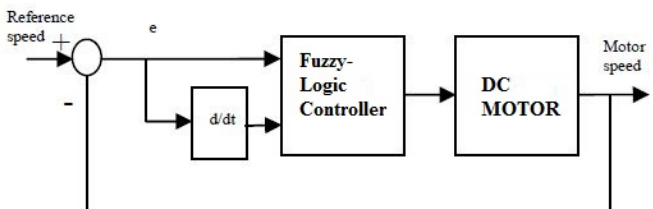


Fig. 5 Block diagram of fuzzy logic controlled DC motor

1. **Artificial Neural Network:** Artificial neural network is computational technique based on human central nervous systems (in human brain) which enables human being for machine learning and pattern recognition. This is a system with interconnected "neurons" that can calculate values from inputs by retrieving information by the network of neurons. In an artificial neural network, simple artificial nodes, called "neurons", "processing elements" or "units", are connected together to form a network which mimics a biological neural network.

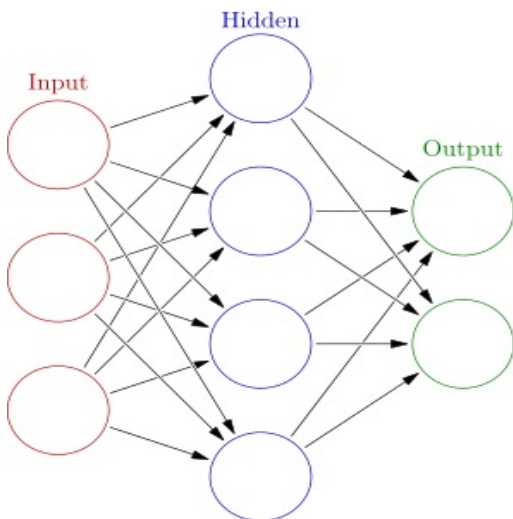


Fig. 6: Basic mechanism of Neural Network

The output of a neuron is a function of the weighted sum of the inputs plus a bias. In following diagram i is input, w is weight factor and output is a function of i and w.

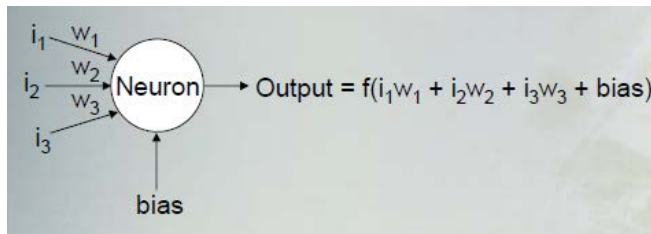


Fig. 7 Basic function of Neural Network

III. A LITRATURE SURVAY

A. DC Drives

1. DC series Motors

a. Fuzzy logic:

SatyaSheel, *et al.* [3], has been proposed high performance fuzzy adaptive PID Speed Control of a converter driven DC motor, A.K.Pal, *et al.* [4] has proposed speed control of dc motor using relay feedback tuned PI, fuzzy PI and self-tuned fuzzy PI controller.InoueKet *et al.*, [5] has explained advanced auto tuning implementation for DC brushless servo motor drive system with learning algorithm-based fuzzy reasoning scheme.

b. Artificial Neural Network

PavelBrandstetter, *et al.* [6], has explained applications of artificial neural network in control of DC drives.MinkovaM.,*et al.* [7], has suggested current limitation in the adaptive neural speed control of a DC motor. El-

SharkawiM.A.,*et al.* [8], has proposed identification and control of a DC motor using back-propagation neural networks. Weerasooriya, *et al.* [9], has suggested laboratory implementation of a neural network trajectory controller for a DC motor. Rubaai, *et al.* [10], has explained online identification and control of a DC motor using learning adaptation of neural networks. Zilong Liu, *et al.* [11], has proposed speed control of a DC motor using BP neural networks.AmitAtri, *et al.* [12], has proposed speed control of DC Motor using neural network configuration. Cirrincione, *et al.* [13] has suggested the control and diagnosis of electrical drives: some applications by using neural networks.

c. Artificial Bee Colony

Akhilesh Kumar Mishra, *et al.*[14], has proposed speed control of DC motors using Artificial Bee Colony Optimization technique.

d. Hybrid

Yang Hui,*et al.*[15], has proposed adaptive double-Loop PID control method of DC motor based on the GA-FNC algorithm.Kukolj,D., *et al.*[16], has proposed artificial intelligence based gain scheduling of PI speed controller in DC motor drive.

2. DC shunt Motors

a. Fuzzy logic

HailongSong,*et al.* [17], has proposed a hybrid adaptive fuzzy variable structure speed controller for brushless DC motor.Jong-baeLee,*et al.*[18], has proposed a low cost speed control system of brushless DC motor using fuzzy logic.Donescu, *et al.*[19], has proposed a systematic design method for fuzzy logic speed controller for brushless DC motor drives. Niasar,*et al.* [20], has proposed ANFIS-Based Controller with Fuzzy Supervisory Learning for Speed Control of 4-Switch Inverter Brushless DC Motor Drive.Tiwary.N, *et al.* [21], has proposed design of Hybrid Fuzzy-PI controller for speed control of Brushless DC motor.Shanmugasundram R., *et al.* [22] has proposed digital implementation of fuzzy logic controller for wide range speed control of brushless DC motor.Sharifian,*et al.*[23] has proposed direct torque control of brushless DC motor drives based on ANFIS controller with fuzzy supervisory learning.Rahmani,*et al.*[24] has proposed fuzzy logic controller optimized by particle swarm optimization for DC motor speed controlTipsuwan,*et al.*[25] has proposedfuzzy logic microcontroller implementation for DC motor speed control

b. Artificial Neural Network

Tipsuwanporn, *et al.*[26], has proposed identification and control of brushless DC motors using on-line trained artificial neural networks.

3. PMDC motors

a. Artificial Neural Network

Khan, M.A., *et al.*[27], has proposed a novel wavelet neural network based robust control of interior permanent magnet motor drives.Hoque M.A., *et al.* [28], has explained artificial neural network based permanent magnet DC motor drives.

b. Hybrid

El-Khouly, *et al.* [29], has proposed Artificial intelligent speed control strategies for permanent magnet DC motor drives. Adel A.A., *et al.* [30], has suggested a hybrid PV-FC-diesel- battery efficient Schemes for four-wheel PMDC Electric Vehicle drive system.

B. AC Drives

1. Single phase Induction Motors

a. Fuzzy logic

GengDayon,*et al.* [31], has discussed modeling and simulating for soft starting of asynchronous motors based on fuzzy adaptive control. Ta-Cao, M,*et al.* [32], has discussed model reference adaptive fuzzy controller and fuzzy estimator for high performance induction motor drive.

b. Artificial Neural Network

Tiago Henrique dos Santos,*et al.* [33], has discussed scalar control of an induction motor using a neural sensorless technique.

c. Hybrid

SollyAryza,*et al.* [34], has discussed a fast Induction Motor speed estimation based on Hybrid Particle Swarm Optimization (HPSO).KenzaBouhoune, *et al.* [35], has discussed Hybrid control of single phase induction machine without capacitor using artificial intelligence technique.

2. Three Phase Induction Motors

a. Fuzzy logic

Ashok Kusagur, *et al.* [36], has discussed AI based design of a fuzzy logic scheme for speed control of induction motors using SVPWM technique.Jagadish H. Pujar,*et al.* [37], has proposed AI based direct torque Fuzzy control of AC

drives.RameshTejavathuet *et al.* [38] has proposed Artificial intelligence based high performance direct torque and flux control of induction motor drive.ShahramJavadet *et al.* [39] has explained Induction Motor Drive Using Fuzzy Logic. RohitGupta,*et al.* [40], has presented the Intelligent Induction Motor Drive.DebirupeHore [41]has explained Fuzzy logic based advance speed control of Induction motor.Guven,*et al.* [42], has discussed a high performance adaptive parallel distributed compensator for induction machine drives.BrahimMetidji,*et al.*[43] has explained a New Fuzzy Direct Torque Control Strategy for Induction Machine Based on Indirect Matrix Converter.Purwanto,*et al.* [44], has explainedSimulation of the application fuzzy logic controller in 3 phase induction motor speed control by selecting membership function parameter.

b. Artificial Neural Network

Mohamadian M., *et al.* [45], has addressed a novel neural network controller and its efficient DSP implementation for vector-controlled induction motor drives.Ms. ChinkiChandhok, *et al.* [46], has suggested Speed Estimation of A.C. Drive by Artificial Neural Networks (ANN).Tien-Chi Chenet *et al.* [47] model reference neural network controller for induction motor speed control.D.K. Bhattacharyya, *et al.* [48], has proposed stepless PWM speed control of AC motors: A neural network approach.Kulawski, *et al.* [49], has proposed adaptive control of non-linear plants using neural networks-application to a flux control in AC drive system.

c. Hybrid

C.Thanga Raj, *et al.* [50], has explained the energy efficient control of three phase induction motor.Uddin, *et al.* [51], has proposed development and Implementation of a Simplified Self-Tuned Neuro-Fuzzy-Based IM Drive.Sarat Kumar Sahoo, *et al.* [52], has suggested salient features of vector control in AC motor drives.ArfatSiddique, *et al.* [53], has suggested the applications of Artificial Intelligence Techniques for Induction Machine Stator Fault Diagnostics.Jalili K., *et al.* [54], has suggestedsensorless vector control of induction motors in fuel cell vehicle using a neuro-fuzzy speed controller and an online artificial neural network speed estimator.AiWu.,*et al.* [55], has suggested an adaptive speed control for induction motor drive using fuzzy neural network based on fuzzy hierarchy error approach.

3. Three phase synchronous motors

a. Fuzzy logic

Parasiliti, *et al.*[56] had discussed Adaptive fuzzy logic control for high performance PM synchronous drive.

b. Artificial Neural Network

Der-FaChenand,*et al.*[57] had discussed the implementation of a novel matrix converter PMSM drive.Won-SikBaik, *et al.*[58],had discussed an optimal efficiency control of reluctance synchronous motor using neural network with direct torque control.SalehKh.,*et al.* [59]had discussed analysis of controlled permanent magnet synchronous motor using artificial neural network.Senjuu, *et al.* [60], had discussed high efficiency drives for synchronous reluctance motors using neural network.Urasaki, N., *et al.* [61], had discussed, neural network based high efficiency drive for interior permanent magnet synchronous motors compensating EMF constant variation.Lim, *et al.* [62] had discussed novel flux linkage control of switched reluctance motor drives using observer and neural network-based correction methods.Al-Taee, *et al.* [63], had discussed real-time efficiency optimization of open-loop controlled synchronous PM motor drive using adaptive neural networks. Campos J.,

et al. [64], had discussed synchronous motor VSS control using recurrent high order neural network.

c. Hybrid

Faa-Jeng Lin, *et al.* [65] had discussed a linear synchronous motor drive using robust fuzzy neural network control.XianqingCao,*et al.* [66] had discussed a novel implementation of neural network and multi-fuzzy controllers for permanent magnet Synchronous motor direct torque controlled drive. GuoZhi-rong,*et al.* [67], had discussed automatic generation: fuzzy neural network speed controller for permanent-magnet synchronous motor drive.GaoWei,*et al.* [68], had discussed sliding mode speed controller for PM synchronous motor drive using dynamic fuzzy neural network.XianqingCao, *et al.* [69], had discussed vector controlled permanent magnet Synchronous motor drive based on neural network and multi fuzzy controllers.

The summary of literature reviewed regarding Application of Artificial Intelligence computational techniques in AC and DC Drives.

IV. Summary of Literature Reviewed for Application of Artificial Intelligence Techniques in AC and DC Drives

| Reference | Drives | AI Techniques | Performance Parameters of Drives |
|---|------------------|---------------------------|---|
| [3]SatyaSheel and Omhari Gupta [4] A.K.Pal and R.K.Mudi, [5]Inoue,K., Yoshitsugu, J.,Shirogane, S and Nakaoka M | DC series Motors | Fuzzy logic control | High performance fuzzy adaptive PID Speed Control of a Converter Driven DC Motor [3] . Speed control of dc motor using relay feedback tuned PI fuzzy PI and self-tuned fuzzy PI controller[4] Advanced auto tuning implementation for DC brushless servo motor drive system with learning algorithm-based fuzzy reasoning scheme.[5]. |
| [6] PavelBrandstetter and PavelBilek [7]Minkova,M.,Minkov, D., Rodgerson, J.L. and Harley, R.G. [8]El-Sharkawi, M.A. and Weerasooriya, Siri, [9]Weerasooriya, Siri and El-Sharkawi, M.A., [10]Rubai, A and Kotaru, R. [11]Zilong Liu, XianyiZhuang and Shuyi Wang [12]AmitAtri and Md. Ilyas [13]Cirrincione | DC series Motors | Artificial Neural Network | Applications of artificial neural network in control of DC drives[6], Current limitation in the adaptive neural speed control of a DC motor,[7] Identification and control of a DC motor using back-propagation neural networks , [8] Laboratory implementation of a neural network trajectory controller for a DC motor[9], Online identification and control of a DC motor using learning adaptation of neural networks[10], Speed control of a DC motor using BP neural networks[11], Speed Control of DC Motor using Neural Network Configuration[12], Control and diagnosis of electrical drives: some applications by using neural networks [13]. |
| [14]Akhilesh Kumar Mishra,AnukaranKhanna ,Navin Kumar Singh and VivekK.Mishra | DC series Motors | Artificial Bee Colony | Speed control of DC motors using Artificial Bee Colony Optimization technique[14] |
| [15]Yang Hui, [16]Kukolj, D. | DC series Motors | Hybrid | Adaptive double-Loop PID control method of DC motor based on the GA-FNC algorithm[15], Artificial intelligence based gain scheduling of PI speed controller in DC motor drives[16], |
| [17]HailongSong,Yong Yu , Ming Yang and Dianguo X [18] Jong-baeLee,Tae-Bin Im ,Ha-Kyong and Sung Young-Ouk Kim [19] Donescu, V, Neacsu, D.O.,Griva, G.andProfumo, F [20] Niasar, A.H.Vahedi, A.and Moghbelli, H [21] Tiwary, N, Rathinam, A and Ajitha, [22] Shammuganandram, R ,Zakariah K.M and Yadaiah, N [23]Sharifian, M.B.B.Shafiei, M.Sadeghi, M.S.andGolestaneh, F [24]Rahmani, R., Mahmodian, M.S.,Mekhilef, S. and Shojaei, A.A [25] Tipsuwan, Y.and Mo-Yuen Chow | DC shunt Motors | Fuzzy logic | A hybrid adaptive fuzzy variable structure speed controller for brushless DC motor[17] A low cost speed control system of brushless DC motor using fuzzy logic[18] A systematic design method for fuzzy logic speed controller for brushless DC motor drives[19] ANFIS-Based Controller with Fuzzy Supervisory Learning for Speed Control of 4-Switch Inverter Brushless DC Motor Drive[20], Design of Hybrid Fuzzy-PI controller for speed control of Brushless DC motor[21] Digital implementation of fuzzy logic controller for wide range speed control of brushless DC motor[22] Direct torque control of brushless DC motor drives based on ANFIS controller with fuzzy supervisory learning[23] Fuzzy logic controller optimized by particle swarm optimization for DC motor speed control[24] Fuzzy logic microcontroller implementation for DC motor speed control[25] |
| | DC shunt Motors | Fuzzy logic | |

| | | | |
|---|--------------------------------|---------------------------|---|
| [26]Tipsuwanporn, V,Piyarat, W and Tarasantisuk, C | DC shunt Motors | Artificial Neural Network | Identification and control of brushless DC motors using on-line trained artificial neural networks[26] |
| [27] Khan, M.A., Uddin, M.N. and Aziz Rahman, M | PMDC motors | Artificial Neural Network | A novel wavelet neural network based robust control of interior permanent magnet motor drives[27] |
| [28] Hoque, M.A.Zaman, M.R.and Rahman, M.A. | | | Artificial neural network based permanent magnet DC motor drives[28] |
| [29]El-Khouly, F.M,AbdelGhaffar, A.S., Mohammed, A.A. and Sharaf, A.M. | PMDC motors | Hybrid | Artificial intelligent speed control strategies for permanent magnet DC motor drives[29], A hybrid PV-FC-diesel- battery efficient Schemes for four-wheel PMDC Electric Vehicle drive system[30], |
| [30]Adel A.A. El-Gammal and Adel M.Shraf, | | | |
| [31]GengDayongandMaWenge | Single phase Induction Motors | Fuzzy logic | Modeling and Simulating for Soft Starting of Asynchronous Motors Based on Fuzzy Adaptive Control[31] |
| [32]Ta-Cao, M. and Hoang Le-Huy | Single phase Induction Motors | Artificial Neural Network | Model reference adaptive fuzzy controller and fuzzy estimator for high performance induction motor drives[32] |
| [33]Tiago Henrique dos Santos, Alessandro Goedtel, Sergio Augusto Oliveira da SilvaandMarceloSuetake, | | | Scalar control of an induction motor using a neural sensorless technique[33] |
| [34]SollyAryza, Ahmed N Abdallah, Zulkeflee bin Khalidin, ZulkarnainLubis and Ma Jie | Single phase Induction Motors | Hybrid | A fast Induction Motor speed estimation based on Hybrid Particle Swarm Optimization (HPSO)[34], Hybrid control of single phase induction machine without capacitor using artificial intelligence techniques[35] |
| [35]KenzaBouhoune, KrimYazid and Mohamed SeghirBoucherit | | | |
| [36]Ashok Kisagur, Dr. S. F. Kodad,Dr. B V. Sankar Ram | Three Phase Induction Motors | Fuzzy logic | AI based design of a fuzzy logic scheme for speed control of induction motors using SVPWM technique[36],AI based Direct Torque FuzzyControl of AC Drives[37], |
| [37]Jagadish H. Pujar and S.F. Kodad, | | | Artificial intelligence based high performance direct torque and flux control of induction motor drives[38], |
| [38]Ramesh, Tejavathu,Panda, A.K. ; Bonala, Sathyam | | | Induction Motor Drive Using Fuzzy Logic[39], Intelligent Induction Motor Drive[40], |
| [39]ShahramAvadi | | | Fuzzy logic based advance speed control of Induction motor[41], |
| [40]Rohit Gupta and Ruchika | | | A high performance adaptive parallel distributed compensator for induction machine drives[42], |
| [41]DebirupeHore | | | A New Fuzzy Direct Torque Control Strategy for InductionMachine Based on Indirect Matrix Converter[43],Simulation of the application fuzzy logic controller in 3 phase induction motor speed control by selecting membership function parameter[44] |
| [42]Guven, M.K.Rehman, H.,Yu, L. and Derdiyok, A. | | | |
| [43]BrahimMetidji, FaridTazrart, Ahmed Azib, Nabil Taib, and ToufikRekioua | | | |
| [44]Purwanto, E,Daniel, M.W.,Harianto and Prabowo, G | | | |
| [45]Mohamadian, M. Nowicki, E. Ashrafpour, F. Chu, A. Sachdeva, R. and Evanik, E | Three Phase Induction Motors | Artificial Neural Network | A novel neural network controller and its efficient DSP implementation for vector-controlled induction motor drives[45]. |
| [46]Ms. ChinkiTChandhok | | | Speed Estimation of A.C. Drive by Artificial Neural Networks (ANN)[46], |
| [47]Tien-Chi Chen and Tsong-TengSheu | | | Model reference neural network controller for induction motor speed control[47], Stepless PWM speed control of AC motors:A neural network approach[48], |
| [48] D.K. Bhattacharyya and Amit Kumar Ray | | | Adaptive control of non-linear plants using neural networks-application to a flux control in AC drive system [49] |
| [49]Kulawski, G.J. andBrdys, M.A | | | |
| [50]C.Thanga Raj | | | Energy efficient control of three phase induction motor.[50] |
| [51]Uddin, M.N | | | Development and Implementation of a Simplified Self-Tuned Neuro-Fuzzy-Based IM Drive[51] |
| [52]Sarat Kumar Sahoo | | | Salient features of vector control in AC motor drives: A review[52] |
| [53]ArfatSiddique | | | Applications of Artificial Intelligence Techniques for Induction Machine Stator Fault Diagnostics: Review[53] |
| [54]Jalili, K.,Farhangi, S and Saievar-Iranizad, E | | | Sensorless vector control of induction motors in fuel cell vehicle using a neuro-fuzzy speed controller and an online artificial neural network speed estimator[54] |
| [55]Ai Wu and Tam, P.K.S | | | An adaptive speed control for induction motor drive using fuzzy neural network based on fuzzy hierarchy error approach[55], |
| [56]Parasiliti, F,Tursini, M andZhang, D.Q | Three Phase Synchronous Motors | Fuzzy logic | Adaptive fuzzy logic control for high performance PM synchronous drive[56]. |
| [57]Der-FaChenand | | | Implementation of a novel matrix converter PMSM drive[57]. |
| [58]Won-SikBaik, Min-Huei Kim, Nam-Hun Kim, Dong-Hee Kim, Kyeong-Ho Choi and Don-Ha Hwang | Three Phase Synchronous Motors | Artificial Neural Network | An optimal efficiency control of reluctance synchronous motor using neural network with direct torque control [58]. |
| [59]Saleh,Kh.Badr, M.A.,Elwer, A.S. and Wahsh, S | | | Analysis of controlled permanent magnet synchronous motor using artificial neural network[59]. |
| [60]Senjuu, T.,Shingaki, T.,Omoda, A. and Uezato, K] | | | High efficiency drives for synchronous reluctance motors using neural network[60]. |
| [61]Urasaki, N, Senjuu, T and Uezato, K | | | Neural network based high efficiency drive for interior permanent magnet synchronous motors compensating EMF constant variation[61]. |
| [62]Lim, H.S Roberson,D.G.Lobo, N.S and Krishnan, R | | | Novel flux linkage control of switched reluctance motor drives using observer and neural network-based correction methods[62]. |
| [63]Al-Taee, M.A.Al-Din, M.S andAl'zubi, H.S, | | | Real-time efficiency optimisation of open-loop controlled synchronous PM motor drive using Adaptive Neural Networks[63]. |
| [64]Campos, J. Loukianov, Alexander G.and Sanchez, Edgar N | | | Synchronous motor VSS control using recurrent high order neural networks[64]. |
| [65]Faa-Jeng Lin and Po-Hung Shen | Three Phase Synchronous Motors | Hybrid | A linear synchronous motor drive using robust fuzzy neural network control[65] |
| [66]Xianqing Cao and Liping Fan | | | A Novel Implementation of Neural Network and Multi-Fuzzy Controllers for Permanent Magnet Synchronous Motor Direct Torque Controlled Drive[66] |
| [67]GuoZhi-rong, Gao Wei and Xie Shun-yi | | | Automatic Generation:Fuzzy Neural Network Speed Controller for Permanent-Magnet Synchronous Motor Drive[67] |
| [68]Gao Wei and Mao Wei | | | Sliding mode speed controller for PM synchronous motor drive using dynamic fuzzy neural network[68] |
| [69]Xianqing Cao and Liping | | | Vector Controlled Permanent Magnet Synchronous Motor Drive Based on Neural Network and Multi Fuzzy Controllers[69] |

| | | | |
|-----|--|--|--|
| Fan | | | |
|-----|--|--|--|

V. CONCLUSION

This paper presents the application of artificial intelligence computational techniques in DC and AC drives such as DC series motors, DC shunt motors, DC compound motors, permanent magnet DC motors, single phase induction motors, three phase induction motors, three phase synchronous motors and other special purpose motors. Presently the maximum research work carryout from application of hybrid techniques in DC and AC drives.

VI. ACKNOWLEDGMENT

The authors would like to thanks Dr. K.S. Verma, Dr. R.P.Payasi, and Dr. D Singh, Kamala Nehru Institute of Technology, Sultanpur, for their valubles suggestions regarding application of artificial intelligence computational techniques in DC and AC drives

VII. REFERENCES

- [1] E. Kozlowska, "Basic principles of fuzzy logic", available at: <http://access.feld.cvut.cz/view.php?cisloclanku=2012080002>.
- [2] Ross T.J., HASSANEIN H., ALI A.N.; Fuzzy logic with engineering applications: design and stability analysis. 3rd ed. Chichester (RoyaumeUni): Wiley, 2010, xxvii, 275 p. ISBN 978-047-0748-510.
- [3] SatyaSheel and OmhariGupta,"High performance fuzzy adaptive PID Speed Control of a Converter Driven DC Motor", *International Journal of Control and Automation*, vol.5 no.1, , March 2012,pp.71-88.
- [4] A.K.Pal and R.K.Mudi, "Speed control of dc motor using relay feedback tuned PI,fuzzy PI and self-tuned fuzzy PI controller", *Control Theory and Informatics*, Vol 2, No.1, 2012, pp. 24-32.
- [5] Inoue,K.,Yoshitsugu, J.,Shirogane. S and Nakaoka M, "Advanced auto tuning implementation for DC brushless servo motor drive system with learning algorithm-based fuzzy reasoning scheme", *1997 International Conference onPower Electronics and Drive Systems*, 1997. Proceedings.,Volume:1,26-29 May 1997 pp.302 – 308.
- [6] PavelBrandstetter and PavelBilek, "Applications of artificial nueral network in control of DC drives", *Advances in Intelligent Systems and Computing* Volume 189, 2013, PP 351-360.
- [7] Minkova, M., Minkov, D, Rodgerson, J.L and Harley, R.G., "Current limitation in the adaptive neural speed control of a DC motor", *AFRICON, 1996., IEEE AFRICON 4th*,Volume 2 ,24-27 Sep 1996, pp..837 – 842.
- [8] El-Sharkawi, M.A.andWeerasooriya, Siri, "Identification and control of a DC motor using back-propagation neural networks", *Energy Conversion, IEEE Transactions on* Volume 6 , Dec 1991,pp.663 – 669.
- [9] Weerasooriya, Siri and El-Sharkawi, M.A., "Laboratory implementation of a neural network trajectory controller for a DC motor", *IEEE Transactions on Energy Conversion* ,Volume:8 , Mar 1993, pp.107 – 113.
- [10] Rubaai, A and Kotaru, R."Online identification and control of a DC motor using learning adaptation of neural networks", *Industry Applications, IEEE Transactions on* Volume 36 May/Jun 2000, pp. 935 – 942.
- [11] Zilong Liu, XianyiZhuang and Shuyi Wang, "Speed control of a DC motor using BP neural networks" *Control Applications, 2003. CCA 2003. Proceedings of 2003 IEEE Conference on* Volume 2 June 2003 pp..832 – 835.
- [12] AmitAtri and Md. Ilyas, "Speed Control of DC Motor using Neural Network Configuration", *International Journal of Advanced Research in Computer Science and Software Engineering*, Volume 2 , May 2012, pp. 209-212.
- [13] Cirrincione,"Control and diagnosis of electrical drives: some applications by using neural networks", *Proceedings, IEEE International Joint Symposia on Intelligence and Systems*, May 1998 pp..210 – 217.
- [14] Akhilesh Kumar Mishra,AnukaranKhanna,Navin Kumar Singh and VivekKMishra, "Speed control of DC motors using Artificial Bee ColonyOptomization technique", *Universal Journal of Electrical and Electronic Engineering* 1(3),2013, pp. 68-75.
- [15] Yang Hui,"Adaptive double-Loop PID control method of DC motor based on the GA-FNC algorithm", *Instrumentation and Control Technology (ISICT)*, 11-13 July 2012 pp324 - 329.
- [16] Kukolj, D., "Artificial intelligence based gain scheduling of PI speed controller in DC motor drives", *Industrial Electronics, 1999. ISIE '99. Proceedings of the IEEE International Symposium on* Volume:1,1999,pp.425– 429.
- [17] Hailong Song ,Yong Yu ,Ming Yang and DianguoXu, "A hybrid adaptive fuzzy variable structure speed controller for brushless DC motor", *IECON 02 [Industrial Electronics Society, IEEE 2002 28th Annual Conference of the Volume 3*, Nov. 2002,pp.2126 – 2130.
- [18] Jong-bae Lee ,Tae-Bin Im ,Ha-Kyong Sung and Young-Ouk Kim, "A low cost speed control system of brushless DC motor using fuzzy logic", *Information, Decision and Control, 1999.IDC 99.Proceedings*. 1999,pp. 433 – 437.
- [19] Donescu, V. Neacsu, D.O.,Griva, G. and Profumo, F, "A systematic design method for fuzzy logic speed controller for brushless DC motor drives", *Power Electronics Specialists Conference, 1996. PESC '96 Record., 27th Annual IEEE Volume 1*, Jun 1996,pp. 689 – 694.
- [20] Niasar, A.H., Vahedi, A. and Moghbelli, H, "ANFIS-Based Controller with Fuzzy Supervisory Learning for Speed Control of 4-Switch Inverter Brushless DC Motor Drive", *Power Electronics Specialists Conference, 2006.PESC '06. 37th IEEE*. June 2006,pp. 1 – 5.
- [21] Tiwary, N.,Rathinam, A. and Ajitha, S,"Design of Hybrid Fuzzy-PI controller for speed control of Brushless DC motor", *Electronics, Communication and Instrumentation (ICECI), 2014 International Conference on*, Jan. 201,pp. 1 – 4.
- [22] Shanmugasundram .R,Zakariah, K.M. and Yadaiah, N. "Digital implementation of fuzzy logic controller for wide range speed control of brushless DC motor", *Vehicular Electronics and Safety (ICVES), 2009 IEEE International Conference on*, Nov. 2009,pp.119 – 124.
- [23] Sharifian, M.B.B, Shafiei, M , Sadeghi, M.S and Golestaneh, F. "Direct torque control of brushless DC motor drives based on ANFIS controller with fuzzy supervisory learning", *Electrical Machines and Systems (ICEMS), 2011 International Conference on*, Aug. 2011,pp.1 – 6.
- [24] Rahmani, R ,Mahmodian, M.S., Mekhilef, S.andShojaei, A.A, "Fuzzy logic controller optimized by particle swarm optimization for DC motor speed control", *Research and Development (SCOReD), 2012 IEEE Student Conference on*, Dec. 2012,pp. 109 – 113.
- [25] Tipsuwan, Y and Mo-Yuen Chow, "Fuzzy logic microcontroller implementation for DC motor speed control", *Industrial Electronics Society, 1999.IECON '99 Proceedings. The 25th Annual Conference of the IEEE* Volume31999,pp. 1271 – 1276.
- [26] Tipsuwanporn, V. ,Piyarat, W. and Tarasantisuk, C, "Identification and control of brushless DC motors using on-line trained artificial neural networks", *Power Conversion Conference, 2002.PCC-Osaka 2002. Proceedings of the Volume3*, 2002,pp.1290-1294.
- [27] Khan, M.A. Uddin, M.N. and Aziz Rahman, M, "A novel wavelet neural network based robust control of interior permanent magnet motor drives", *Industry Applications Society Annual Meeting (IAS), 2011 IEEE*,9-13 Oct. 2011.
- [28] Hoque, M.A.Zaman, M.R.and Rahman, M.A. "Artificial neural network based permanent magnet DC motor drives" *Industry*

- Applications Conference, 1995. Thirtieth IAS Annual Meeting, IAS '95, Conference Record of the 1995 IEEE ,Volume:1, Oct 1995 pp. 98 – 103.*
- [29] El-Khouly, F.M,AbdelGhaffar, A.S., Mohammed, A.A. and Sharaf, A.M.“Artificial intelligent speed control strategies for permanent magnet DC motor drives”, *1994., Conference Record of the Industry Applications Society Annual Meeting 1994 IEEE, , volume 1,2-6 Oct 1994,pp.379 – 385.*
- [30] Adel A.A. El-Gammal and Adel M.Sharaf, “A hybrid PV-FC-diesel-battery efficient Schemes for four-wheel PMDC Electric Vehicle drive system”,*2012, International Journal of Renewable Energy Research, Volume.2, 28 Oct 2011,pp. 54-77.*
- [31] GengDayongandMaWenge, “Modeling and Simulating for Soft Starting of Asynchronous Motors Based on Fuzzy Adaptive Control”, *Intelligent Systems and Applications (ISA), 2011 3rd International Workshop on,28-29 May 2011,pp. 1 – 4*
- [32] Ta-Cao, M. and Hoang Le-Huy,” Model reference adaptive fuzzy controller and fuzzy estimator for high performance induction motor drives” *Industry Applications Conference, 1996. Thirty-First IAS Annual Meeting, IAS '96, Conference Record of the 1996IEEE, volume 3, 6-10 Oct 1996, pp. 380 – 387.*
- [33] Tiago Henrique dos Santos, Alessandro Goedtel, Sergio Augusto Oliveira da Silva and Marcelo Suetake, “Scalar control of an induction motor using a neural sensorless technique”, *Electric Elsevier Power Systems Research, March 2014, Volume 108 pp. 322–330.*
- [34] Solly Aryza, Ahmed N Abdallah, Zulkeflee bin Khalidin, Zulkarnain Lubis and Ma Jie, “ A fast Induction Motor speed estimation based on Hybrid Particle Swarm Optimization (HPSO)”,*Elsevier Physics ProcediaInternational Conference on Solid State Devices and Materials Science, Volume 25,April 1-2, 2012, pp. 2109–2115.*
- [35] KenzaBouhoune, KrimYazid and Mohamed SeghirBoucherit. “Hybrid control of single phase induction machine without capacitor using artificial intelligence techniques”, *Elsevier,EnergyProcedia, Vol. 18,2012, pp.1392-1401.*
- [36] Ashok Kusagur, Dr. S. F. Kodad,Dr. B V. SankarRam,”AI based design of a fuzzy logic scheme for speed control of induction motors using SVPWM technique”,*JJCSNS International Journal of Computer Science and Network Security, volume .9, January 2009,pp.74-80.*
- [37] Jagadish H. Pujar and S.F. Kodad,”AI based Direct Torque FuzzyControl of AC Drives”,*International Journal of Electronic Engineering Research, Volume 1,2009 pp. 233–244.*
- [38] Ramesh, Tejavathu,Panda, A.K. ; Bonala, Sathyam.”Artificial intelligence based high performance direct torque and flux control of induction motor drive”,*Circuits, Power and Computing Technologies (ICCPCT), 2013 International Conference on,pp.225 – 230.*
- [39] ShahramJavadi,“Induction Motor Drive Using Fuzzy Logic”,*Proceedings of the 7th WSEAS International Conference on Systems Theory and Scientific Computation, Athens, Greece, August 24-26, 2007,pp.265-271*
- [40] Rohit Gupta and Ruchiika,“Intelligent Induction Motor Drive”,*International Journal of Computer Applications (0975 – 8887),Volume 50- No.22, July 2012,pp.41-46.*
- [41] DebirupeHore, “Fuzzy logic based advance speed control of Induction motor”, *International Journal of Computers And Technology,Volume 4, Jan-Feb, 2013,pp.124-128.*
- [42] Guven, M.K,Rehman, H.Yu, L. and Derdiyok, A.,“A high performance adaptive parallel distributed compensator for induction machine drives”,*Electric Machines and Drives Conference, 2001. IEMDC 2001. IEEE Internationa,2001,pp 486 – 491.*
- [43] BrahimMetidji, FaridTazrart, Ahmed Azib, Nabil Taib, and ToufikRekioua,“A New Fuzzy Direct Torque Control Strategy for InductionMachine Based on Indirect Matrix Converter”,*International Journal of Research and Reviews in Computing EngineeringVol. 1, No. 1, March 2011,pp 18-22.*
- [44] Purwanto, E,Daniel, M.W,Harianto and Prabowo, G ,“Simulation of the application fuzzy logic controller in 3 phase induction motor speed control by selecting membership function parameter”,*TENCON '02.Proceedings. 2002 IEEE Region 10 Conference on Computers, Communications, Control and Power Engineering,Volume:328-31 Oct. 2002,pp.2050 - 2052.*
- [45] Mohamadian, M. Nowicki, E.Ashrafzadeh, F. Chu, A. Sachdeva, R. and Evanik, E.”A novel neural network controller and its efficient DSP implementation for vector-controlled induction motor drives”,*Industry Applications, IEEE Transactions on Volume:39,Nov.-Dec. 2003,pp.1622 – 1629*
- [46] Ms. ChinkiChandok,“Speed Estimation of A.C. Drive by Artificial Neural Networks (ANN)”,*International Journal of Advanced Research in Computer Science and Software Engineering,Volume 2, November 2012,pp*
- [47] Tien-Chi Chen and Tsong-TerngSheu, “Model reference neural network controller for induction motor speed control”, *IEEE Transactions onEnergy Conversion,Volume:17,Jun 2002, pp.157 – 163.*
- [48] D.K. Bhattacharyya and Amit Kumar Ray,“Stepless PWM speed control of AC motors A neural network approach”, *Elsevier Neurocomputing, Volume 6,October 1994, pp. 523–539.*
- [49] Kulawski, G.J. andBrdys, M.A. “Adaptive control of non-linear plants using neural networks-application to a flux control in AC drive system”,*Control, 1994. Control '94. International Conference on,Volume2 ,21-24 March 1994,pp.1472 – 1477.*
- [50] C.Thanga Raj, S.P.Srivastava and PramodAgarwal, “Energy efficient control of three phase induction motor”,*International Journal of Computer and Electrical Engineering, Vol. 1, No. 1, April 2009,pp. 61-70.*
- [51] Uddin, M.N.,ZhiRuiHuang ,Hossain and A.B.M.S,“Development and Implementation of a Simplified Self-Tuned Neuro-Fuzzy-Based IM Drive”,*Industry Applications, IEEETransactions on,Volume 50,Jan.-Feb 2014,PP.51 – 59.*
- [52] Sarat Kumar Sahoo and A. Ramulu,“Salient features of vector control in AC motor drives: Areview”,*Scientific Research and Essays, Volume 8(34), 11 Septeme,2013,pp.1649-1657.*
- [53] ArfatSiddique andBhimSin,“Applications of Artificial Intelligence Techniques forInduction Machine Stator Fault Diagnostics: Review”*Symposium on Diagnostics for ElectricMachines, Power Electronics and DrivesAllanla, GA, USA ,August 2003,pp.29-34*
- [54] Jalili, K.,Farhangi, S and Saievar-Iranizad, E, ”Sensorless vector control of induction motors in fuel cell vehicle using a neuro-fuzzy speed controller and an online artificial neural network speed estimator”,*Control Applications, 2001. (CCA '01). Proceedings of the 2001 IEEE International Conference on ,2001 ,pp. .259 – 264.*
- [55] Ai Wu and Tam, P.K.S “An adaptive speed control for induction motor drive using fuzzy neural network based on fuzzy hierarchy error approach”,*Electric Machines and Drives, 1999. International Conference IEED '99May ,1999, pp.284 – 286.*
- [56] Parasiliti, F,Tursini, M andZhang, D.Q, “Adaptive fuzzy logic control for high performance PM synchronous drives”,*Electrotechnical Conference, 1996. MELECON '96., 8th Mediterranean Volume 1,13-16 May 1996, pp.323 – 327*
- [57] Der-FaChen andTian-HuaLiu,“Implementation of a novel matrix converter PMSM drive”,*Aerospace and Electronic Systems, IEEE Transactions on,Volume:37,Jul 2001,pp.863 – 875.*
- [58] Won-SikBaik, Min-Huei Kim,, Nam-Hun Kim, Dong-Hee Kim, Kyeong-Ho Choi and Don-Ha Hwang,”An optimal efficiency control of reluctance synchronous motor using neural network with direct torque control”,*Industrial Electronics Society, 2003, IECON '03. The 29th Annual Conference of the IEEE,Volume:2 ,2-6 Nov. 2003,pp. 1590 – 1595.*
- [59] Saleh, Kh,Badr, M.A.,Elwer, A.S. and Wahsh, S,”Analysis of controlled permanent magnet synchronous motor using artificial neural network”,*Electrical Machines and Systems, 2001. ICEMS 2001. Proceedings of the Fifth International Conference on, ,Volume2, Aug 2001,pp.91 – 795.*
- [60] Senju, T.,Shingaki, T.,Omoda, A. and Uezato, K.,”High efficiency drives for synchronous reluctance motors using neural network”,*Industrial Electronics Society, 2000. IECON 2000. 26th Annual Conference of the IEEE, ,volume 2,2000,pp. 777 – 782.*
- [61] Urasaki, N, Senju, T and Uezato, K, ”Neural network based high efficiency drive for interior permanent magnet synchronous motors compensating EMF constant variation”,*Power Conversion*

- Conference, 2002. PCC-Osaka 2002*, volume3,2002, pp. 1273 – 1278.
- [62] *Lim, H.S Roberson, D.G,Lobo, N.S and Krishnan, R*, "Novel flux linkage control of switched reluctance motor drives using observer and neural network-based correction methods",*Industrial Electronics Society, 2005. IECON 2005. 31st Annual Conference of IEEE*,6-10 Nov. 2005.
- [63] *Al-Tuee, M.A,Al-Din, M.S and AlZu'bi, H.S*, "Real-time efficiency optimisation of open-loop controlled synchronous PM motor drive using Adaptive Neural Networks",*EUROCON - International Conference on Computer as a Tool (EUROCON)*, 2011 IEEE,27-29 April 2011,pp 1-4.
- [64] *Campos, J, Loukianov, Alexander G.and Sanchez, Edgar N*, "Synchronous motor VSS control using recurrent high order neural networks",*Decision and Control, 2003. Proceedings. 42nd IEEE Conference on*,volume 4,9-12 Dec. 2003pp.3894 – 3899.
- [65] *Faa-Jeng Lin and Po-Hung Shen*, "A linear synchronous motor drive using robust fuzzy neural network control",*Intelligent Control and Automation, 2004. WCICA 2004. Fifth World Congress on* Volume:5,15-19 June 2004, pp.4386 – 4390.
- [66] Xianqing Cao and LipingFan,"A Novel Implementation of Neural Network and Multi-Fuzzy Controllers for Permanent Magnet Synchronous Motor Direct Torque Controlled Drive",*Intelligent Information Technology Application, 2008. IITA '08. Second International Symposium on*, volume 1,20-22 Dec. 2008. pp.751 – 755.
- [67] GuoZhi-rong, Gao Wei and Xie Shun-yi,"Automatic Generation :Fuzzy Neural Network Speed Controller for Permanent-Magnet Synchronous Motor Drive",*Intelligent Computation Technology and Automation, 2009. ICICTA '09. Second International Conference on*, volume 2 10-11 Oct. 2009, pp. 664 – 667.
- [68] *Gao Wei and Mao Wei*, "Sliding mode speed controller for PM synchronous motor drive using dynamic fuzzy neural network",*Electronic Measurement & Instruments (ICEMI)*, 2011 10th International Conference on, volume 2, 16-19 Aug. 2011, pp. 274 – 277.
- [69] *Xianqing Cao and LipingFan*, "Vector Controlled Permanent Magnet Synchronous Motor Drive Based on Neural Network and Multi Fuzzy Controllers",*Fuzzy Systems and Knowledge Discovery, 2008. FSKD '08.Fifth International Conference on. Volume 3*,18-20 Oct. 2008, pp. 254 – 258.

Impact Assessment of Wind Farms and FACTS Controllers in Emerging Power System

Bindeshwar Singh¹, Ajay Kumar², Vikash Singh Rathore³, and Kevi Singh⁴

Abstract- This paper presents a review on impact assessment of wind farms and FACTS controllers such as SVC, STATCOM, UPFC and SSSC in emerging power system. Authors strongly believe that this survey article will be very much useful to the researchers, scientific, engineers and industrial persons for finding out the relevant references in the field of impact assessment of wind farms and FACTS controllers such as SVC and STATCOM in emerging power system.

Keywords: Wind Farms, Flexible AC Transmission System (FACTS), FACTS Controllers, SVC, STACOM, and Emerging Power System.

I. INTRODUCTION

THE utilization of wind energy for power generation purposes is becoming increasingly attractive and gaining a great share in the electrical power production market worldwide. Injection of the wind power into an electric grid affects the power quality. The performance of the wind turbine and thereby power quality are determined on the basis of measurements and the norms followed according to the guideline specified in International Electro-technical Commission standard, IEC-61400 [1]. Wind farms typically contain a variety of voltage control equipment including tap-changing transformers, switched capacitors, SVCs, STATCOMs, and the generators themselves [2]. With the development of wind turbine technology, large scale wind farms of hundreds MW level are being developed in many countries. These modern wind farms are usually connected to the power grid. The wind power penetration levels in the networks could be high, for example, average wind power penetration levels of 20-30 % with peak penetration level up to 100% [3]. At present, a wide range of flexible controllers, which capitalize on newly available power electronics components, are emerging for custom power applications. Generator excitation controller with only excitation control can improve transient stability for minor faults but it is not sufficient to maintain stability of system for large faults occur near to generator terminals [4]. Researchers worked on other solution and found that FACTS is one of the most

prominent solution that can improve stability by changing electrical characteristics of Power system [5]-[6]. FACTS is a term denoting a whole family of concepts and devices for improved use and flexibility of power systems. Some of these devices have today reached certain maturity in their concept and application, some are as a matter of fact quite established as tools in power systems [7]. The technology behind the FACTS device is also matured with a long history of development. However, the number of real world applications of advanced FACTS devices are still limited [8]. FACTS, based on power electronics have been first developed to improve the performance of long distance AC transmission [9]. For most applications in AC transmission systems and for network interconnections, SVC, FSC, TCSC and GPFC/B2B are fully sufficient to match the essential requirements of the grid. STATCOM and UPFC are tailored solutions for special needs [10].

NOMENCLATURES

| | |
|----------|--|
| FACTS | Flexible Alternating Current Transmission System |
| FC-TCR | Fixed capacitor Thyristor Controlled Reactor |
| TCSC | Thyristor Controlled Series Capacitor |
| TCPAR | Thyristor Controlled Phase Angle Regulator |
| SSSC | Static Synchronous Series Compensator |
| TCPST | Thyristor Controlled Phase Shifting Transformer |
| TSSC | Thyristor Switched Series Capacitor |
| TCSR | Thyristor Controlled Series Reactor |
| TCR | Thyristor Controlled Reactor |
| TSR | Thyristor Switched Reactor |
| SVC | Static Var Compensator |
| STATCOM | Static Synchronous Compensator |
| DSTATCOM | Distribution Static Compensator |
| IPFC | Interline Power Flow Controller |
| UPFC | Unified Power Flow Controller |
| GUPFC | Generalized Unified Power Flow Controller |
| HPFC | Hybrid Power Flow Controller |
| SMES | Superconducting Magnetic Energy Storage Systems |
| BESS | Battery Energy Storage Systems |
| UIPC | Unified Interphase Power Controller |
| PFC | Power System Stabilizers |
| AP | Active Power |
| RP | Reactive Power |
| VSC | Voltage Source Converter |
| VSI | Voltage Source Inverter |
| VS | Voltage Stability |
| VI | Voltage Instability |
| VC | Voltage Collapse |
| VP | Voltage Profile |
| VR | Voltage Regulation |
| SSVS | Steady State Voltage Stability |
| TS | Transient Stability |
| APTC | Available Power Transfer Capacity |
| PQ | Power Quality |
| SSR | Sub-synchronous Resonance |
| SS | Steady State |
| α | Firing Angle |
| HFC | Hybrid Flow Controller |
| PST | Phase Shifting Transformer |
| PSS | Power system stability |

¹ Asst. Professor, Department of Electrical Engineering, Kamla Nehru Institute of Technology (KNIT), Sultanpur-228118, U.P., India

^{2&3}B. Tech. (Electrical Engineering) Student, Department of Electrical Engineering, Kamla Nehru Institute of Technology (KNIT), Sultanpur-228118, U.P., India⁴

M. Tech. (POWER SYSTEMS) Regular Students, Department of Electrical Engineering, GBTU, Noida, U.P., India

II. A LITRATURE SURVAY

A. Wind Farms

P. Ramanathan [11], has been presented a STATCOM control scheme for grid connected wind energy system for power quality improvement. The integration of wind energy into existing power system presents a technical challenges and that requires consideration of voltage regulation, stability, power quality problems. The power quality is an essential customer-focused measure and is greatly affected by the operation of a distribution and transmission network. Z. Chen [12], has proposed the Issues of connecting wind farms into power systems. with the development of wind turbine technology, large scale wind farms of hundreds MW level are being developed in many countries. These modern wind farms are usually connected to the power grid. The wind power penetration levels in the networks could be high, for example, average wind power penetration levels of 20-30% with peak penetration level up to 100%. Which will effectively reducethe requirement on the fossil fuel based conventional power generation, however, it also presents many challenges to modern power systems. R. K. Tyagi [13], has been presented wind energy and role of effecting parameters. The amount of wind energy available at any location depends on two set of factors:-

- a) Climatic factors including: time of day, season, geographic location, topography, and local weather.
- b) Mechanical factors including: diameter of rotor, and type of turbine.

Vardar A *et al* [14], has been presented the Merits and demerits of Wind energy.

a) Merits of wind energy

One of the greatest advantages of wind energy is that it is ample. Secondly, wind energy is renewable. Some other advantages of wind energy are that it is widely distributed, cheap, and also helps in reducing toxic gas emissions. Wind Energy is also advantageous over traditional methods of creating energy, in the sense that it is getting cheaperto produce wind energy. Wind energy may soon be the cheapest way to produce energy on a large-scale. The cost of producing wind energy has come down by at least eighty percent since the eighties. Along with economy, wind energy is also said to diminish the greenhouse effect. Also, wind energy generates no pollution.

b) Demerits of wind energy

However, there are some disadvantages for wind energy, which may put a dampener in its popularity. Though thecosts of creating wind energy are going down, even today a large number of turbines have to be built to generate aproper amount of wind energy. Though wind power is non-polluting, the turbines may create a lot of noise,

which indirectly contributes to noise pollution. Wind can never be predicted. Even the most advanced machinery may come out a cropper while predicting weather and wind conditions. Since wind energy will require knowledge of the weather and wind conditions on long-term basis, it may be a bit impractical. Tamer A. Kawady *et al* [15], has proposed wind farm protection systems: state of the art and challenges . daniel f. Opila *et al* [16] , has proposed wind farm reactive support and voltage control. utility-scale wind generation facilities should be capable of regulating voltage through the provision of dynamic reactive support . Wind farms, however, are comprised of many distributed WTGs and therefore exhibit behaviour that is vastly different to that of traditional large generators.

B. FACTS Controllers

1. Shunt Connected FACTS Controllers

a) SVC

Alisha Banga, *et al*. [17], proposed the modeling and simulation of SVC controller for enhancement of power system stability. SVC are shunt connected static generators / absorbers whose outputs are varied so as to control voltage of the electric power systems. Navid Ghaffarzadeh, *et al*.[18], proposed the investigation and comparison of the effect of FACTS devices, capacitors and lines reactance variations on voltage stability improvement and loadability enhancement in two area power system. in transmission applications, the SVC is used to regulate the grid voltage. If the power system's reactive load is capacitive (leading), the SVC will use thyristor controlled reactors to consume vars from the system, lowering the system voltage. Under inductive (lagging) conditions, the capacitor banks are automatically switched in, thus providing a higher system voltage . Naresh Acharya, *et al*. [19], proposed the facts about FACTS controllers practical installations and benefits. even the utilities in developing countries took the benefit of SVCs since its invention. ABB remains the pioneer in deployment of SVC and has supplied 55% of the total installation of which 13% were being installed in Asian countries. The world's first demonstration of SVC for utility application was installed in 1974, which was commercialized by General Electric (GE). Alok Kumar Mohanty,*et al* [20], proposed the power system stability improvement using FACTS devices. SVCs also may be placed near high and rapidly varying loads, such as arc furnaces, where they can smooth flicker voltage. It is known that the SVCs with an auxiliary injection of a suitable signal can considerably improve the dynamic stability performance of a power system . It is observed that SVC controls can significantly influence nonlinear system behavior especially under high-stress operating conditions and increased SVC gains.

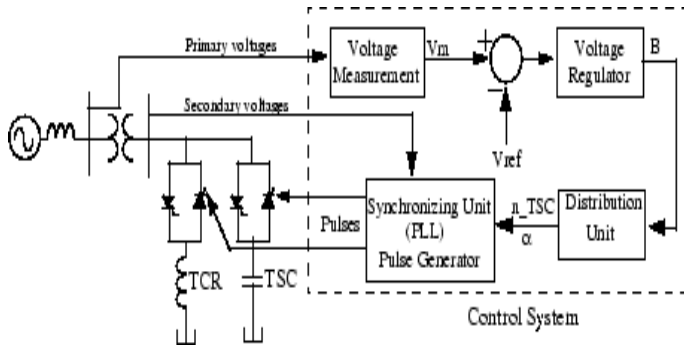


Fig. 1 connection diagram of SVC

b) STATCOM

Arvind Pahade *et al* [21], proposed the transient stability improvement by using shunt FACT device (STATCOM) with RVC control scheme. A STATCOM is a controlled reactive-power source. It provides the desired reactive-power generation and absorption entirely by means of electronic processing of the voltage and current waveforms in a VSC. G.Sundar *et al* [22], proposed the Digital Simulation of multilevel inverter based statcom. The STATCOM is basically a DC-AC voltage source converter with an energy storage unit, usually a DC capacitor. It operates as a controlled SVI connected to the line through a coupling transformer. R.krishna sampath *et al* [23], proposed the dynamic performance of STATCOM under various faults in power system. The STATCOM based on VSC is used for voltage regulation in transmission and distribution systems. The STATCOM can rapidly supply dynamic VAR's during system faults for voltage support.

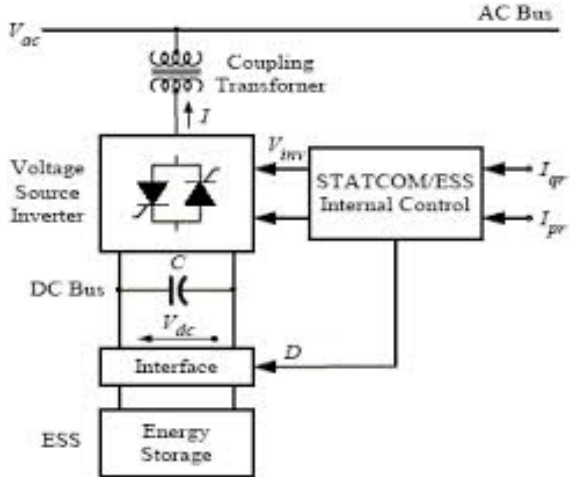


Fig. 2 Connection diagram STATCOM

2. Series- Shunt Connected FACTS Controllers

a) UPFC

Ali Ajami *et al* [24], proposed modelling and controlling of UPFC for power system transient studies. The UPFC is one of the typical FACTS devices that can provide simultaneous control of all or selectively basic parameters of power system (trans-mission voltage, line impedance and phase angle) and dynamic compensation of AC power system. S. Tara Kalyani *et al* [25], proposed simulation of real and reactive power flow control with UPFC connected to a transmission line. The basic components of the UPFC are two voltage source inverters (VSIs) sharing a common dc storage capacitor, and connected to the power system through coupling transformers. One VSI is connected to in shunt to the transmission system via a shunt transformer, while the other one is connected in series through a series transformer. Satakshi Singh [26], proposed the UPFC optimal power flow model. UPFC is able to control both transmitted real and reactive power independently, at the sending and receiving ends of the transmission line. The UPFC model is very flexible; it allows the control of active and reactive powers and voltage magnitude simultaneously. It can also be set to control one or more of these parameters in any combination or to control none of them. K. Manozi kumar reddy [27], proposed multiple control functions of UPFC. The UPFC is assigned two control functions, power flow and AC voltage control. Three PI controllers, i.e. PI power flow controller, PI AC voltage controller and PI DC voltage controller, for the UPFC are designed separately in a sequence which ensures closed loop system stability and a satisfactory control performance .

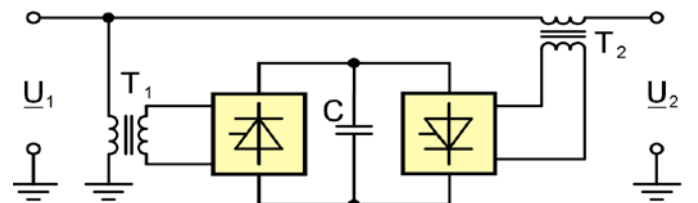


Fig. 3 connection diagram UPFC

3. Series Connected FACTS Controllers

SSSC

P.Suman Pramod Kumar *et al* [28], proposed static synchronous series compensator for series compensation of EHV transmission line. SSSC is one of the important series FACTS devices. SSSC is a solid-state voltage source inverter, injects an almost sinusoidal voltage, of variable magnitude in series with the transmission line. The injected voltage is almost in quadrature with the line current. Hossein Nasir Aghdam [29], proposed analysis of sssc, on congestion management and voltage profile in power system by PSAT toolbox. Outage of transmission lines, congestion, cascading line tripping, and power system stability loss are the major ideas where capability and

utilization of FACTS are considered. The SSSC is a device which can control simultaneously all three parameters of line power flow (line impedance, voltage and phase angle). B. M. Naveen Kumar Reddy *et al* [30], proposed power system stability enhancement using SSSC. The compensator is equipped with a source of energy, which helps in supplying or absorbing active power to or from the transmission line along with the control of reactive power flow. As the name suggests, SSSC is a series compensator. It is connected in series with the transmission line. Three phase series transformers are used to connect the compensator in series with the power system.

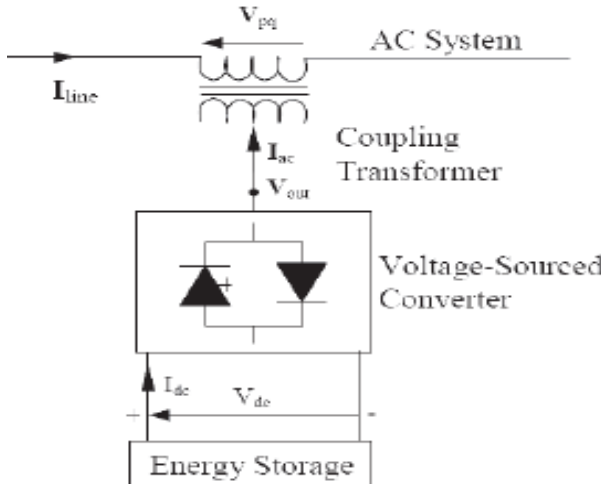


Fig. 4 connection diagram SSSC

III. SUMMERY OF THE PAPER

The summery of literature reviewed regarding with active and reactive power problems and its solutions. So that the FACTS controllers are best solution for this problems. The Wind farms and FACTS controller such as series, series-series, series-shunt, FACTS controllers in power system network are used for the reactive power compensation. With the help of wind farms and FACTS controllers, required reactive power is supplied and the fault is cleared in minimum time and the system stability also increases.

IV. CONCLUSION

This paper presents a survey on impact assessment of wind farms and facts Controllers in Emerging Power System. The PQ problem such as voltage fluctuation, frequency, harmonics etc. can be solved by using FACTS controller such as SVC, TCSC, SSSC, STATCOM, DSTATCOM, UPFC, IPFC, GUPFC, HPFC, GIPFC, TCPAR. Finally it is concluded that the most powerful and versatile FACTS controller from enhancement of power quality parameters are STATCOM & DSTATCOM, are utilized in the system.

V. ACKNOWLEDGMENT

The authors would like to thanks Dr. K.S. Verma, Dr.R.P.Payasi, and Dr. D Singh, Kamala Nehru Institute of Technology, Sultanpur, U.P.,-228118, India for their valubles suggestions regarding A power quality problems in power system environments.

VI. REFERENCES

- [1] P. Ramanathan, "A Statcom-Control Scheme for Grid ConnectedWind Energy System for Power Quality Improvement,"Middle East Journal of Scientific Research 20 (1):57-61, 2014.
- [2] Daniel F.Opila, Abdi M.Zeynu and Ian A. Hiskens, "Wind Farm Reactive Support and Voltage Control," 2010 IREP Symposium-Bulk Power System Dynamics and Control – VIII (IREP), August 1-6, 2010, Buzios, RJ, Brazil.
- [3] Z. Chen, "Issues of Connecting Wind Farms into PowerSystems," 2005 IEEE/PES Transmission and DistributionConference & Exhibition: Asia and PacificDalian, China.
- [4] Cong, L. "Coordinated control of Generator excitation and STATCOM for Rotor angle stability and voltage regulation enhancement of power systems." IEE Proceedings on Generation & Transmission and Distribution, 149(2), pp 659-666, Feb 2003
- [5] Hingorani and N.G. Gyungyi, "Understanding FACTS Devices." IEEE Press, 2000.
- [6] Spista.V, "Design of a Robust State Feedback Controller for a STATCOM Using Zero Set Concept", IEEE transactions on Power delivery, 25(1), pp 456-467, Jan 2010
- [7] Rolf Grünbaum, Bruno Halvarsson and Aleksander Wilk-Wilczynski, "FACTS And HVDC Light for POWER SYSTEM Interconnections,"Presented at PowerDeliveryConference, Madrid, Spain,September 1999
- [8] Nadarajah Mithulanthan and Naresh Acharya, "A proposal for investment recovery of FACTS devices in deregulated electricity markets," Electric Power Systems Research 77 (2007) 695–703
- [9] Hingorani, N. G.: Flexible AC transmission. IEEE Spectrum, pp. 40-45, April 1993
- [10] D. Povh and D. Retzmann, "DEVELOPMENT OF FACTS FOR TRANSMISSION SYSTEMS," The IERE Cetral America Forum.
- [11] P. Ramanathan , "A Statcom-Control Scheme for Grid ConnectedWind Energy System for Power Quality Improvement," Middle-East Journal of Scientific Research, 2014.
- [12] Z.Chen, "Issues of connecting wind firms into power system," 2005 IEEE/PES Transmission and Distribution Conference & Exhibition:Asia and Pacific Dalian, China.
- [13] R. K. Tyagi , "Wind Energy and Role of Effecting Parameters," European Journal of Applied Engineering and Scientific Research, 2012
- [14] Vardar A., Alibas I., Renewable Energy, Vol. 33, pp-1721–1732, 2008.
- [15] Tamer A. Kawady, Naema M. Mansour and Abdel-Maksoud I. Taalab , "Wind Farm Protection Systems: State of the Art and Challenges,"
- [16] Daniel F. Opila ,Abdi M. Zeynu and Ian A. Hiskens, "Wind Farm Reactive Support and Voltage Control," 2010 IREP Symposium-Bulk Power System Dynamics and Control – VIII (IREP), August 1-6, 2010, Buzios, RJ, Brazil.

- [17] Alisha Banga and S.S. Kaushik, "Modeling and simulation of svc controller for enhancement of power system stability," International Journal of Advances in Engineering & Technology, July 2011.
- [18] Navid Ghaffarzadeh, Haniyeh Marefatjou and Iman Soltani, "Investigation and Comparison of the Effect of Fact Devices, Capacitors and Lines Reactance Variations on Voltage StabilityImprovement and Loadability Enhancement in Two Area Power System," International Journal of Applied Power Engineering (IJAPE) Vol.1, No.3, December 2012
- [19] Naresh Acharya, Arthit Sode-Yome and Nadarajah Mithulanathan, "Facts about Flexible AC Transmission Systems (FACTS) Controllers: Practical Installations and Benefits."
- [20] Alok Kumar Mohanty and Amar Kumar Barik, "Power System Stability Improvement Using FACTS Devices," International Journal of Modern Engineering Research (IJMER), Vol.1, Issue.2, pp-666-672.
- [21] Arvind Pahade and Nitin Saxena, "Transient stability improvement by using shunt FACT device (STATCOM)with Reference Voltage Compensation (RVC) control scheme," International Journal of Electrical, Electronics and Computer Engineering 2(1): 7- 12(2013).
- [22] G.Sundar and S.Ramareddy, "Digital Simulation oF Multilevel InverterBased STATCOM," Journal of Theoretical and Applied Information Technology.
- [23] R.krishna Sampath and C.kumar, "Dynamic Performance of STATCOM Under Various Faults in Power System," International Journal of Advanced Computer Research (ISSN (print): 2249-7277 ISSN (online): 2277-7970) Volume-2 Number-4 Issue-6 December-2012.
- [24] Ali Ajami,S.H. Hosseini and G.B. Gharehpétian, "Modelling and Controlling of UPFC for Power System Transient Studies,"
- [25] S. Tara Kalyani and G.Tulasiram Das, "SIMULATION OF REAL AND REACTIVE POWER FLOW CONTROL WITH UPFC CONNECTED TO A TRANSMISSION LINE," Journal of Theoretical and Applied Information Technology.
- [26] Satakshi Singh, "The Unified Power Flow Controller Optimal Power Flow Model," International Journal of Scientific and Research Publications, Volume 2, Issue 8, August 2012.
- [27] K. Manoz kumar reddy, "Multiple Control Functions of UPFC,"International Journal of Advanced Research in Computer Science and Software Engineering.
- [28] P.Suman Pramod Kumar ,N.Vijaysimha and C.B.Saravanan,"static synchronous series compensator for series compensation of EHV transmission line," International Journal of Advanced Research in Electrical, Electronics and Instrumentation Engineering 7, July 2013.
- [29] Hossein Nasir Aghdam, "analysis of static synchronous series compensators , on congestion management and voltage profile in power system by psat toolbox," Research Journal of Applied Sciences, Engineering and Technology 3(7): 660-667, 2011.
- [30] B. M. Naveen Kumar Reddy, Mr. G. V. Rajashekhar and Dr. Himani Goyal,"Power System Stability Enhancement Using Static Synchronous Series Compensator," International Journal of Modern Engineering Research Vol. 3, Issue. 4, Jul - Aug. 2013.

BIBLIOGRAPHIES



Bindeshwar Singh received the M.Tech. In electrical engineering from the Indian Institute of Technology, Roorkee, in 2008. He is now a Ph. D. student at ISM Dhanbad, Jharkhand, India. His research interests are in Coordination of DGs & FACTS controllers in power systems and Power system Engg. Currently, he is an Assistant Professor with Department of Electrical Engineering Kamla Nehru Institute of Technology, Sultanpur, U.P., and India, where he has been since August'2010.
Mobile: 09473795769.

Email id: bindeshwar.singh2025@gmail.com



Ajay Kumar is a B. Tech student in electrical engineering department, KNIT Sultanpur-228118 (U.P.),India..His interests are in Coordination of Wind Farms and FACTS controller in power system.

E-mail ID: ajayrajput10305@gmail.com



Vikash Singh Rathore is a B. Tech student in electrical engineering department, KNIT Sultanpur-228118 (U.P.),India.. His interests are in Coordination of Wind Farms and FACTS controller in power system.

E-mail ID: vikash10356@gmail.com



Kevi Singh is a M.Tech student (Regular). In specialization of Power Systems in department of electrical engineering, GBTU, Noida, U.P. India. His interests are in the areas of Power Systems.

E-mail ID: kevi.singh1990@gmail.com

Comparative Study on Signal Processing Techniques Applied to Human Sleep EEG Signals

A. Meenakshi, B. Dr.R.K.Singh, C. Prof.A.K.Singh, D. Mr.A.K.Jayank

ABSTRACT - Electroencephalogram (EEG) signal is the commonly used signal for classification of sleep stages. Classification of sleep stages is a multiclass classification problem and very useful in the diagnosis of sleep disorders. A variety of methods for analysing sleep EEG signals can be found in the literature. This article provides an overview of these methods and offers guidelines for choosing appropriate signal processing techniques. The three key stages required for the analysis of sleep EEGs namely, pre-processing, feature extraction, and feature classification. The pre-processing section describes the most frequently used signal processing techniques that deal with preparation of the sleep EEG signal prior to further analysis. The feature extraction and classification sections are also dedicated to highlight the most commonly used signal analysis methods used for characterising and classifying the sleep EEGs.

Keywords – Sleep, Signal processing Quantitative analysis , Feature selection/classification.

I. INTRODUCTION

Sleep is a crucial part directly affects our cognitive performance, learning capabilities, and general physical and emotional well-being. Sleep is the primary activity of the brain [1,2]. Sleep problems in early life may result in lasting neuro cognitive deficits. Krueger et al. [3] point out that “during sleep one gives up the opportunities to reproduce, eat, drink or socialise and one is subject to predation. Sleep could only have evolved despite these high evolutionary costs if it serves a crucial, primordial function”. Understanding and measuring brain activity in sleep is an exciting frontier of neuroscience, and poly-somnography (PSG) provides a data-rich source for understanding sleep in both health and disease. PSG combines multiple signals in sleep typically including neurophysiological signals:

- EEG (usually 4–8 channels), EOG and EMG (submentalis and/or tibialis muscle) combined with cardio respiratory signals such as:

- ECG
- Oxy haemoglobin saturation
- Oral-nasal air flow
- Abdominal and thoracic excursions

Visual inspection of these neurophysiological signals forms

the basis for standard sleep staging [4]. Signal processing allows the extraction of detailed information from such signals. Applications of these methods in relation to sleep EEG range from simple time and frequency domain analysis to implementation of sophisticated nonlinear pattern recognition and classification algorithms. Kubicki et al. [5] emphasise that going beyond the well-known and commonly used Rechtschaffen and Kales scoring criteria [4] will not be possible without the use of signal processing techniques and computer aided analyses to reveal further information on the microstructure of sleep. The body of literature developed for the analysis of sleep EEG is vast and therefore this review paper provides a synthesis of a selection of this literature to generate an overview of signal processing techniques applied to human sleep EEG analysis and their relative merits.

The characteristic of the PSG signals to be analysed is rather challenging. The underlying signals are inherently non-stationary and the relationships between the different measurement channels maybe time-varying. Many of the physical processes giving rise to the observed signals are nonlinear in nature with the result that the measured signals exhibit non-Gaussian statistics. To further confound the problem many signal components of interest may be observed in the presence of contaminating noise at a comparatively poor signal noise ratio. The standard principled approach to the development of signal processing algorithms is generally based on modelling the underlying processes and using that model to then develop optimal algorithms. As is common in many biomedical applications, this approach flounders due to a lack of realistic signal models and so a more heuristic approach is flourished leading to the plethora of techniques observed in the field.

Signal processing techniques will be considered in three sections: pre-processing, feature extraction and feature classification, which constitute the basic underlying tasks in the automated analysis of sleep signals. Each section describes its most frequently reported signal analysis methods. An extended Taxonomy Table which summarises the sleep EEG related applications of the surveyed techniques, containing a significantly greater selection of references has also been collated for each section and may be found in the accompanying supplemental materials. A final supplementary Taxonomy Table re-categorises the addressed signal processing techniques based on their applications in well-established areas of sleep research such as obstructive sleep apnoea (OSA) diagnosis and automatic sleep staging. Studies included in this survey are limited to surface EEG signals in

A. PG Scholar, ECD, KNIT Sultanpur

B. HOD, ECD, KNIT Sultanpur

C. Professor, ECD, KNIT Sultanpur

D. Assistant Professor, ECD, KNIT Sultanpur

sleeping humans (including the paediatric population). In short, this review aims to synthesise the complex field of sleep EEG analysis to inform both the signal processing and the sleep research communities.

II. PRE-PROCESSING

There are several objectives when pre-proposing of PSG signals including: normalisation, calibration, detrending and equalisation, but these are aspects which are common to many signal processing applications and require only the most basic of processing strategies. After signal acquisition phase, signals are to be pre-processed. Signal pre-processing is also called as Signal Enhancement. In general, the acquired brain signals are contaminated by noise and artefacts. The artefacts are eye blinks, eye movements (EOG), heart beat (ECG). In addition to these, muscular movements and power line interferences are also mingled with brain signals. Artefact removal can be done using Common Average Referencing (CAR), Surface Laplacian (SL), Independent Component Analysis (ICA), Common Spatial Patterns (CSP), Principal Component Normalization (Freq-Norm), Local Averaging Technique (LAT), Robust Kalman Filtering, Common Spatial Subspace Decomposition (CSSD) etc. The most frequently used methods are ICA, CAR, SL, PCA, CSP and Adaptive Filtering [10].

TABLE 1
COMPARISON OF SIGNAL ENHANCEMENT
METHODS

| S. No. | Meth od | Advantages | Disadvantage s |
|-----------|------------|---|--|
| 1 | ICA | <ul style="list-style-type: none"> • Computationally efficient. • Shows High performance for large sized data. • Decomposes signals into temporal independent and spatial fixed component. | <ul style="list-style-type: none"> • Can't be applicable for under determined cases. • Requires more computations for decomposition. |
| 2 | CAR | <ul style="list-style-type: none"> • Outperforms all the reference methods. • Yields improved SNR. | <ul style="list-style-type: none"> • Finite sample density and incomplete head coverage cause problems in calculating averages. |

| | | | |
|---|--------------------|---|--|
| 3 | SL | <ul style="list-style-type: none"> • Robust against the artefacts generated at regions that are not covered by electrode cap. • It solves electrode reference problem | <ul style="list-style-type: none"> • Sensitive to artefacts • Sensitive to spline patterns |
| 4 | PCA | <ul style="list-style-type: none"> • Helps in reduction of feature dimensions. • Ranking will be done and helps in classification of data . | <ul style="list-style-type: none"> • Not well as ICA. |
| 5 | CSP | <ul style="list-style-type: none"> • Doesn't require <i>a priori</i> selection of sub specific bands and knowledge of these bands | <ul style="list-style-type: none"> • Change in position of electrode may affect classification accuracies. • Requires use of many electrodes |
| 6 | Adaptive filtering | <ul style="list-style-type: none"> • Ability to modify the signal features according to signals being analyzed • Works well for the signals and artefacts with overlapping spectra nature | |

III. FEATURE EXTRACTION

Analyses of time series are often carried out by extracting features from the signal of interest. Features can be defined as parameters which provide information about the underlying structure of a signal. There have been numerous techniques applied to sleep EEG signals for the purpose of feature extraction. Note that in general, studies employ more than one feature in their analyses and hence more often than not, features are complementary. The rest of this section briefly describes some of the most frequently used features and feature extraction techniques in sleep EEG analysis. A review of quantitative analysis techniques applied to EEG signal can be found in [7].

3.1. Temporal features

Temporal features are characteristics obtained from the signal in the time domain. Some of the more widely used temporal features and the associated processing techniques are described below.

3.1.1. Instantaneous statistics

These are among the simplest features which can be derived from a time series. These statistics include measures derived from moments of the waveform including the mean absolute amplitude, standard deviation/variance, skewness and kurtosis, as well as measures relating to the probability density function of the waveform, such as mode, median or the entropy.

3.1.2. Zero-crossing and period-amplitude analysis (PAA)

Zero-crossings are the points at which the waveform crosses the x-axis. They are simple to compute and zero crossing rate encodes frequency information, because data which is dominated by high frequencies has a rapid zero crossing rate, whereas low zero-crossing rates are associated with low frequency processes [7, 8]. This approach can be adopted within frequency bands to mitigate the effects of noise and to reduce the issues associated with signals comprised of multiple components [9].

3.1.3. Hjorth parameters

The parameters are based on variance of the derivatives of the waveform and have been used for some time to characterise EEG waveforms [10]. The Hjorth parameters are sensitive to noise and hence the signal of interest is commonly filtered prior to calculation of these parameters [11].

3.1.4. De-trended fluctuation analysis (DFA)

DFA is a method to characterise long range temporal correlations in a time series [12,13] and can be used as a measure of self-similarity [14]. It is based on identifying trends in the signal's variance when analysed with different block length and is inherently suitable for the analysis of non-stationary, noisy signals such as the sleep EEGs [15,16].

3.2. Spectral features

The most commonly extracted features from sleep EEGs are the spectral features. They are essentially parameters which characterise the signal in the frequency domain. Sleep EEGs are traditionally divided into five frequency bands namely

delta (0–4 Hz), theta (5–7 Hz), alpha (8–12 Hz), sigma (13–15 Hz) and beta (16–30 Hz). Most spectral measures are only meaningful when the underlying signal is stationary which emphasises the importance of prior segmentation of the EEG signals. This section describes some of the most frequently used spectral features.

3.2.1. Non-parametric spectral estimation

3.2.2. Coherence analysis

3.2.3. Parametric spectral estimation

3.2.5. Higher-order spectral analysis (HOSA)

3.3. Time-frequency features

Time-frequency analysis is a powerful tool which allows decomposition of signals into both time and frequency [18]. It thus provides a means for analysing signals which are non-stationary, such as sleep EEGs. In the analysis of such signals one is often interested in the evolution of the frequency content with time. This is particularly important in the analysis of sleep EEGs where many of the events (e.g. arousals, sleep spindles, alpha intrusions) are manifested by sudden changes in amplitude and frequency characteristics. Some of the more commonly used time-frequency methods in the analysis of sleep EEGs are highlighted below.

3.3.1. Short time Fourier transform (STFT)

Is the simplest form of time-frequency analysis [18]. Often one only considers the squared magnitude of the STFT and this squared magnitude is termed the spectrogram. To compute the STFT the signal of interest is uniformly segmented into many short duration overlapping portions, the data in each portion are then windowed and Fourier transformed. The result is a set of Fourier transforms at different points in time revealing how these spectral properties change from one segment to another; that is the evolution of frequencies with time.

3.3.2. The wavelet transform

The wavelet transform is closely related to the STFT. The wavelet transform represents a signal using a function which is scaled and shifted in time. The scaling factor and time shifts can then be translated into frequency and time parameters respectively [19]. The character of the wavelet transform implies that it uses variable size windows to achieve time-frequency decomposition; short duration functions representing high frequency components and long duration functions representing low frequencies.

3.3.3. Matching pursuits (MP)

MP is based on signal description via a collection of mathematical functions (commonly Gaussian modulated sinusoids) called dictionaries. An advantage of MP is the large dictionary size which is not limited to a certain form of function (as opposed to the Fourier transform which uses only sinusoids or the wavelet transform which employs a mother wavelet function) [20]. MP achieves time-frequency decomposition by finding the best matches that fit the structure of the signal from the dictionary.

3.3.4. Empirical mode decomposition (EMD)

EMD is a decomposition technique which provides a signal representation which does not rely upon an assumption of stationarity. In this method, the signal is broken down into basis functions (called the intrinsic mode functions IMFs) which have distinct oscillatory modes. The modes are constrained to have a well-defined instantaneous frequency and these instantaneous frequencies are then computed utilising the Hilbert transform. The calculated instantaneous frequencies can then be combined to produce an energy-time-frequency representation of the signal. This time-frequency plot is known as the Hilbert spectrum [21]. Use of EMD in sleep EEG analysis has not been very wide, even though the method offers the advantage of being well-suited to the analysis of non-stationary signals.

3.4. Nonlinear Features/Complexity Measures

It is traditionally assumed that EEG signals are generated from stochastic processes and hence statistical methods can characterise them. An alternative view suggests that EEG signals may be generated from a deterministic nonlinear process [22]. Since nerve cells are highly nonlinear in nature, this view is intuitively appealing [23].

Nonlinear features can provide complementary information to characterise specific waveforms as well as different stages of sleep. An important issue in nonlinear analysis of time series is the reliability and interpretability of the potential results. Successful application and interpretation of these techniques requires a good understanding of the method and the application [23]. The rest of this section briefly describes some of the nonlinear features/techniques which have been more frequently applied to the analysis of sleep EEGs.

3.4.1. Fractal dimension (FD)

The FD directly measures the complexity of the measured signal. The basic idea comes from quantification of dimensionalities of fractals (i.e. geometries which are self-similar on different scales [28]). Fractals are mathematical objects whose dimension is non-integer; for instance an object

of fractal dimension between one and two might be a line of infinite length which is contained within a finite area. The concept of FD has been expanded to the analysis of time series, the principle being that a simple time-series would have a lower fractal dimension than a more complex one. For a single-channel sleep EEG signal, FD can range from one to two, that is, its dimension is at least one and cannot be greater than two. There are several algorithms for the calculation of FD from a time series which have been used in the analysis of sleep EEGs to date. FDs are suitable for detection of transients in EEG signals since they can be applied to short segments of data and are relatively stable measures of complexity [23].

3.4.2. Correlation dimension

The correlation dimension is commonly considered for use in the analysis of sleep EEGs this relatively wide usage is, in part, a consequence of an efficient and straightforward numerical algorithm for its estimation [31]. The correlation dimension has been applied to the analysis of both neonatal [31, 32] and adult sleep EEGs. Its use in identifying the different stages of sleep is based on the observation that in deeper sleep the measured complexity tends to be lower [21]. Accurate estimation of correlation dimension requires a large sample size (large segments) which limits its applicability; it is therefore generally not suitable for parameterisation of short transient events such as sleep spindles or arousals..

3.4.3. Entropy measures

There are a variety of definitions of entropy measures which have been proposed. Estimating the entropy directly from the time-series requires computation of the joint probability density function between time series, a process which is data intensive, many entropy measures therefore attempt to approximate this quantity in an efficient manner. Approximate entropy (ApEn) is one such widely considered method. ApEn reflects the conditional probability that two time series remain similar to each other for the next m samples, given that they have previously been similar. It has several desirable properties .it is robust in the analysis of short data segments, resilient to outliers and strong transients, is capable of dealing with noise by appropriate estimation of its parameters and can be applied to both stochastic and deterministically chaotic signals.

ApEn is a biased estimate of complexity and the alternative, closely related idea of sample entropy (SampEn) has been suggested. It is claimed that SampEn is consistent, has reduced bias and is largely independent of sample sizes [32]. Both methods have been used in the analysis of sleep EEGs, for instance, SampEn has been used to capture and reflect the distinctive characteristics of sleep in different stages [37].

3.4.4. Lyapunov exponents

The Lyapunov exponents represent the average convergence or divergence rate of trajectories in phase space. These exponents can be positive, zero or negative and their interpretation depends on their signal [25,]. Positive Lyapunov exponents are taken as an indication of chaos. There are as many Lyapunov exponents as there are dimensions in the underlying dynamical equations. Knowledge of the system equations allows one to compute Lyapunov exponents directly, but in practice these equations are not available in EEG analysis problems and the exponents must be estimated from time series data [23]. Commonly only the Largest Lyapunov Exponent (LLE) is considered, since if it is positive then the underlying dynamics will be chaotic.

IV. FEATURE CLASSIFICATION

After feature extraction the signals are classified into various classes using various classifiers. in sleep staging we may have five possible classes namely, wake, stage 1, stage 2, stage 3 sleep and REM, or in automatic spindle detection, we may have two, spindle vs. non-spindle.

In classification, features within each category (or class) share some similarity and maybe classified based on some measure of that similarity. Classification can be undertaken for a diagnostic purpose, e.g. classifying patients with obstructive sleep apnoea vs. controls, or can aid automation (classification of transient events in sleep or classifying sleep stages). Numerous techniques have been proposed and used for sleep EEG signal classification. Table 2 in supplementary materials is dedicated to these methods and their specific applications in the analysis of sleep EEGs.

TABLE 2
COMPARISON OF SIGNAL CLASSIFICATION
METHODS

| S. No. | Method | Advantages | Disadvantages |
|-----------|--|--|---|
| 1 | LDA (Linear Discriminant Analysis) | <ul style="list-style-type: none"> •It provides good generalization. • Performance is more than other linear classifier. | <ul style="list-style-type: none"> •It fails when the discriminatory function not in mean but in variance of the features. • For non- |

| | | | |
|---|---------------------------------------|--|---|
| | | | Gaussian distributions it may not preserve the complex structures. |
| 2 | SVM (Support Vector Machine) | <ul style="list-style-type: none"> • It provides good generalization. • Performance is more than other linear classifier. | <ul style="list-style-type: none"> •Has high computational complexity. |
| 3 | ANN (Artificial Neural Networks) | <ul style="list-style-type: none"> • Ease of use and implementation. • Robust in nature. •Simple computations are involved • Small training set requirements are required. | <ul style="list-style-type: none"> •Difficult to build. •Performance depends on the number of neurons in hidden layer. |
| 4 | NBC (Non Linear Bayesian Classifiers) | <ul style="list-style-type: none"> • Requires only small amount of training data to estimate parameters. • Only variance of class variables is to be computed and no need to compute the entire covariance matrix. | <ul style="list-style-type: none"> •Fails to produce a good estimate for the correct class probabilities. |
| 5 | K-NN (K-Nearest Neighbour) | <ul style="list-style-type: none"> •Very simple to understand. •Easy to implement and debug. | <ul style="list-style-type: none"> • Poor runtime performance if training set is large. • Sensitive to irrelevant and redundant features. • On difficult classification tasks out performed by other classification methods. |

V. CONCLUSION

A clear representation of various signal processing methods used in each level of EEG signal processing is presented in this paper. The results of this study give a way to select methods required for processing signals. And it also discusses the methods that are not suitable, while describing the following phases of EEG/BCI signal processing: 1) Signal pre-processing 2) Feature Extraction and 4) Signal Classification. This information may give guidance on finding the best method.

With the use of various methods of processing, researchers have developed models for animating objects, identifying human emotions. With the adequate knowledge of these new and efficient methods with mingled characteristics to always attain better performances can be developed. These new methods may drive to a new era of EEG/BCI applications including the thought based operating system, finding the intensity of human emotion, detecting the gender of human based on thoughts, automation of house hold appliance usage based on thoughts etc.

VI. REFERENCES

- [1] J.M. Krueger, D.M. Rector, S. Roy, H.P.A. Van Dongen, G. Belenky, J. Panksepp, Sleep as a fundamental property of neuronal assemblies, *Nat. Rev. Neurosci.* 9 (2008) 910–919.
- [2] E. Touchette, D. Petit, J.R. Seguin, M. Boivin, R.E. Tremblay, J.Y. Montplaisir, Associations between sleep duration patterns and behavioral/cognitive functioning at school entry, *Sleep* 30 (2007) 1213–1219.
- [3] A. Rechtschaffen, A. Kales, A manual of standardized terminology, techniques and scoring system for sleep stages of human subjects, U.S. National Institute of Neurological Diseases and Blindness, Neurological Information Network, 1968.
- [4] S. Kubicki, W.M. Herrmann, The future of computer-assisted investigation of the polysomnogram: sleep microstructure, *J. Clin. Neurophysiol.* 13 (1996) 285–294.
- [5] Ali Bashashati, Mehrdad, Fatourechi, Rabab K Ward and Gary E Birch, A survey of signal processing algorithms in brain-computer interfaces based on electrical brain signals, *J. of Neural Engg.*, Vol. 4, 2007.
- [6] A. Isaksson, A. Wennberg, L.H. Zetterberg, Computer analysis of EEG signals with parametric models, *Proc. IEEE* 69 (1981) 451–461.
- [7] M. Carrozzini, A. Accardo, F. Bouquet, Analysis of sleep-stage characteristics in full-term newborns by means of spectral and fractal parameters, *Sleep* 27 (2004) 1384–1393.
- [8] B.A. Geering, P. Achermann, F. Eggimann, A.A. Borbely, Period-amplitude analysis and power spectral analysis: a comparison based on all-night sleep EEG recordings, *J. Sleep Res.* 2 (1993) 121–129.
- [9] R. Armitage, R. Hoffmann, T. Fitch, C. Morel, R. Bonato, A comparison of period amplitude and power spectral analysis of sleep EEG in normal adults and depressed outpatients, *Psychiatry Res.* 56 (1995) 245–256.
- [10] A. Saastamoinen, E. Huupponen, A. Varri, J. Hasan, S.L. Himanen, Computer program for automated sleep depth estimation, *Comput. Methods Programs Biomed.* 82 (2006) 58–66.
- [11] S. Guðmundsson, T.P. Runarsson, S. Sigurdsson, Automatic sleep staging using support vector machines with posterior probability estimates. International Conference on Computational Intelligence for Modelling, Control and Automation, 2005 and International Conference on Intelligent Agents, Web Technologies and Internet Commerce, in: M. Mohammadian (Ed.), IEEE, Vienna, Austria, 2005, p. 6.
- [12] C.K. Peng, S.V. Buldyrev, S. Havlin, M. Simons, H.E. Stanley, A.L. Goldberger, Mosaic organization of DNA nucleotides, *Phys. Rev. E* 49 (1994) 1685–1689.
- [13] Y. Shen, E. Olbrich, P. Achermann, P.F. Meier, Dimensional complexity and spectral properties of the human sleep EEG, *Clin. Neurophysiol.* 114 (2003) 199–209.
- [14] L. Jong-Min, K. Dae-Jin, K. In-Young, P. Kwang-Suk, S.I. Kim, Detrended fluctuation analysis of EEG in sleep apnea using MIT/BIH polysomnography data, *Comput. Biol. Med.* 32 (2002) 37–47.
- [15] S. Leistedt, M. Dumont, J.P. Lanquart, F. Jurysta, P. Linkowski, Characterization of the sleep EEG in acutely depressed men using detrended fluctuation analysis, *Clin. Neurophysiol.* 118 (2007) 940–950.
- [16] P. Welch, The use of fast Fourier transform for the estimation of power spectra: a method based on time averaging over short, modified periodograms, *IEEE Trans. Audio Electroacoust.* 15 (1967) 70–73.
- [17] G.M. Jenkins, D. Watts, *Spectral Analysis and its Applications*, 1968.
- [18] L. Cohen, *Time-Frequency Analysis*, Prentice-Hall, New Jersey, 1995.
- [19] C.K. Chui, *An Introduction to Wavelets*, Academic Press, Inc., 1992.
- [20] J. Zygierek, K.J. Blinowska, P.J. Durka, W. Szelenberger, S. Niemcewicz, W. Androsiuk, High resolution study of sleep spindles, *Clin. Neurophysiol.* 110 (1999) 2136–2147.
- [21] N.E. Huang, Z. Shen, S.R. Long, M.C. Wu, H.H. Shih, Q. Zheng, N.-C. Yen, C.C. Tung, H.H. Liu, The empirical mode decomposition and the Hilbert spectrum for nonlinear and non-stationary time series analysis, *Proc. Math. Phys. Eng. Sci.* 454 (1998) 903–995.
- [22] B.H. Jansen, Quantitative analysis of electroencephalograms – is there chaos in the future, *Int. J. Bio-Med. Comput.* 27 (1991) 95–123.
- [23] D. Gallez, A. Babloyantz, Predictability of human EEG – a dynamic approach, *Biol. Cybern.* 64 (1991) 381–391.
- [24] J.W. Milnor, Attractor, in: Scholarpedia, 2006.
- [25] C.J. Stam, Nonlinear dynamical analysis of EEG and MEG: review of an emerging field, *Clin. Neurophysiol.* 116 (2005) 2266–2301.
- [26] B. Henry, N. Lovell, F. Camacho, Nonlinear dynamics time series analysis, in: M. Akay (Ed.), *Nonlinear Biomedical Signal Processing*, vol. 2, 2001.
- [27] M. Palus, Nonlinearity in normal human EEG: cycles, temporal asymmetry, nonstationarity and randomness, not chaos, *Biol. Cybern.* 75 (1996) 389–396.
- [28] P. Achermann, R. Hartmann, A. Gunzinger, W. Guggenbuhl, A.A. Borbely, All-night sleep EEG and artificial stochastic-control signals have similar correlation dimensions, *Electroencephalogr. Clin. Neurophysiol.* 90 (1994) 384–387.
- [29] T. Kobayashi, S. Madokoro, Y. Wada, K. Misaki, H. Nakagawa, Human sleep EEG analysis using the correlation dimension, *Clin. Electroencephalogr.* 32 (2001) 112–118.
- [30] J. Skinner, M. Molnar, C. Tomberg, The point correlation dimension: performance with nonstationary surrogate data and noise, *Integr. Psychol. Behav. Sci.* 29 (1994) 217–234.
- [31] S.M. Pincus, I.M. Gladstone, R.A. Ehrenkranz, A regularity statistic for medical data-analysis, *J. Clin. Monit.* 7 (1991) 335–345.
- [32] S.M. Pincus, Approximate entropy as a measure of system-complexity, *Proc. Natl. Acad. Sci. U.S.A.* 88 (1991) 2297–2301.
- [33] J. Roschke, J. Fell, P. Beckmann, The calculation of the 1st positive Lyapunov exponent in sleep EEG data, *Electroencephalogr. Clin. Neurophysiol.* 86 (1993) 348–352.
- [34] A. Wolf, J.B. Swift, H.L. Swinney, J.A. Vastano, Determining Lyapunov exponents from a time-series, *Phys. D* 16 (1985) 285–317.
- [35] J. Fell, J. Roschke, P. Beckmann, Deterministic chaos and the 1st positive Lyapunov exponent – a nonlinear analysis of the human electroencephalogram during sleep, *Biol. Cybern.* 69 (1993) 139–146.
- [36] X.Y. Wang, L. Chao, M. Juan, Nonlinear dynamic research on EEG signals in HAI experiment, *Appl. Math. Comput.* 207 (2009) 63–74.
- [37] D.R. Liu, Z.Y. Pang, S.R. Lloyd, A neural network method for detection of obstructive sleep apnea and narcolepsy based on pupil size and EEG, *IEEE Trans. Neural Netw.* 19 (2008) 308–318.

Analysis and Evaluation of Impact of Domestic Load Unbalancing

Pankaj Sharma, Kuldeep Kanaujiya,

I. ABSTRACT

Load unbalancing is one of the major threats in our power distribution sector. This occurs due to the fact that we have mostly single phase loads in our domestic power sector, which are very dynamic in nature. Due to this dynamic property, there arises the problem of load unbalancing which leads to flowing of neutral current which may be of high magnitude. It not only results in loss of precious electrical energy in form of heating but also can cause irreparable damage to neutral. This paper analyses the impact of unbalancing in context of Indian context

II. KEYWORDS

BHU, Domestic, Load, Loss, Neutral, Threat, Unbalance.

III. INTRODUCTION

Our present power distribution system starts from the nearest substation and terminates at the metering point of the customer. In our domestic power sector, for power consumption Voltages level provided to domestic customers is generally 230-240 volts if he has a single phase connection and 400-415 volts if he has a three phase connection. Conductors providing the power can be in form of overhead lines in rural and semi-urban areas while underground in urban areas where we have dense populated areas and finding right-of-way is a difficult task. In Indian context, mostly we have overhead pole configuration for power distribution. Urban and semi urban areas are generally provided with three-phase power connections to serve residential, industrial, and commercial loads. Rural areas are generally provided with only single-phase power connections.

Most domestic power customers are connected to a transformer, which reduces the distribution voltage to the phase-neutral voltage of 230volt which can be used for domestic use. The transformer may be pole-mounted in cities or may be placed on the ground in a closed boundary. In Villages, a pole-mount transformer may serve only one customer due to less density of peoples. In cities and metros, up to a dozen customers may be connected to a single transformer.

In domestic power distribution, we have two types of distribution networks

1. **Radial:** it leaves the sub-station and feeds all the designated area with no connection to any other supply in the process. This is useful in rural areas and the isolated

areas where we have a very low population density. In radial systems, we often have the problem of voltage drop.

2. **Interconnected:** it is usually found in urban areas and metros. It possesses simultaneous multiple connections to other points of supply. These other points of connection are normally open but allow various configurations by closing and opening switches. These switches can be turned on or off by either by a lineman or by remote control from a control center. This scheme has an advantage that benefit of the interconnected model is that a small area is disturbed in the case any fault occurs or maintenance needs to be done.

We have one-third of India, still not able to light up a bulb in their households. Unbalancing in any electrical system is caused by unequally Shunted single-phase load at all three phases. It may also be due to unbalanced primary voltage. Use of Delta-Wye or Wye-Delta transformers may also be criteria for it. Last, but not the least, the use of defective transformers in our electrical distribution system can be responsible for load imbalance. Now we have to see how this can affect the performances of load such as motor. It can cause serious reduction in starting torque due to low voltage in one or more phases. It may cause excessive and unbalanced full load current to flow. There is a chance that it can cause nuisance overload tripping, it may lead to rotor overheating which may cause permanent damage to the rotor winding, if preventive measures be not be adopted. Due to the Backward rotating field caused by unbalanced phase current may result into nuisance. Lastly the possibility of premature failure of motor windings cannot be ignored if proper overload protection is not used and known to be functional. Load unbalancing often disturbs the neutral current as well. On a three-phase system where the dominant loads are single phase, the neutral carries the unbalanced amount of current. Even though the loads may have been balanced at one time, the

normal changing of the system may have caused a large unbalance, leading to a large neutral current. Many times, when sizing loads and distributing them within a panel, only the full load current is considered, not how often that load is on or off. So, at any given time there may be significant unbalance due to loads being on or off. Whether because of

load shifts and changes, or due to the diversity of loads being on or off at the same time, neutral current from unbalance may become high. Problems happen when the neutral wire has been undersized and high currents still occur – possibly leading to a burnt neutral. Quite often this is aided by illegal wiring practices. High neutral currents from unbalance are fairly easy to resolve. Loads need to be powered from appropriate phase to ensure balancing, so relocate or rewire particular loads to bring balance about. If diversity is the problem, then use a power flow monitor such as the Power Profiler to determine the current swings of loads and when the shifts occur. Then rewire or relocate to bring in a better balance. In both cases, keep the neutral conductor at least the same size as the phase conductors. For those who really want to think ahead, make the neutral one size larger. This will help deal with the concern over harmonics.

Considering the practical scenario of India, load unbalancing has been a major problem which has several times resulted in burnt neutrals. A burnt neutral not only requires immediate attention for restoration of electrical supply to user but also wastes valuable time of utility engineer, technician and other workers. One of the techniques used for creation of a three-phase supply from a non three-phase supply is use of ARNO converter. ARNO converter is a device which converts single phase or two phase supply to a three phase supply which can be further used to run three phase machines. ARNO converter is a rotary converter also called a rotating phase converter. Its main application is in electric locomotive for conversion of single phase supply output of main traction transformer to three phase supply to meet the electrical load demand of three phase auxiliary motors. With the changing times, it has been discovered that there are some advantages of static converters on AC locomotives when used in place of ARNO converters. These include output of static converters remains balanced and also voltage variations remain within $\pm 5\%$ of the rated output voltage of the static converter. The efficiency and power factor of the static converter is also considerably more than that of ARNO converter. Due to which considerable energy can be conserved. Absence of moving parts in the static converter makes its construction rigid, maintenance free. Further, absence of pulsating torques results in less mechanical failures of auxiliary machines. Lastly we can use soft switching in traction auxiliary supply machines which gives low switching losses. The low failures on electric locomotive with provision of static converter shows the benefit of static converters in making the auxiliary supply voltage variation and distortion within limits. There is also saving in energy consumed due improved efficiency of static converter. No load test and Full load test reveals that the three phases output of the ARNO converter is highly

unregulated, unbalanced and distorted. Hence this output affects the performance of the auxiliary motors badly. There is an Increase in hysteresis and eddy current losses of the induction motor which in turn further increases losses which requires the need of better ventilation.

Voltage unbalance of 5% can causes the current unbalance of the order of 40%. Hence motor fails to give its standard output. Due to these unbalance currents rotor of induction motors gives increased pulsating torques which results invibrations of the rotor bars and hence about 20% additional losses. It is seen that by replacing the ARNO converter with the modern static converter failure of auxiliary machine reduces considerably as the out voltage variations and balanced supply voltage is obtained. Hence use of solid state static converter in place of ARNO converter in the modern scenario must be preferred. But the problem is that in villages, where this is being used illegally to generate three phase supply from their domestic connections. Even the CFL bulbs having greater advantages of lower power consumption are still to replace traditional incandescent bulbs, thus replacing the ARNO converter with static converters will be a hard nut to crack.

To analyze the effect of load unbalancing which is happening due to use of two phase supply for running three phase machines, a 5 bus system is created.

IV. MODELING

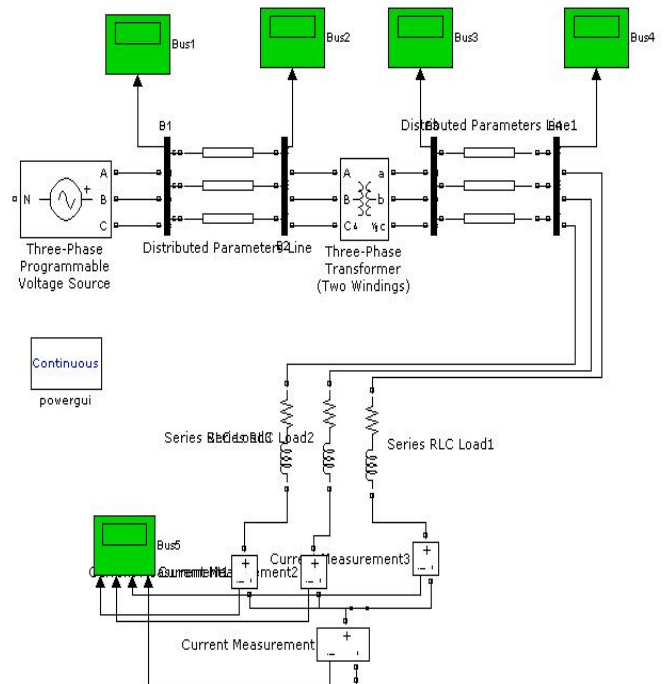


Fig. 1. 5-Bus Model to study the load unbalancing.

TABLE I
READINGS IN CASE OF A BALANCED SYSTEM

In the above figure, we have a bus1 which is an infinite bus then we had a short transmission line of 2000feet. Then there is a transformer to convert the voltage level down to 400volts line to line. Then again we have another short transmission line of 2500 feet. After that we have inductive loads attached to it. In balanced conditions the there is a neutral current of almost zero value.

V. OBSERVATIONS AND CALCULATIONS

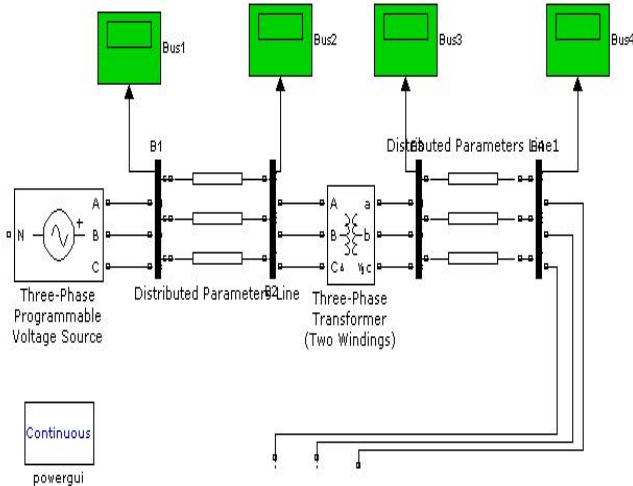


Fig. 2. Model at no load condition.

At no load condition, we have all buses showing magnitude of 1.0 pu which must be as there is no load on the model. All four buses are showing unity per unit voltage level.

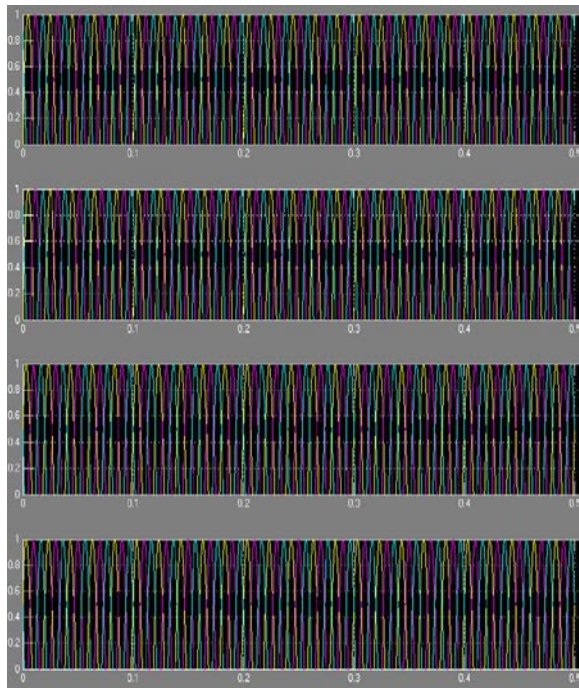
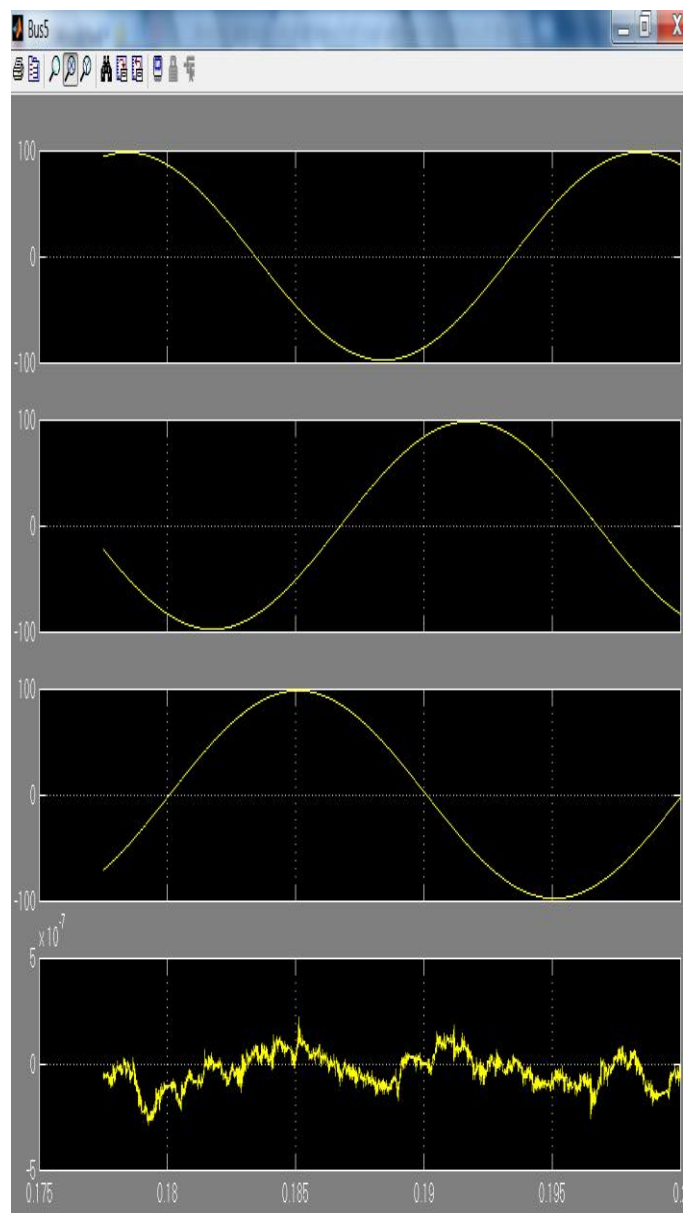


Fig. 3. Simulation results of Model at no load condition.

Fig. 4. Simulation results of Model at balanced load



Let us consider a case of unbalancing where loads are unbalanced in the Ratio 4:5:6

TABLE II
READINGS IN CASE OF AN IMBALANCED SYSTEM

| Reading | R | Y | B | N |
|----------------------------------|-------|-----------|-------|-------|
| Current | 79.79 | 99. 31 | 114 | 28.76 |
| P(Real Power of Load in KW) | 12 | 15 | 18 | - |
| Q(Reactive Power of Load in KVA) | 6 | 7.5 | 9 | - |
| Power Factor | 0.894 | 0.8 94 | 0.894 | - |

We can see that there is a considerable change in current waveforms and further the voltage waveform has also undergone various distortions.

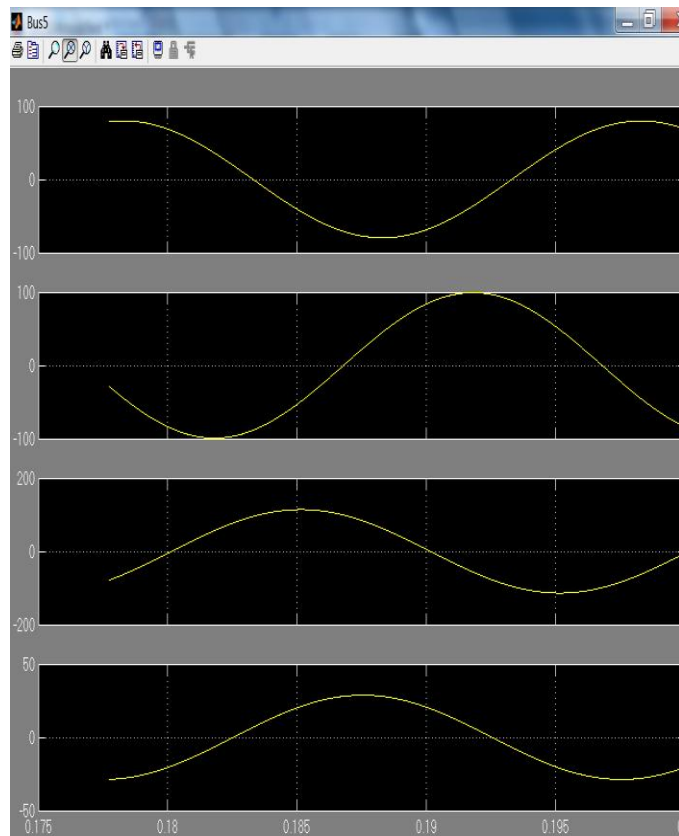


Fig. 5. Current waveforms at unbalanced load.

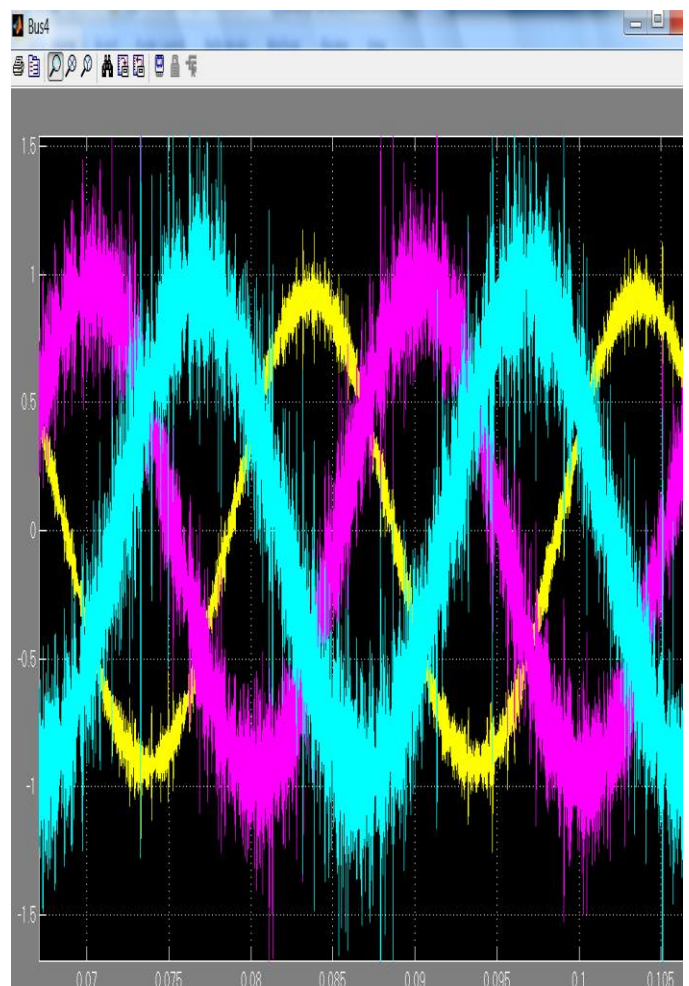


Fig. 6. Voltage waveform at unbalanced load.

We can see that there is a considerable change in current waveforms and further the voltage waveform has also undergone various distortions.

almost 36% of the current flowing in one of the phase of the circuit which is no doubt a big reason to worry.

Load unbalancing is one of the prime causes for the degradation in the power quality. Thus we need to have automatic techniques for load balancing. In most of the India as of now, we manually balance the Load. Since domestic load is very dynamic in nature, thus balancing the load is the ultimate need of the hour. Balancing the load will help us to save the current and power loss which would have taken

place in form of neutral heating and even burning in some cases. Thus we need to keep all phases balanced for uplifting power quality of our domestic power distribution system.

VI. RESULTS AND DISCUSSION

It is obvious from the above interpretation that due to load imbalance, there is a flow of current through the neutral which also distorts the supply voltage profile. This may result into potential damage to the nearby equipments sensitive to power quality. In case of balanced 3-phase loads, there is a neutral current of order of nanoamperes. In the case of unbalanced load condition, we had a neutral current of 28.76 Amperes which is almost 36% of the current flowing in one of the phase of the circuit, which no doubt, is a big reason to worry.

Load imbalance is one of the prime causes for the degradation in the power quality. From the FFT analysis carried out on the 4-Bus system, it can be observed that due to the load imbalance, the THD has reached the level of 14.23%. Thus we need to have automatic techniques for mitigating the evil impact of load balancing on the healthy condition of the system. In Indians scenario, as of now, we balance the Load manually. Since domestic load is of very dynamic nature, thus balancing the load is the ultimate need of the hour. Balancing the load will help us to upgrade the power quality as well as for avoiding the unwanted power loss in the distribution system. Added to this, by means of load balancing, we may avoid the malfunction and unwanted heating of motors. Thus we need to keep all phases balanced for uplifting power quality of our domestic power distribution system.

VII. ACKNOWLEDGMENT

The authors gratefully acknowledge the continuous and esteemed guidance of Dr. M.K.Verma, (Associate Professor, Indian Institute of Technology, Banaras Hindu University, India). Without his

support and guidance this work wouldn't have been possible. The authors are thankful to Head and all other teaching and non-teaching staff of Electrical Engineering Department who gratefully.

We are thankful to Engineer Bala Guru Nathan, Schneider Electric Infrastructure Limited and Engineer Anand Kumar Electrical Division, National aerospace Laboratories, HAL Airport Road, Kodihalli, Bangalore. We are thankful to staffmembers of Electrical and Water Dept, Banaras Hindu University for assisting us whenever required. Lastly the authors thank their family and friends for continuously providing all types of support whenever needed.

VIII. REFERENCES

- [1]. D.K. tanti, M.K.Verma, Brijeshsingh, O.N. mehrotra, "optimal placement of custom power devices in power system network for load and voltage balancing", International Journal Of Electrical Engineering And Technology(IJEET), volume 3, Issue 3, October-December 2012, pp 187-199.
- [2]. "All India Region wise Generating Installed Capacity of Power". CentralElectricity Authority, Ministry of Power, Government of India. February2013.
- [3]. N. Gupta, A. Swarmkar, KR. Niazi. *A novel strategy for phase balancing in three-phase four-wire distribution systems*. IEEE Power and Energy Society General Meeting, ISSN 1944-9925, San Diego (CA), 1-7, 2011.
- [4]. Annette von Jouanne, "assessment of voltage imbalance", IEEE Transaction on power Delivery, Vol. 16, No. 4, October 2001.
- [5]. IEEE Recommended practice for industrial and commercial powersystems analysis Standard 399-1997, IEEE, ISBN 1-55937-968-5 page47.
- [6]. Wikipedia, the free encyclopedia, Electricity distribution. Retrievedfrom World WideWeb.
- [7]. Brown, R. E., "Electric Power Distribution Reliability", Marcel Dekker,Inc., 2002.
- [8]. J. C. Balda, A. R. Oliva, D. W. McNabb and R. D.Richardson,
- [9]. "Measurements of neutral currents andvoltages on a distribution feeder",IEEE Trans Power Delivery, 12(4), October 1997, pp 1799-1804.

Comparative Study of Different Fusion Techniques in Multimodal Biometric Recognition

A. Shalini verma, B. Dr.R.K.Singh, C. Mr.A.K.Singh

Abstract- Multimodal biometric authentication resolves no. of issues present in uni modal biometrics. There are number of ways for the fusion of different modalities in multimodal biometrics. Fusion could be either before matching the scores or after matching the score. The presented research paper deals with the comparative study of different techniques which performs fusion of information after matching.

General Terms

Multi biometrics, fusion schemes

Keyword-Multimodal biometrics, Score level fusion, Rank level fusion, Decision level fusion

I. INTRODUCTION

In the present era of information technology, there is a need to implement authentication and authorization techniques for security of resources. There are number of ways to prove authentication and authorization. Biometric techniques prove the authenticity or authorization of a human being based on his/her physiological or behavioural traits.

Based on the usage of number of traits, they are divided into two categories:

1. Uni modal biometrics – Use of only one trait e.g. face, fingerprint, iris, retinal, gait etc.
2. Multi biometrics – Use of two or more traits or algorithms or samples

Uni modal biometric authentication suffers from the following problems:

1. Noisy sensor data
2. Non-Universality
3. Lack of individuality
4. Lack of invariant representation

All these problems can be overcome with the help of multi biometric authentication. Multi biometric authentication can be achieved in different ways like:

1. Multi-algorithm systems – the same biometric data processed with different algorithms.
¹

2. Multi-sensor systems – the single biometric trait imaged using multiple sensors.
3. Multi-sample systems – a single sensor used to get multiple samples of same biometric trait
4. Multi-modal systems – use of the evidences collected from multiple trait

The first four authentications can be achieved with the help of even single modality, while the fifth authentication can be achieved with the help of multiple modalities. Multimodal biometric authentication requires fusing information of different modalities like fingerprint, face, iris, retina, voice etc... The fusion can be achieved in two different ways. The first is information fusion prior to matching and the second method is fusion after matching [1].

1.1 Fusion prior to matching

Fusion prior to matching can be achieved in two different ways:

1. Sensor level fusion
2. Feature level fusion

Sensor level fusion is applicable only if the multiple sources represent samples of the single biometric trait obtained either using a single sensor or different compatible sensors.

Feature level fusion is achieved by combining different feature sets extracted from multiple biometric sources. Feature sets could be either homogeneous or heterogeneous. The consolidation of feature set creates problems as the feature sets originate from different algorithm and modalities.

1.2 Fusion after matching

Fusion after matching can be achieved in three different ways:

1. Matching score level fusion
2. Rank level fusion
3. Decision level fusion

Matching score level fusion provides richest set of information.

Rank level fusion consolidates the ranks output by the individual subsystems in order to derive a consensus rank of each identity. Rank level fusion provides less information with compare to match score level fusion.

Decision level fusion is carried out at decision level when the decisions output by the individual matcher are available. COTS (Commercial Off The Shelf) matchers provide only the final decision and those decisions are evaluated with the help of rules like “AND” or “OR”, majority voting, Bayesian decision fusion etc. Here the problem is that we have least information about the features or scores of different

A. PG Scholar, ECD, KNIT Sultanpur
Shalinive1990@gmail.com
B. HOD, ECD, KNIT Sultanpur
Singhrabinder57@gmail.com
C. Professor, ECD, KNIT Sultanpur
Anilkumarsingh1961@rediffmail.com

modalities.

The researcher has selected fusion after matching because sensor level fusion and feature level fusion are less informative. Also we cannot ignore any data and also the fusion of data set is complex to achieve.

II. MATCH SCORE LEVEL FUSION

This fusion technique is also known as measurement level or confidence level fusion. It is comparatively easy to consolidate the scores generated by different biometric matchers. This method is the most commonly used method for fusion.

Here we have to identify the pattern only in two classes: genuine (Truly what something is said to be; authentic) or impostor (A person who pretends to be someone else in order to deceive others, esp. for fraudulent gain). In general there are three different methods to achieve match score level fusion. They are:

1. Rule based score fusion
2. Classification based score fusion
3. Estimation based score fusion

As the match score level fusion use scores from different modalities based on different scaling methods, the scores cannot be combined or used directly. It is required to perform score normalization, thereby converting the scores into common domain or scale.

Score normalization can be carried out with different methods. Here are some methods of normalization worked well with different modalities. Slobodan Ribaric and Ivan Fratric carried out experiments for bimodal biometrics with palmprint and facial features [2]. They discovered new normalization technique – piecewise linear normalization. They calculated EER (Equal Error Rate) and minimum TER (Total Error Rate) with different normalization technique. They achieved EER of 2.79 % and min. TER of 5.15 % with this normalization. The chart of comparison is given below:

Table 1. EER and Min. TER under different normalization techniques

| Normalization Technique | Piecewise linear | median-MAD | Tanh | Minmax |
|-------------------------|------------------|------------|------|--------|
| EER | 2.79 | 2.79 | 3.05 | 3.12 |
| Min. TER | 5.15 | 5.42 | 5.74 | 6.39 |

Mingxing He et al. Proposed a new method of normalization for scores in score level fusion, Reduction of High-scores Effect normalization (RHE) [7]. They experimented on four different databases with multi modality of fingerprint, face and fingervein. They revealed that RHE performs better with compare to other techniques of score normalization in score level fusion.

Table 2. Performance of sum rule-based fusion on NIST multimodal database [7]

| FAR (%) | GAR (%) | | | |
|---------|---------|---------|------|------|
| | Minmax | Z-score | Tanh | RHE |
| 0.01 | 97.9 | 98.2 | 97.7 | 99.4 |
| 0.001 | 96.9 | 97.0 | 95.8 | 98.2 |

After performing normalization, the next step is to perform fusion of the scores. Here are some examples of different fusion models for score level fusion. Gian Luca Marcialis and Fabio Roli suggested the following model for score level fusion of fingerprint and face traits [3].

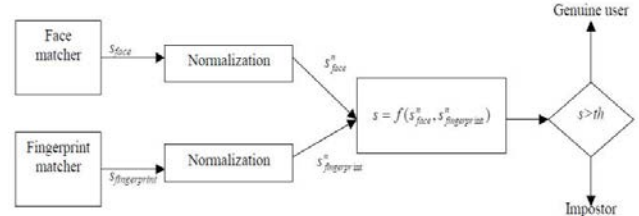


Fig. 1 Score level fusion suggested by Roli and Marcialis [3].

They carried out experiments on multimodal data set made up of 100 subjects with two independent face and fingerprint data sets. With the above given scheme, they achieve improvement in the error rate. Their results showed that fusion has improved the reliability of the system by reducing the gap between expected and real performance.

Feifei Cui and Gongping Yang performed biometric fusion with fingerprint and finger vein recognition [4]. They did this with score level fusion. They collected 2880 fingerprint and finger vein images from 80 fingers. With score level fusion they achieved the following performance:

Table 3. Recognition rate for fingerprint and finger vein fusion.

| Biometrics method | Recognition rate |
|--------------------|------------------|
| Fingerprint | 95.3 % |
| Finger vein | 93.72 % |
| Score level fusion | 98.74% |

These results shows that score level fusion works well with compare to unimodal biometric traits.

Fawaz Alsaade experimented score level fusion with face and voice biometrics. He investigated the results under three data

conditions and with min-max normalization. He used Adaptive Neuro – Fuzzy Inference System (ANFIS) for decision making [5]. He was able to achieve 0 % EER with ANFIS approach with clean data of both face and voice biometrics.

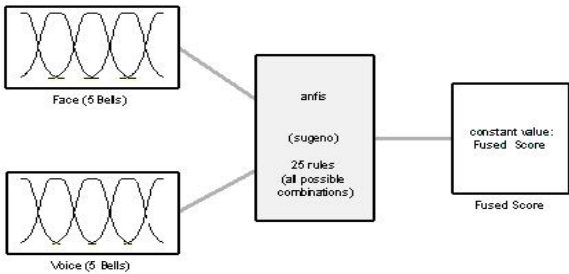


Fig. 2 The ANFIS structure proposed by Fawaz Alsaade [5]

Table 4. Multimodal biometric verification based on clean biometric data [5].

| Modality | EER% |
|---|------|
| Voice (TIMIT Database) | 2.55 |
| Face (XM2VTS Database) | 3.57 |
| Fused: voice and face by BFS (Brute force search) | 0.05 |
| Fused: voice and face by SVM | 0.68 |
| Fused: voice and face by ANFIS | 0 |

Sarat C. Dass et al. proposed a framework to combine the match score from multiple modalities with the use of likelihood ratio statistic computed using generalized densities which were estimated from genuine and impostor match scores[6]. They conducted experiments on two different databases with different number of users. The details of databases are shown in table -5:

Table 5 – Details of databases used by Sarat Dass et al. [6].

| Database | Modalities | No. Users |
|-----------------|--|-----------|
| MSU-Multimodal | Fingerprint, Face, Hand-Geometry | 100 |
| NIST-Multimodal | Fingerprint (Two Fingers), Face (Two matchers) | 517 |

They proposed two different approaches to combine evidences based on generalized densities:

1. Product rule
2. Copula model

With the above given database and these two score fusion methods, they achieved consistently high performance.

Romaissa Mazouni and Abdellatif Rahmoun fused face and speech modalities with five different methods of score level fusion: Particle Swarm Optimization (PSO), Adaptive Neuro Fuzzy Interface Systems (ANFIS), Genetic Algorithm (GA), Brute Force Search (BFS), and Support Vector Machine (SVM) [8]. They did their experiments with three kinds of datasets: Clean data, Varied data, Degraded data. They derived the conclusion that Genetic algorithm (GA) and Particle Swarm Optimization performed best among all five method even in worst conditions.

III. DECISION LEVEL FUSION

Now a day, if you are using commercial off the shelf tools for biometric verification, then decision level fusion is the only option for fusion, as they don't provide the data about the scores or feature neither they provide details about the ranking of different users after comparison. Decision level fusion is also referred as *abstract* level fusion. They only provide the result of matching in the form of whether the user is genuine or imposter. With decision level fusion, there are different rules that can be used to authenticate the user. Lam and Suen proposed majority voting rule [9]. They also proposed behavioral knowledge space method. Xu et al. proposed weighted voting based on Dempster - Shafer theory [10]. Daugman proposed AND/ OR rules for deciding the decision [11].

The general and mostly used approach for decision level fusion is majority voting. Here the input sample is given the identity for which the majority of the matchers are agreed. AND and OR rules are used rarely, because as they combine two different matchers, so sometimes degradation of performance could be there with this method [11]. The main benefit of the majority voting method is that neither you require prior knowledge about the matcher nor the training is required for final decision making [1]. Domingos and Pazzani suggested that naïve Bayesian decision fusion works very well even if the matchers are dependent to each other [12].

IV. RANK LEVEL FUSION

The rank level fusion is generally adopted for the identification of a person rather than verification. In verification, as we have to compare the template only with one template in the database, here we have to generate rank of identities in sorted order with all modalities. Then after with the help of one method of fusion, we have to fuse the ranking for each person available for different modalities. Then the identity with lowest score is identified as the correct person. This method provides more accuracy with compare to just identifying best match with one modality. But the only thing is that, it provides less information for fusion purpose. With compare to match score level fusion, here you can easily compare the ranking from different

modalities. So the decision making is easy.

Md. Maruf Monwar and Marina L. Gavrilova carried out rank level fusion with face, signature and ear biometric traits [13].

They performed experiments with PCA and fisher's LDA. The rank of individual matchers was combined with highest rank, Borda count, and logistic regression approaches. With this approach, the performance was improved performance even with low quality of data. Table 6 shows performance of the experiment.

Table. 6
Comparison of different multibiometric systems [13].

| Systems | Biometric identifiers | Fusion level and approach | EER |
|-------------------------|-----------------------|---------------------------|-------|
| Md. Maruf Monwar et al. | Face, Ear, Signature | Rank ; logical regression | 1.12% |
| Garcia Salicetti et al. | Signature, Voice | Match score; | 1.88% |
| Nandkumar et al. | Fingerprint | Match score | 3.39% |

Ajay kumar and Sumit Shekhar suggested combination of multiple palmprint representations to achieve improvement in the performance with compare to individual performance [14]. They performed various rank level combinations like, Borda Count, Logistic Regression, Highest rank method and Bucklin majority voting approach. With this approach, they performed experiments with NIST BSSR database. The nonlinear fusion approach gave best results for first – rank recognition rates. Average rank one recognition rate was of 99%.

With rank level fusion, three most common approaches are Borda count method, Logistic Regression method and Highest rank method. Out these three methods, Borda count and highest rank method do not use statistical information of the classifier performance. But with Logistic regression method, statistical information is required and weights are assigned to classifiers. These weights depend on the data.

Abaza and Ross performed experiments with two modalities: Fingerprint and Face [15]. They evaluated results with two databases: WVU and NIST. With Modified Highest Rank method, they achieved rank - 1 accuracy of ~ 99 % on WVU dataset. They proposed Q-based rank algorithms for rank level fusion. They were able to improve the performance by ~4 %.

V. CONCLUSION

In today's environment, commercial biometric systems are very popular. And with these commercial systems, the person cannot get rich information about the biometrics data. But they can provide the information, which is sufficient for either rank level, decision level or score level fusion (fusion after matching). At the same time they are also efficient to give acceptable accuracy for verification and identification. From the above discussion, we can summarize that score level fusion provides more information about the biometric data compare to rank level and decision level fusion. But complexity is more. At the same time, decision level fusion provides very less data i.e. only the results of modalities, so it is very easy to implement. But rank level fusion is better than this approach, as it provides rank to different matches and also we can assign weights to some classifiers. So the researcher has concluded that for better results, one should prefer either rank level or score level fusion.

VI. REFERENCES

- [1] Anil Jain, Karthik Nandakumar, Arun Ross, "Score Normalization in Multimodal Biometric Systems", *Pattern Recognition*, 2005.
- [2] Slobodan Ribaric, Ivan Fratric, "A matching score normalization technique for multimodal biometric systems."
- [3] Gian Luca Marcialis, Fabio Roli, "Score-level fusion of fingerprint and face matchers for personal verification under "stress" conditions", *14th IEEE International Conference on Image Analysis and Processing ICIAP 2007*, IEEE (2007), pp. 259-264
- [4] F. Cui, et al., "Score Level Fusion of Fingerprint and Finger Vein Recognition", *Journal of Computational Information Systems* 7: 16 (2011) 5723-5731
- [5] Fawaz Alsaade, "Neuro-Fuzzy Logic Decision in a Multimodal Biometrics Fusion System". *Scientific Journal of King Faisal University (Basic and Applied Sciences)* Vol.11 No.2 1431 (2010)
- [6] Sarat C. Dass, et al., "A Principled Approach to Score Level Fusion in Multimodal Biometric Systems", *AVBPA 2005: 1049-1058*
- [7] M. He, et al., "Performance evaluation of score level fusion in multimodal biometric systems", *Pattern Recognition* (2009)
- [8] Romaissa Mazouni, et al., "On Comparing Verification Performances of Multimodal Biometrics Fusion Techniques", *International Journal of Computer Applications*, Volume 33– No.7 :24-29
- [9] Lam, L. and Suen, C. Y., "Optimal Combination of Pattern Classifiers", *Pattern Recognition Letters*, 16:945-954.
- [10] Xu, L., Krzyzak, A., and Suen, C. Y., "Methods for Combining Multiple Classifiers and their Applications to Handwriting Recognition", *IEEE Transactions on Systems, Man, and Cybernetics*, 22(3):418-435.
- [11] Domingos, P. and Pazzani, M., "On the Optimality of the Simple Bayesian Classifier under Zero-One Loss", *Machine Learning*, 29(2-3): 103-130.
- [12] Md. Maruf Monwar, Marina L. Gavrilova, "Multimodal Biometric System Using Rank-Level Fusion Approach", *IEEE Transactions on Systems, Man and Cybernetics – Part B: Cybernetics*, Vol. 39, No. 4, August 2009, pp. 867-878
- [13] Ajay Kumar, Sumit Shekhar, "Personal Identification Using Multibiometrics Rank-Level Fusion", *IEEE Transactions on Systems, Man and Cybernetics- Part C: Applications and reviews*
Ayman Abaza, Arun Ross, "Quality Based Rank-Level Fusion in Multibiometric Systems", *Proc. of 3rd IEEE International Conference on Biometrics: Theory, Applications and Systems (BTAS)*, (Washington DC, USA), September 2009.

Empirical Study of a Solar Still Coupled with an Evacuated Tube Collector

A.Shitosh Dillu, B. A. K. Gautam, *Student Member, IEEE*, and C. Dr. Amit Medhavi

Abstract-- In this paper, we study Solar distillation is a promising method for clean water supply to rural communities where the quality of water is poor and sunshine is abundant. Due to a lower yield of water distilled in a passive solar still, it is not popularly used and commercialized. Various active methods were developed to overcome this problem.

It has also been observed that the efficiency of an active solar still is lower than the passive solar still in high temperature operations.

Keywords: Solar distillation, solar still

Index Terms--The author shall provide up to 4 keywords (in alphabetical order) to help identify the major topics of the paper. For example; Active solar still, efficiency, performance, solar collector.

I. INTRODUCTION

Fresh water is the basic need of human welfare and it is adversely affected by the pollution created by man-made activities. Recent statistics show that more than 884 million people lack access to safe water. On one hand, demand for fresh water is increasing rapidly, while on the other hand, supply is decreasing over the last decades. This is the right time to develop technology to match the supply and demand for fresh water, Technology must enable to reduce CO₂ and other gaseous emissions and this compels the countries turn to non-polluting renewable energy sources.

Solar distillation is one of methods for water purification and it is more popular particularly in rural areas. The technology is simple and more economical than the other available methods. A solar still operates similar to the natural hydrological cycle of evaporation and condensation. Several types of solar stills were developed over the years.

Simplest one, is called a passive solar still. It has many features, such as simplicity in construction, operation, cost effectiveness, and eco friendly, but it has a low yield (2-4 kg/day/m²). Many researchers made an attempt to enhance the yield of the solar still and one of the methods is an active solar still. In an active solar still, extra thermal energy is fed into the basin water to enhance the water temperature through the concentrated solar collectors or other heat sources. The single basin solar still is coupled with a flat plate solar collector

A) Shitosh Dillu and B.) A.K. Gautam are PG Scholar with dept. mechanical engg. And Dept Electrical Engg., KNIT Sultanpur. Email: ,abhinavgautam97@gmail.com

C) Dr. Amit Medhavi are Asst. Professor with Dept. of Mechanical Engineering, KNIT Sultanpur,U.P

through natural circulation mode and it enhances the productivity by 30-52% compared to the simple solar. More than 50% of productivity enhancement was achieved by a solar still coupled with a flat plate solar collector through forced circulation. The solar still coupled with a parabolic concentrator increases the productivity by 35-45% and it was more in a double effect solar still. The stepped solar still is augmented with a solar pond with a fin and sponges used in the basin. This type of system enhances the productivity up to 80%. The coupling of a single effect solar still of greenhouse type produced two times the distilled water than compared to a simple solar still.

A single basin solar still coupled with a hybrid PVET system gave three times higher yield than a simple solar still. Other active methods, such as heat pipe and multistage evacuated solar distillation also produced higher yields. Most of the above works used a solar pond, solar parabolic concentrator, and heat pipe to increase the daily average yield of the solar still and many works have been reported in a solar still coupled with a flat plate collector. Evacuated tube solar collectors are well known for their higher efficiencies compared to flat plate solar collectors in high temperature operations. The evacuated tube greatly reduces the heat losses due to the vacuum present in the tubes. Research study inferred that water in a glass evacuated tube collector is the most successful due to its simplicity and low manufacturing cost. The current market price of flat plate and heat pump solar water heaters is 30–50% higher than evacuated tube solar water heaters. Tiwari et al. (2007) developed thermal models for a flat plate collector, concentrating collector, evacuated tube collector, and a heat pipe. Their results show that the productivity of the active solar stills is much higher than compared to the passive solar still. Within the active solar stills, the higher output was produced by evacuated tube collector with heat pipe followed by the concentrating collector, evacuated tube collector, and flat plate collector. A thermal model with a flat plate collector was developed and experimentally validated.

The main objective of this work is to present a new design for a solar distillation coupled with an evacuated tube solar collector for productivity enhancement. A solar still coupled with an evacuated tube collector was fabricated and tested. A passive solar still of the same specification was also fabricated and tested for comparative studies and their results are explained in this article in detail.

II. EXPERIMENTAL STUDY

A. Single Basin Passive Solar Still

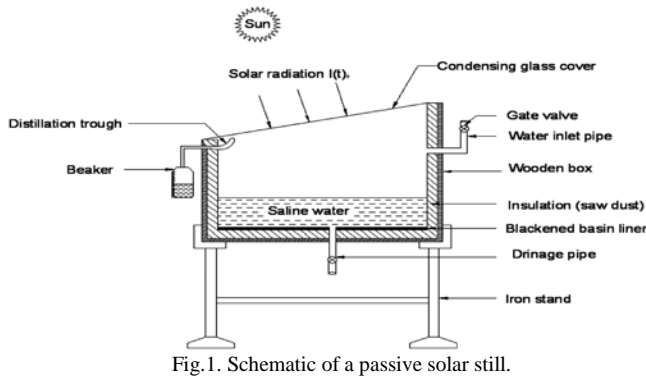


Fig.1. Schematic of a passive solar still.

Fig.1. illustrates the schematic of a single basin solar still.

SOLAR STILL COUPLED WITH EVACUATED TUBE COLLECTOR

The inner surface of the basin is painted in dull black to absorb the maximum solar radiation. A similar type of box structure is made using plywood with an area of $1.05 \text{ m} \times 1.05 \text{ m}$ to enclose the still. The gap of 0.05 m is provided between the still and box. The saw dust is used as the insulation material, which is filled tightly at the bottom and the sides of the solar still. An inlet pipe is fixed at the rear side of the solar still for supply of brackish water, and two pipes are fixed at the bottom and left side of the solar still. The ordinary clear window glass cover is fixed on the still at an inclined angle of 11° . The silicon rubber sealant is used to keep the glass cover intact with the solar still and to prevent leakages. The distillate water condensed from the glass cover is collected in a U-shaped galvanized iron sheet fitted at the lower side of the solar still. Further, rubber pipe is connected to the collection tray for collecting desalinated water in a measuring jar. Holes were drilled in the body of the still to fix the J-type thermocouples to measure the temperatures at various places. The whole unit is mounted on a $1.10 \text{ m} \times 1.10 \text{ m} \times 1.50 \text{ m}$ iron stand. The solar still is oriented toward the south in order to receive the maximum solar radiation throughout the year.

B. Single Basin Active Solar Still

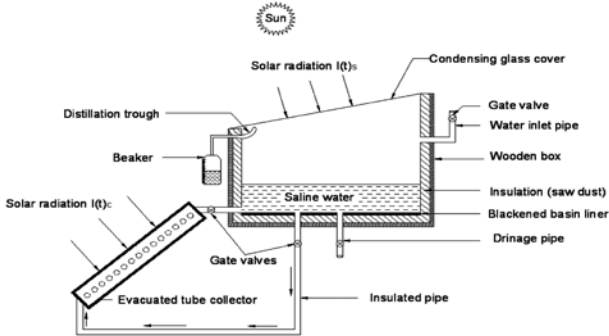


Fig.2. Schematic of an active solar still.

The schematic of the single basin active solar still is shown in Figure 2. The system consists of two main components, namely, an evacuated tube collector and a solar still. Fifteen numbers of double-walled hard borosilicate glass tubes with 1.6 mm thickness, inner diameter of 47 mm , outer diameter of 58 mm , and length of 1.5 m are used in the collector. The evacuated tubes are coupled to a horizontal manifold with an

absorber area of 1.0575 m^2 . The outer tube is transparent and allowing light rays to pass through it. The inner tube is coated with a selective coating of aluminium nickel alloys compound ($\text{Al-N}/\text{Al}$) for better solar radiation absorption ($>93\%$) and minimum emittance ($<6\%$). The polyurethane foam insulation is used on the sides of the horizontal manifold to hold the evacuated tubes. The evacuated tubes are fixed in the manifold using rubber sealant to avoid leakages.

A tubular support structure, The assembly is mounted on an iron frame. The energy absorbed by each tube is transferred to the basin water via the horizontal manifold. The fabricated single slope passive solar still of the same specification is connected to the evacuated collector using insulated piping with gate valves. The bottom and side pipes in the solar still are connected to the inlet and outlet of evacuated tube collector, respectively. The position of thermocouples is fixed similar to the passive solar still. In an active solar still, the water in the basin gets heated directly by the sun and additional thermal energy is supplied from the evacuated tube solar collector. The system operates in a natural circulation mode and does not require any pump for circulation of water. The complete unit is oriented toward the south in order to receive maximum solar radiation throughout the year. The pictorial view of a single basin passive solar still and single basin active solar still is shown in Figure 3.

SOLAR STILL COUPLED WITH EVACUATED TUBE COLLECTOR

Fig. 3 Pictorial view of an experimental setup India. For every-day experiments, the glass cover was cleaned in the morning to avoid the dust deposition over the outer glass cover surface. The underground water is taken as sample and it is filled for desired depth before a day for the commencement of experiment in order to bring the basin water temperature in steady state condition. The experiments were started at 8:00 am and ended at 5:00 pm on clear sunny days. The night-time distilled water collections were measured every day at the commencement of the experiment. The ambient, basin liner, inner surface of the glass cover, outer surface of the glass cover, water temperature, wind velocity, hourly distillate yield, intensity of solar radiation on the still cover, and evacuated tube collector were measured on an hourly basis.

III. CONTROL TECHNIQUE

The intensity of solar radiation was measured by using a solarimeter with a range of $0-1, 200 \text{ W/m}^2$. It was calibrated with the help of a standard pyrometer and has an accuracy of $\pm 5 \text{ W/m}^2$. The wind speed was measured by a digital wind anemometer with the range of $0-15 \text{ m/s}$ and accuracy of $\pm 0.2 \text{ m/s}$. The temperature in various locations of the solar still and evacuated tube collector were recorded using J-type thermocouples with a range of $0-700^\circ\text{C}$ and an accuracy of $\pm 1^\circ\text{C}$ with a digital temperature indicator. The distillate yield is measured by using a plastic measuring jar with a range of $0-1,000 \text{ ml}$ and accuracy of $\pm 10 \text{ ml}$.

IV. RESULTS AND DISCUSSION

The experiments were conducted in different meteorological conditions to find the performance of the active and passive solar stills. The observed value on clear days is taken for the discussion. Figure 3 shows the hourly variation of solar radiation on the still glass cover and evacuated tube collector. It has been observed that the ambient temperature increases proportionally with the intensity of solar radiation and vice versa. It has also been observed that there is a small variation in intensity of solar radiation received by the still glass cover and evacuated tube collector. It is due to the variations in the inclination angle of the solar still and evacuated tube collector.

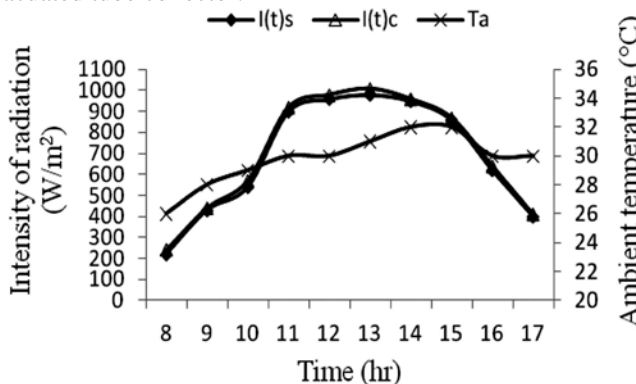


Fig.3 Hourly variation of solar radiation and ambient temperature.

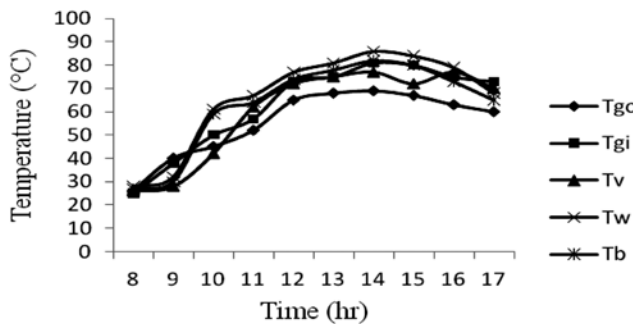


Fig.4 Hourly variation of outer glass, inner glass, vapor, water, and basin temperatures in an active solar still.

Fig. 4 and 5 show the hourly variations in the temperature of the outer glass cover, inner glass cover, vapor, water, and basin temperature of the active and the passive solar stills, respectively.

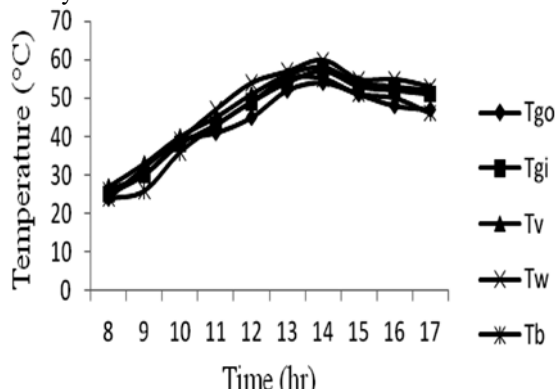


Fig.5 Hourly variation of outer glass, inner glass, vapor, water, and basin temperatures in a passive solar still.

All of them show a similar trend of increasing with the increase of the solar radiation. Only small variations were observed in the basin and water temperatures of both the solar stills. It is due to the low heat capacity of the absorbing material of the basin.

SOLAR STILL COUPLED WITH EVACUATED TUBE COLLECTOR

Temperature was higher than the outer surface glass cover in both of the stills during most parts of the time except during morning hours, because the condensation rate is more than the heat loss rate from the outer surface of the glass cover during the morning hours. It has been observed that commencement of experimental time, the outer surface of glass cover temperature was higher than the inner surface of the glass cover. It is due to the fact that low intensity of solar radiation is initially observed by the outer surface glass cover during morning hours. It has also been observed that the highest value of water temperature reached in the active solar still was 86°C at 14 h and it was higher than the passive solar still value of 60°C at 14 h at 0.04 m water depth on March 13, 2014. A similar trend has also been noticed for the inner surface of the glass cover temperature in active and passive solar stills. The vapor temperature was approximately average of water and inner surface glass cover temperature in both of the solar stills.

The hourly yield for active and passive solar stills during the day time is shown in Figure 7. It has been noticed that a solar still coupled with an evacuated tube collector has a significant increase in yield compared to a passive solar still throughout the day. The day time yield obtained from the passive solar still (2.445 kg) is lower compared to the active solar still (5.6 kg) at 0.04 m water depth on local climatic condition. The day time yield of the active solar still was 129% higher than the passive solar still. The maximum hourly yield of 1.12 and 0.62 kg was recorded in 14 h for the active and passive solar stills, respectively. The higher yield in the active solar still is due to the additional thermal energy supplied from the evacuated tube solar collector. From Figures 4 and 7, it is observed that the maximum intensity of solar radiation (980 W/m²) was recorded at 13 h. This is due to the time taken for water evaporation and condensation phenomena in the solar still basin. It has also been noticed that the intensity of solar radiation is directly proportional to the hourly yield of the solar still.

Fig.7 shows the day and night yield of active and passive solar stills during the day of the experiment. It has been observed that after sunset a higher yield was obtained in the active solar still than the passive solar still. It is due to the fact that the basin water temperature remained hotter in the active solar still than the passive solar still and the distillation continued during the night as well.

Fig. 8 shows the average comparative yield of the active and passive solar stills in different months of the year. It has been noticed that the maximum and minimum yields were based on the intensity of solar radiation. The highest average monthly yields obtained from the active and passive solar stills were 6.62 and 3.16 kg, respectively, in the summer months (March 2014). It has also been observed that monthly average measured yields in the winter

Fig.7 Hourly variation of yield in an active and a passive solar still.

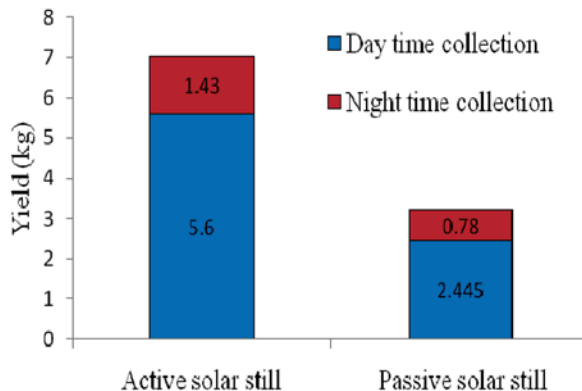
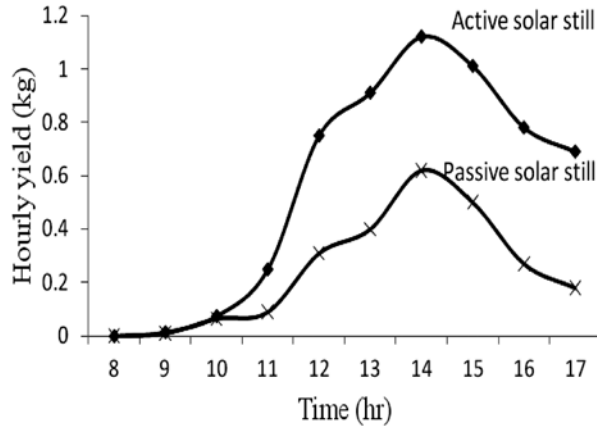


Fig. 7 Day and night yield of an active and a passive solar still. (Color figure available online) season (November 2009) were 4.76 and 2.52 kg, respectively. The low yield was due to partially cloudy conditions some days of the month. The total yields from the active solar still and passive solar still were observed as 911.5 and 512 kg, respectively, from June 2013 to March 2014. It is understood that the active solar still is more efficient than the passive solar still throughout the year. 3.1. Overall Thermal Efficiency of the Solar Still The overall thermal efficiency of the passive solar still is evaluated as (Tiwari et al., 2007):-passive Dmew_L.I.t /s _ As _ 3600/: (1)

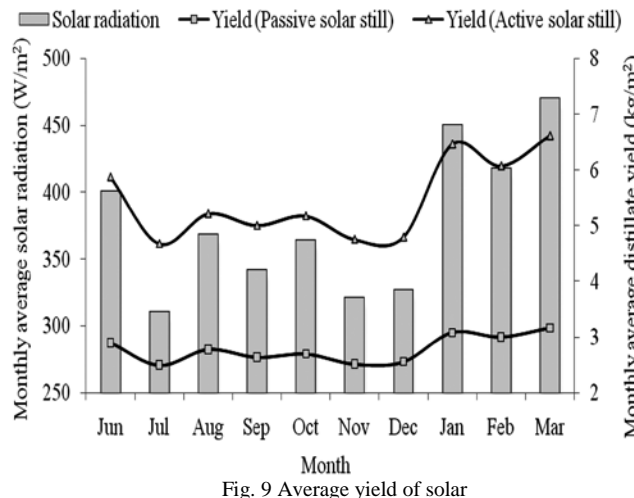


Fig. 9 Average yield of solar

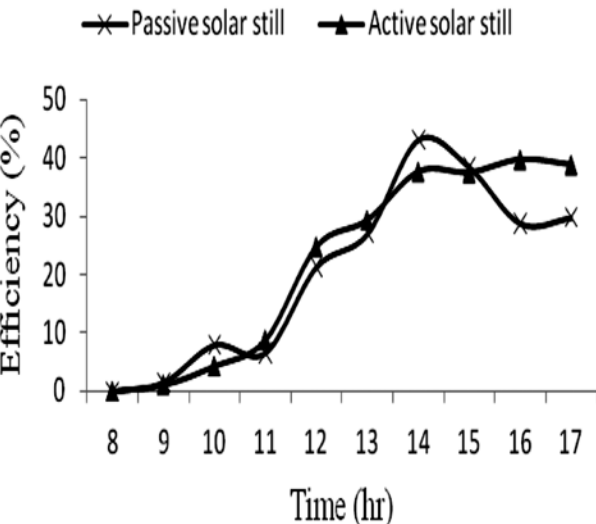


Fig. 10 Hourly variation in thermal efficiency of an active and a passive solar still.

The overall thermal efficiency of the active solar still is evaluated as: Active DMew_ L.I.t /c _ Ac _ 3600/C .I.t /s _ As _ 3600//: (2)

The above Eq. (1) and (2) are used to find the thermal efficiency of the passive and active solar stills using the experimental data. From Figure 10, it is observed that the thermal efficiency of the active solar still (43%) is lower than the passive solar still (37%) in the peak hours for a 0.04m water depth. This is due to the fact that, in high temperature distillation, the amount of heat loss to ambient air is higher than compared to useful energy gain at 13.30 h. But the daily yield of distilled water is maximum in a high temperature active solar still than compared to a low temperature passive solar still.

V. CONCLUSIONS

Based on the experimental investigation of a solar still coupled with an evacuated tube collector and a simple solar still, the following conclusions have been made: The distilled water yield is increased in an active solar still by 129% during the day time and 83% during night time than compared to a passive solar still. The maximum daily production of 7.03 and 3.225 kg are obtained from active and passive solar stills, respectively, at a water depth of 0.04 m. The additional thermal energy supplied by the evacuated tube collector increases the basin water temperature and in turn increases the yield. The active solar still is more efficient than the passive solar still throughout the year. However, the average monthly yield of the active solar still is higher in the winter than the summer.

As for further research work, it can be concluded that:

- The thermal efficiency of the active solar still is lower than the passive solar still; it can be increased by reducing the heat losses from the still.
- Performance study of a solar still coupled with an evacuated tube collector under forced circulation mode.
- Optimizing the number of evacuated tubes in the collector and inclination angle may increase the distillation water yield.

VI. REFERENCES

- [1]. Abdel-Rehim, Z. S., and Lasheen, A. 2007. Experimental and theoretical study of a solar desalination system located in Cairo, Egypt. Desalination 217:52–64.
- [3]. Ahmed, M. I., Hrairi, M., and Ismail, A. F. 2009. On the characteristics of multistage evacuated solar distillation. Renew. Energy 34:1471–1478.
- [5]. Badran, O. O., and Al-Tahaineh, H. A. 2005. The effect of coupling a flat plate collector on the solar still productivity. Desalination 183:137–142.
- [7]. Chaouchi, B., Zrelli, A., and Gabsi, S. 2007. Desalination of brackish water by means of a parabolic solar concentrator. Desalination 217:118–126.
- [9]. El Sebai, A. A., Ramadan, M. R. I., Aboul Enein, S., and Slaem, N. 2008. Thermal performance of a single basin solar still integrated with a shallow solar pond. Energy Convers. Manage. 49:2839–2848.
- [11]. Han, J., Mol, A. P. J., and Lu, Y. 2010. Solar water heaters in China. Energy Policy 38:383–391.
- [12]. Kumar, S., and Tiwari, A. 2008. An experimental study of hybrid photovoltaic thermal (PV/T) active solar still. Int. J. Energy Res. 32:847–858.
- [14]. Kumar, S., and Tiwari, G. N. 2009. Estimation of internal heat transfer coefficients of a hybrid (PV/T) active solar still. Solar Energy 83:1656–1667.
- [16]. Kumar, S., Tiwari, G. N., and Singh, H. N. 2000. Annual performance of an active solar distillation system. Desalination 127:79–88.
- [18]. Lawrence, S. A., and Tiwari, G. N. 1990. Theoretical evaluation of solar distillation under natural circulation with heat exchanger. Energy Convers. Manage. 30:205–213.
- [20]. Morrison, G. L., Budihardjo, I., and Behina, M. 2004. Water-in-glass evacuated tube solar water heaters. Solar Energy 76:135–140.
- [22]. Rai, S. N., and Tiwari, G. N. 1983. Single basin solar still coupled with flat plate collector. Energy Convers. Manage. 23:145–149.
- [24]. Sampathkumar, K., Arjunan, T. V., Pitchandi, P., and Senthilkumar, P. 2010. Active solar distillation—A detailed review. Renew. Sustain. Energy Rev. 14:1503–1526.
- [26]. Singh, H. N., and Tiwari, G. N. 2004. Monthly performance of passive and active solar stills for different Indian climatic condition. Desalination 168:145–150.
- [28]. Singh, S. K., Bhatnagar, V. P., and Tiwari, G. N. 1996. Design parameters for concentrator assisted solar distillation system. Energy Convers. Manage. 37:247–252.
- [30]. Tanaka, H., Nakatake, Y., and Watanabe, K. 2004. Parametric study on a vertical multiple effect diffusion type solar still coupled with a heat pipe solar collector. Desalination 171:243–255.
- [32]. Tiris, C., Tiris, M., Erdalli, Y., and Sohmen, M. 1998. Experimental studies on a solar still coupled with a flat plate collector and a single basin still. Energ. Convers. Manage. 39:853–856.
- [34]. Tiwari, G. N., Dimri, V., Singh, U., Chel, A., and Sarkar, B. 2007. Comparative thermal performance evaluation of an active solar distillation system. Int. J. Energy Res. 31:1465–1482.
- [36]. Velmurugan, V., and Srinivas, K. 2007. Solar stills integrated with a mini solar pond—Analytical simulation and experimental validation. Desalination 216:232–241.
- [38]. Voropoulos, K., Mathioulakis, E., and Belessiotis, V. 2001. Experimental investigation of a solar still coupled with solar collectors. Desalination 138:103–110.
- [40]. Voropoulos, K., Mathioulakis, E., and Belessiotis, V. 2003. Solar stills coupled with solar collectors and storage tankanalytical simulation and experimental validation of energy behaviour. Solar Energy 75:199–205.

NOMENCLATURE

Symbols

- Ac diameter of inner glass tube _ total length of the tubes, m²
- As basin liner still area, m²
- It /c intensity of solar radiation on evacuated tube collector, W/m²
- I.t /s intensity of solar radiation on solar still, W/m²
- L latent heat of vaporization, J/kg
- mew hourly distillate output, kg/m²

Grid Connected Photovoltaic System: A Review

Neha jaiswal¹ IEEE student member , S.M. Tripathi² IEEE member

Abstract—recently, the needs of renewable energy resources are increasing due to the fuel energy crisis and the global warming issues. Solar energy is one of the most important renewable energy.

The installation of PV system aims to obtain the maximum benefit of captured solar energy. In the I-V curve of PV module, there is a point at which the power is maximum for a particular irradiation condition. To achieve the maximum efficiency, it is necessary to track this maximum power point (MPP) called as MPPT (Maximum Power Point Tracking).

Photovoltaic (PV) power supplied to the utility grid is gaining more and more visibility, while the world's power demand is increasing. Integration of PV power generation systems in the grid plays an important role in securing the electric power supply in an environment-friendly manner.

Index Terms-Photovoltaic (PV) System, Maximum power point tracking (MPPT).

I. INTRODUCTION

Photovoltaic (PV) systems are the most promising as a future energy technology. The photovoltaic technology is used to obtain electricity from the sun that is cost competitive and even advantageous with respect to other energy sources [1]. A photovoltaic system converts sunlight into electricity. The basic device of a photovoltaic system is the photovoltaic cell. Cells may be grouped to form panels or modules. Panels can be grouped to form large photovoltaic arrays. The term array is usually employed to describe a photovoltaic panel (with several cells connected in series and/or parallel) or a group of panels. Photovoltaic modules or panels composed of several basic cells (Fig. 1). The term array used henceforth means any photovoltaic device composed of several basic cells [5].

Types of PV Systems

Photovoltaic power systems are generally classified according to their functional and operational requirements, their component configurations, and how the equipment is connected to other power sources and electrical loads. The two principal classifications are[2]

- Stand-alone or off grid systems and
- Grid connected or utility-interactive systems

a) Stand-alone Systems

Stand-alone PV systems are designed to operate independent¹

-
- PG scholar , EED KNIT sultanpur
neha.knit.14@gmail.com
 - Assistant professor, EED,KNIT sultanpur
mani_excel@gmail.com

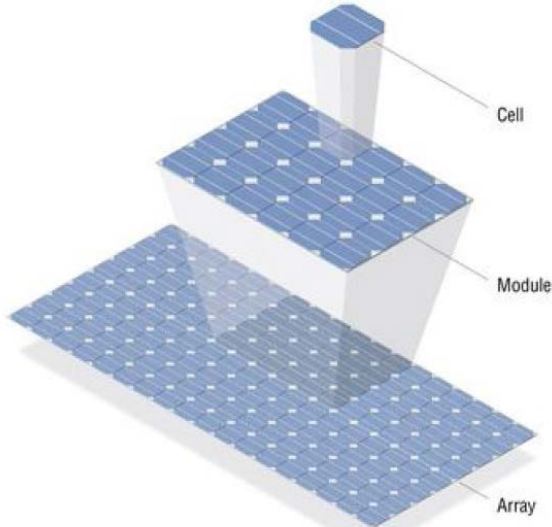


Fig. 1. Figure showing PV Cell, Module, Array

of the electric utility grid, and are generally designed and sized to supply certain DC and/or AC electrical loads. These types of systems may be powered by a PV array only, or may use wind, an engine-generator or utility power as an auxiliary power source in what is called a PV-hybrid system.

i. Stand-alone System With AC and DC Loads

This system can be used to power AC as well as DC loads (Fig. 2). It needs inverter, charge controller, battery in the circuit. The AC supply also may be used for charging only in case of emergency.

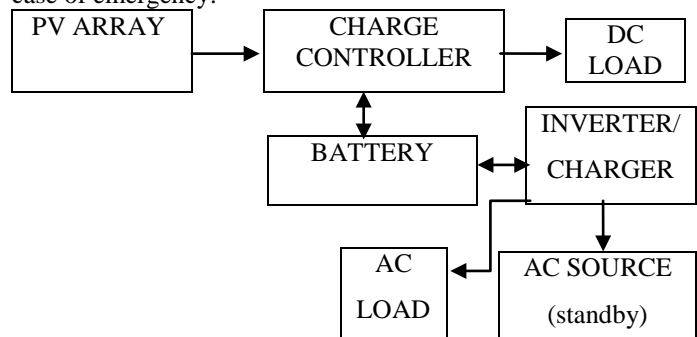


Fig. 2. Stand-alone system with AC and DC loads

ii. Hybrid Stand-alone Systems

In a Hybrid standalone system one or more sources in addition to the PV panels are used. Sources like stand by engines, turbines fuel cells etc may be used in conjunction with PV arrays (Fig. 3). Thus reliance on any source is reduced.

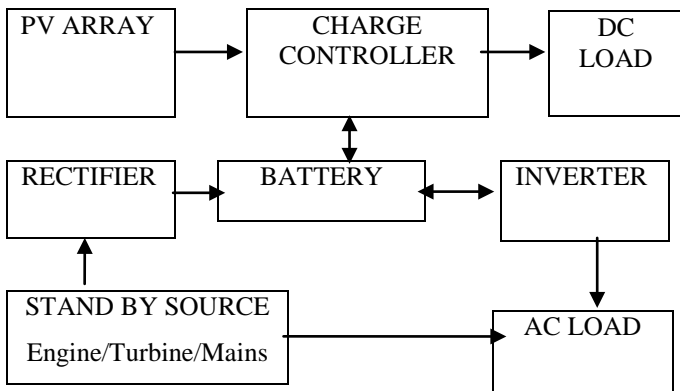


Fig. 3. Hybrid stand-alone systems

(b) Grid Connected System

Grid-connected or utility-interactive PV systems are designed to operate in parallel with and interconnected with the electric utility grid as in Fig. 4. The primary component in grid-connected PV systems is the inverter, or power conditioning unit (PCU). The PCU converts the DC power produced by the PV array into AC power consistent with the voltage and power quality requirements of the utility grid. A bi-directional interface is made between the PV system AC output circuits and the electric utility network, typically at an on-site distribution panel or service entrance. This allows the AC power produced by the PV system to either supply on-site electrical loads, or to back-feed the grid when the PV system output is greater than the on-site load demand.

The grid integration of Renewable Energy Sources (RES) applications based on photovoltaic systems is becoming today the most important applications of PV systems, gaining interest over traditional stand-alone systems [3, 4].

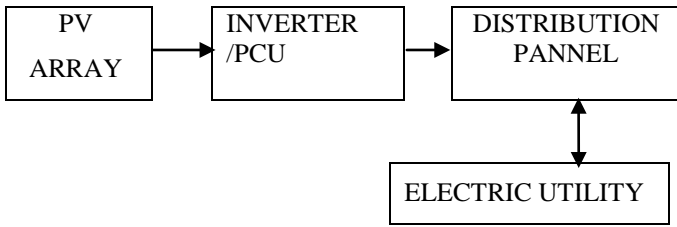


Fig. 4. Grid connected PV system

II. Grid Connected PV System: overview

A. Modeling of PV Array

There is an easy and accurate method of modeling photovoltaic arrays. The method is issued to obtain the parameters of the array model using information from the datasheet [5]. Photovoltaic modules must generally be connected in series in order to produce the voltage required to efficiently drive an inverter [6].

PV cell is a non-linear device and can be represented as a current source in parallel with diode as shown in Fig. 5. Figure shows the equivalent circuit of the ideal photovoltaic

cell. The basic equation which describes the I-V characteristic of the ideal photovoltaic cell is:

$$I = I_{pv,cell} - I_{0,cell} \left[\exp\left(\frac{qV}{akT}\right) - 1 \right] \quad (1)$$

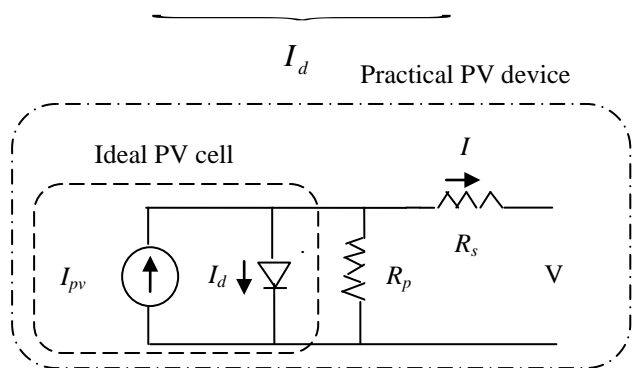


Fig. 5. Single-diode model of the theoretical photovoltaic cell and equivalent circuit of a practical photovoltaic device including the series and parallel resistances.

where $I_{pv,cell}$ is the current generated by the incident light (It is directly proportional to the Sun irradiation), I_d is the Shockley diode equation, $I_{0,cell}$ [A] is the reverse saturation or leakage current of the diode, q is the electron charge [$1.60217646 \times 10^{-19}$ C], k is the Boltzmann constant [$1.3806503 \times 10^{-23}$ J/K], T [K] is the temperature of the $p-n$ junction, and a is the diode ideality constant. Practical arrays are composed of several connected photovoltaic cells and the observation of the characteristics at the terminals of the photovoltaic array requires the inclusion of additional parameters to the basic equation (1):

$$I = I_{pv} - I_0 \left[\exp\left\{\frac{V + R_s I}{N_s V_t}\right\} - 1 \right] \quad (2)$$

where I_{pv} and I_0 are the photovoltaic and saturation currents of the array and $V_t = \frac{N_s k T}{q}$ is the thermal voltage of the

array with N_s cells connected in series. Cells connected in parallel increase the current and cells connected in series provide greater output voltages. If the array is composed of N_p parallel connections of cells the photovoltaic and saturation currents may be expressed as: $I_{pv} = I_{pv,cell} N_p$, $I_0 = I_{0,cell} N_p$. R_s is the equivalent series resistance of the array and R_p is the equivalent parallel resistance. This equation originates the I-V curve seen in Fig. 6, where three remarkable points are highlighted: short

circuit ($0, I_{sc}$), maximum power point (V_{mp}, I_{mp}) and open-circuit ($V_{oc}, 0$).

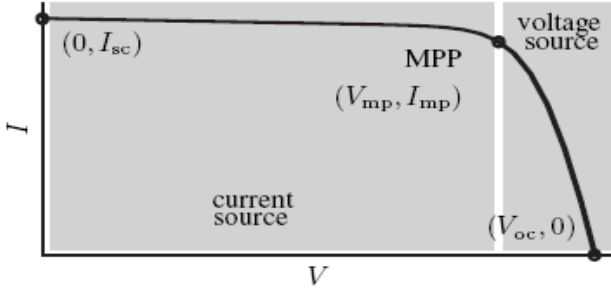


Fig. 6. Characteristic I-V curve of a practical photovoltaic device and the three remarkable points: short circuit ($0, I_{sc}$), maximum power point (V_{mp}, I_{mp}) and open circuit ($V_{oc}, 0$) [5]

B. Grid Connected Inverter Technology

Inverters are very important power electronics equipment in grid connected PV systems. Their major role is to convert DC power into AC power. Furthermore inverter interfacing PV module(s) with the grid ensures that the PV module(s) is operated at the maximum power point (MPPT) [7].

Based on the photovoltaic arrays output voltage, output power level and applications, the photovoltaic grid-connected system can adopt different technologies.

(a) Centralized Inverters

This is the past technology as illustrated in Fig. 7. (a) was based on centralized inverters that interfaced a large number of PV modules to the grid. The PV modules were divided into a string, each generating a sufficiently high voltage to avoid further amplification. These series connections were then connected in parallel, through string diodes, in order to reach high power levels [7]. For this architecture, the PV arrays are connected in parallel to one central inverter. The main advantage of central inverters is the high efficiency (low losses in the power conversion stage) and low cost due to usage of only one inverter. The drawbacks of this topology are the long DC cables required to connect the PV modules to the inverter and the losses caused by string diodes, mismatches between PV modules, and centralized maximum power point tracking [8, 9].

(b) String Inverters

The present technology consists of the string inverters and the ac module. The string inverter, shown in Fig. 7. (b), is a reduced version of the centralized inverter, where a single string of PV modules is connected to the inverter. The input voltage may be high enough to avoid voltage amplification [7]. in this topology the PV strings are connected to separate inverters. If the voltage level before the inverter is too low, a DC-DC converter can be used to boost it. The configuration allows individual MPPT for each string; hence the reliability of the system is improved due to the fact that the system is no

longer dependent on only one inverter compared to the central inverter topology [8].

(c) Multi-String Inverters

As this present and future topology, multi-string inverter configuration became available on the PV market in 2002 being a mixture of the string and module inverters [8]. The multi-string inverter depicted in Fig. 7. (c) is the further development of the string inverter, where several strings are interfaced with their own dc-dc converter to a common dc-ac inverter.

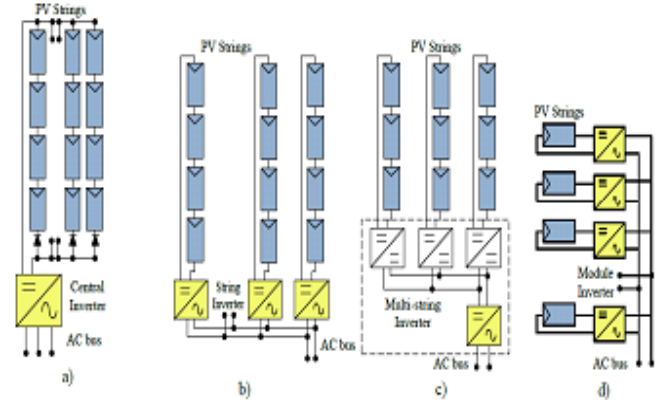


Fig. 7. PV grid connected systems configurations a). Central Inverters; b). String Inverters; c). Multi-String Inverters; d). Module inverters [8]

This is beneficial, compared with the centralized system, since every string can be controlled individually [7, 9]. The topology allows the connection of inverters with different power ratings and PV modules with different current-voltage (I-V) characteristics. MPPT is implemented for each string, thus improved power efficiency can be obtained [8]. This gives a flexible design with high efficiency, and will probably become standard where centralized and string converters are used today [9].

(d) Module Inverters

Module Inverters shown in Fig. 7. (d) is the present and future technology consists of single solar panels connected to the grid through an inverter. A better efficiency is obtained compared to string inverters as MPPT is implemented for every each panel [8]. By incorporating the PV module and the converter into one device, the possibilities of creating a module based “plug and play” device arises, and it can then be used by persons without any knowledge of electrical installations. In this configuration the mismatch losses between the PV modules is removed and it is possible to optimize the converter to the PV module, and thus also allowing individual MPPT of each module.

C. Dual and Single Stage PV Inverter Circuit Topology

PV inverter circuit topology with DC-DC converter is termed as dual stage, and in this topology the DC-DC converter will handle the MPPT and some voltage amplification if needed [9]. Single-stage topology Fig. 8. (a) presents the most reliable and cost effective solution. However this topology is bulky

and less efficient. Meanwhile the AC output power ripple which has double fundamental frequency oscillation unavoidably introduces the double-line-frequency voltage ripple unlike the balanced operation of maximum power point tracking. To minimize the DC voltage ripple and then enhance the solar energy transfer efficiency, a large value DC link capacitor is normally employed, which however cannot fully eliminate this problem and leads to the increase of system size and cost.

Alternatively, a two-stage solution as shown in Fig. 8. (b) consisting of DC-DC converter and DC-AC inverter can operate in a large range of PV voltage ensuring the proper PV energy conversion under wide operational range. Moreover, the inserted DC-DC converter decouples the direct connection

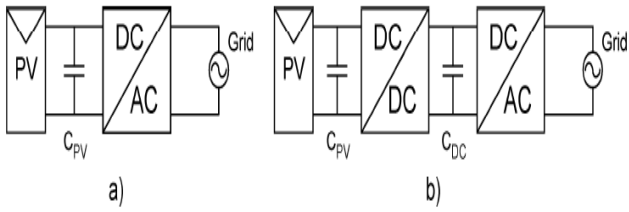


Fig. 8. Single and dual stage inverter topology with coupling capacitances [14]

of PV panel and ac output so that the ac output power ripple will not induce the double-line-frequency ripple of PV voltage. The MPPT efficiency can then be enhanced by using a relatively small input capacitor to just attenuate the high frequency input voltage ripple in the DC-DC voltage conversion. Using a DC-DC converter in front, the efficiency of whole inverter would decrease since more passive and active components are involved in the energy processing when compared to the single-stage topology but when considering the improved MPPT efficiency and wide operation range the two-stage solution is superior to the single-stage inverter [10].

D. DC-DC Converter Topologies

DC-DC converters have a wide range of uses today and are becoming increasingly more important in everyday use. DC power supplies are probably the largest use of the converters and are much more compact and efficient. Generally hard switching converters are used for PV System s because of their simple design and low cost. Hard Switching converters which obey the conventional switching phenomenon. While the switch is turned ON, the voltage across the switch tends to decrease and the current across increase. This results in some switching losses. There are three basic types of DC/DC converters [11].

- i. The boost converter as a step-up converter is used for cases in which a higher output voltage than input is required;
- ii. A buck converter as a step-down converter is used for cases in which a lower output voltage than input is required; and
- iii. A buck-boost converter, which reduces or increases the voltage ratio with a unit gain for a duty ratio of 50%.

For single stages topologies and with low output voltages [9], fly-back converters, boost converters and Cuk converters have shown some challenges when used alone as converters. To handle 400DC which will give approximately 230 V AC voltage as an output to these converters, poor efficiency, switches to be on all the time, high current, large inductor is used and switching power losses are among the factors affecting the performance of these topologies.

On the other hand, when high voltage and galvanic isolation is needed there are other topologies that can be used to provide higher power. As discussed in [11] these topologies have a multistage operation. The multistage converter first inverts the signal to AC for use with a transformer, and then it converts back to DC voltage. Topologies that handling high power [11] include push-pull converter, half bridge converter and full bridge converters. Another configuration to provide high voltages as pointed out in [11] is the Half-Bridge Converter. It has a higher efficiency and a simpler structure with only two switches.

E. Maximum Power Point Tracking (MPPT)

According to its I-V curve, there is a point where the PV module generates the most power. This point is called the Maximum Power Point (MPP), and the corresponding current and voltage are denoted as I_{mp} and V_{mp} , from Fig. 6. The MPP is different as the PV module's I-V curve changes with irradiance and module temperature. Sometimes it changes rapidly due to fast changes in the weather conditions such as partial cloudy day; otherwise it is almost constant in a sunny day without clouds. Because of this characteristic of MPP, some proper algorithms are required for Maximum Power Point Tracking (MPPT).

Existing Control Algorithms

So far several methods of approaching maximum power point tracking have been identified. These can be separated into the following groups.

(i). Perturbation Methods(Hill Climbing/P&O)

Hill climbing involves a perturbation in the duty ratio of the power converter, and P&O a perturbation in the operating voltage of the PV array. In the case of a PV array connected to a power converter, perturbing the duty ratio of power converter perturbs the PV array current and consequently perturbs the PV array voltage. Hill climbing and P&O methods are different ways to envision the same fundamental method [12].

From Fig. 9, it can be seen that incrementing (decrementing) the voltage increases (decreases) the power when operating on the left of the MPP and decreases (increases) the power when on the right of the MPP. Therefore, if there is an increase in power, the subsequent perturbation should be kept the same to reach the MPP and if there is a decrease in power, the perturbation should be reversed. The process is repeated periodically until the MPP is reached. The system then oscillates around the MPP.

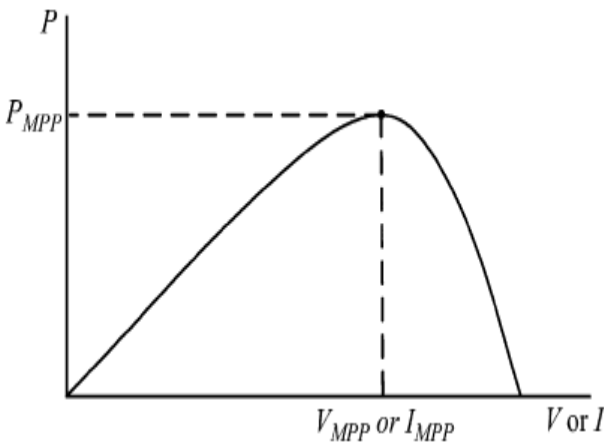


Fig. 9. Characteristic PV array power curve [12]

-tes about the MPP. The oscillation can be minimized by reducing the perturbation step size. Hill climbing and P & O methods can fail under rapidly changing atmospheric conditions.

(ii) Computational Method (Incremental Conductance):

One disadvantage of the perturbation techniques is that oscillations exist around the maximum power point causing loss of power, especially in the case of varying atmospheric conditions. An improvement of the perturbation and observation method is the Incremental Conductance approach; the most frequently used computational method. This technique avoids this problem by looking at the conductance of the array. The incremental conductance approach is based on the fact that the derivative of the output power with respect to the array panel voltage is equal to zero at the maximum power point. The array output voltage is adjusted relative to the peak voltage by measuring and comparing the incremental ($\Delta G, dI/dV$) and instantaneous array conductance ($G, I/V$) (Fig. 10). The algorithm's role is to search the voltage operating point at which the conductance is equal to the incremental conductance and it makes its decision on whether to increase or decrease the duty cycle. Therefore the algorithm searches for the condition where dP/dV is equal to zero or equivalently, where $dI/dV = -I/V$ [13].

(iii). Fractional Open-Circuit Voltage Method

The near linear relationship between V_{mp} and V_{oc} of the PV array, under varying irradiance and temperature levels, has given rise to the fractional V_{oc} method.

$$V_{mp} \approx k_1 V_{oc} \quad (3)$$

usually has to be computed beforehand by empirically determining V_{mp} and V_{oc} for the specific PV array at

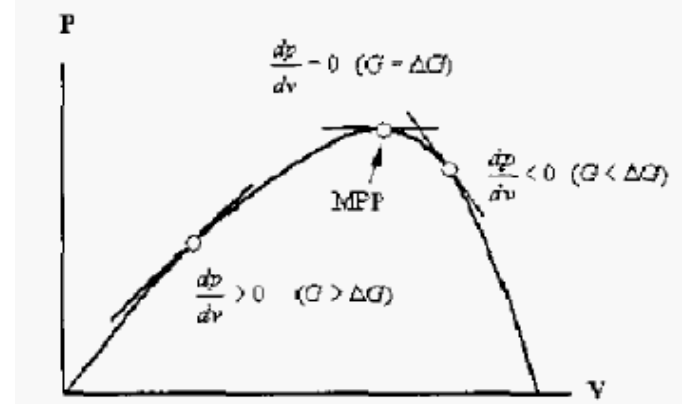


Fig. 10. Operation of the Incremental Conductance Method [13]

different irradiance and temperature levels. The factor k_1 has been reported to be between 0.71 and 0.78. Once k_1 is known, V_{mp} can be computed using (3) with V_{oc} measured periodically by momentarily shutting down the power converter. However, this incurs some disadvantages, including temporary loss of power. To prevent this, uses pilot cells from which V_{oc} can be obtained. Since (3) is only an approximation, the PV array technically never operates at the MPP. Depending on the application of the PV system, this can sometimes be adequate. Even if fractional V_{oc} is not a true MPPT technique, it is very easy and cheap to implement as it does not necessarily require DSP or microcontroller control. This obviously adds to the implementation complexity and incurs more power loss [12].

(iv). Fractional Short-Circuit Current Method

Fractional I_{sc} results from the fact that, under varying atmospheric conditions, I_{mp} is approximately linearly related to the I_{sc} of the PV array

$$I_{mp} \approx K_2 I_{sc} \quad (4)$$

where k_2 is a proportionality constant. Just like in the fractional V_{oc} technique, k_2 has to be determined according to the PV array in use. The constant k_2 is generally found to be between 0.78 and 0.92. Measuring I_{sc} during operation is problematic. An additional switch usually has to be added to the power converter to periodically short the PV array so that I_{sc} can be measured using a current sensor. This increases the number of components and cost [12]. Microcontrollers have made using fuzzy logic control [14, 15] popular for MPPT over the last decade. As mentioned in [16], fuzzy logic controllers have the advantages of working with

imprecise inputs, not needing an accurate mathematical model, and handling nonlinearity. MPPT fuzzy logic controllers perform well under varying atmospheric conditions. Along with fuzzy logic controllers came another technique of implementing MPPT, neural networks [17, 18], which are also well adapted for microcontrollers.

III. CONCLUSIONS

The energy injected into the electric grid by a PV installation depends on the amount of power extracted from the PV power source and the efficient processing of this power by the DC/AC inverter. The influences of the electric grid regulations and standards as well as the PV array operational characteristics on the design of grid-connected PV inverters must be considered.

In the past, large areas of PV modules were connected to the grid by means of centralized inverters. This included many shortcomings for which reason the string inverters emerged. A natural development was to add more strings, each with an individual dc–dc converter and MPPT, to the common dc–ac inverter, thus, the multi-string inverters were brought to light. This is believed to be one of the solutions for the future.

Conventional two-stage PV energy conversion systems are bulky, expensive, provide low efficiency, and are, thus, not suitable for small-scale PV energy conversion utilization. To resolve this problem, a PV energy conversion system with single-stage architecture is there. The single-stage system has advanced features such as small physical volume, low weight, and high efficiency.

Several MPPT techniques taken from the literatures are discussed herein, which is useful in choosing the right MPPT method for specific PV systems.

IV. REFERENCES

- [1] N. Patcharapakiti and S. Premrudeepreechacharn, “Maximum power point tracking using adaptive fuzzy logic control for grid-connected photovoltaic system,” in *IEEE Power Engineering Winter Meeting*, 2002.
- [2] “Procedures for Photovoltaic System Design Review and Approval,” FSEC Standard 203-10 (January 2010)
- [3] A. J. Morrison, “Global Demand Projections for Renewable Energy Resources,” *IEEE Canada Electrical Power Conference*, pp 537-542, 25-26 Oct. 2007.
- [4] Pollikas A., “Implementation of distributed generation technologies in isolated power,” *Renewable and Sustainable Energy Reviews*, vol. 11, pp. 30-56, 2007.
- [5] Marcelo Gradella Villalva, Jonas Rafael Gazoli, Ernesto Ruppert Filho, “Modeling and Circuit based simulation of Photovoltaic array,” *IEEE Transactions on Energy Conversion*, 25: 1998-1208, 2009.
- [6] Toshihisa Shimizu, Masaki Hirakata, Tomoya Kamezawa, and Hisao Watanabe, “Generation Control Circuit for Photovoltaic Modules,” *IEEE Transaction on Power Electronics*, vol. 16, no. 3, May 2001.
- [7] Soeren Baekhoej Kjaer, John K. Pedersen and Frede Blaabjerg, “A Review of Single- Phase Grid-Connected Inverters for Photovoltaic Modules,” *IEEE Transactions of Industry Applications*, vol.41, no.5, pp.1292-1306, September/October 2005.
- [8] Vlad Alexandru Muresan, “Control of Grid Connected PV Systems with Grid Support Functions”, Master’s thesis, Department of Energy Technology - Pontoppidanstræde 101, Aalborg University, Denmark, 2012.
- [9] Svein Erik Evju, “Fundamentals of Grid Connected Photovoltaic Power Electronic Converter Design,” Specialization project, Department of Electric Engineering, Norwegian University of Science and Technology, December 2006.
- [10] Raymond M. Hudson, Michael R. Behnke, Rick Wed, Sigifredo Gonzalez and Jeny Ginn, “Design considerations for three-phase grid connected photovoltaic inverters,” *Conference Record of the Twenty-Ninth, Photovoltaic Specialists Conference, IEEE*, pp 1396-1401, 2002
- [11] N. Mohan, T.M. Undeland and W.P. Robbins, “Power Electronics: Converters Applications and Design,” 3rd edition, *John Wiley & Sons, Inc.*, ISBN: 0-471-22693-9, 2003.
- [12] Trishan Esram and Patrick L. Chapman, “Comparison of Photovoltaic Array Maximum PowerPoint Tracking Techniques,” *IEEE Transactions on Energy Conversion*, vol. 22, no. 2, june, 2007.
- [13] S. Armstrong, and W. G. Hurley, “ Self-Regulating Maximum Power Point Tracking For Solar Energy Systems,” *Proceeding of the 39th International Universities Power Engineering Conference, (ITEC’03),IEEE Computer Society, U.S.A.*, pp:256-260,2003.
- [14] R. M. Hilloowala and A. M. Sharaf, “A rule-based fuzzy logic controller for a PWM inverter in photo-voltaic energy conversion scheme,” in *Proc. IEEE Ind. Appl. Soc. Annu. Meet. ,* pp. 762-769,1992.
- [15] N. Khaehintung, K. Pramotung, B. Tuvirat, and P. Sirisuk, “RISC microcontroller built-in fuzzy logic controller of maximum power point tracking for solar-powered light-flasher applications,” in *Proc. 30th Annu. Conf. IEEE Ind. Electron. Soc.*, pp. 2673-2678, 2004.
- [16] M. Veerachary, T. Senju, and K. Uezato, “Neural-network-based maximum-power-point tracking of coupled-inductor interleaved-boost converter- supplied PV system using fuzzy controller,” *IEEE Trans. Ind. Electron.*, vol. 50, no. 4, pp. 749-758, Aug. 2003
- [17] T. Hiyama, S. Kouzuma, and T. Imakubo, “Identification of optimal operating point of PV modules using neural network for real time maximum power tracking control,” *IEEE Trans. Energy Convers.*, vol. 10, no. 2, pp. 360-367, Jun. 1995.
- [18] L. Zhang, Y. Bai, and A. Al-Amoudi, “GA-RBF neural network based maximum power point tracking for grid-connected photovoltaic systems,” in *Proc. Int. Conf. Power Electron. , Machines and Drives*, pp. 18-23, 2002.

Renewable Grid Integration: Analytical Approach

Jaina Ram¹, Luckey Chouksey

Abstract— The limited fossil fuel energy resource is a critical issue throughout the world. Because of the limited traditional energy sources and the concerns about environmental pollution, there has been significant development in renewable energy sources worldwide, wind energy is also one of them. But we can't use this renewable energy directly from the source because this is not a constant power. Wind energy and solar power are two important and large power generating sources in renewable energy sources. Wind power generation depends on wind speed that can't be fully constant and solar power generation depends on sun light that also can't be constant in 24 hours. So grid integration of renewable power is very important to use power from renewable sources.

The present paper is just an analytical approach for Grid integration of renewable (wind) power. In wind power integration the main trends of modern wind farms are clearly the variable speed operation and a grid connection through a power electronic interface, especially using self excited induction generators. Large wind power can be integrated with grid by CSC HVDC and by using VSC-HVDC the control capabilities of these wind farms are extended and thus the grid requirements are fulfilled.

Keywords— *renewable energy sources (RES); wind power; grid integration; VSC-HVDC; induction generator; power grid*

I. INTRODUCTION

The main impetus for renewable energy growth has been increasing concern over global warming, and a range of policy instruments have been used to promote carbon free technologies. Unsurprisingly, most growth has taken place in locations with generous subsidies, such as California (in the early days), China, Denmark, Germany, Spain and India also. In India two kind of renewable energy sources are available which can produce large power these are solar power and wind power. Large solar power generation has been developed in India years ago. But wind power generation still trying to increase its generation. Nowadays, modern large wind turbines currently replace a large number of small wind turbines and there is a significant attention to offshore wind farms, mainly because of higher average wind speed and no space limitation. With its reproducible, resourceful and pollution-free characteristics, the wind power generation has been developing rapidly and applied widely around the world since the 20th century. Europe (4995 MW) is the global leader in terms of offshore wind energy installation followed by China (390 MW) and Japan (25 MW).

¹But India has only 19600 MW onshore wind power and now trying to increase offshore wind power. A study by Scottish Development International done in January 2012 has indicated

potential to establish around one GW capacity wind farm each along the coastline of Rameshwaram and Kanyakumari in Tamil Nadu. India is estimated to have 350 GW of offshore wind energy capacity. In order to facilitate the flow of renewable energy into the national grid, the Government plans to roll out a Rs 43,000-crore ‘green energy corridor’ project [1].

II. CONCEPT OF VARIABILITY WITH WIND

Renewable energy sources are variable with time and place. Renewable energy has a variability problem and pretending that it does not – at the very least on a public perception level – won't make this issue go away. The wind does not always blow, nor does it always blow steadily and sunlight can be obstructed by clouds. The irregularity of wind flow is a main concern for grid integration. Wind and solar are variable sources of energy and this poses certain unique challenges that need to be addressed. At times an entire region can experience periods of a day or sometimes even a week where winds or solar energy that is usually on average available is largely absent. Wind energy in particular is also variable over short time scales with gusting wind producing peaks and troughs in power output that can cause voltage problems, because of the unevenness of the power being put onto the grid.

Wind and solar energy are referred to as variable power generation sources because their electricity production varies based on the availability of wind and sun. However, they are not the only source of variation in a power system. The demand for electricity, or load, also varies, and the power system was designed to handle that. So, requirement of reactive power is also varies. Short-term changes in load (over seconds or minutes) are generally small and caused by random events that change demand in different directions. Over longer periods (several hours), changes in load tend to be more predictable. So due to variability of wind power frequency and output voltage is also variable, it can't be interfaced with the grid. But offshore wind power plant also has almost constant and high wind speed [3]. If deviation of wind speed is less then it can be controlled by pitch angle controller of wind turbine. So a large wind power (GW) generation is possible from offshore wind power plant. This kind of wind power plant is being situated in sea around 100 Km far from the shore. If one wind mill is generating 5 MW power than its control parameters are different than other which is generating 1 MW. So as wind speed will vary control parameters also vary with the wind speed [4].

1. PG Scholar EED ,IIT BHU ,Varanasi
Jain.jooya.eee12@iitbhuac.in

III. OPERATIONAL ISSUES OF GRID INTERFACE

The transmission system operators have raised many issues with wind power generation, especially for large-scale generation, in order to enable secure and reliable system operation. However wind energy has many advantages over other renewable resources; the integration of wind generation with the grid can introduce many technical challenges and issues due to the intermittent nature of wind generation. These problems have become more pronounced as the penetration level of wind increases. The major issues of wind power integration are related to: high cost converters required, changed approaches in operation of the power system, connection requirements for wind power plants to maintain a stable and reliable supply, extension and modification of the grid infrastructure, and influence of wind power on system adequacy and the security of supply [5]-[6]. These challenges and issues regarding to the wind generation and integration to the grid are discussed below.

- Irregularity of wind
- System Inertia and Frequency Regulation
- Fault Ride-Through Capability of Wind Turbines
- Ramping Due to Wind Speed Variations
- Congestion on the Power Transmission Grids
- Cost
- Storage

IV. TECHNOLOGY OF GRID INTEGRATION WITH RES

The major problem in interfacing such renewable energy sources to the grid is the controlling and transmission of the large wind power. Mainly High Voltage DC transmission system is used to interface the large wind power to the grid. This HVDC is used following three kinds of technologies [7]:

- Conventional HVDC System
- VSC HVDC system
- Hybrid HVDC System

The grid interconnections may be point-to-point or multi-terminal, a configuration for which VSC technology is particularly well-suited and hence may lead to development of offshore dc networks. In general, high-voltage direct current (HVDC) conversion stations are a well-established technology. It is worth to note that HVDC converters are typically based on current source converter (CSC), which has some difficulties in regulating reactive power. By the other hand, a converter based on a Voltage Source Inverter (VSC) structure can manipulate the reactive and active power independently. If the VSC-based converter is not ill designed, is possible to gain some transient stability margin for a conventional generator and to give support to ride through faults.

A. Large RES Integration

The integration of large renewable energy sources can be done by conventional HVDC system or hybrid HVDC system. This kind of integration can't be done by VSC high voltage DC link. Because required rating of converters is very high and available rating of VSC HVDC is lower than it. If RES generating capacity is 2 GW then we have to use conventional thyristor based HVDC system for grid integration. The classic HVDC, like it is used for some decades now, is based on thyristors as power electronics devices (Fig. 1). This thyristor HVDC is also known as Current Source Converter (CSC) HVDC. The thyristor-HVDC is a proven technology and available for transmission power up to some Giga Watts. But the thyristor-rectifier and the thyristor-inverter need reactive power and filtering for an operation with good power quality. It is also a problem to create a voltage-system offshore to supply the offshore wind park with energy during the installation, times of no wind and starting-up operation [8]. The thyristor inverter needs reactive power for the commutation that has to be supplied by a strong supply grid or a reactive power source like a big synchronous generator that is connected to the offshore grid [6].

The thyristor-HVDC-Transmission is more expensive than a conventional AC solution for short distances. Nevertheless, HVDC may well be used for many offshore wind projects, because:

- HVDC provides a power transmission with very high capacity over only two DC cables.
- HVDC has no restrictions for the transmission distance in principle.
- The advantage of CSC HVDC over VSC HVDC is that they are available with high ratings and cost of thyristor based converters is also less than IGBT based converters.

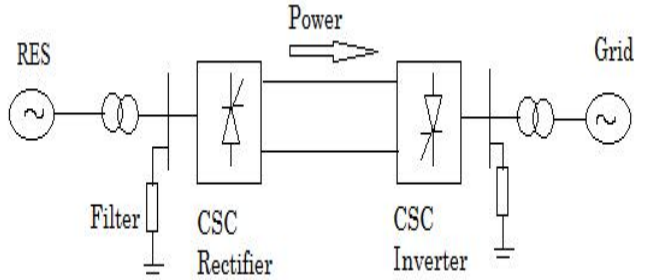


Fig. 1. Grid Integration of RES with CSC HVDC

B. Small RES Integration

The problem faced with conventional thyristor based HVDC system is that self commutation is not available; slow switching; large size filters are required and independent regulation of reactive power is not available. So overcome these problems new technology is invented IGBT base

HVDC.

Because technology is growing up day by day and the IGBT based HVDC is an excellent example of this modern technology. IGBT is a self commutating device and its switching is faster than thyristors. IGBT based converters are called Voltage Source Converters. Another advantage of VSC HVDC is that size of voltage source converters HVDC is less than CSC HVDC because harmonic is improved by IGBT switches, so much less filters are required. VSC HVDC can be used for grid integration with large wind power. The main advantage of VSC HVDC is that it can provide independent control of active and reactive power. It can provide reactive power support to the induction generator for excitation. For integration of grid with small offshore wind power (500 MW) VSC HVDC is best technology. Due to use of this there is no requirement of capacitor bank or STATCOM to provide reactive power support to the induction generators. It can regulate reactive power as wind speed is changes or as induction generator is required [9]-[12].

The grid integration of large wind power with VSC HVDC can be done as shown below.

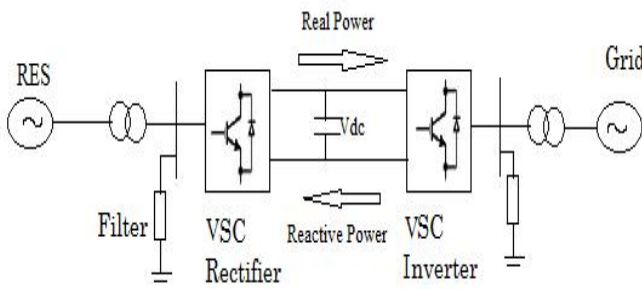


Fig. 2. Grid Integration of RES with VSC HVDC

Fig. 2 shows a VSC-HVDC transmission line, where the RES side IGBT-Unit rectifies the AC RES voltages to get a DC voltage. The inverter on the grid side makes a three phase AC voltage to feed the energy into the public grid.

VSC HVDC provides independent control of reactive power at the converter stations, which could be a great benefit in increasing the power quality in the public grid. The CSC HVDC provides almost no contribution to fault currents, which in many areas are a major limitation on the connection of a new power station. In addition to full power flow control in both directions, the VSC HVDC system can prevent fault propagation, increase low frequency stability, reduce network losses and increase voltage stability. But on the other hand the power range of the VSC HVDC is only about some hundred megawatts, which is not enough for the big wind farms because power rating of IGBT is less. But research is going on so it can be increases with low cost in future. The VSC HVDC-Transmission is more expensive than the CSC HVDC relating to the same nominal power [13]-[17]. But its operation is very fast and smooth, so in modern fast era this technology is very impressive for grid integration of small RES.

C. Comparision between CSC HVDC and VSC HVDC

There are lot of difference between current source converter and voltage source converter HVDC. These differences may be on system ratings basis or may be on system capability basis. The main property of VSC HVDC is to the ability to connect offshore wind farms which is not in CSC HVDC. VSC HVDC also can inject the reactive power at induction generators [16]-[17].

TABLE I.
COMPARISONS BETWEEN HVDC TRANSMISSION
TECHNOLOGIES

| System Descriptions | CSC HVDC | VSC HVDC |
|--|-----------------------|-----------------------|
| System ratings in operation | ± 800 KV, 3000 MW | ± 150 KV, 350 MW |
| System ratings available | ± 800 KV, 6400 MW | ± 300 KV, 1100 MW |
| Future trend of system ratings | Toward higher ratings | Toward higher ratings |
| Operational experience | >50 years | ~ 15 years |
| Converter losses (at full load, per converter) | 0.5-1% | 1-2% |
| Availability (per system) | > 98% | > 98% |
| System capabilities | CSC HVDC | VSC HVDC |
| Transmission capacity | ■■■ | ■■ |
| Power flow control | ■■■ | ■■■ |
| Transient stability | ■■ | ■■■ |
| Voltage stability | ■ | ■■ |
| Power oscillation damping | ■■ | ■■■ |
| Reactive power demand | ■■■ | ■ |
| System perturbation | ■■■ | ■ |
| Reactive power injection possible | No | Yes |
| Easy meshing | No | Yes |
| Limitation in cable line length | No | No |
| Ability to connect offshore wind farms | No | Yes |
| Investment costs per MW | ■■ | ■■■ |

Legenda: ■ — Small; ■■ — Medium; ■■■ — Strong

As shown in above table we find that although VSC HVDC is more expensive than CSC HVDC but it has some reliable and important features. These features attract new researchers to use it.

D. Modeling Concept

Modeling Concept of renewable grid integration can be explained by mathematical modeling of each part. The generalized modeling can be understood by following block diagram.

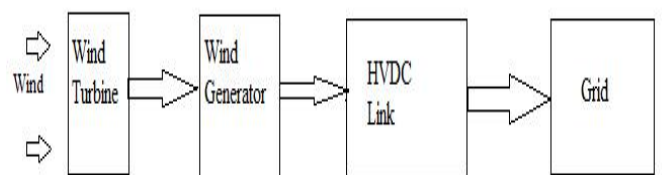


Fig. 3. Block diagram of modeling concept

In first part wind turbine should be modeled. Find out the wind turbine output mechanical power in respective input of wind speed. This mechanical power will depend on wind speed, air density, area swept by turbine blades, pitch angle and tip speed ratio of turbine. Modeling of gear box also can be considered in wind turbine modeling. The output torque of wind turbine should be considered as an input of wind generator. This wind generator will generate electrical power as an output. Part two modeling is modeling of wind generator in respective input of torque developed by wind turbine. The output of wind generator also depends on rotational and core losses of generator. In generalized modeling losses of generator can be avoided. Electrical power developed by wind generator can be fed into grid. This interface can be done by HVDC link efficiently. So in third part modeling of HVDC link can be done. HVDC link can be any kind VSC or CSC as per requirement and suitability in grid interface. Harmonic are produced by wind generator can be removed by filters. Mathematical modeling of filters is can be considerd in HVDC link block. At last modelling of grid also can be done and output of HVDC will be input of grid in grid interface technology. In grid integration with renewable energy grid code requirement must be fulfilled [19]-[21]. After mathematical modelling of each part these blocks can be modelled in simulation tools and analysis can be done.

E. Simulation Tools

Analysis of renewable grid integration can be done by several tools available in laboratory. These tools can be as follows:

- i. PSCAD/EMTDC
- ii. MATLAB/Simulink
- iii. DIgSILENT Power factory
- iv. NEPLAN
- v. Ansoft Simplorer

Any of above tool can be used in analysis of renewable grid integration. The real time simulation can be done by PSCAD/EMTDC. If you use MATLAB/Simulink tool then first you should develop your complete model. After completing the model you can define ratings of different components. Then you can simulate it and find out results. The various results just like as active power, reactive power, wind speed, pitch angle variation can be find out by the MATLAB/Simulink [22].

V. CONCLUSION

In last two decade the wind power has caused many transformations compelling to re-thinking the planning and operational strategies of the power system, restructure the power grid, revise the grid rules, research on suitable and accurate models for the wind turbines, wind farms and the interaction with the power grid, development of new standards and simulation tools, and new demands and enlightenment on the electricity markets. And the evolution continues. The

recent transformations have also driven to a new perception, motivation and admission of a young generation of engineers to the power system area. Grid interface technology for large and small wind power generation is presented in this paper. Operational issues also discussed in presented paper. Then comparative study between CSC HVDC and VSC HVDC is also presented. This study tells that although cost of VSC HVDC is more than CSC HVDC but the few important features are present in VSC. Due to those features VSC HVDC is used mostly for grid integration of offshore wind farm. According to paper VSC HVDC is best technique to interface grid with offshore wind power generation. Modelling concept of renewable grid interface technology is also discussed. The simulation studies can be done by PSCAD/EMTDC, MATLAB, DIgSILENT Power factory or NEPLAN.

REFERENCES

- [1] Report of Ministry of new and renewable energy on projected wind energy, Government of India.
- [2] http://www.ewea.org/fileadmin/ewea_documents/documents/publications/reports/Pure_Power_Full_Report.pdf.
- [3] www.nrel.gov , A report of National Renewable Energy Laboratory , 1617 Cole Boulevard Golden, Colorado 80401.
- [4] F. E. Development, —Role of HVDC Transmission in Future Energy Development,|| 1999.
- [5] Frans Van Hulle —*Large Scale Integration of Wind Energy in European Power Supply: analysis, issues and recommendations,*|| A report by EWEA, Dece. 2005
- [6] J. M. Carrasco, L. G. Franquelo, J. T. Bialasiewicz, S. Member, E. Galván, R. C. P. Guisado, S. Member, M. Ángeles, M. Prats, J. I. León, S. Member, and N. Moreno-alfonso, —Power-Electronic Systems for the Grid Integration of Renewable Energy Sources : A Survey,|| vol. 53, no. 4, pp. 1002–1016, 2006.
- [7] J. M. Carrasco, E. Galvain, R. Portillo, and L. G. Franq, —Power Electronic Systems for the Grid Integration of Wind Turbines,|| vol. 00, pp. 4182–4188.
- [8] M. Inverter, P. Samuel, R. Gupta, and D. Chandra, —Grid Interface of Wind Power With Large Split-Winding Alternator Using Cascaded,|| vol. 26, no. 1, pp. 299–309, 2011.
- [9] A. Sciences and B. Germany, —POWER TRANSMISSION FROM OFFSHORE,|| pp. 51–59.
- [10] F. Iov, P. Srensen, A. Hansen, and F. Blaabjerg, —Grid connection of active stall wind farms using a VSC based DC transmission system,|| pp. 1–10.
- [11] L. Xu, S. Member, L. Yao, and C. Sasse, —Grid Integration of Large DFIG-Based Wind Farms Using VSC Transmission,|| vol. 22, no. 3, pp. 976–984, 2007.
- [12] H. Li, —The Performance Research of Large Scale Wind Farm Connected to External Power Grid,|| no. 2, pp. 2–6, 2009.
- [13] Rieghard Vermaak, Johannes H.J. Potgieter, Maarten J. Kamper, —Grid-Connected VSC-HVDC Wind Farm System and Control Using Permanent Magnet Induction Generators,|| PEDS2009.
- [14] S. Wang, G. Li, M. Zhou, and Z. Zhang, —Research on Interconnecting Offshore Wind Farms Based on Multi-terminal VSC-HVDC,|| pp. 1–7, 2010.
- [15] R. Meere, M. O. Malley, and A. Keane, —VSC-HVDC Link to Support Voltage and Frequency Fluctuations for Variable Speed Wind Turbines for Grid Connection,|| pp. 1–5, 2012.
- [16] X. Chen, H. Sun, J. Wen, W.-J. Lee, X. Yuan, N. Li, and L. Yao, —Integrating Wind Farm to the Grid Using Hybrid Multiterminal HVDC Technology,|| IEEE Trans. Ind. Appl., vol. 47, no. 2, pp. 965–

972, Mar. 2011.

- [17] H. J. Bahirat, S. Member, B. A. Mork, S. Member, and H. K. Høidalen, —Comparison of Wind Farm Topologies for Offshore Applications,| pp. 1–8, 2012.
- [18] D. Level, —REseArch , methodoLogies and technologieS for the effective development of pan-European key GRID infrastructures to support the achievement of a reliable , competitive and sustainable electricity supply Incentive schemes and regulation framework for transmission development in Europe,| 2010.
- [19] S. M. Lukic, S. Member, J. Cao, S. Member, R. C. Bansal, S. Member, F. Rodriguez, S. Member, A. Emadi, and S. Member, —Energy Storage Systems for Automotive Applications,| vol. 55, no. 6, pp. 2258–2267,
- 2008
- [20] K. Mattern, A. Ellis, S. Member, S. E. Williams, A. Nourai, and S. Member, —Application of Inverter-Based Systems for Peak Shaving and Reactive Power Management,| pp. 1–4, 2008.
- [21] Y. Fu, Y. Wang, Y. Luo, H. Li, and X. Zhang, —Interconnection of wind farms with grid using a MTDC network,| *IECON 2012 - 38th Annu. Conf. IEEE Ind. Electron. Soc.*, pp. 1031–1036, Oct. 2012.
- [22] P. Zhan, C. Li, J. Wen, Y. Hua, M. Yao, and N. Li, —Research on hybrid multi-terminal high-voltage DC technology for offshore wind farm integration,| *J. Mod. Power Syst. Clean Energy*, vol. 1, no. 1, pp. 34–41, Jul. 2013

A Review on Micro Hydro Power Plant: Solution for Off-grid Renewable Energy Source in India

Madhvi Mishra¹, Shafat Zia², Priyanka Patel³, Harsh Vikram Singh⁴

Abstract: -In this paper we will review the use of micro hydropowersystem in India and suggest innovative ideas for generation of energy from hydro power. The evolution and advancement in technology has improved the standard of living of every individual. It has improved the lifestyle and level of comfort. It can be abridged that the technological development has helped mankind in many prospects. However, every coin has two sides. The ever increasing industrialization has adverse effects on energy resources. As in today's date India is a large consumer of fossil fuel such as coal, crude oil etc. The rapid increase in use of Non-renewable energies such as fossil fuel, oil, natural gas has created problems of demand & supply. Because of which, the future of Non-renewable energies is becoming uncertain. So to overcome this renewable energy resources are used. Renewable energy is generally defined as energy that comes from resources which are naturally replenished on a human timescale such as sunlight, wind, rain, tides, waves and geothermal heat. Renewable energy replaces conventional fuels in four distinct areas: electricity generation, hot water/space heating, motor fuels, and rural (off-grid) energy services. In this paper Micro hydro power is used for the generation of energy. Electricity from these plants effect the daily life-habits of households and also foster the birth of some new enterprises.

Index Term- Micro hydro, Renewable energy, power plant, Hydroelectricity.

I. INTRODUCTION

In today's date, India is a large consumer of fossil fuel such as coal, crude oil etc. Over a past few decades, energy is needed for everything. The electricity requirement is increasing at an alarming rate due to increased population & industrial growth. This rapid increase in use of energy has created problems of demand & supply. Because of which, the future of Non-renewable energies is becoming uncertain. India ranks sixth in the world in total energy consumption. Because of which, the future of Non-renewable energies is becoming uncertain.
¹

Also India has had a negative Energy Balance for decades, which has resulted in the need to purchase energy from outside the country to fulfil the needs of the entire country. So for the solution of this problem is to the use of renewable energy. Renewable energy replaces conventional fuels in four distinct areas: electricity generation, hot water/space heating, motor fuels, and rural (off-grid) energy services. About 16% of global final energy consumption presently comes from renewable resources, with 10% of all energy from traditional biomass, mainly used for heating, and 3.4% from hydroelectricity. New renewables (small hydro, modern biomass, wind, solar, geothermal, and biofuels) account for another 3% and are growing rapidly. At the National level, at least 30 nations around the world already have renewable energy contributing more than 20% of energy supply. National renewable energy markets are projected to continue to grow strongly in the coming decade and beyond. Renewable energy resources exist over wide geographical areas, in contrast to other energy sources, which are concentrated in a limited number of countries. Rapid deployment of renewable energy and energy efficiency is resulting in significant energy security, climate change mitigation, and economic benefits. In international public opinion surveys there is strong support for promoting renewable sources such as solar power and wind power. While many renewable energy projects are large-scale, renewable technologies are also suited to rural and remote areas and developing, where energy is often crucial in human development. United Nations Secretary-General has said that renewable energy has the ability to lift the poorest nations to new levels of prosperity. Renewable energy replaces conventional fuels in four distinct areas: electricity generation, hot water/heating, motor, and rural (off-grid) energy services:

Power generation. Renewable energy provides 19% of electricity generation worldwide. Renewable power generators are spread across many countries, and wind power alone already provides a significant share of electricity in some areas: for example, 14% in the U.S. state of Iowa, 40% in the northern German state of Schleswig-Holstein, and 49% in Denmark. Some countries get most of their power from renewables, including Iceland (100%), Norway (98%), Brazil (86%), Austria (62%), New Zealand (65%), and Sweden (54%).

-
1. PG scholar, ECD,KNIT sultanpur
 2. PG scholar, ECD,KNIT sultanpur
 3. PG scholar, EED,KNIT sultanpur
 4. Assistant professor,ECD sultanpur

Heating. Solar hot water makes an important contribution to renewable heat in many countries, most notably in China, which now has 70% of the global total (180 GW). Most of these systems are installed on multi-family apartment buildings and meet a portion of the hot water needs of an estimated 50–60 million households in China. Worldwide, total installed solar water heating systems meet a portion of the water heating needs of over 70 million households. The use of biomass for heating continues to grow as well. In Sweden, national use of biomass energy has surpassed that of oil. Direct geothermal for heating is also growing rapidly.

Transport fuels. Renewable biofuels have contributed to a significant decline in oil consumption in the United States since 2006.^[15] The 93 billion liters of biofuels produced worldwide in 2009 displaced the equivalent of an estimated 68 billion litres of gasoline, equal to about 5% of world gasoline production [1].

There some types of renewable energy resources are given below:-

Hydropower: Hydropower represents one of the oldest and largest renewable power sources and accounts for close to 10% of our nation's electricity. Existing hydropower capacity is about 80,000 megawatts (MW – one million watts or one thousand kilowatts). Hydropower plants convert the energy of flowing water into electricity. This is primarily done by damming rivers to create large reservoirs and then releasing water through turbines to produce electricity

Biomass: Biomass is second to hydropower as a leader in renewable energy production. Biomass has an existing capacity of over 7,000 MW. Biomass as a fuel consists of organic matter such as industrial waste, agricultural waste, wood, and bark. Biomass can be burned directly in specially designed power plants, or used to replace up to 15% of coal as a fuel in ordinary power plants. Biomass burns cleaner than coal because it has less sulphur, which means less sulphur dioxide will be emitted into the atmosphere.

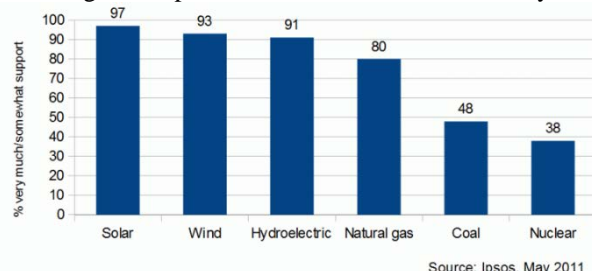
Geothermal: Geothermal power plants use high temperatures deep underground to produce steam, which then powers turbines that produce electricity. Geothermal power plants can draw from underground reservoirs of hot water or can heat water by pumping it into hot, dry rock. High underground high temperatures are accessed by drilling wells, sometimes more than a mile deep. In one sense, this geothermal energy is not renewable, since sometime in the future the core of the earth will cool.

Most geothermal powerplants are located in the western United States. Geothermal heat pumps use compressors to pump heat out of the earth (for winter heating) or into the earth (when running as air conditioners in summer). The energy they pump into and out of the earth is renewable, since it is replaced by the cycle of the seasons. The energy that runs the compressor can either be renewable or conventional.

Solar Energy: Solar energy comes directly from the power of the sun and is used to produce electricity, to produce heat, and for light. Solar contribution to heating and lighting is much larger. Solar-electric power can be produced either by power plants using the sun's heat or by photovoltaic (PV) technology, which converts sunlight directly to electricity using solar cells. PV technology is more practical for residential use. Systems to use the heat of the sun directly can be either active or passive. In active systems, air or liquid circulates through solar collectors and bring heat to where it is used. In passive systems, buildings are built with windows and heat-absorbing surfaces set up to maximize solar heating in winter. Either technology is suitable for residential use. Systems to directly use the light of the sun are most common.

Wind Power: Wind has been the fastest growing energy source in the world over the last decade mainly due to very significant improvements in wind energy technology. Wind power is produced by the energy of the wind turning aerodynamic blades mounted to a hub. The hub is connected to a shaft that turns a generator. Large utility-scale wind turbines range in size from 50 kilowatts to over four megawatts. Smaller wind turbines (under 50 kW) are suitable for residential and agricultural use.

Fuel Cells: A fuel cell is an alternative energy device, but it is not necessarily a renewable energy device. It is only renewable if the source of the fuel used is renewable. A fuel cell is an electrochemical device, like a battery in that it converts the energy from a chemical reaction directly into electricity and heat. But unlike a battery, which is limited to the stored chemicals within, a fuel cell has the capacity of generating energy as long as fuel is supplied. Currently produced fuel cells combine hydrogen and oxygen without combustion to produce electricity. The oxygen comes from the air, while the hydrogen can either be produced from water (using electricity) or extracted from fossil fuels. New fuel cells are being developed that can use fossil fuels directly.



Source: Ipsos, May 2011

Fig. 1. Global public support for energy sources [2]

II. ASPECT OF HYDRO POWER

Hydroelectric Power is a form of renewable energy. Hydroelectric powerplants do not use up resources to create electricity nor do they pollute the air, land, or water, as other

power plants. Hydroelectric power has played an important part in the development of this Nation's electric power industry. Both small and large hydroelectric power developments were instrumental in the early expansion of the electric power industry. Hydroelectric power comes from flowing water winter and spring runoff from mountain streams and clear lakes. Water when it is falling by the force of gravity, can be used to turn turbines and generators that produce electricity. Hydroelectric power is important to our Nation. Growing populations and modern technologies require vast amounts of electricity for creating, building, and expanding. Hydropower is an essential contributor in the national power grid because of its ability to respond quickly to rapidly varying loads or system disturbances, which base load plants with steam systems powered by combustion or nuclear processes cannot accommodate. Hydroelectric power plants are the most efficient means of producing electric energy. The efficiency of today's hydroelectric plant is about 90 percent. Hydroelectric plants do not create air pollution, the fuel falling water is not consumed, projects have long lives relative to other forms of energy generation, and hydroelectric generators respond quickly to changing system conditions. These favourable characteristics continue to make hydroelectric projects attractive sources of electric power [3].

III. HYDROPOWER PLANT

A hydroelectric power plant consists of a high dam that is built across a large river to create a reservoir, and a station where the process of energy conversion to electricity takes place. The first step in the generation of energy in a hydropower plant is the collection of run-off of seasonal rain and snow in lakes, streams and rivers, during the hydrological cycle. The run-off flows to dams downstream. The water falls through a dam, into the hydropower plant and turns a large wheel called a turbine. The turbine converts the energy of falling water into mechanical energy to drive the generator. After this process has taken place electricity is transferred to the communities through transmission lines and the water is released back into the lakes, streams or rivers. This is entirely not harmful, because no pollutants are added to the water while it flows through the hydropower plant [4].

Hydroelectric power comes from water at work, water in motion. It can be seen as a form of solar energy, as the sun powers the hydrologic cycle which gives the earth its water. In the hydrologic cycle, atmospheric water reaches the earth surface as precipitation. Some of this water evaporates, but much of it either percolates into the soil or becomes surface runoff. Water from rain and melting snow eventually reaches ponds, lakes, reservoirs, or oceans where evaporation is constantly occurring. Hydro-turbines convert water pressure into mechanical shaft power, which can be used to drive an electricity generator, or other machinery. The power available is proportional to the product of pressure head and volume

flow rate. The general formula for any hydro system's power output is:

$$P = \eta \rho g Q H$$

where P is the mechanical power produced at the turbine shaft (Watts), η is the hydraulic efficiency of the turbine, ρ is the density of water (kg/m^3), g is the acceleration due to gravity (m/s^2), Q is the volume flow rate passing through the turbine (m^3/s), and H is the effective pressure head of water across the turbine (m). The best turbines can have hydraulic efficiencies in the range 80 to over 90% (higher than most other prime movers), although this will reduce with size. Micro hydrosystems tend to be in the range 60 to 80% efficient.

IV. MICRO HYDRO POWER PLANT

Micro hydro is mainly 'run of river,' so does not involve the construction of large dams and reservoirs. It also has the capacity to make a more immediate impact on the replacement of fossil fuels since, unlike other sources of renewable energy, it can generally produce some electricity on demand (at least at times of the year when an adequate flow of water is available) with no need for storage or backup systems. It is also in many cases cost competitive with fossil-fuel power stations, or for remote rural areas, diesel generated power. Small hydro has a large, and as yet untapped, potential in many parts of the world. It depends largely on already proven and developed technology with scope for further development and optimization. Least-cost hydro is generally high-head hydro since the higher the head, the less the flow of water required for a given power level, and so smaller and less costly equipment is needed. While this makes mountainous regions very attractive sites they also tend to be in areas of low population density and thus low electricity demand and long transmission distances often nullify the low cost advantage. Low-head hydro on the other hand is relatively common, and also tends to be found in or near concentrations of population where there is a demand for electricity [5].

Construction details of a micro hydro plant are site-specific. Sometimes an existing mill-pond or other artificial reservoir is available and can be adapted for power production. In general, micro hydro systems are made up of a number of components. The most important include the intake where water is diverted from the natural stream, river, or perhaps a waterfall. An intake structure such as a catch box is required to screen out floating debris and fish, using a screen or array of bars to keep out large objects. In temperate climates this structure must resist ice as well. The intake may have a gate to allow the system to be dewatered for inspection and maintenance. The intake then tunnels water through a pipeline (penstock) to the powerhouse building containing a turbine. In mountainous areas, access to the route of the penstock may provide considerable challenges. If the water source and

turbine are far apart, the construction of the penstock may be the largest part of the costs of construction. At the turbine, a controlling valve is installed to regulate the flow and the speed of the turbine. The turbine converts the flow and pressure of the water to mechanical energy; the water emerging from the turbine returns to the natural watercourse along a tailrace channel. The turbine turns a generator, which is then connected to electrical loads; this might be directly connected to the power system of a single building in very small installations, or may be connected to a community distribution system for several homes or buildings. Usually micro hydro installations do not have a dam and reservoir, like large hydroelectric plants have, relying on a minimal flow of water to be available year-round.

V. HYDRO POWER PLANT IN INDIA

India is blessed with immense amount of hydro-electric potential and ranks 5th in terms of exploitable hydro-potential on global scenario. As per assessment made by CEA, India is endowed with economically exploitable hydro-power potential to the tune of 1, 48,700 MW of installed capacity. The basin wise assessed potential is as under:-

Basin/Rivers Probable Installed Capacity (MW)

| | |
|--|----------|
| Indus Basin | 33,832 |
| Ganga Basin | 20,711 |
| Central Indian River system | 4,152 |
| Western Flowing Rivers of southern India | 9,430 |
| Eastern Flowing Rivers of southern India | 14,511 |
| Brahmaputra Basin | 66,065 |
| Total | 1,48,701 |

In addition, 56 number of pumped storage projects have also been identified with probable installed capacity of 94 000 MW. In addition to this, hydro-potential from small, mini & micro schemes has been estimated as 6 782 MW from 1 512 sites. Thus, in totality India is endowed with hydro-potential of about 250000 MW. Recognizing that small hydropower projects can play a critical role in improving the overall energy scenario of the country and in particular for remote and inaccessible areas, the Ministry aims to harness at least half of the potential in the country over the next decade to bring the installed capacity of small hydro to about 7 GW by the end of 12th Plan in 2017. In August 2012, the Minister of New and Renewable Energy, Dr. Farooq Abdullah, said that during the 11th Plan, a capacity of 1,419 MW of small hydro was added compared to 536 MW during the 10th Plan. Some 967 small hydro projects with an aggregate capacity of 3,632 MW have been installed in India to the end of April 2013, with 24 states announcing a policy to invite private sector bodies to set up projects. In addition, 281 small hydro projects with an aggregate capacity of 1,061 MW are also under construction in various states.

VI. EFFECT OF MICRO HYDRO POWER PLANT

Small-scale micro hydro power is both an efficient and reliable form of energy, most of the time. There are some advantage of micro hydro power plant are:

Increase of oxygen content in the lower course

Turbines of small-scale hydropower plants spin oxygen into the waters. This benefits fish stock preservation.

Flood control

River valleys assure a lot of peace and relaxation, which is why they are widely appreciated as residential areas. The quality of life, however, is deeply affected by common flooding that often cause much damage. Power plants and their facilities can contribute to flood control.

No reservoir required

Micro hydro is considered to function as a run of river system, meaning that the water passing through the generator is directed back into the stream with relatively little impact on the surrounding ecology.

Cost effective energy solution

Building a small-scale hydro-power system can cost from \$1,000-\$20, 000 depending on site electricity requirement and location. Maintenance fees are relatively small in comparison to other technologies.

Power for developing countries

Because of the low-cost versatility and longevity of micro hydro, developing countries can manufacture and implement the technology to help supply much needed electricity to small communities and villages.

Integrate with the local power grid

If your site produces a large amount of excess energy, some power companies will buy back your electricity overflow. You also have the ability to supplement your level of micro power with intake from the power grid [6].

VII. PROPOSED WORK

The electricity sector in India had an installed capacity of 237.742 GW as of February 2014 the world's fourth largest. Captive power plants generate an additional 39.375 GW. Non Renewable Power Plants constitute 87.55% of installed capacity, and Renewable Power Plants constitute the remaining 12.45% of total installed Capacity. India ranks 5th in terms of exploitable hydro-potential on global scenario.^[1] In 2012, India is the 7th largest producer of hydroelectric power with 114,000 GW hours. With installed capacity of 37 GW, it produces 3.3% of the world's total.^[2] The Working Group of the Planning Commission for the Twelfth Plan has estimated a total requirement of 1403

Billion Units (BU) per annum by the end of 12th Five Year Plan (2016–17), out of which share of hydro generation is expected to be 12%. As per Planning Commission, the capacity addition for the 12th Five Year Plan on an all-India comprises 10,897 MW for Hydro.^[3] By the use of micro hydro power plant we can generate electricity on rural area because this power plant can establish on small area with minimum resources .We proposed that we can establish this type of project near the Himalayan area and basins.

VIII. CONCLUSION

Due to depletion of non-renewable energy resources in present scenario it is necessary to use renewable energy resources such as wind energy, hydro energy and so on. Our proposed frame work give details about micro hydro power plant by

which we can minimize the problem of electricity in rural area with minimum resources.

REFERENCES

- [1] Barnes, D.F., W. M. Floor (1996) 'Rural Energy in Developing Countries: A Challenge for Economic Development, *Annual Review of Energy and the Environment* 21(1): 497-530.
- [2] REN21, Renewables Global Status Report (2006 - 2012)". Ren21.net. Retrieved 2012-10-21.
- [3] Berner, E., G. Gomez and P. Knorringa (2012) "Helping a Large Number of People Become a Little Less Poor: The Logic of Survival Entrepreneurs, *European Journal of Development Research*.
- [4] Howard Schneider (8 May 2013). "World Bank turns to hydropower to square development with climate change". *The Washington Post*. Retrieved 9 May 2013.
- [5] Adam Harvey, Andy Brown, Priyantha Hettiarachi and Allen Inversin, "Micro Hydro Design Manual" Intermediate Technology Publications, United Kingdom, 1993.
- [6] Prof. Dr. Ing. Joachim Raabe, "Hydro Power" VDI-Verlag GmbH, Germany, 1985.

Assessment of Nuclear Power And It's Future In India

H.V. Singh¹, Ashok Kumar², Sandeep Pacheyan³

Abstract- This paper presents a review on impact assessment of nuclear power plants in India and the regulatory process in India is continuously evolving to cater to the new developments. Some of the recent initiatives taken by Department of Atomic Energy(DAE) in that direction are briefly described .Authors strongly believe that this survey article will be very much useful to the researchers, scientific, engineers and industrial persons for finding out the relevant references in the field of impact assessment of nuclear power plants and its future prospects.

Keywords:Nuclear Power Plant, DAE, Nuclear Ageing and Emerging Power System.

I. INTRODUCTION

THE Nuclear energy has had a long history in India. The Atomic Energy Commission (AEC) was set up in 1948, barely a few months after the country became independent after two centuries of British colonialism. A few years later, in 1954 the DAE was formed under the direct charge of the Prime Minister, thereby circumventing many standard procurement and funding procedures. Ever since its inception, the DAE has made confident predictions that atomic energy would play an important role in satisfying India's energy needs, but the actual growth of nuclear power in the country has been extremely modest. In July 2013, the total installed nuclear power generation capacity was 4,780 MW, 2.08 % of the total installed electricity generation capacity of over 2,28,721.73 MW in the country[1]. It has been estimated by DAE that about 220 GW nuclear power will be installed up to the year 2045 [2]. How Long Can a Nuclear Reactor Last? Increasingly dependable and emitting few greenhouse gases, the U.S. fleet of nuclear power plants will likely run for another 50 or even 70 years before it is retired -- long past the 40-year life span planned decades ago -- according to industry executives, regulators and scientists [3]. The heyday of nuclear power plant construction was the 1970s and 1980s. While most of the first generation of reactors have been closed down, the following second generation of reactors are largely still operational. By 11 March 2014, the third anniversary of the Fukushima nuclear disaster, the 25 oldest reactors in Europe (excluding Russia) will be over 35 years old[4].

¹

Tarapur 1 and 2 units in India are arguably one of the oldest operational reactors in the world, nearly 45 years old [5] DAE continues to rely on future projections with zero correlation to its past accomplishments. From its original target of 10,000 MW by year 2000, to its revised target of 20,000 MW by 2020 since 1984, the heated debates on Indo-US nuclear deal were to make Government of India declare that, against existing 4120 MW for 2008, "the U.S. will help us add 40,000 MW of nuclear power by the year 2020." Former Atomic Energy Chairman Anil Kakodkar was to pitch in predicting, how by 2050, the share of nuclear power will constitute 20 to 35 per cent of electricity generation though it now stood at less than 3 per cent. [6]. Nuclear genie continues to be the symbol of progress and power and our scientific and political leadership continues to vouch for its cost-effective and indigenous nature. It reminds one of the 'Atoms for Peace' of 1950s and the famous prognoses of Lewis Strauss, President Eisenhower's Chairman of US AEC, who once called it source of energy "too cheap to meter." [7].

II. DEVELOPMENT OF NUCLEAR POWER

Weston M. Stacey [8], in Nuclear Reactor Physics has proposed that a great deal of care is taken to ensure that the nuclear reactors operate safely. The fundamental objective of this effort is to ensure that radionuclides are not released in the environment to create a health hazard to the general public or operating personnel. 90Sr and 137Cs and the isotopes of iodine are of particular concern. Strontium has a high fission yield and behaves chemically like calcium and is deposited in bone tissue. Both 90Sr and its daughter 90Y produce a very high dose per unit activity, which is quite damaging to the blood cells produced in bone marrow [9]. The iodine radioisotopes are concentrated in the thyroid gland, where they would produce tumours [10]. There are generally three levels of defence used to prevent nuclear fission product release. The first level of defence is to have a good design of nuclear power plant to prevent the occurrence of any event that could result in damage to the fuel or other reactor system. The next level comprise of protective systems (which are designed to halt or bring under control any transients resulting from operator error or component failure that may lead to fuel damage and fission product release within the pressure vessel).

1. Assistant professor, ECD, knit sultanpur
2. Assistant professor, ECD, knit sultanpur
3. UG scholar, knit sultanpur

Reactor scram systems which inject control rods into the core for rapid shutdown upon being activated by any one of several signals being outside the tolerance range, pressure relief systems, and so on, constitute the reactor protective systems. The third level of defense is provided by mitigation systems, which limit the consequences of accidents if they do occur.

III. NUCLEAR POWER IN INDIA

Narora Atomic Power Station (NAPS) are provided with two diverse & independent shut down system. The primary shutdown system has shutoff mechanism at 14 locations in the reactor. Each of the 14 mechanisms has cadmium sandwiched steel as neutron absorbing element. Normally these rods are parked outside core during power operation & fully in on a trip signal. The rods are held out of reactor core by rope & drum arrangement. These rods drop in the core under gravity whenever a trip signal is received, & make the reactor sub-critical in less than 2.3 sec [11]. The secondary shutdown system provides sufficient reactivity worth by promptly filling 12 vertical tubes in the reactor core with a neutron absorbing liquid (Lithium Pentaborate decahydrate). The principle is such that when liquid filled tanks are pressurized than the liquid rises up in liquid tubes located inside reactor. It makes the reactor sub-critical in 1.4 s. Both the shutdown systems are backed by Automatic Liquid Poison addition system injecting controlled quantities of boron into the moderator after receiving the appropriate signal to ensure guaranteed sub-criticality of the reactor for prolonged periods. Whenever there is total blackout of the station & automatic liquid poison system is not available, addition of poison, under gravity, to moderator is incorporated [12]. M.V. Ramana et al [13], has presented clear picture of the current scenario of Indian nuclear program. Despite its inability to live up to its promises, the DAE has always received high levels of financial support from the government. In the late 1950s, over a quarter of all resources devoted to science and technology development in the country went to the DAE [14]. Though it was subsequently overtaken by the Department of Space (DoS), the total amount spent on the DAE, the Defence Research and Development Organisation (DRDO), and the DoS has been increasing as a fraction of all government research and development budgets. In the late 1980s, for example, the proportion was over 60 % of the total. With the nuclear weapon tests conducted in 1998, the DAE's funding has increased dramatically over the last few years [15].

Following are the power stations under construction: -

| S.NO. | PLACE | CAPACITY |
|-------|-------------------|------------|
| 1. | RAPS (7 & 8) | 2X700 MWe |
| 2. | KAKRAPAR (3 & 4) | 2X700 MWe |
| 3. | KUNDAKULAM (1&2) | 2X1000 MWe |

TAPS Tarapur Atomic Power Station

RAPS Rajasthan Atomic Power Station

MAPS Madras Atomic Power Station

Following are the India's Atomic Power Stations operating as on today [16]:

| S.NO. | PLACE | CAPACITY |
|-------|------------------|-----------|
| 1. | TAPS (1 & 2) | 2X160MWe |
| 2. | RAPS (1 & 2) | 2X220MWe |
| 3. | MAPS (1 & 2) | 2X220MWe |
| 4. | NAPS(1 & 2) | 2X220MWe |
| 5. | KAKRAPAR (1 & 2) | 2X220MWe |
| 6. | KAIGA (1 & 2) | 2X220MWe |
| 7. | RAPS (3 & 4) | 2X220MWe |
| 8. | TAPS (3 & 4) | 1X540 MWe |
| 9. | RAPS (5 & 6) | 2X220MWe |
| 10. | KAIGA(3 & 4) | 2X220MWe |

IV. COST COMPARISON OF NUCLEAR POWER PLANT

Heavy Water, the one of the key element of nuclear power has also had hiccups though Heavy Water reactors had been India's hot favourite from the very beginning. All this has led to reactors working on low capacity and facing shut downs and DAE staying happy with turnkey projects and imports. Expensive plutonium separation from used fuel rods continues to be justified for its 'tremendous potential' for treating hazardous radioactive waste and for unlocking the huge energy reserves of low-grade uranium and thorium resources through breeder reactors to unfold India's nuclear renaissance. Over a decade ago, a comparison of energy technologies had concluded that other options such as coal and hydroelectric power were cheaper than nuclear power under realistic assumptions and "even if the projections and scenarios indicate large demand-supply gaps in the future, the most expensive way of bridging these gaps is through nuclear power plants" [17].

Table 4.
Capital costs of operating reactors

| Station | Original cost (Rs, million) | Revised cost(Rs. million) | Criticality year |
|-------------|-----------------------------|---------------------------|------------------|
| TAPS I & II | 929.9 | - | 1969 |
| RAPS I | 339.5 | 732.7 | 1972 |
| RAPS II | 581.6 | 1025.4 | 1980 |
| MAPS I | 617.8 | 1188.3 | 1983 |
| MAPS II | 706.3 | 1270.4 | 1985 |
| NAPS I & II | 2098.9 | 7450 ^[2] | 1989 & 1991 |

| | | | | |
|-----------------|--------|--------|--------------|---|
| Kakrapar I & II | 3825 | 13,350 | 1992 1995 | & |
| Kaiga I & II | 7307.2 | 28,960 | 1999 2000 | & |
| RAPSIII & IV | 7115.7 | 25,110 | 2000 | |

Sources: DAE, 1996, p. 67; DAE, 2002b

The major problem in making independent estimates of the cost of nuclear energy has been the difficulty in getting economic and performance data from the DAE. Like nuclear establishments elsewhere, the DAE has had a history of secrecy [18]. Sanctioned in 1982, the Manuguru Heavy Water Plant (HWP) has an annual capacity of 185 t of HW[19]. The estimated cost of the Manuguru HWP when it was sanctioned was Rs. 4.216 billion. In 1989, the plant cost was revised to Rs. 6.6158 billion. The plant finally started production in December 1991 [20]. According to the Comptroller and Auditor-General(CAG), the “total capital cost including interest during construction and excluding cost of spares came to Rs. 983.38 crores [9.8338 billion] and the increase, with reference to the original estimated cost was 133 percent.” When questioned about the cost escalation, DAE stated that “the grounds for sanction of this project was strategic and not commercial”. The DAE’s initial estimate of the cost of production was Rs. 5,176 per kg of HW (Rs./kgHW). However, because of slippages in the project schedules and consequential delay in commencement of production, the cost of HW worked out to Rs. 7,529/kgHW as of February 1986. This translates to about Rs. 24,880/kgHW at 2002 prices, in the same ball-park as the 1983 figure of Rs. 6,635/kgHW (Rs. 26,960/kgHW when inflated to 2002 prices) cited by the then head of the DAE [21]. However, in its 1994 report on Manuguru, the CAG pointed out “Due to further escalation, the cost would have gone up further -- the figures for costing after commencement of production in December 1991 were not produced to Audit (December 1993).” There appear to be no further public estimates of the cost of the project.

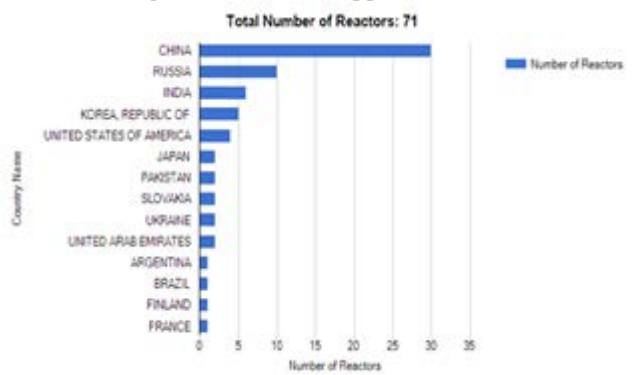
V. RISKS OF NUCLEAR AGEING

The design lifetime is the period of time during which a facility or component is expected to perform according to the technical specifications to which it was produced. Life-limiting processes include an excessive number of reactor trips and load cycle exhaustion. Physical ageing of systems, structures and components is paralleled by technological and conceptual ageing, because existing reactors allow for only limited retroactive implementation of new technologies and safety concepts. Together with ‘soft’ factors such as outmoded organisational structures and the loss of staff know-how and motivation as employees retire, these factors cause the overall safety level of older reactors to become increasingly inadequate by modern standards[22]. Measures to uprate a reactor’s power output can further compromise safety

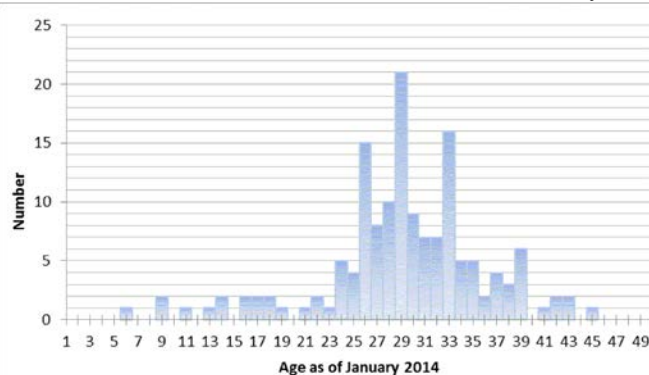
margins, for instance because increased thermal energy production results in an increased output of steam and cooling water, leading to greater stresses on piping and heat exchange systems, so exacerbating ageing mechanisms. Modifications necessitated by power uprating may additionally introduce new potential sources of failure due to adverse interactions between new and old equipment. Thus, both lifetime extension and power uprating decrease a plant’s originally designed safety margins and increase the risk of failures[23].

Physical ageing issues include those affecting the reactor pressure vessel (including embrittlement, vessel head penetration cracking, and deterioration of internals) and the containment and the reactor building, cable deterioration, and ageing of transformers. Conceptual and technological ageing issues include the inability to withstand a large aircraft impact, along with inadequate earthquake and flooding resistance. Some reactor types, such as the British Advanced Gas-Cooled Reactors (AGC) and Russian-designed VVER-440 and RBMK (Chernobyl-type) reactors suffer specific problems[24][25][26]. With nuclear providing always-on electricity that will become more cost-effective if a price is placed on heat-trapping carbon dioxide emissions, utilities have found it is now viable to replace turbines or lids that have been worn down by radiation exposure or wear. Many engineers are convinced that nearly any plant parts, most of which were not designed to be replaced, can be swapped out [27]. “We think we can replace almost every component in a nuclear power plant,” said Jan van der Lee, director of the Materials Ageing Institute(MAI), a nuclear research facility in France and run by the state-owned nuclear giant EDF. “We don’t want to wait until something breaks,” he said. By identifying components that are wearing down and replacing them, he said, suddenly nuclear plants will find that “technically, there is no age limit. “Indeed, as U.S. regulators begin considering the extended operations of nuclear plants the Nuclear Regulatory Commission(NRC) [28] expects the first application for an 80-year license could come within five years or less perhaps the largest lingering question is one of basic science: How do heavy doses of radiation, over generations, fundamentally alter materials like steel and concrete?” It’s taken many years for us to understand the problem,” said Gary Was, the director of the University of Michigan’s Phoenix Energy Institute and an expert in aging materials. “Thirty years ago, we didn’t have techniques to see these changes.” Until recently, such research has not been a priority. But within the past few years, the Department of Energy began a program looking at “long-term operations,” as it is known in the industry. And provisions in the Senate’s climate bill call for DOE to increase these investigations in the hope of extending plant lives “substantially beyond the first license extension period.” DOE collaborates in this research with France’s MAI and the U.S.-based Electric Power Research Institute(EPRI), a non-profit funded by many nuclear utilities. U.S. leadership in the field is natural, given the sheer age of America’s reactors, many of which are

already coming close to exceeding their intended operating lives. The oldest commercial plants in the United States reached their 40th anniversary this year, and the average plant has operated for 30 years. Already, more than half of the nation's more than 100 reactors have seen their initial licenses extended for an additional two decades. Nearly all the country's plants are expected to eventually win such extensions. Manu Mathai[29] explains that the fatal attraction for nuclear power as integral to modern megamachine societies that see modernity as a linear process premised on powerful patronage of science by State. Benjamin Sovacool et al [30] shows how inability to justify enormous funding for poor performance of nuclear power and inability to justify such investments in the name of nuclear weapons led Indian elite to calibrate songs of "nuclear non-alignment" and "nuclear apartheid" to celebrate liberation and equality. Robert Anderson [31] alludes to corruption and infighting within the scientific community and lack of political vision resulting in loss of talent (e.g. Noble laureate Hargobind Khorana or Meghnath Saha) and opportunities.



Reactors under construction worldwide in November 2013 [32]. This political inaptness made slick scientists promise power generation and weaponisation that no other agency could offer, and the resultant political clout has been used by the DAE to bypass democracy. Recent climate change debates have brought another lease of life projecting nuclear power as less carbon-intensive and therefore environment friendly.



Age (based on first grid connection) of operating nuclear reactors in the European Union, Switzerland and Ukraine.

Source: based on IAEA:Power Reactor Information System(PRIS), <http://www.iaea.org/PRIS>, as of 10 January 2014.

Plant lifetime extension and power uprating

Design lifetime is defined by the IAEA as:

The period of time during which a facility or component is expected to perform according to the technical specifications to which it was produced. The Systems, Structures and Components (SSCs) of nuclear reactors often fulfil safety relevant functions, either because the failure of a component may initiate an incident or accident, or because a system function is needed to cope with an incident or accident when it occurs. Because of this, the functioning of systems, structures and components within their specified parameters has to be guaranteed throughout the operation of a reactor. On a long-term basis, the predicted collective lifetime doses due to the fallout from the Chernobyl accident are 1.6×10^4 person-Gy for the evacuated population near the site, 4.7×10^5 person-Gy for the European part of the former USSR, 1.1×10^5 person-Gy for the Asian part of the former USSR, 5.8×10^5 person-Gy for Europe, 2.7×10^4 person-Gy for Asia, 1.1×10^3 person-Gy for the United States, and 1.2×10^6 person-Gy for the entire northern hemisphere. The increase in the estimated 50-year exposure doses in Europe, for example, varied from a fraction of the natural background to a few times the natural background. There is no scientific evidence on which to assess the effect, if any, of such small incremental doses. However, by extrapolating from higher dose levels, it is possible to estimate the long-term health effects of fallout from the Chernobyl accident. The estimated increase above natural incidence of fatal cancers in the respective populations due to the Chernobyl fallout is 2.4% for the evacuated population near the site, 0.12% for the European part of the former USSR, 0.01% for the Asian part of the former USSR, 0.02% for Europe, 0.00013% for Asia, and 0.00005% for the northern hemisphere[24][25][26]. At Fukushima, the spent-fuel rods holding most of the highly radioactive uranium at the site have proved a bigger radiation problem than the reactor cores. This shines a spotlight on the spent-fuel challenges at the sister but older plant in Tarapur, where the discharged fuel has been accumulating for over four decades because the U.S. has refused to either take it or allow India to reprocess it. The mounting Tarapur spent-fuel stockpile poses greater safety and environmental hazards than probably at any other plant in the world. The spent-fuel rods — unlike the reactors have no containment structure, and they endanger public safety in India's densely-populated commercial heartland. The spent-fuel bundles are kept under water in bays at a special facility at Tarapur. But such temporary pools have proven Fukushima's Achilles heel. Until Fukushima, nuclear energy was coming out of a decades-long slump. A tally in January found 65 new nuclear power plants under construction in 15

countries. Only one of these is in the United States. Most of the new construction is in Asia. Still, nuclear power represents 20 percent of U.S. electricity capacity, with 104 plants currently operating. Worse still, the planned import of four different types of new Light Water Reactor (LWR) technology will make India's nuclear-power complex the most diverse in the world. Technological diversity may be good to obviate reliance on one supplier. But the wide-ranging diversity India is getting into will make its safety responsibilities extremely arduous and complex, given the multiplicity of reactor designs it already has in place[33]. It takes a long time to create teams of experienced safety engineers for any reactor model. But when a particular reactor model is still not in operation anywhere, training of engineers cannot even begin. By

contrast, India has immense experience in building, operating and safeguarding indigenous CANDU-style reactors. While the risks and reasons for the risks vary along the bathtub curve, the consequences of failing to manage the risks remain nearly constant—potentially massive releases of radioactivity into the atmosphere with devastating harm to people and places downwind. An aggressive regulator consistently enforcing federal safety regulations provides the best protection against these risks. As the famous Physicist R.P. Feynman wrote in the Appendix F (Personal Observation on the Reliability of the Shuttle) of Roger's Commission on Challenger Shuttle Disaster :

"For a successful technology, reality must take precedence over public relations, for nature cannot be fooled."

VI. SUMMARY OF THE PAPER

The summary of literature reviewed regarding ageing of nuclear power plants with its problems and its solutions. So that the lifetime extension of nuclear plant is good solution for this problems if proper care is taken.

Table 5. 26 Oldest nuclear power stations in the world.

| | Country | Power Station | Reactor Type | Reference Unit Power | Starting Date | Age (years) |
|----|---------|-----------------------|--------------|----------------------|---------------|-------------|
| 1 | IN | Tarapur 1 and 2 | BWR | 320 | 28.10.1969 | 44 |
| 2 | CH | Beznau 1 | PWR | 365 | 17.07.1969 | 44 |
| 3 | UK | Wylfa 1 | GCR | 490 | 24.01.1971 | 43 |
| 4 | ES | Santa Maria de Garona | BWR | 446 | 02.03.1971 | 43 |
| 5 | CH | Muehleberg | BWR | 373 | 01.07.1971 | 42 |
| 6 | SE | Oskarshamn 1 | BWR | 473 | 19.08.1971 | 42 |
| 7 | CH | Beznau 2 | PWR | 265 | 23.10.1971 | 42 |
| 8 | NL | Borssele | PWR | 482 | 04.07.1973 | 40 |
| 9 | SE | Ringhals 2 | PWR | 865 | 17.08.1974 | 39 |
| 10 | BE | Doel 1 | PWR | 433 | 28.08.1974 | 39 |
| 11 | SE | Oskarshamn 2 | BWR | 638 | 02.10.1974 | 39 |
| 12 | SE | Ringhals 1 | BWR | 865 | 14.10.1974 | 39 |
| 13 | BE | Tihange 1 | PWR | 962 | 07.03.1975 | 39 |
| 14 | BE | Doel 2 | PWR | 433 | 21.08.1975 | 38 |
| 15 | UK | Hinkley Point B2 | GCR | 435 | 05.02.1976 | 38 |
| 16 | UK | Hunterston B1 | GCR | 430 | 06.02.1976 | 38 |
| 17 | UK | Hinkley Point B1 | GCR | 435 | 30.10.1976 | 37 |
| 18 | FI | Loviisa 1 | PWR | 495 | 08.02.1977 | 37 |
| 19 | UK | Hunterston B2 | GCR | 430 | 31.03.1977 | 36 |
| 20 | FR | Fessenheim 1 | PWR | 880 | 06.04.1977 | 36 |
| 21 | FR | Fessenheim 2 | PWR | 880 | 07.10.1977 | 36 |

| | | | | | | |
|----|----|-------------|-----|-----|------------|----|
| 22 | FR | Bugey 2 | PWR | 910 | 10.05.1978 | 35 |
| 23 | FI | Olkiluoto 1 | BWR | 880 | 02.09.1978 | 35 |
| 24 | FR | Bugey 3 | PWR | 910 | 21.09.1978 | 35 |
| 25 | CH | Goesgen | PWR | 970 | 02.02.1979 | 35 |
| 26 | FR | Bugey 4 | PWR | 880 | 08.03.1979 | 35 |

BWR = boiling water reactor, PWR = pressurised water reactor, GCR = gas cooled reactor

Age shown as of 11 March 2011 , Source: IAEA PRIS database – <http://www.iaea.org/pris>. 11.03.2014

VII. CONCLUSION

This paper presents a thorough assessment of the nuclear energy trends and its future in India. Although a lot has been invested in this field yet the present data cannot be termed as encouraging though the future might be bright in this area considering the projections made by DAE. Considering the necessity of non-conventional energy, this could be crucial in future and hence India needs to harness it judiciously. Although, no compromises, whatsoever, should be made in terms of Health and Safety of the citizens.

VIII. ACKNOWLEDGEMENT

The authors would like to thank Dr. K.S. Verma ,Dr .H.V.Singh and Ashok Kumar, Kamala Nehru Institute of Technology, Sultanpur, U.P.,-228118, India, for their valuable suggestions regarding Assessment of Nuclear Power And Its Future In India

IX. REFERENCES

- [1] Power ministry , Power Sector at a Glance "ALL INDIA" , http://powermin.nic.in/indian_electricity_scenario/introduction.htm accessed on April 10 2014
- [2] Kakodkar, A., 2004. Nuclear energy in India – retrospect and prospects. An International Journal of Nuclear Power 18 (2–3), 7–12.
- [3] Paul Voosen , How Long Can a Nuclear Reactor Last?ScientificAmerican , November 20, 2009.
- [4] IAEA PRIS database – <http://www.iaea.org/pris>. 11.03.2014
- [5] Nuclear Power Corporation Of India (NPCIL) , Plants Under Operation Tarapur Atomic Power Station (TAPS) <http://www.npcil.nic.in/main/ProjectOperationDisplay.aspx?ReactorID=73> accessed on April 10 2014
- [6] Swaran Singh ,India's nuclear power problem, The Hindu,April 9, 2013
- [7] M. V. Ramana,The Power of Promise, Examining Nuclear Energy in IndiaPenguin Books India Pvt. Ltd
- [8] Weston M. Stacey ,Nuclear Reactor Physics , Second Edition ,WILEY-VCH Verlag GmbH & Co.KGaA, Weinheim
- [9] R. A. Knief, Nuclear Engineering, Taylor & Francis, Washington, DC (1992),Chaps. 13–16.
- [10] H. Cember, Introduction to Health Physics, 3rd ed., McGraw-Hill, NewYork (1996).
- [11] Nuclear Power Corporation (NPC), Narora Nuclear Power Plant, Industrial training manual.
- [12] Nuclear Power Corporation (NPC), Narora Nuclear Power Plant , Shutdown Mechanism Mannual
- [13] M. V. Ramana , Antonette D'Sa and Amulya K.N. Reddy, The Power of Promise, Examining Nuclear Energy in India , Penguin Books
- [14] Abraham, I., 1993. Security, Technology and Ideology: "Strategic Enclaves" in Brazil and India, 1945-1989, Ph.D. dissertation thesis, University of Illinois, Urbana Champaign.
- [15] Joseph, A., 1999. "India plans to be nuke powerhouse by 2020, sets a 20,000 MW target", Economic Times, September 16.
- [16] Nuclear Power Corporation of India Limited (NPCIL) , Plants Under Operation<http://www.npcil.nic.in/main/allprojectoperationdisplay.aspx> accesseed on April 10 2014.
- [17] Reddy, A.K.N., 1990. "Nuclear power: is it necessary or economical?", Seminar, (1), pp. 18-26, June.
- [18] Ramana, M.V., D'Sa, A., and Reddy, A.K.N., 2005. "Economics of nuclear power from heavy water reactors", Economic and Political Weekly, 40(17), pp. 1763-1773, April 23.
- [19] Nuclear Power Corporation of India Limited (NPCIL) , Manuguru Heavy Water Plant
- [20] Comptroller and Auditor-General (CAG), 1994. Report by the Comptroller and Auditor General of India, Comptroller and Auditor General of India, New Delhi.
- [21] Ramanna, R., 1985. "Can nuclear energy claim to be the only source of power in the future?", C.C. Desai Memorial Lecture, Administrative Staff College of India, 4 March.
- [22] Schneider, M., Froggart, A. et al. 2013. World nuclear industry status report 2013. Mycle Schneider Consulting.
- [23] Tehan,N.K. , US Nuclear Regulating Committee , Nuclear Science Symposium Conference Record , 2004 , IEEE
- [24] "Special Issue: Chernobyl," Nucl.Safety 28 (1987).
- [25] "Chernobyl: A Special Report," Nucl. News, 29, 87 (1986); "Chernobyl: The Soviet Report," Nucl. News, SpecialReport (1986).
- [26] Report on the Accident at the Chernobyl Nuclear Power Station, NUREG-1250, U.S. Nucl. Regul. Commission,Washington, DC (1987).
- [27] WASH-1400, Reactor Safety Study: An Assessment of Accident Risks in U.S. Commercial Nuclear Power Plants, NUREG-74/014, U.S. Nuclear Regulatory Commission, Washington, DC(1975).
- [28] Nuclear Regulatory Commission (NRC), Safety Evaluation Report for an Early Site Permit (ESP) at the Vogtle Electric Generating Plant (VEGP) ESP Site, NTIS:NUREG1923; 2009.
- [29] Manu Mathai , Nuclear Power, Economic Development Discourse and the Environment: The Case of India 2013
- [30] Benjamin Sovacool , Scott Valentine The National Politics of Nuclear.Power 2012
- [31] Robert Anderson , Nucleus and Nation 2010.
- [32] Öko-Institut. 2011,Streitpunkt Kernenergie. <http://www.streitpunkt-kernenergie.de/index.php?id=19>.
- [33] Brahma Chellaney, Corrupt means taint the nuclear deal , March 23 2011 , The Hindu , <http://www.thehindu.com/opinion/lead/corrupt-means-taint-the-nuclear-deal/article1562256.ece>

BIBLIOGRAPHIES

HARSH VIKRAM SINGH received the Ph.D. in electronics engineering from the Banaras Hindu University in 2008. His research interests are in Information Security, Steganography & Cryptography, Image Processing, and Digital System Design. Currently, he is an Assistant Professor with Department of Electronics Engineering, Kamla Nehru Institute of Technology, Sultanpur, U.P., and India, where he has been since October 2008.
Mobile: 09415763939.
Email id: harshvikram@gmail.com



Department of Telecommunications and having work experience of 17 years. His area of interest are Microwave, Radar, Antenna, and Electromagnetic theory. Presently working as Associate Professor in Electronics Engineering Department KNIT, Sultanpur.
Mobile: 09415094287.
E-mail: akprasad212@yahoo.co.in



Ashok Kumar Received his B Tech. , M Tech. degree from IET, Lucknow and KNIT, Sultanpur respectively. He has worked at ISRO, Hassan, DRDO Balasore, NTPC New Delhi, HBTI Kannur, KNIT Sultanpur, ITI Raebareilly,



Sandeep Pacheyan is a B.Tech. (Electronics Engineering) Student, Department of Electronics Engineering, Kamla Nehru Institute of Technology (KNIT), Sultanpur-228118, U.P., India. His interests are in the areas of Nuclear Physics. Mobile: 9457228484
E-mail ID: sandeep.pacheyan@gmail.com

POWER QUALITY IMPROVEMENT BY UPQC USING ANN CONTROLLER

A. Ravi Yadav, *student member IEEE*, B. Vivek Soni, *student member IEEE*, C. Vinod Chaudhry, *student member IEEE*, D. Dinesh Kandu, *student member IEEE*

Abstract--In this paper, general introduction to active power filters (APF's), classification and operation of APF's are discussed. The IEEE standards, which define the limits of current and voltage harmonics at various voltage levels, are specified. Various modulation techniques of APF's for generating gate pulses, and various methods implemented to generate the reference template are discussed. Design of interfacing filter and criterion for selection of D.C link capacitor are also discussed. Unified Power Quality Conditioner (UPQC) using PLL with Hysteresis control is discussed and simulated. Case study of a typical steel plant has been given. Simulated proposed UPQC for various non-linear loads of steel plant and results with installation of STATCOM and UPQC are reported.

Index term-Custom power park, Unified Power Quality Conditioner, Static Transfer Switch (STS), Voltage control mode, Voltage Sag

I. INTRODUCTION

With the advent of power semiconductor switching devices, like thyristors, GTO's (Gate Turn off thyristors), IGBT's (Insulated Gate Bipolar Transistors) and many more devices, control of electric power has become a reality. Such power electronic controllers are widely used to feed electric power to electrical loads, such as adjustable speed drives (ASD's), furnaces, computer power supplies, HVDC systems etc. The power electronic devices due to their inherent non-linearity draw harmonic and reactive power from the supply.

¹

In three phase systems, they could also cause unbalance and draw excessive neutral currents. The injected harmonics, reactive power burden, unbalance, and excessive neutral currents cause low system efficiency and poor power factor. In addition to this, the power system is subjected to various transients like voltage sags, swells, flickers etc. These transients would affect the voltage at distribution levels. Excessive reactive power of loads would increase the generating capacity of generating stations and increase the transmission losses in lines. Hence supply of reactive power at the load ends becomes essential. Power Quality (PQ) has become an important issue since many loads at various distribution ends like adjustable speed drives, process industries, printers; domestic utilities, computers, microprocessor based equipment etc. have become intolerant to voltage fluctuations, harmonic content and interruptions. Power Quality (PQ) mainly deals with issues like maintaining a fixed voltage at the Point of Common Coupling (PCC) for various distribution voltage levels irrespective of voltage fluctuations, maintaining near unity power factor power drawn from the supply, blocking of voltage and current unbalance from passing upwards from various distribution levels, reduction of voltage and current harmonics in the system and suppression of excessive supply neutral current. Conventionally, passive LC filters and fixed compensating devices with some degree of variation like thyristor switched capacitors, thyristor switched reactors were employed to improve the power factor of ac loads. Such devices have the demerits of fixed compensation, large size, ageing and resonance. Nowadays equipments using power semiconductor devices, generally known as active power filters (APF's), Active Power Line Conditioners (APLC's) etc. are used for the power quality issues due to their dynamic and adjustable solutions. Flexible AC Transmission Systems (FACTS) and Custom Power products like STATCOM (Static synchronous Compensator), DVR (Dynamic Voltage Restorer), etc. deal with the issues related to power quality using similar control strategies and concepts. Basically, they are different only in

-
- A. PG Scholar, EED, KNIT Sultanpur
 - B. PG Scholar, EED, KNIT Sultanpur
 - C. PG Scholar, EED, KNIT Sultanpur
 - D. PG Scholar, EED, KNIT Sultanpur

the location in a power system where they are deployed and the objectives for which they are deployed.

II. GENERAL THEORY OF ACTIVE FILTER

The various nonlinear loads like Adjustable Speed Drives (ASD's), bulk rectifiers, furnaces, computer supplies, etc. draw non sinusoidal currents containing harmonics from the supply which in turn causes voltage harmonics. Harmonic current cause increased power system losses, excessive heating in rotating machinery, interference with nearby communication circuits and control circuits, etc. It has become imperative to maintain the sinusoidal nature of voltage and currents in the power system. Various international agencies like IEEE and IEC have issued standards, which put limits on various current and voltage harmonics. The limits for various current and voltage harmonics specified by IEEE-519 for various frequencies are given in Table 3.1 and Table 3.2.

**Table 1.1
IEEE 519 Voltage Limits**

| Bus Voltage | Minimum Individual Harmonic Components (%) | Maximum THD (%) |
|------------------|--|-----------------|
| 69 kV and below | 3 | 5 |
| 115 kV to 161 kV | 1.5 | 2.5 |
| Above 161 kV | 1 | 1.5 |

The objectives and functions of active power filters have expanded from reactive power compensation, voltage regulation, etc. to harmonic isolation between utilities and consumers, and harmonic damping throughout the distribution as harmonics propagate through the system. Active power filters are either installed at the individual consumer premises or at substation and/or on distribution feeders. Depending on the compensation objectives, various types of active power filter topologies have evolved, a proper briefing of which is provided in [3-4].

2.2 Classifications of Active Power Filters

2.2(a) Converter based classification-

Current Source Inverter (CSI) Active Power Filter and Voltage Source Inverter Active Power Filter (VSI) (Fig 3.2) are two classifications in this category. Current Source

Inverter behaves as a non-sinusoidal current source to meet the harmonic current requirement of the nonlinear loads. A diode is used in series with the self-commutating device (IGBT) for reverse voltage blocking. However, GTO-based configurations do not need the series diode, but they have restricted frequency of switching. They are considered sufficiently reliable, but have higher losses and require higher values of parallel ac power capacitors. Moreover, they cannot be used in multilevel or multistep modes to improve performance in higher ratings. The other converter used as an AF is a voltage-fed PWM inverter structure. It has a self-supporting dc voltage bus with a large dc capacitor. It has become more dominant, since it is lighter, cheaper, and expandable to multilevel and multistep versions, to enhance the performance with lower switching frequencies. It is more popular in UPS-based applications, because in the presence of mains, the same Inverter bridge can be used as an AF to eliminate harmonics of critical nonlinear loads.

III. OPERATION OF THREE PHASE ACTIVE FILTER

In recent years, the power quality of the AC main system has become a great concern due to the rapidly increased number of electronic equipment. In order to reduce the harmonic contamination in power lines and improve the transmission efficiency Active power filters become essential. A current source is connected in parallel with nonlinear load and controlled to generate the harmonic currents needed for the load. The basic configuration of a three-phase three-wire active power filter is shown in Fig 3.1. The diode bridge rectifier is used as an ideal harmonic generator to study the performance of the Active filter. The current-controlled voltage-source inverter (VSI) is shown connected at the load end. This PWM inverter consists of six switches with antiparallel diode across each switch. The capacitor is designed in order to provide DC voltage with acceptable ripples. In order to assure the filter current at any instant, the DC voltage V_{dc} must be at least equal to $3/2$ of the peak value of the line AC mains voltage.

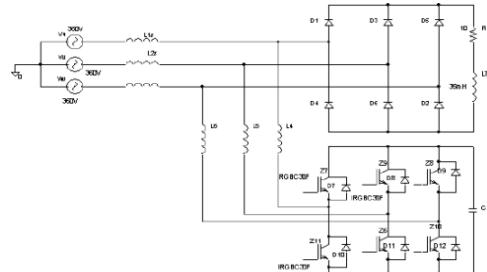


Fig 3.1 Configuration of the three phase, three wire Active filtering system.

Three aspects have to be considered in the design of APF.

- a) The parameters of the inverter such as inverter switches and the values of the link inductances.
- b) Modulation method used and
- c) The control method used to generate the harmonic reference template.

IV. SAMPLE AND HOLD CIRCUIT'S METHODS FOR HARMONICS REFERENCE TEMPLATE

This method is simple, eliminates complicated transformations and mathematical operations such as multiplications and divisions, and permits good transient response. Fig 3.8 shows implementation of Sample and Hold method.

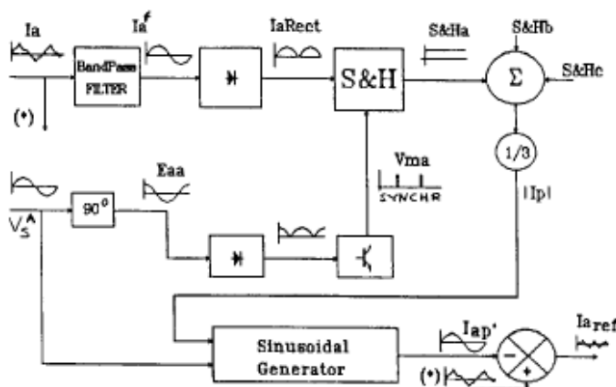


Fig. 4 Control block of Sample and Hold circuit's harmonic reference template

The current in each phase of the load is filtered to get the fundamental phase current. A "Sample and Hold" circuit, synchronized with the peak value of the phase-to-neutral voltage, allows to get three dc signals, which are proportional to the amplitude of the active component of the current for each phase. Three dc signals, with the information of the total active power in the load, are averaged to balance the system. Then, by multiplying the averaged dc signal for a set of balanced reference waveforms (in phase with the mains voltages), three in phase balanced currents for each phase are obtained. Finally, these currents are subtracted from the real load currents to get the compensation currents. These harmonic are then able to correct the harmonic distortion, the power factor and the unbalances of the load.

Let to assume that I_L is the total load current in one phase. This current contains basically three components.

$$I_L = I_P + I_Q + I_H$$

where I_P , I_Q and I_H are fundamental, reactive & harmonic current respectively. The APF will eliminate I_Q and I_H by subtracting I_P from I_L . First the load currents sensed and filtered to eliminate the (I_H) and then the total fundamental currents (one for each phase) are obtained. These currents have to be separated in their active and reactive components.

$$I = I_P + I_Q$$

Where,

$$I_P = I \cos\phi$$

However the angle " ϕ " does need to be known, because the term " $I \cos\phi$ " can be obtained from the time function of the fundamental when the main voltage reaches its maximum value. Fig 4.1 explains graphically the idea.

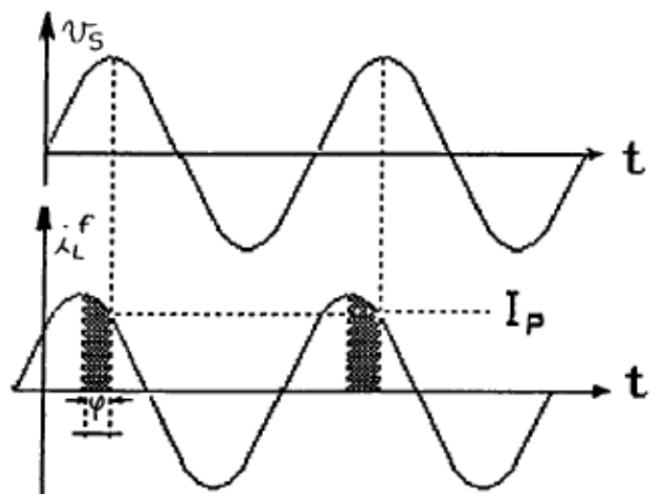


Fig 4.1 Method used to capture I_P .

I_P is captured and "stored" until the next sample of I_P is obtained to replace the old one. This action is executed with the help of "Sample and Hold" circuits, which are synchronized with the synchronization pulses to trigger the S&H are generated through the "zero-crossing" signals, obtained from the set of "in-quadrature voltages". These "in-quadrature voltages" are generated in the control block with the DZ0 connection, signal transformer. The control circuit is also has the capability to avoid flickers and transient phenomena in the source, produced by sudden changes in load current. To do this, control system makes soft variation of I_P during these moments. However, this action will require to have the energy storage components in the APF. Hence the

design of the control system has to take in account the characteristics of the power filter.

V. AN ANN AND ITS APPLICATION IN VOLTAGES REGULATION

The exact workings of the human brain are still a mystery. Yet, some aspects of this amazing processor are known in particular, the most basic element of the human brain is a specific type of cell which, unlike the rest of the body, doesn't appear to regenerate. Because this type of cell is the only part of the body that isn't slowly replaced, it is assumed that these cells are what provide us with our abilities to remember, think, and apply previous experiences to our every action. These cells, all 100 billion of them, are known as neurons. Each of these neurons can connect with up to 200,000 other neurons, although 1,000 to 10,000 are typical. The power of the human mind comes from the sheer numbers of these basic components and the multiple connections between them. It also comes from genetic programming and learning. The individual neurons are complicated. They have a myriad of parts, sub-systems, and control mechanisms. They convey information via a host of electrochemical pathways. There are over one hundred different classes of neurons, depending on the classification method used. Together these neurons and their connections form a process which is not binary, not stable, and not synchronous. In short, it is nothing like the currently available electronic computers, or even artificial neural networks. These artificial neural networks try to replicate only the most basic elements of this complicated, versatile, and powerful organism. They do it in a primitive way. But for the software engineer who is trying to solve problems, neural computing was never about replicating human brains. It is about machines and a new way to solve problem.

5.1 Simple Neuron

A neuron with a single scalar input and no bias appears on the left below.

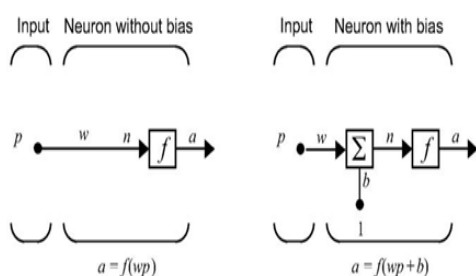
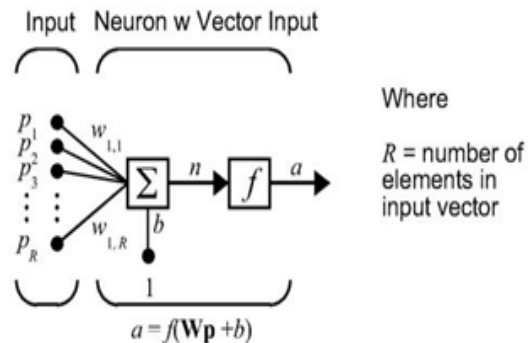


Fig 5.1 simple Neuron

The scalar input p is transmitted through a connection that multiplies its strength by the scalar weight w to form the product wp , again a scalar. Here the weighted input wp is the only argument of the transfer function f , which produces the scalar output a . The neuron on the right has a scalar bias, b . You can view the bias as simply being added to the product wp as shown by the summing junction or as shifting the function f to the left by an amount b .



The neuron has a bias b , which is summed with the weighted inputs to form the net input n . This sum, n , is the argument of the transfer function f . $n = w_1, 1p_1 + w_1, 2p_2 + \dots + w_1, RpR + b$. This expression can, of course, be written in MATLAB code as

$$n = W * p + b$$

However, you will seldom be writing code at this level, for such code is already built into functions to define and simulate entire networks.

VI. PROPOSED UNIFIDE POWER QUALITY CONDITIONER MODEL

Basic block diagram of UPQC is shown in Fig.6, whereas the overall control circuit is shown in the Fig 6.1. The voltage at PCC may be or may not be distorted depending on the other non-linear loads connected at PCC. Here we assume the voltage at PCC is distorted. Two voltage source inverters are connected back to back, sharing a common dc link.

One inverter is connected parallel with the load. It acts as shunt APF, helps in compensating load harmonic current as well as to maintain dc link voltage at constant level.

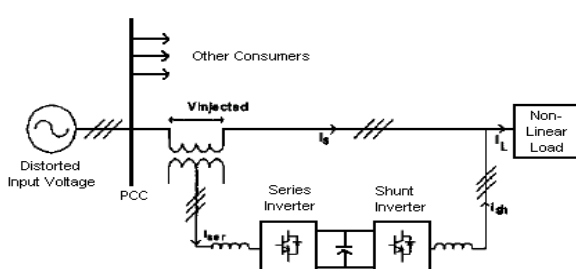


Fig 6 (a). Basic Block Diagram of UPQC

The second inverter is connected in series with utility voltage by using series transformers and helps in maintaining the load voltage sinusoidal.

6.1 Reference generation (Phase Locked Loop)

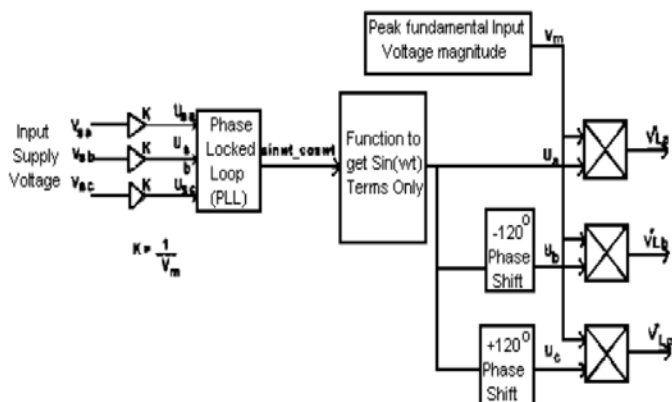


Fig.6 (b) Extraction of unit vector templates

Reference currents and voltages are generated using Phase Locked Loop (PLL). The control strategy is based on the extraction of Unit Vector Templates from the distorted input supply. These templates will be then equivalent to pure sinusoidal signal with unity (p.u.) amplitude. The extraction of unit vector templates is shown in the Fig 6(b).

The 3-ph distorted input source voltage at PCC contains fundamental component and distorted component. To get unit input voltage vectors U_{abc} , the input voltage is sensed and multiplied by gain equal to $1/V_m$, where V_m is equal to peak amplitude of fundamental input voltage. These unit input voltage vectors are taken to phase locked loop (PLL). With proper phase delay, the unit vector templates are generated

$$U_a = \text{Sin}(\omega t)$$

$$U_b = \text{Sin}(\omega t - 120^\circ) \quad (1)$$

$$U_c = \text{Sin}(\omega t + 120^\circ)$$

Multiplying the peak amplitude of fundamental input voltage with unit vector templates of equation (1) gives the reference load voltage signals,

$$V^*_{abc} = V_m \cdot U_{abc} \quad (2)$$

In order to have distortion less load voltage, the load voltage must be equal to these reference signals. The measured load voltages are compared with reference load voltage signals. The error generated is then taken to a hysteresis controller to generate the required gate signals for series APF. The unit vector template can be applied for shunt APF to compensate the harmonic current generated by non-linear load. The shunt APF is used to compensate for current harmonics as well as to maintain the dc link voltage at constant level. To achieve the abovementioned task the dc link voltage is sensed and compared with the reference dc link voltage. A PI controller then processes the error. The output signal from PI controller is multiplied with unit vector templates of equation (1) giving reference source current signals. The source current must be equal to this reference signal. In order to follow this reference current signal, the 3-ph source currents are sensed and compared with reference current signals. The error generated is then processed by a hysteresis current controller with suitable band, generating gating signals for shunt APF.

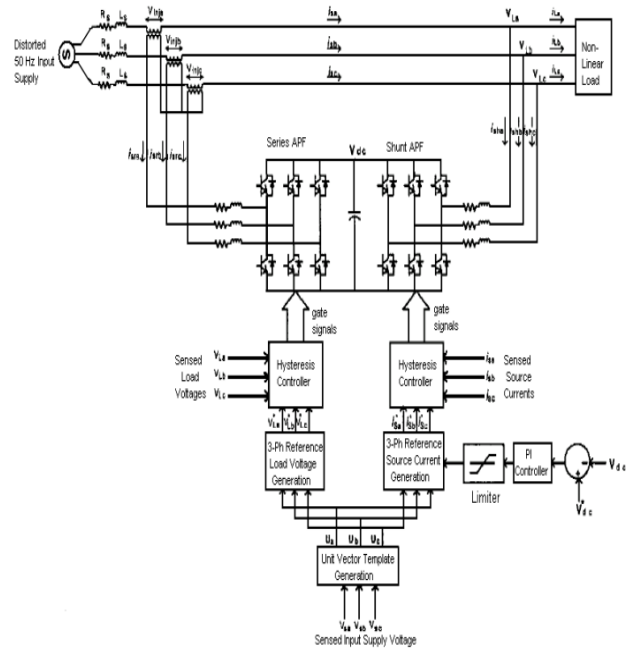


Fig 6.1 Overall Control Circuit Configuration of UPQC

6.2 Modulation method (Hysteresis Control)

The UPQC uses two back-to-back connected three phase VSI's sharing a common dc bus. The hysteresis controller is used here to control the switching of the both VSI's.

Hysteresis control law for Series APF:

If $(V_{act}) > (V_{ref} + HB)$ upper switch of a leg is ON and lower switch is OFF.

If $(V_{act}) < (V_{ref} - HB)$ upper switch of a leg is OFF and lower switch is ON.

Hysteresis control law for Shunt APF:

If $(i_{act}) > (i_{ref} + HB)$ upper switch of a leg is ON and lower switch is OFF. If $(i_{act}) < (i_{ref} - HB)$ upper switch of a leg is OFF and lower switch is ON. Where HB is the hysteresis band.

6.3 Matlab/Simulink Model

The SimPower Systems (SPS) Matlab/Simulink based simulation model of proposed UPQC is shown in Fig 6.2. The load is realized by using a diode bridge rectifier followed by a RL load. The distortion in the supply voltage is introduced by connecting a 5th (20% of the fundamental input) and 7th (10% of fundamental input) harmonic voltage sources in series with the utility voltage. Both the series and shunt APF's are realized by six IGBT switches each, sharing a common dc link.

6.4 Simulation Results

To verify the operating performance of the proposed UPQC, a 3-phase electrical system, a PLL extraction circuit with hysteresis controlled UPQC is simulated using MATLAB software. The simulation results are shown in the Fig. 6.9 and Fig. 6.10. Both the series and shunt APF's are put into the operation at different time instant. First series APF put into the operation at a simulation time of 0.1 sec. At time 0.2 sec. shunt APF is put into the operation, such that both series and shunt APF's are operated as UPQC. Fig 6.5 shows the unit vector templates generated by using proposed control technique. It should be noted that, in spite of distorted voltage at PCC, the unit vector template is pure sinusoidal because of use of PLL. Initially both APF's are not in operation the load voltage is equal to the distorted input voltage deliberately consisting of 5th and 7th order voltage harmonics. As soon as series APF is put into the operation at instant '0.1 sec.', immediately it starts compensating the load voltage by injecting sum of 5th and 7th harmonic voltage through series line transformer, such that the load voltage is perfectly sinusoidal, as shown in the Fig. 6.5

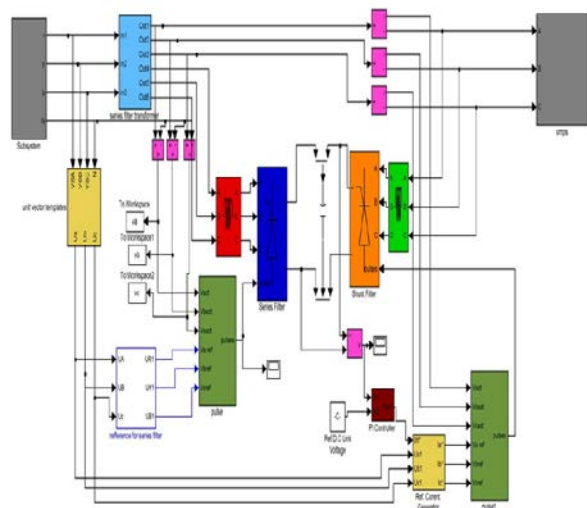


Fig 6.2 Matlab/Simulink Model

The voltage injected by the series APF is shown in the Fig. 6.6, which is nothing but the sum of 5th (20%) and 7th (10%) harmonic voltages in the supply.

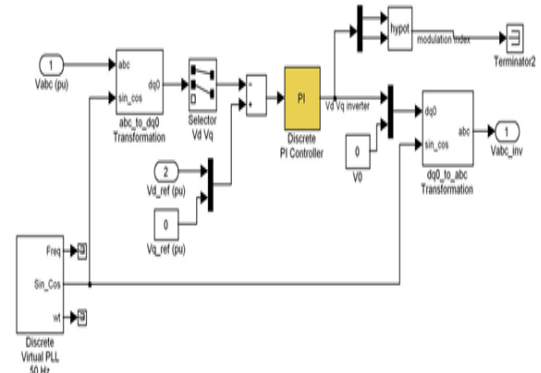


Fig 6.3 Simulink Model series voltage regulator with PI controller

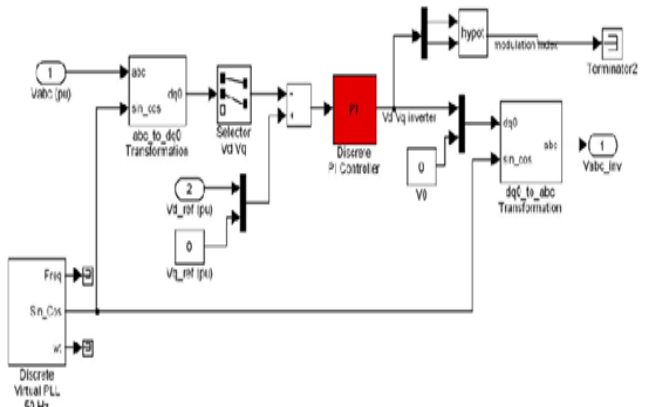


Fig 6.4 Shunt voltage regulator with PI controller

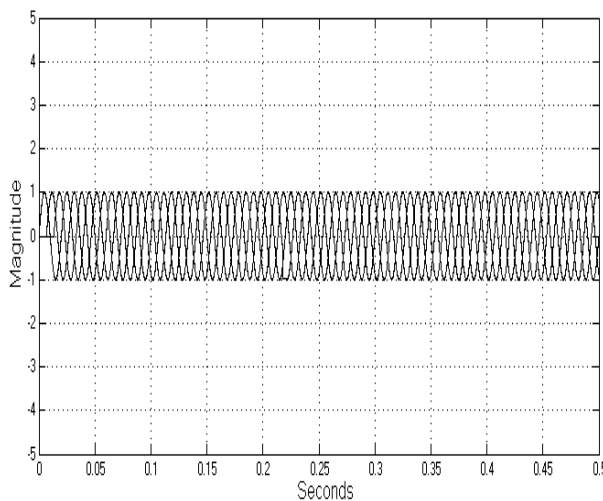


Fig 6.5 Unit Vector Templates

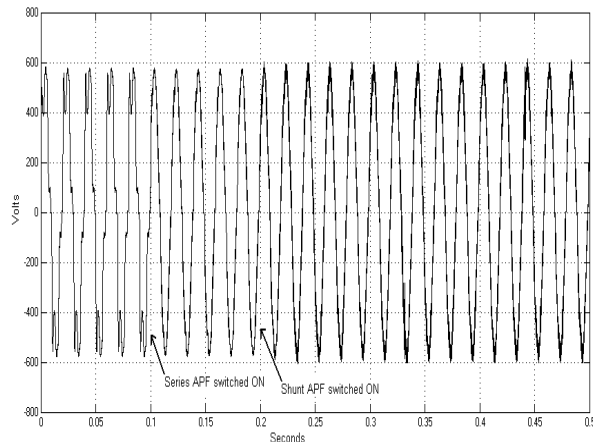


Fig 6.6 Load Voltage

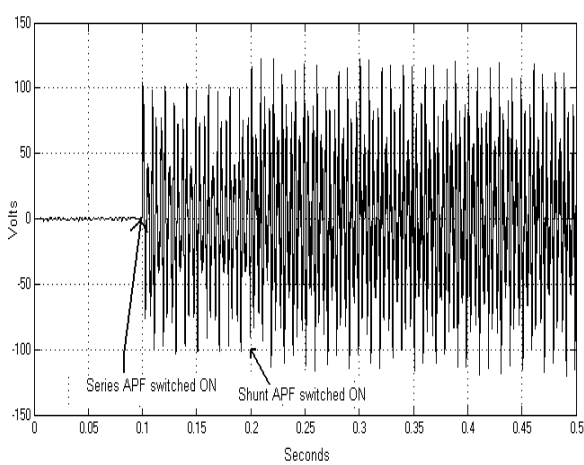


Fig 6.7 Voltage Injected by Series APF

Assuming the dc link capacitor is initially charged at 110V, when series APF starts compensating the load voltage, the dc link voltage starts going down from instant '0.1 sec' to '0.2 sec'. In order to maintain the dc link voltage at required constant level, the shunt APF is put into the operation at instant '0.2 sec'. Within a very short time period the shunt APF maintained the dc link voltage at constant level. In addition to this the shunt APF also helps in compensating the current harmonics generated by the nonlinear load. The load current waveform is shown in Fig 6.7. It is evident that before time '0.1 sec', as load voltage is distorted, so the load current. As soon as the series APF put in to operation at '0.1 sec' the load current profile is also improved. The source current waveform is shown in Fig. 6.9. Before time '0.2 sec', the source current is equal to load current. But after time '0.2 sec', when shunt APF starts maintaining dc link voltage; it injects the compensating current in such a way that the source current becomes sinusoidal. Current injected by the shunt APF is shown in Fig .6.8 Source Voltage and Current are shown in Fig 6.11.

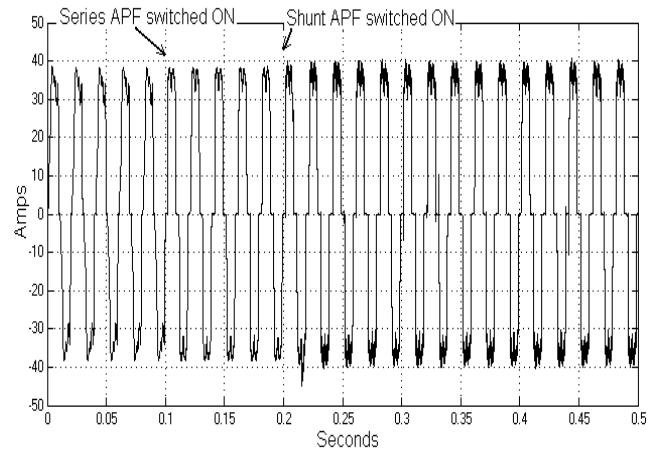


Fig 6.8 Load Current

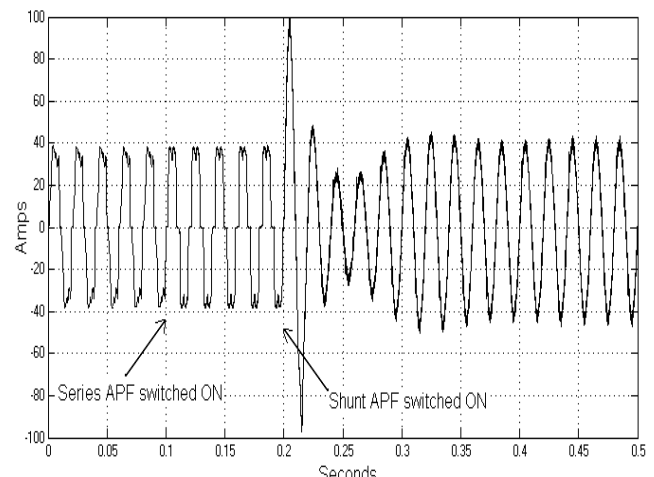


Fig 6.9 Input Source Current

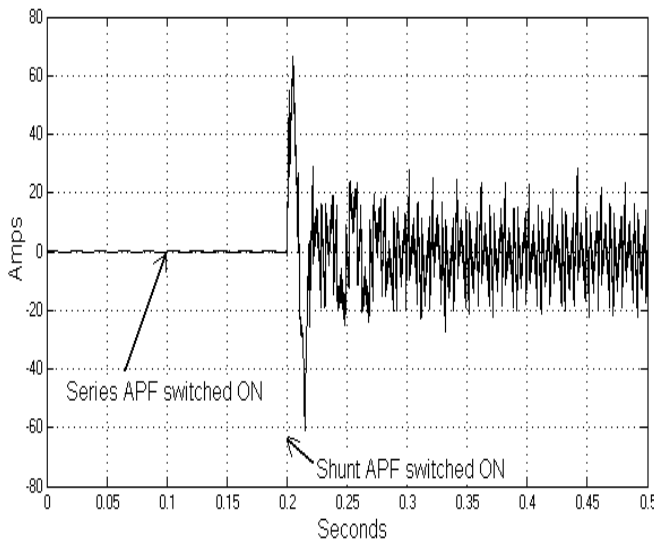


Fig 6.10 Current Injected by Shunt APF

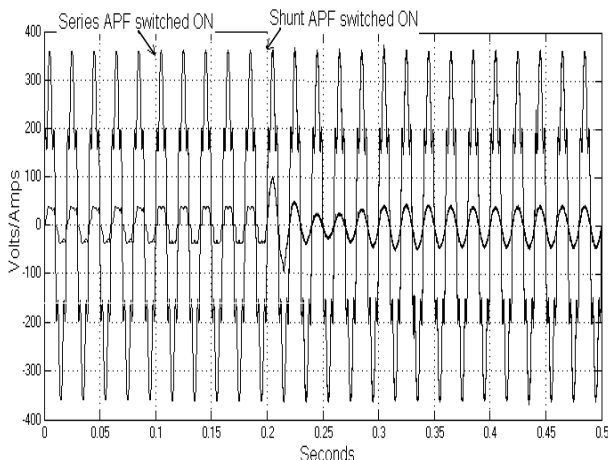


Fig 6.11 Input Source Voltage and Source Current

REFERENCES

- [1] Hirofumi Akagi, Trends in Active Power Line Conditioners, *IEEE Tran. Power Electronics*, vol. 9, no.3, May 1994, pp. 263-268.
- [2] Janko Nastran, Rafael Cajhen, Matija Seliger, and Peter Jereb, Active Power Filter for Nonlinear AC Loads, *IEEE Trans. Power Electronics*, vol.9, no.1, Jan. 1994, pp. 92-96.
- [3] E. Destobbeleer and L.Protin, On the Detection of Load Active Currents for Active Filter Control, *IEEE Trans. Power Electronics*, vol. 11, no.6, Nov. 1996, pp. 768-775.
- [4] Mauricio Aredes, Jorgen Hafner, and Klemens Hermann, Three-Phase Four-Wire Shunt Active Filter Control Strategies, *IEEE Trans. Power Electronics*, vol.12, no.2, Mar. 1997, pp. 311-318.
- [5] Hideaki Fujita and Hirofumi Akagi, the Unified Power Quality Conditioner: The Integration of Series- and Shunt-Active Filters, *IEEE Tran. Power Electronics*, vol. 13, no.2, Mar. 1998, pp.315-322.
- [6] Fang Zheng Peng, George W. Ott Jr., and Donald J. Adams, Harmonic and Reactive Power Compensation Based on the Generalized Instantaneous Reactive Power Theory for Three-Phase Four-Wire Systems, *IEEE Trans,Power Electronics*, vol.13, no.6, Nov. 1998, pp. 1174-1181.
- [7] Kishore Chatterjee, B.G. Fernandes, and Gopal K.Dubey, An Instantaneous Reactiv Volt Ampere Compensator and Harmonic Suppressor System, *IEEE Trans. Power Electronics*, vol. 14, no.2, Mar.1999, pp. 381-392.
- [8] Po-Tai Cheng, Subhashish Bhattacharya, and Deepak D. Divan, Line Harmonics Reduction in High-Power Systems Using Square-Wave Inverters-Based Dominant Harmonic Active Filter, *IEEE Trans. Power Electronics*, vol. 14, no.2, Mar. 1999, pp. 265-272.
- [9] Shyh-Jier Huang and Jinn-Chang Wu, A Control Algorithm for Three-Phase Three-Wired Active power filters under Nonideal mains voltages, *IEEE Trans. Power Electronics*, vol. 14, no. 4, Jul. 1999, pp. 753-760.
- [10] Ambrish Chandra, Bhim Singh, B.N.Singh, and Kamal Al-Haddad, An Improved Control Algorithm of Shunt Active Filter for Voltage Regulation, Harmonic Elimination, Power-factor Correction, and Balancing of Nonlinear loads, *IEEE Trans. Power Electronics*, vol. 15, no.3, May 2000, pp. 495-507.
- [11] Moleykutty George, Modeling and simulation of a current controlled three-phase shunt active power filter using MATLAB/PSB, *AIUB Journal of Science and Engineering*, vol. 3, no.1, Aug. 2004 issue, pp. 11-18.
- [12] M. George, C.L. Seen, Modeling and control of zero-sequence current of parallel three-phase converters using Matlab/power system blockset, *IEEE Power Systems Conf. and Exp. 2004, PSCE 2004*, vol. 3, pp. 1440-1443.

Role of Quality Models in Software Development

Vikash chauhan¹, Dharmendra Lal Gupta²

Abstract—this paper describes software quality, software quality criteria definitions and CISQ's quality model and provides the relevant matter about the requirements of quality in software field. What is the role of basic quality attributes to develop the software business and IT industries, is described. There is direct impact of measurement techniques on software development and how can we improve the quality of business using software quality is also mentioned. Quality in fact aids easy and high productivity, which has brought software metrics to the forefront. Today there are many software quality modes to improve the quality of software but which model is suitable for our project is very important.

Keywords--Quality; software quality; software quality criteria.

I. INTRODUCTION

“If you cannot measure, you cannot control” – Tom DeMarco. According to this statement software quality is related to the measurement. So correct measurements and valid methods are very important for improving the quality of software. Software quality management manages the quality of software and shows software development process. It ensures that the quality of required level is achieved in a software product. It encourages to a company-wide “Quality Culture” where everyone’s responsibility is quality. It enables process fault avoidance and fault prevention throughout in development. It also reduces the curve of learning and help with continuity in case if team members change position in organization. If one does not have any information about quality of software he/she cannot predict the future of software. In 2004, the Standish Chaos report found only 29% project met their quality criteria for success of project and this report also told that cancelled cost of that projects were near about \$55 billion. If quality of software is not good then probability of failure of projects may increase.

II. SOFTWARE QUALITY

There are so many definitions of software quality. First definition is given in the beginning 20th century from Shewhart. “*There are two common aspects of quality: one of them has to do with the consideration of the quality of a thing as an objective reality independent of the existence of man*”

1. Vikash chauhan ,CSD, knit Sultanpur
Vikashit22@gmail.com

2. Dharmendra lal gupta, CSD, knit Sultanpur
Dlguptap2002@gmail.com

The other has to do with what we think, feel or sense as a result of the objective reality. In other words, there is a subjective side of quality” [1].

Dr. Tom DeMarco has proposed that “*a product's quality is a function of how much it changes the world for the better*” [2].

Another software quality definition is given by Feigenbaum “*Quality is a customer determination, not an engineer's determination, not a marketing determination, nor a general management determination. It is based on upon the customer's actual experience with the product or service, measured against his or her requirements - stated or unstated, conscious or merely sensed, technically operational or entirely - subjective and always representing a moving target in a competitive market*” [3].

III. QUALITY CRITERIA DEFINITIONS

Some important quality criteria definitions have been shown in table I.

TABLE I.
Software quality criterias with their definitions

| Acquisition Concern : GENERAL | | |
|----------------------------------|--------------------------|---|
| Acronym | Criterion | Definition |
| MD | Modularity | Program subunits that are developed independently or characteristics of software which provide a structure of Highly cohesive components with optimum coupling of software. |
| SD | Self-Descriptiveness | Those properties of software which provide explanation of the implementation of functions. |
| SI | Simplicity | Simplicity is the extent that it uses data and control structures for organizing the program, and uses easily understood constructors [4]. |
| Acquisition Concern : ADAPTATION | | |
| AP | Application Independence | Those attributes of software which determine its nondependency on computer architecture, system microcode, algorithms and database. |

| | | | | | |
|-----------------------------------|------------------------|--|----|--------------------------|---|
| AT | Augmentability | Those properties of software which provide capability for functions and data for expansion. | | | operational environment. |
| CL | Commonality | Those attributes of software which provide for the use of interface standards for data representations, protocols, and routines. | | | Those attributes of software which provide status monitoring of the development process and operations. |
| Acquisition Concern : PERFORMANCE | | | | | |
| DO | Document Accessibility | Those properties of software which provide for easy access. | AC | Accuracy | Those qualities of software which provide the required precision in calculations and outputs [5] [6] [8]. |
| FO | Functional Overlap | Those qualities of software which provide common functions to both systems. | AM | Anomaly Management | Those qualities of software which provide for continuity of operations under and recovery from non-nominal conditions. |
| FS | Functional Scope | Those attributes of software which provide commonality of functions amongst applications. | AU | Autonomy | Those properties of software which determine its non-dependency on interfaces and functions. |
| FE | Generality | Those properties of software which provide extend to the functions performed with respect to the application. | D | Distributedness | Determine the degree to which software functions are logically geographically separated within the system. |
| ID | Independence | Those qualities of software which determine its nondependency on software environment (libraries, input, output routines, utilities, computing system and operating system). | EC | Effectiveness-Comm. | Those qualities of the software which provide for minimum utilization of communication resources in performing functions. |
| ST | System Clarity | Those attributes of software which provide for clear description of program structure in a understandable manner non-complex. | EP | Effectiveness-Processing | Those properties of software which provide for minimum utilization of processing resources in performing functions. |
| SY | System Compatibility | Those qualities of software which provide the software, hardware, and communication compatibility of two systems. | ES | Effectiveness-Storage | Those qualities of the software which provide for minimum utilization of storage resources. |
| Acquisition Concern : DESIGN | | | | | |
| VR | Virtuality | Those properties of software which present a system that does not require user knowledge of the logical, physical, or topological characteristics. | OP | Operability | Attributes of software that relate to the users' effort for operation and operation control. |
| CP | Completeness | It provides full implementation of the functions required [5] [6] [7]. | RE | Reconfigurability | Those qualities of software which provide for continuity of system operation when one or more storage units, communications processors, or links fail(s). |
| CS | Consistency | Those qualities of software which provide for uniform design and notation implementation techniques [6]. | SS | System Accessibility | Those properties of software which provide for control and audit of access to the data and software. |
| TC | Traceability | Those attributes of software which provide a thread of origin from the implementation to the requirements with respect to the specified development envelope and | TN | Training | Those qualities of software which provide transition from current operation and provide initial familiarization. |

IV. CISQ's QUALITY MODEL

Software quality is a perceptual and conditional subjective attributes and may be differ by different people. The

characteristics of software quality have been defined by Consortium for IT Software Quality (CISQ). CISQ has defined five major characteristics of software needed to provide business value, under the guidance of CISQ's first director; Bill Curtis, co-author of the Capability Maturity

Model framework (CMM) and Capers Jones, CISQ's distinguish advisor. There are following "Whats" that need to be achieved in the house of quality.

A. Efficiency

To measure the execution behavior (storage speed and execution speed) of program is called efficiency. The software architecture attributes and source code are the elements that ensure high performance once the application is in run-time mode. Efficiency is very important in high execution environments such as transaction of money from ATM, RADAR system in defense, artificial satellite systems, mars and moon projects etc., where execution speed plays an important role. A clear picture of the latent business risks and the harm is provided by analysis of source code efficiency and scalability. It is extent to which resources are utilized. If any system has high efficiency it means high software efficiency and usability. The efficiency depends on the machine and operating system environment on which program or software is running and implementation language.

B. Reliability

Here are two groups definitions generally related to software and hardware. According to the first group definition reliability is the measures of the number of error encountered in a program. In a broader definition relates that it is the extent to which a program can be expected to perform its intended functions satisfactorily (according to Thayar 1976). In another critic adds a qualifier: the functions of software must be performed correctly in spite of computer component failures (McCall, Richards, and Walters 1977). In this view correctness and performance of software are closely related to the reliability.

On the other hand hardware reliability has a certain physical and tangible element. Reliability measures potential application failure and the level of risk. The goal for monitoring and checking reliability measure the execution behavior (storage speed and execution speed) of program is called efficiency. It affects users directly and improve the image of IT and business performance.

C. Maintainability:

To measure the effort and time required to fix a bug in the program is called maintainability (McCall, Richards, and Walters 1977). According to Boehm "It is the ease or difficulty with which software can be updated to satisfy new requirements". Measurements of how easily software can be changed because of bugs encountered during operation, user requirements that were not fulfilled, changing requirements according to client etc., and upgrading or "obsoleting" a system (McCall, Richards, and Walters 1977).

Maintainability is a software quality factor that addresses

how well software can be maintained after it has been developed. Here is the question of how well the software adapts to changing requirements or to improvements made to the product. In such terms, maintenance can be closely aligned with flexibility and expandability. It may include notion of transferability (from one development team to another), portability and adaptability. Where change is driven by tight time-to-market schedules and where it is important for IT to remain responsive to business-driven changes measuring and monitoring, maintainability is a must for such mission-critical applications. Size of program plays a very important role in maintainability because according to size of program compilation speed may increase or decrease and processing of program will be affected.

D. Security

Security is very important quality attribute which is related to security of business and it can damage the business. Security is only concerned with unauthorized access to information. It contributes directly to integrity. When a software program is not secure, the confidentiality of the data is compromised, whether or not the software program is subjected to adverse conditions. It measures the likelihood of potential security breaches and unwanted action due to poor coding practices and architectures. It quantifies the risk of encountering critical vulnerabilities that are harmful for our business.

E. Size

We measure the source code size in in terms of Source Lines of Code (SLOC) by counting the lines of a program. The sizing of source code is a software characteristic that obviously impacts maintainability. After Combining with the above quality characteristics, software size can be used to assess the amount of effort produced and to be done by teams, as well as their productivity through correlation with time-sheet data, and other SDLC-related software metrics. It is also used to measure effort both as an actual value and before as an estimate. Before as an estimate and after as an actual value both are measured by SLOC. It comes from the days of assembly coding and FORTRAN.

SLOC provide a much clearer image to software developers on the size of the project. When source code is written, integration and unit testing can be performed so measures of quality and programming productivity can be assessed.

SLOC themselves are not as meaningful as other software metrics. Just because if one project has more lines of code than other does not mean that first project is more complex or give better quality rating. SLOC is a direct metrics which can be measured directly by counting the numbers of lines of a program. This metrics play important role to derive the mathematics formulas of indirect metrics. These indirect metrics define the product quality. When product quality is mainly depend on SLOC, it gives a much better reflection on the overall project's quality; efficiency of the code; ratio of good code to buggy code etc.

In another point of view SLOC is the measuring the actual number of lines of code written in specific amount of time. If we are looking at a project level, the number of lines of code would typically come from the overall lines of code written throughout the project within a specific amount of period of time. If there is a team of many developers then total number of lines of code would obviously be measured on the lines written by the developer or team respectively. If developers are using auto-generated code software it can be lead to incorrect productivity measures. These lines of code are unuseful and should be removed from the calculation to give a better indication of actual number of lines written by the developer or team.

For example if we are using two different languages FORTRAN and C to develop the same function code and C takes 10 lines of code and FORTRAN takes 30 lines of code, it is short coming of SLOC. There may be different measurements for the same function in different programming languages so here function points analysis metrics is better than SLOC.

There are two ways to measure lines of code:

- 1) Physical SLOC = Lines of Source Code + Comments
+ Blank lines
- 2) Logical SLOC = Number of lines of functional code ("statements")

* If blank lines are less the 25% of the section.

Names of SLOC measures:

- K-LOC – 1,000 Lines of Code
- K-SLOC - 1,000 Source Lines of Code
- K-DLOC - 1,000 Delivered Lines of Code
- M-LOC - 1,000,000 Lines of Code
- G-LOC - 1,000,000,000 Lines of Code
- T-LOC - 1,000,000,000,000 Lines of Code

[K – Kilo, M – Mega, G – Giga, T – Tera]

1) Physical SLOC (PLOC)

The most common definition of physical SLOC is a count of lines including comment lines in the text of the program's source code. Blank lines are also counted unless the line of code in a section consists of more than 25% blank lines. In this case blank lines more than 25% are not counted toward lines of code.

2) Logical SLOC (LLOC)

Logical SLOC measures the number of executable "statements", but their specific definitions are tied to particular computer languages (one simple logical SLOC measure for C-like programming languages is the number of statement-terminating semicolons). It is much easier to create tools that measure physical SLOC, and physical SLOC definitions are easy to explain.

By comparing logical SLOC and physical SLOC we find that measurements of physical SLOC are sensitive to logically irrelevant formatting and style conventions, on the other hand logical SLOC is less sensitive to formatting and style conventions. However, logical SLOC can often be significantly different from physical SLOC and SLOC measures are often stated without giving their definition. Let us take some snapshot C code as an example of the ambiguity encountered when determining SLOC:

```
for (j = 0; j < 100; j++) printf("hi"); /* How many lines of code is this? */
```

In this example we have:

- 2 Logical Lines of Code (LLOC) (for statement and printf statement)
- 1 Physical Line of Code (LOC)
- 1 comment line

According to different programmer and coding standards, the above "line of code" could be written on many separate lines in the following way:

```
/* Now find how many lines of code in this? */
for (j = 0; j < 100; j++)
{
    printf("hi");
}
```

In the above example we have:

- 2 Logical Line of Code (LLOC): what about all the work writing non-statement lines?
- 5 Physical Lines of Code (LOC): is placing braces work to be estimated?
- 1 comment line: tools must account for all code and comments regardless of comment placement.

Even the "physical" and "logical" SLOC values can have a large number of different definitions. Robert E. Park (while at the Software Engineering Institute) et al. developed a framework for defining the SLOC values, to enable people to carefully explain and define the SLOC measure criteria used in a project. Considering an example, most software systems reuse code, and determining which (if any) reused code to include is important when reporting a measure.

V. DISCUSSION, CONCLUSION AND FUTURE WORK

In this paper we described the quality, quality criteria of software by which we can improve the performance of software. We have presented CISQ's software quality model that is used to solve software business problems. We have described here what is the role of program size (SLOC), is to develop the software and what impact of SLOC to improve the business is and what the disadvantages of SLOC are. In

present time there are so many software quality models that are being used in software industry to improving the software quality but we have to choose best software quality model according to our requirement. First of all we have to select quality attributes that are used in our project or software after that we have to select software quality models and lastly according to our priority we have to select one of the software quality models and apply it into our project. There may be different combinations of quality attributes to make many different quality models. These quality models have different properties. We have many software quality models at the present time so we have to choose very carefully according to our need. It is not necessary that we should use only one quality model in all projects, we should use such quality model that provides better and efficient result. Software engineering provides us many rules and regulations to select the appropriate software quality models.

In this area of research work there are a lot of queries, and their solutions which may be found in our future work. These queries may be as given below:

1. What are the parameters to relate these quality models?
2. How a business performance is related to the software quality models in real world?

3. How we identify which software quality model is more important than other software quality model and why?

REFERENCES

- [1] W. A. Shewhart, "Economic control of quality of manufactured product", Van Nostrand, 1931.
- [2] DeMarco, T., "Management Can Make Quality (Im)possible", Cutter IT Summit, Boston, April 1999.
- [3] McCall, Jim A., Paul K. Richards, and Gene F. Walters, "Factors in Software Quality", RADC-TR-77-369, Volumes I, II, and III, RADC, Griffiss Air Force Base, NY, November 1977.
- [4] Gilb, T., "Software Metrics", Winthrop, Inc., Cambridge, MA, 1977.
- [5] Boehm, B. W. et al., "Characteristics of Software Quality", North-Holland Publishing Company, New York, NY, 1978.
- [6] Bowen, Thomas P., Gary B. Wigle, and Jay T. Tsai, "Specification of Software Quality Attributes", RADC-TR-85-37, RADC, Griffiss Air Force Base, NY, Volumes I, II, and III, February 1985.
- [7] Walters, G. F., "Applications of Metrics to a Software Quality Management (QM) Program", Software Quality Management, Petrocelli, New York, NY, 1979.

An Overview of Intrusion Detection System for Wireless Ad-hoc Networks

A. Rajesh Kumar, B. B.P. Chaurasia, C. Neeraj Sharma

Abstract-This paper describes a brief survey of current research in intrusion detection for wireless ad-hoc networks. In addition to determining the challenges of providing intrusion detection in this environment, this paper reviews the current efforts to detect attacks against the ad-hoc routing infrastructure, and also detect the attacks directed against the mobile nodes. This paper also include the intrusion detection architectures that may be deployed for different wireless ad-hoc network infrastructures, as well as proposed methods of intrusion response in the wireless ad-hoc network.

Keywords -Ad hoc network; Intrusion Detection System; Wireless network.

I. INTRODUCTION

Wireless ad-hoc networks do not depend on a pre-existing network infrastructure, and are characterized by wireless multi-hop communication. Unlike fixed wired networks, wireless ad-hoc networks have several operational limitations. For example, the wireless link is constrained by transmission range and bandwidth, and the mobile nodes may be constrained by battery life, CPU, and memory. Wireless ad-hoc networks are used in situations where a network must be deployed rapidly, without an existing infrastructure. Applications of wireless ad-hoc networks include the strategic battlefield, emergency search and rescue missions, as well as civilian ad-hoc situations, such as conferences and classrooms. Wireless ad-hoc networks are vulnerable to additional threats above those for a fixed wired network, due to the wireless communication link and the dynamic and cooperative nature of the ad-hoc routing infrastructure.

The wireless link does not provide the same level of protection for data transmission as a wired link, allowing adversaries within radio transmission range to make attacks against the data transmitted over the wireless link without gaining physical access to the link. Passive attacks, such as eavesdropping, may violate the confidentiality of the system. Active attacks, such as deleting, modifying, or injecting erroneous messages or the impersonation of a node, may violate the availability, integrity, authentication, or non-repudiation of the system [15]. Other active attacks against the wireless link include blocking to reject service to mobile nodes, and energy exhaustion attacks, referred to as sleep deprivation torture [12], to exhaust the battery life of mobile nodes. The dynamic and cooperative nature of the ad-hoc routing infrastructure also enforces additional security threats. Attacks against the ad-hoc routing infrastructure may be made from external or internal nodes. Ad-hoc routing algorithms rely on node cooperation, where each node may act as a relay. Dynamic changes to the network topology

make it difficult to identify if a node providing false routing information is Byzantine or is just out of sync with the topological changes. These additional security threats must be considered, when designing security mechanisms for a wireless ad-hoc network.

2. Intrusion Detection in Wireless Ad-hoc Networks

Security mechanisms must be deployed in order to counter threats against wireless ad-hoc networks. While cryptographic mechanisms provide protection against some types of attacks from external nodes, cryptography will not protect against malicious inside nodes, which already have the required cryptographic keys. Therefore, intrusion detection mechanisms are necessary to detect these Byzantine nodes. Intrusion Detection Systems (IDS) may be classified based on the data collection mechanism, as well as the technique used to detect events. While the requirement of intrusion detection for both fixed wired and wireless ad-hoc networks are the same, wireless ad-hoc networks impose additional challenges. In general, the effectiveness of solutions designed for fixed wired networks are limited for wireless ad-hoc networks.

2.1. Classification of IDS

An Intrusion Detection System (IDS) may be classified as either host-based or network-based, depending on the data collection mechanism. Host-based IDS operate on the operating system's audit trails, system and application logs, or audit data generated by loadable-kernel modules that intercept system calls. Network-based IDS operate on packets captured from network traffic. In addition, IDS may be classified based on the detection technique as described below:

- Signature-based detection monitors for the occurrence of predefined signatures or sequences that indicate an intrusion. This technique may exhibit low false positive rates, but does not perform well at detecting previously unknown attacks.
- Anomaly-based detection defines a profile of normal behaviour and classifies any deviation of that profile as an intrusion. The normal profile is updated as the system learns the subject's behaviour. This technique may detect previously unknown attacks, but may exhibit high rates of false positives.

Specification-based detection defines a set of constraints that describe the correct operation of a program or protocol, and monitors the execution of the program with respect to the defined constraints. This technique may provide the capability to detect previously unknown attacks, while exhibiting a low false positive rate.

2.2. Restrictions of IDS Solutions for Wireless Ad-hoc Networks

IDS solutions for fixed wired networks are often hierarchical and deploy network-based sensors at key traffic concentration points, such as switches, routers, and firewalls. These IDS sensors are physically secured, and use the signature-based detection technique to detect attacks. Alerts generated by these distributed IDS sensors are sent to centralized security servers for analysis and correlation. The centralized security server distributes attack signature updates to the network-based IDS sensors. The effectiveness of IDS solutions that were designed for fixed wired networks are limited for wireless ad-hoc networks as described below:

- Wireless ad-hoc networks lack key concentration points where network traffic can be monitored. This limits the effectiveness of a network-based IDS sensor, since only the traffic generated within radio transmission range may be monitored.
- In a dynamically changing ad-hoc network, it may be difficult to rely on the existence of a centralized server to perform analysis and correlation.
- The secure distribution of signatures may be difficult, due to the properties of wireless communication and mobile nodes that operate in disconnect mode.
- It may be difficult to physically secure a mobile host that could be captured, compromised, and later re-join the network as a Byzantine node.

3. Detection of Attacks Against the Routing Infrastructure

In a wireless ad-hoc network, security mechanisms must be deployed to detect attacks against the routing infrastructure. External nodes may inject, replay, or distort routing information in order to partition the network or cause excessive load, while inside nodes may advertise incorrect routing information [15]. In this section we will briefly review previous work proposed to detect attacks against the routing infrastructure of fixed wired networks, as well current research proposed for wireless ad-hoc networks.

3.1. Solutions for Fixed Wired Networks

Solutions to detect attacks against the routing infrastructure of a wireless ad-hoc network may build on solutions previously proposed for fixed wired networks. We will briefly review four solutions to detect attacks against routers and the routing protocols in a fixed wired network as follows:

- **Distributed Probing:** A router may detect neighbouring routers, which act as network sinks or misroute packets, by directly sending to each router test packets that have a destination of the router performing the diagnosis [4]. A router can determine the goodness of a tested router based on whether the tester router receives the test packet back within a certain time interval. If the tested router can distinguish

between test packets and normal traffic, however, it can avoid detection.

- **Principle of Conservation Flow:** The WATCHERS protocol was developed to detect routers that violate the principle of conservation flow, where by all data bytes sent to a node and not destined for that node should exit that node [1]. WATCHER run on each router, and provides the capability to detect bad routers that drop or misroute packets. Using WATCHERS, a router may test a neighbouring router using its own counters, the counters of the tested router, and the counters for each neighbour of the tested router.

- **Statistical Anomaly Detection:** This technique may be used to detect known and unknown attacks against the routing infrastructure. The JiNao statistical analysis module, based on the SRI NIDES/STAT algorithm, was developed to detect insider OSPF routing attacks

[5]. The NIDES/STAT algorithm compares a subject's current behaviour (short-term profile) against its expected behaviour (long-term profile), which is established using a training period and is periodically updated. Using statistical measures of activity intensity (OSPF packet volume), categorical (OSPF packet type), and counting (link-state advertisement age), JiNao was able to detect known attacks with a low false positive.

- **Protocol Analysis:** The behaviour of a routing protocol may be monitored with respect to a state transition diagram that models the protocol states, in order to determine when an anomalous state is entered. In JiNao, protocol analysis is performed using real-time Finite State Machines (FSM) pattern matching modules based on knowledge about known attacks against the OSPF routing protocol, in order to detect three types of insider attacks [5]. State transitions in the JiNao FSMs are based on the events as well as the time of an event.

3.2 Solutions to Detect Attack for Wireless Ad-hoc Networks

A number of solutions to detect attacks against the routing infrastructure of wireless ad-hoc networks were proposed as an extension of the Dynamic Source Routing (DSR) protocol. In the Route Discovery phase of the DSR protocol, a nodes broadcast Route Request (RREQ) message to neighbour's in order to find a route to a destination, and the Route Reply (RREP) message from the destination contains the full source route. In this section we will briefly review some of the proposed solutions as follows:

- **Watchdog:** The watchdog mechanism was implemented on top of DSR to verify that when a node forwards a packet, the next node in the path also forwards the packet otherwise the next node is misbehaving [10]. Watchdog runs on each node, operates by listening in promiscuous mode to transmissions of neighbouring nodes, and assumes bi-directional links. Watchdog maintains a buffer of recently

sent packets, and removes a packet from the buffer when the packet is forwarded by the next hop. If a packet remains in the buffer beyond a threshold value, Watchdog determines that the next hop is misbehaving and sends a message to the source identifying the misbehaving node. Watchdog may not always be effective due to packet collisions, a malicious node deliberately limiting transmission power, or collusion.

- **Control Messages:** A scheme that proposed adding two control messages to the DSR protocol, Route Confirmation Request (CREQ) and Route Confirmation Reply (CREP), requires intermediate nodes, which have a known route to the destination; request that the next hop in the path send a confirmation message back to the source [9]. When an intermediate node responds to a RREQ for which it has a route in its cache, the node sends back an RREP to the source, and will additionally send a CREQ message to the next hop in the destination's path. The next hop sends a CREP message back to the source if it also knows a path to the destination. When the source receives the RREP and the CREP, it can determine the validity of the path. This method may operate with most on-demand routing protocols to detect malicious nodes, such as black hole routers, which falsely advertise being on the shortest path. This scheme may not be always be effective due to colluding nodes.
- **Neighbourhood Watch:** As part of the CONFIDANT protocol, a neighbourhood watch is used to detect (either by listening to the transmission of the next node or observing the route protocol behaviour) intrusive activity made by the next node on the source route, and when a node detects a malicious neighbour, the node sends an alarm message to the other nodes on its friends list [3]. The CONFIDANT protocol works as an extension of reactive source-routing protocols, such as DSR, and uses a reputation system that rates nodes based on malicious behaviour. Alarm messages received from other nodes are evaluated, and the reputation of an accused node is changed only if the source of the alarm is a fully trusted node or the node was similarly accused by several partially trusted nodes.
- **Neighbourhood Watch:** As part of the CONFIDANT protocol, a neighbourhood watch is used to detect (either by listening to the transmission of the next node or observing the route protocol behaviour) intrusive activity made by the next node on the source route, and when a node detects a malicious neighbour, the node sends an alarm message to the other nodes on its friends list [3]. The CONFIDANT protocol works as an extension of reactive source-routing protocols, such as DSR, and uses a reputation system that rates nodes based on malicious behaviour. Alarm messages received from other nodes are evaluated, and the reputation of an accused node is changed only if the source of the alarm is a fully trusted node or the node was similarly accused by several partially trusted nodes.

- **Statistical Anomaly Detection:** Using statistical anomaly detection to detect false routing information generated by Byzantine nodes is another approach that may be well suited for wireless ad-hoc networks. In a proposed solution, a normal profile may be established that correlates the physical movement of a node to changes in the routing table, with the RIPPER as the proposed classification algorithm and “nearest neighbour” as the clustering algorithm for deviation scores [14].

4. Discovery of Attacks Against Mobile Nodes

The requirement for detection of attacks against a mobile node in a wireless ad-hoc network is the same as for hosts in a fixed wired network. In a wired network, hosts are typically protected by network firewalls and network-based IDS. These network-based security mechanisms, however, may not be effective for wireless ad-hoc networks. Without protection from network Firewalls, mobile nodes may be directly exposed to attacks from external as well as internal Byzantine nodes. Therefore each mobile node should run some type of node-based IDS, if the node has the available CPU, memory, and battery capacity. While signature-based detection is the primary technique used in fixed wired networks, the secure distribution of signature updates in a wireless ad-hoc network may be difficult, and mobile nodes may operate in disconnect mode. The ideal node-based IDS should be able to detect unknown attacks without requiring signature updates. Potential solutions for node-based IDS to detect attacks against the node may use anomaly or specification-based detection on the system calls generated by monitored processes running on the node.

Anomaly detection may be used to detect attacks against a network daemon or a set user id (SUID) program by building a normal profile of the system calls made during program execution. An intrusion can be detected by comparing the normal profile of a program against a running process. If the process execution deviates significantly from the established profile, an intrusion is assumed. One disadvantage of anomaly detection for mobile computing is that the normal profile must be periodically updated and calculating deviations from the normal profile may impose a heavy load on mobile devices. A more light-weight approach using profiles consisting of the type of system call and its occurrence of frequency was proposed, in which the DP Matching method (traditionally used in speech recognition) is used to calculate the optimal match between a normal profile and a sample profile [11].

The specification-based technique [6, 7] has demonstrated the capability to detect both known and previously unknown attacks against network daemons and SUID programs on UNIX platforms. In this technique, the execution of designated programs is monitored and the generated system calls are compared against a set of pre-defined constraints. Any deviation from the defined constraints is considered to be the manifestation of an attack. The specification-based IDS can be preloaded on mobile nodes prior to deployment to the

field, and should not require any periodic updates in order to be effective.

5. Different Architectures for Intrusion Detection in Wireless Ad-hoc Networks

The optimal IDS architecture for a wireless ad-hoc network may depend on the network infrastructure itself. Wireless ad-hoc networks may be configured in either a flat or multi-layered network infrastructure. In a flat network infrastructure, all nodes are considered equal and may participate in routing functions. This infrastructure may be suitable to civilian applications, such as a class room or conference. In a multi-layered network infrastructure, all nodes are not considered equal. Nodes within transmission range are organized into a cluster, and elect a Cluster-Head (CH) node to centralize routing information for the cluster. The CH nodes form a virtual backbone for the network, and depending on the protocol intermediate gateway nodes may relay packets between CH nodes. This infrastructure is suitable for military applications.

5.1A Stand-alone IDS Architecture

In a stand-alone IDS architecture, each host runs an IDS that independently detects attacks. The original IDS were stand-alone systems developed to protect specific mainframes. Since stand-alone IDS do not cooperate or share information with other systems, all intrusion detection decision is based on information available to the individual node. The watchdog mechanism [10], could be deployed as a stand-alone IDS mechanism and detect Byzantine nodes within transmission range, but not report these malicious nodes to any other node. The node running watchdog would then forward packets only to neighbouring nodes that do not appear to misbehave. While the effectiveness of this solution is limited, this architecture may be suitable in an environment where not all nodes are capable of running an IDS or have an IDS installed.

5.2 Cooperative and Distributed IDS Architecture

Cooperation among distributed host-based IDS was originally proposed for fixed wired networks in the Cooperating Security Managers [13]. Intrusion detection for fixed wired network is primarily hierarchical and network-based, so there is no need to incur the overhead associated with the exchange of messages required for this architecture. This IDS architecture is more suitable for flat wireless ad-hoc networks, and a distributed and cooperative architecture was proposed for this environment in which IDS agents residing on every node independently make local intrusion detection decisions, but cooperatively participate in global intrusion detection [14]. In this architecture, if a node detects an intrusion with weak or inconclusive evidence, it can initiate a cooperative global intrusion detection procedure, or if a node detects locally an intrusion with strong evidence, it can

independently determine an attack on the network. A cooperative and distributive IDS architecture could be susceptible to attacks from Byzantine nodes, which could independently make false claims of detecting an attack from a correct node with strong evidence, thus making it difficult to derive a distributed consensus. In the CONFIDANT protocol, nodes cooperate and share alarm messages with other nodes in the wireless ad-hoc network that are in a node's friend list [3]. Since alarm messages are evaluated based on their trustworthiness, this solution should minimize the effect of a Byzantine node, which falsely accuses a correct node.

5.3 Hierarchical Architecture of IDS

Hierarchical IDS architectures have been proposed for multi-layered, wireless ad-hoc networks. In a multi-layered wireless ad-hoc network, cluster-head nodes centralized routing for the cluster and may support additional security mechanisms. For example, a three-layered infrastructure may be deployed in the tactical battlefield, consisting of two-layered ground networks and a third layer of Unmanned Aerial Vehicles (UAVs), which provide event correlation for a theatre of operations. Neighbouring ground nodes detecting that ground node V is acting malicious send an accusation message to the UAV, the UAV will determine that node V is compromised after receiving a threshold of K accusations [8]. Then the UAV may respond, such as broadcasting a message to notify all nodes in the theatre.

In addition to correlating events detected by cluster-member nodes, CH nodes may also detect attacks against the virtual backbone's routing infrastructure made by Byzantine CH nodes. In a multi-layered wireless ad-hoc network, the detection of Byzantine CH nodes is essential. A Byzantine CH node could potentially reroute, modify, or drop packets transmitted by cluster member nodes, as well as any packets routed through the CH node on the virtual backbone

6. Intrusion Response in Wireless Ad-hoc Networks

The ideal intrusion response for a wireless ad-hoc network is to isolate Byzantine nodes from the rest of the network. For fixed wired networks, the "electronic quarantine" was developed to dynamically create the filtering rules required for desktop firewalls, packet-filtering intranet firewalls, and application-level Internet firewalls, in order to isolate a compromised host within a fixed wired network [2]. In a dynamically changing wireless ad-hoc topology, the centralized solution proposed by the electronic quarantine would not be effective, since the implementation of intranet firewalls and application-level firewalls may not be feasible. In the distributed and cooperative IDS architecture proposed for wireless ad-hoc networks, one approach suggested that in response to a detected intrusion end-users re-authenticate themselves using an out-of-bound mechanism, and negotiate a new communication channel to exclude compromised nodes [14]. Re-authentication using an out-of-bound mechanism may be appropriate in some but not all environments. The path manager function of the CONFIDANT protocol allows

nodes to delete paths containing malicious nodes and to choose not to forward packets for nodes that have bad ratings [3]. Since nodes share information about malicious nodes with their friend nodes, malicious nodes will eventually be detected and isolated from the wireless ad-hoc network.

A hierarchical approach was proposed for intrusion response in multi-layered wireless ad-hoc networks in the digital battlefield, in which high layer UAVs support centralized certification and counter-certification for a theatre of operations [8]. A data forwarding policy is used in which only packets for authenticated nodes are forwarded. The Certificate Authority can isolate a suspected node from rest of the network by broadcasting a counter certificate for that node.

7. Conclusions

Research in intrusion detection has been conducted for the past fifteen years however its application to wireless ad-hoc networking is fairly recent. This paper presents a brief overview of current research efforts in this area. Commercial IDS solutions are primarily focused on network-based IDS sensors and these security mechanisms may not be effective in a wireless ad-hoc network. Therefore, researchers have started to develop IDS solutions that are applicable for this environment. A number of research efforts concentrated on developing solutions as an extension of the Dynamic Source Routing (DSR) protocol, and using a simulated environment to evaluate the proposed solutions. Research efforts should continue to explore new methods to detect attacks against the various ad-hoc routing protocols, as well as prototyping existing solutions which appear promising.

References

- [1] Bradley, K., Cheung, S., Puketza, N., Mukherjee, B., and Olsson, R. "Detecting Disruptive Routers: A Distributed Network Monitoring Approach," In *Proceedings of IEEE Symposium on Security and Privacy*, May 1998.
- [2] Brutsch, P., Brutsch, T., and Pooch, U. "Electronic Quarantine: An Automated Intruder Response Tool", In *Proceedings of Information Survivability Workshop*, 1998.
- [3] Buchegger, S. and Boudec, J. "Performance Analysis of the CONFIDANT Protocol (Cooperation of Nodes: Fairness in Dynamic Ad-hoc Networks)", In *Proceedings of MOBIHOC '02*, 2002.
- [4] Cheung, S. and Levitt, K., "Protecting Routing Infrastructures from Denial of Service Using Cooperative Intrusion Detection", In *Proceedings of New Security Paradigms Workshop*, 1997.
- [5] Jou, Y., Gong, F., Sargor, C., Wu, X., Wu, S., Chang, H., and Wang, F., "Design and Implementation of a Scalable Intrusion Detection System for the Protection of Network Infrastructure", In *Proceedings of DARPA Information Survivability Conference and Exposition*, 2000.
- [6] Ko, C., Ruschitzka, M., and Levitt, K. "Execution Monitoring of Security Critical Programs in Distributed Systems: A specification-based approach," In *Proceedings of Symposium on Security and Privacy*, 1997.
- [7] Ko, C., Brutsch, P., Rowe, J., Tasfnat, G. and Levitt, K., "System Health and Intrusion Monitoring using a Hierarchy of Constraints", In *Proceedings of 4th International Symposium on Recent Advances in Intrusion Detection*, 2001.
- [8] Kong, J., Luo, H., Xu, K., Gu, D., Gerla, M., and Lu, S., "Adaptive Security for Multi-layer Ad-hoc Networks," *Special Issue of Wireless Communication and Mobile Computing*, 2002.
- [9] Lee, S., Han, B., and Shin, M. "Robust Routing in Wireless Ad Hoc Networks", In *Proceedings of the International Conference on Parallel Processing Workshop (ICPPW'02)*. 2002.
- [10] Marti, S., Giulia, T., Lai, K., and Baker, M., "Mitigating Routing Misbehaviour in Mobile Ad Hoc Networks," In *Proceedings of the Sixth Annual International Conference on Mobile Communication and Networking*, 2000.
- [11] Okazaki, Y., Sato, I., and Goto, S., "A New Intrusion Detection Method based on Process Profiling", In *Proceedings of 2002 Symposium on Applications and the Internet (SAINT '02)*, 2002.
- [12] Stajano F. and Ross, A., "The Resurrecting Duckling: Security for Ad-hoc Networks, *AT&T Software Symposium*, 1999.
- [13] White, G. and Pooch, U., "Cooperating Security Managers: Distributed Intrusion Detection System," *Computers & Security*, vol. 15, no. 5, 1996.
- [14] Zhang, Y. and Lee, W., "Intrusion Detection in Wireless Ad-Hoc Networks," In *Proceedings of the Sixth Annual International Conference on Mobile Communication and Networking*, 2000.
- [15] Zhou, L. and Haas Z., "Securing Ad Hoc Networks," *IEEE Network Magazine*, vol. 13, no. 6, November/December 1999.

Grid connected Photovoltaic system An Assessment of Performance

A. Saurabh Singh Kashyap, *Student Member IEEE*, B. Dr. K. S. Verma, C. Vivek Kumar Soni
D. Rizwan Haider, *Student Member IEEE*, E. Dinesh Singh *Student Member IEEE*

Abstract- The present trend towards extended adoption of energy production from renewable sources is leading to increased attention towards the diffusion of grid-connected photovoltaic (PV) systems. Different technologies are available for the connection of the PV systems to the grid through inverter-based Power Conditioning Units (PCUs). This paper presents the results of a comparative study referred to the characteristics of different types of PCUs, based on the experimental results obtained for a wide range of solar irradiance and operating conditions. The performance of the grid connection has been characterised by using a set of parameters, referred both to the DC and to the AC side of the inverter, such as the efficiency of the maximum power point tracking, the DC/AC efficiency, the power factor and the harmonic distortion of voltage and current at the interface with the grid. The PV systems have been further characterised by considering their ability of avoiding the undesired islanding operation through relatively fast detection of the islanding conditions and fast PV system shutdown. The results are discussed and compared to the specifications provided by the manufacturers and to the limits imposed by some standards.

Key words: grid connection, harmonic distortion, inverter, islanding, maximum power point tracking, photovoltaic systems, power conditioning unit, power quality

I. INTRODUCTION

In the last decades, the energy production from renewable sources has become an increasingly important subject, in a framework aimed at reducing the environmental pollution and at pushing forward the development of technologies for alternative production of energy. The economic barriers that are of obstacle to a widespread evolution of some types of energy production from renewable sources have often been reduced by offering specific incentives towards the construction and operation of new plants and systems. In this framework, Photovoltaic (PV) systems have been subject to special attention. However, the present size of most PV systems is still relatively limited and not sufficient to cover the entire local load. The size limitations make PV systems suitable to operate as local generators in peak-shaving mode, to reduce the load demand seen by the grid.¹

As such they must be rapidly disconnected whenever the grid is switched off (for islanding prevention), as well as in case of over/under voltage or over/under frequency. In these cases, suitable protections shutdown the PV system within time limits specified by specific Standards [2].

The PV system components can be schematically represented as in Figure 1. The DC side includes a number of arrays of PV modules, interfaced with the external grid by means of inverters or, more generally, Power Conditioning Units (PCUs). The main components of the PCU are the Maximum Power Point Tracker (MPPT), the DC/AC converter

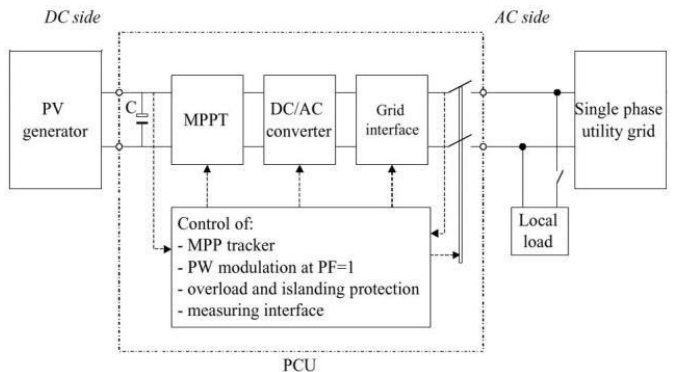


Fig. 1 Layout of a PV system connected to the single-phase grid

Table 1 Power Conditioning Unit Specifications

| Unit | A | B | C | D |
|--|--------|---------|---------|---------|
| transformer | HF | LF | HF | LF |
| nominal DC power PDCn (W) | 2700 | 2770 | 2700 | 1600 |
| MPPT voltage range ΔV_{MPPT} (V) | 66–120 | 268–550 | 150–400 | 140–400 |
| MPPT efficiency η_{MPPT} | 99 % | 99 % | 99 % | 99 % |
| nominal AC power PACn (W) | 2500 | 2600 | 2500 | 1500 |
| nominal efficiency η_{DC-AC} | 93 % | 94 % | 93 % | 93 % |
| power factor PF | 1 | 1 | 1 | 1 |
| THD of nominal AC current THDI | – | 4 % | 3 % | 4 % |
| run-on time t_l (ms) | 10 | 200 | – | 200 |

the internal protections and various control systems required for performing efficient PV system operation. The scope of the MPPT is to optimise the performance of the PV modules by tracking the maximum power point of the current/voltage characteristic with the highest possible accuracy, in function

A. PG Scholar, EED, KNIT Sultanpur
saurabhkashyap@yahoo.com
B. Professor, EED, KNIT Sultanpur
ksv211@rediffmail.com
C. PG Scholar, EED, KNIT Sultanpur
PG Scholar, EED, KNIT Sultanpur

of the conditions affecting the DC power supplied (solar irradiance and temperature). In addition, the electrolytic capacitor C acts as buffering storage device to balance the fluctuations of the single-phase instantaneous power demand at the AC side, that occur at double frequency with respect to the grid frequency, in order to limit the DC voltage ripple at the input section of the PCU. The other controls are aimed at providing AC power supply with acceptable features in terms of high power factor and reduced waveform distortion [3]. In the presence of multiple PV systems operating in a close portion of the distribution system, the PV system interactions have to be specifically analysed [4, 5], since they could lead to malfunctioning of the controls, being each control typically designed on the basis of the individual PV system characteristics.

Various technologies are available for performing the DC/AC conversion [6, 7, 8, 9]. Self commutated inverters (with MOSFETs or IGBTs in bridge configuration) are equipped with Pulse Width Modulation (PWM) and High Frequency (HF) or Low Frequency (LF) transformer. Different solutions are also available for what concerns the number and location of the inverters in the PV system, including a centralised inverter for the whole array of PV modules, string inverters (one inverter for each string of PV modules connected in series) or module integrated inverters (a single inverter for each PV module) [10]. In particular, the adoption of module integrated inverters leads to some benefits, concerning system modularity, increased system availability, and minimisation of the losses due to mismatching of the current/voltage characteristics, because of the individual and independent control of the single inverters. As a counterpart, the inverters integrated in the single modules must withstand the different climatic conditions that occur during the PV system operation and must be individually equipped with islanding protections.

This paper reports on the results of an experimental investigation carried out on a set of relevant technical aspects concerning the connection of PV systems to the external grid. A first aspect is the characterisation of the PCU performance by using a set of parameters, referred both to the DC and to the AC side of the inverter, such as the efficiency of the maximum power point tracking, the DC/AC efficiency, the power factor and the harmonic distortion of voltage and current at the interface with the grid [11]. A further aspect is the characterisation of the ability of the PV system to provide a relatively fast shutdown in order to avoid undesired islanding operation.

The investigation concerns four PV systems connected to the LV three-phase grid. For the sake of comparison, the systems have similar values of the total power (about 20 kW). All the PV plants have been funded by the Italian programme »10,000 PV roofs« [12] and are in operation since 2002.

The PV systems data are summarised in Table 1. Three PV systems (A, B and C) include six single-phase inverters, with groups of two inverters connected in parallel to each single phase. The PV system D includes eight single-phase

inverters, with two groups of three inverters and one group of two inverters connected to the three-phase grid. The PWM inverters belong to different manufacturers. In particular, the inverters A and C use the HF transformer, whereas the inverters B and D adopt the LF toroidal transformer. For the sake of comparison, the active power is normalised with respect to the nominal DC power of the inverter.

2 EXPERIMENTAL TESTS FOR POWER QUALITY CHARACTERISATION

2.1 Definition of the parameters

A global view of the power quality issues has been considered for the experimental study, including the information available from measurements both at the DC side and at the AC side [12]. In particular:

- P_{dc} is the PV power, that is, the input power of the PCU;
- P_{ac} is the active power at the grid side;
- P_{max} is the maximum power calculated on the power-voltage P(U) characteristic obtained by the transient charge of a capacitor (see subsection 2.2);
- U_{ac} is the RMS voltage at the AC side;
- I_{ac} is the RMS current at the AC side;
- I_k is the RMS value of the k-th harmonic order component of the AC current supplied to the load;
- U_k is the RMS value of the k-th harmonic order component of the AC voltage at the point of grid connection;
- n is an even number representing the highest harmonic order considered in the study.

The following parameters have been used for characterising the PCU performance in terms of power quality:

1. the MPPT efficiency is the parameter describing the optimum utilisation of the PV array [12]. It represents how close to the maximum power P_{max} the MPPT is operating and is expressed by

$$MPPT = \frac{P_{dc}}{P_{max}}$$

2. the inverter efficiency is defined in the conventional way as the ratio between the output and the input power

$$Eff = \frac{P_{ac}}{P_{dc}}$$

3. the Total Harmonic Distortion (THD) of the AC current

$$THD_1 = \sqrt{\frac{n}{\sum I_k^2}}$$

4. the THD of the AC voltage

$$THD_u = \sqrt{\frac{n}{\sum U_k^2}} \quad k = 2$$

2.2 Instrumentation

The experimental tests on the PV systems have been carried out in clear days, for a wide range of solar irradiance. The results analysed are extracted from daily measurements. The analysis has been performed by taking into account national and international standards, guidelines and specifications [10, 7, 8, 9]. A dedicated Lab View [12] software has been used for automatic data acquisition. The software is based on a Data Acquisition board (DAQ), integrated into a notebook PC. The DAQ specifications are the sampling rate (500 kSa/s), the resolution of the Analogue Digital Converter (12-bit), the number of channels (8 differential channels) and a voltage range of ± 10 V. Suitable voltage and current probes (used as a signal conditioning stage to extend the range of the measured quantities) must have operational amplifiers with both high input resistance ($> 1 \text{ M}\Omega$), in order to neglect the »loading effect«, and low output resistance ($< 50 \Omega$), for obtaining low time constants with the capacitance of the Sample & Hold circuit in the DAQ board. Typical uncertainty can be within $\pm 0.1\%$ for voltage measurement, $\pm 0.4\%$ for current measurement and about $\pm 0.5\%$ for power measurement. These values have been obtained by performing a suitable calibration procedure, in the laboratory, on the measurement chain composed of DAQ and probes. Without this calibration, the uncertainty would be significantly higher (e.g., 1 % or more).

The software implements Virtual Instruments [11] behaving as storage oscilloscope and multimeter for measurement of RMS voltage (600 V), current active power and power factor. The multimeter also performs harmonic analysis for the calculation of the Total Harmonic Distortion and operates as data logger with user-selected time interval between two consecutive measurements.

2.3 Tracing the PV generator current-voltage characteristic by transient charge of a capacitor

In order to measure in a single sweep the current-voltage $I(U)$ characteristic of a PV generator, proper measuring circuits of the first and the second order (with LC resonant components) can be

used [12, 11]. Concerning the circuit of the first order, which gives the $I(U)$ only according to the generator operation, Figure 2 shows the scheme related to the method of the transient charge of capacitor (initially uncharged). The PV current, during the transient charge, is measured by a four-terminal shunt (or a current probe based on the Hall effect) and converted into a voltage signal, as well as the voltage across the PV generator

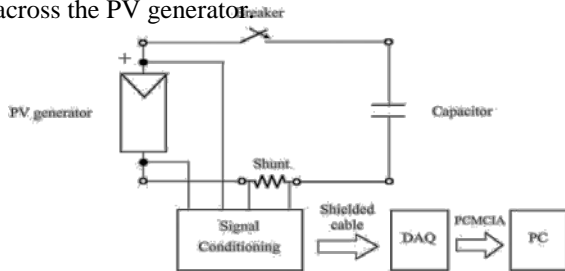


Fig. 2 Data acquisition system for tracing the $I(U)$ characteristic of a PV generator

The PV array can be seen as an equivalent generator. Depending on the operating point imposed by the load, this generator can be conveniently modelled by using the Norton generator (in the region of operation with almost constant current) or the Thévenin generator (in the region of operation with almost constant voltage), obtaining a linear approximation of the actual $I(U)$ characteristic. Then, the transient evolution associated to the capacitor charge can be divided into two parts. The first part can be studied as a capacitor charge with constant current and linear voltage, whereas the second part corresponds to a charge with a real voltage generator, leading to an exponential evolution of both voltage and current.

At the closing of the breaker, the voltage across the capacitor cannot change instantaneously and hence the PV generator changes abruptly its condition from open circuit to short circuit. Figure 3 shows that the current signal is, at first, enough constant and the corresponding voltage linear up to, roughly, the voltage of maximum power U_M (equal to almost 80 % of the open circuit voltage). The duration of this part of transient is approximately inversely proportional to the

$$\Delta t = \frac{U_1}{SC}$$

short circuit current I_{sc} and thus to the solar irradiance. Then, around the maximum power, the subsequent evolution is similar to an exponential, both for current and for voltage: also this duration depends directly on the capacitance.

During the transient charge, in which solar irradiance and temperature are considered constant, the $I(U)$ characteristic is covered in a single sweep from the short circuit to the open circuit condition.

For deeper understanding, it is necessary to mention the junction capacitance of PV generators, which has low value (much lower than microfarads), because a high number of series connections of PV cells (in the modules) and of PV modules (in the strings) is often used to obtain the PV generator. Therefore a sharp peak of current, higher than the short circuit current, arises immediately, during the transient, when the voltage across the PV generator is shorted by the capacitor (Figure 3). With reference to the capacitance of capacitor, values within 1–5 mF can be suitable for obtaining transient durations within 5–100 ms, so that it is possible to neglect the interaction with the junction capacitance and assume constant solar irradiance and temperature.

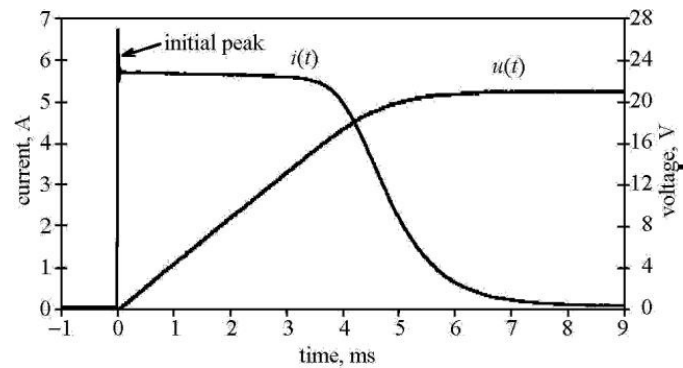


Fig. 3 Transient charge of a capacitor by a PV generator

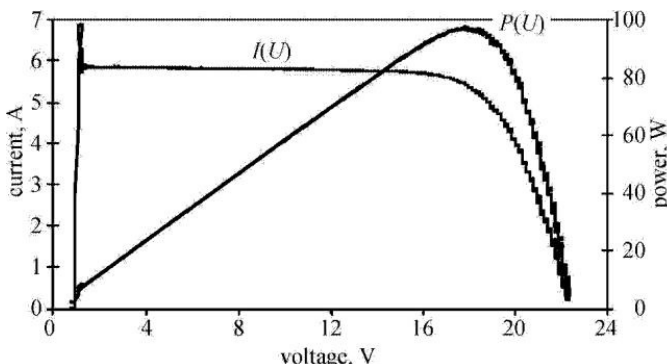


Fig. 4 Current-voltage and power-voltage characteristics

The current-voltage curve of Figure 4 is obtained by plotting the values of current and voltage corresponding to the same time instant. In addition, multiplying the current values by the corresponding voltage gives the points of the power-voltage curve shown in Figure 4.

2.4 MPPT efficiency

The MPPT efficiency is obtained from two tests, carried out as close as possible in order to maintain similar ambient conditions (solar irradiance and temperature). The first test determines the current-- voltage $I(U)$ and power-voltage $P(U)$ characteristic by the transient charge of a capacitor. The maximum power P_{MAX} is determined from the complete $I(U)$ and $P(U)$ curves (Figure 4) . The second test determines the power $P_{DC}(t)$ as product of the DC

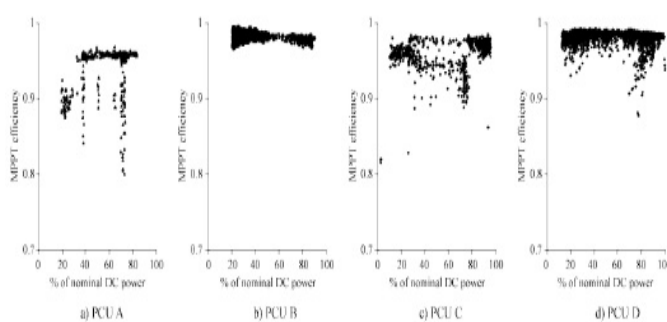


Fig. 5 MPPT efficiency for the PCUs tested

voltage $U_{DC}(t)$ and current $I_{DC}(t)$ signals of the inverter. Since the AC single-phase load demands an instantaneous power fluctuating at double frequency with respect to the grid frequency, voltage and current exhibit a 100 Hz ripple, evaluated as the peak to peak values $2 \sqrt{2} U_{2k}$ and $2 \sqrt{2} I_{2k}$ with respect to the mean values U_0 and I_0 , respectively, for $k = 1, \dots, n/2$. The ripple voltage and the ripple current always have a 180° phase shift, that is, on the $I(U)$ characteristic, if voltage increases, then current decreases. On the other hand, ripple voltage and ripple power can have a 0° or 180° phase shift, respectively if the operating points on the $P(U)$ characteristic are biased on the left ($dP/dU > 0$) or on the right ($dP/dU < 0$) with respect to the MPP.

If the operating points on the $P(U)$ characteristic are not biased, it is difficult to state the phase shift of $p_{DC}(t)$ with respect to $u_{DC}(t)$. The ripple power must be as low as possible, because it decreases the mean value (active power P_{DC}) with respect to the maximum value. The expression of the power P_{DC} is

$$P_{dc} = U_0 I_0 + \sum_{k=1}^{n/2} U_{2k} I_{2k} \cos \phi_{2k} \quad (6)$$

where $\cos \phi_{2k}$ is negative, so that P_{DC} is lower than the product $U_0 I_0$. An approximation (in excess) of the MPPT efficiency can be provided by measuring the DC signals with the peak value of $p_{DC}(t)$ assumed as P_{MAX} , without determining the whole $P(U)$ characteristic. The MPPT efficiency values shown in Figure 5 have been obtained by repeating the measurement of μ_{MPPT} , carried out by the above mentioned approximation, for different conditions of P_{DC} (corresponding to different values of the solar irradiance).

There are various causes that may decrease the MPPT efficiency, the main ones being:

- a) the adoption of simplified MPPT strategies;
- b) the presence of overload due to high solar irradiance or high inverter temperature;
- c) the shading effect on some modules of the PV array.

About MPPT strategies, an example is shown where the MPPT of the PCU A imposes the operation at fixed voltage (about 80 % of U_{oc}), where the open-circuit voltage U_{oc} of the PV array is assessed by means of a fast open-circuit measurement at time intervals of about two seconds (e.g., Figure 6). This practice does not correspond to searching for the true MPP, and as such it leads to relatively low values of the MPPT efficiency.

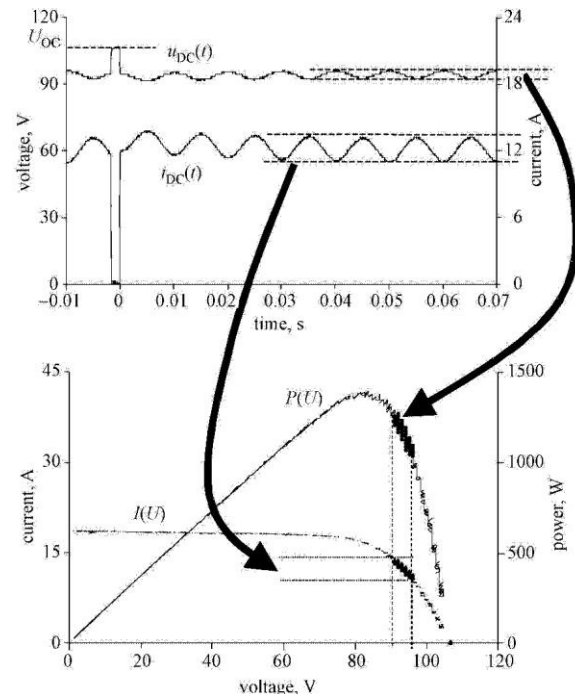


Fig. 6 Voltage and current ripples at the DC side in the presence of overloading

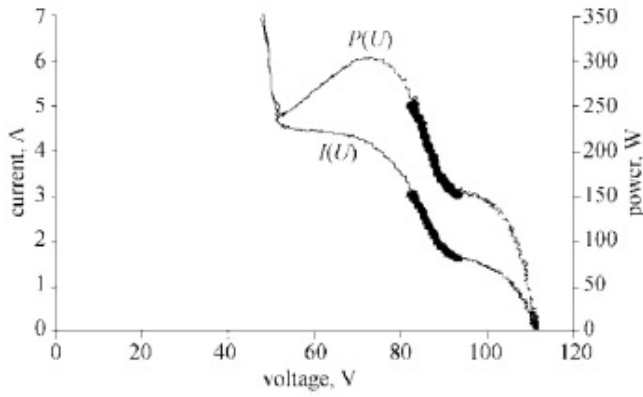


Fig. 7 Operating points imposed by the MPPT in the presence of the shading effect

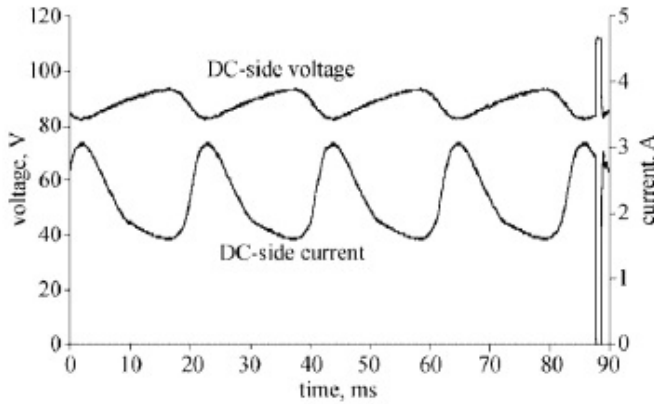


Fig. 8 Voltage and current ripples at the DC side in the presence of shading effect

An example of overload is shown in Figure 6 for the same PCU A. In overload conditions, the MPPT is intentionally disabled, so that the operating point moves away from the MPP, reaching locations at higher voltages with respect to the one corresponding to the MPP, in a region of the I(U) characteristic with high (negative) slope and resulting high amplitude of the current ripple.

For what concerns the shading effect, tests carried out on a façade PV plant with the inverter A have put into evidence a partial shading effect occurring during morning periods in part of the year (from April to September) [12]. This shading effect, concentrated on some cells of a PV array, determines a mismatch of cell current-voltage I(U) characteristics, with an important reduction of the available power, only limited by the bypass diodes, i.e., diodes connected in anti-parallel to a group of PV cells in order to limit the negative impact of the shading effect. Furthermore, the shaded cells can work as a load and the hot spots can rise. In order to evaluate the PCU performance in shading conditions, experimental data have been collected. As shown in Figure 7, representing the right-hand sides of the complete P(U) and I(U) characteristics, the P(U) characteristic changes shape and can exhibit more than

one maximum power point. More specifically, the maximum power corresponds to a voltage lower than the operating voltage range of the MPPT indicated in Table 1. Then, very high amplitudes of the peak-to-peak voltage and current ripples occur (Figure 8) with operating points even located far from the local maximum (Figure 7) and the MPPT efficiency falls down considerably.

2.5 DC/AC efficiency

Figure 9 shows the DC/AC efficiency values for the PCUs tested. The PCUs B and D, with LF toroidal transformer, generally exhibit better performance than the inverters with HF transformer. The PCU B, which exhibits the best performance, has high nominal power and DC voltage within the range 300–350 V, allowing for selecting the turns ratio of the transformer close to unity to obtain the peak value of the grid voltage $U_p = 2U_r \cong 325 \text{ V}$ (with single-phase nominal voltage $U_r = 230 \text{ V}$). The PCU B maintains high DC/AC efficiency also at low DC power ($P_{DC} < 30\% \text{ of nominal DC power}$), where

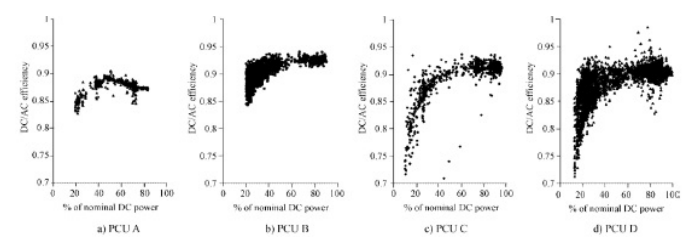


Fig. 9 DC/AC efficiency of the PCUs tested

there is a large number of hours of operation. On the other hand, the PCU D operates at a lower voltage level, i.e., in the range 150–190 V. Moreover, the PCU D has a larger spread of the DC/AC efficiency values due to a wider range of operating conditions, also including overloads caused by high solar irradiance. The relatively lower efficiency of the PCU A is also affected by the systematic shading effect, as shown in the previous subsection, that also produces even harmonics of the AC current; even harmonics are not present in the AC voltage and thus do not contribute to the AC active power production. The PCU C is able to guarantee high DC/AC efficiency at high power, but its efficiency falls down when the power decreases.

2.6. Total Harmonic Distortion

From the power quality point of view, the grid connection of PV plant through inverter implies the presence of distorted current waveforms, even if the voltage at the grid side has negligible distortion when the PV plant is not connected (open connection). The presence of a distorted voltage waveform

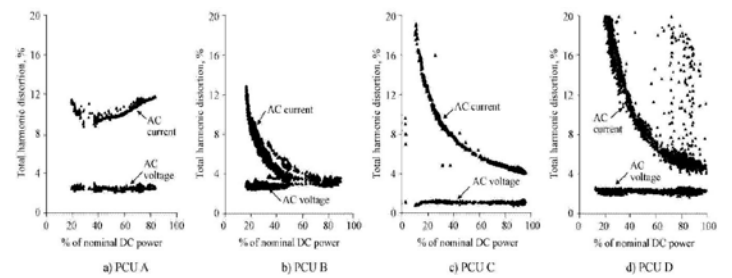


Fig. 10 Total Harmonic Distortion of the current for the PCUs tested

in the open connection leads to the modification of the harmonic spectrum when the PV plant is connected [25]. Clearly, the nature of the current distortion, represented by the most involved harmonic orders, varies from case to case and during time. The worst power quality conditions may occur at low loading [23, 24], but in these cases the current magnitudes are relatively low and do not cause significant problems.

The Total Harmonic Distortion (THD) values of the AC currents are shown in Figure 10. The PCU A has a poor harmonic behaviour, since the THD of its currents never falls below 8 %. The other PCUs exhibit decreasing values for increasing values of the DC power. The THD of the currents for the PCUs C and D show variations in a relatively large range, whereas the THD of the voltage remains close to the same values, as shown in Figure 11.

The PCU D presents a particular behaviour, with the presence of high current THD spots at high power. These spots are due to the effect of the net-work impedance measurement circuit, based on the

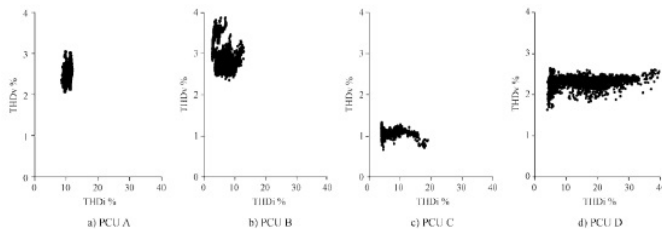


Fig. 11 Current vs. voltage Total Harmonic Distortion for the inverters tested

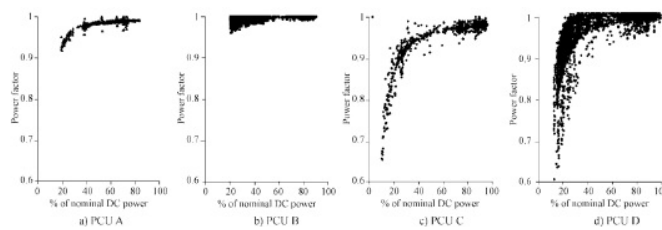


Fig. 12 Power factor of the PCUs tested

temporary switching of a RC circuit at time cadence of about 5 s. This technique, used for islanding detection [26], produces distortion to the cur-rent waveform, deteriorating the current THD. The number of spots detected depends on the time cadence with which the measurements are performed (12 s in this case) and on the length of the time interval used to compute the THD (100 ms). The lack of synchronism between harmonics measurement and network impedance measurement deter-mines the possible presence of capacitive peaks in the current waveform sampled for performing harmonic analysis.

The PCU B exhibits better characteristics with respect to the other PCUs, since the THD of its currents remains relatively low even in the presence of the largest distortion of the voltage, for the entire range of normalised DC powers.

In order to check the fulfilment of the maximum limits allowed for the waveform distortion, Figure 10 shows that the PCUs B and C, as well as the PCU D in most of the cases, satisfy the requirement of current THD lower than 5 % at full load imposed by [18], while the PCU A never reaches the required level. However, from the experimental results it is clear that the indications concerning the harmonic distortion should be more specifically referred to the voltage THD and possibly to various power levels.

2.7 Power Factor

The power factor embeds the contributions of both the phase shift between current and voltage at the fundamental frequency, and the harmonic distortion of the waveforms. All the PCUs tested exhibited a qualitatively similar behaviour above 50 % of the nominal DC power (Figure 12). How-ever, the PCUs C and D exhibit significant reductions of the power factor at low DC power. In particular, the power factor values for the PCUs C and D are lower than the ones proposed by some standards, e.g., the IEEE Standard 929–2000, according to which the PV system should operate at power factor higher than 0.85 when the output exceeds 10 % of the rating [27]. Furthermore, the PCU C presents low power factor but relatively low harmonic distortion content, so that the power factor reduction in this case has to be associated to a scarcely effective phase angle control.

3 AVOIDING THE ISLANDING OPERATION

Islanding operation occurs when, in the absence of supply from the utility grid, the PV plant opera-tes alone to supply the local load. When an island is formed, frequency and voltage may exceed the acceptable ranges, so that frequency and voltage monitoring can recognise the island formation and can switch the PV plant off. However, in case of sufficient balance of generation and load, the monitored quantities may fall into a range for which the protections are unable to work (the non-detection zone) and the island could persist without trip of the protections. Hence, efficient islanding detection must include the addition of specific functions to the common protection schemes, e.g., measurement of the network impedance. Phase criteria based on the detection of zero phase error between the PV output current and the voltage at the PV terminals have been illustrated in [12] in order to reduce the size of the non-detection zones. A further phase-shift method is illustrated in [11]. Different functions have been tested in [11] on typical circuits for islanding protection. However, several test circuits have been proposed in the literature and the standardisation of the criteria for islanding detection is still in progress [6, 12].

The typical parameter representing the ability of automatic shutdown of the PCU after a lack of supply at the utility side of the network is called run-on time [3, 2] and consists of the time elapsed between the instant of utility disconnection and the instant at which the interruption of the current supplied from the PV system has been completed.

A typical categorisation of the islanding events leads to

identifying short-term (< 1 s) and long-term (> 1 s) islanding operation. Long-term islanding operation has to be avoided, mainly for ensuring the system safety. In fact, during islanding the maintenance or repair personnel, arriving to operate on an expected isolated feeder, could be unaware that it is still energised and could then be injured. In addition, after opening the circuit breaker from the utility side, the islanded PV system would lose synchronism with respect to the utility. The analysis of PV system islanding also requires to take into account the possible mutual interference among the islanding prevention methods. That could lead to longer run-on times and possible failure to detect islanding if several PV systems are present in the island.

The islanding tests have been carried out by performing measurements at the AC side of each single inverter. Concerning the PV system protection, some national specifications [33] require introducing redundant islanding protections, with both the local protection at the (output) AC side of each inverter and a centralised protection for the three-phase system at the grid side. The presence of these protections impacts on the time evolution of the shutdown process.

The run-on time has been evaluated by using the circuit of Figure 13. The run-on time evaluation has been carried out in the worst case, where the active powers of inverter and load are equal, $P_{AC} = P_{load}$, and the reactive power is null. This worst case corresponds to the matching condition: at the

moment in which the grid is switched off, the current supplied by the inverter has the same RMS value as the current of the local load, thus making it difficult to detect the islanding condition and to deactivate the PV system. In case of different RMS

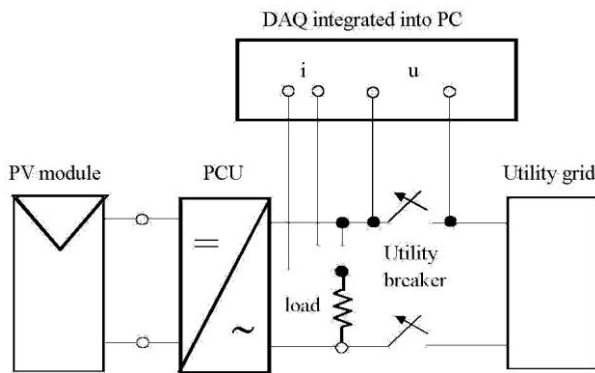


Fig. 13 Circuit for the islanding time detection

currents between inverter and load, the release of relays is easier, since an over-voltage or under voltage occurs after the grid deenergization.

The average values of the run-on times occurred on a set of tests are around 7 ms for the PCU A, 120 ms for the PCUs B and D, and 60 ms for the PCU C. For the PCU A, Figure 14 shows that the PCU switch-off is very fast (6 ms), in line with the values specified in Table 1. Its run-on time could even be too fast with respect to the switch-off duration required by

most standards (about 200 ms), leading to possible untimely trip. For the PCU B, Figure 15 and Figure 16 show the time evolution of the load current and of the voltage at the terminals of the circuit breaker, respectively in case of measurement on the phase and on the neutral pole of the circuit breaker. The run-on time is 84 ms for the case in Figure 15 and 80 ms for the case in Figure 16. Both cases are within the inverter specifications shown in Table 1. However, in a few cases one of the inverters of the PCU B exhibited run-on times up to 280 ms, exceeding the manufacturer's specifications (200 ms). The time evolution of the switch-off for the PCU C is shown in Figure 17 for a run-on time of 63 ms. The PCU D has similar

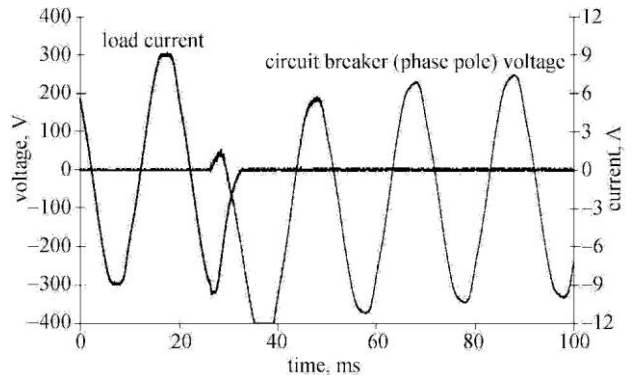


Fig. 14 Shutdown test results on the PCU A

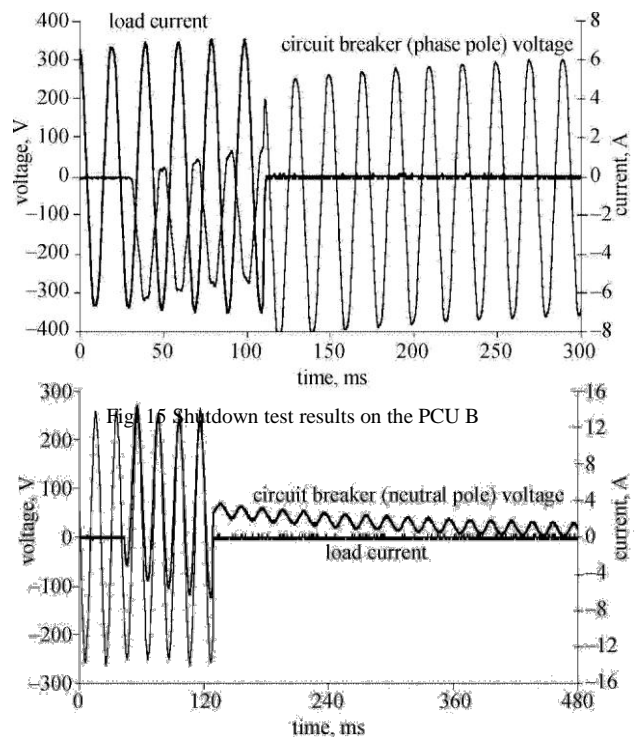


Fig. 15 Shutdown test results on the PCU B

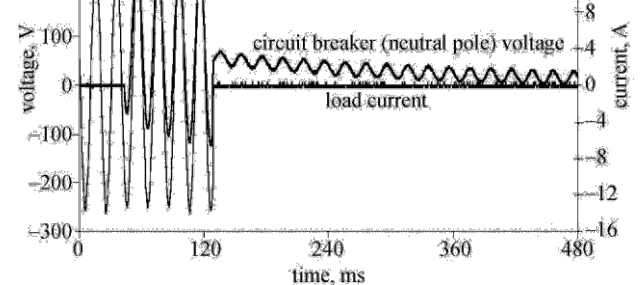


Fig. 16 Shutdown test results on the PCU B (voltage measurement on the neutral pole)

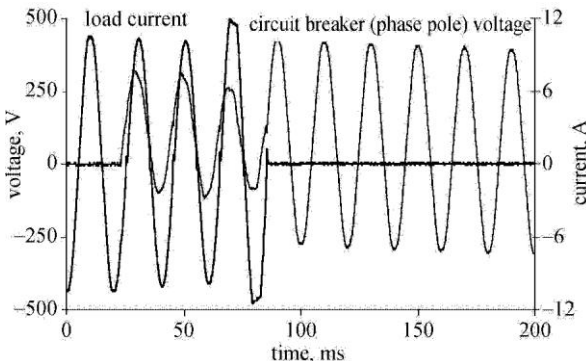


Fig. 17 Shutdown test results on the PCU C

characteristics as the PCU B and exhibited a similar behaviour. The asymmetrical evolution of the voltage, shown in all the cases after the load current interruption, is due to the presence of the RC transient consequent to the discharge of the capacitor connected at the AC inverter terminals.

4 CONCLUSIONS

This paper has presented detailed results concerning the performance of inverter-based PCUs, obtained from an extended experimental analysis. A suitable set of measured quantities has been selected, in order to perform a widespread quality testing of the PCUs. The results of the measurements carried out in actual operating conditions of the PV systems have put into evidence some critical aspects in the performance of the various PCUs. These aspects are mainly linked to the internal strategies implemented for tracking the maximum power point and to possible severe conditions occurring during the actual operation for solar irradiance, temperature, possible shading effect and distortion of the voltage waveform at the point of grid connection. The results obtained show that the performance of PCUs with similar rated values can be significantly different. In some cases, either the declared specifications or the limits imposed by

specific standards were not completely satisfied. These facts should be carefully taken into account by the manufacturers, in order to define suitable inverter and PCU specifications. In particular, the procedures for PCU testing based on the results obtained from laboratory tests could be refined to better reflect the PV system behaviour in real conditions.

REFERENCES

- [1] S. A. Papathanassiou, N. D. Hatziargyriou, Technical Requirements for the Connection of Dispersed Generation to the Grid. Proc. IEEE/PES Summer Meeting 2, July 15–19, 2001, 749–754.
- [2] IEEE Standard for Interconnecting Distributed Resources with Electric Power System, Std. 1547–2003, 28 July 2003.
- [3] M. Prodanovic, T. C. Green, Control and Filter Design of Three-phase Inverters for High Power Quality Grid Connection. IEEE Trans. on Power Electronics 18, 1, Jan. 2003, 373–380.
- [4] J. H. R. Eslin, W. T. J. Hulshorst, A. M. S. Atmadji, P. J. M. Heskes, A. Kotsopoulos, J. F. G. Cobben, P. Van der Sluijs, Harmonic Interaction Between Large Numbers of Photo-voltaic Inverters and the Distribution Network. Proc. IEEE Bologna Power Tech, June 23–26, 2003.
- [5] D. G. Infield, P. Onions, A. D. Simmons, G. A. Smith, Power Quality from Multiple Grid-Connected Single-Phase Inverters. IEEE Trans. on Power Delivery 19, 4, October 2004, 1983–1989.
- [6] F. Sick, T. Erge, Photovoltaics in Buildings: a Design Hand-book. International Energy Agency, 1996.
- [7] H. Wilk, R. Hotopp et al., Photovoltaic Systems. The Fraunhofer Institute for Solar Energy, Comett Book, 1995.
- [8] P. Rooij, Technical Evaluation of Modern Grid Connected Inverters. Proc. PV in Europe: from PV technology to energy solutions, Roma, Italy, October 2002, 868–871.
- [9] E. T. Schönholzer, Inverters for Utility Interactive Photo-voltaic Power Plants. Proc. Melecon 1989, April 11–13, 1989, 16–20.
- [10] Abete, F. Scapino, F. Spertino, Comparison of Power Quality Between Centralised Inverters and Module Integrated Inverters in Grid Connected PV Systems. Proc. 17th European Photovoltaic Solar Energy Conference, Munich, Germany, October 2001, 421–425.
- [11] A. D. Simmons, D. G. Infield, Current Waveform Quality from Grid-connected Photovoltaic Inverters and its Dependence on Operating Conditions. Progress in Photovoltaic 8, 2000, 411–420.
- [12] S. Castello, M. Garozzo, S. Li Causi, A. Sarno, The Italian Roof-top Program: Current Status and First Results. Proc. 17th European PV Solar Energy Conference, Munich, Germany, October 2001

Security Aspects In Vehicular ad hoc Network System (VANET'S)

A. Neeraj Sharma, B. B.P Chaurasia, C. Rajesh Kumar

Abstract— now a day Vehicular Ad Hoc Networks (VANET) Security has directed the attention of research efforts, while compact optimized solutions to protect the network from attacks and adversary yet need to be improved, trying to reach a tolerable level, for the manufacturer and driver to achieve life safety and infotainment. The need for a healthful VANET networks is hardly dependent on their security and privacy features, which are being discussed in this paper. Many challenges has been facing In VANET that been addressed in the research, we also discuss all the possible present challenges and problems; and we made critics for these solutions and proposed suitable solutions for some of these problems.

Keywords- Vehicular Ad Hoc Networks, Attacks, VBKI, Privacy, Authentication, DSRC, ELP, CRL.

I. INTRODUCTION

Our efforts to create comfortable and efficient safer driving conditions have started, The Vehicular Adhoc Network will be the main player in this work, it's directing to efficient driving, road safety, and infotainment. Now a day the world is living a combat, and the battle field lies on the roads, the estimated number of deaths is about 1.2 million people yearly worldwide [1], and injures about forty times of this number, without forgetting that traffic congestion that makes a huge waste of time and fuel [2]. The Vehicular Ad hoc Networks (VANET) subset of Mobile Ad Hoc Networks (MANET), this means that Each and Every Node can move freely within the network coverage Region and stay connected, Every node can communicate with other nodes in Single and Muti Hop, and any node could be Road Side Unit (RSU) as well as Vehicle. In the year 1998, the team of engineers from Delphi Delco Electronics System and IBM Corporation proposed a network vehicle concept aimed at providing a wide range of applications [3]. There advancements in wireless communications technology, the concept of network car have attracted the attention all over the world. At the Latest years, ¹A number Of New projects have been launched, Realize and

Target the dream of car Networking and successful implementation of vehicular networks. The project Network on Wheels (NOW) [3] is a German research project in 2004, The project adopts an IEEE 802.11 standard for wireless access, Their Major objectives of The project is to solve technical issues Which are related to communication protocols and data security for car-to-car communications.



Figure 1. Car-to-Car Communication.

The Car-to-Car Communication Consortium [4] is initiated by six European car manufacturers. Their goal is to create a European industrial standard for car-to-car communications extend across all brands. FleetNet [4] was another European program which ran from 2000 to 2003 this ad hoc research was dominated by efforts to standardize MANET protocols, and the MANET research focused on the network layer [5], their major challenge was how to solve the problem to reach nodes not directly within radio range by employing neighbors as forwarders.

A Radio Signal is used for the communication is Dedicated Short-Range Communications (DSRC), which been allocated as new band in 1999 by the Federal Communications Commission (FCC)[3], the band (the band width) allocated was 75 MHz at 5.9 GHz frequency for Intelligent Transport System (ITS) is applications in north America.

In This paper in section II the analysis of VANET Attackers and attack to show the problems that is being faced in VANET. In section III we examine the VANET challenges as Privacy and Mobility that assumed the difficult security problems of VANET, in section IV we listed requirement of the security which must happen to achieve the System Security, in section [V] we have discussed the current solution for the Attacks and Challenges and Necessary requirement to achieve a secure system, Which been addressed by other

-
- A. PG Scholar, CSE, KNIT Sultanpur
neerajknit2012@gmail.com
 - B. Assistant Professor, CSE, KNIT Sultanpur
bpc1888@gmail.com
 - C. PG Scholar, CSE, KNIT Sultanpur
rajeshchauhanusat@gmail.com

researcher and papers, in section VI we gave further critics for the current solution, and Present our solution for some of these problems.

II. HOW VEHICULAR NETWORKS WORK

The vehicular Adhoc Network System contain a large number of nodes, approximately number of vehicles exceeding 750 million in the world today [6], Those vehicles will be required an authority to govern it, Every vehicle can communicate with other vehicles by using short radio signals DSRC (5.9 GHz), for range can reach 1 KM, that communicate in Ad Hoc Network that means every connected node can freely move, There is no need any kind of wires required, the routers Which used are called Road Side Unit (RSU), these RSU works as a router among the vehicles on the road and connected to The devices of Other Network.

Every vehicle has OBU (on board unit), this is used to connects the vehicle with RSU via DSRC radios signal, and Other device is TPD (Tamper Proof Device), this device holding the vehicle credential Terms, all the information about the vehicle like Driver Identity, Keys, Trip Details, speed, Route...etc.

III. VANET SECURITY ISSUES:

VANET facing many attacks; these attacks are discussed in the following sections:

A. Attacks and Treats:

Under the paper we are concentrated on attacks blemish against the message itself in spite of the vehicle, as physical security is not in the scope of this paper.

1) Message Suppression Attack:

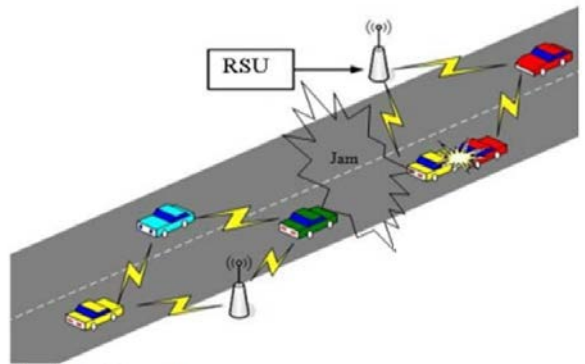
An attacker choicely dropping packets from the network, those packets may hold pointed information for the receiver, the attacker transpose these packets and can able to use them again latter. The goal of such an attacker would be to prevent insurance and registration authorities from learning about collisions involve ness of his vehicle and/or to avoid delivering collision reports to roadside access points [10]. For instance, an attacker may transpose a congestion warning, and use it in another time, so the warning message will not be delivered to the Vehicle and forced to wait in the traffic.

2) Denial of Service attack:

This attack takes place when the attacker takes control over the vehicle's resources or jams of the communication channel which are being used by the Vehicular Network, so it prevents critical information from get in. It also increases the danger to the driver, if it does depend on the application's information. For instance, if Evil-minded wants to create a huge pile up on the highway, it can cause an accident and use the DoS attack to prevent the warning from reaching to the approaching

vehicles [8].and [10].

See figure 2. The authors in [9], proposed a solution by switching among different channels or even communication technologies (e.g., DSRC, UTRATDD, or even Bluetooth for very short ranges), if they are available, when one of them



(typically DSRC) is brought down.

Figure 2. Dos Attack.

3) Sybil Attack:

The Sybil Attack happens when an attacker creates a large number of pseudonymous, demands or acts like it is more than a hundred vehicles (see figure 3), to tell other vehicles that there is congestion ahead, and force them to take different route [7]. A Sybil attack (fig 2) depends on how easily identities may be generated, the degree of the system accepts inputs from entities that do not have a chain of trust linking them to a trusted entity, and whether the system treats all entities identically.

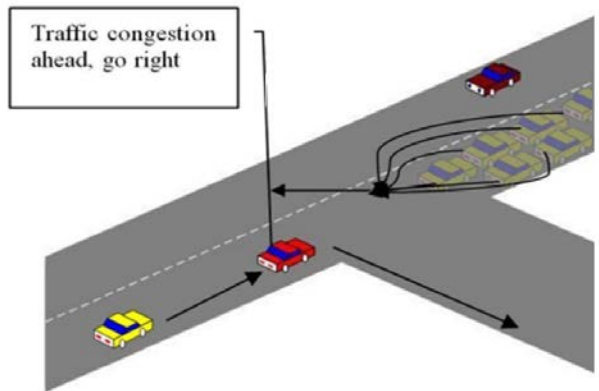


Figure 3. Sybil Attack

4) Replay Attack

The Replay attack takes place when an attacker replays the transmission of earlier information to take advantage of the situation of the message at time of sending [7]. Basic 802.11

securities have no protection against replay.

It does not contain timestamps or sequence numbers. Because of keys may be re-used, this is possible to replay stored messages with the same key without detection to insert factitious messages into the system. The solo packets should be authenticated, not just encrypted.

The Packets should contain timestamps. The aim of such an attack would be to confuse the authorities and possibly prevent identification of vehicles in hit-and-run incidents [10].

5) Alteration Attack:

This attack happens when attacker alters an existing data information. It includes delay in the transmission of information, reply earlier transmission, or alter the actual entry of the data transmitted [7]. For instance, an attacker are able to alter a message tells other vehicles that the Ahead road is clear while the road is congested.

6) Fabrication Attack:

An attacker can placed this attack by transmitting wrong information into the network, the information could be false wrong or the transmitter can claim, this is done by some other person. This attack includes fabricate messages, warnings, certificates, Identities [8].

B. ATTACKERS:

1) Malicious Attacker:

The malicious Attackers is the kind of attack in which attacker try to cause damage via the applications available on the vehicular network. In many different cases, these attackers will have unusual targets, and they will access to the resources of the network [7].

2) Selfish Driver:

The idea for trust in Vehicular Adhoc Network is the vehicles must be trusted initially, these vehicles are trusted to follow the protocols specified by the application, and few drivers try to increase their profit from the network, Imprudent the cost for the system by taking advantage of the network resources illegally [7]. A Selfish Drive pass the wrong message to the other vehicles that there is congestion takes place ahead in the road, so they must choose an alternate way. they should choose an alternate route, so the road will be clear for it.

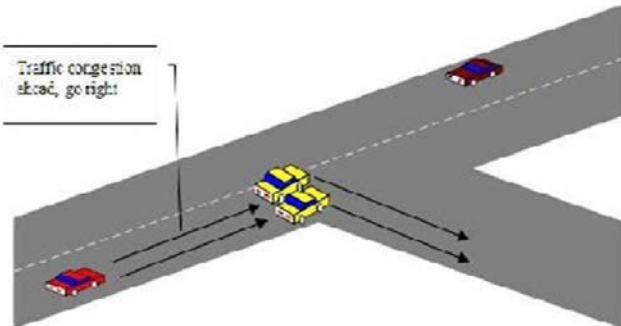


Figure 4. Selfish driver Attack

3) Pranksters:

Include bored people probing for penetrability and hackers seeking discover to reach fame via their damage [7]. For instance, a prankster can convince one vehicle to slow down, and tell the other vehicle behind it to increase the speed.

IV. VEHICULAR NETWORKS CHALLENGES

A. Mobility:

the concept of mobility in VANET came from Ad Hoc Networks allow nodes users to move from network to the another network with in the coverage but still the mobility is limited, While in Vehicular Ad Hoc Networks nodes move at very high speed, The High speed vehicles mobility make connection in its way with any other Vehicles that can be never faced before, and this connection lost for only few seconds as each vehicle goes in its direction, and those two vehicles may never meet again. So securing mobility challenge is hard problem [7].

B. Volatility:

The connectivity among nodes can be convince ephemeral, and possible they will not happen again, Vehicles traveling within the coverage area an established connection with another vehicles, these types of connections will lost as every car has a high mobility, and may be travel in opposite direction[2]. Vehicular networks short of the relatively long life context, so personal contact of users' device to a hot spot will require long life password, and this will be impractical for securing VC.

C. Network Scalability:

The network scalability in the world approximately exceeding the 750 million nodes [6], and this number is rapidly, another problem arise when we know that there is no any global authority govern the standards for the existing network [7], [8], for example: the standards for DSRC in North America is deferent from the DSRC standards in Europe, the standards for the GM Vehicles is deferent from the BMW one (see figure 5).

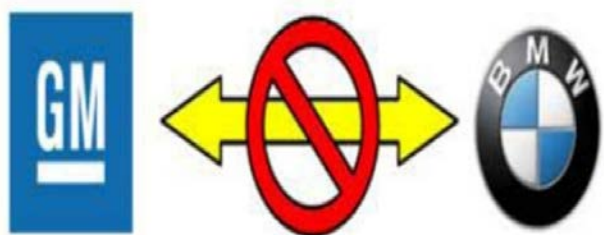


Figure 5. BMW VS. GM Slandered.

D. Bootstrap:

At this moment only few number of car have the equipment required for the DSRC radios signal, so if we make a communication we have to assume that there are limited number of cars that will take participation in the communication, in the future we should concentrate on finding the higher number, to find out a financial benefit that will courage the commercial firms to invest in this technology [7].

V. SECURITY REQUIREMENTS

A. Authentication:

Authentication is the process of confirming the identity Of User. It involve in the confirmation, the identity of a person by validating their document, is verified through the website with a digital certificate, ensure which a product is labeling and claiming to be. In other words, Authentication mostly involves in verifying the validity of at least one identification form.

In VC (vehicular communication) every message should be authenticated, to make sure for its origin and to control authorization level of the vehicles, to do this vehicles will assign every message with its Private Key along with their Certificate, In the receiver end side, the vehicle will receive the message and check for the key and certificate once this is done, the receiver verifies the message [2], [7]. Signing every message with this, causes an overhead, to reduce this overhead we can use the approach ECC (Elliptic Curve Cryptography), the efficient public key cryptosystem.

VANET is a kind of Wireless ad hoc network which has a routable networking environment at the top of the Link Layer ad hoc network. A Vehicular ad hoc network VANET is a self-configuring infrastructure less Network. Vehicular connected by wireless. In Latin Ad hoc means for this purpose. Each device in a VANET is free to move independently .In any direction with in the Connected Region Area, and change its links to other devices frequently. Every Vehicle forward traffic unrelated to its own use, and therefore be a router.

The primary challenge in developing a VANET is equipping every device to continuously maintain the information required to proper traffic route. Such networks may operate by it or can connect to the larger Internet. Mobility within a bounded space, usually with all nodes within a few nodes to each other. Different protocols are developed to evaluated the measures such as the packet drop rate, the overhead is introduced by the routing protocol, end-to-end packet delays, network throughput, Jitter etc.)

B. Availability:

The availability of Vehicular Network should be available all the time, for many applications Vehicular Networks will be required in realtime environment, these applications require

faster response from Sensor Networks or even Ad Hoc Network, a delay in seconds for some applications will change the total meaning Of the message and make the message meaningless and maybe the result will be Harmful[2][7].

Attempting to meet real-time demands makes the system pregnable to the DoS attack. In some messages, a delay in millisecond makes the message meaningless; the problem is much bigger, where the application layer is Incredible, since the potential way to recover with incredible transmission is to store partial messages in hopes to be completed in next transmission.

C. Non-repudiation:

It provide the facility for the ability to identify the attackers when ever after the attack happens [7], [11]. This will prevent the cheaters from denying their crimes. Any car related information ‘related to the car’ like: the trip route, speed, time, any violation will be stored in the TPD, any official side holding authorization can protest this data.

D. Privacy :

This keeps the information of the drivers away from unauthorized observers, this information like real identity, trip path, speed etc.

The privacy can retrieve by using temporary anonymous keys, these keys will changed consecutively such as each key could be used just for one time and expires after this single usage [2].

All these keys will be stored in the TPD, and will be refresh again in next time through which the vehicle makes an official checkup [7]. For obtaining the real identity of the driver, an ELP (Electronic License Plate) is used, this license is stored in the factory for every new vehicle, which will provide an identification number for the vehicle, for the identification of the vehicle identify the vehicle in anywhere, with the RFID technology to hold the ELP.

E. Confidentiality:

The privacy of each driver must be protected; the messages should be encrypted to prevent outsiders from gaining the drivers information [2].

VI. CURRENT PROPOSED SOLUTIONS:

In Vehicular ad-hoc Network (VANET) more security solutions been proposed, and large number of papers were had been introduced to solve the above problems, the authors in [2] and in [8] suggested the use of VPKI (Vehicular Public Key Infrastructure) as a solution, In which each node should have a public/private key. When a vehicle sends a safety message, it signs it with their own private key and adds the Certificate authority (CA's) certificate.

The receivers of the message will obtain the public key of V using the certificate and then verify V's signature using their

certified public key. In order to do (happens) this, the receiver should have the public key of the CA [9];

this solution is cited in [7]. The Author suggested the idea of using the group signature, but this idea has a major drawback which is causing a great overhead, in every moment of time which any vehicle can enters the group area, in the group public key and the vehicle session key of each vehicle which belongs to the group must be changed transmitted and changed, another issue should be considered which the mobility of the VANET prevents the network from making a static group, so the group is changed all the time, and the signatures and keys frequently transmitted and changed in group are also mentioned in [12][13], as the authors proposed a protocol for guarantee the requirements of the security and privacy, and to provide the desired liability and traceability, but the result of the study was not quit encouraging, even 9 ms verification delay in group signature, the average message loss ratio was 45%, another result was the loss ratio reaches as high as 68% when the traffic load is 150 vehicles .

The other solution been suggested is the use of CA and this requires suitable infrastructure structure for it. VANET requires a large number of CA to govern it. Either now we don't have a real authority which govern the world of VANET, the CA been suggested by[6],[8],and [18] , all of these researchers mentioned the CA to handle all the operations of certificate : renewing, revoking and generating, the CA must be responsible in initiating keys, storing, managing and broadcasting and managing the CRL.

Authors in [2] also discussed how to maintain the authentication for the message, where vehicles will sign every message with its private key and attach the respective certificate. Thus, when the other vehicle receives this message, it verifies the key which are being used to sign the message and if all process happens correctly, it verifies the message, and they have proposed the use of ECC to reduce the overhead as mentioned.

Using VPKI in VANET accustomed with some challenges, like certificate of an attacker which should be revoked, authors in[2] discussed the solution of Certificate revocation Solution, this revocation solution is used to revoke the expired certificate to make other vehicles aware of their invalidity.

The most common way to revoke certificates is the distribution of CRLs (Certificate Revocation Lists) which contains all revoked certificates, but this method has some drawbacks: First, CRLs can be very long due to the enormous number of vehicles and their(its) high mobility.

Second, the short lifetime of certificates often creates a vulnerable window, and there is no infrastructure for the CRL. It 'is' also mentioned some protocols for revocations like RTPD (Revocation Protocol of the Tamper-Proof Device), RCCRL (Revocation protocol using Compressed Certificate Revocation Lists), and DRP (Distributed Revocation Protocol).

These types of protocols also been discussed in details in [6],

and been proposed in [5], saying that the use of CRL is not appropriate anymore and these protocols are better, but these methods rely on monitoring, so each vehicle should have to monitor and detect all the vehicles around it, but this method will not be considerable in any of the reputation system, as it is a possible for the number of adversary vehicles to make an accusation and causes of an unnecessary revocation, the best result obtained from DRP simulation is which just 25% if the current road vehicles will receive the warning, which is too low. Author in [2] mentioned a solution which will be helpful to maintain the privacy by using a set of anonymous keys which change frequently every couple of minutes according to the driving speed. Every key can be used only one time and expires after its usage; only a single key one key can be used at a time. These keys are reallocated in the vehicle's TPD for a long time duration; every key is certified by the issuing CA and has a short lifetime (e.g., a specific time period of the year). In addition, it can be traced back to the real identity of the vehicle ELP, the drawback of this solution is that the keys need required storage.

VI. Discussion:

Under this section we will provide additional criteria for the current solutions and provide our solutions for the last problems. The normal message format, see figure 6.

| Payload | | |
|------------------------|-------------------|-----------|
| Location | Time | Signature |
| Certificate of Vehicle | Certificate of CA | |

Figure 6.Messege Format

This message should be encrypted by session key find out from the CA. To decrease the overhead on the receiving vehicle for the verification of the signature, we propose an idea for making a list in TPD contains the certificates of vehicles of the last 100 vehicles which made a successful communication, each certificate can be identified by a 16 byte [14] fingerprint the size of one AES block.

The total for the memory consuming is 1600 byte, 10 minutes is the life time for each signature in the list, so when new message arrives, the vehicle will search in the list, if the certificate is there, no need for verifying the vehicle signature and the vehicle certificate will be moved to the top of the list. If the certificate is not in the list the signature will be verified, if it is correct.

The certificate will be added to the top most positioning in the list. The certificate is removed from the list after 10 minutes or when the vehicle desired to add new certificate in the list.

The list has a maximum capacity of 100 certificates, then the certificate in the rear will be removed, searching in the list is faster than verification the signature for each and every communication, and this will provide some satisfaction level

of trust for the vehicles,

If again any vehicle wants to communicate with a vehicle, it delivered the message without the signature, and then every vehicle will be verified it once. In critical situations for sending emergency messages.

we suggest the following message format(see figure 7):



Fig 7. Emergency message format.

The message is delivered without encryption. The cryptography process requires time for obtaining the keys, decryption and encryption process, and this is not suitable in emergency situation as any delay will make the message useless. To ensure the originality of the message we propose the use of special certificates originated by the vehicle and signed previously by CA, Vanet security Certificate Archetecture as follows: see figure 8.

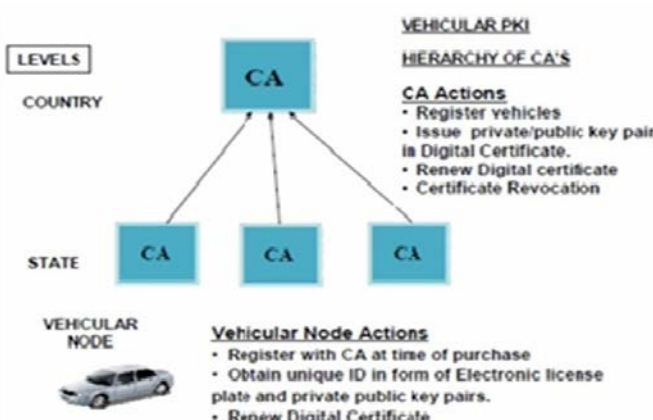


Figure 8. Certificate Issuing Authority

these certificates are on the shelf, and used just in emergency and safety message, these certificates will be ready for use when they are required, these certificates have a short life time period about 1 minute and used for once, so if the certificate is stolen, the adversary can't use it. The generation of these certificates is done by vehicle, and the vehicle signs them by CA any time when the network is available or free The use of these certificates will improve the performance of the communication as resultant the communication will be faster as we eliminated the signature part as the signature requires 5e-4 s/msg for signing, and 7.2e-3 ms/msg for Verification 1, and eliminated the verification of the certificates and eliminated the encryption decryption process.

The importance of the location is to prevent the Sybil attack, and it will tell the receiving vehicle whether the sending

vehicle is on logical place or not, for example: if the vehicle outside the road, or the vehicle can observe accident in front of the receiver while the sender behind of the receiver.

When broadcasting the emergency message, it must be sent with single hop, because in multi hop when the message is not encrypted, the forwarder vehicle can alter the message before send it again. When a vehicle receives this emergency message it verifies the certificate and examine the lifetime of it, it also verifies the location, if the obtained certificate is correct and the location is correct logically, it accept the message, else it report for the nearest CA about this abuse, however.

Using CRL has many drawbacks; to (reduce) decrease these drawbacks we propose the use of Timely geographical CRL list issued by the issuer of CRL, Timely CRL length is for 100 certificate and contains the fresh new revoked certificates of specific area, storing and broadcasting this list to vehicles is easier, as it is smaller and contains the last updating for the revocation,

we assume that the broadcasting in this list takes place in every 1 minute, using DSRC radios signal, any revoked certificate will be added at the topmost position in the list, and if new certificate been revoked the previous last one will be moved a step down in the list.

The list will keep accepting the revoked certificates until it reached the number 100, the maximum capacity for it, at that moment of time this list will be sent to the CA, the CA will take the bottom 50 certificate, and add it to the base CRL which it has, and removes these certificates from the Timely CRL, at which time the Timely CRL will be half full, and can receive new revoked certificates.

The base CRL will not be transmitted frequently as there is no need for revocation information for more than 2 minutes in highways, or 5 minutes for inside the city, as the network has a highly mobility. If a specific vehicle has a certificate revoked and still appears in the Timely CRL this means, vehicle parked on the road side to transmit false information.

VII. CONCLUSIONS AND FUTURE WORK

Vehicular Ad Hoc Networks is an emerging and promising technology, this technology is a fertile region for attackers, who will be trying to challenge the network with their malicious attacks. This paper gave a wide analysis for the current solution and challenges, and critics for these solution, we also proposed a new solutions which will help to maintain a securer VANET network, in the future work we want to expand our idea about certificates of the safety messages, how to be created, discarded, and verified and test it by simulation.

REFERENCES

- [1] http://www.who.int/features/2004/road_safety/en/
- [2] M Raya, P Papadimitratos, JP Hubaux, "Securing Vehicular Communications", IEEE Wireless Communications, Vol.13, October 2006 .

- [3] GMT Abdalla, SM Senouci "Current Trends in Vehicular Ad Hoc Networks", Proceedings of UBIROADS workshop, 2007.
- [4] Car-to-Car Communications, www.car-2-car.org
- [5] H Fussler, S Schnaufer, M Transier , W Effelsberg , "Vehicular Ad-Hoc Networks: From Vision to Reality and Back", Proc. Of IEEE Wireless on Demand Network Systems and Services, 2007.
- [6] M Raya, D Jungels, P Papadimitratos, I Aad, JP Hubaux,"Certificate Revocation in Vehicular Networks "Laboratory for computer Communications and Applications (LCA) School of Computer and Communication Sciences ,EPFL, Switzerland, 2006.
- [7] Al Sakib Khan Pathan: A book: where a chapter is Security in VANET.
- [8] Antonios Stampoulis (antonios.stampoulis@yale.edu), Zheng Chai: A Survey of Security in Vehicular Networks.
- [9] M Raya, J Pierre Hubaux, "The Security of Vehicular Ad Hoc Networks ", Proc. of the 3rd ACM workshop on Security of ad hoc and sensor networks, 2005.
- [10] Security & Privacy for DSRC-based Automotive Collision Reporting.
- [11] Douceur," the Sybil Attack", First International Workshop on Peer-to-Peer Systems, 1st ed USA, Springer, 2003.
- [12] R Lu, X Lin, H Zhu, PH Ho, X Shen, "ECPP: Efficient conditional privacy preservation protocol for secure vehicular", In proceeding The 27th Conference on Computer Communications, INFOCOM 2008.
- [13] X Lin, R Lu, C Zhang, H Zhu, PH Ho, "Security in Vehicular Ad Hoc Networks", IEEE Communications Magazine, April 2008.
- [14] J J Haas, Y C Hu, K P. Laberteaux," Design and analysis of a lightweight certificate revocation mechanism for VANET", Proceedings of the sixth ACM international workshop on Vehicular Internetworking , 2009.

POWER QUALITY IMPROVEMENT USING SHUNT ACTIVE POWER FILTER

A. Dinesh Singh Stu. Member IEEE, B. Dr. K.S Verma, C. Saurabh Singh Kashyap Stu. Member IEEE

Abstract- Most of the pollution issues created in power systems are due to the non-linear characteristics and fast switching of power electronic equipment. Power quality issues are becoming stronger because sensitive equipment will be more sensitive for market competition reasons, equipment will continue polluting the system more and more due to cost increase caused by the built-in compensation and sometimes for the lack of enforced regulations. Efficiency and cost are considered today almost at the same level. Active power filters have been developed over the years to solve these problems to improve power quality. Among which shunt active power filter is used to eliminate load current harmonics and reactive power compensation. In this work both PI controller based three-phase shunt active power filter to compensate harmonics and reactive power by nonlinear load to improve power quality is implemented for three-phase three wire systems. A MATLAB program has been developed to simulate the system operation. Various simulation results are presented under steady state conditions and performance of PI controllers is obtained.

Key Words: Harmonics distortion, Shunt active filters, DC voltage control, mathematical model of the system, simulation result.

1 Introduction

Early equipment was designed to withstand disturbances such as lightning, short circuits, and sudden overloads without extra expenditure. Current power electronics (PE) prices would be much higher if the equipment was designed with the same robustness. Pollution has been introduced into power systems by nonlinear loads such as transformers and saturated coils; however, perturbation rate has never reached the present levels. Due to its nonlinear characteristics and fast switching, PE creates most of the pollution issues. Most of the pollution issues are created due to the nonlinear characteristics and fast

- A. EED, KNIT Sultanpur
- B. Professor , EED, KNIT Sultanpur
- C. EED, KNIT Sultanpur

switching of PE. Active power filters are now seen as a viable alternative over the classical passive filters, to compensate harmonics and reactive power requirement of the non-linear loads. A new scheme has been proposed in [10], in which the required compensating current is determined by sensing load current which is further modified by sensing line currents only [8,12]. Fig1 shows converter topology for active filters.

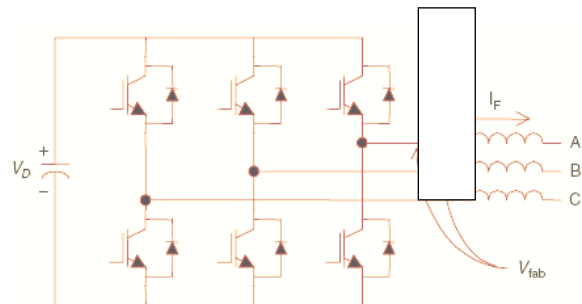


Fig. 1.1 Voltage source converter topology for active filters.

2Shunt Active Power Filter

The shunt-connected active power filter, with a self-controlled dc bus, has a topology similar to that of a static compensator (STATCOM) used for reactive power compensation in power transmission systems. Shunt active power filters compensate load current harmonics by injecting equal-but opposite harmonic compensating current. In this case the shunt active power filter operates as a current source injecting the harmonic components generated by the load but phase-shifted by 180°.

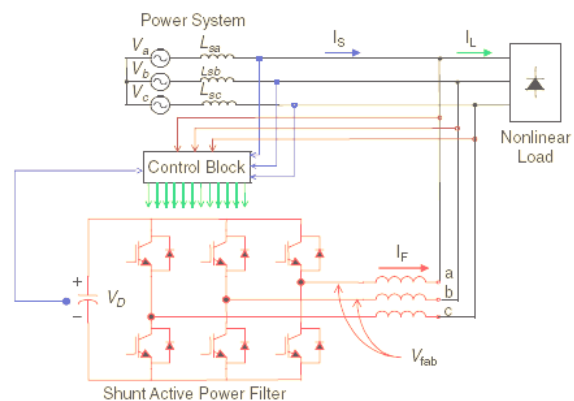


Fig. 2.1 Shunt active power filter topology.

2.1 Basic Compensation Principle

Fig. 2.3 Shows the basic compensation principle of a shunt active power filter. It is controlled to supply a compensating current i_c from / to the utility so that it cancels current harmonics on the AC side and makes the source current in phase with the source voltage.

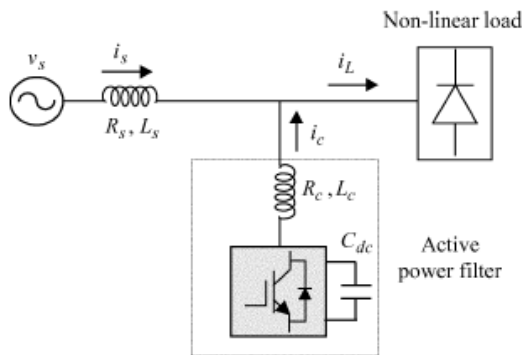


Fig. 2.2 Shunt active power filters Basic compensation principle.

2.2 PI Control Scheme

The control scheme realization, the actual capacitor voltage is compared with a set reference value.

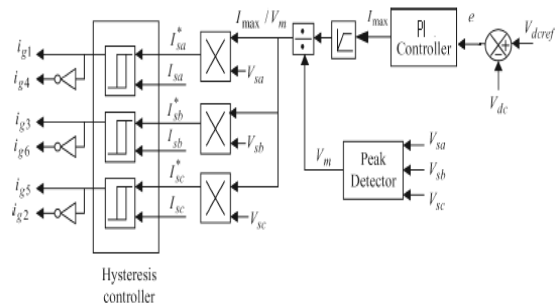


Fig. 2.3 APF Control scheme with PI controller.

The error signal is fed to PI controller. The output of PI controller has been considered as peak value of the reference current. It is further multiplied by the unit sine vectors (u_{sa} , u_{sb} , and u_{sc}) in phase with the source voltages to obtain the reference currents (i_{sa}^* , i_{sb}^* , and i_{sc}^*).

These reference currents and actual currents are given to a hysteresis based, carrierless PWM current controller to generate switching signals of the PWM converter [2]. The difference of reference current template and actual current decides the operation of switches. To increase current of

particular phase, the lower switch of the PWM converter of that particular phase is switched on, while to decrease the current the upper switch of the particular phase is switched on. These switching signals after proper isolation and amplification are given to the switching devices. Due to these switching actions current flows through the filter inductor L_c , to compensate the harmonic current and reactive power of the load, so that only active power drawn from the source.

2.3 DC Voltage Control Loop

The block diagram of the voltage control loop is shown in fig.2.4 Where, $G_c(s)$ is the gain of the PI controller and $K_c(s)$ is the transfer function of the PWM converter.

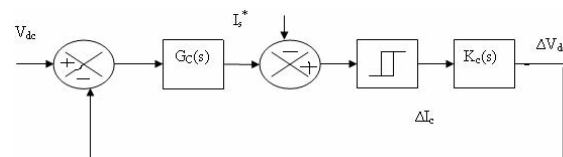


Fig. 2.4 Block diagram of voltage control loop.

Equating the average rate of change of energy quantities of input and output side of the PWM converter.

$$P_{cap} = P_{conv} - P_{ind} \quad 2.3.1$$

In order to linearize the power equation a small perturbation ΔI_c is applied in the input filter current of converter I_c , about a steady state operating point I_c^{co} , the average dc link voltage will also get perturbed by a small amount ΔV_{dc} , about its steady state operating point $V_{dc0}(V_{dcref})$. The transfer function of the PWM converter for a particular operating point can be obtained from above equation as

$$K_c = \frac{V_{dc}}{I_c} = 3 \frac{[V_s - L_c I_{co} - 2 I_{co} R_c]}{C_{dc} V_{dc0} S} \quad 2.3.2$$

3.Selection of PI Controller Parameters

A proportional-integral-derivative controller (PID controller) is control loop feedback mechanism used in industrial control systems. In an industrial process a PID controller attempts to correct the error between

a measured process variable and a desired set point by calculating and then outputting a corrective action that can adjust the process accordingly, the integral mode determines the reaction based on recent errors and the derivative mode determines the reaction based on the rate by which the error has been changing. By adjusting constants in the PID controller algorithm the PID can provide individualized control specific to process requirements including error responsiveness, overshoot of set point and system oscillation.

Proportional mode responds to a change in the process variable proportional to the current measured error value. The proportional response can be adjusted by multiplying the error by a constant K_p , called the proportional gain or proportional sensitivity.

With integral mode, the controller output is proportional to the amount and duration of the error signal. The integral mode algorithm calculates the accumulated proportional offset over time that should have been corrected previously (finding the offset's integral). While this will force the controller to approach the set point quicker than a proportional controller alone and eliminate steady state error, it also contributes to system instability as the controller will always be responding to past values. This instability causes the process to overshoot the set point since the integral value will continue to be added to the output value, even after the process variable has reached the desired set point. The characteristic equation of the voltage control loop is used to obtain the constants of PI controller in this case, can be written as [2]:

$$1 + \left(K_p + \frac{K_i}{S} \right) 3 \left(\frac{V_s - L_c I_{co} S - 2 I_{co} R_c}{C_{dc} V_{dco} S} \right) = 0$$

Thus a second order transfer function can be found for the closed loop system. This characteristic equation is used to find the components of PI controller. The analysis of these characteristic equation shows that K_i determines the voltage response and K_i defines the damping factor of the voltage loop. The current controller has been designed on the basis of 5% overshoot, to step the change in the amplitude of current reference.

4 Modeling Of the System

4.1 Modeling of Pwm Converter

The PWM converter has been modeled as having a three phase AC voltage applied through a filter impedance (R_c, L_c) on its input, and DC bus capacitor on its output. The three phase voltages v_{fa} , v_{fb} , and v_{fc} reflected on the input side can be expressed in terms of the DC bus capacitor voltage V_{dc} and switching functions stating the on/off status of the devices of each leg S_a , S_b and S_c as

$$V_{fc} = \left(\frac{V_{dc}}{3} \right) (2S_a - S_b - S_c) \quad 4.1$$

$$V_{fb} = \left(\frac{V_{dc}}{3} \right) (-S_a + 2S_b - S_c) \quad 4.2$$

$$V_{fa} = \left(\frac{V_{dc}}{3} \right) (-S_a - S_b + 2S_c) \quad 4.3$$

The three phase currents i_{fa} , i_{fb} , and i_{fc} flowing through impedances (R_c, L_c) are obtained by solving the following differential equations

$$P_{ifa} = \frac{1}{LC} (R_c i_{fa} + V_{sa} - V_{fa}) \quad 4.4$$

$$P_{ifb} = \frac{1}{LC} (R_c i_{fb} - V_{sb} - V_{fb}) \quad 4.5$$

$$P_{ifc} = \frac{1}{LC} (R_c i_{fc} + V_{sc} - V_{fc}) \quad 4.6$$

The DC capacitor current can be obtained in terms of phase currents i_{fa} , i_{fb} , and i_{fc} and the switching status (1 for on and 0 for off) of the devices S_a , S_b and S_c

$$3.1 \quad i_{fc} = i_{fa} S_a + i_{fb} S_b + i_{fc} S_c \quad 4.7$$

From this, the model equation of the DC side capacitor voltage can be written as

$$PV_{fc} = \frac{1}{C_{dc}} (i_{fa} S_a + i_{fb} S_b + i_{fc} S_c) \quad 4.8$$

5. Hysteresis Current Controller

The current controller decides the switching patterns of the devices in the APF. The switching logic is formulated as

*

if $i_{sa} < (i_{sa} - hb)$ upper switch is OFF and lower switch is ON in leg "a" of the APF; if $i_{sa} > (i_{sa} - hb)$ upper switch is ON and lower switch is OFF in leg "a" of the APF. Similarly, the switches in the legs "b" and "c" are activated. Here, hb is the width of the hysteresis band around which the reference currents.

In this fashion, the supply currents are regulated within the hysteresis band of their respective reference values.

The performance of active filter is analyzed by solving set of differential equations (4.1) to(4.8), with other expressions by a fourth order Rungakutta method.

6. Simulation Results

A program is developed to simulate the PI controller based shunt active power filter in MATLAB. The complete active power filter system is composed mainly of three-phase source, a nonlinear load, a voltage source PWM converter. All these components are modeled separately, integrated and then solved to simulate the system.

Figures 6.1 - 6.5 show the simulations results of the proposed shunt active power filter controlled by a conventional PI controller with MATLAB program. The parameters selected for simulation studies are given in table 6.1. The three phase source voltages are assumed to be balanced and sinusoidal. The source voltage waveform of the reference phase only (phase-a, in this case) is shown in fig.6.1.

A load with highly nonlinear characteristics is considered for the load compensation. The THD in the load current is 28.05%. The phase-a load current is shown in figure 6.2. The source current is equal to the load current when the compensator is not connected.

| System Parameters | Values |
|---|---------------------|
| Source voltage(V_s) | 100V(peak) |
| System frequency(f) | 50Hz |
| Source impedance(R_s, L_s) | $0.1\Omega, 0.15mH$ |
| Filter impedance(R_c, L_c) | $0.4\Omega, 3.35mH$ |
| Load impedance(R_l, L_l) | $6.7\Omega, 20mH$ |
| DC link capacitance | $2000\mu F$ |
| Reference DClink voltage(V_{dcref}) | 220V |

Table 6.1 System parameters for simulation study.

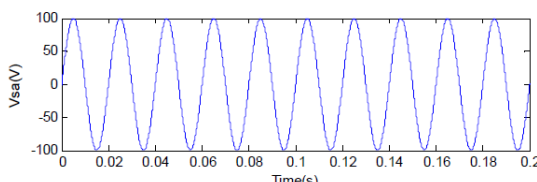


Fig. 6.1 Source voltage.

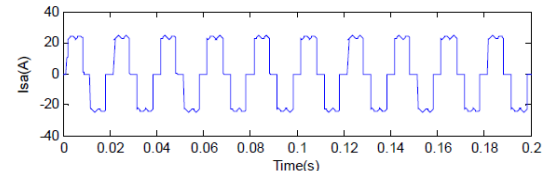


Fig. 6.2 Source current when the compensator is not connected.

The compensator is switched ON at $t=0.05s$ and the integral time square error (ITSE) performance index is used for optimizing the and coefficients of the PI controller. The optimum values (K_p and K_i) are found to be 0.2 and 9.32 respectively, which corresponds to the minimum value of ITSE.

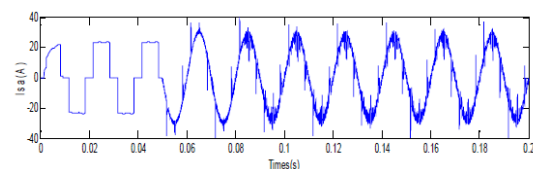


Fig. 6.3 Source current PI controller.

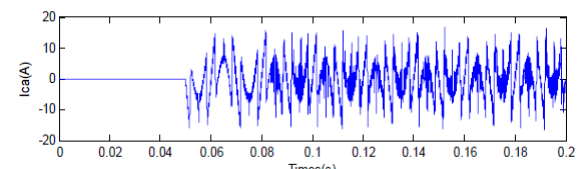


Fig. 6.4 Compensating current of PI controller.

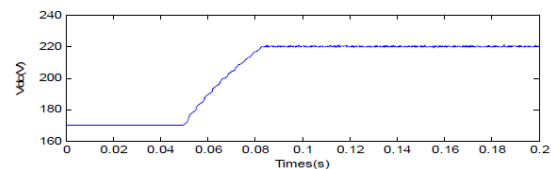


Fig. 6.5 DC Capacitor voltage during switch-on response with PI controller.

From the wave forms it is clear that harmonic distortion is reduced after connecting compensator. PI controller gives better harmonic compensation.

The system studied has also been modeled using Simulink and performance of PI controllers is analyzed,Which Is shown below. From the responses it is depicted that the settling time required by the PI controller is approximately 8 cycles. The source current THD is reduced form 27.88% to 2% in case of PI controller.

REFERENCES

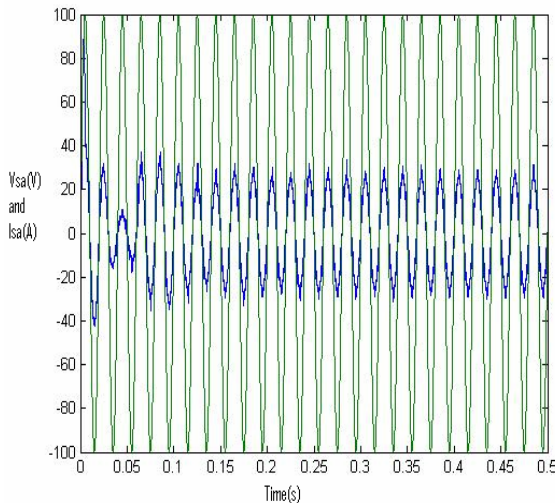


Fig. 6.5 Voltage and current in phase with PI controller after compensation.

7 Conclusions

A shunt active power filter has been investigated for power quality improvement. Various simulations are carried out to analyze the performance of the system. PI controller based Shunt active power filter are implemented for harmonic and reactive power compensation of the non-linear load. A program has been developed to simulate the PI controller based shunt active power filter in MATLAB. It is found from simulation results that shunt active power filter improves power quality of the power system by eliminating harmonics and reactive current of the load current, which makes the load current sinusoidal and in phase with the source voltage. The performance of the controllers has been studied. A model has been developed in MATLAB SIMULINK and simulated to verify the results. The PI controller in steady state except that settling time is very less in case of using of shunt active filter. The THD of the source current is below 5%, the harmonics limit imposed by IEEE standard.

- [1]. W. M. Grady, M. J. Samotyj, and A. H. Noyola, "Survey of active power line conditioning methodologies," *IEEE Transactions on Power Delivery*, vol. 5, no. 3, Jul. 1990, pp. 1536–1542.
- [2]. H. Akagi, Y. Kanazawa, and A. Nabae, "Instantaneous reactive power compensators comprising switching devices without energy storage components," *IEEE Transactions on Industry Applications*, vol. IA-20, no. 3, May/Jun. 1984, pp. 625–630.
- [3]. S. Jain, P. Agarwal, and H. O. Gupta, "Design simulation and experimental investigations on a shunt active power filter for harmonics and reactive power compensation," *Electrical Power Components and Systems*, vol. 32, no. 7, Jul. 2003, pp. 671–692.
- [4]. F. Z. Peng, H. Akagi, and A. Nabae, "Study of active power filters using quad series voltage source PWM converters for harmonic compensation," *IEEE Transactions on Power Electronics*, vol. 5, no. 1, Jan. 1990, pp. 9–15.
- [5]. H. Akagi, "Trends in active power line conditioners," *IEEE Transactions on power Electronics*, vol 9, no 3, 1994, pp 263-268.
- [6]. S. K. Jain, P. Agrawal, and H. O. Gupta, "Fuzzy logic controlled shunt active power filter for power quality improvement," *Proceedings of Institute of Electrical Engineers, Electrical Power Applications*, vol. 149, no. 5, 2002.
- [7]. L.A.Morgan, J.W.Dixon&R.R.Wallace, "A three phase active power filter operating with fixed switching frequency for reactive power and current harmonics compensation," *IEEE Transactions on Industrial Electronics*, vol.42, no.4, August 1995, pp 402-408.
- [8]. B. Singh, A. Chandra, and K. Al-Haddad, "Computer-aided modeling and simulation of active power filters," *Electrical Machines and Power Systems*, vol. 27, 1999, pp. 1227–1241.
- [9]. B. Singh, A. Chandra, and K. Al-Haddad, "A review of active filters for power quality improvement," *IEEE Transactions on Industrial Electronics*, vol.46, no 5, Oct 1999, pp1-12.
- [10]. R. M. Duke and S. D. Round, "The steady state performance of a controlled current active filter," *IEEE Transactions on Power Electronics*, vol. 8, Apr. 1993, pp. 140–146.
- [11]. Mohan, N., Undeland,T.M, and Robbins.,W.P, "Power electronics :converters, applications and design," Singapore,John Wiley and sons, 2003.
- [12]. K. Chatterjee, B. G. Fernandes, and G. K. Dubey, "An instantaneous reactive volt-ampere compensator and harmonic suppressor system," *IEEE Transactions on Power Electronics*, vol. 14, no. 2, Mar. 1999, pp. 381–392.

Improvement of PQ in Electrical Distribution System Using Custom Power Devices: A Survey

A. Sunil Kumar Singh, B. Bindeshwar Singh

Abstract: - *Voltage disturbances are the most common problem due to the increased use of a large numbers of sophisticated electronic equipment in industrial distribution system. The voltage disturbances such as voltage sags, swells, harmonics, unbalance and flickers. High quality in the power supply is needed, since failures due to such disturbances usually have a high Impact on production cost. Now a day's Power quality is main concern for both power companies and customers. This paper discusses the power qualities, various parameters reliability and problem associated with power quality, their effects and solutions. Power Quality in electric networks is one of today's most concerned areas of electric power system. The power quality has serious economic implications for consumers, utilities and electrical equipment manufacturers. The impact of power quality problems is increasingly felt by customers - industrial, commercial and even residential. Some of the main power quality problems are sag, swell, transients, harmonic, and flickers etc. By custom power devices, we refer to power electronic static controllers used for power quality improvement on distribution systems.*

Keywords: Power Quality, Energy Storage System (ESS), D-STATCOM, Voltage Flicker, FACTS, custom power devices, Synchronous Reference Frame (SRF).

Nomenclatures

| | |
|----------|--|
| DSTATCOM | Distribution Static Compensator |
| SRF | Synchronous Reference Frame |
| EAF | Electrical Arc Furnace |
| BESS | Battery Energy Storage System |
| PQ | Power Quality |
| DVR | Dynamic Voltage Restorer |
| FACTS | Flexible AC Transmission Systems |
| UPFC | Unified Power Flow Controller |
| PSCC | Periodical Sampling Current Controller |
| TCC | Triangular carrier Current Controller |
| PFC | Power Factor Correction |
| ASD | Adjustable Speed Drive |
| CPD | Custom Power Devices |
| TPCC | Triangular Periodical Current Controller |

1. INTRODUCTION

One of the most power quality problems today is voltage dip. A voltage dip is a short time (10ms to 1 minute) event during which a reduction in rms voltage magnitude occurs.

¹

A. PG Scholar EED KNIT Sultanpur
B. Ass. Prof. EED KNIT Sultanpur

It is often set usually only by two parameters, Depth/magnitude and duration. The voltage dip magnitude ranges from 10% to 90% of the nominal voltage (Which corresponds to 90% to 10% of remaining voltage) and with a duration of half a cycle to 1 minute. In a three phase system, voltage dip by nature is a three – phase phenomenon, which affects both the phase-to-ground and phase-to-phase voltages. A voltage dip is caused by a fault in the utility system, a fault within the customer's facility or a large increase of load current, like a starting a motor or transformer energizing. Faults due to lightning, is one of the most common causes to voltage dips on overhead lines.

Utility and customer-side disturbances result in terminal voltage fluctuations, transients, and waveform distortions on the electric grid. Power electronic controllers for distribution systems, namely custom power devices, are able to enhance the reliability and quality of power that is delivered to customers [151]. A distribution static compensator or D-STATCOM is a fast response, solid-state power controller that provides flexible voltage control at the point of connection to the utility distribution feeder for power quality (PQ) improvements. It can exchange both active and reactive power with the distribution system by varying the amplitude and phase angle of the converter voltage with respect to the line terminal voltage, if an energy storage system (ESS) is included into the dc bus. The result is a controlled current flow through the tie reactance between the D-STATCOM and the distribution network. This enables the D-STATCOM to mitigate voltage fluctuations and to correct the power factor of weak distribution systems in instantaneous real-time [152]. In general, the D-STATCOM can be utilized for providing voltage regulation, power factor correction, harmonics compensation and load leveling [153].

During the transient conditions the D-STATCOM provides leading or lagging reactive power to active system stability, power factor correction and load balancing and /or harmonic compensation of a particular load [153,154].The D-STATCOM has emerged as a promising device to provide not only for voltage sags mitigation but a host of other power quality solutions such as voltage stabilization, flicker suppression, power factor correction and harmonic control [155]. The D-STATCOM has additional capability to sustain reactive current at low voltage, reduce land use and can be developed as a voltage and frequency support by replacing capacitors with batteries as energy storage [156]. The proposed multi-level control scheme for the integrated D-STATCOM/BESS device is based on concepts of instantaneous power on the synchronous-rotating dq reference frame [157]. This paper presents a model for (D-STATCOM) for voltage flicker mitigation. The most commonly used methods for compensation of voltage flicker is by regulating the Electric

Arc Furnace (EAF) passive components [158-160], static VAR compensator (SVC) and D-STATCOM.

II. DEFINITION OF POWER QUALITY

Power quality is defined as the concept of powering and grounding sensitive equipment in a manner that is suitable to the operation of that equipment. It is a measure of how well electric power can be utilized by customers. Some of the main reasons for the enormous increases in the interest in power quality are:

- Equipment has become more sensitive to voltage disturbances.
- The no of loads fed via power electronic converters has recently increased .These present a challenge in ensuring power quality.
- There is a growing need for standardization and performance criteria.
- The power quality can be measured. Harmonic currents and voltage dips are no longer difficult to measure.

A. Power Quality and Reliability

Power quality and reliability cost the industry large amounts due to mainly sags and short-term interruptions. Distorted and unwanted voltage wave forms, too. And the main concern for the consumers of electricity was the reliability of supply. Here we define the reliability as the continuity of supply. As shown in Fig.1, the problem of distribution lines is divided into two major categories. First group is power quality, second is power reliability. First group consists of harmonic distortions, impulses and swells. Second group consists of voltage sags and outages. Voltage sags is much more serious and can cause a large amount of damage. If exceeds a few cycle, motors, robots, servo drives and machine tools cannot maintain control of process.

Both the reliability and quality of supply are equally important. For example, a consumer that is connected to the same bus that supplies a large motor load may have to face a severe dip in his supply voltage every time the motor load is switched on. In some extreme cases even we have to bear the black outs which is not acceptable to the consumers.

There are also sensitive loads such as hospitals (life support, operation theatre, and patient database system), processing plants, air traffic control, financial institutions and numerous other data processing and service providers that require clean and uninterrupted power. In processing plants, a batch of product can be ruined by voltage dip of very short duration. Such customers are very wary of such dips since each dip can cost them a substantial amount.

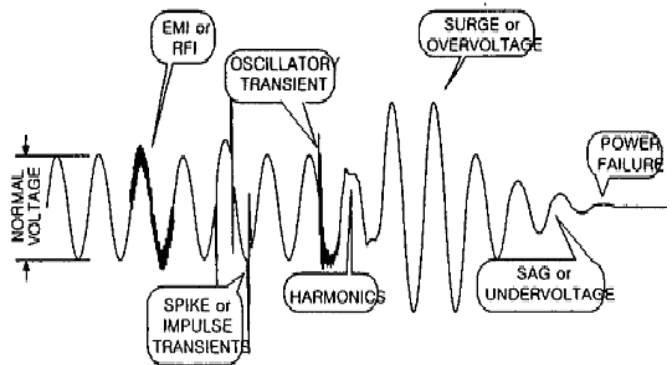


Fig. 1 Power Quality and Reliability

of money. Even short dips are sufficient to cause contactors on motor drives to drop out. Stoppage in a portion of process can destroy the conditions for quality control of product and require restarting of production. Thus in this scenario in which consumers increasingly demand the quality power, the term power quality (PQ) attains increased significance transmission lines are exposed to the forces of nature. Furthermore, each transmission line has its load ability limit that is often determined by either stability constraints or by thermal limits or by the dielectric limits. Even though the power quality problem is distribution side .Problem, transmission lines are often having an impact on the quality of the power supplied. It is however to be noted that while most problems associated with the transmission systems arise due to the forces of nature or due to the interconnection of power systems, individual customers are responsible for more substantial fraction of the problems of power distribution systems.

B. Power Quality- A Big Issue

Power quality in electric networks is one of today's the most concern area of electric power system. The power quality has serious economic implications for consumers, utilities and electrical equipment manufacturers. Modernization and automation of industry involves increasing use of computers, microprocessors and power electronics system such as adjustable speed drives. Integration of non -conventional technique such as fuel cells, wind turbine and photo voltaic with utility grids often requires power electronic interfaces. The power electronic systems also contribute power electronic problems (generating harmonics). Under the deregulated environment, in which electric utilities are expected to compete with each other, the customer satisfaction becomes very important. The impact of power quality problems is increasingly felt by customers.

1. Problem Associated with Power quality

Power quality problems encompass a wide range of disturbances that can disrupt the operation of sensitive industrial loads and causes a loss of production.

- Voltage dip
- Voltage swells/ over voltage.

- Voltage flicker
- Voltage and current harmonic distortion
- Voltage and current transients
- Shorts interruptions
- Power frequency variation

The power quality parameters are the items required for surveying or analyzing power trouble. By measuring the power quality parameters, you can gain a thorough understanding of the power quality status. Threshold values are set on the power quality analyzer to detect the “fault value” or “fault waveform” for the power quality parameters.

a. Frequency fluctuation

This occurs due to a change of effective power balance between supply and consumption, or an excessive increase or decrease of the load. Varying rotation speeds of synchronous generators, the most common type of generator used in utility power systems, may be the cause of frequency fluctuations. The waveform of frequency fluctuation is shown in fig. 2.

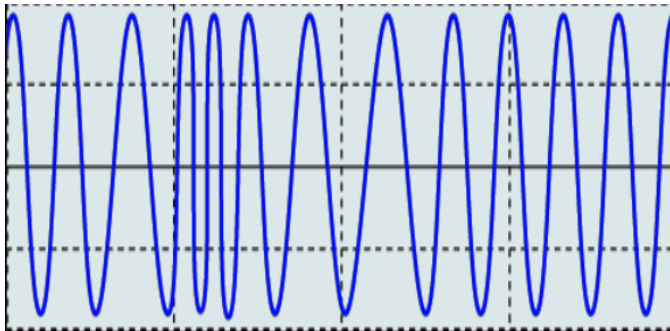


Fig. 2 Waveform of Frequency Fluctuation.

b. Voltage Swell (Surge)

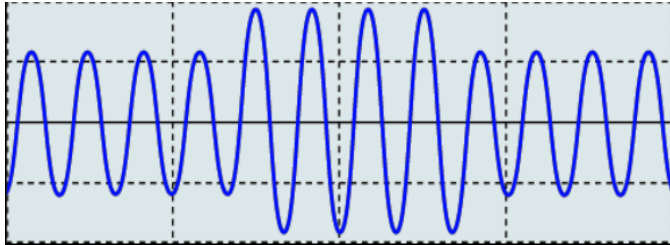


Fig. 3 Waveform of Voltage Swell.

This is the instantaneous voltage increase caused by lightning strikes, opening or closing of a power supply circuit, high capacitor bank switching, ground short circuit, or cutting a heavy load, etc. It may also occur due to the grid connection of a new energy source (solar power, etc.). A sudden increase in voltage may damage or reset the power supply of equipment. A voltage swell is defined as a rise in rms voltage which is between 1.1 and 1.8 p.u. for time duration between 0.5 cycles to 1 minute. A voltage swells is characterized by its magnitude (rms) and duration. The waveform of voltage Swell is shown in fig. 3.

c. Transient overvoltages (Impulse)

This is the voltage change generated by a lightning strike, contact problem and closing of a circuit breaker/relay. It is often a rapid change and consists of high peak voltage. Over-voltage conditions can create high current draw and cause unnecessary tripping of downstream circuit breakers, as well as overheating and putting stress on equipment. Hence, this may cause failure to the power electronics device, which is a common device in household appliances [147]. Damage to equipment's power supply or reset function often occurs near the generation point due to its high voltage. The waveform of transient overvoltage is shown in fig. 4.

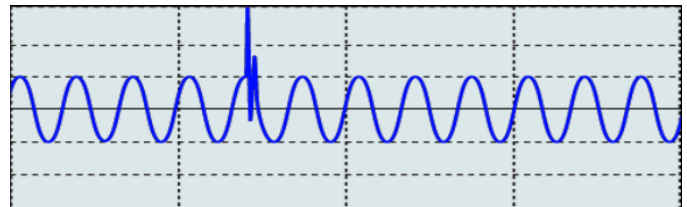


Fig. 4 Waveform of Transient Overvoltage.

d. Voltage Flicker

Flicker is a periodically repeated voltage fluctuation caused by a furnace, arc welding or thyristor controlled load which lies in the range of 0.9 to 1.1 p.u. It may cause lights to flicker and equipment to malfunction. When the flicker value is high, most people feel uncomfortable because of the flickering lights. The voltage flicker can also affect stable operation of electrical and electronic devices such as motor and CRT devices. The typical frequency spectrum of voltage flicker lies in the range from 1 Hz to 30 Hz. The waveform of transient overvoltage is shown in fig..5.

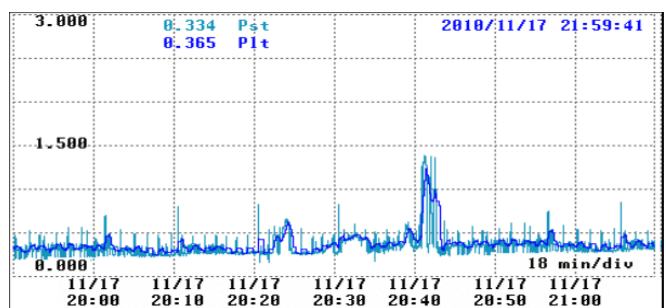


Fig. 5 Waveform of Voltage Flicker.

e. Voltage dip (Sag)

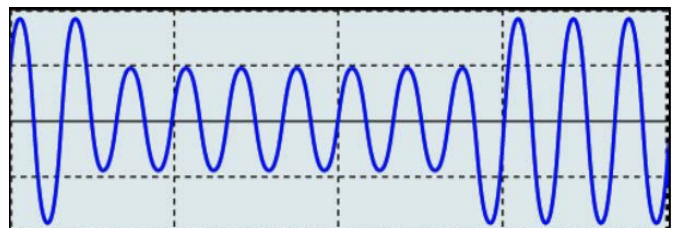


Fig.6 Waveform of Voltage Dip or Voltage Sag.

Voltage sag is defined as the reduction of rms voltage to a value between 0.1 and 0.9 p.u. and lasting for the duration between 0.5 cycles to 1 minute. Voltage sags are mostly caused by system fault and other causes are due to natural phenomenon like thunder and lightning. It is represented by an instantaneous voltage drop caused by the cutting off of the power supply circuit due to a short circuit to the ground or high inrush current generation when starting a large motor(as motor draws a current upto 10 times the full load current during the starting). Also power factor of starting current is generally poor. The waveform of Voltage Sag is shown in fig. 6.

f. Interruptions

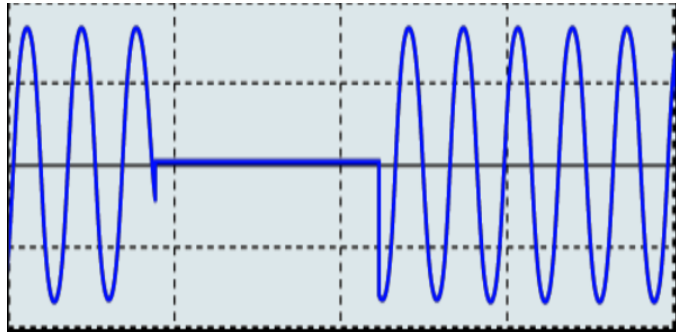


Fig.7 Waveform of Interruption.

If supply voltage or load current decreases to less than 0.1 p.u. for a period of times not more than 1 minute is known as interruption . Some interruption may also be caused by voltage sag conditions when there are faults on the source side.

This is a power outage (a period of general power failure) over an instantaneous, short or long period. It is caused either by accidents such as lightning strikes or tripping of the circuit breaker because of a short-circuit or by the system fault, equipment failure or control malfunction. Some equipments are now a day are used to protect against interruption such as UPS are widely used to protect PCs, but this type of equipment may also cause a stop or reset of equipment. The waveform of Interruption is shown in fig.7.

g. Harmonics

A phenomenon caused by distortions in the voltage and current waveforms that affect many devices with power supplies using semiconductor control devices. When the harmonic component is big, it may cause serious accidents such as overheating or noise in motors or transformers, burn out reactors in phase compensation capacitors, etc. The waveform of harmonics. is shown in fig.8.

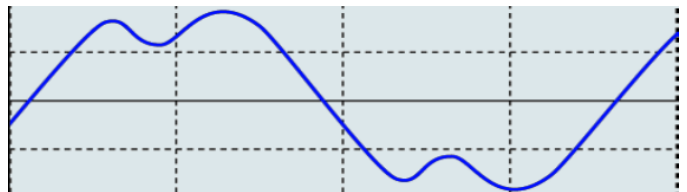


Fig. 8 Waveform of Harmonics.

h. High-order harmonic component

This is a noise component higher than several kHz generated by the semi-conductor control device in the power supply of equipment, and may contain various frequency components. High-order harmonic components may damage the power supply of equipment, reset equipment or introduce abnormal noise in equipment such as TVs or radios. By measuring the high-order harmonic component, it is possible to monitor harmonic noise at the 50th and higher order emitted by switching power supplies, inverters, LED lighting, and other devices. Recently, increases in the switching frequencies used by switching power supplies and Inverters have resulted in the problematic introduction of noise in excess of 10 kHz into power Supply lines. The waveform of High- order harmonic component is shown in fig.9.

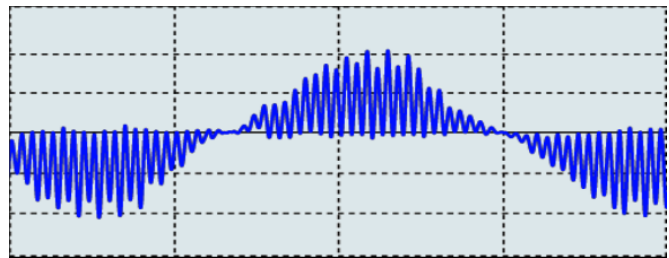


Fig.9 Waveform of High- order harmonic component.

i. Inter-harmonics

This is an instantaneous high current flowing at the time equipment is powered on. Inrush current(An inrush current can be equal to or greater than 10 times the current that flows when the device is in the normal operating state) may cause relays to malfunction, circuit breakers to open, impact on the rectifier, unstable power supply voltage, and/or equipment to malfunction or reset. The waveform of Waveform of Inter-harmonics is shown in fig.10.

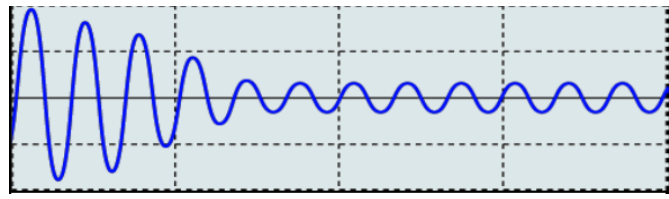


Fig. 10 Waveform of Inter- harmonics.

2. Effects of Poor Power Quality on Power System Devices

Poor electric power quality has many harmful effects on power system devices and end users. What makes these phenomena so important is that its effects are often not known until failure

occurs. Therefore insight into how disturbances are generated and interact into how they affect components is important for preventing failures. Even if failure does not occur, poor power quality and harmonics increase losses and decrease the lifetime of power components and end-use device. Some of the main detrimental effects of poor power quality include the following

- Heating, noise and reduced life on capacitors, surge suppressors, rotating machines, cables, transformers, fuses and customer's equipment.
 - Utility companies are particularly concerned that distributed transformer may need to derate to avoid premature failure due to overheating.
 - Additional losses of transmission lines, cables, generators, ac motors and transformers may occur due to harmonics.
 - Failure of power system components and costumer's load may occur due to unpredicted disturbances such as voltage and/or current magnifications due to parallel resonance and ferroresonance.
1. Malfunction of controllers and protective devices such as fuse and relays is possible.
 2. Inter harmonics may occur which can perturb ripple control signals and can cause flickers at sub-harmonic levels.
 3. Harmonic instability may be caused by large and unpredicted harmonic sources such as arc furnace.

C. Solutions to Power Quality Problems

There are two approaches to the mitigation of power quality problems. The solution to the power quality can be done from customer side or from utility side. First approach is called load conditioning, which ensures that the equipment is less sensitive to power disturbances, allowing the operation even under significant voltage distortion. The other solution is to install line conditioning systems that suppress or counteracts the power system disturbances. A flexible and versatile solution to voltage quality problems is offered by active power filters. Currently they are based on PWM converters and connect to low and medium voltage distribution system in shunt or in series. Series active power filters must operate in conjunction with shunt passive filters in order to compensate load current harmonics. Shunt active power filters operate as a controllable current source and series active power filters operates as a controllable voltage source. Both schemes are implemented preferable with Voltage source PWM inverters, with a dc bus having a reactive element such as a capacitor. Active power filters can perform one or more of the functions required to compensate power systems and improving power quality.

Their performance also depends on the power rating and the speed of response. However, with the restructuring of power sector and with shifting trend towards distributed and dispersed generation, the line conditioning systems or utility side solutions will play a major role in improving the inherent

supply quality; some of the effective and economic measures can be identified as following.

1. Lightening and Surge Arresters

Arresters are designed for lightening protection of transformers, but are not sufficiently voltage limiting for protecting sensitive electronic control circuits from voltage surges.

2. Thyristor Based Static Switches

The static switch is a versatile device for switching a new element into the circuit when the voltage support is needed. It has a dynamic response time of about one cycle. To correct quickly for voltage spikes, sags or interruptions, the static switch can be used to switch one or more of devices such as capacitor, filter, alternate power line, energy storage systems etc. The static switch can be used in the alternate power line applications. This scheme requires two independent power lines from the utility or could be from utility and localized power generation like those in case of distributed generating systems. Such a Scheme can protect up to about 85 % of interruptions and Voltage sags.

3. Energy Storage Systems

Storage systems can be used to protect sensitive production equipments from shutdowns caused by voltage sags or momentary interruptions. These are usually DC storage systems such as UPS, batteries, superconducting magnet energy storage (SMES), storage capacitors or even fly wheels driving DC generators. The output of these devices can be supplied to the system through an inverter on a momentary basis by a fast acting electronic switch. Enough energy is fed to the system to compensate for the energy that would be lost by the voltage sag or interruption. In case of utility supply backed by a Localized generation this can be even better accomplished.

4. Electronic Tap changing Transformer

A voltage-regulating transformer with an electronic load tap changer can be used with a single line from the utility. It can regulate the voltage drops up to 50% and requires a stiff system (short circuit power to load ratio of 10:1 or Better). It can have the provision of coarse or smooth steps intended for occasional voltage variations.

5 Harmonic filters

Filters are used in some instances to effectively reduce or eliminate certain harmonics. If possible, it is always preferable to use a 12-pluse or higher transformer connection, rather than a filter. Tuned harmonic filters should be used with caution and avoided when possible. Usually, multiple filters are needed, each tuned to a separate harmonic. Each filter causes a parallel resonance as well as a series resonance, and each filter slightly changes the resonances of other filters.

6 Constant Voltage transformers

For many power quality studies, it is possible to greatly improve the sag and momentary interruption tolerance of a facility by protecting control circuits. Constant voltage transformer (CVTs) can be used on control circuits to provide constant voltage with three cycle ride through, or relays and ac contactors can be provided with electronic coil hold-in devices to prevent Mis-operation from either low or interrupted voltage.

7. Digital-Electronic and Intelligent Controllers for Load-Frequency Control

Frequency of the supply power is one of the major determinants of power quality, which affects the equipment performance very drastically. Even the major system components such as Turbine life and interconnected-grid control are directly affected by power frequency. Load frequency controller used specifically for governing power frequency under varying loads must be fast enough to make adjustments against any deviation. In countries like India and other countries of developing world, still use the controllers which are based either or mechanical or electrical devices with inherent dead time and delays and at times also suffer from ageing and associated effects. In future perspective, such controllers can be replaced by their Digital -electronic counterparts.

There are so many different methods to mitigate voltage sags/swells, but the use of the custom power devices is considered as a most efficient method. FACTS for transmission systems, the term custom power pertains to the use of power electronics controllers in a distribution system, particularly to deal with a Variety of power quality problems. Just as FACTS improves the power transfer capabilities and stability limits, Custom power make sure customers get pre-specified quality and reliability of supply.

D. Power Quality Standards

Various standards are set to limit the harmonics generated by nonlinear loads. IEEE standard 519 was first issued in 1991. It gave the first guidelines for system harmonics limitations and revised in 1991. It gave the first guidelines for system harmonics limitations and revised in 1992. The 5% voltage distortion limit was recommended below 69 kV, while the limit on current distortion is fixed in the range of 2.5% to 20% depending upon the size of the customer and system voltage. IEEE 519 standard limits harmonics primarily at the service entrance, while IEC 1000-3-2 is applied at the terminals of end-user equipment.

Table 1: Power Quality Standards

| Performance | Standards |
|-------------------------------------|---|
| Classification of power quality | IEC 61000-2-5:1995; IEC 61000-2-1:1990; IEEE 1159:1995 |
| Transients | IEC 61000-2-1:1990; IEEE c62.41:1991; IEEE 1159:1995; IEC 816:1984 |
| Voltage sag/swell and interruptions | IEC 61009-2-1:1990; IEEE 1159:1995 |
| Harmonics | IEC 61000-2-1:1990; IEEE 519:1992; IEC 61000-4-7:1991 |
| Voltage flicker | IEC 61000-4-15:1997 |

III. FUNDAMENTALS OF CUSTOM POWER

Initially for improvement of power quality or reliability of system FACTS devices are used. These devices are such as (STATCOM), (SSSC) and (IPFC) etc. N. G. Hingorani was first to propose FACTS controller to improving power quality. For the improvement of power quality, these devices are modified and He termed them as custom power devices (CPD) (known as custom power devices).The main custom power devices which are used in power distribution system for power quality improvement are (DSTATCOM), (DVR), active filter (AF) and (UPFC) etc. By custom power devices, power electronic static controllers used for power quality development on distribution system. If the Power quality level is not achieved, it can cause costly downtimes and costumer dissatisfaction.

A. Need of Custom Power Devices

The electrical distribution network failures account for about 90% of the average customer interruptions. As the customer's demand for the reliability of power supply is increased day by day. So the reliability of the distribution system has to be increased. However, in the distribution systems have numerous non-linear loads. The purity of the waveform of supplies is lost and producing power quality problems. The sensitivity of today's sophisticated electronics devices makes them more disposed to the quality of power supply due to power disturbances. For some sensitive devices, a temporary disturbance can cause scrambled data, interrupted communications and equipment failure etc. To solve this problem, custom power devices are used.

B. Classification of Custom Power Devices

Custom power devices can be classified on the basis of different type of topologies and the no of phases.

1 Converter based classification:

- VSI
- CSI

2 Topology based classification:

- D-STATCOM
- DVR
- UPFC

3 Supply System Based Classification: -

- Single-phase two-wire systems:
- Three-phase 3-wire systems:
- Three-phase 4-wire systems.

C. Benefits of Custom Power Devices

The benefits due to custom power devices are listed below.

- The power flow in critical line can be improved as the operating margins can be reduced by fast controllability.
- The power carrying capacity of line can be increased to values up to a thermal limit by imposed by current carrying capacity of the conductors.
- The transient stability limit is improved by improving dynamic security of the system and reducing the incidence of blackouts caused by cascading outages.
- They contribute to best possible system operation by improving voltage profile and reducing power losses.
- The problem of starting voltage dip in case of industrial loads like induction motor can also be reduced by these devices.
- The problem of voltage fluctuations and in particular, dynamic over voltages can be overcome by these controllers.
- The steady state or small signal stability region can be increase by providing auxiliary stabilising controllers to damp low frequency oscillations.

D. Drawbacks of Custom Power Devices

- The STATCOM and DSTATCOM are basically designed by using VSI converters, so that voltage and current harmonics are generated in the system. Therefore more excessive heat developed in the due to such harmonics. The reliability of the system will be decreases.
- Since filters are required in the system. Therefore overall Capital cost of system will be increased.
- In parallel operation or coordinated operation of custom power device, voltage and current interaction phenomenon occurs in the system due to unbalance operation.

E. Applications of Each Custom Power Devices

1. Static Shunt Compensator (D -STATCOM)

Power factor improvement
Current Harmonic compensation
Load current balancing
Flicker effect compensation

2. Static Series Compensator (DVR)

Voltage sag and swell protection
Voltage balancing and Voltage regulation
Flicker attenuation

3. Unified Power Flow Controller (UPFC)

Voltages sag and swell correction
Voltage balancing and Voltage regulation
Flicker attenuation and VAR compensation
Harmonic suppression and Current balancing
Active and reactive power control

Ref. [26], has been presented The deregulation of electric power energy has boosted the public awareness toward power quality among the different categories of users to provide an active & flexible solution for power quality problems, various efforts have done from time to time. Among these power quality solution lossless passive filters [37-39] consists of L-C tuned component have been widely used to suppress harmonic. Passive filters are advantageous as its initial cost is low and high efficiency. on the other hand it have various drawbacks of instability, fixed compensation , resonance with supply as well as loads and utility impedance. To overcome these limitations active power filters [40-42] have been used.

Ref. [73], has been addressed the custom power devices to improve the power quality by using a Distribution Static Compensator. It describes the techniques of correcting the supply voltage sag in a distribution system by DSTATCOM. The steady state performance of system with or without DSTATCOM is studied for voltage sag. Power Quality improvement using custom power devices considers the structure, control and the performance of series compensating DVR, the shunt compensating DSTATCOM and the shunt with series UPQC for power quality improvement in electricity distribution.

Ref. [91], has been presented with the restructuring of Power Systems and with shifting trend towards distributed and dispersed Generation, the issue of Power Quality is going to take newer dimensions. The aim is to identify the prominent concerns in the area and thereby to recommend measures that can enhance the quality of the power, keeping in mind their economic viability and technical repercussions. The electromagnetic transient studies are presented for the following two custom power controllers: the distribution static compensator (D-STATCOM), and the dynamic voltage restorer (DVR). Comprehensive results are presented to assess the performance of each device to mitigate the power quality

problems. Modern industrial processes are based a large amount of electronic devices such as programmable logic controllers and adjustable speed drives. The electronic devices are very sensitive to disturbances [1] and thus industrial loads become less tolerant to power quality problems such as voltage dips, voltage swells, and harmonics.

Ref.[93],has been addressed The present researchers are concentrating on the new technologies utilizing power electronics based concepts because these devices are capable of mitigating several power quality problems. The application of power electronics to power distribution system for the benefit of a customer or group of customers is called custom power. Comprehensive results are presented to assess the working of each device as a potential custom power solution. There are different ways to mitigate voltage dips, swell and interruptions in distribution systems. A custom power specification may include provision for (i) no power interruption (ii) Tight Voltage regulation including short duration sags or swells (iii) Low harmonic Voltages and (iv) Acceptance of fluctuating and non linear loads without effect on terminal voltage [94]. These devices are connected either in shunt or in series or in combination of both series and shunt.

Ref. [100], has been addressed analysis of custom power controllers, a new generation of power electronics-based equipment aimed at enhancing the reliability and quality of power flows in low-voltage distribution networks [101], [102]. The modelling approach adopted in the paper is graphical in nature, as opposed to mathematical models embedded in code using a high-level computer language. The well-developed graphic facilities available in an industry standard power system package, namely PSCAD/EMTDC, are used to conduct all aspects of model implementation and to carry out extensive simulation studies. Comprehensive results are presented to assess the performance of each device as a potential custom power solution.

Ref. [132], has been presented The PSCAD program is used to conduct all aspects of model implementation and to carry out extensive simulation studies as example the distribution static compensator (D-STATCOM) was presented as member of custom power and static var compensator (SVC) as example of FACTS. Paper more discussed about DSTATCOM and its modelling and suggested to be used as hybrid system with magnetically controllable reactor (MCR) in future.

F. Topology based classification

On the basis of topology custom power in three types.

- D-STATCOM** it is a 3-phase and shunt connected power electronics based reactive power compensation equipment, which generates and/or absorbs the reactive power. It is connected near the load at the distribution system. Thus DSTATCOM is an effective solution for power systems facing such power quality problems like terminal voltage fluctuations, various transients like voltage sag ,swell,

flicker etc and waveform distortions. To enhance the reliability and quality of power for distribution systems that is delivered to customers, D-STATCOM is used which is a fast response, solid-state power controller that provides flexible voltage control at the point of connection to the utility distribution feeder for PQ improvements.

a. Single-line diagram of D-STATCOM

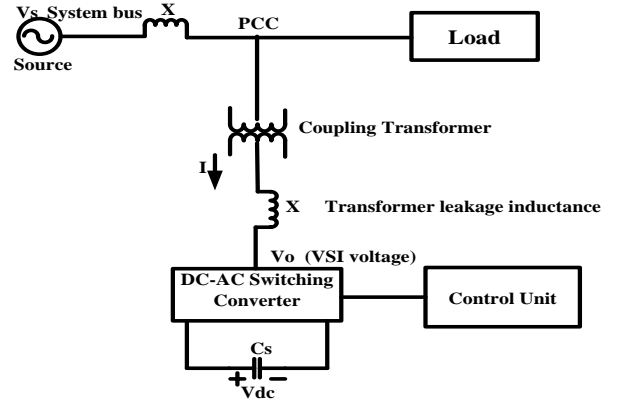


Figure 11 Basic Configuration of DSTATCOM

b. D-STATCOM Components

Voltage Source PWM Inverter, Coupling Transformer, Voltage Regulator, L C Damped Filter, D-STATCOM Controller Unit, Anti Aliasing Filter, PWM Pulse Generation and D C Voltage Source.

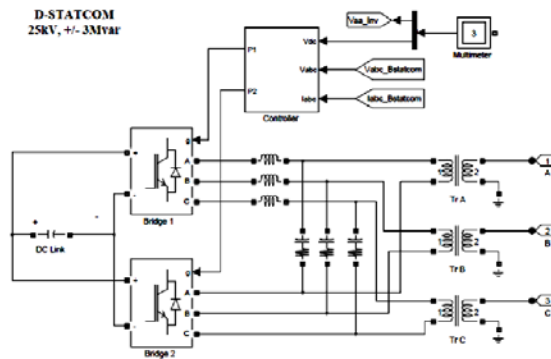


Fig 12 Design or layout of DSTATCOM.

c. Principle of D-STATCOM

Basic operating principle of a DSATCOM is similar to that of synchronous machine. The synchronous machine will provide lagging current when under excited and leading current when over excited. DSTATCOM can generate and absorb reactive power similar to that of synchronous machine and it can also exchange real power if provided with an external device DC source. Exchange of Reactive Power and Exchange of Real Power.

d. Operation of D-STATCOM

The voltage is compared with the AC bus voltage system (V_s), When the AC bus voltage magnitude is above that of the VSI magnitude (V_o); the AC system sees the D-STATCOM as inductance connected to its terminals. Otherwise if the VSI voltage magnitude is above that of the AC bus voltage magnitude, the AC system sees the D-STATCOM as capacitance to its terminals. If the voltage magnitudes are equal, the reactive power exchange is zero.

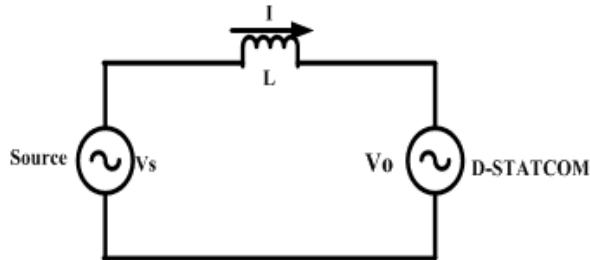


Figure 13 Equivalent circuit

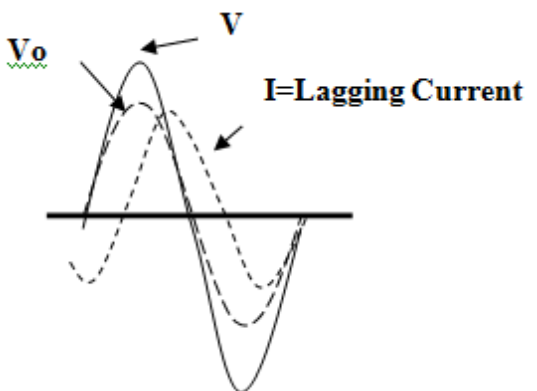
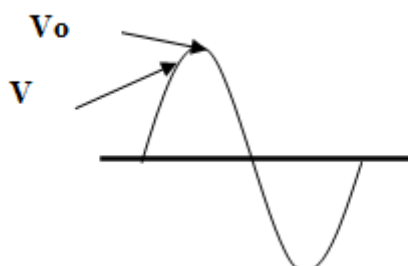
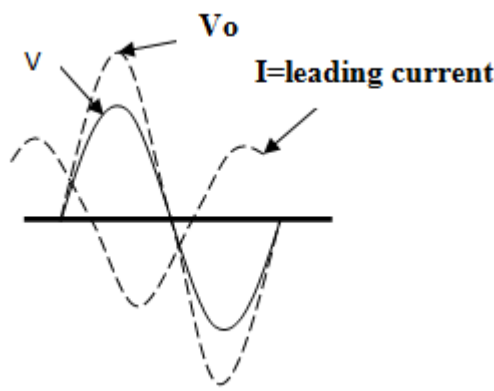


Fig.14 Operation modes of D-STATCOM

e. Control Technique

Synchronous Reference Frame Theory (d-q theory)
The D-Q reference frame theory is used to generate the reference compensating currents for DSTATCOM.

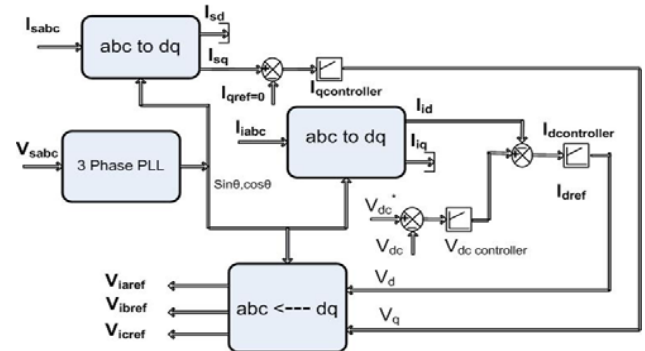


Fig. 15 D-STATCOM controller with d-q theory.

abc to dq0 Transformation
If θ is the transformation angle, then the current transformation from abc to d-q-0 frame is defined as

$$\begin{bmatrix} i_d \\ i_q \\ i_0 \end{bmatrix} = \sqrt{\frac{2}{3}} \begin{bmatrix} \cos \theta & \cos\left(\theta - \frac{2\pi}{3}\right) & \cos\left(\theta + \frac{2\pi}{3}\right) \\ -\sin \theta & -\sin\left(\theta - \frac{2\pi}{3}\right) & -\sin\left(\theta + \frac{2\pi}{3}\right) \\ \frac{1}{\sqrt{2}} & \frac{1}{\sqrt{2}} & \frac{1}{\sqrt{2}} \end{bmatrix} \begin{bmatrix} i_a \\ i_b \\ i_c \end{bmatrix}$$

- f. **PI Controller** proportional and integral (PI) control is used for capacitors dc voltage regulation for DSTATCOM. Advantages of PI controller-Fast action and Eliminate the offset

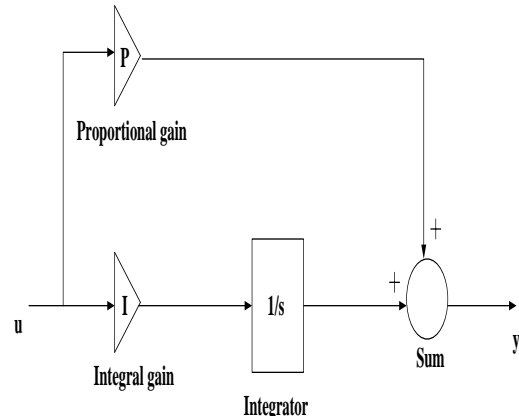


Fig. 16 PI controller

g. Hysteresis controller

In this controller the desired current of a given phase is summed with the negative of the measured current. The error is fed to a comparator having a hysteresis band which is naturally 1% to 5% of the current level. The control logic used is given as $i_{sa} < i_{sa}^* - h_b$, then the upper switch of VSC is turned off and lower switch is turned ON means When the error crosses the lower limit of the hysteresis band, the upper switch of the inverter leg is turned on. But when the current attempts to become less than the upper reference band, the bottom switch is turned on.

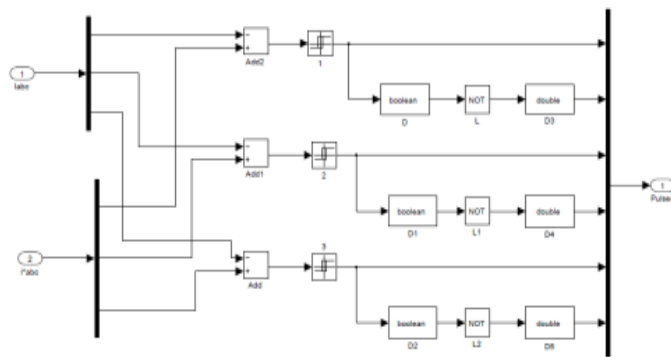


Fig 17 schematic representation of PWM hysteresis control

Thus upper and lower switching devices are switched ON and OFF in complementary manner. The hysteresis band can be varied and a narrow hysteresis band results in very good and fast tracking of currents but switching frequency may becomes too high. A wide hysteresis band may not able to provide effective tracking thus leading to the system becomes unstable. Hysteresis current controller can also be implemented to control the inverter currents. The controller will generate the

reference currents with the inverter within a range which is fixed by the width of the band gap. Figure 3.8 shows the hysteresis band with the actual current and the resulting gate signals. This controller does not have a specific switching frequency and changes continuously but it is related with the band width.

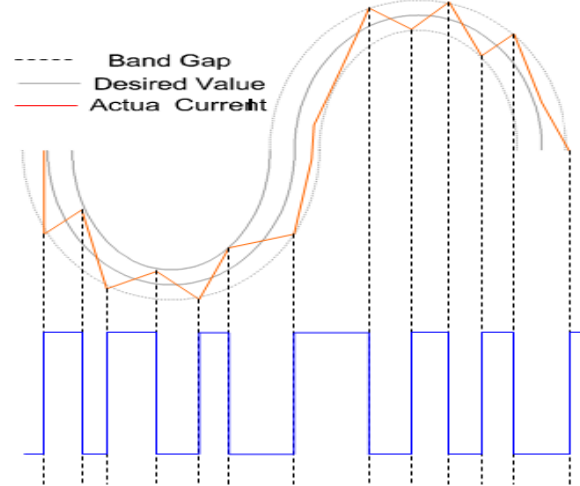


Figure 18 Hysteresis controller

Ref. [1], has been presented the complete background of the compensating devices and power electronic application in compensating devices is presented in this paper and also the compensation using the DSTATCOM modelling is also discussed. Theoretical analyses of the Different types of control strategies use for the control of DSTATCOM are discussed and the necessary block diagrams and the transformations required are discussed. The PI controllers are used for the implementation of the models and are discussed. Simulation results are we discussed and various case studies applied depending on the various loads like resistive, inductive and capacitive on the DSTATCOM simulink models and the simulation results are studied.

Ref. [2], has been addressed an investigation of Hybrid Seven-Level (HSL) H – bridge Inverter is used in a Distribution Static Compensator (DSTATCOM) in Power System (PS), making use of HSLI benefits of low harmonics distortion, Reduced number of switches to achieve the seven- level inverter output over the conventional cascaded seven level inverter and reduced switching losses. In order to improve the power factor, compensate the reactive power and suppress the total harmonics distortion (THD) drawn from a Non-Liner Diode Rectifier Load (NLDRL) of DSTATCOM, we propose a Sub-Harmonics Pulse Width Modulation (SHPWM) technique is used as control for the switches of HSL H – bridge Inverter.

Ref. [17], has been presented Some of the topologies of DSTATCOM for three-phase four-wire system for the mitigation of neutral current along with power quality compensation in the source current are four-leg voltage source converter (VSC), three single-phase VSCs, three-leg VSC with

split capacitors [18], three-leg VSC with zigzag transformer [19]-[21] and three-leg VSC with neutral terminal at the positive or negative of dc bus [22]. The voltage regulation in the distribution feeder is improved by installing a shunt compensator [23]. There are many control schemes reported in the literature for control of shunt active compensators such as instantaneous reactive power theory, power balance theory, synchronous reference frame theory, symmetrical components based, etc. [24], [25]. The synchronous reference frame theory [24] is used for the control of the proposed DSTATCOM. A new topology of DSTATCOM is proposed for a three-phase four-wire distribution system, which is based on three-leg VSC and a Zigzag Phase-Shifting transformer (PST).

Ref. [63], has been presented The topology and control are discussed of a distribution static compensator (DSTATCOM) that can be operated flexibly in the voltage or current control mode. Both these objectives are achieved, irrespective of unbalance and harmonic distortions in load currents or source voltages. The chosen DSTATCOM topology includes three single-phase voltage source inverters connected in parallel to a filter-capacitor, which allows the high-frequency component of the current to pass.

Ref. [74], has been suggested for reactive power compensation of distribution system (DSTATCOM) is based on the cascaded H-bridge multilevel inverter configuration. The mathematical formulation of the multilevel DSTATCOM is presented using state-space representations. A new software phase-locked loop (SPLL) is presented for grid synchronization and the obtained phase angle of the fundamental component of the grid voltage is utilized for deriving the active and reactive power balancing equations of the multilevel DSTATCOM. The proportional-resonant (PR) controller scheme is adopted for the current tracking control of the inverter, and the average dc-link voltage is controlled using a proportional-integral (PI) controller to regulate the active power flow of the DSTATCOM. Besides, the voltage balancing (VB) control among individual H-bridges is achieved by using separate PI regulators to control the difference voltage between the individual dc-link voltage and the average dc-link voltage.

Ref. [80], has been addressed the capabilities of DSTATCOM systems used to improve power quality (PQ) in low voltage (LV) grids with distributed energy resources (DERs). Selected single-phase DERs of varying power are connected into the networks which introduce PQ disturbances such as voltage variations, harmonics and asymmetry. To mitigate deviations in power quality DST ATCOM compensator operating in current control mode has been applied. The possibility of using the DSTATCOM operating in voltage control mode for reducing voltage dips coming from the supplying network has also been studied. Control circuits have been designed for these two modes of operation. Description of the study network, their element models and some selected results of simulation are presented in the paper.

Ref. [81], has been presented DSTATCOM is used for Grid Connected Power System, for Voltage Fluctuation, for Wind power Smoothening and Hydrogen Generation etc. in Marine power System for power quality improvement. Relevant solution which applied nowadays to improve power quality of electric network according to the five aspects of power quality – harmonics, fluctuation and flick of voltage , voltage deviation, unbalance of 3-phase voltage and current frequency deviation.

2. DVR

The DVR was first installed in 1966 .It is normally installed in a distribution system between the supply and the critical load feeder at the PCC. Its primary function is to boost up the load-side voltage in the event of a disturbance in order to avoid any power disruption to that load. DVR is a recently proposed series connected solid state device that injects voltage into the system in order to regulate the load side voltage. A DVR is connected in series with the feeder using a transformer, low voltage winding in connected to the converter. The DVR is required to inject active power into the distribution line during the period of compensation

a. Location of DVR

Location of DVR in Electrical Distribution Network is shown in fig.19.

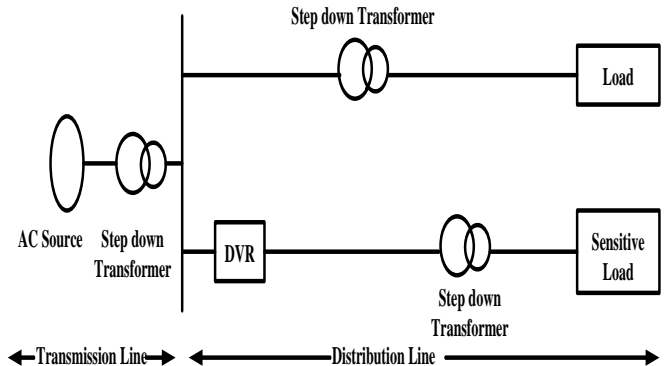


Figure 19 Location of DVR

b. Single-line diagram of DVR

The single line Diagram of DVR (Dynamic Voltage Restorer) is shown in figure 20. This is one of the important Custom power Devices.

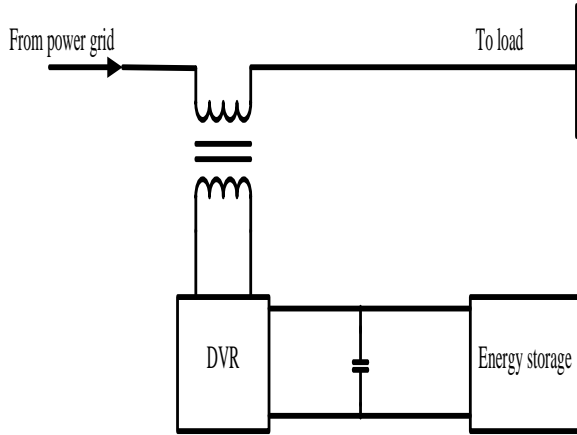


Fig. 20 Basic Configuration of DVR

c. DVR Components

The DVR mainly consists of the following components:
The general configuration of a DVR consists of an injection / booster transformer, a harmonic filter, a voltage source converter (VSC), DC charging circuit and a control and protection system as shown in Fig.21.

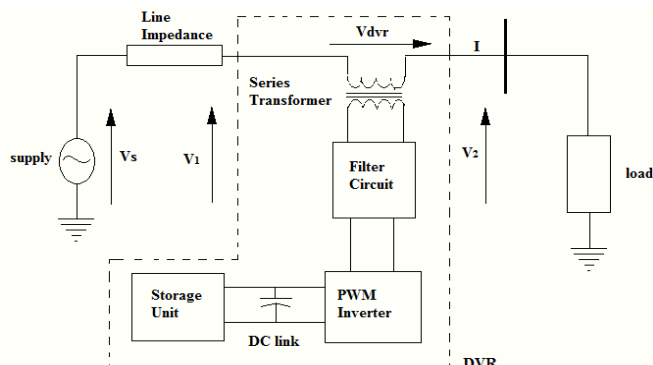


Figure-21 Schematic diagram of DVR

d. Principle of DVR

The basic principle of the DVR is to inject a controlled voltage generated by a forced commuted converter in a series to the bus voltage by means of an injecting transformer. A DC to AC inverter regulates this voltage by sinusoidal PWM technique. The DVR capable of generating or absorbing reactive power but the active power injection of the device must be provided by an external energy source or energy storage system. which is shown in fig.22.

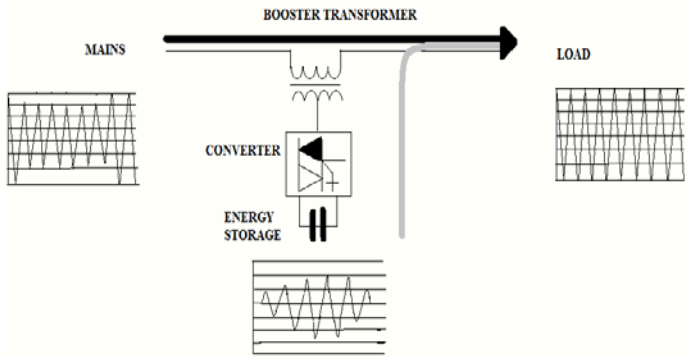


Figure-22 Principle of DVR system

e. Operating Modes of DVR

Protection mode, standby mode and Injection/boost mode are three mode of operation of DVR.

In protection mode, if the current on the load side exceeds a tolerable limit due to any fault or short circuit on the load, DVR will isolate from the system.

In standby mode the voltage winding of the injection transformer is short circuited through converter.

In the Injection/Boost mode the DVR is injecting a compensating voltage through the injection transformer due to the detection of a disturbance in the supply voltage.

f. Voltage Injection Methods of DVR

There are different methods of DVR voltage injection which are:

- i. Pre-sag compensation method
- ii. In-phase compensation method
- iii. In-phase advanced compensation method

i. Pre SAG Compensation

The supply voltage is always tracked and the load voltage is compensated to the pre-sag condition. This scheme results in undisturbed load voltage, but normally requires higher rating of the DVR. Before a sag occur, $V_s = V_L = V_o$. Where

V_s is supply voltage

V_L is load voltage and

V_o is pre sag voltage

The voltage sag results in drop in the magnitude of the supply voltage to V_{s1} . The phase angle of the supply also may shift (see Figure-23). The DVR injects a voltage V_{c1} such that the load voltage ($V_L = V_{s1} + V_{c1}$) remains at V_o i.e. pre sag voltage (both in magnitude and phase). It is claimed that some loads are sensitive to phase jumps and it is essential to compensate for both the phase jumps and the voltage sags.

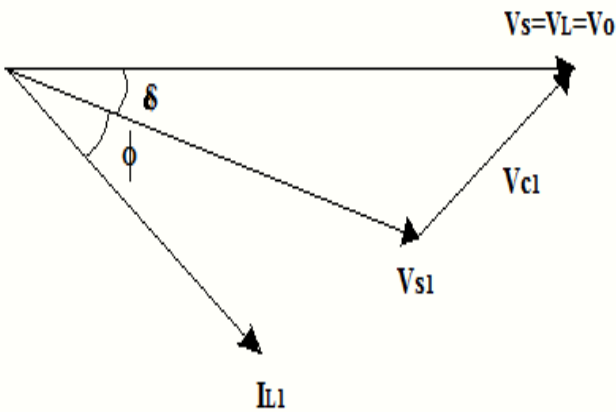


Figure-23 Phasor diagram showing injected voltage by DVR

ii In Phase Compensation

The voltage which is injected by the DVR is always in phase with the supply voltage in spite of the load current and the pre-sag voltage (V_0). This control strategy results in the minimum value of the injected voltage (magnitude). However, the phase of the load voltage is disturbed. The power requirements for the DVR are not zero for this approach.

iii In Phase Advanced Compensation

In this method the real power which is injected by the DVR is reduced by reducing the power angle between the voltage during sag condition and load current. The minimization of injected energy is achieved by making the active power component zero by having the injection voltage phasor perpendicular to the load current phasor. In this technique the values of load current and voltage are fixed in the system so only the phase of the voltage during sag is changed.

Ref. [6], has been presented. The rapid response of this device enables them to operate in real time, providing continuous and dynamic control of the supply including voltage and reactive power regulation, harmonic reduction and elimination of voltage dips. This presents the benefits of multilevel inverters when they are used for DPC based custom power devices. Power flow control mechanism, salient features, advantages and disadvantages of direct power control (DPC) using lookup table. The basic DPC strategy is based on the instantaneous active and reactive power comparators. The active power command is provided from a dc-bus voltage control block, while the reactive power command is directly given from the outside of the controller. Errors between the commands and the estimated feedback power are input to the hysteresis comparators.

Ref. [8], has been addressed describes the problem of voltage sags and swells and its severe impact on non linear loads or sensitive loads. The dynamic voltage restorer (DVR) has become popular as a cost effective solution for the protection of sensitive loads from voltage sags and swells. It first analyzes

the power circuit of a DVR system in order to come up with appropriate control limitations and control targets for the compensation voltage control. The proposed control scheme is simple to design. Swell magnitude is also described by its remaining voltage, in this case, always greater than 1.0. [10, 11, 12]. To production downtime and equipment damage [13-15].

3. UPFC

The UPFC is the fastest, most flexible, and the best-featured FACTS device. It can be seen as a combination of the D-STATCOM and DVR. The Unified Power Flow Controller (UPFC) is used to control the power flow in a transmission system by controlling the impedance, voltage magnitude and phase angle. Therefore, UPFC can be used efficiently and flexibly to optimise line utilization and increase system reliability, to enhance system stability, and to dampen system oscillations. The UPFC can fulfil functions of reactive shunt compensation, active and reactive series compensation and phase shifting.

a. Configuration of UPFC.

The basic structure of the UPFC consists of two voltage source converters (VSCs); where one converter is connected in parallel to the transmission line through a shunt coupling transformer while the other is in series with the transmission line through a series coupling transformer. Both VSCs are connected to each other by a common dc link including a storage capacitor. This is shown in the following fig.24.

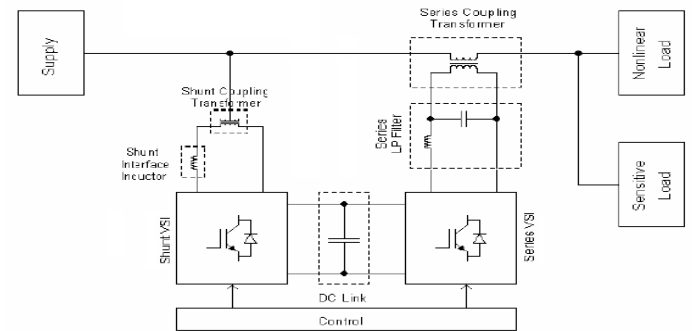


Fig. 24 Basic Configuration of UPFC

b. Principle of UPFC

UPFC generates or absorbs the needed reactive power locally by the switching operations of its converters. Each converter generates or absorbs the reactive power independently, i.e. reactive power does not flow through the dc link. The power transfer between the shunt converters and series convert sets the UPFC rating. The shunt inverter is used for voltage regulation at the point of connection injecting reactive power into the line and to balance the real power flow exchanged between the series inverter and the transmission line. The series

inverter can be used to control the real and reactive line power flow inserting voltage with controllable magnitude and phase in series with the transmission line.

c. Operating Modes of UPFC

Series converter operation the series converter produces an ac voltage of controllable magnitude and phase angle, and injects this voltage at this fundamental frequency in series with the transmission line through a booster transformer. It also exchanges real and reactive power at its ac terminals through the series connected transformer. The active power needed by this converter is provided from the ac power system by the shunt converter through the dc link. The series converter can be used to increase the transmission capability.

Shunt converter operation the basic function of shunt converter is to supply or absorb the active power demanded by the series converter at the dc terminals. It also can generate or absorb controllable reactive power and provide independent shunt reactive compensation for the line. The shunt controller can be used for local voltage control, which in turn improves system voltage stability. The shunt voltage and its current are limited by the rating of shunt converter.

Ref. [82], has been addressed the regulation of voltage at wind farm (WF) terminals and the improvement of power quality and WF stability in a WF to Weak-Grid connection. A situation commonly found in such scheme is that the power generated is comparable to the transport capacity of the grid. This case is known as Wind Farm to Weak Grid Connection, and its main problem is the poor voltage regulation at the point of common coupling (PCC). Thus, the combination of weak grids, wind power fluctuation and system load changes produce disturbances in the PCC voltage, worsening the Power Quality and WF stability. The internal control strategy is based on the management of active and reactive power in the series and shunt converters of the UPFC, and the exchange of power between converters through UPFC DC-Link. Simulations results show the effectiveness of the proposed compensation strategy for the enhancement of Power Quality and Wind Farm stabilityIn this paper we propose and analyze a compensation strategy using an UPFC, for the case of SCIG-based WF, connected to a weak distribution power grid.

Ref. [135], has been addressed different applications of a UPFC for the improvement in power quality is presented. Such as power-factor correction, load balancing and mitigation of voltage and current harmonics, it can regulate the load voltage against voltage sag/swell and voltage dip in a three-phase three-wire distribution system for different combinations of linear and non-linear loads. The synchronous reference frame (SRF) theory is used to get the reference signals for series and shunt active power filters (APFs). The reference signals for the shunt and series APF of UPFC are derived from the control algorithm and sensed signals are used in a hysteresis controller to generate switching signals for shunt and series APFs. The

UPFC is realized using two voltage source inverters (VSI) connected back to back, to a common dc link capacitor.

Ref. [136], has been presented the primary task of UPQC is to minimize grid voltage and load current disturbances along with reactive and harmonic power compensation, additional functionalities such as compensation of voltage interruption and active power transfer to the load and grid have also been identified.

Ref. [141], has been addressed is proposed which is composed of the DC/DC converter and the storage device connected to the DC link of UPFC for balancing the voltage interruption.. The proposed system can improve the power quality at the common connection point of the non-linear load and the sensitive load.

Ref. [143], has been presented unified power flow conditioner (UPFC) is being used as a universal active power conditioning device to mitigate both current as well as voltage harmonics at a distribution end of power system network. The performance of UPFC mainly depends upon how quickly and accurately compensation signals are derived. The performance validation of Current Source Inverter (CSI)-based UPQC using Fuzzy Logic Controller (FLC) and Results are compared with conventional PID Controller and improvements are observed by FLC. The FLC-based compensation scheme eliminates voltage and current magnitude of harmonics with good dynamic response.

G. Converter Based Classification

The heart of the DSTATCOM/ CUSTOM POWER DEVICES is voltage source converter. Ref. [111], has been suggested the IGBT based VSC is capacitor supported and is controlled for the required compensation of the load current. The dc bus voltage of the VSC is regulated during varying load conditions. The performance of the three-phase four-wire DSTATCOM is validated for power factor correction and voltage regulation along with neutral current compensation, harmonic elimination and balancing of linear loads as well as non-linear loads using MATLAB software with its simulink.

This is classified as

1. VSI

In the voltage control mode, the DSTATCOM can force the voltage of a distribution bus to be balanced sinusoids.

Ref. [137], has been suggested a cascaded multilevel Voltage Source Inverter (VSI) based shunt Active Power Filter (APF) for current harmonics and reactive power compensation due to nonlinear loads. The cascaded multilevel active filter switching signals are derived from Triangular carrier Current Controller (TCC), Periodical Sampling Current Controller (PSCC) and proposed Triangular Periodical Current Controller (TPCC). It gives better dynamic performance under transient and steady state operating conditions. The APF system is validated through extensive simulation under steady state and transient

condition with different nonlinear loads. These simulation results reveal that the cascaded active filter effectively compensates the current harmonics and reactive volt amperes to improve the power quality.

Ref. [142], has been addressed the simulation and experimental results are included to highlight the fact that the scheme also enables to maintain a constant output voltage over a wide range of load variations, the PWM VSIs are required to maintain a sinusoidal output waveform for various types of loads, in addition to offering acceptable standards of power quality. A number of closed loop control schemes for PWM inverters with instantaneous feedback, by using analog techniques have been realized to achieve good dynamic performance and low total harmonic distortion (THD) .The instantaneous feedback control with adaptive hysteresis has served to regulate the PWM inverters with direct current and voltage.

2. CSI

A DSTATCOM is a voltage source converter (VSC) based device. When operated in a current control mode, it can improve the quality of power by mitigating poor load power factor, eliminating harmonic content of load and balancing source currents for unbalanced loads [3]-[4] and In the current control mode, it can cancel distortion caused by the load, such that current drawn by the compensated load is pure balanced sinusoid.

Ref. [133], has been addressed we proposed voltage-sourced converter (VSC) with Pulse-width modulation (PWM) provides a faster control that is required for flicker mitigation purpose. The voltage regulation in the distribution feeder is improved by installing a shunt compensator. The proposed DSTATCOM is modelled and its performance is simulated and verified for power factor correction and voltage regulation along with neutral current compensation, harmonic elimination and load balancing with linear loads and non-linear loads. The three phase three wire Distribution Static Compensator (DSTATCOM) is proposed for power quality improvement. DSTATCOM is based on a three leg VSC and is controlled to compensate reactive power, harmonic current and unbalances in the load. IGBT based VSC is capacitor supported and is controlled for the required compensation of the load current. Micro-sources mostly connect to converters to output voltage and frequency demanded. PWM converters can improve the generator power factor to be unit, and produce fewer harmonic. So PWM converters have good effects on improving the power quality. By changing voltage amplitude and phase of PWM converter, generators may create active and reactive power neatly to meet the load demand. And thus maintain the voltage and frequency stability.

H. Supply System Based Classification

1. Single-phase two-wire systems

2. Three-phase 3-wire systems

The last few decades has seen ever increasing demand for energy. The deregulation of power system has allowed autonomous generation of electrical energy [45]-[46]. Thus autonomous asynchronous generator (AAG) with its excitation requirement being met by a capacitor bank connected across its terminals [47]-[52], has become a compatible option. However the poor voltage and frequency regulation is a major bottleneck in its commercialization. This has led to a number of attempts to investigate the voltage and frequency controllers for constant [53]–[59], as well as variable power applications [60]-[62]. The reported controllers supported three phase 3-wire systems.

3. Three-phase 4-wire systems

Three-phase four-wire distribution systems are facing severe power quality problems such as poor voltage regulation, high reactive power and harmonics current burden, load unbalancing, excessive neutral current etc. [112-117]. Three -phase four-wire distribution systems are used in commercial buildings, office buildings, hospitals etc. a new three-phase four-wire DSTATCOM (distribution static compensator) based on three-leg VSC (voltage source converter) and a star/delta transformer is proposed for power quality improvement. The star/delta transformer connection mitigates the neutral current and the 3-leg VSC compensates harmonic current, reactive power and balances the load.

I. Power Quality Problem

A Power quality problem is an occurrence manifested as a nonstandard voltage, current or frequency that results in a failure or a mis-operation of end use equipments. Utility distribution networks, sensitive industrial loads, and critical commercial operations all suffer from various types of outages and service interruptions which can cost significant financial loss per incident based on process down-time, lost production, idle work forces, and other factors. With the restructuring of Power Systems and with shifting trend towards Distributed and Dispersed Generation, the issue of Power Quality is going to take newer dimensions. The aim therefore, in this work, is to identify the prominent concerns in the area and thereby to recommend measures that can enhance the quality of the power, keeping in mind their economic viability and technical repercussions.

1. Voltage SAG OR Voltage DIP

Ref. [16], has been addressed the electromagnetic transient studies are presented for the following two custom power controllers: the distribution static compensator (D-STATCOM), and the dynamic voltage restorer (DVR).

Comprehensive results are presented to assess the performance of each device as a potential custom power solution.

Ref. [64], has been presented DSTATCOM is one of the equipments for voltage sag mitigation in power systems. A new control method for balanced and unbalanced voltage sag mitigation using DSTATCOM has been proposed. This system has two controllers to regulate compensator current and load voltage. Delayed signal cancellation has been used for sequence separation. Performance of proposed method with balanced and unbalanced voltage sag has been considered. A simulation result shows appropriate operation of the proposed control system. Some methods that have been allocated for voltage sag mitigation using DSTATCOM only take balanced voltage sag into account [65-66]. In references [67] and [68] for improvement of these imperfections, sequence components of voltage and current have been separated in synchronous reference frame.

Ref. [82], has been addressed an artificial neural network (ANN) based approach for optimal placement of DSTATCOM to mitigate voltage sag under faults. Optimal location of DSTATCOM has been obtained using a feed forward neural network trained by post fault voltage magnitude of 3- phases at different busses. Case studies have been performed on IEEE 30 bus system and effectiveness of proposed approach of DSTATCOM placement has been established.

Ref. [125], has been presented the DVR, which is the most efficient and effective modern custom power device used in power distribution networks, is employed because of its lower cost, smaller size, and fast dynamic response to the disturbance. This presents the simulation analysis of a DVR in MATLAB / SIMULINK environment and its hardware implementation for voltage sag compensation. The results showed clearly the performance of the DVR in mitigating voltage sags.

Ref. [134], has been addressed the performance, analysis of operating principles of a new generation of power electronics based equipment called Distribution Static Compensator (D-STATCOM) aimed at enhancing the reliability, and quality of power flow in low voltage distribution network. The model is based on the Voltage Source Converter (VSC) principle. The D-STATCOM injects a current into the system to mitigate the voltage sags. LCL Passive Filter was then added to D-STATCOM to improve harmonic distortion and low power factor.

2. Voltage SWELLS

Ref. [149], has been suggested a new configuration of a DVR with an improvement of a controller based on direct-quadrature-zero method has been introduced to compensate voltage swells in the network. The effectiveness of the DVR with its controller was verified using Matlab/Simulink's SimPower Toolbox and then implemented using 5KVA DVR experimental setup. Simulations and experimental results

demonstrate the effective dynamic performance of the proposed configuration. The implementations of the proposed DVR validate the capabilities in mitigating of voltage swells effectiveness. During voltage swells, the DVR injects an appropriate voltage to maintain the load voltage at its nominal value. IEEE 519-1992 and IEEE 1159-1995 describe the voltage sags/swells. In this study the proposed new configuration is shown to possess the ability of mitigating voltage swells in low voltage distribution systems.

3. Voltage FLICKER

Ref. [78], has been presented voltage flicker is a major power quality concern for both power companies and customers. This paper discusses the dynamic performance of a (D-STATCOM) with ESS for mitigation of voltage flicker. The (D-STATCOM) is intended to replace the widely used static var compensator (SVC). A Distribution Static Synchronous Compensator (D-STATCOM) is used to regulate voltage on a 25-kV distribution network. The (D-STATCOM) protects the utility transmission or distribution system from voltage sag and /or flicker caused by rapidly varying reactive current demand. The (D-STATCOM) regulates bus voltage by absorbing or generating reactive power. This voltage is provided by a voltage sourced PWM inverter. The simulation is carried out using MATLAB/SIMULINK and the simulation results illustrate the performance of (D-STATCOM) in mitigation of voltage flicker.

Ref. [79], has been addressed the installation of a 5 MVA, 4.16 kV Distribution level Static Reactive Compensator (D-STATCOM) was completed in July, 1999. The D-STATCOM technology was selected as the preferred option for voltage flicker compensation of a 4,000 Hp shredder motor, which will be operated at the new facility. For voltage flicker applications, the D-STATCOM technology provides rapid-response compensation to correct for the voltage fluctuation characteristics imposed on the interconnected system during the shredder motor operation. In this application, the D-STATCOM System will be operating at 4.16 kV and will provide reliable power quality for both the new steel recycling facility and the interconnecting utility, which provides power to the plant at 26.4 kV.

Ref. [96], has been suggested This paper analysis the dynamic performance of a D-STATCOM with energy storage system for limitation of voltage flicker. A Distribution Static Synchronous Compensator (D-STATCOM) is used to regulate voltage on a 25-kV distribution network. The (D-STATCOM) protects the utility transmission or distribution system from voltage sag and /or flicker caused by rapidly varying reactive current demand. The (D-STATCOM) regulates bus voltage by absorbing or generating reactive power. This voltage is provided by a voltage-sourced PWM inverter. The simulation is carried out using MATLAB/SIMULINK and the simulation results illustrate the performance of (DSTATCOM) in mitigation of voltage flicker.

4. UNDER VOLTAGE

Ref. [148], has been suggested the power quality of a low-voltage grid with two wind turbines is investigated. Periodic power fluctuations reaching 10 % of the rated power are registered; voltage variations are lower than the prescribed IEC flicker limit at steady-state operation. As the turbines are put on-line, the voltage level is lowered by 3 %, which exceeds the flicker limit. The risk for flicker increases if the X/R ratio of the grid is low and if turbines which have a tendency to produce large periodic power fluctuations are used. Which may be caused by the wind shear, (different wind speeds at different heights) or by aerodynamic effects when the blades pass the tower. The main purpose is to investigate the influence of these wind turbines on voltage quality. Voltage quality is examined regarding slow voltage variations as well as transients and harmonics and to determine the origin and magnitude of the periodic components produced by the wind turbines.

5. OVER VOLTAGE

Ref. [146], has been suggested that In most of the IGBT gate drive design for overvoltage protection circuit, however, the problem of short-circuit would still happen. Therefore the overvoltage condition is being simulated to a boost Power Factor Correction (PFC) circuit implementing the IGBT as a switching device. A set of equations is derived for calculating the maximum junction temperature of an IGBT using the device switching characteristics during overvoltage condition. This approach can be used to determine the heat generation of IGBT device as well as identifying the root-cause of the short-circuit failure of hard switching design scheme during overvoltage condition.

6. NOISE

Ref. [144], has been addressed that a singular value decomposition (SVD) is a technique which is used for tracking the harmonics under noisy conditions in power system voltage and current waveforms. This allows real time accurate measurements of the amplitude and phase angle of harmonics present in high noise contaminated power system waveforms. The SVD method is a very powerful tool for identification of harmonics buried in a noisy signal in comparison to traditional FFT For the same number of samples and the same sampling period.

7. FLUCTIONS

Ref. [95], has been addressed the power quality challenges become greater when large volumes of renewable generation capacity are connected to distribution networks, traditionally designed to be passive circuits with unidirectional power flows. This presents two schemes to meet the different power quality challenges in the utility grid due to Distribution Generation. In this first scheme is DSTATCOM and second is three phase Distributed Generation. This work is aimed at demonstrating,

from the planning perspective, the benefits that the adoption of the different compensators might bring the system to a ‘fit and forget’ approach.

8. INTERRUPTION

Ref. [140], has been suggested a review about some of the methods that can be applied in an industrial installation to get a satisfactory operation in any electromagnetic environment with the presence of voltage sags or short interruptions will be showed in an abridged way. Moreover, a voltage sags and short interruptions measures analysis was also made, using a series of samples registered by a distribution utility, to characterize this events, as well as search and guess the future tendencies to improve power quality in the distribution networks.

9. HARMONICS

Ref. [75], has been addressed the modified instantaneous power control scheme of D-STATCOM for power factor and harmonic compensation. To achieve these additional control objectives can help system operators maximize overall system performances. A control scheme with constant power and sinusoidal current compensation [76, 77] is exploited. In order to correct the power factor, a power factor control loop is required and included in the control block. To verify its use, a 22-kV power distribution feeder with a three-phase rectifier load was tested. Results showed that integration of the proposed reactive power control loop can correct the power factor of the controlled feeder to be unity power factor.

Ref. [126], has been addressed by integrating phase shifting into an extremely low zero phase sequence impedance transformer with single or multiple outputs, substantial reduction of triplen, 5th and 7th order harmonics can be achieved.

Ref. [138], has been presented the harmonics generated by nonlinear load when added with reactive load causes more problematic to supply system as it not only affects transformer at supply end, but also to other consumers connected to same supply. Hence an object of great concern not only for consumers but also for distributors. This presents modelling and simulation of a Synchronous Link Converter (SLC) using PWM connected to a single-phase system having both reactive and non-linear load. The SLC acts as Active Power Filter for harmonics compensation and static Synchronous Compensator for variable compensation of load.

Ref. [139], has been presented the effect of harmonics on the power quality of the power supply. The paper also discussed the different configuration of pwm technique for harmonic reduction and improvement of fundamental peak voltage. In addition a, comprehensive comparison of all configurations is made in terms of THD FFT and dominating harmonics components.

J. Others

Ref. [43], has been addressed whether the power is supplied by asynchronous generator or by the grid at the remote location, its quality has become an important aspect for consumers of electricity. Efforts have been made to improve the power quality using passive filters, active filters and the new concept of Custom Power. Use of Custom power devices ensures that a load do not pollute the power supply of the other loads. One such custom power device is the DSTATCOM (Distribution Static Compensator) which is connected in shunt at the load end. The focus on the autonomous generation has increased in the recent years. The paper presents a comprehensive review of the DSTATCOM used for autonomous generation.

Ref. [83], has been addressed large inductive loads require larger rating of DSTATCOM to generate the required reactive power of the load and hence cost is increases, the DSTATCOM provides a continuous and smooth variation in the reactive power generation and can track the change in the VAr requirement very fast. To obtain optimal performance of the combined system, the TSCs are switched through a Fuzzy Logic controller. The DSTATCOM along with Fuzzy Logic Controller operated TSCs is demonstrated for an autonomous. The demand of electrical energy is ever increasing. The accelerated depletion of the fossil fuel and the price of petroleum crude fluctuating widely, has forced the energy planners to look for alternative resources of energy which are replenished by nature [84]-[87]. For remote and rural applications, more and more need is being felt to have off-grid systems based on asynchronous generators, using available renewable energy sources like wind, micro or pico hydro and biomass [88]-[90].

Ref. [103], has been suggested the performance of DSTATCOM depends on capacitor voltage regulation. In DSTATCOM, the nonlinear controller is preferred to linear controller. Regulating and fixing the capacitor DC voltage in DSTATCOM can improve the system dynamic such as capacitor voltage response, current response and modulation index. The regulation of DC capacitor voltage based on optimal PI co-efficient. In conventional scheme, the trial and error method is used to determine PI values. The genetic algorithm is applied for exact calculation of optimized PI co-efficient, to reduce disturbances in DC link voltage. Optimization and simulations are worked out in MATLAB environment. Many different strategies such as proportional-Integral controller, sliding mode controller [4] and nonlinear controller have been suggested to control DSTATCOM. But in DSTATCOM, nonlinear controller is preferred in comparison with linear method [5]. In non-linear controller, the generalized averaged method [6] has been used to determine the nonlinear time invariant continuous model of the system [7]-[9]. This method has been applied to implement a nonlinear control law based on exact linearization via feedback for STATCOM [10].

Ref. [119], has been addressed the three – level neutral point diode clamped inverter is used in a distribution static compensator (DSTATCOM), making use of the multi advantages of low harmonics distortion and reduced switching losses. The pulse width modulation (PWM) inverter is employed as DSTATCOM compensating reactive power and eliminates the harmonics drawn from a non-linear load. A fuzzy gain scheduled proportional and integral (FGPI) dc voltage proposed for inverter dc voltage control to improve the performances of three – levels DSTATCOM and fuzzy logic current controller is proposed to reduce harmonic supply currents for DSTATCOM.

Ref. [127], has been presented the transient response of the DSTATCOM is very important while compensating rapidly varying unbalanced and nonlinear loads. The proper operation of DSTATCOM requires variation of the dc-link voltage within the prescribed limits. Conventionally, a proportional-integral (PI) controller is used to maintain the dc-link voltage the reference value. It uses deviation of the capacitor voltage from its reference value as its input. However, the transient response of the conventional PI dc-link voltage controller is slow. A fast-acting dc-link voltage controller based on the energy of a dc-link capacitor is proposed.

K. Conclusions

In this project the concepts of power quality have been studied and explained. This paper presents a comprehensive survey on the mitigation of power quality problems such as low power factor, shortage of reactive power, poor voltage, voltage and current harmonics due to sudden change in field excitation of synchronous alternator, sudden increased in load, sudden fault occur in the system are solved by FACTS controllers such as STATCOM, and DSTATCOM. This paper also presents current status of mitigation of power quality problems by FACTS controllers. Authors strongly believe that this survey article will be very much useful to the researchers for finding out the relevant references in the field of power quality problems solved by FACTS controllers.

ACKNOWLEDGMENT

REFERENCES

- [1] Kiran Kumar Pinapatruni, and Krishna Mohan, "DQ based Control of DSTATCOM for Power Quality Improvement," *VSRD-IJEECE*, Vol. 2 (5), 2012, 207-227.
- [2] D.Kalyanakumar, Dr.V.Kirbakaran, K.Ramash Kumar "Hybrid Seven Level H- Bridge Inverter "Journal of Theoretical and Applied Information Technology.
- [3] W. Liqiao, L. Ping, L. Jianlin and Z.Zhongchao, "Study on shunt active power filterbased on cascaded multilevel

- [4] converters," 35th *IEEE Power Electr. Spec. Conf. (APEC)*, vol.5, pp. 3512-3516, 20-25 June 2004.
- [5] A. Ghosh and G. Ledwich, *Power Quality Enhancement using Custom Power Devices*, Kluwer Academic Publisher, Boston, MA, 2002.
- [6] A. Ghosh and G. Ledwich, "Load Compensating DSTATCOM in weak AC systems," *IEEE Trans. Power Delivery*, vol.18, No. 4, pp. 1302-1309, Oct. 2003.
- [7] S. Venkateshwarlu, B. P. Muni, A. D. Rajkumar, and J. Praveen "Direct Power Control Strategies for Multilevel Inverter Based Custom Power Devices" World Academy of Science, Engineering and Technology 39 2008.
- [8] V. Blasko "Adaptive Filtering for Selective Elimination of Higher Harmonics from Line Currents of a Voltage Source Converter" IEEEIAS Conference 1998, pp. 1222-1228.
- [9] Rosli Omar, Nasrudin ABD Rahim, Marizan Sulaiman "Modelling and Simulation for voltage Sags/Swells Mitigation using DVR" Journal of Theoretical and Applied Information Technology.
- [10] N.G. Hingorani, "Introducing Custom Power in IEEE Spectrum," 32p, pp. 41-48, 1995.
- [11] IEEE Std. 1159 – 1995, "Recommended Practice for Monitoring Electric Power Quality".
- [12] P. Boonchiam and N. Mithulanthan, "Understanding of Dynamic Voltage Restorers through MATLAB Simulation," Thammasat Int. J. Sc. Tech., Vol. 11, No. 3, July-Sept 2006.
- [13] J. G. Nielsen, M. Newman, H. Nielsen, and F. Blaabjerg, "Control and testing of a dynamic voltage restorer (DVR) at medium voltage level," *IEEE Trans. Power Electron.*, vol. 19, no. 3, p.806, May 2004.
- [14] A. Ghosh and G. Ledwich, "Power Quality Enhancement Using Custom Power Devices," Kluwer Academic Publishers, 2002.
- [15] S. Chen, G. Joos, L. Lopes, and W. Guo, "A nonlinear control method of dynamic voltage restorers," in 2002 IEEE 33rd Annual Power Electronics Specialists Conference, 2002, pp. 88- 93.
- [16] R. Buxton, "Protection from voltage dips with the dynamic voltage restorer," in IEE Half Day Colloquium on Dynamic Voltage Restorers – Replacing Those Missing Cycles, 1998, pp. 3/1- 3/6.
- [17] Mahesh Singh (Lecturer) SSCET BHILAI INDIA Vaibhav Tiwari CSIT BHILAI INDI "Modeling analysis and solution of Power Quality Problems".
- [18] R.Revathi and J.Ramprabu "A ZIGZAG-DELTA PHASE-SHIFTING TRANSFORMER AND THREE-LEG VSC BASED DSTATCOM FOR POWER QUALITY IMPROVEMENT" International Journal of Advances in Engineering & Technology, Jan 2012. ©IJAET ISSN: 2231-1963 553 Vol. 2, Issue 1, pp. 552-563.
- [19] H. Beverly, R. D. Hance, A. L. Kristalinski, and A. T. Visser, "Method and apparatus for reducing the harmonic currents in alternating current distribution networks," U.S. Patent 5 576 942, Nov. 19, 1996.
- [20] H.-L. Jou, J.-C. Wu, K.-D. Wu, W.-J. Chiang, and Y.-H. Chen, "Analysis of zig-zag transformer applying in the three-phase four-wire distribution power system," *IEEE Trans. Power Del.*, vol. 20, no. 2, pp. 1168–1173, Apr. 2005.
- [21] H.-L. Jou, K.-D. Wu, J.-C. Wu, and W.-J. Chiang, "A three-phase four-wire power filter comprising a three-phase three-wire active filter and a zig-zag transformer," *IEEE Trans. Power Electron.*, vol. 23, no.1, pp. 252–259, Jan. 2008.
- [22] H. L. Jou, K. D. Wu, J. C. Wu, C. H. Li, and M. S. Huang, "Novel power converter topology for three-phase four-wire hybrid power filter," *IET Power Electron.*, vol. 1, no. 1, pp. 164–173, 2008.
- [23] H. Fugita and H. Akagi, "Voltage-regulation performance of a shunt active filter intended for installation on a power distribution system," *IEEE Trans. Power Electron.*, vol. 22, no. 1, pp. 1046–1053, May 2007.
- [24] M. C. Benhabib and S. Saadate, "New control approach for four-wire active power filter based on the use of synchronous reference frame," *Electr. Power Syst. Res.*, vol. 73, no. 3, pp. 353–362, Mar. 2005.
- [25] M. I. Milanes, E. R. Cadaval, and F. B. Gonzalez, "Comparison of control strategies for shunt active power filters in three-phase four-wire systems," *IEEE Trans. Power Electron.*, vol. 22, no. 1, pp. 229–236, Jan. 2007.
- [26] Satyaveer Gupt ,Ankit Dixit,Nikhil Mishra,S.P. Singh "CUSTOM POWER DEVICES FOR POWER QUALITY IMPROVEMENT" IJREAS Volume 2, Issue 2 (February 2012) ISSN: 2249-3905.
- [27] C. Sankaran, "Power quality," (CRC Press, New York, 2001).
- [28] J. Stones and A. Collinson, "Power quality," Power Eng. Journal, vol.15, pp.58-64, April 2001.
- [29] M. H. J. Bollen, "What is power quality?," Electric Power Systems Research, vol.66, pp.5-14, July 2003.
- [30] A.El Mofty,K. Youssef, "Industrial power quality problems," in Proc. on IEE Int. Conf & Exhib. on Electricity Distribution, 2001, vol.2, June 2001.
- [31] E.W.Gunther and H. Mehta, "A survey of distribution system power quality-preliminary results," *IEEE Trans. Power Delivery*, vol.10, pp.322-329, Jan.1995.
- [32] J.M.Salzer, "Worldwide review of power disturbances," IEEE Aerospace and Electron. Systems Magazine, vol.3, pp.2-5, April 1988.
- [33] Shailendra Jain, Pramod Agarwal and H.O. Gupta, "A survey of harmonics: Indian scenario," in Proc. on IEEE Conf India Annu. Conf., pp.84-89, Dec.2004.
- [34] A. Rash, "Power quality and harmonics in the supply network: a look at common practices and standards,"

- in Proc. on MELECON'98,* May1998, vol.2, pp.1219-1223.
- [35] R. C. Sermon, "An overview of power quality standards and guidelines from the end-user's point-of-view," *in Proc. Rural Electric Power Conf.*, May2005, pp. B 1/1 -B 1/15.
- [36] C. T. Heydt and W.T. Jewell, "Pitfalls of electric power quality indices," *IEEE Trans. on Power Delivery*, vol. 13, pp.570-578, April 1998.
- [37] A. K. Kapoor and R. Mahanty, "A quasi passive filter for power quality improvement," *in Proc. IEEE Int. Conf on Ind. Technology*, Jan 2000, vol. 1, pp.526-529.
- J. C. Das, "Passive filters - potentialities and limitations," *IEEE Trans. Ind. Application.*, vol.40, pp.232-241, Feb.2004.
- [38] M. Bou-rabee, C.S. Chang,D. Sutanto and K.S.Tam, "Passive and active harmonic filters for industrial power systems" *in Proc. IEEE TENCON*, 1991, pp. 222-226.
- [39] W.M. Grady, M.J. Samotyj and A.H. Noyola, "Survey of active power line conditioning methodologies," *IEEE Trans. Power Delivery*, 1990, 5, pp. 1536-1542.
- [40] H Akagi, "New trends in active filters for power conditioning," *IEEE Trans. Ind . Applcat.*, 1996, 32, pp. 1312-1322.
- [41] B. Singh, AL.K. Haddad and A. Chandra, "A review of active filters for power quality improvement," *IEEE Trans. Ind Elect.*, vol.46, pp. 960-971, 1999.
- [42] M.El-Habrouk, M.K. Darwish and P.Mehta, "Active power filters: A review," *Proc. IEE, Elect. Power Appl.*, vol. 147 pp. 493-413, 2000.
- [43] Ambarnath Banerji, Sujit K. Biswas, Bhim Singh "Review of Static Compensation of Autonomous Systems" International Journal of Power Electronics and Drive System (IJPEDS) Vol.2, No.1, ISSN: 2088-8694.
- [44] B. Singh, "Induction generator – A prospective," *Elect. Mach. Power Syst.*, vol. 23, pp. 163-177, 1995.
- [45] R. C. Dugan, M.F. McGranaghan, S. Santoso and H. W. Beaty, Electrical Power Systems Quality. Tata McGraw Hill Education New Delhi, 2nd. Ed. 2010.
- [46] Ann-Marie Borbely and Jan F. Kreider, Distributed Generation The Power Paradigm for the New Millennium. CRC press, Washington, D.C. 2001.
- [47] G. K. Singh, "Self-excited induction generator research – a survey," *Electric Power System Research*, vol. 69, no.2-3, pp. 107-114, May 2004.
- [48] R. C. Bansal, "Three Phase self excited induction generator: an overview," *IEEE Trans. on Energy Conversion*, vol. 20, no.2, pp. 292-299, June 2005.
- [49] R. C. Bansal, T. S. Bhatti and D. P. Kothari, "Bibliography on the application of Induction Generator in Non- Conventional energy systems," *IEEE Trans. on Energy Conversion*, vol. EC-18, no.3, pp. 433- 439, Sept. 2003.
- [50] D. B. Watson and I. P. Milner, "Autonomous and Parallel operation of self excited induction generator," *International Journal of Electrical Engineering Education*, vol.22, pp.365-374, 1985.
- [51] A. H. Al-Bahrani and N. H. Malik, "Steady State Analysis of parallel operated self-excited induction generator," *IEE Proceedings, Pt. C.* vol. 140, no.1, pp. 49-55, 1993.
- [52] E. G. Marra, and J. A. Pomilio, "Self-excited induction generator controlled by a VS-PWM bi-directional convertor for rural applications," *IEEE Trans. on Industry Applications*, vol. 35, no. 4, pp.877-883, July/August 1999.
- [53] R. Bonert and S. Rajakaruna, "Self-excited induction generator with excellent voltage and frequency control," *Proc. Inst. Elect. Eng. Gen. Transm. Distrib.*, vol. 145. No.1 pp.33-39, January 1998.
- [54] E. Suarez and G. Bortolotto, "Voltage – Frequency control of a self excited induction generator," *IEEE Trans. Energy. Convers.*, vol. 14, no.3, pp. 394- 401, Sept.1999.
- [55] B. Singh, S. S. Murthy and S. Gupta, "Analysis and implementation of an electronic load controller for a selfexcited induction generator," *Proc. Inst. Elect. Eng., Gen. Transm. Distrib.*, vol. 151, no.1, pp. 51-60, Jan 2004.
- [56] B. Singh, S. S. Murthy and S. Gupta, " Transient analysis of self excited induction generator with electronic load controller supplying static and dynamic loads," *IEEE Trans. Ind. Appl.*, vol. 41, no. 5, pp. 1194-1204, Sept.2005.
- [57] B. Singh, S. S. Murthy and S. Gupta, "Analysis and design of electronic load controller for self excited induction generators," *IEEE Trans. Energy Convers.* Vol. 21, no. 1, pp. 285-293, Mar. 2006.
- [58] B. Singh, S. S. Murthy and S. Gupta, "A Voltage and Frequency Controller for self excited induction generator," *Elect. Power Compon. and Syst.* Vol. 34, no. 2, pp. 141-157, Feb 2006.
- [59] J. A. Barrado and R. Grino, "Voltage and Frequency control for a self excited induction generator using a 3-phase 4-wire electronic converters," *in Proc. 12th Int. IEEE Power Electronics Motion Control Conf. Aug. 2006*, pp. 1419-1424.
- [60] B. Singh, S. S. Murthy and S. Gupta, "STATCOM based voltage regulator for self-excited induction generator feeding non-linear loads," *IEEE Trans. Ind. Electron.* Vol. 53, no. 5, pp. 1437-1452, Oct. 2006.
- [61] B. Singh, S. S. Murthy and S. Gupta, "Analysis and Design of STATCOM based voltage regulator for self-excited induction generator," *IEEE Trans. Energy Convers.* Vol. 19, no. 4, pp. 783-790, Dec. 2004.
- [62] M. B. Brennen and A. Abbondati, " Static exciter for induction generator," *IEEE Trans. Ind. Appl.* Vol. 13, no.5, pp. 422-428,Sept. 1977.
- [63] G. Ledwich and A. Ghosh "A flexible DSTATCOM operating in voltage or current control mode" *IEE Proc.-Gener. Trunsm. Disrrhh. Vol. 149, No. 2, Murcli 2002.*
- [64] H. Nasiraghdam A. Jalilian "Balanced and Unbalanced Voltage Sag Mitigation Using DSTATCOM" *Dept of*

- Elec Eng, Iran University of Science and Technology (IUST) Tehran, Iran.*
- [65] B. Singh, A. Adya, J. Gupta, "Power Quality Enhancement with DSTATCOM for Small Isolated Alternator feeding Distribution System", Power Electronics And Drive Systems 2005, (PEDS 2005), Vol1, 16-18 Jan, Pages: 274-279.
- [66] W. L. Chen, Y. Hsu, "Direct Output Voltage Control of a Static Synchronous Compensator Using Current Sensor less d-q Vector-Based Power Balancing Scheme", Transmission and Distribution Conference and Exposition 2003 IEEE 2003 PES, Vol 2., 7-12 Sept, Pages 545-549.
- [67] H. Seong, K. Nam, "Dual Current Control Scheme for PWM Converter Under Unbalanced Input Voltage Condition" IEEE Trans. On Indust.Electronics, Vol.46, No. 5, Oct. 1999.
- [68] C. Hochgraf, R. Lasseter, "Statcom Controls for Operation with Unbalanced Voltages" IEEE Trans, On Power Delivery, Vol. 13, No. 2, April 1998.
- [69] Sachin Goyal, *Student Member, IEEE*, Arindam Ghosh, *Fellow, IEEE* and Gerard Ledwich, *Sr. Member, IEEE* "A Hybrid Discontinuous Voltage Controller for DSTATCOM Applications" *IEEE Power Engineering Society General Meeting 2008*, Pittsburgh USA.
- [70] A. Ghosh and G. Ledwich, Power Quality Enhancement Using Custom Power Devices: Kluwer Academic Publishers, 2002.
- [71] A. Ghosh and G. Ledwich, "Load compensating DSTATCOM in weak AC Systems," IEEE Transaction on Power Delivery, vol. 18, pp. 1302- 1309, October 2003.
- [72] B. Singh, K. Al-Haddad, and A. Chandra, "A Review of Active Filters for Power Quality Improvement," IEEE Transaction on Industrial Electronics, vol. 46, pp. 960-971, 1999.
- [73] K Hussain1, J Praveen " Voltage Sag Mitigation Using Distribution Static Compensator System" International Journal of Engineering and Technology Volume 2 No. 5, May, 2012.
- [74] Lin Xu, Yang Han, Chen Chen, Jun-Min Pan, Gang Yao, Li-Dan Zhou, M. M. Khan "Modeling, Control and Experimental Investigation of a Novel DSTATCOM Based on Cascaded H-bridge Multilevel Inverter" ISSN 0005-1144 ATKAFF 51(1), 41-54(2010)
- [75] Y.UDAYKIRAN, S. RADHA KRISHNA REDDY, JBV Subrahmanyam " A Novel Approach On Instantaneous Power Control of D-STATCOM with Consideration of Power Factor Correction" International Journal of Engineering Research and Applications (IJERA) Vol. 2, Issue 3, May-Jun 2012, pp. 166- 170.
- [76] H. Akagi, *Instantaneous Power Theory and Applications to Power Conditioning*, New Jersey, USA.: Wiley, 2007.
- [77] J. A. Momoh, *Electric Power Distribution, Automation, Protection and Control*, New York, USA: CRC Press, 2008.
- [78] M. SajediHir, Y. Hoseinpoor, P. MosadeghArdabili, T. Pirzadeh "Analysis and Simulation of a D-STATCOM for Voltage Quality Improvement" Australian Journal of Basic and Applied Sciences, 5(10): 864-870, 2011 ISSN 1991-8178.
- [79] Gregory F. Reed, Ph.D. - Member IEEE ,Masatoshi Takeda, Ph.D. - Member, IEEE Fred Ojima, P.E. - Member, IEEE "APPLICATION OF A 5 MVA, 4.16 kV D-STATCOM SYSTEM FOR VOLTAGE FLICKER COMPENSATION AT SEATTLE IRON& METALS"
- [80] Irena Wasia, Rozmyslaw Mienski, Ryszard Pawelek, Piotr Gburczyk "Application of DSTATCOM compensators for mitigation of power quality disturbances in low voltage grid with distributed generation" Institute of Electrical Power Engeering Technical University of Lodz.
- [81] Bhattacharya Sourabh "Applications of DSTATCOM Using MATLAB/Simulation in Power System" *Research Journal of Recent Sciences* Vol. 1(ISC-2011), 430-433 (2012).
- [82] B.Rajani, P.Sangameswara Raju "Enhancement of Power Quality By Optimal Placement of Dstatcom For Voltage Sag Mitigation Using Ann Based Approach" International Journal of Soft Computing and Engineering (IJSCE) ISSN: 2231-2307, Volume-2, Issue-3, July 2012 424 .
- [83] Ambarnath Banerji, Sujit K. Biswas, and Bhim Singh "Fuzzy Logic Based Window Operation of DSTATCOM for an Autonomous Asynchronous Generator" International Journal on Electrical Engineering and Informatics - Volume 3, Number 4, 2011.
- [84] S. Heier, Grid Integration of Wind Energy Conversion Systems, New York: Wiley, 1998.
- [85] M.G. Simoes and F. A. Farret, Renewable Energy Systems, Orlando Fl. : CRC, 2004.
- [86] S. N. Bhadra, D. Kastha, and S. Banerjee, Wind Electrical Systems, New Delhi: OxfordUniversity Press 2007.
- [87] V.Quaschning, "Understanding Renewable Energy Systems," London, UK:EARTHSCAN, 2005.
- [88] S. Sharma and B. Singh, "Isolated Wind Energy Conversion with Asynchronous Generator for Rural Electrification," in Proc. *IEEE PEDES*, Dec. 2010, pp.1-7.
- [89] E.G. Marra and J.A. Pomilio, " Self-Excited Induction Generator Controlled by a VSPWM Bidirectional Converter for Rural Applications," *IEEE Trans. on Ind. App.*, vol. 35, no. 4, pp. 877-883, July/ Aug.1999.
- [90] S. S. Murthy, B. Singh, A. Kulkarni, R. Sivarajan and S.Gupta, " Field Experience on a Novel Pico-Hydel System Using Self Excited Induction Generator and Electronic Load Controller," in Proc. *IEEE PEDS 2003, Fifth international Conf.* on, vol. 2, pp. 842-847.
- [91] Dr. M. Vijay Kumar,,Dr. V.C.Veera Reddy,T.Devaraju "Modeling and Simulation of Custom Power Devices to

- Mitigate Power Quality Problems" International Journal of Engineering Science and Technology Vol. 2(6), 2010, 1880-1885.
- [92] H. Hingorani "Introducing Custom Power" IEEE Spectrum, vol.32 no.6 June 1995 p 41-48.
- [93] Dr. V.C.Veera Reddy ,Dr. M. Vijaya Kumar, T.Devaraju "Role of custom power devices in Power Quality Enhancement" International Journal of Engineering Science and Technology Vol. 2(8), 2010, 3628-3634.
- [94] Anaya-Lara,O.,E.Acha,2002.Modeling and analysis of custom power systems by PSCAD/EMTDC.IEEE Trans..Power Delivery, Issue, 17; 266-272.
- [95] K.Sri chandan, T.Sandhya ,Research Scholar, "Mitigation of Output Power Fluctuations in Utility Grid using Three Phase Distribution Generation" K.Sri chandan et al./International Journal of Engineering Science and Technology Vol 2(12), 2010, 7710-7718.
- [96] F. Gharedaghi, H. Jamali, M. Deysi, A. Khalili "Investigation of D-Statcom Operation in Electric Distribution System" *J. Basic. Appl. Sci. Res.*, 1(12)2900-2907, 2011.
- [97] Esfandiari A and M. Parniani, 2004. "Electric arc furnace power quality improvement using shunt active filter and seriesinductor," IEEE Region10 Conference, 4: 105-108.
- [98] Montanari G.C, M. Loggini, L. Pitti, E. Tironi and D. Zaninelli, 1993. "The effects of series inductors for flicker reduction in electric power systems supplying arc furnaces," IEEE Industry Applications Society and Annual Meeting,1496-1503.
- [99] Marshall M.W, 1997. "Using series capacitors to mitigate voltage flicker problems," 41st Annual Rural Electric Power Conference, pp B3-1-5.
- [100] Olimpo Anaya-Lara and E. Acha "Modeling and Analysis of Custom Power Systems by PSCAD/EMTDC" IEEE TRANSACTIONS ON POWER DELIVERY, VOL. 17, NO. 1, JANUARY 2002.
- [101] "Introducing custom power," IEEE Spectrum, vol. 32, pp. 41–48,June 1995.
- [102] S. Nilsson, "Special application considerations for Custom Power systems," in Proc. IEEE Power Eng. Soc., Winter Meeting 1999, vol. 2. 1999, pp. 1127–1130.
- [103] Madhusmita Das, Mrs. Varsha Singh, Dr. Swapnajit Pattnaik "GA For Improved Dynamic Response Of DSTATCOM" International Journal of Engineering Research and Applications (IJERA) ISSN: 2248-9622 Vol. 2, Issue 3, May-Jun 2012, pp.2145-2152.
- [104] Hung-ChiTsai and Chia-Chi Chu; Nonlinear STATCOM Controller using Passivity-Based Sliding Mode Control , IEEE APCCAS, 4-7 Dec. 2006 Page(s):1996-1999.
- [105] Yazdani, A., Crow, M.L.,and Guo, J.,. A comparison of linear and nonlinear STATCOM control for power quality enhancement, IEEE Power and Energy Society General Meeting-conversion and Delivery of Electrical Energy in the 21st Century, 20-24 July 2008 Page(s):1-6.
- [106] Sanders, S.R., Noworolski, J.M., Liu, X.Z.,and Verghese, G.C., Generalized averaging method for power conversion circuits , *IEEE Transaction on Power Electronics*, Vol. 6,April 1991 page(s):251-259.
- [107] P. Petitclair, S. Bacha, and J. P. Rognon., Averaged modeling and nonlinear control of an ASVC (advanced static VAr compensator), in Proc. *IEEE/PESC'96 Annu.. Meeting*, Jun. 1996, pp.753-758.
- [108] Petitclair,, P..Bacha, and S. Ferrieux. Optimized linearization via feedback control law for a STATCOM ,In *IEEE industry Applications Conference Volume 2*, 5-9 Oct. 1997 page(s):880-885.
- [109] Zhichang Yuan, Qiang Song, Wenhua Liu, and Qingguang Yu . Nonlinear Controller for Cascade H-Bridge Inverter-Based STATCOM In *IEEE Transmission and Distribution Conference 2005* page(s):1 -5.
- [110] J.E.Slotine, and W.Li. *Applied nonlinear control.* (Prentice Hall, New Jersey,1991).
- [111] Bhim Singh, P. Jayaprakash* and D. P. Kothari."Three-Leg VSC and a Transformer Based Three-Phase Four-Wire DSTATCOM forDistribution Systems" Fifteenth National Power Systems Conference (NPSC), IIT Bombay, December 2008.
- [112] *IEEE Recommended Practices and Requirements for Harmonics Fig. 7 Load current and the harmonic spectrum Control in Electric Power Systems*, IEEE Std. 519, 1992. Fig. 8 Source current and the harmonic spectrum Fig. 9 Voltage at PCC and the harmonic spectrum.
- [113] A.Ghosh and G. Ledwich, *Power Quality Enhancement using Custom Power Devices*, Kluwer Academic Publishers, London, 2002.
- [114] R. C. Dugan, M. F. McGranaghan and H. W. Beaty, *Electric Power Systems Quality*. 2ed Edition, McGraw Hill, New York, 2006.
- [115] H. Akagi, E H Watanabe and M Aredes, *Instantaneous power theory and applications to power conditioning*, John Wiley & Sons, New Jersey, USA, 2007.
- [116] Antonio Moreno-Munoz, *Power Quality: Mitigation Technologies in a Distributed Environment*, Springer-Verlag London limited, London, 2007.
- [117] Ewald F. Fuchs and Mohammad A. S. Mausoum, *Power Quality in Power Systems and Electrical Machines*, Elsevier Academic Press, London, UK, 2008.
- [118] Irena Wasik, Rozmyslaw Mienski, Ryszard Pawelek, Piotr Gburczyk "Application of DSTATCOM compensators for mitigation of power quality disturbances in low voltage grid with distributed generation".
- [119] Ganesh Prasad Reddy , K. Ramesh Reddy "Neutral Point Diode Clamped Multi DSTATCOM by Using Fuzzy Gain Scheduling P Fuzzy Logic Controllers" International Journal of Computer Applications (0975 – 8887)Volume 8– No.10, October 2010.

- [120] A. Dell'Aquila, G. Delvino, M. Liserre, P. Zancheta, A new fuzzy logic strategy for active power filter, power electronics and variable speed drives, 18-19 September 2000, Conference Publication No. 475, pp. 392-397.
- [121] S.K. Jain, P. Agrawal, H.O. Gupta, Fuzzy controlled shunt active filter for quality improvement, IEEE. Pro. Electr. Power Appl. 149 (September (5))(2002)317-328.
- [122] C. Charmeela, M.R. Mohan, G. Uma, J. Baskaran, Fuzzy logic controller based three-phase shunt active filter for line harmonics reduction, J. Comput. Sci. 3(2) (2007)76- 80 (ISSN 1549-3636).
- [123] S. Saad, L. Zellouma, L. Herous, Comparison of fuzzy logic and proportional controller of shunt active filter compensating current harmonics and power factor, in: Proceedings of the 2nd International conference on Electrical EngineeringDesign and Technology ICEEDT08, Hammamet, Tunisia, November 8-10, 2008.
- [124] L. Zellouma, S. Saad, Fuzzy logic controller for three phase shunt active filter compensating harmonics and reactive power simultaneously, in: Proceedings of the International Conference on Computer Integrated Manufacturing CIP', Setif, Algeria, 03-04 November, 2007.
- [125] Dr. M. Rajaram , D. Murali "Simulation and Implementation of DVR for Voltage Sag Compensation" International Journal of Computer Applications (0975 – 8887) Volume 23– No.5, June 2011.
- [126] S Ramana Kumar Joga , M. Praveen , B. Durga Prasad " A power quality Improvement of Mitigating Neutral current for VSC Based DSTATCOM Using TIES" International Journal of Engineering Research and Applications (IJERA) Vol. 2, Issue 1,Jan-Feb 2012, pp.579-585.
- [127] D.Sree Vani, K.Gopala Krishna "A Fast-Acting DC-Link Voltage Controller for Three-Phase DSTATCOM to Compensate AC and DC Loads USING FUZZY LOGIC" International Journal of Engineering Research and Applications (IJERA) Vol. 2, Issue 3, May-Jun 2012, pp.2723-2733.
- [128] Miss Sobha rani Injeti, K. Ratna Raju "Power Quality Improvement by UPQC device in Doubly Fed Induction Generator Wind Farm to Weak-Grid Connection" International Journal of Scientific & Engineering Research Volume 2, Issue 12, December-2011 1 ISSN 2229-5518 .
- [129] R.C. Dugan, M.F. McGranahan, S. Santoso, H.W. Beaty —Electrical Power Systems Quality 2nd Edition McGraw-Hill, 2002. ISBN 0-07-138622-X.
- [130] P. Kundur —Power System Stability and Control McGraw-Hill, 1994. ISBN 0-07-035958 .
- [131] Z. Saad-Saoud, M.L. Lisboa, J.B. Ekanayake, N. Jenkins and G. Strbac —Application of STATCOM's to wind farms IEE Proc. Gen. Trans. Distrib. vol. 145, No. 5; Sept. 1998.
- [132] Zakaria Anwar Zakaria; Baichao Chen and Mohammed Osman Hassan"Transient Studies of Custom Power Equipments and Static Var Compensator Using PSCAD"International Journal of Electrical and Electronics Engineering 2:11 2008.
- [133] Rodda Shobha Rani, B. Jyothi "VSC Based DSTATCOM & Pulse-width modulation for Power Quality Improvement" International Journal of Engineering Trends and Technology- Volume2Issue2-2011.
- [134] E.Rambabu, E.Praveena, Prof.P.V.Kishore "Mitigation of Harmonics in Distribution System Using D – STATCOM"International Journal of Scientific & Engineering Research Volume 2, Issue 11, November-2011.
- [135] Yash Pal, A. Swarup, Senior Member, IEEE, and Bhim Singh Fellow, IEEE, "Applications of UPQC for Power Quality Improvement"16th NATIONAL POWER SYSTEMS CONFERENCE, 15th-17th DECEMBER, 2010.
- [136] S. K. Khadem, M. Basu and M. F. Conlon, "Integration of UPQC for Power Quality Improvement in Distributed Generation Network – A Review", ISGT Europe 2011, Manchester UK, Dec 2011.
- [137] Karuppanan P , Rajasekar S , KamalaKanta Mahapatra "Cascaded Multilevel Voltage Source Inverter based active power filter for Harmonics and Reactive power compensation" INTERNATIONAL JOURNAL OF APPLIED ENGINEERING RESEARCH, DINDIGUL Volume 1, No 4, 2011.
- [138] PANKAJ KUMAR GOSWAMI, GARIMA GOSWAMI "A PWM CONTROLLED SYNCHRONOUS LINK CONVERTER SCHEME FOR POWER QUALITY IMPROVEMENT AT NONLINEAR LOAD" International Journal of Engineering Science and Technology (IEST).
- [139] Mahesh A. Patel, Ankit R. Patel, Dhaval R. Vyas and Ketul M. Patel"Use of PWM Techniques for Power Quality Improvement", International Journal of Recent Trends in Engineering, Vol. 1, No. 4, May 2009.
- [140] Nicolás Louzán Pérez, Manuel Pérez Donsión "Technical Methods for the Prevention and Correction of Voltage Sags and Short Interruptions inside the Industrial Plants and in the Distribution Networks" INTERNATIONAL CONFERENCE ON RENEWABLE ENERGY AND POWER QUALITY.
- [141] M. Davudi, S. Torabzad, B. Ojaghi "Power Quality and Power Interruption Enhancement by Universal Power Quality Conditioning System with Storage Device" Australian Journal of Basic and Applied Sciences, 5(9): 1180-1187, 2011.
- [142] N.Radhakrishnan, M.Ramaswamy "A Fuzzy based DSP Implementation for Power Quality Improvement of a three phase AC-AC Converter" International Journal of Computer Applications (0975 - 8887) Volume 1 – No. 24, 2010.
- [143] R V D Rama Rao , Dr.Subhransu Sekhar Dash "Enhancement of Power Quality by using Unified Power Quality Conditioner with PID and Fuzzy Logic

- Controller” *International Journal of Computer Applications (0975 – 8887) Volume 5– No.7, August 2010.*
- [144] Thip Manmek, Colin Grantham and Toan Phung “A REAL TIME POWER HARMONICS MEASURING TECHNIQUE UNDER NOISY CONDITIONS” School of Electrical Engineering and Telecommunication. The University of New South Wales.
- [145] T. Manmek, C. Grantham and B. T. Phung, “ A Novel technique for real time voltage and current harmonic estimation based on the singular value decomposition method”, in Proceeding of the Australasian Universities Power Engineering Conference (AUPEC’2003), Christchurch New Zealand, September 2003, ISBN:0-473-09867-9.
- [146] B.C. Kok, M.S. Looi, H.H. Goh, “Insulated Gate Bipolar Transistor Failure Analysis in Overvoltage Condition” International Conference on Renewable Energies and Power Quality (ICREPQ’12) Santiago de Compostela (Spain), 28th to 30th March, 2012.
- [147] Bollen M.H. J., “Understanding Power Quality Problems”, IEEE Press, Inc. New York, 2000, pp. 139-248.
- [148] Torbjorn Thiringer Student Member“Power Quality Measurements Performed on a Low-Voltage Grid Equipped with Two Wind Turbines” IEEE Transactions on Energy Conversion, Vol. 11, No. 3, September 1996.
- [149] R. Omar, N.A. Rahim and A. Ahmad “Voltage Swells Improvement in Low Voltage Network Using Dynamic Voltage Restorer” American Journal of Applied Sciences 8 (1): 55-62, 2011.
- [150] Perera, M.V.K., 2007. Control of a Dynamic Voltage Restorer to Compensate Single Phase Voltage Sags. Master of Science Thesis Stockholm, Sweden. <http://www.docstoc.com/docs/43551112/Controlof-a-Dynamic-Voltage-Restorer-to-compensate-single>.
- [151] Hingorani N. G. 1995 “Introducing custom power ,” IEEE Spectrum, 1(6): pp 41-48.
- [152] Song Y. H. and A. T. Johns, “Flexible AC transmission system (FACTS),” 1st Ed. United Kingdom: IEEE Press, pp. 39-49, 1999.
- [153] Hingorani N.G. and L. Gyugyi, “ Understanding FACTS: Concepts and Technology of Flexible AC Transmission Systems,” New York IEEE Press, 135-143.
- [154] IEEE PES working Group FACTS Applications, 1996, IEEE Press, (96).
- [155] Reed G. F.,Takeda M. and Iyoda I., “Improved power quality solutions using advanced solid-state switching and static compensation technologies,” IEEE Power Engineering Society, Winter Meeting, New York, NY, USA, IEEE, 2: 1132-1137,1999.
- [156] Taylor G.A., “ Power quality hardware solutions for distribution Systems: Custom Power,” IEEE North Eastern Center Power Section Symposium, Durham, UK,11/1-11/9.
- [157] Schauder C.D. and H. Mehta, “Vector analysis and control of advanced static var compensators,” IEEE Proceedings- C,140(4): 299-306, 1993.
- [158] Esfandiriani A. and M. Parniani, “ Electric arc furnace power quality improvement using shunt active filter and series inductor,” IEEE Region 10 Conference, 4: 105-108.
- [159] Montanari G.C, M. Loggini, L. Pitti, E. Tironi and D. Zaninelli, “ The Effects of series inductors for flicker reduction in electric power systems supplying arc furnaces,” IEEE Industry Applications Society and Annual Meeting,1496-1503,1993.
- [160] Marshall M.W,”Using series capacitors to mitigate voltage flicker problems,” 41st Annual Rural Electric Power Conference, pp.B3-1-5.

Smart Grid wide area power system Load Protection schemes

A. Mrs. Chandarani , B. Dr. K. S. Verma , C. S. P. Singh

Finally this paper shows islanding operation through WAM and results have been verified in MATLAB.

Abstract-- Operation of modern power system specifically under the emerging electric market scenario has become a challenging task. The system may often operate under stressed condition to meet the ever increasing demand due to comparatively limited expansion of its transmission network. Thus it has become more important to optimally utilize available resources and equipment with well design and coordinated protection and control schemes to deal with wide spread disturbance. Traditionally many of existing protection scheme have utilized only local data for disturbance analysis. The recent development in communication technology and synchrophasor measurement have made the design of system wide protection solution possible. Special protection scheme utilizing wide area measurement system (WAMS) is being popularly used to prevent the power system from large disturbance. These wide area protection scheme mainly focus on avoiding frequency instabilities ,voltage instabilities and rotor angle instabilities.

Synchrophasor measurement technique are divided in to two groups Off -line application and On-line application .Off-line applications are usually use to improve and validate the system model to make system planning. Online application are monitoring phase angle and power flow ,voltage magnitude, system frequency, real and reactive power across grid, inter area oscillation monitoring in wide area . Power system frequency is one of the most valuable information for online assessment of system stability . The system frequency is direct measure of balance between generation and demand during the large disturbance the system frequency is rapidly varying in different part of bulk system. Therefore power system operator require an accurate wide area frequency measurement system and adaptive frequency control scheme for large disturbance. In this research paper wide area power system load protection scheme and ensuring design requirement that enhances stability as well as protection and control schemes using traffic between generating units ,server ,connected loads and protection devices using TCP/IP.

Faults detected in Local Areas is communicated to Load Area Manager which takes control action to handle it.

¹

Index terms-- Wide area power system load protection, adaptive frequency control.

I. Introduction:

World wide power system are frequently being operated for maximum economy with possible sacrifice for traditional stability margins . Long lines between generators and loads, changed in generation mix and increase in inter connection have complicated to use of older tools for stability analysis . System disturbances and black out at locations throughout the world have demonstrated the need to simplify how system operators obtain situational awareness necessary to maintain stability and optimize economy. Synchronize phasor measurement provide a new method for improvement visualization of system condition in wide area control . Several discussion on methods that are being used to visualize, analyze and control power system using WAMPSCS. Simple value such as voltage angle ,line flows and breaker status can be viewed real time [1].The disturbance caused by voltage instability in the transmission network has significantly contributed to major blackouts around the world. Its timely identification is very crucial to allow effective control and protection scheme .On this concern a world wide interest in defining effective real time voltage stability by measuring the local voltage and current phasors at an extra high voltage bus .The voltage instability analysis can be performed by considering the classic Thevenin equivalent . The new method depends on the requirement given by system operation and control condition . The N-1 criterion would be described using measurement at either ends and reduced equivalent network can be constructed and use for analytical stability assessment [1-7]. Traditionally many of existing protection schemes have utilized any local data for disturbance analysis . But recent development in communication technology and synchro phasor measurement have made the design of wide area protection solutions .

-
- A. Ph. D Scholar, EED, KNIT Sultanpur
 - B. Professor, EED, KNIT Sultanpur
 - C. Assistant Professor, EED, KNIT Sultanpur

WAMS assisted frequency and voltage stability based adaptive load shedding scheme implemented to decided optimal load shedding , optimal solution for post contingency state [2].

The new approach of load frequency control to decreasing regulating capacity with providing tolerance of frequency fluctuation was analyzed by author Keita Katsura. In this load estimation mechanism is based and it is made to decrease tolerance of frequency fluctuation and tie-line power flow .Load frequency control that decreasing the regulating capacity is proposed in refered research .Non reheat and reheat thermal power LFC power plant in which the area consists of 3 area models.Then random distribution which simulated on load fluctuation in morning and evening is made to arise the model system. By the deviation of disturbance power in load estimation mechanism Fuzzy control is used. Maximum value of random disturbance on the frequency variation is concluded by considering economical load dispatch control[20].

Power system dynamics response for real time transient stability prediction by author James Thorp proposed on IEEE 39 Bus system .In this three phase short circuit to ground faults were simulated on various transmission line.The post fault and pre fault conditions are analyzed and it can be the both current load equivalent and admittance equivalent can predict the swings in real time . Several decoupled integration algorithms like runga-kuttae used for this research[21].

Frequency stability is a part of power system reliability to overcome drastically decreasing performance of frequency.Adaptive load shedding method based on Neural Network was elaborated by author Mauridhi to anticipate and enhance the time response>Loading through UFR means reducing load until balance or standard frequency operation is reached.The schemes are occupied to cut the connected load to a level that can be safely supplied by serviceable generation. In authors analysis Neural network is successfully implemented for signal processing,optimization and intelligent control[22].

Under frequency load shedding UFLS is used in the power industry to resume system facing extreme disturbances to avoid system collapse.An adaptive UFLS method based on Genetic algorithm was developed for finding optimal parameters to minimize

the repetitive trial and error calculations .Simulation demonstrates that the method has better performance than previous schemes and reduces the time and effort of repetitive

simulation .The multi objective optimization successfully optimized f_{\min} , minimized the final frequency overshoot. The GA scheme resulted in less load shed thus , less customers are affected by power interruption[23].

The advent of WAMS and better inter substation communication makes it possible to greatly improve existing protection schemes .One most complex protection scheme is out of step (OOS) protection .Generator angles are periodically tracked by a central controller to identify out of step criteria [6].

In the circumstances dynamics of frequency oscillation and its control become important issue for power system engineers . Based on synchronizing method and Discrete fourier transform (DFT) algorithm time synchronized voltage and current phasor measurement technologies have been developed .System dynamics due to load frequency control (LFC) is extracted from time frequency based wavelet transform [8].

Dynamic parameter indentified on generator for smart grid by author Yunzhi Gheng ,explained hybrid method combing Particle Swarm Optimization (PSO) and Sensitivity Analysis (SA) .In this hybrid Method provides the right balance between convergence and computation speed.The simulation results match the measured curve by adjusting the exciter and governor parameter .It can be formulated as the non-linear curve fitting problem solved by weighted least square methods. Simulation results are carried out on a plant with two identical generators in ERCOT system .In these test case the short circuit fault event is analyzed by sensitivity analysis .Using historical data for each parameter mismatch index between original curve of reactive or active power output .Multicore processor with parallel programming increases speed of method[17].

Recently Similar strategies are implemented for dynamic stability monitoring and model validation in ERCOT by author Jian chen .Post event analysis and small signal stability conditions by monitoring phase angle and oscillation are simulated on real time monitoring software. To validate the existing dynamic model of conventional wind generator .Results shows the simulation and PMU data for low wind output with poorly damped voltage response .Based on the finding in off-line studies and tunning of wind dynamic model to recreate PMU recorded oscillatory response in real time event the voltage regulator of the wind power plant was identified as key cause of oscillations .The oscillatory response is combination of weak grid condition and aggressive voltage control of wind power plant. As

results the potential solutions to mitigate these oscillations include the improvement of system strength and tuning of wind voltage controller [18].

Several work reported in the literature on wide area measurement and protection and control scheme on frequency instability, voltage instability and rotor angle instability .To track slow and dynamic disturbances Fourier transform technique, Probability analysis, Eigen value analysis reported in review study of WAMS scheme. However when real time performance are require these method do not give satisfactory outcome and in this situation fast fourier transform based methods are preferable for its availability and simplicity to implement in DSP.

The new approach of Artificial intelligence (AI) techniques such as neural networks ,fuzzy logic system are being well recognized tool in power system application.

III.Research Problem Formulation:

Wide Area Protection and Fast Control Applications and Benefits

A smart grid system need to have its underlining protection system to be adaptive such a protection system will be capable of changing its characteristics according to system conditions and wide area measurements .Different strategies for the same will be worked out.

Implementing Adaptive load shedding scheme considering frequency instability and voltage instability of system simultaneously through optimal load shedding in availability of WAMS measurements.

- To develop dynamic model of power system and decides optimal load shedding based on frequency instability as well as voltage instability consideration.
- To find disturbance power /power mismatch in contingency case.
- To find severity of disturbance based on frequency instability
- To find an optimal locations and magnitude of load curtailments according to a dynamic voltage stability
- To evaluating stability margins at each load bus.
- To implement load shedding frequency control methods.
- To optimal re-dispatching of generators.

Following steps will be followed:

Review of existing wide area measurement protection and control solutions emphasis on applications, system architecture and technology point of view .

Developing a generic model of power system for determining proposed research on WAMPSCS.

Developing new applications and algorithms for improving voltage and frequency stability.

Establishing a simulating platform for demonstrating and evaluation the operation of wide area monitoring protection and control system using MATLAB .

The purpose of Power System Load Protection Model is to keep the power system stable by isolating only the components that are The under fault, whilst leaving as much of the network as possible still in operation. Joachim Bertsch, Cedric Carnal, Daniel Karlsson, John McDaniel, and Khoi Vu [24] integrate the local protection center into wide solution with System Protection Scheme. These local protection centers forms System Protection Scheme, while the interconnected coordinated system forms a defense plan [8], [9]. Protection systems against voltage instability can use simple binary signals such as —low voltage|| or more advanced indicators such as power transfer margins based on the VIP algorithm [10] or modal analysis. Transients in substations[11] may result in current surges through the substation grounding system. Ground Potential Rise can affect the communication system located near the protective relays or communication facilities outside the substation perimeter. The ElectromagneticInterface and Ground Potential Rise problem, IEEE recently developed a new standard [12] to define an optical digital interface between relay and multiplexer. IEEE [13], ANSI and IEC Standards define transient and Surge Withstand Capabilities that should be met. Protection Model must apply a very pessimistic and pragmatic approach to clear system faults to a normal state and diminish the impact ofthe disturbances, the protection and control actions are required to stop power system degradation and system wide disturbances are growing issue for the power system industry [14], [15]. Development of microprocessor protection [16] device based on IEC61850 on the high speed DSP hardware platform is an unavoidable trend for substation automation. A PLC-based load shedding scheme offers many advantages, such as the use of a distributed network using the power management system, as well as an automated means of load relief. However, in such applications monitoring of the power system is limited to a portion of the network with the acquisition of

scattered data. This drawback [17] is further compounded by the implementation of pre-defined load priority tables at the PLC level that are executed sequentially to curtail blocks of load regardless of the dynamic changes in the system loading, generation, or operating configuration. The system wide operating condition is often missing from the decision-making process resulting in insufficient or excessive load shedding. In addition, response time (time between the detection of the need for load shedding and action by the circuit breakers) during transient disturbances is often too long requiring even more load to be dropped. A number of low-power and low cost technologies have evolved to present themselves as enablers for Smart Grid communications. Among the wireless technologies, IEEE 802.15.3a — UWB [18] communications the shortcoming of this technology lies in its high power requirementsAlso, after several years of deadlock, the IEEE 802.15.3a task group was dissolved in 2006. Therefore, further support for UWB may not be possible in the future if UWB is selected as the communication technology in the Smart Grid Home Area Network. The IEEE 802.11 protocol, commonly referred to as Wi-Fi [18], is suited for higher-data-rate applications over larger areas. The main shortcoming of this technology is similar to that of UWB: the high power requirement of devices using Wi-Fi. Another shortcoming of Bluetooth is its periodical waking up and synchronization with the master device of the Pico net. IEEE 802.15.4 ZigBee [18] is a protocol employed in many home networking solutions including HANs. ZigBee was developed particularly for wireless devices, ensuring low power and long life time. The disadvantage of this technology is that it has short range communication of 10-100m. In interconnected power system communication medium should be very strong to handle the bidirectional traffic between server and clients. As server handles large amount of data and update it rapidly after millisecond so it is not easy for it to make decisions of each control and emergency signal at that specific time intervals. And delay can make power system gets unstable. Therefore for the data transferring reliable medium should be used, having large band width and speed TCP/IP is most well-liked protocol for data communication. It becomes standard protocol in modern era. It took birth in USA in late 70's by a research group and becomes the best among communication protocols. The advantages of TCP/IP networking are its Widespread usage (e.g. Internet), Hardware and software are well developed, Option of application layer protocol and simplicity, IP routing concept's inherent resilience and powerful network management. Strong client server communication architecture using TCP/IP is provided in MATLAB which enhances reliability provides intelligent

control updates wide area manager (WAM) server for each and every instant which uproots the over current and under voltage faults when exceeding required thresholds. WAM provides bidirectional wireless communication channel to local area manager (LAM) for intelligent operations. Each LAM acting as a server communicates with respective area clients through TCP/IP. The Model consists of compulsory loads spreading in the wide area (i.e. Residential, Commercial, Farm, Agricultural and Industrial), each type of loads as mentioned above are further expended into its local clients, consisting of various types of loads, specially the industry and the farm loads consisting of 3-phase motors. Through bidirectional communication, internal faults are tackled by LAM and external faults are handled by WAM.

III. WIDE AREA CONTROL DESIGN

The Wide Area smart grid Architecture for power system load protection consists of various area loads i.e. Residential, Commercial, Farm, Agriculture, and Industrial. The residential and commercial load consists of resistive and inductive loads the farm load, Agriculture load and Industrial load consisting of resistive, inductive and three-phase motor loads. The loads are controlled by wide area manager and further clients of each load are controlled by a local area manager (LAM). Control area Manager of each client receives signals from fault sensing system which send control signals to WAM through TCP/IP sender/receiver and control each area through bidirectional communication as shown in figures 3.1 Figure 3.1 consists of flow chart of the whole wide area smart grid architecture in which the generating sources composed of renewable energy resources including wind power plant and solar panels. The wide area manager is the centralized portion which is the main soul of the complete wide area smart grid architecture which got its intelligent control due to its computational engine and data user defined cases. Due to these circumstances the WAM accurately control its area using TCP/IP through bidirectional communication. The internal flow chart of industrial portion is shown in figure 3.2. Fault sensing system senses the abnormal conditions and sends signal to local controller from where the signal is processed by transmitter to the LAM through TCP/IP. Local controller and LAM shows bidirectional communication architecture in local clients. Each load as shown in the flow chart of industrial area had its own load controller, fault sensing relay system and circuit breaker. That is for the purpose of uprooting only the faulty load portion

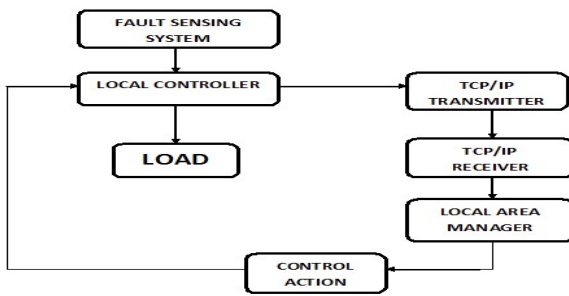


Fig 3.1 Wide Area Block Diagram

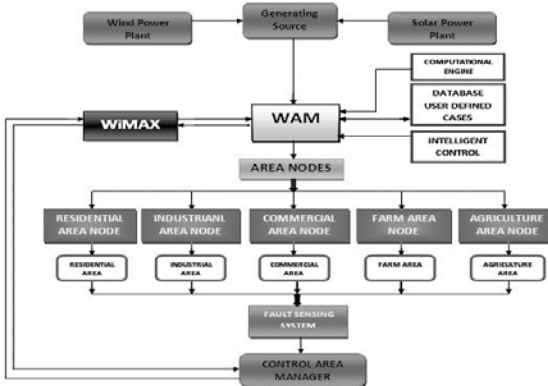


Fig 3.2 Industrial Load Block Diagram

An AC waveform can be mathematically represented by the equation:

$$x(t) = x_m \cos(\phi + \int_{-\infty}^t \omega(\tau) d\tau) \quad (1)$$

where: x_m = magnitude of the sinusoidal waveform

$\omega = 2 * \pi * f$ where f is the instantaneous frequency

ϕ = angular starting point for the waveform

Note that the synchrophasor is referenced to the cosine function. In a phasor notation this waveform is typically represented as:

$$\bar{x} = x_m \leq \phi$$

Since in the synchrophasor definition correlation with the equivalent RMS quantity is desired. A scale factor of $1/\sqrt{2}$ must be applied to the magnitude which results in the phasor representation .

$$\bar{x} = \frac{x_m}{\sqrt{2}} < \phi$$

Adding in the absolute time mark a synchrophasor is defined as the magnitude and angle of a cosine signal as referenced to an absolute point in time.

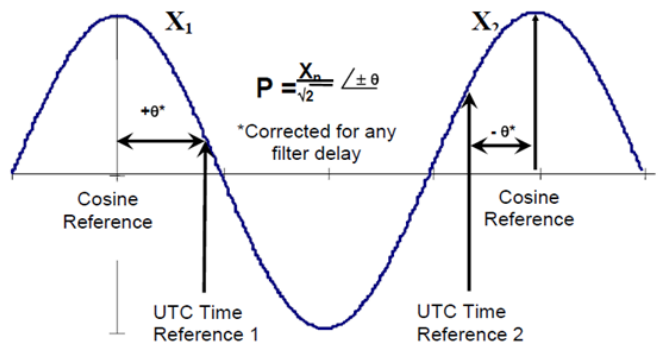


Figure 3.3: Synchrophasor Definition

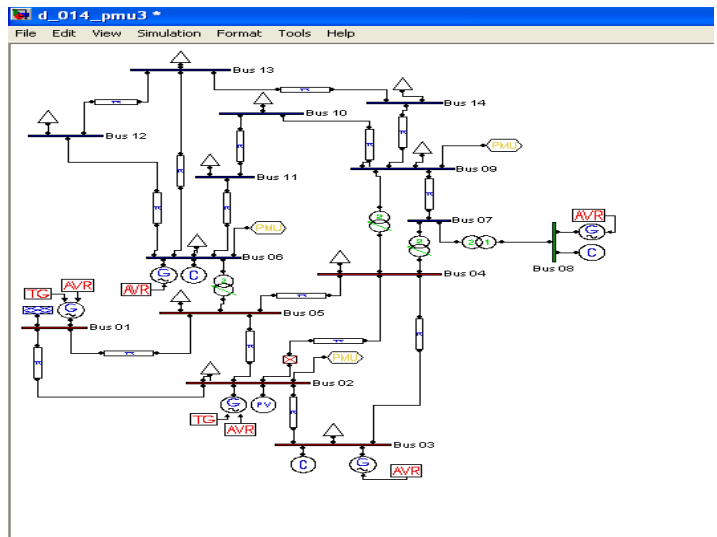


Figure 3.4: IEEE14 Bus PMU Placement using PSAT

IV. PROPOSED SYSTEM IMPLEMENTATION IN MATLAB

The complete scenario of the above mentioned smart grid architecture briefly explains the wide area power system load protection, consisting of five area loads and are controlling by wide area manager (WAM) in MATLAB/Simulink. The system given below have primary protection on the main line along with transmitter and receiver, If the secondary protection on the distribution line fails or if the fault occurs on the main primary line of the generating station then it's the primary protection to trip all the loads. While intelligent protection is one which isolates only the faulty portion, which is also implemented in all loads. The below system also show

five areas which are industrial, commercial, farm, Agricultural and Residential along with their sub-systems

The wide area manager (WAM) receiving data through receiver and sending data through transmitter. The fault sensing system send data through TCP/IP received by receiver of the WAM and sends the control signal via transmitter to the circuit breakers of each area. The internal sub-system of industrial loads is shown in figure4.3, which have three sub areas (i.e. Resistive, motor and R-L loads). The internal Local area manager controls the internal clients of each sub-load. . The internal motor load is shown, although such sub-systems along with faults are simultaneously simulated for other areas too. The internal sub-system of Industrial Motor load. The motor load consists of five motors each consisting of intelligent and smart TCP/IP transmitter and receiver along with relay and circuit breaker. When the over current fault (i.e. phase A to ground) occurs in the three-phase motor the relay sense the fault and convey the data via transmitter to receiver, there after the receiver convey the trip signal to circuit breaker. The circuit breaker operates and isolates the faulty client without the interruption of other clients load. Hence intelligent protection system is justified here because only a faulty load in the zone is isolated without the disturbance of the rest of the Areas load. The overall drift in the voltage and current wave form indicates type of fault (e.g. Phase A to ground).

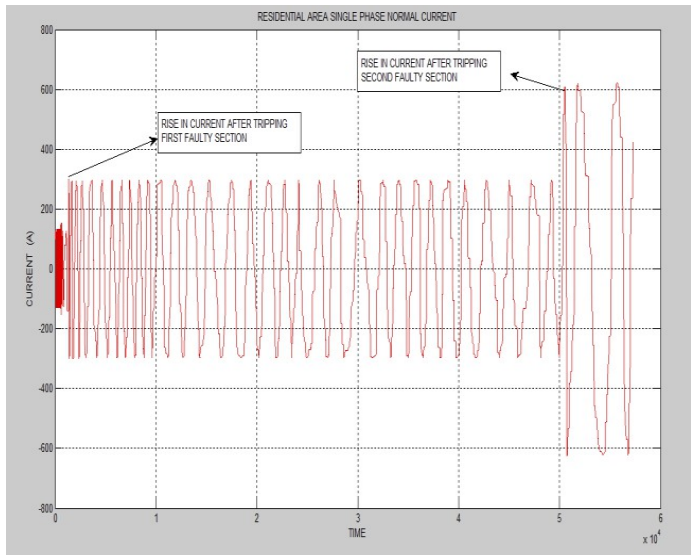


Fig 4.1 Single Phase External Residential Area Load Current

the faulty loads, which are connected parallel to the residential load. Figure 4.1 shows the Residential Area Load, single phase current graph. The Residential Area Load is normal load means no kind of any disturbance or fault occurred at this load. Figure shows that before the maximum peak, the value of current is normal, as the

fault occur the current shoots up to higher value. The reason behind the condition is by tripping

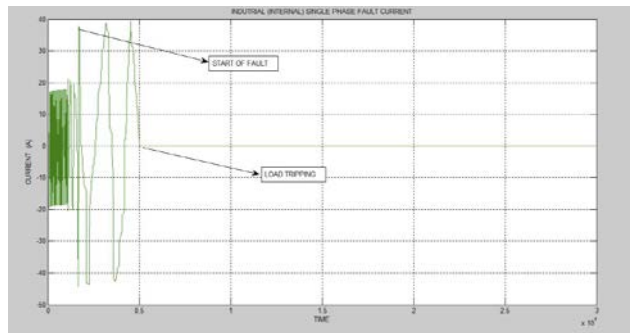


Fig 4.2 Single Phase Internal Fault Current of Industrial Load

Figure. 4.2 mention the single phase Industrial Area internal Load fault current plot. The highest peak shows the phase B to ground fault, after that the load has been tripped by tripping syste Events and protection system operation analysis includes the following checks.

1. Relay and breaker contacts state is tested for a change and indicates that the protection system has detected a fault.
2. When phase to ground fault occurs or over current fault occurs due to any other natural phenomena, the relay will sense the fault and send trip signal to TCP/IP transmitter.
3. The TCP/IP receiver will receive the tripsignal and transfer the signal to the server
4. It's the server to decide the fault occurring side and trip the faulty load through circuit breaker without any interruption in the rest of the system

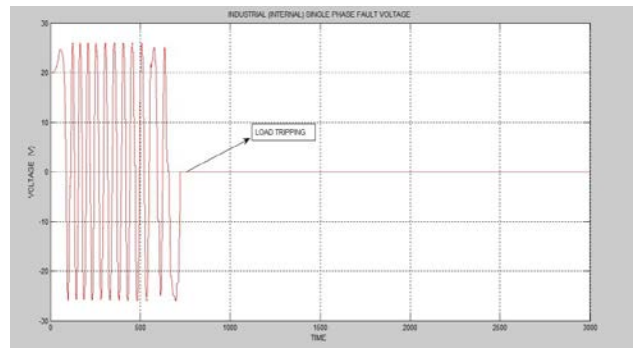


Fig 4.3 Single Phase Internal Fault Voltage of Industrial Load

VI. CONCLUSION

The use of TCP/IP in wide area has greatly improved the observe ability of the power system dynamics. Based on TCP/IP different Wide Area Power System load protection is designed in MATLAB/Simulink. This paper illustrates the benefits of Wide Area PowerSystem

load protection using TCP/IP reduced the risk of system collapse. This scheme would allow the smart grid systems operator more flexibility to operate the power system and utilize the generation resources more efficiently.

References

- [1] Bander Allaf and Roy Moxley , “ Synchrophasors for Improved interconnection operations ,” grid tech 2011-3 rd international exhibition and conference ,19-21 april 2011 ,New delhi.
- [2] Seethalekshmi .k ,S.N Singh ,S.C Srivastav , “WAMS assisted frequency and voltage stability based adaptive load shedding scheme .
- [3] A.G Phadke and J.S Thorp , “ communication needs for wide area measurement application ,”in CRIS 2010, 5th internation conference on 2010 PP-1-7.
- [4] J.De ,La Ree, V CENteno, J.S.Thorp and A.G Phadke , “ synchronized phasor measurement applications in power systems ,” smart grid ,ieee transaction on volume -1PP-20-27 ,2010.
- [5] H Hua lil,Santosh,Sandeep Sukla,James Thorp, “ study of communication and power system infrastructure inter dependent on PMU based wide area monitoring and protection,”
- [6] A Sauhats,Jkucajevs,L.Leite, A Utans, “out of step automation device model validation methodology ,”eeeic,2011,10th international conference on 2011, PP-1-6.
- [7] V.K Agrawal and P.K Agrawal, “challenges faced and lesion learnt in implementation of first synchrophasor project in India,” grid tech 2011-3 rd international exhibition and conference, 19-21 April 2011, New Delhi.
- [8] P.M. Anderson and M. Mirheydar, “ order system frequency response model, Trans. Power Systems, vol. 5, no.3, pp. 720-729,August 1990.
- [9] Masa Hide, Hojo,Tokuo , Oh Mish, “Observation of frequency oscillation in Japan 60 Hz power system base on multiple synchronized PMU ,” 2003 IEEE BOLOGNA Power tech conference,June-23-26,Itely.
- [10] H. You, V. Vital, and Z. Yang, power systems: an approach using rate of frequency decline based load shedding, Trans. Power Systems, vol. 18, no.1, pp. 174-181, February 2003.
- [11] G. Huang and H. Zhang, “ stability reserve studies for deregulated environment, Meeting, vol. 1, pp.301-306, July 2001.[15] R. IEEE Power System Relaying Committee, “ Wide-area protection and emergency controls, Tech. Rep., 2002, [Online]. Available: http://www.pes-psrc.org/.
- [12] P. Kundur, Power System Stability and Control, ser. Power System Engineering Series, McGraw-Hill, New York 1994.
- [13] V. V. Terzija and H. J. Koglin, “ frequency load shedding integrated with a frequency estimation numerical algorithm, IEEE Proc.- Gener. Transm. Distrib., Vol. 149, no.6, pp. 713-717, November 2002.
- [14] S. J. Huang and C. C. Huang, “An adaptive load shedding method with time-based design for isolated power systems, Electrical Power & Energy Systems, vol.22, no.1, pp. 51-58, January 2000.
- [15] B. N. Shi, X. R. Xie, and Y. D. Han, “ WAMS-based load shedding for systems suffering power deficit, Distribution Conf. & Exhibition: Asia and Pacific, Dalian, China 2005.
- [16] Yunzhi Cheng ,Wei Jen Lee , “Dynamic parameter Indentification for smart grid development,IEEE conference ,2011.
- [17] Jian chen ,shun hesein huang , “Use of synchronized phasor measurement for dynamic model validation in ERCOT, IEEE Journal,Vol.1-4673-2729-2012.
- [18] Bharat Bhargava,Armando Salazar“use ofSynchronized phasor measurement for monitoring power system stability and system dynamics in real time.” ,IEEE journal,2008.
- [19] Keita katsuura,Mizutani, “a study of new load frequency control method ,IEEE Tranciton 2000.
- [20] Chin-wen liu, james Thorp , “ new methods for computing power dynamic response for real time transient stability prediction,IEEE tranciton on circuits and systems ,2000.
- [21] Maurani Hery purnoma,crist, “Adaptive load Shedding on neural network ,IEEE tranciton ,2002.
- [22] Dong Mingchui ,Lou, chinwang,wang Chikong , “Adaptive under frequency load shedding,IEEE ,Tsinghua science and Technology, v-13,pp-823-828-2008.
- [23] Joachim Bertsch, Cedric Carnal, Daniel Karlsson, John Mdaniel, and Khoi Vu, —Wide-Area Self-healing Protection and Power System Utilization, Proceedings of the IEEE, VOL. 93, NO. 5, pp. 997-1003, MAY 2005.
- [24] “Dynamic voltage

Non–Isolated Multiphase Bidirectional DC-DC Converter Design for Electric Vehicle Applications

A. Abhijeet Sah, B. Kalpana Chaudhary, C. Avdhesh Kumar

Abstract-- Energy conservation is one of the important issue now days and making our planet pollution free. For these purposes researchers are suggesting alternatives. Battery fed motor vehicles are one of the emerging option rather than conventional fuel vehicles. Bidirectional DC-DC converters are now mostly used in electric vehicles. The main reason behind this is to operate motor in two quadrants as motoring and regenerative for making efficient operation. Bidirectional DC-DC converter consists of buck and boost converter. During motoring mode energy is supplied through a battery and in regenerative mode battery is charged through a DC link created. This paper primarily gives attention on control strategy used for operation. In this gate complimentary control used to trigger initially turned off switch and divert current through anti parallel connected diode of initially active switch so that main switch can be triggered under zero voltage switching.

Index Terms-- Bidirectional DC-DC converter, closed loop control signal.

I. INTRODUCTION

Non-isolated bidirectional DC-DC converter basically comprises of a buck converter and boost converter in half bridge configuration. In recent years researchers have been attracted towards bidirectional DC-DC converters [1]. The main idea behind this is to make earth as pollution free from fossil-fuels emission. In Battery fed non isolated DC-DC converter the energy requirement is fulfilled by battery and power flow takes place between source and load through a DC link connected. Bidirectional DC-DC converter provides a control strategy for both motoring and regenerative modes and it increases overall efficiency level of the whole system. In this paper a whole calculation of inductor, capacitor parameters is shown and for different values of circuit parameters a different

A. & C. Abhijeet Sah and Avdhesh Kumar are Masters student in Department of Electrical Engineering, Indian Institute of Technology, Banaras Hindu University Varanasi-221005, India (e-mail: abhijeet.eee12@iitbhu.ac.in).

B. Dr. Kalpana Chaudhary is Assistant Professor in Department of Electrical Engineering, Indian Institute of Technology, Banaras Hindu University Varanasi-221005, India (e-mail: kchaudhary.eee@iitbhu.ac.in).

output is studied. As far as control is concerned a gate signal complimentary control scheme to turn on main switch and divert all current through anti parallel connected diode of initially operating switch. Thus this will help in turn ON main switch under zero voltage switching technique [2]. By this both turn on and off is obtained under zero voltage switching technique due to diverted current [3], [4]. In practical purposes multiphase bidirectional converters are connected to meet high power applications.

II. CIRCUIT DESCRIPTION & CONTROL STRATEGY

SINGLE PHASE TOPOLOGY

Mode-1: In this mode of operation switch S_d is turned on and converter works as boost converter. The inductor current increases linearly and inductor current is given by equation.

$$V_{\text{input}} = L \frac{di_L}{dt} \quad (1)$$

Mode-2: In this mode of operation both switch S_u and S_d are turned off and inductor current is passed through upper diode D_u and armature current increases as supply voltage is applied across motor terminals.

$$\frac{dV_{\text{input}}}{dt} = \frac{i_a}{C_{\text{out}}} \quad (2)$$

Mode-3: Now upper switch S_d is turned on and circuit acts as buck converter. The energy is supplied by motor and direction of inductor current is opposite to mode 1 operation. During this interval inductor current is given by following equation.

$$\frac{di_L}{dt} = -\frac{V_{\text{out}}}{L} + \frac{V_{\text{input}}}{L} \quad (3)$$

Mode-4: Now both switches are turned off and inductor current is freewheeled through diode D_d .

$$\frac{dV_{\text{input}}}{dt} = \frac{i_L}{C_{\text{out}}} - \frac{i_a}{C_{\text{out}}} \quad (4)$$

$$\frac{di_a}{dt} = \frac{V_{input}}{L} - \frac{E_b}{L} - \frac{r_a}{L} i_a \quad (5)$$

Fig.1. (c) PWM generation circuit

Fig (b) below shows gate complimentary control scheme for non-isolated DC-DC converter. Initially when upper switch is on battery supplies to motor and inductor current increases and goes from negative to positive and converter works in “buck” mode and battery is charged through inductor current. There is some dead time, in this time both switches are off and inductor current will tend to change its direction. Now inductor current is decreasing because lower switch is conducting and motor supplies energy to charge inductor as in “boost” mode.

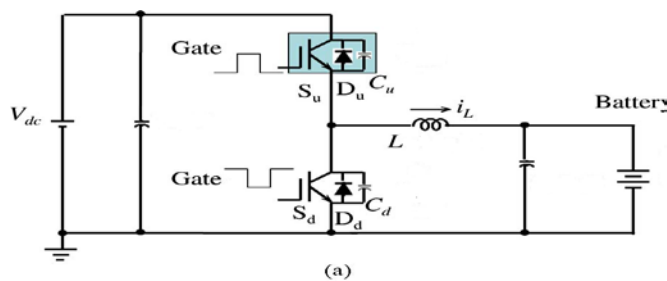


Fig. 1. (a) Bidirectional DC-DC converter circuit

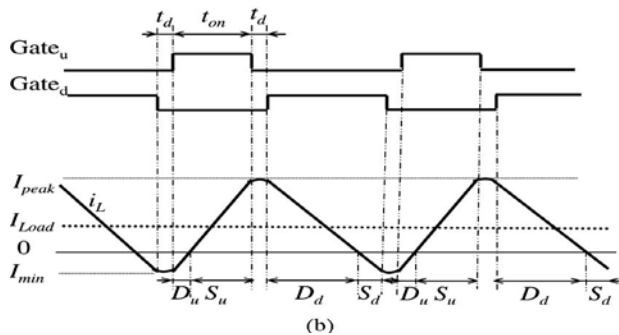
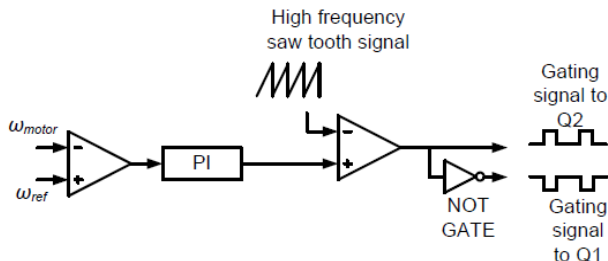


Fig. 1. (b) Complimentary Gate pulses.



III. MULTI PHASE TOPOLOGY

In multi-phase topology comprises several advantages over a single-phase, such as low ripple on the low- and high-side capacitors, improved system efficiency. Fig. shows the switch pulse diagram of three-phase non-isolated bidirectional dc-dc converter.

In this converter upper switch as the main switch and lower switch as auxiliary switch, upper and lower switches in a phase-leg are complementary to each other [5]. Complementary switching control scheme allows the inductor current to continuously flow through opposite direction, near zero inductor current condition. Phase signals are interleaved with one third of period apart [6].

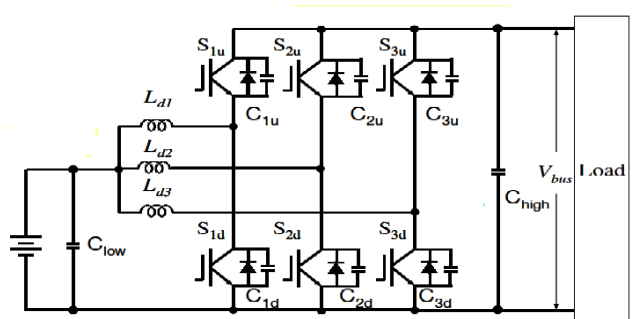


Fig. 1. (d) Bidirectional DC-DC converter circuit for 3 phases

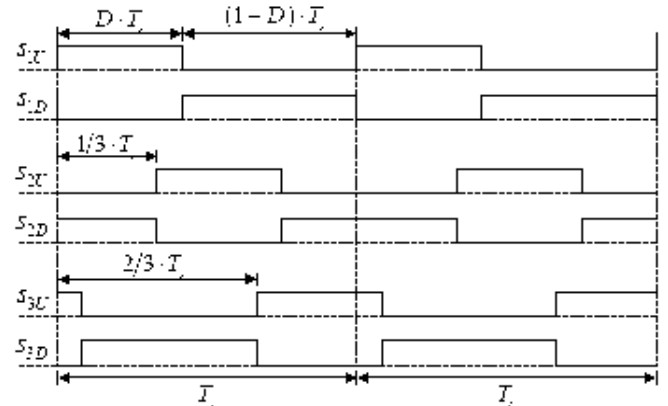


Fig.1.(e)Timing diagram of 3 phase Bidirectional DC-DC Converter

IV. CLOSED LOOP OPERATION

It is desired to control speed of dc motor drive, to control its speed it is required to control output voltage. To control output voltage in bidirectional DC-DC converter it is required to control gating signal of switches. For this motor speed is sensed and compared with a reference speed ssignal and corresponding error signal is generated [7]. This error signal is passed through a PI controller and compared with sawtooth signal of switching frequency and pulse width modulation (PWM) signal is obtained. Since the converter operates in two modes i.e. motoring as well as regeneration, therefore two controllers are required during separate modes. But a simplified approach to implement the controller is to merge both the controllers into a single unified controller with a mode switching logic according to the power flow demand. The voltage conversion ratio of the converter can be expressed as:

$$\frac{V_{out}}{V_{input}} = \frac{1}{1-D_{boost}} \quad (6)$$

$$\frac{V_{input}}{V_{out}} = D_{buck} \quad (7)$$

V. CONVERETR PARAMETER DESIGN

The bidirectional DC-DC converter is designed on the basis of output power requirement and input supply. The main parameters are to design inductor, capacitor and snubber circuit. The value of inductor depends upon ripple current, switching frequency and voltage across inductor [8], [9].

$$\Delta I = \frac{1}{2} \cdot \frac{V_{input}-V_{out}}{L_c} \cdot \frac{V_{input}}{V_{out}} \cdot L \quad (8)$$

$$I_{LOAD} = \frac{P}{V_{out}} \quad (9)$$

$$I_{max} = I_{LOAD} + \Delta I \quad (10)$$

$$I_{min} = I_{LOAD} - \Delta I \quad (11)$$

$$I_{rms} = \sqrt{I_{LOAD}^2 + \frac{\Delta I^2}{2}} \quad (12)$$

VI. SIMULATION RESULTS

This simulation is obtained in MATLAB Simulink R2009A. For simulation purpose following component values are considered.The parameter values of bidirectional DC-DC convereter are listed.

| S. No | Bidirectional Converter Parameters | | |
|----------|------------------------------------|---------------------------|--------------------------|
| | Parameters | Single phase | Three phase |
| 1 | Inductor | 100 μH | 70 μH |
| 2 | Capacitor In Capacitor Out | 150 μF 50 μF | 70 μF 50 μF |
| 3 | Switching Frequency | 25 KHz | 15 KHz |
| 4 | Supply voltage | 24 V | 48 V |
| 5 | Duty cycle | 33% | 50% |
| 6 | Battery Capacity | 12 Ah | 15 Ah |

VII. STEADY STATE RESULTS

The inductor current waveform obtained and ripple current $\Delta I=8.0$ A and inductor current waveform shown in fig.3. corresponding power supplied from battery is also shown.this simulation is obtained for 25KHz switching frequency and complimentary gate signal is obained is simulation.

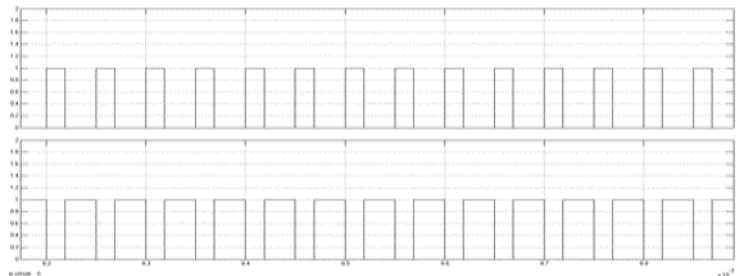


Fig. 2 Complimentary gate signal for mosfets

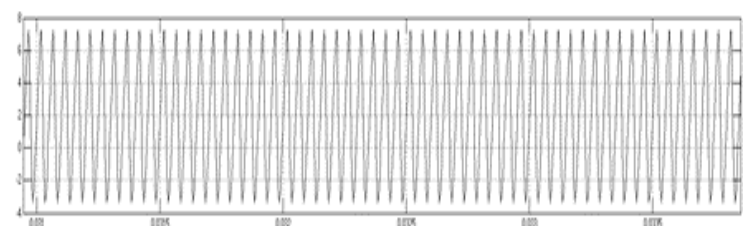


Fig. 3 Steady state inductor current

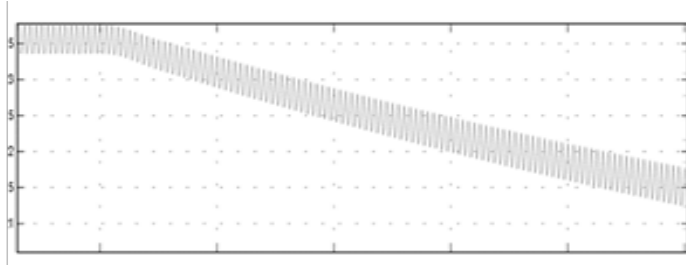


Fig. 4 Inductor current when load is suddenly decrease

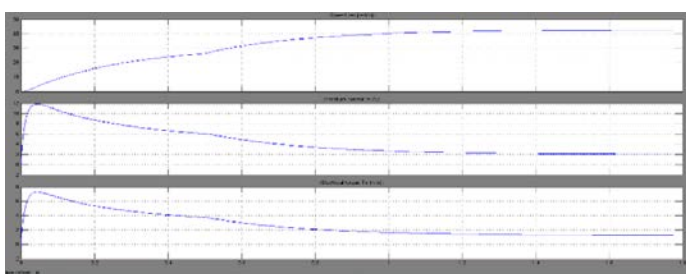


Fig. 5 Motor speed, armature current and torque and t=0.5sec speed is increased from 25 rad/sec to 40 rad/sec

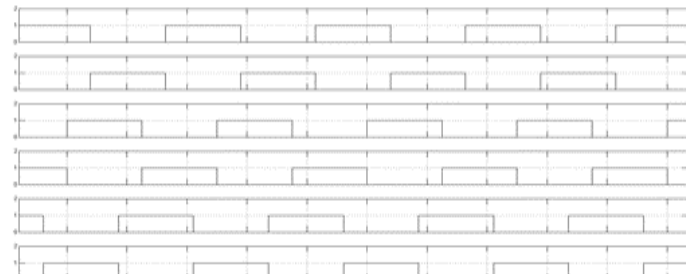


Fig. 6 Gate pulses for three phase topology for duty cycle 50 %

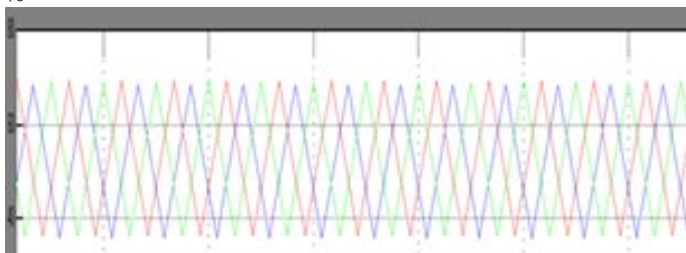


Fig. 7 Inductor currents in three phases respectively

VIII. CONCLUSION

This paper describes circuit component optimization technique to achieve significant switching loss reduction for a multiphase complimentary-switching-type bidirectional dc–dc converter. The main features of this DC–DC converter consists of low switching losses, regenerative mode of operation and zero voltage switching techniques. This simulation is performed on MATLAB Simulink R2013a and these results also compared with simulated results of another software Caspoc 2013. This Bidirectional DC-DC Converter obtains efficiency of 97%.

IX. REFERENCES

- [1]. Junhong Zhang, Jih-Sheng Lai, Rae-Young Kim and Wensong Yu, "High-Power Density Design of a Soft-Switching High-Power Bidirectional dc–dc Converter," *IEEE Trans. Power Electron.*, VOL.22 , no. 4, pp. 1045–1053 July 2007.
- [2]. O. Garcia, P. Zumel, A. de Castro, and J. A. Cobo, "Automotive DC-DC bidirectional converter made with many interleaved buck stages," *IEEE Trans. Power Electron.*, vol. 21, no. 3, pp. 578–586, May 2006.
- [3]. Y. Zhang and P. C. Sen, "A new soft-switching technique for buck, boost, and buck-boost converters," *IEEE Trans. Ind. Appl.*, vol. 39, no . 6, pp. 1775–1781, Nov./Dec. 2003.
- [4]. C. P. Henze, H. C. Martin, and D. W. Parsley, "Zero-Voltage switching in high frequency power converters using pulse width modulation," in *Proc. IEEE APEC*, 1988, pp. 33–40
- [5]. Premananda Pany, R.K. Singh and R.K. Tripathi, " Bidirectional DC- DC converter fed drive for electric vehicle system," *IJEST Vol. 3, No. 3, 2011, pp. 101-110.*
- [6]. Wensong Yu, Hao Oian, Jih-Shengh Lai, "Design of High-Efficiency Bidirectional DC-DC Converter and High Efficiency Measurement," *Power Electronics, IEEE Transactions on*, vol.25, no. 3, pp. 650-658, March 2010.
- [7]. M.C. Joshi and Susonva Samanta, " Modeling and Control of Bidirectional DC-DC Converter Fed PMDC Motor for Electric Vehicles", Annual IEEE India Conference (INDICON) 2013.
- [8]. X. Huang, X. Wang, T. Nergaard, J.-S. Lai, X. Xu, and L. Zhu, "Parasitic ringing and design issues of digitally controlled high power interleaved boost converters," *IEEE Trans. Power Electron.*, vol. 19, no. 5, pp. 1341–1352, Sep. 2004.
- [9]. Ki-Man Kim, Sang-Hoon Park, jung-Hyo Lee, Chul-Ho Jung, ChungYuen Won,"Mode change method of bi-directional DC DC converter for electric vehicle" *IEEE ICPE2011*.pp.2687-2693, 2011 .

DYNAMIC VOLTAGE RESTORER (DVR) FOR MITIGATION OF VOLTAGE SAG/SWELL IN DISTRIBUTION SYSTEM

Dinesh Chandra Kandu, *student member, IEEE*, Ravi Yadav, *student member, IEEE*, Rizwan Haider *student member, IEEE* and Ankit Srivastava, *member, IEEE*

Abstract—Dynamic Voltage Restorer (DVR) is a custom power devices that are used for the protection of sensitive loads against voltage disturbances in power distribution system. The efficiency of the DVR directly depends on the performance of the efficiency control technique involved in switching the inverters. Unlike previous approaches, this paper presents a hysteresis voltage control technique of DVR based on bipolar and unipolar Pulse Width Modulation (PWM). The hysteresis voltage control has a fast response, simple operation and variable switching frequency. The role of DVR to compensate load voltage is investigated during the different fault conditions like voltage sag, single phase to ground, and three phases to ground faults. The validity of proposed method and achievement of desired compensation are confirmed by the results of the simulation in MATLAB/ Simulink.

Index Terms— Dynamic Voltage Restorer (DVR), power quality, voltage sag, voltage swell, hysteresis voltage control, Total Harmonic Distortion (THD), Hysteresis Band

I. INTRODUCTION

The IEEE Standard Dictionary of Electrical and Electronics defines power quality as “the concept of powering and grounding sensitive electronic equipment in a manner that is suitable to the operation of that equipment.” Power quality may also be defined as “the measure, analysis, and improvement of bus voltage, usually a load bus voltage, to maintain that voltage to be a sinusoid at rated voltage and frequency.” Another definition of power quality reported in [1] is as follows:

Power quality is “the provision of voltages and system design so that the user of electric power can utilize electric energy from the distribution system successfully without interference or interruption.” A broad definition of power quality borders on system reliability, dielectric selection on equipment and conductors, long-term outages, voltage unbalance in three-phase systems, power electronics and their interface with the electric power supply and many other areas.

A.Dinesh Chandra Kandu,
B.Ravi Yadav
C.Rizwan Haider
D.Ankit Srivastava

Power quality problems like harmonic, voltage sag and voltage swell are major concern of the industrial and commercial electrical consumers due to enormous loss in terms of time and money. Voltage sag/swell that occurs more frequently than any other power quality problems is known as the most important power quality problems in the power distribution systems. IEEE 519- 1992 and IEEE 1159-1995 describe the voltage sags /swells as shown in Fig.3. Voltage sag is defined as the reduction of rms voltage to a value between 0.1 and 0.9p.u and lasting for duration between 0.5 cycles to 1 minute. [3]

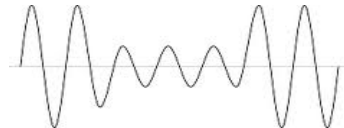


Fig. 1: Voltage Sag.

A voltage swell is defined as a raise in rms voltage which is between 1.1 and 1.8p.u for time duration between 0.5 cycles to 1 minute. [3]

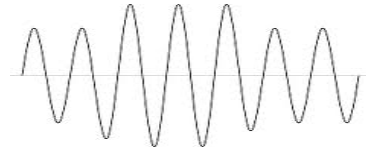


Fig. 2: Voltage Swell.

Table 1: IEEE definitions of Voltage Sags and Swells

| <i>Disturbance</i> | <i>Voltage</i> | <i>Duration</i> |
|--------------------|----------------|-----------------|
| Voltage sag | 0.1-0.9 p.u | 0.5-30 cycle |
| Voltage Swell | 1.1-1.8 p.u | 0.5-30 cycle |

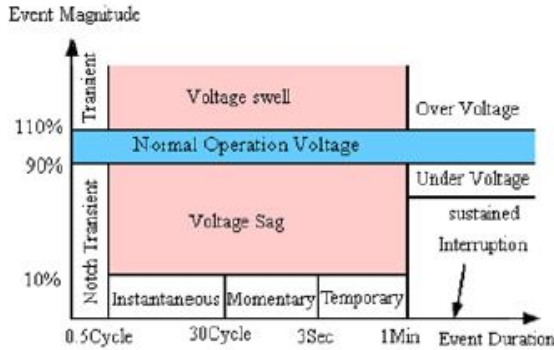


Fig. 3: Voltage Reduction Standard of IEEE Std. 1159-1995.

There are various control methods proposed for DVR, such as compensation of voltage sags with phase jump suggested in (John Godsk Nielsen et al, 2001), A.Teke, et al., 2010, presents the design and analyzed fuzzy logic (FL) controlled dynamic voltage restorer (DVR), A new approach to estimate symmetrical components for controlling the DVR was suggested by Marei et al (2007). Fawzi (2007) recommended the use of DVR based on hysteresis voltage control. Also, in reference (Ezoji et al, 2008) hysteresis voltage control based on unipolar pulse width modulation (PWM) has been used to control DVR. The hysteresis voltage control in terms of quick controllability and easy implementation hysteresis band voltage control has the highest rate among other control methods. This paper presents a Hysteresis Voltage Control technique based on bipolar and unipolar PWM to improve the quality of load voltage. The proposed method is validated through modeling in MATLAB/Simulink.

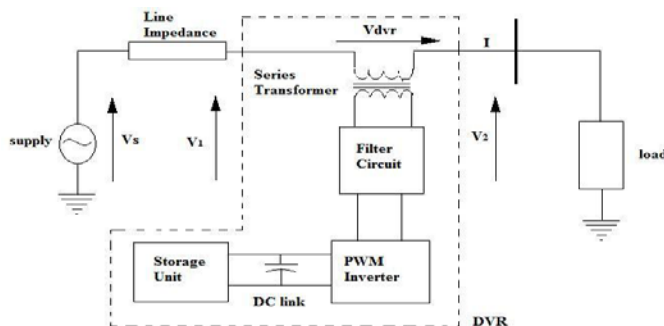


Fig. 4: Schematic diagram of DVR.

II. BASIC ARRANGEMENT OF DVR

The DVR mainly consists of the following components (Fig. 4):

- An Injection transformer
- DC charging unit
- Storage Devices
- A Voltage Source Converter (VSC)
- Harmonic filter
- A Control and Protection system

A .Injection Transformer

Three single phase transformers are connected in series with the distribution feeder to couple the VSC (at the lower voltage level) to the higher distribution voltage level. It links the DVR system to the distribution network via the HV-windings and transforms and couples the injected compensating voltages generated by the voltage source converters to the incoming supply voltage. In addition, the Injection transformer also serves the purpose of isolating the load from the DVR system (VSC and control mechanism).

B.DC charging unit

The dc charging circuit is used after sag compensation event. The energy source is charged again through dc charging unit. It is also used to maintain dc link voltage at the nominal dc link voltage.

C.Voltage Source Converter

A VSC is a power electronic system consists of a storage device and switching devices, which can generate a sinusoidal voltage at any required frequency, magnitude, and phase angle. It could be a 3 phase - 3 wires VSC or 3 phases - 4 wires VSC. Either a conventional two level converter or a three level converter is used. For DVR application, the VSC is used to momentarily replace the supply voltage or to generate the part of the supply voltage which is absent. There are four main types of switching devices: Metal Oxide Semiconductor Field Effect Transistors (MOSFET), Gate Turn-Off thyristors (GTO), Insulated Gate Bipolar Transistors (IGBT), and Integrated Gate Commutated thyristors (IGCT). Each type has its own benefits and drawbacks.

The IGCT is a recent compact device with enhanced performance and consistency that allows building VSC with very large power ratings. The function of storage devices is to supply the required energy to the VSC via a dc link for the generation of injected voltages. The different kinds of energy storage devices are Superconductive magnetic energy storage (SMES), batteries and capacitance.

D.Harmonic Filter

As DVR consist of power electronic devices, the possibility of generation self-harmonics is there so harmonic filter is also become a part of DVR. The main task of harmonic filter is to keep the harmonic voltage content generated by the VSC to the acceptable level.

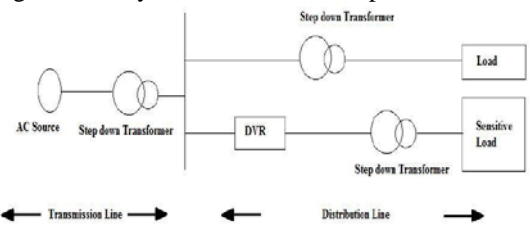


Fig. 5: Location of DVR.

III.EQUATIONS RELATED TO DVR

Here (Fig. 6) the impedance Z_{LINE} depends on the fault level of the load. When the system voltage (V_{SOURCE}) drops or reduced from any specific value, the DVR injects a series voltage i.e. V_{DVR} through the injection transformer such that the desired load voltage V_{LOAD} can be maintained. Now the injected voltage of the DVR can be written as

$$V_{DVR} = V_{LOAD} + Z_{LINE} I_{LOAD} - V_{SOURCE} \quad (1)$$

Where

V_{LOAD} = Desired load voltage

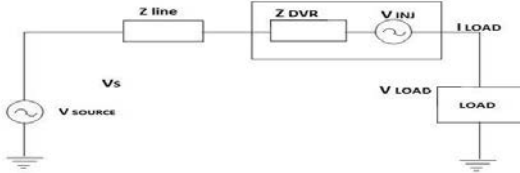


Fig. 6: Equivalent circuit diagram of DVR.

Z_{LINE} = Line impedance

I_{LOAD} = Load current

V_{SOURCE} = System voltage during any fault condition

If we take I_{LOAD} as I_L , V_{SOURCE} as V_{TH} , V_{LOAD} as V_L , Z_{LINE} as Z_{TH} then, The load current I_L is given by,

$$I_L = \frac{[P_L + jQ_L]}{V} \quad (2)$$

When V_L is considered as a reference equation can be rewritten as,

$$V_{DVR} \angle \alpha = V_L \angle 0 + Z_{TH} (\beta - \theta) - V_{TH} \angle \delta \quad (3)$$

α , β , δ are angles of V_{DVR} , Z_{TH} , V_{TH} respectively and θ is Load power angle

$$\theta = \tan^{-1} \frac{Q_L}{P} \quad (4)$$

The complex power injection of DVR can be written as

$$S_{DVR} = V_{DVR} I^* L \quad (5)$$

IV. CONVENTIONAL VOLTAGE INJECTION METHODS OF DVR

The voltage injection or compensation methods by means of a DVR mainly depend upon the limiting factors such as; DVR power ratings, different conditions of load, and different types of voltage sag [4].

There are different methods of DVR voltage injection which are

- Pre-sag compensation method
- In-phase compensation method
- In-phase advanced compensation method
- Minimum Energy Injection

A Pre Sag Compensation

The supply voltage is always tracked and the load voltage is

compensated to the pre-sag condition. This scheme results in undisturbed load voltage, but normally requires higher rating of the DVR. Before a sag occur, $V_s = V_L = V_o$. Here V_s is supply voltage, V_L is load voltage and V_o is pre sag voltage. The voltage sag results in drop in the magnitude of the supply voltage to V_{s1} . The phase angle of the supply also may shift (see Fig. 7). The DVR injects a voltage V_{ci} such that the load voltage ($V_L = V_{s1} + V_{ci}$) remains at V_o i.e. pre sag voltage (both in magnitude and phase). It is claimed that some loads are sensitive to phase jumps and it is essential to compensate for both the phase jumps and the voltage sags.

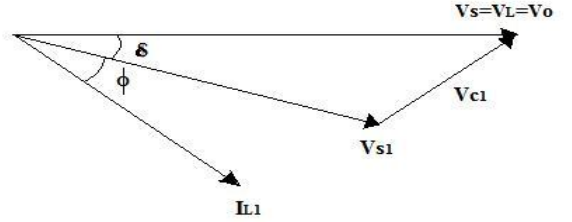


Fig. 7: Phasor diagram showing injected voltage by DVR.

B. In-phase compensation method

The voltage which is injected by the DVR is always in phase with the supply voltage in spite of the load current and the pre-sag voltage (V_o) shown in fig. 8. This control strategy results in the minimum value of the injected voltage (magnitude). However, the phase of the load voltage is disturbed. For loads which are not sensitive to the phase jumps, this control strategy results in optimum utilization of the voltage rating of the DVR. The power requirements for the DVR are not zero for this approach.

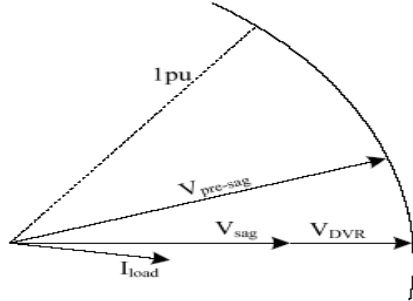


Fig. 8: In-Phase Compensation Techniques.

C. In-phase advanced compensation method

In this method the real power which is injected by the DVR is reduced by reducing the power angle between the voltage during sag condition and load current. The minimization of injected energy is achieved by making the active power component zero by having the injection voltage phasor perpendicular to the load current phasor. In this technique the values of load current and voltage are fixed in the system so only the phase of the voltage during sag is

changed. This technique is only appropriate for a limited range of sag because this technique uses only reactive power and unfortunately, but all the sags cannot be mitigated without real power.

D. Minimum Energy Injection

In this injection method the injected voltage is in quadrature with load current. The power requirements of DVR are zero if the injected voltage by DVR is in quadrature with load current, neglecting losses. Minimum energy compensation strategy which considers the voltage limitation could control the active power exchange between DVR and the external system. The compensation capability of DVR could be maintained by the strategy not only when the injection voltage is under the voltage limitation but also when the injection voltage is above the voltage limitation. Both magnitude and phase control can be achieved by small or minimum energy injection.

V. CONTROL TECHNIQUES

The unit vector templates are very simple control strategy. The distorted supply is used to generate the unit vector templates. The schematic diagram of unit vector templates (uvt) generation is shown in fig. 9. These templates nothing but pure sinusoidal signal with amplitude unity (p.u.) will be equal to pure sinusoidal signal with the unit (p.u) amplitude. The sinusoidal template can be extracted by multiplying a gain equal to $1/V_m$ (peak amplitude of the input fundamental voltage). With input supply voltage V_s .

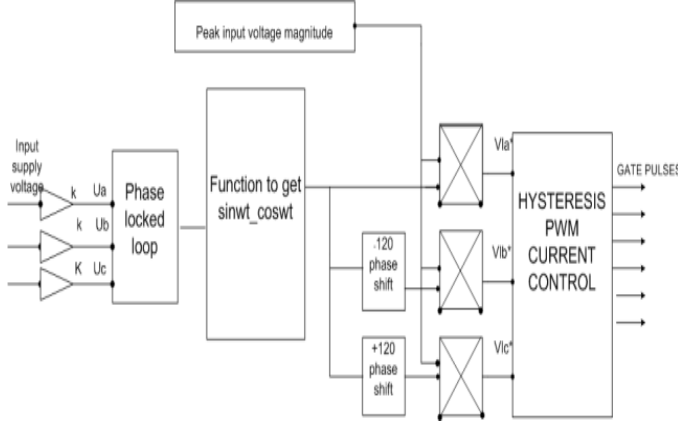


Fig. 9: Control technique of DVR, based on Unit Vector Templates (uvt).

The phase locked loop input is unit voltage vectors. A unit vector template can be determined by adjusting appropriate phase delay.

$$\left\{ \begin{array}{l} V_a = \sin \omega t \\ V_b = \sin(\omega t - 120^\circ) \\ V_c = \sin(\omega t + 120^\circ) \end{array} \right\} \quad (6)$$

$$K = \frac{1}{V_m} \quad (7)$$

V_m is multiplied with template of the unit vector of equation (6) to give the load reference voltage signal

$$V * L_{abc} = V_m * V_{abc}$$

The purpose of load voltage compared to the reference signal voltage. The error is process through hysteresis controller and generating the required gate signals for inverter. [12]

A. Hysteresis Voltage Control

This control technique is used for determine switching signals for inverters gates. It is also used for improve the load side voltage. The control signal is produced by the error signal i.e. generating between a reference voltage of DVR (V_{ref}) and an injection voltage (V_{inj}). The above and lower bands for reference voltage are called Hysteresis Band (HB). If the difference between the inverter voltages and reference voltage reaches to the upper limit, the voltage is forced to decrease and vice versa.

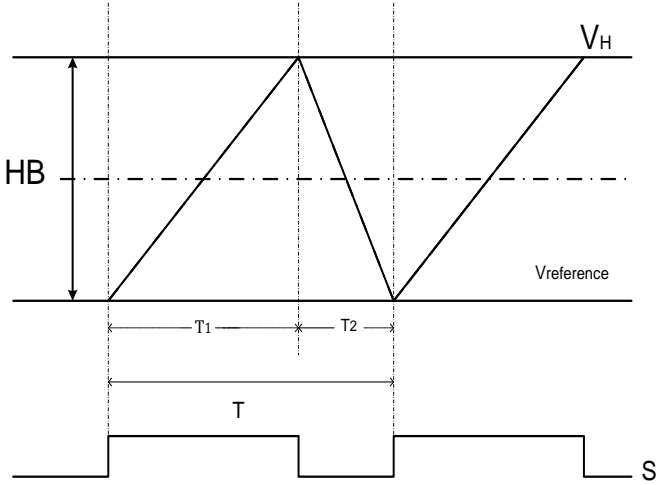


Fig. 10: Hysteresis Band Voltage Control.

$$T_C = 1/f_C = T_1 + T_2$$

Where HB is called Hysteresis Band, f_C is called switching frequency and T_1 and T_2 are the turn-on and turn-off time respectively. The relation between switching frequency and Hysteresis Band (HB) has inversely proportional. The Hysteresis Band (HB) is defined as $(HB = V_H - V_L)$.

VI. SIMULATION MODEL AND RESULTS

A. System Data

To validate the proposed algorithm, the series injection device (dynamic voltage restorer) simulated using Power System Block set in MATLAB/SIMULINK. The system parameters are shown in Table 2.

Table 2: Simulation System Parameters

| | |
|---------------------------|---|
| Supply Voltage, Vs | 415 V |
| Supply frequency | 50 Hz |
| DC Bus voltage, Vdc | 120 V |
| Filter | R=0.8,C=430 μ F |
| DC side capacitor, C | 5000 μ F |
| Load | R-L Load (30 ohm and 5mH connected in series) |
| Series filter transformer | 10 KVA |

1) Simulink Model for DVR

Test system shown in Fig. 11 is simulated for 1sec. Waveforms of source voltage, load voltage; unit vectors templates, error voltage and load voltage are shown from Fig. 14 to Fig. 19.

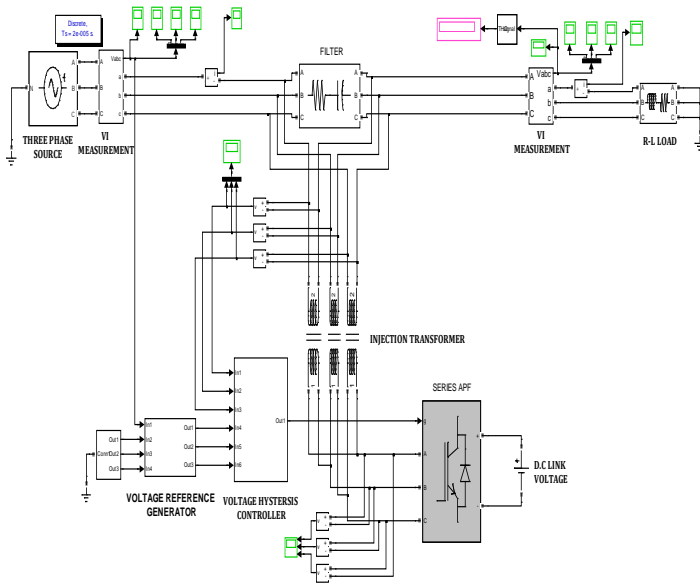


Fig. 11: Simulink Model for DVR.

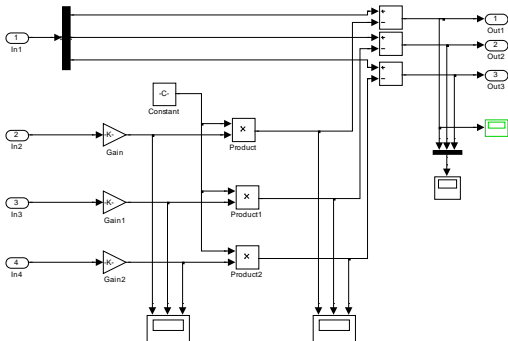


Fig. 12: Simulink Model for Reference Voltage Generator.

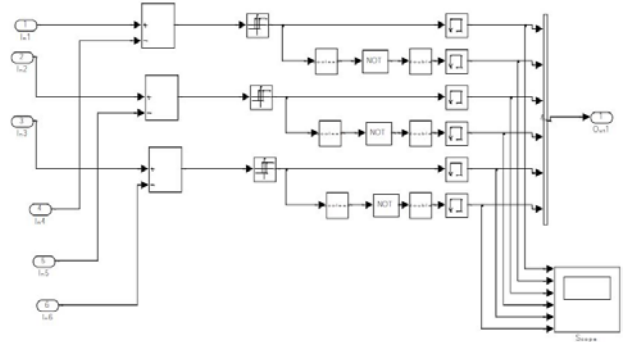


Fig. 13: Simulink model for Hysteresis Voltage controller

II) Results for DVR

• During Voltage Sag

Fig. 14 shows source voltages during sag. Fig. 15 shows unit vector templates generation. Fig. 16 shows load voltages during sag. Fig. 17 shows reference voltage. Fig. 18 error voltages. Fig. 19 shows load voltage after compensation. Thus results shows Series injection device effectively compensates voltage sag and maintains load voltage constant.

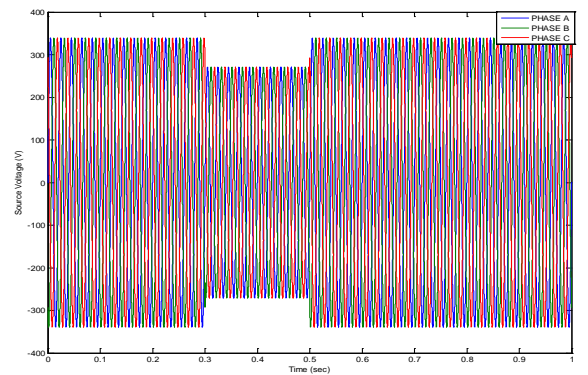


Fig. 14: Source Voltages during sag from 0.3sec to 0.5 sec.

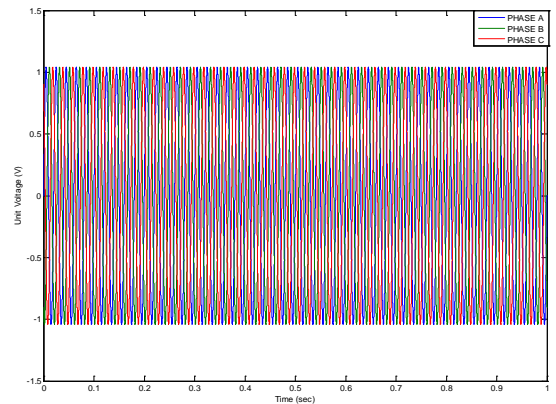


Fig. 15: Unit Vector Template

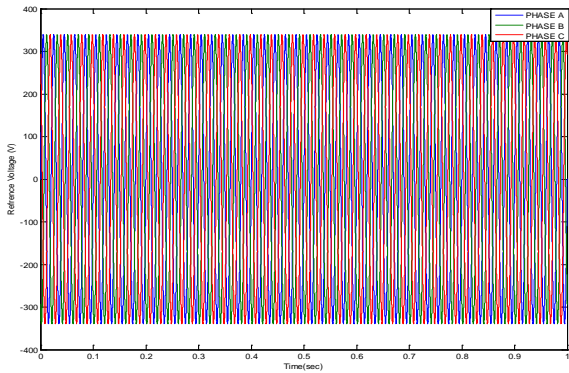


Fig. 16: Load Voltage without DVR.

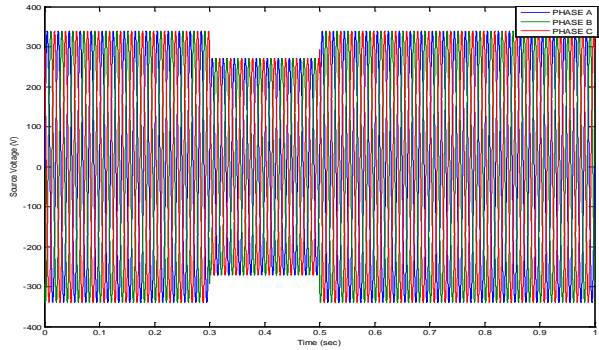


Fig. 17: Reference Voltage.

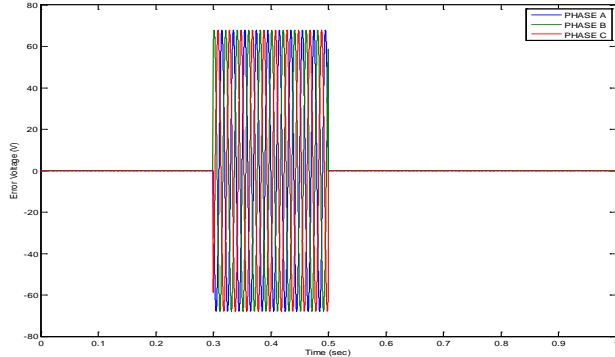


Fig. 18: Error Voltage.

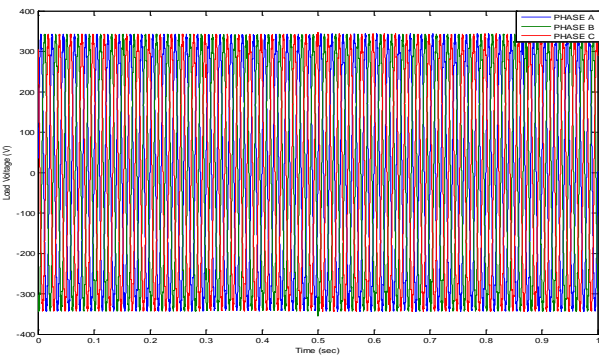


Fig. 11: Output Voltage with DVR.

- During Voltage Swells

Fig. 20 shows load voltages during swell. Fig. 21 shows error voltage and Fig. 22 shows load voltage after compensation. Thus results shows Series injection device effectively compensates voltage swell and maintains load voltage constant. Simulated in discrete-time domain with the system sampling time at 0.5sec.

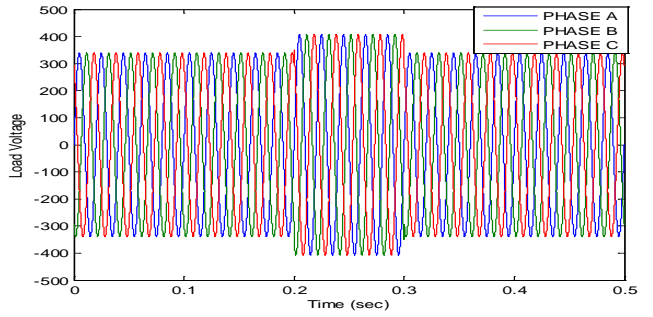


Fig. 20: Load voltage without DVR during swell from 0.2 sec to 0.3 sec.

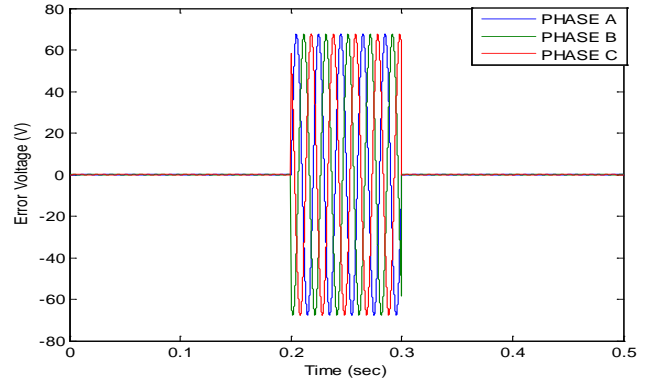


Fig. 21: Error voltage.

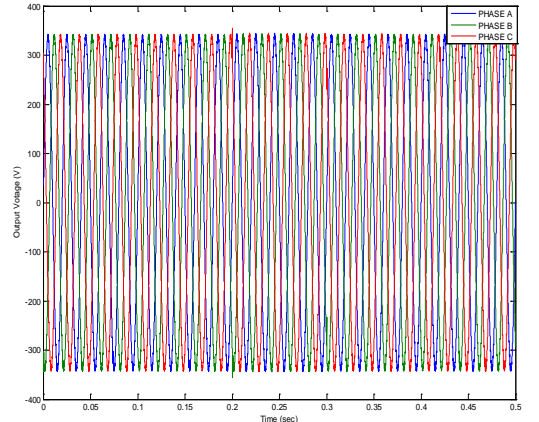


Fig. 22: Load voltage with DVR.

VII. CONCLUSION

This paper presents a hysteresis voltage control technique based on unipolar and bipolar Pulse Width Modulation (PWM) For DVR to improve the quality of load voltage. The validity of proposed method is approved by results of the simulation in MATLAB/Simulink. From the simulation responses,

- 1) Reference voltage generator, Hysteresis PWM voltage controllers are performing satisfactorily.
- 2) The three phase terminal voltages, three phase reference voltages are used to generate the switching patterns for DVR.
- 3) The source voltage waveform is in phase with the utility voltage and free from harmonic components. The load voltage waveform is maintained constant.
- 4) During the voltage sag, voltage is dip observed from 0.3s to 0.5s; magnitude changed from 338.8 V to 271.1 V. And when DVR is connected between the systems, the load voltage is maintained.
- 5) During the voltage swell, voltage is raises observed from 0.2s to 0.3s; magnitude changed from 338.8 V to 389.6 V. And when DVR is connected between the systems, the load voltage is maintained. Different advance control technique can be used in DVR for future work.

VIII. REFERENCES

- [1] C. Sankaran "Power Quality", CRC Press 2002.
- [2] N.G. Hingorani, "Flexible AC Transmission," IEEE Spectrum, vol. 30, pp. 40-44, 1993.
- [3] N.G. Hingorani and L Gyugyi "Understanding FACTS – Concepts and Technology of Flexible AC Transmission Systems," IEEE Press, New York, 2000.
- [4] S. Masoud Barakati, Arash Khoshkbar Sadigh, Ehsan Mokhtarpour "Voltage Sag and Swell Compensation with DVR based on Asymmetrical Cascade Multicell Converter" (NAPS), pp.1-7, 2011.
- [5] A.Teke K.Bayindir M.Tumay Department of Electrical and Electronics Engineering, Cukurova University, Adana, Turkey "Fast sag/swell detection method for fuzzy logic controlled dynamic voltage restorer" generation transmission and distribution IET, vol. 4, pp. 1-12, 2010.
- [6] B. Ferdi, S. Dib, R.Dehini University of Bechar, Algeria. "Adaptive PI Control of Dynamic Voltage Restorer Using Fuzzy Logic" Journal of Electrical Engineering: Theory and Application Vol.1, pp. 165-173, 2010.
- [7] P.Ajay-D-Vimal Raj, M.Sudhakaran, S.Senthil Kumar, Sapta Rishi Roy, T.G.Palanivelu "multi level inverter based dynamic voltage restorer with pi and fuzzy logic controller" NSC, pp. 65-70, Dec. 2008.
- [8] H. Ezoji, A. Sheikholeslami, M. Tabasi and M. M. Saeednia, "Simulation of Dynamic Voltage Restorer Using Hysteresis Voltage Control," (EJSR), vol. 27 no. 1, pp. 152-166, 2009.
- [9] D. Daniel Sabin, Senior Member, IEEE, and Ambra Sannino, IEEE "A Summary of the Draft IEEE P1409 Custom Power Application Guide" Transmission and Distribution Conference and Exposition, IEEE PES, vol. 3, pp. 931-936, 2003.
- [10] R. Anil Kumar, G. Siva Kumar, B. Kalyan Kumar "Compensation of Voltage Sags and Harmonics with Phase-Jumps through DVR" Member, IEEE, pp. 1361-1366, 2009.
- [11] K.R. Padiyar "Facts controllers in power transmission and distribution" new age international (P) Ltd publishers, 2007.
- [12] Bingsen Wang, Giri Venkataraman and Mahesh Illindala, "Operation and Control of a Dynamic Voltage Restorer Using Transformer Coupled H-Bridge Converters", IEEE transactions on power electronics, vol. 21, pp. 1053-1061, July 2006.
- [13] Rajkumar M., Usha Rani P. and Dr. S. Rama Reddy "Modeling and simulation of ZSI based DVR for voltage compensation," in ICCSET March, 2011.
- [14] Eimi Diyana binti Rosli, Muhamad Nabil bin Hidayat and Rahimi bin Baharom "Direct single phase ac-ac dynamic voltage restorer," IEEE Press, pp. 1257-1262, 2013.
- [15] V. Jayalakshmi and Dr. N. O. Gunasekar "Implementation of discrete PWM control scheme on Dynamic Voltage Restorer for the mitigation of voltage sag /swell," IEEE Press, pp. 1036-1040, 2013.

A Comparative Analysis of Various LNA Topologies Used in CMOS - LNA Design

A.Rajneesh Kr. Iodhi ,B. Dr. R.K. Singh , C.Anjani Kr. Mishra and D. Vikram Singh

Abstract — This paper analyses various CMOS UWB LNA topologies. The paper presents an exclusive guideline for UWB LNA research work. The paper describes selection procedure of LNA configuration for desired specifications as the UWB LNA has a major tradeoff among five main design parameters viz Bandwidth, NF, Gain, Power dissipation and Linearity.

Keywords -- CMOS LNA, Topology, UWB.

I. Introduction

The communication system that comprises of transmitter and receiver will experience not only attenuation but also the interference at the receiver end. The signal strength will be normally in milli-volt range hence unable to drive the demodulator circuitry; hence it is mandatory to amplify the signal before giving it to the demodulator circuit. But the amplifier will not only amplify the signal but also amplify the noise as well. Hence amplifier with minimum noise addition is required. So LNA is essential & first active block in receiver front end chain.

A) Ultra-Wide Band

Over the last decade, the availability of the 3.1– 10.6-GHz spectrum for ultra-wideband (UWB) communications has driven both research and industry toward the development of a novel set of mass-market applications. Indeed, the high achievable through put capacity of the multi-gigahertz bandwidth provides high-data rate (HDR) (100 Mb/s) wireless connection at short ranges (1– 10m) for ad hoc connectivity among portable consumer electronics and communication devices. A different mode of operation exploits the high time resolution of UWB pulse signals to enable localization/tracking capabilities for low-data rate (LDR) communications. In these applications, oriented to wireless sensor networks (WSNs), the data rate can be from 1 Kbps to 1 Mbps with an operating range around 100–300m. To manage the ultra-wide spectrum and operate at a low power at the same time poses severe challenges in the design of an UWB transceiver. Such issues can be managed if high technology performance is combined with proper circuit solutions and suitable transceiver architecture [1]. Many published works deal with the 3–5-GHz bandwidth, demonstrating the feasibility of both standalone circuit blocks [1], and fully integrated transceiver solutions, whereas less works are available in the 3–10-GHz range due to a more critical

RF section. Especially for LNAs used in Ultra Wideband Application must provide the Wide bandwidth, moderate but Flat Gain over entire BW, low NF, Good Linearity, Lower

II. Design Overview for LNAs

A) Overview of existing LNA structure

The LNA design includes three sections to be designed

1. Input matching network.
2. Main amplifier section.
3. Output matching network.

The role of the input matching network is to make the input return loss (S_{11}) minimized without introducing additional noise. The interface between the antenna and the LNA entails an interesting issue that divides analog designers and microwave engineers. Considering the LNA as a voltage amplifier, we may expect that the ideal value of its input impedance is infinite. From the noise point of view, we may require a transformation network to precede the LNA so as to obtain minimum NF. From signal power point of view, we may utilize conjugate matching between the antenna and the LNA. While each of these choices has certain merits and drawbacks, the last one is dominant in today's systems, i.e., the LNA is designed to have a 50Ω resistive input impedance.

Amplifier section ensures a high gain, high linearity, low noise factor and low power consumption and at the same time it provides input impedance that can be conducive to the realization of broadband matching. The output buffer guarantee the output impedance is 50Ω in order to test.

The design of matching network circuitry is called the topology of LNA. Many elementary wide-band amplifiers exploit the wide-band trans-conductance of the MOS transistor to determine their performance, amplifiers that can be modeled as circuits with 2 Voltage Controlled Current Source (VCCS) are generated in a systematic fashion. Methodology is already exploited in past, which renders all 2VCCS wide-band amplifiers that can be found in a database containing all the potentially useful 2VCCS circuits, which was made available from previous work of Klumperink [2].

This is done selecting into the 2VCCS database all two-port circuits having certain non-zero transmission parameters {A, B, C, D} according to a set of properly defined amplifier functional requirements and given the source/load impedance. Limiting ourselves to the important case of elementary 2VCCS circuits exploiting 2 MOSFETs leads to 2 well-known and 2 unknown wide-band amplifier circuits [2].

B) Design Considerations for UWB LNAs

The main design target of an LNA for UWB applications is to provide 50Ω input matching on the whole 3.1–10.6-GHz frequency band, thus minimizing signal reflections back to the receiver antenna. Of course, high gain and low NF are also necessary to reduce the noise contribution of subsequent stages and improve the receiver sensitivity.

For UWB amplifiers, the importance of a small group delay, which is a direct measure of phase variation, is not always pointed out. A small-varying group delay guarantees that the UWB signal experiences the same time delay over the wide frequency band, so that the signal may be recovered properly. If the group delay varies significantly with frequency, the time-domain waveform will be distorted,

A. M.tech Scholar, ECD, KNIT, Sultanpur
rajneesh.nra@gmail.com

B. Associate professor, ECD KNIT,Sultanpur

C. M.tech, ECD, KNIT, Sultanpur
Anjani.mishra31@gmail.com

D. M.tech Scholar, ECD, KNIT, Sultanpur
Vik081189@gmail.com

especially in case of UWB pulse signals that occupy a several-gigahertz spectrum. Thus, different from a narrowband amplifier design, a 3–10 GHz UWB LNA has to provide flat gain, as well as flat group delay throughout the operating bandwidth.

Finally, limits on power consumption and cost suggest simplifying the topology and reducing the use of on-chip large passive components. As a consequence, differential circuits, which are often adopted for their immunity to common-mode spurious signals and assembling parasitic, are less attractive since they introduce a twofold penalty. Indeed, a differential LNA requires around twice the current budget compared to a single-ended version to achieve a similar performance. Moreover, it also needs a wideband passive network to provide the single-ended-to-differential conversion between the antenna and LNA. To this aim, both off-chip baluns and integrated transformers are not viable solutions since the former exhibit high-frequency limitations and the latter introduce losses that directly add to the NF of the LNA, heavily degrading the performance of the whole receiver. Moreover, off-chip baluns and integrated transformers increase complexity and silicon area, respectively. The choice to implement a single-ended LNA, even if not compulsory, then gives a fundamental advantage in fulfilling the severe specifications imposed by low-power and low-cost UWB applications[1].

III. Various LNA Topologies

The two well-known topology structure found in [2] are common source (CS) topology and common gate topology (CG). There are various other possible topologies as well which is discussed here in detail along with existing CG and CS configurations.

Here we would like to indicate that along with basic topology some topology are resulted due to Bandwidth extension techniques, Input matching techniques and Noise cancellation techniques when applied on basic topologies.

A) Distributed Amplifier (DA) topology

The distributed topology incorporating T-lines was originally proposed by Ginzton [3]. Insufficient technological capability to design area-efficient distributed circuits delayed the usability of these circuits for a long time. They made their reappearance in 1980's in a variety of advanced processes, such as GaAs or other III-V technologies, and recently, in CMOS process.

Examples include distributed amplifiers, distributed mixers, and distributed oscillators. The renewed interest in distributed circuits is mainly due to the capability of designing on-chip T-lines, and high-Q inductors [3]. As a fundamental property, integrated circuits incorporating on-chip T-lines trade delay for bandwidth. In frequency domain, the transistor's parasitic capacitances are absorbed into the constants of the T-line. Hence, until the cut-off frequency of the line itself is reached, the circuit's bandwidth remains approximately constant.

The generalized schematic for distributive amplifiers is shown in fig-1

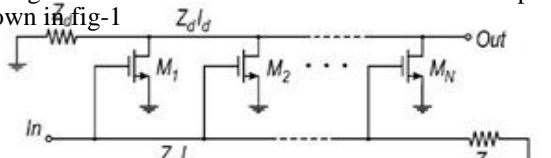


Fig. 1 - Generalized structure of distributed LNA[1]

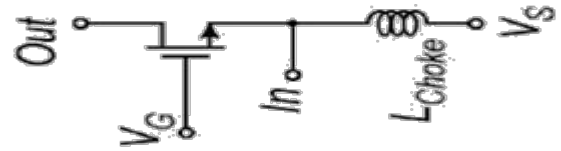


Fig. 2 - Common gate configuration [5].

Distributed circuits are capable of providing a wideband input/output matching. This property is essential in the UWB LNA design.

The main advantages of a distributed amplifier (DA) are its intrinsic broadband characteristic that goes all the way down to DC, and good input and output matching. But, high power consumption and large area have limited its application space. However, when one considers the trade-off between the five main design parameters of an LNA: power drain, gain, bandwidth, noise, and linearity, it becomes evident that the traditional way of biasing a MOS DA in strong inversion, is not the optimal choice for reducing power consumption. So it will be beneficial to bias DA in moderate inversion region [4].

The major drawbacks of DAs is the large silicon area, which is due to the presence of several on-chip inductors and/or transmission lines and high power consumption that is related to the number of stages required to enhance the gain, often approaching hundreds of milli-watts [1].

B) Common Gate (CG) Topology

Figure 2 shows the conventional CG-LNA where the inductor resonates with the parasitic capacitance of the Impedance-matching device and the input pad. Within the signal bandwidth, the reactive part of the input impedance is then cancelled and the real part of the input impedance is determined by $1/(g_m + g_{mb})$.

Also, the input-matching network of the CG-LNA is a parallel resonance as opposed to the series resonance of the inductor-degenerated LNA. Hence, a low Q (quality factor) of the input-matching network results in a wider bandwidth and the CG-LNA is more robust to process, voltage, and temperature (PVT) variations [5].

The power gain of CG-LNAs is relatively low due to the impedance-matching constraint. Ignoring the trans conductance of the back-gate transistor (g_{mb}), input impedance matching requires $1/g_m = R_s$ and the CG LNA's effective trans conductance under an input-matching condition is

$$g_m^{\text{CG-LNA}} = g_m / 2$$

CG-LNAs exhibit superior stability and reverse isolation due to the absence of the Miller effect. Although CG-LNAs feature desirable properties for wideband operation, their high NF under the input-matching condition prevents its extensive use. The NF including channel noise, induced gate noise, and resistive load under the input-matching condition is expressed as

$$NF_{CG-LNA} \approx 1 + \frac{\gamma}{\alpha} + \frac{\delta\alpha}{5} \left(\frac{\omega_0}{\omega_T} \right) + \frac{4R_s}{R_L} \quad (1)$$

Where, γ , α & β are bias-dependent parameters, R_L is the load impedance, R_s is the source impedance, and ω_0 and ω_T are operating and unity current gain frequencies,

respectively. The dominant noise source in the CG-LNA is due to the channel noise of the MOSFET device. The gate induced noise in a CG-LNA is usually negligible in contrast to an inductor-degenerated LNA under simultaneous noise and power match condition. The fourth term shows that a large resistive load is desirable for low NF, but this condition is usually detrimental for wideband operation of LNAs.

In summary, CG-LNAs achieve a broadband impedance match, superior reverse isolation, stability, and a high linearity. Recently reported CG feedback amplifiers aim at decoupling the noise and power (input) match trade-off without degrading other relevant LNA parameters.

Negative-feedback around a common-base amplifier has been employed to break the lower bound of noise performance. The simplified CMOS version schematic of the LNA is shown in Fig. 3(d). In this topology, the feedback network is passive, limiting the choice of the g_m of the impedance-matching device. Low gain and a large parasitic capacitance at the output node makes this approach unsuitable for wideband LNAs.

Positive feedback in combination with passive g_m boosting can achieve the best theoretical noise performance with low power. Fig. 3(e) requires half the power consumption for the same power gain and features further suppression of channel noise from the impedance-matching device.

All the reported works are based on feedback amplifiers taking advantage of the high f_t scaled CMOS devices. However, none of these designs achieve the full decoupling of noise and power match in CG-LNAs. Also, other design parameters (e.g., stability, reverse isolation, and wide bandwidth) are sacrificed in order to improve noise performance.

Low-Noise Techniques Employing Feedback in CG-LNA-

The capacitor cross-coupled CG-LNA in Fig. 3(b) reduces its NF and power consumption by employing negative feedback g_m boosting with inverting amplification, A_{neg} , reduces the noise contribution due to the channel noise by a factor of $1 + A_{\text{neg}}$ under input-matching condition. At the same time, the intrinsic transconductance of the impedance-matching device can be halved, which reduces the power consumption by the same factor. The drawbacks of the capacitor cross-coupled CG-LNA

are that the passive g_m boosting dictates that the inverting amplification must be less than 1 taking into account the parasitic capacitance C_{gs} . Furthermore, the unilateral behaviour of the CG-LNA is affected by the scheme where input-output feed-through and stability is deteriorated. Shunt-shunt positive feedback is used to add a degree of freedom in determining the g_m of the impedance-matching device, as shown in Fig. 3(c).

However, the amplifier's stability must be carefully evaluated when the positive feedback is employed. Also, increasing the loop gain in positive feedback reduces the overdrive voltage of the transistor, and consequently, its linearity.

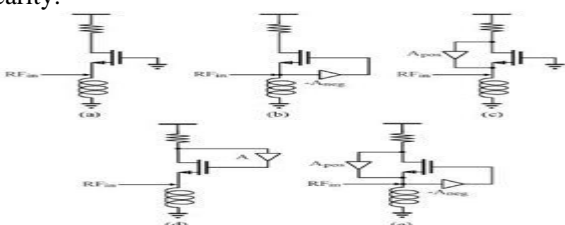


Fig.3 - Conventional CG-LNA and low-noise techniques employing feedback [5].

C) Inductively degenerated common source topology (IDCS)

The basic inductively degenerated common-source (IDCS) LNA shown in Fig. 4 (a) has typically been the best choice for narrowband applications due to its noise and gain performance. Both the input matching and the resonator load are capable of handling bandwidths (BW) of several hundred MHz. However, the ultra-wideband (UWB) systems, which have recently gained a lot of interest due to their capability to transmit high-speed data for short ranges, set new challenges. The band allocated for the UWB covers the frequencies between 3.1-10.6 GHz. According to Multiband OFDM Alliance (MBOA) the UWB is divided into 14 sub-bands, which are collected to 5 band groups (BG) [1]. At first, the UWB devices must support the lowest three sub-bands. Thus, the LNA should have at least 1.6-GHz operational band, which is difficult to achieve with the IDCS LNA.

Fig 4(b) shows one of the first CMOS LNAs designed for the UWB. The core of that LNA is also based on IDCS topology. To have a wide operation BW, a Chebyshev input matching technique and a shunt-peaked load are utilized. The drawback of using wideband input matching is the number of on-chip inductors. Wideband input matching circuit in Fig. 4(b) becomes more troublesome when designing a balanced or differential LNA. Then, all inductors at the input matching cannot be differential which leads to even larger number of inductors. To minimize the noise from input matching circuit and to prevent

the current signal leakage into the resonator L_2C_2 , inductors having high Q-value are required. As a result, the area of the input matching circuit becomes large.

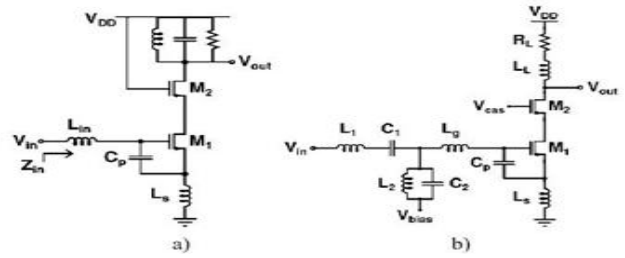


Fig. 4 (a) - Conventional inductively degenerated common source configuration for narrow band applications (b) inductive degenerated CS for UWB [6].

A drawback of this approach for UWB is the large group-delay variation that the signal can experience, due to several resonances in the input-matching network. Moreover, it requires moderate to large silicon area and introduces a high insertion-loss that degrades the amplifier NF and gain.

Complement UWB inductively degenerated common source topology

The use of complementary, or known as current re-use, method has been demonstrated in CMOS low noise amplifier (LNA) design to achieve broadband input matching where the equivalent 50Ω input impedance is made possible by the coupled gate-drain inductors and the loading capacitor. Since

the external resistive drain bias circuit is not more needed in the complementary topology, not only the signal loss can be minimized but also noise performance of the amplifier can also be improved. However, since the two coupled inductors are themselves large and lossy, the unavoidable signal attenuation will raise the amplifier's noise figure. The ultra-wideband LNA mainly utilizes shunt-shunt resistive feedback to achieve input matching; however, the use of the feedback resistor inevitably deteriorates the amplifier's noise. In this letter, we propose a new wideband CMOS LNA design method that is combining the complementary topology with asymmetrical inductive source degeneration. By omitting the use of large inductors and a feedback resistor, superb noise performance can now be expected.

D) Cascode Topology

The cascode is a combination of a common-source device with a common-gate load. This has the effect of increasing the voltage gain of the LNA and the output impedance while providing shielding as well. The additional cascode device consists of a transistor M₂ biased as common-gate, providing a large active load to improve voltage gain at high frequency. It is normal to set the cascode device with the same W/L (channel width versus length) ratio as the first single-stage LNA.

In the design of a cascaded CMOS LNA, NF and linearity of a LNA are directly affected by the gate width (M₁& M₂) and V_{gs} of common-source transistor. The transistor M₁ dominates the noise performance. However, the transistor M₂ contributes to the linearity performance as well as the improvement of the reverse isolation due to high output impedance. Furthermore, a multi-finger layout pattern is applied to reduce the gate-induced noise.

The cascode amplifier is shown in the Fig 5. Where M₁ is CS amplifier and M₂ is CG load.

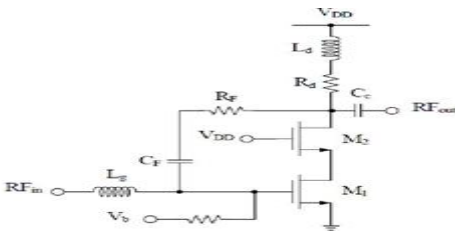


Fig. 5 - Cascode configuration [7].

Cascoded Common Source Amplifier

The most commonly used topology for LNA design today is the cascode amplifier with inductive source degeneration shown in the Fig. 5. This type of cascode amplifier is called the telescopic cascode amplifier since the cascode transistor is the same type as the input transistor. On the other hand, a folded cascode amplifier has a cascode transistor with a different type from the input transistor. The cascode topology results in a higher gain, due to the increase in the output impedance, as well as better isolation between the input and output ports. The cascode transistor M₂ suppresses the Miller capacitance of M₁ thereby increasing the reverse isolation. The suppression of the parasitic capacitances of the input transistor also improves the high frequency operation of the amplifier.

The formula for the input impedance of the cascaded common-source LNA is given in (1) where g_m, C_{gs}, L_g and

L_s are the input transistor's transconductance, input transistor's gate-to-source capacitance, gate inductance, and source inductance respectively. At the resonant frequency, given in (2), the formula for the input impedance reduces to (3).

The width of the input transistor M₁ that will give the required transconductance was set based on (2). The degenerating inductor L_s, which gives the LNA its purely real input impedance, was computed based on(3).With the value of L_s determined, the value of the gate inductance, L_g, that will set the resonant frequency, can be

calculated. The width of the cascode transistor M₂, was set equal to the width of the input transistor to take advantage of the reduced junction capacitance in the layout. Finally, the output matching network, composed of the drain inductor, L_d, and the

output capacitors, C₁ and C₂, can be designed. Fig. 5 shows the final schematic design of the cascaded common-source with device sizes and bias voltages. [10]

The cascaded common-source also achieved the lowest power dissipation since it contains only one current branch [10].

$$Z_{in} = \left(\frac{g_m}{c_{gs}} \right) * (L_s) + \frac{1}{s.c_{gs}} + s.(L_g + L_s) \quad (2)$$

$$\omega_0 = \frac{1}{\sqrt{(L_s + L_g) * C_{gs}}} \quad (3)$$

$$Z_{in} = \left(\frac{g_m}{c_{gs}} \right) * (L_s) \quad (4)$$

The cascaded architecture allows us to achieve simultaneously high gain, low noise, and high linearity over a wide frequency range. Since this design doesn't use any off-chip components, it can be easily integrated as one part of a complete low-voltage transceiver.

E) Folded Cascode Topology

With the unparalleled advantages in terms of gain, isolation, stability, and impedance matching, a cascode stage is considered one of the most widely used topologies for the implementation of LNA circuits at multi-gigahertz frequencies. However, with the stacking architecture of the common-source and common gate transistors, relatively large bias voltage is required in the LNA design, and the performance degrades significantly as the supply voltage decreases.

The basic circuit schematic of folded-cascode LNA is composed of one NMOS transistor and one PMOS transistor. Fig. 6 shows the schematic of the topology. The supply voltage

of traditional cascode circuits must be more than 2V_T. In this circuit, a single 0.8V voltage source is used to supply the whole circuit. The gate bias of input common-source stage is fed

through the inductors L₁, L₂ and L₃ by the 0.8V voltage source. Here, several additional bypass capacitors are connected to the supply voltage source to make DC bias not susceptible to RF signals and hence noise figures sustain evaluated values.

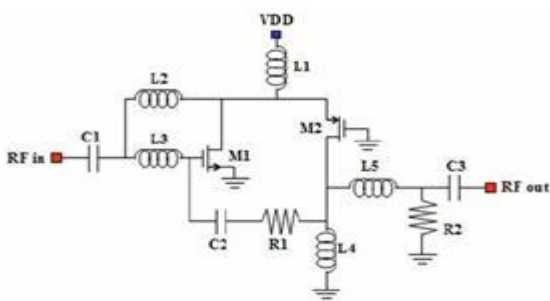


Fig. 6 - Folded cascode configuration [8].

Conventional cascade topology requires a large supply voltage because of stacking a large number of transistors. To avoid this problem, one can use a PMOS transistor instead of NMOS transistor.

By stacking folded-cascode stage on the top of the common source (CS) amplifier, the total transconductance is increased with the same current consumption.

Compared with other low-voltage LNA topologies, the folded cascode one possesses exclusive advantages in terms of amplifier linearity, noise figure, and bias stability. However, the inherently low gain is one of the major concerns, especially for applications where the current consumption is limited. In this study, gain-enhancement techniques are proposed for the folded cascode topology and high-gain LNAs are realized for low-voltage and low-power RF applications.

The best linearity where only one single transistor exists in each DC path which increases the voltage swing and consequently improves the circuit linearity. This improves the circuit linearity, increases the input trans conductance and consequently the power gain.

F) Cascade Topology

The cascading topology many a times found in multi section or multi stage circuit topology, where two or more stages are connected in cascade to achieve the high gain. Many a times it is also found in some of the IEEE papers that two transistors are connected in cascade for higher amplification purpose. Mostly in cascode structure CG and CS stages are connected in cascading only.

The supply voltage requirement is more in cascade topology. And it will consume large silicon area as compared to cascode topology. In some of the paper confusion is there in between two terms cascade and cascode structure.

G) Current reuse topology

The typical schematic of current-reuse LNA is shown in the Fig. 7. The technique of current-reuse can reduce the power consumption of LNA while preserve high-gain. However, since the second stage of the traditional current-reused LNA topology requires a DC bias as well as biasing resistor, they will result in extra noise and signal leakage [9].

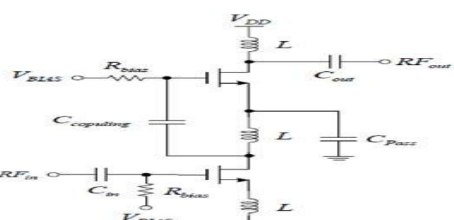


Fig. 7 - Conventional current reuse configuration [9]

By using the current-reuse technique, the power consumption, noise and the IIP3 can be improved. Current Reuse topology can be used with any circuit configuration like cascode topology, common source or common gate, and feedback topologies or even with multi stage cascaded structures to reduce the DC power consumption.

Recently, current reuse cascaded amplifier has been presented in literature as a suitable configuration for LNA implementation because of its low DC power consumption, high and flat gain , low NF and high reverse isolation. The current reuse circuit is followed by a CG stage used as a buffer to improve the output impedance matching and flatten the LNA gain.

A major drawback of this design is its high input and output impedances, thus requiring external impedance matching networks. This prevents the use of this LNA in fully integrated applications. Due to the high gain property, the strong Miller effect reduces the reverse isolation of this LNA. In the actual design, two identical stages are cascaded to improve the reverse isolation.

H) Differential topology

The capacitor cross-coupled gm-boosted UWB LNA features the differential configuration, and can provide the input matching and low noise figure, but the power gain of 6.1-8.5dB (or 5.2-8.2dB) is insufficient to suppress the noise of the subsequent components. Owing to employing the noise cancelling, the LNA has achieved input matching, high power gain, and low noise figure under the wideband condition. However, the single-end configuration will cause severe 2nd-order nonlinearity which is very detrimental for zero-IF receivers. In order to suppress this nonlinearity, the noise-cancelling technique is employed in pseudo-differential configuration. However, this configuration suffers from variable input common-mode level and is only suitable for the narrow band LNA [11].

The differential capacitive cross coupled LNA is shown in Fig 8.

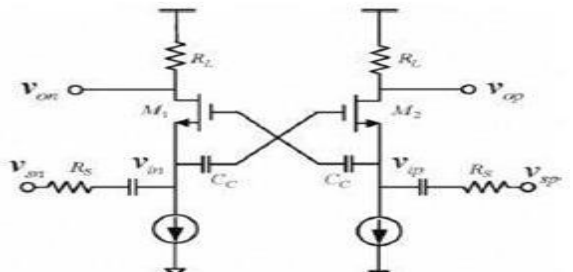


Fig. 8. Differential capacitive cross coupled configuration [11].

LNA exhibits superior performances over the frequency range of 3.1-10.6 GHz to the LNA's reported in [1-3]. The differential configuration can highly diminish the 2nd-order nonlinearity and make the input common-mode level invariable. The shunt-series triple resonance peaking technique is adopted to achieve wideband flat gain in our LNA.

The noise-cancelling technique can decouple the input matching with the NF by cancelling the output noise from the matching device. The simplified illustration of the noise-cancelling principle is shown in Figure 9.

By employing the noise-cancelling technique, the traditional link between the input matching and the noise figure is decoupled, and the equivalent transconductance is increased.

They are so power-hungry and hence not suitable for low-power applications. Single-stage LNA's consume low power but their output bandwidth cannot provide the flat-high-gain response. When the LNA is selected to operate in the differential receiving mode, the circuit presents a balanced response. Both M_1 and M_2 are configured as common-gate (CG) amplifiers. The differential signal from the off-chip balun is AC-coupled to the source nodes of M_1 and M_2 , which are connected to the ground through two external large inductors for DC current sink.

The differential LNA is preferred over other topologies as it offers better immunity to environmental noise, improved linearity, low power consumption. Firstly, the effect of the parasitic ground inductances is reduced by the virtual ground formed at the tail. Secondly the differential amplification of the signal ensures attenuation of the common mode signal and in most systems this common mode signal will be noise.

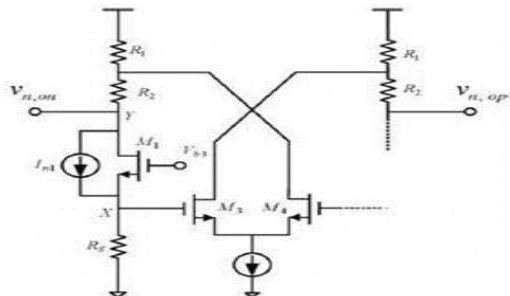


Fig. 9 - Noise cancelling principal of differential topology [11]

Thirdly, the use of mixers and image rejection schemes require to be fed from a differential source.

IV. Conclusions

In case of UWB LNA topology, only few topologies are basic, while others are the modifications of basic narrowband

V. References

- [1] G. Sapone, G. Palmisano, "A 3–10-GHz Low-Power CMOS Low-Noise Amplifier for Ultra-Wideband Communication", IEEE Transactions On Microwave Theory And Techniques, Vol. 59, No. 3, March 2011.
- [2] E.A.M. Klumperink, "Finding all the elementary circuits exploiting transconductance", IEEE Transaction on Circuits and Systems, CAS-II, Vol. 48, No. 11, pp. 1039-1053, Nov. 2001.
- [3] P.Heydari, D.Lin, "A Performance Optimized CMOS Distributed LNA for UWB Receivers", Custom Integrated Circuits Conference, IEEE 2005.
- [4] F.Zhang, P.Kinget, "Low Power Programmable Gain CMOS Distributed LNA for Ultra Wideband Applications", Symposium on VLSI Circuits Digest of Technical Papers, 2005.
- [5] J.Kim, S.Hoyos, and Jose S.Martinez, "Wideband Common-Gate CMOS LNA Employing Dual Negative Feedback With Simultaneous Noise, Gain, and Bandwidth Optimization", IEEE Transactions On Microwave Theory And Techniques, Vol. 58, No.

LNA and majority are the result of bandwidth extension and noise cancelling techniques. Even two or more topology can be simultaneously applied in design to achieve the desired specifications of LNA. This paper presented guidelines for selection of LNA topologies for designing LNA. A table showing comparison of various LNA topologies is as shown in Table 1.

| Topology | Band Width | Gain | Noise figure | Power Consumption | Impedance matching | Linearity | Area |
|------------------------|------------|----------|--------------|-------------------|--------------------|-----------|----------|
| Distribution Amplifier | High | High | High | High | Better | Good | High |
| Common Gate(CG) | High | low | High | Moderate | better | Best | Moderate |
| Common Source(CS) | Low | High | Low | High | Best | Good | Moderate |
| Cascode CS | High | High | Low | Moderate | Best | Best | Moderate |
| Folded Cascode | High | Low | Low | High | Best | Best | High |
| Resistive Feedback | High | Moderate | Low | High | Better | Better | High |
| Differential Amplifier | Low | Low | Low | High | Good | Better | Moderate |
| Current Reuse | Better | High | High | Low | Good | Good | Better |

Table 1 - Comparison of various LNA topologies

- 9, September 2010.
- [6] J.Kaukovuori, J.Ryynanen, and K.Halonen, "CMOS Low-Noise Amplifier Analysis and Optimization for Wideband Applications", IEEE2006.
 - [7] R.Wang, M.Lin, C.Lin, C.Yang, "A IV Fullband Cascoded UWB LNA with Resistive Feedback" RFIT2007-IEEE International Workshop on Radio-Frequency Integration Technology, Dec. 9-11, 2007, Singapore 2007.
 - [8] R.Wang, S.Chen, C.Lin, Y.Lin, "A 0.8V Folded-Cascode Low Noise Amplifier for Multiband Applications" IEEE.2008.
 - [9] C. Wu, Y. Lin, "A Low-Power CMOS Low Noise Amplifier for UWB Applications", Proceedings of 2010 IEEE International Conference on Ultra-Wideband (ICUWB2010), IEEE 2010.
 - [10] M. Lorenzo, M. Leon, "Comparison of LNA Topologies for WiMAX Applications in a Standard 90-nm CMOS Process" 12th International Conference on Computer Modelling and Simulation, IEEE 2010.
 - [11] Z. Liu, G. Chen, R. Zhang, "Design of a Noise cancelling Differential CMOS LNA for 3.1-10.6 GHz UWB Receivers" IEEE 2009

Identification of Inrush Current of Transformer using Discrete Wavelet Transforms

Shah Mohammad, Dr. D.N. Vishwakarma, Senior member IEEE

Abstract-- In this paper there is a technique used for the protection of power transformer. In principle, a wavelet transform technique used to extract the feature component of transformer currents. The powerful toolbox of discrete wavelet transform technique is used to distinguish between inrush current and internal fault of transformer. The potential benefit of applying discrete wavelet transform for improving the performance of the protection relay have been recognized in recent years.

Index Terms-- Power transformer, Differential protection, inrush currents, internal faults, wavelet transform.

I. INTRODUCTION

Power transformer is amongst the most important components in a power system. Avoiding damage to Power transformers is vital, otherwise continuity in power delivery may be seriously disrupted. Furthermore, repair or replacement is expensive and time consuming. Basically, in transformer protection differential protection relay is used, However, a key problem of differential protection is accurate and rapid discrimination of magnetizing inrush current from an internal fault current. It is evident that relaying protection should be initiated in response to internal fault but not to inrush current. To avoid the needless trip by magnetizing inrush current, many different restrain methods are proposed in recent years. The statistic survey shows that 70-80% of transformer failures results from interturn fault. This implies that the detection of interturn fault at early stage will minimize the failure of transformer and improve considerably the reliability of system operation.[1] This paper presents a new protection scheme for transformer fault. The proposed algorithm extracts fault and inrush generated transient signals using DWT. When a fault occurs in the system, the specially designed relay captures the fault transient currents via CTs installed at the primary and secondary sides of transformer respectively. The signals are then tuned by DWT Multiresolution filter bank to filter out the unwanted components Units [2]. In this daubechies wavelets are used to construct five level of filter bank to extract the transient. From the DWT outputs, the Differential and average currents between the primary and the secondary are derived and the spectral energies of those currents are calculated to produce the operational and restraint signals.

Finally the relay compares the levels of two signals to determine whether the fault is an internal or external to the transformer. By this, we can say that this technique is able to clearly distinguish an inrush current from internal fault [4].

Authors are with Department of Electrical Engineering, Indian Institute of Technology, Banaras Hindu University varanasi-221005, India (e-mail: shah.eee12@iitbhu.ac.in, dnv.eee@iitbhu.ac.in).

II. WAVELET THEORY AND ITS ANALYSIS

A. Discrete wavelet transform

One example of a signal transformation is the transformation from the time domain to the frequency domain. The oldest and probably best known method for this is the Fourier Transform developed in 1807 by Joseph Fourier. An another method with some entice properties is the wavelet transform, first mentioned by Alfred Haar in 1909. Since then a lot of research into wavelets and the wavelet transform is Performed. When the time localization of the spectral components are needed, a transform giving the time-frequency representation of the signal is needed. The solution tool is wavelet transform. Wavelet is capable of giving the time and frequency information simultaneously, hence giving a time- frequency representation of signal. The analysis of a non-stationary signal using the FT give unsatisfactory results. Better results can be obtained using wavelet analysis. One advantage of wavelet analysis is the ability to perform local analysis.

The wavelet transform is divided into Continuous wavelet transform (CWT) and Discrete Wavelet Transform (DWT) The continuous wavelet transform is given by [7].

$$CWT(a,b) = \frac{1}{\sqrt{a}} \int_{-\infty}^{+\infty} x(t)g\left(\frac{t-b}{a}\right) \quad (1)$$

The transformed signal CWT (a, b) is a function of the translation parameter a and the scale parameter b. The mother wavelet is denoted by g. The signal energy is normalized at

every scale by diving $(\frac{1}{\sqrt{a}})$

The discrete wavelet transform is given by

$$DWT(m,k) = \frac{1}{\sqrt{a_o^m}} \sum_n x(n)g\left(\frac{k-n a_o^m}{a_o^m}\right) \quad (2)$$

In which g(n) is the mother wavelet, scaling and translation parameter a and b, respectively, are functions of an integer Parameter,given by

$$m, a=a a_o^m \quad e \quad b=n a_o^m$$

In wavelet technique multi resolution analysis (MRA) is used. By using this approach called MRA it is possible to analyze a signal at different frequencies with different resolutions. The change in resolution is schematically displayed in Fig below. You can see in below that in every boxes have a certain non zero area. Every box in above Figure corresponds to a value of the wavelet transform in the time-frequency plane. Let's take a closer look at below Figure First thing to notice is that although the widths and heights of the boxes change, the area is constant. That is each box represents

an equal portion of the time-frequency plane, but giving different proportions to time and frequency.

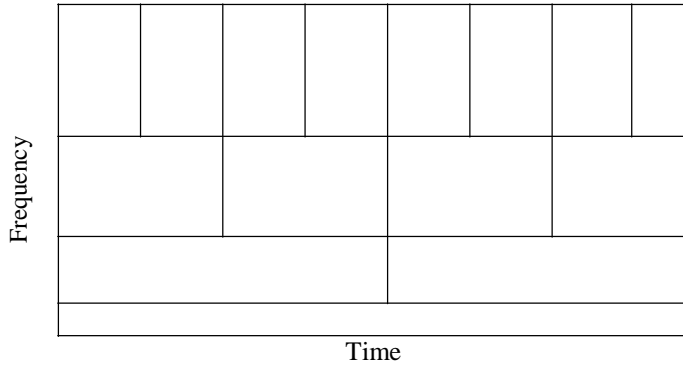


Fig. 1. Multi Resolution Analysis

III. STRUCTURE OF MULTI LAYER RESOLUTION

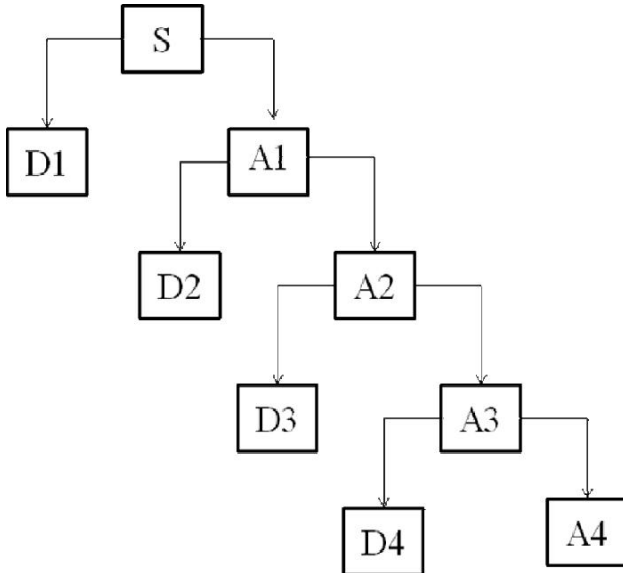


Fig. 2 Four layer Multi resolution analysis

As we can see from above figure is decomposition of signal, in which A denotes the high approximate component of signal and D denotes the detail component of signal. The low frequency component is further decomposed in multi resolution analysis. And high frequency component is not taken into account.

The relationship of decomposition is given

$$\text{by } S = A_4 + D_4 + D_3 + D_2 + D_1$$

The discrete wavelet transform (DWT) uses filter banks for the construction of the Multi resolution time-frequency plane. Filter banks will be introduced in further. The DWT uses multi resolution filter banks and special wavelet filters for the analysis and reconstruction of signals.

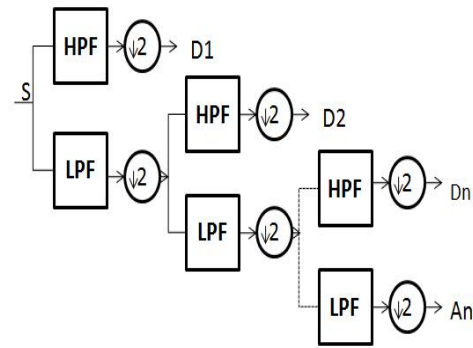
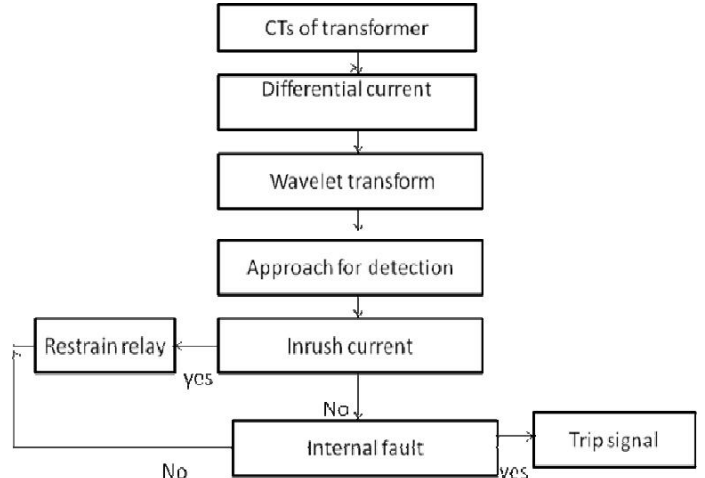


Fig. 3. Implementation of DWT

DWT is computed by successive low pass and high pass filtering of the discrete time-domain signal. The signal S is decomposed in two parts. High pass filter [HPF] and low pass filter [LPF]. Then the output of LPF is further cut in half of the frequency bandwidth and sent to second stage. This procedure is repeated until the original signal is decomposed to a pre-defined certain level.

IV. FLOWCHART OF THE PROPOSED ALGORITHM



The flowchart shown above is given an overview of wavelet transform, that how the procedure is takes place when we are using Discrete Wavelet Transform (DWT).

V. SIMULATION OF POWER TRANSFORMER

Three phase transformer of 200 MVA, 220/110 are modelled using MATLAB. The parameters used for the simulation of these transformers through MATLAB were taken.

A three phase source with a 150 km transmission line are used in this model, and the simulation was done by means of Sim Power Systems (MATLAB) software.

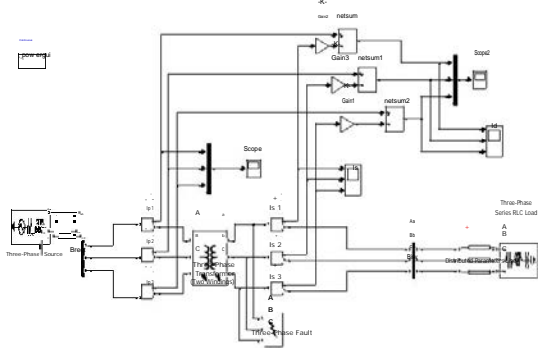


Fig. 4. Simulated power system for internal fault condition.

Inrush condition can be obtain by transformer secondary open. Internal fault can be obtain, Transformer secondary shorted and single-phase ground fault and double phase-ground faults and three phase fault.

the simulation waveform of inrush current and three phase fault are shown below.

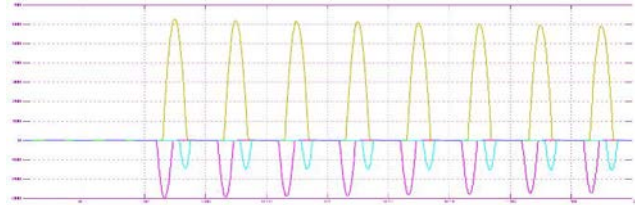


Fig. 5. Simulated power system of inrush condition (3-ph.)

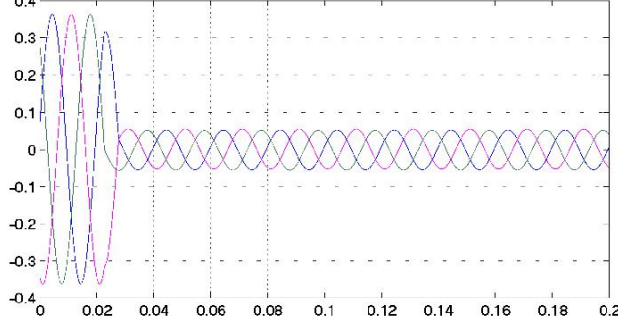


Fig. 6. Simulated power system of internal fault condition (3-ph.)

VI. WAVELET ANALYSIS METHOD TO IDENTIFY INRUSH CURRENT

There are many type of wavelet function in wavelet toolbox. And according to our needs we choose from them. Here we use DB5 of daubechies series constructed by famous wavelet analysis scholars Daubechies Ingrid to transform the original waveform.

From figure (7) show wavelet transform of inrush current and internal fault. among them d1, d2, d3, d4 shows high coefficient of wavelet transform waveform in the first, second, third and fourth scale, and A4 shows wavelet discrete signal. We can easily see from wavelet discrete waveform that, there is more difference in three phase fault and inrush graph.

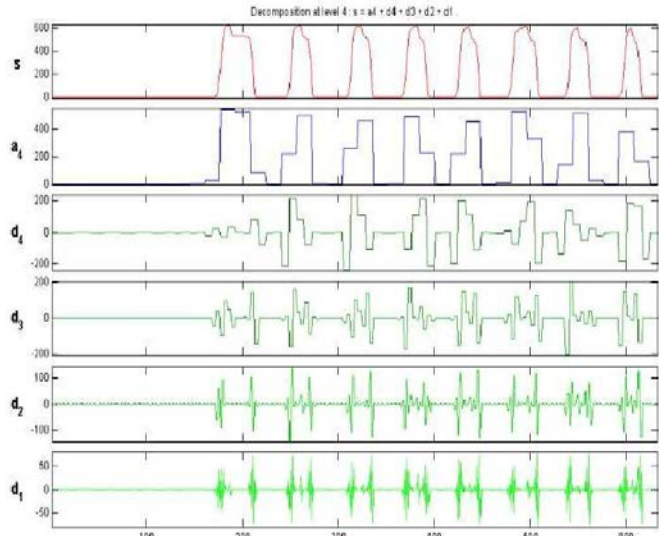


Fig. 7. Wavelet transform of inrush current-A phase

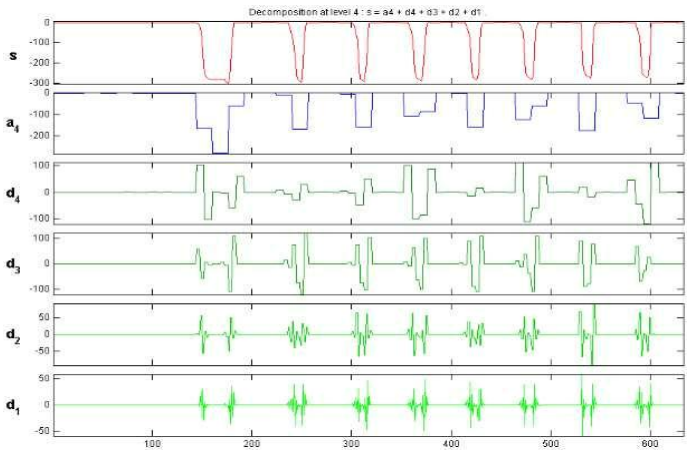


Fig 8. Wavelet transform of inrush current-B phase

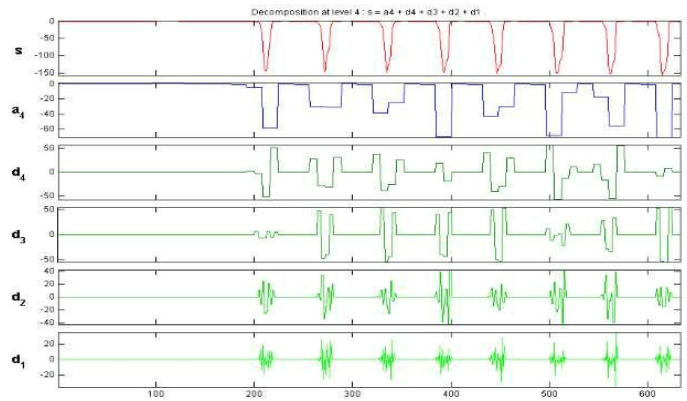


Fig 9. Wavelet transform of inrush-C phase

Here we take a only one phase of three phase current of inrush as well as three phase faults. As we see in inrush wavelet graph the d1 shows approx equal graph but in case of three phase fault graph, there is a larger pulse component in fault starting, but this component quickly decay, so it is very easy to identify for transformer to identify inrush current and the fault current well.

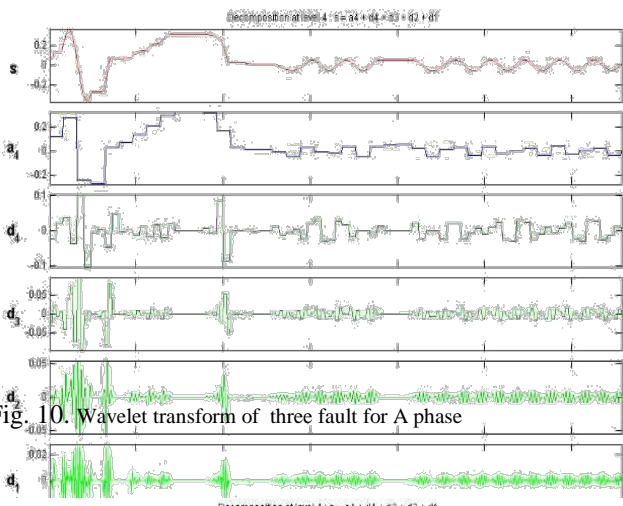


Fig. 10. Wavelet transform of three fault for A phase

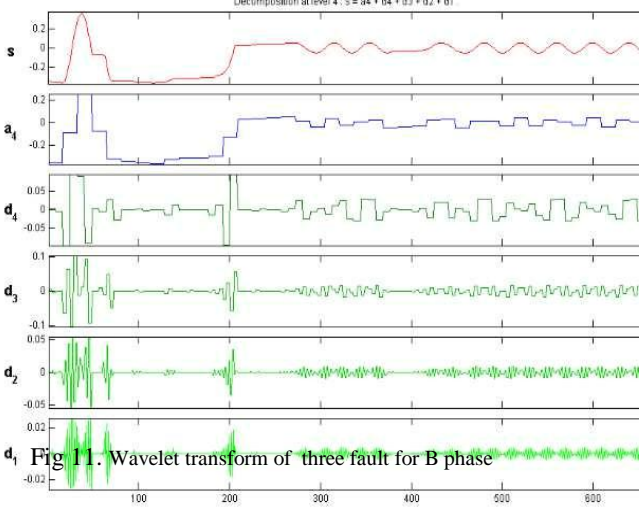


Fig. 11. Wavelet transform of three fault for B phase

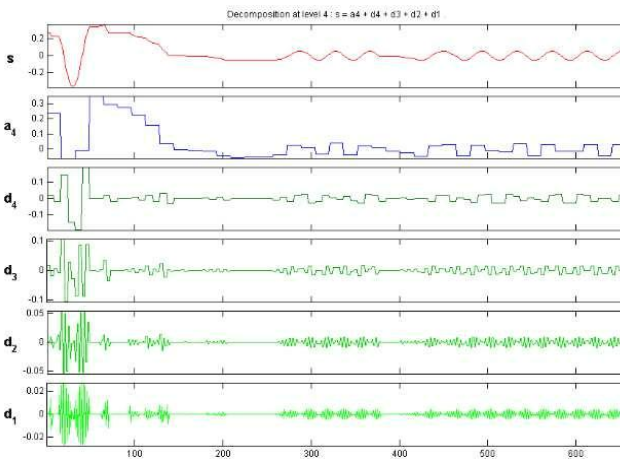


Fig. 12. Wavelet transform of three fault for C phase

VII. ACKNOWLEDGMENT

The authors are very thankful to Dr. S.P. Singh, professor and head Department of Electrical Engineering IIT-BHU, for providing necessary facilities for carrying out my research work.

VIII. CONCLUSION

This paper introduces a modern differential protection scheme for power transformer. This paper established easy model of matlab software, carries out fast simulation and puts out forward a method of using discrete wavelet transform to differentiate between inrush current and internal fault. This is the method which can easily identified without doing any long calculation. It is possible, with less computation.

REFERENCES

- [1] B.Ram and D.N. Viswakarma, "power system protection and switchgear",Tata McGraw-hill publishing company limited, new delhi,1995.
- [2] Okan OZGO NENEL, Guven ONBILGIN, Cagri KOCAMAN"Transformer Protection Using the Wavelet Transform" Turk J Elec Engin, VOL.13, NO.1 2005, c TUBITAK
- [3] A. Rahmati, and M. Sanaye-Pasand, "New Method for Discrimination of Transformers Internal Faults from Magnetizing Inrush Currents Using Wavelet Transform" IEEE 2008 .
- [4] M. Jamali, M. Mirzaie, S. Asghar Gholamian and S. Mahmodi Cherati,"A Wavelet-Based Technique for Discrimination of Inrush Currents from Faults in Transformers Coupled with Finite Element Method" IEEE 2011.
- [5] Jiang F; Bo, Z.Q.; chin, P.S.M.; redfern, M.A.; chin, Z.Power Transformer Protection Based On Transient Detection Using Discrete Wavelet Transform DWT, IEEE power engg. Society winter meeting 2000, vol-3.
- [6] Moises Gomez-Moranle, Denise W. Nicoletti "A Wavelet-based Differential Transformer Protection" IEEE Transactions on Power Delivery, Vol. 14, No. 4, October 1999.
- [7] Jefferson Prates Marques , Aecio Oliveira, Ghendy Cardoso junior, Algorithm using Discrete Wavelet Transform to Power Transformers Protection IEEE 2013.

Torque Ripples Minimization of Switched Reluctance Motor for Hybrid Electric Vehicle Applications

A.Avdhesh kumar, B.Kalpana Chaudhary, and C.Abhijeet Sah

Abstract-- This paper reports on a method to improve the torque profile of the switched reluctance motor. The analysis and study of rotor geometry modifications is the method; the importance of rotor pole shaping is justified through CASPOC simulation and FEM analysis. Simulated torque profiles from rippled to the improved are presented.

Index Terms-- Switched reluctance motor (SRM), CASPOC simulation, torque ripple (TR), rotor pole shaping (RPS), stator pole arc (β_s), rotor pole arc (β_r).

I. INTRODUCTION

In the past few years, the switched reluctance motor (SRM) has gained much interest over other types of electric motors in drives applications due to its several advantages like a simple structure, Low cost, Possible operation in all four quadrant operation, Rotor and robustness, high speed operation, high reliability and efficient variable speed drive. Switched reluctance motor has no form of excitation on rotor, which eliminates the requirements of brushes or slip rings [2]. Although SRM has several advantages over the other types of electric machine like permanent magnet synchronous motor (PMSM), brushless D.C. (BLDC), Induction motor and D.C. motor but SRM has not been widely used until recently because of the problem of high torque ripples [2,5]. The paper investigated the impact of changing rotor pole arc on torque ripples in 6/4 three phase SRM.

A.Avdhesh kumar
B.Kalpana Chaudhary
C.Abhijeet Sah

the pole width of stator and rotor both, widening the stator back iron thickness etc. by implementing the rotor pole arcs modification. The torque ripples mainly occurs at the instant of commutation, when torque production mechanism is being transferred from one active phase to another [2]. Torque ripple minimization of SRM drives can be done by modification at design level either machine side or converter side.

Torque ripple minimization on machine side at design level can and simulating on CASPOC and ANSYS.

II. INDUCTANCE AND TORQUE PROFILE OF CONSIDERED SRM

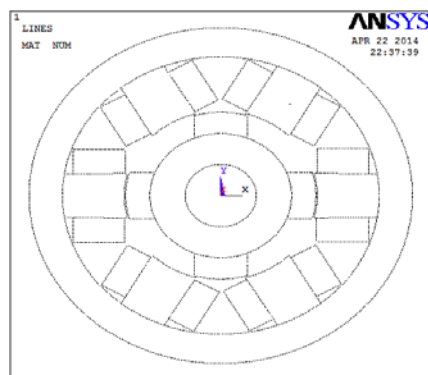


Figure.1 ANSYS design of SRM with stator winding

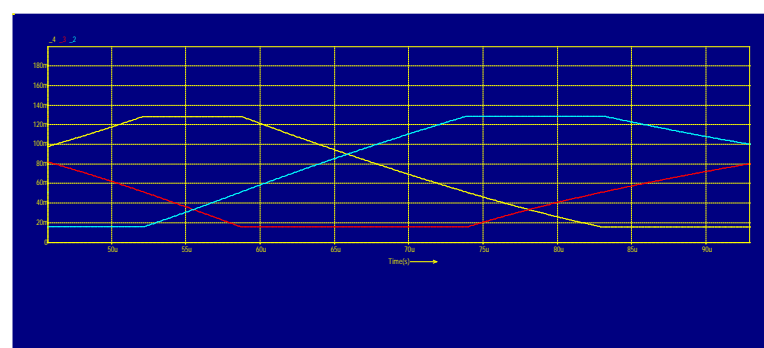


Figure.2. stator inductance of three successive phase

be done by doing some modification in machine at design level like,: Changing the rotor pole arc geometry, Changing

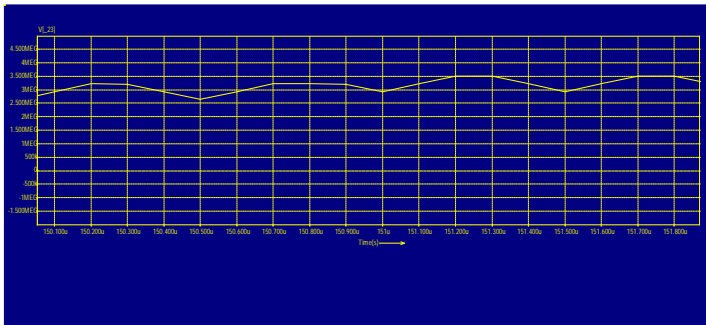


Figure.3. Torque profile with ripples observed of reference SRM ($\beta_s=30$ & $\beta_r=32$ degree)

1) Main Dimensions of Reference SRM

Stator outer diameter 269 mm

Overall axial length 184.16 mm

Shaft length 156 mm

Rotor diameter 134.5 mm

Stack length 100 mm

Number of stator pole 6

Number of rotor pole 4

Stator rotor air gap 0.5 mm

Number of phases 3

Stator pole arc 30 degree

Rotor pole arc 32 degree

III. THE IMPACT OF CHANGING ROTOR POLE ARC ON THE TORQUE RIPPLES OF SRM

Fig. 1 illustrates a 6/4 Switched reluctance motor (SRM) and SRM is symmetrical and modelled with all the three phases. As per design consideration, the rotor pole shape of SRM cannot be made “square” as the conventional tendency in a.c/d.c. machines. The best SRM design requires long narrow poles, proved on discussion basis [7] and [8], but, the rotor pole shaping of considered SRM is presented in this subsection of this paper by rigorous CASPOC simulation results. The considered SRM [1] produce torque profile as in figure.3-4.

The shaping of the rotor pole arcs are modified for two different sets of iteration, keeping the stator pole arc constant. This paper investigate the minimum torque ripple by optimization of design of rotor pole arc by iterating the rotor pole arc from its minimum arc to maximum rotor pole arcs [5] and simulating on CASPOC. There is two sets of iteration of rotor pole arc, one is for 30 degree, and other for 32 degree of stator pole arc respectively.

Rotor pole arcs should be slightly greater than stator pole arcs in order to maintain the self-starting feature of SRM, otherwise inductance profile will introduce a overlap region and torque production would be zero due to zero slope of the inductance profile. Rotor pole arcs can be modified up to its maximum range of rotor pole arcs [5]

IV. CASPOC SIMULATION RESULT

Table. I-II shows the CASPOC simulated result for different rotor pole arcs.

Table.I.

| S.N. | Stator pole arc (β_s) in mech. degree | Rotor pole arc (β_r) in mech. degree | Torque | |
|------|---|--|--------|---------------|
| | | | Ripple | Ripple factor |
| 1 | 30 | 30 | 31.608 | 146.225 |
| 2 | 30 | 32 | 1.523 | 4.152 |
| 3 | 30 | 34 | 1.505 | 4.140 |
| 4 | 30 | 36 | 2.589 | 9.855 |
| 5 | 30 | 38 | 1.43 | 3.896 |
| 6 | 30 | 40 | 1.040 | 1.881 |

Table.II..

| S.N. | Stator pole arc (β_s) in mech. degree | Rotor pole arc (β_r) in mech. degree | Torque | |
|------|---|--|--------|---------------|
| | | | Ripple | Ripple factor |
| 1 | 32 | 32 | 2.031 | 7.071 |
| 2 | 32 | 34 | 1.455 | 3.602 |
| 3 | 32 | 36 | 1.250 | 2.859 |
| 4 | 32 | 38 | 1.584 | 5.294 |
| 5 | 32 | 40 | 1.309 | 3.365 |

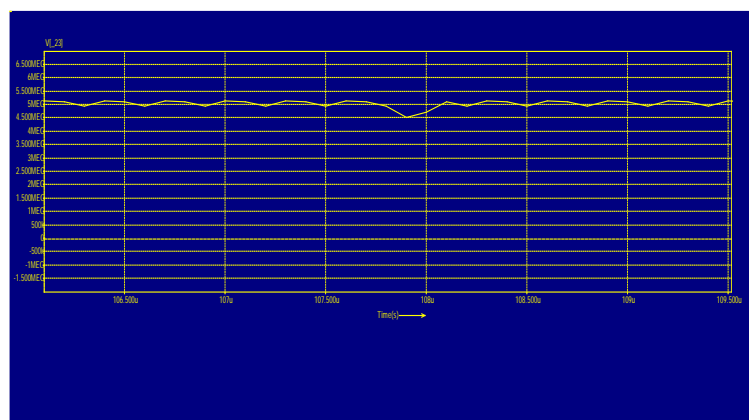


Figure.4. Improved torque profile ($\beta_s=32$ degree & $\beta_r=36$ degree)

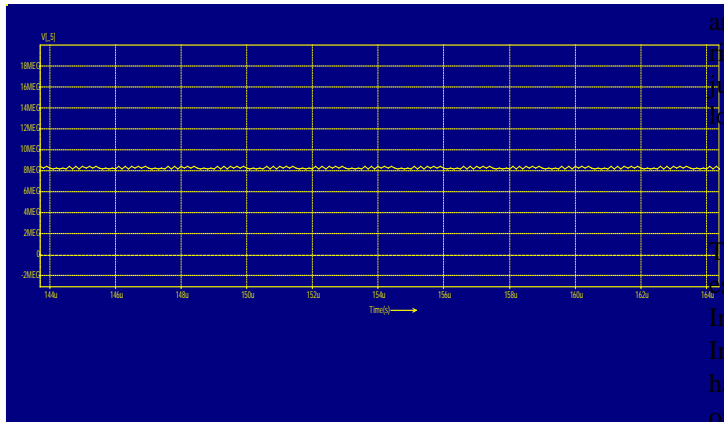


Figure 5 . Improved torque profile ($\beta_s=30$ degree & $\beta_r =40$ degree)

V. RESULT AND DISSCUSSION

It is obvious from the above interpretation that due to increasing the rotor pole arcs, torque ripples reduced up to requisite level in order to achieve uniform or smooth torque profile for SRM drives. The modification of rotor pole arcs and CASPOC simulation gives the prediction of best optimum operating point corresponding rotor pole arcs.

As per analysis and simulation, none of the stator and rotor pole arc combination gives the ripple free torque profile but the combination ($\beta_s=30$ degree & $\beta_r =40$ degree) and ($\beta_s=32$ degree & $\beta_r =36$ degree) are the best combination of minimum torque ripples for SRM drive fed Hybrid Electric Vehicle Applications.

VI. CONCLUSION

The paper studies, analysis and simulation the trend of torque ripple minimization like Changing the rotor pole arc geometry, Changing the pole width of stator and rotor both and widening the stator back iron thickness etc. which can be used to minimize the ripples in the torque characteristic of the SRMs.

Rotor pole geometry modification affects the ripples in the torque characteristic effectively, however, none of rotor pole

arc combination gives torque characteristics without torque ripples. The trend of modification of rotor pole arcs are justified by CASPOC simulation, the results illustrates very low torque ripple for higher rotor pole arcs.

VII. ACKNOWLEDGMENT

The authors gratefully acknowledge the continuous and esteemed guidance of Dr. K. Chaudhary, (Assistant Professor, Indian Institute of Technology, Banaras Hindu University, India). Without his support and guidance this work wouldn't have been possible. The authors are thankful to Head and all other teaching and non-teaching staff of Electrical Engineering Department who gratefully.

VIII. REFERENCES

- [1] Akira Chiba,"Torque Density and Efficiency Improvements of a Switched Reluctance Motor Without Rare-Earth Material for Hybrid Vehicles", IEEE Transactions on Industry Applications, VOL. 47, NO. 3, MAY/JUNE 2011.
- [2] "Approaches for Minimizing the Torque Ripples in the Switched Reluctance Motor"__ Proceedings of the 14th International Middle East Power Systems Conference (MEPCON'10), Cairo University, Egypt, December 19-21, 2010, Paper ID 245,_596.
- [3] "Analysis and Improvement of Torque Profile in the Switched Reluctance Drives".
- [4] "Design Procedure for Switched-Reluctance Motors", IEEE Transactions on Industry Applications, VOL. 24, NO. 3, May/June 1988
- [5] R. Krishnan — Fellow, IEEE, "Switched Reluctance Motor Drives, modeling, simulation, analysis, design and application". CRC Press, Boca Raton London New York Washington , D.C.
- [6] T. J. E. Miller, "Switched Reluctance Motors and their control", Magna Physics Publishing, Oxford Science Publications, New York, 1992.Industry Applications, VOL. 24, NO. 3, May/June 1988
- [7] T.J.E.Miller, " Brushless permanent magnet and reluctance motor drives". Clarendon press, Oxford, 1989
- [8] R. Arumugam,J.F.Lindsay and R.Krishnan."sensitivity of pole arc/ pole pitch ratio on SRM" IEEE-IAS proceedings,Pittsburg.P.A.Ocober 1988.

Suboptimal control of a higher order system by Balance Truncation method

A. Abdul HafeezPrem, B. NarayanVerma

ABSTRACT-- This paper discusses suboptimal control method using model reduction technique. Modeling of large real time systems results in large number of differential or difference equations that lead to state variable or transfer function models that represents a higher order system. It is very difficult to handle such a higher order system model for the analysis and design purposes. This paper presents Balance Truncation method technique that is used to reduce the higher order model to a lower order one and then optimal control technique is applied on reduced model for finding suboptimal control result.

I. INTRODUCTION

Optimal control is an attractive approach to control design for general systems. Although there is extensive literature on the theory of optimal control, it is very difficult to obtain the optimal feedback law for real world processes. Therefore many methods to calculate approximations of the optimal feedback law have been proposed over the last four decades. Scientists and engineers are often confronted with the analysis, design and synthesis of real life problems. The first step in such studies is the development of a 'mathematical model' which can be a substitute for the real problem.

In any modeling task there are two often conflicting factors, simplicity and accuracy. On one hand, if a system model is oversimplified, presumably for computational effectiveness, incorrect conclusions may be drawn from it in representing an actual system. On the other hand, a highly detailed model would lend to a great deal of unnecessary complications and should a feasible solution be attainable, the extent of resulting details may become so vast that further investigations on the system behavior would become impossible with questionable practical values.

A. Abdul Hafeez (Assistant Professor) KNIPSS Sultanpur, U.P. India (email:-hafeez3755@gmail.com)

B. Narayan Verma, KNIT Sultanpur U.P. India (email:-pnvknit@gmail.com)

Clearly a mechanism by which a compromise can be made between a complex, more accurate model and a simple and less accurate model, is needed for which different model reduction techniques are used that gives the model whose performance is similar to original model on which we apply the optimal control that gives the optimal control laws of system in simple way.

Suboptimal control concept is originated from finding optimal control law for a complex system by obtaining low order reduced model of system whose performance is similar to original system and finding its optimal control law.

II. OPTIMAL CONTROL

Optimal control deals with the problem of finding a control law for a given system such that a certain optimality criterion is achieved. A control problem includes a cost functional that is a function of state and control variables. An optimal control is a set of differential equations describing the paths of the control variables that minimize the cost functional.

The formulation of optimal control problem requires:-

1. A mathematical description (or model) of the process to be controlled (generally in state variable form).
2. A specification of the performance index.
3. A statement of boundary conditions and the physical constraints on the states and/or controls.

Consider a dynamical system in input-state-output form

$$\begin{aligned} \dot{x}_{(t)} &= Ax_{(t)} + Bu_{(t)} \\ y_{(t)} &= Cx_{(t)} + Du_{(t)} \end{aligned} \quad (1)$$

Here, we have a system with n states, m inputs and p outputs. That is, $x_{(t)} \in R^n$, $u_{(t)} \in R^m$ and $y_{(t)} \in R^p$ for all time instants $t \in R$.

Let the performance index 'J' as a function of free parameter $k_1, k_2, k_3, \dots, k_n$ of the system with fixed configuration

$$J = J(k_1, k_2, k_3, \dots, k_n)$$

Here we have to find the set of value of k for which 'J' is optimized

$$\frac{\partial J}{\partial K_i} = \mathbf{0} \quad i=1, 2, 3, 4, \dots, n; \quad (2)$$

give the necessary condition so that 'J' is to be minimum from the solution of the equation (2) find the subset that satisfy the sufficient condition which require that the Hessian Matrix given below is positive definite.

$$H = \begin{pmatrix} \frac{\partial^2 J}{\partial K_1^2} & \frac{\partial^2 J}{\partial K_1 \partial K_2} & \cdots & \frac{\partial^2 J}{\partial K_1 \partial K_n} \\ \frac{\partial^2 J}{\partial K_2 \partial K_1} & \frac{\partial^2 J}{\partial K_2^2} & \cdots \cdots & \frac{\partial^2 J}{\partial K_2 \partial K_n} \\ \cdots & \cdots & \cdots \cdots & \cdots \\ \frac{\partial^2 J}{\partial K_n \partial K_1} & \frac{\partial^2 J}{\partial K_n \partial K_2} & \cdots \cdots & \frac{\partial^2 J}{\partial n} \end{pmatrix}$$

If there are two or more sets of K_i satisfying the necessary as well as sufficient conditions of minimization then compute the corresponding J for each set the set that has smallest 'J' gives the optimal parameter. The minimization problem will be more easily solved if we can express performance index in terms of transform domain quantities for quadratic performance index given in integral square error (ISE) this can be done by using Parseval's theorem which allow us to write equation (3) as given in [1].

$$\int_0^\infty (x_{(t)}^2) dt = \frac{1}{2\pi} \int_{-\infty}^\infty (x_{(s)} x_{(-s)}) ds \quad (3)$$

Where $x_{(s)}$ is Laplace transform of $x_{(t)}$

III. METHODS OF MODEL ORDER REDUCTION

In this paper, we are discussing about time domain techniques, which are given below:

1) Modal Analysis Approach

2) Aggregation Method

A. *Modal Analysis Approach-*

This method attempts to retain the dominant eigenvalues of the original system and then obtains the remaining parameter of the low order model in such a way that its response, to a certain specified input should approximate closely to that of high order system. In other words we neglect the effect of far off poles and zeros from the dominant poles and zeros. The methods proposed by Davison (1966), Marshall (1966), Mitra (1967) and Aoki (1968) all belong to this category.

1) *Balanced Model Truncations:-*

Balanced Model Truncations requires a state truncation of a system which is represented in balanced state space form. The balanced state space representation is an input-state-output representation of the form for which the controllability grammian and the observabilitygrammian are equal and diagonal.

Suppose that a minimal and stable state space representation of a dynamical system is given then we define two matrices.

The controllability grammian associated with the system (A, B, C, D) is the matrix

$$P = \int_{-\infty}^0 (e^{At} B^T B e^{A^T t}) dt \quad (4)$$

Since the system is assumed to be stable, the eigenvalues of A has a negative real part, and from this it follows that the integral in (4) is well defined. Note that P is an $n \times n$ real matrix, it is symmetric.

The observabilitygrammian associated with the system (A, B, C, D) is the matrix

$$Q = \int_{-\infty}^0 (e^{A^T t} C^T C e^{At}) dt \quad (5)$$

Again, the stability assumption implies that the integral in (5) is well defined. Q is an $n \times n$ real symmetric matrix.

Fortunately, to compute the controllability and observabilitygrammians of a state space system (1), it is not necessary to perform the integration as in (4) and (5) it can be obtain from the Lyapunov equation [4].

Given a minimal and stable system, its controllability grammian P is the unique positive definite solution of the Lyapunov equation

$$AP + PA^T + BB^T = 0 \quad (6)$$

Similarly, the observabilitygrammian Q is the unique positive definite solution of

$$A^T Q + QA + C^T C = 0 \quad (7)$$

If the system we have is minimal, then grammians P and Q are the unique solutions to (6) and (7), respectively. The computation of the grammians is therefore equivalent to the algebraic problem to find solutions of Lyapunov equations (6) and (7). A minimal state space representation (1) is called balanced if the controllability and observabilitygrammians are equal and diagonal,*i.e*, if

$$P = Q = \text{diag}(\sigma_1, \sigma_2, \dots, \sigma_n)$$

where σ_i are real and positive numbers that are ordered according to

$$\sigma_1 \geq \sigma_2 \geq \sigma_3 \geq \dots \geq \sigma_n$$

To find the balanced representation of the system (1), let us assume that we calculated the controllability and observability grammians for the stable system (1) and let us see how these grammians transform if we change the basis of the state space.

Consider a state space transformation

$$x_{(t)} = T x'_{(t)} \quad (8)$$

for system (1) with T a non-singular matrix of dimension $n \times n$. Since such a transformation only amounts to rewriting the state variable in a new basis, this transformation does not affect the input-output behavior of system associated with (1). By substituting (8) in (1) and solving for $x'_{(t)}$, equation (1) can be written as

$$\dot{x}'_{(t)} = T^T A T x'_{(t)} + T^T B u_{(t)}$$

$$y_{(t)} = C T x'_{(t)} + D u_{(t)} \quad (9)$$

In fact, we describe all minimal input-state-output representations of system by varying T over the set of non-singular matrices. The transformation

$$A \quad T^T A T = A' \quad (10) \quad \rightarrow$$

is called a similarity transformation of the matrix A . The characteristic polynomial of the A matrix occurring in (1) is the polynomial $p_{(s)} = \det(sI - A)$. We can write this polynomial in various formats as in [3]

Thus, consider again the state space transformation (8). As we have seen, this results in the transformed state space parameters (A' , B' , C' , D') and transformed grammians take the form

$$P' = T^T P (T^T)^T \quad Q' = T^T Q T \quad (11)$$

This shows that the grammians depend strongly on the basis of the state space.

However, their product is

$$P' Q' = T^T P (T^T)^T T^T Q T = T^T P Q T \quad (12)$$

This shows that the eigenvalues of PQ are invariant under state space transformations.

Let $\lambda_1, \lambda_2, \lambda_3, \dots, \lambda_n$ denote the eigenvalues of the product PQ . Then λ_i are positive real numbers for $i = 1, 2, \dots, n$ so that it makes sense to consider their square roots.

$$\sigma_i = \sqrt{\lambda_i} = \lambda_i^{1/2} \quad (13)$$

That showed that these numbers are system invariants: they do not change by transforming the basis of the state space. In the literature, these system invariants play a crucial role and are called the Hankel singular values of the system (1). To show that balanced state space representations actually exist, we need to construct a non-singular state transformation matrix T that simultaneously diagonalizes the controllability and the observability grammians P and Q .

If (1) is a stable, balanced state space system, then the k^{th} order truncation

$$\dot{x}^*_{(t)} = A_{11} x^*_{(t)} + B_1 u_{(t)}$$

$$y_{(t)} = C_1 x^*_{(t)} + D u_{(t)}$$

is called the k^{th} order balanced modal truncation

This simple approximation method provides very efficient and good approximate models. It eliminates the poorly controllable and poorly observable states from a state space model. The number k may in practice be determined by inspecting the ordered sequence of Hankel singular values $\sigma_1, \sigma_2, \dots, \sigma_n$. A drop in this sequence (i.e., a number k for which $\sigma_{k+1} / \sigma_k \ll 1$) may give you a reasonable estimate of the order of a feasible approximate model. If $\sigma_k > \sigma_{k+1}$ (as will be the case in many practical situations) the k^{th} order balanced truncation turns out to have good properties.

IV. RESULT

The state space representation of a system is

$$\dot{x} = Ax + Bu; \quad \text{where } A = n \times n \text{ matrix}$$

$$y = Cx$$

Where

$x \in \mathbb{R}^n$ is the state vector

$u \in \mathbb{R}^m$ is the control input vector

$y \in \mathbb{R}^p$ is the output vector

Here we have to find out the step response of system for open loop closed loop optimal control and closed loop suboptimal control and compare these responses.

A system in state space is represented by:

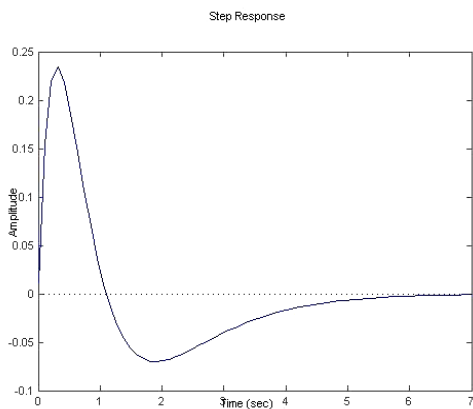
$$\begin{aligned}\dot{x}_1 &= \begin{pmatrix} 0 & 1 & 0 \\ 0 & 0 & 1 \\ -6 & -11 & -6 \end{pmatrix} \begin{pmatrix} x_1 \\ x_2 \\ x_3 \end{pmatrix} + \begin{pmatrix} 0 \\ 0 \\ 2 \end{pmatrix} u(t) \\ y(t) &= [1 \ 0 \ 0] x(t) \\ A &= \begin{pmatrix} 0 & 1 & 0 \\ 0 & 0 & 1 \\ -6 & -11 & -6 \end{pmatrix} \\ C &= [1 \ 0 \ 0] \quad \text{and} \quad D = [0]\end{aligned}$$

Using MATLAB programming:-

Eigen value of this system is given as

$$\{-1.0000, -2.0000, -3.0000\}$$

And its step input response is



Close loop system (Optimal control)

Using lqr function we convert the open loop system in close loop system whose feedback gain matrix is given as

$$K = [0.1623 \ 0.2913 \ 0.2080]$$

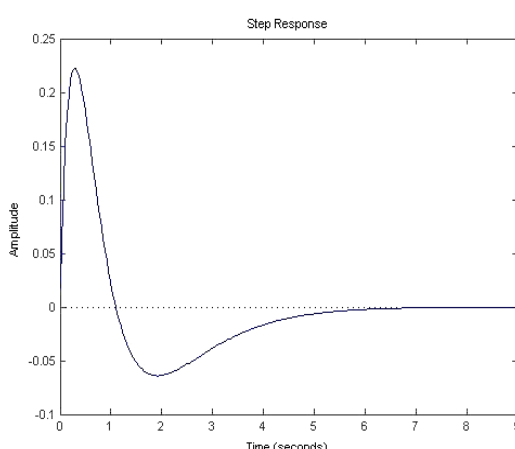
and

$$P = 1.1446 \begin{pmatrix} 1.8137 & 1.1446 & 0.0811 \\ 1.9974 & 0.1457 & \\ 0.0811 & 0.1457 & 0.1040 \end{pmatrix}$$

Eigen values is given as

$$\{-3.8138, -1.4869, -1.1153\}$$

Its step input response is given as:-



V. CONCLUSION

In case of balance truncation method there is reduction in order of system matrix but only small difference in response of system such that peak overshoot are slightly higher. Settling time decrease in case of balance truncation there is a difference of 0.075 in output

From the above example we conclude that if we apply model reduction techniques and choose a suitable method then response of system remain almost same and system remain stable .There is only change in output that will be within limit so we can apply reduce order model instead of full model such that complexity of calculation in optimal control reduce.

VI. REFERENCES

- [1] E. Bryson, "Optimal Control – 1950 to 1985," IEEE Control Systems Magazine, Vol. 16, Page(s):26–33, 1996,
- [2] Andrés A. Peters and Mario E. Salgado, "Performance Bounds In H_∞ Optimal Control For Stable SISO Plants With Arbitrary Relative Degree" IEEE transactions on automatic control, Vol. 54(8), August 2009.
- [3] Aoki M."Control of Large Scale Dynamic Systems by Aggregation", IEEE Trans.Auto. Contr., AC-13, Page(s):246-253,Junuary 1968.
- [4] Mohammed S.R. Abu Hatab "Model Order Reduction Using LMI" M.Tech Thesis The Islamic University of Gaza, 2009.

Lists of Sponsors for NPESC-2014

1. IEEE U. P. SECTION



2. TECHNICAL EDUCATION QUALITY IMPROVEMENT PROGRAMME



3. UTTAR PRADESH TECHNICAL UNIVERSITY, LUCKNOW (U. P.)



**1. BUDDHA INSTITUTE OF TECHNOLOGY, GORAKHPUR
(U.P.)**



**BUDDHA INSTITUTE OF TECHNOLOGY
GORAKHPUR**

APPROVED BY AICTE & AFFILIATED TO UPTU, LUCKNOW

Website : www.bit.ac.in email : bit.gkp@gmail.com

(A Premier Institute of Purvanchal Region of U.P.) **Code No. 525**



Imparting Quality Education in Different Branches of Engineering

Civil, CS, IT, EC & ME

Special features ;

- (i) The only Engineering Institution that provides facility to the students for summer training in foreign countries.
- (ii) Free education for 10 bright girl students of weaker section of society.
- (iii) Placement more than 60% students in reputed organizations.

2. ABES INSTITUTE OF TECHNOLOGY, GHAZIABAD (U. P.)



ABES IT GROUP OF INSTITUTIONS

ABES Institute of Technology - Code: 290

3. RKM GROUP OF COMPANIES(DELHI, MUMBAI, AHMEDABAD, & USA)

RKM
Start Think Real

About RKM IT SERVICES PVT. LTD.
is the unit of RKM Group of Company an emerging information Technology Service provider; dedicated to developing a suite of software products that will be useful for small and medium businesses, entrepreneurs and business professionals. We offer ERP services in consulting, implementation and support. We also design and deliver custom business critical software & Web Portals to help customers to achieve their strategic equipped objectives.

We offering

- Assurance Services
- BI & Performance Management
- Business Process Outsourcing
- Cloud Services
- Connected Marketing Solutions
- Consulting
- Eco-sustainability Services
- Engineering & Industrial Services
- Enterprise Solutions, Small & Medium Business,
- IT Infrastructure Service, IT Service
- Mobility Solutions and Services, Platform Solution.

Rajendra Mishra


Chairman & CEO
RKM Group of Company
Rajendra Mishra is chairman & CEO of RKM Company, a Million worth of management consulting, technology services and outsourcing company.
Email : rajendra@ansolutions.com
Share On :  www.facebook.com/Rajendra.mishra11  www.twitter.com/rjmishra11

Chairman & CFO

We are in industries as a IT Solutions Provider.

| | |
|------------------------------|--|
| Banking & Financial Services | High Tech |
| Construction | Insurance, Life Sciences, Manufacturing, Media & Information |
| Energy & Utilities | Services, Metals & Mining, Retail & Consumer Products |
| Government | Telecom |
| Healthcare | Travel, Transportation & Hospitality |

We have Branches at Delhi, Mumbai, Ahmedabad & USA
Mail us : info@rkmsolution.com, info.mumbai@rkmsolution.com, info.ahmedabad@rkmsolution.com
Visit us website : www.rkmsolution.com, www.rkmglobalsolutions.com, www.rkmtechsupport.com,
Contact Us : (O) +91-011-26340160/77 (Mob) +91-9853750780, +91-8744050780, +91-9212022200

4. KANPUR INSTITUTE OF TECHNOLOGY, KANPUR (U. P.)



KANPUR INSTITUTE OF TECHNOLOGY
ISO 9001:2008 Certified NBA Accredited

190 COMPANIES
offered JOBS to KITians

Courses offered :
GATE Code - 165
B.Tech. | B.Tech. | M.Tech. | MCA | MBA
GATE Code - 550
B.Pharma | B.Pharma

MAJOR RECRUITERS - In a Record Breaking Year 86+ Reputed Companies Visited KIT

KANPUR INSTITUTE OF TECHNOLOGY(165)
KANPUR INSTITUTE OF TECHNOLOGY & PHARMACY(550)

A-1, UPSEDC Industrial Area, Raoula, Kanpur • Ph. : 0512-2410068, 2450063
E-mail : info@kit.ac.in

No. 1
Institute in Campus, Results & Placements

Courses Offered : B.Tech. | M.Tech. | MCA | MBA
B.Pharma | M.Pharma

MAJOR RECRUITERS - In a Record Breaking Year 86+ Reputed Companies Visited KIT

KANPUR INSTITUTE OF TECHNOLOGY(165)
KANPUR INSTITUTE OF TECHNOLOGY & PHARMACY(550)

A-1, UPSEDC Industrial Area, Raoula, Kanpur • Ph. : 0512-2410055, 2430068 • e-mail : info@kit.ac.in

YOU DREAM YOUR CAREER
KIT

10 mbps Broad Band Internet, 24 hours Internet, All day Library, 24 hours Backup, Sports activities, Gofodays Hostel Facility, Bus Facilities, Digital Library

Courses Offered : B.Tech. | M.Tech. | MCA | MBA
B.Pharma | M.Pharma

MAJOR RECRUITERS - In a Record Breaking Year 86+ Reputed Companies Visited KIT

KANPUR INSTITUTE OF TECHNOLOGY(165)
KANPUR INSTITUTE OF TECHNOLOGY & PHARMACY(550)

A-1, UPSEDC Industrial Area, Raoula, Kanpur • Ph. : 0512-2410055, 2430068 • e-mail : info@kit.ac.in

A4 size (advt-1)

A4 size (advt-2)

A4 size (advt-3)

5. XNETIC TRADERS (Pvt.) Limited

Xnetic Traders (Pvt.) Ltd.



New Thinking New World

6. PUNJAB NATIONAL BANK, KNIT, SULTANPUR BRANCH



11. BANK OF BARODA, KNIT, SULTANPUR BRANCH

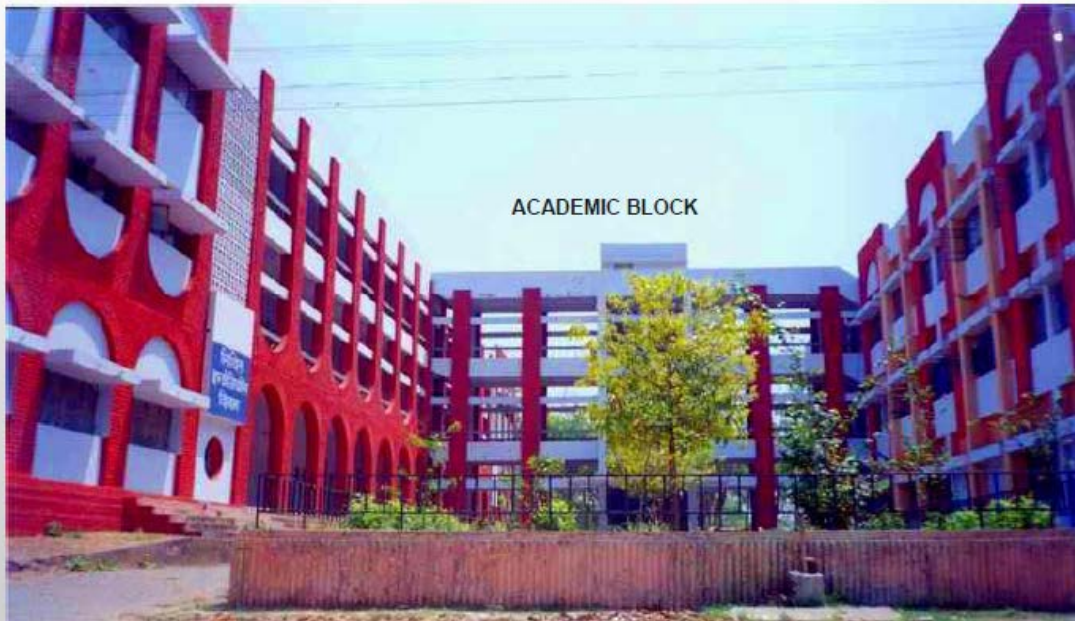


EDITORS:
S. P. Singh & B. Singh

© 2014, NPESC-2014, KNIT, Sultanpur (U .P.). Personal use of this material is permitted. However, permission to reprint/republished this material for advertising or promotional purpose or for creating new collective works for resale or redistributions to the servers or lists, or to reuse any copyrighted component of this work in other works must be obtained from NPESC-2014, KNIT Sultanpur (U . P.)



**HEARTIEST WELCOME
AT
K N I T SULTANPUR (UP) INDIA
(An Autonomous Govt. Institute)**



KAMLA NEHRU INSTITUTE OF TECHNOLOGY (KNIT), SULTANPUR U.P.